INFORMATION TO USERS

This manuscript has been reproduced from the microfilm master. UMI films the text directly from the original or copy submitted. Thus, some thesis and dissertation copies are in typewriter face, while others may be from any type of computer printer.

The quality of this reproduction is dependent upon the quality of the copy submitted. Broken or indistinct print, colored or poor quality illustrations and photographs, print bleedthrough, substandard margins, and improper alignment can adversely affect reproduction.

In the unlikely event that the author did not send UMI a complete manuscript and there are missing pages, these will be noted. Also, if unauthorized copyright material had to be removed, a note will indicate the deletion.

Oversize materials (e.g., maps, drawings, charts) are reproduced by sectioning the original, beginning at the upper left-hand corner and continuing from left to right in equal sections with small overlaps. Each original is also photographed in one exposure and is included in reduced form at the back of the book.

Photographs included in the original manuscript have been reproduced xerographically in this copy. Higher quality 6" x 9" black and white photographic prints are available for any photographs or illustrations appearing in this copy for an additional charge. Contact UMI directly to order.

UMI

University Microfilms International
A Bell & Howell Information Company
300 North Zeeb Road. Ann Arbor, MI 48106-1346 USA
313/761-4700 800/521-0600

Reproduced with permission of the copyright owner. Further reproduction prohibited without permission.

Reproduced with permission of the copyright owner. Further reproduction prohibited without permission.

Order Number 9502499

A geologic and environmental investigation of the occurrence of chrysotile asbestos in the Coalinga region of western Fresno County, California

DeReamer, John Harris, Jr., Ph.D.

University of Cincinnati, 1994

U·M·I
300 N. Zeeb Rd.
Ann Arbor, MI 48106

Reproduced with permission of the copyright owner. Further reproduction prohibited without permission.

Reproduced with permission of the copyright owner. Further reproduction prohibited without permission.

A GEOLOGIC AND ENVIRONMENTAL INVESTIGATION OF THE OCCURRENCE OF CHRYSOTILE ASBESTOS IN THE COALINGA REGION OF WESTERN FRESNO COUNTY, CALIFORNIA

A Dissertation submitted to the
Division of Research and Advanced Studies
of the University of Cincinnati

in partial fulfillment of the
requirements for the degree of

DOCTOR OF PHILOSOPHY

in the Department of Geology
of the College of Arts and Sciences

1994

by

John Harris DeReamer, Jr.

B.A., University of Kentucky, 1973

M.A., University of Kentucky, 1976

M.S., University of Cincinnati, 1984

Reproduced with permission of the copyright owner. Further reproduction prohibited without permission.

UNIVERSITY OF CINCINNATI

25 May , 19 94

I, John Harris DeReamer, Jr. ,
hereby submit this as part of the requirements for the degree of:

Doctor of Philosophy

in Arts & Sciences, Geology

It is entitled A Geologic and Environmental Invetigation of the Occurrence of Chrysotile Asbestos in the Coalinga Region of Western Fresno County, California .

Approved by:

Reproduced with permission of the copyright owner. Further reproduction prohibited without permission.

ABSTRACT

This dissertation presents the results of a geologic and environmental investigation of the occurrence and distribution of chrysotile asbestos in the Coalinga region of western Fresno County, California. The regional investigation included a comprehensive review of available literature; a regional field and aerial reconnaissance investigation of potential sources of asbestos including natural outcrop areas and areas disturbed by mining operations; a review and interpretation of historical aerial photography including black and white and color/infrared imagery; a macroscopic and microscopic assessment of the unique physical and petrographic characteristics of the region's chrysotile deposits; and a regional sediment sampling program for analysis of asbestos content of chrysotile outcrop areas, asbestos mine and mill site areas, streambed sediment transport pathways, and alluvial fan surface and subsurface deposits. The regional investigation also included a watershed asbestos soil erosion modeling program to evaluate the potential relative contribution of asbestos sediment derived by erosion from a range of identified potential sources. The regional geologic and environmental investigation was conducted to help evaluate the source or sources of asbestos detected in water samples from the California Aqueduct. The Aqueduct was constructed along the western margin of the San Joaquin Valley and the Arroyo Pasajero - Coalinga region in the 1960's. Parts of the Aqueduct receive run-off from the mountains and foothills that form the western margin of the San Joaquin Valley in the Coalinga region.

The results of the regional geologic and environmental investigation generally show the following:

The Coalinga region contains massive amounts of tectonically and diapirically emplaced deposits of a flakey, friable assemblage of minerals known as serpentinite. The largest deposit is known as the New Idria Formation and forms the core of the Joaquin Ridge Anticline. This formation outcrops over an elliptically-shaped 48-square mile area in a mountainous area located approximately 17 miles northwest of Coalinga and 15 miles west of the California Aqueduct. The serpentinite deposit is in faulted diapiric contact with Cretaceous-aged sandstones and shales of the Panoche Formation and became emergent approximately 17 to 20 million years ago in the Miocene era. Eroded asbestos-bearing sediment from this ultramafic deposit has subsequently been incorporated in some

Reproduced with permission of the copyright owner. Further reproduction prohibited without permission.

of the Miocene and younger sedimentary formations in the central San Joaquin Valley region.

The results of polarized light microscope analyses of typical samples from the New Idria Formation show that the flakey serpentinite matrix consists of 80 to 90% of a fibrous polymorph of serpentinite known as chrysotile asbestos. Much of the chrysotile is found as a fibrous form of another serpentinite polymorph known as antigorite and/or picrolite; however, subsequent transmission electron microscope analyses of the serpentinite polymorphs has shown that the serpentinite is primarily formed by very short fibers identified as chrysotile that may generally be less than 5 microns in length.

The results of field and aerial reconnaissance investigations and interpretation of historical aerial photography including color/infrared imagery has helped document the extent of the region's potential asbestos source areas including more than 50 square miles of naturally occurring asbestos-bearing serpentinite outcrop areas as well as the extent of those areas affected by 17 mining operations, 5 milling operations, and 334 exploration pit areas. The serpentinite outcrop area has experienced three phases of mining including mercury mining in the late 1800's; chromite mining in the 1940's and 1950's; and asbestos mining in the 1960's and 1970's.

The results of the review and interpretation of aerial photography were also used to identify sampling stations for a regional soil sampling and asbestos analysis program. In the Arroyo Pasajero watershed, the results of an outcrop, mine site, and streambed sampling program have shown that the concentration of chrysotile asbestos sediment in the streambed pathway decreases from approximately 80% near the serpentinite outcrop area to less than 1% approximately 30 to 40 miles downstream of the outcrop area where the asbestos-bearing stream channel flows on to the Arroyo Pasajero alluvial fan on the eastern side of Coalinga.

The results of the watershed soil erosion modeling program provides quantitative estimates that, in the Arroyo Pasajero watershed basin, approximately 2% of the asbestos in the streambed pathway may be attributed to erosion from anthropic sources such as mine and mill sites and other areas affected by mining and/or exploration operations. Based on the numerical modeling work using the Modified Universal Soil Loss Equation (MUSLE), the vast majority of the asbestos sediment in the streambed pathway may be attributed to erosion of anthropically undisturbed outcrop areas. The drainage area of the

Reproduced with permission of the copyright owner. Further reproduction prohibited without permission.

Arroyo Pasajero watershed includes approximately 6.8 square miles of serpentinite outcrop areas with approximately 12% of that area, or 530 acres, attributed to disturbances from mining operations.

The MUSLE is useful for providing estimates of relative contributions of sediment erosion; however, the MUSLE does not specifically allow for contributions from mass wasting along the sides walls of over-steepened gullies which appears to be the predominant form of erosion in the serpentinite outcrop areas. The results of the numerical modeling also do not include consideration of an estimated 16,500 cubic yards of asbestos-bearing tailings that may have been dumped into the streambed pathway in the 1930's and 1940's as a result of chromite milling operations which included washing large quantities of the serpentinite matrix for recovery of grains of disseminated chromite ore.

The results of the geologic and environmental investigation have shown that naturally-occurring serpentinite outcrop areas are the primary source of eroded asbestos sediment found in the region's intermittent streambed drainage pathways. The results of the regional investigation, including the watershed soil erosion modeling program, indicates that remediation of individual mine and/or mill sites may have negligible affect on reducing the amount of eroded asbestos sediment in the intermittent streambed pathways. The regional investigation has also shown that the primary sources of asbestos to the California Aqueduct may be located upstream of the Arroyo Pasajero drainage area in areas where run-off from asbestos-bearing geologic deposits in the Diablo Range mountains and foothills is allowed by engineering design to flow into the Aqueduct..

Reproduced with permission of the copyright owner. Further reproduction prohibited without permission.

ACKNOWLEDGMENTS

I would like to take this opportunity to express my sincere appreciation to Levine-Fricke Environmental Engineers and Hydrogeologists of Emeryville, California for providing the opportunity and support for completing this dissertation project. Much of the work presented in this dissertation was part of a regional investigation conducted by Levine-Fricke, Inc. on behalf of Southern Pacific Land Company (SPLC) in response to a USEPA (United States Environmental Protection Agency) mandated Consent Decree issued as part of SPLC's Coalinga Asbestos Mill Site remedial investigation which included, as a separate deliverable, an evaluation of potential sources of chrysotile asbestos in the Coalinga region. As the lead geologist for the Levine-Fricke regional investigation, I was responsible for developing a regional geologic perspective on the occurrence of chrysotile asbestos in the regional environment. The results of that investigation were reported in Levine-Fricke, May 9, 1989: "Offsite Source Characterization, Regional Soil Sampling, and Watershed Modeling Report." Levine-Fricke and Dr. Wayne A. Pryor, chairman of my dissertation committee, subsequently encouraged me to complete the regional investigation as a dissertation project. I particularly wish to express my appreciation to James D. Levine, President of Levine-Fricke, Inc., and Charles E. Robinson, Principal, Levine-Fricke, Inc., for their continuing support and encouragement at all stages of this project. In addition to providing moral support, Levine-Fricke also contributed to completion of most of the figures and tables presented in this dissertation and Mr. Robinson directed most of the numerical modeling work. I would also like to express my appreciation to Dr. Wayne A. Pryor and my dissertation committee including Dr. Atilla I. Kilinc and Dr. J. B Maynard for their support and guidance in completing this environmental geologic dissertation. I would also like to express my sincere appreciation to my wife, Susan DeReamer, who has graciously allowed me the opportunity to spend the many hours required for completion of this manuscript. This is noteworthy because Susan was also simultaneously completing her undergraduate degree in nursing and graduated in May of 1994 - while also providing for the birth of our son, Ian Harris DeReamer, in December of 1993 and while also providing for her three children from her first marriage. I wish to express my heartfelt appreciation for my new family, including stepchildren Chase, Cara, and Alex Southard, and my new son, Ian Harris DeReamer, to whom this endeavor is dedicated. I also wish to express my fond appreciation for all my friends in California and for my grateful memories of the great Northern California lifestyle.

Reproduced with permission of the copyright owner. Further reproduction prohibited without permission.

TABLE OF CONTENTS

Reproduced with permission of the copyright owner. Further reproduction prohibited without permission.

CHAPTER ONE CONTENTS

DISSERTATION BACKGROUND, ORGANIZATION, AND SCOPE AND PURPOSE OF INVESTIGATION

Page

1.0 DISSERTATION BACKGROUND 1-1

2.0 DISSERTATION ORGANIZATION 1-7

3.0 PURPOSE OF REGIONAL GEOLOGIC AND ENVIRONMENTAL INVESTIGATION 1-10

4.0 ENVIRONMENTAL HEALTH CONCERNS 1-11

5.0 SCOPE OF REGIONAL AND ENVIRONMENTAL INVESTIGATION 1-12

Reproduced with permission of the copyright owner. Further reproduction prohibited without permission.

CHAPTER TWO CONTENTS

SUMMARY OF GEOLOGIC AND ENVIRONMENTAL SETTING INCLUDING LITERATURE REVIEW AND SOIL MAPPING

Page

1.0 CHAPTER ORGANIZATION 2-1

2.0 SUMMARY OF GEOLOGIC AND ENVIRONMENTAL SETTING 2-3
2.1 Diablo Range Serpentinite Masses 2-3
2.2 New Idria Formation and Table Mountain Serpentinite Masses 2-5
2.3 Detrital Serpentinite Deposits and Regional Stratigraphy 2-9
2.4 Crustal Shortening 2-11
2.5 Evidence of Uplift and Erosion of the New Idria Formation 2-11
2.6 Arroyo Pasajero Drainage of the New Idria Formation 2-13
2.7 Mining Activities 2-13
2.8 Chromite Mining 2-14
2.9 Asbestos Mining 2-15
2.10 Tailings Piles, Dumps, Mines Sites, and Naturally Occurring Asbestos Sources 2-16
2.11 California Aqueduct and Alluvial Fan Sedimentation 2-18

3.0 GEOLOGIC SETTING 2-19
3.1 Geologic Origin and Description of the New Idria Formation 2-19
3.1.1 Diapiric Fold Structure of Joaquin Ridge Anticline 2-19
3.1.2 Thickness of the New Idria Formation 2-20
3.1.3 Reflectance Characteristics of the New Idria Formation and Other Serpentinite Deposits 2-20
3.1.4 Regional Drainage of the New Idria Formation 2-21
3.1.5 Alluvial Fan Sedimentation, Farming Practices, and the California Aqueduct 2-22

Reproduced with permission of the copyright owner. Further reproduction prohibited without permission.

CHAPTER TWO CONTENTS (continued)

	Page
4.0 ENVIRONMENTAL SETTING	**2-23**
4.1 Regional Overview	2-23
4.2 Johns-Manville Coalinga Asbestos Mill and the Pine Canyon Drainage Area	2-24
4.3 Atlas Mine and Mill and the White Creek Drainage Area	2-26
4.4 Landslide and/or Serpentinite Debris Flow Complexes	2-27
5.0 HISTORICAL GEOLOGY AND STRATIGRAPHY	**2-29**
5.1 Previous Studies	2-29
5.2 Paleogeography and Sedimentary Basins	2-30
5.3 Deposition of the Big Blue Member of the Temblor Formation (Miocene)	2-33
5.4 Other Serpentinite-Bearing Sedimentary Formations	2-36
5.5 Summary of Regional Stratigraphic Units	2-38
6.0 REGIONAL TECTONIC SETTING	**2-45**
6.1 Anticlines and Synclines	2-45
6.2 Extrusive Serpentinite Structures	2-45
6.3 Regional Structural Setting	2-47
6.4 Compressional Tectonics, Crustal Shortening, and the San Andreas Fault Zone	2-48
6.5 Miocene "Unroofing" and Erosion of the New Idria Formation	2-49
6.6 Regional Folding and Rate of Crustal Shortening	2-50
7.0 REGIONAL FAULTING AND SEISMIC ACTIVITY	**2-52**
7.1 Regional Faulting	2-52
7.2 Seismicity	2-52
7.3 Geologic Implications of Regional Seismicity	2-54

Reproduced with permission of the copyright owner. Further reproduction prohibited without permission.

CHAPTER TWO CONTENTS (continued)

	Page
8.0 GEOMORPHOLOGY	**2-56**
8.1 Regional Overview	2-56
8.1.1 Arroyo Pasajero Watershed	2-56
8.1.2 Pleasant Valley and Uplift of the Coalinga Anticline	2-57
8.1.3 Arroyo Pasajero Alluvial Fan	2-59
8.1.4 Arroyo Pasajero Section of the California Aqueduct	2-60
8.1.5 Subsidence and Channel Entrenchment on the Alluvial Fan	2-61
8.1.6 New Idria Formation Outcrop Area	2-61
8.1.7 Watershed Soils and Geologic Units	2-62
8.2 Joaquin Ridge-Pine Canyon Area	2-63
8.2.1 Field Observations of Landslides and/or Serpentinite Debris Flows	2-64
8.2.2 Recent Geologic Mapping	2-65
8.2.3 Relative Age of the Landslides and/or Serpentinite Debris Flow Deposits	2-66
8.2.4 Chromite Mining of Landslide Deposits	2-67
8.2.5 Origin of the Landslide and/or Serpentinite Debris Flow Complexes	2-67
8.2.6 Erosion of the Earthflow and/or Debris Flow Complexes	2-68
8.2.7 Approximate Age of the Pine Canyon Earthflow Complexes	2-69
8.2.8 Field Evidence of Continuing Uplift	2-69
8.3 Joaquin Ridge/White Creek Area	2-70
8.4 Diablo Range Alluvial Fans	2-71
8.4.1 Asbestos As A Natural Constituent of Diablo Range Alluvial Fans	2-71
8.4.2 Arroyo Pasajero Alluvial and Quaternary Asbestos Sediment	2-73
8.4.3 Depositional Facies and Drainage Pathways	2-75
8.4.4 Alluvial Fan Soil Survey Results	2-78
8.5 Arroyo Pasajero Alluvial Fan Depositional Environments and Sedimentation Rates	2-79
8.6 Cantua Creek, Salt Creek and Arroyo Hondo Alluvial Fans	2-81

Reproduced with permission of the copyright owner. Further reproduction prohibited without permission.

CHAPTER TWO CONTENTS (continued)

	Page
9.0 MINING AND MILLING OPERATIONS	**2-83**
9.1 Mercury Mining	2-83
9.2 Benitoite and Magnesite Mines	2-84
9.3 Chromite Mines and Mills	2-84
9.3.1 James-Corbett-Byles Mine	2-86
9.3.2 Railroad Mine	2-86
9.3.3 Butler Estate Chromite Mine	2-86
9.3.4 Big Ridge Mine	2-88
9.3.5 Rhodes/Byles/Gribble Mine	2-88
9.3.6 Tromby No.1 and No. 2	2-89
9.4 Asbestos Mining	2-89
9.4.1 Union Carbide Operation	2-90
9.4.2 Johns-Manville Coalinga Asbestos Operation	2-91
9.4.2.1 Mines and Mill Facility	2-91
9.4.2.2 Mining and Milling Practices	2-91
9.4.3 Atlas Corporation Operation	2-93
9.4.4 Hidden Splendor Operation	2-93
9.4.5 Todd Industries Operation	2-94
9.4.6 Basic Industries Operation	2-94
9.4.7 Other Asbestos Mining Operations	2-94
9.4.8 Asbestos Exploration Practices	2-95
10.0 SOILS	**2-97**
10.1 Arroyo Pasajero Soils Overview	2-97
10.2 Serpentinite Soils	2-98
10.2.1 Historical Background	2-98
10.2.2 Serpentinite Soil Mapping	2-99
10.2.3 Pine Canyon Area Soils	2-101
10.2.4 White Creek Area Soils	2-105

Reproduced with permission of the copyright owner. Further reproduction prohibited without permission.

CHAPTER TWO CONTENTS (continued)

	Page
11.0 CONCLUSIONS	2-109
12.0 REFERENCES	2-112

Reproduced with permission of the copyright owner. Further reproduction prohibited without permission.

CHAPTER THREE CONTENTS

RESULTS OF FIELD AND AERIAL RECONNAISSANCE INVESTIGATIONS AND INTERPRETATION OF AERIAL PHOTOGRAPHY

Page

1.0 INTRODUCTION **3-1**

1.1 Johns-Manville Coalinga Asbestos Mill Site and Pine Canyon Drainage Area 3-3

1.2 Atlas Mine and Mill Site and the White Creek Drainage Area 3-5

1.3 Landslide and/or Serpentinite Debris Flow Complexes 3-6

2.0 SUMMARY INTERPRETATION OF RECONNAISSANCE AERIAL PHOTOGRAPHS AND FIELD OBSERVATIONS **3-9**

2.1 White Creek Area 3-10

2.2 Pine Canyon Area 3-16

2.3 Los Gatos Creek Drainage Pathway 3-21

2.4 Arroyo Pasajero Alluvial Fan 3-22

2.5 Salt and Cantua Creek Drainage Area 3-24

3.0 SUMMARY OF AERIAL PHOTOGRAPHY INCLUDING LOW TO MEDIUM ALTITUDE BLACK AND WHITE AND HIGH ALTITUDE COLOR INFRARED IMAGERY **3-26**

4.0 CONCLUSIONS OF FIELD OBSERVATIONS AND INTERPRETATION OF AERIAL PHOTOGRAPHY **3-33**

5.0 REFERENCES **3-36**

Reproduced with permission of the copyright owner. Further reproduction prohibited without permission.

CHAPTER FOUR CONTENTS

MACROSCOPIC AND MICROSCOPIC CHARACTERISTICS OF CHRYSOTILE ASBESTOS DEPOSITS

Page

1.0 INTRODUCTION AND SUMMARY **4-1**

2.0 PHYSICAL AND CHEMICAL CHARACTERISTICS OF CHRYSOTILE ASBESTOS **4-6**

3.0 POLARIZED LIGHT MICROSCOPE CHARACTERISTICS OF COALINGA CHRYSOTILE DEPOSITS **4-8**

3.1 Non-Standard Optical Properties 4-9

3.2 Results of Detailed Petrographic Analyses for Identification of Particular Source Areas 4-10

4.0 RESULTS OF X-RAY DIFFRACTION ANALYSIS **4-13**

5.0 REFERENCES **4-14**

Reproduced with permission of the copyright owner. Further reproduction prohibited without permission.

CHAPTER FIVE CONTENTS

RESULTS OF REGIONAL SOIL SAMPLING AND ASBESTOS ANALYSIS PROGRAM

Page

1.0 INTRODUCTION 5-1
1.1 Purpose and Scope of Soil Sampling and Asbestos Analyses Programs 5-2
1.2 Summary Observations and Conclusions 5-5
1.3 Chapter Organization 5-9

2.0 SAMPLING METHODOLOGY 5-11
2.1 Sample Collection 5-11
2.2 Equipment Decontamination 5-13
2.3 Sample Preservation, Shipment and Archiving 5-13
2.4 Sample Documentation 5-13

3.0 ANALYTICAL METHODS 5-15
3.1 Asbestos Analyses 5-15
3.1.1 PLM Methodologies 5-16
3.1.2 TEM Methodology 5-20
3.1.3 Comparison of PLM and TEM Methods 5-22
3.2 Particle Size Analyses 5-25
3.3 Organic Matter Analyses 5-25

4.0 QUALITY ASSURANCE/QUALITY CONTROL PROGRAM 5-27
4.1 Data Validation 5-28
4.2 Laboratory QC Samples 5-28
4.2.1 PLM Laboratory QC Checks 5-29
4.2.2 TEM Laboratory QC Checks 5-30
4.2.3 Organic Matter Laboratory QC Checks 5-30
4.3 Field Quality Control Checks 5-31
4.3.1 PLM Field Duplicates 5-32
4.3.2 TEM Field Duplicates 5-33

Reproduced with permission of the copyright owner. Further reproduction prohibited without permission.

CHAPTER FIVE CONTENTS (continued)

Page

4.3.3 Organic Matter Field Duplicate 5-34
4.4 Data Compilation, Reduction and Summary 5-34

5.0 RESULTS AND INTERPRETATION OF REGIONAL SOIL SAMPLING DATA 5-36
5.1 Outcrop Areas 5-38
5.1.1 New Idria Formation 5-38
5.1.2 Big Blue Member of the Temblor Formation (Miocene) 5-39
5.1.3 Other Asbestos-Bearing Formations 5-40
5.2 Non-Asbestos-Bearing Soils 5-41
5.3 Streambed Stations 5-41
5.3.1 White Creek 5-42
5.3.2 Pine Canyon 5-44
5.3.3 Los Gatos Creek 5-45
5.3.4 Warthan, Jacalitos, and Zapato-Chino Creeks 5-48
5.3.5 Arroyo Pasajero Channel 5-49
5.4 Arroyo Pasajero Alluvial Fan and Settling Basin Subsurface Sampling 5-49
5.4.1 Subsurface Sampling Program 5-49
5.4.2 Alluvial Fan Rates of Sediment Deposition 5-51
5.4.3 Mining and Milling Activities That Predate the Late 1950's 5-53
5.4.4 Results of Alluvial Fan and Settling Basin Soil Boring Program 5-54
5.4.5 Department of Water Resources Sampling Program 5-56

6.0 SUMMARY INTERPRETATION OF JOHNS-MANVILLE COALINGA ASBESTOS MILL SITE SOIL SAMPLING DATA 5-57
6.1 Coalinga Asbestos Mill Site Stream Channels 5-58
6.1.1 West Fork of Pine Canyon at Johns-Manville Coalinga Site 5-59
6.1.2 East Fork of Pine Canyon at Johns-Manville Coalinga Site 5-61

Reproduced with permission of the copyright owner. Further reproduction prohibited without permission.

CHAPTER FIVE CONTENTS (continued)

Page

6.2 Potential Borrow Source Materials 5-63
6.3 Geomorphic Excavation Pits 5-63
6.4 Anthropically-Affected Surface Areas 5-65
6.4.1 Tailings Pile in East Fork of Pine Canyon Creek 5-65
6.4.2 Ore Storage/Loading Area 5-66
6.4.3 Mill Site Operations Area 5-66
6.4.4 Railroad Mine 5-67
6.4.5 Access Roads 5-68

7.0 CONCLUSIONS 5-70

8.0 REFERENCES 5-76

Reproduced with permission of the copyright owner. Further reproduction prohibited without permission.

CHAPTER SIX CONTENTS

WATERSHED ASBESTOS SOIL EROSION AND SEDIMENT TRANSPORT MODELING

	Page
1.0 INTRODUCTION	**6-1**
1.1 Scope and Methodology of Watershed Modeling	6-2
1.2 Other Workers and Entrenched Channel Sediment Erosion	6-4
1.3 Regional Context	6-6
1.4 Major Conclusions	6-10
2.0 EROSION AND SEDIMENT TRANSPORT BY SURFACE WATER PROCESSES	**6-12**
2.1 Weathering	6-12
2.2 Splash Erosion	6-13
2.3 Sheet Erosion	6-14
2.4 Rill Erosion	6-15
2.5 Gully Erosion and Mass Wasting	6-15
2.6 Channel, Streambed and Streambank Erosion	6-16
2.7 Sediment Transport Concepts	6-17
3.0 ESTIMATION OF EROSION OF ASBESTOS-CONTAINING SEDIMENTS IN THE LOS GATOS WATERSHED	**6-19**
3.1 Erosion Estimation Methods	6-19
3.2 MUSLE and USLE Hydrologic Input Parameters	6-23
3.2.1 The MUSLE Hydrologic Model Input Parameters	6-24
3.2.2 The USLE Hydrologic Model Input Parameters	6-25
3.3 Soil Erodibility Estimation	6-26
3.3.1 Estimation of Relative Soil Erodibility	6-26
3.3.2 Determination of K Factor Values for Asbestos-Bearing Soils	6-28
3.3.3 Sensitivity Analysis of K Factors	6-32
3.4 Effects of Length and Steepness on Erosion	6-34
3.5 Vegetative Cover Impacts on Erosion	6-35
3.6 Erosion Control Practices	6-38
3.7 Asbestos Content of Sub-Basin Materials	6-38

Reproduced with permission of the copyright owner. Further reproduction prohibited without permission.

CHAPTER SIX CONTENTS (continued)

Page

3.8 Calculation of the MUSLE and the USLE Asbestos Sediment Estimations 6-40
3.9 Average Yearly Sediment Yield Calculations 6-40
3.10 Findings of the MUSLE and the USLE Asbestos Soil Loss Estimations 6-41
3.10.1 Estimates of Anthropic Contributions to Asbestso Erosion .. 6-42
3.10.2 Possible Effects on Asbestos Erosion from Varied Paramters 6-47
3.11 Chromite Mill Tailings 6-48

4.0 DISCUSSION OF SURFACE WATER TRANSPORT PATHWAY 6-51
4.1 Previous Regional Evaluations of Arroyo Pasajero Sediments 6-51
4.2 Anthropic Increases in Asbestos Erosion Relative to Natural Sources in the Arroyo Pasajero and Surrounding Regions 6-53
4.2.1 Potential Discharges to the California Aqueduct 6-54

5.0 CONCLUSIONS 6-56

6.0 REFERENCES 6-58

Reproduced with permission of the copyright owner. Further reproduction prohibited without permission.

CHAPTER SEVEN CONTENTS

SUMMARY OF OBSERVATIONS AND CONCLUSIONS

Page

1.0 INTRODUCTION 7-1

2.0 SUMMARY OF BACKGROUND ASSESSMENT AND GEOLOGIC SETTING 7-2

3.0 SUMMARY OF GEOLOGIC OBSERVATIONS AND CONCLUSIONS 7-6

3.1 Diapiric Uplift of Diablo Range Serpentinite Masses 7-6
3.2 Miocene "Unroofing" of Serpentinite Deposits 7-8
3.3 New Idria Formation and Table Mountain Serpentinite Masses 7-9
3.4 Geologic Age of Serpentinite Deposits 7-10
3.5 Regional Structure and Asbestos-Bearing Sedimentary Formations 7-10
3.6 Extruded Serpentinite Masses 7-11
3.7 Detrital Serpentinite Deposits and Regional Stratigraphy 7-12
3.8 Continuing Uplift and Erosion of the New Idria Formation 7-13
3.9 Petrographic Characteristics of the New Idria Formation Chrysotile Asbestos Deposits 7-14
3.10 Erosion and Transport of Asbestos-Bearing Sediment to the Arroyo Pasajero Alluvial Fan and California Aqueduct 7-15
3.11 Results of Arroyo Pasajero Watershed Asbestos Soil Erosion Modeling 7-15
3.12 Summary of other Potential Sources of Chrysotile Asbestos to the California Aqueduct 7-17

4.0 FINAL SUMMARY 7-18

Reproduced with permission of the copyright owner. Further reproduction prohibited without permission.

LIST OF FIGURES

No.	Title
1-1	Regional Schematic Diagram
2-1	General Location Map with Natural Asbestos Sources
2-2A	Regional Geologic Map Showing the New Idria Formation; Other Asbestos Containing Formations; and the California Aqueduct
2-2B	Explanation of Figure 2A
2-3	Geologic and Watershed Map of Joaquin Ridge and the New Idria Formation
2-4	Geologic Map of the "Big Blue" Outcrop Near Cantua, Salt and Martinez Creeks
2-5	Generalized Stratigraphic Column of Coalinga Region Showing Asbestos-Containing Formations
2-6A	Regional Geologic Map Showing Locations of Cross Sections A-A' and B-B'
2-6B	Generalized Cross Sections Showing Structural Relationship of the Intrusive New Idria Serpentinite with Flanking Sedimentary Formations
2-6C	Explanation of Figure 6B
2-7	Joaquin Ridge Location Map Showing Johns-Manville Coalinga Asbestos and Atlas Sites and Other Mining Operations (modified from Santa Rita Peak Topographic Map, 1984)

Reproduced with permission of the copyright owner. Further reproduction prohibited without permission.

FIGURES CONTINUED

2-8A Joaquin Ridge Location Map Highlighting Location of Mines, Exploration Pits, and Drainage Channels (modified from Santa Rita Peak Topographic Map, 1984)

2-8B Joaquin Ridge Watersheds and Intermittent Drainage Channels in Mill and Mine Areas

2-9 Regional Geologic Map Showing Epicenter Locations of 1982 and 1983 Coalinga Seismic Events

2-10 Geomorphic Sketch Map of Pleasant Valley

2-11 Land Subsidence in the San Joaquin Valley, California, 1926 - 1970

2-12 Geologic Map of Joaquin Ridge-Pine Canyon Area, Including Johns-Manville Coalinga Asbestos Mill Site

2-13 Soil Map of White Creek and Pine Canyon Drainage Areas of Joaquin Ridge (from unpublished SCS data, 1987)

2-14 Soil Map of Joaquin Ridge-Pine Canyon Area, Including Johns-Manville Coalinga Asbestos Mill Site (from unpublished SCS data, 1987)

4-1 Photograph of typical serpentinite hand sample.

4-2 Photograph of serpentinite sample known as "mountain leather'.

4-3 Photomicrograph of lath-shaped bundle.

4-4 Photomicrograph of lath-shaped bundle with fibrous structure visible with increased magnification.

Reproduced with permission of the copyright owner. Further reproduction prohibited without permission.

FIGURES CONTINUED

4-5 Photomicrograph showing antigorite, lizardite, and chrysotile polymorphs.

4-6 Photomicrograph with increased magnification and crossed nichols.

4-7 Photomicrograph showing coincidental occurrence of antigorite, lizardite, and chrysotile.

4-8 Photomicrograph of coincidental occurrence of antigorite, lizardite, and chrysotile

4-9 Photomicrograph of lath-shaped bundle as picrolite with inclusion of lizardite.

4-10 Photomicrograph of chrysotile fibers and splinters viewed under cross-nichols.

4-11 Photomicrograph of splinter of chrysotile with high birefringence under crossed nichols.

4-12 Photomicrograph of mesh-like structure of platelet of lizardite particle.

4-13 Photomicrograph of similar particle as seen in 4-12 with vaguely discernible, acicular needle-like structures.

4-14 Photomicrograph of particle seen in 4-13 under crossed nichols.

4-15 Millimeter scale observed under 31 X magnification.

4-16 Millimeter scale observed under 125 X magnification.

4-17 Results of X-Ray Diffraction Analysis

Reproduced with permission of the copyright owner. Further reproduction prohibited without permission.

FIGURES CONTINUED

5-1 General Location Map Showing Asbestos Concentrations of Streambed Sampling Stations (SS Series)

5-2 General Location Map Showing Asbestos Concentrations of Outcrop Sampling Stations (OC Series)

5-3 Geologic Sketch Map of Outcrop Belt of Big Blue Formation Near Cantua Creek Southward Across Salt and Martinez Creeks

5-4 Geomorphic Map of Pleasant Valley with Streambed Sampling Results

5-5 Data Organization Chart

5-6 PLM Plot, Elongate Serpentine Asbestos Results versus Serpentine Asbestos Results

5-7 PLM Plot, Chrysotile Asbestos Results versus Serpentine Asbestos Results

5-8A Comparison of Results for Samples Analyzed by Both PLM and TEM

5-8B Comparison of Results for Samples Analyzed by Both PLM and TEM That Have Results Less Than or Equal To 20%

5-9 Frequency Distribution of PLM Results for New Idria Formation

Reproduced with permission of the copyright owner. Further reproduction prohibited without permission.

FIGURES CONTINUED

5-10 Frequency Distribution of PLM Results for the "Big Blue" Deposits

5-11 Elongate Serpentine Asbestos (% Area), Pine Canyon Creek to White Creek to Los Gatos Creek to Arroyo Pasajero (Trend Analysis)

5-12 Elongate Serpentine Asbestos (% Area), White Creek to Los Gatos Creek to Arroyo Pasajero (Trend Analysis)

5-13 Frequency Distribution of PLM Results - Alluvial Fan Core Samples

5-14 Frequency Distribution of PLM Results - West Fork Above the Site (Upstream Pine Canyon Creek)

5-15 Frequency Distribution of PLM Results - West Fork Along the Site (Downstream Pine Canyon Creek)

5-16 Frequency Distribution of PLM Results - On-Site Serpentine Landslide Area

5-17 Frequency Distribution of PLM Results - Upper Borrow Source Area

5-18 Frequency Distribution of PLM Results - Lower Borrow Source Area

5-19 Frequency Distribution of PLM Results - Tailings Pile

5-20 Frequency Distribution of PLM Results - Ore Storage Area

5-21 Frequency Distribution of PLM Results - Mill Site Operations Area

5-22 Frequency Distribution of PLM Results - Railroad Mine

Reproduced with permission of the copyright owner. Further reproduction prohibited without permission.

FIGURES CONTINUED

5-23 Frequency Distribution of PLM Results - Mill Site Access Roads

6-1 Arroyo Pasajero Drainage Basin

6-2 Joaquin Ridge Location Map Showing Coalinga Asbestos and Atlas Sites and Other Mining Operations

6-3 Sub-Basin Delineation of Los Gatos Creek Subwatershed

6-4 Oblique Perspective of Arroyo Pasajero Sediment Ponding Basin

6-5 Normal Annual Precipitation Map

6-6 Pre-Mining Erodibility Factor K MUSLE and USLE Model Input Parameters

6-7 Post-Mining Erodibility Factor K MUSLE and USLE Model Input Parameters

6-8 Intermittent Streams or Gully Drainages in Asbestos-Bearing Serpentinite Soils

6-9 Pre- and Post-Mining Ground Cover Interpretations - MUSLE and USLE Input Parameters Used in "C" Factor Development

6-10 Pre-Mining Canopy Cover Interpretations - MUSLE and USLE Input Parameters Used in "C" Factor Development

6-11 Post-Mining Canopy Cover Interpretations - MUSLE and USLE Input Parameters Used in "C" Factor Development

6-12 Roads Identified on Asbestos-Bearing Soils in the Los Gatos Watershed

6-13 California Aqueduct Inflow and Sampling Stations Locations

Reproduced with permission of the copyright owner. Further reproduction prohibited without permission.

LIST OF TABLES

No.	Title
2-1	Geologic Time Scale and Emergence of the New Idria Formation in Central California
5-1	Summary of Number of Samples Analyzed
5-2	Soil Asbestos Data Summary
5-3	Particle Size and Organic Matter Data Summary
5-4	Laboratory QC Data Summary of PLM Analyses by Med-Tox
5-5	Laboratory QC Data Summary of PLM Analyses by McCrone
5-6	Laboratory QC Data Summary of TEM Analyses by Med-Tox
5-7	Laboratory QC Data Summary of Organic Matter Analyses by Dellavalle
5-8	QA/QC Intra-Laboratory Data Summary of PLM Analyses by Med-Tox
5-9	QA/QC Inter-Laboratory Data Summary of PLM Analyses by Med-Tox and McCrone
5-10	QA/QC Intra-Laboratory Data Summary of TEM Analyses by Med-Tox
5-11	PLM-TEM Data Comparison (PLM Data Greater than or Equal to 1%)

Reproduced with permission of the copyright owner. Further reproduction prohibited without permission.

TABLES CONTINUED

5-12 TEM Results When PLM Results Equal Trace Results

5-13 PLM Asbestos Data Summary of Outcrop Areas

5-14A PLM Asbestos Data Summary of Serpentinite Soil Samples from the New Idria Formation

5-14B PLM Asbestos Data Summary of Samples from Mine Surfaces in the New Idria Formation

5-14C PLM Asbestos Data Summary of Samples from Intermittent Streambeds That Run Through the New Idria Formation

5-15 PLM Asbestos Data Summary of Samples from the "Big Blue" Deposits

5-16 PLM Asbestos Data Summary of Alluvial Fan Core Samples

5-17 Summary of Pre-Asbestos Mining versus Post-Asbestos Mining TEM Results for Alluvial Fan Core Samples

5-18 Summary of Pre-Asbestos Mining versus Post-Asbestos Mining TEM Results for Settling Basin Soil Boring Core Samples

5-19 PLM Asbestos Data Summary of Streambed Sediment from the West Fork from Locations Upstream of the Mill Site

5-20 PLM Asbestos Data Summary of Streambed Sediment from the West Fork from Locations Along and Downstream of the Mill Site

Reproduced with permission of the copyright owner. Further reproduction prohibited without permission.

TABLES CONTINUED

5-21 PLM Asbestos Data Summary of Samples from Streambanks Formed by Serpentinite Landslide and/or Debris Flow Deposits in the Mill Site Area

5-22 PLM Asbestos Data Summary of the Upper Borrow Source Area

5-23 PLM Asbestos Data Summary of the Lower Borrow Source Area

5-24 PLM Asbestos Data Summary of the Tailings Pile

5-25 PLM Asbestos Data Summary of the Ore Storage Area

5-26 PLM Asbestos Data Summary of the Mill Site Operations Area

5-27 PLM Asbestos Data Summary of the Railroad Mine

5-28 PLM Asbestos Data Summary of the Mill Site Access Roads

6-1 Summary of Average Soil Type Characteristics Including Laboratory Data and Field Observations

6-2 Summary of K Factor Values and Potential Adjustments for Asbestos Source Materials Based on Data as Reported and/or Used by SPLC and Others

6-3 MUSLE & USLE C-Factor Computation Sheet

6-4 Estimated Effect of Roads and Exploration Pits on Foliage and Associated Erosion

6-5 Watershed Asbestos Content - Pre & Post Mining

6-6A Individual Mine Impact on Asbestos Soil Erosion Summary - Unadjusted K

Reproduced with permission of the copyright owner. Further reproduction prohibited without permission.

TABLES CONTINUED

6-6B Individual Mine Impact on Asbestos Soil Erosion Summary - Unadjusted K Percentage of Individual Mine Impact on Pre-Asbestos Soil Erosion Summary - Unadjusted K

6-6C Individual Mine Impact on Asbestos Soil Erosion Summary - Unadjusted K Percentage of Individual Mine Impact on Post Asbestos Soil Erosion Summary - Unadjusted K

6-6D Individual Mine Impact on Asbestos Soil Erosion Summary - Adjusted K Yearly Average Asbestos Erosion

6-6E Individual Mine Impact on Asbestos Soil Erosion Summary - Adjusted K Percentage of Individual Mine Impact on Pre-Asbestos Soil Erosion Summary - Adjusted K

6-6F Individual Mine Impact on Asbestos Soil Erosion Summary - Adjusted K Percentage of Individual Mine Impact on Post-Asbestos Soil Erosion Summary - Adjusted K

6-7A MUSLE Individual Mine Impact on Asbestos Soil Erosion Summary - Adjusted K - Yearly Average Asbestos Erosion

6-7B MUSLE Individual Mine Impact on Asbestos Soil Erosion Summary - Unadjusted K Yearly Average Asbestos Erosion

6-8A MUSLE Total Pre-Mining Asbestos Sediment Yield Calculated by the MUSLE Adjusted and Unadjusted K

6-8B MUSLE Total Post-Mining Asbestos Sediment Yield Calculated by the MUSLE - Adjusted and Unadjusted K

6-8C MUSLE Total Mine and Road/Pits Impact on Asbestos Soil Erosion Summary - adjusted and Unadjusted K

6-8D MUSLE Total Pre-Mining and Post-Mining Asbestos Sediment Yield Calculated by the MUSLE Adjusted and Unadjusted K Portion of Currently Eroded Asbestos Increase to Natural Asbestos Erosion

Reproduced with permission of the copyright owner. Further reproduction prohibited without permission.

TABLES CONTINUED

6-8E MUSLE Total Pre-Mining and Post-Mining Asbestos Sediment Yield Calculated by the MUSLE Adjusted and Unadjusted K Portion of Currently Eroded Asbestos

6-9A Mines in the Los Gatos Creek Drainage Basin

6-9B Mines in the Los Gatos Creek Drainage Basin

6-9C Mines in the Los Gatos Creek Drainage Basin

6-10 Estimation of Chromite Milling Serpentinite Soil Matrix Discharge

6-11 Estimated Asbestos Concentration Increase to Natural Asbestos Concentration in Water-Dependent Transport Pathways from Anthropic Asbestos Erosion

6-12 Estimated Asbestos Concentration Increase to Natural Asbestos Concentrations in Water-Dependent Transport Pathways from Anthropic Asbestos Erosion

6-13 Inlets at Foothill Drainage Areas Where Runoff Enters the California Aqueduct

6-14 California Aqueduct Water Quality Asbestos Sampling Data

Reproduced with permission of the copyright owner. Further reproduction prohibited without permission.

LIST OF APPENDICES

Appendix A	Field Photographs
Appendix B	Aerial Photographs and Interpretations
Appendix C	Inventory of Reviewed Aerial Photography
Appendix D	Analytical Laboratory Reports of Reconnaissance Petrographic, PLM, and TEM Analyses
Appendix E	Examples of Typical Laboratory Data Reports
Appendix F	Alluvial Fan Soil Boring Location Map and Soil Boring Lithologic Logs
Appendix G	K-Factor Nomographs

Reproduced with permission of the copyright owner. Further reproduction prohibited without permission.

CHAPTER ONE

DISSERTATION BACKGROUND, ORGANIZATION, AND SCOPE AND PURPOSE OF INVESTIGATION

1.0 DISSERTATION BACKGROUND

This dissertation presents the results of my contributions to a geologic and environmental investigation of the occurrence and distribution of chrysotile asbestos in the Coalinga and Arroyo Pasajero watershed region of the central San Joaquin Valley in western Fresno County, California. This work was conducted to help evaluate the relative contribution of asbestos to the regional environment and the California Aqueduct from a range of natural and/or man-made potential sources. Much of the work presented in this dissertation was originally presented as part of an investigation conducted by Levine-Fricke, Inc. (an environmental engineering consulting company based in Emeryville, California) on behalf of the Southern Pacific Land Company (SPLC) in response to requirements from the U.S. Environmental Protection Agency (EPA). The general area of investigation is illustrated in Figures 1-1 and 2-1.

SPLC was identified in 1986 by the EPA as being a potential contributor of asbestos to the California Aqueduct in the vicinity of the Coalinga and Arroyo Pasajero section of the California Aqueduct. SPLC was identified as being owners of an abandoned asbestos milling operation located in the Upper Pine Canyon area adjacent to the primary outcrop area of an asbestos-bearing geologic formation known as the New Idria Formation. This area is located approximately 17 miles northwest of the town of

Reproduced with permission of the copyright owner. Further reproduction prohibited without permission.

Coalinga in western Fresno County, California. The abandoned asbestos milling operation on SPLC land was identified as the Coalinga Asbestos Mill Site. SPLC had leased the land area of the Coalinga Asbestos Mill Site to the Johns-Manville Corporation in the 1960's. When Johns-Manville abandoned their Pine Canyon mill site operations in the early 1970's, they left an unremediated facility with numerous potential sources of asbestos including ore storage and processing piles and an estimated 400,000 cubic yards of asbestos tailing materials deposited in a gorge-like canyon fork of Upper Pine Canyon Creek. The tailings pile was partially protected from erosion by the steep sidewalls of the gorge-like canyon and by a sediment retaining dam constructed near the base of the tailings pile. However, as a result of an intermittent drainage pathway running through the middle of the tailings pile, some of the asbestos tailings were subject to erosion and sediment transport downstream through the intermittent Pine Canyon drainage system.

The Coalinga Asbestos Mill Site was designated by the EPA as being one of two Superfund Sites in the region that were responsible for the erosion and transport of asbestos-bearing sediment into the waters of the California Aqueduct. The other Site was identified as the Atlas Mine and Mill Site. These mine and mill sites are located in the Joaquin Ridge mining district of the New Idria Formation outcrop area in a mountainous area approximately 17 miles northwest of Coalinga and 15 miles west of the western margin of the San Joaquin Valley and the California Aqueduct. In this area, the Aqueduct was constructed along the upper western margin of the valley at an elevation of approximately 340 feet near the base of the region's asbestos-bearing foothills and mountains. The New Idria Formation outcrop area is located in a mountainous area at an elevation that ranges from approximately 4,400 to 5,400 feet and there is approximately 5,000 feet of relief between the primary asbestos outcrop mining areas and Aqueduct. The Aqueduct was designed with inlet structures to

Reproduced with permission of the copyright owner. Further reproduction prohibited without permission.

capture runoff from the adjoining mountains and in some area, the runoff contains elevated concentrations of asbestos sediment and suspended asbestos fibers that is allowed by engineering design to drain into the Aqueduct.

In accordance with an Administrative Order on Consent (Consent Order), SPLC agreed on November 16, 1987 to conduct a regional investigation of the occurrence of chrysotile asbestos in the Coalinga region to evaluate the relative contribution of asbestos to the California Aqueduct by watershed erosion from a range of potential sources including: the Coalinga Asbestos Mill Site in Pine Canyon; the Atlas Mine and Mill Site in the White Creek drainage area of the New Idria Formation; and hundreds of other potential sources including abandoned mining operations and many square miles of natural, undisturbed chrysotile outcrop areas.

Levine-Fricke, Inc. (Levine-Fricke) of Emeryville, California was retained by SPLC to conduct the regional investigation agreed to in the Consent Order. The results of the Levine-Fricke investigation were presented to the EPA in a draft technical report titled: "Offsite Source Characterization, Regional Soil Sampling, And Watershed Soil Erosion Modeling Report" (Levine-Fricke, May 9, 1989).

I was part of the engineering team assembled by Levine-Fricke to conceptualize, manage, implement, and complete the required investigations. As the project's lead geologist, my responsibilities included evaluating the scope and magnitude of the region's potential sources and working with the project's engineers to develop numerical estimates of the relative contributions of identified potential sources in the Arroyo Pasajero watershed. I was also responsible for evaluating the geology of other nearby watersheds were runoff from asbestos-bearing materials may have been allowed to drain into the California Aqueduct. This work included interpretation of additional

Reproduced with permission of the copyright owner. Further reproduction prohibited without permission.

asbestos sediment sampling data obtained from the California Department of Water Resources for aqueduct water samples and sediment samples collected from other upstream and downstream sections of the California Aqueduct.

As the project's lead geologist, I was responsible for the collection and interpretation of geologic data; for the preparation of geologic illustrations; and for writing a majority of the technical report prepared by Levine-Fricke (May 9, 1989).

For the geologic aspects of this project, I developed an approach that included conducting a comprehensive review of available geologic literature and maps regarding the occurrence of chrysotile asbestos in the Cologne region. I had access to the geologic library at the University of California at Berkeley and other sources of geologic and technical reports. I supplemented my literature review with a review of aerial photography available at Whittier University (Fairchild Collection) and the University of California at Santa Barbara (UCSB). The UCSB library is a national repository of aerial photography. Additional aerial photographs were procured from the U.S. Department of Agriculture, Soil Conservation Service and from the USGS.

My review of aerial photographs was supplemented with several low altitude aerial reconnaissance flights made by private plane over the area of investigation. These aerial reconnaissance flights were supplemented with several preliminary ground reconnaissance surveys of asbestos-bearing outcrop areas; mining areas; and mill site areas. My preliminary evaluations indicated to me and to others that there were in fact numerous potential sources including vast a chrysotile-bearing outcrop area of the New Idria Formation that covered an estimated 50 square miles that contained numerous areas affected by mining and/or mineral exploration operations.

Reproduced with permission of the copyright owner. Further reproduction prohibited without permission.

The results of my field and aerial reconnaissance surveys were used for my identification of field sampling stations for evaluation of asbestos content of identified potential sources of asbestos including chrysotile outcrop areas, mining areas, and mill site areas. The asbestos sampling program also included collection of samples from streambed sediment stations and from alluvial fan surface and subsurface sampling stations.

I was also responsible for working with several asbestos analytical laboratories that were used for EPA-certified asbestos analyses of several hundred bulk soil and/or streambed sediment samples. I also worked closely with the laboratories on petrographic interpretation of microscopic and submicroscopic analyses of the collected samples. This was done to increase our understanding of the unique optical characteristics of the region's chrysotile asbestos deposits and to help facilitate the routine analysis of the hundreds of analyzed samples. For this dissertation project, I have supplemented the asbestos analytical results of the participating subcontracting laboratories (McCrone Environmental Services of Norcross, Georgia and Med-Tox Associates of San Diego, California) with a series of photomicrographs that illustrate some of the unique petrographic characteristics of the regions' chrysotile asbestos deposits.

Although the Coalinga Asbestos Mill Site had a tailings pile that filled a canyon with an estimated 400,000 cubic yard of asbestos tailings, there was a retaining dam at the base of the tailings pile. Field observations indicated that the retaining dam was effective in retaining asbestos-bearing sediment from being washed into the canyon's intermittent stream pathway. This indicated that the Coalinga Asbestos Mill Site's contribution of asbestos to the regional environment was small in comparison with the region's other un-contained potential sources.

Reproduced with permission of the copyright owner. Further reproduction prohibited without permission.

In order to provide quantitative estimates of the relative contribution of asbestos sediment from identified sources, I worked with the project's engineering team on development of a numerical modeling program that could be used to evaluate the relative contributions by erosion from each of the identified potential sources. The modeling program was designed to evaluate potential watershed contributions by using the Modified Universal Soil Loss Equation for numerical modeling of asbestos-bearing soil erosion and sediment transport in the greater Arroyo Pasajero watershed.

For the soil erosion modeling work, it was my responsibility to review and interpret available aerial photographs for identification of potential asbestos sources; to identify representative sampling stations for characterization of asbestos content of potential source materials including mine sites, mill sites, ore storage areas, tailing piles, natural outcrop areas, streambed sediment deposits, and alluvial fan surface and subsurface deposits; to collect or supervise the collection of field samples for laboratory analyses; to work with several EPA-approved laboratories as subcontractors for the asbestos analyses of the numerous samples required for characterization of the asbestos content of identified potential source areas; to work with the project engineers on evaluation of field and soil conditions for development of "K" factor estimates of soil erodibility of identified potential source materials; and to work with the project engineers on identification of additional watershed soil erosion modeling parameters including interpretation of aerial photographs for development of estimates of vegetative coverings of watershed sub-basins.

Reproduced with permission of the copyright owner. Further reproduction prohibited without permission.

2.0 DISSERTATION ORGANIZATION

This dissertation is organized into six chapters as described in the following sections:

Chapter Two: Regional Geologic and Environmental Setting

This chapter provides my review of the regional geologic and environmental setting including a review of what is known about the occurrence of chrysotile asbestos in the Coalinga region including identification of potential upland source areas and mining operations. This chapter includes my comprehensive review of available literature including geologic reports and maps.

Chapter Three: Regional Field and Aerial Reconnaissance Investigation.

This chapter provides the results of my regional field and aerial reconnaissance investigation of potential asbestos source areas including natural outcrop areas and asbestos-bearing mine and mill site operations areas. This section includes a summary of my field observations of identified potential source areas; stream sediment transport pathways; and alluvial fan depositional areas. The aerial reconnaissance section includes my review and interpretation of aerial photography including low altitude reconnaissance photography and high altitude color/infrared imagery. I used the results of the field and aerial reconnaissance investigations to identify the location of sampling stations for the collection of representative soil and/or sediment samples for analysis of chrysotile asbestos content.

Reproduced with permission of the copyright owner. Further reproduction prohibited without permission.

Chapter Four: Macroscopic and Microscopic Characteristics of Coalinga Chrysotile Asbestos Deposits.

This chapter provides a summary of the results of my macroscopic and microscopic assessment of a typical, relatively unweathered chrysotile sample from a mine surface exposure in outcrop area of the New Idria Formation. The microscopic assessment includes a series of photomicrographs that help document the unique petrographic characteristics of the three serpentinite polymorphs associated with the region's chrysotile deposits including antigorite, lizardite, and chrysotile. This chapter also includes a summary of the microscopic (PLM) and sub-microscopic (TEM) characteristics of numerous bulk soil samples analyzed by two EPA-approved supporting laboratories using EPA-approved analytical methods.

Chapter Five: Regional Soil Sampling and Asbestos Analysis Program.

This chapter provides my summary of the results of the regional sampling program which includes the results of 385 samples analyzed using PLM analytical methods and 73 samples analyzed using TEM analytical methods. The analyzed samples included samples collected from the New Idria Formation including undisturbed outcrop areas; mine site areas; mill site ore storage and tailings pile areas; streambed sediment samples; alluvial fan surface samples; and alluvial fan subsurface samples. The sampling program also included samples collected from non-asbestos bearing outcrops of the marine shales and sandstones of the Cretaceous-aged Panoche Formation (i.e., pre-Miocene aged formations). The data was used for characterization of asbestos content of various identified sources for use in a regional asbestos soil erosion modeling program as reported in Chapter Five. The analysis of the resulting data included an analysis of the correlation of PLM and TEM data for samples analyzed by both methods.

Reproduced with permission of the copyright owner. Further reproduction prohibited without permission.

Chapter Six: Arroyo Pasajero Watershed Asbestos Soil Erosion Modeling.

This chapter provides a summary of the results of my contributions to the numerical modeling and estimation of the relative contributions of asbestos sediment transported from identified potential source areas to the Arroyo Pasajero alluvial fan and California Aqueduct as a result of watershed erosion. I have provided a summary of my contributions to the development soil erodibility "K" factors and other watershed modeling parameters including interpretation of aerial photography for mapping of vegetative coverings and identification of drainage sub-basins. I have also provided a summary of the results of the Levine-Fricke watershed soil erosion modeling work which was conducted from a regional perspective to evaluate the relative contributions from various man-made sources such as mine sites and mill sites versus natural (undisturbed) outcrop sources. This chapter also provides a summary of the numerical modeling work that was conducted by myself and the project's engineering team to evaluate potential relative differences in the amount of asbestos-bearing sediment eroded in pre-mining versus post-mining time scenarios to evaluate the potential contribution to erosion as a result of regional mining operations. The results of my alluvial fan surface and subsurface investigation were used to confirm the results of the numerical modeling pre-mining and post-mining evaluations.

Chapter Seven: Summary Observations and Conclusions

This chapter provides a summary of my observations and conclusions of the results of the regional environmental investigation. Summary observations and conclusions are presented regarding the regions' geologic history including the diapiric emplacement of massive deposits of chrysotile asbestos; observations and conclusion regarding the extent and physical characteristics of potential sources of asbestos to the regional environment

Reproduced with permission of the copyright owner. Further reproduction prohibited without permission.

including natural outcrop areas, areas affected by asbestos mining and milling operations and other mining and mineral exploration activities of the past; observations and conclusions regarding the macroscopic and microscopic characteristics of the region's geologic deposits of chrysotile asbestos; observations and conclusions regarding the results of regional soil sampling and asbestos analyses; observations and conclusions regarding the results of numerical modeling assessments of the relative contributions of a range of identified potential sources of asbestos-bearing sediment being delivered to the Arroyo Pasajero section of the California Aqueduct; and observations and conclusion regarding the occurrence of other potential sources of asbestos to the California Aqueduct in areas located upstream of the Arroyo Pasajero section of the Aqueduct.

3.0 PURPOSE OF REGIONAL GEOLOGIC AND ENVIRONMENTAL INVESTIGATION

The regional geologic and environmental investigation was conducted to provide information on the occurrence and distribution of chrysotile asbestos deposits in the Coast Range mountains, foothills, and alluvial fan regions of the Coalinga region in western Fresno County, California. This area is located along the western margin of the central San Joaquin Valley as illustrated in Figures 1-1, 2-1, and 2-2.

This is an area were there are massive occurrences of ultramafic and sedimentary deposits of the primary mineral chrysotile asbestos. These deposits are known as serpentinite and are of both economic and environmental health significance. The ultramafic deposits of serpentinite have yielded massive quantities of commercial grade chrysotile asbestos ore and other ores, primarily chromite and mercury. Mining chromite, mercury, and other rare minerals has been taking place in this district since the late 1800's. Chromite mining operations were increased in the 1940's and 1950's

Reproduced with permission of the copyright owner. Further reproduction prohibited without permission.

as a result of the strategic value of chromite ore. Mining operations for chrysotile asbestos occurred in the 1960's when it was discovered that the primary matrix of the chromite ore deposits consisted of 80 to 90 percent or more of an almost pure form of chrysotile. The chrysotile occurred as very short fibers, generally 5 to 10 microns in length or shorter, which were bundled in a flakey, whitish-gray matrix that was not previously recognized as having commercial value.

4.0 ENVIRONMENTAL HEALTH CONCERNS

The environmental health concerns of the naturally occurring and commercially disturbed deposits of asbestos-bearing serpentinite in the Coalinga region were recognized by the United States Environmental Protection Agency and other agencies in the 1980's when elevated concentrations of chrysotile asbestos were discovered in the waters of the California Aqueduct in the Coalinga region. The California Aqueduct was constructed in the mid to late 1960's near the base of the foothills that form the western margin of the San Joaquin Valley. The Aqueduct was designed with inlet structures to capture run-off from the foothill regions to increase the yield of water to the Aqueduct and to increase the economic value of the project by protecting previously flood-prone alluvial fan areas. Run-off from the foothill watersheds has subsequently been found to contain high concentrations of chrysotile asbestos. Chrysotile asbestos has also been detected at elevated concentrations in the air of the Coalinga region. Airborne concentrations of chrysotile have been found to cause a form of lung cancer, mesothelioma, and subsequently has been controlled by environmental regulations. Research is currently being conducted to evaluate potential health risks from ingestion of chrysotile asbestos in water. Preliminary health evaluations do not indicate any significant gastro-intestinal impacts. Significant health

Reproduced with permission of the copyright owner. Further reproduction prohibited without permission.

risks are partly evaluated in terms of potential increases in the rates of cancer on the order of 1 in 100,000 or 1 in 1,000,000.

5.0 SCOPE OF REGIONAL AND ENVIRONMENTAL INVESTIGATION

My contribution to the regional geologic and environmental investigation included a field and aerial reconnaissance assessment of potential chrysotile asbestos source areas located in the semi-arid Joaquin Ridge highland areas; a soil and streambed sediment sampling program conducted to provide an assessment of the intermittent stream pathways that drain potential chrysotile source areas located in the Joaquin Ridge mining district and the intermittent streams which serve as migration pathways for the downstream transport and dispersion of chrysotile asbestos from the potential source areas; and an investigation of the chrysotile content of the Arroyo Pasajero surface and subsurface alluvial fan deposits of the central San Joaquin Valley.

My field and aerial reconnaissance investigation included an investigation of the primary chrysotile asbestos outcrop area which covers more than fifty square miles and is regionally known as the New Idria Formation. The outcrop area of the New Idria Formation includes the Joaquin Ridge mining district located in a mountainous area approximately 17 miles northwest of the town of Coalinga. My regional geologic assessment also included an investigation of the sedimentary serpentinite deposits of the Big Blue Hills and other asbestos-containing sedimentary formations that flank the Joaquin Ridge foothills; and an investigation of the geologically recent alluvial fan deposits of the Arroyo Pasajero, Cantua Creek, and other alluvial fan systems found along the western margin of the central San Joaquin Valley in the Coalinga region.

Reproduced with permission of the copyright owner. Further reproduction prohibited without permission.

In addition to field and aerial reconnaissance investigations, my geologic research included a review of available literature and technical reports including discussions of the regional geology, tectonic setting, and local seismicity; a review of the physical and mineralogical characteristics of the asbestos-containing New Idria Formation; and a discussion of regional mining operations (primarily mercury, chromite and asbestos) that have been active in the area since 1853. Additional work included microscopic analyses for asbestos content of outcrop samples, mill site samples, streambed drainage pathway sediment samples, and alluvial fan samples. Data from the asbestos sample analyses was used for numerical modeling of relative rates of erosion from identified potential asbestos source areas.

Reproduced with permission of the copyright owner. Further reproduction prohibited without permission.

CHAPTER TWO

SUMMMARY OF GEOLOGIC AND ENVIRONMENTAL SETTING INCLUDING LITERATURE REVIEW AND SOIL MAPPING

1.0 CHAPTER ORGANIZATION

This chapter provides background information on the regional geologic and environmental setting including a comprehensive review of available literature including geologic and technical reports and soil mapping. The information presented in this chapter has the following organization:

Section 2.0 provides an overview of the regional geology including brief summaries of what is known of the natural occurrence of asbestos in the mountains, foothills, and alluvial fans of the western margin of the central San Joaquin Valley in the Coalinga region.

Section 3.0 provides a synopsis of the geologic setting including brief discussions of what has been reported regarding the origin of the region's asbestos deposits.

Section 4.0 provides detailed information on the regional geology, including discussions of the occurrence of asbestos sediment in geologic units that date from the present back to the Miocene time period (approximately 17 to 20 million years ago).

Reproduced with permission of the copyright owner. Further reproduction prohibited without permission.

Section 5.0 provides a summary of the historical geology and regional stratigraphy.

Sections 6.0 and 7.0 provide information on the tectonics and seismicity of the Coalinga region, which is located approximately 17 miles northeast of the San Andreas Fault Zone.

Section 8.0 provides a review of the geomorphology of the Arroyo Pasajero watershed basin, including descriptions of the asbestos sediment source areas, the intermittent streambed drainage pathways, and the Arroyo Pasajero and other alluvial fans.

Section 9.0 provides information on the occurrence of mining in the asbestos outcrop areas of the New Idria Formation.

Section 10.0 discusses the physical characteristics of the soils that have been mapped by the SCS (Soil Conservation Service) and by myself and others in the asbestos outcrop areas of the White Creek and Pine Canyon drainage sub-basins.

Section 11.0 presents the major conclusions of my regional geologic investigation of the occurrence of chrysotile asbestos in the Coalinga and western Fresno County region.

Section 12.0 provides a list of references.

Reproduced with permission of the copyright owner. Further reproduction prohibited without permission.

2.0 SUMMARY OF GEOLGIC AND ENVIRONMENTAL SETTTING

2.1 Diapiric Emplacement of Diablo Range Serpentinite Masses

The southern Diablo Range mountains of the central Coast Range in the vicinity of Coalinga contain more than 50 known ultramafic serpentine deposits that contain a high percentage of chrysotile asbestos (EPA, Potential Sources Report, 1987; Dickenson, 1966a; Mumpton and Thompson, 1975; Davis, 1962; Rice, 1963). The majority of these deposits are located on the northeastern side of the San Andreas Fault Zone as illustrated in Figure 2-1. The serpentine deposits are primarily composed of a sheared, flakey, readily-friable matrix of serpentinite that contains up to 96% chrysotile asbestos (Mumpton and Thompson, 1975; Soil Conservation Service, Soil Lab Data Report, 1987). The serpentinite bodies were derived from the metamorphic and hydrothermal alteration of oceanic crustal material that underlies the continental crust in the Coast Range region (Dietz, 1963; Page, 1966 and 1981; Mumpton and Thompson, 1975). The serpentinite bodies were emplaced in the upper crust of the earth's surface by diapiric or upward solid-flow. The upward movement of the semi-plastic, diapiric serpentinite bodies contributed to the warping and folding of the overlying geologic formations. In the Coalinga region, these upwardly warped and folded formations formed elliptically-shaped, dome-like anticlinal structures that are oriented subparallel to the trend of the nearby San Andreas Fault Zone (Eckel and Myers, 1946; Dibblee, 1971; Zigler, Wentworth, and Zoback, 1987). These deposits are illustrated in the geologic maps and illustrations presented in Figures 2-1, 2-2A, 2-3, 2-4, and 2-5.

The diapiric emplacement of the serpentinite masses and the anticlinal deformation of the geologic formations occurred in response to a system of crustal compression that

Reproduced with permission of the copyright owner. Further reproduction prohibited without permission.

resulted from the tectonic convergence of the Pacific oceanic plate and the North American continental plate (Dickenson, 1966a; Cowan and Mansfield, 1970; Page, 1981). The massive serpentinite deposits were derived from the metamorphic and hydrothermal alteration of oceanic crustal material that was thrust under the continental plate (Hess, 1955; Dietz, 1962; Page, 1966). These massive, metamorphosed assemblages of serpentine minerals were less dense than the surrounding host rock; and because of their semi-plastic, buoyant nature and the occurrence of crustal compression, the serpentinite masses were forced upward toward the surface (Dickenson, 1966a). These upwardly mobile masses have migrated into the cores of anticlinal structures that are generally oriented subparallel to the northwest-southeast trend of the San Andreas Fault Zone. Continued crustal compression and diapiric uplift allowed the serpentinite masses to pierce or rupture the anticlinal structures and the overlying rock formations. The asbestos-bearing serpentinite masses were subsequently forced out or extruded from the cores of faulted, anticlinal structures. In addition to diapiric structures, some of the serpentinite deposits were extruded from large fissures or cracks associated with local faulting (Eckel and Myers, 1946; Dickenson, 1966a).

The "unroofing" or surface exposure of these serpentinite masses allowed great quantities (estimated to be as much as ten cubic miles by Eckel and Meyers, 1946) of the semi-plastic material to be extruded or forced out of the anticlinal structures by means of solid-flowage. Much of the extruded, asbestos-bearing serpentinite was subsequently eroded and redeposited in local sedimentary environments as detrital serpentinite debris. An analysis of the regional stratigraphy demonstrates that this detrital serpentinite debris has been incorporated in many of the local sedimentary rock formations that are Miocene or younger in age (i.e., 20 million years old or less)

Reproduced with permission of the copyright owner. Further reproduction prohibited without permission.

including the Big Blue Member of the Temblor Formation (Miocene) and relatively recent Quaternary alluvial fan sediments that were deposited prior to historic time.

As a result of their relationship with faulted, uplifted anticlinal structures, most of the southern Diablo Range serpentinite bodies are located near the tops of mountains and ridges in areas associated with steep relief and rugged terrain (Eckel and Myers, 1946; Dickenson, 1966a; Cowan and Mansfield, 1970; Dibblee, 1971). The climate of the region is characterized as Mediterranean with a short rainy season in the winter and a long hot dry period in the remaining months. The areas of higher elevation, including the serpentinite outcrop areas, typically receive the region's highest annual rainfalls and strongest seasonal winds. This contributes to apparently high rates of erosion of the asbestos-bearing serpentinite soils. This also explains why asbestos is an integral component of the sediments derived from the mountain areas and deposited in the alluvial fan areas.

2.2 New Idria Formation and Table Mountain Serpentinite Masses

The New Idria Formation is the largest known serpentinite deposit in the Coalinga region. This asbestos-containing formation is exposed over an elliptically-shaped, 48-square-mile area that forms the crest of the Joaquin Ridge highland trend (Eckel and Myers, 1946). The mountainous area is located approximately 20 miles northwest of Coalinga (Jenkins, 1971). Another major deposit is the Table Mountain serpentinite body, which originally may have covered more than 30 square miles as a result of extrusion and surface spreading (Dickenson, 1966a). The Table Mountain serpentinite deposit is located approximately 17 miles south of Coalinga. Both of these serpentinite deposits are related to faulted, anticlinal structures. The location of these

Reproduced with permission of the copyright owner. Further reproduction prohibited without permission.

regional serpentinite deposits and the regional geology and structure are illustrated in Figures 2-1, 2-2A, and 2-6B.

The New Idria Formation forms the exposed core of the Joaquin Ridge Anticline (Zigler, Wentworth, and Bartow, 1986). Diapiric uplift of the serpentinite body over great lengths of geologic time has allowed large volumes of serpentinite debris to be extruded and eroded from the elliptically-shaped, 48-square-mile outcrop area (Anderson and Pack, 1915; Eckel and Myers, 1946; Read, 1959; Casey and Dickenson, 1976). The Table Mountain deposit was formed by serpentinite debris that was extruded from a series of faults and fissures associated with the Table Mountain structure (Dickenson, 1966a). Geophysical and geological investigations of the New Idria Formation indicate that the diapiric, serpentinite mass extends from the surface to a depth of more than 15,000 feet (Byerly, 1966). The fact that the serpentinite body forms the core of an anticlinal structure indicates that the serpentinite mass may extend much deeper. The extrusive Table Mountain serpentinite deposit originally covered more than 30 square miles with serpentinite debris that ranged from 50 to 250 feet thick. Fluvial erosion and dissection of the Table Mountain structure has diminished the areal extent of this serpentinite deposit to about 20 square miles (Dickenson, 1962 and 1966a).

It has been estimated that in early Miocene time (approximately 17 to 20 million years ago) approximately 5 to 10 cubic miles of serpentinite debris was extruded from the New Idria/Joaquin Ridge structure (Eckel and Myers, 1946). This estimate is based on calculations regarding the areal extent and thickness of sedimentary asbestos deposits of Miocene age in the Coalinga region. The extruded material was eroded and deposited as detrital serpentinite debris in a shallow marine environment that was part of the inland and/or continental margin sea that once covered the central San

Reproduced with permission of the copyright owner. Further reproduction prohibited without permission.

Joaquin Valley area. This asbestos-containing body of detrital serpentinite debris is known as the Big Blue Member of the Temblor Formation (Miocene). The Big Blue Member ranges in thickness from 300 to 1,000 feet. The soft, weakly consolidated, asbestos-containing formation now forms the Big Blue Hills which are located approximately 10 miles north of Coalinga. The location and extent of the "Big Blue" deposits is illustrated in Figures 2-2A, 2-6A, and 2-6B. The stratigraphic occurrence and areal extent of sedimentary asbestos deposits (including the Big Blue Member and other formations) that originated from the New Idria serpentinite mass has been reported by the following: Anderson and Pack, 1915; Eckel and Myers, 1946; Hoots, Bear, and Kleinpell, 1954; Read, 1959; Page, 1966; Casey and Dickenson, 1976).

The Big Blue Hills are part of an easterly dipping monocline (dipping approximately 20 to 30 degrees) that flanks the New Idria - Joaquin Ridge structure and also forms the western margin of the central San Joaquin Valley. (See Figure 2-6A and 2-6B). This area is located approximately eight miles east of the New Idria Formation outcrop at the crest of the Joaquin Ridge Anticline. The monocline is formed by Cretaceous and younger strata including the Temblor Formation (Lower Miocene); the Santa Margarita Formation (Upper Miocene); the Jacalitos-Etchegoin Formation (Pliocene); and the Tulare Formation (Pliocene-Pleistocene). All of these sedimentary formations are known to contain at least a minor component of detrital serpentinite debris, and all of the strata are eroding as a result of uplift and exposure associated with the margin of the monoclinal structure (Anderson and Pack, 1915; Eckel and Myers, 1946; Hoots, Bear, and Kleinpell, 1954; Read, 1959; Page, 1966; Casey and Dickenson, 1976; Brown, 1984).

Reproduced with permission of the copyright owner. Further reproduction prohibited without permission.

In some of these formations and/or sedimentary deposits as in the Big Blue Member of the Temblor Formation the detrital serpentinite debris is a locally major component. The ubiquitous presence of detrital serpentinite debris in all of these sedimentary formations is indicative of the serpentinite mineralogy of the sediment source areas (i.e., the ultramafic serpentinite deposits of the New Idria Formation and the Table Mountain structure and possibly the erosional reworking of sedimentary serpentinite deposits such as the Big Blue Member (Anderson and Pack, 1915; Taliaferro, 1943; Eckel and Myers, 1946; Read, 1959; Page, 1966; Miller, Green, and Davis, 1971; Casey and Dickenson, 1976). The regional geology and stratigraphy is illustrated in the geologic cross sections illustrated in Figures 2-6A, 2- 6B, and 2-6C.

In Pliocene-Pleistocene time (i.e., approximately 1.8 million years ago) and in more recent Quaternary time, large volumes of serpentinite debris were similarly extruded by solid-flowage from the New Idria and Table Mountain anticlinal structures (Dickenson, 1966a; Cowan and Mansfield, 1970). The extruded serpentinite debris formed large landslides and/or serpentinite debris flow complexes that flank the highland serpentinite source areas of both of these structures. The extruded serpentinite debris from the Table Mountain structure is unique in that the deposit originally covered more than 30 square miles and had a thickness ranging from 50 to 250 feet and a total volume estimated to exceed 0.48 cubic miles (Dickenson, 1966a, p. 456). The surficial debris sheet deposit originally extended from the summit carapace, down a ramping slope, and over a piedmont plain (an area now known as the Kettleman Plain which is a southerly extension of the Pleasant Valley floodplain (Dickenson, 1966a, p. 455). Geologically recent (i.e., within the last 1.8 million years) landslides and/or serpentinite debris flows associated with the New Idria Formation are also known to cover more than five square miles with a similar thickness (Eckel and Myers, 1946; Dibblee, 1971). These deposits are generally found in the headlands of

Reproduced with permission of the copyright owner. Further reproduction prohibited without permission.

canyons that, as a result of erosion, are encroaching on the Joaquin Ridge outcrop of the New Idria Formation (Cowan and Mansfield, 1970).

2.3 Detrital Serpentinite Deposits and Regional Stratigraphy

An analysis of the stratigraphic section in the Coalinga region demonstrates that large volumes of detrital serpentinite debris has been deposited in many local sedimentary formations that post-date the Miocene age of the Temblor Formation. The ubiquitous occurrence of detrital serpentinite debris throughout the stratigraphic setting and regional environment indicates that the primary serpentinite deposits (i.e., the New Idria, Table Mountain, and other un-named intrusive serpentinite masses as illustrated in Figure 2-1) have been subject to an almost continuous sequence of extrusion and erosion since Miocene time.

Sedimentary rock units in the Coalinga region that have been reported to contain detrital serpentinite debris include geologically recent Quaternary alluvial deposits; alluvial deposits of the Tulare Formation (Pliocene-Pleistocene); alluvial and shallow marine deposits of the Jacalitos-Etchegoin Formation (Early Pliocene); marine and non-marine deposits of the Santa Margarita Formation (Late Miocene); and marine and non-marine deposits of the Big Blue Member of the Temblor Formation (Early Miocene) (Anderson and Pack, 1915; Taliaferro, 1943; Eckel and Myers, 1946; Read, 1959; Page, 1966; Miller, Green, and Davis, 1971; Mansfield, 1972; Casey and Dickenson, 1976). In the Arroyo Pasajero watershed basin, these asbestos-containing sedimentary formations are exposed and subject to fluvial and wind erosion over an estimated 130-square-mile area (Jenkins, 1971). Sediments eroded from the Arroyo Pasajero watershed basin have been deposited as an alluvial fan which covers an estimated 300-square mile area (Munn, Busacca, and Trott, 1981). Approximately

Reproduced with permission of the copyright owner. Further reproduction prohibited without permission.

two-thirds of this alluvial fan area has been cultivated for commercial agricultural purposes (National High Altitude Photographs or NHAP, 1981).

These Miocene and younger asbestos-containing formations are also exposed in the foothills that form the western margin of the central San Joaquin Valley (Jenkins, 1971). In the Central Valley region (excluding the Arroyo Pasajero watershed and alluvial fan), these foothills include Kettelman Hills, Guijarral Hills, Anticline Ridge, the Big Blue Hills, Ciervo Hills, Monocline Ridge, Tumey Hills, Panoche Hills, and Leguna Seca Hills. (See USGS, Santa Cruz Sheet, 1:250,000 Scale Topographic Map, Jenkins, 1971). Collectively, the asbestos-containing sedimentary formation outcrops of these foothills cover an estimated additional 120 square miles (Jenkins, 1971). Collectively, the alluvial fans of the western central San Joaquin Valley between Los Banos and Kettleman City (i.e., the area that encompasses the alluvial fans of the Leguna Seca Hills south to the Kettleman Hills) cover an estimated 1,500 square miles (Jenkins, 1971; and Miller, Green, and Davis, 1971) and the asbestos-containing sedimentary formations (i.e., the Big Blue Member and younger, overlying geologic units) collectively cover an estimated 250 square miles.

Reproduced with permission of the copyright owner. Further reproduction prohibited without permission.

2.4 Crustal Shortening

Regional studies of the tectonic setting of south-central California (including studies of seismic and earthquake activity and crustal deformation) show that the central Coast Ranges have experienced up to 30 percent crustal shortening during the late Neogene and Quaternary time periods. Crustal shortening has resulted from compressional deformation from transpressive tectonics (i.e., the transform convergence of the Pacific oceanic plate and the North American continental plate) (Mount and Suppe, 1987). The compressive deformation of the tectonic plates has resulted in faulting, folding, and regional uplift. Recent earthquake activity in the Coalinga area and deformation of late Pleistocene and Holocene deposits (by faulting, folding, and uplift) indicate that these processes are continuing today (Burford, 1965; Barbat, 1971; Page, 1966 and 1984; Reimer et al, 1985; Minster and Jordan, 1987; Mount and Suppe, 1987; Zoback et al., 1987; Harbert and Cox, 1987; Bartow, 1987). In the coastal range region, it has been estimated that the occurrence of crustal stress and strain associated with the tectonic convergence of the North American plate and the Pacific plate has resulted in a relative crustal shortening rate of approximately 0.5 mm per year (Sauber, et al., 1988, p. 326). Recent tectonic studies of the Coalinga region indicate that uplift of the Diablo Range in its present configuration started in Pliocene time, accelerated in the Pleistocene, and is likely continuing today (Rymer and Ellsworth, 1985, p. 7).

2.5 Evidence of Uplift and Erosion of the New Idria Formation

A review of the literature cited in the previous section on crustal shortening (re: seismic and earthquake activity and crustal deformation) and field investigations of the New Idria Formation indicate that the diapiric, anticlinal structure is continuing to be

Reproduced with permission of the copyright owner. Further reproduction prohibited without permission.

uplifted. This is indicated by the fact that the soft, friable matrix of flakey serpentinite continues to persist as a topographic high with more than a 2,200 feet of topographic relief at the crest of the Joaquin Ridge anticlinal structure. In some areas, the serpentinite is migrating by slow plastic flowage into the headlands of encroaching canyons. The core of the anticline consists of readily friable serpentinite, and the flanks of the anticline are formed by erosion-resistant Cretaceous sandstones and shales (Eckel and Myers, 1946; Dibblee, 1971). The ridgetop outcropping of the serpentinite mass, with over 2,000 feet of topographic relief, is exposed on both sides of the ridge (Cowan and Mansfield, 1970; USGS, 1984, Santa Rita Peak 7.5 Minute Topographic Quadrangle) - somewhat like a giant ice cream cone. Because of this rugged relief, the weakly consolidated, flakey serpentinite matrix is highly susceptible to sheet, rill and gully erosion and mass wasting in the form of landslide and/or debris flow complexes (Dibblee, 1971). However, inspite of the deposits's susceptibility to erosion and mass wasting, the deposit continues to persist as a topographic high. If the deposit was not continuing to be uplifted, it is likely that the processes of erosion and mass wasting over great lengths of geologic time would have diminshed the serpentinite deposit's topographic relief.

In addition to the erosional processes of surface runoff and mass wasting, the long, hot summers of the region contribute to the desiccation and drying of the naturally occurring asbestos outcrops. The dried asbestos is very friable, and the strong seasonal winds may contribute to the wind erosion of the very small, clay-sized (2 to 3 microns in length) fibers (Mumpton and Thompson, 1975).

Asbestos-rich sediments derived from the New Idria/Joaquin Ridge highland area (including those from the weathered surface outcrop of the New Idria Formation, from the eroding margins of serpentinite landslides and debris flows, from asbestos and

Reproduced with permission of the copyright owner. Further reproduction prohibited without permission.

chromite milling tailings, from fresh exposures from road cuts and open-pit mining operations, and from other geologic sources including ultramafic and sedimentary serpentinite deposits) are eroded by fluvial and eolian (i.e., wind blown) processes. In the Coalinga region, these sediments have historically been deposited on the Arroyo Pasajero and Cantua Creek alluvial fans that have formed on the western margin of the central San Joaquin Valley (Miller, Green and Davis, 1971; Munn, Busacca, and Trott, 1981; Atwater et al., 1986). (See Figure 2-2A and Jenkins, 1971).

2.6 Arroyo Pasajero Drainage of the New Idria Formation

The southeastern third of the New Idria Formation is drained by four regional watersheds including the Arroyo Pasajero watershed to the southeast, the Cantua Creek watershed to the northeast, the San Benito River watershed to the west, and the Silver Creek - Panoche Creek watershed to the north. Approximately 6.8 square miles of the New Idria Formation drain into the Arroyo Pasajero watershed and an area of approximately 4.3 square miles drains into the Cantua Creek watershed. In the Arroyo Pasajero, the New Idria Formation is drained by the White Creek and Pine Canyon sub-basins. The White Creek sub-basin drains approximately 5.8 square miles of the New Idria Formation and the Pine Canyon sub-basin drains approximately 1.0 square mile. See geologic map of Joaquin Ridge as illustrated in Figure 2-3.

2.7 Mining Activities

In addition to geologic processes, the region's mining and surface mineral exploration operations (e.g. cinnabar, chromite, chrysotile asbestos, and other serpentinite related minerals) may have contributed to the increased erosion potential of asbestos-containing sediments from disturbed surfaces of the New Idria Formation and from

Reproduced with permission of the copyright owner. Further reproduction prohibited without permission.

roads, dumps, and tailings piles. The southeastern third of the formation is associated with rich chromite and chrysotile asbestos ore deposits that were heavily explored and mined during the 1950's, 60's, and 70's (Eckel and Myers, 1946; Rice, 1957; Matthews, 1961; Munro and Reim, 1962; Merritt, 1962; Rice, 1963; Mumpton and Thompson, 1975). A review of topographic maps (USGS, 1984) and aerial photographs (National High Altitude Photographs, 1981) shows that the southeastern third of the New Idria Formation is associated with over 400 bulldozer exploration pits; 17 open-pit mining operations; 5 milling operations; and countless miles of exploration access roads. The reason that most of these mining and milling operations were located in the White Creek drainage basin of the Arroyo Pasajero was not because of higher asbestos concentrations, but because of the sloping hillside areas where bench-cut mining techniques could be used and because these areas were more readily accessible from roads than other less accessible regions (personal communication, Dr. F. Mumpton, April 24, 1989). The locations of mine sites and mill sites in the Joaquin Ridge area are illustrated in Figures 2-7, 2-8A, and 2-8B.

2.8 Chromite Mining

In the 1950's, more than 64,000 tons of disseminated chromite ore was mined from six (or more) open-pit chromite mines operating in the White Creek and Pine Canyon sub-basins (Matthews, 1961; EPA, "Potential Sources Report", 1987). The asbestos-containing ore was excavated by bulldozers and mechanical shovels and was concentrated by as many as five gravity settling milling operations located on White Creek (the Holman mill, the Russell and Chambers mill, and three additional mills that were discovered during reconnaissance of the region). Government records indicate that approximately 24,000 tons of concentrated ore from these mining operations was shipped to the national strategic minerals stockpile in Oregon. None of the chromite

Reproduced with permission of the copyright owner. Further reproduction prohibited without permission.

mines have been restored to their pre-mining conditions. It is estimated that approximately 47,000 tons or more of waste serpentinite debris from the chromite concentrating gravity settling operations was dumped into the White Creek drainage pathway. This estimate is based on a review of chromite mining production records, a review of the reported chromite mining processes and the gravity settling processes, a review of aerial photographs, and discussions with local miners. The operation pads (and some remnant machinery), retaining dams, and primary streambed discharge points (i.e., the areas where the serpentinite debris was dumped into the streambed) associated with some of these chromite milling operations can still be located from ground investigations and from aerial photographs. Information regarding the occurrence of chromite milling operations in the Joaquin Ridge area is provided by Rice, 1957; Matthews, 1961; Munro and Reim, 1962; Merritt, 1962; Rice, 1963; and Mumpton and Thompson, 1975. Excavation pits and mines have been mapped by the USGS (1984) and are readily apparent in field and aerial photographs (See USGS, Santa Rita Peak, 7.5 Minute Topographic Quadrangle Map).

2.9 Asbestos Mining

In the late 1950's and early 1960's, it was discovered that the chromite-bearing serpentinite matrix of the New Idria Formation was composed of a high percentage of economically recoverable, short fiber chrysotile asbestos (typically 2 to 3 microns in length). At least five companies set up asbestos mining operations at that time in the Joaquin Ridge area (Union Carbide Nuclear Company, Atlas Corporation, Johns-Manville Coalinga Asbestos Company, Todd Industries, and Hidden Splendor Mining Company). These companies extracted asbestos ore from an estimated 10 mines, using methods similar to those used in chromite mining operations. None of these mines has been restored. In the White Creek and Pine Canyon area, two milling

Reproduced with permission of the copyright owner. Further reproduction prohibited without permission.

operations were set up to process the asbestos ore prior to commercial distribution. The White Creek mill was operated by the Atlas Corp., and the Pine Canyon mill was operated by the Johns-Manville Coalinga Asbestos Company. Asbestos from the Union Carbide mines was processed by a mill located in King City in San Benito County. Asbestos from the Todd Industries mine was processed at a pilot mill located in Coalinga.

A few companies explored the asbestos potential of the sedimentary serpentinite deposits of the Big Blue Hills located north of Coalinga in the foothills of the Martinez Creek, Salt Creek, and Cantua Creek drainage area. However, these mines were never commercially developed to the extent of the asbestos mines of Joaquin Ridge (Rice, 1957; Munro and Reim, 1962; Merritt, 1962; Rice, 1963; and EPA, Potential Sources Report, 1987).

2.10 Tailings Piles, Dumps, Mine Sites, and Naturally Occurring Asbestos Sources

The Atlas and Johns-Manville Coalinga Asbestos mill facilities are associated with significant tailings deposits. At the Johns-Manville Coalinga Asbestos Site, mill tailings covering approximately 10 acres are located in a narrow canyon that acts to contain the tailings pile. Gullies up to approximately eight feet wide and six feet deep have been eroded by runoff from approximately 100 acres which currently drain through the tailings pile. A sediment-retaining dam at the base of the tailings pile retains debris eroded from the pile. This is evident because of the significant asbestos deposits upstream of the dam (estimated at approximately 4,000 cubic yards and, in places, more than 4 feet in depth) compared to the isolated pockets of asbestos sediments found downstream of the tailings dam. Some tailings not consolidated in

Reproduced with permission of the copyright owner. Further reproduction prohibited without permission.

Pine Canyon are also located adjacent to the mill facility and have an approximate area of 2 acres. The Atlas tailings were deposited in a broad, open area that is more susceptible to air erosion than the Johns-Manville Coalinga Asbestos tailings pile in Pine Canyon. The Atlas pile covers a much broader area (approximately 112 acres compared to 10 acres for the Johns-Manville Coalinga Asbestos pile) that is not protected or contained by the sidewalls of a canyon or any sediment-retaining dam structures.

It is important to note that the overall sizes of the piles and related dumps of both of these sites are relatively small in comparison with: (1) the approximately seven square miles of naturally exposed serpentinite of the New Idria Formation containing greater or approximately equal asbestos concentrations as the Sites in the Arroyo Pasajero watershed; and (2) the more than 80 square miles of naturally occurring ultramafic serpentinite deposits which are located throughout the region and contain similar asbestos concentrations as the Sites (Mumpton and Thompson, 1975; Mumpton, 1989; Eckel and Meyers, 1946; Dibblee, 1971; and Miller, Green and Davis, 1971).

These and other sources with lower asbestos concentrations cover approximately 1700 square miles and are discussed in detail in following sections. It should also be noted that despite the relatively small overall size of the mining sites compared to the areal extent of the natural chrysotile in the New Idria Formation and other asbestos-bearing deposits, milled chrysotile waste material, present at the sites, without any mitigation may erode faster than a significant portion of the naturally occurring serpentine outcrops. Further discussion and estimation of asbestos soil erosion rates is presented in Chapter Six .

Reproduced with permission of the copyright owner. Further reproduction prohibited without permission.

2.11 California Aqueduct and Alluvial Fan Sedimentation

In the early 1960's, the construction of the California Aqueduct on the western margin of the central San Joaquin Valley acted as a barrier to the natural eastward drainage and dispersion of asbestos-bearing sediments on the Arroyo Pasajero and Cantua Creek alluvial fans. The accumulation of sediments from these alluvial fans on the western margin of the Aqueduct has far exceeded the original engineering calculations of projected sediment load for the Arroyo Pasajero and Cantua Creek fan drainage systems. A sediment settling and ponding basin constructed adjacent to the Aqueduct to contain runoff and sediments from the Arroyo Pasajero has accumulated sediment much more quickly than projected by the original engineering design. During periods of heavy rainfall, asbestos-bearing floodwaters and sediments may be drained into the Aqueduct.

There has been no provision, however, for the ponding of sediments or runoff from the Cantua Creek drainage system, which includes the Salt and Martinez creeks. The Salt Creek, Martinez Creek, and Cantua Creek each drain a portion of the asbestos-bearing "Big Blue" foothill area. The Cantua Creek system also drains approximately 4.3 square miles of the New Idria Formation outcrop on the northeastern flank of Joaquin Ridge. Asbestos-bearing sediments and runoff from the intermittent Cantua Creek drainage system enter the Aqueduct through permanently open concrete gates as indicated in Figure 1-1.

Reproduced with permission of the copyright owner. Further reproduction prohibited without permission.

3.0 GEOLOGIC SETTING

3.1 Geologic Origin and Description of the New Idria Formation

The New Idria/Joaquin Ridge highland area is located in western Fresno County near the San Benito County line. The Joaquin Ridge area has generally been included in regional geologic studies of the Coalinga district which geographically includes: (1) the western margin of the central San Joaquin Valley which includes outcrops of asbestos-containing sedimentary formations - most notably the Big Blue Member of the Temblor Formation (Miocene); (2) the New Idria Formation, the Table Mountain serpentinite deposit, and approximately 50 additional, un-named ultramafic serpentinite deposits exposed in the rugged foothills of the southern Diablo Range; (3) the Parkfield segment of the San Andreas Fault Zone; and (4) a system of northwest trending, "en echelon" anticlines and synclines which are oriented sub-parallel to the trend of the San Andreas Fault Zone. (Note: In this context, "en echelon" refers to a system of parallel structural features).

3.1.1 Diapiric Fold Structure of Joaquin Ridge Anticline

The New Idria Formation has been defined as a serpentinite plug that was tectonically emplaced as a diapiric fold structure that forms the core of the Joaquin Ridge Anticline (Eckel and Myers, 1946, p. 87-88; and Zigler, Wentworth, and Bartow, 1986). The serpentinite core of the anticline now forms the crest of the rugged Joaquin Ridge highland area which is located on the border of San Benito County and Fresno County. As a diapiric serpentinite mass, the Formation is in thrust-faulted contact with steeply dipping Cretaceous strata (sandstones and shales) that form the flanks of the

Reproduced with permission of the copyright owner. Further reproduction prohibited without permission.

anticline. These stratigraphic and structural relationships are illustrated on the geologic maps and cross-sections presented in Figures 2-2A, 2-2B, 2-4, and 2-5.

3.1.2 Thickness of the New Idria Formation

The total thickness of the New Idria Formation is unknown; however, gravity data indicate that the asbestos-containing serpentinite formation extends to a depth of approximately 15,000 feet, with the deepest portion occurring near the southeastern half of the Formation (Mumpton and Thompson, 1975, p. 134; Byerly, 1966; Bishop and Chapman, 1967, Bouguer Gravity Map). The fact that the serpentinite deposit forms the core of a linear anticlinal structure related to a tectonically active continental margin suggests that the deposit may extend even deeper into the lower crust.

3.1.3 Reflectance Characteristics of the New Idria Formation and Other Serpentinite Deposits

As a result of the unique reflectance characteristics of the light bluish gray serpentinite matrix, the New Idria Formation can be readily identified on black and white, color, and color infrared aerial photographs of the region. Research has shown that mapping of the visible and near-infrared (0.35 to 2.5 micrometers) reflection spectrometry of serpentinized rocks is a potentially rapid and reliable technique for targeting areas for asbestos exploration (Hunt and Evarts, 1981). As a result of the unique reflectance characteristics of the serpentinite minerals (i.e., lizardite, antigorite, and chrysotile asbestos), other asbestos-containing formations in the area (including the sedimentary Big Blue Member of the Miocene Temblor Formation, the extrusive Table Mountain serpentinite deposit located approximately 30 miles south-southeast of the New Idria deposit, and other un-named primary serpentinite deposits similar to the New Idria

Reproduced with permission of the copyright owner. Further reproduction prohibited without permission.

Formation) can also be identified. The results of my review and interpretation of aerial photographs and high altitude/color infrared imagery are presented in Chapter Three.

3.1.4 Regional Drainage of the New Idria Formation

The New Idria Formation outcrops over an elliptically-shaped 48-square-mile area that forms the crest of the Joaquin Ridge highland trend. The formation is drained by four regional watershed basins including the watershed of eastern San Benito County and the Arroyo Pasajero, Cantua Creek, and Panoche Creek watersheds of western Fresno County. The Arroyo Pasajero and Cantua Creek watersheds are located on the western margin of the central San Joaquin Valley in an area that includes the rugged foothills of the Southern Diablo Range to the west and a system of coalescing alluvial fans (including the Cantua Fan and Arroyo Pasajero Fan) to the east. See the Arroyo Pasajero watershed map of Figure 2-1; the regional geologic map of Figure 2-2A; and the geologic map of Joaquin Ridge of Figure 2-3.

Approximately 6.8 square miles of the New Idria Formation drain to the southeast into the Arroyo Pasajero watershed, approximately 9 square miles drain to the north and northeast into the Cantua Creek and Panoche Creek watersheds, and the remainder drain to the west into the San Benito River watershed. (See Figure 2-3). In the Arroyo Pasajero drainage system, the New Idria Formation is drained by the White Creek and Pine Canyon sub-basins located in the upper watershed of Los Gatos Creek. Approximately 5.8 square miles of the New Idria Formation are drained by the White Creek sub-basin, and approximately 1.0 square mile is drained by the Pine Canyon sub-basin. The White Creek and Pine Canyon areas are associated with rugged terrain and approximately 3,000 feet of relief (with elevations ranging from 1,600 feet above sea

Reproduced with permission of the copyright owner. Further reproduction prohibited without permission.

level at the juncture of Pine Canyon Creek and White Creek to 4,566 feet above sea level in the New Idria Formation outcrop on Joaquin Ridge).

3.1.5 Alluvial Fan Sedimentation, Farming Practices, and the California Aqueduct

The historical (normal) patterns of alluvial fan deposition for the Arroyo Pasajero and Cantua Creek Fans have been altered by regional farming and irrigation practices and by the construction of the California Aqueduct, which has acted as a barrier to the natural (west to east) distribution of alluvial fan sediments to medial and distal alluvial fan environments. As a consequence, significant volumes of medial fan Arroyo Pasajero sediments (approximately 15 million cubic yards) have been deposited and retained in a floodwater and sediment settling basin constructed adjacent to the Aqueduct (Simons, Li and Associates, 1985). During most storm events, asbestos-containing sediment from the Arroyo Pasajero drainage system is retained at least temporarily in this settling basin.

During times of very high rainfall, asbestos-containing runoff and sediment from the Arroyo Pasajero may be drained into the Aqueduct through inlet structures located near the intersection of the Aqueduct and Gale Avenue. Asbestos-containing sediment and floodwaters from the Cantua Fan wash directly into the Aqueduct through two permanently open concrete gates.

Reproduced with permission of the copyright owner. Further reproduction prohibited without permission.

4.0 ENVIRONMENTAL SETTING

4.1 Regional Overview

The Johns-Manville Coalinga Asbestos Mill and the Atlas Mine and Mill are located approximately 18 miles northwest of Coalinga near the crest of the Joaquin Ridge highland trend. This mountainous area is associated with steep relief and rugged terrain which is typical of the mountains of the southern Diablo Range. The serpentinite mass of the New Idria Formation forms the core and the crest of the Joaquin Ridge anticlinal structure. Many additional mines and mills are located on the southern flank of Joaquin Ridge in far western Fresno County in the White Creek and Pine Canyon sub-basins of the Los Gatos Creek drainage basin of the Arroyo Pasajero watershed. Los Gatos Creek and other watershed tributaries (Warthan Creek, Jacalitos Creek, Zapato-Chino Creek) join downstream from the Joaquin Ridge area near Coalinga to form the Arroyo Pasajero alluvial fan system on the western margin of the central San Joaquin Valley. Sediment eroded from these drainage basins is deposited on the alluvial fan.

The geologic and topographic maps presented in Figures 2-2A, 2-3, 2-7, 2-8A, and 2-8B illustrate the location of the Atlas Mine and Mill and Johns-Manville Coalinga Asbestos Mill in relationship to the New Idria Formation outcrop and other mining operations that include the Butler Estate Chromite Mine and the Jensen, Christie, James Corbett Byles, Archer, and Union Carbide mining operations. Also illustrated are the New Idria Formation drainage divides of the Arroyo Pasajero, Cantua Creek, and San Benito Creek watershed basins and the general drainage network of the Arroyo Pasajero watershed, including the Arroyo Pasajero alluvial fan and the California Aqueduct.

Reproduced with permission of the copyright owner. Further reproduction prohibited without permission.

4.2 Johns-Manville Coalinga Asbestos Mill and the Pine Canyon Drainage Area

The Johns-Manville Coalinga Asbestos Mill is located in the Pine Canyon sub-basin of the Los Gatos Creek - Arroyo Pasajero drainage system. (See watershed drainages illustrated in Figure 2-3). The Pine Canyon sub-basin drains approximately one square mile of the New Idria Formation, and the White Creek sub-basin drains approximately 5.8 square miles of the New Idria Formation.

The Johns-Manville Coalinga Asbestos Mill is located on the southeastern flank of Joaquin Ridge in the headlands of Pine Canyon (T19S, R13E, Sec.1, Fresno Co.; Santa Rita Peak 7.5 Minute Topographic Quadrangle Map). This location is approximately 0.5 miles downslope from the Joaquin Ridge outcrop of the asbestos-containing New Idria Formation. The asbestos milling facility was constructed on top of a large complex of asbestos-bearing serpentinite landslides and/or debris flows that are the predominant geomorphic feature of the upper Pine Canyon area. These serpentinite earthflow deposits originated from the steep slopes of the New Idria outcrop (with slopes having a vertical to horizontal ratio of 1 to 5.8). The general drainage pathways of the Johns-Manville Coalinga Asbestos Mill site area are less steep because of the canyon-filling affect of the earthflow deposits which have contributed a streambed slope with a vertical to horizontal ratio of 1 to 9.1. In the general area of the Johns-Manville Coalinga Asbestos Mill, some of the earthflow deposits have developed soils with deep, clay-rich argillic horizons that support a grassy cover. These soils have asbestos concentrations which are generally less than one percent. These soils have developed on top of the asbestos-containing debris flow and landslide deposits as a result of the accumulation of organic debris and other soil-forming materials.

Reproduced with permission of the copyright owner. Further reproduction prohibited without permission.

Tailings from the Coalinga asbestos milling operation were deposited in a small gorge that had formed on the eastern margin of the Pine Canyon earthflow complex. The tailings are contained by the sidewalls of the gorge and by a sediment retaining dam that was constructed at the base of the tailings pile. Additional tailings from chromite milling operations were deposited in the general area of the mill.

In addition to the New Idria Formation, the Johns-Manville Coalinga Asbestos Mill is located approximately 0.6 to 0.7 miles downslope from two large-scale, open-pit mining operations - the Jensen Asbestos Mine and the Butler Estate Chromite Mine. The Jensen Mine covers approximately 29 acres, and the Butler Mine covers approximately 43 acres. The Butler Mine was a deep-pit mining operation that was carved out of a steep hillside that marks the drainage divide between the Pine Canyon and the White Creek drainage areas. The Jensen Mine was a bench-mining operation and is located on a serpentinite debris flow deposit. The terrain in the vicinity of the Jensen and Butler Mines has vertical to horizontal slope ratios of 1 to 3.52 and 1 to 3.96, respectively. These mines, including uncontained waste ore dumps, are drained by Pine Canyon Creek upstream of the Johns-Manville Coalinga Asbestos Mill. See Figure 2-7 which is a general location map modified from the Santa Rita Peak (USGS, 1984) topographic map.

Field observations by myself and by others have confirmed that asbestos-containing sediments from both of these mines are being eroded and transported downstream through the Upper Pine Canyon drainage system. Erosion of the Butler waste ore dumps appears particularly severe. As a result of its ridgetop location and other factors (i.e., an over-steepened waste-ore dump, the unconsolidated nature of the serpentinite debris, and lubrication of glide planes from water seeping into the pile),

Reproduced with permission of the copyright owner. Further reproduction prohibited without permission.

slumping and debris flows from the Butler waste-ore pile are moving into the Upper Pine Canyon drainage channels.

4.3 Atlas Mine and Mill and the White Creek Drainage Area

The Atlas Mine and Mill is located in the White Creek mining district approximately three miles west-northwest of the Johns-Manville Coalinga Asbestos Mill of Upper Pine Canyon. The Atlas Mine and Mill is located within the outcrop area of the New Idria Formation near the crest of Joaquin Ridge (T18S, R13E, Sections 31 and 32; Santa Rita Peak 7.5 Minute Topographic Quadrangle). The Atlas Mine and Mill covers approximately 200 acres and includes three large-scale, open-pit asbestos mines and a large tailings pile complex that is much larger than the tailings pile of the Johns-Manville Coalinga Asbestos Mill. The Atlas tailings form a complex of merged, dune-like piles that are uncontained on all sides and are migrating downslope in dune-like fashion. Field observations show that the uncontained piles are subject to wind erosion and gullying. The terrain of the Atlas Mine and Mill is a steep area that has a vertical to horizontal slope ratio of 1 to 5.8.

In addition to the Atlas Mine and Mill, the White Creek drainage area includes at least five other large-scale, open-pit mines and three chromite milling operations. These mines include the James/Corbett/Byles Mine, the Big Ridge Mine, the Rhodes/Byles/Gribble Mine, the Tromby Mines (Nos. 1 and 2), the Archer Mine, and part of the Butler Estate Chromite Mine. The chromite milling operations included the Holman Mill, the Chambers and Russell Mill, and several previously unreported mills located on White Creek.

Reproduced with permission of the copyright owner. Further reproduction prohibited without permission.

The White Creek sub-basin also includes several large scale landslide and/or serpentinite debris flow complexes that cover approximately four square miles and are very steep. Some surfaces have slopes which are equal to or greater than the angle of repose (i.e., 34 degrees) which causes the serpentinite debris to be unstable and subject to mass wasting. These landslides are relatively barren of vegetation and are subject to significant gullying. The tailings piles of the Atlas milling operation are merging with these naturally occurring earth flow complexes.

4.4 Landslide and/or Serpentinite Debris Flow Complexes

Landslides and/or serpentinite debris flow deposits from the New Idria Formation have been mapped throughout the Joaquin Ridge area since the early 1900s. The landslide and/or serpentinite debris flow deposits are particularly abundant in the central and southeastern areas of the New Idria Formation outcrop (Eckel and Myers, 1946; Matthews, 1961; Cowan and Mansfield, 1970; Dibblee, 1971). Extensive landslides and slope wash material occur throughout the general serpentinite area of the New Idria Formation outcrop, with most of the landslides occurring along the southern boundary of the serpentinite mass. One of the largest landslides occurs just southeast of the Butler Estate (or "Mistake") Chromite Mine in the Pine Canyon drainage basin (Matthews, 1961, p. 13). Several other large landslide and/or serpentinite debris flow complexes have been mapped in the White Creek and Cantua Creek drainage basins. Some of these complexes cover as much as several square miles.

The largest landslide and/or serpentinite debris flow complex that has been mapped in this area covers approximately three square miles of the New Idria Formation outcrop in the White Creek drainage area (Dibblee, 1971). This large complex is being dissected by approximately 16 miles of intermittent stream channels that are associated

Reproduced with permission of the copyright owner. Further reproduction prohibited without permission.

with significant gully erosion. The Cantua Creek drainage area includes four mapped serpentinite debris flow complexes that have moved into the heads of four small canyons. These serpentinite debris flow deposits cover approximately 3.2 square miles.

Reproduced with permission of the copyright owner. Further reproduction prohibited without permission.

5.0 HISTORICAL GEOLOGY AND STRATIGRAPHY

5.1 Previous Studies

The Coalinga region has been the focus of a range of geologic investigations related to: (1) the exploration for the vast petroleum and mineral resources of the district; (2) regional geologic investigations related to the San Andreas Fault Zone and the evolution of the Coast Range geomorphic province; and (3) recent geologic and geophysical investigations of the 1983 Coalinga earthquake and related seismic events. Petroleum investigations generally have focused on the subsurface structure (i.e., anticlines, synclines, and faults) in relationship to the regional stratigraphy and the distribution of sedimentary facies. Information from these studies has helped to define the structural and sedimentary evolution of the regional basins and related depositional centers. Mineral resource investigations have generally focused on the occurrence, distribution, and economic potential of the explored mineral deposits, and on the physical and chemical characteristics of the deposits. Regional geologic investigations have been conducted to evaluate the Parkfield segment of the San Andreas Fault Zone, the evolution of the Coast Range geomorphic province, and the occurrence and potential for seismic events along the western margin of the San Joaquin Valley. These studies have contributed to an improved understanding of the thrusting, faulting, and folding that dominates the southern Coast Range Province. Information from these studies collectively provides a foundation for understanding the geologic emplacement of the New Idria Formation serpentinite mass and the subsequent exposure and sedimentary redistribution of serpentine minerals throughout the region.

Reproduced with permission of the copyright owner. Further reproduction prohibited without permission.

5.2 Paleogeography and Sedimentary Basins

An analysis of the stratigraphy and geologic structure of the Coalinga region shows that in Cretaceous time (approximately 65 to 120 million years ago), the area now occupied by the central San Joaquin Valley and the southern Diablo Range mountains was occupied by a marine basin associated with deposition of marine sandstones, siltstones, and shales. In Cretaceous time, the source of most of the marine sediments was the land mass of the Sierra Nevada mountains that were located to the east. As a result of the uprising of the Coast Range mountains and withdrawal or regression of marine environments that covered the central valley of Central California, the Sierra Mountains now form the eastern margin of the central San Joaquin Valley. The sediments derived from the Sierra Nevada land mass were deposited across an area that, because of crustal compression, eventually became an asymmetric structural trough that has been filled with a prism of upper Mesozoic and Cenozoic sediments (i.e., basin and/or valley fill sediments deposited over the past 100 million years). This prism of clastic sedimentary rocks ranges up to 9 km thick (Bartow, 1987, pp. 1-3) and includes both marine and non-marine sediments.

In Cretaceous time, the eastern margin of this structural trough was formed by the North American continental land mass and the ancestral Sierra Nevada mountains, and the western margin was open to the Pacific Ocean. Because of changes in sea level and climate and because of regional tectonic uplift from thrusting and folding, the western margin of the structural trough was uplifted. This uplift acted to restrict the circulation of marine waters from the open Pacific Ocean. Continued uplift in the area now occupied by the Coast Range geomorphic province resulted in the emergence of a (Coast Range) land mass that acted to restrict marine circulation. As a result of the emergence of this land mass, there was a gradual transition from a marine environment

Reproduced with permission of the copyright owner. Further reproduction prohibited without permission.

to a non-marine environment in the area now occupied by the central San Joaquin Valley. This transition from marine to non-marine depositional environments is reflected in the physical characteristics of the Miocene and younger stratigraphic units including the Temblor Formation (Miocene), Santa Margarita Formation (Late Miocene), Etchegoin and Jacalitos Formations (Early Pliocene), San Joaquin Formation (Late Pliocene), and the Tulare Formation (Pliocene and Pleistocene). (See Section 3.5 which describes the regional stratigraphy; and Miller, Green, and Davis, 1971; Barbat, 1971; Lettis, 1982; and Bartow, 1987.)

In Miocene time (approximately 17 to 20 million years ago), the occurrence of faulting, folding, and crustal compression related to movement along the San Andreas Fault Zone and the diapiric upwelling of the New Idria serpentinite mass contributed to the formation of anticlinal structures such as the Joaquin Ridge Anticline. In the marine environment that existed at that time, these anticlines had dome-like structures which were surrounded by and overlain by shallow water environments. Continued uplift and a lowering of sea level allowed the Joaquin Ridge Anticline and other dome-like structures to become emergent. These emergent structures (which are generally oriented parallel to the present trend of the San Andreas Fault Zone, i.e., north-northwest to south-southeast) were subject to erosion and eroded sediments were deposited in nearby shallow marine embayments and non-marine alluvial depositional areas. This was the time when the New Idria Formation became emergent and great quantities of asbestos-containing serpentinite debris was extruded, eroded, and deposited in nearby sedimentary environments. Some of these deposits have been mapped as the Big Blue Member of the Temblor Formation (Miocene). As indicated in the following discussions, other post-Miocene sedimentary formations also contain asbestos sediment that was derived from the ultramafic asbestos-containing

Reproduced with permission of the copyright owner. Further reproduction prohibited without permission.

serpentinite formations and from erosion of uplifted, asbestos-containing sedimentary formations.

Renewed crustal compression and folding during the Pliocene-Pleistocene time period (approximately one to three million years ago) contributed to the formation of the anticlinal and monoclinal structures that mark the western margin of the central San Joaquin Valley. These structures are generally oriented northwest to southeast (i.e., obliquely to the trend of the San Andreas Fault Zone) and include Kettleman Hills, Guijarral Hills, Anticline Ridge, Big Blue Hills, Ciervo Hills, Panoche Hills, and Leguna Seca Hills. These structures have contributed to the present configuration of the sediment source areas (i.e., mountains and foothills) and local depositional centers of the western central San Joaquin Valley. Detailed discussions of the regional paleogeography and the transition from marine to non-marine depositional environments are provided by Arnold and Anderson (1908); Clark (1935); Taliaferro (1943); Hoots, Bear and Kleinpell (1954); Read (1959); Page (1966 and 1981); Miller, Green and Davis (1971); Barbat (1971); Lettis (1982); and Bartow (1987).

Today, the western central San Joaquin Valley has a series of coalescing alluvial fans that are composed of sediments derived from the erosion of Cretaceous-aged and younger sedimentary and ultramafic rock formations exposed in the foothills and mountains of the southern Diablo Range of the Coast Range geomorphic province (Miller, Green, and Davis, 1971). In the Arroyo Pasajero watershed basin, the sediment source areas include an estimated 42 square miles of Franciscan geologic units, and 7 square miles of asbestos-bearing ultramafic serpentinite deposits. Approximately 130 square miles of the lower foothills in the Arroyo Pasajero watershed are outcrops of Miocene, Pliocene and Pleistocene sedimentary deposits (Jenkins, 1971). Geologic research has shown that Miocene and younger sedimentary

Reproduced with permission of the copyright owner. Further reproduction prohibited without permission.

deposits, including the Big Blue Member of the Temblor Formation and overlying sedimentary formations (Santa Margarita Formation, Etchegoin and Jacalitos Formations, San Joaquin Formation, and Tulare Formation) all contain locally high to trace concentrations of asbestos sediment. The geologically recent alluvial fan sediments are mineralogically most similar to the sediments of the underlying Tulare Formation (Miller, Green, and Davis, 1971) which are both known to contain chrysotile asbestos.

5.3 Deposition of the Big Blue Member of the Temblor Formation (Miocene)

During the early Miocene Epoch (approximately 17 to 20 million years ago), large quantities (approximately 5 to 10 cubic miles) of serpentinite debris from the New Idria Formation were extruded by solid-flowage from the diapiric core of the Joaquin Ridge Anticline. This serpentinite debris was eroded and redeposited as asbestos-containing detrital sediments of the Big Blue Member of the Miocene Temblor Formation. The detrital serpentinite debris of the Big Blue was deposited in a shallow marine environment by a combination of continental and submarine debris flows and/or slides. These deposits occurred in response to erosion and mass wasting associated with doming or diapiric, anticlinal uplift of the New Idria Formation serpentinite mass. (See Casey and Dickinson, 1976, pp. 73-74; Harding, 1976, p. 371; Read, 1959, pp. 42-44; Anderson and Pack, 1915, p. 84; Eckel and Myers, 1946, pp. 94-95; Arnold and Anderson, 1908, p. 29). The following quote from Eckel and Myers (1946, p. 95, compiled from their field investigation and reports from Anderson and Pack, 1915; Bramlette, 1934; and Woodring, Stewart, and Richards, 1940) indicates the vast extent of the detrital serpentinite debris that originated from the uplift, extrusion and erosion of the New Idria serpentinite deposit:

Reproduced with permission of the copyright owner. Further reproduction prohibited without permission.

As reported by Eckel and Meyers (1946, p. 95):

"A more widespread and conspicuous layer of serpentine debris is the well-known `Big Blue,' of late middle Miocene Age, which is interbedded with more normal sediments along the western foothills of the San Joaquin Valley, opposite the Idria dome. The Big Blue consists almost entirely of serpentine flakes and boulders, and in the Big Blue Hills, about 8 miles east of the southeast end of the Idria serpentine body, it attains a maximum thickness of 1,000 feet.... As the thickest part of the Big Blue is nearest to the Idria serpentine body, which is the large serpentine mass exposed nearby, this body in all probability is the source of the serpentine debris. The same conclusion has been reached by previous workers in the area. The enormous volume of the serpentine debris originally contained in the Big Blue - probably between 5 and 10 cubic miles - contrasted with the nearly complete absence of serpentine debris in the older Tertiary beds of the region, indicates that this debris came from a large serpentine mass that was uplifted and exposed rather suddenly. That is rendered all the more probable by the fact that the Big Blue includes serpentine boulders at least 40 feet in diameter, which now lie 8 miles from the Idria serpentine body."

As indicated above, the Big Blue Member of the Temblor Formation is exposed in outcrop in the foothills of the Diablo Range on the western margin of San Joaquin Valley in the vicinity of Coalinga. In this area, the layered rock units form a monocline that dips (approximately 30 degrees towards the east) in the direction of the San Joaquin Valley. The limits of the "Big Blue" outcrop are illustrated in Figures 2A and 2-4. In the vicinity of the Big Blue Hills, located about 8 miles east of the southeast end of the New Idria Formation outcrop, the Big Blue Member is approximately 800 feet thick and consists almost entirely of serpentinite flakes and boulders (Harding, 1976, p. 371; Eckel and Myers, 1946, p. 95; Anderson and Pack, 1915, p. 84; Casey and Dickenson, 1976, pp. 65-74). When viewed from the air, the Big Blue has the same light bluish-gray color as the New Idria Formation and other serpentinite outcrops in the region.

Reproduced with permission of the copyright owner. Further reproduction prohibited without permission.

A review of the regional geology shows that the New Idria Formation is the only massive source of detrital serpentinite debris in the region capable of providing the large volumes of serpentine sediments preserved in the Big Blue Member (Eckel and Meyers, 1946, p. 95; Casey and Dickenson, 1976, pp. 73-74). This interpretation is supported by: (1) the restricted geographic distribution of the asbestos-bearing detrital serpentinite debris of the Big Blue Member; (2) the close geographic relationship of the Big Blue Member with the New Idria Formation which is structurally located approximately 8 miles to the east; and (3) the trend of paleocurrent data which indicate sediment transport and deposition in a direction away from the New Idria Formation source area (Casey and Dickenson, 1976, pp. 74-75).

As reported by Harding (1976, p. 371), the extrusion of the New Idria Formation through the overlying sedimentary strata at the crest of an anticlinal structure during the Early Miocene Epoch provides evidence of a system of regional compression and folding that has continued through the modern era.

Based on detailed mapping of the Big Blue Member in the Salt, Martinez, and Cantua Creek areas, Casey and Dickenson (1976, p. 74) reported that:

"The enormous volume and remarkable purity of the serpentinite debris in the Big Blue Formation (sic) indicates that it was derived from a large mass exposed as a solitary source. We suspect a major episode of diapiric protrusion of serpentinite in the vicinity of Joaquin Ridge during the middle to late Miocene. The required timing coincides closely with the onset of rapid motion along the late Cenozoic San Andreas fault.... We envision forceful diapiric upwelling of protrusive serpentinite along the anticlinal trend to stratigraphic levels much higher than those now exposed at the crest of the fold.... As an unstable mound of serpentinite debris built up at the surface, gigantic serpentinite flows moved away laterally, while undergoing concurrent erosion, to form the sedimentary serpentinites of the Big Blue Formation.... Structural

Reproduced with permission of the copyright owner. Further reproduction prohibited without permission.

piercement of the adjacent Mesozoic strata in the limbs of the Joaquin Ridge anticline has been demonstrated by detailed mapping.... The crest of the diapir, where protrusive serpentinite emerged at the surface during the Miocene after penetrating the Mesozoic and Paleogene sequences, may have reached a structural level perhaps 5 km above that of the present exposures."

5.4 Other Serpentinite-Bearing Sedimentary Formations

An analysis of lithologic data from post-Cretaceous sedimentary formations in the Coalinga region shows that detrital serpentinite debris has been deposited throughout the region for approximately the past 20 million years. Some facies of the Big Blue Member of the Temblor Formation (Miocene) are known to be composed almost entirely of serpentinite debris. The percentage of serpentinite debris decreases significantly in the sedimentary formations that overlie the Big Blue. This correlates with the gradual geologic change from marine to non-marine to continental depositional environments in the San Joaquin Valley sedimentary basin. In Miocene time, the present San Joaquin Valley area was occupied by an inland sea that flanked the New Idria "dome" from which serpentinite debris was extruded. Regional uplift associated with a gradual lowering of sea level allowed the marine basin to gradually change to a non-marine basin in the late Miocene and early Pliocene. This basinal transition is indicated by the upward transition from marine to non-marine sediments of the upper Miocene Reef Ridge Formation, the lower Pliocene Jacalitos Formation, and the upper Pliocene San Joaquin Formation which grades into brackish or fresh-water strata in its upper part (Munn, Bussaca, and Trott, 1981, p. 9). The overlying Tulare Formation is composed of lacustrine (lake), fluvial, and alluvial fan sediments. The mineralogy (or provenance) of these sedimentary deposits reflects the mineralogy of the sediment source areas which included: (1) erosion of uplifted Cretaceous and younger sedimentary strata that make up the Diablo Range mountains; and (2)

Reproduced with permission of the copyright owner. Further reproduction prohibited without permission.

erosion of the primary, extrusive serpentinite bodies such as the New Idria Formation which are known to exist throughout the region. As the basin changed from a marine to a non-marine depositional environment, additional land areas were exposed to erosion. Eroded sediment from these additional land areas had the effect of diluting the concentration of the asbestos sediments derived from the serpentinite source areas such as the New Idria Formation. This is reflected in the asbestos concentrations of the Miocene Big Blue Member (which ranges up to 90% asbestos) and the decreasing asbestos concentrations of geologically younger sedimentary formations which overlie the Big Blue Member. Quaternary alluvial fan sediments in the Arroyo Pasajero (as determined from analysis of subsurface core samples - see soil sampling results of Chapter Four) generally have trace asbestos concentrations (i.e., less than 1%).

Post-Cretaceous sedimentary formations in the Coalinga region that are known to contain detrital serpentinite debris (i.e., asbestos sediment) are illustrated in Figure 2-5 and include:

Quaternary Alluvium (Pleistocene/Holocene)
- *deposited in the last 600,000 years*

Tulare Formation (Pliocene/Pleistocene)
- *deposited approximately 1 to 3 million years ago*

Etchegoin/Jacalitos Formation (Early Pliocene)
- *deposited approximately 3 to 5 million years ago*

Santa Margarita Formation (Late Miocene)
- *deposited approximately 5 to 12 million years ago*

Temblor Formation (Early Miocene)
- *deposited approximately 17 to 20 million years ago*

These sedimentary rock formations are exposed over an estimated 150 square mile area on the uplifted margins of the anticlinal and monoclinal structures that form the

Reproduced with permission of the copyright owner. Further reproduction prohibited without permission.

western margin of the central San Joaquin Valley (Jenkins, 1971; Miller, Green and Davis, 1971). These structures comprise the foothills that have formed at the base of the Diablo Range mountains. These asbestos-containing foothills include Kettleman Hills, Guijarral Hills, Anticline Ridge, Big Blue Hills, Ciervo Hills, Panoche Hills and Leguna Seca Hills. The sedimentary formations exposed in these foothills are poorly consolidated and are susceptible to wind and fluvial erosion and mass wasting. Sediment eroded from these formations has historically been deposited downslope on the alluvial fans of western Fresno County, including the fans of Cantua Creek and Arroyo Pasajero. These alluvial fan deposits collectively cover more than 1,500 square miles (Miller, Green, and Davis, 1971).

5.5 Summary of Regional Stratigraphy

In addition to the diapiric New Idria Formation, the Coalinga area contains a thick sequence of sedimentary rocks ranging in age from Late Jurassic to Holocene (163 million years ago to the present). The geologic units (as reported by Alfors, 1983, pp. 108-109; and Mansfield, 1972)) are briefly described below. The regional stratigraphy is illustrated in the stratigraphic column of Figure 2-5. Those stratigraphic units that have been reported to contain detrital serpentinite debris (i.e., sedimentary rocks that contain serpentine minerals) are identified in the following summary of stratigraphic units in the Coalinga region and the stratigraphic column of Figure 2-5. The following units are described in sequence from the older to younger units. This ordering reflects the depositional sequence of the described sedimentary units which have been reported to contain detrital serpentinite debris which contains asbestos sediment. As a result of regional uplift, most of these units are exposed on the eastern flanks of the Diablo Range mountains and foothills that form the western margin of the central San Joaquin Valley. Geologic research shows that the New Idria

Reproduced with permission of the copyright owner. Further reproduction prohibited without permission.

Formation is an ultramafic serpentinite mass that intruded the Cretaceous-aged Panoche Formation and subsequently became emergent (by diapiric uplift) in early Miocene time (approximately 17 to 20 million years ago). Subsequently, large volumes of serpentinite debris have been extruded from this ultramafic mass. This explains why only Miocene and younger sedimentary formations in the Coalinga region are expected to contain asbestos sediment.

Franciscan Complex (Jurassic to Late Cretaceous):

In the Coalinga area, the Franciscan Complex ranges in age from Jurassic to Late Cretaceous and consists of sandstones and shales, altered mafic volcanic rock, and chert. Northwest of Coalinga, the large New Idria serpentinite diapiric fold structure is in thrust fault contact with Franciscan and Great Valley sequence rocks. Smaller masses of serpentinite occur in other Franciscan terrain in the Coalinga area. The thickness of the Franciscan Complex in the Coalinga area is uncertain but has been estimated to exceed 50,000 feet.

The New Idria Formation is an ultramafic intrusion that became emergent in Early Miocene time (approximately 17 to 20 million years ago). At the surface, the ultramafic deposit is an elliptically-shaped, asbestos-rich, serpentinite mass approximately 12 miles long and 4 miles wide; the axis of the ellipse is oriented northwest/ southeast. The formation forms the core of the Joaquin Ridge Anticline, and gravity data indicate that the serpentinite extends to a depth of approximately 15,000 feet. The occurrence of the serpentinite in the core of a faulted, anticlinal structure suggests that the deposit may extend to an even greater depth. Petrographic analyses indicate that the serpentine was derived from the low-temperature alteration of dunite.

Reproduced with permission of the copyright owner. Further reproduction prohibited without permission.

Great Valley Sequence (Late Jurassic to Late Cretaceous):

The Great Valley Sequence near Coalinga consists of about 28,000 feet of thin-bedded mudstone, sandstone, and conglomerate. The age is similar to that of the Franciscan Complex which is dated Late Jurassic to Late Cretaceous. The sequence includes at least three formations: Gravelly Flat Shale, Panoche Formation, and Moreno Shale.

The Panoche Formation (Late Cretaceous) forms the rubbly ridges surrounding the Johns-Manville Coalinga Asbestos Mill Site in Upper Pine Canyon. This formation is composed of thin-bedded clay-rich shales, siltstones, and sandstones. The thin clay shale beds are one to five inches thick and are soft and weathered. The rocks are composed of fine fragments of quartz, feldspar, biotite, chlorite, and clay materials.

Lodo Formation (Paleocene to Early Eocene):

The Lodo Formation consists of about 1,150 feet of claystone of Paleocene and Early Eocene age in the type area (i.e., where the unit was first described). South of the type area, sandstone units are included, and the formation has been divided into four distinct units: Cerros Sandstone, Cerros Shale, Cantua Sandstone, and Arroyo Hondo Shale. The aggregate maximum thickness of these units is approximately 6,190 feet.

Yokut Sandstone (Middle Eocene):

The Yokut Sandstone consists of a shallow water beach sand deposit that gradually onlaps the Arroyo Hondo Shale. Maximum thickness is about 300 feet.

Reproduced with permission of the copyright owner. Further reproduction prohibited without permission.

Domengine Sandstone (Middle Eocene):

The Domengine Sandstone is a poorly-sorted arkosic sandstone with interbedded claystone and siltstone units. It unconformably overlaps the Yokut Sandstone and the Lodo Formation and averages 70 feet in thickness.

Kreyenhagen Shale (Late Eocene to Oligocene):

The Kreyenhagen Shale is a diatomaceous shale that attains a maximum thickness of almost 3,000 feet. The unit conformably overlies the Domengine Sandstone.

Tumey Formation (Oligocene):

The Tumey Formation is an arkosic sandstone unit with an overlying diatomaceous shale member. The formation is about 950 feet thick.

Temblor Formation (Early Miocene):

The Temblor Formation consists of petroliferous sandstone, calcareous sandstone, and diatomaceous and foraminiferal shale with a total thickness of about 550 feet. The unit unconformably overlies the Kreyenhagen Shale and the Tumey Formation.

Big Blue Member of the Temblor Formation:

At the top of the Temblor Formation is a unit that contains fine to coarse serpentinite fragments. This unit attains a maximum thickness of 1,000 feet. Reported to consist almost entirely of serpentinite flakes and boulders of serpentinite debris up to 40 feet

Reproduced with permission of the copyright owner. Further reproduction prohibited without permission.

in diameter where the unit outcrops in the Big Blue Hills north of Coalinga (Eckel and Myers, 1946, p. 95) and in outcrops in the Cantua Creek, Salt Creek, and Martinez Creek drainage areas (Read, 1959, pp. 42-48; Casey and Dickenson, 1976, pp. 65-74).

Santa Margarita Formation (Late Miocene):

The Santa Margarita Formation consists of fine- to coarse-grained sandstone with some gravel at the base and top of the formation. The unit is approximately 700 feet thick. Reported to contain large lenses of serpentinite debris in outcrops north of Cantua Creek (Read, 1959, p. 48).

McLure Shale (Late Miocene):

The McLure Shale consists of about 1,000 feet of siliceous shale and is equivalent in age to the Santa Margarita Formation. Although not reported, this unit probably contains asbestos sediment.

Reef Ridge Shale (Late Miocene):

The Reef Ridge Shale is similar in composition to the McClure Shale but is less resistant and is equivalent in age to the Santa Margarita Formation. Although not reported, this unit probably contains asbestos sediment.

Reproduced with permission of the copyright owner. Further reproduction prohibited without permission.

Etchegoin-Jacalitos Formation (Early Pliocene):

The Etchegoin-Jacalitos Formation consists of relatively soft shale, gravel, and sandstone and unconformably overlies older units. Reported to contain flakes and pebbles of serpentine in the outcrops exposed north of Cantua Creek (Read, 1959, p. 53).

San Joaquin Formation (Late Pliocene):

The San Joaquin Formation consists of silty sandstone, siltstone, and clay shale and has a maximum thickness of over 1,800 feet. Although not reported, this unit probably contains asbestos sediment.

Tulare Formation (Pliocene-Pleistocene):

The Tulare Formation is generally a non-marine sandstone and conglomerate of fluvial origin and lacustrine deposits of sandstone, clay, and limestone. Maximum thickness is 3,500 feet. Reported to contain "serpentine flakes" and fine-grained serpentinite debris in outcrops exposed along western margin of San Joaquin Valley (in the Coalinga area) and near Tumey Gulch located about 15 miles northeast of the New Idria "dome" (Anderson and Pack, 1915; Eckel and Myers, 1946, p. 95; Read, 1952, p. 57; Bull, 1964, p. 93).

Reproduced with permission of the copyright owner. Further reproduction prohibited without permission.

Quaternary Deposits

The Quaternary Deposits are geologically recent deposits (including both Pleistocene and Holocene deposits) comprised of stream terrace sands, gravels, and boulders and valley fill alluvium found along streams and in alluvial fans. The stream deposits include clay, silt, sand, and gravel deposits. The alluvial fan deposits are mostly silt and clay with some coarser grained sediments associated with intermittent alluvial fan channels. Recent deposits also include the occurrence of landslides that are common in the Cantua Creek Valley and in other areas flanking the New Idria Formation. Quaternary deposits in the Coalinga region commonly contain detrital serpentinite debris derived from the erosion of uplifted ultramafic serpentinite bodies such as the New Idria Formation and the Table Mountain serpentinite. Detrital serpentinite debris is also derived from the erosion of asbestos-bearing sedimentary formations such as the Big Blue Member of the Temblor Formation (Miocene).

Reproduced with permission of the copyright owner. Further reproduction prohibited without permission.

6.0 REGIONAL TECTONIC SETTING

6.1 Anticlines and Synclines

Joaquin Ridge and other Diablo Range mountains in the Coalinga region are part of the southern Coast Ranges geomorphic province which, in the latitude of Coalinga, consists of a series of northwest-trending anticlinal and synclinal structures that are generally oriented sub-parallel to the trend of the San Andreas Fault Zone. The zone of fold deformation associated with crustal up warping (forming anticlinal structures) and down warping (forming synclinal structures) extends from the San Andreas Fault Zone north and east to the subsurface of the San Joaquin Valley.

6.2 Extrusive Serpentinite Structures

As indicated in Figure 2-1, more than 50 extrusive serpentinite bodies (including the New Idria Formation, Table Mountain, and many other un-named deposits) have been identified and mapped in the region (EPA, 1987, Potential Sources Report; Dibblee,1976). These serpentinite deposits have been extruded through the exposed core of the Joaquin Ridge Anticline (i.e., New Idria Formation) and through local faults and fissures on the northeast side of the San Andreas Fault Zone (i.e., Table Mountain serpentinite and other unnamed extrusive deposits as mapped by Dibblee (1976).

The ultramafic serpentinite masses were derived from the metamorphic and hydrothermal alteration of oceanic crust that was thrust under the North American plate (Page, 1966 and 1981). This thrusting was accomplished by means of subduction of the oceanic plate (from Pacific sea floor spreading) under the continental

Reproduced with permission of the copyright owner. Further reproduction prohibited without permission.

plate. Subduction may also have occurred as a result of "rafting" of the continental plate over the oceanic plate, as a result of extension of the continental plate in association with emplacement of the Sierra Nevada batholith located to the east (Barbat, 1971). The metamorphosed hydrothermally altered serpentinite masses were less dense than the surrounding country rock in which they were formed; consequently, the "buoyant" masses were mobilized in an upward direction. These diapiric serpentinite masses pierced the overlying rock strata (sometimes causing doming of the overlying and adjacent units) (Eckel and Myers, 1946) or were forced upward through faults and fissures (Dibblee, 1976; Dickenson, 1976).

The occurrence of crustal compression (a function of plate tectonics related to sea-floor spreading) allowed the diapiric serpentinite masses to form the semi-plastic cores of some of the anticlinal structures which, in the Diablo Range, form linear trends of upwardly folded layers of rock. Continued crustal compression caused the semi-plastic serpentinite masses to pierce the near-surface rock units; and locally, the semi-plastic serpentinite masses were extruded by solid-flowage at the surface from the ruptured core of an anticlinal structure or along faults and fissures (Eckel and Myers, 1946, p. 94; Dickenson, 1962, p. 34 and 1966a; Dietz, 1962, p. 34). These semi-plastic serpentinite masses are estimated to have originated from the subduction of oceanic crustal material from depths of approximately 8-12 miles. As a result of the upward mobilization and surface extrusion of metamorphically and hydrothermally altered serpentinite deposits from great depths, these formations (including the New Idria and Table Mountain deposits) appear to be relatively uniform in respect to their mineralogical constituents. These serpentinite formations contain similar asbestos concentrations as the anthropic mines and milling operations which exploited these same deposits.

Reproduced with permission of the copyright owner. Further reproduction prohibited without permission.

6.3 Regional Structural Setting

In a regional context, the Joaquin Ridge/White Creek/Pine Canyon area is approximately 15 miles northeast of the Parkfield segment of the San Andreas Fault Zone. The Joaquin Ridge Anticline is flanked to the north by the Vallecitos Syncline and to the south by the White Creek Syncline. These structures are generally sub-parallel to the trace of the San Andreas Fault. The eastern margin of the Joaquin Ridge structure is flanked by an easterly dipping monocline or ramp (dipping approximately 20 to 30 degrees to the east). This monocline comprises the foothills which form the western margin of the central San Joaquin Valley. These foothills include the Big Blue Member of the Temblor Formation (Miocene) and other younger asbestos-containing sedimentary formations. Because of regional uplift, these foothills have been subject to erosion by the intermittent streams and creeks that drain the eastern watershed of the Diablo Range mountains. See geologic map of the Big Blue Hills as illustrated in Figure 2-4.

The Johns-Manville Coalinga Asbestos Mill is located approximately 0.9 miles south of the structural axis of the northwest trending Joaquin Ridge Anticline (Zigler, Wentworth, and Bartow, 1986); 0.6 miles southeast of the faulted contact of the New Idria Formation with the steeply dipping strata of the Franciscan Complex (Jurassic to Cretaceous) and Panoche Formation of the Cretaceous Great Valley sequence; and approximately 3 miles northeast of the structural axis of the tightly folded White Creek Syncline. The monocline that forms the western margin of the San Joaquin Valley north of Coalinga is located approximately eight miles east of the Johns-Manville Coalinga Asbestos Mill Site. See geologic maps and structural cross sections illustrated in Figures 2-2A, 2- 6A, and 2-6B.

Reproduced with permission of the copyright owner. Further reproduction prohibited without permission.

6.4 Compressional Tectonics, Crustal Shortening, and the San Andreas Fault Zone

The regional and localized geologic structures in the Diablo Range in the southern part of the Coast Ranges geomorphic province (including the Joaquin Ridge and Coalinga Anticlines and the White Creek Syncline) have evolved as a function of the complex interaction of intermittent folding, high-angle reverse faulting, thrusting, and strike-slip faulting that has occurred throughout the province from the early Cretaceous Period until the present (Taliaferro, 1943; Dickenson, 1966; Page, 1966; Harding, 1976; Dibblee, 1977; Wentworth et al., 1983). Present day seismic activity in the region occurs as a function of stress and strain related to the transform and compressive forces associated with the tectonic convergence of the oceanic and continental tectonic plates of the Circum-Pacific orogenic system.

In the Coalinga region, local structures are influenced by the interaction of two components including: (1) the transform San Andreas Fault Zone which is oriented north 38 degrees west; and (2) a system of regional compression oriented north 35 degrees east. These compressive forces are a result of the transform convergence of the Pacific oceanic and North American continental plates. The San Andreas Fault Zone is associated with a right-lateral, strike-slip, fault system (oriented north 38 degrees west) that is thought to have been active since late Tertiary time (Harding, 1976, p. 356). The right-lateral displacement associated with the San Andreas fault system within the Coast Ranges province has been estimated to range from 200 to 300 miles (Dibblee, 1966, pp. 375-384). Regionally, the Coast Ranges province has compressive thrusting, folding and crustal shortening that is oriented north 35 degrees east.

Reproduced with permission of the copyright owner. Further reproduction prohibited without permission.

As indicated by the regional stratigraphy and the distribution of sedimentary facies in relationship to the trend of anticlinal and synclinal fold axes, folding in the Coalinga region has occurred primarily in two episodes (in the Early Miocene and the Pleistocene). The trend of these regional structural components is a result of the compressive forces resulting from the transform convergence of the Pacific oceanic plate and the North American continental plate. These forces are the result of transpressive tectonics which has been described as "decoupled transcurrent and compressive deformation, operating simultaneously and largely independent" (Mount and Suppe, 1987, p. 1,146).

In a summary of the regional geology related to the Coalinga earthquake of 1983, Wentworth et al. (1983, p. 115) realized that at least some of the west-northwest trending folds in the Coalinga region were formed in early Tertiary time (approximately 60 to 65 million years ago). These folds were presumably controlled by proto-San Andreas movement in pre-Eocene time (more than 57 million years ago). Wentworth et al. reported that during this pre-Eocene time period, the Vallecitos trough was accumulating marine sediments, and the New Idria "high" became emergent and subject to erosion. The domal structure of the Joaquin Ridge Anticline influenced the distribution of local sedimentary facies including marine and non-marine environments of deposition. The north-south oriented structures of the western margin of the central San Joaquin Valley, including the Coalinga Anticline, were mostly formed during the Pliocene - Pleistocene time period.

6.5 Miocene "Unroofing" and Erosion of the New Idria Formation

In early Miocene time (approximately 17 to 20 million years ago), a localized influx of detrital serpentinite debris was deposited along the northeastern flank of the Joaquin

Reproduced with permission of the copyright owner. Further reproduction prohibited without permission.

Ridge Anticline (as evidenced by the asbestos-containing Big Blue Member of the Temblor Formation which is Miocene in age) (Casey and Dickenson, 1976). Wentworth et al. (1983) reported that the influx of serpentinite-rich sediments indicated deformation of the New Idria serpentinite diapir in association with the beginning of right-lateral shearing and faulting associated with the San Andreas Fault Zone in the Coalinga area.

6.6 Regional Folding and Rate of Crustal Shortening

An analysis of the regional system of folding in conjunction with a quantitative analysis of present-day crustal strain (using U.S. Coast and Geodetic Survey data on the apparent movement of triangulation stations) shows that modern folding in the region has resulted in crustal shortening oriented in the direction of north 35 degrees east. This shortening is occurring at the rate of 1 to 5 cm per kilometer over a time period of approximately 20 years (Burford, 1965, reported in Page, 1966, p. 275). As reported by Page (1966, p. 275), in the Coalinga area, this regional compressive strain is integrated with the effect of transform, strike-slip shear forces which allow north-south crustal shortening and east-west extension.

An analysis of seismic and geologic data related to the 1983 Coalinga earthquake and data from crustal shortening studies show that regional compression associated with crustal shortening and compressional thrusting at great depth is presently occurring throughout the southern Coastal Range province (Burford, 1965; Page, 1966; Minster and Jordan, 1978; Mount and Suppe, 1987; Zoback et al., 1987; Harbert and Cox, 1987; Bartow, 1987). This means that the area is continuing to experience regional uplift and, consequently, relatively high rates of erosion of less-resistant rock units that are located in topographically high areas.

Reproduced with permission of the copyright owner. Further reproduction prohibited without permission.

An analysis of leveling data across the Pleasant Valley and Anticline Ridge areas near Coalinga has shown that the anticlinal structure was uplifted approximately 0.5 meters as a result of the 1983 Coalinga earthquake (King and Stein, 1983, p. 165). Additional data indicate that the anticlinal structure has been uplifted at the rate of approximately 0.5 millimeters per year over the past million years (Sauber, et al., 1988, p. 326). This uplift has affected the morphology and pathway of the streams that flow through the Pleasant Valley area (King and Stein, 1983, p. 176). See Figure 2-10.

Recent work by the USGS (King and Stein, 1983) on the evolution of river terraces related to Los Gatos Creek indicates that the Coalinga area has been experiencing regional uplift over the past 500,000 years. The persistence of the soft, readily erodable, serpentinite matrix of the New Idria Formation as a regional high (i.e., forming the crest of the Joaquin Ridge highlands) and the occurrence of serpentinite debris flow deposits on the flanks of the New Idria Formation that are estimated to be 250,000 to 300,000 years old provides additional evidence that the region has been experiencing uplift for hundreds of thousands of years. The recent seismic events of the Coalinga region are related to the regional folding and crustal shortening that is occurring in the Coast Ranges geomorphic province. This regional folding and crustal shortening is occurring in response to a component of tectonic convergence across the Pacific-North American plate margin that resulted from a change in plate motion about three to five million years ago (Harbert and Cox, 1988, p. 4).

Reproduced with permission of the copyright owner. Further reproduction prohibited without permission.

7.0 REGIONAL FAULTING AND SEISMIC ACTIVITY

7.1 Regional Faulting

A review of geologic maps and available literature shows that the Johns-Manville Coalinga Asbestos Mill Site is located in an area associated with several regionally mapped surface faults, including the Parkfield segment of the San Andreas Fault Zone, the Waltham Canyon Fault, the Nunez Canyon Fault, and the intrusive thrust fault contacts related to the tectonic emplacement of the New Idria serpentinite mass. The notable surface faults include the San Andreas Fault Zone (which marks the transform boundary between the Pacific oceanic plate and the North American continental plate) and the thrust faults associated with the margins of the New Idria Formation. In addition to regional surface faults, the Joaquin Ridge area also contains an abundance of minor tear faults that occurred as a result of the diapiric, anticlinal structure of the New Idria serpentinite body. These faults are illustrated in the regional geologic map of Figure 2-2A and thrust faults associated with diapiric emplacement of the New Idria Formation are illustrated in Figure 2-6B.

7.2 Seismicity

Historically, most ground shaking in the Joaquin Ridge area, including White Creek and Pine Canyon, appears to have occurred as a function of seismic events related to the Parkfield segment of the San Andreas Fault Zone. This fault zone is located approximately 17 miles southwest of Joaquin Ridge and the Johns-Manville Coalinga Asbestos Mill Site. In June 1966, the Parkfield segment experienced an earthquake (Richter magnitude 6.1) that ruptured the San Andreas Fault.

Reproduced with permission of the copyright owner. Further reproduction prohibited without permission.

More recently, there has been a series of strong earthquakes in the vicinity of Coalinga with epicenters located on the northeast flank of the Coalinga Anticline (May 1983, Richter magnitude 6.5 M) and the northeast flank of the Joaquin Ridge Anticline (October 1982, Richter magnitude 5.4 M). These more recent earthquakes were unusual in that: (1) they were not related to movement on the San Andreas Fault; (2) they occurred in an area where earthquakes were not expected; and (3) there was no observed rupturing of any surface faults related to the initial, primary events.

As illustrated in Figure 2-9, the epicenter of the 1983 Coalinga earthquake was located 13.5 miles to the east-southeast of the location of the Johns-Manville Coalinga Asbestos Mill. The epicenter of the October 1982 Joaquin Ridge event was located on the northerly flank of the Joaquin Ridge Anticline, approximately one mile north of the Johns-Manville Coalinga Asbestos Mill.

Stove (1983, Figure 1) constructed an isoseismal map that illustrates the regional distribution of the seismic intensity of the May 2, 1983 Coalinga earthquake. The map shows that the Johns-Manville Coalinga Asbestos Mill Site lies in a transitional zone between Modified Mercalli Zones VI and VII. These are zones associated with slight to negligible predicted damage in buildings and structures of good design and appropriately reinforced construction (California Division of Mines and Geology, February 1979).

Following the May 2, 1983 earthquake, a series of smaller earthquakes (ranging in magnitude from 5.0 to 6.4 M) in June and July 1983 resulted in surface rupturing in the vicinity of Nunez Canyon and Los Gatos Creek Road. As indicated in Figure 2-11, this area is located approximately 8.75 miles northwest of Coalinga and 6.5 miles southeast of the Johns-Manville Coalinga Asbestos Mill Site in Pine Canyon.

Reproduced with permission of the copyright owner. Further reproduction prohibited without permission.

Subsequent geologic investigations (Hart and McJunkin, 1983, pp. 210-219) provided evidence that the surface rupturing was associated with an east-dipping reverse fault that was tectonically related to folding, faulting, and general crustal shortening in the Coalinga area and elsewhere along the western margin of the San Joaquin Valley. Evidence of a pre-existing fault along the Nunez rupture zone was provided by subtle geomorphic features (i.e., scarps and sidehill benches) indicating previous Holocene faulting.

7.3 Geologic Implications of Regional Seismicity

The 1983 series of strong earthquakes (Richter magnitudes of 6.0 M or greater; Modified Mercalli intensities of VI or greater) which occurred in the vicinity of Coalinga came as a surprise to many earth scientists because the epicenters were located in a geographic area that has few recognized faults and sparse historical seismicity, and because the initial strong earthquakes were not related to any observable surface ruptures. The occurrence of such strong seismic events with epicenters located along the western margin of the San Joaquin Valley suggests that undetected faults within the boundary zone between the Coast Ranges province and the Sierran crustal block have probably been the source of other significant seismic events. However, the persistent concentration of small earthquakes along slipping segments of known major faults (San Andreas, Hayward, Calaveras) has generally caused attention to be focused only on areas of known seismicity (Eaton, 1985, pp. 44-45; Wong and Ely, 1983, p. 89), with little attention focused on the seismically less active boundary between the Coast Ranges province and the Sierran Block.

As reported by Eaton (1985), the geologic and geophysical modeling of seismic data associated with the Coalinga events suggests the following:

Reproduced with permission of the copyright owner. Further reproduction prohibited without permission.

(1) The zone of interaction between the Pacific and North American plates (expressed as transpressional deformation) appears to extend entirely across the Coast Ranges;

(2) A ductile, aseismic detachment zone located deep beneath the upper crust allows decoupling of the overlying brittle crust from the underlying plate. With decoupling, deformation will occur in the overlying brittle crust; however, the deformation will be controlled by physical properties within the crust rather than by physical properties of the decoupled shear zone and the underlying plate; and

(3) Particularly strong sections of the crust will resist internal deformation, and earthquakes will be concentrated along their boundaries. Weaker portions of the crust will undergo internal deformation and generate earthquakes internally as well as along their boundaries.

The points above suggest that the earthquake activity in the Coalinga area is related to a series of subhorizontal thrust faults resulting from a component of convergent motion across the Pacific - North American plate boundary. This accounts for the occurrence of active, low angle blind thrusts not associated with significant surface faulting. An exception is the Nunez fault (a north-trending, east-dipping reverse fault) which may be a secondary "backthrust" associated with the hanging wall block of a primary low-angle thrust fault at depth (i.e., 10 to 15 kilometers deep). As reported by Hart and McJunkin (1983, p. 206), the Nunez fault may also be related to a compressive system of folds located to the east that have been active during Quaternary time.

Reproduced with permission of the copyright owner. Further reproduction prohibited without permission.

8.0 GEOMORPHOLOGY

8.1 Regional Overview

8.1.1 Arroyo Pasajero Watershed

The Arroyo Pasajero watershed centers around the town of Coalinga in western Fresno County and includes drainage from four major intermittent streams including Los Gatos Creek, Warthan Creek, Jacalitos Creek, and Zapato-Chino Creek. (See regional watershed map as illustrated in Figure 2-1). These streams drain a total area of more than 500 square miles. The upper reaches of these streams and their tributaries head in the highland areas of the Diablo Range mountains which are formed by steeply dipping Cretaceous sandstones and shales and by metamorphic and igneous rocks of the Franciscan Complex (Jurassic to Cretaceous). The mountains are formed by a series of linear, anticlinal structures and ridges that are subparallel to the northeast-southwest trend of the San Andreas Fault Zone, which is located approximately 15 miles southwest of Coalinga. The streams are organized in a structurally influenced trellis and dendritic drainage pattern that has been modified by regional uplift associated with the Coast Range orogeny (i.e., mountain building) episode that occurred during the Pliocene to Pleistocene time period.

Three of these streams (Los Gatos Creek, Warthan Creek, and Jacalitos Creek) come together in the vicinity of Coalinga, which is located on an alluvial floodplain surrounded by the foothills of the Diablo Range to the west and the low rounded hills of Anticline Ridge and Guijarral Hills to the east. This floodplain is known as Pleasant Valley and covers approximately 20 square miles. Los Gatos Creek is the main tributary, and flow from these three intermittent creeks has contributed to the

Reproduced with permission of the copyright owner. Further reproduction prohibited without permission.

development of a drainage pathway that cuts through a gap between Guijarral Hills and Anticline Ridge (an area locally known as the Turk Narrows). These hills have formed on the western margin of Pleasant Valley in conjunction with the tectonic uplift of the Coalinga Anticline (Munn, Busaca, and Trott, 1981).

8.1.2 Pleasant Valley and Uplift of the Coalinga Anticline

The structural axis of the Coalinga Anticline was reportedly uplifted approximately 0.5 meters during the 1983 Coalinga earthquake (King and Stein, 1983, p. 165). This uplift, which is continuing, is thought to have occurred in response to folding of the anticlinal structure in conjunction with earthquake activity in the region. Over the past million years, this uplift has been estimated to occur at a rate of approximately 0.5 millimeters per year (Lettis, 1982 and Sauber, et al, 1988, p. 326). Uplift of the anticlinal structure has extended into the Pleasant Valley area and has affected the morphology and drainage pathways of Los Gatos Creek and Zapato-Chino Creek.

The Pleasant Valley floodplain may be thought of as a hinged ramp that is affected by uplift of the Coalinga Anticline which is marked by the trend of Anticline Ridge. When the anticline is uplifted (as a result of compressive folding associated with the transform convergence of the North American Plate and the Pacific Plate), the western margin of the Pleasant Valley floodplain is also uplifted with most of the uplift occurring on that part of the ramp that is closest to the structural axis of the anticline. This uplift has in the geologic past redirected the drainage pathway of Los Gatos Creek. As reported by King and Stein (1983, p. 166), Los Gatos Creek used to flow along a drainage pathway closer to Anticline Ridge but now follows a course developed on the west and south side of Pleasant Valley before it flows to the east

Reproduced with permission of the copyright owner. Further reproduction prohibited without permission.

toward Guijarral Hills and the Arroyo Pasajero alluvial fan. See the geomorphic sketch map of Pleasant Valley presented in Figure 2-10.

Between Coalinga and Guijarral Hills (a distance of approximately five miles), the hydraulic gradient of Los Gatos Creek is significantly reduced and the intermittent stream follows a broad, sinuous, meandering pathway. The average bedslope for this reach is reported to be 0.003 ft/ft (Simons, Li and Associates, 1985, p. 3.1). The reduction in the hydraulic gradient of the streambed has occurred in conjunction with an abrupt meandering of the streambed, a noticeable widening of the intermittent channel (to approximately 500 feet, set within an entrenched meander floodplain that widens to approximately 1,200 feet), and the abundant deposition of sand-sized material as the intermittent channel crosses the structural axis of the Coalinga Anticline. The meandering streambed in this area is entrenched approximately 40 feet and is associated with several inset terraces. Some of the terraces are related to the episodic uplift of the Pleasant Valley floodplain in association with episodic uplift of the Coalinga Anticline. As reported by King and Stein (1983), the occurrence of lake or marsh deposits on the northwest side of Guijarral Hills in the Pleasant Valley floodplain provides some evidence that uplift associated with the anticlinal structure has, in the prehistoric past, contributed to the temporary damming of the Pleasant Valley drainage pathways (i.e., Los Gatos Creek and Zapato-Chino Creek).

Field observations show that the average size of the material deposited in this reach of Los Gatos Creek changes from sandy gravel and cobbles on the east side of the town of Coalinga to mostly coarse silt and sand in the area of the Turk Narrows (i.e., the gap between Anticline Ridge and Guijarral Hills). The predominant deposition of sandy material in this reach of Los Gatos Creek has occurred in response to a decrease in the capacity of the intermittent stream to transport coarser material. This decrease

Reproduced with permission of the copyright owner. Further reproduction prohibited without permission.

in transport capacity has generally occurred in association with a marked increase in the width of the meandering channel and a decrease in the hydraulic gradient (i.e., bedslope). In this reach, the sandy streambed sediment occurs in braided stream deposits that are subject to scouring and cut and fill processes that tend to winnow (i.e., suspend and transport downstream) the fine silt and clay fractions.

8.1.3 Arroyo Pasajero Alluvial Fan

On the west side of Anticline Ridge and Guijarral Hills, Los Gatos Creek is joined by Zapato-Chino Creek. Collectively, these streams form the Arroyo Pasajero drainage channel which discharges its runoff to the Arroyo Pasajero alluvial fan. This alluvial fan is one of the largest alluvial fans that has formed on the western margin of the San Joaquin Valley. The fan covers more than 300 square miles and has been forming for more than 600,000 years. On the eastern side of Anticline Ridge and Guijarral Hills, the Arroyo Pasajero channel has become entrenched approximately 30 to 40 feet. The entrenched channel has formed in response to streambed downcutting associated with tectonic uplift of the Coalinga Anticline and the phenomenon of widespread subsidence along the western margin of the San Joaquin Valley between Los Banos and the Kettleman Hills (King and Stein, 1983, p. 167; Ireland, 1986, p. 7). In the last 60 years, subsidence in the Huron area has been more than 20 feet. See Figure 2-11. The combined occurrence of tectonic uplift and subsidence has contributed to an increased hydraulic gradient for this portion of the Arroyo Pasajero drainage channel, and this increased hydraulic gradient has contributed to the occurrence of streambed and streambank erosion in the region.

Reproduced with permission of the copyright owner. Further reproduction prohibited without permission.

A surface and subsurface investigation of the alluvial fan and settling basin sediments in the medial alluvial fan area near the California Aqueduct and the town of Huron shows that these sediments are mostly silt and clay deposits interbedded with some fine-grained sand intervals. These deposits generally have no visible evidence of asbestos in comparison with the visible evidence of asbestos in the gravelly, sandy streambed sediment of Los Gatos Creek on the northwest side of the town of Coalinga. The lack of coarser grained sediment in the alluvial fan deposits is probably a result of the "trapping" of coarser grained sediment in the area of the Pleasant Valley floodplain. As described above, in the Pleasant Valley area, Los Gatos Creek has a decrease in the capacity (or competency) to transport coarser grained sediment as a result of a reduced hydraulic gradient resulting from streambed sediment deposition and the occurrence of tectonic uplift of the structural axis of the Coalinga Anticline.

8.1.4 Arroyo Pasajero Section of the California Aqueduct

Elevations within the Arroyo Pasajero watershed range from 225 feet at the toe of the Arroyo Pasajero alluvial fan to approximately 5,000 feet in the upper Los Gatos Creek watershed on Joaquin Ridge. The California Aqueduct was constructed across the medial portion of the Arroyo Pasajero fan at an elevation of approximately 325 feet above sea level. The construction of the Aqueduct has acted as a barrier to the natural drainage of the alluvial fan and has interrupted the natural dispersion of floodwaters and sediments to the distal parts of the alluvial fan. These floodwaters and sediments are currently being ponded in a three-square-mile settling basin that has been constructed adjacent to and upslope of the Aqueduct on the east side of Huron. The settling basin was originally constructed to contain sediments and floodwaters from a 100-year storm; but because of higher-than-projected sedimentation rates (nearly four times greater than expected), the settling basin is being filled with fine-grained

Reproduced with permission of the copyright owner. Further reproduction prohibited without permission.

sediments, and its holding capacity has been diminished to contain runoff and sediments from only a seven-year storm. During storm events, runoff and sediment may be drained into the Aqueduct through four gated inlet structures located at the southern end of the settling basin.

8.1.5 Subsidence and Channel Entrenchment on the Alluvial Fan

The slopes of the upper watershed areas are steep and may exceed 60% to 70%. In the lower watershed areas where there is much less relief, the stream channels have become entrenched 30 to 40 feet. This is particularly evident on the west side of Coalinga where the Arroyo Pasajero channel has become entrenched by downcutting through the fine-grained strata of the upper alluvial fan. The lower-most exposed strata may be part of the Tulare Formation (Pleistocene). As indicated above, this downcutting may be related to tectonic uplift associated with the Coalinga Anticline or from subsidence related to the local lowering of the ground-water table as a result of overdraft by agricultural water wells. Some of the subsidence may be related to the near-surface wetting and collapse of soil structure associated with large-scale irrigation systems (Ireland, 1986). The lower-most slopes of the watershed are formed by the alluvial fan. The slope of the alluvial fan decreases from about 0.8% at the head of the fan in the Guijarral Hills area to less than 0.4% in the medial fan near Huron.

8.1.6 New Idria Formation Outcrop Area

The upper watershed drainage area of Los Gatos Creek includes 6.8 square miles of the New Idria Formation which outcrops on the crest of Joaquin Ridge. Approximately 5.8 square miles of the New Idria Formation are drained by the White Creek tributary network, and 1.0 square mile is drained by the Pine Canyon tributary

Reproduced with permission of the copyright owner. Further reproduction prohibited without permission.

network. The White Creek drainage area includes nine inactive mining operations and four inactive milling operations, and the Pine Canyon area includes three inactive mining operations and one inactive milling operation.

8.1.7 Watershed Soils and Geologic Units

Hill slopes formed by the asbestos-containing serpentinite of the New Idria Formation appear to be susceptible to high rates of sheet, rill, and gully erosion and mass wasting in the form of large landslides and/or debris flows. As reported by Munn, Busacca, and Trott (1981, p. 7) and confirmed by field sampling activities during this investigation, the surface erosion potential of the naturally occurring serpentinite soils of the New Idria Formation appears to be higher than indicated by K factor data because of the weak, unconsolidated structure of the serpentinite soils combined with steep slopes and the sparse natural vegetative cover which consists of sparse manzanita and coffeeberry bushes, but no grass.

Most of the other upper watershed areas are underlain by soils developed on Cretaceous marine sandstones and shales. Field observations indicate that these soils are generally resistant to erosion and may support a good vegetative covering including grasses and oak trees in upper drainage areas.

The middle and lower elevation slopes in the Arroyo Pasajero watershed are mostly composed of soils developed on weakly consolidated Tertiary sandstones, siltstones, and shales of marine and continental origin. These soils (not described in this report) are developed on the Oligocene and Eocene Kreyenhagen shale, the middle and lower Miocene Temblor sandstone, the middle Miocene Monterey shale, the upper Miocene Reef Ridge Formation, the lower Pliocene Jacalitos Formation, the middle Pliocene

Reproduced with permission of the copyright owner. Further reproduction prohibited without permission.

Etchegoin Formation, and the upper Pliocene San Joaquin Formation. Soils of the alluvial fan and the lower-most slopes of the outer foothills (Guijarral Hills and Anticline Ridge) are developed on alluvial deposits of the Pleistocene Tulare Formation and geologically recent alluvium.

The weakly consolidated Tertiary marine rocks are generally less resistant than the underlying Cretaceous sandstones and shales. Consequently, the Tertiary formations have been worn into low, rounded hills associated with broad, sediment-filled valleys and stream channels.

Overlying the Tertiary sediments are the fresh-water lacustrine (lake), fluvial, and alluvial deposits of the Pliocene-Pleistocene Tulare Formation. The Tulare Formation includes the lacustrine Corcoran Clay unit which has been radiometrically dated at approximately 600,000 years old. In the San Joaquin Valley near Coalinga, the Tulare Formation is overlain by Quaternary-aged alluvial sediments deposited by a system of coalescing alluvial fans that have formed at the base of the outer foothills.

8.2 Joaquin Ridge-Pine Canyon Area

A field investigation including reconnaissance geologic mapping of the Joaquin Ridge and Pine Canyon area was completed using aerial photographs, topographic maps, and a detailed ground survey, including an examination of stream channels. The field investigation shows that the Upper Pine Canyon area is underlain by a complex system of on-lapping and over-lapping landslides and/or serpentinite debris flows that originated from several different areas of the asbestos-containing New Idria Formation. The upper detachment zones of the landslides are being dissected by sheet, rill, and gully erosion. The lower two thirds of the landslides have stream-channel

Reproduced with permission of the copyright owner. Further reproduction prohibited without permission.

margins that are being eroded by gullying and mass wasting, and by entrenchment or downcutting of the intermittent streambed channels.

8.2.1 Field Observations of Landslides and/or Serpentinite Debris Flows

The Johns-Manville Coalinga Asbestos Mill Site is located in Upper Pine Canyon on the southern flank of Joaquin Ridge. The geology of the Johns-Manville Coalinga Asbestos Mill site area is illustrated in Figure 2-12. This area is located approximately 0.6 miles downslope from the serpentinite outcrop of the New Idria Formation. The Mill and the Upper Pine Canyon area are underlain by a complex system of several on-lapping and over-lapping inactive Quaternary landslides and/or debris flows composed of serpentinite minerals (including chrysotile asbestos). The location of these landslide and/or debris flow complexes were mapped by Levine-Fricke (May 9, 1989) are readily identified in aerial photographs. These landslide and/or serpentinite debris flow deposits originated from the area of the outcrop of the New Idria Formation and the detachment zones have subject to asbestos and chromite ore mining. In addition to an assemblage of serpentinite minerals, the landslides and debris flows contain blocks of metamorphic rock derived from the Franciscan Complex (Jurassic to Cretaceous). This assemblage of metamorphosed oceanic crustal material and marine sedimentary rocks rims the southeast margin of the serpentinite outcrop on Joaquin Ridge. The metamorphosed rocks contain blueschist-facies mineral assemblages (which were derived from metamorphosed oceanic crustal material) and silica-carbonate (hydrothermally altered serpentine), which may contain cinnabar and magnesite deposits (Eckel and Myers, 1946, p. 96).

Soils of the Upper Pine Canyon area have variable asbestos concentrations, depending upon the origin of parent materials, the extent of weathering processes and possibly

Reproduced with permission of the copyright owner. Further reproduction prohibited without permission.

other factors. The Quaternary landslide and/or debris flow deposits in the vicinity of the Railroad Mine have generally high asbestos concentrations (e.g., greater than 50 percent). However, landslide soils in other areas of the mill location have developed deep clay-rich argillic horizons with relatively low asbestos concentrations (e.g., less than one percent). These clay-rich soils also support a grassy vegetative cover.

The southeastern margin of the New Idria Formation in the Pine Canyon area is also rimmed by steeply-dipping interbedded marine sandstones and shales of the Panoche Formation (Late Cretaceous) of the Great Valley sequence. Some of the sedimentary rock units are fractured and locally overturned (reflecting the complex structural and tectonic history of the region). In the Upper Pine Canyon area, the competent sandstone units of the Panoche Formation form erosion-resistant ridges and vegetated dip slopes, and the intervening shaley units form the moderately steep and rubbly hillsides.

8.2.2 Recent Geologic Mapping

Geologic mapping of the Upper Pine Canyon area (Levine-Fricke, May 9, 1989) shows that four to five landslides converge in the vicinity of the Johns-Manville Coalinga Asbestos Mill Site. These landslide deposits extend throughout the Upper Pine Canyon area. In their entirety, these Upper Pine Canyon landslides cover approximately 1.0 square mile. Analysis of samples of deeply weathered landslide materials from excavation pits shows asbestos concentrations ranging from less than 1% in the deeply weathered, upper soil horizons to more than 80% in the less weathered soil horizons (as determined by PLM and TEM methods). The landslide deposits in the general vicinity of the Johns Manville Coalinga Asbestos Mill Site area

Reproduced with permission of the copyright owner. Further reproduction prohibited without permission.

have very well developed soils profiles with thick (eight feet or more), clay-rich argillic horizons.

The landslide deposits extend downslope approximately 1.6 to 1.8 miles from the zones of detachment from the main serpentinite body of the New Idria Formation. The upper detachment zones generally occurred at an elevation of approximately 4,000 to 4,400 feet, and the toe of the landslide complex was mapped at approximately 2,600 feet (above mean sea level). The combined flows have a maximum width of approximately 0.6 miles in the highland area near the zones of detachment. In the on-site vicinity of the Johns-Manville Coalinga Asbestos Mill Site, the combined flows have a maximum width of approximately 1,000 feet as they are constrained by the canyon walls of Upper Pine Canyon. Stream channels have formed at the margins of the serpentinite debris flows, and the development of these channels has contributed to erosion of the asbestos-containing serpentinite debris flow materials.

8.2.3 Relative Ages of the Landslides and/or Serpentinite Debris Flow Deposits

The relative ages of the landslides was assessed by an analysis of cross-cutting relationships, surface morphology and relative degree of surface dissection, and degree of soil profile development. Based on these observations, the landslides were estimated to be approximately 50,000 to 250,000 years old, and the northerly flows were observed to be relatively older than the northwesterly flows. The northwesterly flows post-date the northerly flows, as indicated by an on-lapping of the northerly flows and an assemblage of immature geomorphic features, including relatively flat topographic expression and minimal degree of dissection. The northerly flows were

Reproduced with permission of the copyright owner. Further reproduction prohibited without permission.

observed to contain large blocks of heavily fractured sandstone and shale derived from the upslope outcropping of the Panoche Formation (Upper Cretaceous).

8.2.4 Chromite Mining of Landslide Deposits

The northwesterly debris flow deposits located downslope from the asbestos mill of Upper Pine Canyon have been prospected for chromium boulders that may have originated from the vicinity of the Butler Estate Chromite Mine (located approximately 0.7 miles northwest of the Johns-Manville Coalinga Asbestos Mill Site). This mine is located along the southeast margin of the diapiric/faulted contact of the New Idria Formation with the Cretaceous Panoche Formation. The prospected and mined area covers approximately five acres and is known as the Railroad Mine.

8.2.5 Origin of the Landslide and/or Serpentinite Debris Flow Complexes

As reported by Cowan and Mansfield (1970, p. 2,617) for upland canyons that are encroaching on the sidewalls of the diapiric structure of the New Idria Formation, continuous erosion of the upper-most reaches of Pine Canyon drainage channels probably "breached the contact between sedimentary rock and serpentinite to the extent required to allow (downslope) flowage to begin. Larger flow deposits on the southern margin of the (New Idria Formation) parent body (in the vicinity of the Atlas Mine and Mill) are several square kilometers in area and are not confined to a single canyon. These features indicate that continual or intermittent uplift of the parent body may also have initiated flowage. Thus, both uplift and canyon erosion seem to have been important processes in the development of serpentinite flows." The resulting flows migrated downslope into the heads of the encroaching, upland canyons.

Reproduced with permission of the copyright owner. Further reproduction prohibited without permission.

Continued downslope movement of the flows was influenced by existing canyon topography.

Cowan and Mansfield (1970, p. 2,617 - 2,623) observed that the serpentinite flows on the northeast side of Joaquin Ridge have a form that resembles that of solidified lava flows and debris flow deposits. The flows consist of rounded blocks of serpentinized peridotite and dunite enclosed in a matrix of flakey, asbestos-containing serpentinite; the flakey, asbestos-containing serpentinite matrix comprises approximately 75% of the flow volumes, and the lowest ends of the flows (i.e., the "snouts") have assumed the form of a semi-plastic material in critical equilibrium.

8.2.6 Erosion of the Earthflow and/or Debris Flow Complexes

In Pine Canyon, the emplacement of the older, northerly serpentinite flow deposits displaced the canyon's original drainage channel, and subsequent drainage channels formed along the margins of the flow deposit. The emplacement of the younger serpentinite flow deposits (which originated from the northwest canyon area in the vicinity of the Butler Estate Chromite Mine) similarly affected the Upper Pine Canyon drainage system by contributing to the formation of additional drainage channels. The subsequent drainage network is dissecting the upper landslide areas and the zones of detachment, and stream channels have become entrenched and are eroding the margins of the asbestos-containing landslide deposits.

Reproduced with permission of the copyright owner. Further reproduction prohibited without permission.

8.2.7 Approximate Age of the Pine Canyon Earthflow Complexes

Although an exact age has not been determined using radiometric data methods, the serpentinite flows in Pine Canyon are estimated to be approximately 50,000 to 250,000 years old based on analysis of the development of soil profiles and the development of surface dissection by fluvial processes. Additional features indicating a very old age include the occurrence of coarse pebble lag deposits formed by winnowing of fine material by eolian processes (i.e., deflation); and the occurrence of cemented conglomerates found in the streambeds of the channels formed at the margins of the serpentinite flows.

An analysis of geomorphic data indicates that the Pine Canyon flows have been stabilized for many years, and there is no direct evidence of any recent movement. Most of the digger pine trees that have grown on the flows are standing upright, and as reported for the flows on the north side of Joaquin Ridge (Cowan and Mansfield, 1970, p. 2,623), the trunks of the trees are neither strongly bent nor markedly inclined from the vertical plane of reference. This indicates that no significant downslope movement has occurred during the growth of the trees.

8.2.8 Field Evidence of Continuing Uplift

Field evidence of continuing uplift and erosion of the New Idria Formation is provided by a geomorphic analysis of the serpentinite outcrop area. Previous geologic investigations have confirmed that the flakey serpentinite matrix of the New Idria Formation forms the diapiric core of the Joaquin Ridge Anticline. This flaky, weakly consolidated, readily friable serpentinite matrix has persisted as a topographically high area in spite of long-term erosional processes. Throughout Quaternary time, the New

Reproduced with permission of the copyright owner. Further reproduction prohibited without permission.

Idria Formation has formed the crest of the Joaquin Ridge highlands. In the White Creek area, the serpentinite outcrop has more than 2,000 feet of surface relief over a relatively short distance (approximately two miles) (USGS, 1984; Jenkins, 1971; and Eckel and Myers, 1946, Plate 1). Because of this steep gradient and other physical characteristics (i.e., a flakey, weakly consolidated matrix; extensive internal fracturing and faulting; and a high subsurface water content which tends to lubricate glide planes), the outcrop area is subject to severe erosion and mass wasting, including large landslide and/or debris flow complexes. The downslope movement of these earthflows contributes to the formation of erosional gullies that tend to dissect the landslide and outcrop areas. Without continuing uplift, these erosional processes would eventually minimize the topographic relief of the outcrop area.

8.3 Joaquin Ridge/White Creek Area

White Creek is the principal drainage system for the southeastern portion of the New Idria Formation. The White Creek watershed drains approximately 5.8 square miles of the New Idria Formation in an area that has included extensive mining, milling, and surface mineral exploration operations. The area is associated with steep relief (up to 2,200 feet) which contributes to: (1) significant sheet, rill, and gully erosion; and (2) the formation of large landslide and/or debris flow complexes. A large serpentinite landslide complex that covers approximately 3.2 square miles has been mapped in the lower third of the White Creek outcrop area (Eckel and Myers, 1946, Pl. 8; Dibblee, 1971).

As indicated in the above discussion of the serpentinite flows in Pine Canyon, the upper landslide areas are being dissected by the development of the surface drainage system, and erosional stream channels are forming along the margins of the landslides.

Reproduced with permission of the copyright owner. Further reproduction prohibited without permission.

Figure 2-8 illustrates the detailed drainage network that is dissecting and eroding the asbestos-containing serpentinite matrix of the New Idria Formation in the White Creek area. During storm events, large quantities of asbestos-containing sediments are being eroded by sheet, rill and gully erosion and by mass wasting. These sediments are being transported downstream through the intermittent White Creek - Los Gatos Creek drainage systems. These asbestos-bearing serpentinite sediments have historically been deposited along the Los Gatos Creek drainage pathway and on the Arroyo Pasajero alluvial fan.

8.4 Diablo Range Alluvial Fans

8.4.1 Asbestos As A Natural Constituent of Diablo Range Alluvial Fan Deposits

The western margin of the central San Joaquin Valley in the Coalinga region is formed by a series of coalescing alluvial fans that include the Arroyo Pasajero, Cantua Creek, Arroyo Hondo, Panoche Creek, Little Panoche Creek, Leguna Seca Creek, the Ortigalita Creek, and other lesser alluvial fans that drain the eastern flanks and foothills of the Diablo Range mountains. The alluvial fans associated with these drainage systems collectively cover more than 1,500 square miles (Miller, Green, and Davis, 1971). These fans have been formed by the alluvial deposition of sediments derived from erosion of the formations that comprise the eastward-draining mountains and foothills (Bull, 1964; Jenkins, 1971; Miller, Green, and Davis, 1971; Atwater, et al., 1986). These formations include the New Idria Formation, the Table Mountain serpentinite deposit, and other un-named ultramafic serpentinite deposits (Figure 3, EPA, Potential Sources Report, 1987) that are known to contain chrysotile asbestos. The exposed foothills that form the western margin of the central San Joaquin Valley also include at least five sedimentary formations containing serpentinite sediment with

Reproduced with permission of the copyright owner. Further reproduction prohibited without permission.

varying concentrations of chrysotile asbestos. These formations include the Big Blue Member of the Temblor Formation (Miocene), Santa Margarita Formation (Late Miocene), Etchegoin and Jacalitos Formation (Early Pliocene), Tulare Formation (Late Pliocene and Pleistocene), and Quaternary alluvium.

The sediments of these Miocene and younger sedimentary formations reflect the mineralogy of sediment source areas that include asbestos-bearing serpentinite deposits (such as the New Idria Formation) and sedimentary serpentinite deposits (such as the Big Blue Member) which have been exposed to erosional processes by regional uplift. The New Idria Formation and the Big Blue Member have asbestos concentrations that range up to 90% or higher. The serpentinite mass of the New Idria Formation outcrops over a 48-square-mile area at the crest of Joaquin Ridge. This intrusive serpentinite deposit has been exposed to erosion and mass wasting for approximately 17 million years. Sediment eroded from this natural source of asbestos has been incorporated in the flanking sedimentary deposits of the Big Blue Member (Miocene) and younger formations including the Santa Margarita, Etchegoin, Jacalitos, and Tulare Formation and the Quaternary deposits of the modern alluvial fans.

The asbestos-containing sedimentary formations are exposed in the uplifted foot-hills that form the western margin of the central San Joaquin Valley from Kettle-man City north to Los Banos. These foothills include Kettleman Hills, Guijarral Hills, Anticline Ridge, Big Blue Hills, Ciervo Hills and Monocline Ridge, Panoche Hills, and Leguna Seca Hills. The alluvial fan deposits of these foothills and drainage basins have asbestos that originated from erosion of the asbestos-containing ultramafic and sedimentary formations described above. Asbestos concentrations in Miocene and younger sedimentary formations range from trace amounts to levels greater than 90%.

Reproduced with permission of the copyright owner. Further reproduction prohibited without permission.

The Quaternary alluvial fan sediments have asbestos concentrations that are generally 1% or less.

8.4.2 Arroyo Pasajero Alluvial Fan and Quaternary Asbestos Sediment

The Arroyo Pasajero alluvial fan is one of the largest alluvial fans that has formed on the western margin of the central San Joaquin Valley. The modern alluvial fan surface presently covers more than 300 square miles and has been forming for more than 600,000 years (Munn, Busacca, and Trott, 1981; Atwater, et al., 1986). The regional watershed basin that supplies sediment to the alluvial fan covers 512 square miles. This area includes close to seven square miles of the asbestos-containing New Idria Formation. In addition to the New Idria Formation, the Arroyo Pasajero watershed basin encompasses approximately 130 square miles of outcrops of Miocene, Pliocene, and Pleistocene sedimentary deposits (Jenkins, 1971). Geologic research has shown that Miocene and younger sedimentary deposits including the Big Blue Member of the Temblor Formation and overlying sedimentary formations (Santa Margarita Formation, Etchegoin and Jacalitos Formations, San Joaquin Formation, and Tulare Formation) all contain locally high to trace concentrations of asbestos sediment. The geologically recent alluvial fan sediments are mineralogically most similar to the sediments of the underlying Tulare Formation (Miller, Green, and Davis, 1971), both of which are known to contain asbestos-bearing sediment.

An analysis of cross-cutting relationships shows that the Arroyo Pasajero alluvial drainage system has existed since at least early Pleistocene time (i.e., up to 1.8 million years ago) (Munn, Busacca, and Trott, 1981, p. 14). This drainage system has been delivering sediment derived from sediment source areas of the Arroyo Pasajero watershed to the central San Joaquin basin and its alluvial depositional environments

Reproduced with permission of the copyright owner. Further reproduction prohibited without permission.

throughout this time period. PLM and TEM analysis of medial and distal subsurface alluvial fan sediments (sampled from eight cores from depths as great as 42.5 feet) show that ancient alluvial fan sediment contains chrysotile asbestos in concentrations that are generally 1% or less (i.e., trace concentrations).

In addition to serpentinite source areas located near the crest of Joaquin Ridge (i.e., the New Idria Formation outcrop area) and on the lower flanks of Joaquin Ridge and Anticline Ridge (i.e., the Big Blue Member of the Temblor Formation and other post-Miocene sedimentary formations), erosion of the Los Gatos Creek and the Arroyo Pasajero intermittent drainage channels in the vicinity of Anticline Ridge has been recognized as an additional source of asbestos for the Arroyo Pasajero alluvial fan including the Arroyo Pasajero section of the California Aqueduct and the sediment settling basin that is adjacent to the Aqueduct on the east side of Huron (U.S. Department of Interior, Bureau of Reclamation, 1984, p. 26). Stream bed and stream bank erosion of the Arroyo Pasajero channel is particularly significant on the east side of Anticline Ridge. In this reach of the Arroyo Pasajero, the average slope of the stream bed is 15.4 feet per mile. This slope allows storm waters to achieve sufficient velocities to cause bank cutting and bottom cutting of the intermittent channel (U.S. Department of Interior, Bureau of Reclamation, 1984, p. 28). The stream bed and stream bank sediments are Quaternary alluvial sediments that are mineralogically similar to the modern alluvial sediments of the region. Geologic research and asbestos analysis of subsurface alluvial fan sediments have shown that these Quaternary sediments have a small percentage of asbestos, ranging from trace concentrations to several percent. It has been estimated that 37% to 62% of the sediment currently being deposited on the Arroyo Pasajero alluvial fan and in the settling basin has been derived from the occurrence of this stream bed and stream bank erosion (Munn, Busacca, and Trott, 1981, p. 62; U.S. Department of Interior, Bureau of Reclamation,

Reproduced with permission of the copyright owner. Further reproduction prohibited without permission.

1984, p. 17; Simons, Li and Associates, 1985, pp. 4-13 to 4-22; Boyle Engineering, 1988, p. 4-11).

Surface sampling conducted by the California DWR (1986) using TEM methods has shown that the modern alluvial fan surface sediment has asbestos concentrations that range from trace levels to slightly more than 1% (i.e., up to 1.3%). An analysis of subsurface data correlated with pre-mining and post-mining time periods has shown there is no statistical difference in asbestos concentrations of the subsurface areas which were sampled and analyzed. Moreover, samples from these depths had asbestos concentrations similar to surface sampling results by the California DWR (1986). This is in agreement with what is known about the regional geology, i.e., that the Coalinga region has many square miles of natural asbestos source areas that have been subject to erosion for as much as 17 million years, and these eroded sediments are a natural constituent of post Miocene sedimentary formations as well as the alluvial sediments that have been deposited in the Arroyo Pasajero throughout the alluvial fan's geologic history.

8.4.3 Depositional Facies and Drainage Pathways

A review of soil maps (U.S. Department of Agriculture, Soil Conservation Service [USDA, SCS], 1952) and other data including NASA and NHAP high altitude, color infrared photographs, USGS topographic maps, and information from technical reports and publications on depositional processes and sediments of Los Gatos Creek and the Arroyo Pasajero alluvial fan show that the modern Arroyo Pasajero has had three general drainage pathways oriented to the north, northeast, and southeast. These drainage pathways have sandy alluvial sediments from old stream channel, overbank, and levee deposits. Depositional areas adjacent to and downslope from these drainage

Reproduced with permission of the copyright owner. Further reproduction prohibited without permission.

pathways have finer grained sediments (i.e., fine silts and clays) that were deposited by alluvial fan floodwaters. Alluvial fan depositional processes are such that alluvial sediments are deposited by a combination of stream channel, mud flow, and flood-water deposits (USDA, SCS, 1952; Reading, 1978; Munn, Busacca, and Trott, 1981). The fan sequence as a whole becomes thinner and finer in distal environments.

At any particular time, only a relatively small area of the Arroyo Pasajero alluvial fan surface receives sediment during depositional events. As an area accumulates sediment, floodwaters and mud flows tend to migrate to laterally adjacent environments that are topographically lower (Munn, Busacca, and Trott, p. 46). This process contributes to the basic geometric symmetry that is observed in the radial profile of the Arroyo Pasajero and other alluvial fans that have formed in semi-arid environments.

A review of USDA, SCS (1952) soil maps, USGS topographic maps, and aerial photographs (USDA, 1950; and USDA, 1957) show that prior to the construction of the California Aqueduct in 1965, the Arroyo Pasajero debouched floodwaters and alluvial sediment along a drainage pathway oriented to the northeast of the town of Huron. Alluvial sediment was deposited in a medial to distal alluvial fan environment over an irregular lobe-shaped area that covered approximately 15 square miles. The current depositional area is located on the north and northeast side of the town of Huron. Sediment deposited in this area was deposited in a combination of stream channel, mud flow, and floodwater deposits. The size of the depositional area was related to the magnitude and duration of flood events. During very high flood events (such as a 100-year flood), alluvial floodwaters drained to the northeast across distal alluvial fan environments to the Fresno Slough and the Kings River (a distance of

Reproduced with permission of the copyright owner. Further reproduction prohibited without permission.

approximately 17 miles) (USDA, SCS, 1952, p. 5; U.S. Department of Interior, Bureau of Reclamation, p. 19).

The historic patterns of Arroyo Pasajero alluvial fan deposition have been altered by regional farming and irrigation practices and by construction of the California Aqueduct, which has acted as a barrier to the natural (west to east) distribution of alluvial fan sediments to medial and distal alluvial fan environments. During flood events, floodwaters and sediment flowing in a northeasterly direction are directed by an east-west training dike into a settling basin constructed on the upslope (western) side of the California Aqueduct. The training dike is approximately one mile long. Since construction of the Aqueduct, approximately 15 million cubic yards of sediment has been deposited into this settling basin (California DWR, San Joaquin Division, Draft Report, June 1984). The settling basin covers approximately three square miles and is located approximately two miles east of the town of Huron. The terminus of the Arroyo Pasajero channel is located in the general vicinity of T20S, R17E, Sec. 34 (USGS, Huron 7.5 Minute Topographic Quadrangle) which is located approximately one mile northwest of the town of Huron, near the intersection of Lassen Avenue and Marmon Avenue. The braided alluvial deposits of this terminus cover approximately one square mile. A review of high altitude, color infrared photographs (NASA, 1979, Flight 70-076) shows that the present depositional area of the Arroyo Pasajero alluvial fan covers an estimated eight square miles. Previous reports have indicated that the present depositional area is approximately six square miles (U.S. Department of Interior, Bureau of Reclamation, 1984) with the locus of the depositional area over the past 50 years shifting towards the east approximately 2.5 miles (Munn, Busacca, and Trott, 1991, p. 46). This depositional area includes the terminus of the Arroyo Pasajero channel, the area between the terminus and the training dike, and the settling basin area adjacent to the Aqueduct. As sediment is deposited in this area, the ground

Reproduced with permission of the copyright owner. Further reproduction prohibited without permission.

elevation rises, and floodwaters are consequently expected to gradually shift in a southerly direction towards the town of Huron and the central portion of the settling basin (U.S. Department of Interior, Bureau of Reclamation, 1984, p. 22).

8.4.4 Alluvial Fan Soil Survey Results

A review of soil surveys of the Coalinga area (USDA, 1952; and USDA, SCS, 1987 unpublished data), supplemented by information from recent National High Altitude Photographs (NHAP, 1981), shows that soils developed on the outer and medial alluvial fan surface of the Arroyo Pasajero originated from sediments deposited in association with a system of migrating, intermittent, alluvial fan channels. The channels are generally broad, shallow, and braided and are associated with an assemblage of depositional environments including streambed deposits, overbank and levee deposits, and floodwater deposits.

The soils in the medial alluvial fan positions are classified by the USDA as Panoche loam and clay loam soils with slightly developed profiles. As reported by the USDA (1952, pp. 50-53), thin layers in the soil profiles are caused by stratification of coarse and finer alluvium during flood event deposition. As mapped by the USDA, the surface distribution of the coarser Panoche soils is associated with inactive, intermittent stream channels that migrated across the alluvial fan surface in response to normal fluvial/alluvial fan processes. Deposition of sediments in the alluvial fan area appear to have been rather evenly, laterally distributed throughout the fan's long-term, depositional history, as evidenced by the distinctly symmetrical expression of the fan on topographic maps.

Reproduced with permission of the copyright owner. Further reproduction prohibited without permission.

The USDA (1952, Eastern Map Sheet) soil survey of the Arroyo Pasajero alluvial fan illustrates three distinct, historical Arroyo Pasajero channel trends oriented to the north, the northeast, and the southeast. The Arroyo Pasajero channel is currently oriented to the northeast. The University of California College of Agriculture (Harradine, 1950, pp. 3-4) reported that in the 1940's, floodwaters from the Arroyo Pasajero were dissipated on the alluvial fan soils located west and south of Huron.

As described by Bull (1964) for other alluvial fans in western Fresno County, the Arroyo Pasajero channel is entrenched approximately 20 to 30 feet in the upper fan environment known as the fan head or apex. This "fanhead trench" merges with the medial alluvial fan surface on the northwest side of Huron. In this area (located west of the intersection of Marmon and Lassen Avenues - see the Huron and Guijarral Hills 7.5' Topographic Maps), the Arroyo Pasajero channel broadens into a braided distributary channel that is approximately 1,000 to 2,000 feet wide. Because of broadening of the channel, the Arroyo Pasajero loses its ability (or competency) to transport coarser grained sediments. Consequently, large volumes of coarser grained sediments are deposited in this general area; and floodwaters and finer grained, suspended sediments (i.e., fine silt and clay-sized particles), no longer confined by the narrow fanhead trench, are allowed to disperse across the medial alluvial fan surface.

8.5 Arroyo Pasajero Alluvial Fan Depositional Environments and Sedimentation Rates

As reported by Reading (1981, pp. 15-20), alluvial fans are cone-shaped sedimentary deposits that develop at the base of drainage areas that have an abundant supply of sediment. The amount of sediment is related to the relief of the drainage basin, the type of soils and vegetative covering associated with the sediment source areas, and

Reproduced with permission of the copyright owner. Further reproduction prohibited without permission.

climatic conditions. In the semi-arid Coalinga region (where annual rainfall ranges from 8 to 17 inches per year), the Arroyo Pasajero and other alluvial fans are forming as a result of rapid erosion from infrequent rainfall in the highland areas. In the highland areas, sediment washed into the intermittent stream channels by sheet, rill, and gully erosion is transported down-stream under turbulent flow conditions. When the flow reaches the apex of the alluvial fan, the main distributary channel generally broadens, the hydraulic gradient and the competency to transport sediment is greatly reduced, and sediment deposition occurs in the form of braided channel deposits, over-bank or levee deposits, and sheetflood deposits. The coarsest sediments (i.e., sand and silt) are deposited in the upper fan environments in channel facies and at the terminus of the distributary channel. The finest grained sediments (i.e., silt and clay) are deposited in the medial and distal fan environments associated with overbank and sheetflood facies.

Alluvial fan depositional processes are such that the fan tends to accumulate sediment in a manner that contributes to the balanced, long-term development of the fan's cone-shaped geometry. At any one time, only a relatively small area of the alluvial fan receives sediment. As these areas accumulate sediment, the distributary channels in the upper and medial fan environments tend to laterally migrate to depositional areas that are topographically lower. Channeled debris flow deposits of the upper fan environments grade downdip into sheetflood deposits, and as the distributary channels migrate across the fan surface, these types of deposits overlap and stack on top of each other. Alluvial sedimentation rates can thus be considered in terms of short- and long-term rates. Long-term rates are related to the geometrically balanced development of the alluvial fan over thousands of years. Short-term rates occur as a function of position on the fan in relation to areas of active sediment deposition.

Reproduced with permission of the copyright owner. Further reproduction prohibited without permission.

Recent studies of the Arroyo Pasajero alluvial fan (Atwater et al., 1986, p. 106; and Munn, Busacca, and Trott, 1981, p. 14), including a stratigraphic analysis of 10 continuously-cored soil borings collected for this study, show that the fan generally lacks any well-developed buried soil profiles and has widespread late Holocene deposits in the upper and medial alluvial fan environments in the vicinity of Huron. Radiocarbon dates of charcoal material recovered from several subsurface samples from the Arroyo Pasajero and Arroyo Hondo fans indicate a medial alluvial fan depositional rate of approximately one foot of thickness per 100 years (Atwater et al., 1986, Table 4; Munn, Busacca, and Trott, 1981, p. 14).

Angular charcoal debris recovered from Arroyo Pasajero alluvial fan sediment at a depth of 4.92 feet from a soil boring located near the intersection of Gale Avenue and the Southern Pacific Railroad crossing of the Arroyo Pasajero channel gave a C^{14} age of 490 years before present (plus or minus 60 years) (Atwater et al., 1986, Figure 3). A charcoal sample recovered from a depth of 10.5 feet from an area located near the apex of the Arroyo Hondo Fan (which is located approximately 17 miles northeast of the Arroyo Pasajero Fan) gave a C^{14} age of 1,040 years before present (plus or minus 200 years) (Munn, Busacca, and Trott, 1981, p. 14). Both of these fans have a similar geologic history, and the above data indicate that both fans have similar rates of deposition in the upper and medial alluvial fan environments (i.e., approximately 0.01 foot of thickness per year).

8.6 Cantua Creek, Salt Creek and Arroyo Hondo Alluvial Fans

The alluvial fans located adjacent to the Arroyo Pasajero include the Salt Creek, Cantua Creek and Arroyo Hondo fans. Cantua Creek drains an estimated 50 square miles. Salt Creek and Arroyo Hondo Creek drain an estimated 24 and 25 square

Reproduced with permission of the copyright owner. Further reproduction prohibited without permission.

miles, respectively. The Cantua Creek watershed includes an estimated 4.3 square miles of the New Idria Formation on the northeast flank of Joaquin Ridge. The Cantua Creek, Salt Creek, and Arroyo Hondo Creek also drain approximately 5 square miles of the Big Blue Member of the Temblor Formation (Miocene).

The New Idria Formation, the Big Blue Member, and other younger asbestos-containing sedimentary formations are sources of asbestos sediment for the Salt, Cantua Creek, and Arroyo Hondo alluvial fans. These alluvial fans collectively cover an estimated 128 square miles. As reported by Bull (1964) and the SCS (Draft Geology Report, 1988), the formation of these alluvial fans are the result of deposition of detrital material from erosion of the foothills and mountains of the Diablo Range, including the New Idria Formation and the Big Blue Member. The California Aqueduct transects the upper medial portions of the fans. During storm events, runoff from the Salt Creek, Cantua Creek, and Arroyo Hondo accumulates on the upslope side of the Aqueduct. A recent study (SCS, 1988, Draft Geology Report - Cantua Creek Sediment Study) has shown that an estimated 45 acre-feet per year of sediment from Salt Creek and Cantua Creek has been deposited adjacent to the Aqueduct. There has been no provision for ponding of sediment and floodwaters from these watersheds and alluvial fans. Consequently, sediment and runoff drain directly into the Aqueduct through ungrated inlet structures as indicated in Figure 1-1.

Sampling of the Cantua Creek and Salt Creek alluvial fans (California DWR, 1986) has shown that the alluvial soils have low concentrations of asbestos (i.e., generally less than one percent). The SCS (Draft Geology Report, 1988) reports that most of the sedimentary materials in the fans is the result of sheet and rill, streambank, and gully erosion in the upland areas and from furrow irrigation in cultivated areas of the upper alluvial fans.

Reproduced with permission of the copyright owner. Further reproduction prohibited without permission.

9.0 MINING AND MILLING OPERATIONS

The New Idria Formation has been prospected for mineral deposits (primarily cinnabar, chromite, chrysotile asbestos, magnesite, and benitoite - a gem mineral) since 1853. Mining in the area of San Benito County and Fresno County has generally occurred in three stages: mercury mining predominated from the 1800's through the early 1900's; chromite mining (spurred by the federal government's strategic mineral purchasing program) was active in the 1940's and 1950's; and asbestos mining occurred in the 1960's and 1970's. Many cinnabar, chromite, and asbestos mines were located throughout eastern San Benito and western Fresno Counties. This report discusses those operations related to the Cantua Creek and Los Gatos Creek drainage systems of western Fresno County. These mining and related operations have been conducted in the southeastern third of the New Idria Formation outcrop, as indicated on Figures 2-8A, and 2-8B.

9.1 Mercury Mining

Many early geologic reports (Eckel and Myers, 1946) characterize the area as the New Idria Quicksilver District. During the time period between 1858 and 1944, the district reportedly produced over 437,195 flasks of mercury which was produced from veins and stocks found in fractures in hydrothermally altered rocks near the faulted contact of the serpentinite minerals and the surrounding sedimentary country rock (Eckel and Myers, 1946, p. 83). The most productive deposits were found in hydrothermally altered beds of the Panoche Formation beneath the New Idria thrust fault and associated tear faults which offset the thrust. The New Idria thrust fault is mapped on the northern side of the formation at the contact of the serpentinite with rocks of the Franciscan and Panoche Formations. (Eckel and Myers, 1946, Plate 1).

Reproduced with permission of the copyright owner. Further reproduction prohibited without permission.

In the 1800's and early 1900's, mercury mining practices consisted of extensive open cuts and adits (Eckel and Myers, 1946, p. 105). In the southeastern portion of the New Idria Formation, significant mercury mines (Eckel and Myers, 1946, pp. 105-121) included the Archer Mine, the Del Mexico Mine, and the Rita Mine. As described by Eckel and Myers (1946), in the early 1940's the Archer Mine consisted of over 750 open cuts and the Del Mexico Mine consisted of over 800 open cuts. The Archer Mine is located in the White Creek drainage area, and the Del Mexico and Rita Mines are located in the Cantua Creek drainage area.

9.2 Benitoite and Magnesite Mines

The Gem Mine, discovered in the early 1900's, was explored for the gem mineral benitoite. Benitoite is the California state mineral and is known to occur only in the Gem Mine area. The Gem Mine is located approximately 1.5 miles northwest of the Atlas Site. Another early 1900's mining operation in the White Creek area was a magnesite mine (White Creek Magnesite Mine - T19S, R13E, Sec. 5) (EPA, Potential Sources Report, 1987). It is not known how much ore was extracted from either of these operations.

9.3 Chromite Mines and Mills

In the late 1940's and 1950's, the focus of mining in the area shifted to exploration for chromite ore which was designated a strategic mineral essential to the defense of the United States (Rice, 1957, p. 121). Chromite is the only ore mineral of chromium, and many primary deposits are associated with serpentine formations derived from ultrabasic igneous rocks rich in peridotite and dunite. In the New Idria Formation,

Reproduced with permission of the copyright owner. Further reproduction prohibited without permission.

chromite ore occurs as disseminated grains (average grain size is 5 millimeters) in the asbestos-containing serpentinite matrix and as massive pods, lumps, or chimneys.

Chromite mining operations in the White Creek and Pine Canyon drainage sub-basins in the 1950's (spurred by the federal government's strategic minerals purchasing program) were associated with at least six open-pit mines and as many as five gravity settling, ore concentrating milling operations. These chromite milling operations were located on the banks of White Creek at approximately one-to two-mile intervals downstream from the serpentinite outcrop area. The loose ore was screened to separate much of the flakey serpentinite matrix from the heavier disseminated chromite crystals. The screened material was further concentrated by using a water-based gravity settling operation to remove the disseminated chromite from the serpentinite matrix. A review of aerial photographs and an interview with a local miner (personal communication, Charlie Akers, 1988) indicates that much of the waste material from these chromite ore concentrating operations was probably dumped into the streambed ponding basins that provided the water for the wet-milling process. It has been estimated that approximately 43,000 tons of serpentinite debris may have been dumped into White Creek during the 1940's and 1950's. Seasonal runoff may have subsequently washed thousands of tons of waste ore downstream each year, and the entrained sediments may have been deposited on the Arroyo Pasajero alluvial fan. Aerial photographs and field surveys suggest that some of the waste serpentinite ore may remain as bed load material in the White Creek streambed.

In the Los Gatos watershed, six chromite mines were active. These were the James-Corbett-Byles Mine, the Railroad Mine, the Butler Estate Chromite Mine, the Big Ridge Mine, the Rhodes/Byles/Gribble Mine, and Tromby No.1 and 2. Ore from the

Reproduced with permission of the copyright owner. Further reproduction prohibited without permission.

Butler Estate Mine was transported to the Johns-Manville Coalinga Asbestos Mill where it was milled by Marmac Resources Company during the mid-1970's.

9.3.1 James-Corbett-Byles Mine

The James-Corbett-Byles Mine (T19S, R13E, Sec. 3, NE 1/4) began operation in 1910, and during the period of 1945 to 1955, this mine produced approximately 11 tons of lump ore and 530 tons of concentrates. The ore was mined from a large benched cut approximately 160 feet long and 80 feet deep (EPA, Potential Sources Report, 1987). The concentrated ore was probably processed at the James mill located about 10.5 miles west of the mine on the San Benito River (Matthews, 1961, p. 9). Very little other information is available about the James-Corbett-Byles mining operation.

9.3.2 Railroad Mine

The Railroad Mine (T19S, R13E, Sec. 1, NW 1/4) began operation in the early 1950's and reportedly was explored for chromite ore boulders. The Railroad Mine consisted of two open cuts that measured 105 by 50 feet and 120 by 70 feet. As reported by the EPA (Potential Sources Report, 1987), approximately 60 tons of chromite ore was shipped from the site.

9.3.3 Butler Estate Chromite Mine

The major chromite mine in the area was the Butler Estate (or "Mistake") Chromite Mine (T18S, R13E, Sec. 34, SW 1/4) which is located in the Pine Canyon sub-basin approximately 0.7 miles northwest of the Johns-Manville Coalinga Asbestos Mill Site.

Reproduced with permission of the copyright owner. Further reproduction prohibited without permission.

In the early 1950's, the Butler Estate Chromite Mine began large-scale open-pit exploration stripping operations for massive and disseminated chromite ore (Cr_2O_3). A deep pit was excavated (approximately 850 feet by 550 feet by 250 feet deep) and the asbestos-containing dumps and overburden (approximately 60% chrysotile: Matthews, 1961, p. 19) were deposited in an unstable pile located adjacent to the mine. A field inspection of the tailings pile on March 9, 1988 revealed that the pile is generally unstable, with an over-steepened slope face and large fissures and slumps forming on the upper surface. A large debris flow is forming at the base of the pile, and asbestos-containing sediments were observed throughout the streambed to the channel's juncture with the western fork of Pine Canyon Creek.

The Butler Estate Chromite Mine is located at the top of a ridge on the Pine Canyon side of the White Creek - Pine Canyon drainage divide. When mining activities were initiated in the 1950's, access to the mine was from the White Creek sub-basin. Disseminated chromite ore (average grain size approximately five millimeters) from the mine was processed at the Hollman and the Chambers and Russell gravity concentrating mills located along White Creek. Raw ore (containing a high percentage of asbestos) was stockpiled in large piles located adjacent to the gravity concentrating mills on the banks of White Creek. It is not known what was done with the spent ore, but considering what is known about mining practices in the area and the location of the mill sites, the material was probably dumped into the stream channel and eroded by seasonal runoff. During the period of 1952 to 1961, approximately 63,000 long tons of chromite ore was mined from the deposit (Matthews, 1961, pp. 8-17).

From approximately 1975 to 1977, Marmac Resource Company (Marmac) milled chromite ore at the Johns-Manville Coalinga Asbestos Mill site. Marmac transported asbestos-containing chromite ore from the Butler Mine to the Johns-Manville Coalinga

Reproduced with permission of the copyright owner. Further reproduction prohibited without permission.

Site, where the chromite-rich fractions were concentrated using a gravity concentrating mill. Chromite tailings generated by this process were discharged as a water slurry to a series of settling ponds located at the Johns-Manville Coalinga Site. All milling operations at the Johns-Manville Coalinga Site are believed to have ceased by approximately October 1977.

9.3.4 Big Ridge Mine

This chromite operation was located at the crest of a northwest-trending ridge that forms the northeast flank of Condon Peak (T18S, R12E, Sec. 36). Chromite ore was excavated from a line of pits located on the ridge crest. The mine began producing ore in 1917 but was most active in the years 1956 and 1957. Approximately 1,270 tons of chromite ore was produced in 1956 and 1957 (EPA, Potential Sources Report, 1987). Although not reported by the EPA, the ore was probably processed at a mill located on White Creek. This mine may have been the Jeanne Mine (operated by the Aurora Quicksilver Company), as reported by Walker and Griggs (1953, p. 79).

9.3.5 Rhodes/Byles/Gribble Mine

This chromite operation was located in far western Fresno County on the southwestern flank of Condon Peak (T18S, R12E, Sec. 35, S 1/2). This area is drained by the Los Gatos Creek system but is not located in the White Creek sub-basin. It is not known when this mine became active, how much ore was produced, or where the ore was processed (EPA, Potential Sources Report, 1987).

Reproduced with permission of the copyright owner. Further reproduction prohibited without permission.

9.3.6 Tromby No. 1 and No. 2

This chromite mining operation was located close to the Big Ridge mining operation described above (T18S, R12E, Sec. 36). Little more is known about this operation (EPA, Potential Sources Report, 1987).

9.4 Asbestos Mining

In the mid-1950's, an investigation by the California Division of Mines and Geology of the Butler Estate Chromite Mine (Matthews, 1961) provided evidence that the serpentinite matrix of the New Idria Formation being processed for disseminated chromite was actually chrysotile asbestos. Laboratory studies indicated the matted, flakey material to contain short-fiber chrysotile asbestos. Subsequent exploration of the southeastern third of the New Idria Formation by the Union Carbide Nuclear Company demonstrated that the asbestos ore could be profitably mined (by open-pit quarrying) and milled to produce a marketable short-fiber product of superior grade. It was recognized that the immense asbestos deposit would yield hundreds of millions of tons of ore that could be easily processed using dry-milling processes (Rice, 1963, p. 6; Munro and Reim, 1962).

The Union Carbide Nuclear Company began filing claims in 1959 and in the next three years the area experienced an intensive land rush for asbestos mining claims. Other significant asbestos-mining companies active in the area included: (1) the Johns-Manville Coalinga Asbestos Company, in which the Johns-Manville Corporation owned an 85 percent interest and the Kern County Land Company owned a 15 percent interest; (2) the Atlas Minerals Division of the Atlas Corporation; (3) the Hidden Splendor Mining Company; (4) Todd Industries; and (5) the Asbestos Corporation

Reproduced with permission of the copyright owner. Further reproduction prohibited without permission.

Ltd. The Table Mountain serpentinite deposit, located in the Parkfield District south of Coalinga, was explored by the Johns-Manville Sales Corporation (Rice, 1963, p. 6; Davis, 1963, p. 5).

The location of these mines and an inventory of related exploration pits are illustrated in Figures 2-8A and 2-8B. A review of the Santa Rita Peak 7.5 Minute Topographic Map and other sources (EPA, Potential Sources Report, 1987) shows the southeastern third of the New Idria Formation outcrop area has approximately 18 large-scale open-pit mines, 400 exploration pits, 3 asbestos and 3 chromite milling operations, and many miles of unpaved roads throughout the area. (Note: The USGS map does not show the location of all the chromite milling operations that may have been in the area.) In the Los Gatos Creek - Arroyo Pasajero watershed basin, which includes the Pine Canyon and White Creek sub-basins, there are approximately 12 open-pit mines, 203 exploration pits, and more than 50 miles of exploration access roads.

9.4.1 Union Carbide Operation

The Union Carbide Nuclear Company set up a mining operation in eastern San Benito County in 1960. This operation was located approximately 0.75 miles west of the San Benito - Fresno County border (T18S, R12E, Sec. 25) but probably also included a few mines located to the east in Fresno County. The main mine is in the San Benito River watershed. EPA research (EPA, Potential Sources Report, 1987) indicates that the Union Carbide Nuclear Company probably also operated mines located on the north side of Joaquin Ridge in Fresno County (T18S, R13E, Sections 28 and 29). This area is located in the Cantua Creek watershed. Ore from the Union Carbide Nuclear Company was processed at a milling facility located in King City in San Benito County. It is not known what tonnage capacity the milling facility was

Reproduced with permission of the copyright owner. Further reproduction prohibited without permission.

designed for; however, the mining operations were large-scale, with the lateral dimensions of the main pit measuring in excess of 2,000 by 3,000 feet (Merritt, 1962; Munro and Reim, 1962; Rice, 1963).

9.4.2 Johns-Manville Coalinga Asbestos Operation

9.4.2.1 Mines and Mill Facility

The Johns-Manville Coalinga Asbestos Company set up a milling operation in Pine Canyon in 1962 that processed ore from two mines - the Jensen Mine (T18S, R34E, Sec. 34) and the Christie Mine (T18S, R27E, Sec. 27). The mill plant and the Jensen Mine are located in the Pine Canyon drainage system of the Los Gatos Creek watershed; the Christie Mine is located in the Cantua Creek watershed. The Jensen Mine area measures approximately 1,000 by 1,000 feet, and the Christie Mine measures approximately 2,000 by 2,100 feet. The mill facility in Pine Canyon (T19S, R13E, Sec. 1) was designed to process approximately 15,000 tons per year. The tailings pile in the eastern fork of Pine Canyon Creek measures approximately 500 by 1,200 feet, and is confined by the steep walls of Pine Canyon. The downstream transport of tailings from the pile is restricted by the presence of a retaining dam located near the base of the pile (Merritt, 1962; Munro and Reim, 1962; Rice, 1963; EPA, 1987).

9.4.2.2 Mining and Milling Practices

As reported by Munro and Reim (1962, pp. 48-49), the soft nature of the serpentinite ore permitted simple mining and milling operations. A bulldozer was used to excavate surface materials and weathered ore (to a depth of approximately 20 to 30 feet) to

Reproduced with permission of the copyright owner. Further reproduction prohibited without permission.

form benched surfaces cut into the hillsides. The benched surfaces were flat and accessible to dump trucks. A front-end loader would mine ore from the face of the bench cut and directly load the ore into a waiting truck. The ore was then trucked to a wet-rock storage area and spread out for partial sun-drying. After partial sun-drying, the ore was passed through a trommel screen to remove solid particles, and then conveyed to a rotary dryer. Milling of the dry ore was accomplished through the combined use of hammers, grinders and screeners, and the fibrous product was collected by an air separator and packaged in 100-pound bags.

Atlas Site milling and mining operations were reportedly initiated in the mid-1960s and ceased in the late 1970s. Open pit mines were operated at the site and ore generated at these locations was milled in a central on-site mill. Mill tailings reportedly were deposited into a single pile. Because of the Atlas Site's relatively high elevation and the absence of topographical features which would provide protection against wind erosion, mill tailings have been distributed by wind at the Atlas Site across an area which covers more than 100 acres. Distinguishing the Atlas Site's tailings and mining materials from the natural serpentinite is difficult because of the generally similar morphology of the natural and anthropic materials. The approximate total drainage area affecting the Atlas Site is estimated to exceed 250 acres, and obvious erosional features such as rills and gullies are readily observable throughout the site.

The Johns-Manville Coalinga Site's tailings cover approximately ten acres. A sediment trapping dam at the base of the tailings pile appears to significantly diminish the off-site transport of tailings which might otherwise be eroded from the tailings pile. Wind erosion appears to be less of a concern at the Johns-Manville Coalinga Site because it is located at more protected lower elevation with generally lower wind speeds. The Johns-Manville Coalinga Site operations reportedly began in the early 1960s and

Reproduced with permission of the copyright owner. Further reproduction prohibited without permission.

ceased in the mid-1970s. Most of the tailings found at the site were dumped in a steeply sloped portion of the eastern fork of the intermittent Pine Canyon Creek.

9.4.3 Atlas Corporation Operation

In 1963, the Atlas Corporation set up a similar milling operation in the White Creek area to process ore from several mines located near the mill facility (mill site - T18S, R13E, Sec. 32; mines - T18S, R13E, Sec. 31). The Atlas facility was designed to produce 15,000 tons of asbestos fiber per year and had the capacity to expand to 25,000 tons (Merritt, 1962; Munro and Reim, 1962; Rice, 1963; EPA, 1987). The associated mine and mill facilities were significantly larger than the Pine Canyon facility. As reported by the EPA (Potential Sources Report, 1987), two of the Atlas mines have surface dimensions that measure 800 by 1,000 feet and 1,000 by 1,600 feet, respectively. The dimensions of a third mine were not reported. The tailings pile complex measures approximately 1,500 by 4,300 feet. The tailings pile is uncontained on three sides and is located in an open area near the crest of Joaquin Ridge. Because of its open location, the tailings pile is unprotected from the strong winds that sweep over Joaquin Ridge; and the large surface area is subject to sheet, rill and gully erosion.

9.4.4 Hidden Splendor Operation

The Hidden Splendor Mining Company originally owned and operated many of the leases that were procured by the Atlas Corporation. Not much more is known about the Hidden Splendor operations. The only reference to its operation is contained in a 1962 report on asbestos mining in California (Merritt, 1962, p. 59). There is no

Reproduced with permission of the copyright owner. Further reproduction prohibited without permission.

reference to the Hidden Splendor operation in the EPA Potential Sources Report (1987).

9.4.5 Todd Industries Operation

Another asbestos mine, operated by Todd Industries, was located just east of the San Benito - Fresno County border (T18S, R12E, Sec. 25). The mine is located approximately 0.5 miles northwest of the Atlas site. In 1961, asbestos ore was mined from a 40-acre tract and was transported 33 miles by truck to a milling facility located in Coalinga. The Todd Industries mill facility was designed to produce approximately 3,000 tons of asbestos fiber per year and reportedly was the first plant to produce asbestos fiber in the Coalinga area (Merritt, 1962, p. 60).

9.4.6 Basic Industries Operation

A pilot mining operation located on the San Benito/Fresno County border was set up by Basic Resources Company in 1959 (T18S, R13E, Sec. 30). As reported by the EPA (Potential Sources Report, 1987), initial screening of the asbestos ore was conducted at the mining site and then the ore was trucked to a pilot mill site in Coalinga. There is no more reported information for this operation.

9.4.7 Other Asbestos Mining Operations

A few companies explored the asbestos potential of two additional serpentinite deposits, including the detrital serpentinite debris of the Big Blue Member of the Temblor Formation and the extrusive Table Mountain serpentinite deposit.

Reproduced with permission of the copyright owner. Further reproduction prohibited without permission.

Beginning in 1962, the Asbestos Corporation Ltd. explored the serpentinite deposits of the Big Blue Hills located north of Coalinga. As reported by Davis (1963, p. 5), the Asbestos Corporation was planning to develop a short fiber chrysotile deposit located near the mouth of Cantua Creek. This site is located approximately 20 miles north of Coalinga. As reported by the California Division of Mines and Geology (Rice, 1963, p. 6), this sedimentary deposit of serpentinite debris apparently "flowed" into the inland sea that occupied the San Joaquin Valley area during Miocene time. The deposit reportedly had a maximum thickness of 1,000 feet and was predominantly composed of flakey, chrysotile-rich serpentinite debris. It is not known to what extent this deposit was developed.

In 1962, the Johns-Manville Sales Corporation explored the Table Mountain serpentinite body as a potential source for chrysotile ore (Rice, 1963, p. 6). This extrusive serpentinite body is located approximately 15 miles south of Coalinga in the Parkfield District. It is not known if this deposit was ever commercially exploited.

9.4.8 Asbestos Exploration Practices

A large portion of the southeastern area of the New Idria Formation outcrop was heavily explored by the above companies for the highest grade asbestos deposits. The exploration programs consisted of geologic mapping, trenching and sampling, drilling, magnetic surveys, and the stripping of areas proposed for mining (Munro and Reim, 1962, pp. 47-48). A review of the Santa Rita Peak 7.5 Minute Topographic Quadrangle Map and a review of aerial photographs of the Joaquin Ridge area provide dramatic evidence of how extensively the area has been explored and mined.

Reproduced with permission of the copyright owner. Further reproduction prohibited without permission.

In addition to the previously described mining operations, several hundred exploration pits are evident on the Santa Rita Peak topographic map. Most of these exploration pits were cut by bulldozers and other earth-moving machinery. An inventory of these exploration pits shows that approximately 45 pits are located in the Pine Canyon watershed and approximately 158 pits are located in the White Creek watershed. The area also contains more than 50 miles of exploration access roads. The total area of the above exploration pits and access roads is estimated to be approximately 166 acres, or 4 percent of the New Idria formation area which is drained by these watersheds. See mine and exploration pit locations illustrated in Figures 2-8A and 2-8B.

As indicated by USGS topographic maps of the Joaquin Ridge area, the Cantua Creek and San Benito River watersheds have also been extensively explored. Other areas in the region that have been similarly explored include the sedimentary Big Blue Member of the Temblor Formation (Miocene) and the extrusive Table Mountain serpentinite deposit located south of Coalinga in the Parkfield District (Rice, 1963, p. 6).

Reproduced with permission of the copyright owner. Further reproduction prohibited without permission.

10.0 SOILS

10.1 Arroyo Pasajero Soils Overview

Soil development in the Arroyo Pasajero watershed has been influenced by a variety of factors including geology and mineralogy of the parent material, slope and geomorphic position, and slope stability (Munn, Busacca, and Trott, 1981, p. 11). Sedimentary soils have developed on sedimentary rocks and alluvial deposits. Serpentine or serpentinite soils are those that have developed on the surfaces of ultramafic serpentinite rock outcrops. The Arroyo Pasajero watershed includes approximately 513 square miles, and in this area sedimentary soils account for approximately 98% of the watershed's soils and serpentinite soils account for approximately 2% of the watershed's soils. Most of the non-serpentinitic soils in the Arroyo Pasajero watershed have formed on Cretaceous-aged and younger sedimentary rocks of predominantly marine origin. The Cretaceous and Paleogene (i.e., Paleocene, Eocene, and Oligocene) rocks consist of marine sandstones and shales that are not known to contain asbestos. Rocks that are Miocene in age and younger, including Pliocene, Pleistocene, and Holocene, may contain varying amounts of asbestos depending on their sedimentary relationship with asbestos-bearing geologic formations such as the New Idria Formation and the Big Blue Member of the Temblor Formation (Miocene).

In the Coalinga region, the occurrence of regional uplift and faulting and folding resulting from crustal compression in the Coast Range geomorphic province (in conjunction with worldwide changes in sea level) contributed to a gradual transition from a marine environment to a non-marine environment in the area now occupied by the central San Joaquin Valley. The post-Cretaceous formations include non-marine sedimentary sequences that are softer and less consolidated than the underlying

Reproduced with permission of the copyright owner. Further reproduction prohibited without permission.

Cretaceous-aged marine sandstones and shales. The soils associated with the post-Cretaceous aged formations are generally more susceptible to erosion than the soils associated with the Cretaceous-aged formations. The post-Cretaceous formations generally occur in the lower and middle elevation areas of the watershed, while the Cretaceous-aged formations occur in the higher upland areas. The upland watershed areas also include large areas of rock outcrop that are barren of any soil.

The upland watershed of the Los Gatos Creek drainage basin in the northwest quadrant of the Arroyo Pasajero watershed includes the serpentinite outcrop area of the New Idria Formation. This ultramafic outcrop area covers approximately 6.8 square miles, with approximately 5.8 square miles occurring in the White Creek drainage area and 1.0 square mile occurring in the Pine Canyon drainage area.

10.2 Serpentinite Soils

10.2.1 Historical Background

The ultramafic serpentinite deposits of the New Idria Formation have contributed to the development of serpentinite soils which have physical and chemical properties that support little plant growth. Geologists and botanists who observed the serpentinite outcrop areas of the New Idria Formation in the late 1800's and early 1900's were quick to describe the area as being the serpentine barrens -"vast wasteland areas of almost barren summits associated with sparse, restricted vegetation with dry gray soils furrowed by ancient streams into innumerable canyons - a scene of unmixed desolation - the most spectacular serpentine barren in the West" (Kruckeberg, 1984). These early geologists mapped the extent of the serpentinite outcrop area and studied the mineralogical and chemical characteristics of the metamorphic serpentinite deposits in

Reproduced with permission of the copyright owner. Further reproduction prohibited without permission.

their search for economic minerals. Early soil scientists and botanists focused on the unique physical and chemical characteristics of the azonal soils that developed on the weathered slopes of the serpentinite outcrop. Soil scientists recognized that the serpentinite soils were generally skeletal (poorly developed) soils which strongly reflected the elemental composition of the parent material which included chrysotile asbestos, lizardite, antigorite, chromite, and magnesite in conjunction with iron, magnesium, silica and other elements such as nickel, chromium, and magnesium.

Botanists focused on the occurrence of the sparse, restricted vegetation associated with the New Idria serpentinite in conjunction with the availability of the serpentinite soils to colonization by plant life for the past 10 to 15 million years. Botanists reported that the stressful and highly selective nature of the serpentinite soils was a direct result of the soil chemistry which included high levels of exchangeable magnesium, low levels of exchangeable calcium, and high levels of heavy metals including chromium and nickel. Other stressful factors have been reported to include high temperature effects, moisture stress, and stress related to the residual soils derived from serpentinite outcrops on steeply sloping surfaces. For additional information, the reader is referred to Kruckeberg's (1984) book on the vegetation and soils of California's serpentines.

10.2.2 Serpentinite Soil Mapping

The Soil Conservation Service (SCS) of the USDA is currently mapping soils in the Arroyo Pasajero - Coalinga area, and a new soil survey is scheduled to be published in the 1990's (Kerry Arroues, SCS, personal communication, 1987). Although none of the new information has been published to date, the SCS has provided this investigation with preliminary soil descriptions for parts of the New Idria serpentinite

Reproduced with permission of the copyright owner. Further reproduction prohibited without permission.

outcrop area. Based on the field and laboratory observation of unique physical and mineralogical characteristics, the SCS has proposed a new soil series classification for the serpentinite soils of the Joaquin Ridge area in western Fresno County. This classification has been designated as Atravesada, which gets its name from the Loma Atravesada hills on the northeastern flank of Joaquin Ridge.

The SCS has described its preliminary soil mapping effort as third-order mapping. This means that the field mapping activities were limited by the amount of effort that could be expended for the mapping of defined areas. Consequently, the preliminary soil maps are based on the interpretation of aerial photographs with the interpretive mapping being supported by limited field data. The third-order mapping guidelines also limit to two the number of modifiers that can be used to describe a particular type of soil (personal communication, Paul Nazar, SCS, Los Banos Office, 1988). As indicated in the following discussion, this is important for SCS soil type #769 - Atravesada Pits and Dumps which can also be characterized as Atravesada Pits, Dumps, and Gullies. For the purposes of modeling of erosion of asbestos-containing soil types, this investigation has provided a separate map designation for the soils associated with naturally occurring gully complexes, as indicated by a review of aerial photographs that predate asbestos mining activities. This soil type is described below as AGC Atravesada Gully Complex. These are the soils associated with the deeply furrowed, barren, canyon-like areas described by geologists and botanists in the late 1800's and early 1900's.

The third-order type of mapping provides for a good approximation of existing soil types which, as suggested by the SCS, can be improved by more detailed mapping as required for more specific purposes, such as modeling of erosion in a defined area. The results of SCS soil mapping of the New Idria Formation outcrop area in the White

Reproduced with permission of the copyright owner. Further reproduction prohibited without permission.

Creek and Pine Canyon drainage areas are presented in Figures 2-13 and 2-14. The SCS soil mapping data of the White Creek and Pine Canyon areas has been reduced to match the scale of the 1 to 24,000 scale USGS topographic map of the area (USGS, Santa Rita Peak 7.5 Minute Topographic Quadrangle, 1984).

10.2.3 Pine Canyon Area Soils

The SCS has mapped three general soil types in the vicinity of the Johns-Manville Coalinga Asbestos Mill Site in Upper Pine Canyon: Atravesada (SCS #767); Atravesada Pits and Dumps (SCS #769); and Xerorthents with a Lilten association (SCS #742). In addition, based on geomorphic and geologic investigations of the Johns-Manville Coalinga Mill Site, the Johns-Manville Coalinga Mill Site area is underlain by another soil type not recognized or mapped by the SCS. This soil type has been designated by this investigation as Landslide Surface Soils (LSS). Surface sampling and excavation pits have shown that the Landslide Surface Soils have unique characteristics that are significantly different from the Atravesada soil type defined by the SCS and consequently should be mapped as a separate soil type. The characteristics of these four soil types in the vicinity of the Mill Site are discussed below, and their surface distributions are illustrated in Figures 2-13 and 2-14.

The Atravesada soils have developed from weathered and eroded material derived from serpentinite minerals including serpentinite landslide and/or debris flow deposits. The asbestos content of the Atravesada soils ranges up to 96%, as reported by the SCS. The Atravesada Pits and Dumps type of soil at the Mill Site is associated with the waste ore, ore storage, and general operations areas, the tailings pile, and the Railroad Mine. The Xerorthents - Lilten soils (SCS #742) are soils that have developed on the steep to very steep hillside slopes underlain by the thinly interbedded,

Reproduced with permission of the copyright owner. Further reproduction prohibited without permission.

upturned sandstones and shales of the Panoche Formation (Cretaceous) which form the steep side walls of the canyon in the vicinity of the Johns-Manville Coalinga Site. The Landslide Surface Soils are clay-rich soils with argillic horizons that have developed on the upper surfaces of some of the landslide and debris flow deposits in the Johns-Manville Coalinga Site area. These soils appear organic-rich, support an abundant grassy covering, and have very low asbestos concentrations - generally less than 1%.

Atravesada (SCS #767)

The Atravesada classification includes the skeletal, poorly developed soils of the serpentinite outcrop areas and the skeletal soils of the serpentinite landslide and debris flow deposits that occur throughout the outcrop region. The Atravesada soils have poorly developed profiles and high concentrations of chrysotile asbestos. According to SCS descriptions, the Atravesada soil is composed of sandy loam with an asbestos content that can range up to 96%. Gravel content ranges up to 15%. Field observations indicate that the textural classification is a sandy loam. Laboratory data show that clay and silt size fractions are much less than suggested by field observations and the sand size fraction ranges up to 90% or more, as indicated by particle size analyses for Atravesada serpentinite soil samples. This may be related to the occurrence of platey aggregates of chrysotile asbestos which tend to slide past one another when rolled and/or compressed (indicating a moderate to high plasticity).

Atravesada soils are generally a light yellowish gray to a reddish brown. The Atravesada soil type has a blocky soil structure with a variable organic matter content that ranges from less than 1% to more than 5%. The SCS reports that the soil permeability is moderately rapid, and water erosion potential is moderate to high.

Reproduced with permission of the copyright owner. Further reproduction prohibited without permission.

Field observations show that the Atravesada soil type has a rapid permeability with low runoff. Vegetation is generally sparse and is restricted to those plants tolerant of soils enriched in magnesium. These plants include manzanita bushes, coffee berry bushes, and some digger pine and Coulter pine trees. The Atravesada soil generally does not support a grassy covering.

Atravesada Pits and Dumps (SCS #769)

The asbestos ore and tailings at the Johns-Manville Coalinga Asbestos Mill Site are classified as Atravesada Pits and Dumps (SCS #769). This classification also includes the Railroad Mine area which was bulldozed during prospecting for massive chromite boulders in the 1950's. The soils included in the Pits and Dumps classification are very heterogeneous and characterized by great variations within short distances. Typically, the dumps are composed of serpentinite material masses with Atravesada loam inclusions. The Dumps and Pits materials are generally a grayish white with bright reflectance characteristics. According to SCS definitions for this soil class, permeability is moderate and runoff is variable with a moderate to high water-erosion potential. Field observations show that the permeability for this soils class is rapid, and available water capacity is very high. The Atravesada Pits and Dumps soil type has a blocky soil structure with an organic matter content that is generally less than 1%. Generally, the pits and dumps soil type lacks vegetation. As with the Atravesada soil type, laboratory data show that clay and silt size fractions are much less than that indicated by field observations.

Reproduced with permission of the copyright owner. Further reproduction prohibited without permission.

Xerorthents - Lilten Association (SCS #742 and #770)

The soils developed on the hillside slopes of the Pine Canyon drainage are classified as Xerorthents (SCS # 742) with a Lilten (SCS # 770) association. Both of these soil types are well-drained and formed in weathered material dominantly derived from clay shales and sandstones of the Panoche Formation. Xerorthents are on scarps, and Lilten soils are on the hillside slopes.

Xerorthent soils are shallow to deep, well drained, and can vary widely in texture and color. The soil is derived from sandstone and shale and is composed of clay loam, gravelly clay loam, sandy and silty loam, and clay. Permeability is very low to very high. The Lilten soil is deep and well-drained and calcareous throughout. Lilten soil permeability is low; available water capacity is moderate to high, and surface runoff is rapid to very rapid. The Lilten soil has a high shrink-swell potential and limited load supporting capacity. These soil types may have a clay content that ranges up to 40% or more and generally have a coarse platey structure with an organic matter content that is generally less than 1%. These soils generally support a moderate plant community of trees, shrubs, and grasses.

Landslide Surface Soils (LSS)

The Johns-Manville Coalinga Asbestos Mill area is underlain by soils that have developed on the surfaces of landslide and/or debris flow deposits that underlie the area. These landslide deposits have developed soils with deep, clay-rich (70 to 80% or greater) argillic horizons that commonly have accumulations of calcium carbonate in horizons beneath the argillic horizons. The soils are a dark brown color when wet and are generally classified as silty clays with less than 10% gravel. The LSS soil type has

Reproduced with permission of the copyright owner. Further reproduction prohibited without permission.

a blocky soil structure and an organic matter content ranging up to 3%. The landslide surface soils support a thick grassy covering that covers approximately 90% of the surface with roots that extend approximately three inches below the surface. These soils formed in deeply weathered material derived from landslide and/or debris flow deposits. Excavation pits in these soils show that the clay-rich argillic horizons generally extend to depths greater than 8 to 10 feet. There is little or no evidence of asbestos in these soils. Laboratory analyses show that these soils have an asbestos concentration that is generally less than 1%. The low asbestos concentration of the LSS soils is probably related to several factors including: (1) the accumulation of organic matter and other soil materials over many thousands of years; (2) deep weathering of the landslide surfaces; and (3) the occurrence of non-asbestos containing materials that were pushed downslope in front and on top of the serpentinite debris flow deposits. Some of the LSS deposits may have Atravesada inclusions.

10.2.4 White Creek Area Soils

In preliminary mapping of soils in the White Creek drainage area of the New Idria Formation, the SCS has identified seven soil types, while this investigation has identified an additional soil type that is described in this section. The SCS soil types include Atravesada (SCS #767), Atravesada Pits and Mine Complex (SCS #765), Atravesada Pits and Dumps (SCS #769), Hentine - Franciscan Rock Complex (SCS #774), Xerorthents (SCS #742), Lilten (SCS #770), and Xerofluvents (SCS #741). Based on field investigations, some areas mapped as Atravesada Dumps (SCS #769) are areas associated with naturally occurring gully erosion that existed prior to mining operations and consequently should be appropriately designated. In this report, these areas are designated as Atravesada Gully Complex (AGC). The mapping of these soil

Reproduced with permission of the copyright owner. Further reproduction prohibited without permission.

types is illustrated on Figure 2-14. A review of aerial photographs from 1950 and 1928 shows that some of the SCS #769 units were existing AGC units prior to the initiation of asbestos mining activities and consequently some of the SCS #769 units are also designated "(AGC)" in Figure 2-14.

Atravesada (SCS #767)

The Atravesada soils are serpentinitic soils with a high asbestos content and other characteristics as described for the Atravesada soil type of Pine Canyon.

Atravesada Pits and Mine Complex (SCS #765)

As reported by the SCS, this unit is 50% Atravesada loam and 50% Pits - Mine Complex. The components are so intermingled that the SCS was not able to map them separately at the scale used. This soil type occurs on slopes that range up to 15 degrees and is related to the occurrence of mining operations. This unit includes exploration pits and other general areas affected by anthropic activities. Field observations indicate that the textural classification is sandy loam. As with other Atravesada soil types, laboratory data show that clay and silt size fractions are much less than that suggested by field observations. This may be related to the occurrence of platey aggregates of chrysotile asbestos which tend to slide past one another when rolled and/or compressed (indicating a moderate to high plasticity). Color is a grayish white with bright reflectance characteristics. Permeability is rapid, soil structure is very blocky, and organic matter content is generally less than 0.5%. These soils generally lack vegetation. The chrysotile asbestos content is high as for the Atravesada soil type (SCS #767; asbestos concentration up to 96%).

Reproduced with permission of the copyright owner. Further reproduction prohibited without permission.

Atravesada Pits and Dumps (SCS #769)

The pits, dumps and tailings associated with mining operations in the White Creek area have similar characteristics previously described for the Pine Canyon area.

Xerorthent - Lilten Association (SCS #742 and SCS #770)

The soils developed on the hillside slopes of the drainage area adjacent to the New Idria Formation are composed of Xerorthents (SCS #742) with a Lilten (SCS #770) association, with characteristics as described previously for the Pine Canyon area.

Hentine - Franciscan Rock Outcrop Complex (SCS #774)

Hentine soils are associated with Franciscan rock outcrops of serpentine and serpentinite, and are generally shallow and well drained. The Hentine soil formed in weathered material dominantly derived from hard fractured serpentine rock and included areas of serpentinite. Permeability is moderately slow. Runoff is rapid to very rapid, and the water erosion potential is very high. Surface layer is generally a thin (less than two inches) gravelly clay loam that is brown in color. Gravel content may increase with depth. The Hentine soil type has inclusions of Atravesada soil types with variable chrysotile asbestos contents. Geologically, this area has been mapped as a Tertiary syenite intrusion (Fowkes, 1982, p. 158) that is approximately a quarter mile in diameter. The syenite deposit has inclusions of serpentinite and other minerals. Color infrared images and reconnaissance aerial photographs of the area indicate that the serpentinite inclusions account for approximately 20 percent to 30 percent of the Hentine surface area.

Reproduced with permission of the copyright owner. Further reproduction prohibited without permission.

Xerofluvents (SCS #741)

The Xerofluvents (SCS #741) are sediments deposited in the intermittent drainage pathway of White Creek at the base of the New Idria Formation outcrop area. These channeled deposits are generally gravelly sands and sandy gravels that contain an abundant amount of detrital serpentinite debris with asbestos contents that range up to 80%. Color is generally a dark yellowish gray when wet and light yellowish when dry.

Atravesada Gully Complex (AGC)

These are Atravesada-type serpentinitic soils that are associated with the surfaces of areas affected by naturally occurring gully erosion, as indicated by a review of aerial photographs that predate the occurrence of asbestos mining operations. Because of this natural occurrence, these soil types qualify for a classification that differs from the Atravesada soil types as defined by the SCS, including Atravesada (SCS #767), Atravesada Pits and Mine Complex (SCS #765), and Atravesada Pits and Dumps (SCS #769). The Atravesada Gully Complex (AGC) soils are variable in their physical characteristics because of their association with gully erosion and mass wasting. These soils are generally light colored with a high asbestos content as with Atravesada #767 (up to 96% chrysotile asbestos). Texture may be variable, ranging from a sandy loam to a coarse sand. This soil type has a blocky soil structure with an organic matter content that is generally less than 1%. The areas affected by gully erosion occur on slopes that range up to 65 degrees and are generally barren of vegetation.

Reproduced with permission of the copyright owner. Further reproduction prohibited without permission.

11.0 CONCLUSIONS

Major conclusions of this review of the regional geologic and environmental setting are as follows:

The occurrence and distribution of asbestos throughout the Coalinga area is primarily related to the natural erosion of the New Idria Formation, Table Mountain, and more than 50 other unnamed ultramafic serpentinite deposits which collectively cover approximately 80 square miles. These deposits consist of a soft, flakey matrix of short-fiber chrysotile asbestos. Most of these deposits are located near the tops of ridges or mountains, in areas which are naturally subject to mass wasting (i.e., landslides and debris flows), surface water erosion, and wind erosion.

Serpentinitic sediments eroded over the past 16 million years have become incorporated within sedimentary deposits and alluvial fans in the western San Joaquin Valley covering more than an estimated 1500 square miles. Because of this, these geologic features also contain asbestos which is subject to wind erosion, surface water erosion, and disturbance by vehicles and other machinery. Over geologic time, erosion of regionally widespread serpentinite outcrops has resulted in erosional processes delivering asbestos-bearing sediments to the Arroyo Pasajero alluvial fan. Consequently, because of these relatively large natural asbestos-containing areas (compared to anthropically disturbed areas) and the long time period of natural erosion, the contribution of asbestos to the Arroyo Pasajero alluvial fan sediments resulting from anthropic mining and milling activities (covering approximately 1.1 square miles in the Los Gatos Creek drainage) would not be expected to have significantly increased asbestos concentrations in post-mining alluvial sediments when compared to the pre-mining alluvial asbestos concentrations.

Reproduced with permission of the copyright owner. Further reproduction prohibited without permission.

Open-pit mining, milling, and related activities (e.g., mineral exploration pits and road construction) conducted in the New Idria Formation may have increased the erosion of asbestos-containing sediments from this geologic source area. However, given the limited areas which have been anthropically affected (16%, in comparison to the total naturally exposed outcrop areas), the fact that natural asbestos-containing areas have always naturally eroded asbestos to the environment, and the fact that the naturally exposed asbestos deposits, as well as disturbed areas, are prone to erosion and mass wasting, the above anthropic activities are expected to have caused a relatively minor increase in total erosion from asbestos source areas.

The Arroyo Pasajero watershed basin includes two sub-basins that drain approximately 6.8 square miles of the New Idria Formation which is exposed over an elliptically-shaped, 48-square-mile area that forms the crest of the Joaquin Ridge highland trend. The White Creek sub-basin drains approximately 5.8 square miles of the New Idria Formation, and the Pine Canyon sub-basin drains approximately 1.0 square mile. The White Creek sub-basin includes the Atlas Asbestos Mine and Mill and as many as six additional open-pit mining operations and three milling operations. The Pine Canyon sub-basin includes the Johns-Manville Coalinga Asbestos Mill and three open-pit mining operations.

In the 1960's, the California Aqueduct was constructed across the medial portions of the Arroyo Pasajero and Cantua Creek alluvial fans. The construction of the Aqueduct has acted as a barrier to the natural dispersion of floodwaters and sediments across the medial and distal portions of these alluvial fans. During normal storm events, sediment and stream flow from the Arroyo Pasajero watershed are now retained by a settling basin constructed adjacent to and upslope of the California

Reproduced with permission of the copyright owner. Further reproduction prohibited without permission.

Aqueduct. However, because of higher than originally projected sedimentation rates, the settling basin is being filled more quickly than expected and its ponding capacity is reduced. During periods of high runoff, asbestos-containing floodwaters and sediments from the settling basin previously were allowed to discharge into the Aqueduct; however, current operational procedures for the aqueduct facilities limit such discharges only to situations involving runoff from very large storms (greater than 50 year return period).

Sediment and stream flow water from the Cantua Creek watershed contain relatively high concentrations of asbestos because of erosion from the New Idria Formation outcrop area and from the asbestos-containing Big Blue Member of the Temblor Formation. During storm events, asbestos-bearing sediment and water are allowed, by engineering design, to directly enter the Aqueduct. There has been no design provision for ponding basins or a by-pass at the intersection of the Aqueduct and the Cantua Creek Fan or other asbestos-containing fan drainage systems.

Analytical data from the analysis of Aqueduct water and sediment samples (as sampled and reported by the California Department of Water Resources) indicates that some areas of the Aqueduct located upstream from the Arroyo Pasajero section have higher concentrations of chrysotile asbestos with some samples ranging as high as 25,500 million fibers per liter (MFL). This further indicates the occurrence of upstream sources of asbestos to the California Aqueduct.

Reproduced with permission of the copyright owner. Further reproduction prohibited without permission.

12.0 REFERENCES

Alfors, John T. 1983. Regional Geology of the Coalinga, California Area: California Division of Mines and Geology, Special Publication No. 66: 105-112.

Anderson, R., and Pack, R. 1915. Geology and Oil Resources of the West Border of the San Joaquin Valley North of Coalinga, California: U.S. Geological Survey, Bulletin 603, Washington D.C., 187 pp.

Arnold, R., and Anderson, R. 1910. Geology and Oil Resources of the Coalinga District, California: U.S. Geological Survey, Bulletin 398, Washington D.C., 354 pp.

Arnold, R., and Anderson, R. 1908. Preliminary Report on the Coalinga Oil District, Fresno and Kings Counties, California: U.S. Geological Survey, Bulletin 357, Washington D.C., 142 pp.

Atwater, Brian F.; Adam, D. P.; Bradbury, J. P.; Forester, R. M.; Mark, R. K.; Lettis, W. R.; Fisher, G. R.; Gobalet, K. W.; and Robinson, S. W. 1986. A Fan Dam for Tulare Lake, California and Implications for the Wisconsin Glacial History of the Sierra Nevada: Geological Society of America Bulletin, vol. 97: p. 97-109.

Barbat, W. F. 1971. Megatectonics of the Coast Ranges, California: Geological Society of America Bulletin, vol. 82: p. 1,541-1,562.

Bartow, Alan J. 1987. The Cenozoic Evolution of the San Joaquin Valley, California: U.S. Geological Survey, Open-File Report 87-581, 74 pp.

Reproduced with permission of the copyright owner. Further reproduction prohibited without permission.

Bishop, Charles C., and Chapman, Rodger H. 1967. Bouguer Gravity Map of California, Santa Cruz Sheet: California Division of Mines and Geology, San Francisco.

Boyle Engineering, Corporation. 1988. Draft Summary Letter Report for Hydrologic Analysis: Arroyo Pasajero Drainage and Sediment Control Plan.

Bramlette, M. N. 1934. Heavy Mineral Studies on Correlation of Sands at Kettleman Hills, California: American Association of Petroleum Geologists Bulletin, vol. 18: p. 1,564 - 1,572.

Brown, Robert D. 1984. Chapter Three - Tectonic Setting: in Coalinga, California, Earthquake of May 2, 1983, Reconnaissance Report: Earthquake Engineering Research Institute, Berkeley, California, pp. 51-53.

Bull, W. B. 1964. Geomorphology of Segmented Alluvial Fans in Western Fresno County, California: U.S. Geological Survey, Professional Paper 352-E.

Burford, R. O. 1965. Strain Analysis Across the San Andreas Fault and Coast Ranges of California: Proceedings of 2nd International Symposium on Recent Crustal Movements, Aulanko, Finland, pp.100-110.

Byerly, P. E. 1966. Interpretations of Gravity Data from the Central Coast Ranges and San Joaquin Valley, California: Geological Society of America Bulletin, vol. 79: p. 1,947-1,960.

Reproduced with permission of the copyright owner. Further reproduction prohibited without permission.

California Department of Water Resources. 1986. Laboratory reports of asbestos analyses of Aqueduct sediment and water samples in the San Joaquin - Arroyo Pasajero region.

California Department of Water Resources, San Joaquin Division. 1984. Draft Report: Arroyo Pasajero Ponding Basin Sediment Excavation.

California Division of Mines and Geology (CDMG). 1979. How Earthquakes Are Measured: California Geology, CDMG Note 23, February, 1979.

Casey, Tom A., and Dickenson, William R. 1976. Sedimentary Serpentinite of the Miocene Big Blue Formation near Cantua Creek, California in The Neogene Symposium: Society of Economic Paleontologists and Mineralogists, pp. 65-74.

Clark, Bruce. 1935. Tectonics of the Mount Diablo and Coalinga Areas, Middle Coast Ranges of California: Geological Society of America Bulletin, vol. 46: 1,025-1,078.

Cowan, Darrel S., and Mansfield, Charles F. 1970. Serpentinite Flows on Joaquin Ridge, Southern Coast Ranges, California: Geological Society of America Bulletin, vol. 81: p 2,615-2,628.

Davis, Fenelon F. 1963. Highlights in California Mining: Mineral Information Service. California Division of Mines and Geology, vol. 16, no. 2: 1-8.

Dibblee, T. W. 1971. Geologic Map of the New Idria Quadrangle, California-Open File Map. Reston, Va.: U.S. Geologic Survey.

Reproduced with permission of the copyright owner. Further reproduction prohibited without permission.

Dickenson, William R. 1962. Brecciated serpentine extrusion on Table Mountain in Central California Coast Ranges: Geological Society of America, Abstracts for 1962, Los Angeles.

Dickenson, William R. 1966a. Table Mountain serpentinite extrusion in California Coast Ranges: Geological Society of America Bulletin, vol. 77, no. 5: 451-471.

Dickenson, William R. 1966b. Plate Tectonics and the Continental Margin of California in Geology of Northern California: California Division of Mines and Geology, Chapter 1, pp. 1-28.

Dietz, Robert S. 1963. Actualistic Concept of Geosynclines and Mountain Building: Geological Society of America, Abstracts for 1962, p. 34, Los Angeles.

Eaton, J. P. 1985. Seismic Setting, Location, and Focal Mechanism of the May 2, 1983 Coalinga Earthquake, in Borcherdt, R. D., ed., The Coalinga Earthquake Sequence Commencing May 2, 1983: U.S. Geological Survey Open-File Report 83-511, pp. 20-26.

Eckel, E. B., and Myers, W. B., 1946. Quicksilver Deposits of the New Idria District, San Benito and Fresno Counties, California: California Journal of Mines and Geology, vol. 42: 81-124.

Fowkes, E. J. 1982. An Educational Guidebook to the Geologic Resources of the Coalinga District: West Hills College, Coalinga, California.

Reproduced with permission of the copyright owner. Further reproduction prohibited without permission.

Harbart, William, and Cox, Allan. 1987. Late Neogene Motion of the Pacific Plate: Journal of Geophysical Research, submitted January 1987.

Harding, T. P. 1976. Tectonic Significance and Hydrocarbon Trapping of Sequential Folding Synchronous with San Andreas Faulting, San Joaquin Valley, California: American Association of Petroleum Geologists Bulletin, vol. 60, no. 3: 356-378.

Harradine, Frank F. 1950. Soils of Western Fresno County, California: University of California - College of Agriculture, Division of Soils, Berkeley, 86 p.

Hart, Earl W., and McJunkin, Richard D. 1983. Surface Faulting Northwest of Coalinga, California, June and July 1983: California Division of Mines and Geology, Special Publication no. 66, pp. 201-220.

Hess, Harry H. 1955. Serpentines, Orogeny and Epeirogeny in Geological Society of America, Special Paper 62: Crust of the Earth, pp. 391-408.

Hoots, Harold W.; Bear, Ted L.; and Kleinpell, William D. 1954. Geological Summary of the San Joaquin Valley, California in Jahns, Richard H., ed., Geology of Southern California: California Department of Natural Resources - Division of Mines, Bulletin 170, pp.113-129.

Hunt, G. R., and Evarts, R. C. 1981. The Use of Near-Infrared Spectroscopy to Determine the Degree of Serpentinization of Ultramafic Rocks: Geophysics, vol. 46, no. 3: 316-321.

Reproduced with permission of the copyright owner. Further reproduction prohibited without permission.

Ireland, R. L. 1986. Land Subsidence in the San Joaquin Valley, California, as of 1983: U.S. Geological Survey, Water-Resources Investigations Report 85-4196, Sacramento, 50 pp.

Jenkins, Olaf P., ed. 1971. Santa Cruz Sheet, Geologic Map of California, compiled by Charles W. Jennings and Rudolph G. Strand: California Division of Mines and Geology, Scale 1:250,000.

King, Geoffrey, and Stein, Ross. 1983. Surface Folding, River Terrace Deformation Rate and Earthquake Repeat Time in a Reverse Faulting Environment: The Coalinga, California, Earthquake of May, 1983 in California Division of Mines and Geology, Special Publication No. 66: 165-176.

Kruckeberg, A. R. 1984. California Serpentines: Flora, Vegetation, Geology, Soils, and Management Problems: University of California Publications in Botany, Vol. 78, University of California Press, Berkeley, 180 p.

Lettis, W. R. 1983. Late Cenozoic Stratigraphy and Structure of the Western Margin of the Central San Joaquin Valley, California: U.S. Geological Survey Open File Report 82-526.

Levine-Fricke. May 9, 1989. "Off-Site Source Characterization; Regional Soil Sampling and Watershed Modeling Report".

Mansfield, C. F. 1972. Petrography and Sedimentology of the Late Mesozoic Great Valley Sequence near Coalinga, California: Stanford University, Department of Geology, Ph.D. thesis.

Reproduced with permission of the copyright owner. Further reproduction prohibited without permission.

Matthews, R. A. 1961. Geology of the Butler Estate Chromite Mine, Southwestern Fresno County, California: California Division of Mines and Geology, Special Report No. 71, 20 pp.

Miller, R. E., Green, J. H., and Davis, G. H. 1971. Geology of the Compacting Deposits in the Los Banos - Kettleman City Subsidence Area, California, Geological Survey Professional Paper 497-E: U.S. Department of the Interior, 46 p.

Minster, J. Bernard, and Jordan, Thomas H. 1978. Present-day plate motions: Journal of Geophysical Research, Vol. 83, No. B11: 5,331-5,354.

Merritt, Paul C. 1962. California Asbestos Goes to Market: Mining Engineering, vol. 14, no. 9: 57-62.

Mount, Van S., and Suppe, John. 1987. State of Stress Near the San Andreas Fault: Implications for Wrench Tectonics: Geology, vol. 15: 1,143-1,146.

Mumpton, F. A. 1989, April 24, 1989. Personal communication with John DeReamer.

Mumpton, F. A., and Thompson, C. S. 1975. Mineralogy and Origin of the Coalinga Asbestos Deposit: Clays and Clay Minerals, vol. 23: 131-143.

Munn, John R.; Busacca, Alan J., and Trott, Kenneth E. 1981. California Aqueduct Sedimentation Study for the Arroyo Pasajero and Tributary Watersheds: California Department of Conservation, 72 pp.

Reproduced with permission of the copyright owner. Further reproduction prohibited without permission.

Munro, Robert C., and Reim, Kenneth M. 1962. Coalinga Asbestos Fiber - A Newcomer to the Asbestos Industry: Canadian Mining Journal, vol. 83, no. 8: 45-50.

Page, B. M. 1966. Geology of the Coast Ranges in Geology of Northern California, California Division of Mines and Geology Bulletin 190, pp. 255-276.

Page, B. M. 1981. The Southern Coast Ranges: in The Geotectonic Development of California (Rubey vol. 1), Prentice Hall, Englewood Cliffs, New Jersey, pp. 329-417.

Read, William H. 1959. Geology of the Lillis Ranch Quadrangle. Berkeley: University of California, M.S. thesis, 83 pp.

Reading, H. G. 1981. Sedimentary Environments and Facies: Elsevier, New York, 569 p.

Rice, Salem J. 1957. Asbestos in Wright, Lauren A., ed., Mineral Commodities of California, California Department of Natural Resources - Division of Mines, Bulletin 176: 49-58.

Rice, Salem J. 1963. California Asbestos Industry: Mineral Information Service, vol. 16, no. 9, pp. 1-7: California Division of Mines and Geology.

Rymer, Michael J., and Ellsworth, William L. Mechanics of the May 2, 1983, Coalinga, California Earthquake: U.S. Department of the Interior, Geological Survey, Open-File Report 85-44, 437 p.

Reproduced with permission of the copyright owner. Further reproduction prohibited without permission.

Rymer, Michael J.; Harms, Katherine K.; Clark, Malcolm M., and Lienkaemper, James J. 1985. Surface Faulting Associated with the June 11 Aftershock of the May 2, 1983 Coalinga Earthquake in Borcherdt, R. D., ed., The Coalinga Earthquake Sequence Commencing May 2, 1983: U.S. Geological Survey Open-File Report 83-511, pp. 57-60.

Sauber, J.; Lisowski, M.; and Solomom, S. C. 1988. Geodetic Measurement of Deformation East of the San Andreas Fault in Central California: Eos, vol. 69, no. 16: 326.

Simons, Li and Associates. 1985. Final Report - Stream Channel Erosion Study - Arroyo Pasajero, Submitted to California Department of Water Resources, March 20.

Stove, Carl W. 1983. Intensity Distribution and Isoseismal Map: California Division of Mines and Geology, Special Publication No. 66: 1-4.

Taliaferro, N. L. 1943. Geologic History and Structure of the Central Coast Ranges of California in Geologic Formations and Economic Development of the Oil and Gas Fields of California: California Division of Mines and Geology, Bulletin 118: 119-163.

U.S. Department of Agriculture, Soil Conservation Service. 1987. Draft Geology Report - Cantua Creek Sediment Study, December, 16 p.

U.S. Department of Agriculture. 1952. Soil Survey - Coalinga Area, California, 91 pp.

Reproduced with permission of the copyright owner. Further reproduction prohibited without permission.

U.S. Department of the Interior, Bureau of Reclamation. 1984. Arroyo Pasajero Flood and Silt Deposition Study - Special Report on Flood Protection for San Luis Canal, January, 81 p.

U.S. Environmental Protection Agency. 1987. Inventory of Potential Asbestos Sources in the New Idria - Coalinga Study Region for the Atlas and Coalinga Sites, Fresno County, California: Prepared by Woodward-Clyde Consultants, San Francisco, 11 pp.

U.S. Geological Survey. 1984. Santa Rita Peak Quadrangle, 7.5 Minute Topographic Map. Reston, Va: U.S. Geological Survey.

Van Eysinga, F.W.B. 1983. Geologic Time Table, Third Edition: Elsevier Scientific Publishing Company, Amsterdam.

Walker, George W., and Griggs, Allan B. 1953. Chromite Deposits of the Southern Coast Ranges of California: California Department of Natural Resources, Division of Mines, Bulletin 134, part 2, ch. 2: 39-88.

Wentworth, Carl M.; Walter, Allan W.; Bartow, J. Alan; and Zoback, Mark D. 1983. Evidence on the Tectonic Setting of the 1983 Coalinga Earthquakes from Deep Reflection and Refraction Profiles Across the Southeastern End of Kettleman Hills: California Division of Mines and Geology, Special Publication No. 66: 113-126.

Wong, Ivan G., and Ely, Richard W. 1983. Historical Seismicity and Tectonics of the Coast Ranges-Sierran Block Boundary: Implications to the 1983 Coalinga, California

Reproduced with permission of the copyright owner. Further reproduction prohibited without permission.

Earthquakes: California Division of Mines and Geology, Special Publication No. 66: 89-104.

Woodring, W. P.; Stewart, R., and Richards, R. W. 1940. Geology of the Kettleman Hills Oil Field, California: U.S. Geological Survey Professional Paper 195, 170 p.

Zigler, J. L.; Wentworth, C. M., and Bartow, J. A. 1986. Structure Contour Map of the Tops of the Kreyenhagen Formation and Cretaceous strata in the Coalinga Area, Fresno and Kings Counties, California. Reston, Va: U.S. Geological Survey.

Zoback, Mark D.; Zoback, Mary Lou; Mount, Van S.; Suppe, John; Eaton, Jerry; Healy, John H.; Oppenheimer, David; Reasenberg, Paul; Jones, Lucile; Raleigh, C. Barry; Wong, Ivan G.; Scotti, Oona; and Wentworth, Carl. 1987. New Evidence on the State of Stress of the San Andreas Fault System: Science, vol. 238: p. 1,105 - 1,111.

Reproduced with permission of the copyright owner. Further reproduction prohibited without permission.

CHAPTER THREE

RESULTS OF FIELD AND AERIAL RECONNAISSANCE INVESTIGATIONS AND INTERPRETATION OF AERIAL PHOTOGRAPHY

1.0 INTRODUCTION

This chapter presents a summary of field observations of the occurrence and distribution of chrysotile asbestos despotism throughout the area of investigation including the primary outcrop area of the asbestos-bearing New Idria Formation; mine and mill site areas located in the Joaquin Ridge mining district (i.e., mining operations located in the White Creek and Pine Canyon drainage sub-basins of the New Idria Formation); streambed deposits in the White Creek and Pine Canyon drainage pathways; streambed deposits in the Los Gatos Creek and Arroyo Pasajero drainage pathway; and alluvial deposits in the sediment settling basin constructed adjacent to the California Aqueduct and other alluvial fan areas. This chapter also provides a summary of a review and interpretation of available aerial photography including high altitude color/infrared imagery.

Copies of annotated field photographs are included in Appendix A. These photographs include photos taken from the field sampling program as well photos taken during several low altitude aerial reconnaissance flights taken by private plane over the Arroyo Pasajero alluvial fan, Los Gatos Creek stream pathway, and Joaquin

Reproduced with permission of the copyright owner. Further reproduction prohibited without permission.

Ridge highland outcrop area. These photos provide an excellent perspective of existing field conditions in the areas of investigation.

The review of field photographs is supplemented with a review and interpretation medium and high altitude aerial photography. A few select aerial photographs with annotated interpretations are included in Appendix B. The reviewed aerial photographs included aerial photos dating from 1928 through 1987. An inventory of reviewed aerial photographs is provided in Appendix C. My detailed summaries and interpretations of specific aerial photographs are also provided in Appendix C. Access to the reviewed aerial photographs was provided by several regional aerial photography archival collections including Whittier College, Whittier, California; University of California at Santa Barbara; and California Department of Water Resources, Sacramento, California. Additional photos were obtained from the USGS and from US Department of Agriculture, Soil Conservation Service (SCS).

The primary asbestos outcrop area of investigation, including the areas of the Johns-Manville Coalinga Asbestos Mill Site and the Atlas Mine and Mill Site, is located approximately 18 miles northwest of Coalinga near the crest of the Joaquin Ridge highland trend. This mountainous area is associated with steep relief and rugged terrain which is typical of the mountains of the southern Diablo Range. The serpentinite mass of the New Idria Formation forms the core and the crest of the Joaquin Ridge highland area. Many additional mine and milling operations are located in this general mining area. Most of these mine and mill sites are located in the White Creek and Pine Canyon sub-basins of the Los Gatos Creek drainage basin of the Arroyo Pasajero watershed. Los Gatos Creek and other watershed tributaries (Warthan Creek, Jacalitos Creek, Zapato-Chino Creek) come together in the Pleasant Valley area near Coalinga. In the Pleasant Valley area near Coalinga, the gradient of

Reproduced with permission of the copyright owner. Further reproduction prohibited without permission.

the gradient of the Los Gatos Creek drainage pathway is significantly reduced as a result of valley fill conditions and possibly as a result of a upward ramping effect caused by localized uplift along the structural axis of the Coalinga Anticline. Downstream of Coalinga, this drainage pathway becomes the Arroyo Pasajero channel which flows onto the Arroyo Pasajero alluvial fan in the vicinity of the town of Huron.

1.1 Johns-Manville Coalinga Asbestos Mill Site and the Pine Canyon Drainage Area

The Johns-Manville Coalinga Asbestos Mill is located in the Pine Canyon sub-basin of the Los Gatos Creek - Arroyo Pasajero drainage system. (See watershed drainages illustrated in Figure 2-3). The Pine Canyon sub-basin drains approximately one square mile of the New Idria Formation, and the White Creek sub-basin drains approximately 5.8 square miles of the New Idria Formation.

The Johns-Manville Coalinga Asbestos Mill is located on the southeastern flank of Joaquin Ridge in the headlands of Pine Canyon (T19S, R13E, Sec.1, Fresno Co.; Santa Rita Peak 7.5 Minute Topographic Quadrangle Map). This location is approximately 0.5 miles downslope from the Joaquin Ridge outcrop of the asbestos-containing New Idria Formation. The asbestos milling facility was constructed on top of a large complex of asbestos-bearing serpentinite landslide and/or debris flow deposits that are the predominant geomorphic feature of the upper Pine Canyon area. These serpentinite earthflow deposits originated from the steep slopes of the New Idria outcrop (with slopes having a vertical to horizontal ratio of 1 to 5.8). The general drainage pathways of the Johns-Manville Coalinga Asbestos Mill site area are less steep because of the canyon-filling affect of the earthflow deposits which have

Reproduced with permission of the copyright owner. Further reproduction prohibited without permission.

contributed a streambed slope with a vertical to horizontal ratio of 1 to 9.1. In the general area of the Johns-Manville Coalinga Asbestos Mill, some of the earthflow deposits have developed soils with deep, clay-rich argillic horizons that support a grassy cover. These soils have asbestos concentrations which are generally less than one percent. These soils have developed on top of the asbestos-containing debris flow and landslide deposits as a result of the accumulation of organic debris and other soil-forming materials.

Tailings from the Coalinga asbestos milling operation were deposited in a small gorge that had formed on the eastern margin of the Pine Canyon earthflow complex. The tailings are contained by the sidewalls of the gorge and by a sediment retaining dam that was constructed at the base of the tailings pile. Additional tailings from chromite milling operations were deposited in the general area of the mill.

In addition to the New Idria Formation, the Johns-Manville Coalinga Asbestos Mill is located approximately 0.6 to 0.7 miles downslope from two large-scale, open-pit mining operations - the Jensen Asbestos Mine and the Butler Estate Chromite Mine. The Jensen Mine covers approximately 29 acres, and the Butler Mine covers approximately 43 acres. The Butler Mine was a deep-pit mining operation that was carved out of a steep hillside that marks the drainage divide between the Pine Canyon and the White Creek drainage areas. The Jensen Mine was a bench-mining operation and is located on a serpentinite debris flow deposit. The terrain in the vicinity of the Jensen and Butler Mines has vertical to horizontal slope ratios of 1 to 3.52 and 1 to 3.96, respectively. These mines, including uncontained waste ore dumps, are drained by Pine Canyon Creek upstream of the Johns-Manville Coalinga Asbestos Mill. See Figure 9A which is a general location map modified from the Santa Rita Peak (USGS, 1984) topographic map.

Reproduced with permission of the copyright owner. Further reproduction prohibited without permission.

Field observations confirm that asbestos-containing sediments from both of these mines are being eroded and transported downstream through the Upper Pine Canyon drainage system. Erosion of the Butler waste ore dumps appears particularly severe. As a result of its ridgetop location and other factors (i.e., an over-steepened waste-ore dump, the unconsolidated nature of the serpentinite debris, and lubrication of glide planes from water seeping into the pile), slumping and debris flows from the Butler waste-ore pile are moving into the Upper Pine Canyon drainage channels.

1.2 Atlas Mine and Mill Site and the White Creek Drainage Area

The Atlas Mine and Mill Site is located in the White Creek mining district approximately three miles west-northwest of the Johns-Manville Coalinga Asbestos Mill of Upper Pine Canyon. The Atlas Mine and Mill is located within the outcrop area of the New Idria Formation near the crest of Joaquin Ridge (T18S, R13E, Sections 31 and 32; Santa Rita Peak 7.5 Minute Topographic Quadrangle). The Atlas Mine and Mill covers approximately 200 acres and includes three large-scale, open-pit asbestos mines and a large tailings pile complex that is much larger than the tailings pile of the Johns-Manville Coalinga Asbestos Mill. The Atlas tailings form a complex of merged, dune-like piles that are uncontained on all sides and are migrating downslope in dune-like fashion. Field observations show that the uncontained piles are subject to wind erosion and gullying. The terrain of the Atlas Mine and Mill is a steep area that has a vertical to horizontal slope ratio of 1 to 5.8.

In addition to the Atlas Mine and Mill, the White Creek drainage area includes at least five other large-scale, open-pit mines and three chromite milling operations. These mines include the James/Corbett/Byles Mine, the Big Ridge Mine, the

Reproduced with permission of the copyright owner. Further reproduction prohibited without permission.

Rhodes/Byles/Gribble Mine, the Tromby Mines (Nos. 1 and 2), the Archer Mine, and part of the Butler Estate Chromite Mine. The chromite milling operations included the Holman Mill, the Chambers and Russell Mill, and several previously unreported mills located on White Creek.

The White Creek sub-basin also includes several large scale landslide and/or serpentinite debris flow complexes that cover approximately four square miles and are very steep. Some surfaces have slopes which are equal to or greater than the angle of repose (i.e., 34 degrees) which causes the serpentinite debris to be unstable and subject to mass wasting. These landslides are relatively barren of vegetation and are subject to significant gullying. The tailings piles of the Atlas milling operation are merging with these naturally occurring earth flow complexes.

1.3 Landslide and/or Serpentinite Debris Flow Complexes

Landslides and/or serpentinite debris flow deposits from the New Idria Formation have been mapped throughout the Joaquin Ridge area since the early 1900s. The landslide and/or serpentinite debris flow deposits are particularly abundant in the central and southeastern areas of the New Idria Formation outcrop (Eckel and Myers, 1946; Matthews, 1961; Cowan and Mansfield, 1970; Dibblee, 1971). As reported by Matthews (1961, p. 13), extensive landslides and slope wash material occur throughout the general serpentinite area of the New Idria Formation outcrop, with most of the landslides occurring along the southern boundary of the serpentinite mass. One of the largest landslides occurs just southeast of the Butler Estate (or "Mistake") Chromite Mine in the Pine Canyon drainage basin (Matthews, 1961, p. 13). As indicated in Figure 2-4, several other large landslide and/or serpentinite debris flow

Reproduced with permission of the copyright owner. Further reproduction prohibited without permission.

complexes have been mapped in the White Creek and Cantua Creek drainage basins. Some of these complexes cover as much as several square miles.

The largest landslide and/or serpentinite debris flow complex that has been mapped in this area covers approximately three square miles of the New Idria Formation outcrop in the White Creek drainage area (Dibblee, 1971). This large complex is being dissected by approximately 16 miles of intermittent stream channels that are associated with significant gully erosion. The Cantua Creek drainage area includes four mapped serpentinite debris flow complexes that have moved into the heads of four small canyons. These serpentinite debris flow deposits cover approximately 3.2 square miles.

Based on interpretation of aerial photographs and reconnaissance geologic mapping completed as part of this study has shown that the Upper Pine Canyon area is underlain by a complex system of at least four on-lapping and over-lapping landslides and/or serpentinite debris flows associated with several detachment zones. These slides cover approximately 0.7 square miles and were mapped on the basis of topographic position, development of surface drainage features, relative degree of soil-profile development, and cross-cutting stratigraphic relationships.

Previous mapping of the landslide/serpentinite debris flows in Pine Canyon indicated two detachment zones which were located approximately 1.8 miles to the west-northwest and northwest of the toe of the flows (Eckel and Myers, 1946, Pl. 8; Dibblee, 1971). However, reconnaissance geologic mapping completed for this study shows that the serpentinite debris flow deposits in Pine Canyon cover a much broader area than previously reported by Dibblee (1971) or Eckel and Myers (1946). Mapping conducted by Levine Fricke (May 9, 1989) shows that the Upper Pine Canyon

Reproduced with permission of the copyright owner. Further reproduction prohibited without permission.

drainage area consists of a complex system of on-lapping and over-lapping landslide and debris flow deposits. These slide and/or debris flow deposits are estimated to be approximately 50,000 to 250,000 years old, based upon the interpretation of soil profiles and the degree of surface dissection.

Reproduced with permission of the copyright owner. Further reproduction prohibited without permission.

2.0 SUMMARY INTERPRETATION OF RECONNAISSANCE AERIAL PHOTOGRAPHS AND FIELD OBSERVATIONS

An analysis of reconnaissance aerial photographs (see photographs numbered 1 through 119 included in Appendix A), integrated with detailed field observations, shows that the occurrence of asbestos-containing sediment in the intermittent Los Gatos Creek drainage pathways, including White Creek and Pine Canyon Creek, is related to:

(1) the occurrence of gully erosion on steeply sloping serpentinite surfaces located in the New Idria Formation outcrop area including naturally occurring serpentinite outcrops, serpentinite soils, and serpentinite earthflow deposits; mining related serpentinite dumps and tailings; and serpentinite areas adjacent to roads;

(2) the occurrence of sheet and rill erosion of the poorly vegetated and steeply sloped and anthropically undisturbed serpentinite surfaces of the New Idria Formation; and

(3) the occurrence of sheet and rill erosion of anthropically disturbed serpentinite surfaces including mines, tailings piles, and exploration pits.

An additional source may be approximately 43,000 tons of serpentinite debris that may have been dumped into ponding basins constructed in the intermittent White Creek streambed by chromite milling operations that operated in the 1940's and early 1950's.

Reproduced with permission of the copyright owner. Further reproduction prohibited without permission.

2.1 White Creek Area

Most of the asbestos in the Los Gatos Creek drainage pathway has originated from the White Creek drainage area of the New Idria Formation. This is evident from field observations and from a review of aerial photographs (see Appendices A and B) which show that the White Creek channel is partly choked with gravel and sand-sized detrital serpentinite debris throughout most of its length. This means that the channel contains more sediment than it has the capacity to transport. Field observations and aerial photographs also show the extent of the natural erosion associated with the occurrence of deep gullies that have formed on steeply sloping surfaces in the lower two thirds of the serpentinite outcrop area. A review of geologic maps (Dibblee, 1971) and topographic maps (USGS, 1984) shows that the White Creek drainage area of the New Idria Formation includes a large serpentinite landslide and debris flow complex that covers approximately 3.2 square miles. These landslides and the landslide detachment zones are being eroded by a drainage network of more than 18 miles of intermittent streams. These intermittent streams and steeply inclined hillsides have slopes that range up to 65 degrees. The intermittent streams are dissecting the upper third of the outcrop areas and are deeply incised in the lower two thirds where the channels have formed deep, V-shaped gullies.

Approximately 16% (i.e., 0.96 square miles) of the surface of the New Idria Formation in the White Creek drainage area has been disturbed by mining and other anthropic activities. As indicated on the Santa Rita Peak 7.5 Minute Topographic Quadrangle map (USGS, 1984), the White Creek drainage area includes 158 exploration pits, 8 mines, 2 chromite milling operations, 1 asbestos milling operation, 1 mercury retorting operation, and many miles of unimproved roads. A review of the literature (Matthews, 1961), aerial photographs, and field survey observations indicate that there

Reproduced with permission of the copyright owner. Further reproduction prohibited without permission.

may have been three additional chromite milling operations on White Creek which have not been documented on the USGS topographic map.

Field photographs and reconnaissance aerial photographs of the White Creek and Pine Canyon drainage basins of the Joaquin Ridge mining area and the Arroyo Pasajero alluvial fan are presented in Appendix A. Field photographs were taken from the ground and the reconnaissance aerial photographs were taken from an airplane at low altitude. Higher altitude aerial photographs are included in Appendix B and are discussed in Section 3.0. A detailed summary of low and high altitude aerial photographs is included in Appendix C.

A review of field observations and aerial photographs of the White Creek area shows the following:

1. The serpentinite outcrop area in the White Creek drainage basin is associated with an extensive network of more than 18 miles of gullies which are generally barren of vegetation. These gullies are concentrated in the lower two thirds of the serpentinite outcrop area. At the base of the serpentinite outcrop area, the White Creek channel branches into a network of distributary channels that head into the New Idria Formation. These channels are armored with large cobbles and boulders. As the channels head into the serpentinite outcrop area, the width of most channels decreases to the point where the channel is formed by a V-shaped, steeply sloped gully with sidewalls that are unstable (approximately 50 to 60 degrees; i.e., beyond the angle of repose). These slopes are susceptible to slumping and mass wasting. These gullies range up to 300 to 400 feet deep. Some of the gullies appear to have formed at the margins of serpentinite landslide and debris flows deposits. The sidewalls of the gullies are entirely formed by the weakly consolidated serpentinite matrix of the New

Reproduced with permission of the copyright owner. Further reproduction prohibited without permission.

Idria Formation. As noted above, slumping and mass wasting of the sidewalls of these gullies is common. See Photos 1 through 6 and 8 through 20.

2. The serpentinite outcrop area in the White Creek drainage basin has been associated with at least 10 surface mining operations including chromite mines, asbestos mines, a mercury mine, and a magnesite mine. These mines and a net-work of exploration access roads are generally barren of vegetation and are subject to erosion and mass wasting. These mines were open-pit mining operations that included benching operations and deep-pit operations. The chromite mines were generally deep-pit operations, and the asbestos mines were generally bench-cut operations. Overburden from the mining operations was generally dumped down-slope in large piles or dumps and abandoned. No attempts appear to have been made to reclaim (i.e., regrade and revegetate) any of the mining operations. See Photos 21 through 32 and 34 through 36.

3. The serpentinite soils in the White Creek drainage basin are associated with a sparse vegetation that mostly consists of manzanita and coffee berry bushes, some Digger pine trees, and almost no grassy ground covering. The undisturbed surfaces have weathered to a loose, reddish-brown soil. The soils are mostly composed of primary minerals (i.e., serpentinite). The undisturbed serpentinite soils have coarse, sandy textures with low plasticity and blocky soil structures. See Photos 48 and 49.

4. The serpentinite soils and mine surface soils have a blocky soil structure and are mostly composed of coarse sand-sized aggregates of chrysotile asbestos. These soils have some plasticity as a result of the platey aggregates of asbestos. See Photos 50 and 51.

Reproduced with permission of the copyright owner. Further reproduction prohibited without permission.

5. The anthropically disturbed surfaces associated with mining operations have virtually no vegetation. The soils associated with these surfaces are very coarse and platey and are composed of primary minerals that are weakly consolidated and readily friable. These soils have a platey, blocky structure and are generally classified as sandy material that has a low plasticity when compressed. The anthropically disturbed surfaces, including mines, dumps, and tailings piles, commonly have a thin caliche-like crust that is not normally observed on undisturbed surfaces. This crust may have developed as a result of the precipitation of magnesium carbonate in response to the upward movement and evaporation of water at the surface. The disturbed surfaces were generally observed to be slightly moist several inches below the surface. The crusts were generally observed to be approximately one to two inches thick. See Photos 52 and 53.

6. The Atlas Site has a tailings pile complex that is composed of four to five uncontained, coalescing piles that cover approximately 280 acres which appear to be migrating downslope in dune-like fashion. These piles, like the piles and dumps of other mining operations, are subject to erosion and mass wasting. Field evidence indicates that the piles are highly susceptible to the effects of wind erosion and are migrating in dune-like fashion. The field evidence consists of the occurrence of strong winds that are frequently encountered in the Atlas area (which is approximately 1/4-mile down-slope from the crest of Joaquin Ridge) in conjunction with the occurrence of manzanita bushes and pine trees that have been partially covered with wind-blown asbestos sediment, open areas of serpentinite soils adjacent to the tailings piles that have been covered with wind-blown asbestos sediment, and smoothing of the break in slope where the tailings piles are encroaching on natural serpentinite soils. Because of this sediment migration, the Atlas tailings piles are merging with the naturally occurring serpentinite soils and landslides of the New Idria Formation. The tailings

Reproduced with permission of the copyright owner. Further reproduction prohibited without permission.

debris was deposited in a broad, open area with a natural slope of approximately 30 degrees. The tailings piles have slopes of approximately 40 to 50 degrees. Because of these steeply sloping surfaces, the Atlas tailings piles are unstable and subject to sheet and rill erosion, gullying, and slumping and mass wasting. See Photo 54.

7. Some intervals of the intermittent White Creek streambed appear to be choked with sand-sized serpentinite debris. Some of this serpentinite debris may have been the result of chromite milling operations that occurred during the 1940's and 1950's. Field observations and reconnaissance aerial photographs show the locations of at least five abandoned chromite mill sites. On the Santa Rita Peak 7.5 Minute Topographic Quadrangle map, four of these chromite milling operations are located at:

(1) T.19 S., R.13 E., Sec. 4, SW 1/4;
(2) T.19 S., R.13 E., Sec. 9, NW 1/4;
(3) T.19 S., R.13 E., Sec. 17, SE 1/4; and
(4) T.19 S., R. 13 E., Sec. 21, NE 1/4.

A fifth abandoned chromite milling operation is located on the Sherman Peak 7.5 Minute Quadrangle map at T.19 S., R.13 E., Sec. 25, SE 1/4. This location is approximately 0.25 miles upstream of White Creek's juncture with Pine Canyon Creek.

These areas have been identified on the basis of the following: (1) the occurrence of abandoned mill site machinery and asbestos-affected operation pads visible from ground surveys; (2) the occurrence of earthen dams constructed across White Creek with the purpose of capturing and damming water for use in the chromite milling process; (3) the occurrence of a sudden widening of the streambed in relationship to the deposition of a broad band of serpentinite debris in the streambed and on the

Reproduced with permission of the copyright owner. Further reproduction prohibited without permission.

adjacent streambanks as is visible in aerial photographs; and (4) the occurrence of roads leading to these affected areas. See Photos 55 through 60.

8. Streambed sediment in the intermittent White Creek channel has been deposited as channel sand and channel gravel deposits. The sandy sediments are mostly detrital serpentinite debris that has been deposited in elongate braided channel sand deposits and as a matrix in the gravelly deposits. These deposits line the intermittent White Creek channel throughout its entire length. Some of the serpentinite debris occurs as white, platey chips and as pale green, lath-shaped particles. Moist deposits are bluish gray to yellowish gray and have a mushy, fibrous texture indicating a high asbestos content. The White Creek channel is generally broad and shallow and ranges from 30 to 40 feet wide in the most narrow areas to as much as 150 feet wide. This means that under high flow conditions, the channel may have the capacity to transport large volumes of sediment. In sharp contrast, the Pine Canyon intermittent streambed is much narrower and is relatively barren of deposited sediment. See Photos 59 through 63.

9. The concentration and volume of the asbestos sediment in the White Creek channel visually appears to diminish only slightly downstream from the base of the New Idria Formation outcrop to the juncture of White Creek and Los Gatos Creek. This is evident from field observations and from high altitude aerial photographs which show a bright, bluish-white ribbon of sediment that lines the White Creek channel from the New Idria Formation outcrop area downstream to the juncture with Los Gatos Creek. See high altitude, color infrared (CIR) photos NASA/MSC, 1971, Flight 5, Roll 29, Frame 3477 and NHAP, 1981, Flight 445, Frame 75 in Appendix A-2 and the discussion of high altitude aerial photographs of the following Section 3.0. Downstream of the juncture of White Creek and Los Gatos Creek, the White Creek

Reproduced with permission of the copyright owner. Further reproduction prohibited without permission.

sediments are diluted by sediment and runoff from Los Gatos Creek, which contributes to attenuation of the reflectance characteristics of the white ribbon of sediment that lines White Creek.

2.2 Pine Canyon Area

1. The Pine Canyon channel is much smaller than the White Creek channel. The Pine Canyon channel ranges from less than 10 feet wide in the upper canyon areas to approximately 20 to 30 feet wide in the lower canyon areas near the juncture with White Creek. The bottom of the channel is generally associated with bare rock or a very thin veneer of gravelly sediment. Asbestos-bearing sediment visually appears to be deposited in very thin isolated pockets that are partially accreting sand-sized sediment. Some of these deposits are composed of coarse asbestos sediment that includes fibrous white chips and platelets locally referred to as "mountain leather" and pale green, flat, "splintery" lath-shaped minerals. These deposits are not common, and sampling teams had to expend considerable effort to locate these isolated deposits. This is in sharp contrast to the abundance of sediment in the White Creek channel where one does not have to walk more than a few feet to find a channel sand deposit suitable for sampling. Asbestos-containing streambed sediment in Pine Canyon is most common in depositional areas located upstream of the Johns-Manville Coalinga Site in the uppermost reaches of the Upper Pine Canyon drainage system. These depositional areas are generally in close proximity to either the Jensen Mine and/or the Butler Estate Chromite Mine. See Photos 37 through 40, 61, 64, 65, 67, and 69.

2. The asbestos concentration of the fine-grained sediment deposits found in Pine Canyon visually appear to decrease downstream from the Jensen Mine and the Butler Estate Chromite Mine, both of which are located less than one mile upstream from the

Reproduced with permission of the copyright owner. Further reproduction prohibited without permission.

Johns-Manville Coalinga Site. This was indicated by an increase in the brownish color of the downstream sediment and the downstream decrease in the platy textural characteristics associated with the whitish-gray asbestos sediment found near potential asbestos source areas including the piles and dumps associated with the Butler Estate Chromite Mine and the Jensen Mine, the erosional margins of the serpentinite debris flows and landslides of the Upper Pine Canyon area, and the johns-Manville Coalinga Site tailings pile. See Photos 37 through 40 and 66 through 70.

3. The Upper Pine Canyon area, including the Johns-Manville Coalinga Site, is underlain by an extensive complex of serpentinite landslide and/or debris flow deposits. Some of the deposits originated from different source areas and side canyons and in the Mill Site area and some of these deposits overlap each other. Drainage channels have formed on the eastern and western margins of the landslide complex, forming the east and west forks of Pine Canyon Creek at the Johns-Manville Coalinga Site. Some of these channels have cut through landslide and/or serpentinite debris flow deposits that originated from side canyon areas (i.e., the canyon that leads to the Butler Mine and the side canyon located to the west of the Railroad Mine area). Both the east and west forks are associated with steep gullies and streambeds that are semi-armored with cobbles and boulders. See Photos 40, 66, and 67.

4. The streambanks of the east and west forks of Upper Pine Canyon contain some deposits of detrital serpentinite debris that visually appear to have a high asbestos content. One of these deposits occurs upstream of the Johns-Manville Coalinga Site and was sampled as Station OC-10X (with an elongate serpentine asbestos concentration of 85%). See Photo 68. These fluvial deposits form part of the streambanks, are subject to erosion, and may be an additional natural source of asbestos in the Pine Canyon drainage pathway.

Reproduced with permission of the copyright owner. Further reproduction prohibited without permission.

5. The tailings pile in the east fork of Pine Canyon Creek has two bermed, ponding basins which were built by Marmac to capture runoff for use in the company's milling operation. Drainage from these ponding basins has contributed to the occurrence of a gulley-like channel that has formed in the lower half of the tailings pile. A sediment retaining dam in the east fork approximately 300 yards downstream from the tailings pile appears to be effective in preventing the downstream movement of asbestos sediment eroded from the tailings pile. Approximately 4,000 cubic yards of tailing material has been deposited in an arroyo on the upstream side of the retaining dam, with very little evidence of tailings material deposited downstream of the retaining dam. See Photos 41 through 44 and 65.

6. A series of excavation pits showed that the upper Johns-Manville Coalinga Site landslide areas have developed deep soil profiles (i.e., 10 to 12 feet) with no visual evidence of asbestos. The Johns-Manville Coalinga Site excavation pits generally featured a dark grayish brown soil that was classified in the field as a silty clay with medium to high plasticity. The surfaces of the landslide deposits in the Johns-Manville Coalinga Site area support a good vegetative covering (80 to 90 percent) of grass and some trees. The soil type and the vegetative covering associated with the Johns-Manville Coalinga Site landslide deposits differ from the Atravesada soils defined and mapped by the SCS (unpublished soil survey, Fresno County, 1987). Consequently, SPLC has differentiated these soils as a separate, mappable soil type designated as SPLC #LSS (Landslide Surface Soil). The development of the deep soil profiles of these landslide deposits appears to have occurred in response to the accumulation of organic debris and other soil materials in conjunction with the weathering of serpentinite from physical, chemical, and biological processes. The occurrence of water from runoff and springs located upgradient of the Site may have also contributed

Reproduced with permission of the copyright owner. Further reproduction prohibited without permission.

to the development of the deep soil profiles observed in the Coalinga Site excavation pits. See Photos 46, 47, and 67.

7. The west fork upstream of the Johns-Manville Coalinga Site has many stream-bed deposits of asbestos sediment. The physical and textural characteristics of these deposits are similar to the physical and textural characteristics of asbestos sediment associated with the piles and dumps of the Butler Mine and the Jensen Mine. See Photos 37 through 40.

8. The Butler Mine is located at the head of the west fork of Upper Pine Canyon on the side of a steep ridge that forms the divide between the White Creek and Pine Canyon drainage basins. The Butler Mine covers approximately 43 acres and consists of a large open pit that is 200 to 300 feet deep. This pit was carved into the steeply sloping hillside using large mechanical shovels, one of which has been abandoned on the pile. Serpentinite debris that was excavated from the pit was dumped in a large, unstable pile that is slumping and flowing into the head of the west fork of Upper Pine Canyon. This pile appears to be a source of much of the coarse serpentinite debris found in the west fork upstream of the Johns-Manville Coalinga Asbestos Mill Site. See Photos 37, 38, 70, and 71.

9. The Jensen Mine is located near the head of the east fork of Upper Pine Canyon and is located on the surface of a serpentinite landslide and/or debris flow deposit that is rich in asbestos ore. The mine covers approximately 29 acres and consists of a series of benches cut into the landslide deposit. Unused ore was dumped in an elongate pile that forms the margin of one of the tributary channels to the west fork. Coarse serpentinite debris from this pile is slumping into the drainage channel and is being washed downstream into and through the west fork of the Mill Site. This pile is

Reproduced with permission of the copyright owner. Further reproduction prohibited without permission.

another source of much of the coarse asbestos sediment in the drainage channels located upstream of the Johns-Manville Coalinga Site. See Photos 39, 40, 69, 72, and 73.

10. The serpentinite landslide deposit which includes the Jensen Mine is particularly rich in asbestos as evidenced by the restricted manzanita vegetative covering and the coarse serpentinite debris that forms the poorly developed soil profile observed in an excavation pit (XP-6). This deposit is being eroded by stream channels that have formed on the margins of the deposit. This naturally occurring erosion is a significant natural source of asbestos sediment to the east fork. Field observations and streambed sampling show that the east fork of Pine Canyon upstream of the Mill Site has scattered deposits of this naturally occurring asbestos sediment. Much of the sediment in the east fork upstream of the tailings pile has been cemented together with what appears to be a calcite-dolomite conglomerate. See Photo 45.

Johns-Manville is believed to have installed a stream diversion in the early 1960's to divert flow from the east fork into the west fork upstream of the Mill Site. This diversion has minimized downstream flow in the east fork through the area that contains the tailings pile. The diversion was also used to build a road to provide access to the Jensen Mine location. Part of this access road was built on top of the diversion. As a result of the diversion, much of the asbestos-bearing streambed sediment in the east fork immediately upstream of the Mill Site may have been deposited prior to the initiation of mining activities, and would therefore represent natural background levels of asbestos in the east fork of Upper Pine Canyon.

Reproduced with permission of the copyright owner. Further reproduction prohibited without permission.

2.3 Los Gatos Creek

1. There is little visible evidence of asbestos in Los Gatos Creek upstream of its juncture with White Creek. This is evident in both aerial photographs and in streambed sampling activities. Immediately downstream of this point, sediment containing asbestos was observed in gravelly sand deposits that line the streambed channel. The concentration and volume of asbestos sediment in Los Gatos Creek visually appears to decrease downstream from the maximum level observed at the Los Gatos Creek juncture with White Creek. See Photo 74.

2. Several miles downstream of its juncture with White Creek, Los Gatos Creek widens to a width that ranges up to 150 feet. The streambed sediment generally consists of coarse sand and gravel. In several places, the channel has been modified by bulldozing of the streambed sediment to the sides of the channel, possibly to protect the streambanks from erosion. This practice may contribute to increased flow rates and increased erosion downstream. See Photos 75 and 76.

3. On the northwest side of the town of Coalinga, the Los Gatos Creek channel narrows to a width of approximately 20 to 30 feet. The streambed sediment is mostly fine gravel (less than 1/8 inch diameter) with a silty sandy matrix. Asbestos sediment appears as pale white, sand-sized chips and platelets and as sand-sized grains of pale green, lathe-shaped minerals. See Photos 77 and 78.

4. On the east side of the town of Coalinga, Los Gatos Creek is joined by Warthan Creek. The intermittent channel formed by the joining of these two stream groups gradually widens to a width of 500 feet. This broad channel meanders over a four-mile reach that heads east across the Pleasant Valley floodplain and east to the Arroyo

Reproduced with permission of the copyright owner. Further reproduction prohibited without permission.

Pasajero alluvial fan by cutting through a gap between Anticline Ridge and Guijarral Hills. This is an area where the intermittent streambed is entrenched approximately 30 to 40 feet and is associated with several in-set terraces. In this reach of Los Gatos Creek, there is a noticeable change in the particle size distribution of the streambed sediment. Between the town of Coalinga and the Anticline Ridge area, the streambed sediment in this reach of Los Gatos Creek generally consists of sand-sized material. See Photos 79 through 84.

5. On the east side of Anticline Ridge (approximately eight miles east of the town of Coalinga) in an area located downstream of the junctions with Warthan, Jacalitos, and Zapato-Chino Creeks, the Los Gatos Creek channel becomes the Arroyo Pasajero channel. On the east side of the Guijarral Hills area, this channel is entrenched approximately 25 to 35 feet into the Tulare Formation over a three- to four-mile distance. In this area, the yellowish-brown streambed sediment is mostly coarse silt and sand, with no gravel and no visible evidence of asbestos. This is in contrast to the asbestos-bearing pale white sandy gravel of Los Gatos Creek in the vicinity of the town of Coalinga. Streambed and streambank erosion from this entrenched portion of the Arroyo Pasajero channel reportedly accounts for up to 62% of the sediment deposited downstream on the alluvial fan adjacent to and updip of the California Aqueduct (60% as reported by Munn, Busacca, and Trott, 1981, p. 63; Simons, Li and Associates, 1985, p. 6.1; Boyle Engineering Corporation, 1988, p. 4-11). See Photos 85 through 89.

2.4 Arroyo Pasajero Alluvial Fan

1. At the point where the Arroyo Pasajero channel is no longer entrenched (on the west side of Huron), the channel widens to approximately 1,500 feet. This is the

Reproduced with permission of the copyright owner. Further reproduction prohibited without permission.

terminus of the Arroyo Pasajero channel. At this point, most of the coarse silt and sand-sized sediment is deposited in a lobe-shaped, braided alluvial fan deposit. This deposit is subject to scouring and cut and fill processes. During flood events, floodwaters and suspended sediment are transported by sheetflow in a northeasterly direction for several miles to the point where the flow is diverted into a settling basin constructed adjacent to and updip of the California Aqueduct. The sediment deposited in the settling basin is mostly silty clay to clay-sized material, with no visible evidence of asbestos. This clay has a high plasticity. Except for areas occupied by the Arroyo Pasajero channel, the terminus of the channel, and the settling basin, most of the alluvial fan surface has been cultivated by large-scale agricultural businesses. This large-scale farming has been made possible, in part, by the availability of water provided by the California Aqueduct. See Photos 90, 91 and 104 through 106.

2. Continuously cored soil borings located in the alluvial fan in areas located updip and downdip of the Aqueduct encountered both coarse and fine-grained sediments associated with alluvial channel, overbank, and floodwater deposits. Some of the medium-grained intervals were associated with a "fluffy" texture and some of the coarser-grained intervals were associated with dark bluish-gray serpentine pebbles. However, none of the subsurface alluvial fan sediments showed any visible evidence of asbestos. See Photos 93 to 100. The relatively low asbestos concentrations in alluvial fan sediments near the Aqueduct may be explained by (1) the dilution of asbestos-containing sediments from the New Idria Formation with non-asbestos sediments from other parent materials in the Arroyo Pasajero watershed, and (2) the deposition of coarse serpentinite sediments in the Los Gatos Creek streambed in an area west of the Coalinga Anticline's structural axis.

Reproduced with permission of the copyright owner. Further reproduction prohibited without permission.

3. Continuously cored soil borings located in the settling basin located adjacent to and updip of the California Aqueduct encountered very fine-grained settling basin fill and floodwater deposits that were underlain by stratified alluvial fan sediments that included both coarse and fine-grained intervals. None of the sediments encountered in the settling basin borings showed any visible evidence of asbestos. See Photos 99 through 106.

2.5 Salt and Cantua Creek Drainage Areas

1. The asbestos-bearing Big Blue Member of the Temblor Formation is well exposed in the uplifted foothills that form the monoclinal western margin of the central San Joaquin Valley on the north side of Coalinga. The monoclinal structure is dipping approximately 20 to 30 degrees to the east. Because of this structure, many of the incompetent sedimentary formations that overlie the Big Blue (including the Santa Margarita, Jacalitos, and Etchegoin Formations) have formed landslides and badlands. These badlands are areas that support very little vegetation and are highly susceptible to erosion and mass wasting, making them of little use for agricultural and cattle grazing purposes. See Photos 107 through 111.

2. In the Salt and Martinez Creek areas, the Big Blue is well exposed in areas associated with hillside slumping. In these areas, the detrital serpentinite debris of the Big Blue has the same physical and textural characteristics as the serpentinite of the New Idria Formation and the asbestos tailings piles. In the Salt Creek area, the Big Blue has formed the nearly vertical, light bluish-gray sidewalls of a small gorge that is approximately 150 to 200 feet deep. See Photos 112 and 113.

Reproduced with permission of the copyright owner. Further reproduction prohibited without permission.

3. In some areas of the Cantua Creek drainage area, ancient landslides of the Big Blue are forming the streambanks of the intermittent Cantua Creek channel. Field observations show that during periods of high runoff, these streambanks are subject to erosion. See Photos 115 through 118.

4. The upland drainage area of the Cantua Creek watershed includes approximately seven square miles of the New Idria Formation outcrop on the northeast flank of Joaquin Ridge, including several mines and serpentinite debris flow complexes. Considering the size of this drainage area (slightly greater than the combined areas of the upper Pine Canyon and White Creek watersheds), this upland drainage area may be a very significant source of asbestos to the regional surface water pathway. Runoff from the Cantua Creek and Salt Creek alluvial channels is drained into the California Aqueduct through two permanently open concrete gates. See Photo 119. TEM analysis of water samples from the California Aqueduct show that there are asbestos sources upstream of the Arroyo Pasajero, and these source areas include the Salt and Cantua Creek drainage inlets to the Aqueduct.

Reproduced with permission of the copyright owner. Further reproduction prohibited without permission.

3.0 SUMMARY OF AERIAL PHOTOGRAPHY INCLUDING LOW TO MEDIUM ALTITUDE BLACK AND WHITE AND HIGH ALTITUDE COLOR INFRARED IMAGERY

Available aerial photographic images of Joaquin Ridge and the Coalinga region were reviewed on an historical basis for selected time periods dating from 1928 through 1987. The results of this review are presented in Appendices B and C which include images from seven series of aerial photographs from selected time periods from 1950 through 1987. These images are useful for illustrating the vast extent of geologic deposits of asbestos-containing serpentinite minerals in the Coalinga region and the extent to which these deposits have been affected by erosion associated with natural geologic processes and anthropic activities, including mining, milling, exploration, and road construction.

Interpretation of color infrared images of the Joaquin Ridge area and the Arroyo Pasajero regional watershed basin indicates that most of the asbestos in the Arroyo Pasajero surface drainage pathways has originated from the White Creek drainage area of the New Idria Formation. This conclusion is based on the interpretation of serpentinite reflectance characteristics on color infrared images integrated with results from asbestos analysis of surface samples from serpentinite soils, mine surfaces, tailings piles, and intermittent streambed sediment. The asbestos-containing serpentinite deposits have a bright bluish-white reflectance which enables the rapid identification of this material (Hunt and Russell, 1981). In images of the White Creek and Pine Canyon drainage areas of the New Idria Formation, the White Creek drainage pathway appears to have the same bright bluish-white reflectance characteristic as the serpentinite source areas. The Pine Canyon drainage pathway has a dull grayish-yellow reflectance characteristic which has a very low association with the signature

Reproduced with permission of the copyright owner. Further reproduction prohibited without permission.

reflectance characteristics of the serpentinite source areas in the Pine Canyon drainage area. Correlation of these reflectance characteristics with asbestos sampling results and field observations show that the White Creek drainage pathway has an abundance of asbestos-containing streambed sediment throughout its entire reach, and the Pine Canyon drainage pathway has limited pockets of asbestos-containing streambed sediment that are attenuated in their occurrence and concentration downstream from the serpentinite source areas. The streambed deposits of asbestos-containing streambed sediment in Pine Canyon are of limited dimensions and concentrations which do not allow their identification in color infrared images. See Appendix B for reproductions of aerial photography and color infrared images.

Appendix C includes a detailed summary of the submitted photographs and an annotated summary of reviewed images that date back to 1928. The pre-1950 images are generally only available for review in archival collections and their quality is generally not as good as the quality of images that post-date 1950. However, the pre-1950 images are useful for documenting the general surface conditions of the New Idria Formation outcrop area and the Arroyo Pasajero alluvial fan area prior to the initiation of significant mining activities that occurred from the 1940's through the 1970's.

Many of the attached photographs are high resolution, high altitude color infrared images that cover large areas (100 square miles or more per image). The color infrared images are particularly useful for documenting potential asbestos source areas because of the unique, bright bluish-white reflectance characteristic of the asbestos-containing serpentinite deposits. The high altitude images are also useful for illustrating the geographic and geologic relationship of the New Idria Formation's

Reproduced with permission of the copyright owner. Further reproduction prohibited without permission.

diapiric structure with exposed sedimentary serpentinite deposits such as the "Big Blue" on the western margin of the central San Joaquin Valley.

The attached aerial photographs include stereo pairs of low altitude black and white images and high altitude color infrared images that provide detailed coverage of the White Creek and Pine Canyon areas of Joaquin Ridge from the years 1986, 1981, 1979, 1973, 1971, 1957, and 1950. Collectively, these images are useful for illustrating the geologic and geographic relationship of the New Idria Formation's outcrop area (which forms the crest of Joaquin Ridge) with the surrounding region, encompassing the drainage pathways that lead from the outcrop areas to downstream depositional areas which include the Los Gatos Creek drainage pathway, the Pleasant Valley floodplain and the town of Coalinga, and the Arroyo Pasajero alluvial fan.

The submitted images of the White Creek and Pine Canyon drainage areas of the New Idria Formation are useful for documenting the post-1950's historical sequence of mining and milling activities in the Joaquin Ridge area, including the Atlas Mine and Mill Site (in the White Creek drainage area), the Johns-Manville Coalinga Asbestos Mill Site (in the Pine Canyon area), and other mining and exploration activities that occurred in the Joaquin Ridge area. These images are also useful for documenting surface conditions throughout the Joaquin Ridge area including: (1) the occurrence and extent of areas affected by erosion and mass wasting of the serpentinite outcrop area; and (2) the occurrence and extent of vegetated versus non-vegetated areas including estimates of percent vegetation covering. The images submitted with this report are also useful for evaluating anthropic and non-anthropic related changes in surface conditions in the serpentinite outcrop area of Joaquin Ridge.

Reproduced with permission of the copyright owner. Further reproduction prohibited without permission.

Interpretation of images from 1950 and 1981, integrated with information from field surveys, were used as a basis for mapping the above parameters including identification of areas affected by mining and other anthropic activities and identification of areas affected by natural erosion and mass wasting. These images were also used as a basis for mapping estimates of percent vegetation covering throughout the White Creek and Pine Canyon serpentinite outcrop areas and for mapping asbestos concentrations of asbestos-containing serpentinite source areas. The results of these mapping efforts are reported in Chapter Five, which presents the results of numerical modeling of erosion of asbestos-containing serpentinite deposits in the White Creek and Pine Canyon drainage areas of the New Idria Formation.

Some of the attached images also include coverage of the California Aqueduct from the Arroyo Pasajero region north to the San Luis Reservoir near Los Banos in Merced County. These images are useful for illustrating the Aqueduct's relationship with outcrops of additional potential asbestos source areas that are located north of the Arroyo Pasajero region. These areas include geologic outcrops of the Big Blue Member of the Temblor Formation and other sedimentary asbestos deposits that are exposed in uplifted geologic formations of the foothill mountains which form the western margin of the central San Joaquin Valley. The Aqueduct was generally constructed on the upper medial portions of the alluvial fans which have formed at the base of these foothill mountains and ridges. Runoff from some of the asbestos containing foothill drainage basins runs directly into the Aqueduct as an additional source of Aqueduct water.

The following observations are provided in detail in the Appendix C summary of the attached aerial photographs and are included here as a review. Detailed flight information including flight numbers, frame numbers, and image format (i.e., high

Reproduced with permission of the copyright owner. Further reproduction prohibited without permission.

altitude color infrared or low altitude black and white) is reported in Appendix C in conjunction with a sequential frame analysis for images from each included series.

Notable features in the high altitude, color infrared images include the New Idria Formation outcrop on the crest of Joaquin Ridge, the White Creek, Pine Canyon Creek, Los Gatos Creek drainage pathway leading to the town of Coalinga, out-crops of the asbestos-containing Big Blue Member of the Temblor Formation, other asbestos-containing sediments, and the alluvial fans that have formed on the western margin of the San Joaquin Valley. The images of Joaquin Ridge show the diapiric structure of the New Idria Formation's serpentinite deposit in conjunction with the close geographic relationship of the New Idria Formation, the "Big Blue," and the town of Coalinga, which is contained in a semi-enclosed basin formed by the Pleasant Valley floodplain.

Images of Joaquin Ridge show that the serpentinite matrix of the New Idria Formation has a bright bluish-white reflectance characteristic. Non-vegetated areas are particularly bright, and this characteristic facilitates identification of mines, tailings piles, and barren surfaces associated with geologic occurrences of gully erosion. This signature characteristic also facilitates the identification of hundreds of exploration pits and many miles of exploration access roads. In area that are vegetated, the restricted vegetation associated with the magnesium-rich serpentinite soils appears as a dark bluish-green surface that is readily differentiated from the vegetation associated with non-serpentine soils. The Johns-Manville Coalinga Asbestos Mill Site is located near the southeast margin of the serpentinite outcrop, and the Atlas Mine and Mill Site is located near the center of the serpentinite outcrop area that is drained by White Creek.

Reproduced with permission of the copyright owner. Further reproduction prohibited without permission.

Elongate barren areas are associated with naturally occurring gully erosion in steeply sloped drainage pathways in the New Idria Formation. Irregularly shaped, expansive barren areas are associated with mining operations and asbestos mill sites. Notable mines include the Atlas Mine and Mill Site, the Union Carbide Mine, the Gem Mine, the Big Ridge Mine, the Tromby Mines, the White Creek Magnesite Mine, the Archer Mine, the James-Corbett-Byles Mine, the Butler Estate Chromite Mine, the Jensen Mine, the Christie Mine, the Railroad Mine, and other un-named mines. Areas that appear as white dots are areas affected by exploration pits. Notable mill sites include the Atlas Mine and Mill Site in the White Creek drainage area and the Johns-Manville Coalinga Asbestos Mill Site in the Pine Canyon drainage area. Four to five abandoned chromite milling operations can be identified in the streambed of White Creek. These locations are associated with what appears as a sudden broadening of the White Creek stream-bed as a result of earthen dams that were constructed to retain water for the gravity settling chromite milling operations.

In all of the color infrared images, the White Creek streambed appears as a light bluish-gray ribbon that has the same reflectance characteristic as the barren serpentinite surfaces of the New Idria Formation and the "Big Blue". Close examination of the White Creek drainage pathway shows five areas where the streambed appears to widen. These are areas associated with chromite milling operations that were conducted along the banks of White Creek in the 1940's and 1950's. The tailings pile in the east fork of Pine Canyon Creek can be seen as a small sliver of white material that is located on the lower left margin of the New Idria Formation outcrop. Particularly notable is the absence of any light bluish-gray sediment marking the pathway of the Pine Canyon Creek. The visible path-way leading from the Johns-Manville Coalinga Asbestos Mill Site is a dirt road and not a streambed. This shows that very little asbestos-containing sediment is being

Reproduced with permission of the copyright owner. Further reproduction prohibited without permission.

transported through the Pine Canyon drainage pathway in comparison with White Creek.

Some of the high altitude, color infrared images feature the California Aqueduct and its relationship with the uplifted sedimentary formations that form the western margin of the San Joaquin Valley from the Cantua Creek region north to the O'Neill Forebay and San Luis Reservoir region in Merced County. Some of these sedimentary formations have reflectance characteristics which are similar to the reflectance characteristics of the "Big Blue". These formations have been mapped as being of the same age as the "Big Blue" (i.e., Miocene), and because of their close geographic and geologic relationships, some of these formations may have asbestos-containing sedimentary serpentinite deposits similar to that of the "Big Blue".

Some of the high altitude, color infrared images provide excellent coverage of the Arroyo Pasajero alluvial fan and the Pleasant Valley region, including the California Aqueduct near the town of Huron. These images show the braided terminus of the Arroyo Pasajero intermittent stream channel and the California Aqueduct blocking the eastward flow of sediment and floodwaters to distal alluvial fan environments. These images also show the entrenched meandering pathway of Los Gatos Creek as it flows to the east across the Pleasant Valley floodplain and across the structural axis of the Coalinga Anticline which is marked by a gap in the trend of Anticline Ridge and Guijarral Hills.

Reproduced with permission of the copyright owner. Further reproduction prohibited without permission.

4.0 CONCLUSIONS OF FIELD OBSERVATIONS AND INTERPRETATIONS OF AERIAL PHOTOGRAPHY

1. Field observations of the White Creek and Pine Canyon drainage areas of the New Idria Formation show that the serpentinite outcrop area is associated with a friable, platy, fractured matrix of weakly consolidated serpentinite. This asbestos-containing material is readily identifiable in aerial photographs because of the bright reflectance characteristics of the serpentinite minerals. Some of the serpentinite outcrop areas are associated with steep slopes that range up to 65 degrees. These steeply sloping surfaces are unstable and are subject to accelerated rates of naturally occurring (geologic) erosion and mass wasting. Most of the mass wasting is associated with the occurrence of gully erosion in conjunction with serpentinite landslide and debris flow deposits. The existence of these gullies and barren outcrop areas is apparent in historic (i.e., 1940's and 1950's) photographs which pre-date most mining activities in the White Creek and Pine Canyon drainage areas.

2. The serpentinite soils in outcrop areas have shallow, poorly developed profiles with a blocky structure and little vegetative cover. The serpentinite soils generally have a coarse, sandy matrix that is mostly composed of primary minerals (i.e., chrysotile asbestos). Some of the Pine Canyon deposits have developed deep, mature soil profiles that support a thick, grassy vegetative covering, with little or no visible evidence of asbestos-containing sediment. The development of these soils is probably a result of the net accumulation of soil materials and organic debris in conjunction with weathering phenomenon, possibly including the sub-surface flow of water from upgradient springs.

Reproduced with permission of the copyright owner. Further reproduction prohibited without permission.

3. Most of the asbestos in the Los Gatos Creek drainage pathway originated from the White Creek drainage area of the New Idria Formation. This is apparent from field photographs, reconnaissance aerial photographs and high altitude color infrared images. The White Creek channel is choked with asbestos-containing serpentinite debris throughout most of its length. This is in sharp contrast with the streambed sediment of Pine Canyon Creek which shows little evidence of asbestos-containing sediment downstream from the potential source areas in Upper Pine Canyon.

4. Downstream of the White Creek juncture with Los Gatos Creek, the asbestos concentration of the Los Gatos Creek streambed sediment visually appears to decrease to very low levels in comparison with the streambed sediment of White Creek. On the east side of the town of Coalinga downstream from the juncture of Los Gatos Creek with Warthan Creek, there is little or no visible evidence of asbestos in the Los Gatos Creek streambed sediment. This appears to be the result of dilution with sediments derived from the Warthan Creek drainage area. The lack of coarser-grained sediment in alluvial fan deposits may be a result of tectonic uplift associated with the structural axis of the Coalinga Anticline. Uplift of this anticline has significantly reduced the streambed hydraulic gradient in the Pleasant Valley floodplain, reducing the stream's capacity to transport sand-sized (and coarser) sediment.

5. The post-1970 photographs include high altitude, color infrared imagery. Because of the bright bluish-white reflectance characteristic of the serpentinite minerals, these photos are particularly useful for documenting the occurrence and distribution of serpentinite deposits throughout the Coalinga region, including the New Idria Formation, the White Creek-Los Gatos Creek drainage pathway, and some of the sedimentary serpentinite deposits of the Diablo Range foothills on the western margin of the central San Joaquin Valley. Some of the photos also show the occurrence of

Reproduced with permission of the copyright owner. Further reproduction prohibited without permission.

sedimentary serpentinite deposits such as the "Big Blue", which outcrops on the north side of Coalinga and in the foothills adjacent to the California Aqueduct.

6. In the Joaquin Ridge area, the high altitude, color infrared images feature the New Idria Formation and a bright ribbon of sediment in the White Creek drainage pathway that has the same reflectance characteristic as the New Idria Formation's serpentinite outcrop area and the serpentinite deposits of the "Big Blue". No other drainage pathways have the same, bright bluish-white reflectance characteristic. This suggests that the Pine Canyon drainage pathway has transported very little serpentinite debris in comparison with White Creek. These images suggest that the White Creek drainage pathway is the major source of waterborne asbestos to the Arroyo Pasajero watershed. Downstream of the juncture with White Creek, the bright reflectance characteristic of the streambed sediment in Los Gatos Creek appears to be attenuated, and this is probably from dilution and mixing of the asbestos-containing streambed sediment with sediment derived from non-asbestos sediment source areas.

Reproduced with permission of the copyright owner. Further reproduction prohibited without permission.

5.0 REFERENCES

Boyle Engineering, Corporation. 1988. Draft Summary Letter Report for Hydrologic Analysis: Arroyo Pasajero Drainage and Sediment Control Plan.

Cowan, Darrel S., and Mansfield, Charles F. 1970. Serpentinite Flows on Joaquin Ridge, Southern Coast Ranges, California: Geological Society of America Bulletin, vol. 81: p 2,615-2,628.

Dibblee, T. W. 1971. Geologic Map of the New Idria Quadrangle, California-Open File Map. Reston, Va.: U.S. Geologic Survey.

Eckel, E. B., and Myers, W. B., 1946. Quicksilver Deposits of the New Idria District, San Benito and Fresno Counties, California: California Journal of Mines and Geology, vol. 42: 81-124.

Levine-Fricke. May 9, 1989. "Off-Site Source Characterization, Regional Soil Sampling, and Watershed Modeling Report".

Matthews, R. A. 1961. Geology of the Butler Estate Chromite Mine, Southwestern Fresno County, California: California Division of Mines and Geology, Special Report No. 71, 20 pp.

Munn, John R.; Busacca, Alan J., and Trott, Kenneth E. 1981. California Aqueduct Sedimentation Study for the Arroyo Pasajero and Tributary Watersheds: California Department of Conservation, 72 pp.

Reproduced with permission of the copyright owner. Further reproduction prohibited without permission.

U.S. Department of Agriculture, Soil Conservation Service. 1987. Unpublished - Soil Survey, Western Fresno County, California

U.S. Geological Survey. 1984. Santa Rita Peak Quadrangle, 7.5 Minute Topographic Map. Reston, Va: U.S. Geological Survey.

Reproduced with permission of the copyright owner. Further reproduction prohibited without permission.

CHAPTER FOUR

MACROSCOPIC AND MICROSCOPIC CHARACTERISTICS OF COALINGA CHRYSOTILE ASBESTOS DEPOSITS

1.0 INTRODUCTION AND SUMMARY

This chapter provides an overview of the macroscopic and microscopic characteristics of the chrysotile asbestos deposits of the New Idria Formation in the Coalinga region.

A comprehensive report of the petrographic and mineralogical characteristics of the chrysotile deposits of New Idria Formation has been published by Mumpton and Thompson (Mineralogy and Origin of the Coalinga Asbestos Deposit: Clays and Clay Minerals, 1975, vol. 23: 131-143). Mumpton and Thompson analyzed more than 2600 samples including approximately 500 samples collected from the surface and/or near surface weathering zone and approximately 2100 drill core subsurface samples. Their analyses included petrographic studies; X-ray powder diffraction studies; and electron microscope studies. Additional mineralogical assessments of the New Idria serpentinite deposits have been presented by Eckel and Meyers (Quicksilver Deposits of the New Idria District, San Benito and Fresno Counties, California: California Journal of Mines and Geology, 1946, vol. 42: pp. 81-124); Coleman (Mineralogy and Petrology of the New Idria District, California: Ph.D. Dissertation, Stanford University, 1957); and Fowkes (An Educational Guidebook to the Geologic

Reproduced with permission of the copyright owner. Further reproduction prohibited without permission.

Resources of the Coalinga District: West Hills College, Coalinga, California, 260 pp, 1982).

Except for hydrothermally altered marginal contacts, most of the New Idria Formation is composed primarily of an unconsolidated matrix of a suite of soft, flakey serpentinite minerals including lizardite, antigorite, and chrysotile. Macroscopically, the serpentinite appears to be formed primarily of platey agglomerates representative of the antigorite species of serpentinite. Microscopic analyses including polarized light microscopy and transmission electron microscopy indicate that when dissagregated, the apparent platey polymorphs are formed of a fibrous mineral identified as chrysotile asbestos.

The semi-plastic serpentinite matrix includes large blocks and boulders of serpentinized peridotite and dunite and a suite of accessory minerals including disseminated grains of chromite and magnesite. The flakey matrix is pervasive and visually forms as much as 80% to 90% of the serpentinite deposit. Chemically, asbestos ore from the formation is generally homogeneous with a recoverable asbestos fiber content ranging from 35 to 74% (Mumpton and Thompson, 1975, pp. 132 and 135).

As reported by Mumpton and Thompson (1975, pp. 134 - 135) and as generally observed in the field in the asbestos mining areas:

"The Coalinga asbestos ore is a mixture of several physically different types of serpentine materials, with gradations between the types being the rule rather than the exception. The four main types of material are: (1) hard, dense, dark-blue and green fragments of blocky serpentinite, ranging from fractions of an inch to tens of feet in

Reproduced with permission of the copyright owner. Further reproduction prohibited without permission.

diameter; (2) large, tough, leathery sheets of matted chrysotile, resembling mountain leather, up to several square feet in size; (3) small, brittle, bladed and platy fragments of green serpentine, up to several square inches in size; and (4) soft, friable greenish-white agglomerates of flakey asbestos, varying from about 1/4 to 1 inch diameter, and containing small quantities of both the green-bladed material and the hard, dense, serpentinite rock fragments."

A mixture of Type 3 and Type 4 material is illustrated in the photograph of Figure 4-1. A large sheet of "mountain leather" that measures up to 5 inches in length is illustrated in the photograph of Figure 4-2. .

Based on field observations of this investigations and as reported by others, the soft, friable greenish-white agglomerates of flakey asbestos generally makes up the bulk of the ore encountered in the primary chrysotile mining areas, particularly in the southeastern third of the outcrop area in the Los Gatos Creek drainage area. There appears to be a remarkable consistency of this material throughout the investigated area.

The great bulk of the New Idria serpentinite has been highly sheared and pulverized and consists of soft, friable sheets and clumps of asbestiform material admixed with a fine serpentine powder. The friable ore has little strength or coherence and crumbles with a touch. Hard, dense competent masses of serpentinite, ranging from fractions of an inch to tens of feet in diameter, are scattered throughout the body and stand out as resistant knobs and ridges. Many are rounded and take the shape of resistant boulders encased in softer, friable material.

Reproduced with permission of the copyright owner. Further reproduction prohibited without permission.

Additional minerals that have been reported associated with the New Idria Formation include ankerite, magnetite, magnesite, limonite, diopside, topazalite, andradite garnet, melanite garnet, uvarite garnet, spessarite garnet, metacinnabar, cinnabar, marcasite, pyrite, quartz, calcite, chromite, kammerite, syenite, amphibole, glaucophane, mica, chrysocolla, and silicified carbonates (Eckel and Myers, 1946; Coleman, 1957; and Fowkes, 1982, pp. 137-167).

In the vicinity of the White Creek and Pine Canyon drainage areas, the New Idria Formation is mostly composed of a highly fractured matrix of flakey serpentinite minerals. Chrysotile is the principal matrix component and forms the bulk of the highly sheared, pulverized, flakey matrix. In addition to serpentine minerals, the deposit has been reported to contain up to 7% brucite, with an approximate formula of $(Mg_{10}Fe_2)(OH)_{24}$, and minor quantities of magnetite, calcite, chromite, and uvarovite (titanium) garnet (Mumpton and Thompson, 1975). As suggested by Mumpton and Thompson (1975, p. 141), the occurrence of brucite may be related to the transformation of an olivine rich dunite plus water to form serpentinite plus brucite with an attendant increase in rock volume of approximately 40%. This increase in volume has likely contributed to the diapiric structure of the New Idria deposit and other serpentinite deposits in the central Coast Range Diablo Range mountains.

In some areas of the New Idria deposit, as in the Butler Estate Chromite Mine, lenticular layers may contain up to 25% disseminated chromite ore (Matthews, 1961). Other minerals (including mercury-bearing cinnabar and metacinnabar) are found in hydrothermally altered deposits associated with the faulted margins of the New Idria Formation with the surrounding sedimentary country rock of the Panoche Formation (Cretaceous) and Franciscan assemblage (Jurassic - Cretaceous).

Reproduced with permission of the copyright owner. Further reproduction prohibited without permission.

Weathering Characteristics

The surface weathering zone of the New Idria serpentinite extends to a depth of approximately 20 to 30 feet. In this reddish-brown zone, portions of the serpentinite have been transformed into brown crumbly masses surrounded by tan or grayish-white friable asbestos ore.

On fresh exposures including mine surfaces, serpentinite ore storage piles, and tailings piles, the serpentinite has a well-developed crust from the precipitation of hydromagnesite. The hydromagnesite is precipitated to form a durable, "caliche-like" cemented crust resistent to wind erosion and erosion from rain drop impacts and minor sheet and rill erosion from surface run-off. The hydromagnesite is precipitated as a result of the upward movement and surface evaporation of magnesium-rich groundwater. This crust appears to be limited to fresh exposures and was not generally observed on naturally weathered and undisturbed surfaces.

Reproduced with permission of the copyright owner. Further reproduction prohibited without permission.

2.0 PHYSICAL AND CHEMICAL CHARACTERISTICS OF CHRYSOTILE ASBESTOS

Chrysotile asbestos forms soft, silky fibers that have a layered silicate structure. It's ideal chemical formula is $[Mg_6Si_4O_{10}(OH)_8]$. This allows substitution not only in the X and Y positions in an ideal formula of $X_6Y_4O_{10}(OH)_8$ but also in the positions allocated to OH where F and Cl may enter (Faust and Fahey, 1962, p. 2). X represents atoms in the octehedral coordination that may include primarily magnesium and also nickel, cobalt, manganese, ferrous iron, zinc, chromium, and titanium; and Y represents primarily silicon (Faust and Fahey, 1962, p. 1). Substitution may involve Al for Si or Al or Fe (2+ or 3+) for Mg. The hydrous magnesium silicate structure consists of double layers, each consisting of a layer of linked SiO_4 tetrahedra that are coordinated to a second layer of linked $MgO_2(OH)_4$ octahedra through the sharing of oxygen atoms. This structure is recognized as trioctahedral structure (Faust and Fahey, 1962). Three species of serpentinite are generally recognized including lizarditie, antigorite, and chrysotile. These species are recognized by some workers as being a solution series (Faust and Nagy, 1967). Three species of chrysotile are recognized including orthochrysotile, clinochrysotile, and parachrysotile (Whittaker and Zussman, 1956). In the chrysotile polymorph, the composite layer rolls up to form long hollow tubes (or fibrils), possibly as a result of uneven charges in the crystal structure layers. The diameters of the individual tubes are approximately 25 nanometers; the length-to-diameter ratio can vary from approximately 5:1 to well over 10,000:1. (W. McCrone, 1980, p.5).

The anthropic chrysotile asbestos found at the Johns-Manville Coalinga Asbestos Mill Site consists of milled and unmilled ore. The unmilled ore consists of soft, friable greenish white aggregates that can contain up to 30% to 70% commercially

Reproduced with permission of the copyright owner. Further reproduction prohibited without permission.

recoverable chrysotile. When dried, this material breaks up readily into a fine powder, containing flakes of matted chrysotile and small particles of hard, gritty serpentinite (Mumpton and Thompson, 1975, p. 137).

Reproduced with permission of the copyright owner. Further reproduction prohibited without permission.

3.0 POLARIZED LIGHT MICROSCOPE CHARACTERISTICS OF COALINGA CHRYSOTILE DEPOSITS

The bulk soil samples from the New Idria Formation and other chrysotile asbestos source areas in the Coalinga region are different from the asbestos products routinely analyzed by analytical testing laboratories. The bulk soil sample matrices tend to be more complex and the minerals present within these samples have been found to exhibit certain properties which make chrysotile identification non-routine. The serpentine minerals associated with these samples appear to include chrysotile, antigorite, and lizardite. These serpentine minerals may have the same basic chemical composition but different crystal structures (i.e., platey versus fribrous) which may result from a regular pattern of substitution and/or octahedral coordination in the lattice framework (Faust and Fahey, 1962).

In the New Idria Formation, most of the chrysotile asbestos macroscopically, visually appears as lizardite and/or antigorite forms of serpentine. These polymorphs macroscopically appear as small white chips and platelets and as pale green lath-shaped minerals. Using a binocular scope, these chips, platelets, and lath-shaped minerals were observed to be composed of a material that was easily fibrillated upon slight crushing. Using the PLM method, some of this material was readily confirmed as chrysotile asbestos and some of the material appeared as a fibrous form of antigorite. Using the TEM method, most of the fibrous material was confirmed as chrysotile asbestos based on identification of a cylindrical crystal structure (Med-Tox Associates, 1988). Macroscopically, the chrysotile asbestos was observed to be aggregated as plate and lath-shaped bundles.

Reproduced with permission of the copyright owner. Further reproduction prohibited without permission.

3.1 Non-Standard Optical Properties

Both Med-Tox Associates of San Diego, California and McCrone Environmental Services of Norcross, Georgia were subcontracted to conduct preliminary evaluations of the microscopic characteristics of chrysotile samples collected from the New Idria Formation. Both of the subcontractors noted in their preliminary evaluations that when these samples were analyzed by PLM-dispersion staining (a standard asbestos particle identification technique based on the difference between the dispersion of the refractive index for a particle and the liquid medium in which the particle is immersed), many of the fibers displayed a greater range of optical properties than normally associated with standard chrysotile asbestos. As reported by Walter C. McCrone (The Asbestos Particle Atlas, 1980), chrysotile is normally associated with distinctive fine flexible, curly fibrils and bundles of fibrils with distinctive dispersion staining colors, usually blue-magenta parallel to the fiber axis. Chrysotile in the New Idria Formation samples had optical properties more like fibrous antigorite (i.e., picrolite) than normal chrysotile. Many of the fibrils appeared in lath-shaped and platelet-shaped bundles that had a wider range of dispersion colors. Subsequent analyses of these samples by TEM (with analyses conducted by Med-Tox Associates) identified most of the elongate serpentine minerals to be chrysotile. Consequently, the laboratories have qualified their analytical reports by characterizing the chrysotile asbestos concentrations as serpentine asbestos (McCrone) or elongate serpentine asbestos (Med-Tox). Preliminary petrographic reports by McCrone (1988) and by Med-Tox (1988), including a series of photomicrographs of the New Idria Formation's chrysotile asbestos deposits, are included in Appendix D.

Black and white microphotographs that were taken as part of my contribution to this project are attached as Figures 4-3 to 4-16. The microphotographs of the chrysotile

Reproduced with permission of the copyright owner. Further reproduction prohibited without permission.

particles illustrate the bladed and platelet characteristics of the antigorite (as picrolite) and lizardite polymorphs that have been observed as the predominant form of chrysotile in the New Idria Formation deposits. When fully disaggregated, these bladed and platelet aggregates of serpentinite are found to consist of mostly fibrous chrysotile asbestiform particles as identified using TEM analyses as reported by Med-Tox Associates. Some of the photographed particles display all three serpentinite polymorphs including lizardite, antigorite, and chrysotile as illustrated in Figures 4-5 and 4-7. This microscopic observation illustrates the close relationship of the three serpentinite polymorphs in the chrysotile deposits of the New Idria Formation. This microscopic relationship also reinforces the macroscopic observations of lath-shaped bundles and platelet-shaped particles that make up the bulk of the region's chrysotile deposits.

3.2 Results of Detailed Petrographic Analyses for Identification of Particular Source Areas

Detailed petrographic characterization analyses of 12 bulk soil samples from the Pine Canyon drainage area were completed with the purposes of defining the physical, morphological, and mineralogical characteristics of asbestos-containing serpentinite materials from particular source areas including:

PG-1	Railroad Mine - Central Deposit
PG-2	East Fork Upstream of Tailings Pile
PG-3A	West Fork Upstream of Diversion Channel
PG-3B	West Fork Tributary Downstream from Butler Mine
PG-4	Unprocessed Asbestos Ore
PG-5	Tailings Pile - Processed Ore

Reproduced with permission of the copyright owner. Further reproduction prohibited without permission.

PG-7	Lower Pine Canyon Creek - Channel Sand Deposit
PG-8A	White Creek - Channel Gravel Deposit
PG-8B	White Creek - Channel Sand Deposit
OC-17	New Idria Formation - Outcrop Sample - Atlas Mine Surface
OC-24	New Idria Formation - Outcrop Sample - Butler Mine Surface
OC-28	New Idria Formation - Outcrop Sample - Jensen Mine Surface

These samples were analyzed by McCrone Environmental Services (1988) to identify, if possible, parameters which might be used to distinguish asbestos from various source areas (i.e., processed tailings material versus unprocessed ore sampled from an exposed mine surface). The results from this investigation are discussed below with the results of laboratory analyses including photo-documentation and summary tables presented in Appendix D. (See Asbestos Laboratory Report, McCrone Environmental Services, May 4, 1988).

The asbestiform minerals associated with the New Idria Formation include chrysotile and chrysotile polymorphs of antigorite and lizardite. Petrographic analyses have demonstrated that these serpentinite minerals have non-standard physical and optical properties. Macroscopically, these minerals generally appear as grayish-white matted plates and/or pale green elongate grains of lath-shaped minerals which become fibrous upon crushing.

Most of the chrysotile and apparent lizardite and antigorite minerals occur in the sand-sized fraction (i.e., 0.05 to 2.0 mm) of the bulk samples. When these samples were analyzed with a polarized light microscope with dispersion staining, preliminary indications were that many of the fibrous minerals exhibited optical properties more like fibrous antigorite (i.e., picrolite) than chrysotile asbestos. However, subsequent

Reproduced with permission of the copyright owner. Further reproduction prohibited without permission.

analysis of the samples with transmission electron microscopy (TEM) verified that most of the elongate serpentine minerals were in fact chrysotile.

As reported by McCrone, the serpentine asbestos of the 12 samples generally consisted of plates of matted fibers which became more fibrous with crushing. The analyzed samples also contained green elongated grains of massive serpentine which also became fibrous when crushed. Associated minerals included magnetite, carbonate, mica, and aggregates of unidentified sub-microscopic particles that are probably clumps of clay. The streambed sediment samples were also observed to contain grains of quartz and feldspar which were probably derived from natural erosion of the sandstones and shales of the Panoche Formation (Cretaceous) which flanks the New Idria Formation diapiric serpentinite deposit.

Based on the petrographic analysis of microscope samples, McCrone determined that neither asbestos morphology or associated mineralogy appeared to be effective parameters for distinguishing the source areas of particular asbestos samples. McCrone did note a decrease in grain size of tailings versus unprocessed ore. However, McCrone reported that this observation could not be extended to the interpretation of streambed sediment because of the tendency towards mechanical grain size reduction during waterborne transport. Thus, it does not appear to be possible to relate downstream asbestos-containing sediments to any specific upstream source areas.

Reproduced with permission of the copyright owner. Further reproduction prohibited without permission.

4.0 RESULTS OF X-RAY DIFFRACTION ANALYSIS

A typical mine surface sample was analyzed using x-ray diffraction. The results of the x-ray diffraction analysis are presented in Figure 4-17. The results indicate that the predominate serpentinite polymorph present in the analyzed sample is antigorite. (See Brindley and Brown, 1980: Table 1.4 - X-ray powder data for serpentinite minerals). This is in agreement with field observations and macroscopic observations of a friable mineral matrix of platy agglomerates that range from 1/4 inch in diameter to a fine powder. When observed using PLM, these platy agglomerates appeared as a fibrous form of antigorite known as picrolite. Close PLM analyses of the platey particles often revealed splintering of fine fibrils and/or bundles of fine fibrils on the ends of the particles. Subsequent TEM analyses of these types of samples have shown that the splintery particles as well as the platey particles, when fully disaggregated, are classified as chrysotile asbestos by the USEPA on the basis of asbestiform, cylindrical crystal structures with aspect ratios (i.e., length to width) of 1 to 3 or greater. The results of the x-ray diffraction analysis of a typical serpentinite sample conducted for this project further confirms the close relationship between the antigorite and chrysotile polymorphs of the Coalinga region's serpentinite deposits. The relationship and/or predominance of the identified serpentinite polymorphs of the New Idria Formation deserves further investigation.

Reproduced with permission of the copyright owner. Further reproduction prohibited without permission.

5.0 REFERENCES

Brindley, G. W., and Brown, G. 1980. Crystal Structures of Clay Minerals and Their X-Ray Identification: Mineralogical Society Monograph No. 5: London, England.

Coleman, R. G. 1957. Mineralogy and Petrology of the New Idria District, California: PhD thesis, Stanford, California.

Eckel, E. B., and Myers, W. B., 1946. Quicksilver Deposits of the New Idria District, San Benito and Fresno Counties, California: California Journal of Mines and Geology, vol. 42: 81-124.

Faust, George T., and Fahey, Joseph J., 1962. The Serpentine Group of Minerals: Studies of the Natural Phases in the System MgO-SiO_2-H_2O and the Systems Containing the Cogeners of Magnesium: Geological Survey Professional Paper 384-A, 92 p.

Faust, George T., and Nagy, Bartholomew S., 1967. Solution Studies of Chrysotile, Lizardite, and Antigorite: Geological Survey Professional Paper 384-B, 13 p.

Fowkes, E. J. 1982. An Educational Guidebook to the Geologic Resources of the Coalinga District: West Hills College, Coalinga, California, 260 pp.

Matthews, R. A. 1961. Geology of the Butler Estate Chromite Mine, Southwestern Fresno County, California: California Division of Mines and Geology, Special Report No. 71, 20 pp.

Reproduced with permission of the copyright owner. Further reproduction prohibited without permission.

McCrone Environmental Services, Inc. September 24, 1987. Preliminary Investigation Asbestos Analysis Report.

McCrone Environmental Services, Inc. October 8, 1987. Preliminary Asbestos Analysis Photodocumentation Report.

McCrone Environmental Services, Inc. May 4, 1988. Asbestos Analysis and Photodocumentation Report.

McCrone, Walter C. 1980. The Asbestos Particle Atlas: Ann Arbor Science Publishers, Inc.: Ann Arbor, Michigan. 122 pp.

Med-Tox Associates, Inc. June 3, 1988. Memorandum: Points of Clarification on PLM and TEM Asbestos Analyses of Soils

Mumpton, F. A., and Thompson, C. S. 1975. Mineralogy and Origin of the Coalinga Asbestos Deposit: Clays and Clay Minerals, vol. 23: 131-143.

Whittaker, Eric J., and Zussman, Jack, 1956. The Characterization of Serpentine Minerals by X-Ray Diffraction: Mineralogica Magazine, vol. 31, pp. 107-126.

Reproduced with permission of the copyright owner. Further reproduction prohibited without permission.

CHAPTER FIVE

RESULTS OF REGIONAL SOIL SAMPLING AND ASBESTOS ANALYSIS PROGRAM

1.0 INTRODUCTION

This chapter provides a summary of the results of the regional soil sampling and asbestos analysis program that was conducted under my supervision and management as part of the Levine-Fricke (May 9, 1989) investigation. This program included the laboratory analysis for chrysotile asbestos content of samples collected from potential asbestos source areas located within the Arroyo Pasajero watershed basin and other potential asbestos source areas in the Coalinga region. The sampled potential asbestos sources included naturally occurring outcrop areas; mine site areas; mill site areas including ore storage piles and tailings piles; stream pathway sediment deposits; and alluvial fan surface and subsurface deposits. The sampling program also included the asbestos analysis of samples collected from the well-exposed (and nearly vertical) stream banks of an entrenched channel section of the lower Arroyo Pasajero drainage pathway. The sampling station locations and potential source areas were identified as a result of my regional field and aerial reconnaissance investigations as reported in Chapter Three.

The analytical program included analyses of 385 bulk soil and/or sediment samples for evaluation of chrysotile asbestos content using EPA approved PLM (Polarized Light Microscopy) and TEM (Transmission Electron Microscopy) analytical methods. The PLM and TEM analyses were conducted by two EPA-approved asbestos analytical

Reproduced with permission of the copyright owner. Further reproduction prohibited without permission.

laboratories including McCrone Environmental Services of Norcross, Georgia and Med-Tox Associates of San Diego, California.

The soil sampling and asbestos analytical programs were designed to provide data for an asbestos soil erosion numerical modeling program to evaluate the relative contributions of identified potential asbestos source areas including natural outcrop areas and anthropically (man-made) disturbed areas including asbestos mine and mill site areas. The results of the asbestos soil erosion modeling program are summarized in Chapter Six.

1.1 Purpose and Scope of Soil Sampling and Asbestos Analysis Program

The regional soil sampling and asbestos analysis program was designed to provide data regarding the asbestos content and other soil characteristics of asbestos-containing materials at mill sites, mining sites, naturally occurring asbestos outcrop areas and other asbestos bearing and non-asbestos bearing areas in the Arroyo Pasajero watershed and adjoining potential asbestos source areas.

The soil sampling and asbestos analysis program included collection and analysis of approximately 35 samples collected from the New Idria Formation outcrop area including mine and mill sites; 40 stream pathway samples; and 45 alluvial fan surface and/or subsurface samples. An additional 202 samples were collected and analyzed from the Johns-Manville Coalinga Asbestos Mill Site area as part of that site's remedial investigation. The location and analytical results of regional asbestos sampling stations are illustrated in Figures 5-1 through 5-4. The location and results of samples collected from the Johns-Manville Coalinga Asbestos Mill Site are illustrated in Levine-Fricke, May 9, 1989: Chapter 2, Figures 3 and 4.

Reproduced with permission of the copyright owner. Further reproduction prohibited without permission.

Information obtained from this soil sampling and analytical program was used for development of numerical modeling estimates of relative asbestos contributions to the regional Arroyo Pasajero watershed environment and the California Aqueduct. The numerical modeling work was conducted to provide estimates of the relative contributions by erosion from various mill sites and mining sites in comparison to other "natural" sources of asbestos in the ultramafic and sedimentary outcrop potential source areas located in the watershed. The results of the numerical modeling work are summarized in Chapter Six.

The regional sampling program was designed to focus on: (1) sampling of asbestos-bearing soils from the New Idria Formation and other geologic sources including the Big Blue Member of the Temblor Formation (Miocene); (2) sampling of asbestos-bearing materials at mine and mill sites; (3) sampling of streambed sediment from tributaries throughout the Arroyo Pasajero watershed basin with emphasis on the Los Gatos Creek sub-basins that drain the New Idria Formation; and (4) sampling of subsurface alluvial fan sediment that was deposited prior to the initiation of large-scale mining activities in the Joaquin Ridge area. The sampling program also included the collection and analysis of samples from non-asbestos bearing geologic units and deposits for confirmation purposes and for use in the modeling effort.

The regional soil sampling and asbestos analytical program included the following activities:

- Sampling of potential asbestos source materials to characterize the extent of asbestos in areas affected by human activities (i.e., mining spoils and dumps, mill tailings, and road surfaces, etc.).

Reproduced with permission of the copyright owner. Further reproduction prohibited without permission.

- Sampling of potential asbestos source materials at locations unaffected by human activities (i.e., natural outcrop areas of the New Idria Formation and the Big Blue Member of the Temblor Formation).

- Sampling of soils and sediments in the Arroyo Pasajero alluvial fan and the settling basin constructed adjacent to and upslope of the California Aqueduct. The alluvial fan and settling basin sampling programs included sampling of continuously cored soil borings which provided a basis for establishing the background asbestos concentrations of subsurface sediments deposited prior to the initiation of asbestos-mining activities in the early 1960's and chromite mining in the 1940's.

- Laboratory analysis of soil and sediment samples using EPA-approved polarized light microscopy (PLM) and transmission electron microscopy (TEM) methods for measurement of percent asbestos content. Some samples were also analyzed for particle size distribution and organic matter content for use in the watershed modeling program.

- Interpretation and/or correlation of analytical results of samples analyzed by both PLM and TEM methods.

- Field classification and description of soil texture, color, structure, particle size distribution, plasticity, mineralogy and visible evidence of asbestos.

- Qualitative correlation of soil sampling asbestos analytical results with field observations and interpretation of aerial photography as summarized in Chapter Three.

Reproduced with permission of the copyright owner. Further reproduction prohibited without permission.

Most of the samples for asbestos analysis were collected over a four-month period. Alluvial fan subsurface samples were collected in December of 1987 and most of the streambed, mine and mill site, and outcrop area samples were collected in February and March of 1988. As a result of project planning, I was able to personally collect all of the alluvial fan surface, subsurface, and exposed streambank samples; mine and mill site samples; and outcrop area samples. In order to speed up the collection of sediment samples from the stream pathways toward the end of the sampling program, I directed the work of two sampling teams. One of the sampling teams collected samples from the lower reaches of the Arroyo Pasajero drainage system in the vicinity of Coalinga and Pleasant Valley. The second team which, included myself, collected stream sediment samples from the upper reaches of the White Creek and Pine Canyon drainage pathways near the identified potential source areas. I identified sampling locations on USGS quadrangle topographic maps in advance of actual sample collection. I identified these locations on the basis of my field and aerial reconnaissance investigations as discussed in Chapter Three. Notes were made on USGS topographic maps to further indicate and/or confirm specific sampling locations at the time of sampling.

1.2 Summary Observations and Conclusions

The results of the regional soil sampling and asbestos analysis program provide a basis for the following observations and/or conclusions.

-- The results of laboratory analyses of asbestos-bearing materials in the mine and mill site areas, outcrop areas, and stream pathways generally confirm field observations and interpretations of color/infrared aerial photographs of the occurrence of asbestos-containing materials; particularly were asbestos is present in

Reproduced with permission of the copyright owner. Further reproduction prohibited without permission.

concentrations of 10% or more. This is to say that in areas were the concentration of asbestos is approximately 10% or greater, such deposits can be identified in the field or in interpretation of aerial photography - particularly in color/infrared imagery.

-- Outcrop areas identified as serpentinite or serpentine soils associated with the New Idria Formation in the upper Pine Canyon and White Creek watersheds have an average chrysotile asbestos concentration of 84% (using the polarized light microscopy estimate of percent area asbestos reported as elongate serpentine asbestos as previously defined). Undisturbed and anthropically affected serpentinite materials (e.g., open-pit mines) have essentially the same asbestos concentration as the undisturbed outcrop areas, i.e., approximately 84%.

-- Soil samples obtained from the Big Blue Member of the Temblor Formation, a sedimentary deposit located approximately 10 miles north of the town of Coalinga, have an average elongate serpentine asbestos concentration of 66%, consistent with geologic observations regarding this detrital serpentinite formation.

-- Field observations and laboratory analyses of streambed sediments indicate that White Creek, which drains approximately 5.8 square miles of the New Idria Formation, is the primary channel for the surface water erosion of asbestos within the Arroyo Pasajero watershed. White Creek sediments generally contain between 60 and 85% elongate serpentine asbestos.

-- There is little visible evidence of asbestos in the lower reaches of the Pine Canyon drainage pathway and this observation is supported by the results of laboratory analyses. Asbestos concentrations of Pine Canyon Creek sediment range from 85% to trace levels (i.e., less than 1%). The highest concentrations are generally found in the

Reproduced with permission of the copyright owner. Further reproduction prohibited without permission.

Pine Canyon streambed deposits located closest to the outcrop and/or mine and mill site locations. The concentration of asbestos-bearing sediment in Pine Canyon Creek generally decreases with respect to distance downstream from upland serpentinite source areas. White Creek has sediments containing concentrations of approximately 60% at the confluence with Pine Canyon Creek where Pine Canyon Creek sediments in the same area have only trace asbestos concentrations.

-- Asbestos-bearing materials in the tailings pile in the east fork of Pine Canyon Creek at the Johns-Manville Coalinga Asbestos Mill Site have an average asbestos concentration of 64%. Field observations of streambed sediment show that the presence of a sediment trapping dam at the base of the tailings pile has been effective in limiting the downstream transport of asbestos originating from the Johns-Manville Coalinga Asbestos Mill Site, particularly from the site's tailings pile.

-- Pine Canyon Creek drains into White Creek, which in turn drains to Los Gatos Creek. Eventually, Los Gatos Creek becomes the Arroyo Pasajero. Sediment sample analyses from this drainage pathway indicate that asbestos concentrations decrease steadily to trace levels with respect to distance downstream from the outcrop areas. This reduction in asbestos concentrations is apparently a result of the dilution of asbestos materials with non-asbestos containing sediments from other tributaries to Los Gatos Creek (e.g., Warthan, Jacalitos, and Zapato-Chino Creeks) and possibly as a result of the deposition of asbestos-containing sediments in portions of the Los Gatos Creek channel upstream of the Arroyo Pasajero.

-- Analyses of surface and subsurface samples obtained from continuously cored soil borings within the Arroyo Pasajero alluvial fan indicate that sediments deposited during pre-mining and post-mining time periods have asbestos concentrations which

Reproduced with permission of the copyright owner. Further reproduction prohibited without permission.

have similar average concentrations, i.e., approximately 1% or less, and are not statistically significantly different from each other.

-- Analysis of sediment samples collected from the near-vertical stream bank exposures of unconsolidated Quaternary alluvial fan sediments - exposed along the entrenched sections of the lower Arroyo Pasajero channel - had approximately the same concentration of asbestos as present day alluvial fan sediment (i.e., approximately 1%).

-- Laboratory analyses have indicated that PLM analyses of the region's chrysotile asbestos deposits are non-routine in that the analyzed samples display a wide range of optical characteristics than is normally encountered in the analysis of "standard" types of chrysotile asbestos. As discussed in Chapter Three, this may be a result of the occurrence of serpentinite polymorphs including antigorite, lizardite, and chrysotile. When disaggregated and analyzed using TEM methods, most of this material is identified as chrysotile asbestos based on the occurrence of asbestiform structures.

-- There is little correlation with PLM and TEM results of analyses for samples with concentrations of asbestos that exceed 1%. For samples with concentrations of asbestos that exceed 1%, the PLM method appears to provide the most accurate analytical data of asbestos concentrations.

Reproduced with permission of the copyright owner. Further reproduction prohibited without permission.

1.3 Chapter Organization

This chapter has the following organization.

Section 2.0 reviews the methods used for sample collection and handling.

Section 3.0 describes the EPA-approved analytical methods used for laboratory asbestos PLM and TEM analyses.

Sections 4.0 and 5.0 provide a summary of the results of laboratory analyses samples collected from the regional and Johns-Manville Coalinga Asbestos Mill Site sampling programs.

Section 6.0 presents the observations and/or conclusions of the regional soil sampling and asbestos analysis program.

Figures 5-1 through 5-4 illustrate the results of the asbestos laboratory analyses.

Figure 5-5 is a data organization chart that illustrates the types of materials that were included in the sampling and asbestos analysis program. Figures 5-6 through 5-8 are correlation figures that illustrate the poor relationship between PLM and TEM data. Figures 5-9 through 5-23 illustrate the range of PLM analytical results for various types of deposits. Figures 5-11 and 5-12 illustrate the downstream trends in asbestos concentrations in sampled streambed sediment with results ranging from more than 60% in the White Creek pathway (close to the asbestos outcrop areas) to less than 1% in the Arroyo Pasajero section of the drainage pathway leading to the Arroyo Pasajero Alluvial Fan.

Reproduced with permission of the copyright owner. Further reproduction prohibited without permission.

Table 5-1 provides a summary of the number of samples analyzed for asbestos using PLM and TEM. Table 5-1 also provides a summary of the number of samples analyzed for particle size distribution and organic matter.

Table 5-2 provides a comprehensive summary of asbestos analytical results including PLM and TEM data. Table 5-3 provides a summary of the results of particle size distribution analyses and organic matter analyses.

Tables 5-4 through 5-10 provide the results of a range of QA/QC (Quality Assurance/Quality Control) analyses that were conducted to evaluate the PLM and TEM data sets. Tables 5-11 and 5-12 provide a comparison of PLM and TEM data for samples that were analyzed by both of these methods. Tables 5-13 through 5-28 provide an assessment of the range and modal characteristics of the various categories from which samples were collected and analyzed such as outcrop samples, mill site samples, streambed samples, and alluvial fan samples.

Typical reports of laboratory analyses for asbestos content, total organic content, and particle size distribution are included in Appendix E. A complete set of copies of original laboratory reports of PLM and TEM asbestos analyses, particle size distribution analyses, and organic matter analyses are included in Levine-Fricke, May 9, 1989.

Reproduced with permission of the copyright owner. Further reproduction prohibited without permission.

2.0 SAMPLING METHODOLOGY

This section provides a description of the methods that were used for sample collection and a description of the asbestos analytical methods used by the supporting laboratories.

2.1 Sample Collection

Surface materials were sampled with a hand trowel. A mattock (pick ax) was used as necessary to loosen recalcitrant soils. Samples collected from streambed and road surface stations were obtained from the upper two inches. For all other surface soil samples, at least one inch of overburden material was removed from the excavation point to expose a fresh sampling surface. At all stations, only fine-grained materials were sampled and analyzed. I did this to exclude the sampling of gravels and cobbles. In order to ensure the collection of a representative samples at each identified sampling station, a grid and random number system was used to collect and composite samples. For each sampling station, six sub-samples were randomly selected from within a 2 x 3 meter grid. These subsamples were placed in a clean polyethylene bucket and vigorously mixed with a trowel until the material visually appeared to be homogeneous. Approximately 400 grams of the homogeneous material was then scooped out of the bucket, placed into a clear freezer-grade polyethylene zip-lock bag, labeled, and then placed in a second zip-lock bag. The sampling tools were then decontaminated and a clean bucket was used for compositing the next sample. Excess soils excavated from sample holes were returned to the holes from which they were excavated.

Reproduced with permission of the copyright owner. Further reproduction prohibited without permission.

Potential borrow source excavation pits, for evaluation of asbestos content of clay soils for potential use as a clay cap at the Johns-Manville Coalinga Asbestos Mill Site were excavated with a backhoe. Soils from the excavation pits were either sampled from the backhoe bucket or from the sidewall of the excavation pit where distinct changes, if any, occurred in soil materials. Each borrow pit sample was made up of six subsamples collected from different parts of the backhoe bucket or the excavation pit sidewall. These subsamples were composited, bagged, and labeled in the same manner as described above for surface samples.

At the alluvial fan and settling basin stations, I was able to obtain subsurface soil samples from soil borings drilled using a drill rig and hollow-stem augers. The soil borings were continuously sampled using a split-barrel 3-inch diameter drive sampler lined with 2.5-foot-long clear plastic tubes. I designed this sampling method to help with the preservation of the physical and sedimentary characteristics of each sample core. After removal from the sampling tool, the plastic tube liners were sealed with aluminum foil and red plastic end caps and sealed with tape. The shoe (i.e., bottom end) of the sampling tool was decontaminated by rinsing with tap water, scrub washed with an Alconox solution, and rinsed three times with distilled water. Approximately three inches from each cored interval was recovered from the tool shoe. This material was placed in a clear, freezer-grade, polyethylene zip-lock bag, labeled, and then placed in a second zip-lock bag.

The cores were described in the field and in the laboratory. Intervals targeted for sampling were sampled from a shoe sample or from an opened end of one of the tubes. Approximately three inches of cored material was composited in a clean plastic bucket as described above. Approximately 200 grams of the composited material was placed in a zip-lock bag, labeled, and placed in a second zip-lock bag before shipping to the

Reproduced with permission of the copyright owner. Further reproduction prohibited without permission.

designated laboratory. The excess composited material was placed in a plastic soil sampling jar, labeled, and sealed with black plastic tape.

2.2 Equipment Decontamination

Prior to the collection of each sample, all sampling equipment was rinsed with tap water, washed with Alconox, and rinsed three times with distilled water. All plastic buckets used for compositing samples were similarly decontaminated and allowed to dry before being re-used.

2.3 Sample Preservation, Shipment and Archiving

All samples were packed, stored, and shipped in an ice chest. With the exception of those samples analyzed for organic matter, the samples were not chilled, since asbestos and the analyzed metals are non-volatile and non-biodegradable. All samples were shipped under chain-of-custody to the laboratory by a certified shipper, such as Federal Express.

2.4 Sample Documentation

Filed observations were recorded in my field notebook. Recorded notes included descriptions of sampling station locations, visual observations of potential asbestos content in sampled materials, and descriptions of soil structure and texture, particle size distribution, vegetative covering, color, soil classification, moisture content, and any other pertinent field data. Lithologic soil descriptions were recorded using the Unified Soil Classification System and the Munsell Color Chart for soils.

Reproduced with permission of the copyright owner. Further reproduction prohibited without permission.

Soil boring logs denoting physical characteristics (color, grain size distribution, mineralogy) and any observable sedimentary structures (bedding characteristics, laminations, vertical grain size trends) were recorded for each continuously cored soil boring. Sampling locations were carefully described and I was able to photograph most locations in order to help further document field conditions.

Reproduced with permission of the copyright owner. Further reproduction prohibited without permission.

3.0 ANALYTICAL METHODS

Samples were analyzed for asbestos content using EPA-approved PLM and TEM methods. Some samples were also analyzed for organic matter content and particle size distribution (hydrometer and sieve methods) for use in the watershed soil erosion modeling project. Two EPA-approved laboratories were used for the PLM and/or TEM analyses of bulk soil samples. The two laboratories included McCrone Environmental Services of Norcross, Georgia and Med-Tox Associates of San Diego, California. As the lead geologist for this project, I was the primary contact with these laboratories and my responsibilities included working with the laboratories in advance of the regional sampling program so that they could be better prepared for the routine analysis of the large number of samples to their laboratories. I was also responsible for working with the laboratories to ensure that they were consistent with their reporting and interpretation of the unique petrographic characteristics of the New Idria Formation type of chrysotile as discussed in Chapter Four.

3.1 Asbestos Analyses

Asbestos analytical results may vary widely, depending upon such factors as sample matrices, fiber size, and specific laboratory analysis procedures. PLM and TEM are the two laboratory methods most commonly used for asbestos analysis of bulk soil samples. Both of these methods were used in this regional soil sampling program. The primary method for asbestos analyses was a PLM technique based on EPA's Interim Method for the Determination of Asbestos in Bulk Insulation Samples (EPA-600/M4-82-020), modified for use with soil samples. This PLM procedure is reasonably accurate for measuring optically visible fiber concentrations and has the

Reproduced with permission of the copyright owner. Further reproduction prohibited without permission.

added benefits of being rapid, sensitive, and relatively inexpensive to perform (i.e., PLM analyses typically ranged from approximately $20 to $30 per sample).

Additionally, 73 samples or approximately 19% of all PLM samples were analyzed using a TEM procedure based on the draft EPA method of Yamate, Agarwal, and Gibbons, as modified for bulk soil samples. TEM analyses were only performed on a portion of the PLM samples, primarily to detect the presence of fibers too small to be observed by PLM, and to confirm the identification of asbestos minerals. TEM analyses are also more expensive than PLM analyses with the cost of TEM analyses ranging from approximately $300 to $400 per sample.

3.1.1 PLM Methodologies

The bulk soil samples from the New Idria Formation and other chrysotile asbestos source areas in the Coalinga region are different from the asbestos products routinely analyzed by analytical testing laboratories. The bulk soil sample matrices tend to be more complex and the minerals present within these samples have been found to exhibit certain properties which make chrysotile identification non-routine. The serpentine minerals associated with these samples include chrysotile, antigorite, and lizardite. All of these serpentine minerals have the same basic chemical composition [$(Mg,Fe)_3SiO_5(OH)_4$], but different crystal structures. In the New Idria Formation, it appears that most of the chrysotile asbestos occurs as a polymorph of lizardite and/or antigorite forms of serpentine. These polymorphs macroscopically appear as small white chips and platelets and as pale green lath-shaped minerals. Using a binocular scope, these chips, platelets, and lath-shaped minerals were observed to be composed of a material that was easily fibrillated upon slight crushing. Using the PLM method, some of this material was readily confirmed as chrysotile asbestos and some of the

Reproduced with permission of the copyright owner. Further reproduction prohibited without permission.

material appeared as a fibrous form of antigorite. The results of an x-ray diffraction analysis of one sample indicated antigorite as the predominant polymorph. Using the TEM method, most of the fibrous material was confirmed as chrysotile asbestos based on identification of a cylindrical crystal structure and/or an aspect ratio (length to width) of 3 to 1. Macroscopically, the chrysotile asbestos was observed to be aggregated as platelets and as lath-shaped bundles.

Two laboratories were used for the asbestos analyses for this project. The primary laboratory for the bulk soil asbestos analyses was Med-Tox Associates (San Diego, California), A second laboratory was used for QA/QC purposes. The quality control laboratory was McCrone Environmental Services (Norcross, Georgia) Prior to commencing with routine PLM analyses as part of this sampling program, McCrone Environmental Services evaluated the physical characteristics and optical properties of the serpentinite minerals contained in soils from the proposed sampling areas. Petrographic analyses indicated that the serpentinite minerals had morphological characteristics ranging from acicular fibers to rounded, somewhat flattened fragments. Many of the rounded, flattened fragments became quite fibrous upon crushing. This fibrous habit is indicative of chrysotile asbestos and a fibrous form of antigorite known as picrolite. Macroscopically, the chrysotile and antigorite commonly appeared as coarse sand and silt-sized, white, matted plates and white or pale green, elongated, lath-shaped minerals.

Both Med-Tox and McCrone noted in their preliminary evaluations that when these samples were analyzed by PLM-dispersion staining (a standard particle identification technique based on the difference between the dispersion of the refractive index for a particle and the liquid medium in which the particle is immersed), many of the fibers displayed a greater range of optical properties than normally associated with standard

Reproduced with permission of the copyright owner. Further reproduction prohibited without permission.

chrysotile asbestos. Chrysotile in these samples had optical properties more like fibrous antigorite (i.e., picrolite) than normal chrysotile. However, subsequent analyses of these samples by TEM identified most of the elongate serpentine minerals to be chrysotile.

To more accurately characterize PLM results for samples from the study area, Med-Tox reported their analytical results in terms of both "elongate serpentine asbestos" and "chrysotile asbestos" categories for each sample. As defined by Med-Tox, elongate serpentine asbestos includes all serpentine minerals with an aspect ratio of at least 3:1, including fibers with classical as well as non-standard chrysotile optical properties. Using this broad definition, the elongate serpentine asbestos category represents an upper limit for PLM-detectable concentrations of chrysotile. Conversely, the chrysotile asbestos category only includes fibers with classical chrysotile PLM properties, and therefore represents a lower limit for PLM-detectable concentrations of chrysotile. Med-Tox's PLM method detection limit was 1% for both the elongate serpentine asbestos and chrysotile asbestos categories. Sample concentrations were reported as "trace" if elongate serpentine asbestos or chrysotile asbestos was detected at concentrations less than 1%, or as ND if no elongate serpentine asbestos or chrysotile asbestos was observed.

McCrone analyzed 60 of the PLM samples as blind inter-laboratory splits using the PLM method. McCrone reported chrysotile and all fibrous chrysotile-like minerals as "serpentine asbestos", based on optical properties and morphological characteristics. This category included fibrous grains, matted clumps of fibers, and green elongate chips which gave rise to fibers when crushed. McCrone reported their serpentine asbestos results as a percentage range (i.e., <1%, 1-10%, >80%, etc.). The percent asbestos was measured for either: (1) total bulk soil samples or (2) gravel, sand, and

Reproduced with permission of the copyright owner. Further reproduction prohibited without permission.

silt/clay fractions that were obtained from mechanical sieving of the bulk samples. For sieved samples, each size fraction was weighed and analyzed separately, and the total asbestos percentage was calculated by multiplying the percent asbestos concentration range for each size fraction by its respective weight percent. The resultant products were then summed to give the estimated total percent asbestos for the bulk sample. The results of the asbestos analyses of the sieved samples showed that asbestos occurs in all size fractions, including gravel, sand, and silt and clay size particle size ranges.

A comparison of results from replicate samples that were analyzed by both Med-Tox and McCrone showed that the serpentine asbestos data reported by McCrone agreed more closely with Med-Tox's elongate serpentine asbestos results than with Med-Tox's chrysotile asbestos results, based on RPDs (relative percent differences) and regression analyses calculated for each set of duplicates. See Table 5-9. The RPD between McCrone's serpentine asbestos category and Med-Tox's elongate serpentine asbestos category was 63%, compared to 90% for McCrone's serpentine asbestos category and Med-Tox's chrysotile asbestos category. The correlation coefficient between elongate serpentine and serpentine asbestos was 0.81, compared to a correlation coefficient of 0.74 between serpentine asbestos and chrysotile asbestos.

Since the elongate serpentine asbestos was determined by TEM analyses to consist mostly of chrysotile, and the elongate serpentine asbestos data was found to agree most closely with serpentine asbestos data from replicate (duplicate) samples analyzed by McCrone, the elongate serpentine asbestos category was used as the main reference category in this soil sampling program. Given the above findings, and the fact that elongate serpentine asbestos PLM values were always higher than chrysotile asbestos PLM values, use of elongate serpentine asbestos data provided a conservative upper limit of the PLM-detectable asbestos concentrations of soil samples. Moreover, since elongate serpentine

Reproduced with permission of the copyright owner. Further reproduction prohibited without permission.

asbestos concentrations were generally higher than TEM concentrations for duplicate samples, the elongate serpentine asbestos category is believed to have provided a more conservative measurement of asbestos than was reported by TEM analyses. It is also important to note that those materials identified as elongate serpentine asbestos by Med-Tox were confirmed as being chrysotile asbestos using the TEM method. Thus, unless otherwise indicated, the elongate serpentine asbestos category, with reported units of percent area, has been used to describe asbestos concentrations in subsequent discussions in this investigation.

3.1.2 TEM Methodology

Med-Tox conducted TEM analyses to identify sub-microscopic structures as either chrysotile, non-asbestos, or indeterminate. No amphibole asbestos was identified in any of the samples. All chrysotile structures were described as fibers, bundles, clumps, or matrices. Asbestos structure concentrations (i.e., structures per unit mass) and mass concentrations (percent mass per unit mass) were reported for all structures and for those structures greater than five microns in size.

Although the TEM analysis method can detect fibers too small to be detected by PLM, it has major limitations as a quantitative procedure. These limitations affect TEM results reported in terms of fiber concentrations and mass concentrations. For example, due to the vigorous sample preparation procedures necessary for TEM analysis (i.e., grinding, extracting, and ultrasonicating bulk sample matrices), asbestos fibers tend to get broken up; and therefore TEM results reported as fiber concentrations may not reflect **in situ** fiber concentrations of the original bulk soil sample.

Reproduced with permission of the copyright owner. Further reproduction prohibited without permission.

Although an effort is made to obtain representative sub-samples of the original bulk soil samples for subsequent sample preparation and analysis, significant variability also may be introduced into the TEM measurement given the heterogeneity of most bulk soil samples. Furthermore, the actual TEM grid squares which are subsequently viewed for counting asbestos structures represent a minute fraction of the original bulk sample; thus, additional variability may be added to the TEM analytical results if the grid squares which are counted are not very representative of the sample aliquot which has been placed on the filter for TEM analysis.

Asbestos mass concentrations are also subject to significant possible errors, since asbestos mass values are based on calculated fiber volumes and an assumed chrysotile density (i.e., 2.6 g/cm^3 was used by Med-Tox). Volume estimates are calculated by assuming all fibrils and bundles to be cylinders with diameter and length dimensions as perceived on screen. However, structure diameters measured at a typical TEM magnification of 20,000X are often crude, since the perceived fiber image on screen may range from only a few tenths of a millimeter to a few millimeters, and carbon deposited on asbestos structures during sample preparation can significantly exaggerate the apparent diameter of thin fibers. For these reasons, fiber diameter measurements may not be very accurate. Possible errors associated with diameter measurements are compounded since diameter values must be squared to calculate fiber volumes.

The presence of matted clusters and bundles adds more uncertainty to TEM mass calculations, since the entire length of some fibers cannot be observed and the total number of fibers in some structures is not discernable. In a few cases, Med-Tox calculated TEM asbestos mass concentrations which exceeded 100%. According to Med-Tox, these results are a statistical anomaly and reflect method imprecision;

Reproduced with permission of the copyright owner. Further reproduction prohibited without permission.

however, they probably represent actual asbestos concentrations which are close to 100%. Therefore, for subsequent data interpretations, percent mass values exceeding 100% were treated as being equal to 100%.

3.1.3 Comparison of PLM and TEM Methods

Approximately 19% of the samples analyzed by PLM were also analyzed by TEM. As noted earlier, TEM analyses were primarily used to detect the presence of asbestos which might not be visible by PLM, and to confirm sample asbestos mineralogy. However, it was also of interest to assess possible trends in asbestos concentrations obtained using the two analytical methods. Therefore, PLM results reported as elongate serpentine (percent area) were plotted against TEM (percent mass) data for all samples analyzed by both methods, in order to indicate possible trends in the data. Data plotted in this manner would be expected to fall more or less along a straight line if both the TEM and PLM analytical methods produced similar sample asbestos concentrations. A total of 75 pairs of sample results were plotted. See Figure 5-10A. The results indicate that the data points were widely scattered, with no apparent correlation between TEM and PLM results. Since the majority of the PLM-TEM data points had relatively low values, a similar plot was made for those data with TEM and PLM results less than or equal to 20%. A total of 51 data points fell within this range. Figure 5-8B shows that for samples with relatively low asbestos concentrations, there is no apparent correlation between TEM and PLM analysis results.

The TEM and PLM data were inspected for possible systematic differences by comparing relative asbestos concentrations of the samples analyzed by both analytical methods. The soil sampling data base included a total of 54 sets of PLM and TEM data where PLM elongate serpentine concentrations were greater than or equal to the

Reproduced with permission of the copyright owner. Further reproduction prohibited without permission.

PLM method detection limit of 1%. See Table 5-11. Soil sampling data were compared by assuming that the asbestos percent area concentrations would be equivalent to percent mass concentrations. This assumption is consistent with EPA's interpretation of PLM asbestos data (see EPA, 1988, p. 4-2), and provides a conservative estimate of mass concentrations, since the specific gravities of other minerals present in the bulk soil samples tend to be the same or higher than that of chrysotile (i.e., 2.6).

For each of the 54 sets of samples analyzed by both PLM and TEM methods, the TEM and PLM data were compared to see which value was higher. This analysis showed that asbestos concentrations reported by PLM tended to be the same or higher than those reported by TEM for 76% of the data sets (i.e., for 41 of the 54 pairs of data). This data shows that asbestos concentrations reported as elongate serpentine asbestos by the PLM method generally provided a conservative (i.e., higher) estimate of sample asbestos concentrations compared to the TEM method. See Table 5-11.

To further evaluate the relationship between TEM and PLM analytical results, sample results were screened for those data sets where PLM elongate serpentine asbestos results were reported at trace concentrations (i.e., at a concentration level below the 1% method detection limit). This category is of particular concern since it may represent the threshold of PLM-visible asbestos. A total of 35 samples fell within this category. See Table 5-12. By comparing the paired data as described above, it was observed that TEM percent mass data were higher than the PLM detection limit for 63% of the data pairs (i.e., for 22 of the 35 sample pairs). However, the average TEM percent mass concentration for these 22 samples was only 3.5%, which is a concentration only slightly higher than the PLM detection limit. Based on the available information, it appears that samples from the study area which were reported

Reproduced with permission of the copyright owner. Further reproduction prohibited without permission.

to contain elongate serpentine asbestos at trace levels using PLM analyses generally have similar asbestos concentrations by TEM, notwithstanding the much greater resolution capabilities afforded by the latter method. Of further significance, no samples were present in the data base where elongate serpentine asbestos was reported as ND (not detected) using PLM, but detectable by TEM.

To summarize the above discussions, no significant correlation was apparent between TEM and PLM analytical results. TEM analysis results for bulk soil samples may be highly variable as a result of sample preparation procedures, the amount of sample actually analyzed with respect to total sample volume, and possible errors associated with the calculation of percent mass values. As noted in Tables 5-8 and 5-10, PLM and TEM RPDs for field duplicate samples were found to be 42% and 80% respectively, indicating the PLM method to be more precise than the TEM method for bulk soil sample analyses. The PLM-detectable elongate serpentine asbestos results appeared to be generally higher than corresponding TEM results for duplicate samples, suggesting that PLM analyses provide conservative estimates (i.e., higher values) of asbestos concentrations in bulk soil samples. However, for samples with reported asbestos concentrations near the PLM detection limit, TEM results averaged only 2.5% higher than the PLM detection limit. TEM analyses indicated that the elongate serpentine asbestos fraction identified by PLM is composed predominantly of chrysotile asbestos. Therefore, most data interpretations and conclusions in this report have been presented in terms of elongate serpentine asbestos concentrations reported from PLM analyses.

Reproduced with permission of the copyright owner. Further reproduction prohibited without permission.

3.2 Particle Size Analyses

Soil samples were analyzed for particle size distributions by mechanical sieving and the hydrometer method by Dellavalle Laboratory (Fresno, California). The particle size distribution data was required for the soil erosion modeling work reported in Chapter Six. The laboratory procedures included dispersing and disaggregating samples by shaking in water and by application of a sodium hexametaphosphate solution. Samples were dried at 105° F. After drying, samples were mechanically disaggregated using a rolling pin and/or mechanical soil grinder. Particle size distributions were determined by mechanically separating sand-sized fractions through sieves with standard mesh sizes. The portion of the sample passing through the #200 sieve was placed in a 1-liter cylinder and treated with a sodium hexametaphosphate solution overnight. Hydrometer readings were then taken over various time periods, to determine the silt and clay sized-fractions of each sample. Particle size analysis results were graphed by the laboratory as a cumulative frequency plot indicating the percent passing versus particle size fraction. Information from these graphs was then used to calculate the sand, silt, and clay-sized fractions for each sample. Results from the particle size analyses are summarized in Table 5-3.

3.3 Organic Matter Analyses

Soil samples for were analyzed for organic matter content by Dellavalle Laboratory. Organic matter content data was also used for the soil erosion modeling work. Initial sample preparation for organic matter analyses involved drying the sample and mechanically disaggregating it as described above for particle size analyses. The sample was further ground with a mortar and pestle to pass through a 40 mesh sieve. A portion of the sample was then weighed, transferred to a flask, and potassium

Reproduced with permission of the copyright owner. Further reproduction prohibited without permission.

dichromate and sulfuric acid solutions were added. After a standard time period, the remaining dichromate solution was titrated with ferrous sulfate to determine the organic matter content of the soil. Results of organic matter analyses are summarized in Table 5-3 along with particle size data.

Reproduced with permission of the copyright owner. Further reproduction prohibited without permission.

4.0 QUALITY ASSURANCE/QUALITY CONTROL PROGRAM

This section reviews the QA/QC procedures used in the soil sampling program. The data were evaluated in accordance with QA/QC objectives for accuracy, precision and reproducibility, based primarily on a review of field and laboratory quality control (QC) samples. Data reviewed in this manner were evaluated for acceptability and then compiled for qualitative and quantitative analyses. The compiled data were then evaluated and interpreted as discussed in Sections 5.0 and 6.0.

The following broad data classes were generated:

- PLM asbestos analysis results for QC samples.

- TEM asbestos results for QC samples.

- Split sample results comparing TEM and PLM analysis methods.

- QC results for organic matter and metals analyses.

- PLM asbestos analysis results for regional areas (i.e., outcrop areas, streambeds, and alluvial fan sampling locations).

- PLM asbestos analysis results for CAM-site areas (i.e., tailings and ore areas, streambeds, and potential borrow source locations).

Reproduced with permission of the copyright owner. Further reproduction prohibited without permission.

4.1 Data Verification and Validation

Quality control data (i.e., laboratory and field duplicates) were statistically evaluated and compared to the complete data set for each analytical parameter. Except in very few cases, the data were found to be acceptable and were retained for further analyses. Outlying data points have been identified in the data compilation tables included with this chapter.

Quality control samples included field and laboratory duplicates for precision assessment and method comparability purposes, laboratory spikes for accuracy assessments, and method blanks, where appropriate, for estimates of possible asbestos contamination associated with sample analyses. The QA/QC objectives for accuracy were defined in terms of percent spike recovery. Duplicate sample results were used to evaluate the analytical precision for analyses of asbestos, organic matter, and metals. The results of duplicate and/or replicate samples were expressed as relative percent differences (RPDs), and average RPDs and standard deviations were calculated.

4.2 Laboratory QC Samples

As part of each laboratory's QA/QC program, QC samples were prepared and analyzed by each laboratory to evaluate the precision and accuracy of the analytical methodology as well as the possibility of contamination. The laboratory QC samples included analyses of blanks, spikes, and duplicate samples. Tables 5-4 through 5-10 summarize the laboratory QC checks. Med-Tox prepared and analyzed 29 laboratory duplicates by PLM. McCrone prepared and analyzed 7 laboratory duplicates by PLM. Med-Tox prepared and analyzed 5 duplicates, 2 laboratory method blanks, and one

Reproduced with permission of the copyright owner. Further reproduction prohibited without permission.

spike by TEM analysis. Dellavalle analyzed and prepared 7 duplicates and 5 matrix spikes for organic matter analyses.

4.2.1 PLM Laboratory QC Checks

Table 5-4 compares the results of intra-laboratory duplicates prepared and analyzed by Med-Tox for PLM asbestos concentrations. Both elongate serpentine asbestos and chrysotile asbestos results were compared. For the elongate serpentine asbestos results, only one set of duplicates (Sample AL-41A) exceeded the quality control objective of 2.77 x the RPD standard deviation. The outlying duplicate pair had PLM asbestos concentrations of 2% and 3% with an RPD of 40%. Although this RPD exceeded the quality control objective, the measured asbestos concentrations were very close to the analytical detection limit of 1%, and therefore the RPD for this pair is not indicative of any analytical error in the PLM technique. For the chrysotile asbestos results, the RPD for one set of duplicates (Sample AL-39B) had reported concentrations of 25% and 70%, and an RPD of 95%. This RPD value exceeded the quality control objective and was therefore excluded from use in subsequent data evaluations. Except for the chrysotile asbestos duplicates noted above, Med-Tox's laboratory QC samples met quality control objectives for completeness, accuracy, and precision for PLM analyses.

Table 5-5 compares the results of seven intra-laboratory duplicates prepared and analyzed by McCrone. McCrone's PLM data was generally presented on their laboratory reports as a range of serpentine asbestos concentrations (e.g., 10-20%), or as less than or greater than a particular value (e.g., <1% or >85%). For calculating RPDs, midpoints of each range were compared (or the endpoints in the case of open-ended ranges). With the exception of one sample (PC11A), all of McCrone's

Reproduced with permission of the copyright owner. Further reproduction prohibited without permission.

serpentine asbestos laboratory QC duplicates met the quality control objective for completeness, accuracy, and precision. Serpentine asbestos concentrations for sample PC11A were reported as 10-20% and 5-15%. Although the RPD for this pair of analyses exceeded 2.77 times the standard deviation, it should be noted that McCrone's reported concentration ranges overlap considerably. Thus, the duplicate analyses for sample PC11A are not significantly different.

4.2.2 TEM Laboratory QC Checks

Med-Tox's laboratory QC program included evaluating the accuracy of their TEM analyses by analyzing standards obtained from the National Bureau of Standards, Standard Reference Material No. 1876 (asbestos fibers on air filters). Table 5-6 summarizes data for intra-laboratory duplicates prepared and analyzed by Med-Tox. No sets of values exceeded the QC objective for precision.

Med-Tox prepared and analyzed spiked samples to verify the correct identification of asbestos mineral species and to assess measured asbestos mass concentrations. The spike recovery (i.e., TEM method accuracy) was 62%. Two laboratory method blanks (asbestos-free water samples) were prepared and analyzed by Med-Tox, and both were determined to be below the detection limit for both mass concentration and structure concentration. Based on the above quality control results, Med-Tox's TEM results were found to be acceptable.

4.2.3 Organic Matter Laboratory QC Checks

Table 5-7 summarizes the results of sample duplicates and spikes prepared and analyzed by Dellavalle for the determination of organic matter. Of the seven duplicate

Reproduced with permission of the copyright owner. Further reproduction prohibited without permission.

pairs analyzed, three pairs had RPDs which exceeded the quality control objectives of an RPD less than or equal to 25%. Samples BP-5, BS-35, and AL-17B had RPDs of 67%, 29%, and 67%, respectively. However, these samples had reported organic matter concentrations of less than 1%. Considering that the absolute differences between organic matter concentrations for duplicate analyses of these samples were very low (0.1 to 0.2%), the organic matter analyses are believed to be adequate for the entire data set.

4.3 Field Quality Control Checks

As an additional quality control check, replicate samples were prepared in the field for submission to the laboratories as blind QC samples. These field replicates were submitted as inter-laboratory and intra-laboratory blind duplicates. These field quality control samples were intended to further assess intra-laboratory analytical precision by reducing possible laboratory bias, and to compare PLM analyses results reported by the principal and QC laboratories. Approximately 16% of the asbestos PLM samples were submitted to Med-Tox as intra-laboratory field duplicates, and 20% were submitted as duplicate to McCrone as inter-laboratory field duplicates. Med-Tox also received blind intra-laboratory field duplicates for TEM sample analyses. Dellavalle Laboratory analyzed 13% of their samples for organic matter as intra-laboratory duplicates, and Enseco analyzed all of their samples as intra-laboratory duplicates.

Field duplicates were generated by preparing proportionately larger composite samples at the sampling location, and dividing this single well-mixed composite sample into portions which were the same size as were prepared for non-replicate samples (i.e., approximately 400 grams). Field duplicates were then labeled with sample ID

Reproduced with permission of the copyright owner. Further reproduction prohibited without permission.

numbers which did not reveal their true identity. The results of field quality checks are discussed in the following sections.

4.3.1 PLM Field Duplicates

Forty-nine samples were prepared and submitted to Med-Tox as intra-laboratory PLM duplicates. See Table 5-8. Sixty samples were prepared and sent to McCrone as blind inter-laboratory duplicates for comparison with PLM results reported by Med-Tox. See Table 5-9. All sample results that exceeded the data precision criteria, based on RPD greater than 2.77 x RPD standard deviation values, were denoted with asterisks (*) in Tables 5-8 and 5-9. As previously discussed, Med-Tox reported PLM results as elongate serpentine asbestos and chrysotile asbestos. No amphibole asbestos was detected in any samples from the study area. Three sets of field duplicates reported as elongate serpentine asbestos and five sets of duplicates reported as chrysotile asbestos had RPDs exceeding QC objectives for precision.

Table 5-9 summarizes the inter-laboratory PLM results from Med-Tox and McCrone. The results of inter-laboratory replicates were compared and reviewed for systematic differences, if any, between asbestos results reported by Med-Tox and McCrone. Because Med-Tox reported PLM data in terms of an elongate serpentine asbestos category and a chrysotile asbestos category, a comparison was made between results for each of these categories and the results for the serpentine asbestos category reported by McCrone. As is apparent from the flagging of calculated RPDs that exceed the QC objectives, the elongate serpentine asbestos results of Med-Tox correlate better with McCrone's serpentine asbestos results than does the correlation of Med-Tox's chrysotile asbestos results with McCrone's serpentine asbestos results. Correlation coefficients were determined for these comparisons, and the elongate

Reproduced with permission of the copyright owner. Further reproduction prohibited without permission.

serpentine asbestos category versus serpentine asbestos category had a correlation coefficient of 0.81 and the chrysotile asbestos category versus serpentine asbestos category had a correlation coefficient of 0.74. See Table 5-11.

4.3.2 TEM Field Duplicates

Fourteen samples were sent to Med-Tox as blind intra-laboratory duplicates for TEM asbestos analyses, as well as PLM analyses. Table 5-12 summarizes TEM results for these samples. Med-Tox reported their TEM results as four categories: (1) total asbestos structure concentration for all structures; (2) total asbestos structure concentration for structures greater than 5 microns in size; (3) total asbestos mass concentration for all structures; and (4) total asbestos mass concentrations for structures greater than 5 microns in size. For ease of comparison and correlation, mass concentrations were tabulated as percentages, and structure concentrations were tabulated as trillion structures per gram for all structures and billion structures per gram for those structures greater than 5 microns in size.

The mass concentration for all structures and the structure concentration for all structures were compared between original samples and field duplicates (i.e., intra-laboratory blind duplicates). Sample results which exceeded the data precision criteria were noted with an asterisk (*). All RPDs calculated for reported structure concentrations were within the quality control objective for TEM precision. Of the 14 sets of blind duplicates, two samples (SB3-15.2/SB3-15.3 and SS-34/SS-84) exceeded the data precision acceptance criteria for mass concentration for all structures.

Reproduced with permission of the copyright owner. Further reproduction prohibited without permission.

4.3.4 Organic Matter Field Duplicate

One sample, AL52, was analyzed in duplicate (identified as AL83). See Table 5-8. Both samples had an organic matter content of 0.2%, meeting the quality control objective for precision.

4.4 Data Compilation, Reduction and Summary

PLM asbestos data for the study area were organized as shown in Figure 5-8. The asbestos results are summarized in Table 5-2. PLM asbestos data for the QA/QC laboratory, McCrone Laboratory, were reported as mid-point values of the reported range, as discussed in Section 3.1.1. Table 5-3 summarizes particle size and organic matter analyses, with particle size data reduced to differentiate between various fractions. PLM results were further subdivided into groups as shown in Figure 5-5.

PLM asbestos data was compiled for data evaluation purposes. Sample groups were characterized by calculating arithmetic means and modal concentration ranges for PLM elongate serpentine data. Mean concentrations were used in subsequent watershed modeling activities. A review of the data indicated that some of the mean asbestos concentrations were skewed due to one or a few relatively high or low PLM results. To further characterize the data, the modal concentration range (the concentration range of most frequent occurrence) was also determined for each data group. Both of these measures of central tendency are reported in this document.

To aid in the interpretation of the asbestos concentration data, the elongate serpentine asbestos results for each sample group were plotted on bar graphs displaying elongate serpentine asbestos concentration ranges versus percent occurrence (number of

Reproduced with permission of the copyright owner. Further reproduction prohibited without permission.

occurrences divided by the total set of occurrences). To calculate modal ranges, sample results were generally arranged into the following classes: 0 - 1%; 2 - 3%; 4 - 5%; 6 -10%; 11 - 20%; 21 - 30%; 31 - 40%; 41 - 60%; 61 - 80%; and 81 - 100%. Smaller size classes were defined at the lower concentration ranges in order to provide greater resolution of the data near the PLM detection limit.

Reproduced with permission of the copyright owner. Further reproduction prohibited without permission.

5.0 RESULTS AND INTERPRETATION OF REGIONAL SOIL SAMPLING DATA

The regional soil sampling program included sampling of sediment and soils from outcrops of asbestos-bearing geologic formations including the New Idria Formation and the Big Blue Member of the Temblor Formation (Miocene), from streambeds that drain these geologic source areas, and from the Arroyo Pasajero alluvial fan. The regional sampling program also included sampling of non-asbestos-bearing soils developed on the marine shales and sandstones of the Panoche Formation (Cretaceous) which underlies most of the upper watershed areas. The regional sampling program data are summarized in Tables 5-2 and 5-3, and sampling locations are indicated in Figures 5-1 to 5-4. This section briefly reviews the sampling results for the entire off-site sampling program, followed by more detailed discussions of sampling results for specific sampling areas.

As indicated by the results of this sampling program, integrated with a review of aerial photographs and geologic maps of the Coalinga region, the outcrop areas associated with the New Idria Formation and the Big Blue Member are the primary sources of asbestos for the Arroyo Pasajero and Cantua Creek watershed basins. Thirty-five samples were obtained from the New Idria Formation serpentinite outcrop area, including 15 samples from undisturbed serpentinite soils and from anthropically disturbed areas associated with mining operations. Seven samples were collected from undisturbed serpentinite outcrop areas of the Big Blue Member. These serpentinite samples collectively had a mean elongate serpentine asbestos concentration of 66%, and a modal concentration range of 81-100%. The collective elongate serpentine asbestos data for both geologic source areas are summarized in Table 5-13. Sampling station locations are shown in Figures 5-2 (labeled as OC Stations) and 5-3 (labeled as

Reproduced with permission of the copyright owner. Further reproduction prohibited without permission.

CC Stations). In addition to these two geologic formations, as many as 50 additional asbestos-bearing ultramafic serpentine deposits and 4 additional asbestos-bearing sedimentary formations have been identified throughout the Coalinga region. Many of these asbestos sources are visible in high altitude color infrared (CIR) photographs of the Coalinga region. Sampling of these areas was beyond the scope of this investigation.

Results from the regional streambed samples (see stations designated SS in Figures 5-1 and 5-2) showed that asbestos-containing sediment is being transported downstream from the New Idria Formation outcrop area primarily through the White Creek and Los Gatos Creek tributaries to the Arroyo Pasajero. Except for the Upper White Creek intermittent drainage pathway, the concentration of asbestos in the streambed sediment in the Pine Canyon-White Creek-Los Gatos Creek drainage pathway was generally observed to decrease with increased distance from the New Idria Formation outcrop area.

The upper White Creek streambed samples had the highest asbestos concentrations. In the upper reach of White Creek (i.e., from the New Idria Formation outcrop area downstream to the White Creek juncture with Pine Canyon), the streambed sediment samples decreased from 85% to 65% elongate serpentine asbestos. The Pine Canyon Creek samples from the regional sampling program had elongate serpentine asbestos concentrations that decreased from 85% to less than 1%, with the highest concentrations from samples collected upstream from the Johns-Manville Coalinga Asbestos Mill Site. In the lower reach of White Creek (i.e., from the juncture with Pine Canyon Creek downstream to the White Creek juncture with Los Gatos Creek), the asbestos concentration of streambed sediment samples decreased from 65% to 30% elongate serpentine asbestos.

Reproduced with permission of the copyright owner. Further reproduction prohibited without permission.

In the middle reach of Los Gatos Creek (i.e., from the juncture with White Creek downstream to the Los Gatos Creek juncture with Warthan Creek), the asbestos concentration of streambed sediment samples decreased from 20% to 10% elongate serpentine asbestos. In the lower reach of Los Gatos Creek (i.e., downstream from the juncture with Warthan Creek) in the vicinity of Coalinga and east to the alluvial fan area near Huron, the streambed sediment had elongate serpentine asbestos concentrations that were generally less than 1%.

Subsurface samples from the Arroyo Pasajero alluvial fan (see stations designated AF) and the settling basin (see stations designated SB) had a mean elongate serpentine asbestos concentration of less than 1%, and a modal concentration range of 0 to 1%. See Figure 5-13 and Table 5-16.

5.1 Outcrop Areas

5.1.1 New Idria Formation

Twenty-eight surface samples (see stations designated OC) were collected from the New Idria Formation outcrop area in the White Creek and Pine Canyon watersheds located on the southeastern flank of Joaquin Ridge. These outcrop sampling stations were located in serpentinite soils and intermittent drainage channels in natural, undisturbed areas and at locations affected by mining or milling operations. The mean elongate serpentine asbestos concentration for all serpentinite soil samples collected in the New Idria Formation outcrop area was 86%, with a modal concentration range of 81% to 100%. See Table 5-14A. The mean elongate serpentine asbestos concentration of all mine surface samples collected in the New Idria Formation

Reproduced with permission of the copyright owner. Further reproduction prohibited without permission.

outcrop area was 81%, with a modal concentration range of 61% to 100%. See Table 5-14B. The mean elongate serpentine asbestos concentration of all intermittent streambed samples collected in the New Idria Formation outcrop area was 60%, with a median concentration of 65%. The asbestos concentrations for the intermittent streambed samples in the outcrop area ranged from 25% to 85%, without any clear modal class. See Table 5-14C. The relatively high concentrations of asbestos for this collective group of samples agree with field observations of asbestos-containing materials contained in the above sampled sediment types.

5.1.2 Big Blue Member of the Temblor Formation (Miocene)

Seven samples (see samples designated CC) were collected from sedimentary outcrops of the Big Blue Member of the Temblor Formation (Miocene) in the area of the Big Blue Hills. This area is located approximately 10 miles north of Coalinga along the western margin of the San Joaquin Valley. This area is also approximately 8 miles northeast of the New Idria Formation outcrop area of Joaquin Ridge. The samples were collected from outcrops of the "Big Blue" in the vicinity of Martinez, Salt, and Cantua Creeks. See Figure 5-3. The "Big Blue" samples had a mean elongate serpentine asbestos concentration of 66%, and a modal concentration range of 81 to 100%. See Figure 5-10 and Table 5-15. The naturally occurring asbestos deposits in this area are similar in appearance to fresh ore material observed in the White Creek and Pine Canyon mining areas. The Big Blue was sampled because a review of the regional geology, high altitude color infrared aerial photographs, and data from previous sampling of Aqueduct water by the California Department of Water Resources (DWR, 1986) in the vicinity of Salt and Cantua Creeks indicated that this sedimentary deposit may be a significant asbestos source for the region.

Reproduced with permission of the copyright owner. Further reproduction prohibited without permission.

5.1.3 Other Asbestos-Bearing Formations

A review of the regional geology showed that several additional sedimentary formations that overlie the Temblor Formation (Miocene) in the Coalinga region commonly contain locally high to trace amounts of detrital serpentinite debris that most likely originated from the New Idria Formation. Based on geological considerations combined with the results of this sampling program (i.e., confirmation of chrysotile asbestos in serpentinite soil samples), these detrital serpentinite deposits are likely to contain chrysotile asbestos. The potential asbestos-bearing sedimentary formations include the Santa Margarita Formation (Late Miocene), Etchegoin-Jacalitos Formation (Early Pliocene), Tulare Formation (Pliocene-Pleistocene), and undifferentiated Quaternary alluvial sediments. These formations outcrop in the lower foothills that border Coalinga and the Pleasant Valley area. These formations also outcrop along the western margin of the central San Joaquin Valley and are particularly well-exposed in the Cantua Creek - Big Blue Hills area north of Coalinga. Although not sampled in this study, these formations are expected to contain varying concentrations of asbestos because the sediment source areas for these sedimentary deposits included the New Idria Formation and other ultramafic serpentinite deposits in the region. Another source for the detrital serpentinite debris in post-Miocene aged sedimentary formations includes erosional reworking of the sedimentary serpentinite deposits of the "Big Blue" in association with regional uplift and exposure of the upper Temblor Formation (Miocene) during the Pliocene and Pleistocene period of crustal deformation in the Coast Range geomorphic province.

Reproduced with permission of the copyright owner. Further reproduction prohibited without permission.

5.2 Non-Asbestos-Bearing Soils

Three samples (OC-11, OC-22, and OC-26) were located in the marine sedimentary soils developed on the thinly interbedded sandstones and shales of the Panoche Formation (Cretaceous). Two of these stations were located in the upper Diaz Canyon area, and one station was located in the White Creek area near the Archer Mine. The Diaz Canyon area is located updip and east of asbestos mining areas, and therefore has not been affected by mining or milling activities. The Panoche Formation forms the upturned bedrock that flanks the New Idria Formation serpentinite deposit of Joaquin Ridge in the upper watershed areas. The Cretaceous age of the Panoche Formation predates the Miocene age when the New Idria Formation became emergent. Consistent with the age of the Panoche Formation, no asbestos was detected in these samples.

5.3 Streambed Stations

Approximately 40 samples were collected from the streambeds of White Creek, Pine Canyon Creek, Los Gatos Creek, and other tributaries to the Arroyo Pasajero, including Warthan Creek, Jacalitos Creek, and Zapato-Chino Creek. See Figure 5-1. The samples were collected from fine-grained channel sand deposits. The streambed samples ranged from 85% elongate serpentine asbestos in the upper White Creek area (upstream from the juncture of White Creek with Pine Canyon Creek) to less than 1% elongate serpentine asbestos in the lower watershed area near the alluvial fan, as described below. Because of the semi-arid environment in the Coalinga region and the low annual rainfall, most of the streams in the area are classified as intermittent and are observed to be flowing only in response to runoff from precipitation.

Reproduced with permission of the copyright owner. Further reproduction prohibited without permission.

5.3.1 White Creek

Approximately 5.8 square miles of the New Idria Formation are drained by the White Creek drainage system. This drainage system consists of a network of more than 18 miles of intermittent stream channels which drain areas of 100 acres or more within the upper White Creek watershed. Five of the first order tributaries head near the Atlas Site and others head near and flow along the erosional margins of the many serpentinite landslide and/or debris flow deposits in the White Creek area. The serpentinite landslide and/or debris flow complex in the White Creek drainage area covers more than three square miles. These weakly consolidated deposits are being dissected by the dendritic drainage network of the intermittent stream channels. The headward erosion of the intermittent stream channels along the margins of the serpentinite debris flow deposits has contributed to the occurrence of severe gullying and mass wasting of the serpentinite soils since prehistoric times. The continued headward erosion of these intermittent channels is partly related to the continuous uplift and extrusion of the New Idria Formation serpentinite deposit in relationship to crustal compression associated with the San Andreas fault and the tectonic convergence of the Pacific oceanic plate and the North American continental plate.

In addition to the Atlas Site, other open-pit mining operations associated with large disturbed surface areas in the White Creek watershed include the James-Corbett-Byles Mine, the Big Ridge Chromite Mine, the Tromby No. 1 and No. 2 Chromite Mines, the White Creek Magnesite Mine, and part of the Butler Estate Chromite Mine. (See Part One, Figure 7A, which is a mine site location map). The Butler Estate Chromite Mine is drained primarily by the Pine Canyon watershed. However, a relatively small part of the Butler Mine is located on the drainage divide between the White Creek

Reproduced with permission of the copyright owner. Further reproduction prohibited without permission.

watershed and the Pine Canyon watershed. Therefore, the Butler Mine is included in discussions of mining operations in both watersheds.

The White Creek channel was also associated with as many as five chromite milling operations that were active in the 1940's and 1950's. These wet-process, gravity settling chromite milling operations used water to separate the relatively dense chromite grains from the asbestos-bearing serpentinite matrix. Water was captured by earthen dams constructed across White Creek. The remnants of some of these dams still exist and act to restrict flow during storm events. After the disseminated chromite grains were separated from the flaky serpentinite ore by the gravity settling milling process, the waste serpentinite material was reportedly dumped into White Creek (personal communication, Charlie Akers, 1988). The mill operators reportedly had problems with the flaky serpentinite chromite "gangue" which "tended to plug mill discharge screens, lower the recovery of chromite, and adversely affect the clean separation of chromite from the gangue (i.e., unprocessed ore)" (Matthews, 1961).

The chromite milling operations have been described by Matthews (1961, p. 8, 9, and 17, and Photos 2 and 3), however there has been no published discussion of the impact of these milling operations on the amount of sediment in the White Creek streambed. Field observations and aerial photographs show that the upper White Creek drainage pathway is choked with an abundance of fine sand and coarse, silt sized sediment. Chromite production figures indicate that as much as 47,000 tons or more of chromite tailings were generated by milling operations during the late 1940's and early 1950's (Matthews, 1961; EPA, Inventory of Potential Sources Report, 1987; Rice, 1957; Walker and Griggs, 1953). It is not known if most of this material has been washed downstream to the alluvial fan, or if most of it remains in the White Creek-Los Gatos Creek drainage pathway. Considering the semi-arid environment and the infrequent

Reproduced with permission of the copyright owner. Further reproduction prohibited without permission.

but high flow rates of major storm events in the Coalinga region, either of the above possibilities is feasible.

Figures 5-11 and 5-12 illustrate the downstream trend in elongate serpentine asbestos concentrations measured at various points along White Creek's intermittent streambed beginning near the base of the New Idria Formation outcrop and going downstream to the White Creek juncture with Los Gatos Creek. Samples taken in the White Creek streambed downstream of the New Idria outcrop area had elongate serpentine asbestos concentrations as high as 85%. Elongate serpentine asbestos concentrations decreased gradually to approximately 60% between the outcrop margin and the juncture of White Creek with Pine Canyon Creek. Downstream of the juncture with Pine Canyon Creek, the elongate serpentine asbestos concentrations of the sampled White Creek streambed sediment decreased to 30%, as measured at sampling station SS-20.

5.3.2 Pine Canyon

The Upper Pine Canyon drainage network drains approximately 1.0 square mile of the New Idria Formation in an area that includes most of the Butler Estate Chromite Mine and the Jensen Asbestos Mine. The Upper Pine Canyon area also includes a large landslide and/or debris flow complex that underlies most of the Johns-Manville Coalinga Asbestos Mill Site, including the Railroad Mine. This landslide and/or debris flow complex is composed of several mappable components that originated in the New Idria Formation outcrop area. Some of the debris flow components are rich in serpentinite minerals. The upper detachment zones of this landslide and/or debris flow complex are being dissected by a dendritic drainage network. The middle and lower portions of the deposits are associated with gully-like erosional channels that have formed on the margins of the landslide and/or debris flow deposits.

Reproduced with permission of the copyright owner. Further reproduction prohibited without permission.

Field observations and a review of topographic maps of the Joaquin Ridge area show that the upper Pine Canyon area is less steep than the upper White Creek area, and gully erosion is less severe in the Pine Canyon area in comparison with gully erosion in the White Creek area.

The Pine Canyon streambed sediment samples exhibited a decreasing trend in asbestos concentrations as samples were located farther downstream from the New Idria Formation and the Johns-Manville Coalinga Asbestos Mill Site. See Figure 5-11. The Pine Canyon streambed samples located downstream from the Johns-Manville Coalinga Asbestos Mill Site had elongate serpentine asbestos concentrations that ranged from 25% to 5% or less near Pine Canyon Creek's juncture with White Creek (approximately 5.5 miles downstream from the Johns-Manville Coalinga Asbestos Mill Site). The generally low asbestos concentrations of the Pine Canyon Creek samples located downstream of the Johns-Manville Coalinga Asbestos Mill Site are in agreement with field observations that there is much less asbestos in this reach of the Pine Canyon drainage pathway in comparison with the abundance of asbestos in the White Creek drainage pathway. This observation is in agreement with other evidence including aerial photographs and consideration of the number and extent of potential sources in the Pine Canyon drainage area in comparison with the White Creek drainage area.

5.3.3 Los Gatos Creek

For interpretation purposes, Los Gatos Creek has been divided into three sections. The upper section is located upstream of the juncture of White Creek with Los Gatos Creek, the middle section is located between the White Creek-Los Gatos Creek

Reproduced with permission of the copyright owner. Further reproduction prohibited without permission.

juncture and the Warthan Creek-Los Gatos Creek juncture, and the lower section is located east of Coalinga between the juncture of Warthan Creek with Los Gatos Creek and the juncture of Zapato-Chino Creek with Los Gatos Creek. Downstream of this stream juncture, the channel is known as the Arroyo Pasajero. See Figure 2-1 and 5-1.

The three samples collected within the upper section of the intermittent Los Gatos Creek streambed had non-detectable or trace levels of elongate serpentine asbestos. The upper drainage area of this part of Los Gatos Creek does not drain any of the New Idria Formation outcrop area as mapped by Jennings, 1971. However, the drainage area does include approximately 2-square-miles of the metamorphic Franciscan Complex and 0.25-square-miles of an ultramafic serpentinite deposit (see geologic map cited above). This area includes the inactive Rhodes-Byles-Gribble Chromite Mine located on the southwestern flank of Condon Peak (T.18 S., R.12 E., Sec. 35, S 1/2). As indicated by reconnaissance surveys of the White Creek and Pine Canyon drainage areas, the northern portion of the upper Los Gatos Creek drainage area may include remnants of serpentinite debris flow deposits that flank the serpentinite outcrop area. Based on field observations and sampling results, the metamorphic and ultramafic terrain of the Rhodes-Byles-Gribble Mine area does not appear to be contributing readily detectable quantities of asbestos containing sediment to the streambed sediment of Upper Los Gatos Creek.

The middle section of Los Gatos Creek had elongate serpentine asbestos concentrations that decreased downstream from 20% to 10%. The middle section of Los Gatos Creek meanders downstream from the juncture with White Creek through the lower half of the Los Gatos Creek Valley and across the northeastern quadrant of the Pleasant Valley floodplain. In the streambed interval between Highway 198 and Calaveras Avenue, the particle size distribution of the streambed sediment is observed

Reproduced with permission of the copyright owner. Further reproduction prohibited without permission.

to change from a sandy gravel with abundant pebbles and cobbles to gravelly sand with a large percentage of fines and only a trace of pebbles and cobbles.

The lower section of Los Gatos Creek had elongate serpentine asbestos concentrations that were all less than 1%. The lower section of Los Gatos Creek, which extends from the juncture of Los Gatos Creek with Warthan Creek to the juncture of Los Gatos Creek with Zapato-Chino Creek, consists of 4.6 miles of a meandering intermittent streambed that heads east from Coalinga across the Pleasant Valley floodplain and across the structural axis of the Coalinga Anticline. The intermittent stream crosses the structural axis of the Coalinga Anticline by flowing through a gap between Anticline Ridge and Guijarral Hills. This gap is located approximately six miles east of the town of Coalinga. See Figures 5-1 and 5-4.

Because of uplift associated with the upward folding of the Coalinga Anticlinal Structure, the hydraulic gradient and sediment transport capacity for this part of Los Gatos Creek has been reduced. Consequently, most of the coarse silt and sand-sized sediment transported by Los Gatos Creek has apparently been deposited on the west side of the structural axis of the anticline (i.e., in the broad, entrenched, meandering floodplain of Los Gatos Creek on the southwestern side of Pleasant Valley). The "trapped" sediment is deposited in braided sand deposits that are subject to scouring and cut and fill processes that tend to winnow the fine silt and clay fractions.

The uplift of the anticlinal structure has contributed to the entrenchment of the Los Gatos Creek drainage pathway on both sides of the anticline. On the west side of the anticline in the Pleasant Valley floodplain, the meandering Los Gatos Creek drainage pathway is entrenched approximately 40 feet and is associated with several inset terraces. On the east side of the anticline, the channel straightens and narrows to

Reproduced with permission of the copyright owner. Further reproduction prohibited without permission.

approximately 200 feet and is entrenched approximately 25 to 35 feet. The valley floor on the east side of the anticline in the vicinity of Huron has subsided approximately 20 feet in the past 30 years. This subsidence may have contributed to an increased hydraulic gradient on the east side of the anticline, and consequently increased streambed and streambank erosion. Field observations show that on the west side of the anticline the entrenched drainage pathway is dominated by depositional processes, whereas on the east side of the anticline the entrenched drainage pathway is dominated by erosional processes.

On the east side of the gap between Anticline Ridge and Guijarral Hills, Los Gatos Creek is joined by Zapato-Chino Creek. At this point, Los Gatos Creek becomes the Arroyo Pasajero Channel which has formed at the apex of the Arroyo Pasajero alluvial fan. In this area, the Arroyo Pasajero channel has become entrenched approximately 30 to 40 feet. Erosion of the streambed and streambanks and general downcutting of the Arroyo Pasajero channel in this area reportedly has occurred in response to an increased hydraulic gradient related to: (1) regional subsidence that has occurred in response to the overdraft of aquifers by agricultural pumping for irrigation purposes; (2) the collapse of pore space in sedimentary layers that have been wetted by agricultural irrigation; and (3) deep seated subsidence related to tectonic uplift of the Coalinga Anticline (Ireland, 1986; Munn, Busacca, and Trott, 1981; Bull, 1964).

5.3.4 Warthan, Jacalitos, and Zapato-Chino Creeks

Warthan and Jacalitos Creeks both join the lower section of Los Gatos Creek in the vicinity of Coalinga. See Figure 5-1. Two samples were collected on Warthan Creek, and both samples had non-detectable asbestos concentrations. Two samples were also collected on Jacalitos Creek. The upper sample contained a trace amount of asbestos

Reproduced with permission of the copyright owner. Further reproduction prohibited without permission.

and the lower sample's asbestos concentration was reported to be non-detectable. Two samples were collected on Zapato-Chino Creek, which joins the Arroyo Pasajero channel approximately nine miles east of Coalinga. Elongate serpentine asbestos concentrations reported for the upper and lower reaches of Zapato-Chino Creek were non-detectable and trace, respectively.

5.3.5 Arroyo Pasajero Channel

Three samples were collected from the Arroyo Pasajero channel in the area where the channel has become entrenched east of Guijarral Hills and Interstate 5 and downstream from the juncture with Zapato-Chino Creek. These samples showed elongate serpentine asbestos concentrations that ranged from trace levels to 1%. See Figure 5-1.

5.4 Arroyo Pasajero Alluvial Fan and Settling Basin Subsurface Sampling

5.4.1 Subsurface Sampling Program

The alluvial fan boring program included three borings located in the California Aqueduct settling basin (SB1, SB2 and SB3) and five borings located in the Arroyo Pasajero alluvial fan (AF1, AF2, AF3, AF4 and AF5). Two additional borings (AF6 and AF7) were located in the Pleasant Valley flood plain of Los Gatos Creek near the town of Coalinga. For the Arroyo Pasajero alluvial fan borings, two borings (AF1 and AF2) were located several miles east of the Aqueduct in the distal/medial portion of the fan and three borings (AF3, AF4, and AF5) were located in a line of cross-section oriented perpendicular to the trend of the Arroyo Pasajero stream channel in a medial portion of the alluvial fan on the northwest side of Huron.

Reproduced with permission of the copyright owner. Further reproduction prohibited without permission.

As indicated on the Alluvial Fan Sampling Station and Soil Map included in Appendix F, the alluvial fan and settling basin borings were located in fine- and medium-textured soils that had been mapped by the U.S. Department of Agriculture (USDA) in the soil survey of Coalinga and the Huron area in 1952. Based on textural characteristics and position on the alluvial fan surface, the USDA correlated the textural characteristics and soil type classification with alluvial fan depositional environments including old stream channel and drainage channel trends and overbank (or levee) and floodwater deposits. In addition to these soils types, the settling basin borings were located in sediment deposited as settling basin fill (i.e., floodwater deposits) that have been deposited on top of the soils mapped in the 1952 soil survey.

Lithologic logs for each of the continuously cored borings are presented in Appendix E. These logs include descriptions of the physical and textural characteristics of the encountered intervals. The logs also include interpretations of depositional environments based on textural characteristics and the distribution and geometry of alluvial fan depositional facies including alluvial channel, overbank, crevasse splay, and floodwater deposits. The textural characteristics, depositional interpretations, and asbestos concentrations of the sampled intervals are summarized in Appendix E.

As indicated on the boring logs of Appendix E, the settling basin and alluvial fan cores were sampled at depth intervals that were correlated with pre-asbestos mining and post-asbestos mining time periods, based on: (1) an interpretation of the stratigraphic layering of sediment in each core; (2) the relationship of depth with an approximation of alluvial fan sedimentation rates; and (3) information regarding the construction date of the California Aqueduct's sedimentation basin in relation to the initiation of asbestos mining and milling operations in the Joaquin Ridge area.

Reproduced with permission of the copyright owner. Further reproduction prohibited without permission.

For the settling basin cores, each core was sampled at three distinct intervals, including (1) 5 feet above the contact of sedimentation basin sediment fill with the underlying native materials, and (2) at 5 feet and at 10 feet below the contact of basin fill with the underlying native materials. Additional intervals were sampled based on lithologic and textural characteristics. This sampling program was intended to provide data regarding the concentrations of asbestos in sediments that could be correlated with pre-asbestos mining and post-asbestos (or concurrent) mining time periods.

The alluvial fan cores were similarly analyzed at depth intervals that were correlated with pre-asbestos and post-asbestos mining time periods. These sampled intervals are indicated in the boring logs included in Appendix E and the summary table of Appendix E.

5.4.2 Alluvial Fan Rates of Sediment Deposition

A C_{14} age date for angular charcoal debris recovered from a core located in an upper alluvial fan environment has indicated an upper alluvial fan depositional rate of approximately 0.01 foot per year (Atwater et al., 1986). Medial alluvial fan environments located at the terminus of an alluvial channel may accumulate sediment at a much higher rate (as much as one or two feet per year) over brief time periods. However, as these environments accumulate sediment, flood waters will shift to topographically lower areas and deposit their entrained and suspended sediments in laterally adjacent environments. This process contributes to the geologically long term uniform development of an alluvial fan.

Reproduced with permission of the copyright owner. Further reproduction prohibited without permission.

A review of aerial photographs and topographic maps (from the 1950's and 1970's) of the Arroyo Pasajero alluvial fan in the vicinity of Huron indicates that during this time period the Arroyo Pasajero channel has been debouching sediment to approximately a 15-square-mile area. Since construction of the Aqueduct, approximately 15,000,000 cubic yards of fine sand, silt, and clay sized material has been deposited in the settling basin constructed upslope of and adjacent to the California Aqueduct over an 18 year period (Simons, Li and Associates, 1985, p. 1). The settling basin covers an area of approximately 3 square miles (Scoping Report - Arroyo Pasajero Flood Detention Basin, Bureau of Reclamation, 1988, p. 2). This indicates a depositional rate of approximately 833,000 cubic yards per year for the settling basin area, which converts to an average deposition rate of approximately 0.27 feet per year for the settling basin. Prior to construction of the Aqueduct, this amount of material was deposited over approximately a 15-square-mile area. By extending the settling basin depositional rate to this 15-square-mile area, calculations show that this portion of the alluvial fan was probably receiving sediment at an average rate of 0.05 feet per year.

Since most asbestos and chromite mining and milling activities in the Arroyo Pasajero watershed began after 1940, post-mining/milling sediment deposition has occurred for approximately 48 years. An average deposition rate of 0.05 feet per year over this time period would result in approximately 2.4 feet of sediment accumulation in the medial and distal alluvial form. However, because of the variability of alluvial fan depositional processes as described above, localized depositional centers may accumulate sediment at a much higher rate over shorter periods of time (i.e., time periods as short as each depositional event).

The age interpretation of sediment deposited in the upper two feet of the modern alluvial fan surface is made more problematic by the widespread occurrence of field

Reproduced with permission of the copyright owner. Further reproduction prohibited without permission.

leveling, cultivation and disking which has acted to homogenize or mix the upper 18 to 24 inches of soil. Given the above factor, we have assumed that, outside of the Arroyo Pasajero settling basin, any samples located more than three feet below the current alluvial fan surface in the medial and distal alluvial fan environments (as sampled in the alluvial fan boring program) probably represent pre-asbestos mining (and also pre-chromite mining) sediment deposition.

5.4.3 Mining and Milling Activities That Predate the Late 1950's

Chromite mining and milling activities occurred through the 1970's in the White Creek and Pine Canyon drainage areas. Asbestos mining and milling activities in this area occurred in the 1960's and 1970's. As noted in this chapter, 47,000 tons or more of chromite ore tailings may have been generated by chromite milling activities and disposed of in the White Creek stream channel. Because of the overlap in time between the chromite mining and milling activities and the asbestos mining and milling activities, and because of uncertainties regarding the amount of time required to transport serpentinite bedload sediment the distance from the source areas to the settling basin (a streambed distance of approximately 55 miles), it is not possible to differentiate temporally between these activities in the asbestos analysis of alluvial fan sediment deposition.

Other mining operations that occurred in the White Creek and Pine Canyon drainage areas prior to the 1950's included the mining of magnesite (White Creek Magnesite Mine, EPA, Inventory of Potential Sources Report, 1987) in the 1930's and the prospecting for benitoite and neptunite crystals in the early 1900's (Gem Mine, EPA, Inventory of Potential Sources Report, 1987). The Archer Mercury Mine was discovered in 1904, was worked again in the 1940's, and lately (since the mid 1970's)

Reproduced with permission of the copyright owner. Further reproduction prohibited without permission.

by Steve Hansen who lives at the Archer Camp. The James-Corbett-Byles Mine was first mined in 1910 and worked again in the 1940's and 1950's (EPA, Inventory of Potential Sources Report, 1987).

5.4.4 Results of Alluvial Fan and Settling Basin Subsurface Sampling Program

A total of 44 alluvial fan and settling basin subsurface samples were analyzed by the PLM method, including 6 intra-laboratory and 4 inter-laboratory replicates (submitted blindly to Med-Tox and McCrone, respectively). A total of 32 samples were analyzed using the TEM method, including 8 intra-laboratory replicates (submitted blindly to Med-Tox).

The PLM analyses indicated that most sedimentation basin and alluvial fan samples have trace (i.e., less than 1%) or non-detectable concentrations of asbestos (see Table 5-16 and Figure 5-13). When only PLM measurements greater than the detection limit are considered, the average elongate serpentine asbestos concentration for both pre-mining and post-mining samples is 2%, with both groups having a maximum value of 3%. These samples ranged in depth from less than one foot to approximately 35 feet below the existing ground surface. No discernable trend between pre-asbestos mining and post-asbestos mining samples could be identified based on a qualitative review of the data. Given the relatively few samples with PLM results above the detection limit, statistical analysis were not performed on the alluvial fan PLM data.

The TEM analyses detected asbestos in all of the 32 alluvial fan samples that were analyzed by this method. Asbestos concentrations (reported as percent mass of all detected asbestos structures) ranged from 0.3% (sample AF2-15) to 10% (AF3-25), but were generally within the range of 1 to 3%. Based on a simple inspection of the

Reproduced with permission of the copyright owner. Further reproduction prohibited without permission.

TEM data for each boring, no trends could be observed regarding asbestos concentration with respect to sample depths. The data was further evaluated by statistical tests, as discussed below.

TEM sample results were divided into pre-asbestos mining and post-asbestos mining groups, as with the PLM data, and differences in asbestos concentration between these two groups were assessed using a t-Test. Where more than one pre-asbestos mining or post-asbestos mining sample result was available for a given sampled interval (i.e., for replicate sample analyses), the values were averaged prior to performing this statistical test. Statistical t-Tests were performed for data from all alluvial fan borings (AF-1, AF-2, AF-3, AF-4, AF-5, SB-1, SB-2, SB-3) (Table 5-17) and for just the settling basin borings (SB-1, SB-2, SB-3) (Table 5-18). For both of these groups, the t-Test results indicated that there was no significant difference between pre-asbestos mining and post-asbestos mining sample asbestos concentrations (significance level = 95%).

A qualitative analysis of the PLM and TEM results for the alluvial fan and settling basin subsurface samples from cores AF1, AF2, AF3, AF4, AF5, SB1, SB2, and SB3 suggests that there is no difference in asbestos concentrations for categories based on textural criteria (i.e., sand, silt, and clay size fractions). See Appendix E. This indicates that the alluvial fan depositional processes tend to equally distribute the asbestos sediment to most alluvial fan depositional environments including sheet flood, overbank, alluvial channel, crevasse splay, and settling basin fill deposits. For both PLM and TEM data, there does not appear to be a relationship between textural criteria and asbestos concentrations.

Reproduced with permission of the copyright owner. Further reproduction prohibited without permission.

5.4.5 California Department of Water Resources Sampling Program

The California Department of Water Resources (DWR) collected approximately 51 samples from the settling basin and the open fields located upslope and downslope of the California Aqueduct (California DWR, 1986). These samples were analyzed for asbestos by TEM methods. Most of the DWR samples had concentrations of less than 1%. Five of the DWR samples showed concentrations of slightly more than 1% (i.e., 1.1% to 1.3%). Qualitatively, these data suggest that the surface asbestos concentrations are slightly lower than the subsurface asbestos concentrations indicated by the alluvial fan subsurface core samples. However, considering that the asbestos analyses of this regional investigation and the asbestos analyses of DWR's investigation were performed by different laboratories which may have used different analytical procedures, the DWR surface soil sampling results were not statistically compared with subsurface data from this investigation; and given the variability associated with bulk soil asbestos analyses, the observed differences between surface and subsurface data probably reflect analytical differences.

Reproduced with permission of the copyright owner. Further reproduction prohibited without permission.

6.0 RESULTS AND INTERPRETATION OF COALINGA ASBESTOS MILL SITE SOIL SAMPLING DATA

Approximately 200 samples were collected as part of the Johns-Manville Coalinga Asbestos Mill (CAM) site sampling program. Most of these samples were collected from areas associated with previous mining and milling activities at the site. These areas included asbestos tailings, ore storage and loading areas, access roads through the site, and the Railroad Mine. Samples were also collected from potential borrow source areas and from streambeds and streambanks that have formed on the erosional margins of the serpentinite landslide and/or debris flow complex that underlies most of the site. The analytical results of asbestos analysis for samples collected from the Johns-Manville Coalinga Asbestos Mill Site are illustrated in Levine-Fricke, May 9, 1989: Chapter 2, Figures 4 and 5 (D-size fold-out sheets). These mill site results are summarized in this report in Tables 5-2 and 5-3.

Stations with the PC designation were located in the east and west forks of the intermittent stream channels that flank the CAM site. Stations designated PC-#B were located in the streambed and stations designated PC-#A and PC-#C were located in the streambanks in either native soils or landslide deposits, as indicated by sample type in Table 5-2. Stations designated BS were surface stations located in potential borrow source soil areas. Stations designated BP were excavation pits located in potential borrow source soil areas. Stations designated XP were excavation pits completed as part of a geomorphic investigation of the serpentinite landslide and debris flow deposits of Upper Pine Canyon. Stations designated AL were located near the margins of areas associated with historic milling and mining activities at the CAM site. These stations were located based on field observations and interpretation of aerial photographs. The AL stations were located to further define the boundaries of

Reproduced with permission of the copyright owner. Further reproduction prohibited without permission.

anthropically affected asbestos areas. Stations designated AL-#A were generally located outside of these areas, and stations designated AL-#B were generally located within these anthropically affected areas.

6.1 Coalinga Asbestos Mill Site Stream Channels

A total of 23 samples were collected from the streambeds of the intermittent channels that have formed on the margins of the serpentinite landslide and/or debris flow deposits that underlie most of the Johns-Manville Coalinga Asbestos Mill Site. These channels originate in the serpentinite outcrop area of the New Idria Formation which is located approximately 0.6 miles upslope from the site. These intermittent channels serve as potential pathways for the waterborne transport of asbestos from anthropic and non-anthropic sources located on-site and up-gradient of the site. As identified in the regional geologic investigation and the review of aerial photographs, the off-site sources in the Pine Canyon area include the New Idria Formation outcrop area, the serpentinite debris flows that have migrated downslope from the outcrop area, the Butler Estate Chromite Mine (or Mistake Mine), and the Jensen Mine. The on-site sources include the serpentinite debris flow deposits (including the five-acre area previously mined as the Railroad Mine), ore brought to the Mill Site as part of asbestos and chromite milling operations, and tailings produced by asbestos and chromite milling.

The on-site/near-site stream sediment samples in Pine Canyon (designated with the prefix PC) were obtained from the east and west forks of Pine Canyon upstream of, adjacent to, and downstream of former asbestos and chromite milling operations at the site. Relatively little sediment was observed in the east fork streambed below tailings at the site. However, localized pockets of sediment were found and sampled.

Reproduced with permission of the copyright owner. Further reproduction prohibited without permission.

Analysis of on-site and near-site streambed samples suggest that sediments located above the CAM site generally have equivalent concentrations of asbestos (95% confidence interval of 41% to 80%) than sediment located downstream from the Coalinga Site (95% confidence interval of 29% to 68%). This data indicates that the Coalinga Asbestos Mill Site is not discharging significant quantities of asbestos-bearing sediments to Pine Canyon Creek. In addition, based on the sediments observed upstream of the sediment trapping dam, this dam, constructed at the base of the tailings pile, is believed to be helping to reduce sediment discharge from the site.

6.1.1 West Fork of Pine Canyon at Johns-Manville Coalinga Site

A total of 13 samples were collected in the west fork streambed from areas located upstream, alongside, and downstream of the Coalinga Asbestos Mill Site milling and mining operations areas, including the Railroad Mine. These samples were identified as PC-1 through PC-6 and PC-9, PC-10, PC-11, PC-13, PC-41, PC-42, and PC-43. Potential asbestos sources that are drained by the west fork include:

(1) New Idria Formation outcrop area (located upgradient of the site);

(2) Erosional margins of Upper Pine Canyon serpentinite debris flows (upstream and throughout the site);

(3) Butler Estate Chromite Mine (upstream of the site);

(4) Jensen Mine (upstream of the site);

Reproduced with permission of the copyright owner. Further reproduction prohibited without permission.

(5) Chromite ore and mill tailings associated with Marmac's on-site milling operations; and

(6) Erosion of serpentinite landslide material associated with the Railroad Mine.

Sediment samples have been analyzed numerically with three different comparisons. First the mean concentrations were generated to provide an indication of data trends. Second, modal concentration ranges were discerned to provide an under-standing of data trends which could eliminate analogous sampling and analytical results. Lastly, data was scrutinized statistically to determine, with a 95% certainty by use of the student t-test, if data sets were statistically discrete. Results of these analyses are discussed below.

For streambed sediment samples located in the west fork upstream from the Site, the mean elongate serpentine asbestos concentration was 58%, with a modal concentration range of 41 to 80%, and a 95% confidence interval ranging from 40% to 75%. See Table 5-19 and Figure 5-13. For streambed sediment samples located in the west fork in areas adjacent to and downstream of the anthropically affected Mill Site areas, the mean elongate serpentine asbestos concentration was 49%, with a modal concentration range of 41 to 80%, and a 95% confidence interval ranging from 29% to 68%. See Table 5-20 and Figure 5-15. Sampling of Upper Pine Canyon streambanks formed by serpentinite landslide and/or debris flow deposits showed that these natural deposits had a mean elongate serpentine concentration of 16%. See Table 5-21 and Figure 5-16. Based on the above results, elongate serpentine asbestos concentrations of streambed sediments in the west fork was found to have a higher mean value and have statistically equivalent concentration upstream of the Coalinga Asbestos Mill Site than alongside of and/or downstream of anthropically affected areas at the Coalinga

Reproduced with permission of the copyright owner. Further reproduction prohibited without permission.

Asbestos Mill Site. The above results also show that erosion of the streambanks formed by serpentinite landslide and/or debris flow deposits located upstream, along side, and downstream of the Site, may be a significant source of asbestos containing sediment in the upper Pine Canyon area.

6.1.2 East Fork of Pine Canyon at Johns-Manville Coalinga Site

Nine stations were located in the east fork of Pine Canyon as part of the On-Site/Near-Site sampling program. Five of the stations were located upstream of the tailings pile and other anthropically affected areas and four stations were located downstream from the tailings pile and the sediment retaining dam. Potential asbestos sources that are drained by the east fork include:

(1) New Idria Formation outcrop area located upstream of the Johns-Manville Coalinga Site;

(2) Erosional margins of Upper Pine Canyon serpentinite landslide and/or debris flow deposits located upstream of and throughout the Johns-Manville Coalinga Site; and

(3) the Johns-Manville Coalinga Site tailings pile.

Five samples from the on-site/near-site sampling of the east fork were located upstream of the areas affected by the mill site operations and/or the east fork tailings pile. These samples (PC-56, PC-57, PC-58, PC-59, AL-32B) had an elongate serpentine asbestos concentration that averaged 47%. The results of these samples correlate with field observations of asbestos-containing sediment in the east fork channel upstream of the Johns-Manville Coalinga Asbestos Mill Site. A review of

Reproduced with permission of the copyright owner. Further reproduction prohibited without permission.

aerial photographs shows that the source of this sediment was erosion of the margin of a serpentinite landslide and/or debris flow deposit that is upgradient from the Site.

Four stations were located in the streambed downstream of the east fork tailings pile (between the sediment trapping dam and the junction of the east and west forks of Pine Canyon Creek). In this part of Pine Canyon, the streambed is mostly bare rock with only scattered pockets of fine-grained sediment. These pockets generally measure several feet in diameter and are less than one inch thick. Some of this sediment may have been deposited when the sediment trapping dam was breached in 1983. However, most of the dam remained intact, preventing large quantities of sediment from being transported downstream. In February 1987 the dam was repaired, further limiting sediment discharge from the tailings pile and other upstream sources. The four samples collected downstream of the sediment trapping dam were located at approximately 500-foot intervals and had elongate serpentine asbestos concentrations that decreased downstream from 75% to 5%. The sample with the highest concentration was located closest to the dam. Field observations of very little sediment in the east fork streambed downstream from the sediment trapping dam agree with aerial photographs indicating little or no asbestos in the lower reaches of the east fork (i.e., approximately 0.3 miles downstream from the sediment trapping dam).

A short distance from the juncture of the east and west forks of Pine Canyon, one sample, PC14-B, had a reported asbestos concentration of 80%. Given the relatively higher asbestos concentrations found in the west fork channel upstream of this juncture, it appears likely that sample PC14-B represents asbestos-bearing sediments transported via the west fork, as opposed to sediments originating from the east fork tailings pile.

Reproduced with permission of the copyright owner. Further reproduction prohibited without permission.

6.2 Potential Borrow Source Materials

Potential borrow source and borrow pit samples were obtained at locations previously identified by field investigations (based on observations of physical characteristics and PLM asbestos analyses) to possibly be suitable as a source of cover materials for tailings and ore at the Site. Potential borrow source surface soil samples (designated with the prefix BS) were taken in areas north and south of the former milling and mining areas of the Johns-Manville Coalinga Site. Borrow pit samples (designated with the prefix BP or XP) were taken from excavation pits located in the borrow source areas. These samples were used to evaluate the volume of potential borrow source materials available for remediation use. Thirty samples were obtained from areas located north of the mill (designated as the upper borrow source area). Nine BS samples were collected from areas downgradient from the Railroad Mine area (designated as the lower borrow source area).

For samples from the upper borrow source area, the elongate serpentine asbestos concentration ranged from 0% to 2% with a modal concentration range of 0 to 1%, and a mean concentration of 1%. See Figure 5-17 and Table 5-22. The lower borrow source area had an elongate serpentine asbestos concentration that ranged from trace levels (i.e., less than 1%) to 10% with a modal concentration range of 6 to 10%, and a mean value of 6%. See Figure 5-18 and Table 5-23.

6.3 Geomorphic Excavation Pits

The Excavation Pit series of samples (designated XP) were taken as part of a geomorphologic field investigation of the soil profiles associated with the serpentinite landslide and/or debris flow deposits of Upper Pine Canyon. Additionally, some of

Reproduced with permission of the copyright owner. Further reproduction prohibited without permission.

these samples were located in areas targeted as potential borrow sources, and were therefore used in conjunction with the BP and BS samples to evaluate the suitability of potential borrow materials at the Site.

Results from the excavation pit series of samples indicate varying concentrations of asbestos that appear to correlate with observations of the development of soil profiles. Areas associated with deep, well developed soil profiles generally had low concentrations of asbestos and areas associated with shallow, poorly developed soil profiles had slightly higher concentrations of asbestos.

Excavation Pit XP-1, located near the center of a flat area marking a break in slope at the base of Railroad Mine area, had asbestos concentrations that ranged from 60% to 70%. Excavation Pit samples XP-2, XP-3, and XP-5 had asbestos concentrations that ranged from less than 1% to 5% with one sample having a concentration of 10%. The northernmost Excavation Pit sample (XP-6) was found to have the highest elongate serpentine asbestos concentration, 90%. Excavation Pit XP-6 is located approximately 1,000 feet upgradient of the Site on the western flank of a serpentinite debris flow deposit in the New Idria Formation that has been recognized as a rich source of asbestos ore. This serpentinite deposit was the source of the asbestos ore mined by the Jensen Mine. Gully erosion of the margins of this deposit is presently contributing asbestos-containing sediment to both the east fork and the west fork intermittent drainage pathways. The high values for asbestos for samples from XP-6 correlate well with field observations of a rich serpentinite soil that supports a restricted manzanita vegetative community and aerial photographs which show reflectance characteristics that indicate a rich serpentinite deposit.

Reproduced with permission of the copyright owner. Further reproduction prohibited without permission.

6.4 Anthropically-Affected Surface Areas

Asbestos limiting samples (designated with the prefix AL) were generally taken along the boundaries of tailings, ore storage/loading areas, and the Railroad Mine, in order to further define the lateral extent of anthropically-related asbestos materials at the Site. Stations designated AL-#A were generally located outside of these areas, and stations designated AL-#B were generally located within the anthropically-affected areas. Exact locations were based on consideration of field observations and aerial photographs of the Site.

6.4.1 Tailings Pile in East Fork of Pine Canyon Creek

Nineteen surface samples were collected in the tailings located in the east fork of Pine Canyon. These samples had a mean elongate serpentine concentration of 64%, and a modal concentration range of 61% to 80%. See Table 5-24. Nineteen surface samples were also collected outside the perimeter of the tailings. These outer samples had a mean elongate serpentine concentration of 11%. However, two "outer boundary" stations (AL-17A and AL-18A) located near the western margin of the tailings pile had relatively high elongate serpentine asbestos concentrations (40%) compared to the other outer boundary samples (typically with trace asbestos concentrations). Therefore, the western margin of the tailings pile was re-defined to include the areas around these two sampling stations. Nevertheless, the areal extent of asbestos tailings was determined to be practically the same as had been previously identified in the 1986 sampling program. The tailings at this location cover approximately 10.8 acres, with an estimated volume of 411,000 cubic yards.

Reproduced with permission of the copyright owner. Further reproduction prohibited without permission.

6.4.2 Ore Storage/Loading Area

The ore storage/loading area is a gently sloping area north of the former milling facility and northwest of the tailings pile. This part of the Site was apparently used for the stockpiling of ore during the dry season (when ore could be transported to the Site via the steep mountain roads leading down from mines in the New Idria Formation). Additionally, ore is believed to have been loaded from this area into the mill facility for further processing. The five surface samples collected from within this area had an average elongate serpentine asbestos concentration of 70%, with a modal concentration range of 61 to 80%. See Table 5-25. Seven samples were collected outside of this location. These seven samples had a mean elongate serpentine concentration of 5%. The ore storage/loading area has an estimated area of 4.9 acres, and a volume of 38,000 cubic yards of ore.

6.4.3 Mill Site Operations Area

The Mill Site operations area is a gently sloping area extending to the west, south, and southeast of the former chromite and asbestos milling facilities. It is bounded on the north by the ore storage/loading area, on the west by the west fork of Pine Canyon, and on the east by the tailings pile in the eastern fork of Pine Canyon. This area contains several small ponds associated with Marmac's former chromite milling operation. The ponds contain chromite tailings which have been covered over with fill and have become revegetated. Additionally, much of this area appears to have been graded over at some time in the past. The tailings at this part of the Site have an estimated volume of 4,000 cubic yards and cover an area of approximately 4.1 acres.

Reproduced with permission of the copyright owner. Further reproduction prohibited without permission.

Nine samples were collected from surface soils within this area. These samples had a mean elongate serpentine asbestos concentration of 15%, with a modal concentration range of 11 to 20%. See Figure 5-20 and Table 5-26.

6.4.4 Railroad Mine

The Railroad Mine is located approximately 300 yards southwest of the former mill facility at the Site, near the west fork of Pine Canyon Creek. It is believed to have been prospected for lump chromite ore beginning in the 1950s. Field mapping and interpretation of aerial photographs show that the Railroad Mine material was deposited by landslides and/or debris flows originating from a side canyon located to the west of the present Railroad Mine area. This deposit overlies the main Mill Site landslide/debris flow deposit and consequently is younger and has a different geologic history.

Based on field observations, most of the overburden from the Railroad Mine appears to have been pushed downslope to the southeast of the excavated area. However, some of the Railroad Mine soils were pushed in a westerly direction into the west fork of Pine Canyon. A drainage pipe was reportedly installed at the base of the overburden in order to pass upstream flow (personal communication, Charlie Akers, 1988). According to Mr. Akers (who worked the Railroad Mine Deposit), this material has subsequently been washed away. Traces of the material are evident on the western side of the streambank where the pile had covered the hillside's natural vegetation. Most of this overburden consisted of weathered soils that formed on the landslide deposit that was excavated as the Railroad Mine.

Reproduced with permission of the copyright owner. Further reproduction prohibited without permission.

Ten surface samples were collected from locations within the Railroad Mine where overburden soils had been removed previously. These samples had a mean elongate serpentine asbestos concentration of 49% with a modal concentration range of 61 to 80%. See Figure 5-22 and Table 5-27. The data were variable, possibly reflecting differences in soil types and/or mining-related activities at this part of the Site. Ten surface samples were also collected near the perimeter of the Railroad Mine to assess the asbestos concentrations of the unmined serpentine soils at this part of the Site. These 10 samples had a mean elongate serpentine concentration of 9%. Additionally, three subsurface samples were collected from the geomorphic exploration pit XP-1 located approximately 200 feet downslope from the Railroad Mine. The XP-1 samples had asbestos concentrations of 60% (2 to 3 feet), 60% (4 to 5 feet), and 70% (5.5 to 6.5 feet). These results are similar to the average asbestos concentration measured at the Railroad Mine.

Since the Railroad Mine consists of a natural serpentinite soil deposit, its volume has not been estimated. However, the areal extent of the Railroad Mine (i.e., where overburden has been removed and prospecting has taken place) is approximately five acres.

6.4.5 Access Roads

Nine samples were collected from the unpaved surfaces of roads that pass through the Site near the former milling facility. Six of these samples had trace asbestos concentrations (i.e., < 1%). The sample with the highest concentration (AL-37) had an elongate serpentine asbestos concentration of 10%. Sample AL-37 was located approximately 25 feet north of the ore storage/loading area at the Site. The mean elongate serpentine asbestos concentration for all nine samples was 2%, with a modal

Reproduced with permission of the copyright owner. Further reproduction prohibited without permission.

concentration range of 0 to 1%. See Figure 5-23 and Table 5-28. These results indicate that, except in localized areas, road surfaces are not significant source areas for asbestos at the Johns-Manville Coalinga Site.

Reproduced with permission of the copyright owner. Further reproduction prohibited without permission.

7.0 CONCLUSIONS

The regional soil sampling program included a regional reconnaissance investigation of the occurrence and distribution of asbestos-containing sediments and soils in the New Idria Formation outcrop area drained by Los Gatos Creek and from intermittent streambed and alluvial fan deposits in the Arroyo Pasajero watershed basin. The on-site/near-site sampling program was conducted in order to characterize asbestos-containing materials at the Johns-Manville Coalinga Site. The regional sampling program included: petrographic, PLM, and TEM analyses of bulk sediment and soil samples; field observations of potential asbestos source areas and drainage pathways, and a review and interpretation of aerial photography including color infrared imagery. Principal findings of this investigation are summarized below.

Regional Off-Site Sampling Program

1. The presence of asbestos throughout the regional study area is overwhelmingly attributable to natural geologic sources, including the New Idria Formation. Approximately 80 to 90% of the formation is composed of a soft, friable, platey matrix of serpentinite minerals including chrysotile and chrysotile polymorphs of lizardite and antigorite. The formation's surface outcrop covers more than 48 square miles, the depth of the deposit extends to more than 15,000 feet, and it has been estimated that the formation would yield hundreds of millions of tons of asbestos ore (Matthews, 1962, p. 19; Rice, 1963, p. 6). Field observations and laboratory analysis show that the bulk of the New Idria Formation's serpentinite matrix consists of mostly short-fiber chrysotile asbestos.

Reproduced with permission of the copyright owner. Further reproduction prohibited without permission.

The mean elongate serpentine asbestos concentration for serpentinite soil samples collected in the New Idria Formation outcrop area was 86%, with a modal concentration range of 80% to 100%. The mean elongate serpentine asbestos concentration for mine surface samples collected in the New Idria Formation outcrop area was 81%, with a modal concentration range of 80% to 100%. Thus, mined surfaces and unmined serpentinite soils had very similar asbestos concentrations.

2. White Creek drains approximately 5.8 square miles of the New Idria Formation in an area that includes 8 mining operations, 5 milling operations, and approximately 3 square miles of serpentinite landslide and debris flow deposits. Of all the streambeds which were sampled, the intermittent White Creek channel was found to have the greatest quantity of asbestos-bearing sediment, which generally ranged from 60% to 85%. This concentration is approximately the same as that measured in the New Idria Formation serpentinite outcrop area. The White Creek channel is generally broad (up to 150 feet wide) and braided into channel sand and channel gravel deposits ranging up to 300 feet long and 30 to 60 feet wide. The abundance of sediment in the broad, intermittent channel is indicative of the relatively large volumes of asbestos-containing sediment that has been deposited in and transported through the White Creek drainage pathway.

3. Pine Canyon Creek drains approximately 1.0 square mile of the New Idria Formation in an area that includes 3 mining operations, 1 milling operation, and approximately 0.5 square miles of serpentinite landslide and debris flow deposits. Compared to White Creek, Pine Canyon Creek has relatively little asbestos-bearing streambed sediment. Field observations show that there is very little sediment deposition in the Pine Canyon drainage pathway. The scattered, isolated areas that are accreting fine-grained sediment are generally less than 10 feet in diameter. The

Reproduced with permission of the copyright owner. Further reproduction prohibited without permission.

streambed generally consists of barren rock which is sometimes covered with a thin veneer (i.e., 1 to 2 inches) of sandy gravel with little evidence of asbestos-containing sediment. Upstream of the Johns-Manville Coalinga Asbestos Mill Site, streambed sediment has asbestos concentrations that range from 85% to 60% in the west fork and 35% to 65% in the east fork. Downstream of the Johns-Manville Coalinga Site, the asbestos concentrations of the streambed sediments decrease in a downstream direction from 25% to 5% or less near the juncture of Pine Canyon Creek with White Creek. The Pine Canyon channel is generally shallow and very narrow (ranging from approximately 10 to 30 feet wide).

4. At the juncture of White Creek and Pine Canyon Creek, White Creek has a wider channel (80 feet versus 20 feet), greater sediment deposition, and higher asbestos concentrations than Pine Canyon Creek. Samples taken from this area show that White Creek has an elongate serpentine asbestos concentration that ranges from 60% to 80% on the upstream side of the juncture, while Pine Canyon has a concentration that ranges from trace levels to 5% in samples collected a short distance upstream of the juncture. The width of these intermittent streambed channels is related to the areal extent of the upstream drainage basins and the erosional characteristics of the channels. The White Creek drainage area is much larger than the Pine Canyon drainage area, hence the larger channel (and a greater capacity for sediment transport) for the intermittent White Creek streambed.

5. In the White Creek streambed interval between Pine Canyon Creek and Los Gatos Creek, asbestos concentrations decrease downstream from 65% to 30%. In the Los Gatos Creek streambed interval between White Creek and Warthan Creek on the east side of Coalinga, asbestos concentrations decrease from 20% to 10%. Further downstream, between Warthan Creek and the Arroyo Pasajero alluvial fan, the

Reproduced with permission of the copyright owner. Further reproduction prohibited without permission.

asbestos concentration of streambed sediment in Los Gatos Creek and the Arroyo Pasajero was mostly less than 1%. Streambed sediment samples from Los Gatos Creek tributaries other than White Creek all had asbestos concentrations of less than 1%.

6. The petrographic characteristics of 12 samples were evaluated in an effort to identify possible distinguishing characteristics for particular asbestos source areas (e.g., tailings, mine surfaces, etc.). However, based on these petrographic analyses, neither asbestos morphology or associated mineralogy appear to be effective parameters for distinguishing the source of asbestos in any particular sample. Particle size analyses of these samples did indicate a decrease in grain size of processed asbestos ore versus unprocessed asbestos ore. However, this observation could not be extended to the interpretation of streambed sediment because of the tendency towards mechanical grain size reduction during waterborne transport.

7. Subsurface samples from continuously cored soil borings in the Arroyo Pasajero alluvial fan and settling basin indicate that pre-asbestos mining and post-asbestos mining elongate serpentine asbestos concentrations are not significantly different. Both pre-asbestos mining and post-asbestos mining subsurface samples had average asbestos concentrations which were less than 1%.

8. Surface soil samples from an additional geologic source, the "Big Blue" sedimentary asbestos deposit exposed in the Big Blue Hills north of Coalinga, had asbestos concentrations which ranged from 25% to 90%, with a mean concentration of 66%. These data show that asbestos concentrations of the "Big Blue" can range as high as that measured for the New Idria Formation. The "Big Blue" is drained by Cantua Creek and Salt Creek, which discharge to the California Aqueduct.

Reproduced with permission of the copyright owner. Further reproduction prohibited without permission.

Coalinga Asbestos Mill Site On-Site/Near Site Sampling Program

1. Tailings and unmilled ore at the Johns-Manville Coalinga Asbestos Mill Site have average elongate serpentine asbestos concentrations of 64% and 70%, respectively. Unaffected areas adjacent to the tailings pile and ore storage/loading area generally have elongate serpentine asbestos concentrations of 1% or less.

2. The Railroad Mine, located in Quaternary-aged serpentinite landslide deposits at the Site, has an average elongate serpentine asbestos concentration of 49%. Unaffected areas adjacent to the Railroad Mine have elongate serpentine asbestos concentrations which range from 30% to less than 1%. Subsurface samples from an excavation pit (XP-1) located approximately 200 feet southeast of the base of the Railroad Mine had elongate serpentine asbestos concentrations ranging from 60% to 70%. These results indicate that, in the area of the Railroad Mine, the serpentinite landslide deposits and related soils have relatively high, naturally occurring concentrations of asbestos.

3. Sediment from the east fork upstream of the Coalinga Site had an elongate serpentine asbestos concentration that ranged from 35% to 50%; sediment from the west fork upstream from the Coalinga Site had an elongate serpentine asbestos concentration range of 60% to 85%. Sediment located downstream of the johns-Manville Coalinga Site had an elongate serpentine asbestos concentration that decreased downstream from 25% to 5% or less.

4. The four stations located downstream of the east fork tailings pile (between the sediment trapping dam and the junction of the east and west forks of Pine Canyon Creek) had a mean elongate serpentine asbestos concentration of 47%. These stations

Reproduced with permission of the copyright owner. Further reproduction prohibited without permission.

were spaced at approximately 500-foot intervals and showed a distinct trend of decreasing asbestos concentrations with distance downstream (i.e., elongate serpentine concentrations decreased from 75 to 5%). Very little sediment was found in the east fork streambed downstream from the sediment trapping dam. Over this reach, the streambed is mostly bare rock with only scattered pockets of fine-grained sediment. These pockets generally measure several feet in diameter and are less than one inch thick. These sampling results and field observations suggest that remedial actions taken at the Site are mitigating potential erosion from the tailings pile in the east fork of Pine Canyon.

5. Potential borrow source soils are located at two general areas near the former asbestos mill at the Site. These areas are the upper borrow source area (located upslope from the former mill area) and the lower borrow source area (located downslope from the Railroad Mine). The upper borrow source soils had an average asbestos concentration of 1%, with a modal range of 0% to 1%. The lower borrow source soils had an average asbestos concentration of 6%, with modal range of 6% to 10%. The borrow source soils are generally silty clays (CL) with deep, well-developed and well-drained soil profiles that supported a grassy vegetative cover over approximately 90% of the surface.

Reproduced with permission of the copyright owner. Further reproduction prohibited without permission.

8.0 REFERENCES

Bull, W.B. 1964. Geomorphology of Segmented Alluvial Fans in Western Fresno County, California. U.S. Geological Survey, Professional Paper 352-E.

California Department of Water Resources. 1986. Analysis of Soil Samples for Asbestos. Prepared by EMS Laboratories, South Pasadena, CA. Ref. No. B55469. February 28.

Ireland, R.L. 1986. Land Subsidence in the San Joaquin Valley, California, as of 1983: U.S. Geological Survey, Water-Resources Investigations Report 85-4196, Sacramento.

Levine-Fricke. May 9, 1989. "Off-Site Source Characterization, Regional Soil Sampling, and Watershed Modeling Report".

Matthews, R.A. 1961. Geology of the Butler Estate Chromite Mine, Southwestern Fresno County, California. California Division of Mines and Geology, Special Report no. 71.

McCrone Environmental Services. 1988. Asbestos Analysis Report. McCrone Project No. ME-4260. Prepared for Levine•Fricke. May 4.

Munn, John R.; Busacca, Alan J., and Trott, Kenneth E. 1981. California Aqueduct Sedimentation Study for the Arroyo Pasajero and Tributary Watersheds. California Department of Conservation.

Reproduced with permission of the copyright owner. Further reproduction prohibited without permission.

Simons, Li and Associates. 1985. Stream Channel Erosion Study, Arroyo Pasajero, Final Report. Submitted to California Department of Water Resources. March 20.

U.S. Department of Interior, Bureau of Reclamation. 1988. Scoping Report for the Arroyo Pasajero Flood Detention Basin: Interim Standard Operational Procedure, Environmental Impact Report, Fresno County, California. January.

U.S. Environmental Protection Agency. 1987a. Inventory of Potential Asbestos Sources in the New Idria-Coalinga Study Region for the Atlas and Coalinga Sites, Fresno County, California. U.S. EPA Contract No. 68-01-6939. Prepared by Woodward-Clyde Consultants. September 15.

U.S. Geological Survey. 1984. Santa Rita Peak Quadrangle, 7.5 Minute Topographic Map. Reston, Virginia.

Walker, George W., and Griggs, Allan, B. 1953. Chromite Deposits of the Southern Coast Ranges of California: California Department of Natural Resources, Division of Mines, Bulletin 134, Part 2, 39-88.

Reproduced with permission of the copyright owner. Further reproduction prohibited without permission.

CHAPTER SIX

WATERSHED ASBESTOS SOIL EROSION AND SEDIMENT TRANSPORT MODELING

1.0 INTRODUCTION

This chapter provides a summary of the results of a watershed soil erosion and sediment transport modeling program conducted to estimate the relative contributions of anthropic and natural sources of asbestos bearing sediment to the surface water pathways leading to the California Aqueduct within the Arroyo Pasajero watershed. Anthropic sources are those sources that can be attributed to human-related activities including mining, milling, and road building and other activities. Natural sources are those sources that can be attributed to areas that have not been disturbed by human activities. The approximate limits of the Arroyo Pasajero watershed, including the New Idria Formation outcrop area and the sediment settling basin constructed adjacent to the California Aqueduct, are illustrated in Figure 6-1.

The numerical modeling work was originally conducted as part of Levine-Fricke's (May 9, 1989) engineering evaluation of the occurrence of chrysotile asbestos in the Arroyo Pasajero section of the California Aqueduct. My contributions to this modeling work included a review of available literature including maps, soil reports, and technical reports of soil erosion modeling work; development of soil erodibility factors based on field observations of soil structure and interpretation of laboratory

Reproduced with permission of the copyright owner. Further reproduction prohibited without permission.

analyses of particle size distribution; development of nomograph-based "K" factors for various types of mapped soil materials; development of numerical "K" factor adjustments that may be applied to identified K factors on the basis of type and percentage of vegetative and/or canopy coverings as interpreted from field observations and aerial photographs; field identification and mapping of soil types as well as the type and extent of potential asbestos source areas; and identification and/or interpretation of drainage routes and drainage sub basins based on a review of USGS topographic maps.

1.1 Scope and Methodology of Watershed Modeling

The work described in this chapter provides a quantitative basis for evaluating potential asbestos source area contributions of asbestos to the Arroyo Pasajero alluvial fan and California Aqueduct. The identified potential sources of asbestos include anthropic and natural sources located primarily in the White Creek - Pine Canyon Creek - Los Gatos Creek drainage area of the Arroyo Pasajero watershed.

The Arroyo Pasajero watershed covers an estimated 512 square miles and includes several sub basins located in upland areas that are known to contain potential sources of chrysotile asbestos including natural outcrop areas and areas affected by mining and milling operations. These potential source areas are located in the Los Gatos Creek drainage sub basin which includes the White Creek and Pine Canyon Creek drainage pathways. The White Creek drainage sub-basin drains approximately 5.8 square miles of the asbestos-bearing New Idria Formation and Pine Canyon Creek drains approximately 1 square mile of the New Idria Formation. The Pine Canyon drainage also includes the Johns-Manville Coalinga Asbestos Mill Site which includes approximately 400,000 cubic yards of asbestos tailings that has been placed in a gorge-

Reproduced with permission of the copyright owner. Further reproduction prohibited without permission.

like canyon with a retaining dam constructed at the base of the tailings pile. The White Creek drainage area includes the asbestos Atlas Mine and Mill Site, which covers approximately 280 acres, and numerous other areas affected by other mining and/or milling operations, which collectively cover an additional 250 acres. The location of mine and mill site areas are illustrated in Figure 6-2.

The modeling work focused on the potential of asbestos-bearing sediment erosion in the Los Gatos Creek drainage areas which includes the White Creek and Pine Canyon outcrop areas of the New Idria Formation. Regional erosion and sediment transport in the Los Gatos Creek subwatershed area of the greater Arroyo Pasajero watershed was evaluated by using the U.S. Department of Agriculture's (USDA, 1971) Universal Soil Loss Equation (USLE) and the U.S. Army Corps of Engineers' HEC-1 Model integrated with the Modified Universal Soil Loss Equation (MUSLE) (Williams and Berndt, 1972 and 1977). The USLE, MUSLE, and HEC-1 numerical models were constructed with input from sampling data, published information including USGS topographic maps, USDA SCS soil reports and technical modeling reports, field mapping and field observations, and interpretation of aerial photographs.

This information was used in conjunction with estimation methods developed by the USDA and others to characterize the USLE and MUSLE input parameters (including "K" factor estimates of soil erodibility, vegetative cover, soil erosion prevention practices, asbestos content, and slope length and gradient erosional factors) for 30 subwatersheds which drain portions of the asbestos-bearing New Idria Formation in the Los Gatos Creek watershed. The approximate limits of the identified 30 subwatersheds were identified as a result of field and aerial reconnaissance investigations and interpretations of topographic maps. These subwatershed areas are the primary source areas for historic and current upland erosion of asbestos in the

Reproduced with permission of the copyright owner. Further reproduction prohibited without permission.

Arroyo Pasajero watershed basin. The approximate limits of these subwatersheds are illustrated in Figure 6-3.

Asbestos concentrations for representative natural asbestos-bearing soils, mine surfaces, mill site ore storage piles, tailings piles, and other asbestos-bearing materials were estimated based on the analytical results from a regional soil and sediment sampling and asbestos analysis program summarized in Chapter Five. This sampling program targeted various mappable types of surface materials (i.e., undisturbed asbestos-bearing outcrop and serpentinite soil areas, mine surface areas, mining debris and/or tailings piles, etc.) that may contribute asbestos sediment to the local and regional drainage pathways as a result of surface water runoff erosional processes.

Soil erosion estimates were developed for pre-mining (natural) and post-mining (anthropic) conditions in order to compare relative impacts of mining, milling and road construction to the natural asbestos erosional discharges in the study area. Relative anthropic impacts on total asbestos eroded from the region were estimated by taking the difference between pre-mining and post-mining asbestos erosion estimates and dividing this quantity by the total pre-mining asbestos erosion estimate. This was done to help evaluate if remediation of identified mine site and other man-disturbed areas could significantly reduce the overall amount of asbestos soil erosion in comparison with natural rates of erosion.

1.2 Other Workers and Entrenched Channel Sediment Erosion

Other researchers (U.S. Department of Interior, bureau of Reclamation, 1984; Munn, Busacca, and Trott, 1981; California Department of Water Resources, 1984, 1986, and 1987; Simons, Li, and Associates, 1985; and Boyle Engineering Corporation,

Reproduced with permission of the copyright owner. Further reproduction prohibited without permission.

1988a, b, and c) have studied sediment erosion in the Arroyo Pasajero watershed area including the Los Gatos Creek watershed sub-basin. This work has helped characterize the Arroyo Pasajero's sediment sources in order to aid the California Department of Water Resources (DWR) and the U.S. Bureau of Reclamation (USBR) in their evaluation of possible erosion and sedimentation control measures for Arroyo Pasajero runoff to the San Louis Canal section of the California Aqueduct. These reports indicate that a substantial portion of sediments (37% to 62%) transported by the Arroyo Pasajero to the California Aqueduct have originated from erosional downcutting from several entrenched channel sections of the Arroyo Pasajero drainage pathway. The entrenched sections of channel are located in areas downstream of the town of Coalinga near the apex of the Arroyo Pasajero alluvial fan as illustrated in Figure 6-4. This section of entrenched channel is located near the general area of where the channel crosses the axis of the Coalinga Anticline. In this area, the channel may be entrenched as a result of uplift associated with this anticlinal structure. The entrenched channeling may also be a results of subsidence in the San Joaquin Valley as a result of withdrawal of large quantities of ground water for agricultural purposes. Subsidence in some near-by areas of the valley has been reported to be as much as thirty (30) feet or more (Bull, 1964). (See Figure 2-11).

Results of the soil sampling and asbestos analysis program of this project indicated that alluvial sediments eroded from the streambed and stream bank areas of the entrenched channel section of the Arroyo Pasajero contain asbestos concentrations of approximately 1% or less. These concentrations are similar to the concentrations of asbestos in surface and subsurface alluvial fan sediment deposits that could be correlated with pre-mining and post-mining time periods. These pre-mining and post-mining sediments, obtained from an alluvial fan core boring program, were generally found to contain approximately 1% or less chrysotile asbestos. This is significant

Reproduced with permission of the copyright owner. Further reproduction prohibited without permission.

because approximately 1% appears to be the background concentration of asbestos in most investigated alluvial fan areas including surface and subsurface areas. This is also significant because it appears that the process of channel downcutting is acting to dilute potential upstream contributions of asbestos to alluvial fan depositional environments.

1.3 Regional Context

Natural asbestos sediments are being and have been eroded from the New Idria Formation, Big Blue Member of the Temblor Formation, and numerous other un-named chrysotile deposits along the western margin of the San Joaquin Valley for very long periods of geologic time. These asbestos-bearing sediments are a natural component of historic alluvial fan sediments located downgradient from potential source areas. Recently eroded asbestos-bearing sediments have been transported and discharged into the California Aqueduct by regional runoff or collected in a sediment settling basin constructed adjacent to the Aqueduct since construction of the Aqueduct was completed in 1967.

Geologic Sources of Chrysotile Asbestos

Asbestos-containing sediments have been deposited in alluvial fans along the San Joaquin Valley's western margin for approximately 600,000 years. The areal extent of these alluvial fans are estimated to cover more than approximately 1500 square miles. The sources of asbestos-bearing sediment include the New Idria Formation, the Big Blue Member of Temblor Formation, and numerous other ultramafic and sedimentary deposits exposed in the mountains and foothills of the Diablo Range Mountains. The Arroyo Pasajero alluvial fan, which receives drainage from approximately 6.8 square

Reproduced with permission of the copyright owner. Further reproduction prohibited without permission.

miles of the New Idria Formation outcrop area, covers approximately 300 square miles. A review of "modern day" depositional centers on the Arroyo Pasajero alluvial fan shows that sediments correlated with the post-mining time period have been deposited over approximately 8 to 15 square miles of the modern day alluvial fan surface.

The New Idria Formation, other ultramafic serpentinite deposits, and sedimentary serpentinite deposits such as the Big Blue Member of the Temblor Formation (Miocene) have been eroding and contributing asbestos to sedimentary deposits in the region for approximately the past 17 to 20 million years. During recent geologic history (over the last 600,000 years), alluvial fans on the western margin of the central San Joaquin Valley have been formed by asbestos-containing sediment derived from the above geologic source areas. The asbestos concentration of the New Idria Formation has been found to range up to 80 to 100%. The asbestos-containing alluvial fans of the western margin of the central San Joaquin Valley include the Arroyo Pasajero alluvial fan; the Cantua Creek alluvial fan; the Panoche Creek alluvial fan; and other minor fan systems that have developed at the base of the Diablo Range foothills from Laguna Seca Hills southward to the Kettleman Hills. These alluvial fan and other asbestos-containing sedimentary deposits cover an estimated 1,500 square miles.

Arroyo Pasajero Upland Drainage and Alluvial Fan Depositional Areas

The watershed modeling work of this project focuses on the Arroyo Pasajero watershed drainage basin and Arroyo Pasajero alluvial fan depositional areas. The Arroyo Pasajero drainage basin includes the White Creek - Pine Canyon Creek - Los Gatos Creek sub-basin area which collectively drains approximately 6.8 square miles

Reproduced with permission of the copyright owner. Further reproduction prohibited without permission.

of the New Idria Formation. Potential anthropic sources of asbestos, (i.e., mine and mill site areas), are illustrated in Figure 6-2. Overall, the Arroyo Pasajero watershed basin covers a total of approximately 512 square miles. The approximate extent of the Arroyo Pasajero watershed is illustrated in Figure 6-1.

The alluvial fan created by the deposition of sediments eroded from the watershed basin covers approximately 300 square miles (Munn, Busacca, and Trott, 1981), with alluvial sediments extending to more than 600 feet in depth in some places (Miller, Green and Davis, 1971). At any particular time, only a relatively small area of the alluvial fan surface receives sediment as a result of runoff and erosion from upland watershed sources during storm events. In general, as an alluvial fan area accumulates sediments, the depositional area gains elevation and flood waters shift to areas of slightly lower elevation, thus shifting alluvial depositional areas across the fan surface over time. This process contributes to the general cone-like geometry of a typical alluvial fan system.

Construction of the California Aqueduct

In 1967, the DWR and the USBR completed the San Luis Canal section of the California Aqueduct, which transects the alluvial fans of the western margin of the Central San Joaquin Valley. Construction of the California Aqueduct across the Arroyo Pasajero alluvial fan restricted the Arroyo Pasajero's current depositional area from an estimated 15 square miles to approximately 8 square miles. The present depositional area is further restricted by construction of a training dike (a soil berm to direct flows). Water from the Arroyo Pasajero is captured by a 3-square-mile settling basin constructed to reduce the discharge of water and sediment into the California Aqueduct. The general drainage pathways of the Arroyo Pasajero watershed,

Reproduced with permission of the copyright owner. Further reproduction prohibited without permission.

including the alluvial fan training dike and sediment settling basin, is illustrated in Figure 6-1.

Construction of the Aqueduct has had the affect of stopping the transport of alluvial sediments to other medial and distal alluvial fan depositional environments. The California Aqueduct also acts to restrict the natural drainage of other alluvial fans along the western margin of the San Joaquin Valley, creating the potential for runoff and asbestos-bearing sediment to enter the Aqueduct at various locations. This potential has been increased as a result of the design and construction of inlet culverts which direct drainage directly into the Aqueduct (often without the benefit of sediment-settling basins such as constructed for the Arroyo Pasajero).

Reproduced with permission of the copyright owner. Further reproduction prohibited without permission.

1.4 Major Conclusions

This section provides a summary of conclusions of the erosion and sediment transport modeling work.

- The watershed modeling work indicates that mining, milling, exploration pit construction, and road construction activities in the Arroyo Pasajero drainage area have increased the currently existing surface water erosion of asbestos by an estimated maximum of 6 to 7% above natural background levels in the Los Gatos Creek drainage sub-basin and/or sub-watershed area and approximately 2% in the Arroyo Pasajero alluvial fan areas. However, alluvial fan concentrations of asbestos are generally 1% or less, and a 2% contribution to 1% is approximately 0.02% which may be considered insignificant. Field investigations have shown that an inventory of potential mining area sources in the Arroyo Pasajero watershed area include 11 mine sites; 5 mill sites; and approximately 203 exploration pit areas. These areas collectively cover approximately 700 acres or approximately 1.1 square miles in comparison with approximately 6.8 square miles of the New Idria Formation outcrop area in the Arroyo Pasajero watershed area.

- The results of alluvial fan surface and subsurface sampling and asbestos analyses indicate that asbestos concentrations in alluvial fan sediments have not been significantly increased as a result of mining activities. This is indicated by surface and subsurface concentrations of asbestos that are approximately 1% or less. This is supported by the numerical results of modeling which indicate that anthropic activities in the Los Gatos Creek drainage areas have increased the surface water erosion and transport of asbestos into the Arroyo Pasajero alluvial fan section of the California Aqueduct by a maximum of approximately 2% above contributions

Reproduced with permission of the copyright owner. Further reproduction prohibited without permission.

resulting from erosion of natural sources including the entrenched channel section of the Arroyo Pasajero drainage pathway.

- The relatively small extent to which mining, milling, and related activities are estimated by modeling to have increased erosion may be explained by two factors. First, undisturbed serpentinite outcrops and serpentine soils with naturally high asbestos concentrations support sparse vegetation. The removal of this sparse vegetation as a result of anthropic activities does not numerically appear to substantially increase soil erosion. Second, the erodibility of mine surfaces appears to be significantly less than that of natural asbestos soils, apparently because the natural soils have been weathered for a longer period, causing a finer and more erodible particle size distribution than the coarse, blocky soil structure of recently exposed mine surfaces. As a result of bench-cutting operations, mining also appears to decrease run-off potential in many areas.

- Modeling work conducted by other researchers has indicated that as much as 60% of the sediment deposited in the Arroyo Pasajero section of the California Aqueduct has originated from erosional downcutting from an entrenched section of the Arroyo Pasajero stream pathway. The natural asbestos content of these sediments acts to further decrease and/or dilute the contributions from upstream sources.

Reproduced with permission of the copyright owner. Further reproduction prohibited without permission.

2.0 EROSION AND SEDIMENT TRANSPORT BY SURFACE WATER PROCESSES

Asbestos-containing sediments have been eroded and transported from the relatively remote upland geologic source areas of the New Idria Formation downstream to the Arroyo Pasajero alluvial fan for approximately 600,000 years. That is the estimated age of the Arroyo Pasajero alluvial fan based on stratigraphic information and carbon-dating of bits of charcoal debris found in deep alluvial fan borings (Atwater, et al, 1986). The different characteristics of erosional phenomena in the region are discussed in the following sections including conceptual definitions of various related sediment transport mechanisms.

2.1 Weathering

The serpentinite soils and outcrops of the New Idria Formation are subject to a Mediterranean climate (i.e., a semiarid environment with low annual rainfall, short winters and long, hot summers) which contributes to the development of immature (i.e., poorly developed) soil profiles. The USDA has identified the soil derived from the asbestos-bearing serpentinite as the Atravesada series, which is described as being "formed in weathered material derived dominantly from soft serpentinite with a high content of asbestos" with chrysotile asbestos contents ranging as high as 96% (USDA, SCS, 1988b). The results of some asbestos outcrop sample analyses of the regional soil sampling program of this investigation have indicated results ranging as high as 100%.

The asbestos-bearing serpentinite soils occurring on the New Idria Formation, designated by the SCS as Atravesada soils, result primarily from the weathering of

Reproduced with permission of the copyright owner. Further reproduction prohibited without permission.

ultramafic serpentinite minerals in conjunction with the accumulation of organic matter and other soil materials. Weathering processes break down the New Idria Formation's blocky structure into more easily erodible soils that allow mobilization and transport of the constituent soil particles. Mumpton and Thompson report that the surface "weathering zone extends to a depth of 20 to 30 feet and is present throughout the formation" (Mumpton and Thompson, 1975).

Unlike many soils in more humid climates, relatively little soil development occurs in this region because of limited biological activity in the upper soil profile. This is a result of the sporadic, albeit intense, rainfall events which occur in the region, as well as the chemical composition of the Atravesada soils and parent serpentinite rock which are toxic to many plants and generally do not support ground cover. The primary weathering process is believed to be wetting and drying cycles which have been found to leach magnesium and other constituents from the parent rock and disaggregating the blocky structure of the formation's poorly consolidated to unconsolidated mineral deposits. Freezing and thawing cycles, which occur less frequently, tend to have a similar affect, breaking down the formation's blocky structure by expanding frozen water separating the formation's structure (Goldman, Jackson, and Bursztynsky, 1986; Kruckeberg, 1984; Mumpton and Thompson, 1975).

2.2 Splash Erosion

Raindrop impact causes splash erosion. The pounding action of rain causes soil aggregates to break apart, thus allowing soil particles to become mobilized. Larger raindrop sizes tend to increase the magnitude of splash erosion, since the greater momentum of the larger raindrops causes greater impact. Vegetative cover can absorb much of the raindrop energy, thus minimizing the effects of splash erosion. The loss

Reproduced with permission of the copyright owner. Further reproduction prohibited without permission.

or absence of vegetation allows rainfall to have its greatest effect on erosion (Goldman, Jackson, and Bursztynsky, 1986).

Because of its unique mineralogical characteristics, the Atravesada soils and exposed surfaces of the New Idria Formation do not generally support grasses, other ground cover, or dense canopy. Natural growth in the area consists primarily of sparse manzanita shrubbery. Most areas of the New Idria Formation are therefore exposed to some splash erosion. Anthropic activities such as mining and road construction have exacerbated the natural situation by removing the limited natural growth in the specific area of such activities (Kruckeberg, 1984).

2.3 Sheet Erosion

Sheet erosion is caused by the accumulation and shallow surface flow of water on soil surfaces. Water accumulates in the upper soil horizons as the soil becomes saturated or if the soil's infiltration capacity is exceeded. The accumulated surface water then flows downhill, transporting soil particles detached by splash erosion. Soil particles also may become detached by the flowing water (scouring), but this is minor, because the forces required to detach most soil particles is generally greater than the force of flowing water associated with sheet erosional processes (Goldman, Jackson, and Bursztynsky, 1986). Because of the steep topography and the absence of ground cover (such as grasses) on the New Idria Formation, sheet erosion is a significant erosional phenomenon in the region.

Reproduced with permission of the copyright owner. Further reproduction prohibited without permission.

2.4 Rill Erosion

Sheet erosion becomes more concentrated as the water on a sloping surface increases and is directed by minor surface features. Redirected surface flow eventually develops into small concentrated streams of flowing water known as rills. Most rills do not exceed a few inches in depth and are visually well defined. Rills tend to migrate back and forth across a slope, causing the slope to be eroded evenly. Water flowing through rills may contain enough energy to detach soil particles from the soil matrix, as well as to transport the newly detached soil particles. Rill erosion increases on steep slopes where longer uninterrupted flow lengths exist. Field observations show that rill erosion commonly occurs on the serpentinite soils of the New Idria Formation outcrop area (Goldman, Jackson, and Bursztynsky, 1986; Kirby and Morgan, 1980).

2.5 Gully Erosion and Mass Wasting

Gullies are surface channels that have formed from rills that have become entrenched in the soil surface. As a result of being entrenched, they generally do not migrate back and forth across a sloping surface; however, they are subject to headward encroachment and possibly branching. Gullies are usually deep, steep-walled upland channels. The Atravesada soils of the New Idria region contain many well-defined gullies throughout the steep topography of the region. The New Idria Formation's intermittent streams can be considered as large gullies that act to channel runoff through the serpentinite outcrop area.

During periods of precipitation, serpentinite soils can become saturated along the margins of gullies and stream channels. Saturated conditions contribute to slumping and sloughing of asbestos-bearing material into the intermittent stream and/or drainage

Reproduced with permission of the copyright owner. Further reproduction prohibited without permission.

pathways. Asbestos-bearing sediment is then transported downstream by a variety of streambed sediment transport processes. The slumping phenomena is an example of mass wasting (soil mass failures due to gravity). Mass wasting is evident throughout the drainage network of the New Idria region, evidenced by its many steep canyons formed by gully and mass wasting erosion (Goldman, Jackson, and Bursztynsky, 1986; Kirby and Morgan, 1980).

In addition to the mass wasting occurring along gullies and stream channels, larger scale mass wasting occurs in the New Idria Formation. This larger scale mass wasting occurs in the form of major landslides and debris flows which have occurred throughout the New Idria Formation. These landslides and debris flows tend to crush and pulverize the serpentinite soil structures. The large-scale landslide deposits also disrupt existing surface water flow patterns, causing additional erosion.

2.6 Channel, Streambed, and Stream Bank Erosion

Channel erosion results from scouring or mass wasting of a stream's bottom or banks because of a change in the stream's flow direction, an increase in flow quantity, or an increase in the flow's speed or turbulence (Goldman, Jackson, and Bursztynsky, 1986). Almost all streams draining the upper Los Gatos Creek watershed have not achieved a stable erosional condition because of their intermittent nature and existence in steep topography.

Streambed and stream bank erosion are both associated with flowing streams. The streams found in the New Idria area are generally intermittent and flow primarily in response to precipitation events, with only brief periods of flow associated with minor ground-water discharge to the streams. The intermittent streams and drainage

Reproduced with permission of the copyright owner. Further reproduction prohibited without permission.

pathways behave much like large gullies with scouring and mass wasting. Streambed erosion refers to scouring occurring on the stream's bottom. Stream bank erosion refers to scouring and mass wasting occurring on a stream's banks. In the asbestos-bearing outcrop areas, both of these phenomena result from the streams being located in steep terrain, flowing through relatively soft serpentinite landslide material, and flowing infrequently enough to prevent the streams from coming to a lower erosion, steady-state condition. While portions of the streams draining the New Idria Formation have developed some armoring (rocks and boulders which protect the streambeds and stream banks from erosion), significant areas still appear to be cutting deeper into the formation's surface.

2.7 Sediment Transport Concepts

After soil is mobilized from a soil matrix by erosion, its fate is controlled by sediment transport phenomena. A few of the concepts of sediment transport which are pertinent to this modeling of soil erosion in the Arroyo Pasajero watershed are briefly defined below (Simons, Li and Associates, 1982).

Bedload - Sediment that moves by saltation (jumping or bouncing), rolling, or sliding in the bed layer (bottom layer) of the stream; usually the larger materials being transported by a stream.

Wash load - Sediment that is supported by the stream waters' turbulence and generally flows in suspension with the stream waters; usually the smaller materials are transported, such as clay- and silt-sized particles.

Reproduced with permission of the copyright owner. Further reproduction prohibited without permission.

Total load - The sum of the bed load and the wash load.

Sediment transport capacity - The maximum material which could be transported by a stream at a given point. If the total load exceeds the sediment transport capacity, sediment deposition occurs.

Armoring - Larger rocks and boulders which protect smaller erodible and transportable materials from being eroded. Armor can prevent a stream from reaching its sediment transport capacity by protecting the more erodible particles from scouring.

Gross erosion - All sediments that are mobilized from splash, sheet, rill, gully, streambed, stream bank and channel erosion.

Sediment yield or total sediment discharge - Gross erosion minus deposited sediments upstream of a given point in a stream. Deposition of sediments occurs in stretches of a stream where the total load exceeds the sediment transport capacity.

Sediment delivery ratio - The ratio of total sediment discharge to gross erosion. Much of the gross erosion is deposited in stream reaches where the slope flattens and the stream's flow velocity and turbulence decrease, lessening the stream's transport capacity below the load being transported.

Reproduced with permission of the copyright owner. Further reproduction prohibited without permission.

3.0 ESTIMATION OF EROSION OF ASBESTOS-CONTAINING SEDIMENTS IN THE LOS GATOS WATERSHED

This section describes the modeling conducted to estimate the relative magnitude of natural and anthropically related water erosion of asbestos-containing materials in the Los Gatos Creek watershed. Historic and current conditions were analyzed to estimate the effects on erosion from road construction, exploration pit construction, mining, and asbestos milling activities. Pre-mining or natural conditions were compared with post-mining or anthropically influenced conditions to estimate the effects of mining, milling, and exploration prospecting and road construction on asbestos erosion.

3.1 Erosion Estimation Methods

Soil loss prediction techniques have been developed over many years as a result of studying erosion processes and conducting soil erosion research. Early erosion estimation techniques were primarily qualitative in nature and illustrated that agricultural practices differed in their ability to control soil erosion. Initially, equations using a single independent variable were developed to describe soil loss. Multiple factor equations developed as more data became available and researchers were better able to describe contributing factors. These empirical analyses culminated in the equation most widely used today for soil loss prediction - the Universal Soil Loss Equation (USLE), which was developed by the United States Department of Agriculture (USDA) (Kirby and Morgan, 1980). The USLE was developed from analyses of over 10,000 erosion plots for differing erosion rates resulting from different erosional influences such as rainfall, slope, vegetation cover, erosion control practices and development of quantifiable estimates of soil erodibility. A range of

Reproduced with permission of the copyright owner. Further reproduction prohibited without permission.

input parameters were empirically developed by directly measuring soil loss from soil plots while altering the parameter being evaluated. Development of the USLE parameters in this manner assumes that the various parameters have little or no effect on the other parameters in the USLE equation, but influence erosion independently from one another. This assumption simplifies actual erosional processes to enable the USLE to provide quantifiable estimates of soil loss.

The USLE soil loss estimation technique was originally developed for use on agricultural lands. However, as the model became more widely used, model input parameters were developed to be used on non-agricultural lands to aid in the evaluation of soil conservation practices on non-agricultural lands (Wischmeier, 1976; Kirby and Morgan, 1980). This equation estimates total average yearly rill and sheet erosion and provides a basis for most soil loss predictive techniques.

The USLE is expressed by the general formula:

$$A = R \times K \times LS \times C \times P$$

where: A = soil loss (tons/acre/year)
R = rainfall erosion index (100 ft x tons/acre x in/hr)
K = soil erodibility factor (tons/acre/units of R above)
LS = slope length and steepness factor (dimensionless)
C = vegetative cover factor (dimensionless)
P = erosion control practice factor (dimensionless)

This project used a conversion factor of 0.561 cubic yards/ton to convert USLE results from units of weight to volume. According to geotechnical soil density tests

Reproduced with permission of the copyright owner. Further reproduction prohibited without permission.

(Southern Pacific Land Company, 1986, p. 32) this soil weight is representative and typical for the light serpentinite soils found in this region. This was done in order to conform with other engineering estimates of the amount of asbestos-bearing sediment being delivered to areas adjacent to the California Aqueduct. Much of the sediment deposited adjacent to the is the Arroyo Pasajero section of the California Aqueduct is subsequently subject to excavation and removal in order to protect the Aqueduct.

Williams and Berndt (1975) modified the USLE for predicting sediment yield from watersheds for an individual storm. Their modification, the Modified Universal Soil Loss Equation (MUSLE), was developed empirically by evaluating sediment delivery from 778 individual storms from 18 watersheds ranging from 3 to 4,380 acres in size (Williams, 1975). Sediment yield was compared to the peak and total runoff flows from different storms. While USLE predicts the average annual gross erosion, MUSLE predicts erosion sediment yield for an individual storm event resulting from splash, sheet, rill, and gully erosion.

The MUSLE is widely used and accepted throughout the western United States. It is used in many non-agricultural applications. Previous non-agricultural sediment yield evaluations of the Arroyo Pasajero drainage and the bordering Salt and Cantua Creek drainages have selected the MUSLE for their evaluation method. These studies include: Simons, Li and Associates, 1985; Boyle Engineering, 1988a and b; and USDA, 1988a.

Reproduced with permission of the copyright owner. Further reproduction prohibited without permission.

The MUSLE is expressed by the general formula:

$$A = 95 \times (Q \times V)^{0.56} \times K \times LS \times C \times P$$

where: A = soil loss (tons/storm)

Q = peak discharge (cfs)

V = storm volume (acre-feet)

K = soil erodibility factor (tons/acre/units of R above)

LS = slope length and steepness factor (dimensionless)

C = vegetative cover factor (dimensionless)

P = erosion control practice factor (dimensionless)

As with USLE calculations, a conversion factor of 0.561 cubic yards/ton was used to convert MUSLE results from units of weight to volume. The MUSLE improves the erosion estimation of the USLE by replacing the rainfall erosion index (R) with the runoff factor ($(Q \times V)^{0.56}$), which allows for more detailed evaluation and consideration of site-specific hydrological influences on erosion. This makes the MUSLE applicable to the arid regions of the west, where most erosion is caused by high intensity storms.

In addition to estimating soil loss and erosion from individual storms, annual sediment yield may also be estimated using the MUSLE. This may be accomplished by calculating the sediment yields for a range of storm events and, in conjunction with their corresponding probabilities, weighting their contributions to the average annual sediment yield (Simons, Li and Associates, 1982).

The MUSLE/USLE models, like all mathematical models, are analytical devices which are useful in evaluating modeled conditions but, by their nature, cannot model all

Reproduced with permission of the copyright owner. Further reproduction prohibited without permission.

possible variations in natural conditions. As with any modeling technique, the MUSLE and USLE use certain simplifying assumptions (i.e., independence of individual parameters), which make the results approximations of actual conditions. However, the MUSLE/USLE models have been selected because of their ability to incorporate the effects of more relevant variables (e.g., erodibility, vegetation cover) than other models.

An attempt was made to minimize potential uncertainty associated with this soil erosion modeling program in two ways: (1) by using the results only in a relative manner, so that any variability affecting the calculation of absolute asbestos contributions from both natural and anthropic sources is canceled out; and (2) by performing a series of sensitivity analyses which tested the impact of variability in certain key modeling parameters on the overall results.

Although the MUSLE modifies the USLE, input parameters for each model are similar except for the replacement of the rainfall erosion index (R) with the runoff energy factor $((Q \times V)^{0.56})$. The input parameters for both models are discussed in the following sections.

3.2 MUSLE and USLE Hydrologic Input Parameters

The MUSLE and USLE hydrologic model input parameters are the main input parameters distinguishing these models from each other. USLE uses a rather general input parameter (R) developed for different regions of the country, relating a 2 year, 6 hour storm to a hydrologic input parameter which provides for USLE's average annual sediment estimations. On the other hand, MUSLE uses specific hydrology from the watershed being modeled, taking the total flow quantity (Q) and peak flow (V) from a

Reproduced with permission of the copyright owner. Further reproduction prohibited without permission.

specific storm, and estimating the storm's sediment yield. The MUSLE hydrologic input parameters are discussed in section 3.2.1, while the USLE hydrologic input parameters are discussed in section 3.2.2.

3.2.1 The MUSLE Hydrologic Model Input Parameters

The MUSLE uses the runoff energy factor to consider the effects of differing hydrologic settings on erosion. This factor is calculated by the product of the peak flow (cfs) and total flow (acre feet) to the 0.56 power. In order to calculate this factor, both the peak and total flows should be estimated and then compared to actual runoff conditions to check accuracy. U.S. Army Corps of Engineers HEC-1 model was used to estimate peak and total flows (Levine-Fricke, May 9, 1989, Chapter 3).

The Los Gatos Creek drainage system, including White Creek and Pine Canyon Creek, consists of intermittent streams, with little or no surface flow during most of the year. However, seasonal rainfall events may cause stream flows to increase suddenly, generating relatively large peak flows of short duration.

The Los Gatos Creek drainage area drains approximately 6.8 square miles of the New Idria Formation. Approximately 5.8 square miles of the New Idria Formation outcrop area in the Los Gatos Creek watershed drains through the White Creek drainage pathway, while Pine Canyon drains approximately 1.0 square miles. These intermittent tributaries drain the New Idria's steep terrain at elevations ranging from approximately 2,600 feet above sea level to approximately 4,900 feet above sea level. Normal annual precipitation ranges from approximately 17 to 19 inches/year, with the higher elevations receiving the greatest rainfall.

Reproduced with permission of the copyright owner. Further reproduction prohibited without permission.

The U.S. Army Corps of Engineers HEC-1 Flood Hydrograph Package (HEC-1 Model) was used to estimate storm water runoff characteristics in response to storm events of varying intensity and duration. (Levine-Fricke, Draft - January 9, 1989, Chapter 3). The HEC-1 Model simulates a watershed's response to precipitation by representing the basin as an interconnected system of sub basins with distinct hydrologic and hydraulic characteristics. The region draining Los Gatos Creek upgradient of the Nunez Canyon stream gauging station was hydrologically divided into 52 sub-basins, with the hydrologic parameters (including ground slope, channel shape, and boundary roughness) used as input for each HEC-1 Model subwatershed. The approximate limits of the sub-basins in the Los Gatos Creek drainage area are illustrated in Figure 6-3. The HEC-1 model's flow prediction for a single historic event was compared to actual stream flows measured at the Los Gatos Creek gauging station at Nunez Canyon. The model subsequently was used to calculate storm water runoff flow rates, volumes, and stream hydrographs for a range of 24-hour rainfall intensities, covering 2, 5, 10, 25, 50 and 100 year storms. (Levine-Fricke, May 9, 1989, Chapter 3).

3.2.2 The USLE Hydrologic Model Input Parameters

In contrast to the MUSLE, the USLE hydrologic parameter (the rainfall erosion index) is less precise and relatively simple to calculate. The rainfall erosion index estimates the erosive force and intensity of rain in a normal year. Two storm types were calculated to assess sensitivity of the storm type to the relative erosion. The rainfall erosion indices for the USDA Type I and II storms were calculated with the following equations:

Reproduced with permission of the copyright owner. Further reproduction prohibited without permission.

Type I Storm: $R = 16.55 \times p^{2.2}$

Type II Storm: $R = 27 \times p^{2.2}$

where: p = 2-year 6-hour rainfall (inches)

These equations were developed specifically for California and have been shown to be reasonable approximations of the actual rainfall erosion index (Wischmeier and Smith, 1978).

In a manner similar to the storm estimation for each sub basin used for the HEC-1 analysis for the MUSLE, the 2-year 6-hour storm was estimated by multiplying the Hernandez 7SE rain station 2-year 6-hour storm times the weighting factor calculated from the Corps of Engineers isopleth map (1971) which is attached as Figure 6-5.

3.3 Soil Erodibility Estimation

3.3.1 Estimation of Relative Soil Erodibility

The soil erodibility factor "K" is a measure of a soil particle's susceptibility to detachment and transport by rainfall and runoff. According to USDA and other research, texture (i.e., particle size distribution) is the principal factor affecting erodibility (K), but soil structure, organic matter content and permeability also affect a soil's susceptibility to erosion. As a result of these factors, different soils erode at different rates. The K factor was developed by the USDA during development of the USLE to help quantify the erosion rates of different soils (Goldman, Jackson, and Bursztynsky, 1986).

Reproduced with permission of the copyright owner. Further reproduction prohibited without permission.

K factor estimates of various types of mapped asbestos-bearing soil materials were specifically developed for this project. The K factors were used to determine whether the natural serpentinite materials (e.g., serpentinite Atravesada soils and Atravesada gully complex) erode slower, faster, or at a rate equivalent to anthropic materials under similar situations (similar rainfall, vegetation protection, and slope). Other K factor estimates developed by USDA (SCS) and Boyle Engineering were considered and evaluated, but the emphasis in this program was to insure that K factor comparison and impact on relative asbestos contribution from the different sources was completed in a consistent fashion to minimize potential bias and inaccuracies from inconsistent calculation techniques. Consequently, only the K factors which were developed in a consistent manner for this project using the same analytical procedures for uniformity for interpretation of results were used in the modeling program

The standard USDA erosion test plot for measurement of soil erodibility involves the collection of eroded soil from a standard unit plot (72.6 feet long at a slope of 9% and free of vegetation for at least 2 years) under a representative range of storm sizes and antecedent moisture conditions, in order to measure an average K factor (USDA, 1978). However, because of the area's remote and rugged terrain, and the infrequency of sufficiently intense rainfall events, neither this method nor variations involving smaller plots or artificial rainfall generators (rainulators) are well suited to evaluate K factors for soils in the vicinity of the New Idria Formation.

Because of the complexities and level of effort required to estimate soil erodibility by direct measurement, the USDA has developed a nomograph for estimating soil erodibility in situations where it is unrealistic, too costly, or unnecessary to undertake actual erodibility measurements (Wischmeier and Smith, 1978; and Erickson, 1978).

Reproduced with permission of the copyright owner. Further reproduction prohibited without permission.

It has been determined that particle size distribution is the principal factor which affects determination of K factor values. The silt- and very fine sand-size fractions (0.002 to 0.05 mm (silt) and 0.05 to 1.0 mm (very fine sand)) have been found to be the particle sizes most susceptible to erosion during rainfall and runoff. Clay-size particles (less than 0.002 mm) tend to be cohesive with the clay-size particles sticking together in clumps. Other parameters which can affect determination of a soil's relative erodibility include organic matter content, soil structure, rock and coarse particle content (i.e., particles greater than 2.0 mm in size), and soil permeability. Detailed explanations of K factor parameters are provided by Goldman, Jackson, and Bursztynsky, 1986; Kirby and Morgan, 1980; and Erickson, 1978.

The nomograph method was used for determining the K soil erodibility factor. K factors for pre-mining and post-mining conditions were estimated using the USDA triangular nomograph for the different asbestos-bearing soils and materials found on the New Idria Formation. The results of my nomograph estimates are presented in Appendix G. These estimates were adjusted according to USDA guidelines (Erickson, 1978). In order to be conservative, the USLE and MUSLE erosion estimates were performed with both unadjusted and adjusted K values.

Figures 6-6 and 6-7 delineate the pre-mining and post-mining extent of the different soils and materials in the Los Gatos Creek sub-basins draining the New Idria Formation outcrop area. These figures were developed from my interpretation of black and white and color/infrared aerial photographs from 1950 and 1981, respectively. These figures were also developed from preliminary USDA soils mapping data; geologic mapping by Dibblee (1971); and field observations and field mapping conducted by myself.

Reproduced with permission of the copyright owner. Further reproduction prohibited without permission.

3.3.2 Determination of K Factor Values for Asbestos-Bearing Soils

USLE (and MUSLE) K factors were estimated for five general soil types in the Los Gatos Creek drainage areas that are known to contain chrysotile asbestos. These soil types are summarized in Table 6-1 and are listed here from highest estimated (unadjusted) erodibility to lowest estimated erodibility including: tailings piles associated with asbestos milling operations (K = 0.16); landslide surface soils in Upper Pine Canyon in the vicinity of the Johns-Manville Coalinga Asbestos Mill Site (K = 0.14); naturally occurring serpentinite soils that have formed in the New Idria Formation outcrop area (K = 0.13); Railroad Mine soils (K = 0.12); and mine surfaces in the New Idria Formation outcrop area (K = 0.10).

The K factors which are summarized in Table 6-1 are based on the triangular nomograph method recommended by the USDA (Erickson, 1978) (see Appendix G for nomograph estimations). This method is based primarily on the determination of the sand-, silt-, and clay-size fractions of surface soil samples using sieve and hydrometer particle size analyses of fractions less than 2.0 mm in diameter.

Serpentinite soil samples from anthropically undisturbed areas had slightly higher K factor values because these weathered soils had finer grain size distributions. K factor values for samples from asbestos tailings generally had the highest K factors because of relatively large silt-size fractions. The particle size distribution of tailings materials is generally gap-graded (i.e., includes both a significant coarse size fraction and a fine size fraction) because much of the sand-size fraction was removed as product in the milling process and the silt- and clay-size fractions and the coarse fragment fractions were discarded as unusable material.

Reproduced with permission of the copyright owner. Further reproduction prohibited without permission.

Adjustments for K Factor Values

The triangular nomograph method provides for adjustments to K factor values for:

(a) organic matter contents other than 2%;

(b) soils with greater than 15% very fine sand fractions;

(c) rock fragment and coarse particle size contents greater than 15% (i.e., particles greater than 2.0 mm);

(d) estimates of high or low soil permeability; and

(e) soil structures other than blocky or platy (Goldman, Jackson, and Bursztynsky, 1986; Erickson, 1978).

For the asbestos-bearing materials characterized for the USLE and the MUSLE, application of the organic matter adjustment factor generally resulted in an increase in K factor values (i.e., increasing the estimate of soil erodibility), while application of the coarse particle size and permeability adjustment factors generally resulted in a decrease in K factor values (i.e., lowering the estimate of soil erodibility). Fine granular structures, of the sort associated with asbestos tailings, have been found by empirical experiment to be less erodible than the "standard" nomograph soil. The K factor for asbestos tailings were decreased in accordance with the empirically derived nomograph's suggested adjustments for a fine granular structure (as opposed to a blocky or platy structure). When adjustments for all factors were applied to the serpentinite matrix soil types, the net result was to decrease K factor values. Mine surfaces (excluding the Railroad Mine) had an adjusted K factor value that decreased from 0.10 to 0.07. The Railroad Mine had an adjusted K factor that decreased from 0.12 to 0.09. Serpentinite soils had an adjusted K factor value that decreased from 0.13 to 0.09, and tailings piles had an adjusted K factor value that decreased from 0.16

Reproduced with permission of the copyright owner. Further reproduction prohibited without permission.

to 0.08. Table 6-2 provides a summary of the K factor adjustments made to erodibility estimations.

The appropriateness of adjusting the K factors to the lower values may be questionable because of: (1) the unique physical and mineralogical characteristics of these soil types, including variable organic contents and the platy and fibrous characteristics of the chrysotile asbestos particles which comprise up to 96% to 100% of some of the soil samples; and (2) the unique behavior of the soils in wet conditions (ability to hold large amounts of moisture and apparent low shear strength). These soil characteristics apparently contribute to high levels of gully erosion (mass wasting) compared to the levels of sheet and rill erosion found in the region. Surface soils may be absorbing high amounts of water and becoming heavy and then slipping due to gravitational forces, while scouring and detachment appear to have minimal impacts (as implied by the lower values of the adjusted K factor estimates). According to Paul Nazar of the USDA (SCS), the USDA did not report the adjusted K factor in its Preliminary Soils Report (USDA, June 7, 1988, Table J). The adjusted K factor was estimated to be 0.16 (personal communication between J. DeReamer and Paul Nazar, Aug. 22, 1988).

Since unadjusted K factor values based on particle size analyses without adjustments downward may provide better estimates (closer to USDA reported values) of the relative erodibility of the serpentinite soil types' unique characteristics, the modeling of both the unadjusted and adjusted K factors has been implemented to assess the potential implications of these adjustments and to provide a broader range of K factor magnitudes.

Reproduced with permission of the copyright owner. Further reproduction prohibited without permission.

Table 6-2 provides a summary of the K factor estimations that were developed for use in the USLE and MUSLE modeling. Additionally, Table 6-2 summarizes information regarding Boyle Engineering Inc.'s and the USDA's (SCS's) determinations of K values. Neither Boyle nor the USDA considered all adjustments to the K factor determinations.

3.3.3 Sensitivity Analysis of K Factors

To more fully evaluate the possible contribution of asbestos from anthropic sources in the region, sensitivity analyses of K factors were used for the USLE and MUSLE estimates. Three basic assumptions were considered as noted in the following sections:

(1) Adjusted and Unadjusted K Factor Values

Sediment erosion was modeled using both adjusted and unadjusted K factors, in order to evaluate the sensitivity of the interpretations used to derive this parameter, and to use K factor values that may be closer to those reported and used by others (USDA, SCS, 1988b; and Boyle Engineering, 1988). This was done as a result of the results of particle size distribution analyses (indicating a coarse particle size distribution) and field observations of soil structure which indicated that K factors for mine surfaces and other anthropic sources may be significantly less susceptible to erosion than natural sources

Reproduced with permission of the copyright owner. Further reproduction prohibited without permission.

(2) Atravesada Gully Complex Soils

The results of my field observations and reconnaissance surveys indicated that the degree to which the Atravesada Gully Complex (AGC) soils are weathered ranges from very minimal (i.e., similar to the subsurface soils exposed by mining activities) to comparatively well weathered (i.e., similar to undisturbed Atravesada surface soils). Therefore, the K factor for AGC soils was assumed to be equivalent to that for mines as well as for Atravesada soils.

(3) Mine Surfaces

The K factors which were developed for mine surfaces were lower than those for natural serpentine soils. See Table 6-2 and Appendix G. These results suggest that mine surfaces in the Los Gatos Creek drainage areas are less erodible than non-anthropically affected surface soils. However, to provide a worst case estimate of soil erosion from mine surfaces, sediment erosion was also modeled by assuming that the K factors for mines and serpentine soils were equivalent.

A total of six K factor combinations were used in the sensitivity analyses of K factors in the MUSLE and USLE models, based on the above assumptions. These combinations are as follows:

1) adjusted K: $K_{AGC} = K_{mine}$

2) adjusted K: $K_{AGC} = K_{serpentine\ soil}$

3) adjusted K: $K_{AGC} = K_{serpentine\ soil} = K_{mine}$

Reproduced with permission of the copyright owner. Further reproduction prohibited without permission.

4) unadjusted K: $K_{AGC} = K_{mine}$

5) unadjusted K: $K_{AGC} = K_{serpentine\ soil}$

6) unadjusted K: $K_{AGC} = K_{serpentine\ soil} = K_{mine}$

3.4 Effects of Length and Steepness on Erosion

The slope length-gradient factor (SL) of the USLE and the MUSLE represents the effects of slope and slope length on the erosional process. Water runs down steeper slopes faster and the additional energy causes more erosion than water running down slower, flatter slopes. Similarly, longer slope lengths allow water to gain momentum and higher speeds, causing more erosion than water running down shorter slope lengths. Factors for slope and slope length were originally investigated separately during the development of the USLE. However, because these effects are similar and related, most methods for estimating these parameters for watersheds combine the length and slope parameters into a single model input. This combined parameter is critical because it accounts for more variation than any other factor except watershed practice (P) which is discussed in Section 3.6.

Williams and Berndt (1977) reviewed three methods for estimating this parameter. Fifty-three watersheds were reviewed in detail, critically assessing the different methods for estimating the SL parameter for a watershed. Based on this analysis, Williams and Berndt developed the following equation as best estimating the LS USLE parameter:

Reproduced with permission of the copyright owner. Further reproduction prohibited without permission.

$$LS = (L_s/72.6)^{0.5} \times (0.065 + 0.0454 \times S_g + 0.0065 \times S_{g^2})$$

where: LS = length-slope gradient factor for USLE (or MUSLE)

L_s = length of sub-basin (miles)

S_g = sub-basin slope (dimensionless)

Using this equation, the LS parameter for all the sub-basins was calculated from measurements taken from the USGS Santa Rita Peak Quadrangle (see Figure 6-8) for both the MUSLE and the USLE. As defined by the input parameters, the LS does not change because of anthropic activity, as mines do not affect the overall slope of an entire sub watershed. Therefore, pre-mining and post-mining conditions contained the same LS input parameters.

3.5 Vegetative Cover Impacts on Erosion

Vegetative cover impedes erosion in two different ways. First, the impact of rain (splash erosion) can be largely absorbed by the vegetative canopy (trees or brush) or by the vegetative ground cover (grasses or other vegetative growth in contact with the ground surface). Second, sheet and rill erosion can be significantly reduced and controlled by ground cover. Water accumulating and running down the slope will be slowed and the detachment and transport erosional processes reduced by any vegetative impediments to water flow. The forces of direct precipitation causing splash erosion can also be largely absorbed by ground cover.

The USLE and MUSLE use the vegetative cover factor (C) to estimate these effects on erosion. The USDA publication "Predicting Rainfall Erosion Losses" (Wischmeier

Reproduced with permission of the copyright owner. Further reproduction prohibited without permission.

and Smith, 1978) provides a nomograph for deriving C factors for pasture, range, or idle land, based on the percent coverage of foliage canopy and ground cover. The foliage canopy includes tall weeds with an average height of 20 inches, appreciable brush or bushes with an average raindrop fall of 6.5 feet, and trees with an average drop fall of 13 feet. These canopy types are divided into different percentages of cover, including 0, 25, 50, 75 and 100 percent. The ground cover is divided into two types, grasses and broadleaf herbaceous plants, with percent coverages of 0, 20, 40, 60 and 95+ percent.

As discussed in earlier sections, the vegetative canopy of this region contains mostly brush, including chaparral community species. Because of this specific type of plant growth, the USDA C factor nomograph for pasture, range, and idle land was adapted for the New Idria region by averaging values for the canopy types of tall weeds and appreciable brush, with the ground cover assumed to be grasses. Table 6-3 contains a summary of C factors determined for four general categories (based on percent coverage) of vegetated areas in the New Idria region.

Figure 6-9 summarizes estimates of pre-mining and post-mining ground cover densities for the region modeled by the USLE and the MUSLE. The data were obtained from soils mapping, aerial photographs and field surveys. Of particular significance is the fact that Atravesada soils generally do not support ground cover, while other, less asbestos-containing regions do support grasses.

Estimates of pre-mining and post-mining canopy densities are represented on Figures 6-10 and 6-11. Development of these figures relied heavily on interpretation of the 1950 and 1981 aerial photographs of the region. In the case of the Big Ridge Mine and the White Creek Magnesite Mine, both of which existed prior to 1950, the canopy

Reproduced with permission of the copyright owner. Further reproduction prohibited without permission.

density was estimated from observations of the canopy density observed in the vicinity of the mines.

The increase in erosion resulting from road and exploration pit construction was evaluated by estimating these surface features' impacts on foliage. Pre-mining conditions were altered by the estimated impact from road and exploration pit construction. Roads appearing on the aerial photographs and USGS Santa Rita Peak Quadrangle were plotted onto a map of the asbestos-containing sub-basins as illustrated in Figure 6-12. The road lengths were measured with Auto-CADD and the number of exploration pits were counted for each sub basin. The pre-mining canopy and ground cover factors were adjusted assuming: (1) a 12-foot average road width for all roads; (2) a 300 square foot average disturbed area for each exploration pit; and (3) that the roads were built in areas of canopy and ground cover typical for each watershed. This adjustment used the following equation:

$$cl_{gf} = [(A-a)/A] \times c_{gf}$$

where: cl_{gf} = Road and Exploration Pit Impacted Ground or Canopy Cover

A = area of sub basin

a = area of roads and pits in sub basin

c_{gf} = pre-mining ground or canopy cover

Following the estimation of the post-road and exploration pit ground and canopy cover densities, new post-road and exploration pit C factors were calculated and used as input into the MUSLE and USLE analyses. These ground cover and canopy cover estimates for post-road and exploration pit conditions are shown in Table 6-4.

Reproduced with permission of the copyright owner. Further reproduction prohibited without permission.

3.6 Erosion Control Practices

The soil erosion control practice factor (P) is defined as the ratio of soil lost with erosion control practices to soil lost with no erosion control practices. Erosion control practices include mulching, contour plowing, terrace construction, sedimentation ponds, surface water control structures, and many other technologies used to limit the impact of water on erosion.

A number of erosion control practices are in place at different locations in the sub basins evaluated, including terracing of mine sites, stream diversion and tailings dam construction. However, to conservatively overestimate mining and asbestos milling impacts, none of these control practices were considered, and the practice factor was assumed to be 1 (no reduction for erosion control practices). Actual mine and mill site erosion control practices known to be present are discussed briefly in Section 3.10.2 along with other assumptions specific for each site.

3.7 Asbestos Content of Subwatershed Materials

As explained in Chapter Five, elongate serpentine asbestos results determined by PLM analyses was selected as the most conservative (i.e., showing the highest measured asbestos) analytical technique for measurement of asbestos. Therefore, all modeling work used the average PLM elongate serpentine asbestos concentrations for different asbestos-containing substances found in the region. For the purpose of watershed modeling, PLM results reported as percent area were assumed to be equivalent to percent mass. This assumption probably overestimates actual asbestos percent mass concentrations, since other minerals occurring in bulk samples from the study area

Reproduced with permission of the copyright owner. Further reproduction prohibited without permission.

(e.g., chlorite, mica, actinolite, feldspar, quartz, magnetite, and chromite) have similar or higher specific gravities in comparison to chrysotile (approximately 2.6).

Asbestos-containing materials evaluated by the soil sampling program included serpentinite soils, asbestos mill tailings, mine surfaces (including the Railroad Mine), and landslide soils. For the purposes of the USLE and MUSLE, serpentinite soils and mine surfaces were assumed to have an average asbestos concentration of 84% because of the similar mean asbestos concentrations (86% for serpentinite soils and 81% for mine surfaces). This assumption slightly overestimates mining impacts on erosion and underestimates erosion of natural asbestos-bearing surfaces.

The New Idria Formation contains some areas with low asbestos content. These areas are formed by non-asbestos-bearing inclusions of syenite. The soil materials that have formed on these inclusions of syenite have been mapped as Hentine soils. The asbestos concentration assumed for Hentine soils was 30%. These soils are known to contain varying concentrations of asbestos, depending on the presence or absence of Atravesada soil inclusions in the area. The 30% concentration level was selected based on field observations, interpretation of reflectance characteristics from high and low altitude aerial photos, and from USDA soil descriptions. However, because of the variability of asbestos concentrations in these soils, sediment erosion was also modeled using an assumed Hentine asbestos concentration of 0% to test the sensitivity of the estimates of relative asbestos contributions from other (e.g., anthropic) sources.

Table 6-5 provides a summary of the asbestos concentration data used for each of the 30 Los Gatos Creek sub-basins. This data was weighted in accordance with interpretation of the distribution of identified material types within each sub-basin.

Reproduced with permission of the copyright owner. Further reproduction prohibited without permission.

3.8 Calculation of the MUSLE and the USLE Asbestos Sediment Estimations

MUSLE and USLE estimates of asbestos erosion from individual mines and mills in the Los Gatos Creek watershed are summarized in Tables 6-6 and 6-7, respectively. These tables are organized to present the results of the K factor sensitivity analysis (i.e., with a total of six K factor assumptions as described above in Section 3.3) and Hentine soil assumptions (asbestos concentrations of 0 and 30%). Complete spreadsheet calculations for these models are included in Levine-Fricke (May 9, 1989).

Estimations of asbestos erosion increases resulting from the construction of roads and exploration pits, based on MUSLE and USLE analyses, are presented in Table 6-4. These analyses were completed for adjusted and unadjusted K factors and variable Hentine soil asbestos concentrations in a similar manner to the estimates of potential mining effects on erosion.

3.9 Average Yearly Sediment Yield Calculations

MUSLE estimates sediment yield for specific storm events. Since, longer term or average effects from anthropic impacts on erosion are of primary concern, average yearly sediment production was estimated. These estimations allowed the comparison of each different storm's estimated relative asbestos contributions (from anthropic and natural sources) to the estimated average yearly relative asbestos contributions to minimize absolute variabilities associated with sediment yield estimates generated for individual storm events. This analysis found little or no sensitivity to the different storm events compared to the estimated yearly average relative contributions.

Reproduced with permission of the copyright owner. Further reproduction prohibited without permission.

A watershed's average annual sediment yield can be represented by the integration of the watershed's extreme storm event sediment yields with their associated probabilities. Larger storms have lower associated probabilities of occurrence, and therefor have potentially correspondingly smaller effect on yearly average erodibility. The integration estimation equation used to estimate the average yearly sediment yield from the calculated sediment yields (Simons, Li and Associates, 1982) is:

Average Yearly Sediment Yield =

$$0.015 \times Y_{100} + 0.015 \times Y_{50} + 0.04 \times Y_{25} + 0.08 \times Y_{10} + 0.2 \times Y_5 + 0.4 \times Y_2$$

where: Y_n = MUSLE sediment yield for the subscript year return period

The estimations of yearly average asbestos sediment yield are included in Table 5-8.

3.10 Findings of the MUSLE and the USLE Asbestos Soil Loss Estimations

Each of the mines and asbestos mills located in the Los Gatos Creek watershed and identified in EPA's Potential Sources Report (1987) were evaluated separately and collectively for their impacts on the natural asbestos erosion occurring in the sub-basins. Furthermore, the effects of roads and pits on asbestos erosion were estimated separately to cover other anthropic activities in the region.

The results and findings of the MUSLE and USLE soil erosion estimations are summarized and discussed below. The individual mine and mill sites are discussed briefly, followed by a general discussion of the overall findings of the effects of the different parameters analyzed by the MUSLE and USLE soil loss calculations.

Reproduced with permission of the copyright owner. Further reproduction prohibited without permission.

3.10.1 Estimates of Anthropic Contributions to Asbestos Erosion

Anthropic Effects on Asbestos Erosion

All mining and milling sites in the Los Gatos Creek watershed appear to cover a total area of approximately 530 acres, or 12% of the 6.8-square-mile area drained by White Creek and Pine Canyon Creek. All roads and exploration pits cover an estimated 166 acres, or less than 4% of this 6.8 square mile area. A summary of what is known of mining operations in the Los Gatos Creek drainage basin is provided in Table 6-8. This table is provided for historical perspective.

Loss of vegetative protection apparently has a greater effect (increasing erosion) on sediment erosion estimates than the exposure of the less weathered mining soil surface (potentially lessening erosion) caused by the removal of the surface soil materials for mining purposes. The total increase in asbestos erosion associated with the mines, asbestos mills, exploration pits, and road construction sites was estimated to be as high as approximately 6.5% (with 3.8% from roads and exploration pits). See Table 6-11.

Atlas Mine and Mill Site

The Atlas Mine and Mill Site covers the largest single disturbed area of the New Idria Formation surface and appears to have caused the largest increase in asbestos erosion of the mine and mill sites located in the Los Gatos Creek watershed. Because significant quantities of mill tailings apparently have migrated off-site as a result of localized wind erosion (i.e., tailings piles migrating in dune-like fashion), the Atlas Site is believed to have had a significant impact on local floral cover, making the precise

Reproduced with permission of the copyright owner. Further reproduction prohibited without permission.

boundaries of the site difficult to define. The aerial extent of the disturbed vegetation (and anthropic effects on erosion) covers approximately 280 acres, which is more than half of the 530-acre surface area disturbed by all mining and milling activities in the study area.

Because the Atlas Site encompasses such a high percentage of anthropically disturbed surfaces that are not, strictly speaking, mine surfaces, the worst-case analysis, which does not assume the lower erodibility associated with the unweathered surfaces, may more accurately reflect site conditions than the best estimates, which do make that assumption. For these reasons, a MUSLE estimate of 1.63%, derived by averaging the unadjusted worst-case and best estimates, was used to calculate the effects on relative asbestos contribution in the transport discussion of this chapter.

Johns-Manville Coalinga Asbestos Mill Site

The Johns-Manville Coalinga Asbestos Mill Site is unique in that it is primarily a mill site, with only a 5-acre mined surface area (referred to as the Railroad Mine) located approximately one-half mile downslope of the New Idria Formation. See Figure 6-2. In comparison, the other mine and mill sites are located on the New Idria Formation, where differences between the asbestos content of anthropic and non-anthropic materials are small.

The average adjusted K MUSLE estimate of 0.31% was used to calculate the effects on relative asbestos contribution, as discussed in Section 4 of this chapter.

This percentage overestimates the increase in asbestos erosion from the Coalinga Asbestos Mill Site, considering the fact that a tailings dam exists downstream of the

Reproduced with permission of the copyright owner. Further reproduction prohibited without permission.

tailings pile in the eastern fork of Pine Canyon Creek, effectively trapping asbestos sediments at the site. This site feature contains an estimated 4,000 yds^3 of asbestos-containing sediments measuring approximately 2 - 4 feet in depth upstream of the dam, while downstream of the dam only small isolated pockets of sediment are evident. The dam tends to slow the flow rate of the Pine Canyon Creek causing the asbestos plates and chips to settle with other sediments. The dam breached in 1983. While the dams trapping efficiency was diminished somewhat by this breach, the dam was repaired in 1988 and its trapping efficiency was restored. The presence of the dam has not been considered in the MUSLE and USLE asbestos soil loss estimations, thus making the analyses overestimate Coalinga Asbestos Mill Site contributions.

Basic Resources

The Basic Resources Mine covers approximately 33 acres near the crest of Joaquin Ridge. This mine's location causes it to receive more rainfall than the other mines at lower elevations as indicated in Figure 6-5 (U.S. Army Corps of Engineers, 1971). This additional rainfall causes the hydrologic parameters of the MUSLE and the USLE to be higher for this site compared to other sites which receive less rainfall.

The site is located, in part, on an area naturally without vegetation to protect the soil from direct rainfall. This caused the pre-mining condition to erode relatively high levels of asbestos, making the impacts from mining less severe than if the site had been more densely vegetated.

The average adjusted K MUSLE estimate of 0.14% was used to calculate the effects on relative asbestos contribution, as discussed in Section 4 of this chapter.

Reproduced with permission of the copyright owner. Further reproduction prohibited without permission.

Big Ridge Mine

Operation of this chromite mine pre-dates the 1950 aerial photographs generally used to characterize pre-mining conditions. The pre-mining conditions have therefore been conservatively assumed to be equivalent to the area adjacent to the mine, with no vegetation-free areas. This assumption causes the increases attributed to mining to be maximized by minimizing pre-mining asbestos erosion from the mine site.

This mine covers approximately 40 acres. The average adjusted K MUSLE estimate of 0.13% was used to calculate the effects on relative asbestos contribution, as discussed in Section 4 of this chapter.

Tromby Mines

These two chromite mines are at relatively lower elevations and receive less rainfall than most of the other mines. They cover approximately 59 acres. The average adjusted K MUSLE estimate of 0.30% was used to calculate the effects on relative asbestos contribution, as discussed in Section 4 of this chapter.

James Corbett Biles/Archer Mines

These mines cover approximately 8 acres. The average adjusted K MUSLE estimate of 0.13% was used to calculate the effects on relative asbestos contribution, as discussed in Section 4 of this chapter.

Reproduced with permission of the copyright owner. Further reproduction prohibited without permission.

Mine "?" (Section 28 Mine)

This mine is listed in the EPA Potential Sources Report as the Section 28 Mine. It is located at the top of Joaquin Ridge, and approximately 10 acres drain to the White Creek basin. The average adjusted K MUSLE estimate of 0.14% was used to calculate the effects on relative asbestos contribution, as discussed in Section 4 of this chapter.

Butler Estate Chromite Mine

Most of this chromite mine drains to Pine Canyon and is located at the margin of the New Idria Formation. The mine covers an estimated 43 acres. The average adjusted K MUSLE estimate of 0.49% was used to calculate the effects on relative asbestos contribution in the transport discussion in Section 4 of this chapter.

Jensen Mine

The Jensen mine supplied the Coalinga Asbestos Mill with asbestos ore and covers an estimated 29 acres. The average adjusted K MUSLE estimate of 0.31% was used to calculate the effects on relative asbestos contribution, as discussed in Section 4 of this chapter.

White Creek Magnesite Mine

This mine covers approximately 25 acres of the lower elevations of the New Idria Formation's surface soils. The boundaries of this mine were estimated based upon apparent disturbances of canopy cover as seen on aerial photographs. Pre-mining

Reproduced with permission of the copyright owner. Further reproduction prohibited without permission.

conditions were assumed to be similar to the surrounding foliage. This assumption overestimates asbestos contributions from mining activities because of the possibility of less dense foliage in the pre-mining condition. The average adjusted K MUSLE estimate of 0.20% was used to calculate the effects on relative asbestos contribution, as discussed in Section 4 of this chapter.

3.10.2 Possible Effects on Asbestos Erosion from Varied Parameters

The MUSLE and the USLE estimations did not prove to be sensitive to the range of K factors explored. As previously discussed, the range of relative increases to asbestos erosion found by the estimations and worst-case estimations were not great. The erodibility of soil does not appear to be a sensitive enough parameter to radically change the overall findings of potential increases to asbestos erosion expected from the anthropic activities (mining and milling). Mining actually was found to lower soil erodibility because the lower strata exposed by the removal of the weathered surface soils has a blockier and apparently less erodible structure. Milling appears to increase erodibility of the asbestos ore, but the soil maintains significant fractions of gravel and sand-size materials which still result in a lower estimated adjusted erodibility than natural serpentinite soils.

The worst-case USLE and MUSLE estimations ignore the lower erodibility of surface mining. The results of the estimations do not appear to indicate that the K factor estimations are critical to the overall findings of the minor increase of the estimated erosion of asbestos. The natural conditions and overall large area of the asbestos-containing soils appear to be the dominant reasons for the apparently small effect of the erodibility K factor estimate on the asbestos erosion of the region.

Reproduced with permission of the copyright owner. Further reproduction prohibited without permission.

3.11 Chromite Mill Tailings

The occurrence of chromite milling operations in the Los Gatos Creek Watershed are summarized in Table 6-9. These milling operations were generally established immediately adjacent to White Creek to provide water for the wet chromite milling process. This process relied on screening and water gravity settling techniques to separate the heavier chromite-rich ore from the lighter asbestos-containing soil matrix in which the chromite ore is found. Information presented in the following discussion suggests that disposal of chromite tailings in White Creek could contribute similar or greater amounts of asbestos to the Arroyo Pasajero as erosion of other anthropic sources.

The California Regional Water Quality Control Board (RWQCB) conducted a survey of two of the mill sites on the Los Gatos drainage (Holman and Joaquin) and obtained pictures which showed eroding pond areas constructed in the White Creek drainage pathway (Joseph A. O'Donnell, memo to file, January 7, 1974). Because the condition and amount of tailings contained in any chromite tailing ponds is undetermined, the current fate of the tailings is uncertain. However, because the chromite tailing ponds were constructed in the White Creek drainage pathway, which meanders like most creeks, virtually all of the chromite tailings would eventually be eroded and transported downstream by White Creek.

The report titled "Geology of the Butler Estate Chromite Mine" (1961) discusses the geology of the largest chromite mine in Fresno County, providing the quantities of tons shipped and tons mined. This report was used to estimate the quantity of waste tailings processed by the different chromite mills in the Los Gatos Creek watershed. The ratio of tons of ore shipped to tons of waste tailings was then assumed to apply to

Reproduced with permission of the copyright owner. Further reproduction prohibited without permission.

the other chromite mines in the region, thereby providing an estimation of the total tons of waste tailings. The total quantity of asbestos generated from the chromite milling operations is estimated to be approximately 16,500 cubic yards. See Table 6-9.

Several assumptions are needed to compare the quantity of asbestos potentially eroded by chromite milling with the volume of asbestos eroded as a result of other anthropic activities (i.e., mining, asbestos milling, and road and exploration pit construction). First, the potential increase in asbestos erosion due to mining and road and exploration pit construction is assumed to be approximately 6.53%, based on MUSLE analyses. Second, for post-mining time periods, the yearly average asbestos erosion is estimated to be approximately 5,080 cubic yards, based on MUSLE calculations with adjusted K factors. The estimated erosion rate probably over-represents asbestos erosion over the past 30 years, since anthropic activities evolved gradually to their current magnitude; thus, the average yearly asbestos erosion from mining and road construction during construction of the various mines probably was substantially less than the currently estimated increase of 6.53%.

Applying these assumptions to estimate the cumulative anthropic increase to asbestos erosion from mining, asbestos milling, exploration pits, and road construction sites yields the following:

$$30 \text{ years} \times 6.53\% \times 5{,}080 \text{ yds}^3 \text{ per year} = 9{,}952 \text{ yds}^3.$$

The above estimate of 9,952 cubic yards of asbestos is approximately one-half of the estimated amount of asbestos potentially eroded from chromite milling activities (16,500 cubic yards). The above analyses suggest that disposal of tailings from chromite milling operations potentially has contributed significant quantities of

Reproduced with permission of the copyright owner. Further reproduction prohibited without permission.

anthropic asbestos to the surface water pathway. The above analyses suggest that the potential chromite milling disposal practices appear to be greater than all other anthropic sources combined.

Reproduced with permission of the copyright owner. Further reproduction prohibited without permission.

4.0 DISCUSSION OF SURFACE WATER TRANSPORT PATHWAY

Sections 2 and 3 of this chapter presented the MUSLE and USLE modeling estimates of naturally occurring and anthropic asbestos erosion from the Los Gatos Creek drainage area. This section considers the effects of other known natural asbestos sources within the Arroyo Pasajero drainage on the estimated increases from anthropically eroded asbestos through the water-dependent transport pathways.

Two water-dependent transport pathways were considered: (1) transport of asbestos-containing sediment to the San Luis Canal section of the California Aqueduct, which is a source of potable and irrigation water; and (2) deposition of asbestos-containing sediment onto the Arroyo Pasajero alluvial fan, where it is subject to wind erosion and airborne transport in the western San Joaquin Valley.

Previous work by the DWR and USBR to estimate the origin of sediments being deposited into the settling basin abutting the Arroyo Pasajero section of the California Aqueduct is briefly reviewed and then used to estimate the dilution of the estimated anthropic asbestos increase (originally calculated by MUSLE in Section 3 of this chapter) by natural asbestos-bearing materials being eroded from pre-historic alluvial fan deposits of the Arroyo Pasajero.

4.1 Previous Regional Evaluations of Arroyo Pasajero Sediments

Shortly after the largest storm on record for this region (January 25-26, 1969), the DWR and the USBR became aware that the quality of storm runoff and sediments generated by the Arroyo Pasajero drainage system were significantly underestimated during the design of the California Aqueduct. The consequences are that the sediment

Reproduced with permission of the copyright owner. Further reproduction prohibited without permission.

retaining basin has been filled much more rapidly than had been anticipated. Since 1969, the DWR and USBR have been studying various alternatives to address the original low estimation of the storm flows and sediments generated by the 512-square-mile Arroyo Pasajero drainage basin. The basin must typically now be cleared of excess sediment on a yearly basis in order to protect the Aqueduct and make room for sediment that may be delivered during the next year's storms.

The California Aqueduct was originally designed to collect part of the Arroyo Pasajero flows (up to a 3-day, 100-year storm) and sediments (generated over a 50 year period) in a three square mile settling basin abutting the California Aqueduct, near the town of Huron. Flows beyond the capacity of the settling basin's capacity were to be discharged into the California Aqueduct or siphoned to the Aqueduct's eastern side, to flow on to the Arroyo Pasajero's alluvial fan areas which had been protected by the construction of the Aqueduct (USBR, 1988; Boyle Engineering, 1988) (see Figure 6-4). As a result of the affects of flooding on private and Federal lands, the practice of discharging to the downstream (eastern) side of the Aqueduct has been stopped.

Hydrological analyses of the Arroyo Pasajero conducted by several engineering studies have shown that the original design volume for the 100-year, 3-day storm was approximately one-fifth of the current estimate of this flow volume. As a result, the 50-year sediment and 100-year storm water storage capacity is filled with sediments and the basin is currently capable of storing less than the flow of a 10-year storm (Boyle Engineering, 1988; USBR, 1984; DWR, 1984).

Reproduced with permission of the copyright owner. Further reproduction prohibited without permission.

4.2 Anthropic Increases in Asbestos Erosion Relative to Natural Sources in the Arroyo Pasajero and Surrounding Regions

The MUSLE and USLE provided estimates of the relative increases in asbestos erosion in the Los Gatos Creek drainage area, due to anthropic activities (i.e., mining, asbestos milling, and construction of roads and exploration pits). However, other sources of asbestos in downstream areas are also subject to erosion. Therefore, the potential upland anthropic contributions to regional surface water and air pathways would be expected to be diluted as a result of downstream contributions.

Asbestos-containing soils and sediments from various sources in the Los Gatos Creek drainage area generally can not be distinguished from each other by petrographic analyses of sample morphology and mineralogy. Moreover, the mechanical mixing, sorting, and disaggregation processes which occur during sediment transport via water and air pathways make it infeasible to distinguish among asbestos sediments from various sources. Therefore, to evaluate potential anthropic contributions to erosion in a more regional context, the MUSLE estimates were adjusted to reflect the dilution by other asbestos-bearing sediments eroded from the Arroyo Pasajero alluvial fan. Studies conducted by DWR and USBR indicate that 37% to 62% of the sediments being deposited near the San Luis Canal originate from streambed and stream bank erosion of the entrenched Los Gatos Creek and Arroyo Pasajero channel, west of the town of Coalinga.

As previously discussed, the Arroyo Pasajero alluvial fan reflects the mineralogy of upland sediment source areas, including the New Idria Formation and younger sedimentary formations. Sampling of historic and recent alluvial fan sediments has indicated similar asbestos concentrations in these sediments, at concentrations of

Reproduced with permission of the copyright owner. Further reproduction prohibited without permission.

approximately 1% or less. The relatively low asbestos concentrations of modern and historic alluvial sediments may be explained, in part, by the dilution of asbestos-bearing sediments from upland source areas with non-asbestos sediments derived from other watersheds which do not drain serpentinite formations.

Therefore, because of the similar asbestos concentrations in current sediments and historical sediments found in the alluvial fan, considering regional transport pathways in the Arroyo Pasajero, the relative anthropic asbestos increase from upland sources would be reduced by an amount proportional to the erosion of these historic alluvial sediments.

4.2.1 Potential Discharges to the California Aqueduct

The discharge of asbestos to the California Aqueduct was identified as being a part of the regional surface water transport pathway. The water transport pathway calculation assumes that sediment discharges from the Arroyo Pasajero contribute approximately 50% of the total asbestos which enters the California Aqueduct. This percentage is believed to be an over-estimate, based on regional geologic observations, the occurrence of numerous upstream inlets to the Aqueduct, and the results of Aqueduct sediment sampling and asbestos analyses.

Sampling results by DWR have documented relatively high asbestos concentrations, some as great as 25,500 million fibers per liter, in samples of Aqueduct water at locations upstream of the Arroyo Pasajero inlets. This is a result of the presence of numerous asbestos-bearing formations which drain into the Aqueduct via inlet structures designed to collect surface water runoff and sediments. An inventory of inlet structures to the Aqueduct is provided in Table 6-13 and Aqueduct water

Reproduced with permission of the copyright owner. Further reproduction prohibited without permission.

asbestos sampling data is summarized in Table 6-14. The location of selected inlet structures and Aqueduct sampling stations in relationship to the Arroyo Pasajero section of the Aqueduct are illustrated in Figure 6-13.

All mining, asbestos milling, and road and exploration pit construction activities are estimated to have increased natural asbestos concentrations as much as 2% in California Aqueduct waters. The Atlas and Coalinga Sites are estimated to contribute as much as 0.5% and 0.1%, respectively, to this estimated increase.

Reproduced with permission of the copyright owner. Further reproduction prohibited without permission.

5.0 CONCLUSIONS

The Modified Universal Soil Loss Equation (MUSLE) and the Universal Soil Loss Equation (USLE), two related and widely accepted erosion and sediment prediction models, were used to estimate the highest amount of asbestos that could be eroded by the anthropic disturbance of the New Idria Formation draining to Los Gatos Creek. Conservative model parameters were estimated to purposely overestimate erosion, while maintaining realistic assumptions based upon interpretations of available information, as presented in this chapter. These widely accepted models predicted similar relative anthropic asbestos contributions compared to predicted natural asbestos contributions. All anthropic increases to natural asbestos erosion from the New Idria Formation were estimated to total approximately 6.5%, with the Atlas Site contributing 1.6% and the Johns-Manville Coalinga Asbestos Mill Site contributing 0.3% to this increase, based on existing conditions.

The limited increase in current erosion from anthropic activities appears to be attributed to conditions found in the region. First, the natural vegetative cover on the New Idria Formation soils is sparse because of the toxic effects of asbestos on plants. Therefore, the erosion increase caused by the anthropic elimination of vegetative cover is minimal because the thin natural original cover affords little protection against erosion. Second, the erodibility of mine surfaces decreases compared to the natural asbestos soil, apparently because the natural soils have been weathered for a longer period, causing a finer and more erodible particle size distribution than the soil structure of the recently exposed mine surfaces. This phenomena actually decreases erosion. When the effects of both vegetation loss and surface soil removal are combined, erosion is estimated (by the MUSLE and USLE) to increase slightly beyond natural erosion. The small predicted asbestos increases in the Arroyo Pasajero alluvial

Reproduced with permission of the copyright owner. Further reproduction prohibited without permission.

fan are consistent with the observation that sediments deposited before and after the occurrence of mining and milling activities in the Los Gatos Creek area have similar asbestos concentrations.

Sediment erosion from mining, asbestos milling, exploration pits, and road construction sites in the Los Gatos Creek drainage area is estimated to increase asbestos concentrations in the California Aqueduct by a maximum of approximately 2%. The Atlas Site's contribution to this increase is estimated to be as high as approximately 0.5%, while the Johns-Manville Coalinga Site's maximum contribution to this increase is estimated to be approximately 0.1%. The estimate of the Johns-Manville Coalinga Asbestos Mill Site's asbestos contribution is overestimated because the MUSLE analysis does not consider the tailings dam downstream from the Coalinga Asbestos Mill Site, which appears to effectively capture and prevent the discharge of much asbestos.

Reproduced with permission of the copyright owner. Further reproduction prohibited without permission.

6.0 REFERENCES

Atwater, Brian F.; Adam, D. P.; Bradbury, J. P.; Forester, R. M.; Mark, R. K.; Lettis, W. R.; Fisher, G. R.; Gobalet, K. W.; and Robinson, S. W. 1986. A Fan Dam for Tulare Lake, California and Implication s for the Wisconsin Glacial History of the Sierra Nevada. Geological Society of America Bulletin, vol. 97: p. 97 - 109.

Boyle Engineering Corporation. 1988a. Draft Summary Letter Report for Hydrologic Analysis: Arroyo Pasajero Drainage and Sediment Control Plan.

Boyle Engineering Corporation. 1988b. Draft Summary Letter Report for Watershed Mapping, Task 8.0: Arroyo Pasajero Drainage and Sediment Control Plan. Prepared for the U.S. Department of the Interior, Bureau of Reclamation.

Boyle Engineering Corporation. 1988c. Draft Summary Letter Report for Sediment Analysis: Arroyo Pasajero Drainage and Sediment Control Plan.

Bull, W.B. 1964a. Geomorphology of Segmented Alluvial Fans in Western Fresno County, California: Erosion and Sedimentation in Semiarid Environment. Geological Survey Professional Paper 352-E.

Bull, W.B. 1964b. Alluvial Fans and Near-Surface Subsidence in Western Fresno County, California: Studies of Land Subsidence. Geological Survey Professional Paper 437-A.

California Department of Water Resources, San Joaquin District. 1984. Arroyo Pasajero Alternatives: An Appraisal-Level Report on Alternative Solutions to the

Reproduced with permission of the copyright owner. Further reproduction prohibited without permission.

Flooding-Sedimentation-Asbestos Problem at the Intersection of Arroyo Pasajero and San Luis Canal.

California Department of Water Resources. 1986. Office Memorandum. February.

California Department of Water Resources 1987. Reconnaissance Study and Cost Estimate for Los Gatos Creek Alternative. April.

Dibblee, T.W. 1971. Geologic Map of the New Idria Quadrangle, California - Open File Map: U.S. Geological Survey. Reston, Virginia.

Erickson, A.J. 1978. Aids For Estimating Soil Erodibility "K" Value Class and Soil Loss Tolerance. U.S. Department of Agriculture, Soil Conservation Service.

Goldman, S.J.; Jackson, K.; Bursztynsky, P.E.; and Taras, A. 1986. Erosion and Sediment Control Handbook. McGraw-Hill Book Company.

Kirby, M.J., and Morgan, R.P.C. 1980. Soil Erosion. John Wiley and Sons.

Kruckeberg, A.R. 1984. California Serpentines: Flora, Vegetation, Geology, Soils, and Management Problems. University of California Publications in Botany, vol. 78.

Levine-Fricke. May 9, 1989. "Off-site source characterization; regional soil sampling; and watershed modeling report".

Reproduced with permission of the copyright owner. Further reproduction prohibited without permission.

McGuire, M.J.; Bowers, A.E., and Bowers, D.A. 1982. Asbestos Analysis Case History: Surface Water Supplies in Southern California. Journal of the American Water Works Association, vol. 74, no. 5, pp. 471-478.

Matthews, R.A. 1961. Geology of the Butler Estate Chromite Mine, Southwestern Fresno County, California. California Division of Mines and Geology, Special Report 71.

Miller, R. E.; Green, J. H.; and Davis, G. H. 1971. Geology of the Compacting Deposits of the Los Banos - Kettleman City Subsidence Area, California. Geological Survey Professional Paper 497-E: U.S. Department of the Interior, 46 p.

Mumpton, F.A., and Thompson, C.S. 1975. Mineralogy and Origin of the Coalinga Asbestos Deposit. Clays and Clay Minerals, 23: 131-143.

Munn, J.R. Jr.; Busacca, A.J., and Trott, K.E. 1981. California Aqueduct Sedimentation Study for the Arroyo Pasajero and Tributary Watersheds.

O'Donnel, J.A. 1974. Memo to file, California Regional Water Quality Control Board, Region 5. January 7.

Simons, Li & Associates, Inc. 1982. Engineering Analysis of Fluvial Systems.

Simons, Li & Associates, Inc. 1985. Final Report: Stream Channel Erosion Study Arroyo Pasajero.

Reproduced with permission of the copyright owner. Further reproduction prohibited without permission.

Southern Pacific Land Company. 1986. Remedial Investigation for Southern Pacific Land Company Property, Coalinga, California. Prepared by Levine-Fricke, November 17.

U.S. Department of Agriculture, Soil Conservation Service. 1971. SCS National Engineering Handbook, Chapter 4. Washington, D.C.

U.S. Department of Agriculture, Soil Conservation Service. 1988a. Cantua Creek Sediment Study, Fresno County, California, December 1987. Davis, California.

U.S. Department of Agriculture, Soil Conservation Service. 1988b. Preliminary Soils Mapping.

U.S. Department of Interior, Bureau of Reclamation. 1984. Arroyo Pasajero Flood and Silt Deposition Study: San Luis Unit-CVP-California. Special Report on Flood Protection for San Luis Canal.

U.S. Department of Interior, Bureau of Reclamation. 1988. Scoping Report: The Arroyo Pasajero Flood Detention Basin: Interim Standard Operational Impact Report/Environmental Impact Statement.

U.S. Environmental Protection Agency. 1987. Inventory of Potential Asbestos Sources in the New Idria-Coalinga Study Region for the Atlas and Coalinga Sites, Fresno County, California.

Reproduced with permission of the copyright owner. Further reproduction prohibited without permission.

Williams, J.R. 1975. Sediment-Yield Prediction with Universal Equation Using Runoff Energy Factor. U.S. Department of Agriculture: Present and Prospective Technology for Predicting Sediment and Yield Sources, pp. 244-252.

Williams, J.R., and Berndt, H.D. 1972. Sediment-Yield Computed with Universal Equation Book. Journal of the American Society of Civil Engineers, Hydraulics Division.

Williams, J.R., and Berndt, H.D. 1977. Determining the Universal Soil Loss Equations Length-Slope Factor for Watersheds, in Soil Erosion: Prediction and Control, Special Publication No. 21, Soil Conservation Society of America.

Wischmeier, W.H., and Smith, D.D. 1978. Predicting Rainfall Erosion Losses - A Guide to Conservation Planning. U.S. Department of Agriculture, Agriculture Handbook No. 537.

Reproduced with permission of the copyright owner. Further reproduction prohibited without permission.

CHAPTER SEVEN

SUMMARY OF OBSERVATIONS AND CONCLUSIONS

1.0 INTRODUCTION

This chapter presents a summary of the most important observations and conclusions of this regional environmental investigation and assessment of the geologic occurrence and distribution of chrysotile asbestos deposits in the southern Diablo Range/Coast Range mountains, foothills, and alluvial fan regions of the Coalinga region in western Fresno County, California. This area is located along the western margin of the central San Joaquin Valley as illustrated in Figure 1-1 and 2-1.

This investigation included a review of the regional geologic setting using available literature and geologic reports; a regional field and aerial reconnaissance investigation of potential asbestos source areas including natural outcrop areas and asbestos-bearing mine and mill site operations areas; a review and interpretation of aerial photography including black and white and color/infrared imagery; a macroscopic and microscopic evaluation of the unique characteristics of the chrysotile asbestos deposits of the Coalinga region; a regional asbestos outcrop, streambed sediment, and alluvial fan sediment sampling and asbestos analysis program; and a watershed asbestos soil erosion modeling project to provide a quantitative estimate of the relative amounts of asbestos being eroded from anthropic sources (i.e., mining operations and mill sites) in comparison with natural sources (i.e., natural outcrop areas).

Reproduced with permission of the copyright owner. Further reproduction prohibited without permission.

Major conclusions from each of these areas of investigation are summarized in the following sections.

2.0 SUMMARY OF BACKGROUND ASSESSMENT AND GEOLOGIC SETTING

The Coalinga region is an area were there are massive occurrences of ultramafic and sedimentary deposits of the primary mineral chrysotile asbestos. The chrysotile deposits are known as serpentinite and are of both economic and environmental health significance. These deposits are generally concentrated in rugged upland and mountainous areas that are poorly vegetated. The ultramafic deposits of serpentinite have yielded massive quantities of commercial grade chrysotile asbestos ore and other ores, primarily chromite and mercury. Mining of chromite, mercury, and other rare minerals has been taking place in this district since the late 1800's. Chromite mining operations were increased in the 1940's and 1950's as a result of the strategic value of chromite ore. Mining operations for chrysotile asbestos occurred in the 1960's when it was discovered that the primary matrix of the chromite ore deposits consisted of 80 to 90 percent or more of an almost pure form of chrysotile. The chrysotile occurs as very short fibers, generally 5 to 10 microns in length or shorter, which are bundled in a flaky, whitish-gray matrix not previously recognized as having commercial asbestos value.

In the 1960's and 1970's, an estimated 1 million tons or more of commercial grade chrysotile asbestos may have been produced by asbestos mining and milling operations in the region. Essentially all mining activities in the region were discontinued by the end of the 1970's.

Reproduced with permission of the copyright owner. Further reproduction prohibited without permission.

The chrysotile deposits of the region are characterized as massive, tectonically emplaced deposits that may have originated from metamorphism of olivine-rich crustal material. The chrysotile deposits are found as diapiric bodies that have migrated into the cores of anticlinal structures, most notably the Joaquin Ridge Anticline which is located along the western margin of the San Joaquin Valley approximately 17 miles northwest of Coalinga. The largest deposit is known as the New Idria Formation. This deposit outcrops over a 48 square-mile area at the crest of the Joaquin Ridge highlands in an area associated with rugged terrain and elevations that range from approximately 4200 to 5400 feet above mean sea level. The margin of the San Joaquin Valley, located approximately 15 miles east of the New Idria Formation outcrop area, is formed by Miocene and younger sedimentary formations that outcrop at an elevation of approximately 500 to 1500 feet. The elevation of the floor of the adjoining San Joaquin Valley ranges from approximately 280 to 400 feet along the valley's western margin.

The structural trend of the Joaquin Ridge Anticline and serpentinite outcrop area is located approximately 20 miles northeast of the structural trend of the San Andreas fault system. Faulting and folding in this seismically active area appears to be a result of crustal compression resulting from convergence of the Pacific Plate with the North American Plate.

Stratigraphic data shows that the diapiric serpentinite body of the New Idria Formation became emergent in Miocene time, approximately 17 to 20 million years ago. Massive amounts of chrysotile asbestos-bearing serpentinite was extruded from the diapiric core of the Joaquin Ridge anticlinal structure which is formed by Cretaceous shales and sandstones of the Panoche Formation. The extruded

Reproduced with permission of the copyright owner. Further reproduction prohibited without permission.

serpentinite debris was subsequently reworked in a transitional marine environment as indicated by sedimentary deposits of almost pure serpentinite that flank the Joaquin Ridge structure. As much as 5 to 10 cubic miles of serpentinite debris may have been extruded from the core of the Joaquin Ridge structure. This is indicated by the thickness of some of the asbestos-bearing sedimentary deposits that flank the Joaquin Ridge structure including as the Big Blue Member of the Temblor Formation (Miocene) which ranges up to 1,000 feet in thickness in sedimentary deposits that are found approximately 8 miles southeast of the main serpentinite body of the New Idria Formation. These Miocene-aged deposits of sedimentary serpentinite are found in layered units that are exposed in the foothills that flank the Joaquin Ridge structure. These sedimentary deposits are currently inclined approximately 30 degrees as a result of diapiric uplift of the core of the Joaquin Ridge structure. Asbestos-bearing sediment eroded from the region's ultramafic (primary) and sedimentary (secondary) sources in the highland areas is transported downstream and may ultimately be deposited in alluvial fan depositional environments in the San Joaquin Valley and/or in the California Aqueduct.

The California Aqueduct was constructed in the 1960's along the western margin of the San Joaquin Valley at an elevation of approximately 340 feet with sufficient gradient to allow flow in a southerly direction (i.e., toward Southern California and Los Angeles). In order to increase the yield of water to the Aqueduct, many of the intermittent streams that drain the mountainous areas that form the western margin of the valley were allowed by engineering design to drain directly into the Aqueduct. This design also had the affect of increasing the economic benefits of the project by protecting land areas on the eastern (downgradient) side of the Aqueduct that had previously been subject to seasonal flooding. Water from the Aqueduct was then

Reproduced with permission of the copyright owner. Further reproduction prohibited without permission.

made available to irrigation systems to agriculturally develop some of these previously flood-prone areas.

In the central part of the valley, the Aqueduct was constructed across a series of alluvial fans at an even-contour elevation of approximately 340 feet. Construction of the Aqueduct has had an affect of damming run-off waters and/or sediments in areas where intermittent streams were not allowed to cross the Aqueduct. One of the largest alluvial fans that was cut off by the Aqueduct was the Arroyo Pasajero alluvial fan located near the town of Huron and approximately 17 miles east of Coalinga.

The Arroyo Pasajero drainage basin, i.e., the area from which the alluvial fan receives sediment and run-off waters, covers approximately 500 square miles and includes approximately 7 square miles of the asbestos-bearing New Idria Formation outcrop area.

In the Arroyo Pasajero section of the Aqueduct, flood waters and sediment from the Arroyo Pasajero drainage basin were captured by engineering design in a retaining basin constructed adjacent to the Aqueduct. The retaining basin covers approximately 3 to 5 square miles. Overflow in the retaining basin was designed to be accommodated through a system of inlet structures to the Aqueduct and/or through a system of siphons to pass flood waters to the other side of the Aqueduct. In the 1980's, as a result of siphon pass-through water flooding of the LeMoore Naval Air Station and other areas located approximately 7 miles east of the Arroyo Pasajero section of the Aqueduct, the flood water siphons were ordered closed by the federal government with all future flood waters to be drained into the Aqueduct.

Reproduced with permission of the copyright owner. Further reproduction prohibited without permission.

In the 1980's, the USEPA began investigating the occurrence of elevated concentrations of chrysotile asbestos detected in the waters of the California Aqueduct. The source of the asbestos was identified by the EPA as being several asbestos mining operations located in the Los Gatos Creek drainage sub-basin of the Arroyo Pasajero watershed basin. The identified sites included the Johns-Manville Coalinga Asbestos Mill Site and the Atlas Mine and Mill Site. These two sites were subsequently listed on the USEPA National Priority List (NPL) for Superfund remedial investigation and cleanup. The EPA action initially discounted and/or ignored other potential sources of asbestos to the Aqueduct including asbestos-bearing drainage areas located upstream of the Arroyo Pasajero section of the Aqueduct as well as other mining operations and/or natural outcrop areas located in the Arroyo Pasajero watershed basin.

Subsequent research conducted by myself and by others has demonstrated that there are numerous other potential sources that qualitatively and quantitatively account for a majority of the asbestos that is being delivered by erosional processes to the California Aqueduct. These additional sources were identified as a result of field and aerial reconnaissance investigations, asbestos sample analyses, and quantitative sediment erosion modeling as summarized in the following sections.

3.0 SUMMARY OF GEOLOGIC OBSERVATIONS AND CONCLUSIONS

3.1 Diapiric Emplacement of Diablo Range Serpentinite Masses

A review of available literature, geologic maps, and aerial photography shows that the southern Diablo Range mountains of the central Coast Range in the vicinity of Coalinga contain more than 50 known ultramafic serpentinite deposits that contain a

Reproduced with permission of the copyright owner. Further reproduction prohibited without permission.

high percentage of chrysotile asbestos. The deposits are primarily composed of a sheared, flaky, readily-friable matrix of serpentinite that contains up to 96% chrysotile asbestos. The serpentinite bodies were derived from the metamorphic and hydrothermal alteration of oceanic crustal material that underlies the continental crust in the Coast Range region. Geologic research conducted by other researchers has shown that the serpentinite bodies were emplaced in the upper crust of the earth's surface by diapiric or upward semi-solid flow. The upward movement of the semi-plastic, diapiric serpentinite bodies contributed to the warping and folding of the overlying geologic formations. In the Coalinga region, these upwardly warped and folded formations formed elliptical-shaped, dome-like anticlinal structures that are oriented sub parallel to the trend of the nearby San Andreas Fault Zone.

The diapiric emplacement of the serpentinite masses and the anticlinal deformation of the geologic formations occurred in response to a system of crustal compression that resulted from the tectonic convergence of the Pacific oceanic plate and the North American continental plate. The massive serpentinite deposits were derived from the metamorphic and hydrothermal alteration of oceanic crustal material that was thrust under the continental plate. These massive, metamorphosed assemblages of serpentine minerals were less dense than the surrounding host rock; and because of their semi-plastic, buoyant nature and the occurrence of crustal compression, the serpentinite masses were diapirically forced upward toward the surface. These upwardly mobilized masses migrated into the cores of anticlinal structures that are generally oriented sub parallel to the northwest-southeast trend of the San Andreas Fault Zone. Continued crustal compression and diapiric uplift allowed the serpentinite masses to pierce or rupture the overlying rock formations. The asbestos-bearing serpentinite masses were subsequently forced out or extruded from the cores of faulted, anticlinal structures. In

Reproduced with permission of the copyright owner. Further reproduction prohibited without permission.

addition to diapiric structures, some of the serpentinite deposits were extruded from large fissures or cracks associated with local faulting.

3.2 Miocene "Unroofing" of Serpentinite Deposits

The "unroofing" or surface exposure of these serpentinite masses allowed great quantities (estimated to be as much as ten cubic miles) of the semi-plastic material to be extruded or forced out of the anticlinal structures by means of solid-flowage. Much of the extruded, asbestos-bearing serpentinite was subsequently eroded and redeposited in local sedimentary environments as detrital serpentinite debris. An analysis of the regional stratigraphy demonstrates that this detrital serpentinite debris has been incorporated in many of the local sedimentary rock formations that are Miocene or younger in age (i.e., 20 million years old or less) including the Big Blue Member of the Temblor Formation (Miocene) and relatively recent Quaternary alluvial fan sediments that were deposited prior to historic time.

As a result of their diapiric relationship with anticlinal structures, most of the southern Diablo Range serpentinite bodies are located near the tops of mountains and ridges in areas associated with steep relief and rugged terrain. These areas typically receive the region's highest annual rainfalls and strongest seasonal winds, which contribute to higher rates of erosion of the asbestos-bearing serpentinite soils. This explains why asbestos is an integral component of the sediments derived from the mountain areas and deposited in the alluvial fan areas.

Reproduced with permission of the copyright owner. Further reproduction prohibited without permission.

3.3 New Idria Formation and Table Mountain Serpentinite Masses

The New Idria Formation is the largest known serpentinite deposit in the Coalinga region. This asbestos-containing formation is exposed over an elliptically-shaped, 48-square-mile area that forms the crest of the Joaquin Ridge highland trend. The area is located in the mountains approximately 20 miles northwest of Coalinga. Another major deposit is the Table Mountain serpentinite body, which originally covered more than 30 square miles. The Table Mountain serpentinite deposit is located approximately 17 miles south of Coalinga. Both of these serpentinite deposits are related to faulted, anticlinal structures.

The New Idria Formation forms the exposed core of the Joaquin Ridge Anticline. Diapiric uplift of the serpentinite body over great lengths of geologic time has allowed large volumes of serpentinite debris to be extruded and eroded from the elliptically-shaped, 48-square-mile outcrop area. The Table Mountain deposit was formed by serpentinite debris that was extruded from a series of faults and fissures associated with the Table Mountain structure.

Geophysical and geological investigations of the New Idria Formation indicate that the diapiric, serpentinite mass extends from the surface to a depth of more than 15,000 feet. The fact that the serpentinite body forms the core of an anticlinal structure indicates that the serpentinite mass may extend much deeper. The extrusive Table Mountain serpentinite deposit originally covered more than 30 square miles with serpentinite debris that ranged from 50 to 250 feet thick. Fluvial erosion and dissection of the Table Mountain structure has diminished the areal extent of this serpentinite deposit to about 20 square miles.

Reproduced with permission of the copyright owner. Further reproduction prohibited without permission.

3.4 Geologic Age of Serpentinite Deposits

It has been estimated that in early Miocene time (approximately 17 to 20 million years ago) approximately 5 to 10 cubic miles of serpentinite debris was extruded from the New Idria/Joaquin Ridge structure. This estimate is based on calculations regarding the areal extent and thickness of sedimentary asbestos deposits of Miocene age in the Coalinga region. The extruded material was eroded and deposited as detrital serpentinite debris in a shallow marine environment that was part of an inland sea that once occupied the central San Joaquin Valley area. This asbestos-containing body of detrital serpentinite debris is known as the Big Blue Member of the Temblor Formation (Miocene). The Big Blue Member ranges in thickness from 300 to 1,000 feet. The soft, weakly consolidated, asbestos-containing formation now forms the Big Blue Hills which are located approximately 10 miles north of Coalinga.

3.5 Regional Structure and Asbestos-Bearing Sedimentary Formations

The Big Blue Hills are part of an easterly dipping monocline (dipping approximately 20 to 30 degrees) that flanks the New Idria - Joaquin Ridge anticlinal structure. The monoclinal structure also forms the western margin of the central San Joaquin Valley. This area is located approximately eight miles east of the New Idria Formation outcrop at the crest of the Joaquin Ridge Anticline. The monocline is formed by Cretaceous and younger strata including the Temblor Formation (Lower Miocene); the Santa Margarita Formation (Upper Miocene); the Jacalitos-Etchegoin Formation (Pliocene); and the Tulare Formation (Pliocene-Pleistocene). All of these sedimentary formations are known to contain at least a minor component of detrital serpentinite debris, and all of the strata are eroding as a result of uplift and exposure associated with the margin of the monoclinal structure. In some of these formations, as in the Big Blue Member,

Reproduced with permission of the copyright owner. Further reproduction prohibited without permission.

the detrital serpentinite debris is a locally major component. The ubiquitous presence of detrital serpentinite debris in all of these sedimentary formations is indicative of the serpentinite mineralogy of the sediment source areas (i.e., the ultramafic serpentinite deposits of the New Idria Formation and the Table Mountain structure and possibly the erosional reworking of sedimentary serpentinite deposits such as the Big Blue Member.

3.6 Extruded Serpentinite Masses

In Pliocene-Pleistocene time (i.e., approximately 1.8 million years ago) and in more recent Quaternary time, large volumes of serpentinite debris were similarly extruded by solid-flowage from the New Idria and Table Mountain anticlinal structures. The extruded serpentinite debris formed large landslides and/or serpentinite debris flow complexes that flank the highland serpentinite source areas of both of these structures. The extruded serpentinite debris from the Table Mountain structure is unique in that the deposit originally covered more than 30 square miles and had a thickness ranging from 50 to 250 feet and a total volume estimated to exceed 0.48 cubic miles. The surficial debris sheet deposit originally extended from the summit carapace, down a ramping slope, and over a piedmont plain (an area now known as the Kettleman Plain which is a southerly extension of the Pleasant Valley floodplain. Geologically recent (i.e., within the last 1.8 million years) landslides and/or serpentinite debris flows associated with the New Idria Formation are known to cover more than five square miles with a similar thickness. These deposits are generally found in the headlands of canyons that, as a result of erosion, are encroaching on the Joaquin Ridge outcrop of the New Idria Formation.

Reproduced with permission of the copyright owner. Further reproduction prohibited without permission.

3.7 Detrital Serpentinite Deposits and Regional Stratigraphy

An analysis of the stratigraphic section in the Coalinga region demonstrates that large volumes of detrital serpentinite debris has been deposited in many local sedimentary formations that post-date the Miocene age of the Temblor Formation. The ubiquitous occurrence of detrital serpentinite debris throughout the stratigraphic setting and regional environment indicates that the primary serpentinite deposits (i.e., the New Idria, Table Mountain, and other un-named intrusive serpentinite masses) have been subject to an almost continuous sequence of extrusion and erosion since Miocene time.

Sedimentary rock units in the Coalinga region that have been reported to contain detrital serpentinite debris include geologically recent Quaternary alluvial deposits; alluvial deposits of the Tulare Formation (Pliocene-Pleistocene); alluvial and shallow marine deposits of the Jacalitos-Etchegoin Formation (Early Pliocene); marine and non-marine deposits of the Santa Margarita Formation (Late Miocene); and marine and non-marine deposits of the Big Blue Member of the Temblor Formation (Early Miocene). In the Arroyo Pasajero watershed basin, these asbestos-containing sedimentary formations are exposed and subject to fluvial and wind erosion over an estimated 130-square-mile area. Sediments eroded from the Arroyo Pasajero watershed basin have been deposited as an alluvial fan which covers an estimated 300-square mile area. As indicated by my review of available aerial photographs, approximately two-thirds of this alluvial fan area has been cultivated for commercial agricultural purposes.

These Miocene and younger asbestos-containing formations are also exposed in the foothills that form the western margin of the central San Joaquin Valley. In the Central Valley region (excluding the Arroyo Pasajero watershed and alluvial fan),

Reproduced with permission of the copyright owner. Further reproduction prohibited without permission.

these foothills include Kettelman Hills, Guijarral Hills, Anticline Ridge, the Big Blue Hills, Ciervo Hills, Monocline Ridge, Tumey Hills, Panoche Hills, and Leguna Seca Hills. Collectively, the asbestos-containing sedimentary formation outcrops of these foothills cover an estimated additional 120 square miles. Collectively, the alluvial fans of the western central San Joaquin Valley between Los Banos and Kettleman City (i.e., the area that encompasses the alluvial fans of the Leguna Seca Hills south to the Kettleman Hills) cover an estimated 1,500 square miles and the asbestos-containing sedimentary formations (i.e., the Big Blue Member and younger, overlying geologic units) collectively cover an estimated 250 square miles.

3.8 Continuing Uplift and Erosion of the New Idria Formation

Field observations of the New Idria Formation indicate that the diapiric, anticlinal structure is continuing to be uplifted. This is indicated by the fact that the soft, friable matrix of flaky serpentinite continues to persist as a topographic high by forming the crest of the Joaquin Ridge anticlinal structure. The core of the anticline consists of readily friable serpentinite, and the flanks of the anticline are formed by erosion-resistant Cretaceous sandstones and shales. The ridgetop outcropping of the serpentinite mass has over 2,200 feet of topographic relief and is exposed on both sides of the ridge. Because of this rugged relief, the weakly consolidated, flakey serpentinite matrix is highly susceptible to sheet, rill and gully erosion and mass wasting in the form of landslide and/or debris flow complexes. In addition, the long, hot summers of the region contribute to the desiccation and drying of the naturally occurring asbestos outcrops. The dried asbestos is very friable, and the strong seasonal winds may contribute to the wind erosion of the very small, clay-sized (2 to 3 microns in length) fibers.

Reproduced with permission of the copyright owner. Further reproduction prohibited without permission.

3.9 Petrographic Characteristics of New Idria Formation Chrysotile Asbestos Deposits

The bulk soil samples from the New Idria Formation and other chrysotile asbestos deposits in the Coalinga region are different from the asbestos products routinely analyzed by analytical testing laboratories. The bulk soil sample matrices tend to be more complex and the minerals present within these samples have been found to exhibit certain properties which make chrysotile identification non-routine. The serpentine minerals associated with these samples include chrysotile, antigorite, and lizardite. All of these serpentine minerals have the same basic serpentine chemical composition [$(Mg,Fe)_6Si_4O_{10}(OH)_8$], but different crystal structures. In the New Idria Formation, most of the chrysotile asbestos occurs as a polymorph of lizardite and/or antigorite forms of serpentine. These polymorphs macroscopically appear as small white chips and platelets and as pale green lath-shaped minerals. Using a binocular scope, these chips, platelets, and lath-shaped minerals were observed to be composed of a material that was easily fibrillated upon slight crushing. Using PLM analytical methods, some of this material was readily confirmed by subcontracting laboratories as chrysotile asbestos and some of the material appeared as a fibrous form of antigorite. Using the TEM method, most of the fibrous material was confirmed by the subcontracting laboratories as chrysotile asbestos based on identification of a cylindrical crystal structure. Macroscopically, the chrysotile asbestos was observed to be aggregated as plate and lath-shaped bundles.

Reproduced with permission of the copyright owner. Further reproduction prohibited without permission.

3.10 Erosion and Transport of Asbestos-Bearing Sediment to the Arroyo Pasajero Alluvial Fan and the California Aqueduct

Asbestos-rich sediments derived from the New Idria/Joaquin Ridge highland area (including those from the weathered surface outcrop of the New Idria Formation, from the eroding margins of serpentinite landslides and debris flows, from asbestos and chromite milling tailings, from fresh exposures from road cuts and open-pit mining operations, and from other geologic sources including ultramafic and sedimentary serpentinite deposits) are eroded by fluvial and eolian (i.e., wind blown) processes. In the Coalinga region, these sediments have historically been deposited on the Arroyo Pasajero and Cantua Creek alluvial fans that have formed on the western margin of the central San Joaquin Valley.

3.11 Results of Arroyo Pasajero Watershed Asbestos Soil Erosion Modeling

The Arroyo Pasajero watershed was identified by the USEPA as being a primary source of asbestos-bearing alluvial sediment being transported into the California Aqueduct in the Arroyo Pasajero Alluvial Fan section of the Aqueduct. The Arroyo Pasajero watershed includes 6.8 square miles of the New Idria Formation outcrop area of Joaquin Ridge highlands. In this watershed, run-off from the New Idria Formation flows into two sub-basins including the White Creek and Pine Canyon sub-basins. The White Creek sub-basin drains approximately 5.8 square miles of the New Idria Formation and the Pine Canyon sub-basin drains approximately 1.0 square mile. The results of my field and aerial reconnaissance investigations have shown that, collectively, this watershed outcrop area includes approximately 700 acres of man-made potential asbestos source areas including 2 mercury mining operations; 6 chromite mine and/or milling operations; 5 asbestos mining operations; 2 asbestos

Reproduced with permission of the copyright owner. Further reproduction prohibited without permission.

milling operations with ore storage and tailings piles; more than 200 bulldozed exploration pits; and approximately 50 miles of unimproved exploration access roads. Essentially all of mine and milling operations in this area were out of operation by the middle of the 1970's.

The relative contribution of asbestos-bearing sediment derived by erosion from the identified potential source areas was evaluated using the Modified Universal Soil Loss Equation (MUSLE). This numerical modeling program included my development of estimates of the aerial extent of asbestos-bearing potential sources including field sampling and laboratory analyses for approximations of asbestos concentrations; field estimates of soil and/or surface material erodibility including development of soil erosion K factors; and interpretation of aerial photographs for estimates of vegetative coverings. Additional parameters included estimates of length, slope, and streambed gradient factors. The results of the numerical modeling work indicated that approximately 2 percent of asbestos-bearing sediment delivered to the California Aqueduct in the Arroyo Pasajero region originates from the erosion of anthropically-disturbed outcrop areas including mine and mill sites.

The results of numerical modeling estimates of asbestos soil erosion for pre-mining and post-mining time periods indicate that there has been no significant change in the amount of asbestos-bearing sediment erosion. These numerical estimates agree with the results of my alluvial fan surface and subsurface investigation and laboratory analyses which also indicate no significant change in the concentration of asbestos in alluvial fan surface and subsurface sediment.

Reproduced with permission of the copyright owner. Further reproduction prohibited without permission.

3.12 Summary of Other Potential Sources of Chrysotile Asbestos to the California Aqueduct

When asbestos was first discovered in water samples from the California Aqueduct in 1980, the source of the fibers was thought to be sediments washed into the Aqueduct through drain inlets from the Arroyo Pasajero during significant storm events. Further studies conducted by the California Department of Water Resources (DWR) in 1984 identified additional sources of asbestos. Specifically, the Cantua Creek and Salt Creek inlets, located approximately 24 miles upstream of the Arroyo Pasajero drainage inlets at Gale Avenue, were identified as additional sources of asbestos to the Aqueduct. The results of my geologic investigations and my review of the existing water sampling data show that other asbestos sources exist both upstream and downstream of the Arroyo Pasajero drainage inlets to the Aqueduct.

Approximately 80 to 90 miles of the California Aqueduct were built across the alluvial fans and creeks and intermittent streams which drain the Diablo Range foothills on the western margin of the San Joaquin Valley. Some of these creeks and intermittent streams drain asbestos-bearing ultramafic and sedimentary formations such as the New Idria Formation and Big Blue Member of the Temblor Formation (Miocene). These formations and other minor sources, including the Santa Margarita Formation (Late Miocene), Etchegoin-Jacalitos Formation (Early Pliocene) and the Tulare Formation (Pliocene-Pleistocene), are exposed in outcrops from uplifted formations that form the Diablo Range foothills. These foothills include Kettleman Hills, Guijarral Hills, Anticline Ridge, Big Blue Hills, Ciervo Hills, Panoche Hills, and Leguna Seca Hills. These uplifted formations are readily subject to erosion and mass wasting along the

Reproduced with permission of the copyright owner. Further reproduction prohibited without permission.

banks of the intermittent streams that drain the poorly consolidated sedimentary deposits.

The results of geologic and reconnaissance investigations show that intermittent streams along the western margin of the San Joaquin Valley that drain the New Idria Formation and/or other asbestos-bearing sedimentary formations include: (1) the Arroyo Pasajero; (2) Martinez Creek; (3) Salt Creek; (4) Cantua Creek; (5) Arroyo Hondo Creek; (6) Tumey Gulch Creek; and (7) the Silver Creek tributary to Panoche Creek. Other intermittent streams that drain the Panoche Hills and Leguna Seca Hills include Leguna Seca Creek and Ortigalita Creek. While the discharge waters from most of these have not been tested for asbestos (with the Salt Creek and Cantua Creek systems being an exception), the fact that they receive run-off from asbestos-bearing formations in upland areas suggests that their discharge waters are likely to significant concentrations of suspended asbestos and/or asbestos-bearing bedload sediment.

4.0 FINAL SUMMARY

The occurrence and distribution of asbestos throughout the Coalinga area is primarily related to the natural erosion of massive, diapirically and/or tectonically emplaced deposits of serpentinite including the New Idria Formation and more than 50 other unnamed extrusive serpentinite deposits. The region also includes numerous sedimentary geologic units that contain significant concentrations of asbestos-bearing detrital serpentinite derived from the region's primary source areas including the New Idria Formation which became emergent in Miocene time (i.e., approximately 17 to 20 million years ago). The surface exposures of these deposits collectively cover approximately 80 square miles. These serpentinite deposits consist of a soft, flakey

Reproduced with permission of the copyright owner. Further reproduction prohibited without permission.

matrix of short-fiber chrysotile asbestos. Most of these serpentinite deposits are located near the tops of ridges or mountains, in areas which are naturally subject to mass wasting (i.e., landslides and debris flows), surface water erosion, and wind erosion.

Serpentinitic sediments eroded over the past 16 to 17 million years have become incorporated within sedimentary deposits and alluvial fans in the western San Joaquin Valley covering more than an estimated 1500 square miles. Because of this, these geologic features also contain asbestos which is subject to wind erosion, surface water erosion, and disturbance by vehicles and other machinery. Over geologic time, erosion of these regionally widespread serpentinite outcrop areas has resulted in the deposition of asbestos-containing sediment in the region's sedimentary stratigraphic formations and in the alluvial sediments of the Arroyo Pasajero and adjoining alluvial fan systems located along the western margin of the central San Joaquin Valley in the Coalinga region.

Petrographic analyses of the Coalinga region's chrysotile deposits have shown that the chrysotile minerals have unique macroscopic and microscopic properties. In the New Idria Formation, most of the chrysotile asbestos occurs as a polymorph of lizardite and/or antigorite forms of serpentine. These polymorphs macroscopically appear as small white chips and platelets and as pale green lath-shaped minerals. Using a binocular scope, the chrysotile asbestos was observed to be aggregated as plate and lath-shaped bundles. These materials were observed to be easily fibrillated and/or to release fibrous structures upon slight crushing. Using PLM analytical methods, some of this material was readily confirmed as chrysotile asbestos and some of the material appeared as a fibrous form of antigorite. Using the TEM method, most of the fibrous

Reproduced with permission of the copyright owner. Further reproduction prohibited without permission.

material was confirmed as chrysotile asbestos based on identification of cylindrical, asbestiform crystal structures.

The results of numerical modeling of asbestos-bearing soil erosion in the Arroyo Pasajero watershed indicates that the occurrence of mining and milling operations in the asbestos-bearing outcrops areas contributes approximately 2 percent of the total estimated amount of asbestos being delivered by streambed sediment transport processes to the Arroyo Pasajero alluvial fan and the California Aqueduct. Approximately 1.1 square miles of the 6.8 square miles of the New Idria Formation that is drained by the Arroyo Pasajero watershed has been affected by mining and/or mill site operations. These mining and mill site operations include 2 mercury mines; 6 chromite mines; 5 asbestos mines; more than 200 bull-dozed exploration pits; and approximately 50 miles of unimproved exploration access roads. The individual contribution of any one particular site and/or potential source area appears to be small, i.e., 1 percent or less, in comparison to the contribution from natural and/or undisturbed asbestos-bearing outcrop areas.

The results of an alluvial fan surface and subsurface sampling and analysis program indicates that there has been no statistically significant increase in the concentration of chrysotile asbestos in alluvial sediments as a result of upland mining and milling operations. Pre-mining and post-mining alluvial sediments appear to have approximately 1 percent or less concentrations of chrysotile asbestos.

In the 1960's, the California Aqueduct was constructed across the medial portions of the Arroyo Pasajero and Cantua Creek alluvial fans. The construction of the Aqueduct has acted as a barrier to the natural dispersion of floodwaters and sediments across the medial and distal portions of these alluvial fans. During normal storm

Reproduced with permission of the copyright owner. Further reproduction prohibited without permission.

events, sediment and stream flow from the Arroyo Pasajero watershed are now retained by a settling basin constructed adjacent to and on the upstream side of the California Aqueduct. However, because of higher than originally projected sedimentation rates, the settling basin is being filled more quickly than expected and its ponding capacity is reduced. As much as 60% or more of the sediment being delivered to the ponding basin appears to be coming from erosion of an entrenched section of the Arroyo Pasajero channel at the head of the Arroyo Pasajero alluvial fan. These sediments have a natural asbestos concentration that ranges from less than 1% to trace levels. This and other eroding sedimentary deposits may be an additional source of asbestos to the Aqueduct.

During periods of high runoff, asbestos-containing floodwaters and sediments from the settling basin previously were allowed to discharge into the Aqueduct; however, current operational procedures for the aqueduct facilities limit such discharges only to situations involving runoff from very large storms (greater than 50 year return period). Current practices call for the annual removal of hundreds of thousands of cubic yards of excess sediment from the ponding basin area.

Sediment and stream flow waters from the Cantua Creek watershed, located directly north of the Arroyo Pasajero watershed, contain relatively high concentrations of asbestos because of erosion from the New Idria Formation outcrop area and from the asbestos-containing Big Blue Member of the Temblor Formation. The Big Blue Member is exposed in the monoclinal outcrop areas that form the foothills located directly upgradient from the California Aqueduct. During storm events, asbestos-bearing sediment and water are allowed, by engineering design, to directly enter the Aqueduct in the Cantua Creek area and other asbestos-bearing alluvial areas located upstream of the Arroyo Pasajero section of the Aqueduct. There has generally been

Reproduced with permission of the copyright owner. Further reproduction prohibited without permission.

no design provision for ponding basins or by-pass structures at the intersection of the Aqueduct and alluvial drainage channels in the Coalinga region.

The results of the regional geologic investigations and the results of a regional soil sampling and asbestos analysis program collectively demonstrate that there are vast sources of chrysotile asbestos in the Diablo Range mountains of central California. The results of watershed soil erosion modeling show that the individual mine and mill site contributions of chrysotile asbestos to the California Aqueduct in the Arroyo Pasajero watershed area are generally less than 1 percent when compared to contributions from natural and/or undisturbed areas. The results of numerical modeling for pre-mining and post-mining time periods and the results of alluvial fan surface and subsurface sample analyses indicates that there has been no significant change in the amount of asbestos-bearing sediment being eroded from the New Idria Formation source areas and being deposited in the Arroyo Pasajero alluvial fan environments. This indicates that remediation of individual man-disturbed areas containing chrystotile asbestos are likely to have negligible affects on the over-all occurrence of chrysotile asbestos in the regional environment. The collective remediation of most mine and mill site areas may have a greater collective impact on reducing the occurrence of asbestos fibers in runoff waters that enter the California Aqueduct; however, the extent of the region's natural, undisturbed primary (ultramafic) and secondary (sedimentary) deposits will continue to be the predominant sources of asbestos to the California Aqueduct and the regional environment.

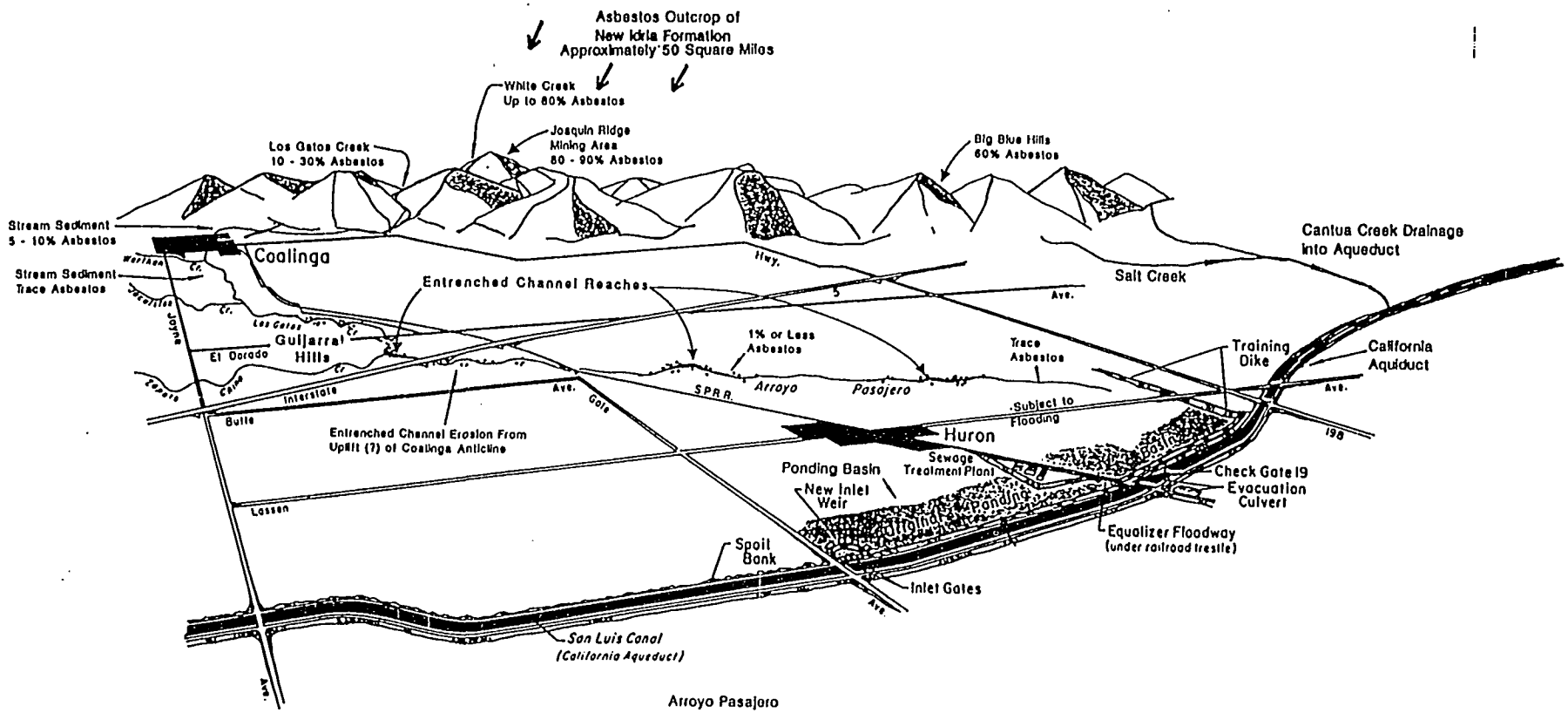
Reproduced with permission of the copyright owner. Further reproduction prohibited without permission.

Reproduced with permission of the copyright owner. Further reproduction prohibited without permission.

FIGURES

Reproduced with permission of the copyright owner. Further reproduction prohibited without permission.

Reproduced with permission of the copyright owner. Further reproduction prohibited without permission.



SOURCE: STATE OF CALIFORNIA, DEPARTMENT OF WATER RESOURCES, SAN JOAQUIN DISTRICT

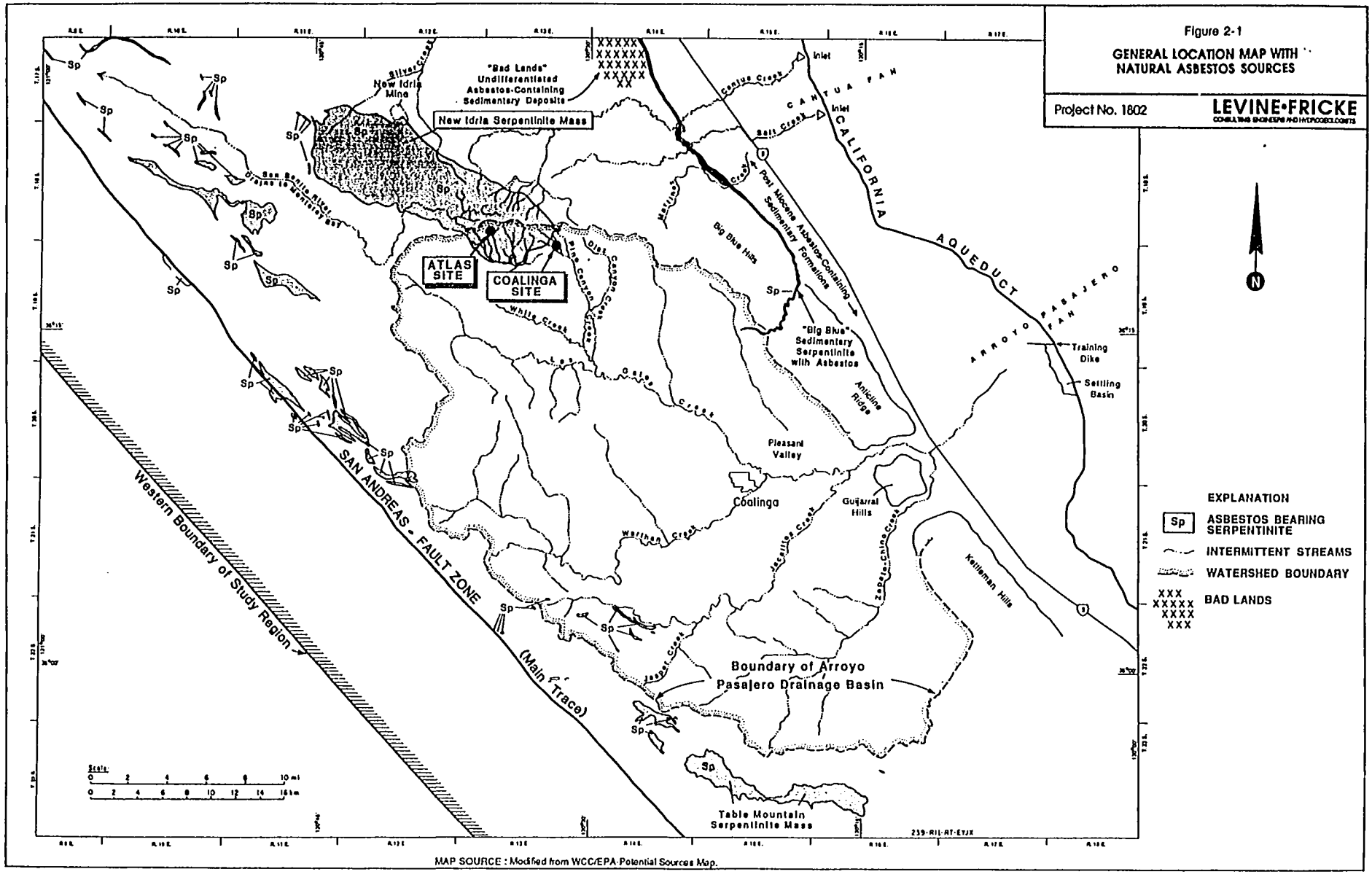
Figure 1-1

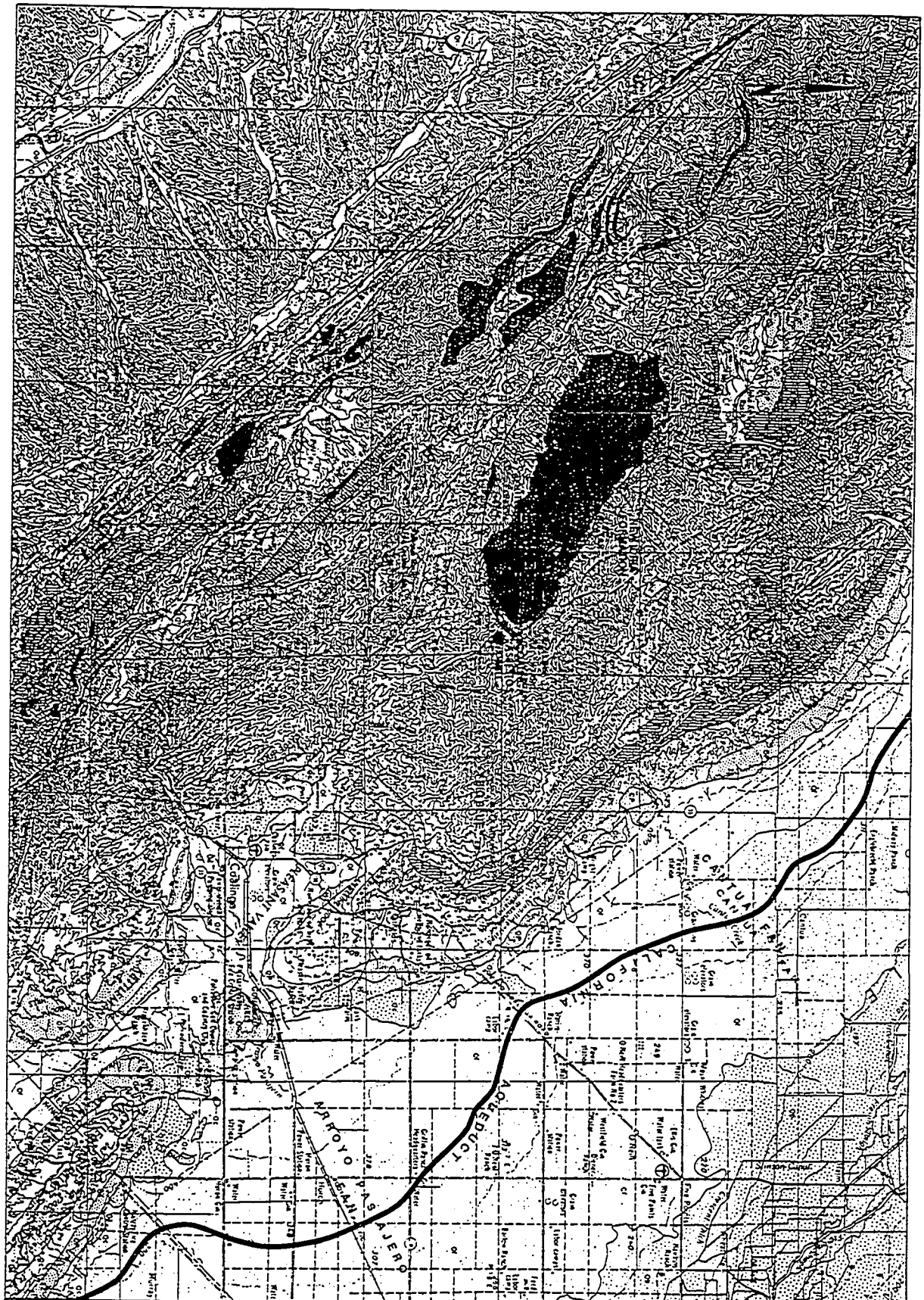
REGIONAL
SCHEMATIC
DIAGRAM

Project No. 1802

LEVINE·FRICKE
CONSULTING ENGINEERS AND HYDROGEOLOGISTS

Reproduced with permission of the copyright owner. Further reproduction prohibited without permission.





MAP SOURCE: Modified from Jenkins, 1971.

SCALE 1 : 250,000

0 5 10 MILES

0 5 10 KILOMETERS

Figure 2-2A

REGIONAL GEOLOGIC MAP SHOWING THE NEW IDRIA FORMATION; OTHER ASBESTOS- CONTAINING FORMATIONS AND THE CALIFORNIA AQUEDUCT

Project No. 1802

LEVINE•FRICKE

CONSULTING ENGINEERS AND HYDROGEOLOGISTS

PAGE 1 of 2

Reproduced with permission of the copyright owner. Further reproduction prohibited without permission.

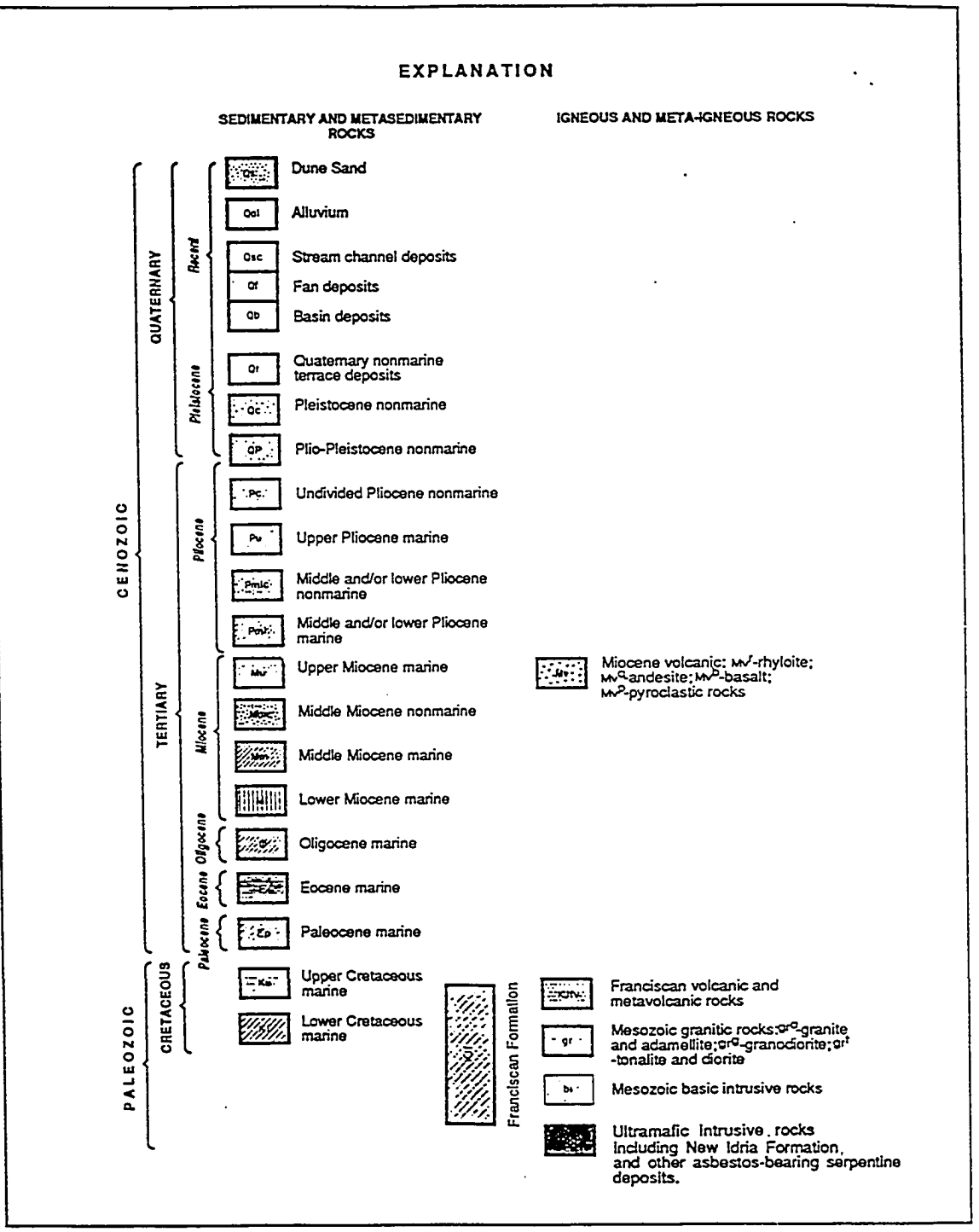


Figure 2-2B : EXPLANATION OF REGIONAL GEOLOGIC MAP SHOWING THE NEW IDRIA FORMATION AND THE CALIFORNIA AQUEDUCT

Reproduced with permission of the copyright owner. Further reproduction prohibited without permission.

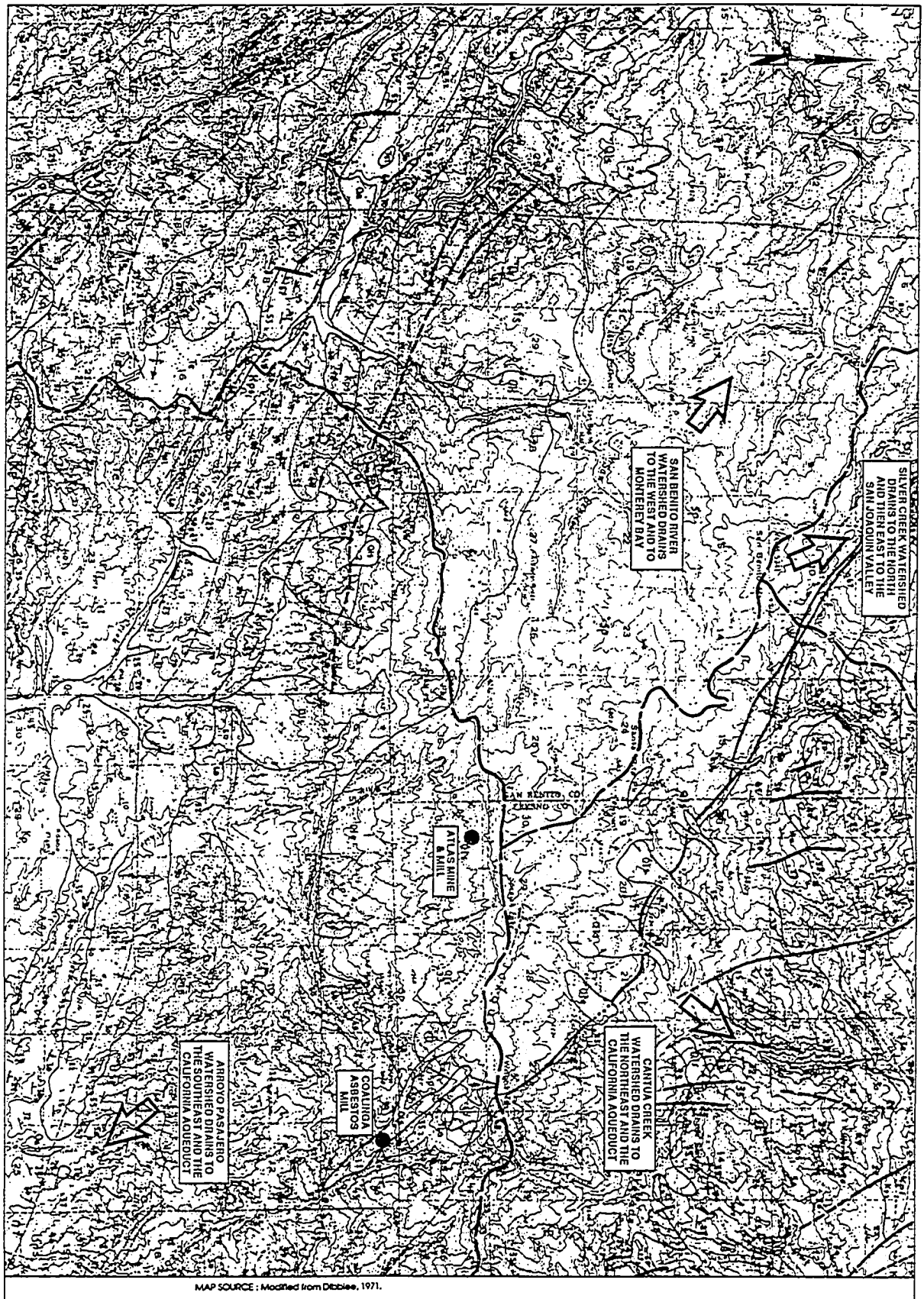


Figure 2-3

GEOLOGIC AND WATERSHED MAP OF JOAQUIN RIDGE AND NEW IDRIA FORMATION

Project No. 1802

LEVINE•FRICKE

CONSULTING ENGINEERS AND HYDROGEOLOGISTS

Reproduced with permission of the copyright owner. Further reproduction prohibited without permission.

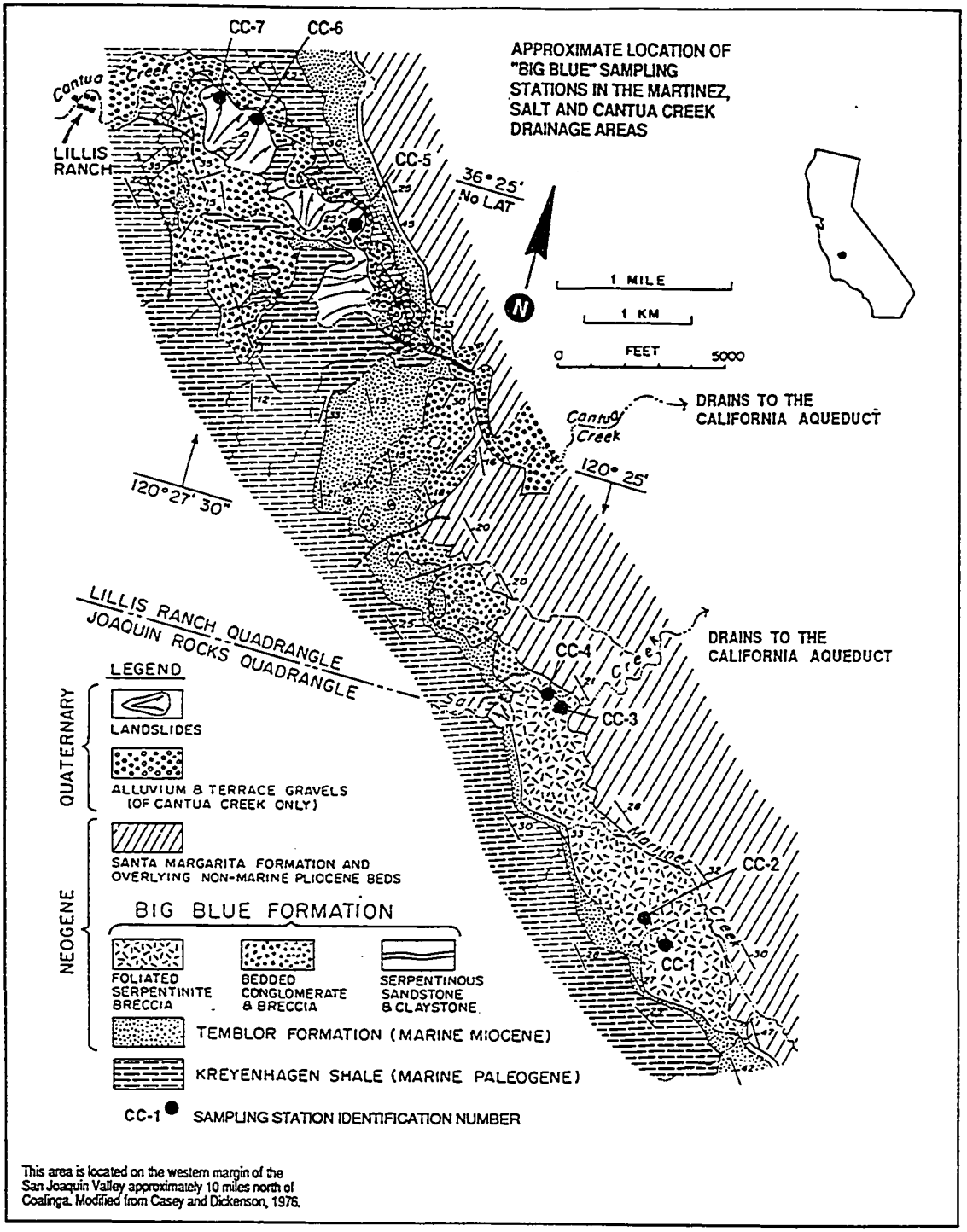


Figure 2-4 : GEOLOGIC MAP OF BIG BLUE OUTCROP NEAR CANTUA, SALT, AND MARTINEZ CREEKS

Reproduced with permission of the copyright owner. Further reproduction prohibited without permission.

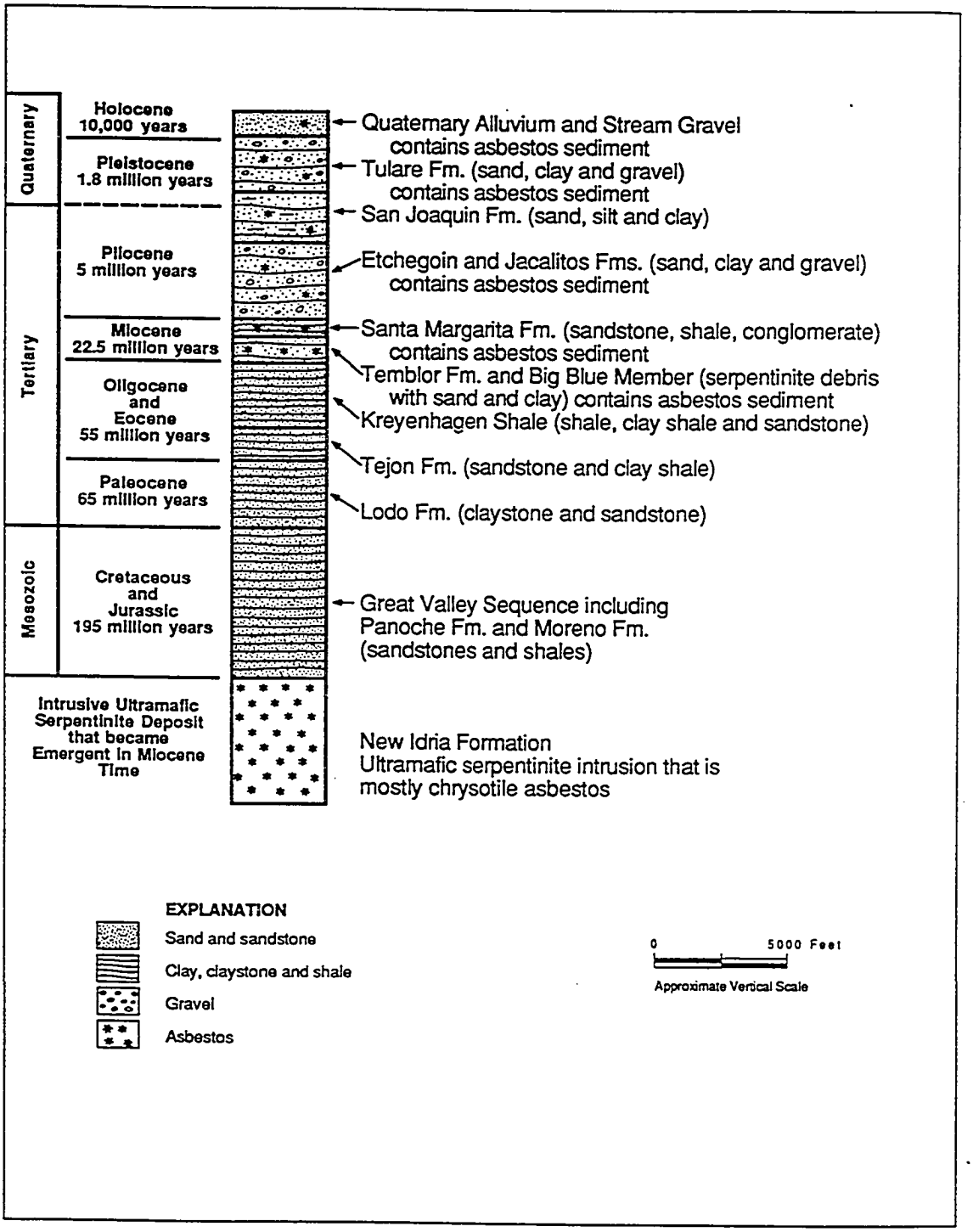
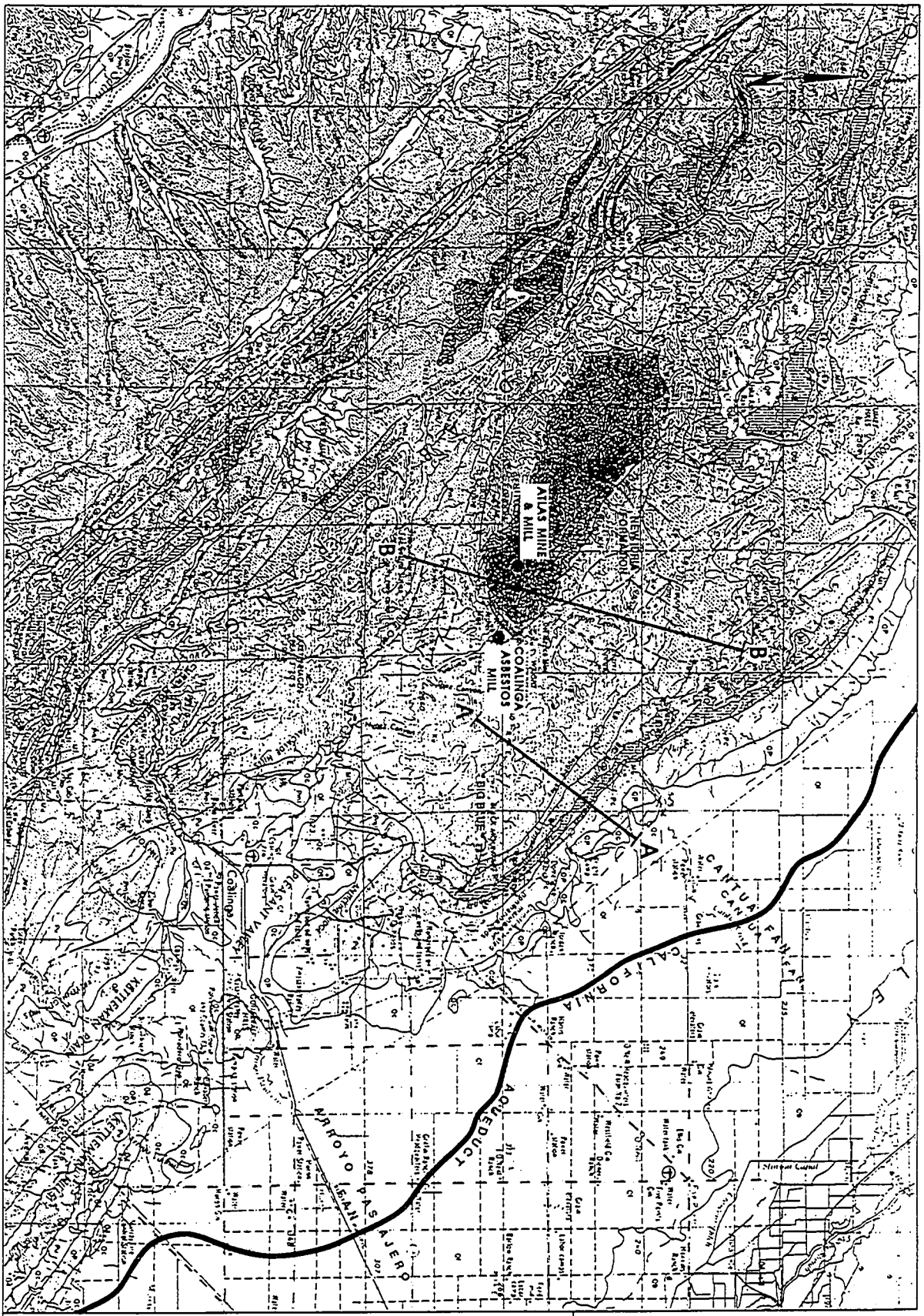


Figure 2-5 : GENERALIZED STRATIGRAPHIC COLUMN OF COALINGA REGION SHOWING ASBESTOS-CONTAINING FORMATIONS

Project No. 1802

LEVINE • FRICKE
CONSULTING ENGINEERS AND HYDROGEOLOGISTS

Reproduced with permission of the copyright owner. Further reproduction prohibited without permission.



MAP SOURCE : Modified from Jenkins, 1971.

SCALE 1 : 250,000

0 5 10 MILES

0 5 10 KILOMETERS

Figure 2-6A

REGIONAL GEOLOGIC MAP SHOWING LOCATIONS OF CROSS-SECTIONS A-A', B-B'

Project No. 1802

LEVINE•FRICKE

CONSULTING ENGINEERS AND HYDROGEOLOGISTS

Reproduced with permission of the copyright owner. Further reproduction prohibited without permission.

Reproduced with permission of the copyright owner. Further reproduction prohibited without permission.

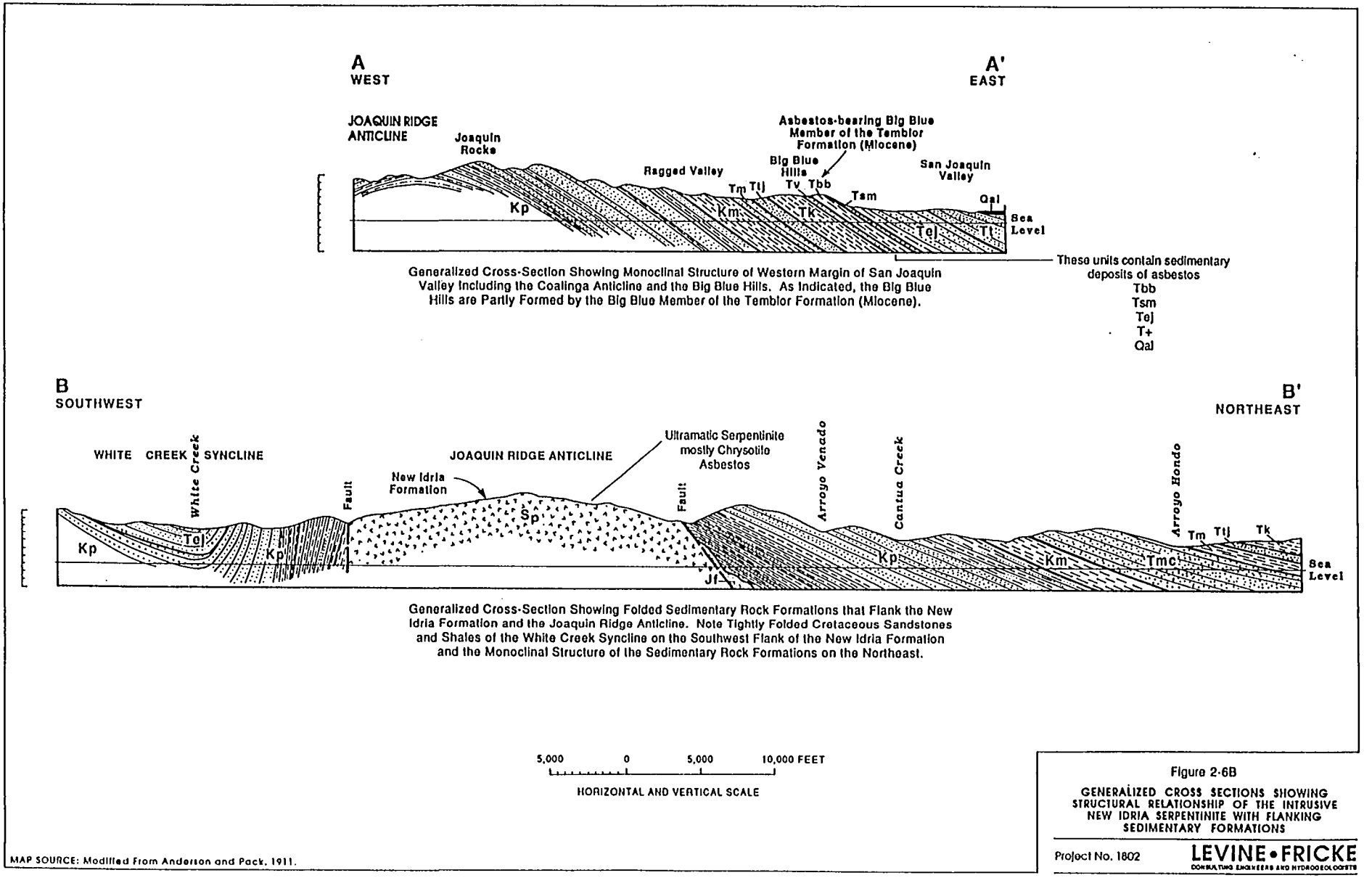


Figure 2-6B

GENERALIZED CROSS SECTIONS SHOWING STRUCTURAL RELATIONSHIP OF THE INTRUSIVE NEW IDRIA SERPENTINITE WITH FLANKING SEDIMENTARY FORMATIONS

Project No. 1802

LEVINE • FRICKE
CONSULTING ENGINEERS AND HYDROGEOLOGISTS

EXPLANATION

GEOLOGY

SEDIMENTARY ROCKS

Quaternary

Recent

Qal — ALLUVIUM AND STREAM GRAVEL

Pleistocene

Tt — TULARE (?) FORMATION (Sand, clay, and gravel, with some sandstone and clay shale)

Tej — ETCHEGOIN AND JACALITOS FORMATIONS (Sandstone, clay shale, and conglomerate, with clay, sand, and gravel)

UNCONFORMITY ?

Tsm — SANTA MARGARITA (?) FORMATION (Fossiliferous sandstone, clay shale, and conglomerate

UNCONFORMITY

Tertiary

Miocene/Pliocene ?

Tbb / Tv — VAQUEROS FORMATION WITH BIG BLUE SERPENTINOUS MEMBER (Sandstone, with conglomerate, clay, and diatomaceous shale, the last composing an important part of the formation in The Vallacitos, where the formation may include some later beds of the Monterey group. North of Coalinga contains shale formed of flakes of serpentine with some boulders of serpentine, the whole forming the Big Blue serpentinous member (Tbb). These units have subsequently been mapped as the Temblor Formation and the Big Blue Member (Jenkins, 1971; Dibblee, 1971).

UNCONFORMITY

Oligocene

Tk — KREYENHAGEN SHALE (Diatomaceous and foraminiferal shale, clay shale, and a little sandstone)

UNCONFORMITY ?

Eocene

Ttj — TEJON FORMATION (Quartzose and arkosic sandstone, pebble beds, carbonaceous clay, and clay shale)

UNCONFORMITY

Tm / Tmc — MARTINEZ (?) FORMATION WITH CANTUA SANDSTONE MEMBER (Dark-gray to black clay and clay shale with a little interstratified sandstone, some of it concretionary. At base the Cantua sandstone member (Tmc), consisting of massive concretionary sandstone with irregular zones of dark clay shale)

UNCONFORMITY

Upper Cretaceous (Chico group)

Km — MORENO FORMATION (Foraminiferal and diatomaceous shale, clay shale, concretionary sandstone, and a little conglomerate)

UNCONFORMITY

Kp — PANOCHE FORMATION (Concretionary sandstone, clay shale, and conglomerate)

UNCONFORMITY

Jurassic

Jf — FRANCISCAN FORMATION (Sandstone, shale, chert, and various altered rocks and schists, with interbedded volcanic rocks. Post-Franciscan intrusive rocks, notably serpentine, are mapped with the Franciscan north of Panoche Pass)

Pre-Tertiary

IGNEOUS ROCKS

S — SERPENTINE (Mapped separately only near Idria; north of that place mapped the Franciscan formation)

MAP SOURCE: Modified from Anderson and Pack, 1911.

Figure 2-6C : EXPLANATION FOR GENERALIZED CROSS-SECTIONS (FIGURE 6A) SHOWING STRUCTURAL RELATIONSHIPS OF THE NEW IDRIA SERPENTINE WITH FLANKING SEDIMENTARY FORMATIONS

Reproduced with permission of the copyright owner. Further reproduction prohibited without permission.

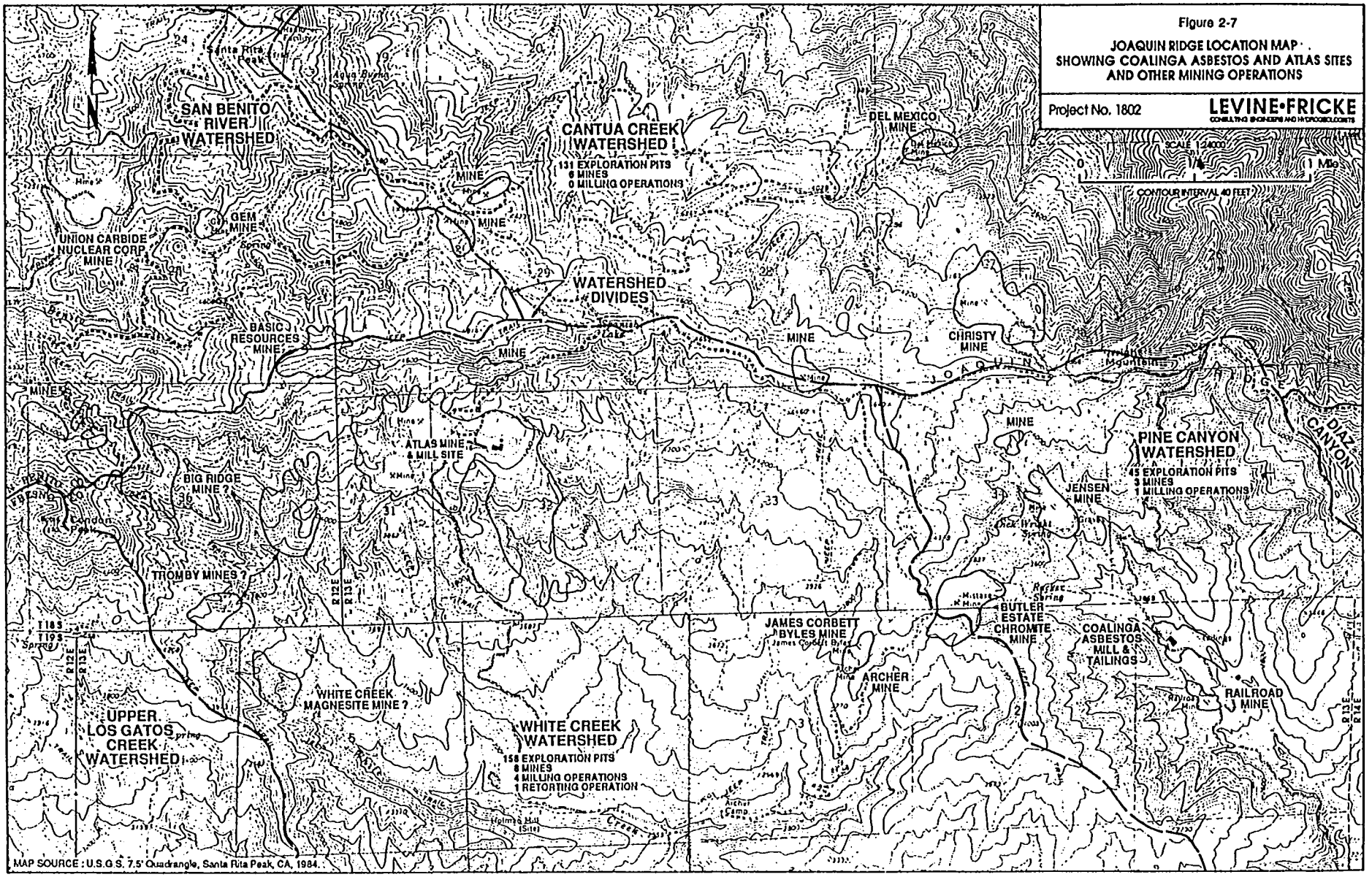


Figure 2-7

JOAQUIN RIDGE LOCATION MAP · . SHOWING COALINGA ASBESTOS AND ATLAS SITES AND OTHER MINING OPERATIONS

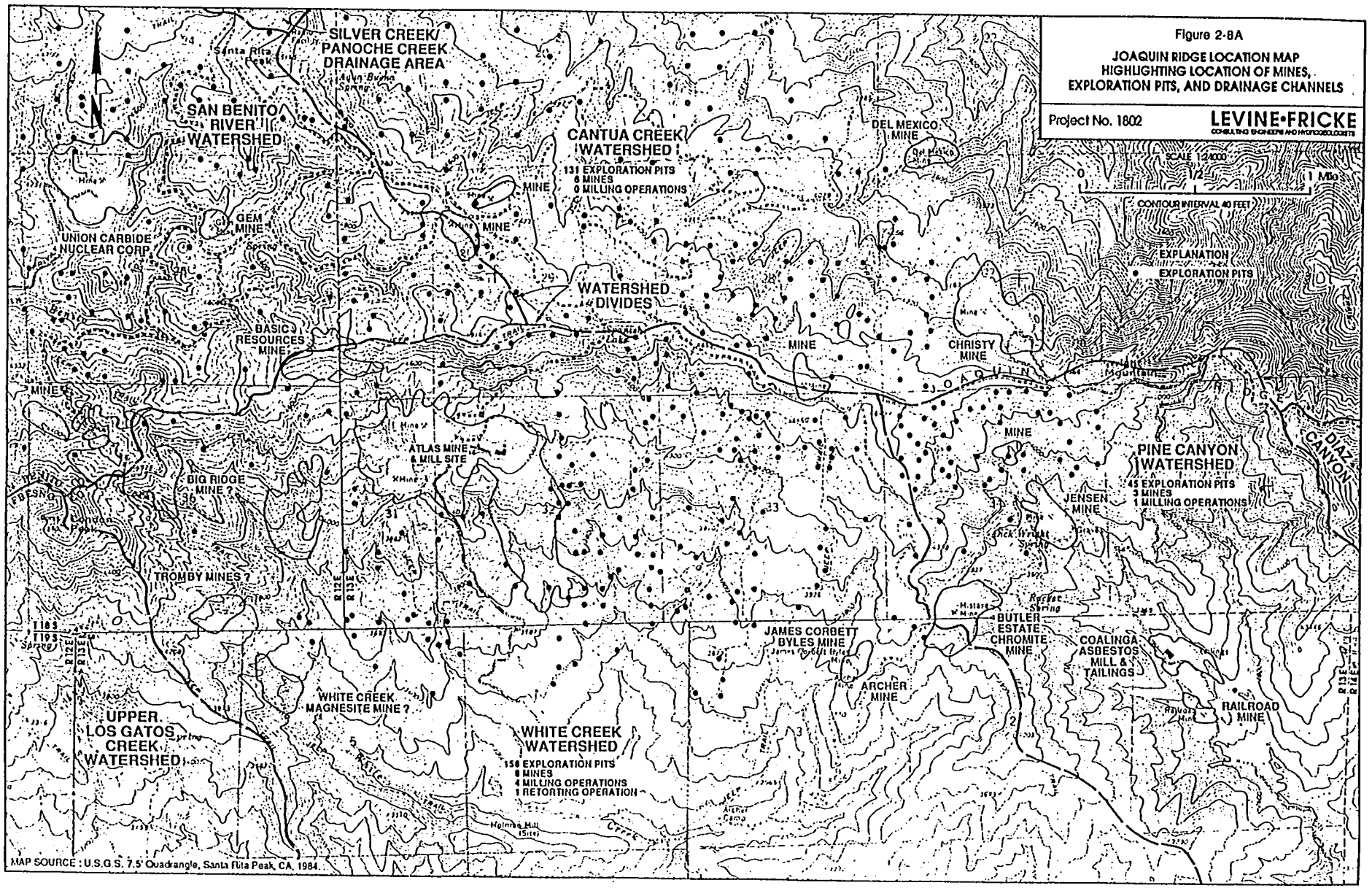
Project No. 1802

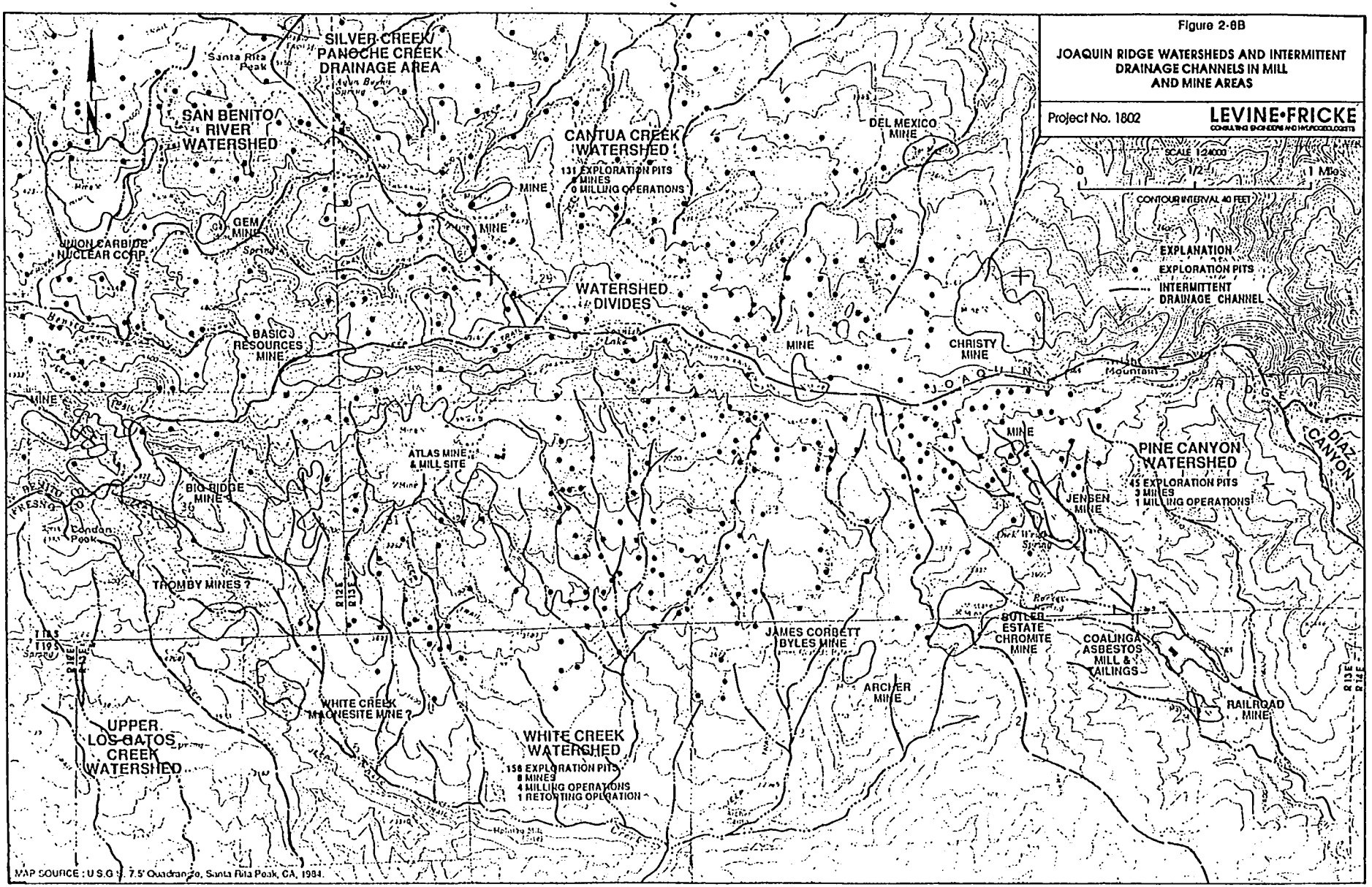
LEVINE•FRICKE

CONSULTING ENGINEERS AND HYDROGEOLOGISTS

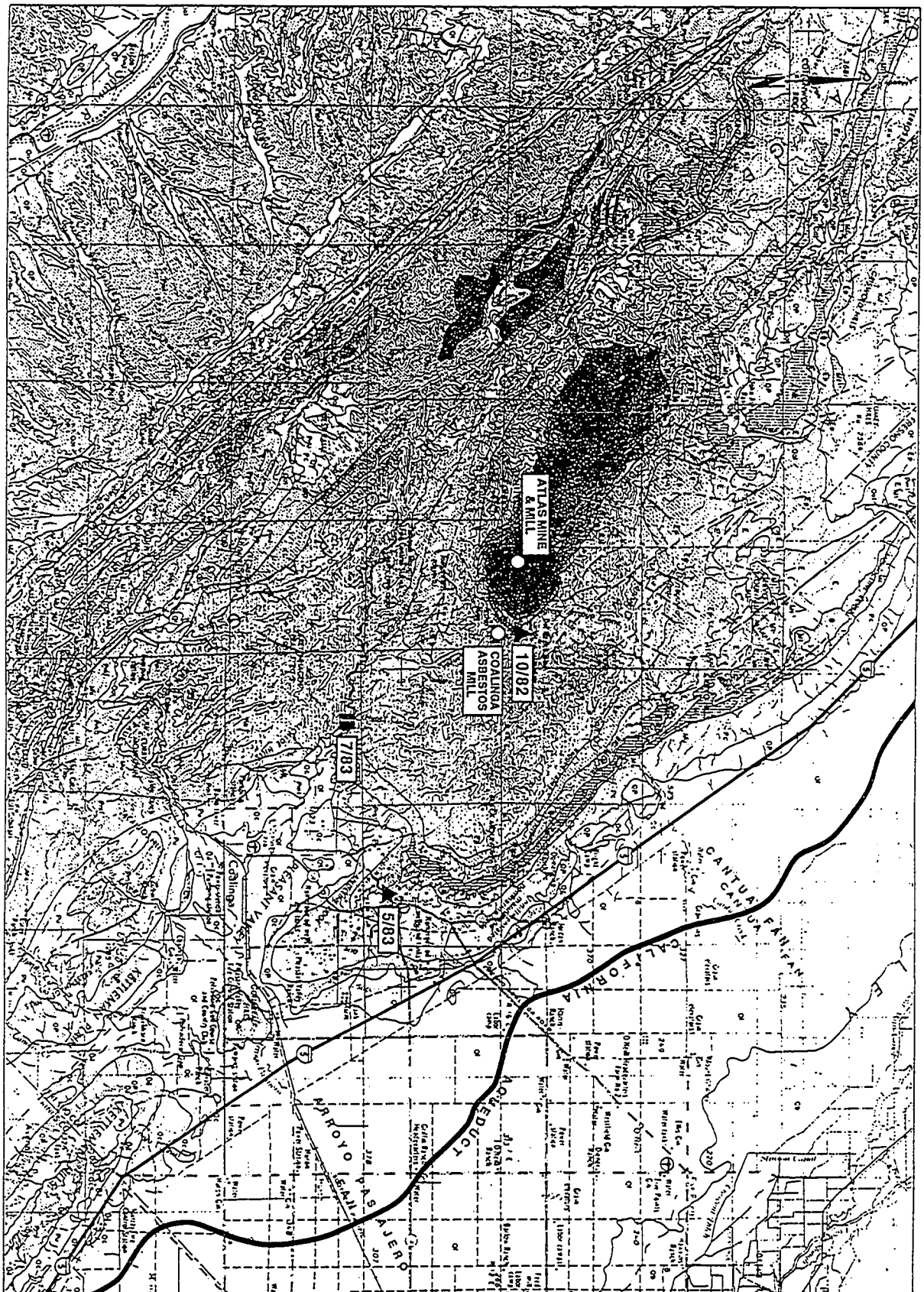
Reproduced with permission of the copyright owner. Further reproduction prohibited without permission.

Reproduced with permission of the copyright owner. Further reproduction prohibited without permission.





Reproduced with permission of the copyright owner. Further reproduction prohibited without permission.



MAP SOURCE : Modified from Jenkins, 1971.

SCALE 1 : 250,000

0 5 10 MILES

0 5 10 KILOMETERS

Figure 2-9

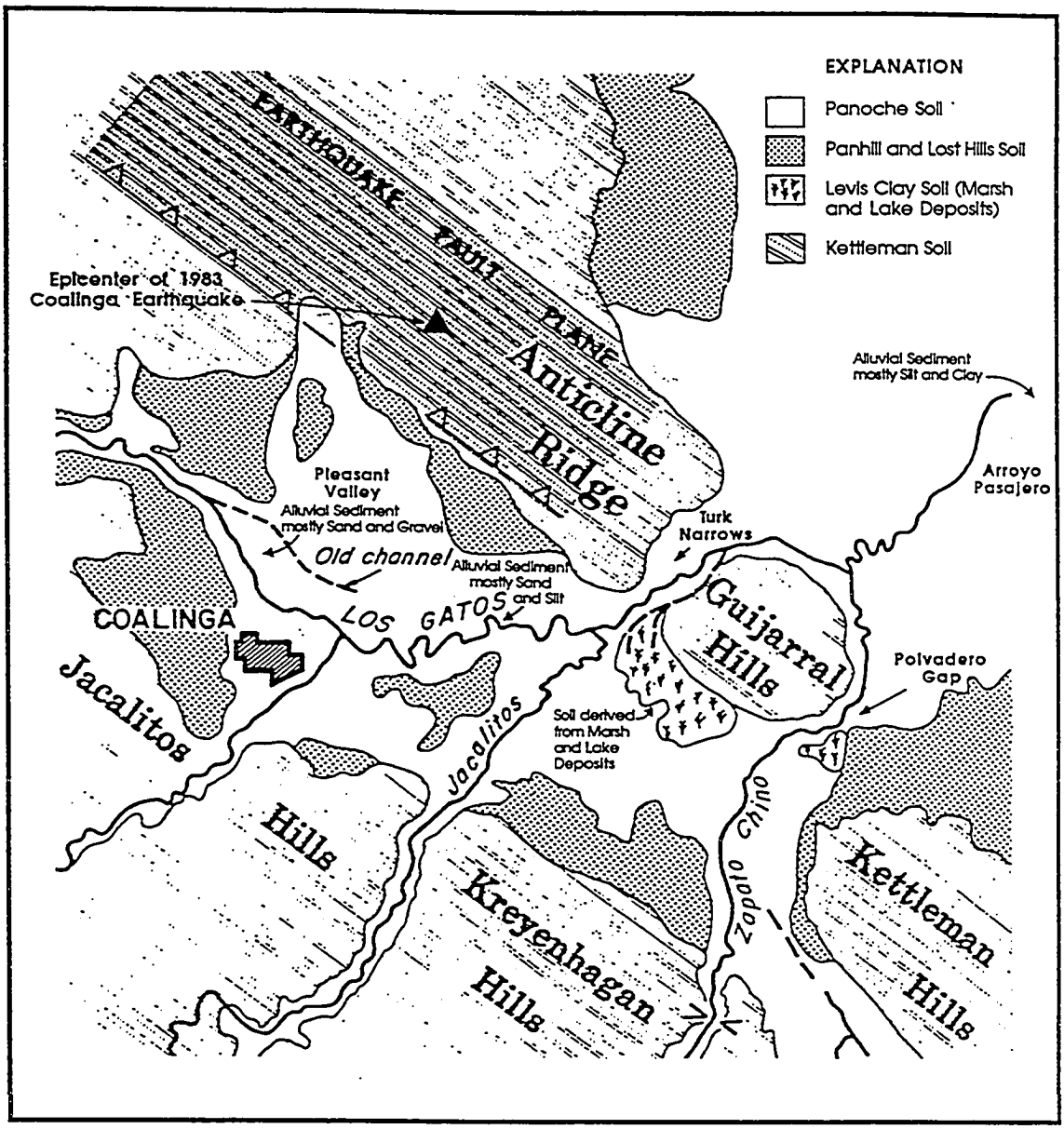
REGIONAL GEOLOGIC MAP SHOWING EPICENTER LOCATIONS OF 1982 AND 1983 COALINGA SEISMIC EVENTS

Project No. 1802

LEVINE • FRICKE

CONSULTING ENGINEERS AND HYDROGEOLOGISTS

Reproduced with permission of the copyright owner. Further reproduction prohibited without permission.



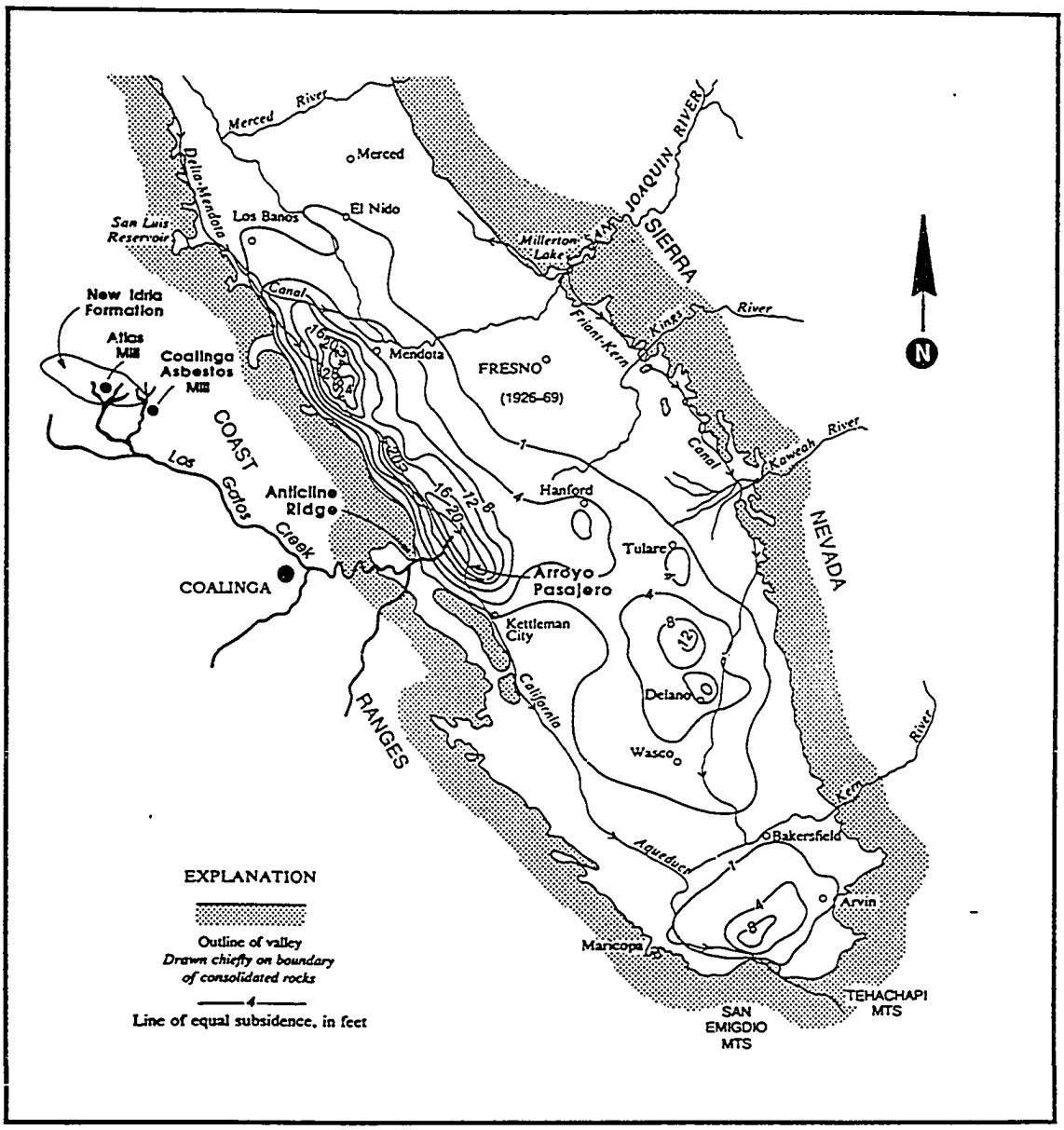
Modified from: King and Stein, 1983

Figure 2-10 : GEOMORPHIC SKETCH MAP OF PLEASANT VALLEY

Project No. 1802

LEVINE•FRICKE
CONSULTING ENGINEERS AND HYDROGEOLOGISTS

Reproduced with permission of the copyright owner. Further reproduction prohibited without permission.



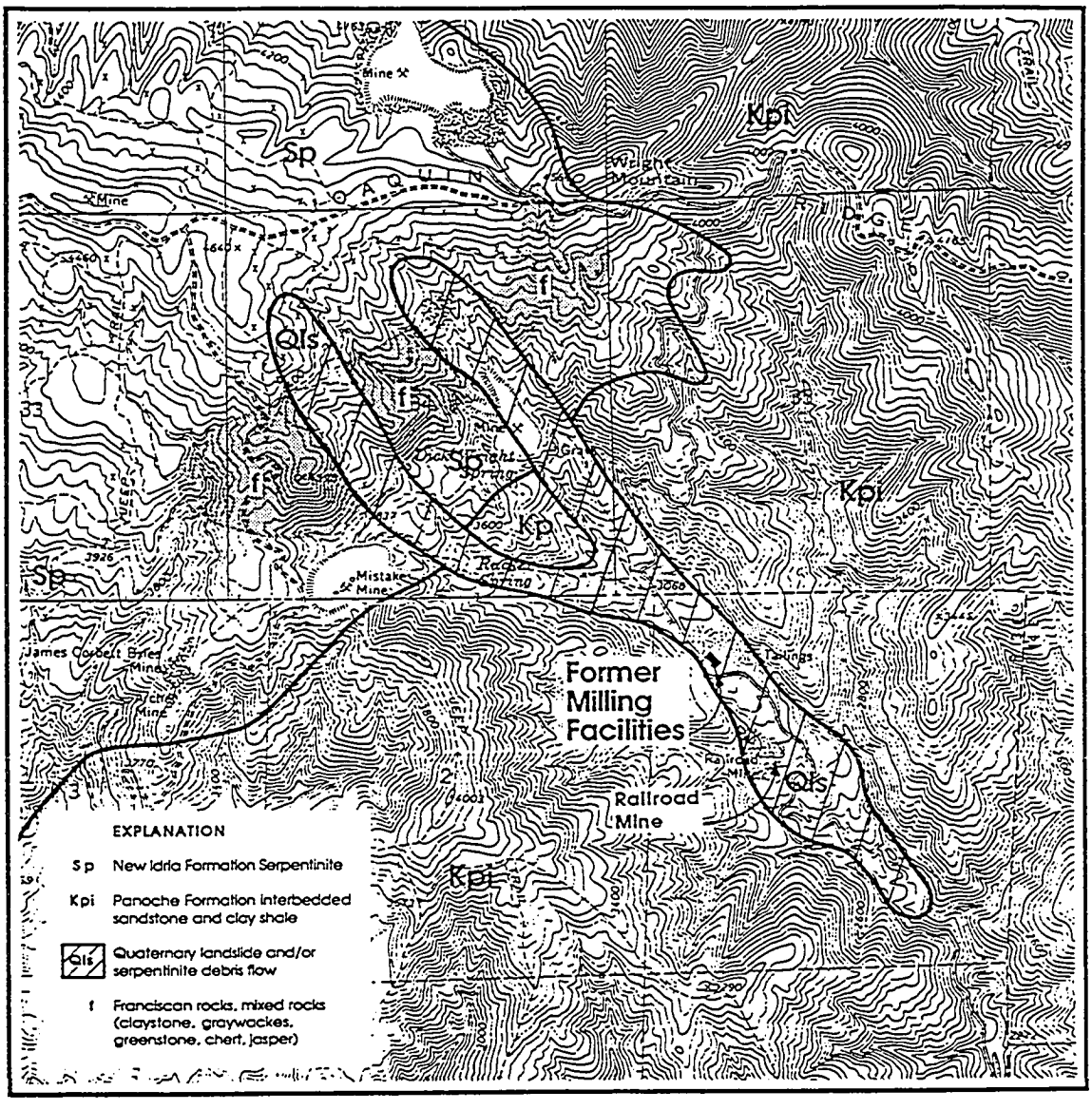
Modified from: Ireland, 1986

Figure 2-11 : LAND SUBSIDENCE IN THE SAN JOAQUIN VALLEY, CALIFORNIA, 1926-1970

Project No. 1802

LEVINE•FRICKE
CONSULTING ENGINEERS AND HYDROGEOLOGISTS

Reproduced with permission of the copyright owner. Further reproduction prohibited without permission.



N

0 1/2 1 Mile

Modified from Dibblee, 1972; and USGS, 1984.

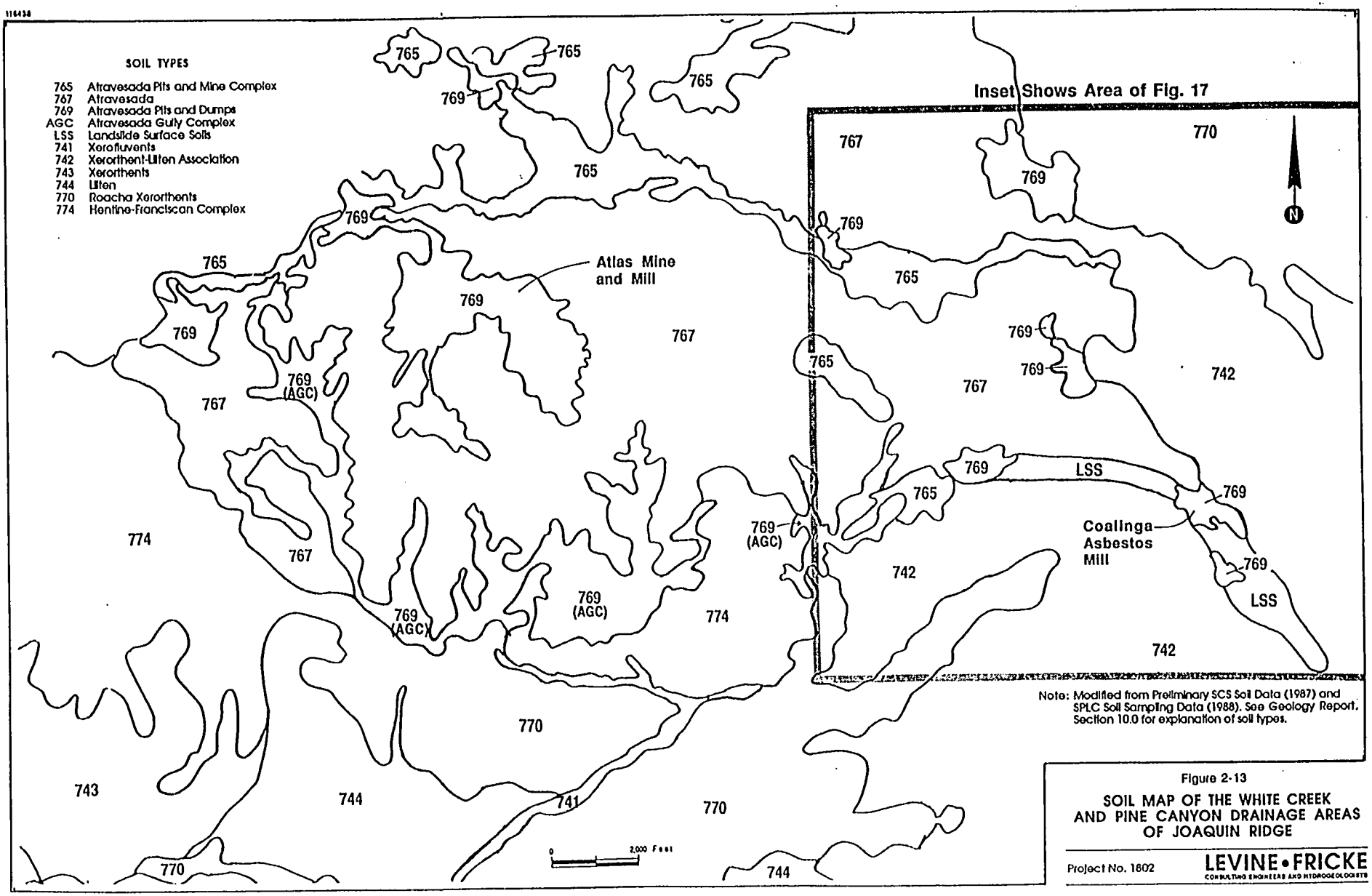
Figure 2-12 : GEOLOGIC MAP OF JOAQUIN RIDGE - PINE CANYON AREA INCLUDING COALINGA ASBESTOS MILL SITE (Modified from USGS Geologic and Topographic Maps)

Project No. 1018

LEVINE•FRICKE
CONSULTING ENGINEERS AND HYDROGEOLOGISTS

Reproduced with permission of the copyright owner. Further reproduction prohibited without permission.

Reproduced with permission of the copyright owner. Further reproduction prohibited without permission.



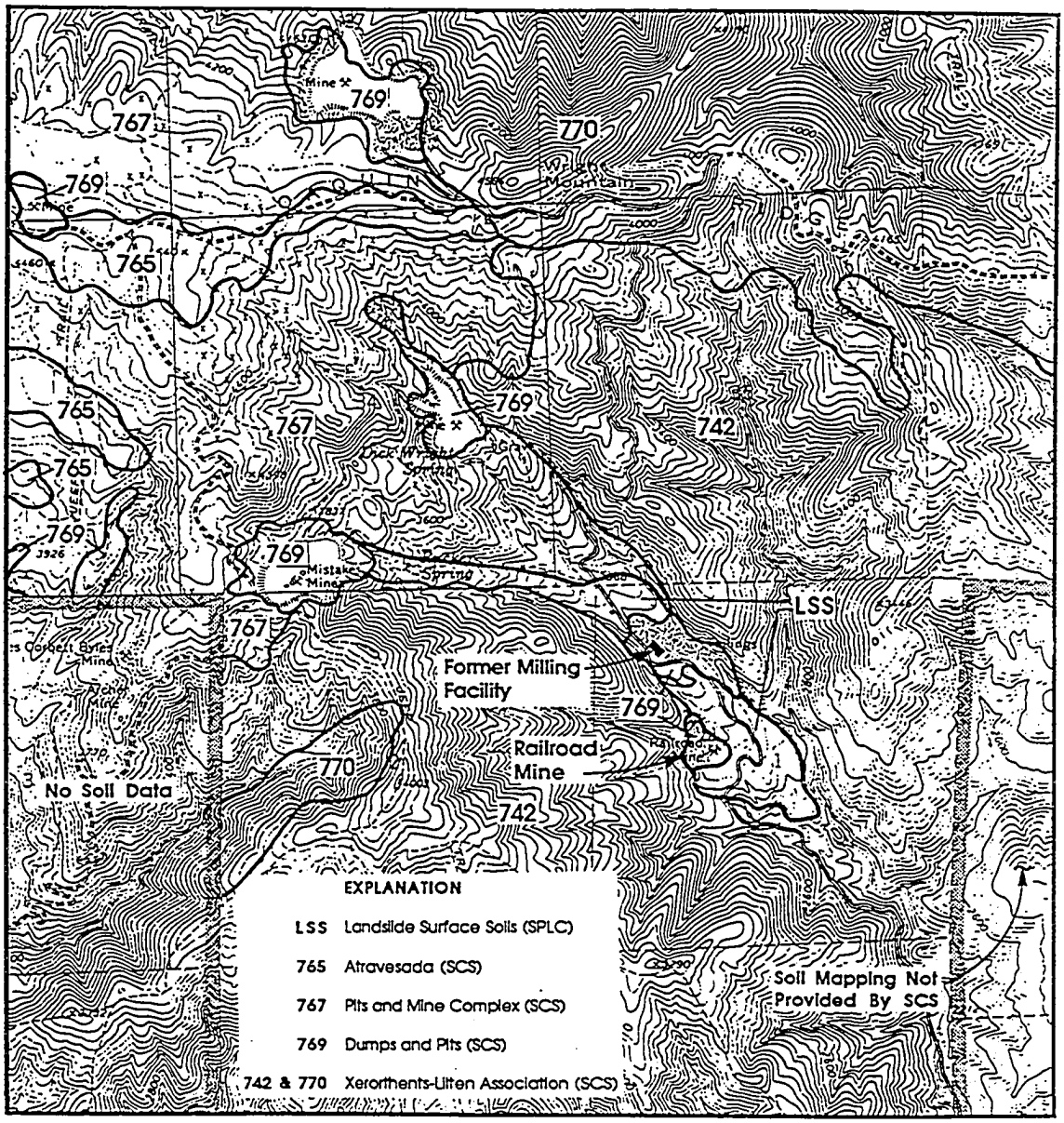
Note: Modified from Preliminary SCS Soil Data (1987) and SPLC Soil Sampling Data (1988). See Geology Report, Section 10.0 for explanation of soil types.

Figure 2-13

SOIL MAP OF THE WHITE CREEK AND PINE CANYON DRAINAGE AREAS OF JOAQUIN RIDGE

Project No. 1802

LEVINE•FRICKE
CONSULTING ENGINEERS AND HYDROGEOLOGISTS



Modified from:
Soil Conservation Service (SCS):
Unpublished Soil Data, 1987;
and USGS, 1984.

Supplemented with:
Southern Pacific Land Company
Soil Sampling Data, 1988.

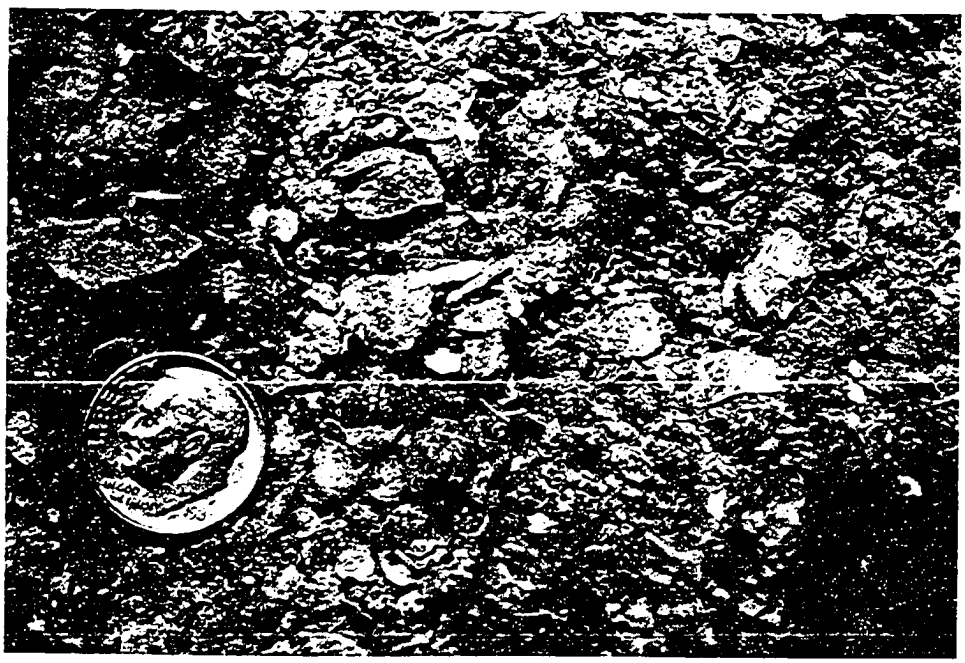
Figure 2-14 : SOIL MAP OF JOAQUIN RIDGE - PINE CANYON AREA INCLUDING COALINGA ASBESTOS MILL SITE

Project No.1805

LEVINE•FRICKE
CONSULTING ENGINEERS AND HYDROGEOLOGISTS

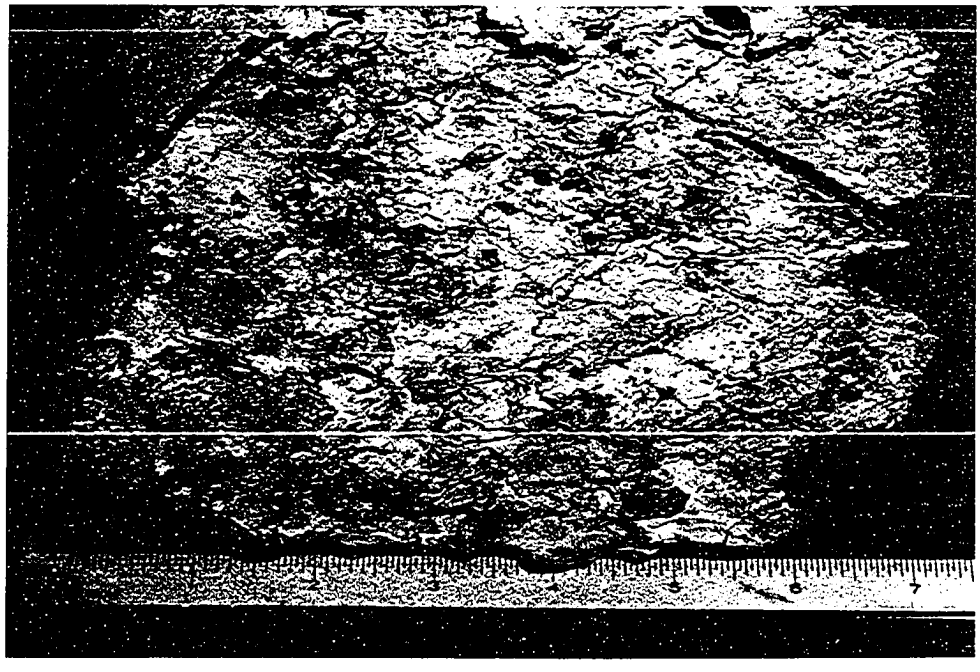
Reproduced with permission of the copyright owner. Further reproduction prohibited without permission.

Figure 4-1. Typical ore sample from a fresh exposure of serpentinite. Chrysotile ore is generally made up of light greenish-gray to light gray agglomerates and/or platelets typical of the antigorite polymorph of serpentinite. Sample contains approximately 3 to 5% lath-shaped particles approximately 3/16 inch or less in length with a pale green color. Platelets are approximately 1/4 inch in diameter and are the thickness of several sheets of paper and/or a thin sheet of cardboard based on field observations. Platelets tend to rapidly disaggregate when gently crushed with hand pressure.



Reproduced with permission of the copyright owner. Further reproduction prohibited without permission.

Figure 4-2. Hand-sized sheet of "mountain leather" polymorph of serpentinite also known as antigorite. Sheet is pale white to brownish white and is similar to a thick sheet of paper. This type of sample can sometimes be encountered by digging in fresh exposures. Sheets of "mountain leather" have been reported in sizes ranging up to several feet in diameter.



Reproduced with permission of the copyright owner. Further reproduction prohibited without permission.

Figure 4-3. Lath-shaped bundle approximately 1.0 millimeters in length as viewed with slightly crossed nichols. Center bundle has fibrous-lamellae structure. Evidence of splintering and/or splaying of chrysotile fibers is observed on left margin of fibril bundle. Magnification is 31X.



Reproduced with permission of the copyright owner. Further reproduction prohibited without permission.

Figure 4-4. Same particle as seen in Photo 4-3 with magnification increased to 125X. Fibrous structure of lamellae is more apparent with increased magnification. Fibrous splintering is apparent at margins of particle. Particle ends have blue and blue-magenta colors length-wise with fiber with cross nichols indicative of chrysotile.



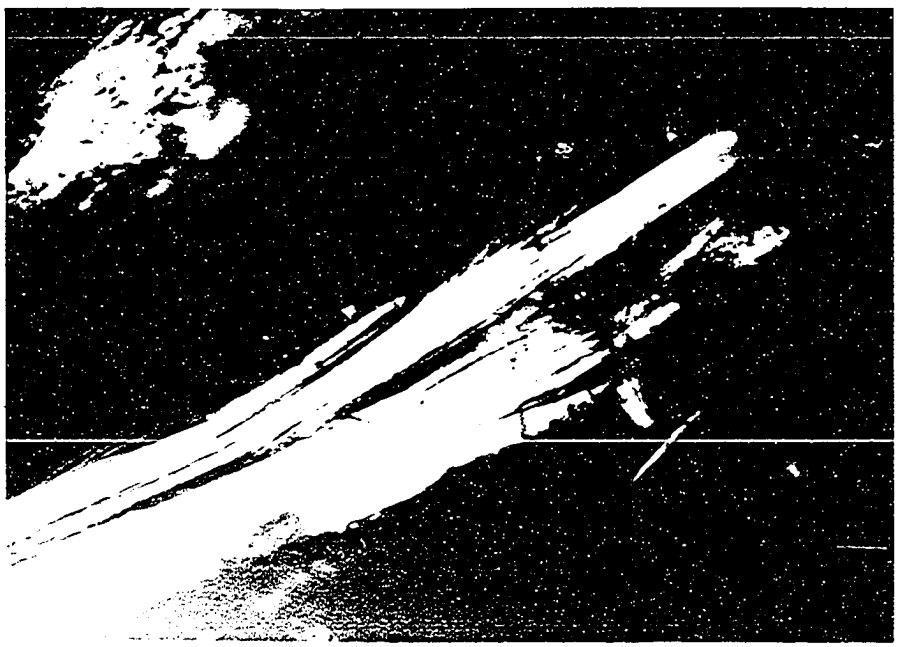
Reproduced with permission of the copyright owner. Further reproduction prohibited without permission.

Figure 4-5. This particle, photographed at 125 X magnification with slightly cross nichols, illustrates all three serpentinite polymorphs including antigorite (as picrolite), lizardite, and chrysotile. The particles show a wide range of birefringence with crossed nichols and a rotating stage. Chrysotile is identified as the very thin fibers observed at the margins of the center particle. The fibrous-lamellae structure of the main body of the center particle is indicative of what is interpreted the picrolite expression of antigorite. Possible relicts of olivine (?) appear in plate-like particles of lizardite observed at the right end of the lath-shaped bundle in the center of the picture. Such relicts of olivine were previously reported by Mumpton and Thompson (1975). An ultra-fine fibrous structure is vaguely apparent in the plate-like particle observed in the upper left corner.



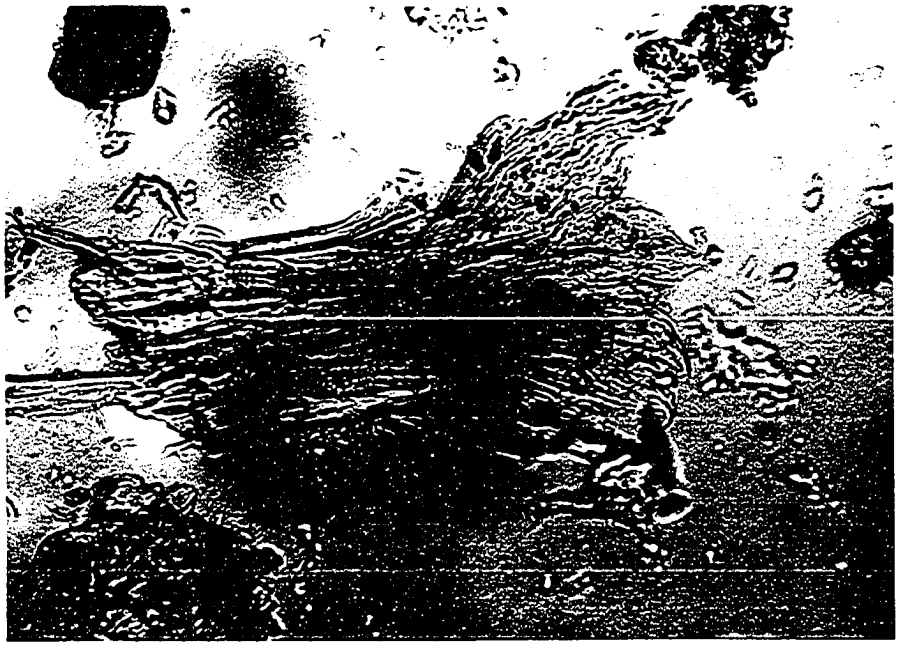
Reproduced with permission of the copyright owner. Further reproduction prohibited without permission.

Figure 4-6. Same particle as in Photo 4-5 with crossed nichols at 125X magnification. Fibrous structure is readily apparent in this photograph.



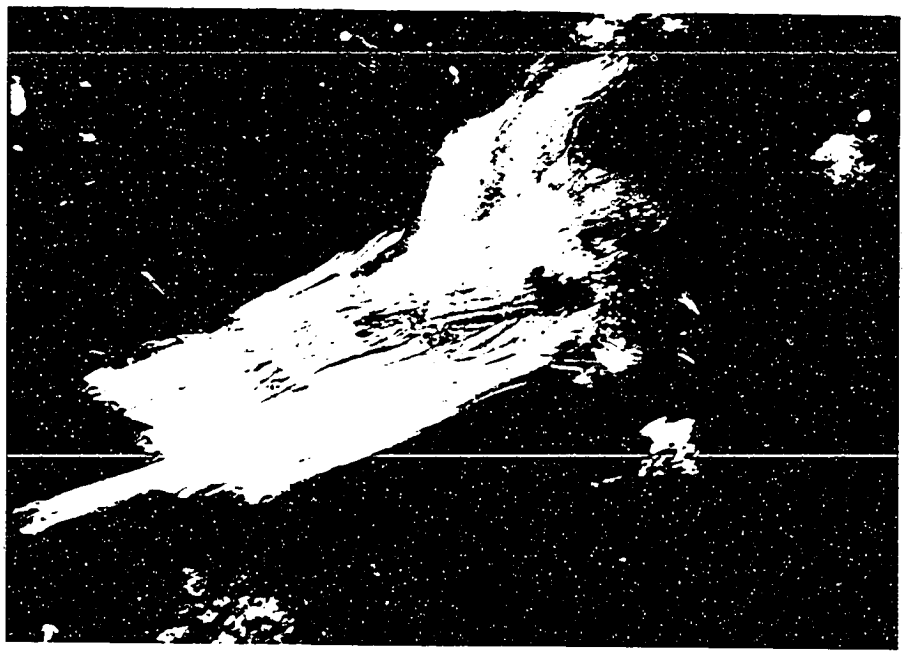
Reproduced with permission of the copyright owner. Further reproduction prohibited without permission.

Figure 4-7. This photograph illustrates the coincidental occurrence of antigorite (as picrolite), lizardite, and chrysotile. A fibrous characteristic is observed in all three polymorphs. Lizardite appears as a plate-like particle at upper right margin of the central bundle. Antigorite and/or picrolite is recognized as the lath-shaped bundle of apparent fibrils that forms the main body of the central particle. Fibrous splinters of chrysotile are observed at the margins of the central particle.



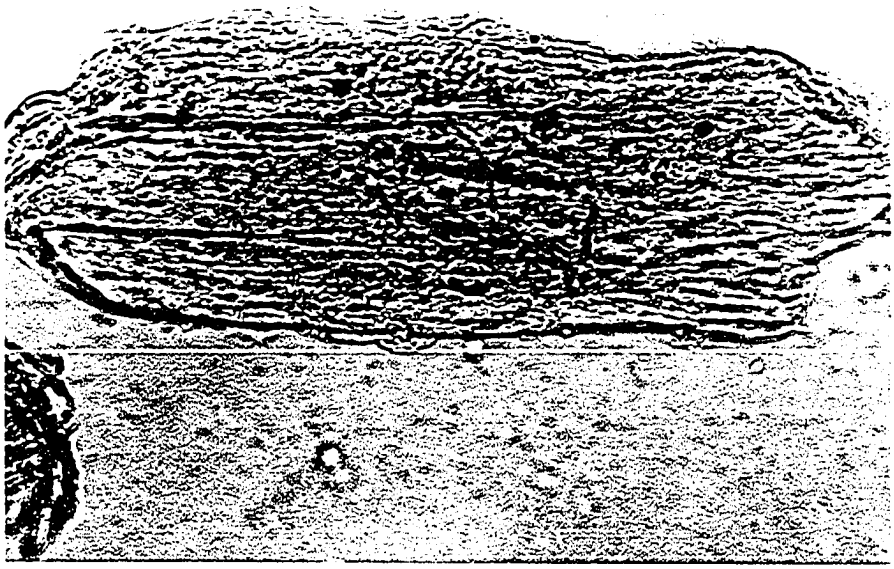
Reproduced with permission of the copyright owner. Further reproduction prohibited without permission.

Figure 4-8. Same particle as Photo 4-7 as viewed under crossed nichols at 125X magnification. Particle shows a wide range of birefringence. Notice splaying of fibrils at margin of particle.



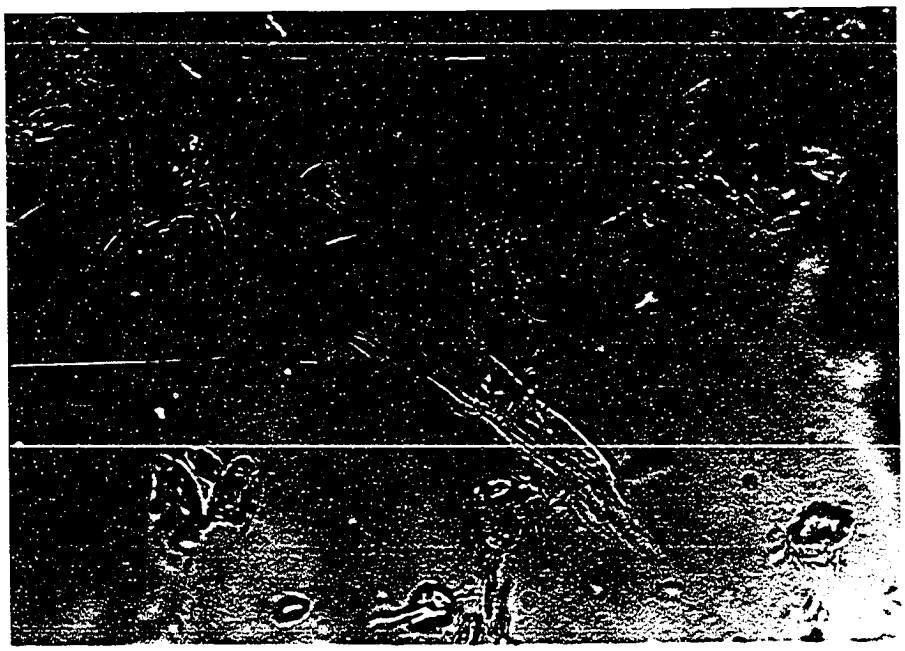
Reproduced with permission of the copyright owner. Further reproduction prohibited without permission.

Figure 4-9. Lath-shaped bundle that appears to have picrolite and/or antigorite structure with inclusions of lizardite as tiny particles embedded in the center of the lath-shaped bundle. Size of the lizardite particles are estimated to be approximately 0.08 millimeters or less in size.



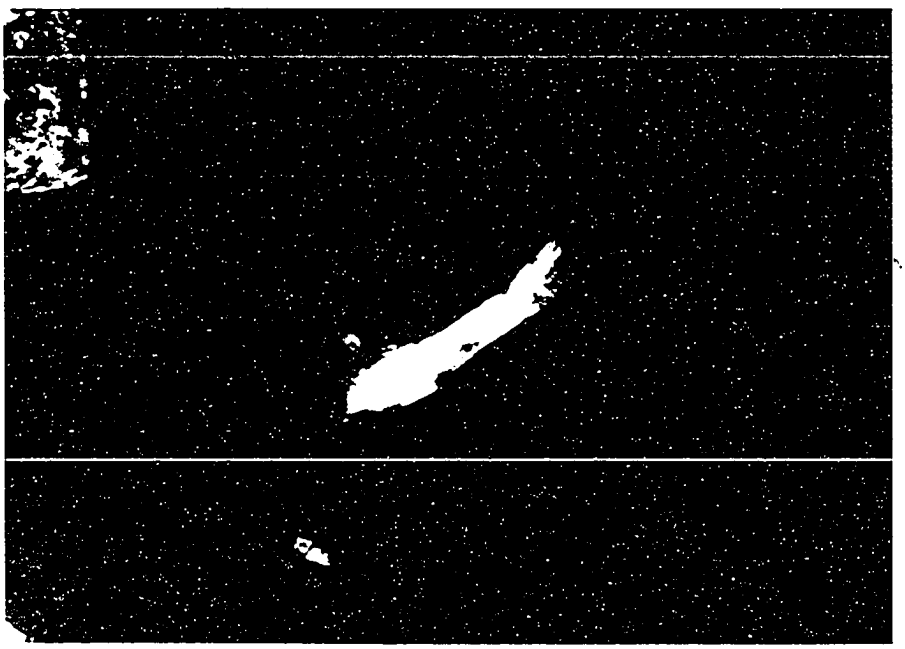
Reproduced with permission of the copyright owner. Further reproduction prohibited without permission.

Figure 4-10. Chrysotile fibers and splinters observed under crossed nichols at 312X magnification. Bundle of fibers in center of picture is approximately 0.10 millimeters in length. Fiber in upper left corner has good blue and magenta colors length-wise to fiber.



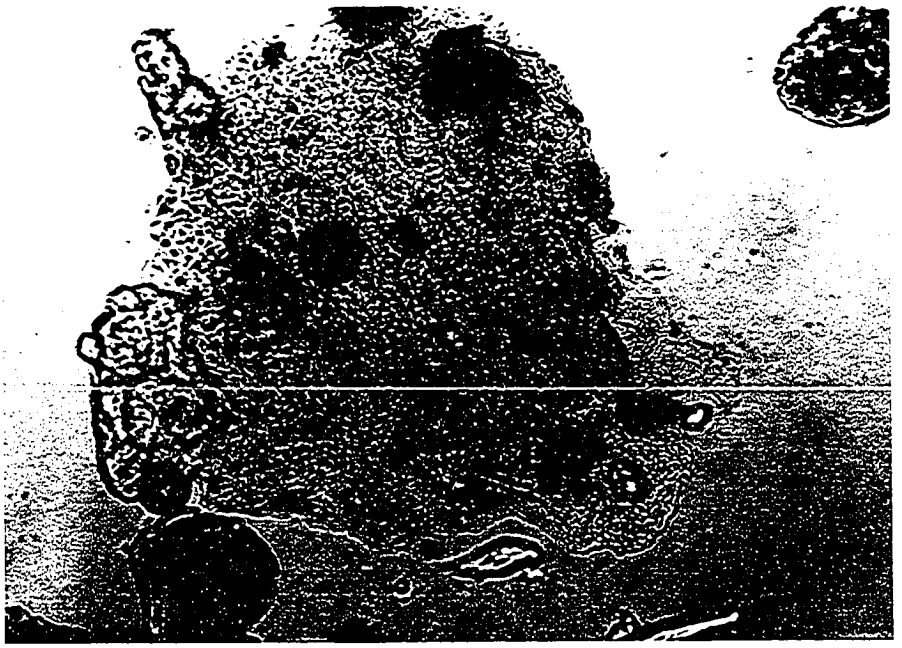
Reproduced with permission of the copyright owner. Further reproduction prohibited without permission.

Figure 4-11. Splinter of chrysotile with high birefringence viewed under crossed nichols. Magnification is 312X.



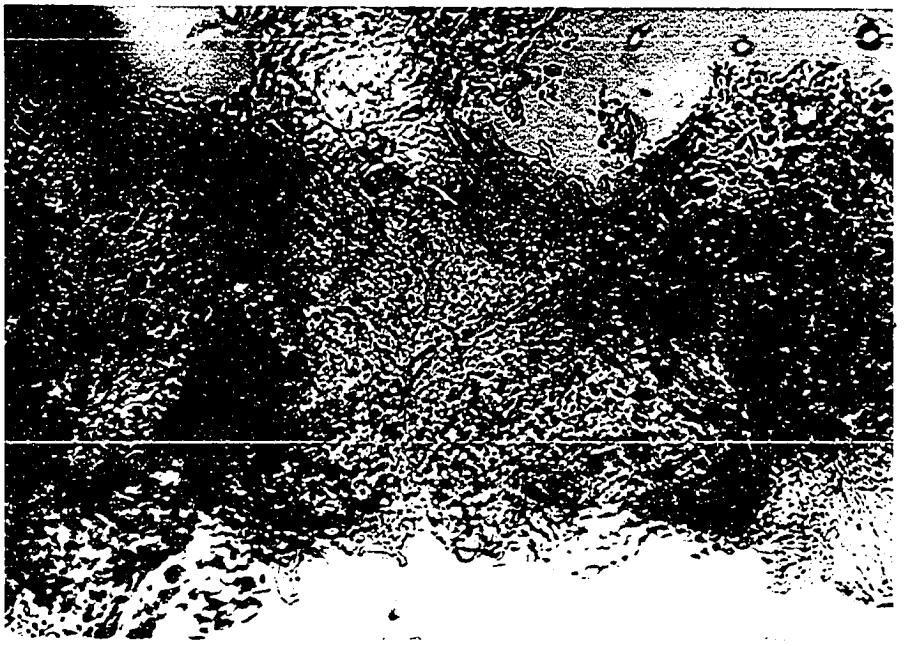
Reproduced with permission of the copyright owner. Further reproduction prohibited without permission.

Figure 4-12. Mesh-like structure of platelet of lizardite aand/or antigorite particle as previously described by Mumpton and Thompson (1975). Acicular needle-like structures as vaguely discernible under 125X magnification. with slightly crossed nichols. Particle is approximately 0.50 millimeters in diameter.



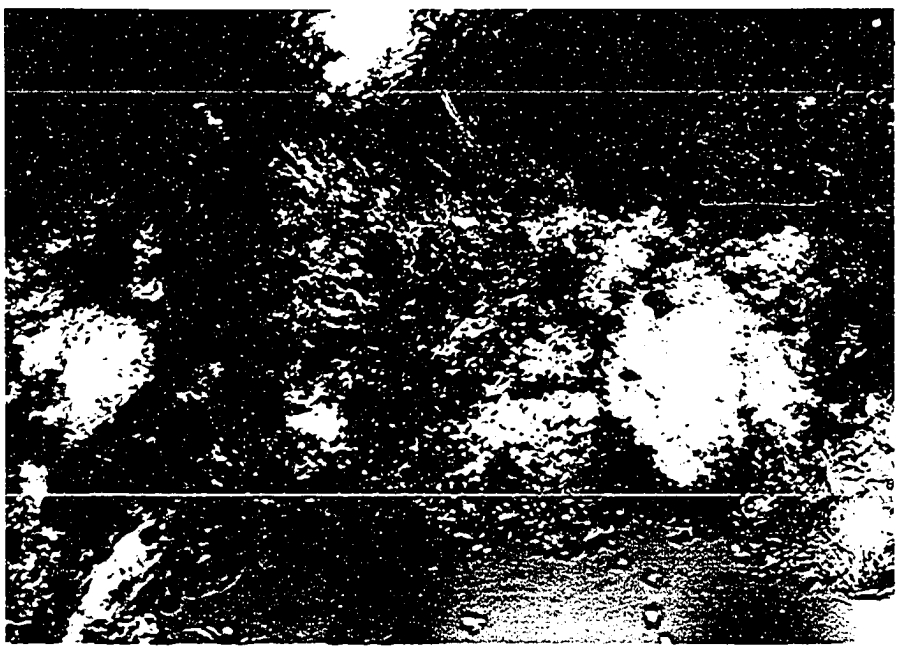
Reproduced with permission of the copyright owner. Further reproduction prohibited without permission.

Figure 4-13. Similar particle as seen in Photo 4-12. Ultra-fine mesh structure appears to have fibrils embedded in matrix.



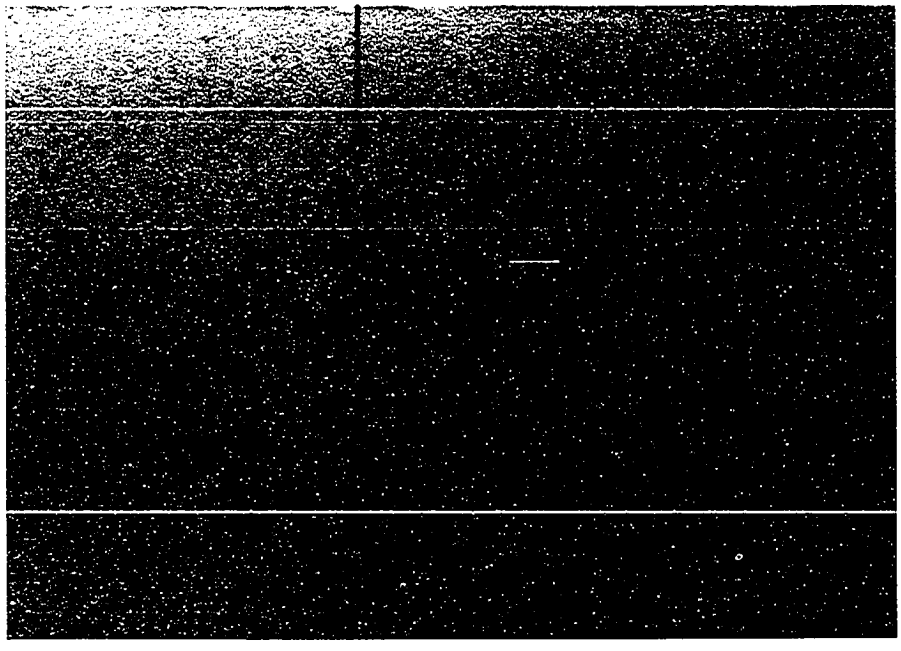
Reproduced with permission of the copyright owner. Further reproduction prohibited without permission.

Figure 4-14. Same particle as seen in Photo 4-12 but under fully cross nichols. Fibrous structure is more apparent under crossed nichols. Particle shows high birefringence.



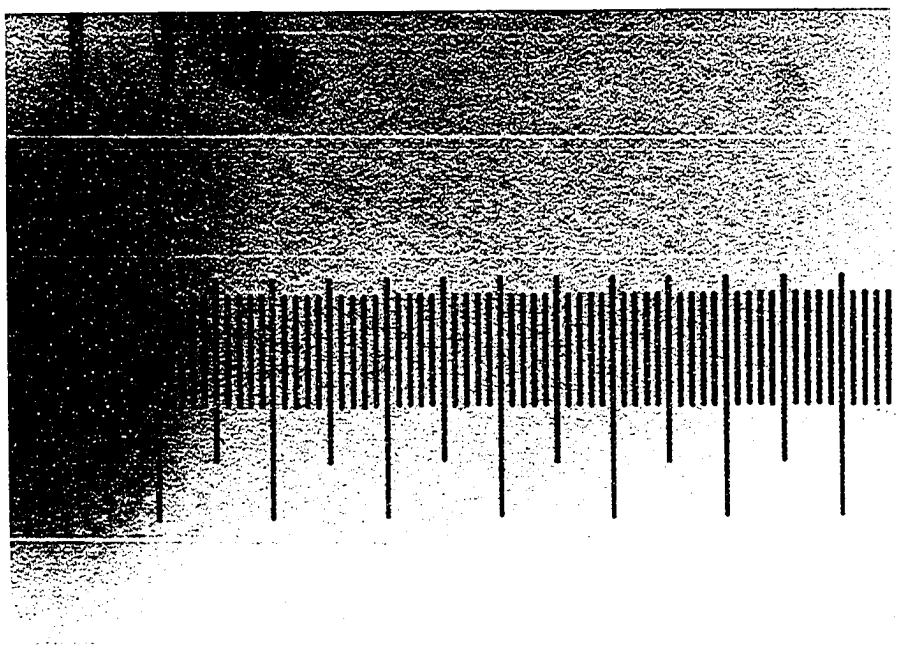
Reproduced with permission of the copyright owner. Further reproduction prohibited without permission.

Figure 4-15. Millimeter scale observed under 31X magnification.



Reproduced with permission of the copyright owner. Further reproduction prohibited without permission.

Figure 4-16. Millimeter scale observed under 125X magnification.



Reproduced with permission of the copyright owner. Further reproduction prohibited without permission.

Reproduced with permission of the copyright owner. Further reproduction prohibited without permission.

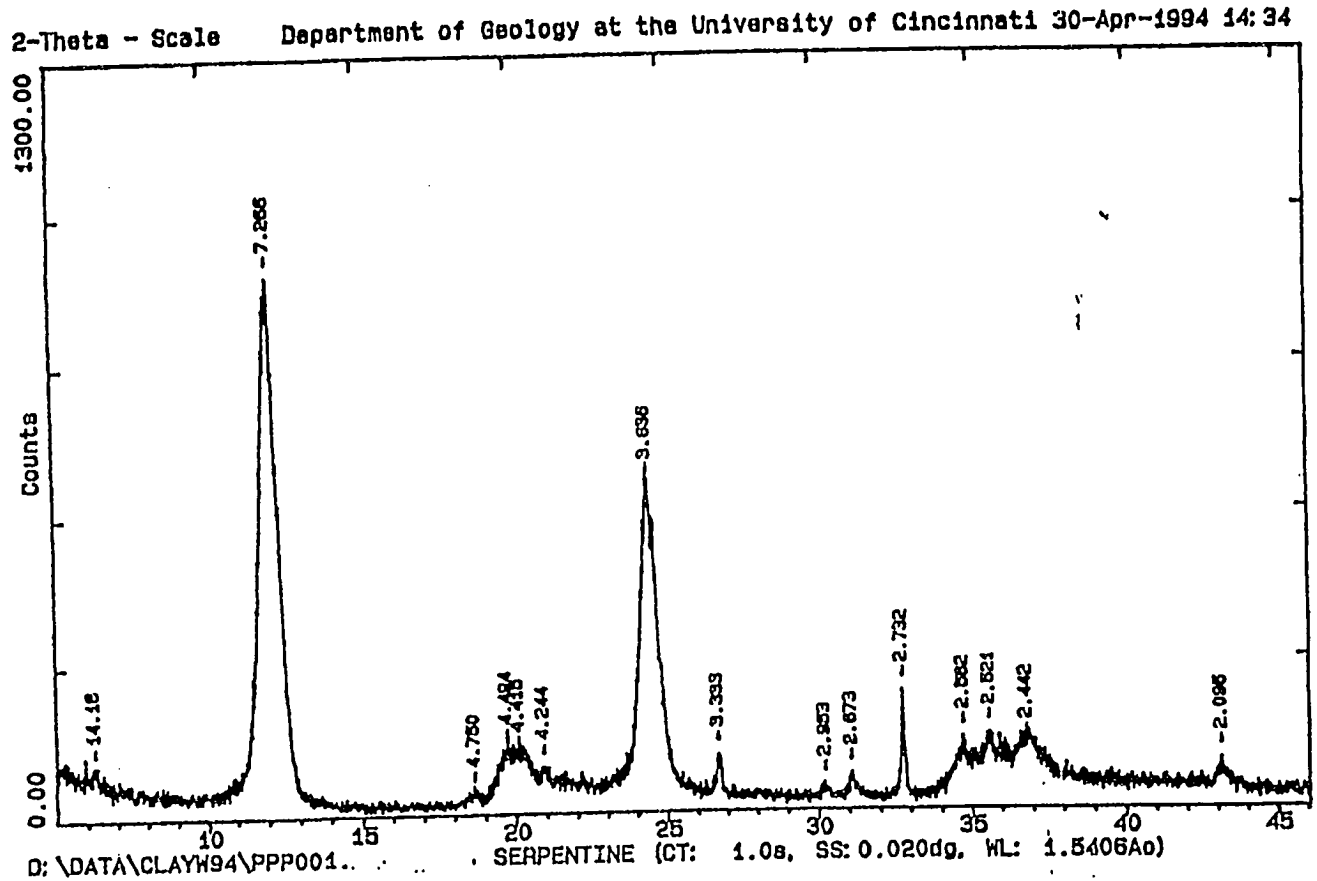


Figure 4-17: X-Ray Diffraction of Coalinga Serpentinite Sample. Identified as antigorite.

Reproduced with permission of the copyright owner. Further reproduction prohibited without permission.

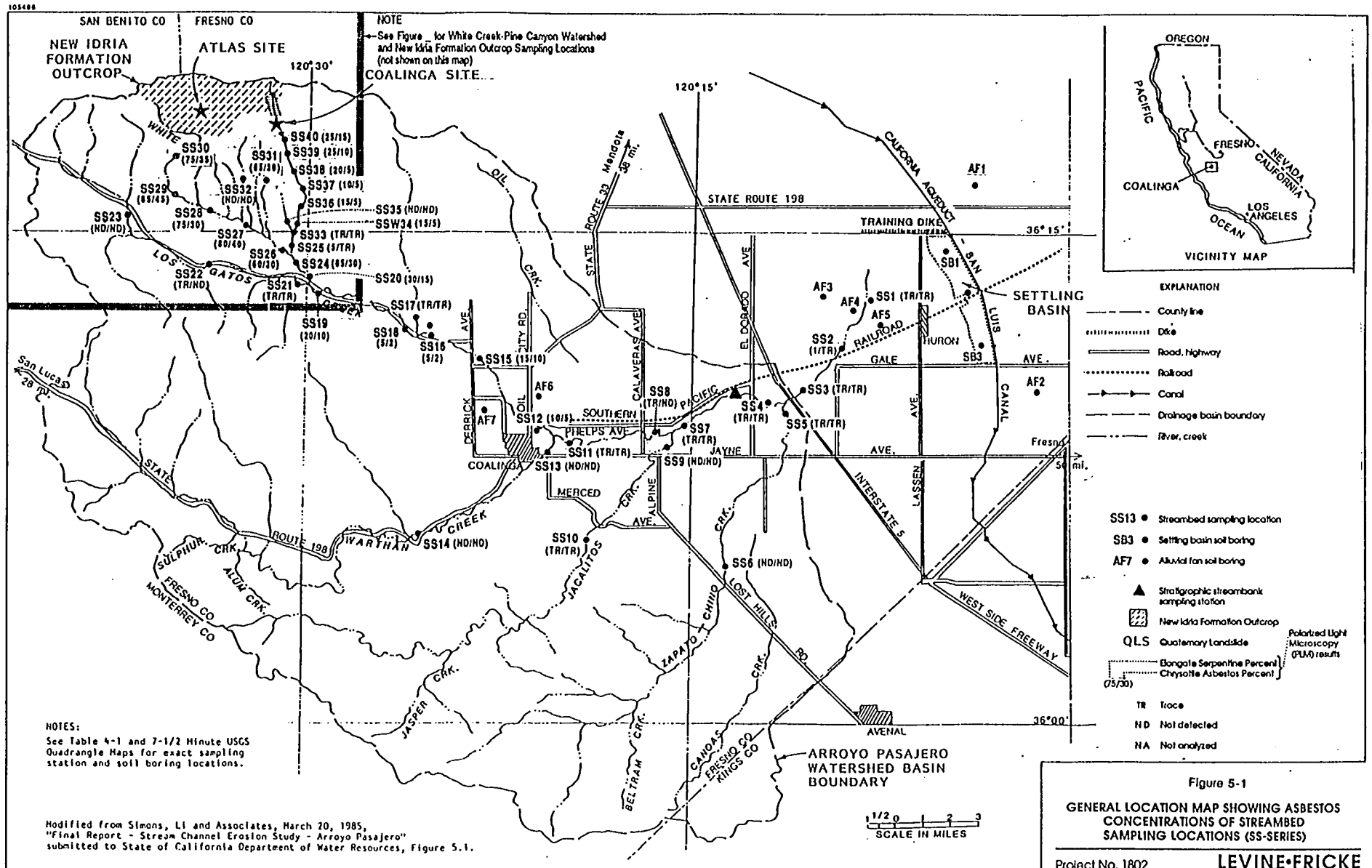


Figure 5-1

GENERAL LOCATION MAP SHOWING ASBESTOS CONCENTRATIONS OF STREAMBED SAMPLING LOCATIONS (SS-SERIES)

Project No. 1802

LEVINE•FRICKE
CONSULTING ENGINEERS AND HYDROGEOLOGISTS

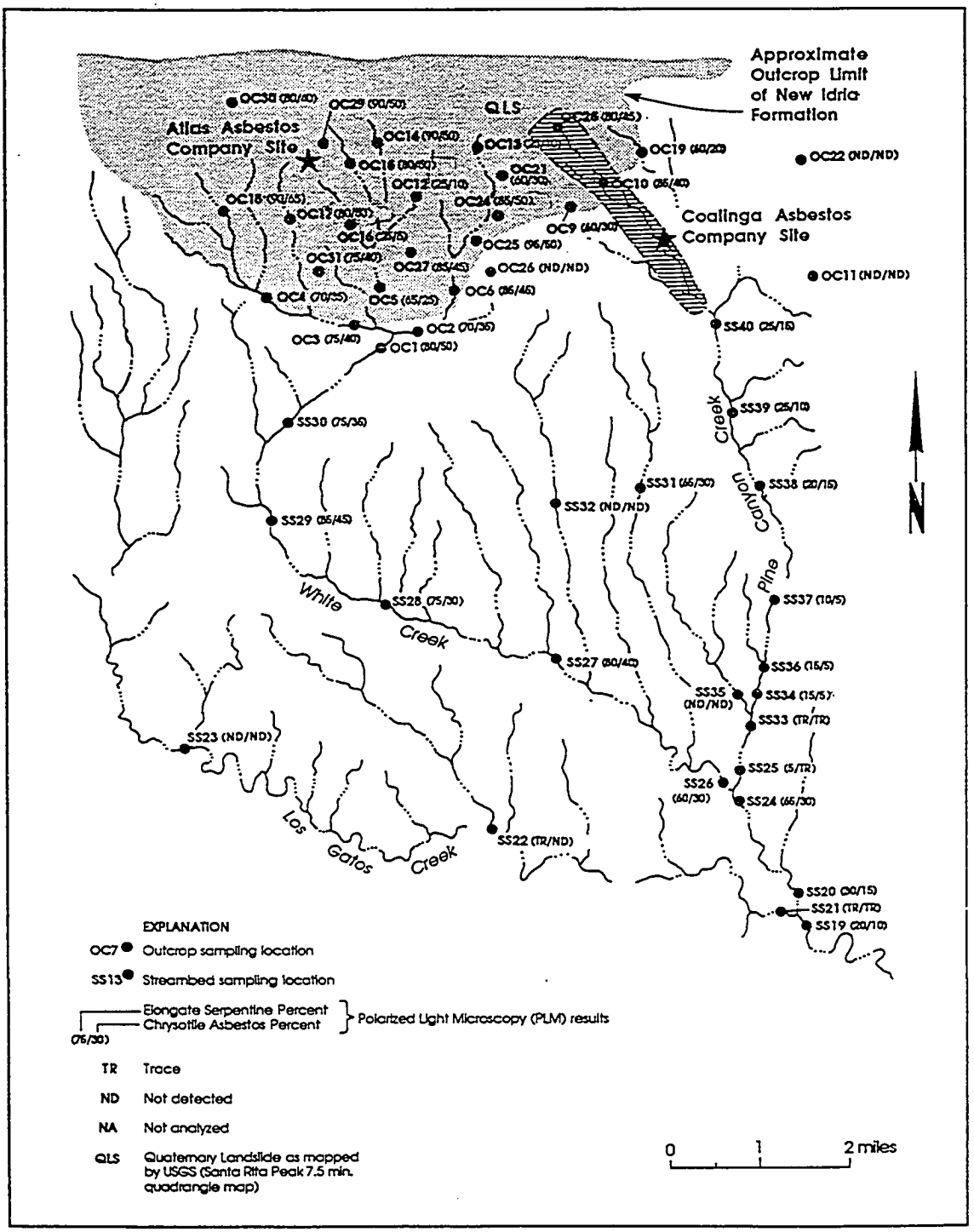


Figure 5-2 : GENERAL LOCATION MAP SHOWING ASBESTOS CONCENTRATIONS OF OUTCROP SAMPLING STATIONS (OC SERIES)

Reproduced with permission of the copyright owner. Further reproduction prohibited without permission.

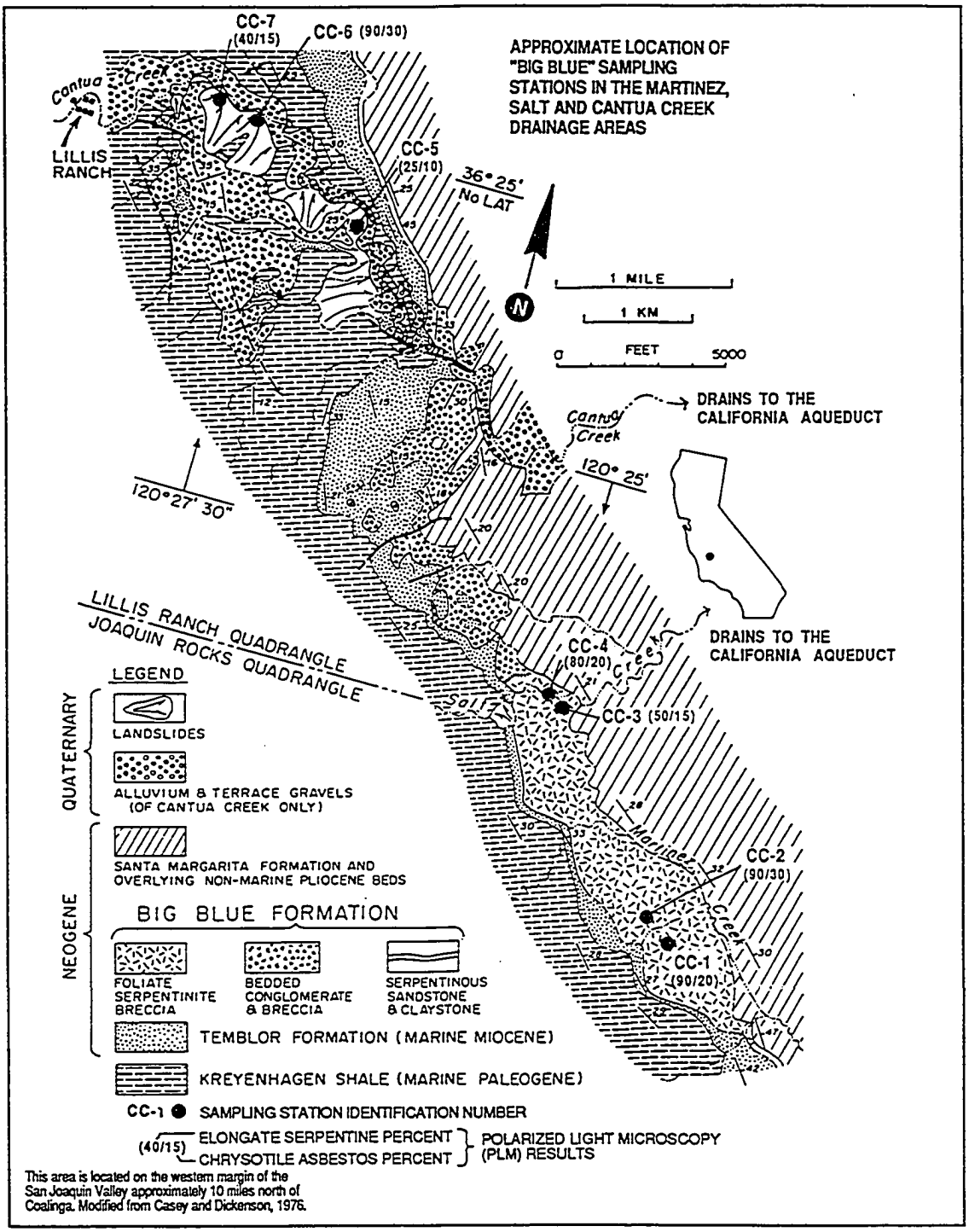
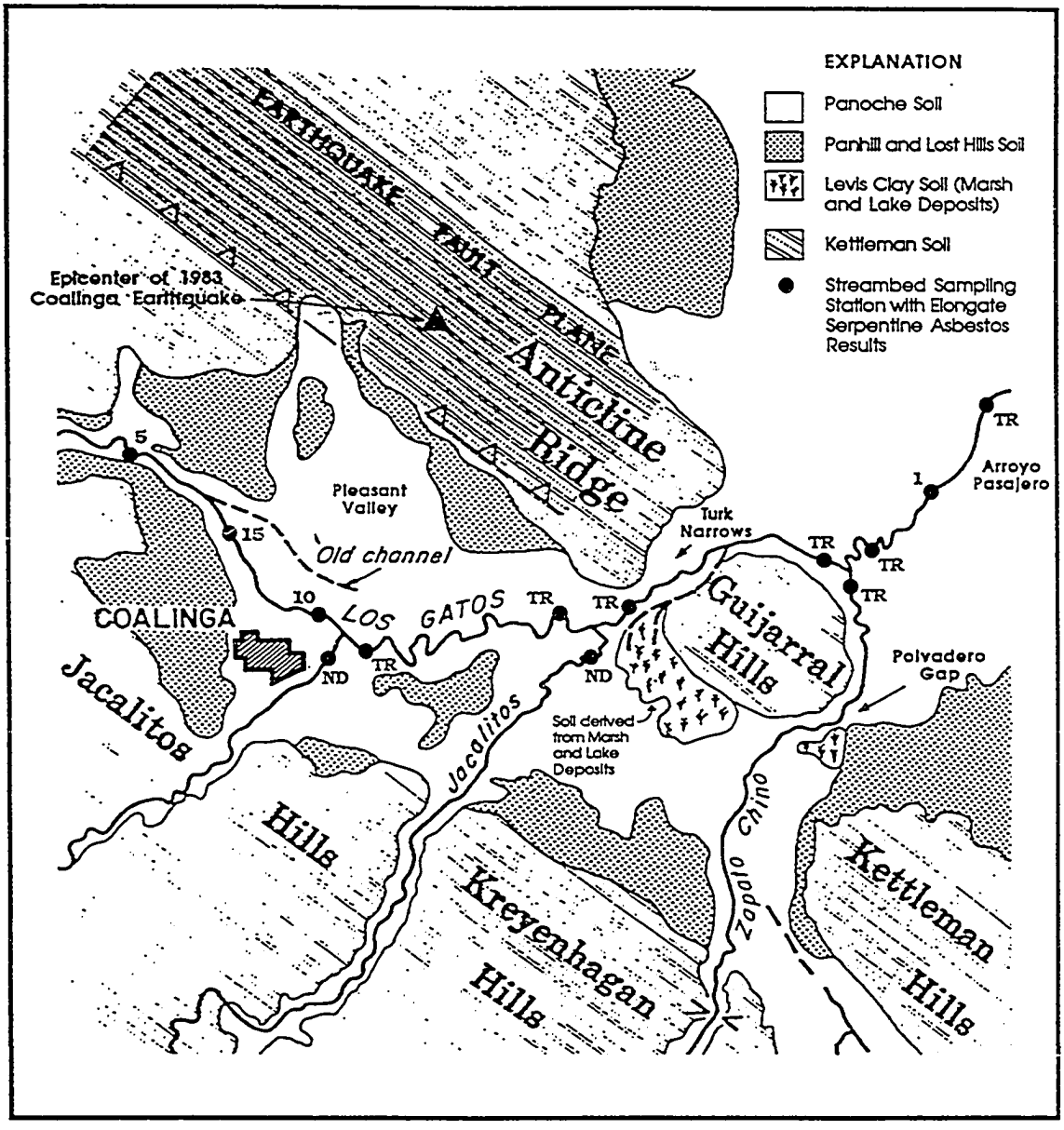


Figure 5-3 : GEOLOGIC SKETCH MAP OF OUTCROP BELT OF BIG BLUE FORMATION NEAR CANTUA CREEK SOUTHWARD ACROSS SALT AND MARTINEZ CREEKS

Reproduced with permission of the copyright owner. Further reproduction prohibited without permission.



Modified from: King and Stein, 1983

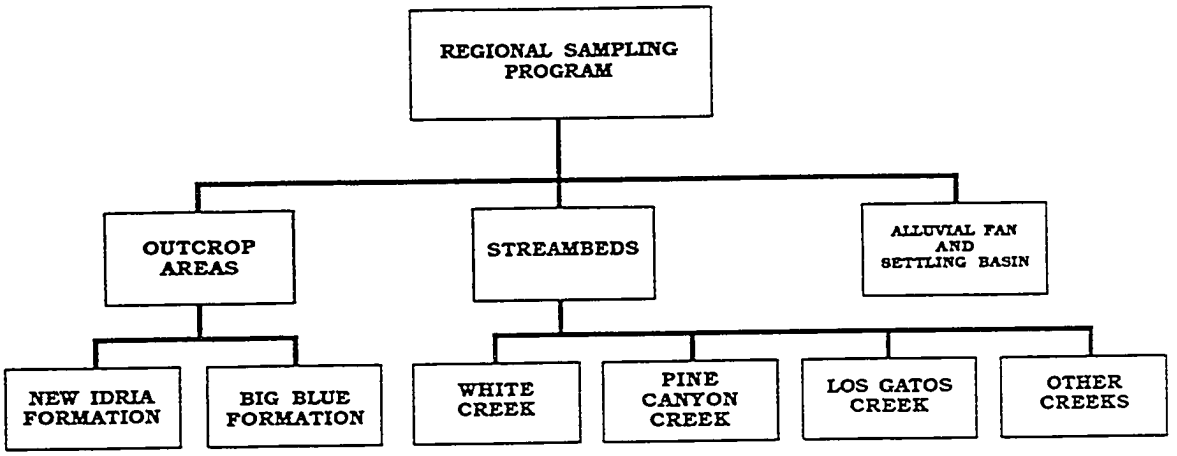
Figure 5-4 : GEOMORPHIC SKETCH MAP OF PLEASANT VALLEY

Project No. 1802

LEVINE•FRICKE
CONSULTING ENGINEERS AND HYDROGEOLOGISTS

Reproduced with permission of the copyright owner. Further reproduction prohibited without permission.

DATA ORGANIZATIONAL CHART



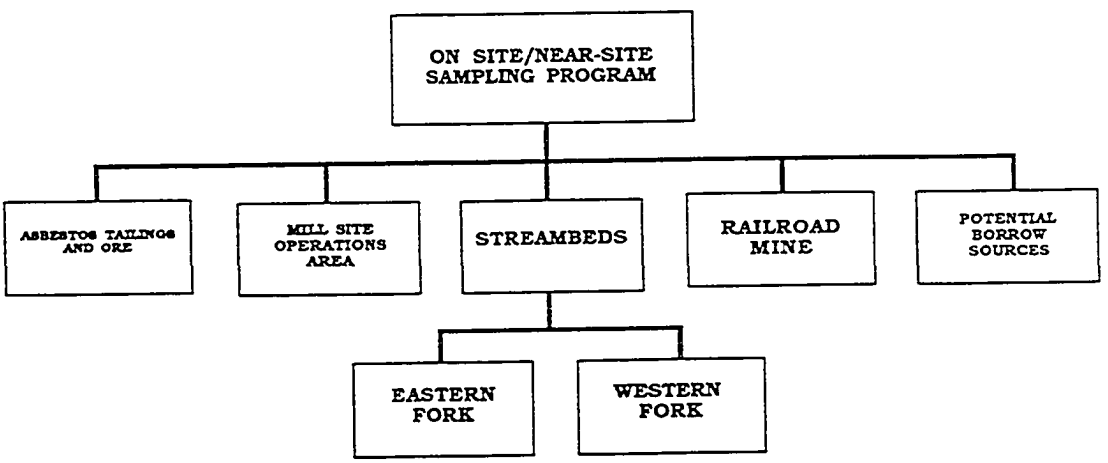


Figure 5-5

Reproduced with permission of the copyright owner. Further reproduction prohibited without permission.

Reproduced with permission of the copyright owner. Further reproduction prohibited without permission.

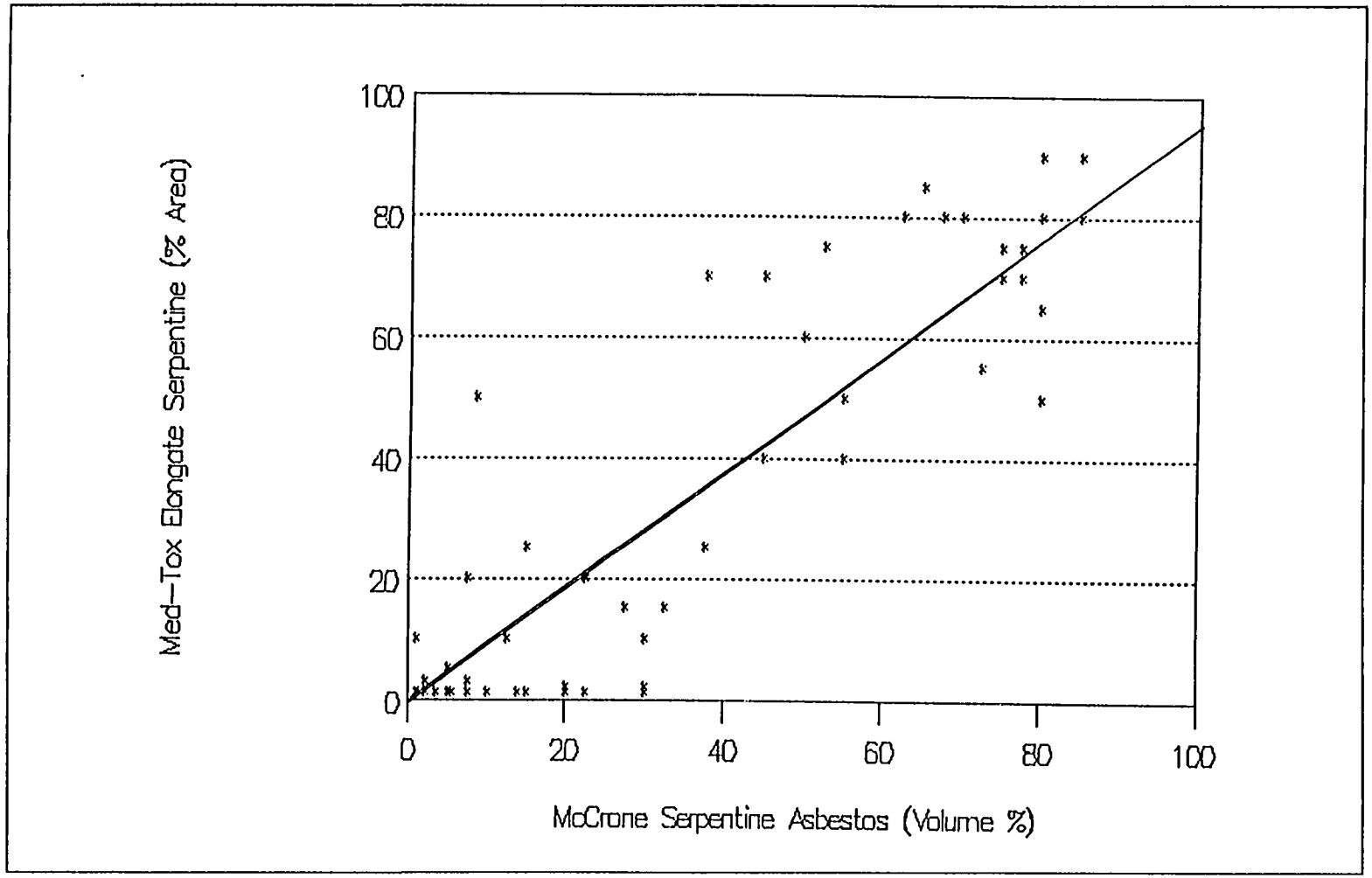


Figure 5-6 : PLM PLOT, ELONGATE SERPENTINE ASBESTOS RESULTS VERSUS SERPENTINE ASBESTOS RESULTS

Reproduced with permission of the copyright owner. Further reproduction prohibited without permission.

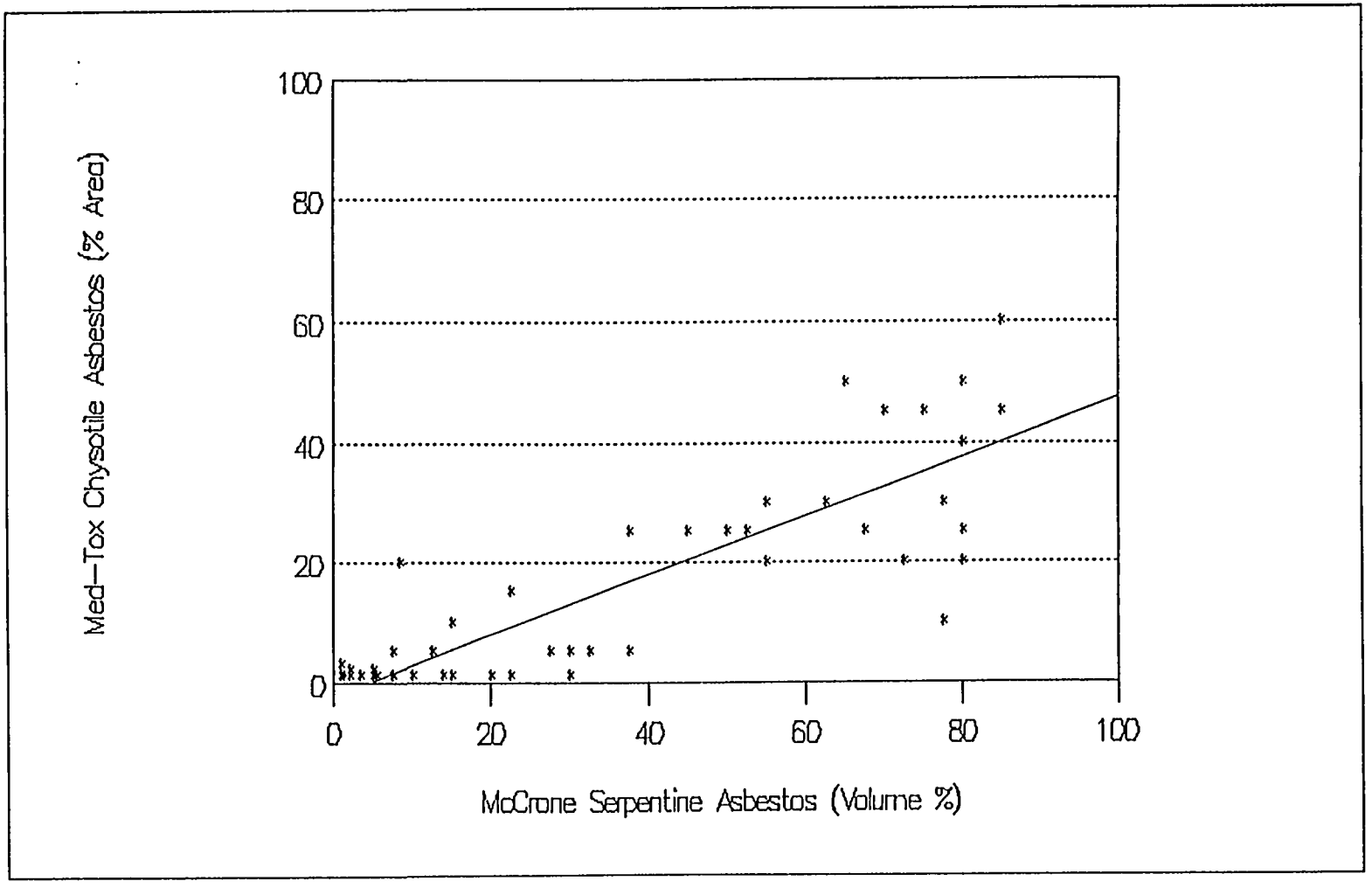


Figure 5-7 : PLM PLOT, CHRYSOTILE ASBESTOS RESULTS VERSUS SERPENTINE ASBESTOS RESULTS

Reproduced with permission of the copyright owner. Further reproduction prohibited without permission.

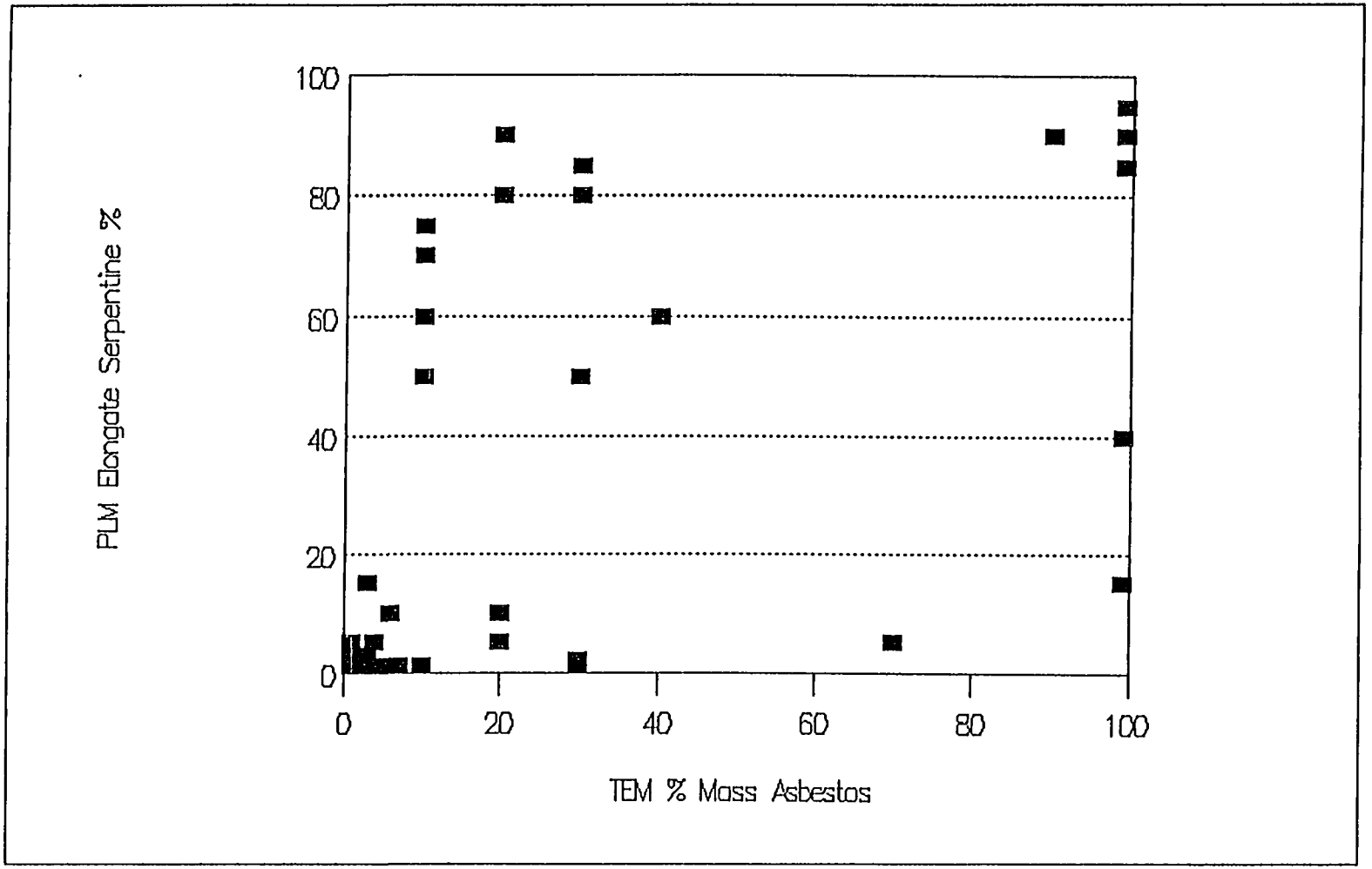


Figure 5-8A : COMPARISON OF RESULTS FOR SAMPLES ANALYZED BY BOTH PLM AND TEM
NO. OF SAMPLES = 75

Reproduced with permission of the copyright owner. Further reproduction prohibited without permission.

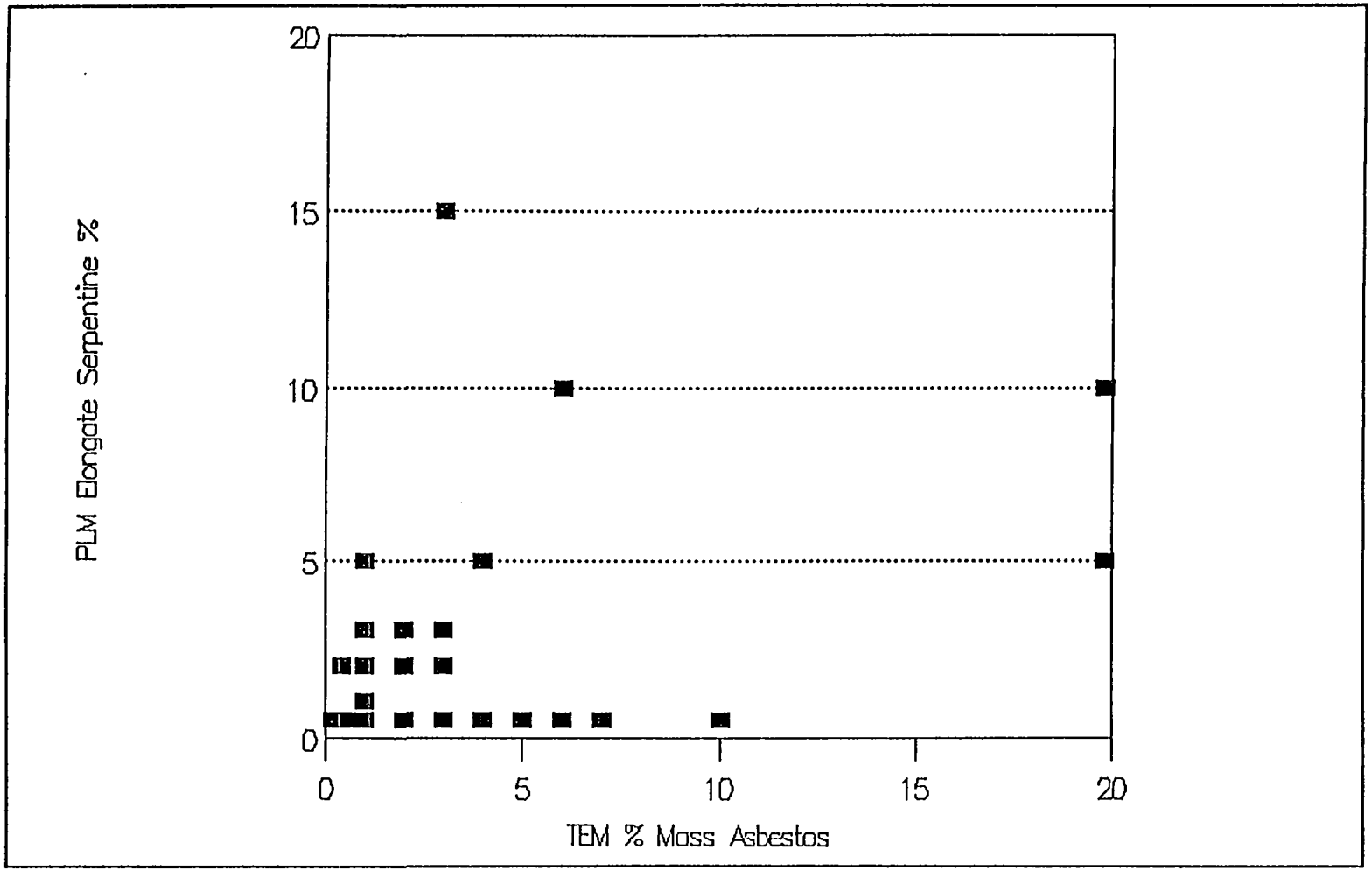


Figure 5-8B : COMPARISON OF RESULTS FOR SAMPLES ANALYZED FOR BOTH PLM AND TEM THAT HAVE RESULTS LESS THAN OR EQUALTO 20%
NO. OF SAMPLES = 51

Reproduced with permission of the copyright owner. Further reproduction prohibited without permission.

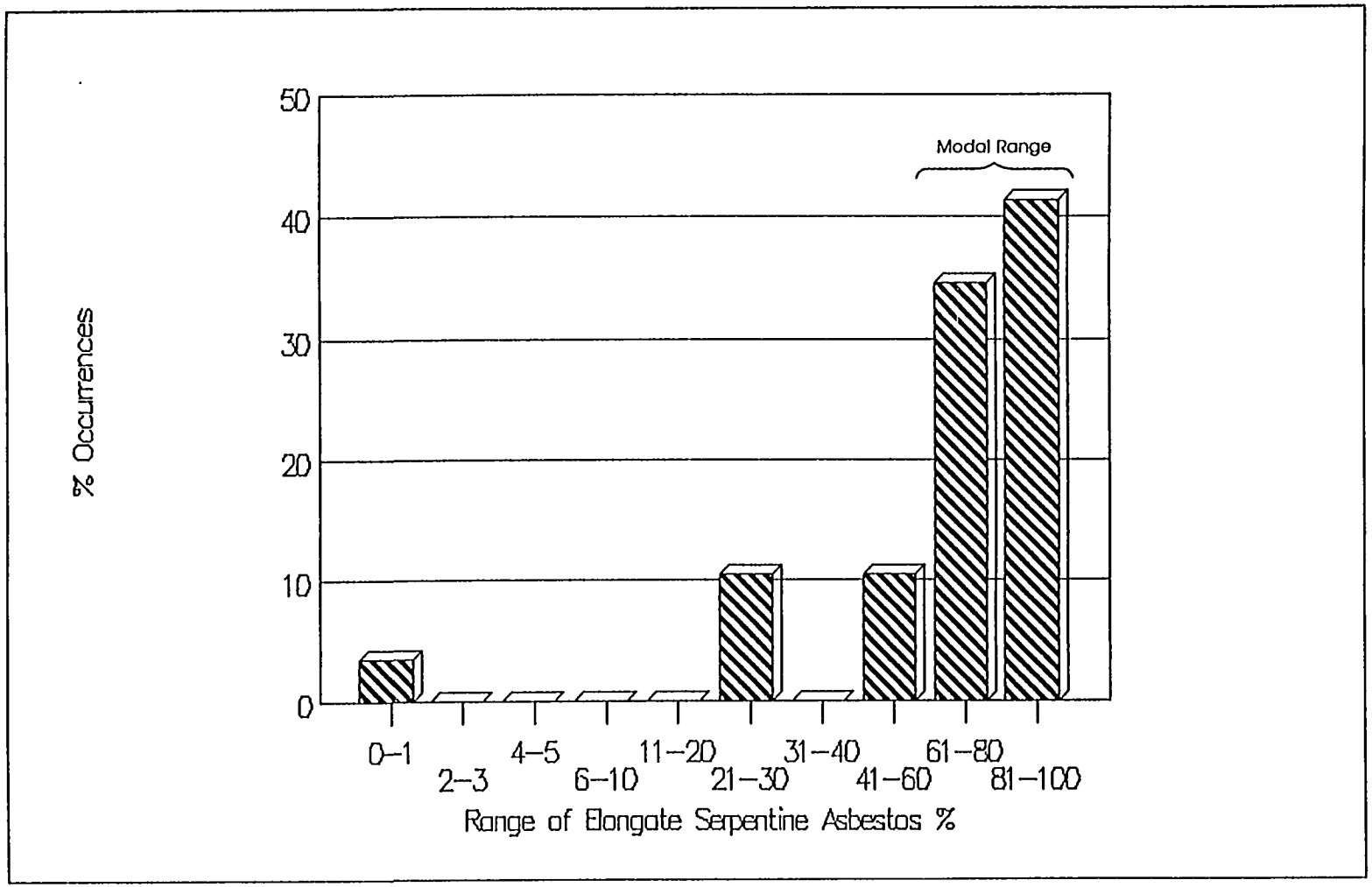


Figure 5-9 : FREQUENCY DISTRIBUTION OF PLM RESULTS - NEW IDRIA FORMATION
NO. OF SAMPLES = 28

Reproduced with permission of the copyright owner. Further reproduction prohibited without permission.

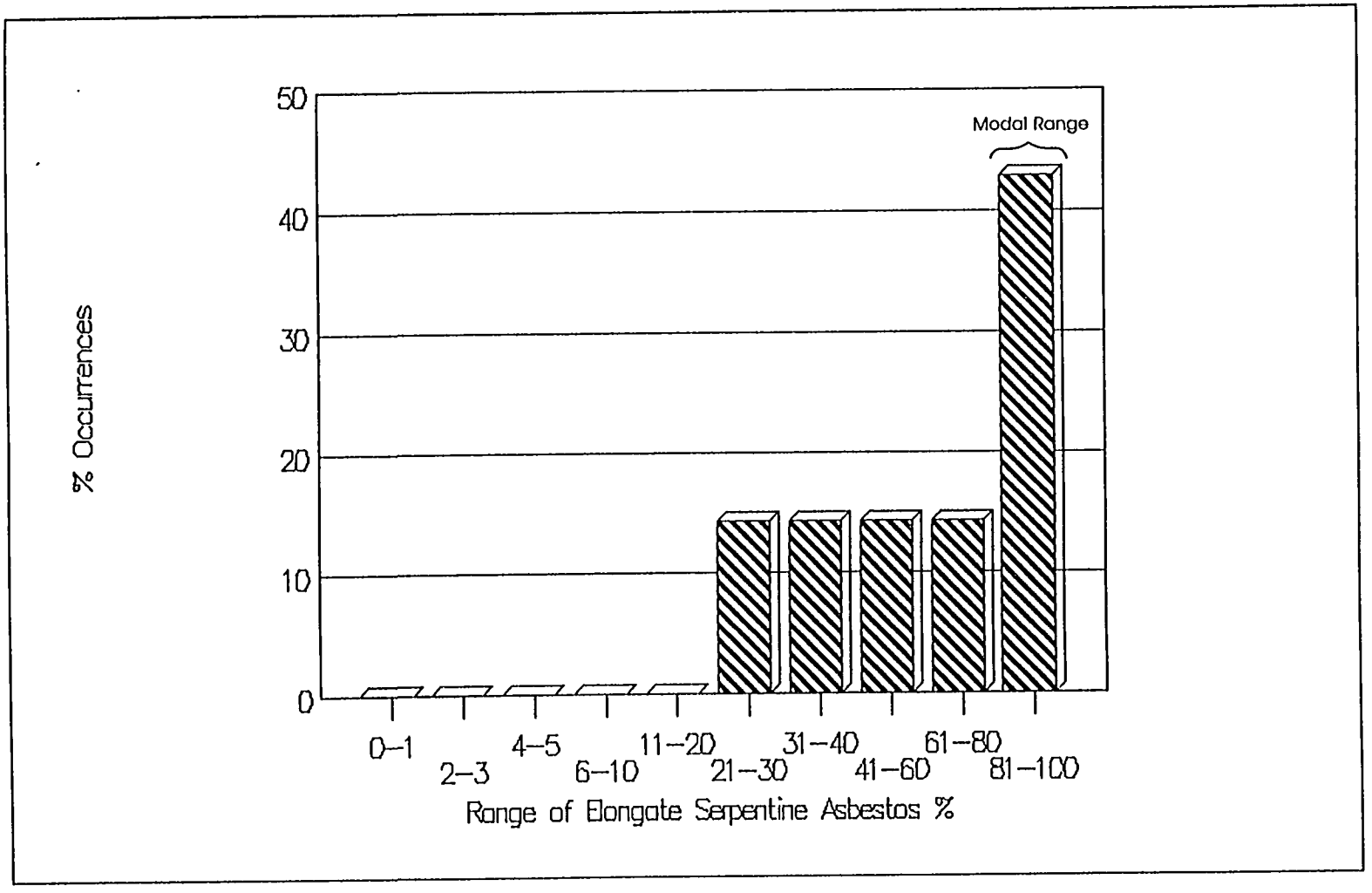


Figure 5-10 : FREQUENCY DISTRIBUTION OF PLM RESULTS - "BIG BLUE" FORMATION
NO. OF SAMPLES = 7

Reproduced with permission of the copyright owner. Further reproduction prohibited without permission.

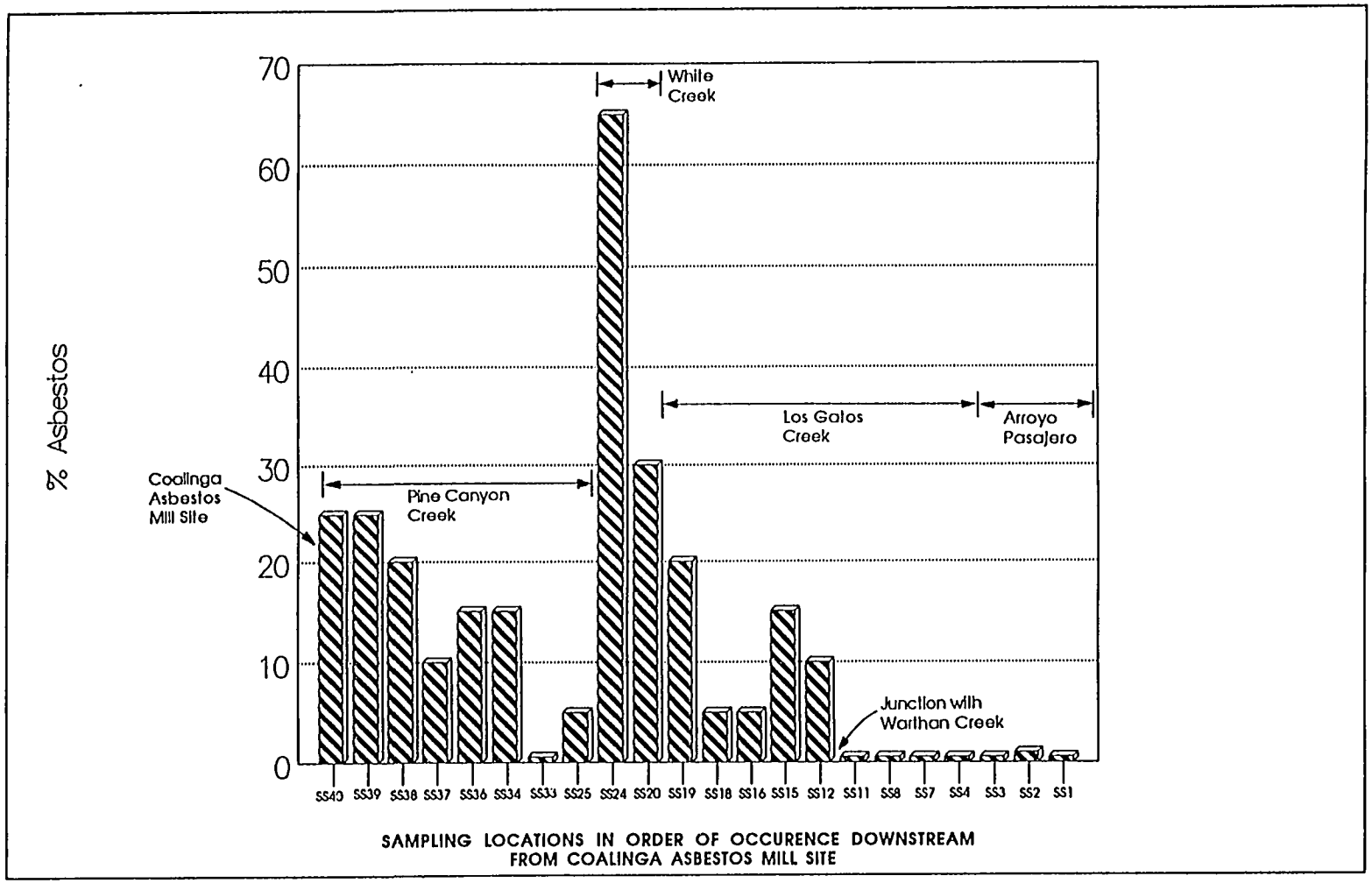


Figure 5-11 : ELONGATE SERPENTINE ASBETOS (% AREA)
PINE CANYON CREEK TO WHITE CREEK TO LOS GATOS CREEK TO ARROYO PASAJERO

Reproduced with permission of the copyright owner. Further reproduction prohibited without permission.

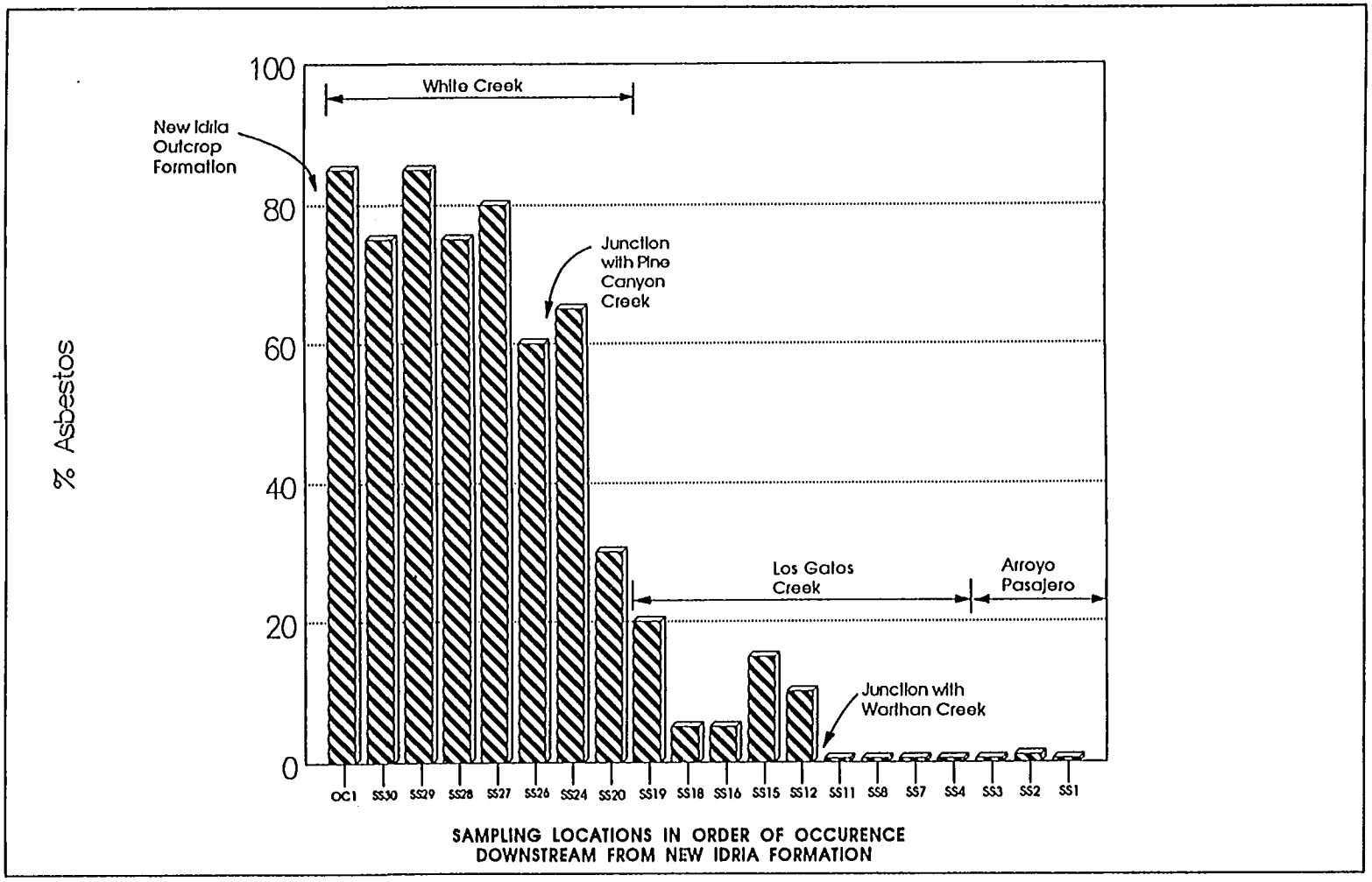


Figure 5-12 : ELONGATE SERPENTINE ASBETOS (% AREA)
WHITE CREEK TO LOS GATOS CREEK TO ARROYO PASAJERO

Reproduced with permission of the copyright owner. Further reproduction prohibited without permission.

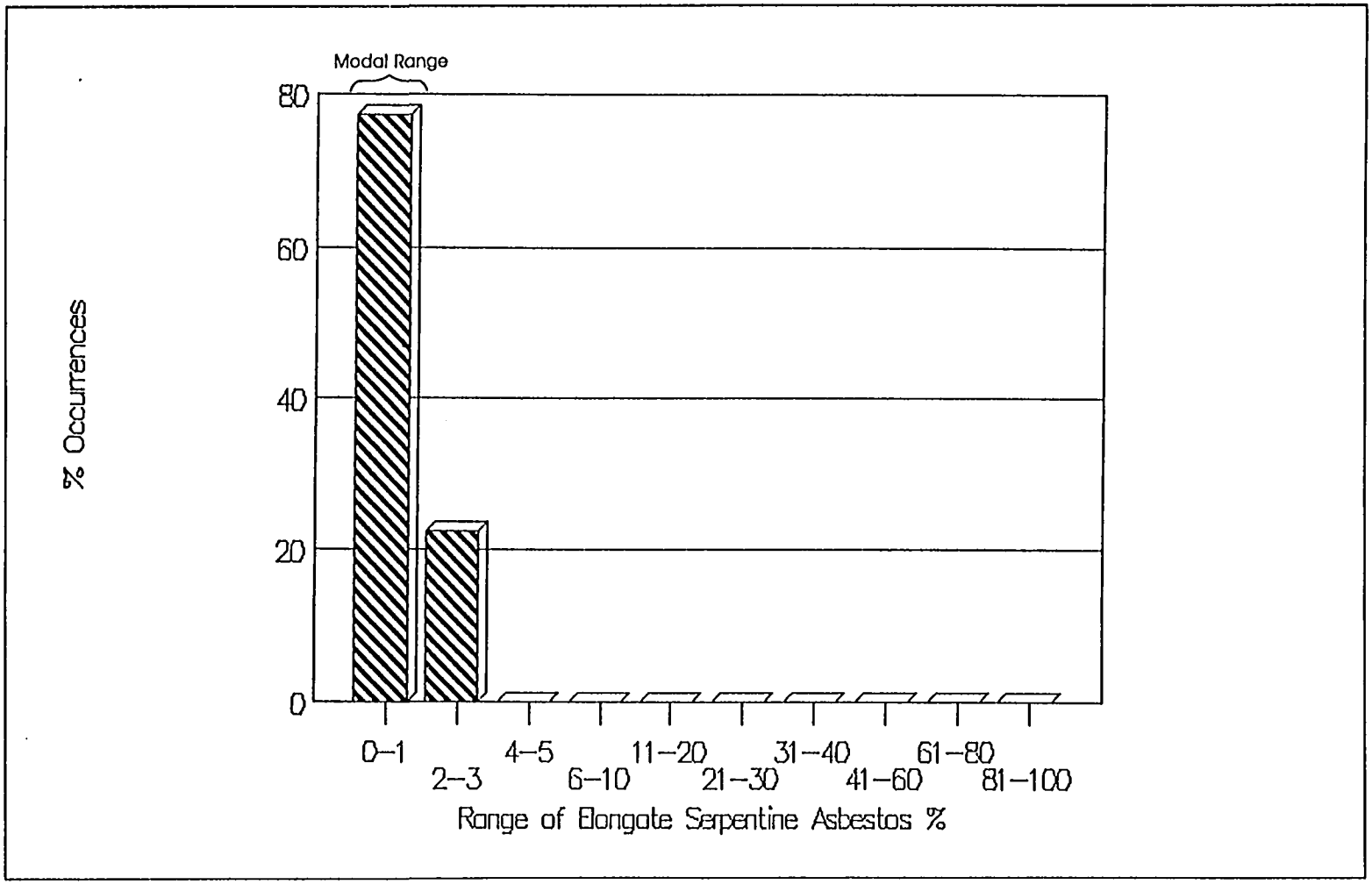


Figure 5-13 : FREQUENCY DISTRIBUTION OF PLM RESULTS - ALLUVIAL FAN CORE SAMPLES
NO. OF SAMPLES = 40

Reproduced with permission of the copyright owner. Further reproduction prohibited without permission.

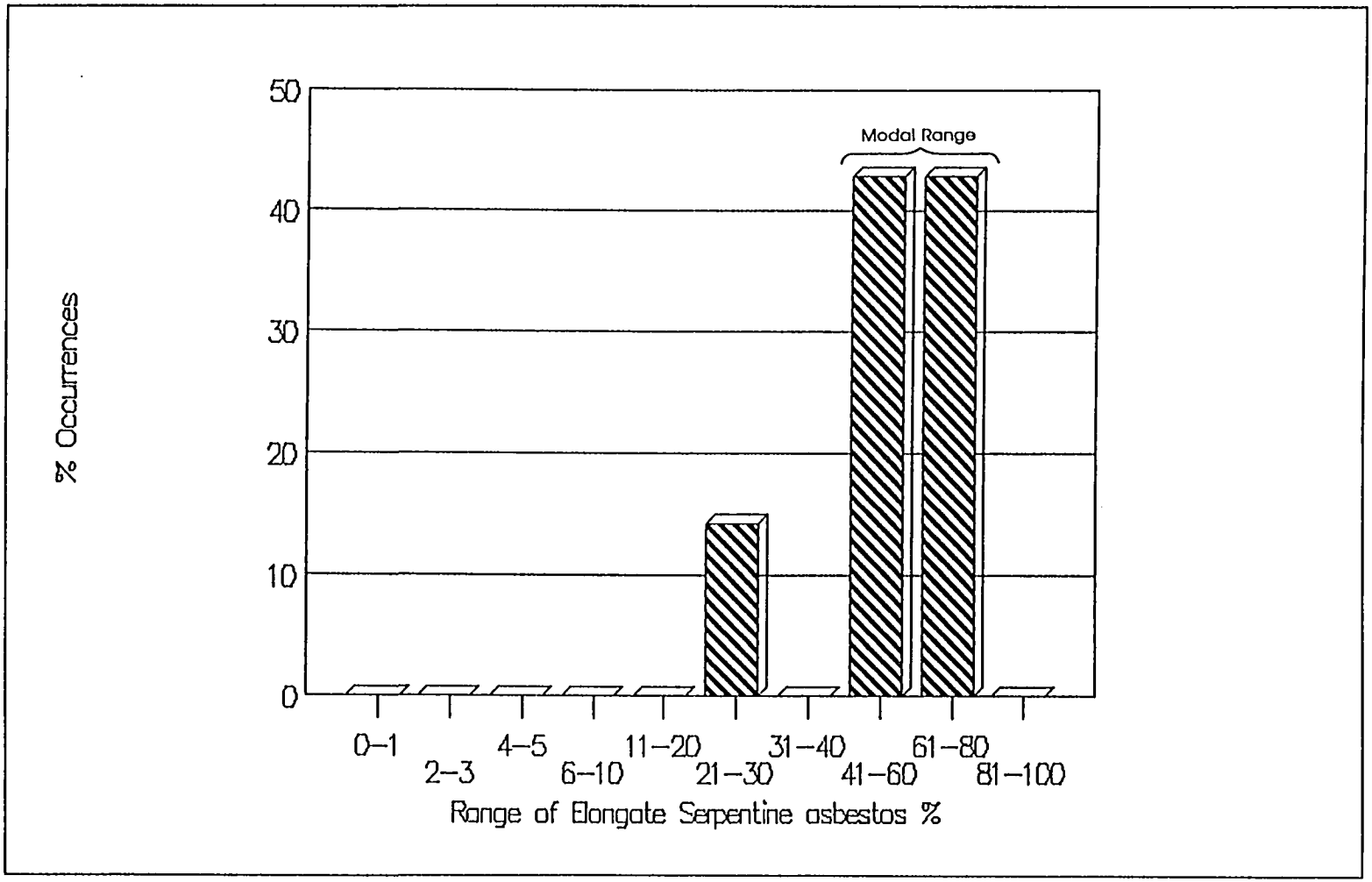


Figure 5-14 : FREQUENCY DISTRIBUTION OF PLM RESULTS - WEST FORK ABOVE THE SITE (UPSTREAM PINE CANYON CREEK)
NO. OF SAMPLES = 7

Reproduced with permission of the copyright owner. Further reproduction prohibited without permission.

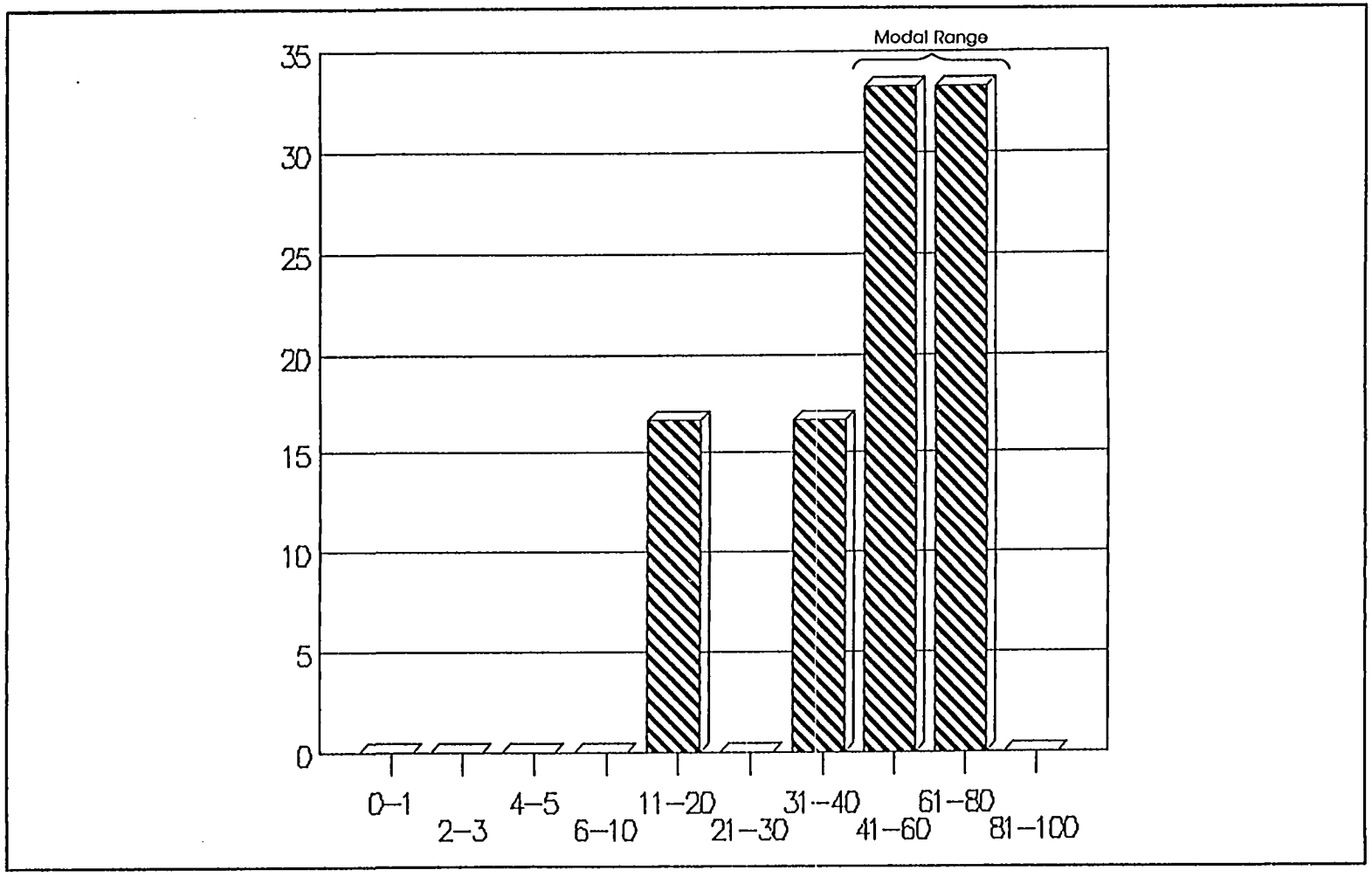


Figure 5-15 : FREQUENCY DISTRIBUTION OF PLM RESULTS - WEST FORK ALONG THE SITE (DOWNSTREAM PINE CANYON CREEK)
NO. OF SAMPLES = 6

Reproduced with permission of the copyright owner. Further reproduction prohibited without permission.

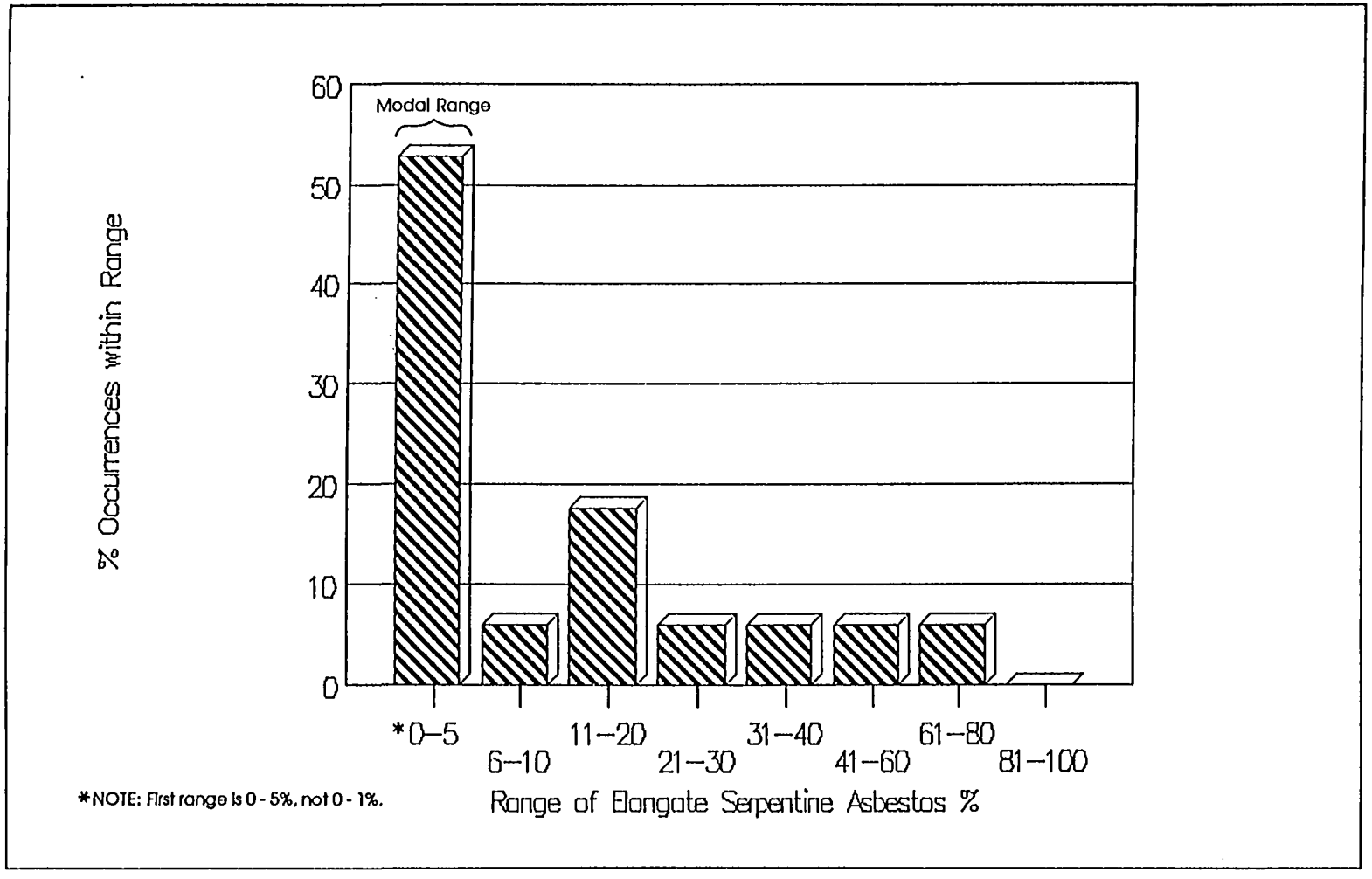


Figure 5-16 : FREQUENCY DISTRIBUTION OF PLM RESULTS - ON-SITE SERPENTINE LANDSLIDE AREA (NATURALLY OCCURING MATERIAL IN STREAMBANKS)

Reproduced with permission of the copyright owner. Further reproduction prohibited without permission.

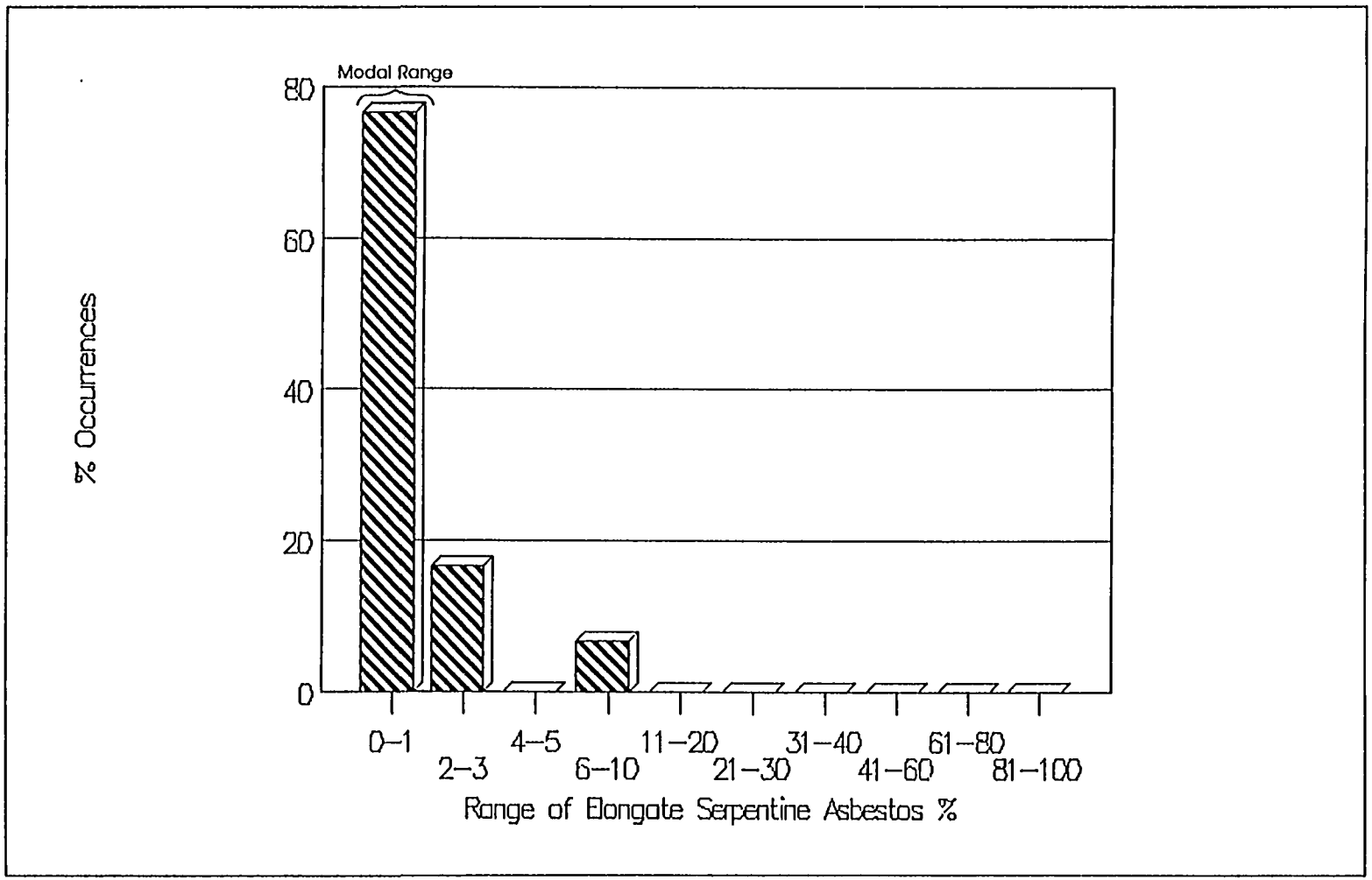


Figure 5-17 : FREQUENCY DISTRIBUTION OF PLM RESULTS - UPPER BORROW SOURCE AREA
NO. OF SAMPLES = 30

Reproduced with permission of the copyright owner. Further reproduction prohibited without permission.

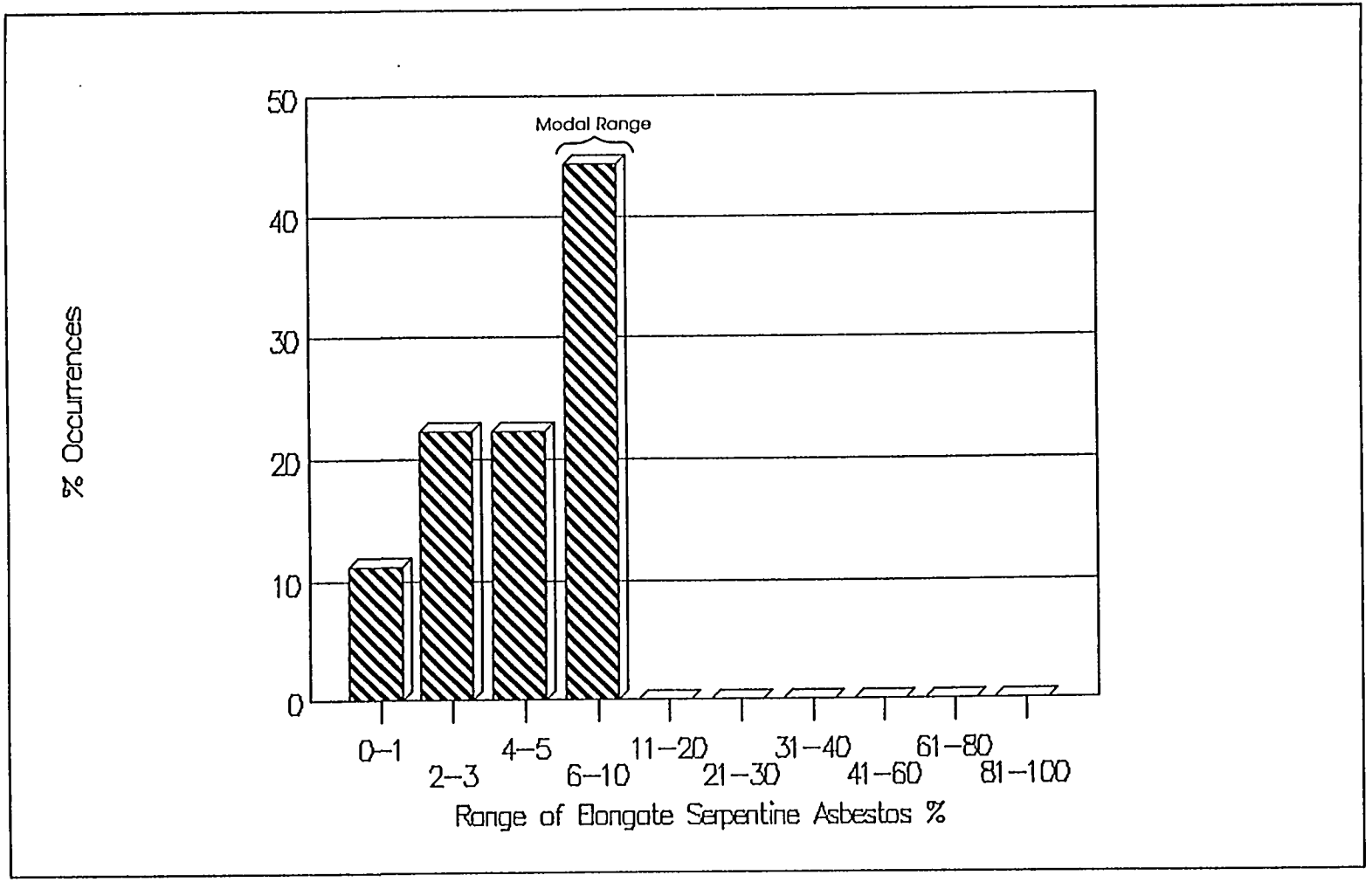


Figure 5-18 : FREQUENCY DISTRIBUTION OF PLM RESULTS - LOWER BORROW SOURCE AREA
NO. OF SAMPLES = 9

Reproduced with permission of the copyright owner. Further reproduction prohibited without permission.

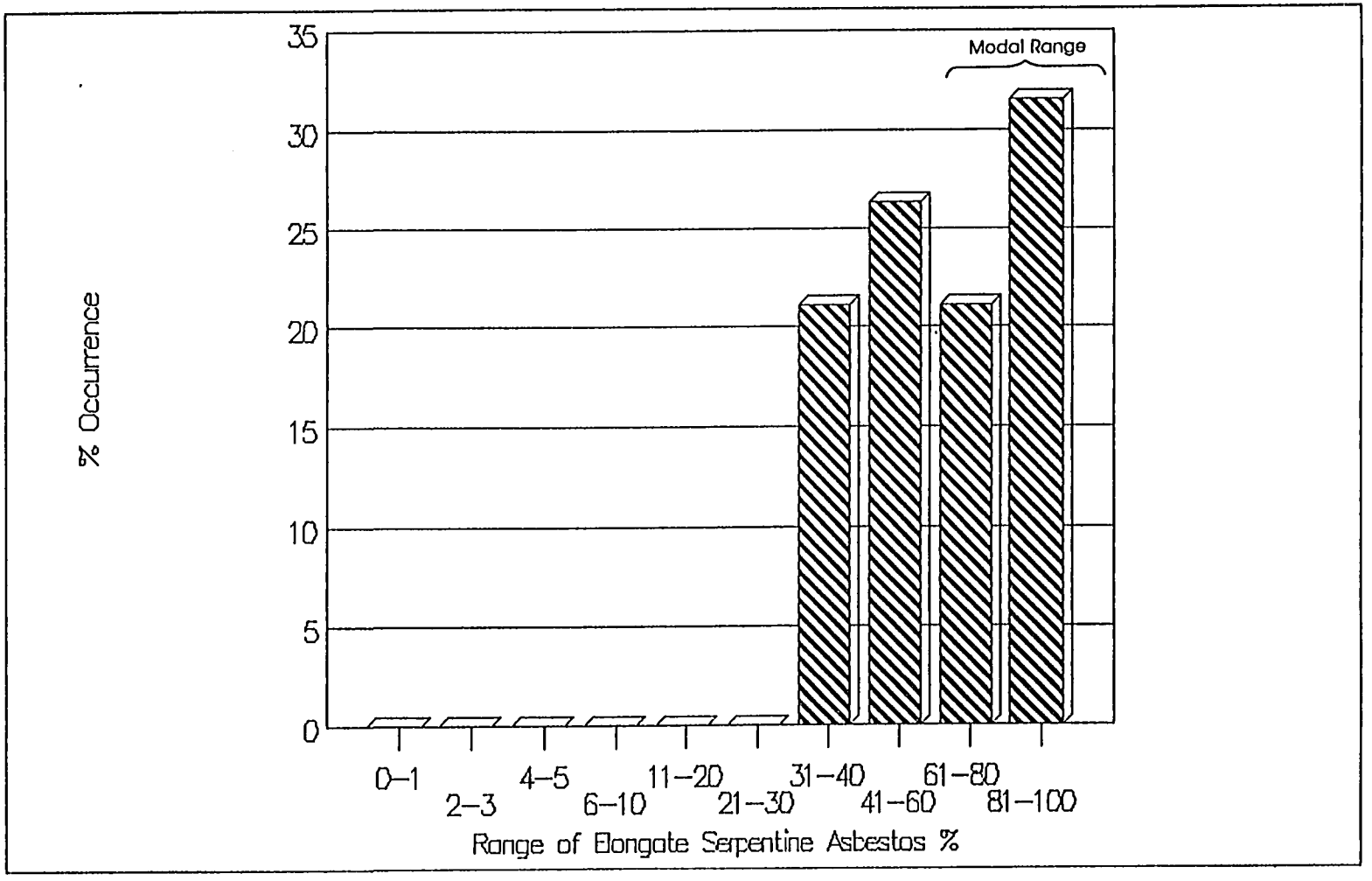


Figure 5-19 : **FREQUENCY DISTRIBUTION OF PLM RESULTS - TAILINGS PILE**
NO. OF SAMPLES = 19

Reproduced with permission of the copyright owner. Further reproduction prohibited without permission.

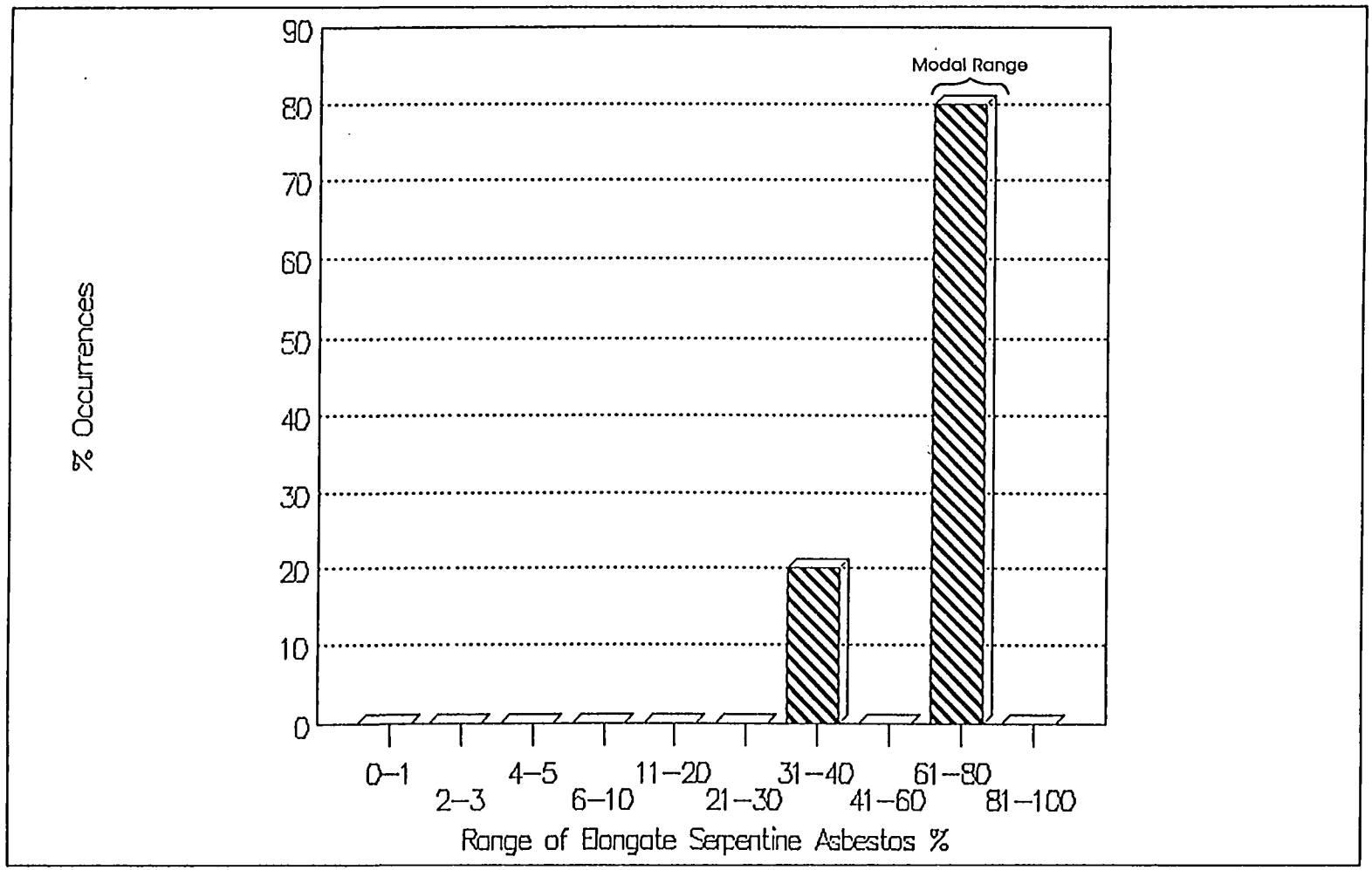


Figure 5-20 : FREQUENCY DISTRIBUTION OF PLM RESULTS - ORE STORAGE AREA
NO. OF SAMPLES = 5

Reproduced with permission of the copyright owner. Further reproduction prohibited without permission.

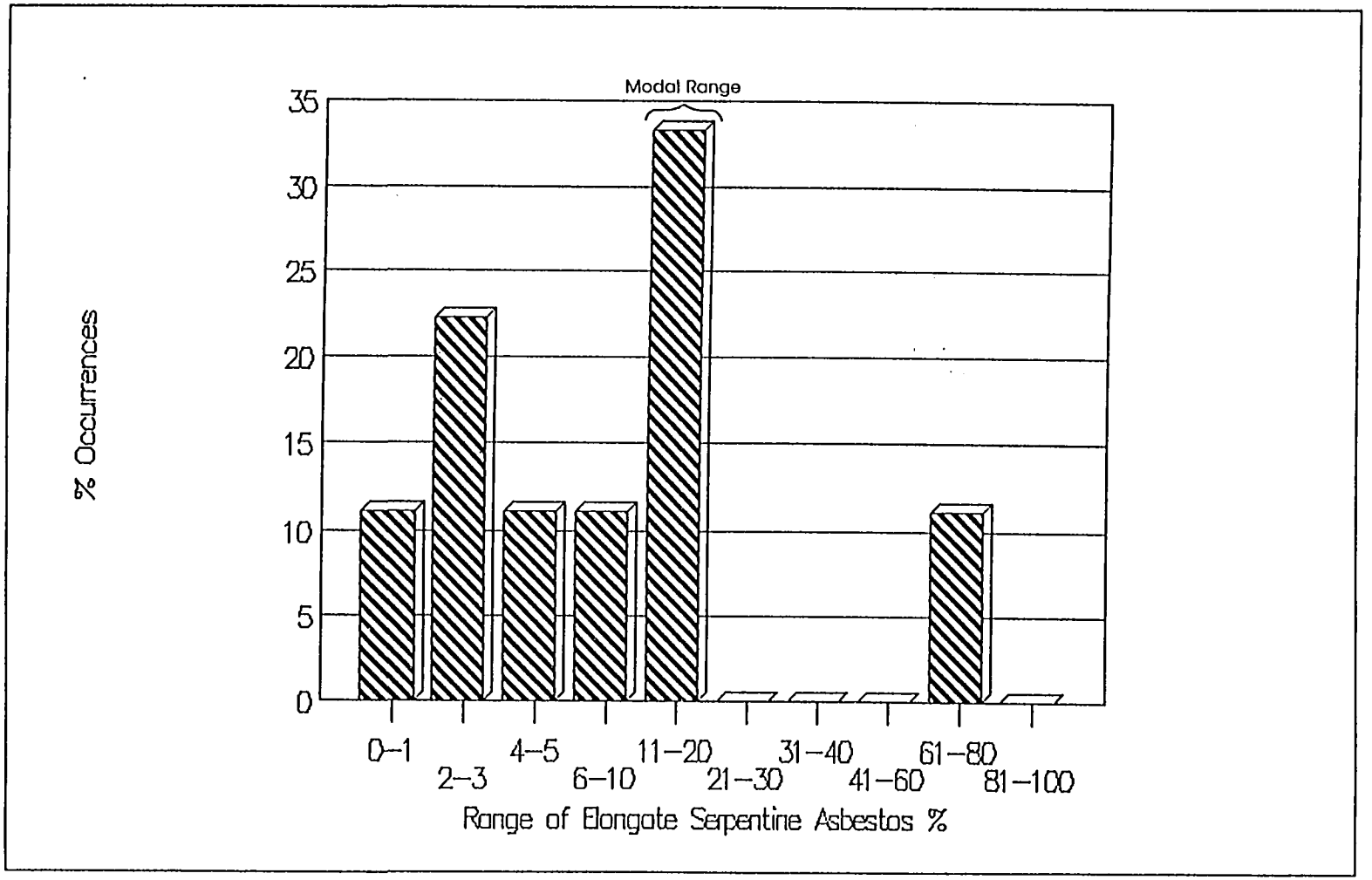


Figure 5-21 : FREQUENCY DISTRIBUTION OF PLM RESULTS - MILL SITE OPERATIONS AREA
NO. OF SAMPLES = 9

Reproduced with permission of the copyright owner. Further reproduction prohibited without permission.

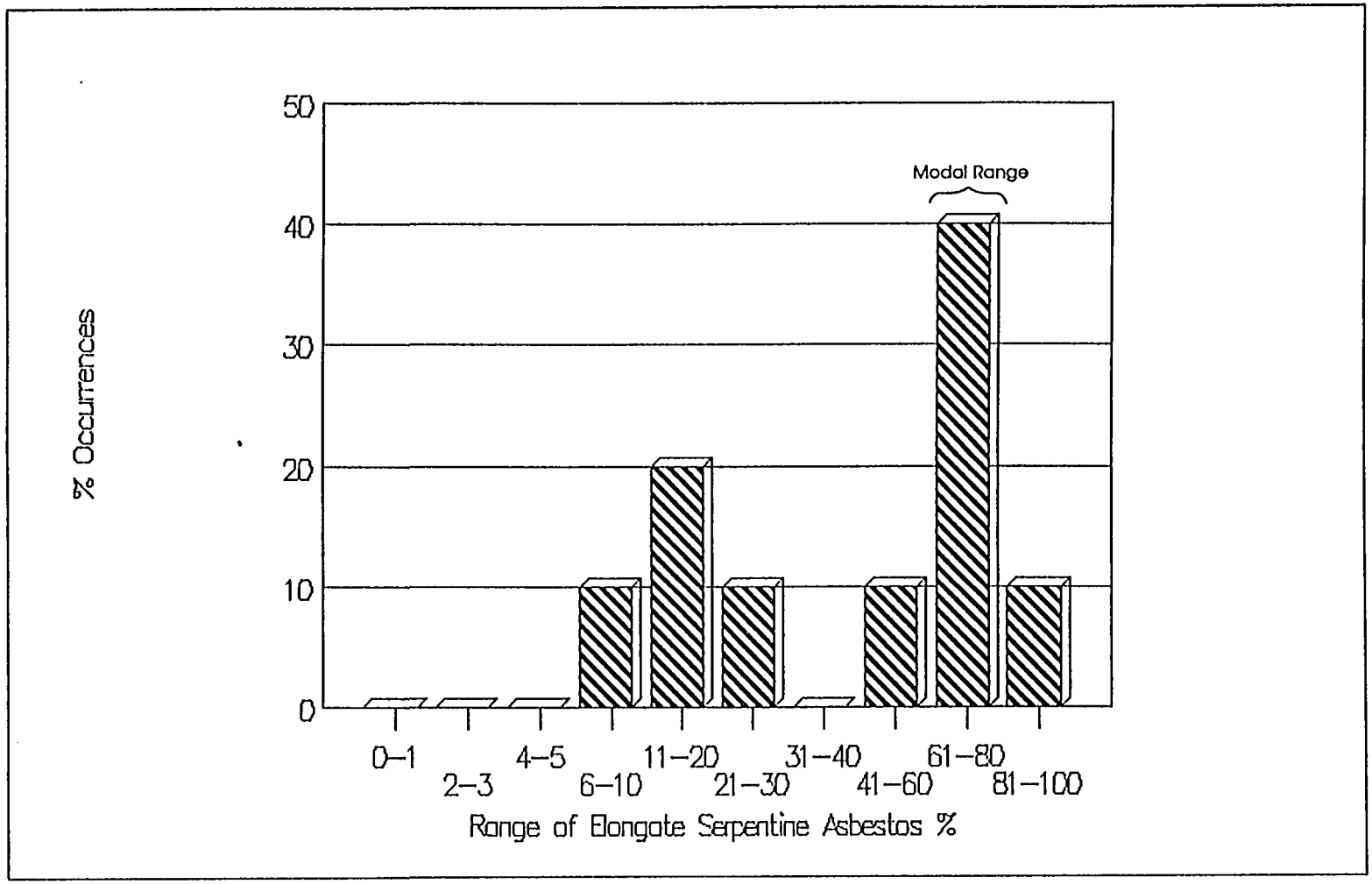


Figure 5-22 : FREQUENCY DISTRIBUTION OF PLM RESULTS - RAILROAD MINE
NO. OF SAMPLES = 10

Reproduced with permission of the copyright owner. Further reproduction prohibited without permission.

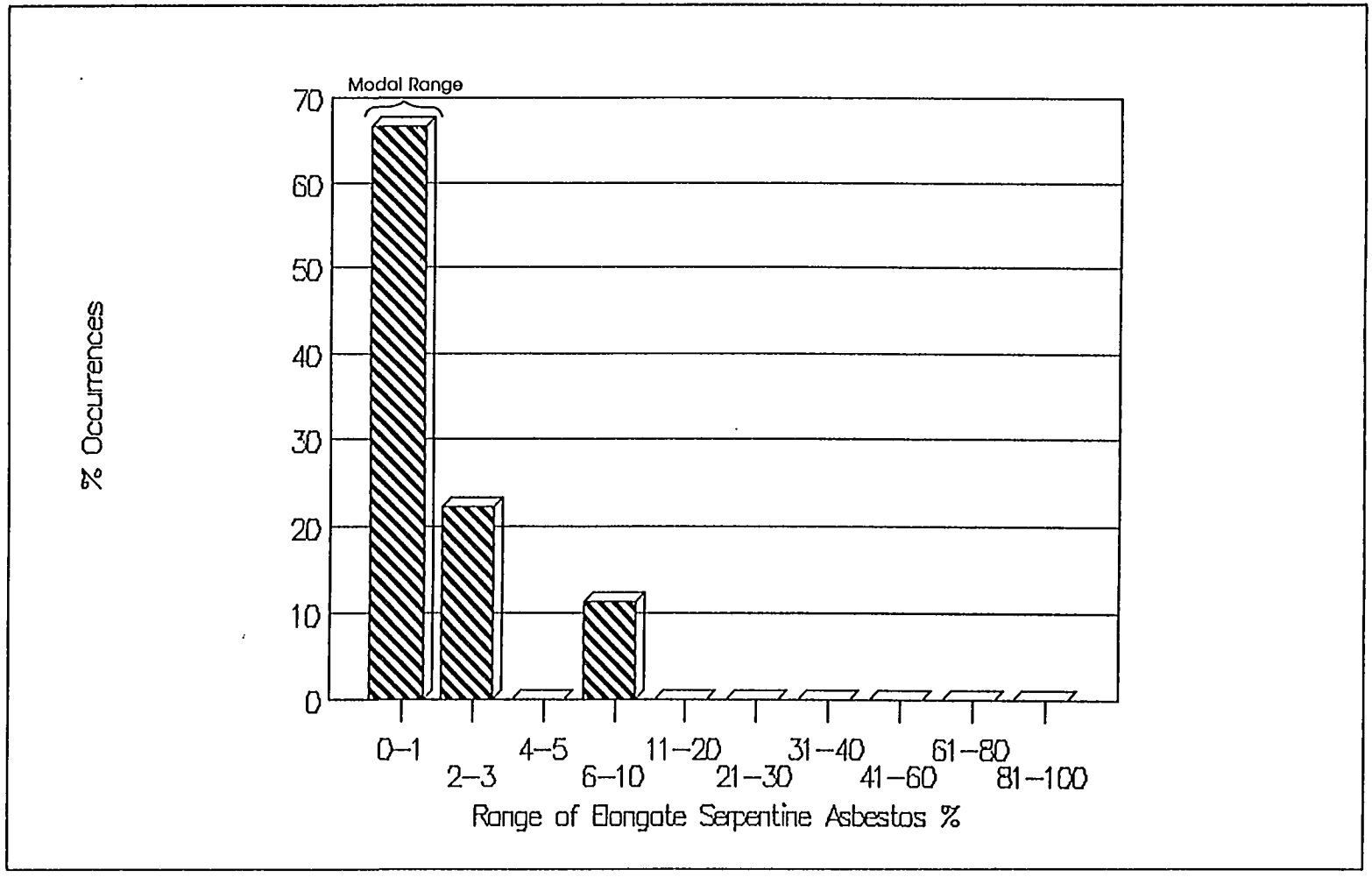
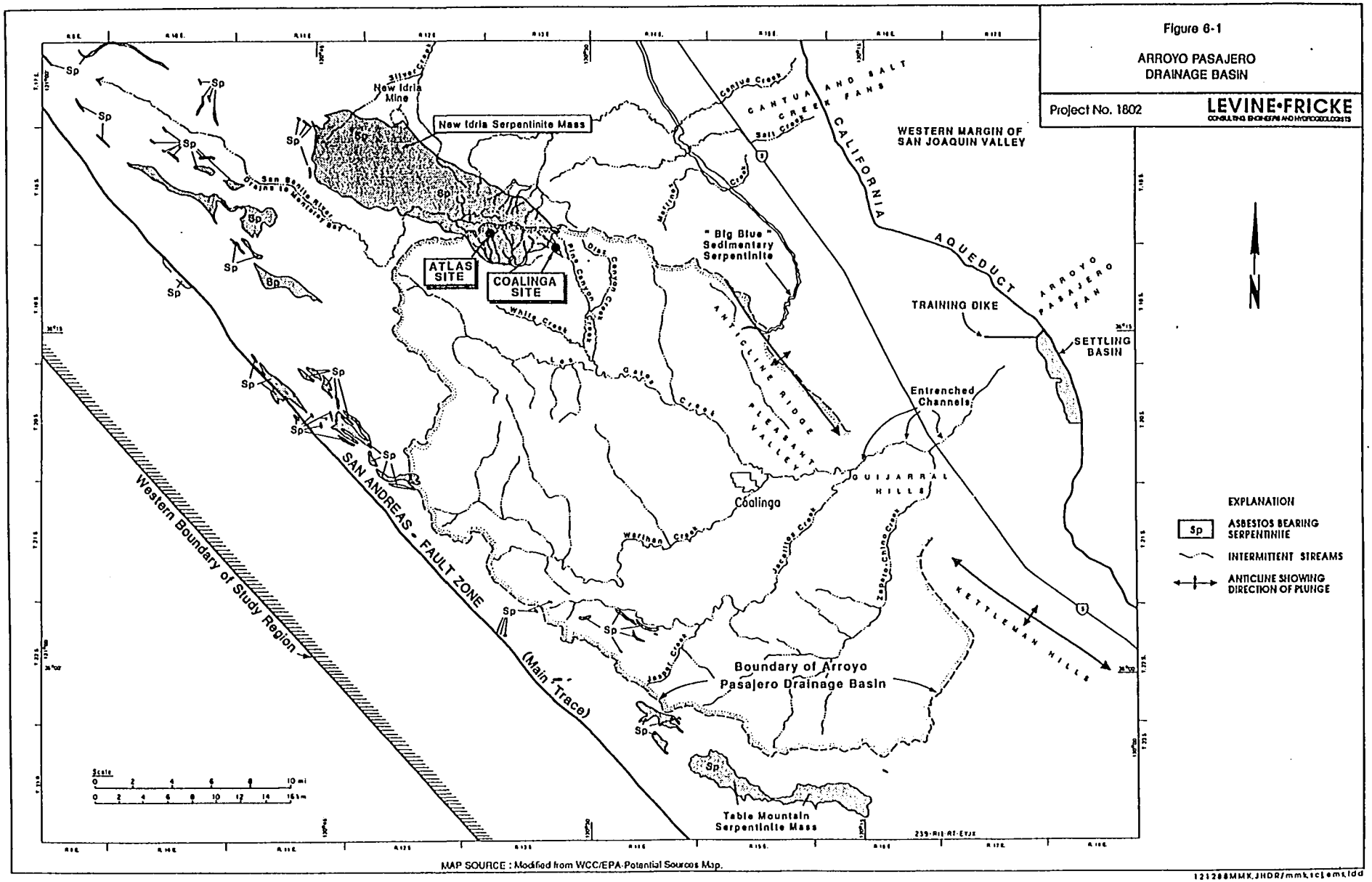
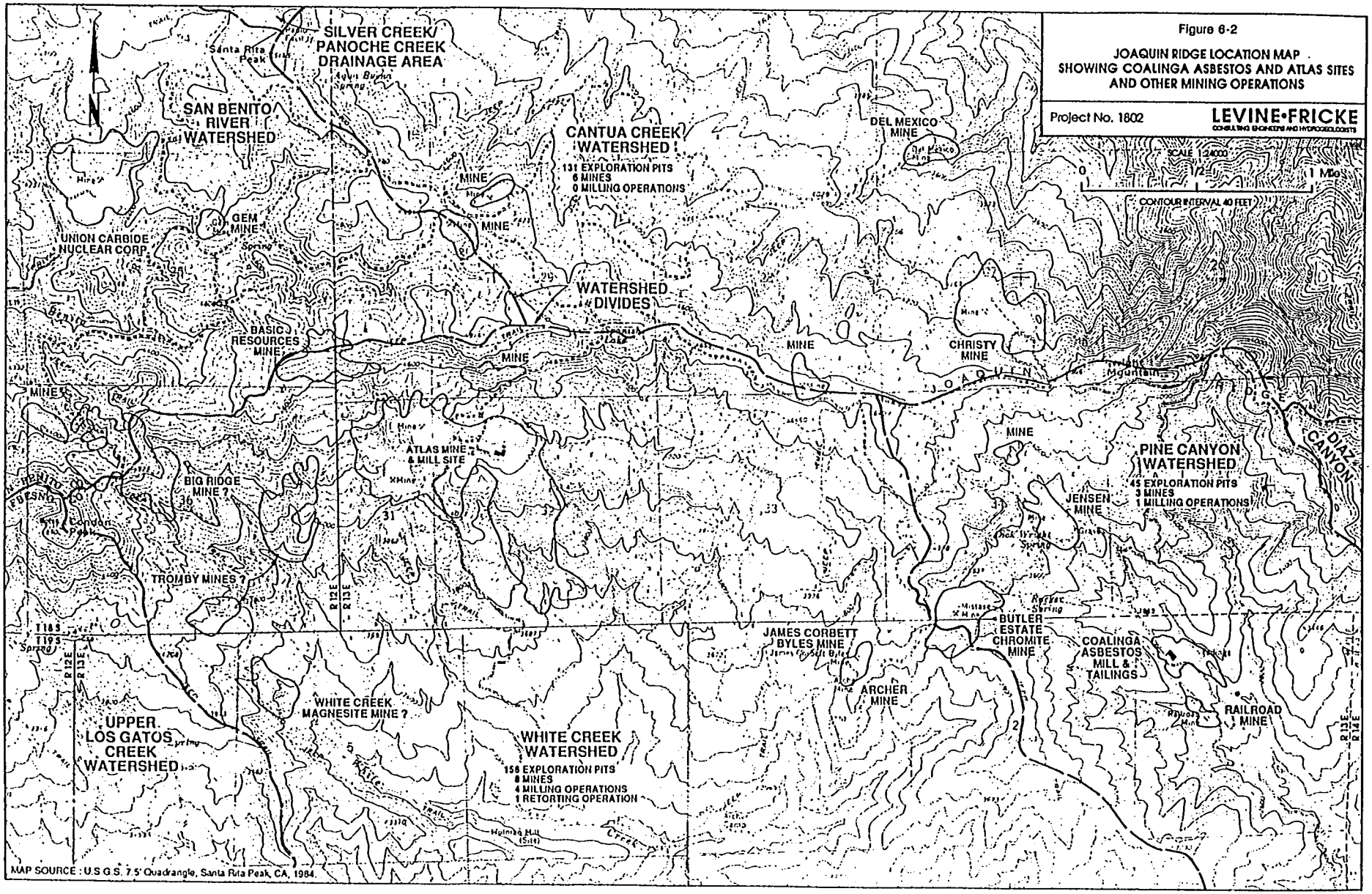


Figure 5-23 : FREQUENCY DISTRIBUTION OF PLM RESULTS - MILL SITE ACCESS ROADS
NO. OF SAMPLES = 9

Reproduced with permission of the copyright owner. Further reproduction prohibited without permission.



Reproduced with permission of the copyright owner. Further reproduction prohibited without permission.



Reproduced with permission of the copyright owner. Further reproduction prohibited without permission.

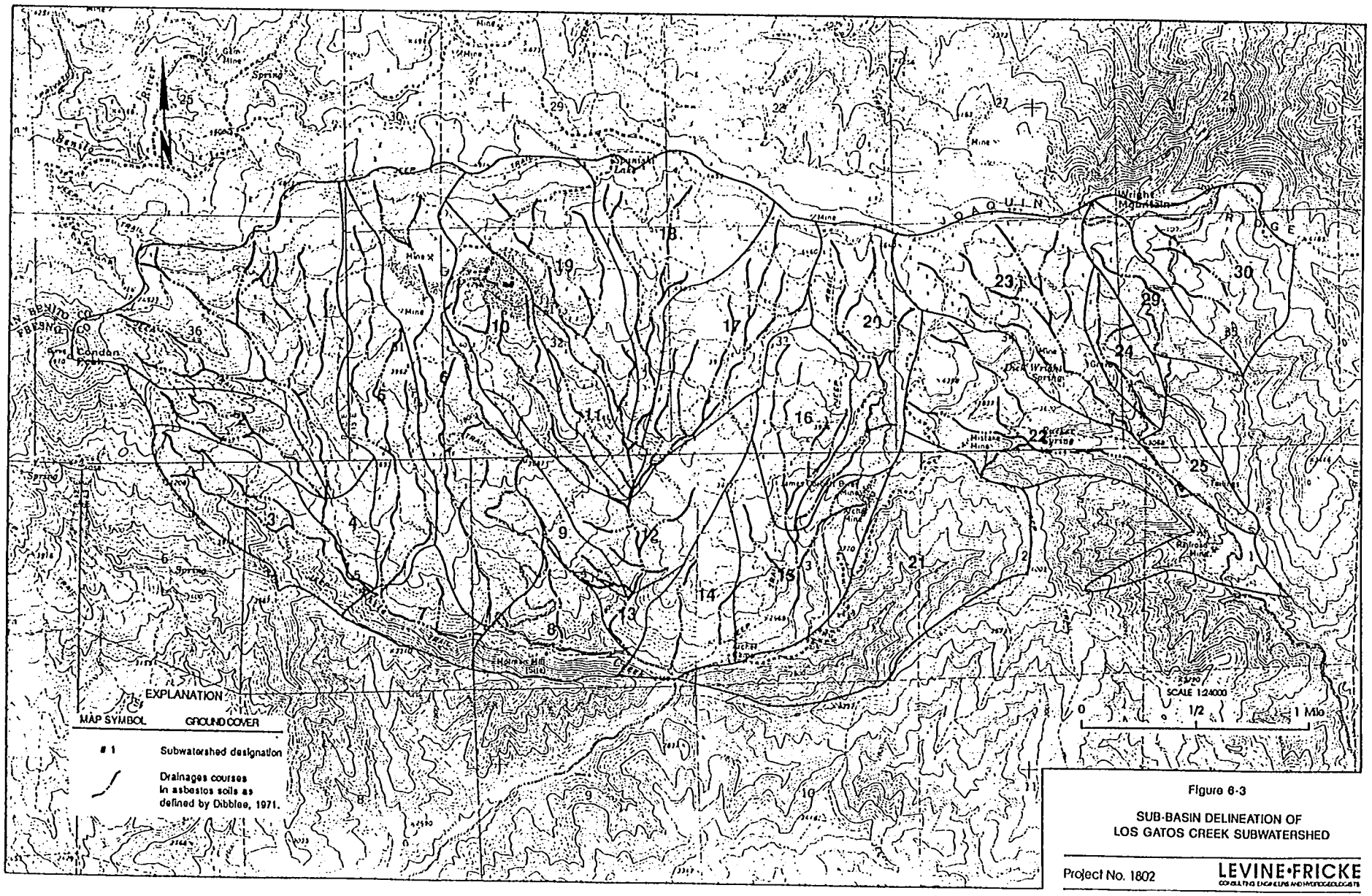


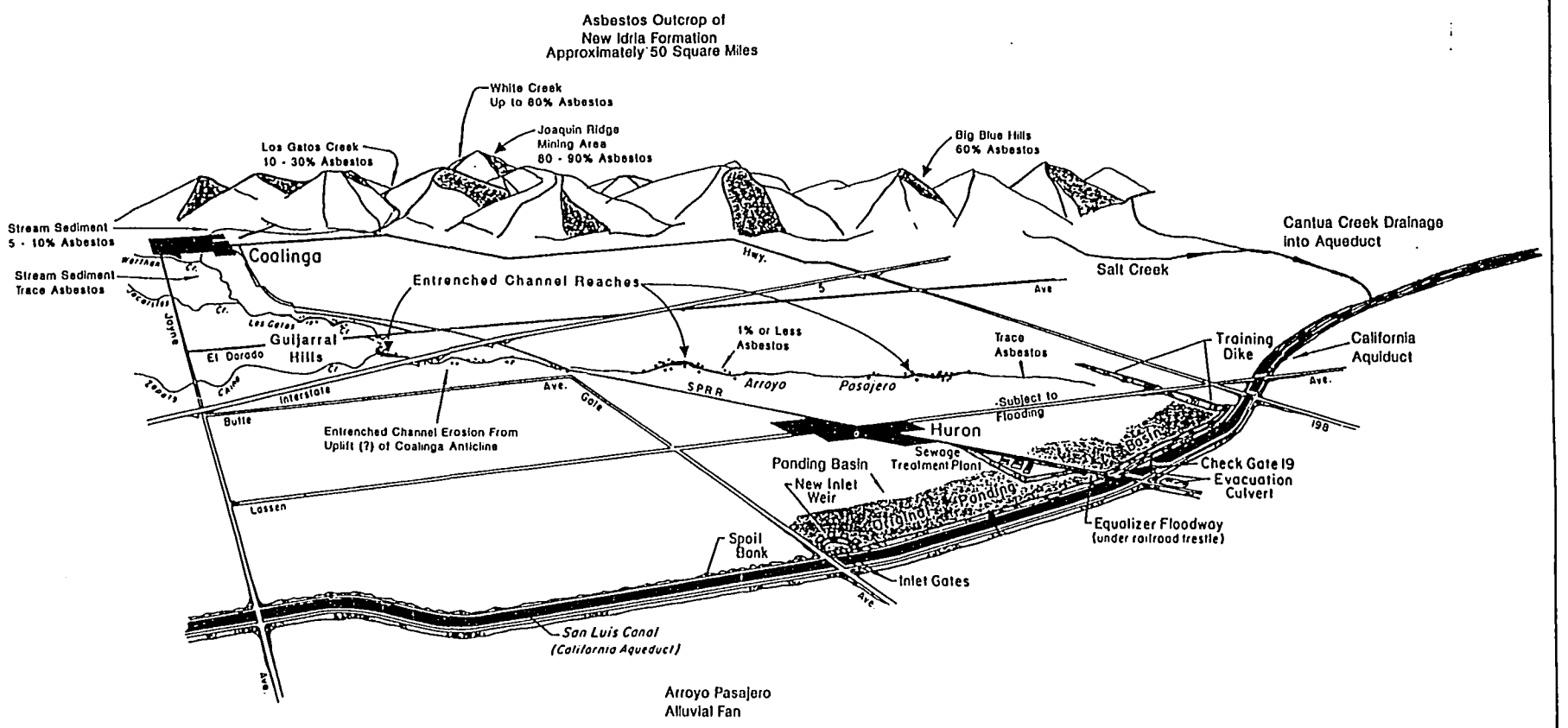
Figure 6-3

SUB-BASIN DELINEATION OF
LOS GATOS CREEK SUBWATERSHED

Project No. 1802

LEVINE•FRICKE
CONSULTING ENGINEERS AND HYDROGEOLOGISTS

Reproduced with permission of the copyright owner. Further reproduction prohibited without permission.



SOURCE: STATE OF CALIFORNIA, DEPARTMENT OF WATER RESOURCES, SAN JOAQUIN DISTRICT

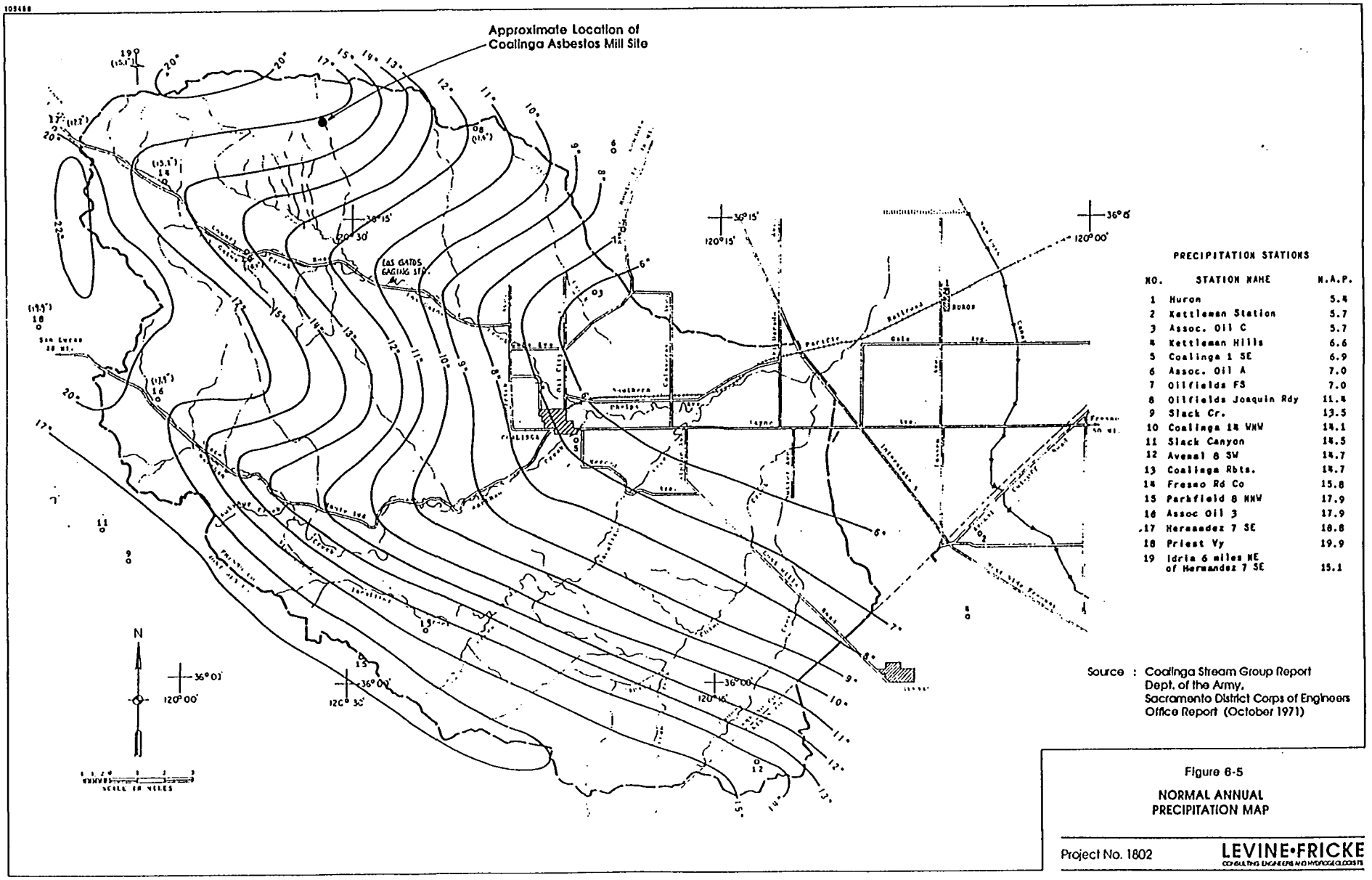
Figure 6-4

OBLIQUE PERSPECTIVE OF ARROYO PASAJERO
SEDIMENT PONDING BASIN

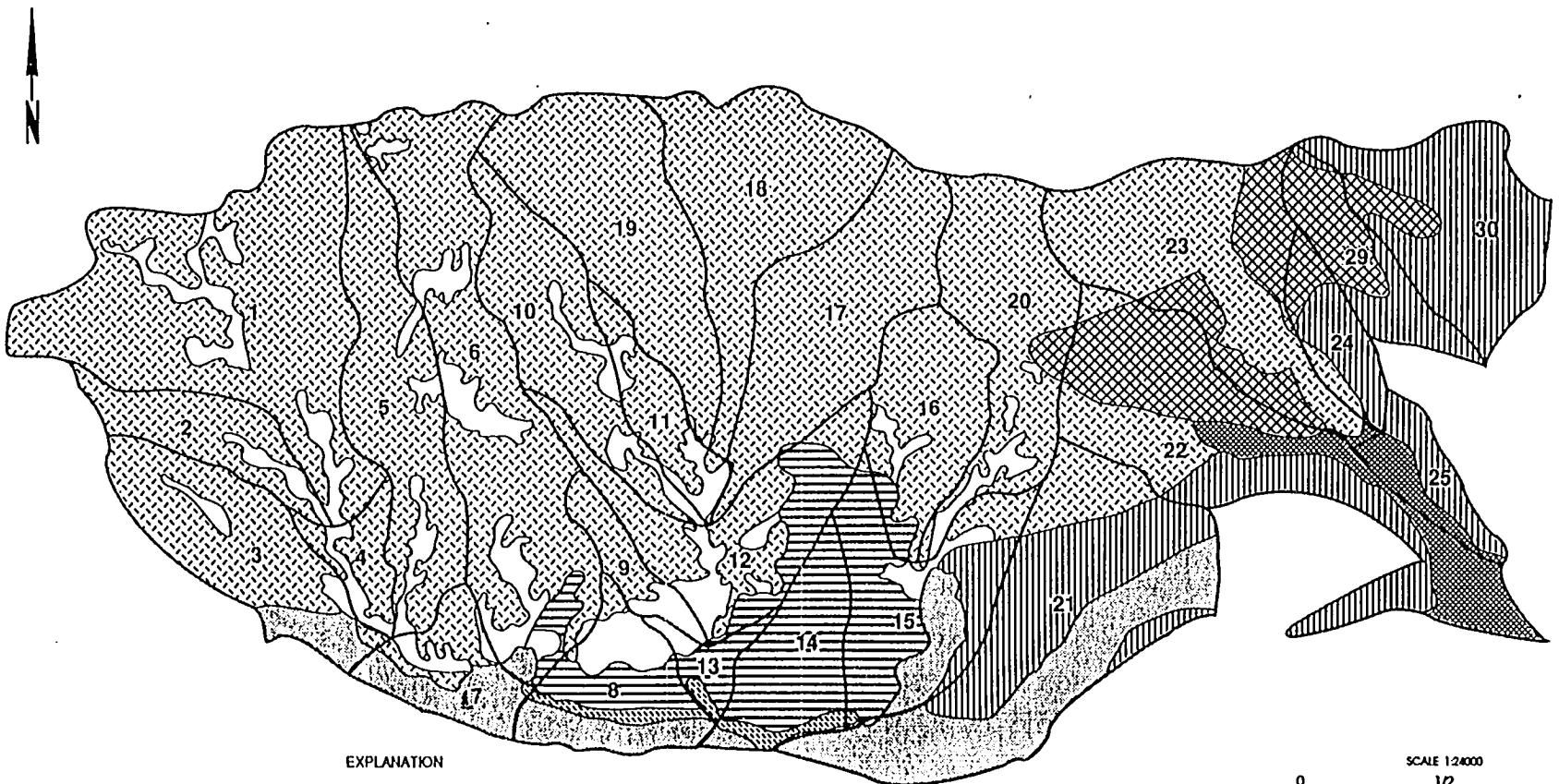
Project No. 1802

LEVINE•FRICKE
CONSULTING ENGINEERS AND HYDROGEOLOGISTS

Reproduced with permission of the copyright owner. Further reproduction prohibited without permission.



Reproduced with permission of the copyright owner. Further reproduction prohibited without permission.



EXPLANATION

MAP SYMBOL	ERODABILITY FACTOR UNADJUSTED	ERODABILITY FACTOR ADJUSTED	MATERIAL TYPE
1	0.13	0.09	SERPENTINITE SOILS *
2	0.10	0.07	MINE SURFACES*
3	0.13 0.10	0.09 0.07	ATRAVASADA GULLY COMPLEX*
4	0.16	0.08	ASBESTOS MILL TAILINGS*
5	0.12	0.09	RAILROAD MINE*

MAP SYMBOL	ERODABILITY FACTOR	MATERIAL TYPE
6	0.11	HENTINE **
7	0.28	XERORTHENTS-LILTEN **
8	0.24	FRANCISCAN**
9	0.25	ROACHA-XERORTHENTS-LILTEN **
10	0.14	BORROW SOURCE-LAND SLIDE*
11	0.32	XEROFLUVENTS **

* - "K"-FACTOR AVERAGE DERIVED FROM SPLC SOIL SAMPLES WITH SCS 1984 TRIANGULAR NOMOGRAPH

** - "K"-FACTOR TAKEN FROM UNPUBLISHED SCS SOILS REPORT.

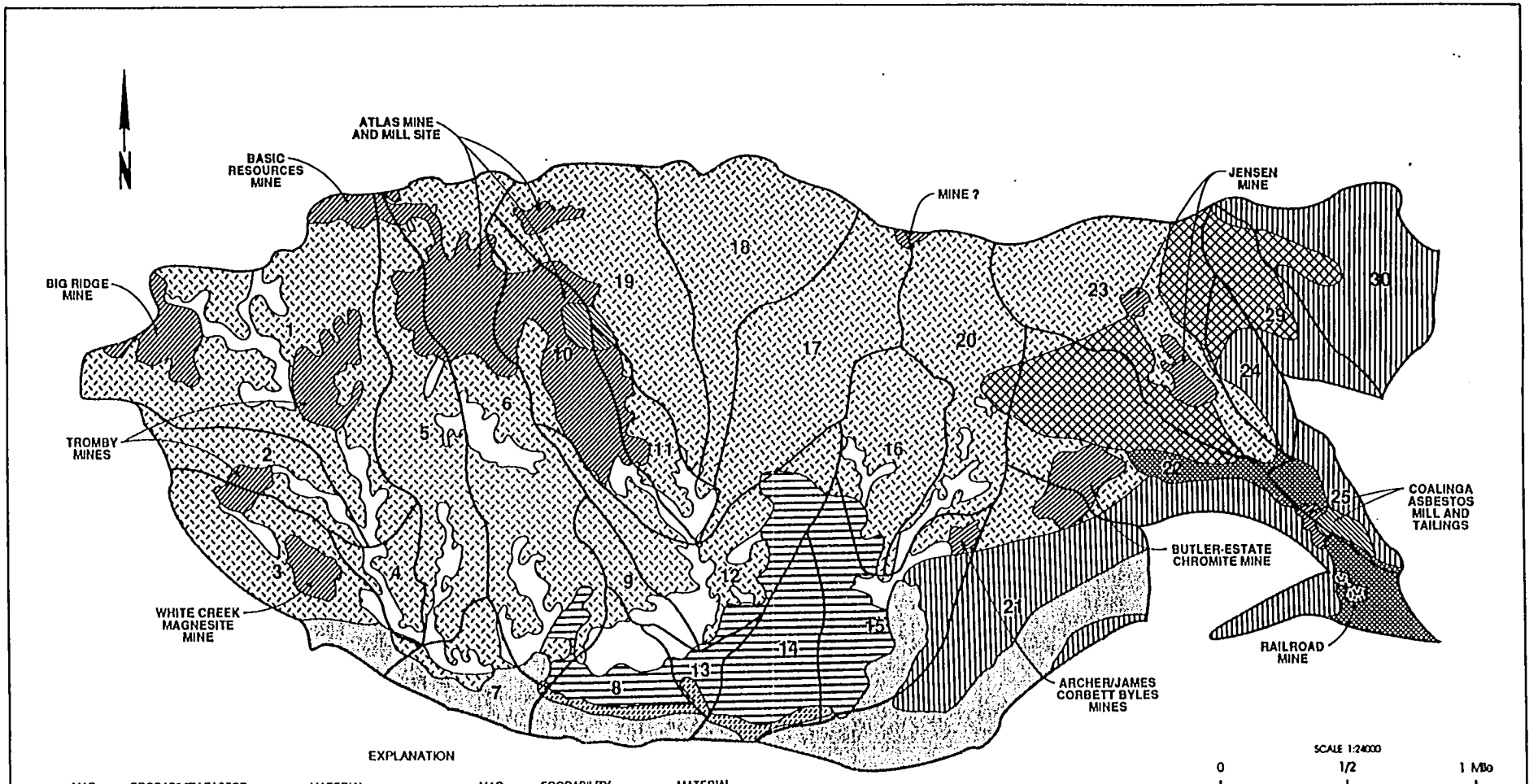
Figure 6-6

PRE-MINING ERODABILITY FACTOR "K" MUSLE & USLE MODEL INPUT PARAMETER

Project No. 1602

LEVINE•FRICKE
CONSULTING ENGINEERS AND HYDROGEOLOGISTS

Reproduced with permission of the copyright owner. Further reproduction prohibited without permission.



EXPLANATION

MAP SYMBOL	ERODABILITY FACTOR UNADJUSTED	ERODABILITY FACTOR ADJUSTED	MATERIAL TYPE
1	0.13	0.09	SERPENTINITE SOILS *
2	0.10	0.07	MINE SURFACES*
3	0.13 0.10	0.09 0.07	ATRAVASADA GULLY COMPLEX*
4	0.16	0.08	ASBESTOS MILL TAILINGS*
5	0.12	0.09	RAILROAD MINE*
6	0.11		HENTINE **
7	0.28		XERORTHENTS-LILTEN **
8	0.24		FRANCISCAN**
9	0.25		ROACHA-XERORTHENTS-LILTEN **
10	0.14		BORROW SOURCE-LAND SLIDE*
11	0.32		XEROFLUVENTS **

* - "K"-FACTOR AVERAGE DERIVED FROM SPLC SOIL SAMPLES WITH SCS 1984 TRIANGULAR NOMOGRAPH METHODOLOGY.

** - "K"-FACTOR TAKEN FROM UNPUBLISHED SCS SOILS REPORT.

Figure 6-7

POST-MINING ERODABILITY FACTOR "K" MUSLE & USLE MODEL INPUT PARAMETER

Project No. 1802

LEVINE•FRICKE
CONSULTING ENGINEERS AND HYDROGEOLOGISTS

Reproduced with permission of the copyright owner. Further reproduction prohibited without permission.

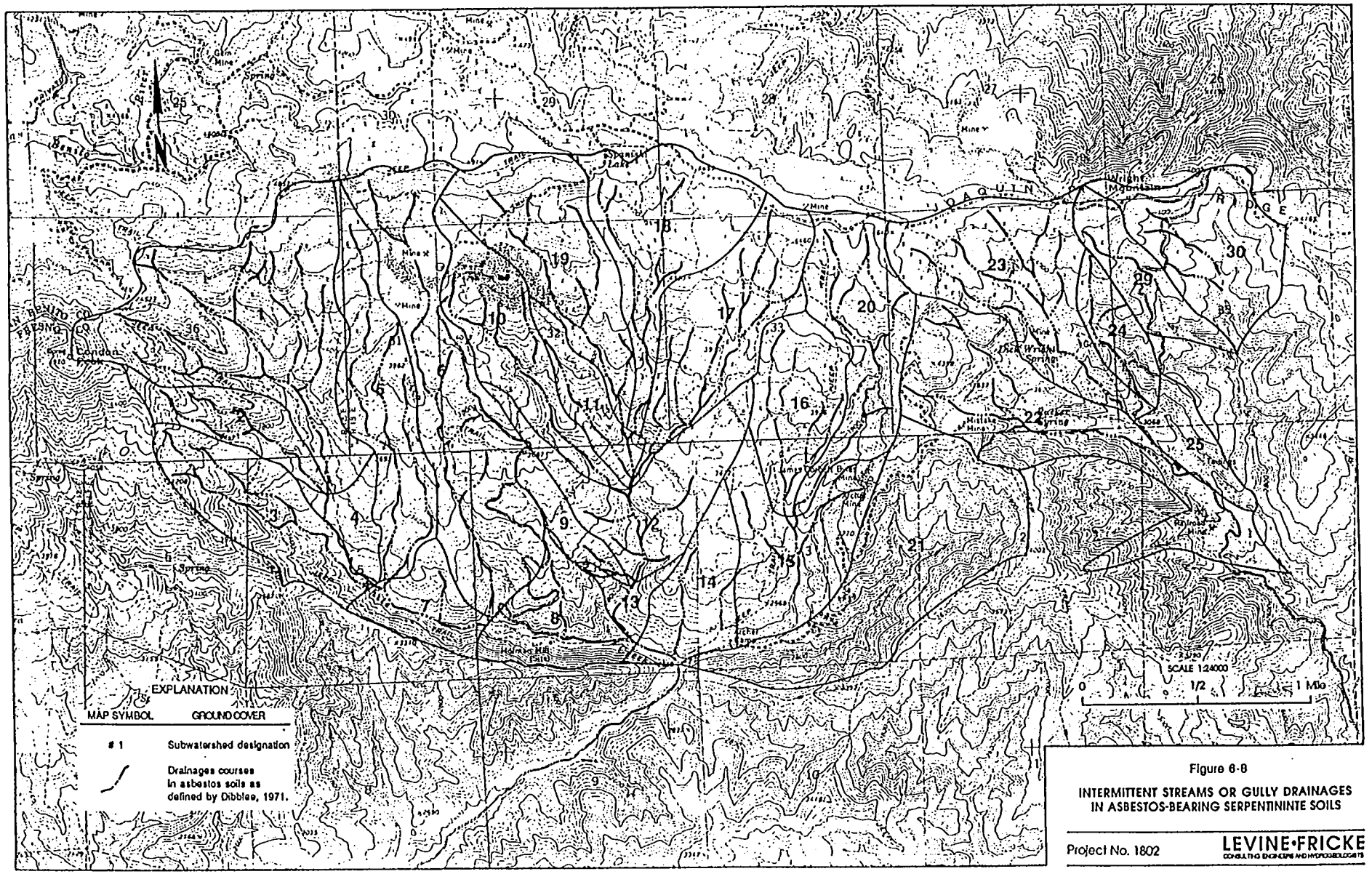


Figure 6-8

INTERMITTENT STREAMS OR GULLY DRAINAGES IN ASBESTOS-BEARING SERPENTININTE SOILS

Project No. 1802

LEVINE•FRICKE
CONSULTING ENGINEERS AND HYDROGEOLOGISTS

Reproduced with permission of the copyright owner. Further reproduction prohibited without permission.

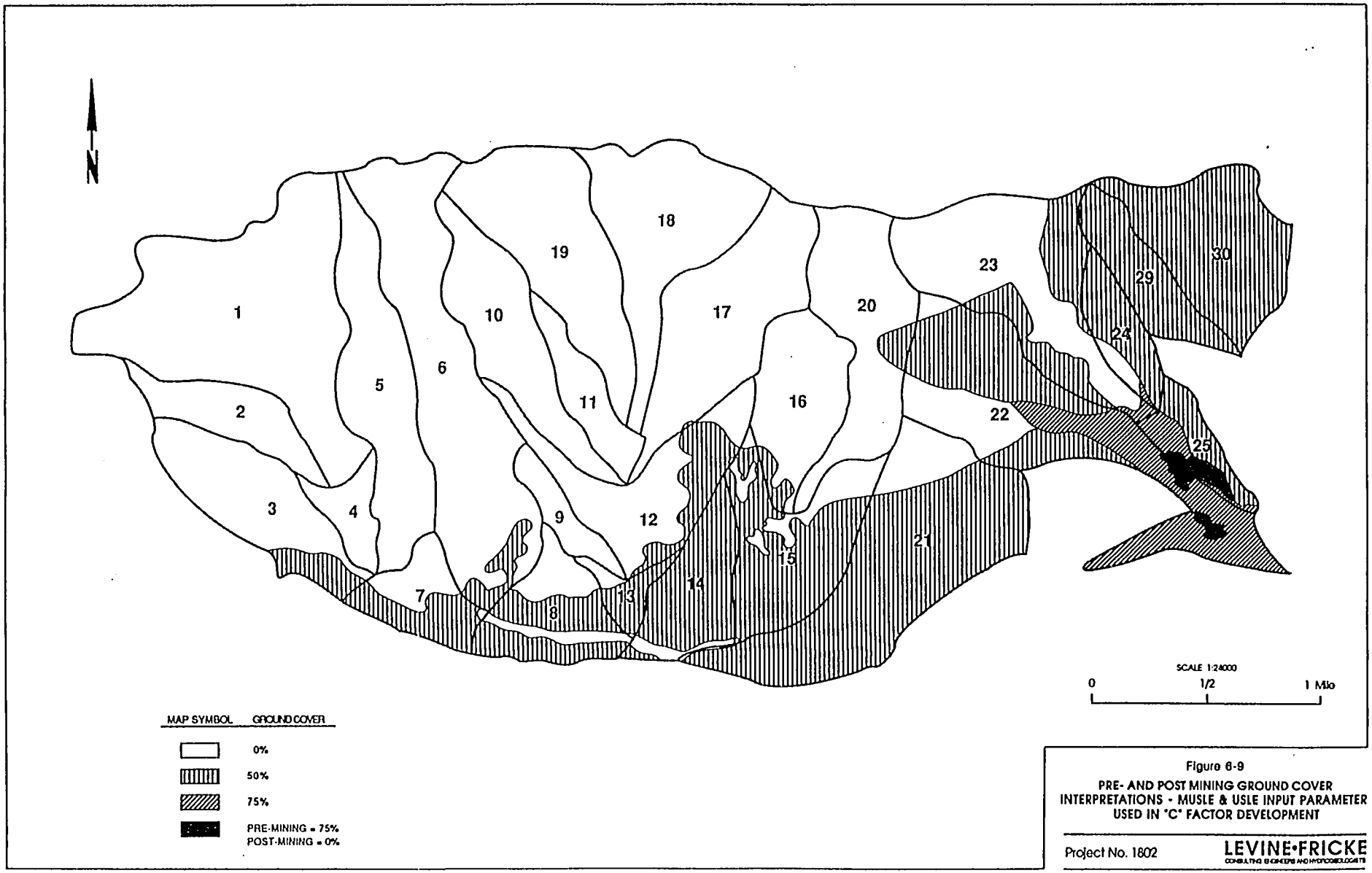


Figure 6-9

PRE- AND POST MINING GROUND COVER INTERPRETATIONS - MUSLE & USLE INPUT PARAMETER USED IN "C" FACTOR DEVELOPMENT

Project No. 1802

LEVINE•FRICKE

CONSULTING ENGINEERS AND HYDROGEOLOGISTS

Reproduced with permission of the copyright owner. Further reproduction prohibited without permission.

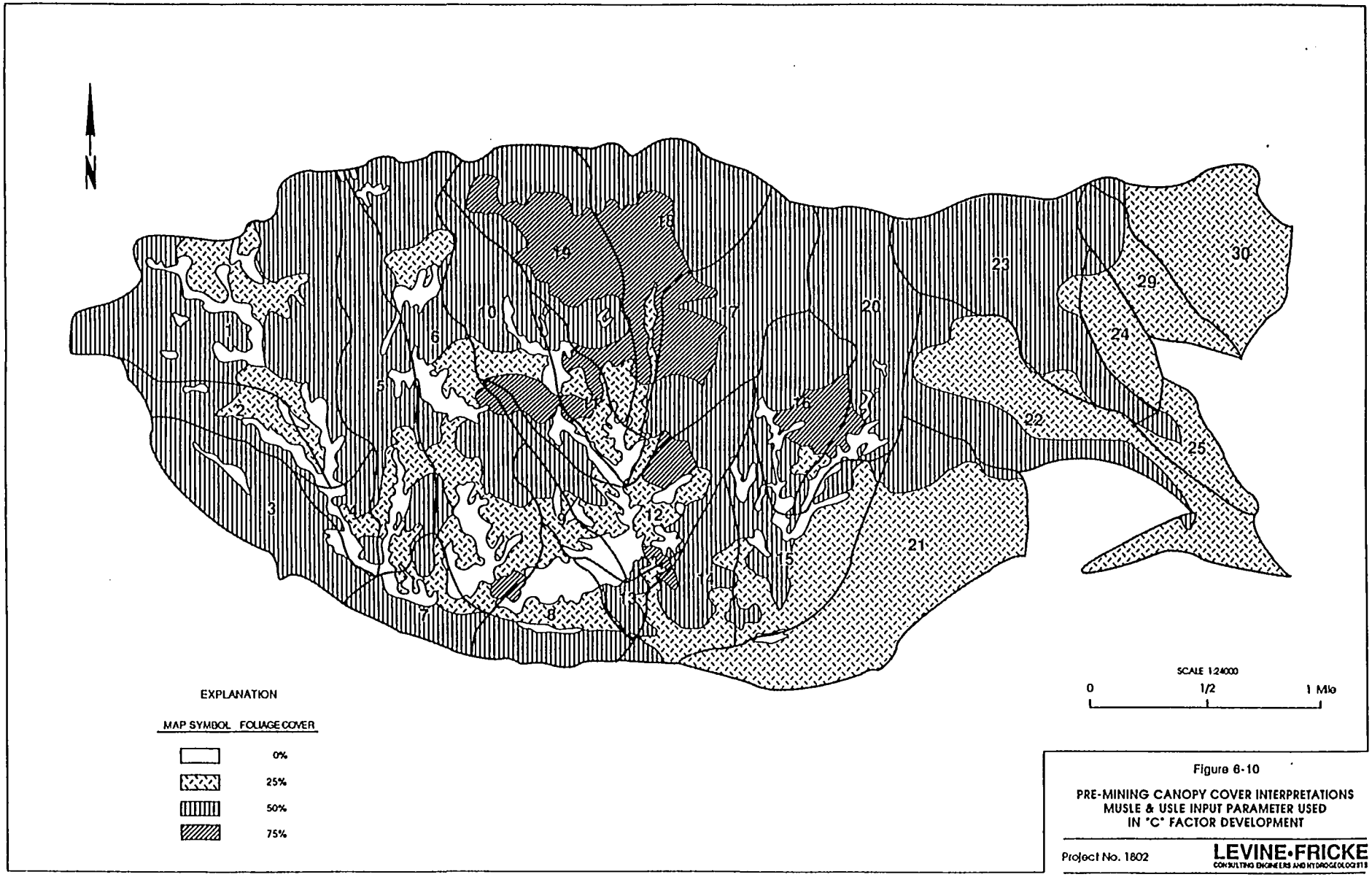


Figure 6-10

PRE-MINING CANOPY COVER INTERPRETATIONS
MUSLE & USLE INPUT PARAMETER USED
IN "C" FACTOR DEVELOPMENT

Project No. 1802

LEVINE•FRICKE
CONSULTING ENGINEERS AND HYDROGEOLOGISTS

Reproduced with permission of the copyright owner. Further reproduction prohibited without permission.

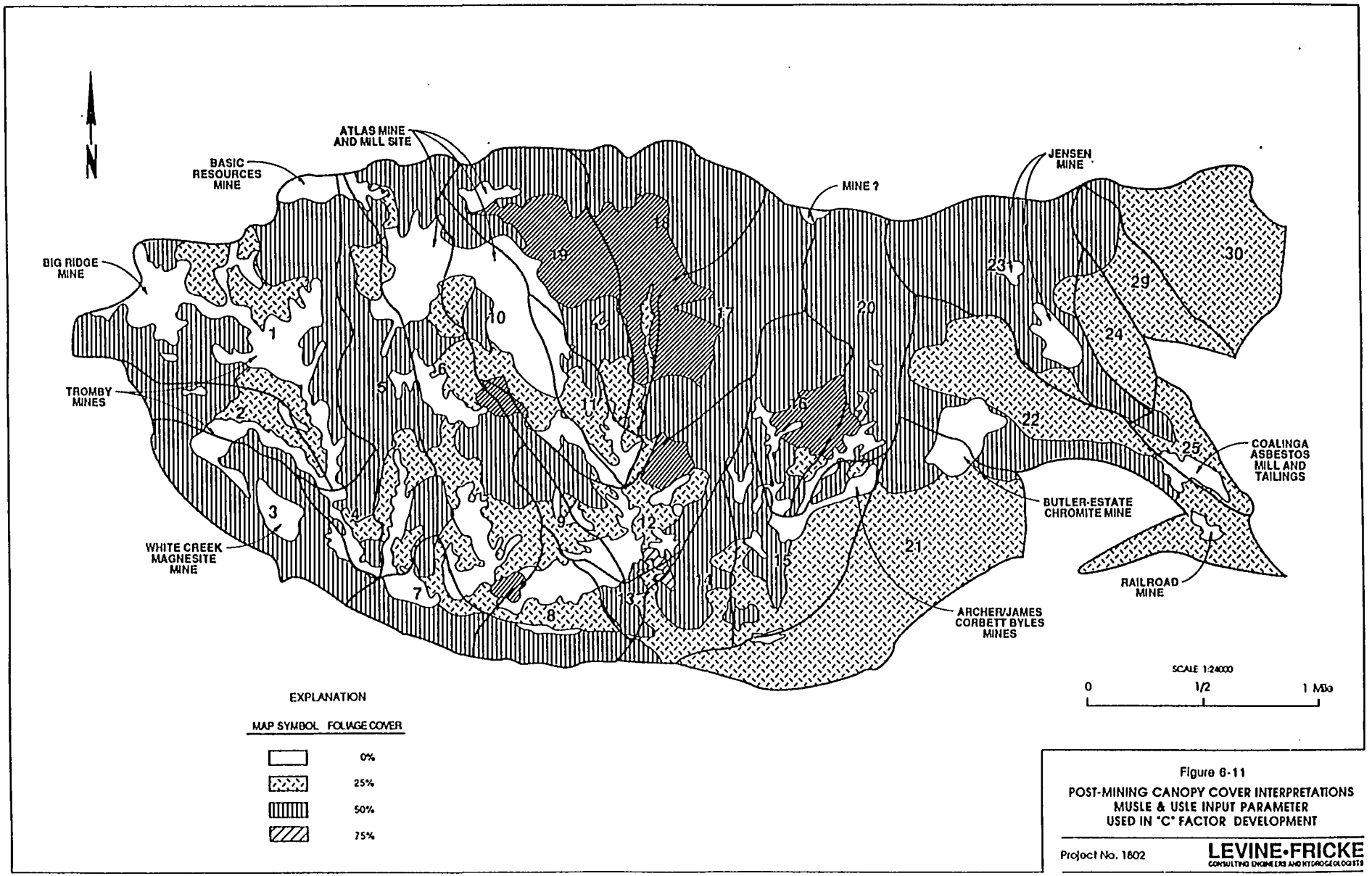


Figure 6-11
POST-MINING CANOPY COVER INTERPRETATIONS
MUSLE & USLE INPUT PARAMETER
USED IN "C" FACTOR DEVELOPMENT

Project No. 1802

LEVINE•FRICKE
CONSULTING ENGINEERS AND HYDROGEOLOGISTS

Reproduced with permission of the copyright owner. Further reproduction prohibited without permission.

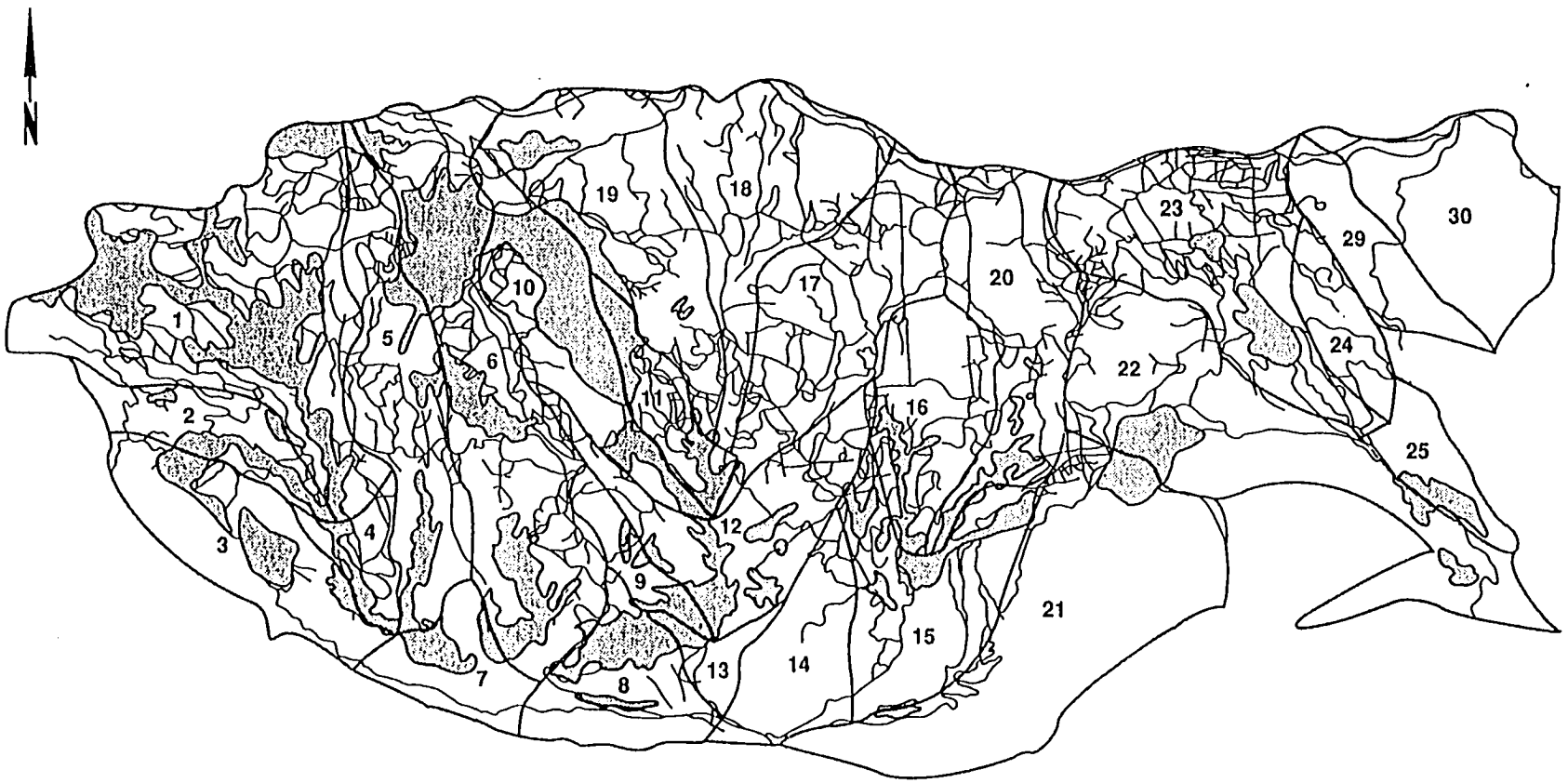


Figure 6-12

ROADS IDENTIFIED ON ASBESTOS-BEARING SOILS IN THE LOS GATOS WATERSHED

Project No. 1802

LEVINE•FRICKE

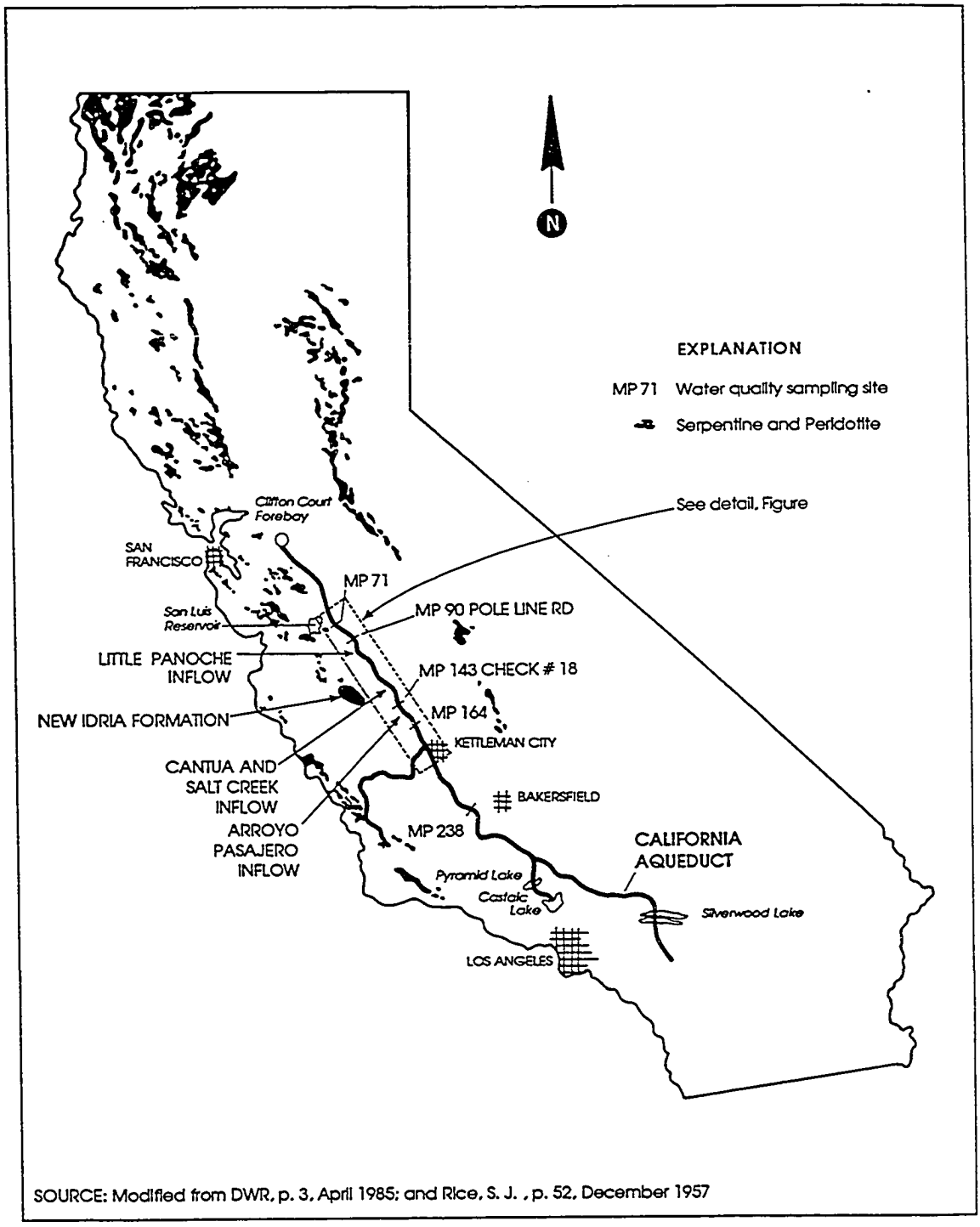


Figure 6-13: CALIFORNIA AQUEDUCT INFLOW AND SAMPLING STATIONS LOCATIONS

Reproduced with permission of the copyright owner. Further reproduction prohibited without permission.

TABLES

Reproduced with permission of the copyright owner. Further reproduction prohibited without permission.

Subdivisions of Geologic Time				Apparent Ages (millions of years before the present)
Eras	Periods	Epochs	Ages	
CENOZOIC	Quaternary	(Recent)		
		Pleistocene		* 1 — 1.8 (?)
	Tertiary	Pliocene		5
		Miocene		* 2 — 22.5
		Oligocene		38
		Eocene		55
		Paleocene		65
MESOZOIC	Cretaceous			* 3 — 141
	Jurassic			
	Triassic			195

* 1 Pliocene - Pleistocene Coast Range Orogeny. Regional faulting and folding help form Joaquin Ridge Anticline and the monoclinal structure of the western margin of Central San Joaquin Valley. Because of uplift and exposure, asbestos-containing ultramafic and sedimentary formations contribute asbestos sediments to the alluvial fans of western Fresno County.

* 2 Rapid movement along San Andreas Fault. New Idria Formations becomes emergent as a diapiric serpentine mass that forms core of Joaquin Ridge Anticline. Serpentinite mass becomes extrusive and is subject to erosion and mass wasting. Detrital serpentinite debris containing asbestos sediment as transported to the east and deposited in a shallow marine environment as the Big Blue Member of the Tambior Formation. Miocene and younger sedimentary formations in the region accumulate asbestos sediment.

* 3 Most of Central California overlain by Pacific Ocean.

Modified from Longwell, Flint, and Sanders, 1969, p.132 and F. Van Eysinga, 1983

Table 2-1 : GEOLOGIC TIME SCALE AND EMERGENCE OF THE NEW IDRIA FORMATION IN CENTRAL CALIFORNIA

Reproduced with permission of the copyright owner. Further reproduction prohibited without permission.

TABLE 5-1

SUMMARY OF NUMBER OF SAMPLES ANALYZED

Polarized Light Microscopy (PLM)	374
Transmission Electron Microscopy (TEM)	92
Particle Size Distribution	120
Organic Matter Content	49

Reproduced with permission of the copyright owner. Further reproduction prohibited without permission.

Reproduced with permission of the copyright owner. Further reproduction prohibited without permission.

Table 5-2

SOIL ASBESTOS DATA SUMMARY

Statn. No.	Sample ID Number	Sample Type	Date Samples Collected	****RESULTS FOR PLM METHOD******* MED-TOX Elongate Serpentine %	MED-TOX Chrysotile Asbestos %	McCRONE Serpentine Asbestos %	**********TOTAL ASBESTOS RESULTS FOR TEM METHOD********** MED-TOX (% Mass)	> 5 um (% Mass)	Struct. Conc. (1.0E+12 struct./g)	> 5 um Struct. Conc. (1.0E+9 struct./g)	Remarks
PC1	PC1A	LNS	16-Mar-88	3	TRACE	N/A	3	ND	4	<500	
	PC1B	STB	16-Mar-88	75	45	75	10	ND	8	<900	Blind Duplicate
	PC93B	STB	16-Mar-88	75	30	N/A	5	ND	7	<900	Blind Duplicate
	PC1C	LNS	16-Mar-88	15	5	N/A	3	ND	4	<500	
PC2	PC2A	LNS	16-Mar-88	20	5	7.5	N/A	N/A	N/A	N/A	Blind Duplicate
	PC92A	LNS	16-Mar-88	TRACE	TRACE	N/A	N/A	N/A	N/A	N/A	Blind Duplicate
	PC2B	STB	16-Mar-88	50	20	55	30	ND	3	<500	Blind Duplicate
	PC92B	STB	16-Mar-88	75	30	N/A	10	ND	4	<500	Blind Duplicate
	PC2C	MNS	16-Mar-88	TRACE	TRACE	5	N/A	N/A	N/A	N/A	Blind Duplicate
	PC92C	MNS	16-Mar-88	ND	ND	N/A	N/A	N/A	N/A	N/A	Blind Duplicate
	PC2AX	LNS	16-Mar-88	50	20	8.5	10	ND	7	<900	Blind Duplicate
	PC92AX	LNS	16-Mar-88	35	15	N/A	N/A	N/A	N/A	N/A	Blind Duplicate
PC3	PC3A	LNS	16-Mar-88	20	TRACE	N/A	N/A	N/A	N/A	N/A	
	PC3B	STB	16-Mar-88	75	30	N/A	10	ND	6	<700	
	PC3C	LNS	16-Mar-88	TRACE	ND	N/A	N/A	N/A	N/A	N/A	
PC4	PC4B	STB	24-Feb-88	60	20	N/A	N/A	N/A	N/A	N/A	
PC5	PC5B	STB	24-Feb-88	50	20	N/A	N/A	N/A	N/A	N/A	
PC6	PC6B	STB	24-Feb-88	40	10	N/A	N/A	N/A	N/A	N/A	
PC7	PC7A	LNS	24-Feb-88	40	10	N/A	N/A	N/A	N/A	N/A	
	PC7C	LNS	24-Feb-88	40	15	N/A	N/A	N/A	N/A	N/A	
PC8	PC8A	LNS	25-Feb-88	ND	ND	N/A	N/A	N/A	N/A	N/A	
	PC8C	LNS	25-Feb-88	15	5	N/A	N/A	N/A	N/A	N/A	
PC9	PC9A	LNS	25-Feb-88	10	3	N/A	N/A	N/A	N/A	N/A	

SOURCE: LEVINE-FRICKE

Reproduced with permission of the copyright owner. Further reproduction prohibited without permission.

SOIL ASBESTOS DATA SUMMARY

Statn. No.	Sample ID Number	Sample Type	Date Samples Collected	****RESULTS FOR PLM METHOD******* MED·TOX Elongate Serpentine %	MED·TOX Chrysotile Asbestos %	McCRONE Serpentine Asbestos %	**********TOTAL ASBESTOS RESULTS FOR TEM METHOD********** MED·TOX (% Mass)	> 5 um (% Mass)	Struct. Conc. (1.0E+12 struct./g)	> 5 um Struct. Conc. (1.0E+9 struct./g)	Remarks
	PC9C	LNS	25·Feb·88	50	20	N/A	N/A	N/A	N/A	N/A	
PC10	PC10A	LNS	25·Feb·88	4	2	N/A	N/A	N/A	N/A	N/A	
	PC10B	STB	25·Feb·88	12	6	N/A	N/A	N/A	N/A	N/A	
	PC10C	LNS	25·Feb·88	TRACE	TRACE	N/A	N/A	N/A	N/A	N/A	
PC11	PC11A	LNS	25·Feb·88	TRACE	TRACE	15	N/A	N/A	N/A	N/A	Blind Duplicate
	PC92A	LNS	25·Feb·88	5	2	N/A	N/A	N/A	N/A	N/A	Blind Duplicate
	PC11B	STB	25·Feb·88	70	10	77.5	N/A	N/A	N/A	N/A	Blind Duplicate
	PC92B	STB	25·Feb·88	85	45	N/A	N/A	N/A	N/A	N/A	Blind Duplicate
	PC11C	LNS	25·Feb·88	25	10	15	N/A	N/A	N/A	N/A	Blind Duplicate
	PC92C	LNS	25·Feb·88	5	2	N/A	N/A	N/A	N/A	N/A	Blind Duplicate
PC12	PC12A	LNS	24·Feb·88	TRACE	TRACE	N/A	N/A	N/A	N/A	N/A	
	PC12C	LNS	24·Feb·88	5	TRACE	N/A	N/A	N/A	N/A	N/A	
PC13	PC13B	STB	25·Feb·88	50	20	N/A	N/A	N/A	N/A	N/A	
PC14	PC14A	MNS	24·Feb·88	TRACE	TRACE	7.5	N/A	N/A	N/A	N/A	Blind Duplicate
	PC91A	MNS	24·Feb·88	5	2	N/A	N/A	N/A	N/A	N/A	Blind Duplicate
	PC14B	STB	24·Feb·88	80	25	67.5	N/A	N/A	N/A	N/A	Blind Duplicate
	PC91B	STB	24·Feb·88	75	35	N/A	N/A	N/A	N/A	N/A	Blind Duplicate
	PC14C	LNS	24·Feb·88	4	2	5	N/A	N/A	N/A	N/A	Blind Duplicate
	PC91C	LNS	24·Feb·88	5	2	N/A	N/A	N/A	N/A	N/A	Blind Duplicate
PC15	PC15A	MNS	15·Mar·88	ND	ND	N/A	N/A	N/A	N/A	N/A	
	PC15B	STB	15·Mar·88	5	TRACE	N/A	N/A	N/A	N/A	N/A	
	PC15C	LNS	15·Mar·88	5	TRACE	N/A	N/A	N/A	N/A	N/A	
PC16	PC16A	MNS	15·Mar·88	ND	ND	N/A	N/A	N/A	N/A	N/A	
	PC16B	STB	15·Mar·88	50	30	N/A	N/A	N/A	N/A	N/A	
	PC16C	LNS	15·Mar·88	3	2	N/A	N/A	N/A	N/A	N/A	

Reproduced with permission of the copyright owner. Further reproduction prohibited without permission.

SOIL ASBESTOS DATA SUMMARY

Statn. No.	Sample ID Number	Sample Type	Date Samples Collected	****RESULTS FOR PLM METHOD******* MED-TOX Elongate Serpentine %	MED-TOX Chrysotile Asbestos %	McCRONE Serpentine Asbestos %	**********TOTAL ASBESTOS RESULTS FOR TEM METHOD********** MED-TOX (% Mass)	> 5 um (% Mass)	Struct. Conc. (1.0E+12 struct./g)	> 5 um Struct. Conc. (1.0E+9 struct./g)	Remarks
PC17	PC17B	STB	15-Mar-88	60	25	N/A	N/A	N/A	N/A	N/A	
PC18	PC18A	MNS	15-Mar-88	4	TRACE	N/A	N/A	N/A	N/A	N/A	
	PC18C	LNS	15-Mar-88	5	2	N/A	N/A	N/A	N/A	N/A	
PC19	PC19A	MNS	15-Mar-88	2	TRACE	N/A	N/A	N/A	N/A	N/A	
	PC19C	MNS	15-Mar-88	TRACE	TRACE	N/A	N/A	N/A	N/A	N/A	
PC20	PC20A	MNS	15-Mar-88	25	5	37.5	N/A	N/A	N/A	N/A	Blind Duplicate
	PC91A	MNS	15-Mar-88	3	TRACE	N/A	N/A	N/A	N/A	N/A	Blind Duplicate
	PC20B	STB	15-Mar-88	70	25	N/A	N/A	N/A	N/A	N/A	Blind Duplicate
	PC91B	STB	15-Mar-88	70	30	N/A	N/A	N/A	N/A	N/A	Blind Duplicate
	PC20C	MNS	15-Mar-88	2	TRACE	30	N/A	N/A	N/A	N/A	
	PC91C	MNS	15-Mar-88	TRACE	TRACE	N/A	N/A	N/A	N/A	N/A	
PC41	PC41A	LNS	24-Feb-88	70	45	75	10	ND	5	<600	Blind Duplicate
	PC93A	LNS	24-Feb-88	30	25	N/A	30	ND	4	<600	Blind Duplicate
	PC41B	STB	24-Feb-88	80	30	62.5	12	ND	4	<500	Blind Duplicate
	PC93B	STB	24-Feb-88	50	20	N/A	4	ND	2	<300	Blind Duplicate
PC42	PC42B	STB	24-Feb-88	30	10	N/A	N/A	N/A	N/A	N/A	
PC43	PC43B	STB	24-Feb-88	50	20	N/A	N/A	N/A	N/A	N/A	
PC56	PC56	STB	19-Sep-88	50	20	N/A	N/A	N/A	N/A	N/A	
PC57	PC57	STB	19-Sep-88	50	15	N/A	N/A	N/A	N/A	N/A	
PC58	PC58	STB	19-Sep-88	50	15	N/A	N/A	N/A	N/A	N/A	
PC59	PC59	STB	19-Sep-88	50	20	N/A	N/A	N/A	N/A	N/A	
BS1	BS1	LNS	04-Feb-88	2	TRACE	N/A	N/A	N/A	N/A	N/A	
BS2	BS2	LNS	04-Feb-88	TRACE	TRACE	N/A	N/A	N/A	N/A	N/A	
BS3	BS3	LNS	29-Jan-88	TRACE	TRACE	N/A	N/A	N/A	N/A	N/A	

Reproduced with permission of the copyright owner. Further reproduction prohibited without permission.

SOIL ASBESTOS DATA SUMMARY

Statn. No.	Sample ID Number	Sample Type	Date Samples Collected	****RESULTS FOR PLM METHOD******* MED-TOX Elongate Serpentine %	MED-TOX Chrysotile Asbestos %	McCRONE Serpentine Asbestos %	**********TOTAL ASBESTOS RESULTS FOR TEM METHOD********** MED-TOX (% Mass)	> 5 um (% Mass)	Struct. Conc. (1.0E+12 struct./g)	> 5 um Struct. Conc. (1.0E+9 struct./g)	Remarks
BS4	BS4	LNS	29-Jan-88	TRACE	ND	N/A	N/A	N/A	N/A	N/A	
BP5	BP5 1.5B	LNS	1-Jul-87	2	1	20	30	ND	8	<800	
	BP5 8-10B	LNS	1-Jul-87	TRACE	TRACE	30	30	ND	6	<700	
BP6	BP6 1.0	LNS	1-Jul-87	TRACE	ND	10	N/A	N/A	N/A	N/A	
BS7	BS7	LNS	29-Jan-88	TRACE	TRACE	N/A	N/A	N/A	N/A	N/A	
BS8	BS8	LNS	29-Jan-88	TRACE	ND	N/A	N/A	N/A	N/A	N/A	
BS9	BS9	LNS	29-Jan-88	TRACE	TRACE	10	N/A	N/A	N/A	N/A	Blind Duplicate
	BS81	LNS	29-Jan-88	6	1	N/A	N/A	N/A	N/A	N/A	Blind Duplicate
BS10	BS10	LNS	29-Jan-88	3	TRACE	N/A	N/A	N/A	N/A	N/A	
BS11	BS11	LNS	28-Jan-88	1	TRACE	N/A	N/A	N/A	N/A	N/A	
BS12	BS12	LNS	28-Jan-88	4	2	N/A	N/A	N/A	N/A	N/A	
BP13	BP13 1.5-2.5	LNS	1-Jul-87	TRACE	TRACE	N/A	N/A	N/A	N/A	N/A	
	BP13 4-5	LNS	1-Jul-87	TRACE	TRACE	N/A	N/A	N/A	N/A	N/A	
	BP13 8-10	LNS	1-Jul-87	TRACE	TRACE	N/A	N/A	N/A	N/A	N/A	
BP14	BP14 3-4B	LNS	1-Jul-87	TRACE	TRACE	N/A	6	ND	3	<400	
	BP14 11-12B	LNS	1-Jul-87	1	TRACE	22.5	30	ND	9	<900	
	BP14 13.3B	LNS	1-Jul-87	TRACE	ND	<2	N/A	N/A	N/A	N/A	
BP15	BP15 3-4	LNS	1-Jul-87	TRACE	TRACE	14	N/A	N/A	N/A	N/A	
	BP15 10-11	LNS	1-Jul-87	TRACE	TRACE	5.5	N/A	N/A	N/A	N/A	
BS16	BS16	LNS	23-Jan-88	ND	ND	N/A	N/A	N/A	N/A	N/A	
BS17	BS17	LNS	28-Jan-88	TRACE	TRACE	N/A	N/A	N/A	N/A	N/A	
BP18	BP18 3-4	LNS	1-Jul-87	3	TRACE	N/A	N/A	N/A	N/A	N/A	

Reproduced with permission of the copyright owner. Further reproduction prohibited without permission.

SOIL ASBESTOS DATA SUMMARY

Statn. No.	Sample ID Number	Sample Type	Date Samples Collected	****RESULTS FOR PLM METHOD******* MED-TOX Elongate Serpentine %	MED-TOX Chrysotile Asbestos %	McCRONE Serpentine Asbestos %	**********TOTAL ASBESTOS RESULTS FOR TEM METHOD********** MED-TOX (% Mass)	> 5 um (% Mass)	Struct. Conc. (1.0E+12 struct./g)	> 5 um Struct. Conc. (1.0E+9 struct./g)	Remarks
	BP18 8-9	LNS	1-Jul-87	7	TRACE	N/A	N/A	N/A	N/A	N/A	
BS19	BS19	LNS	23-Jan-88	TRACE	ND	N/A	N/A	N/A	N/A	N/A	
BS20	BS20	LNS	28-Jan-88	TRACE	TRACE	N/A	N/A	N/A	N/A	N/A	
BS21	BS21	LNS	28-Jan-88	TRACE	TRACE	N/A	N/A	N/A	N/A	N/A	
BS22	BS22	LNS	28-Jan-88	2	TRACE	N/A	N/A	N/A	N/A	N/A	
BS23	BS23	LNS	28-Jan-88	2	TRACE	N/A	N/A	N/A	N/A	N/A	
BS24	BS24	LNS	12-Feb-88	5	TRACE	N/A	N/A	N/A	N/A	N/A	Blind Duplicate
	BS88	LNS	12-Feb-88	10	5	N/A	N/A	N/A	N/A	N/A	Blind Duplicate
BS25	BS25	LNS	12-Feb-88	2	1	N/A	N/A	N/A	N/A	N/A	
BS26	BS26	LNS	12-Feb-88	TRACE	TRACE	N/A	N/A	N/A	N/A	N/A	
BS27	BS27	LNS	12-Feb-88	10	5	N/A	N/A	N/A	N/A	N/A	
BS28	BS28	LNS	12-Feb-88	10	3	N/A	N/A	N/A	N/A	N/A	
BS29	BS29	LNS	12-Feb-88	10	5	30	N/A	N/A	N/A	N/A	
BS30	BS30	LNS	12-Feb-88	5	3	N/A	4	ND	2	<400	
							2	ND	3	<500	Lab Replicate
BS31	BS31	LNS	12-Feb-88	10	3	N/A	N/A	N/A	N/A	N/A	
BS32	BS32	LNS	12-Feb-88	3	TRACE	N/A	N/A	N/A	N/A	N/A	
BS33	BS33	LNS	29-Jan-88	2	1	N/A	N/A	N/A	N/A	N/A	
BS34	BS34	LNS	29-Jan-88	TRACE	ND	N/A	N/A	N/A	N/A	N/A	
BP35	BP35/1-2	LNS	01-Jul-87	TRACE	TRACE	N/A	N/A	N/A	N/A	N/A	
	BP35/3-4	LNS	01-Jul-87	TRACE	TRACE	N/A	N/A	N/A	N/A	N/A	
AL1	AL1	RD	29-Jan-88	TRACE	TRACE	N/A	N/A	N/A	N/A	N/A	

Reproduced with permission of the copyright owner. Further reproduction prohibited without permission.

SOIL ASBESTOS DATA SUMMARY

Statn. No.	Sample ID Number	Sample Type	Date Samples Collected	****RESULTS FOR PLM METHOD******* MED-TOX Elongate Serpentine %	MED-TOX Chrysotile Asbestos %	McCRONE Serpentine Asbestos %	**********TOTAL ASBESTOS RESULTS FOR TEM METHOD********** MED-TOX (% Mass)	> 5 um (% Mass)	Struct. Conc. (1.0E+12 struct./g)	> 5 um Struct. Conc. (1.0E+9 struct./g)	Remarks
AL2	AL2A	RD	28-Jan-88	TRACE	TRACE	N/A	N/A	N/A	N/A	N/A	
	AL2B	RD	28-Jan-88	1	TRACE	N/A	N/A	N/A	N/A	N/A	
AL3	AL3A	RD	28-Jan-88	TRACE	TRACE	N/A	N/A	N/A	N/A	N/A	
	AL3B	RD	28-Jan-88	TRACE	ND	N/A	N/A	N/A	N/A	N/A	
AL4	AL4A	LNS	4-Feb-88	TRACE	TRACE	N/A	N/A	N/A	N/A	N/A	
	AL4B	AO	4-Feb-88	80	60	>85	N/A	N/A	N/A	N/A	Blind Duplicate
	AL82	AO	4-Feb-88	85	60	N/A	N/A	N/A	N/A	N/A	Blind Duplicate
AL5	AL5A	LNS	4-Feb-88	2	TRACE	N/A	N/A	N/A	N/A	N/A	
	AL5B	AO	4-Feb-88	80	30	N/A	N/A	N/A	N/A	N/A	
AL6	AL6A	LNS	4-Feb-88	20	5	N/A	N/A	N/A	N/A	N/A	
	AL6B	CO	4-Feb-88	40	20	N/A	N/A	N/A	N/A	N/A	
AL7	AL7	LNS	4-Feb-88	10	3	N/A	N/A	N/A	N/A	N/A	
AL8	AL8	CMT	4-Feb-88	2	TRACE	N/A	N/A	N/A	N/A	N/A	
AL9	AL9	CMT	4-Feb-88	15	5	N/A	N/A	N/A	N/A	N/A	
AL10	AL10	LNS	5-Feb-88	TRACE	TRACE	N/A	N/A	N/A	N/A	N/A	
AL11	AL11A	LNS	5-Feb-88	TRACE	TRACE	2	N/A	N/A	N/A	N/A	Blind Duplicate
	AL84	LNS	5-Feb-88	TRACE	TRACE	N/A	N/A	N/A	N/A	N/A	Blind Duplicate
	AL11B	CMT	5-Feb-88	15	5	N/A	N/A	N/A	N/A	N/A	
AL12	AL12A	LNS	5-Feb-88	4	1	N/A	N/A	N/A	N/A	N/A	
	AL12B	CMT	5-Feb-88	TRACE	TRACE	N/A	N/A	N/A	N/A	N/A	
AL13	AL13A	LNS	5-Feb-88	TRACE	TRACE	N/A	N/A	N/A	N/A	N/A	
	AL13B	CMT	5-Feb-88	3	TRACE	N/A	N/A	N/A	N/A	N/A	
AL14	AL14A	LNS	5-Feb-88	5	2	N/A	N/A	N/A	N/A	N/A	

Reproduced with permission of the copyright owner. Further reproduction prohibited without permission.

SOIL ASBESTOS DATA SUMMARY

Statn. No.	Sample ID Number	Sample Type	Date Samples Collected	****RESULTS FOR PLM METHOD******* MED-TOX Elongate Serpentine %	MED-TOX Chrysotile Asbestos %	McCRONE Serpentine Asbestos %	**********TOTAL ASBESTOS RESULTS FOR TEM METHOD********** MED-TOX (% Mass)	> 5 um (% Mass)	Struct. Conc. (1.0E+12 struct./g)	> 5 um Struct. Conc. (1.0E+9 struct./g)	Remarks
	AL14B	CMT	5-Feb-88	5	2	N/A	N/A	N/A	N/A	N/A	
AL15	AL15A	LNS	5-Feb-88	1	TRACE	N/A	N/A	N/A	N/A	N/A	
	AL15B	CMT	5-Feb-88	10	5	N/A	N/A	N/A	N/A	N/A	
AL16	AL16A	CMT	5-Feb-88	70	30	N/A	N/A	N/A	N/A	N/A	
	AL16B	LNS	5-Feb-88	TRACE	TRACE	N/A	0.5	ND	0.04	<60	
AL17	AL17A	LNS	19-Feb-88	40	30	55	N/A	N/A	N/A	N/A	Blind Duplicate
	AL85A	LNS	19-Feb-88	55	15	N/A	N/A	N/A	N/A	N/A	Blind Duplicate
	AL17B	AMT	18-Feb-88	65	25	>80	N/A	N/A	N/A	N/A	Blind Duplicate
	AL85B	AMT	18-Feb-88	95	50	N/A	N/A	N/A	N/A	N/A	Blind Duplicate
AL18	AL18A	LNS	19-Feb-88	40	25	45	N/A	N/A	N/A	N/A	Blind Duplicate
	AL86A	LNS	19-Feb-88	35	10	N/A	N/A	N/A	N/A	N/A	Blind Duplicate
	AL18B	AMT	18-Feb-88	50	25	>80	N/A	N/A	N/A	N/A	Blind Duplicate
	AL86B	AMT	18-Feb-88	85	45	N/A	N/A	N/A	N/A	N/A	Blind Duplicate
AL19	AL19A	LNS	19-Feb-88	10	5	N/A	20	ND	5	<600	
	AL19B	AMT	18-Feb-88	40	20	N/A	200	ND	2	<500	
AL20	AL20A	MNS	19-Feb-88	10	5	N/A	N/A	N/A	N/A	N/A	
	AL20B	AMT	18-Feb-88	45	20	N/A	N/A	N/A	N/A	N/A	
AL21	AL21A	MNS	18-Feb-88	3	1	N/A	N/A	N/A	N/A	N/A	
	AL21B	AMT	18-Feb-88	35	20	N/A	N/A	N/A	N/A	N/A	
Al22	AL22A	MNS	18-Feb-88	15	5	27.5	N/A	N/A	N/A	N/A	Blind Duplicate
	AL87A	MNS	18-Feb-88	30	10	N/A	N/A	N/A	N/A	N/A	Blind Duplicate
	AL22B	AMT	18-Feb-88	75	25	52.5	N/A	N/A	N/A	N/A	Blind Duplicate
	AL87B	AMT	18-Feb-88	80	40	N/A	N/A	N/A	N/A	N/A	Blind Duplicate
AL23	AL23A	MNS	18-Feb-88	15	5	N/A	N/A	N/A	N/A	N/A	

Reproduced with permission of the copyright owner. Further reproduction prohibited without permission.

SOIL ASBESTOS DATA SUMMARY

Statn. No.	Sample ID Number	Sample Type	Date Samples Collected	****RESULTS FOR PLM METHOD******* MED-TOX Elongate Serpentine %	MED-TOX Chrysotile Asbestos %	McCRONE Serpentine Asbestos %	**********TOTAL ASBESTOS RESULTS FOR TEM METHOD********** MED-TOX (% Mass)	> 5 um (% Mass)	Struct. Conc. (1.0E+12 struct./g)	> 5 um Struct. Conc. (1.0E+9 struct./g)	Remarks
	AL23B	MNS	18-Feb-88	70	20	N/A	N/A	N/A	N/A	N/A	
AL24	AL24A	MNS	18-Feb-88	20	15	22.5	N/A	N/A	N/A	N/A	Blind Duplicate
	AL88A	MNS	18-Feb-88	35	15	N/A	N/A	N/A	N/A	N/A	Blind Duplicate
	AL24B	AMT	18-Feb-88	55	20	72.5	N/A	N/A	N/A	N/A	Blind Duplicate
	AL88B	AMT	18-Feb-88	80	40	N/A	N/A	N/A	N/A	N/A	Blind Duplicate
AL25	AL25A	MNS	18-Feb-88	TRACE	TRACE	N/A	N/A	N/A	N/A	N/A	
	AL25B	AMT	18-Feb-88	75	40	N/A	N/A	N/A	N/A	N/A	
AL26	AL26A	MNS	18-Feb-88	30	5	N/A	N/A	N/A	N/A	N/A	
	AL26B	AMT	18-Feb-88	90	60	N/A	N/A	N/A	N/A	N/A	
AL27	AL27A	MNS	13-Feb-88	TRACE	TRACE	N/A	N/A	N/A	N/A	N/A	
	AL27B	AMT	13-Feb-88	85	50	N/A	N/A	N/A	N/A	N/A	
AL28	AL28A	MNS	13-Feb-88	TRACE	ND	N/A	N/A	N/A	N/A	N/A	
	AL28B	AMT	13-Feb-88	80	45	N/A	N/A	N/A	N/A	N/A	
AL29	AL29A	MNS	13-Feb-88	TRACE	TRACE	N/A	N/A	N/A	N/A	N/A	
	AL29B	AMT	13-Feb-88	85	50	N/A	N/A	N/A	N/A	N/A	
AL30	AL30A	MNS	13-Feb-88	TRACE	TRACE	N/A	N/A	N/A	N/A	N/A	
	AL30B	AMT	13-Feb-88	85	55	N/A	N/A	N/A	N/A	N/A	
AL31	AL31A	MNS	13-Feb-88	TRACE	TRACE	2	N/A	N/A	N/A	N/A	Blind Duplicate
	AL85A	MNS	13-Feb-88	TRACE	TRACE	N/A	N/A	N/A	N/A	N/A	Blind Duplicate
	AL31B	AMT	13-Feb-88	50	20	>80	N/A	N/A	N/A	N/A	Blind Duplicate
	AL85B	AMT	13-Feb-88	100	70	N/A	N/A	N/A	N/A	N/A	Blind Duplicate
AL32	AL32A	MNS	13-Feb-88	TRACE	TRACE	N/A	N/A	N/A	N/A	N/A	
	AL32B	STB	13-Feb-88	35	10	N/A	N/A	N/A	N/A	N/A	
AL33	AL33	LNS	28-Jan-88	1.5	1	N/A	N/A	N/A	N/A	N/A	

Reproduced with permission of the copyright owner. Further reproduction prohibited without permission.

SOIL ASBESTOS DATA SUMMARY

Statn. No.	Sample ID Number	Sample Type	Date Samples Collected	****RESULTS FOR PLM METHOD******* MED-TOX Elongate Serpentine %	MED-TOX Chrysotile Asbestos %	McCRONE Serpentine Asbestos %	**********TOTAL ASBESTOS RESULTS FOR TEM METHOD********** MED-TOX (% Mass)	> 5 um (% Mass)	Struct. Conc. (1.0E+12 struct./g)	> 5 um Struct. Conc. (1.0E+9 struct./g)	Remarks
AL34	AL34	LNS	28-Jan-88	TRACE	TRACE	N/A	N/A	N/A	N/A	N/A	
	AL34B	CMT	4-Feb-88	TRACE	TRACE	N/A	N/A	N/A	N/A	N/A	
AL35	AL35A	LNS	4-Feb-88	TRACE	TRACE	N/A	N/A	N/A	N/A	N/A	
	AL35B	CMT	4-Feb-88	TRACE	ND	5	N/A	N/A	N/A	N/A	Blind Duplicate
	AL81	CMT	4-Feb-88	1	TRACE	N/A	N/A	N/A	N/A	N/A	Blind Duplicate
AL36	AL36A	LNS	4-Feb-88	1	TRACE	N/A	N/A	N/A	N/A	N/A	
	AL36B	AO	4-Feb-88	70	15	N/A	N/A	N/A	N/A	N/A	
AL37	AL37	RD	4-Feb-88	10	5	N/A	N/A	N/A	N/A	N/A	
AL38	AL38A	NS	12-Feb-88	2	TRACE	N/A	N/A	N/A	N/A	N/A	
	AL38B	RR	12-Feb-88	25	10	N/A	N/A	N/A	N/A	N/A	
AL39	AL39A	LNS	12-Feb-88	3	TRACE	N/A	N/A	N/A	N/A	N/A	
	AL39B	RR	12-Feb-88	75	25	N/A	N/A	N/A	N/A	N/A	
AL40	AL40A	LNS	5-Feb-88	5	2	N/A	70	ND	6	<700	
	AL40B	RR	5-Feb-88	15	5	N/A	100	10	4	800	
AL41	AL41A	LNS	5-Feb-88	3	TRACE	N/A	N/A	N/A	N/A	N/A	
	AL41B	RR	5-Feb-88	15	3	N/A	N/A	N/A	N/A	N/A	
AL42	AL42A	LNS	5-Feb-88	2	TRACE	N/A	N/A	N/A	N/A	N/A	
AL43	AL43A	LNS	5-Feb-88	5	2	N/A	N/A	N/A	N/A	N/A	
	AL43B	RR	5-Feb-88	8	2	N/A	N/A	N/A	N/A	N/A	
AL44	AL44A	LNS	5-Feb-88	15	5	N/A	N/A	N/A	N/A	N/A	
	AL44B	RR	5-Feb-88	70	50	N/A	N/A	N/A	N/A	N/A	
AL45	AL45A	LNS	12-Feb-88	30	15	N/A	N/A	N/A	N/A	N/A	

Reproduced with permission of the copyright owner. Further reproduction prohibited without permission.

SOIL ASBESTOS DATA SUMMARY

Statn. No.	Sample ID Number	Sample Type	Date Samples Collected	****RESULTS FOR PLM METHOD******* MED·TOX Elongate Serpentine %	MED·TOX Chrysotile Asbestos %	McCRONE Serpentine Asbestos %	**********TOTAL ASBESTOS RESULTS FOR TEM METHOD********** MED·TOX (% Mass)	> 5 um (% Mass)	Struct. Conc. (1.0E+12 struct./g)	> 5 um Struct. Conc. (1.0E+9 struct./g)	Remarks
	AL45B	RR	12·Feb·88	85	50	N/A	N/A	N/A	N/A	N/A	
AL46	AL46A	LNS	12·Feb·88	25	10	N/A	N/A	N/A	N/A	N/A	
	AL46B	RR	12·Feb·88	80	55	N/A	N/A	N/A	N/A	N/A	
AL47	AL47	RD	12·Feb·88	TRACE	TRACE	N/A	N/A	N/A	N/A	N/A	
AL48	AL48	RD	12·Feb·88	3	TRACE	N/A	N/A	N/A	N/A	N/A	
AL49	AL49	RD	12·Feb·88	2	TRACE	N/A	N/A	N/A	N/A	N/A	
AL50	AL50A	LNS	12·Feb·88	TRACE	TRACE	N/A	N/A	N/A	N/A	N/A	
	AL50B	RR	12·Feb·88	70	50	N/A	N/A	N/A	N/A	N/A	
AL51	AL51A	LNS	12·Feb·88	TRACE	TRACE	N/A	N/A	N/A	N/A	N/A	
	AL51B	RR	12·Feb·88	50	20	N/A	N/A	N/A	N/A	N/A	
AL52	AL52	AO	4·Feb·88	80	60	>85	N/A	N/A	N/A	N/A	Blind Duplicate
	AL83	AO	4·Feb·88	90	70	N/A	N/A	N/A	N/A	N/A	Blind Duplicate
AL53	AL53	CMT	5·Feb·88	15	5	N/A	N/A	N/A	N/A	N/A	
AL54	AL54A	AMT	19·Feb·88	90	60	N/A	90	ND	4	<900	
	AL54B	AMT	19·Feb·88	60	30	N/A	40	ND	4	<600	
SB1	SB1·17.5	SBF	3·Dec·87	TRACE	TRACE	N/A	4	ND	3	<400	
	SB1·32.5	AFS	5·Dec·87	TRACE	TRACE	N/A	3	ND	2	<300	
							2	ND	2	<200	Lab Replicate
	SB1·39.9	AFS	5·Dec·87	TRACE	ND	N/A	1	ND	1	<100	Blind Duplicate
	SB1·40.0	AFS	5·Dec·87	TRACE	TRACE	N/A	0.5	ND	0.4	<50	Blind Duplicate
SB2	SB2·15.0	SBF	3·Dec·87	TRACE	TRACE	N/A	1	ND	1	<80	
	SB2·35.0	AFS	3·Dec·87	2	TRACE	N/A	1	ND	1	<90	

Reproduced with permission of the copyright owner. Further reproduction prohibited without permission.

SOIL ASBESTOS DATA SUMMARY

Statn. No.	Sample ID Number	Sample Type	Date Samples Collected	****RESULTS FOR PLM METHOD******* MED-TOX Elongate Serpentine %	MED-TOX Chrysotile Asbestos %	McCRONE Serpentine Asbestos %	**********TOTAL ASBESTOS RESULTS FOR TEM METHOD********** MED-TOX (% Mass)	> 5 um (% Mass)	Struct. Conc. (1.0E+12 struct./g)	> 5 um Struct. Conc. (1.0E+9 struct./g)	Remarks
	SB2-42.5	AFS	3-Dec-87	TRACE	ND	N/A	1	ND	0.3	<40	
SB3	SB3-6.7	SBF	3-Dec-87	TRACE	TRACE	N/A	2	ND	1	<200	Blind Quadruplicate
	SB3-6.8	SBF	3-Dec-87	TRACE	TRACE	N/A	4	ND	3	<400	Blind Quadruplicate
	SB3-6.9	SBF	3-Dec-87	2	1	N/A	2	ND	2	<300	Blind Quadruplicate
	SB3-7.0	SBF	3-Dec-87	TRACE	TRACE	1.5	3	ND	3	<400	Blind Quadruplicate
	SB3-15.0	AFS	4-Dec-87	TRACE	TRACE	3.5	4	ND	3	<400	Blind Quadruplicate
	SB3-15.1	AFS	4-Dec-87	TRACE	TRACE	N/A	1	ND	3	<100	Blind Quadruplicate
	SB3-15.2	AFS	4-Dec-87	TRACE	TRACE	N/A	6	ND	3	<400	Blind Quadruplicate
	SB3-15.3	AFS	4-Dec-87	TRACE	TRACE	N/A	1	ND	3	<70	Blind Quadruplicate
	SB3-19.7	AFS	4-Dec-87	TRACE	TRACE	N/A	5	ND	3	<400	
	SB3-27.8	AFS	4-Dec-87	3	2	2	1	ND	1	<100	
AF1	AF1-0.3	AFS	1-Dec-87	1	TRACE	N/A	N/A	N/A	N/A	N/A	
	AF1-5.3	AFS	1-Dec-87	2	TRACE	N/A	N/A	N/A	N/A	N/A	
	AF1-10.0	AFS	1-Dec-87	TRACE	TRACE	N/A	3	ND	2	<200	
	AF1-14.5	AFS	1-Dec-87	TRACE	TRACE	1.5	3	ND	2	<300	
AF2	AF2-1.5	AFS	1-Dec-87	TRACE	TRACE	N/A	N/A	N/A	N/A	N/A	
	AF2-5.0	AFS	1-Dec-87	TRACE	TRACE	N/A	2	ND	3	<400	
	AF2-10.0	AFS	1-Dec-87	TRACE	TRACE	N/A	3	ND	2	<300	
	AF2-15.0	AFS	1-Dec-87	TRACE	TRACE	N/A	0.3	ND	0.3	<50	
AF3	AF3-2.5	AFS	1-Dec-87	2	TRACE	N/A	N/A	N/A	N/A	N/A	
	AF3-7.5	AFS	1-Dec-87	3	TRACE	N/A	2	ND	3	<400	
	AF3-13.3	AFS	2-Dec-87	2	TRACE	N/A	4	ND	3	<300	
	AF3-25.0	AFS	2-Dec-87	TRACE	TRACE	N/A	10	ND	2	<300	
AF4	AF4-5.0	AFS	2-Dec-87	TRACE	TRACE	N/A	3	ND	3	<400	
	AF4-10.0	AFS	2-Dec-87	TRACE	TRACE	N/A	N/A	N/A	N/A	N/A	

Reproduced with permission of the copyright owner. Further reproduction prohibited without permission.

SOIL ASBESTOS DATA SUMMARY

Statn. No.	Sample ID Number	Sample Type	Date Samples Collected	****RESULTS FOR PLM METHOD******* MED-TOX Elongate Serpentine %	MED-TOX Chrysotile Asbestos %	McCRONE Serpentine Asbestos %	**********TOTAL ASBESTOS RESULTS FOR TEM METHOD********** MED-TOX (% Mass)	> 5 um (% Mass)	Struct. Conc. (1.0E+12 struct./g)	> 5 um Struct. Conc. (1.0E+9 struct./g)	Remarks
	AF4-15.0	AFS	2-Dec-87	TRACE	TRACE	N/A	2	ND	1	<200	
	AF4-22.5	AFS	2-Dec-87	TRACE	TRACE	N/A	2	ND	2	<300	
AF5	AF5-2.4	AFS	2-Dec-87	TRACE	ND	N/A	3	ND	2	<300	Blind Duplicate
	AF5-2.5	AFS	2-Dec-87	TRACE	TRACE	N/A	4	ND	2	<300	Blind Duplicate
	AF5-10.0	AFS	2-Dec-87	TRACE	ND	N/A	N/A	N/A	N/A	N/A	
	AF5-15.0	AFS	2-Dec-87	TRACE	ND	N/A	4	ND	4	<500	Blind Duplicate
	AF5-15.1	AFS	2-Dec-87	2	ND	N/A	2	ND	2	<300	Blind Duplicate
	AF5-20.1	AFS	2-Dec-87	2	TRACE	N/A	N/A	N/A	N/A	N/A	
	AF5-20.2	AFS	2-Dec-87	TRACE	TRACE	N/A	1	ND	2	<300	
AF6	AF6-5.0	PVFP	4-Dec-87	1	TRACE	N/A	N/A	N/A	N/A	N/A	
	AF6-10.0	PVFP	4-Dec-87	TRACE	TRACE	N/A	0.09	ND	0.07	<50	
	AF6-15.0	PVFP	4-Dec-87	2	TRACE	N/A	0.4	ND	1	<80	
AF7	AF7-2.5	PVFP	4-Dec-87	2	TRACE	N/A	1	ND	1	<100	
	AF7-10.0	PVFP	4-Dec-87	2	TRACE	N/A	2	ND	3	<400	
SS1	SS1	STB	28-Mar-88	TRACE	TRACE	N/A	N/A	N/A	N/A	N/A	
SS2	SS2	STB	28-Mar-88	1	TRACE	<1	1	ND	0.4	<50	Blind Duplicate
	SS81	STB	28-Mar-88	TRACE	TRACE	N/A	1	ND	0.5	<60	Blind Duplicate
							0.2	ND	0.4	<60	Lab Replicate
SS3	SS3	STB	28-Mar-88	TRACE	TRACE	N/A	N/A	N/A	N/A	N/A	
SS4	SS4	STB	28-Mar-88	TRACE	TRACE	N/A	N/A	N/A	N/A	N/A	
SS5	SS5	STB	28-Mar-88	TRACE	TRACE	N/A	N/A	N/A	N/A	N/A	
SS6	SS6	STB	28-Mar-88	ND	ND	N/A	N/A	N/A	N/A	N/A	
SS7	SS7	STB	29-Mar-88	TRACE	TRACE	N/A	N/A	N/A	N/A	N/A	
SS8	SS8	STB	29-Mar-88	TRACE	ND	N/A	N/A	N/A	N/A	N/A	

Reproduced with permission of the copyright owner. Further reproduction prohibited without permission.

SOIL ASBESTOS DATA SUMMARY

Statn. No.	Sample ID Number	Sample Type	Date Samples Collected	****RESULTS FOR PLM METHOD****** MED-TOX Elongate Serpentine %	MED-TOX Chrysotile Asbestos %	McCRONE Serpentine Asbestos %	**********TOTAL ASBESTOS RESULTS FOR TEM METHOD********** MED-TOX (% Mass)	> 5 um (% Mass)	Struct. Conc. (1.0E+12 struct./g)	> 5 um Struct. Conc. (1.0E+9 struct./g)	Remarks
SS9	SS9	STB	29-Mar-88	ND	ND	N/A	N/A	N/A	N/A	N/A	
SS10	SS10	STB	30-Mar-88	TRACE	TRACE	N/A	N/A	N/A	N/A	N/A	
SS11	SS11	STB	29-Mar-88	TRACE	TRACE	N/A	N/A	N/A	N/A	N/A	
SS12	SS12	STB	29-Mar-88	10	5	12.5	2	ND	0.2	<40	Blind Duplicate
	SS82	STB	29-Mar-88	5	3	N/A	1	ND	0.3	<50	Blind Duplicate
SS13	SS13	STB	29-Mar-88	ND	ND	N/A	N/A	N/A	N/A	N/A	
SS14	SS14	STB	30-Mar-88	ND	ND	N/A	N/A	N/A	N/A	N/A	
SS15	SS15	STB	30-Mar-88	15	10	N/A	N/A	N/A	N/A	N/A	
SS16	SS16	STB	30-Mar-88	5	2	N/A	20	ND	0.4	<60	
SS17	SS17	STB	30-Mar-88	TRACE	TRACE	N/A	N/A	N/A	N/A	N/A	
SS18	SS18	STB	30-Mar-88	5	2	N/A	N/A	N/A	N/A	N/A	
SS19	SS19	STB	30-Mar-88	20	10	N/A	N/A	N/A	N/A	N/A	
SS20	SS20	STB	30-Mar-88	30	15	N/A	N/A	N/A	N/A	N/A	
	SS20X	STB	31-Mar-88	75	30	N/A	N/A	N/A	N/A	N/A	
SS21	SS21	STB	30-Mar-88	TRACE	TRACE	N/A	N/A	N/A	N/A	N/A	
SS22	SS22	STB	30-Mar-88	TRACE	ND	N/A	0.2	ND	0.2	<30	
SS23	SS23	STB	31-Mar-88	ND	ND	N/A	N/A	N/A	N/A	N/A	
SS24	SS24	STB	31-Mar-88	65	30	N/A	N/A	N/A	N/A	N/A	
SS25	SS25	STB	31-Mar-88	5	TRACE	N/A	9	ND	4	<500	
SS26	SS26	STB	31-Mar-88	60	30	N/A	6	ND	0.3	<40	
SS27	SS27	STB	04-Apr-88	80	40	N/A	N/A	N/A	N/A	N/A	
SS28	SS28	STB	04-Apr-88	75	30	77.5	20	ND	1	<70	Blind Duplicate

Reproduced with permission of the copyright owner. Further reproduction prohibited without permission.

SOIL ASBESTOS DATA SUMMARY

Statn. No.	Sample ID Number	Sample Type	Date Samples Collected	****RESULTS FOR PLM METHOD******* MED-TOX Elongate Serpentine %	MED-TOX Chrysotile Asbestos %	McCRONE Serpentine Asbestos %	**********TOTAL ASBESTOS RESULTS FOR TEM METHOD********** MED-TOX (% Mass)	> 5 um (% Mass)	Struct. Conc. (1.0E+12 struct./g)	> 5 um Struct. Conc. (1.0E+9 struct./g)	Remarks
	SS83	STB	04-Apr-88	ND	ND	N/A	N/A	N/A	N/A	N/A	Blind Duplicate
SS29	SS29	STB	05-Apr-88	85	45	N/A	N/A	N/A	N/A	N/A	
SS30	SS30	STB	05-Apr-88	75	35	N/A	N/A	N/A	N/A	N/A	
SS31	SS31	STB	07-Apr-88	65	30	N/A	N/A	N/A	N/A	N/A	
SS32	SS32	STB	07-Apr-88	ND	ND	N/A	N/A	N/A	N/A	N/A	
SS33	SS33	STB	31-Mar-88	TRACE	TRACE	N/A	N/A	N/A	N/A	N/A	
SS34	SS34	STB	31-Mar-88	15	5	32.5	7	ND	5	<600	Blind Duplicate
	SS84	STB	31-Mar-88	15	5	N/A	100	ND	4	<600	Blind Duplicate
SS35	SS35	STB	31-Mar-88	ND	ND	N/A	N/A	N/A	N/A	N/A	
SS36	SS36	STB	31-Mar-88	15	5	N/A	N/A	N/A	N/A	N/A	
SS37	SS37	STB	31-Mar-88	10	5	N/A	N/A	N/A	N/A	N/A	
SS38	SS38	STB	31-Mar-88	20	5	N/A	N/A	N/A	N/A	N/A	
SS39	SS39	STB	31-Mar-88	25	10	N/A	N/A	N/A	N/A	N/A	
SS40	SS40	STB	31-Mar-88	25	15	N/A	N/A	N/A	N/A	N/A	
OC1	OC1	STB	30-Mar-88	85	50	N/A	20	ND	2	<400	
OC2	OC2	STB	05-Apr-88	70	35	N/A	N/A	N/A	N/A	N/A	
OC3	OC3	STB	30-Mar-88	60	30	N/A	N/A	N/A	N/A	N/A	
OC4	OC4	STB	06-Apr-88	70	35	N/A	N/A	N/A	N/A	N/A	
OC5	OC5	STB	30-Mar-88	65	25	N/A	N/A	N/A	N/A	N/A	
OC6	OC6	STB	05-Apr-88	85	45	N/A	N/A	N/A	N/A	N/A	
OC9	OC9	STB	29-Mar-88	60	30	N/A	N/A	N/A	N/A	N/A	
OC10	OC10	STB	29-Mar-88	85	40	N/A	N/A	N/A	N/A	N/A	

Reproduced with permission of the copyright owner. Further reproduction prohibited without permission.

SOIL ASBESTOS DATA SUMMARY

Statn. No.	Sample ID Number	Sample Type	Date Samples Collected	****RESULTS FOR PLM METHOD******* MED-TOX Elongate Serpentine %	MED-TOX Chrysotile Asbestos %	McCRONE Serpentine Asbestos %	**********TOTAL ASBESTOS RESULTS FOR TEM METHOD********** MED-TOX (% Mass)	> 5 um (% Mass)	Struct. Conc. (1.0E+12 struct./g)	> 5 um Struct. Conc. (1.0E+9 struct./g)	Remarks
	OC10X	SPS	29-Mar-88	85	45	N/A	N/A	N/A	N/A	N/A	
OC11	OC11	MNS	28-Mar-88	ND	ND	N/A	N/A	N/A	N/A	N/A	
OC12	OC12	STB	06-Apr-88	25	10	N/A	N/A	N/A	N/A	N/A	
OC13	OC13	STB	06-Apr-88	25	10	N/A	N/A	N/A	N/A	N/A	
OC14	OC14	SPS-QLS	30-Mar-88	90	50	N/A	N/A	N/A	N/A	N/A	
OC15	OC15	SPS-QLS	30-Mar-88	80	50	N/A	30	ND	1	<700	
OC16	OC16	STB	06-Apr-88	25	5	N/A	N/A	N/A	N/A	N/A	
OC17	OC17	ATLAS	30-Mar-88	80	50	80	30	ND	1	<70	
	OC83	ATLAS	30-Mar-88	85	40	N/A	N/A	N/A	N/A	N/A	
OC18	OC18	SPS-QLS	07-Apr-88	90	65	N/A	300	ND	6	<800	
	OC18B	SPS	07-Apr-88	90	45	>85	N/A	N/A	N/A	N/A	Blind Duplicate
	OC85	SPS	07-Apr-88	95	50	N/A	N/A	N/A	N/A	N/A	Blind Duplicate
OC19	OC19	FRC-SPS	28-Mar-88	60	20	N/A	N/A	N/A	N/A	N/A	
OC21	OC21	FRC-SPS	29-Mar-88	60	30	N/A	N/A	N/A	N/A	N/A	
OC22	OC22	MNS	28-Mar-88	ND	ND	N/A	N/A	N/A	N/A	N/A	
OC24	OC24	BUTLER	29-Mar-88	85	50	65	30	ND	0.3	<40	Blind Duplicate
	OC82	BUTLER	29-Mar-88	70	30	N/A	N/A	N/A	N/A	N/A	Blind Duplicate
OC25	OC25	BYLES	05-Apr-88	95	50	N/A	200	ND	4	<500	
	OC25B	SPS	05-Apr-88	95	50	N/A	N/A	N/A	N/A	N/A	
OC26	OC26	MNS	05-Apr-88	ND	ND	N/A	N/A	N/A	N/A	N/A	
OC27	OC27	SPS-QLS	07-Apr-88	85	45	N/A	200	ND	4	<500	
OC28	OC28	JENSEN	29-Mar-88	80	45	70	20	ND	0.4	<60	Blind Duplicate
	OC-81	JENSEN	29-Mar-88	75	40	N/A	N/A	N/A	N/A	N/A	Blind Duplicate
OC29	OC29	ATLAS-TLS	30-Mar-88	90	50	N/A	N/A	N/A	N/A	N/A	

Reproduced with permission of the copyright owner. Further reproduction prohibited without permission.

SOIL ASBESTOS DATA SUMMARY

Statn. No.	Sample ID Number	Sample Type	Date Samples Collected	****RESULTS FOR PLM METHOD******* MED-TOX Elongate Serpentine %	MED-TOX Chrysotile Asbestos %	McCRONE Serpentine Asbestos %	**********TOTAL ASBESTOS RESULTS FOR TEM METHOD********** MED-TOX (% Mass)	> 5 um (% Mass)	Struct. Conc. (1.0E+12 struct./g)	> 5 um Struct. Conc. (1.0E+9 struct./g)		Remarks
OC30	OC30	ATLAS	30-Mar-88	80	40	N/A	N/A	N/A	N/A	N/A		
OC31	OC31	SPS	05-Apr-88	75	40	N/A	N/A	N/A	N/A	N/A		
OC32	OC32	ATLAS	30-Mar-88	60	30	N/A	N/A	N/A	N/A	N/A		
CC1	CC1	TBB	18-May-88	90	20	N/A	N/A	N/A	N/A		N/A	
CC2	CC2	TBB	18-May-88	90	30	N/A	N/A	N/A	N/A		N/A	
CC3	CC3	TBB	18-May-88	50	15	N/A	N/A	N/A	N/A			
CC4	CC4	TBB	18-May-88	80	20	N/A	N/A	N/A	N/A			
CC5	CC5	TBB	18-May-88	25	10	N/A	N/A	N/A	N/A			
CC6	CC6	TBB	18-May-88	90	30	N/A	N/A	N/A	N/A			
CC7	CC7	TBB	18-May-88	40	15	N/A	N/A	N/A	N/A			
XP1	XP1/2-3	LBS	10-Mar-88	60	25	50	10	ND	9	<1100		Blind Duplicate
	XP91/2-3	LBS	10-Mar-88	50	20	N/A	N/A	N/A	N/A	N/A		Blind Duplicate
	XP1/4-5	LBS	10-Mar-88	60	25	50	10	ND	7	<800		Blind Duplicate
	XP91/4-5	LBS	10-Mar-88	65	25	N/A	N/A	N/A	N/A	N/A		Blind Duplicate
	XP1/5.5-6.5	LBS	10-Mar-88	70	25	45	10	ND	12	<1500		Blind Duplicate
	XP91/5.5-6.5	LBS	10-Mar-88	65	25	N/A	N/A	N/A	N/A	N/A		Blind Duplicate
XP2	XP2/1-2	LBS	11-Mar-88	5	2	N/A	N/A	N/A	N/A	N/A		
	XP2/4-5	LBS	11-Mar-88	TRACE	TRACE	N/A	N/A	N/A	N/A	N/A		
XP3	XP3/2-3	UBS	11-Mar-88	1	TRACE	<1	1	ND	2	<300		Blind Duplicate
	XP92/2-3	UBS	11-Mar-88	TRACE	TRACE	N/A	N/A	N/A	N/A	N/A		Blind Duplicate
	XP3/4-5	UBS	11-Mar-88	3	1	7.5	3	ND	6	<800		Blind Duplicate
	XP92/4-5	UBS	11-Mar-88	4	2	N/A	N/A	N/A	N/A	N/A		Blind Duplicate
	XP3/6-7	UBS	11-Mar-88	10	3	<1	6	ND	3	<500		Blind Duplicate
	XP92/6-7	UBS	11-Mar-88	5	2	N/A	N/A	N/A	N/A	N/A		Blind Duplicate

Reproduced with permission of the copyright owner. Further reproduction prohibited without permission.

SOIL ASBESTOS DATA SUMMARY

Statn. No.	Sample ID Number	Sample Type	Date Samples Collected	****RESULTS FOR PLM METHOD******* MED-TOX Elongate Serpentine %	MED-TOX Chrysotile Asbestos %	McCRONE Serpentine Asbestos %	**********TOTAL ASBESTOS RESULTS FOR TEM METHOD********** MED-TOX (% Mass)	> 5 um (% Mass)	Struct. Conc. (1.0E+12 struct./g)	> 5 um Struct. Conc. (1.0E+9 struct./g)	Remarks
XP5	XP5/1-2	UBS	11-Mar-88	TRACE	ND	<2	7	ND	4	<500	Blind Duplicate
	XP93/1-2	UBS	11-Mar-88	TRACE	ND	N/A	N/A	N/A	N/A	N/A	Blind Duplicate
	XP5/4-5	UBS	11-Mar-88	TRACE	ND	<1	0.3	ND	0.2	<30	Blind Duplicate
	XP93/4-5	UBS	11-Mar-88	TRACE	TRACE	N/A	N/A	N/A	N/A	N/A	Blind Duplicate
XP6	XP6/4-5	SPS-QLS	11-Mar-88	90	40	>80	20	ND	89	<1000	Blind Duplicate
	XP94/4-5	SPS-QLS	11-Mar-88	90	40	N/A	N/A	N/A	N/A	N/A	Blind Duplicate
PG	PG1	RR	19-Feb-88	N/A	N/A	82.5	N/A	N/A	N/A	N/A	
	PG2	EF	19-Feb-88	N/A	N/A	57.5	N/A	N/A	N/A	N/A	
	PG3A	WF	19-Feb-88	N/A	N/A	45	N/A	N/A	N/A	N/A	
	PG3B	WF	16-Feb-88	N/A	N/A	60	N/A	N/A	N/A	N/A	
	PG4	AO	19-Feb-88	N/A	N/A	>80	N/A	N/A	N/A	N/A	
	PG5	AMT	19-Feb-88	N/A	N/A	>80	N/A	N/A	N/A	N/A	
	PG7	LPC	29-Jan-88	N/A	N/A	7.5	N/A	N/A	N/A	N/A	
	PG8A	WC	29-Jan-88	N/A	N/A	25	N/A	N/A	N/A	N/A	
	PG8B	WC	29-Jan-88	N/A	N/A	50	N/A	N/A	N/A	N/A	

N/A = Not Analyzed
Trace = Detected but less than 1% (Method Detection Limit for PLM - Med-Tox)
ND = Not Detected

LNS = Landslide Native Soil
MNS = Marine Native Soil
STB = Streambed
RD = Road Surface
CMT = Chromite Mill Tailings
AMT = Asbestos Mill Tailings
AO = Asbestos Ore
LPC = Lower Pine Canyon

SPS = Serpentine Soils
RR = Railroad Mine
AFS = Alluvial Fan Sediment
LBS = Lower Borrow Source
UBS = Upper Borrow Source
WF = West Fork
EF = East Fork
SPS-QLS = Serpentine Soils, Quaternary Landslide

WC = White Creek
SBF = Settling Basin Fill
PVFP = Pleasant Valley Flood Plain
ATLAS = Atlas Mine
JENSEN = Jensen Mine
ATLAS-TLS = Atlas Mine Tailings
BYLES = Byles Mine

CO = Chromite Ore
BUTLER = Butler Mine
TBB = Temblor Big Blue Formation
FRC-SPS = Franciscan-Serpentinite Complex

SOURCE: LEVINE-FRICKE

Table 5-3

PARTICLE SIZE AND ORGANIC MATTER DATA SUMMARY

Sample ID Number	Date Samples Collected	Organic Matter %	Gravel > 4.75 mm %	Coarse Sand < 4.75 mm > 1.18 mm %	Medium and Fine Sand <1.18 mm > 0.075 mm %	Clay and Silt < 0.075 mm %	Remarks
PC1A	23-Feb-88	N/A	4.2	36.4	52.4	7	
PC1B	23-Feb-88	N/A	20.9	43.5	34	1.6	
PC1B	16-Mar-88	N/A	2.2	21.3	70.6	5.9	
PC2A	16-Mar-88	N/A	32.9	45.2	19.3	2.6	
PC2B	16-Mar-88	N/A	18.9	26.9	48.3	5.9	
PC2B	23-Feb-88	N/A	15.5	38	43.1	3.4	
PC2C	16-Mar-88	N/A	28.9	35.2	32.4	3.5	
PC3B	16-Mar-88	N/A	4.2	24.3	65.7	5.8	
PC3C	16-Mar-88	N/A	7.1	53.8	34.4	4.7	
PC5B	23-Feb-88	N/A	5.6	23.6	63.1	7.7	
PC13B	25-Feb-88	N/A	27.6	20.2	46.4	5.8	
PC14B	25-Feb-88	N/A	26	6.2	53.5	14.3	
PC15C	15-Mar-88	N/A	19.2	31.7	42.3	6.8	
PC16C	15-Mar-88	N/A	23.5	45	28.1	3.4	
PC19A	15-Mar-88	N/A	22.5	53.6	21.3	2.6	
PC20B	15-Mar-88	N/A	20.9	41.3	35.7	2.1	
BS2	04-Feb-88	1.7	12.4	32.4	48.3	6.9	
BP5/1.5	01-Jul-88	2.2	5.6	25.3	55.5	13.6	
BP5/8-10	01-Jul-88	0.1	2	29.2	60.2	8.6	OM Duplicate = 0.2%
BS7	29-Jan-88	0.8	4.2	25.8	59.1	10.9	
BS7.5	29-Jan-88	0.9	N/A	N/A	N/A	N/A	
BS12	29-Jan-88	1.2	23.2	30.9	43.5	2.4	
BP13/1.5-2.5	01-Jul-88	0.1	4.6	44.8	47.9	2.7	
BP13/4-5	01-Jul-88	0.1	1.2	28.9	61.5	8.4	
BP14/3-4	01-Jul-88	1.1	15.2	27	48.3	9.5	
BP14/11-12	01-Jul-88	0.1	11.5	32.6	50.6	5.3	
BP15/3-4	01-Jul-88	0.2	4.3	30.7	58.2	6.8	
BP15/10-11	01-Jul-88	0.1	8.9	32.4	53.4	5.3	
BP18/3-4	01-Jul-88	0.5	9.5	42.2	44.7	3.6	
BP18/8-9	01-Jul-88	0.1	3.9	28.9	60.5	6.7	
BS23	28-Jan-88	3	11.7	38.5	44.7	5.1	
BS24	12-Feb-88	1.6	4.5	28.5	60.1	6.9	
BS34	29-Jan-88	1	15.4	28.1	47.8	8.7	

SOURCE : LEVINE-FRICKE

Reproduced with permission of the copyright owner. Further reproduction prohibited without permission.

PARTICLE SIZE AND ORGANIC MATTER DATA SUMMARY

Sample ID Number	Date Samples Collected	Organic Matter %	Gravel > 4.75 mm %	Coarse Sand < 4.75 mm > 1.18 mm %	Medium and Fine Sand <1.18 mm > 0.075 mm %	Clay and Silt < 0.075 mm %	Remarks
BP35/1-2	01-Jul-88	1.3	14.8	33.1	45.4	6.7	
BS35/3-4	01-Jul-88	0.4	3.8	37.5	52.1	6.6	OM Duplicate = 0.3%
AL4A	04-Feb-88	0.5	5.5	46.5	43.7	4.3	
AL6A	04-Feb-88	0.5	7.2	38.6	49.7	4.5	OM Duplicate = 0.4%
AL7	04-Feb-88	0.7	1.8	45.1	49.6	3.5	
AL17A	19-Feb-88	1.6	14.3	31	51	3.7	OM Spike recovery = 115%
AL17B	18-Feb-88	0.2	15	5.3	65.4	14.3	OM Duplicate = 0.4%
AL20A	19-Feb-88	1.9	16.8	43.1	35.5	4.6	
AL20B	18-Feb-88	0.2	4.8	11.8	69.2	14.2	
AL29A	13-Feb-88	0.9	18.6	42	33.4	6	
AL29B	13-Feb-88	0.1	7.3	2.6	80.6	9.5	OM Duplicate = 0.1%
AL30A	13-Feb-88	1.2	4.1	34.6	49.3	12	
AL30B	13-Feb-88	0.2	5.4	7	72.1	15.5	
AL36A	04-Feb-88	1.4	10.4	28	55.7	5.9	
AL36B	04-Feb-88	0.9	4.5	24.6	64.7	6.2	
AL42A	05-Feb-88	1.7	8.7	20.2	60.4	10.7	
AL43B	05-Feb-88	1	9.4	25.5	59.8	5.3	
AL44A	05-Feb-88	2.2	16.1	19.3	59.8	4.8	
AL44B	05-Feb-88	0.1	12.9	26.5	57.4	3.2	
AL50A	12-Feb-88	1.2	4.9	31.4	49.1	14.6	
AL50B	12-Feb-88	0.3	6.3	25.8	60.5	7.4	
AL51A	12-Feb-88	1.4	6.4	29.3	54.7	9.6	OM Spike recovery = 106.3
AL51B	12-Feb-88	0.7	9.8	28.7	56	5.5	
AL52	04-Feb-88	0.2	4.1	21.6	66.8	7.5	OM Spike recovery = 115%
AL83	04-Feb-88	0.2	4.9	22.5	66.7	5.9	Blind Duplicate of AL52
SB1-17.5	05-Dec-88	N/A	0	1.8	87.6	10.6	
SB2-15.0	05-Dec-88	N/A	0	20.3	63.5	16.2	
SB2-35.9	05-Dec-88	N/A	0	5.6	75.4	19	
SB2-42.5	05-Dec-88	N/A	0	9.2	79.81	10.99	
SB3-6.7	05-Dec-88	N/A	0	1.8	87.1	11.1	
SB3-15.2	05-Dec-88	N/A	0	0	97.4	2.6	
SB3-27.5	04-Dec-88	N/A	0	0.56	82.7	16.74	

Reproduced with permission of the copyright owner. Further reproduction prohibited without permission.

PARTICLE SIZE AND ORGANIC MATTER DATA SUMMARY

Sample ID Number	Date Samples Collected	Organic Matter %	Gravel > 4.75 mm %	Coarse Sand < 4.75 mm > 1.18 mm %	Medium and Fine Sand <1.18 mm > 0.075 mm %	Clay and Silt < 0.075 mm %	Remarks
AF1-0.3	01-Dec-88	1	0	9.9	69.5	20.6	
AF2-1.0	01-Dec-88	0.6	0	19.7	63	17.3	OM Spike recovery = 87.5%
AF3-2.5	01-Dec-88	0.5	0	7.4	70.1	22.5	OM Spike recovery = 107.5
AF4-5.0	02-Dec-88	0.3	0	2	85.2	12.8	
AF5-2.5	02-Dec-88	0.4	0	9.1	60.9	30	
AF6-5.0	02-Dec-88	0.1	0	1	81.99	17.01	OM Duplicate = 0.1%
AF7-10.0	02-Dec-88	1.6	0	19.3	65.57	15.13	
SS1	28-Mar-88	N/A	0.1	3.7	95.31	0.89	
SS4	28-Mar-88	N/A	0	0.8	93.9	5.3	
SS6	28-Mar-88	N/A	12.9	21.4	62.3	3.4	
SS8	29-Mar-88	N/A	0	0.9	98	1.1	
SS10	30-Mar-88	N/A	18.7	48.3	32.85	0.15	
SS12	29-Mar-88	N/A	5.4	34.2	58.6	1.8	
SS14	30-Mar-88	N/A	34.3	25.6	37.3	2.8	
SS16	30-Mar-88	N/A	28.6	48.8	21.4	1.2	
SS18	30-Mar-88	N/A	9.7	7.4	78.8	4.1	
SS22	30-Mar-88	N/A	4.1	5.1	87.6	3.2	
SS24	31-Mar-88	N/A	18.1	13.5	56.3	12.1	
SS26	31-Mar-88	N/A	12.2	15.3	69	3.5	
SS28	31-Mar-88	N/A	8.5	10.1	78.1	3.3	
SS30	31-Mar-88	N/A	12.1	8.6	72.8	6.5	
SS30 DUP	07-Apr-88	N/A	1.9	2.5	90	5.6	
SS31	07-Apr-88	N/A	17.6	31.4	45.8	5.2	
SS32	07-Apr-88	N/A	7.7	33.4	53.7	5.2	
SS34	31-Mar-88	N/A	10.3	29.2	50.9	9.6	
SS38	31-Mar-88	N/A	7.4	31.1	56.5	5	
SS40	31-Mar-88	N/A	2.4	10.8	77.5	9.3	
OC2	05-Apr-88	N/A	16.6	24.5	55.2	3.7	
OC4	05-Apr-88	N/A	6.3	17	73.2	3.5	
OC6	05-Apr-88	N/A	2.4	19.6	74.2	3.8	
OC10	29-Mar-88	N/A	33.1	15.1	48.2	3.6	
OC10X	29-Mar-88	N/A	4	45.3	49.1	1.6	
OC11	28-Mar-88	N/A	34.8	29.8	33.8	1.6	

Reproduced with permission of the copyright owner. Further reproduction prohibited without permission.

PARTICLE SIZE AND ORGANIC MATTER DATA SUMMARY

Sample ID Number	Date Samples Collected	Organic Matter %	Gravel > 4.75 mm %	Coarse Sand < 4.75 mm > 1.18 mm %	Medium and Fine Sand <1.18 mm > 0.075 mm %	Clay and Silt < 0.075 mm %	Remarks
OC12	06-Apr-88	N/A	13.3	32.8	51.6	2.3	
OC14	30-Mar-88	N/A	0	2.1	79.8	18.1	
OC15	30-Mar-88	N/A	25.6	14.8	55.2	4.4	
OC16	06-Apr-88	N/A	3.4	20.1	71.7	4.8	
OC17	30-Mar-88	N/A	19.9	26.6	50.3	3.2	
OC18	07-Apr-88	N/A	7.3	27.3	60.3	5.1	
OC22	28-Mar-88	N/A	38	31.8	27.8	2.4	
OC24	29-Mar-88	N/A	20.2	50.1	28	1.7	
OC26	05-Apr-88	N/A	16	60.9	21.5	1.6	
OC27	07-Apr-88	N/A	6.7	43.3	47.9	2.1	
OC28	29-Mar-88	N/A	25.5	24.4	47.7	2.4	
OC30	29-Mar-88	N/A	11.5	24.2	61.1	3.2	
OC32	29-Mar-88	N/A	14.2	34.2	48.3	3.3	
XP1/2-3	10-Mar-88	N/A	6.3	23.9	65.2	4.6	
XP1/4-5	10-Mar-88	N/A	4.5	16.7	72.8	6	
XP1/5.5-6.5	10-Mar-88	N/A	6.2	28	60.5	5.3	
XP2/1-2	11-Mar-88	N/A	52.5	29.4	17.7	0.4	
XP2/4-5	11-Mar-88	N/A	22.3	38.5	36.7	2.5	
XP3/2-3	11-Mar-88	N/A	43.6	41.2	14.5	0.7	
XP3/4-5	11-Mar-88	N/A	36.9	49.6	12.9	0.6	
XP3/6-7	11-Mar-88	N/A	33.9	40.9	23	2.2	
XP5/1-2	11-Mar-88	N/A	43.1	33.3	20.4	3.2	
XP5/4-5	11-Mar-88	N/A	37.7	37.2	23.3	1.8	
XP6/4-5	11-Mar-88	N/A	51	21.3	25.8	1.9	

N/A = Not Analyzed

"Spike" And "Duplicate" refer to internal laboratory QA/QC.

SOURCE: LEVINE-FRICKE

Reproduced with permission of the copyright owner. Further reproduction prohibited without permission.

Table 5-4

LABORATORY QC DATA SUMMARY OF PLM ANALYSES BY MED-TOX

Sample ID	Lab No.	#1 Elongate Serpentine %	#2 Elongate Serpentine %	RPD Elongate Serpentine	#1 Chrysotile Asbestos %	#2 Chrysotile Asbestos %	RPD Chrysotile Asbestos
AL1	69461	1	1	0.0	1	1	0.0
AL3B	69465	1	1	0.0	1	1	0.0
BP13/4-5	69493	1	1	0.0	1	1	0.0
BP13/8-10	69494	1	1	0.0	1	1	0.0
AL41A	69688	2	3	40.0 *	1	1	0.0
AL36B	69684	70	60	15.4	15	20	28.6
AL37	69685	10	10	0.0	5	5	0.0
AL27B	69985	85	90	5.7	50	70	33.3
AL28B	69987	80	90	11.8	45	80	56.0
AL29B	69989	85	90	5.7	50	80	46.2
AL30B	69991	85	90	5.7	55	70	24.0
AL39B	69999	75	90	18.2	25	70	94.7 *
AL88B	70267	80	80	0.0	40	40	0.0
PC14B	71129	80	75	6.5	25	35	33.3
PC93B	72062	75	80	6.5	30	40	28.6
PC3B	72043	75	70	6.9	30	30	0.0
XP94/4-5	72072	90	90	0.0	40	40	0.0
PC20A	72056	25	30	18.2	5	5	0.0
PC19C	72055	1	1	0.0	1	1	0.0
OC32	73308	60	60	0.0	30	30	0.0
SS1	73329	1	1	0.0	1	1	0.0
SS20	73318	25	30	18.2	15	15	0.0
SS14	73344	1	1	0.0	1	1	0.0
SS35	73346	1	1	0.0	1	1	0.0
OC3	73352	60	60	0.0	30	30	0.0
OC5	73353	65	60	8.0	25	30	18.2
OC18	73599	90	85	5.7	65	60	8.0
SS32	73611	1	1	0.0	1	1	0.0
OC85	73606	95	90	5.4	50	40	22.2
Average RPD				2.7			11.1
Standard Deviation				8.9			22.5
Std. Dev. x 2.77				24.7			62.4

* = samples with an RPD > Std. Dev. x 2.77

Med-Tox's PLM Results of Trace and ND were tabulated as 1% (Method Detection Limit)

SOURCE: LEVINE-FRICKE

Reproduced with permission of the copyright owner. Further reproduction prohibited without permission.

Table 5-5

LABORATORY QC DATA SUMMARY OF PLM ANALYSES BY MCCRONE

Sample ID	#1 Serpentine Asbestos Percent	#2 Serpentine Asbestos Percent	RPD Serpentine Asbestos Percent
OC17	80	65	20.7
PG3A	45	50	10.5
PC2B	55	57.5	4.4
AL35B	5	4	22.2
PC11A	15	10	40.0 *
OC18B	85	80	6.1
PC41B	62.5	55	12.8
Average RPD			16.7
Standard Deviation			12.3
Std. Dev. x 2.77			34.0

Notes:

* = samples with an RPD that exceed QA/QC criterion of Std. Dev x 2.77

McCrone's PLM data was generally reported as a range of asbestos concentrations (e.g. 10-20%). For QC purposes, median asbestos concentrations were calculated for comparisons.

McCrone's PLM data was occasionally reported as less than or greater than a particular value. For QC purposes, the particular value was tabulated for comparisons

SOURCE: LEVINE-FRICKE

Reproduced with permission of the copyright owner. Further reproduction prohibited without permission.

Reproduced with permission of the copyright owner. Further reproduction prohibited without permission.

Table 5-6

LABORATORY QC DATA SUMMARY OF TEM ANALYSES BY MED-TOX

Sample ID	Mass Conc. %	Duplicate Mass Conc. %	Average Mass Conc. %	RPD Mass Conc.	Struct. Conc. bill.Struct./g	Duplicate Struct. Conc. bill.Struct./g	Average Struct. Conc. bill.Struct./g	RPD Struct. Conc.
AF1-10.0	3	2	2.5	40.00	2000	2000	2000	0.00
SB1-32.5	3	2	2.5	40.00	2000	2000	2000	0.00
BP5-1.5B	30	30	30	0.00	8000	9000	8500	11.76
BS-30	4	2	3	66.67	2000	3000	2500	40.00
SS-81	1	0.2	0.6	133.33	500	400	450	22.22
Average RPD				56				15
Standard Deviation				49				17
Std. Dev. x 2.77				137				47

Note:

RPD = Relative percent difference

"Duplicate" refers to laboratory replicates

SOURCE: LEVINE-FRICKE

Table 5-7

LABORATORY QC SUMMARY OF ORGANIC MATTER ANALYSES BY DELLAVALLE

Sample ID	Original Organic Matter %	Duplicate Organic Matter %	Average Organic Matter %	RPD Organic Matter
BP5/8-10	0.1	0.2	0.15	66.7 *
BS35/3-4	0.4	0.3	0.35	28.6 *
AL6A	0.5	0.4	0.45	22.2
AL17B	0.2	0.4	0.3	66.7 *
AL29B	0.1	0.1	0.1	0.0
AL83	0.2	N/A	N/A	N/A
AL52	0.2	0.2	0.2	0.0
AF6-5.0	0.1	0.1	0.1	0.0

Notes:

AL83 was submitted as a blind intra-laboratory duplicate

N/A = not analyzed in duplicate (RPD not calculated)

* = samples with an RPD that exceeds the QC objectives

Sample ID	Spike Result % Recovery
AL17A	115
AL51A	106.3
AF2-1.0	87.5
AF3-2.5	107.5
AL52	115
Average Spike Recovery	106.3 %

SOURCE: LEVINE-FRICKE

Reproduced with permission of the copyright owner. Further reproduction prohibited without permission.

Table 5-8

QA/QC INTRA-LABORATORY DATA SUMMARY OF PLM ANALYSES BY MED-TOX

Sample ID Number	Blind Duplicate Number	Elongate Serpentine Asbestos				Chrysotile Asbestos			
		%	Blind Dup. %	Average %	RPD	%	Blind Dup. %	Average %	RPD
PC-1B	PC-93B	75	75	75	0.0	45	30	37.5	40.0
PC-2A	PC-92A	20	1	10.5	181.0 *	5	1	3	133.3 *
PC-2B	PC-92B	50	75	62.5	40.0	20	30	25	40.0
PC-2C	PC-92C	1	1	1	0.0	1	1	1	0.0
PC-2AX	PC-92AX	50	35	42.5	35.3	20	15	17.5	28.6
PC-11A	PC-92A	1	5	3	133.3	1	2	1.5	66.7
PC-11B	PC-92B	70	85	77.5	19.4	10	45	27.5	127.3
PC-11C	PC-92C	25	5	15	133.3	10	2	6	133.3 *
PC-14A	PC-91A	1	5	3	133.3	1	2	1.5	66.7
PC-14B	PC-91B	80	75	77.5	6.5	25	35	30	33.3
PC-14C	PC-91C	5	4	4.5	22.2	2	2	2	0.0
PC-20A	PC-91A	25	3	14	157.1 *	5	1	3	133.3 *
PC-20B	PC-91B	70	70	70	0.0	25	30	27.5	18.2
PC-20C	PC-91C	2	1	1.5	66.7	1	1	1	0.0
PC-41A	PC93A	70	30	50	80.0	45	25	35	57.1
PC-41B	PC-93B	80	50	65	46.2	30	20	25	40.0
BS-9	BS-81	1	6	3.5	142.9	1	1	1	0.0
BS-24	BS-88	5	10	7.5	66.7	1	5	3	133.3 *
AL-4B	AL-82	80	85	82.5	6.1	60	60	60	0.0
AL-11A	AL-84	1	1	1	0.0	1	1	1	0.0
AL-17A	AL-85A	40	55	47.5	31.6	30	15	22.5	66.7
AL-17B	AL-85B	65	95	80	37.5	25	50	37.5	66.7
AL-18A	AL-86A	40	35	37.5	13.3	25	10	17.5	85.7
AL-18B	AL-86B	50	85	67.5	51.9	25	45	35	57.1
AL-22A	AL-87A	15	30	22.5	66.7	5	10	7.5	66.7
AL-22B	AL-87B	75	80	77.5	6.5	25	40	32.5	46.2
AL-24A	AL-88A	20	35	27.5	54.5	15	15	15	0.0
AL-24B	AL-88B	55	80	67.5	37.0	20	40	30	66.7
AL-31A	AL-85A	1	1	1	0.0	1	1	1	0.0
AL-31B	AL-85B	50	100	75	66.7	20	70	45	111.1
AL-35A	AL-81	1	1	1	0.0	1	1	1	0.0
AL-52	AL-83	80	90	85	11.8	60	70	65	15.4
SS-2	SS-81	1	1	1	0.0	1	1	1	0.0
SS-12	SS-82	10	5	7.5	66.7	5	3	4	50.0
SS-28	SS-83	75	1	38	194.7 *	30	1	15.5	187.1 *
SS-34	SS-84	15	15	15	0.0	5	5	5	0.0
OC-17	OC-83	80	85	82.5	6.1	50	40	45	22.2
OC-18B	OC-85	90	95	92.5	5.4	45	50	47.5	10.5
OC-24	OC-82	85	70	77.5	19.4	50	30	40	50.0
OC-28	OC-81	80	75	77.5	6.5	45	40	42.5	11.8
XP1/2-3	XP91/2-3	60	50	55	18.2	25	20	22.5	22.2
XP1/4-5	XP91/4-5	60	65	62.5	8.0	25	25	25	0.0
XP1/5.5-6.5	XP91/5.5-6.5	70	65	67.5	7.4	25	25	25	0.0
XP3/2-3	XP92/2-3	1	1	1	0.0	1	1	1	0.0
XP3/4-5	XP92/4-5	3	4	3.5	28.6	1	2	1.5	66.7
XP3/6-7	XP92/6-7	10	5	7.5	66.7	3	2	2.5	40.0
XP5/1-2	XP93/1-2	1	1	1	0.0	1	1	1	0.0
XP5/4-5	XP93/4-5	1	1	1	0.0	1	1	1	0.0
XP6/4-5	XP94/4-5	90	90	90	0.0	40	40	40	0.0
Average RPD					42.3				42.7
Standard Deviation					52.4				47.3
Std. Dev. x 2.77					145.1				131.1

Note:

* = samples with RPD's > Std. Dev. x 2.77.

Med-Tox's PLM results of Trace and ND were tabulated as 1%.

SOURCE: LEVINE-FRICKE

Reproduced with permission of the copyright owner. Further reproduction prohibited without permission.

Table 5-9

QA/QC INTER-LABORATORY DATA SUMMARY OF PLM ANALYSES BY MED-TOX & McCRONE

Sample ID Number	Elongate Serpentine %	Chrysotile Asbestos %	McCRONE Serpentine Asbestos %	RPD Elongate & McCRONE	RPD Chrysotile & McCRONE
PC-1B	75	45	75	0.0	50.0
PC-2A	20	5	7.5	90.9	40.0
PC-2B	50	20	55	9.5	93.3
PC-2C	1	1	5	133.3	133.3
PC-2AX	50	20	8.5	141.9	80.7
PC-11A	1	1	15	175.0 *	175.0 *
PC-11B	70	10	77.5	10.2	154.3 *
PC-11C	25	10	15	50.0	40.0
PC-14A	1	1	7.5	152.9	152.9
PC-14B	80	25	67.5	16.9	91.9
PC-14C	5	2	5	0.0	85.7
PC-20A	25	5	37.5	40.0	152.9 *
PC-20B	70	25	37.5	60.5	40.0
PC-20C	2	1	30	175.0 *	187.1 *
PC-41A	70	45	75	6.9	50.0
PC-41B	80	30	62.5	24.6	70.3
BP-5 1.5	2	1	20	163.6	181.0 *
BP-5 8-1	1	1	30	187.1	187.1 *
BP-6 1.0	1	1	10	163.6	163.6 *
BS-9	1	1	10	163.6	163.6 *
BP-14 11	1	1	22.5	183.0 *	183.0 *
BP-14 13	1	1	2	66.7	66.7
BP-15 3-	1	1	14	173.3 *	173.3 *
BP-15 10	1	1	5.5	138.5	138.5
BS-29	10	5	30	100.0	142.9
AL-4B	80	60	85	6.1	34.5
AL-11A	1	1	2	66.7	66.7
AL-17A	40	30	55	31.6	58.8
AL-17B	65	25	80	20.7	104.8
AL-18A	40	25	45	11.8	57.1
AL-18B	50	25	80	46.2	104.8
AL-22A	15	5	27.5	58.8	138.5
AL-22B	75	25	52.5	35.3	71.0
AL-24A	20	15	22.5	11.8	40.0
AL-24B	55	20	72.5	27.5	113.5
AL-31A	1	1	2	66.7	66.7
AL-31B	50	20	80	46.2	120.0
AL-35A	1	1	5	133.3	133.3
AL-52	80	60	85	6.1	34.5
SB-3 7.0	1	1	1.5	40.0	40.0
SB-3 15.	1	1	3.5	111.1	111.1
SB-3 27.	3	2	2	40.0	0.0
AF-1 14.	1	1	1.5	40.0	40.0
SS-2	1	1	1	0.0	0.0
SS-12	10	5	12.5	22.2	85.7
SS-28	75	30	77.5	3.3	88.4
SS-34	15	5	32.5	73.7	146.7
OC-17	80	50	80	0.0	46.2
OC-18B	90	45	85	5.7	61.5
OC-24	85	50	65	26.7	26.1
OC-28	80	45	70	13.3	43.5
XP1/2-3	60	25	50	18.2	66.7
XP1/4-5	60	25	50	18.2	66.7

Elongate Serpentine versus Serpentine Asbestos

Regression Output:

Constant	-1.58541
Std Err of Y Est	14.41899
R Squared	0.814826
No. of Observations	60
Degrees of Freedom	58
X Coefficient(s)	0.981625
Std Err of Coef.	0.061445

==========

Chrysotile Asbestos versus Serpentine Asbestos

Regression Output:

Constant	-1.61575
Std Err of Y Est	9.012186
R Squared	0.738656
No. of Observations	60
Degrees of Freedom	58
X Coefficient(s)	0.491714
Std Err of Coef.	0.038405

R Squared = Correlation Coefficient

SOURCE: LEVINE-FRICKE

Reproduced with permission of the copyright owner. Further reproduction prohibited without permission.

QA/QC INTER-LABORATORY DATA SUMMARY OF PLM ANALYSES BY MED-TOX & McCRONE

Sample ID Number	Elongate Serpentine %	Chrysotile Asbestos %	McCRONE Serpentine Asbestos %	RPD Elongate & McCRONE	RPD Chrysotile & McCRONE
XP1/5.5-	70	25	45	43.5	57.1
XP3/2-3	1	1	1	0.0	0.0
XP3/4-5	3	1	7.5	85.7	152.9 *
XP3/6-7	10	3	1	163.6	100.0
XP5/1-2	1	1	2	66.7	66.7
XP5/4-5	1	1	1	0.0	0.0
XP6/4-5	90	40	80	11.8	66.7
Average RPD				63.0	90.1
Standard Deviation				60.7	53.2
Std. Dev. x 2.77				168.2	147.5

Note:
* = samples with an RPD > Std. Dev. x 2.77

Med-Tox's PLM Results of Trace and ND were tabulated as 1% (Method Detection Limit)

McCRONE's PLM data was generally reported as a range of asbestos concentrations (e.g. 10-20%).
For QC purposes, median asbestos concentrations were calculated for inter-laboratory comparisons.

McCRONE's PLM data was occasionally reported as less than or greater than a particular value.
For QC purposes, the particular value was tabulated for inter-laboratory comparisons.

McCRONE's and Med-Tox's PLM data have units of % volume and % area, respectively.
Those units of measurement are assumed to be equivalent.

SOURCE: LEVINE-FRICKE

Reproduced with permission of the copyright owner. Further reproduction prohibited without permission.

Table 5-10

QA/QC INTRA-LABORATORY DATA SUMMARY OF TEM ANALYSES BY MED-TOX

Original Sample ID	"Duplicate" ID	Original Mass Conc. %	Duplicate Mass Conc. %	RPD Mass Conc.	Original Struct. Conc. (trill.struct./g)	Duplicate Struct. Conc. (trill.struct./g)	RPD Struct. Conc.
PC1B	PC93B	10	5	68	8	7	13
PC2B	PC92B	30	10	100	3	4	29
PC41A	PC93A	10	30	100	5	4	22
PC41B	PC93B	10	4	84	4	2	67
SB1-39.9	SB1-40.0	1	0.5	55	1	1	0
SB3-6.7	SB3-6.8	2	4	82	1	3	100
SB3-6.9	SB3-7.0	2	3	36	2	3	40
SB3-15.0	SB3-15.1	4	1	115	3	1	100
SB3-15.2	SB3-15.3	6	1.0	141 *	3	1	100
AF5-2.4	AF5-2.5	3	4	41	2	2	0
AF5-15.0	AF5-15.1	4	2	52	4	2	67
SS2	SS81	1	0.4	24	0.4	0.5	22
SS12	SS82	2	1.0	54	0.2	0.3	40
SS34	SS84	7	100	174 *	5	4	22
Average RPD				80			44
Standard Deviation				42			36
Std. Dev. x 2.77				117			100

"Duplicate" refers to samples submitted as blind duplicate to the laboratory

* = Samples with an RPD > Std. Dev x 2.77

SOURCE: LEVINE-FRICKE

Reproduced with permission of the copyright owner. Further reproduction prohibited without permission.

Table 5-11

PLM-TEM DATA COMPARISON
(PLM DATA GREATER THAN OR EQUAL TO 1%)

Sample ID Number	PLM Elongate Serpentine (% Area)	TEM Asbestos % Mass	PLM < TEM	PLM >= TEM
PC1A	3	3		*
PC1B	75	10		*
PC93B	75	5		*
PC1C	15	3		*
PC2B	50	30		*
PC92B	75	10		*
PC2AX	50	10		*
PC3B	75	10		*
PC41A	70	10		*
PC93A	30	30		*
PC41B	80	12		*
PC93B	50	4		*
BP5 1.5B	2	30	*	
BP14 11-12B	1	30	*	
BS30	5	4		*
AL19A	10	20	*	
AL19B	40	100	*	
AL40A	5	70	*	
AL40B	15	100	*	
AL54A	90	90		*
AL54B	60	40		*
SB2-35.0	2	1		*
SB3-6.9	2	2		*
SB3-27.8	3	1		*
AF3-7.5	3	2		*
AF3-13.3	2	4	*	
AF5-15.1	2	2		*
AF6-15.0	2	0.4		*
AF7-2.5	2	1		*
AF7-10.0	2	2		*
SS2	1	1		*
SS12	10	2		*
SS82	5	1		*
SS16	5	20		*
SS25	5	9	*	
SS26	60	6	*	
SS28	75	20		*
SS34	15	7		*
SS84	15	100		*
OC1	85	20		*
OC15	80	30		*
OC17	80	30		*
OC18	90	100	*	
OC24	85	30		*
OC25	95	100	*	
OC27	85	100	*	
OC28	80	20		*
XP1/2-3	60	10		*
XP1/4-5	60	10		*
XP1/5.5-6.5	70	10		*
XP3/2-3	1	1		*
XP3/4-5	3	3		*
XP3/6-7	10	6		*
XP6/4-5	90	20		*
Total Occurrences		54	12	42
% of Total		100%	22%	78%

SOURCE: LEVINE-FRICKE

Reproduced with permission of the copyright owner. Further reproduction prohibited without permission.

Table 5-12

TEM RESULTS WHEN PLM RESULTS
EQUAL TRACE RESULTS

Sample ID Number	TEM Asbestos % Mass
BP5 8-10B	30
BP14 3-4B	6
AL16B	0.5
SB1-17.5	4
SB1-32.5	3
SB1-39.9	1
SB1-40.0	0.5
SB2-15.0	1
SB2-42.5	1
SB3-6.7	2
SB3-6.8	4
SB3-7.0	3
SB3-15.0	4
SB3-15.1	1
SB3-15.2	6
SB3-15.3	1
SB3-19.7	5
AF1-10.0	3
AF1-14.5	3
AF2-5.0	2
AF2-10.0	3
AF2-15.0	0.3
AF3-25.0	10
AF4-5.0	3
AF4-15.0	2
AF4-22.5	2
AF5-2.4	3
AF5-2.5	4
AF5-15.0	4
AF5-20.2	1
AF6-10.0	0.09
SS81	1
SS22	0.2
XP5/1-2	7
XP5/4-5	0.3
Average	3.4 %
Total # of Samples	35

SOURCE: LEVINE-FRICKE

Reproduced with permission of the copyright owner. Further reproduction prohibited without permission.

Table 5-13

PLM ASBESTOS DATA SUMMARY
OUTCROP AREAS

Elongate Serpentine Concentration Range (% Area)	No. of Samples within concentration Range (n = 35)	Percent Occurrences *
0-1	0	0.00
2-3	0	0.00
4-5	0	0.00
6-10	0	0.00
11-20	0	0.00
21-30	4	11.11
31-40	1	2.78
41-60	4	11.11
61-80 (Modal Range)	11	30.56
81-100 (Modal Range)	15	41.67

*Percent Occurrences = 100 x No. of Samples Within the Concentration Range divided by the Total No. of Samples.

Sample ID	Elongate Serpentine (% Area)
OC-1	85
OC-2	70
OC-3	60
OC-4	70
OC-5	65
OC-6	85
OC-9	60
OC-10	85
OC-10x	85
OC-12	25
OC-13	25
OC-14	90
OC-15	80
OC-16	25
OC-17	80
OC-18	90
OC-18B	90
OC-19	60
OC-21	60
OC-24	85
OC-25	95
OC-25B	95
OC-27	85
OC-28	80
OC-29	90
OC-30	80
OC-31	75
OC-32	60
CC-1	90
CC-2	90
CC-3	50
CC-4	80
CC-5	25
CC-6	90
CC-7	40
Mean	69 %

Note: For purposes of calculating means, elongate serpentine concentrations reported as Trace and ND were assumed to be 0.5% and 0.0%, respectively.

SOURCE: LEVINE-FRICKE

Reproduced with permission of the copyright owner. Further reproduction prohibited without permission.

Table 5-14A

PLM ASBESTOS DATA SUMMARY
SERPENTITNITE SOIL SAMPLES FROM THE NEW IDRIA FORMATION

Elongate Serpentine Concentration Range (% Area)	No. of Samples within concentration Range (n = 8)	Percent Occurrences *
0-1	0	0.00
2-3	0	0.00
4-5	0	0.00
6-10	0	0.00
11-20	0	0.00
21-30	0	0.00
31-40	0	0.00
41-60	0	0.00
61-80	2	25.00
81-100 (Modal Range)	6	75.00

*Percent Occurrences = 100 x No. of Samples Within the Concentration Range divided by the Total No. of Samples.

Sample ID	Elongate Serpentine (% Area)
OC-10x	85
OC-14	90
OC-15	80
OC-18	90
OC-18B	90
OC-25B	95
OC-27	85
OC-31	75
Mean	86 %

Note: For purposes of calculating means, elongate serpentine concentrations reported as Trace and ND were assumed to be 0.5% and 0.0%, respectively.

SOURCE: LEVINE-FRICKE

Reproduced with permission of the copyright owner. Further reproduction prohibited without permission.

Table 5-14B

PLM ASBESTOS DATA SUMMARY
MINE SURFACES IN THE NEW IDRIA FORMATION

Elongate Serpentine Concentration Range (% Area)	No. of Samples within concentration Range (n = 7)	Percent Occurrences *
0-1	0	0.00
2-3	0	0.00
4-5	0	0.00
6-10	0	0.00
11-20	0	0.00
21-30	0	0.00
31-40	0	0.00
41-60	1	14.29
61-80 (Modal Range)	3	42.86
81-100 (Modal Range)	3	42.86

*Percent Occurrences = 100 x No. of Samples Within the Concentration Range divided by the Total No. of Samples.

Sample ID	Elongate Serpentine (% Area)
OC-17	80
OC-24	85
OC-25	95
OC-28	80
OC-29	90
OC-30	80
OC-32	60
Mean	81 %

Note: For purposes of calculating means, elongate serpentine concentrations reported as Trace and ND were assumed to be 0.5% and 0.0%, respectively.

SOURCE: LEVINE-FRICKE

Reproduced with permission of the copyright owner. Further reproduction prohibited without permission.

Table 5-14C

PLM ASBESTOS DATA SUMMARY
INTERMITTENT STREAMBEDS
THAT RUN THROUGH THE NEW IDRIA FORMATION

Elongate Serpentine Concentration Range (% Area)	No. of Samples within concentration Range (n = 11)	Percent Occurrences *
0-1	0	0.00
2-3	0	0.00
4-5	0	0.00
6-10	0	0.00
11-20	0	0.00
21-30	3	27.27
31-40	0	0.00
41-60	2	18.18
61-80	3	27.27
81-100	3	27.27

*Percent Occurrences = 100 x No. of Samples Within the Concentration Range divided by the Total No. of Samples.

Sample ID	Elongate Serpentine (% Area)
OC-1	85
OC-2	70
OC-3	60
OC-4	70
OC-5	65
OC-6	85
OC-9	60
OC-10	85
OC-12	25
OC-13	25
OC-16	25
Mean	60 %

Note: For purposes of calculating means, elongate serpentine concentrations reported as Trace and ND were assumed to be 0.5% and 0.0%, respectively.

SOURCE: LEVINE-FRICKE

Reproduced with permission of the copyright owner. Further reproduction prohibited without permission.

Table 5-15

PLM ASBESTOS DATA SUMMARY
SAMPLES FROM THE "BIG BLUE"

Elongate Serpentine Concentration Range (% Area)	No. of Samples within concentration Range (n = 7)	Percent Occurrences *
0-1	0	0.00
2-3	0	0.00
4-5	0	0.00
6-10	0	0.00
11-20	0	0.00
21-30	1	14.29
31-40	1	14.29
41-60	1	14.29
61-80	1	14.29
81-100 (Modal Range)	3	42.86

*Percent Occurrences = 100 x No. of Samples Within the Concentration Range divided by the Total No. of Samples.

Sample ID	Elongate Serpentine (% Area)
CC-1	90
CC-2	90
CC-3	50
CC-4	80
CC-5	25
CC-6	90
CC-7	40
Mean	66 %

Note: For purposes of calculating means, elongate serpentine concentrations reported as Trace and ND were assumed to be 0.5% and 0.0%, respectively.

SOURCE: LEVINE-FRICKE

Reproduced with permission of the copyright owner. Further reproduction prohibited without permission.

Table 5-16

PLM ASBESTOS DATA SUMMARY
ALLUVIAL FAN CORE SAMPLES

Elongate Serpentine Concentration Range (% Area)	No. of Samples within concentration Range (n = 40)	Percent Occurrences *
0-1 (Modal Range)	31	77.50
2-3	9	22.50
4-5	0	0.00
6-10	0	0.00
11-20	0	0.00
21-30	0	0.00
31-40	0	0.00
41-60	0	0.00
61-80	0	0.00
81-100	0	0.00

*Percent Occurrences = 100 x No. of Samples Within the Concentration Range divided by the Total No. of Samples.

PRE-ASBESTOS MINING SAMPLES
(N = 29)

Sample ID	Elongate Serpentine (% Area)
SB1-32.5	Trace
SB1-39.9	Trace
SB1-40.0	Trace
SB2-35.0	2
SB2-42.5	Trace
SB3-15.0	Trace
SB3-15.1	Trace
SB3-15.2	Trace
SB3-15.3	Trace
SB3-19.7	Trace
SB3-27.8	3
AF1-5.3	2
AF1-10.0	Trace
AF1-14.5	Trace
AF2-5.0	Trace
AF2-10.0	Trace
AF2-15.0	Trace
AF3-7.5	3
AF3-13.3	2
AF3-25	Trace
AF4-5.0	Trace
AF4-10.0	Trace
AF4-15.0	Trace
AF4-22.5	Trace
AF5-10.0	Trace
AF5-15.0	Trace
AF5-15.1	2
AF5-20.1	2
AF5-20.2	Trace
Mean	<1 %

Note: For purposes of calculating means, elongate serpentine concentrations reported as Trace and ND were assumed to be 0.5% and 0.0%, respectively.

POST-ASBESTOS MINING SAMPLES
(N = 11)

Sample ID	Elongate Serpentine (% Area)
SB1-17.5	Trace
SB2-15.0	Trace
SB3-6.7	Trace
SB3-6.8	Trace
SB3-6.9	2
SB3-7.0	Trace
AF1-0.3	1
AF2-1.5	Trace
AF3-2.5	2
AF5-2.4	Trace
AF5-2.5	Trace
Mean	<1 %

SOURCE: LEVINE-FRICKE

Reproduced with permission of the copyright owner. Further reproduction prohibited without permission.

Table 5-17

SUMMARY OF PRE-ASBESTOS MINING VERSUS POST-ASBESTOS MINING TEM RESULTS
FOR ALLUVIAL FAN CORE SAMPLES
including t-Test for signficant difference

Pre-mining samples analyzed by TEM		Post-mining samples analyzed by TEM	
Sample ID	Asbestos % Mass	Sample ID	Asbestos % Mass
SB1-32.5	3	SB1-17.5	4
SB1-39.9	0.8	SB2-15.0	1
SB2-35.0	1	SB3-7.0	3
SB2-42.5	1	AF5-2.5	3
SB3-15.0	3		
SB3-19.7	5		
SB3-27.8	1		
AF1-10.0	3		
AF1-14.5	3		
AF2-10.0	3		
AF2-15.0	0.3		
AF3-13.3	4		
AF3-25	10		
AF4-15.0	2		
AF4-22.5	2		
AF5-15.0	3		
AF5-20.2	1		
# of values	17		4
Average % Mass	2.71		2.75
Sample Variance	4.87		1.19

Combined Results	
Average Variance *	4.28
Std. Error	1.15
Degrees of Freedom	19
Calculated t value	0.03
Tabulated t at 95% Confidence Interval for df = 19	2.09
Result of t-Test	Passed

Conclusion: There exists no significant difference between the two sets of values.

* = Average Variance is the weighted average of the population variance

SOURCE: LEVINE-FRICKE

Reproduced with permission of the copyright owner. Further reproduction prohibited without permission.

Table 5-18

SUMMARY OF PRE-ASBESTOS MINING VERSUS POST ASBESTOS MINING TEM RESULTS
FOR SETTLING BASIN CORE SAMPLES
including t-Test for signficant difference

Pre-mining samples analyzed by TEM		Post-mining samples analyzed by TEM	
Sample ID	Asbestos % Mass	Sample ID	Asbestos % Mass
SB1-32.5	3	SB1-17.5	4
SB1-39.9	0.8	SB2-15.0	1
SB2-35.0	1	SB3-7.0	3
SB2-42.5	1		
SB3-15.0	3		
SB3-19.7	5		
SB3-27.8	1		
# of values	7		3
Average % Mass	2.11		2.67
Sample Variance	2.19		1.56

Combined Results

Average Variance *	2.03
Std. Error	0.98
Degrees of Freedom	8
Calculated t value	0.56
Tabulated t at 95% Confidence Interval for df = 8	2.31
Result of t-Test	Passed

Conclusion : There exists no significant difference between the two sets of values.

* = Average Variance is the weighted average of the population variance

SOURCE: LEVINE-FRICKE

Reproduced with permission of the copyright owner. Further reproduction prohibited without permission.

Table 5-19

PLM ASBESTOS DATA SUMMARY
STREAMBED SEDIMENT FROM THE WEST FORK FROM LOCATIONS
UPSTREAM OF THE MILL SITE

Elongate Serpentine Concentration Range (% Area)	No. of Samples within concentration Range (n = 7)	Percent Occurrences *
0-1	0	0.00
2-3	0	0.00
4-5	0	0.00
6-10	0	0.00
11-20	0	0.00
21-30	1	14.29
31-40	0	0.00
41-60 (Modal Range)	3	42.86
61-80 (Modal Range)	3	42.86
81-100	0	0.00

*Percent Occurrences = 100 x No. of Samples Within the Concentration Range divided by the Total No. of Samples.

Sample ID	Elongate Serpentine (% Area)
PC-4B	60
PC-3B	75
PC-2B	50
PC-1B	75
PC-41B	80
PC-42B	30
PC-43B	30
Mean	57 %

Note: For purposes of calculating means, elongate serpentine concentrations reported as Trace and ND were assumed to be 0.5% and 0.0%, respectively.

SOURCE: LEVINE-FRICKE

Reproduced with permission of the copyright owner. Further reproduction prohibited without permission.

Table 5-20

PLM ASBESTOS DATA SUMMARY
STREAMBED SEDIMENT FROM THE WEST FORK FROM LOCATIONS ALONG AND DOWNSTREAM OF THE MILL SITE

Elongate Serpentine Concentration Range (% Area)	No. of Samples within concentration Range (n = 6)	Percent Occurrences *
0-1	0	0.00
2-3	0	0.00
4-5	0	0.00
6-10	0	0.00
11-20	1	16.67
21-30	0	0.00
31-40	1	16.67
41-60 (Modal Range)	2	33.33
61-80 (Modal Range)	2	33.33
81-100	0	0.00

*Percent Occurrences = 100 x No. of Samples Within the Concentration Range divided by the Total No. of Samples.

Sample ID	Elongate Serpentine (% Area)
PC-5B	50
PC-6B	40
PC-9B	70
PC-10B	12
PC-11B	70
PC-13B	50
Mean	49 %

Note: For purposes of calculating means, elongate serpentine concentrations reported as Trace and ND were assumed to be 0.5% and 0.0%, respectively.

SOURCE: LEVINE-FRICKE

Reproduced with permission of the copyright owner. Further reproduction prohibited without permission.

Table 5-21

PLM ASBESTOS DATA SUMMARY
SAMPLES FROM STREAMBANKS FORMED BY SERPENTINITE LANDSLIDE AND/
DEBRIS FLOW DEPOSITS IN THE MILL SITE AREA

Elongate Serpentine Concentration Range (% Area)	No. of Samples within concentration Range (n = 17)	Percent Occurrences *
0-5 (Modal Range)	9	52.94
6-10	1	5.88
11-20	3	17.65
21-30	1	5.88
31-40	1	5.88
41-60	1	5.88
61-80	1	5.88
81-100	0	0.00

*Percent Occurrences = 100 x No. of Samples Within the Concentration Range divided by the Total No. of Samples.

Sample ID	Elongate Serpentine (% Area)
PC-1A	15
PC-1C	3
PC-2A	20
PC-3A	Trace
PC-3C	20
PC-7A	40
PC-9A	10
PC-9C	50
PC-10A	4
PC-10C	Trace
PC-11A	Trace
PC-11C	25
PC-12A	Trace
PC-12C	5
PC-15C	5
PC-16C	3
PC-41A	70
Mean	16 %

Note: For purposes of calculating means, elongate serpentine concentrations reported as Trace and ND were assumed to be 0.5% and 0.0%, respectively.

SOURCE: LEVINE-FRICKE

Reproduced with permission of the copyright owner. Further reproduction prohibited without permission.

Table 5-22

PLM ASBESTOS DATA SUMMARY
UPPER BORROW SOURCE AREA

Elongate Serpentine Concentration Range (% Area)	No. of Samples within concentration Range (n = 30)	Percent Occurrences *
0-1 (Modal Range)	23	76.67
2-3	5	16.67
4-5	0	0.00
6-10	2	6.67
11-20	0	0.00
21-30	0	0.00
31-40	0	0.00
41-60	0	0.00
61-80	0	0.00
81-100	0	0.00

*Percent Occurrences = 100 x No. of Samples Within the Concentration Range divided by the Total No. of Samples.

Sample ID	Elongate Serpentine (% Area)
BS-33	2
BS-34	Trace
BS-10	3
BS-11	1
BP-18/3-4	3
BP-18/8-9	7
BP-35/1-2	Trace
BP-35/3-4	Trace
BS-19	Trace
BS-20	Trace
BP-15/3-4	Trace
BP-15/10-	Trace
BS-16	ND
BP-14/3-4	Trace
BP-14/11-	1
BP-14/13.	Trace
XP-5/1-2	Trace
XP5/4-5	Trace
BS-2	Trace
BS-3	Trace
Mean	1 %

Note: For purposes of calculating means, elongate serpentine concentrations reported as Trace and ND were assumed to be 0.5% and 0.0%, respectively.

Sample ID	Elongate Serpentine (% Area)
BS-4	Trace
B5-5/1.5B	2
BP-5/8-10B	Trace
BP-6/1.0	Trace
BS-7	Trace
BS-8	Trace
BS-9	Trace
XP-3/2-3	1
XP3/4-5	3
XP3/6-7	10

SOURCE: LEVINE-FRICKE

Reproduced with permission of the copyright owner. Further reproduction prohibited without permission.

Table 5-23

PLM ASBESTOS DATA SUMMARY
LOWER BORROW SOURCE AREA

Elongate Serpentine Concentration Range (% Area)	No. of Samples within concentration Range (n = 9)	Percent Occurrences *
0-1	1	11.11
2-3	2	22.22
4-5	2	22.22
6-10 (Modal Range)	4	44.44
11-20	0	0.00
21-30	0	0.00
31-40	0	0.00
41-60	0	0.00
61-80	0	0.00
81-100	0	0.00

*Percent Occurrences = 100 x No. of Samples Within the Concentration Range divided by the Total No. of Samples.

Sample ID	Elongate Serpentine (% Area)
BS-28	10
BS-29	10
BS-30	5
BS-31	10
BS-32	3
BS-24	5
BS-25	2
BS-26	Trace
BS-27	10
Mean	6 %

Note: For purposes of calculating means, elongate serpentine concentrations reported as Trace and ND were assumed to be 0.5% and 0.0%, respectively.

SOURCE: LEVINE-FRICKE

Reproduced with permission of the copyright owner. Further reproduction prohibited without permission.

Table 5-24

PLM ASBESTOS DATA SUMMARY
TAILINGS PILE

Elongate Serpentine Concentration Range (% Area)	No. of Samples within concentration Range (n = 19)	Percent Occurrences *
0-1	0	0.00
2-3	0	0.00
4-5	0	0.00
6-10	0	0.00
11-20	0	0.00
21-30	0	0.00
31-40	4	21.05
41-60	5	26.32
61-80	4	21.05
81-100 (Modal Range)	6	31.58

*Percent Occurrences = 100 x No. of Samples Within the Concentration Range divided by the Total No. of Samples.

Sample ID	Elongate Serpentine %
AL-17A	40
AL-17B	65
AL-18A	40
AL-18B	50
AL-19B	40
AL-20B	45
AL-25B	75
AL-24B	55
AL-23B	70
AL-22B	75
AL-21B	35
AL-26B	90
AL-27B	85
AL-28B	80
AL-29B	85
AL-30B	85
AL-31B	50
AL-54A	90
AL-54B	60
Mean	64 %

Note: For purposes of calculating means, elongate serpentine concentrations reported as Trace and ND were assumed to be 0.5% and 0.0%, respectively.

SOURCE: LEVINE-FRICKE

Reproduced with permission of the copyright owner. Further reproduction prohibited without permission.

Table 5-25

PLM ASBESTOS DATA SUMMARY
ORE STORAGE AREA

Elongate Serpentine Concentration Range (% Area)	No. of Samples within concentration Range (n = 5)	Percent Occurrences *
0-1	0	0.00
2-3	0	0.00
4-5	0	0.00
6-10	0	0.00
11-20	0	0.00
21-30	0	0.00
31-40	1	20.00
41-60	0	0.00
61-80 (Modal Range)	4	80.00
81-100	0	0.00

*Percent Occurrences = 100 x No. of Samples Within the Concentration Range divided by the Total No. of Samples.

Sample ID	Elongate Serpentine (% Area)
AL-5B	80
AL-4B	80
AL-36B	70
AL-52	80
AL-6B	40
Mean	70 %

Note: For purposes of calculating means, elongate serpentine concentrations reported as Trace and ND were assumed to be 0.5% and 0.0%, respectively.

SOURCE: LEVINE-FRICKE

Reproduced with permission of the copyright owner. Further reproduction prohibited without permission.

Table 5-26

PLM ASBESTOS DATA SUMMARY
MILL SITE OPERATIONS AREA

Elongate Serpentine Concentration Range (% Area)	No. of Samples within concentration Range (n = 9)	Percent Occurrences *
0-1	1	11.11
2-3	2	22.22
4-5	1	11.11
6-10	1	11.11
11-20 (Modal Range)	3	33.33
21-30	0	0.00
31-40	0	0.00
41-60	0	0.00
61-80	1	11.11
81-100	0	0.00

*Percent Occurrences = 100 x No. of Samples Within the Concentration Range divided by the Total No. of Samples.

Sample ID	Elongate Serpentine (% Area)
AL-8	2
AL-9	15
AL-11B	15
AL-12B	Trace
AL-13B	3
AL-14B	5
AL-15B	10
AL-16A	70
AL-53	15
Mean	15 %

Note: For purposes of calculating means, elongate serpentine concentrations reported as Trace and ND were assumed to be 0.5% and 0.0%, respectively.

SOURCE: LEVINE-FRICKE

Reproduced with permission of the copyright owner. Further reproduction prohibited without permission.

Table 5-27

PLM ASBESTOS DATA SUMMARY
RAILROAD MINE

Elongate Serpentine Concentration Range (% Area)	No. of Samples within concentration Range (n = 10)	Percent Occurrences *
0-1	0	0
2-3	0	0
4-5	0	0
6-10	1	10
11-20 (Modal Range)	2	20
21-30	1	10
31-40	0	0
41-60	1	10
61-80 (Modal Range)	4	40
81-100	1	10

*Percent Occurrences = 100 x No. of Samples Within the Concentration Range divided by the Total No. of Samples.

Sample ID	Elongate Serpentine (% Area)
AL-38B	25
AL-39B	75
AL-40B	15
AL-41B	15
AL-43B	8
AL-44B	70
AL-45B	85
AL-46B	80
AL-50B	70
AL-51B	50
Mean	49 %

Note: For purposes of calculating means, elongate serpentine concentrations reported as Trace and ND were assumed to be 0.5% and 0.0%, respectively.

SOURCE: LEVINE-FRICKE

Reproduced with permission of the copyright owner. Further reproduction prohibited without permission.

Table 5-28

PLM ASBESTOS DATA SUMMARY
MILL SITE ACCESS ROADS

Elongate Serpentine Concentration Range (% Area)	No. of Samples within concentration Range (n = 9)	Percent Occurrences *
0-1 (Modal Range)	6	66.67
2-3	2	22.22
4-5	0	0.00
6-10	1	11.11
11-20	0	0.00
21-30	0	0.00
31-40	0	0.00
41-60	0	0.00
61-80	0	0.00
81-100	0	0.00

*Percent Occurrences = 100 x No. of Samples Within the Concentration Range divided by the Total No. of Samples.

Sample ID	Elongate Serpentine (% Area)
AL-49	2
AL-48	3
AL-47	Trace
AL-37	10
AL-1	Trace
AL-2	Trace
AL-3	Trace
AL-2B	Trace
AL-3B	Trace
Mean	2 %

Note: For purposes of calculating means, elongate serpentine concentrations reported as Trace and ND were assumed to be 0.5% and 0.0%, respectively.

SOURCE: LEVINE-FRICKE

Reproduced with permission of the copyright owner. Further reproduction prohibited without permission.

Reproduced with permission of the copyright owner. Further reproduction prohibited without permission.

Table 6-1

SUMMARY OF AVERAGE SOIL TYPE CHARACTERISTICS INCLUDING
LABORATORY DATA AND FIELD OBSERVATIONS

SOIL TYPE	K	PARTICLE SIZES < 2.0 MM Clay	Silt	Sand	COARSE PARTICLES > 2.0 MM	OM	STRUCTURE	PERMEABILITY	COMMENTS
SERPENTINITE SOIL	0.13	0.8%	6.0%	93.2%	>16%	0.5%	Blocky	Moderately Rapid	Field observations indicate gully erosion is severe. Vegetation is restricted primarily to sparse manzanita shrubbery with no grassy covering.
MINE SURFACES	0.10	1.3%	2.7%	96.1%	>35%	0.2%	Very Blocky	Rapid	Field observations indicate steep mine surfaces are primarily susceptible to mass wasting erosion. Less steep mine surfaces appear to erode from sheet and rill erosion. Mine surfaces generally have little vegetation.
TAILINGS PILES	0.16	1.4%	9.3%	89.3%	>11%	0.15%	Very Fine Granular	Rapid	Field observations indicate the Atlas tailings piles are primarily susceptible to wind erosion and gullying and mass wasting from runoff. Atlas piles appear to be migrating like sand dunes with wind-blown particles covering nearby vegetation. Runoff from the Atlas mines and piles drains into steep gullies. Coalinga pile is contained by the steep side walls of Pine Canyon and appears to be less susceptible to wind erosion than the Atlas piles. Coalinga pile has one gully that has formed in the middle of the pile. Runoff from the Coalinga pile is partly trapped by a retaining dam. Tailings generally have little vegetation. Undisturbed surfaces of the Atlas and Coalinga Sites commonly have a thin crust.
RAILROAD MINE	0.12	2.2%	5.0%	92.8%	>23%	0.5%	Blocky	Moderately Rapid	Field observations indicate the Railroad Mine is primarily susceptible to sheet and rill erosion and supports little vegetation.
LANDSLIDE SURFACE SOILS	0.14	3.2%	6.9%	89.9%	>23%	1.5%	Very Blocky	Moderate	Field observations indicate the Mill Site landslide surface soils are not readily erodible because the gently sloping surfaces support a thick, grassy covering with rootlets that extend approximately 3 inches below the surface. This contrasts with the gully erosion associated with the intermittent streams that have formed at the margins of the Mill Site landslide deposits.

NOTES:
K is the unadjusted K factor value determined by SPLC from the SCS triangular nomograph method (Erickson, 1977).
Particle size data are based on sieve and hydrometer analyses of particles less than 2.0 mm in size. Size ranges are per SCS (1987) guidelines.
Coarse particle content indicates percentage of coarse particles greater than 2.0 mm in size.
Laboratory data show that the serpentinite soil samples have greater sand content than indicated by field observations. This is because of the platey, fibrous characteristics of the sand-sized chrysotile aggregates that make up the bulk of these types of soil samples. The platey aggregates tend to resist disaggregation by laboratory dispersion techniques but not by rubbing or crushing. Lab data do not support field classifications which indicate heavier textures (i.e., higher clay content).
OM indicates percentage of organic matter content as determined by laboratory analysis.
Soil structure determined by field observation and reference to SCS (1987) reports.
Permeability estimated by reference to SCS (1987) reports and SPLC (1988) field observations.

SOURCE: LEVINE-FRICKE

Reproduced with permission of the copyright owner. Further reproduction prohibited without permission.

Table 6-2

SUMMARY OF K FACTOR VALUES AND POTENTIAL ADJUSTMENTS FOR ASBESTOS SOURCE MATERIALS BASED ON DATA AS REPORTED AND/OR USED BY OTHERS

SOURCE	SOIL TYPE	NUMBER OF SAMPLES	K FACTOR VALUES AS REPORTED OR USED FOR MODELLING	UNADJUSTED K FACTOR VALUES	ADJUSTED K FACTOR VALUES	VERY FINE SAND ADJUSTMENT	ORGANIC MATTER ADJUSTMENT	COARSE PARTICLE ADJUSTMENT	SOIL STRUCTURE ADJUSTMENT	PERMEABILTY ADJUSTMENT
SCS	ATRAVESADA (SERPENTINITE SOIL)	1	0.28	0.26	0.17	NONE	NONE	- 0.06	NONE	- 0.03
EPA	SERPENTINITE SOIL	4	0.28	0.22	0.14	NONE	NONE	- 0.05	NONE	- 0.03
	MINE SURFACES	1	0.18	0.17	0.15	NONE	+ 0.05	- 0.04	NONE	- 0.03
	TAILINGS PILES	3	0.28	0.20	0.13	NONE	+ 0.08	- 0.05	- 0.06	- 0.03
BOYLE	SERPENTINITE SOIL	7	0.23	0.28	0.23	NONE	NONE	- 0.05	NONE	NONE
SPLC	SERPENTINITE SOIL	3	0.13	0.13	0.09	NONE	NONE	- 0.01	NONE	- 0.03
	MINE SURFACES	5	0.10	0.10	0.07	NONE	+ 0.05	- 0.05	NONE	- 0.03
	TAILINGS PILES	4	0.16	0.16	0.08	NONE	+ 0.05	- 0.04	- 0.06	- 0.03
	RAILROAD MINE	4	0.12	0.12	0.09	NONE	+ 0.04	- 0.04	NONE	- 0.03

SOURCES:
SCS - Soil Conservation Service, 1987, Soil Characterization and Lab Data Reports, Preliminary Soil Mapping, Atravesada Soil Series, Fresno County, California.
EPA - Environmental Protection Agency, 1986, Soil Sampling Data Report for the Atlas and Coalinga Sites, Fresno County, California and personal communications.
BOYLE - Boyle Engineering Corporation, 1988, Draft - Summary Letter Report for Sediment Analysis, Arroyo Pasajero Drainage and Sediment Control Plan and personal communications.
SPLC - Southern Pacific Land Company, 1988, Off-Site Report, Volume Two, Regional and On-Site/Near-Site Soil Sampling Results.

NOTES:
Unadjusted K factor values were determined from the SCS triangular nomograph method (Erickson, 1977) using particle size data reported from the above sources.

SCS reported an organic matter content that ranged from 2 to 5%; an average value of 2% was assumed.
SCS reported a gravel content that ranged up to 15% and a coarse sand content of 1%; a coarse particle content of 10% was assumed.
SCS reported permeability as moderately rapid; this classification was assumed for all serpentinite soils, mine surfaces, and tailings piles.
- This assumption is supported by the results of the EPA rainulator tests which indicated rapid permeability.

EPA particle size data reported for composite samples for each EPA soil type were used for determination of the K factor values:
- The EPA composite sample for mine surfaces (C-02) consisted of 1 sample.
- The unadjusted K factor value for the EPA serpentinite soils was determined from averages from 4 composite sample (C-03, C-04, C-05, C-06). Each of these composite samples were composited from 4 sub-samples.
- The unadjusted K factor value for the EPA asbestos tailings piles soil type was determined from averages from 3 composite samples (C-07, C-08, C-09). These 3 composite samples were composited from a total of 14 sub-samples.

EPA reported organic matter contents for serpentine soils that ranged from 0.5 to 2.9%; an average value of 2% was assumed.
EPA reported an average organic matter content for mine surfaces of 0.2%.
EPA reported organic matter content values for tailings piles that ranged from 0.18 to 0.43%; an average value of 0.3% was assumed.
EPA did not indicate percentages of coarse particle composition; an average value of 10% was assumed for all EPA soil types.
- This assumption was based on field observations and SCS and SPLC data regarding the occurrence of coarse particles.

SPLC reported K factor values were reported using data from the following:
- 3 samples for the serpentinite soil type; 5 samples for the mine surface soil type; 4 samples for the asbestos tailings type.
- 6 sub-samples were composited to form each of the above SPLC samples for each soil type.

SPLC organic matter content values for serpentinite soils ranged from 0.4 to 0.5%; an average of 2% was assumed in accordance with SCS and EPA data.
SPLC organic matter content values for mine surfaces ranged from 0.1 to 0.4%; an average value of 0.2% was assumed.
SPLC organic matter content values for tailings piles ranged from 0.1 to 0.2%; an average value of 0.15% was assumed.
SPLC organic matter content values for the Railroad Mine ranged from 0.1 to 1.0%; an average value of 0.5% was assumed.

SPLC particle size data for serpentinite soils indicated an average very coarse particle content of 16%.
SPLC particle size data for mine surfaces indicated an average very coarse particle content of 35%.
SPLC particle size data for tailings piles indicated an average very coarse particle content of 11%.
SPLC particle size data for the Railroad Mine indicated an average very coarse particle content of 23%.

A blocky soil structure was assumed for serpentinite soils and mine surfaces; this is in accordance with with SCS data and SPLC field observations.
A fine granular soil structure was assumed for asbestos tailings piles; this is in accordance with SPLC field observations of the milled materials.
Organic matter adjustments, soil structure adjustments, and permeability adjustments were applied in accordance with Goldman et al, 1986, Chapter 5.
Coarse particle adjustments were applied in accordance with Erickson, 1977, Chart 4 (as revised in 1979).
Unadjusted and adjusted K factor values determined by SPLC using the SCS triangular nomograph method of Erickson, 1977.
Number of samples indicates the number of samples used to determine a K factor value as indicated.
EPA and SPLC used composited samples - see text for explanation.

SOURCE: LEVINE-FRICKE

Reproduced with permission of the copyright owner. Further reproduction prohibited without permission.

Table 6-3
MUSLE & USLE FACTOR - C-FACTOR COMPUTATION SHEET

CANOPY COVER	% GROUND COVER-VEGETATION 0	20	40	60	80	100
0	0.450	0.200	0.100	0.042	0.013	0.003
25	0.300	0.175	0.090	0.039	0.012	0.003
50	0.300	0.145	0.078	0.036	0.012	0.003
75	0.225	0.120	0.070	0.033	0.011	0.003

NOTES:

Taken from Soil Conservation Service Field Manual, 1977, Table A.4. "c" Factors For Permanent Pasture, Rangeland, Idle Land and Grazed Woodland.

Vegetation-Ground Cover interpreted as grass.
Canopy Cover is interpreted to be the average - between tall weeds and short bushes and appreciable brush or bushes.

SOURCE: LEVINE-FRICKE

Reproduced with permission of the copyright owner. Further reproduction prohibited without permission.

Table 6-4

ESTIMATED EFFECT OF ROADS AND EXPLORATION PITS ON FOLIAGE AND ASSOCIATED EROSION

WATER-SHEDS	WATERSHED AREA (SQ. MI.)	ROAD LENGTH IN WAT.SHD. (MI.)	ESTIMATED ROAD WIDTH AVERAGE (FT)	ESTIMATED ROAD AREA (SQ. MI.)	EX. PIT (#)	ESTIMATED AVERAGE AREA (SQ. FT.)	ESTIMATED EX. PIT AREA (SQ. MI.)	TOTAL AREA ROADS PITS (SQ. MI.)	PRE-MINE CANOPY COVER (%)	PRE-MINE GROUND COVER (%)	ROAD & PIT IMPACTED CANOPY (%)	ROAD & PIT IMPACTED GRND COV. (%)	ROAD & PIT CANOPY IMPACT (%)	ROAD & PIT GRND CVR IMPACT (%)	PRE-MINE C COVER FACTOR	ROAD & PIT IMPACTED C FACTOR	% CHANGE IN EROSION IN WA. SH
1	0.79	8.7	12	0.01977	14	300	0.00015	0.01992	38.00	0.00	37.04	0.00	-0.96	0.00	0.3412	0.3415	0.09
2	0.17	2.1	12	0.00477	2	300	0.00002	0.00479	33.50	0.00	32.56	0.00	-0.94	0.00	0.3528	0.3558	0.85
3	0.32	2.3	12	0.00523	0	300	0.00000	0.00523	45.50	8.00	44.76	7.87	-0.74	-0.13	0.2488	0.2517	1.17
4	0.08	1.1	12	0.00250	0	300	0.00000	0.00250	37.50	0.00	36.33	0.00	-1.17	0.00	0.3400	0.3437	1.09
5	0.39	6.7	12	0.01523	13	300	0.00014	0.01537	39.50	0.00	37.94	0.00	-1.56	0.00	0.3336	0.3386	1.50
6	0.67	8.9	12	0.02023	11	300	0.00012	0.02035	33.25	3.00	32.24	2.91	-1.01	-0.09	0.3252	0.3291	1.20
7	0.16	0.8	12	0.00182	0	300	0.00000	0.00182	34.75	28.50	34.36	28.18	-0.39	-0.32	0.1301	0.1317	1.23
8	0.21	2.1	12	0.00477	0	300	0.00000	0.00477	29.75	31.00	29.07	30.30	-0.68	-0.70	0.1264	0.1278	1.11
9	0.08	0.8	12	0.00182	1	300	0.00001	0.00183	23.25	0.00	22.72	0.00	-0.53	0.00	0.3843	0.3864	0.39
10	0.29	3.8	12	0.00864	7	300	0.00008	0.00871	42.50	0.00	41.22	0.00	-1.28	0.00	0.3240	0.3281	1.27
11	0.13	1.9	12	0.00432	10	300	0.00011	0.00443	34.25	0.00	33.08	0.00	-1.17	0.00	0.3504	0.3541	1.06
12	0.34	3.7	12	0.00841	8	300	0.00009	0.00850	36.75	14.50	35.85	14.14	-0.92	-0.36	0.2108	0.2157	2.32
13	0.05	0.6	12	0.00136	0	300	0.00000	0.00136	33.50	38.50	32.59	37.45	-0.91	-1.05	0.0917	0.0964	5.13
14	0.25	1.7	12	0.00386	3	300	0.00003	0.00390	40.00	47.00	39.38	46.27	-0.62	-0.73	0.0668	0.0686	2.69
15	0.32	4.9	12	0.01114	1	300	0.00001	0.01115	29.25	41.00	28.25	39.57	-1.02	-1.43	0.0854	0.0901	5.50
16	0.25	4.9	12	0.01114	10	300	0.00011	0.01124	52.88	4.00	50.50	3.82	-2.38	-0.18	0.2613	0.2747	5.05
17	0.41	9.1	12	0.02068	27	300	0.00029	0.02097	55.75	0.00	52.90	0.00	-2.85	0.00	0.2823	0.2913	3.01
18	0.43	8.0	12	0.01818	27	300	0.00029	0.01847	66.75	0.00	63.88	0.00	-2.87	0.00	0.2498	0.2584	3.44
19	0.42	6.0	12	0.01364	20	300	0.00022	0.01385	58.00	0.00	56.09	0.00	-1.91	0.00	0.2760	0.2817	2.07
20	0.36	6.3	12	0.01432	11	300	0.00012	0.01444	45.75	3.50	43.92	3.36	-1.83	-0.14	0.2850	0.2914	2.25
21	0.65	4.5	12	0.01023	3	300	0.00003	0.01026	28.25	47.00	27.80	46.26	-0.45	-0.74	0.0710	0.0720	1.41
22	0.59	6.1	12	0.01386	6	300	0.00006	0.01393	34.06	55.60	33.26	54.29	-0.80	-1.31	0.0484	0.0517	6.82
23	0.5	11.4	12	0.02591	39	300	0.00042	0.02633	48.50	15.50	45.95	14.68	-2.55	-0.82	0.1824	0.1933	5.98
24	0.11	2.3	12	0.00523	3	300	0.00003	0.00526	26.50	41.50	25.23	39.52	-1.27	-1.98	0.0855	0.0919	7.49
25	0.11	0.5	12	0.00114	0	300	0.00000	0.00114	28.50	59.75	28.21	59.13	-0.29	-0.62	0.0398	0.0408	2.51
29	0.16	1.5	12	0.00341	3	300	0.00003	0.00344	33.25	50.00	32.53	48.92	-0.72	-1.08	0.0621	0.0648	4.35
30	0.36	2.3	12	0.00523	0	300	0.00000	0.00523	25.00	50.00	24.64	49.27	-0.36	-0.73	0.0654	0.0666	1.83
				0.25682	219		0.00236	0.25917									

SOURCE: LEVINE-FRICKE

Reproduced with permission of the copyright owner. Further reproduction prohibited without permission.

Table 6-5

WATERSHED ASBESTOS CONTENT - PRE & POST MINING

WATER-SHEDS	SERP.SOIL MINE SURFS 84	ORE-STORAGE 70	ASBEST. TAILINGS 64	FRANC-ISCAN 60	R.R-MINE 48	HEN-TINE 30	OPER. AREA 8	BARROW/ L.S 3	0	WATER-SHEDS WT.AVG.
1	100	0	0	0	0	0	0	0	0	84.00
2	100	0	0	0	0	0	0	0	0	84.00
3	84	0	0	0	0	0	0	0	16	70.56
4	100	0	0	0	0	0	0	0	0	84.00
5	100	0	0	0	0	0	0	0	0	84.00
6A	94	0	0	0	0	4	0	0	2	80.16
6B	94	0	0	0	0	0	0	0	6	78.96
7A	44	0	0	0	0	3	0	0	53	37.86
7B	44	0	0	0	0	0	0	0	56	36.96
8A	38	0	0	0	0	30	0	0	32	40.92
8B	38	0	0	0	0	0	0	0	62	31.92
9	100	0	0	0	0	0	0	0	0	84.00
10PRE AT	100	0	0	0	0	0	0	0	0	84.00
10PST AT	95	0	5	0	0	0	0	0	0	83.00
11PRE AT	100	0	0	0	0	0	0	0	0	84.00
11PST AT	95	0	5	0	0	0	0	0	0	83.00
12A	71	0	0	0	0	29	0	0	0	68.34
12B	71	0	0	0	0	0	0	0	29	59.64
13A	37	0	0	0	0	63	0	0	0	49.98
13B	37	0	0	0	0	0	0	0	63	31.08
14A	7	0	0	0	0	90	0	0	3	32.88
14B	7	0	0	0	0	0	0	0	93	5.88
15A	23	0	0	0	0	45	0	0	32	32.82
15B	22	0	0	0	0	0	0	0	78	18.48
16A	92	0	0	0	0	8	0	0	0	79.68
16B	92	0	0	0	0	0	0	0	8	77.28
17	100	0	0	0	0	0	0	0	0	84.00
18	100	0	0	0	0	0	0	0	0	84.00
19PRE AT	100	0	0	0	0	0	0	0	0	84.00
19PST AT	98	0	2	0	0	0	0	0	0	83.60
20	93	0	0	7	0	0	0	0	0	82.32
21	15	0	0	0	0	0	0	0	85	12.60
22PRE CO	20	0	0	32	0	0	0	23	25	36.69
22PST CO	20	1	1	32	1	0	1	19	25	38.55
23	66	0	0	31	0	0	0	3	0	74.13
24	0	0	0	33	0	0	0	0	67	19.80
25PRE CO	0	0	0	0	0	0	0	45	55	1.35
25PST CO	0	0	12	0	0	0	0	33	55	8.67
29	0	0	0	55	0	0	0	0	45	33.00
30	0	0	0	11	0	0	0	0	89	6.60

NOTES:

A = Hentine = 30%
B = Hentine = 0%
PRE = Pre-mining
PST = Post-mining
AT = Atlas Mine
CO = Coalinga Mine
All other values are for both pre- and post-mining

SOURCE: LEVINE-FRICKE

Table 6-6A

INDIVIDUAL MINE IMPACT ON ASBESTOS SOIL EROSION
SUMMARY - UNADJUSTED K

	UNADJUSTED K	2 YR Mine Impact (cu yd)	5 YR Mine Impact (cu yd)	10 YR Mine Impact (cu yd)	25 YR Mine Impact (cu yd)	50 YR Mine Impact (cu yd)	100 YR Mine Impact (cu yd)	AVERAGE YEAR Mine Impact (cu yd)	YEARLY AVERAGE ASB. EROSION (*) (cu yd)
CLNDA									
	A - K=K, AGC=K	8.95	26.52	45.06	66.00	84.00	103.04	16.89	18.20
	B - K=K, AGC=K	8.95	26.52	45.06	66.00	84.00	103.04	16.89	18.20
	A - K=K, AGC=KSS	8.95	26.52	45.06	66.00	84.00	103.04	16.89	18.20
	B - K=K, AGC=KSS	8.95	26.52	45.06	66.00	84.00	103.04	16.89	18.20
	A - K=KSS, AGC=KSS	11.73	34.80	59.14	86.59	110.24	143.26	23.15	25.04
	B - K=KSS, AGC=KSS	11.73	34.80	59.14	86.59	110.24	143.26	23.15	25.04
ATLAS									
	A - K=K, AGC=K	30.92	102.61	173.45	308.58	384.38	480.03	66.78	72.45
	B - K=K, AGC=K	30.89	101.89	173.18	308.13	383.86	473.32	66.21	71.83
	A - K=K, AGC=KSS	26.19	90.19	144.57	246.74	301.39	370.38	53.36	58.14
	B - K=K, AGC=KSS	26.20	93.14	144.14	246.14	300.09	371.83	53.46	58.00
	A - K=KSS, AGC=KSS	62.57	220.15	461.14	710.13	999.76	1134.36	145.15	158.66
	B - K=KSS, AGC=KSS	61.43	219.63	460.74	708.51	997.60	1132.05	145.73	159.74
BASIC									
	A - K=K, AGC=K	3.97	14.51	25.10	42.01	57.17	71.74	9.23	10.09
	B - K=K, AGC=K	3.97	14.51	25.10	42.01	57.17	71.74	9.23	10.09
	A - K=K, AGC=KSS	3.14	11.70	19.98	33.66	45.05	58.01	7.38	8.02
	B - K=K, AGC=KSS	3.14	11.70	20.01	33.66	45.05	58.05	7.42	8.07
	A - K=KSS, AGC=KSS	11.02	44.17	76.69	124.58	174.90	220.14	28.36	30.82
	B - K=KSS, AGC=KSS	11.02	44.14	76.64	124.58	174.48	220.19	28.34	30.81
BORDOS									
	A - K=K, AGC=K	3.55	12.98	21.83	35.62	48.38	60.38	7.93	8.57
	B - K=K, AGC=K	3.55	12.98	21.83	35.62	48.38	60.38	7.93	8.57
	A - K=K, AGC=KSS	3.55	12.98	21.83	35.62	48.38	60.38	7.93	8.57
	B - K=K, AGC=KSS	3.55	12.98	21.83	35.62	48.38	60.38	7.93	8.57
	A - K=KSS, AGC=KSS	10.10	37.72	64.91	108.45	147.11	185.41	24.02	26.10
	B - K=KSS, AGC=KSS	10.10	37.72	64.91	108.45	147.11	185.41	24.02	26.10
TROMBY									
	A - K=K, AGC=K	3.55	12.98	21.83	35.62	48.38	60.38	7.93	8.57
	B - K=K, AGC=K	3.55	12.98	21.83	35.62	48.38	60.38	7.93	8.57
	A - K=K, AGC=KSS	3.55	12.98	21.83	35.62	48.38	60.38	7.93	8.57
	B - K=K, AGC=KSS	3.55	12.98	21.83	35.62	48.38	60.38	7.93	8.57
	A - K=KSS, AGC=KSS	10.10	37.72	64.91	108.45	147.11	185.41	24.02	26.10
	B - K=KSS, AGC=KSS	10.10	37.72	64.91	108.45	147.11	185.41	24.02	26.10
TILES									
	A - K=K, AGC=K	8.95	26.52	45.06	66.00	84.00	103.04	16.89	18.20
	B - K=K, AGC=K	8.95	26.52	45.06	66.00	84.00	103.04	16.89	18.20
	A - K=K, AGC=KSS	8.95	26.52	45.06	66.00	84.00	103.04	16.89	18.20
	B - K=K, AGC=KSS	8.95	26.52	45.06	66.00	84.00	103.04	16.89	18.20
	A - K=KSS, AGC=KSS	20.93	75.47	125.34	201.66	271.05	338.53	46.76	50.50
	B - K=KSS, AGC=KSS	20.93	75.47	125.34	201.66	271.05	338.53	46.76	50.50
MINE?									
	A - K=K, AGC=K	3.55	12.98	21.83	35.62	48.38	60.38	7.93	8.57
	B - K=K, AGC=K	3.55	12.98	21.83	35.62	48.38	60.38	7.93	8.57
	A - K=K, AGC=KSS	3.55	12.98	21.83	35.62	48.38	60.38	7.93	8.57
	B - K=K, AGC=KSS	3.55	12.98	21.83	35.62	48.38	60.38	7.93	8.57
	A - K=KSS, AGC=KSS	10.10	37.72	64.91	108.45	147.11	185.41	24.02	26.10
	B - K=KSS, AGC=KSS	10.10	37.72	64.91	108.45	147.11	185.41	24.02	26.10
PUTLR									
	A - K=K, AGC=K	5.46	15.00	25.07	36.00	47.74	59.15	9.59	10.16
	B - K=K, AGC=K	5.46	15.00	25.07	36.00	47.74	59.15	9.59	10.16
	A - K=K, AGC=KSS	5.46	15.10	25.07	36.00	48.07	59.54	9.65	10.23
	B - K=K, AGC=KSS	5.46	15.10	25.07	36.00	48.07	59.54	9.65	10.23
	A - K=KSS, AGC=KSS	8.20	22.96	38.24	55.44	73.40	90.69	14.63	15.56
	B - K=KSS, AGC=KSS	8.20	22.96	38.24	55.44	73.40	90.69	14.63	15.56
JENSN									
	A - K=K, AGC=K	6.71	18.30	33.08	48.38	64.74	80.47	12.46	13.21
	B - K=K, AGC=K	6.69	18.40	33.08	48.38	64.74	80.47	12.46	13.21
	A - K=K, AGC=KSS	6.69	18.30	33.08	48.38	64.74	80.47	12.46	13.21
	B - K=K, AGC=KSS	6.69	18.30	33.08	48.38	64.74	80.47	12.46	13.21
	A - K=KSS, AGC=KSS	7.28	21.70	35.98	53.14	70.98	87.98	13.80	14.80
	B - K=KSS, AGC=KSS	7.28	21.70	35.98	53.14	70.98	87.98	13.80	14.80
WHTCRK									
	A - K=K, AGC=K	8.71	25.03	39.46	54.00	70.31	108.25	16.10	17.02
	B - K=K, AGC=K	8.71	25.09	39.46	54.00	70.31	108.25	16.10	17.02
	A - K=K, AGC=KSS	8.71	25.08	39.46	54.00	70.31	108.25	16.10	17.02
	B - K=K, AGC=KSS	8.71	25.08	39.46	54.00	70.31	108.25	16.10	17.02
	A - K=KSS, AGC=KSS	15.14	43.59	69.57	111.38	137.93	188.13	27.98	29.60
	B - K=KSS, AGC=KSS	15.14	43.59	69.57	111.38	137.93	188.13	27.99	29.60
	A - K=K, AGC=K	5.93	19.00	30.22	47.58	59.95	71.27	11.70	12.45
	B - K=K, AGC=K	5.93	19.00	30.22	47.58	59.95	271.27	11.70	15.48
	A - K=K, AGC=KSS	5.54	19.06	29.73	45.00	56.99	67.75	11.13	11.91
	B - K=K, AGC=KSS	5.54	19.06	29.73	45.00	56.99	67.75	11.13	11.91
	A - K=KSS, AGC=KSS	10.98	35.47	56.42	88.03	111.91	133.04	21.95	23.19
	B - K=KSS, AGC=KSS	10.98	35.47	56.42	88.03	111.91	133.04	21.95	23.19

NOTES:

A = Mentine = 30%
B = Mentine = 0 %
K = K-MINE
AGC = ATRAVESADA GULLY COMPLEX
KSS = K-SERP. SOIL

(*) Equation for average yield: Yave = 0.015 x Y100 + 0.015 x Y50 + 0.04 x Y25 + 0.08 x Y10 + 0.2 x Y5 + 0.4 x Y2
(Yave = average yield, Y# = yield of that year)

SOURCE: LEVINE-FRICKE

Reproduced with permission of the copyright owner. Further reproduction prohibited without permission.

Table 6-6B

INDIVIDUAL MINE IMPACT ON ASBESTOS SOIL EROSION SUMMARY - UNADJUSTED K PERCENTAGE OF INDIVIDUAL MINE IMPACT ON PRE-ASBESTOS SOIL EROSION SUMMARY - UNADJUSTED K

	UNADJUSTED K	2 YR Mine Impact <=>	5 YR Mine Impact <=>	10 YR Mine Impact <=>	25 YR Mine Impact <=>	50 YR Mine Impact <=>	100 YR Mine Impact <=>	AVERAGE YEAR <=>	YEARLY AVERAGE ASB. EROSION<=> <=>
CLNOR									
	A - K=K, AGC=K	0.22%	0.26%	0.27%	0.24%	0.26%	0.24%	0.26%	0.26%
	B - K=K, AGC=K	0.22%	0.26%	0.27%	0.24%	0.26%	0.24%	0.26%	0.26%
	A - K=K, AGC=KSS	0.21%	0.26%	0.26%	0.24%	0.26%	0.24%	0.26%	0.26%
	B - K=K, AGC=KSS	0.21%	0.26%	0.26%	0.24%	0.26%	0.24%	0.26%	0.26%
	A - K=KSS, AGC=KSS	0.34%	0.34%	0.34%	0.31%	0.34%	0.31%	0.34%	0.34%
	B - K=KSS, AGC=KSS	0.34%	0.34%	0.35%	0.31%	0.34%	0.32%	0.34%	0.34%
ATLAS									
	A - K=K, AGC=K	0.96%	1.01%	1.06%	1.12%	1.08%	1.06%	1.35%	1.04%
	B - K=K, AGC=K	0.97%	1.02%	1.06%	1.14%	1.09%	1.09%	1.37%	1.06%
	A - K=K, AGC=KSS	0.80%	0.91%	0.84%	0.88%	0.85%	0.80%	1.08%	0.83%
	B - K=K, AGC=KSS	0.81%	0.92%	0.85%	0.90%	0.86%	0.82%	1.09%	0.84%
	A - K=KSS, AGC=KSS	1.91%	2.14%	2.34%	2.54%	2.47%	2.46%	2.90%	2.25%
	B - K=KSS, AGC=KSS	1.94%	2.16%	2.37%	2.57%	2.51%	2.49%	2.95%	2.28%
BASIC									
	A - K=K, AGC=K	0.13%	0.14%	0.15%	0.15%	0.16%	0.16%	0.19%	0.14%
	B - K=K, AGC=K	0.13%	0.15%	0.15%	0.16%	0.16%	0.16%	0.19%	0.15%
	A - K=K, AGC=KSS	0.10%	0.11%	0.12%	0.12%	0.13%	0.13%	0.15%	0.11%
	B - K=K, AGC=KSS	0.10%	0.11%	0.12%	0.12%	0.13%	0.13%	0.15%	0.11%
	A - K=KSS, AGC=KSS	0.36%	0.42%	0.45%	0.46%	0.48%	0.48%	0.57%	0.43%
	B - K=KSS, AGC=KSS	0.37%	0.44%	0.46%	0.47%	0.49%	0.48%	0.57%	0.44%
BORDGE									
	A - K=K, AGC=K	0.10%	0.12%	0.13%	0.13%	0.14%	0.13%	0.16%	0.12%
	B - K=K, AGC=K	0.10%	0.12%	0.13%	0.13%	0.14%	0.14%	0.16%	0.12%
	A - K=K, AGC=KSS	0.11%	0.13%	0.13%	0.14%	0.14%	0.14%	0.17%	0.13%
	B - K=K, AGC=KSS	0.11%	0.13%	0.13%	0.14%	0.14%	0.14%	0.17%	0.13%
	A - K=KSS, AGC=KSS	0.37%	0.39%	0.39%	0.39%	0.40%	0.40%	0.48%	0.37%
	B - K=KSS, AGC=KSS	0.37%	0.39%	0.39%	0.39%	0.41%	0.41%	0.49%	0.37%
TROMBY									
	A - K=K, AGC=K	0.26%	0.23%	0.23%	0.23%	0.23%	0.23%	0.28%	0.22%
	B - K=K, AGC=K	0.27%	0.23%	0.50%	0.23%	0.30%	0.23%	0.28%	0.22%
	A - K=K, AGC=KSS	0.27%	0.23%	0.23%	0.23%	0.30%	0.23%	0.28%	0.22%
	B - K=K, AGC=KSS	0.27%	0.23%	0.50%	0.23%	0.30%	0.23%	0.28%	0.22%
	A - K=KSS, AGC=KSS	0.64%	0.71%	0.73%	0.73%	0.74%	0.74%	0.96%	0.72%
	B - K=KSS, AGC=KSS	0.65%	0.71%	0.74%	0.73%	0.76%	0.74%	0.96%	0.72%
BILES									
	A - K=K, AGC=K	0.10%	0.12%	0.13%	0.13%	0.14%	0.13%	0.16%	0.12%
	B - K=K, AGC=K	0.10%	0.12%	0.13%	0.13%	0.14%	0.14%	0.16%	0.12%
	A - K=K, AGC=KSS	0.11%	0.13%	0.13%	0.14%	0.14%	0.14%	0.17%	0.13%
	B - K=K, AGC=KSS	0.11%	0.13%	0.13%	0.14%	0.14%	0.14%	0.17%	0.13%
	A - K=KSS, AGC=KSS	0.37%	0.39%	0.39%	0.39%	0.40%	0.40%	0.48%	0.37%
	B - K=KSS, AGC=KSS	0.37%	0.39%	0.39%	0.39%	0.41%	0.41%	0.49%	0.37%
MINE7									
	A - K=K, AGC=K	0.17%	0.15%	0.14%	0.13%	0.13%	0.13%	0.19%	0.15%
	B - K=K, AGC=K	0.17%	0.15%	0.14%	0.14%	0.14%	0.13%	0.20%	0.15%
	A - K=K, AGC=KSS	0.17%	0.15%	0.14%	0.14%	0.13%	0.13%	0.19%	0.14%
	B - K=K, AGC=KSS	0.17%	0.15%	0.14%	0.14%	0.13%	0.13%	0.20%	0.15%
	A - K=KSS, AGC=KSS	0.20%	0.19%	0.18%	0.20%	0.20%	0.20%	0.30%	0.21%
	B - K=KSS, AGC=KSS	0.20%	0.19%	0.18%	0.20%	0.20%	0.20%	0.30%	0.21%
BUTLR									
	A - K=K, AGC=K	0.21%	0.20%	0.20%	0.19%	0.19%	0.19%	0.26%	0.19%
	B - K=K, AGC=K	0.21%	0.20%	0.20%	0.19%	0.20%	0.19%	0.26%	0.20%
	A - K=K, AGC=KSS	0.19%	0.19%	0.19%	0.18%	0.19%	0.17%	0.25%	0.19%
	B - K=K, AGC=KSS	0.19%	0.20%	0.19%	0.19%	0.19%	0.19%	0.26%	0.19%
	A - K=KSS, AGC=KSS	0.39%	0.41%	0.41%	0.41%	0.41%	0.41%	0.56%	0.41%
	B - K=KSS, AGC=KSS	0.39%	0.41%	0.41%	0.41%	0.41%	0.41%	0.56%	0.41%
JENSN									
	A - K=K, AGC=K	0.17%	0.18%	0.18%	0.23%	0.23%	0.24%	0.33%	0.24%
	B - K=K, AGC=K	0.17%	0.18%	0.18%	0.23%	0.23%	0.24%	0.33%	0.24%
	A - K=K, AGC=KSS	0.17%	0.18%	0.18%	0.23%	0.23%	0.24%	0.33%	0.24%
	B - K=K, AGC=KSS	0.17%	0.18%	0.18%	0.23%	0.23%	0.24%	0.33%	0.24%
	A - K=KSS, AGC=KSS	0.40%	0.42%	0.40%	0.40%	0.39%	0.41%	0.56%	0.42%
	B - K=KSS, AGC=KSS	0.41%	0.43%	0.41%	0.40%	0.39%	0.41%	0.56%	0.42%
WHTCRK									
	A - K=K, AGC=K	0.18%	0.19%	0.19%	0.17%	0.17%	0.16%	0.24%	0.18%
	B - K=K, AGC=K	0.18%	0.19%	0.18%	0.18%	0.17%	0.17%	0.24%	0.18%
	A - K=K, AGC=KSS	0.17%	0.18%	0.17%	0.16%	0.16%	0.15%	0.23%	0.17%
	B - K=K, AGC=KSS	0.17%	0.18%	0.17%	0.16%	0.16%	0.15%	0.23%	0.17%
	A - K=KSS, AGC=KSS	0.33%	0.34%	0.33%	0.32%	0.31%	0.29%	0.44%	0.32%
	B - K=KSS, AGC=KSS	0.34%	0.35%	0.33%	0.32%	0.31%	0.29%	0.44%	0.32%

NOTES:
<=> YEARLY AVERAGE ASBESTOS EROSION/YEARLY AVERAGE PRE-MINING ASBESTOS EROSION * 100

SOURCE: LEVINE-FRICKE

Reproduced with permission of the copyright owner. Further reproduction prohibited without permission.

Table 6-6C

INDIVIDUAL MINE IMPACT ON ASBESTOS SOIL EROSION SUMMARY - UNADJUSTED K PERCENTAGE OF INDIVIDUAL MINE IMPACT ON POST-ASBESTOS SOIL EROSION SUMMARY - UNADJUSTED K

	UNADJUSTED K	2 YR Mine Impact (<>)	5 YR Mine Impact (<>)	10 YR Mine Impact (<>)	25 YR Mine Impact (<>)	50 YR Mine Impact (<>)	100 YR Mine Impact (<>)	AVERAGE YEAR (<>)	YEARLY AVERAGE ASB. EROSION(<>) (<>)
CLNOA									
	A - K=K, AGC=K	0.27%	0.26%	0.26%	0.24%	0.26%	0.24%	0.25%	0.25%
	B - K=K, AGC=K	0.28%	0.26%	0.26%	0.24%	0.26%	0.24%	0.25%	0.25%
	A - K=K, AGC=KSS	0.27%	0.25%	0.26%	0.25%	0.26%	0.24%	0.25%	0.25%
	B - K=K, AGC=KSS	0.27%	0.26%	0.26%	0.24%	0.26%	0.24%	0.25%	0.25%
	A - K=KSS, AGC=KSS	0.34%	0.33%	0.33%	0.29%	0.32%	0.30%	0.32%	0.32%
	B - K=KSS, AGC=KSS	0.35%	0.33%	0.33%	0.30%	0.33%	0.30%	0.32%	0.32%
ATLAS									
	A - K=K, AGC=K	0.94%	0.98%	1.04%	1.10%	1.05%	1.04%	1.00%	1.01%
	B - K=K, AGC=K	0.95%	1.00%	1.05%	1.11%	1.07%	1.05%	1.01%	1.02%
	A - K=K, AGC=KSS	0.78%	0.79%	0.80%	0.86%	0.81%	0.79%	0.80%	0.80%
	B - K=K, AGC=KSS	0.80%	0.80%	0.84%	0.88%	0.85%	0.80%	0.81%	0.82%
	A - K=KSS, AGC=KSS	1.03%	1.04%	1.08%	1.41%	1.13%	1.14%	1.11%	1.12%
	B - K=KSS, AGC=KSS	1.05%	1.06%	1.10%	1.44%	1.16%	1.15%	1.13%	1.14%
BASIC									
	A - K=K, AGC=K	0.12%	0.14%	0.15%	0.15%	0.16%	0.15%	0.14%	0.14%
	B - K=K, AGC=K	0.12%	0.14%	0.15%	0.15%	0.16%	0.16%	0.14%	0.14%
	A - K=K, AGC=KSS	0.09%	0.11%	0.11%	0.12%	0.12%	0.11%	0.11%	0.11%
	B - K=K, AGC=KSS	0.10%	0.11%	0.11%	0.12%	0.12%	0.11%	0.11%	0.11%
	A - K=KSS, AGC=KSS	0.39%	0.41%	0.43%	0.44%	0.45%	0.45%	0.41%	0.42%
	B - K=KSS, AGC=KSS	0.39%	0.42%	0.43%	0.45%	0.46%	0.46%	0.42%	0.43%
BORDGE									
	A - K=K, AGC=K	0.10%	0.12%	0.12%	0.13%	0.13%	0.13%	0.12%	0.12%
	B - K=K, AGC=K	0.10%	0.12%	0.13%	0.13%	0.13%	0.13%	0.12%	0.12%
	A - K=K, AGC=KSS	0.11%	0.13%	0.13%	0.13%	0.14%	0.14%	0.13%	0.13%
	B - K=K, AGC=KSS	0.11%	0.13%	0.13%	0.14%	0.14%	0.14%	0.13%	0.13%
	A - K=KSS, AGC=KSS	0.36%	0.36%	0.36%	0.37%	0.38%	0.38%	0.36%	0.36%
	B - K=KSS, AGC=KSS	0.36%	0.36%	0.36%	0.37%	0.38%	0.38%	0.36%	0.36%
TROMBY									
	A - K=K, AGC=K	0.26%	0.28%	0.29%	0.28%	0.29%	0.29%	0.28%	0.28%
	B - K=K, AGC=K	0.26%	0.28%	0.29%	0.28%	0.29%	0.29%	0.28%	0.28%
	A - K=K, AGC=KSS	0.26%	0.28%	0.29%	0.28%	0.29%	0.29%	0.28%	0.28%
	B - K=K, AGC=KSS	0.26%	0.28%	0.29%	0.28%	0.29%	0.29%	0.28%	0.28%
	A - K=KSS, AGC=KSS	0.61%	0.68%	0.69%	0.69%	0.71%	0.70%	0.68%	0.69%
	B - K=KSS, AGC=KSS	0.62%	0.69%	0.70%	0.70%	0.72%	0.71%	0.69%	0.69%
BILES									
	A - K=K, AGC=K	0.10%	0.12%	0.13%	0.13%	0.13%	0.13%	0.12%	0.12%
	B - K=K, AGC=K	0.10%	0.12%	0.13%	0.13%	0.13%	0.13%	0.12%	0.12%
	A - K=K, AGC=KSS	0.11%	0.13%	0.13%	0.13%	0.14%	0.14%	0.13%	0.13%
	B - K=K, AGC=KSS	0.11%	0.13%	0.13%	0.14%	0.14%	0.14%	0.13%	0.13%
	A - K=KSS, AGC=KSS	0.36%	0.36%	0.36%	0.37%	0.38%	0.38%	0.36%	0.36%
	B - K=KSS, AGC=KSS	0.36%	0.36%	0.36%	0.37%	0.38%	0.38%	0.36%	0.36%
MINET									
	A - K=K, AGC=K	0.17%	0.14%	0.14%	0.13%	0.13%	0.13%	0.14%	0.14%
	B - K=K, AGC=K	0.17%	0.15%	0.14%	0.13%	0.13%	0.13%	0.14%	0.14%
	A - K=K, AGC=KSS	0.16%	0.14%	0.14%	0.13%	0.13%	0.13%	0.14%	0.14%
	B - K=K, AGC=KSS	0.17%	0.15%	0.14%	0.13%	0.13%	0.13%	0.14%	0.14%
	A - K=KSS, AGC=KSS	0.24%	0.21%	0.20%	0.19%	0.19%	0.19%	0.21%	0.21%
	B - K=KSS, AGC=KSS	0.25%	0.22%	0.21%	0.19%	0.19%	0.19%	0.21%	0.21%
BUTLR									
	A - K=K, AGC=K	0.20%	0.19%	0.20%	0.17%	0.19%	0.17%	0.19%	0.19%
	B - K=K, AGC=K	0.21%	0.19%	0.20%	0.18%	0.19%	0.18%	0.19%	0.19%
	A - K=K, AGC=KSS	0.20%	0.19%	0.19%	0.17%	0.19%	0.17%	0.19%	0.19%
	B - K=K, AGC=KSS	0.20%	0.19%	0.20%	0.17%	0.19%	0.17%	0.19%	0.19%
	A - K=KSS, AGC=KSS	0.21%	0.20%	0.20%	0.18%	0.20%	0.18%	0.20%	0.20%
	B - K=KSS, AGC=KSS	0.22%	0.20%	0.21%	0.18%	0.20%	0.18%	0.20%	0.20%
JENSN									
	A - K=K, AGC=K	0.26%	0.24%	0.23%	0.23%	0.23%	0.23%	0.24%	0.24%
	B - K=K, AGC=K	0.27%	0.25%	0.24%	0.23%	0.23%	0.23%	0.24%	0.24%
	A - K=K, AGC=KSS	0.26%	0.24%	0.23%	0.23%	0.23%	0.23%	0.24%	0.24%
	B - K=K, AGC=KSS	0.26%	0.24%	0.23%	0.23%	0.23%	0.23%	0.24%	0.24%
	A - K=KSS, AGC=KSS	0.44%	0.40%	0.39%	0.38%	0.38%	0.38%	0.40%	0.40%
	B - K=KSS, AGC=KSS	0.45%	0.41%	0.39%	0.38%	0.38%	0.38%	0.41%	0.40%
WHTCRK									
	A - K=K, AGC=K	0.18%	0.18%	0.17%	0.17%	0.16%	0.16%	0.18%	0.17%
	B - K=K, AGC=K	0.19%	0.19%	0.18%	0.17%	0.17%	0.16%	0.18%	0.18%
	A - K=K, AGC=KSS	0.17%	0.17%	0.16%	0.16%	0.15%	0.14%	0.16%	0.16%
	B - K=K, AGC=KSS	0.17%	0.17%	0.17%	0.16%	0.16%	0.15%	0.17%	0.16%
	A - K=KSS, AGC=KSS	0.32%	0.33%	0.32%	0.31%	0.30%	0.29%	0.31%	0.31%
	B - K=KSS, AGC=KSS	0.32%	0.33%	0.32%	0.31%	0.30%	0.29%	0.32%	0.31%

NOTES:
(<>) YEARLY AVERAGE ASBESTOS EROSION/YEARLY AVERAGE POST-MINING ASBESTOS EROSION * 100

SOURCE: LEVINE-FRICKE

Reproduced with permission of the copyright owner. Further reproduction prohibited without permission.

Table 6-6D

INDIVIDUAL MINE IMPACT ON ASBESTOS SOIL EROSION SUMMARY - ADJUSTED K
YEARLY AVERAGE ASBESTOS EROSION

	ADJUSTED K	2 YR Mine Impact (cu yd)	5 YR Mine Impact (cu yd)	10 YR Mine Impact (cu yd)	25 YR Mine Impact (cu yd)	50 YR Mine Impact (cu yd)	100 YR Mine Impact (cu yd)	AVERAGE YEAR	YEARLY AVERAGE ASB. EROSION(*) (cu yd)
CLNGR									
	A - K=K, AGC=K	7.77	22.04	39.15	57.60	81.73	95.58	14.68	15.01
	B - K=K, AGC=K	7.77	22.04	39.15	57.60	81.73	95.58	14.68	15.01
	A - K=K, AGC=KSS	7.77	22.04	39.15	57.60	81.73	95.58	14.68	15.01
	B - K=K, AGC=KSS	7.77	22.04	39.15	57.60	81.73	95.58	14.68	15.01
	A - K=KSS, AGC=KSS	7.69	22.04	39.76	58.48	83.04	97.03	14.90	15.99
	B - K=KSS, AGC=KSS	7.69	22.04	39.76	58.48	83.04	97.03	14.90	15.99
ATLAS									
	A - K=K, AGC=K	18.92	62.04	108.66	156.36	221.93	290.27	40.37	43.36
	B - K=K, AGC=K	18.90	61.93	108.49	156.05	221.56	289.67	40.30	43.28
	A - K=K, AGC=KSS	15.76	49.48	85.29	145.14	176.96	217.50	32.09	34.75
	B - K=K, AGC=KSS	15.71	49.50	85.32	145.20	177.04	217.61	32.10	34.76
	A - K=KSS, AGC=KSS	140.02	140.79	256.85	454.06	575.58	706.83	95.58	102.41
	B - K=KSS, AGC=KSS	39.92	140.45	256.19	452.91	574.05	724.83	95.29	102.15
BASIC									
	A - K=K, AGC=K	2.09	10.84	18.77	31.76	40.72	53.65	6.94	7.54
	B - K=K, AGC=K	2.09	10.84	18.77	31.76	40.72	53.65	6.94	7.54
	A - K=K, AGC=KSS	1.59	8.38	15.10	28.65	34.63	44.78	5.97	6.19
	B - K=K, AGC=KSS	1.60	8.40	15.13	28.70	34.80	44.71	5.98	6.19
	A - K=KSS, AGC=KSS	8.14	30.67	53.15	89.91	121.00	154.71	19.65	21.36
	B - K=KSS, AGC=KSS	8.19	30.66	53.11	89.75	120.92	154.60	19.64	21.35
BGRDGE									
	A - K=K, AGC=K	2.47	9.22	15.86	26.84	35.93	45.41	5.88	6.359
	B - K=K, AGC=K	2.47	9.22	15.86	26.84	35.93	45.41	5.88	6.359
	A - K=K, AGC=KSS	1.63	9.01	16.85	28.20	38.26	48.71	6.25	6.749
	B - K=K, AGC=KSS	1.63	9.01	16.85	28.20	38.26	48.71	6.25	6.749
	A - K=KSS, AGC=KSS	6.99	26.11	44.87	75.08	101.84	129.50	16.60	18.07
	B - K=KSS, AGC=KSS	6.99	26.11	44.87	75.08	101.84	129.50	16.60	18.07
TROMBY									
	A - K=K, AGC=K	3.56	13.45	23.97	40.10	80.00	99.05	14.0000	15.5000
	B - K=K, AGC=K	3.56	13.45	23.98	40.10	80.00	99.05	14.0000	15.5000
	A - K=K, AGC=KSS	3.68	13.96	24.79	41.63	80.01	101.54	14.5000	15.5599
	B - K=K, AGC=KSS	3.69	13.96	24.79	41.63	80.01	101.54	14.5000	15.5599
	A - K=KSS, AGC=KSS	14.03	51.97	88.59	148.38	191.13	238.58	33.0000	35.5599
	B - K=KSS, AGC=KSS	14.03	51.97	88.59	148.38	191.13	238.58	33.0000	35.5599
BILES									
	A - K=K, AGC=K	2.47	9.22	15.86	26.84	35.93	45.41	5.88	6.359
	B - K=K, AGC=K	2.47	9.22	15.86	26.84	35.93	45.41	5.88	6.359
	A - K=K, AGC=KSS	1.63	9.01	16.85	28.20	38.26	48.71	6.25	6.749
	B - K=K, AGC=KSS	1.63	9.01	16.85	28.20	38.26	48.71	6.25	6.749
	A - K=KSS, AGC=KSS	6.99	26.11	44.87	75.08	101.84	129.50	16.60	18.07
	B - K=KSS, AGC=KSS	6.99	26.11	44.87	75.08	101.84	129.50	16.60	18.07
MINET									
	A - K=K, AGC=K	3.35	10.87	17.32	26.57	34.65	42.30	5.35	7.37
	B - K=K, AGC=K	3.35	10.87	17.32	26.57	34.65	42.30	5.35	7.37
	A - K=K, AGC=KSS	3.37	10.94	17.43	26.75	34.87	42.56	5.38	7.41
	B - K=K, AGC=KSS	3.37	10.94	17.43	26.75	34.87	42.56	5.38	7.41
	A - K=KSS, AGC=KSS	5.04	16.18	25.80	39.64	51.71	63.12	10.24	10.37
	B - K=KSS, AGC=KSS	5.04	16.18	25.80	39.64	51.71	63.12	10.24	10.97
RUTLR									
	A - K=K, AGC=K	6.60	19.66	33.44	48.41	66.52	79.03	12.50	13.40
	B - K=K, AGC=K	6.60	19.66	33.44	48.41	66.52	79.03	12.50	13.40
	A - K=K, AGC=KSS	6.60	19.66	33.44	48.41	66.52	79.03	12.50	13.40
	B - K=K, AGC=KSS	6.60	19.66	33.44	48.41	66.52	79.03	12.50	13.40
	A - K=KSS, AGC=KSS	7.00	20.85	35.49	51.39	70.65	84.47	13.26	14.22
	B - K=KSS, AGC=KSS	7.00	20.85	35.49	51.39	70.65	84.47	13.26	14.22
JENSN									
	A - K=K, AGC=K	8.23	23.88	37.58	60.95	75.43	103.04	15.33	16.[illegible]
	B - K=K, AGC=K	8.23	23.88	37.58	60.95	75.43	103.04	15.33	16.[illegible]
	A - K=K, AGC=KSS	8.23	23.88	37.58	60.95	75.43	103.04	15.33	16.[illegible]
	B - K=K, AGC=KSS	8.23	23.88	37.58	60.95	75.43	103.04	15.33	16.[illegible]
	A - K=KSS, AGC=KSS	11.57	36.21	56.97	92.45	114.51	156.39	23.[illegible]	24.[illegible]
	B - K=KSS, AGC=KSS	12.57	36.21	56.97	92.45	114.51	156.39	23.[illegible]	24.[illegible]
WHTCRK									
	A - K=K, AGC=K	4.31	16.01	26.47	40.10	50.52	60.06	9.05	10.47
	B - K=K, AGC=K	4.31	16.01	26.47	40.10	50.52	60.06	9.05	10.47
	A - K=K, AGC=KSS	4.75	15.99	24.48	38.53	48.55	57.71	9.48	10.06
	B - K=K, AGC=KSS	4.75	15.99	24.48	38.53	48.55	57.71	9.48	10.06
	A - K=KSS, AGC=KSS	8.28	26.39	42.94	67.59	85.16	101.24	16.60	17.64
	B - K=KSS, AGC=KSS	8.28	26.39	42.94	67.59	85.16	101.24	16.60	17.64

NOTES:

A = Mentone = 30%
B = Mentone = 0 %
K = K-MINE
AGC = ATRAVASADA GULLY COMPLEX
KSS = K-SERP. SOIL

(*) Equation for average yield: Yave = 0.015 x Y100 + 0.015 Y50 + 0.04 x Y25 + 0.08 x Y10 + 0.2 x Y5 + 0.4 x Y2
(Yave=average yield, Y#=yield of #that year)

SOURCE: LEVINE-FRICKE

Reproduced with permission of the copyright owner. Further reproduction prohibited without permission.

Table 6-6E

INDIVIDUAL MINE IMPACT ON ASBESTOS SOIL EROSION SUMMARY - ADJUSTED K
PERCENTAGE OF INDIVIDUAL MINE IMPACT ON PRE-ASBESTOS SOIL EROSION SUMMARY - ADJUSTED K

	ADJUSTED K	2 YR Mine Impact (<>)	5 YR Mine Impact (<>)	10 YR Mine Impact (<>)	25 YR Mine Impact (<>)	50 YR Mine Impact (<>)	100 YR Mine Impact (<>)	AVERAGE YEAR (<>)	YEARLY AVERAGE ASB. EROSION(<>) (<>)
CLNDA									
	A - K=K, AGC=K	0.33%	0.31%	0.30%	0.29%	0.31%	0.29%	0.31%	0.31%
	B - K=K, AGC=K	0.34%	0.32%	0.30%	0.29%	0.30%	0.30%	0.32%	0.32%
	A - K=K, AGC=KSS	0.33%	0.31%	0.31%	0.29%	0.31%	0.29%	0.30%	0.31%
	B - K=K, AGC=KSS	0.33%	0.31%	0.30%	0.29%	0.31%	0.29%	0.31%	0.31%
	A - K=KSS, AGC=KSS	0.33%	0.31%	0.30%	0.29%	0.31%	0.29%	0.31%	0.31%
	B - K=KSS, AGC=KSS	0.34%	0.31%	0.30%	0.29%	0.30%	0.29%	0.31%	0.31%
ATLAS									
	A - K=K, AGC=K	0.90%	0.94%	0.98%	0.93%	0.89%	0.98%	0.85%	0.06%
	B - K=K, AGC=K	0.80%	0.95%	0.90%	0.95%	0.91%	0.89%	0.87%	0.09%
	A - K=K, AGC=KSS	0.66%	0.66%	0.68%	0.71%	0.67%	0.65%	0.67%	0.67%
	B - K=K, AGC=KSS	0.67%	0.67%	0.70%	0.73%	0.68%	0.66%	0.68%	0.68%
	A - K=KSS, AGC=KSS	1.67%	1.87%	2.09%	2.00%	2.17%	2.16%	1.94%	1.94%
	B - K=KSS, AGC=KSS	1.70%	1.91%	2.09%	2.07%	2.21%	2.10%	1.97%	2.01%
BASIC									
	A - K=K, AGC=K	0.12%	0.15%	0.15%	0.16%	0.16%	0.16%	0.15%	0.15%
	B - K=K, AGC=K	0.12%	0.15%	0.16%	0.16%	0.17%	0.17%	0.15%	0.15%
	A - K=K, AGC=KSS	0.10%	0.12%	0.13%	0.13%	0.13%	0.13%	0.12%	0.12%
	B - K=K, AGC=KSS	0.10%	0.12%	0.13%	0.13%	0.13%	0.13%	0.12%	0.12%
	A - K=KSS, AGC=KSS	0.34%	0.41%	0.42%	0.44%	0.46%	0.45%	0.41%	0.41%
	B - K=KSS, AGC=KSS	0.35%	0.42%	0.43%	0.45%	0.47%	0.46%	0.42%	0.42%
BORDGE									
	A - K=K, AGC=K	0.10%	0.12%	0.13%	0.13%	0.14%	0.14%	0.12%	0.13%
	B - K=K, AGC=K	0.11%	0.13%	0.13%	0.14%	0.14%	0.14%	0.13%	0.13%
	A - K=K, AGC=KSS	0.11%	0.13%	0.13%	0.14%	0.14%	0.14%	0.13%	0.13%
	B - K=K, AGC=KSS	0.11%	0.13%	0.13%	0.14%	0.14%	0.14%	0.13%	0.13%
	A - K=KSS, AGC=KSS	0.29%	0.35%	0.36%	0.37%	0.39%	0.38%	0.34%	0.35%
	B - K=KSS, AGC=KSS	0.30%	0.35%	0.37%	0.38%	0.39%	0.39%	0.35%	0.36%
TROMBY									
	A - K=K, AGC=K	0.29%	0.30%	0.31%	0.30%	0.31%	0.30%	0.30%	0.30%
	B - K=K, AGC=K	0.29%	0.31%	0.31%	0.31%	0.31%	0.31%	0.31%	0.30%
	A - K=K, AGC=KSS	0.29%	0.31%	0.31%	0.30%	0.31%	0.30%	0.30%	0.30%
	B - K=K, AGC=KSS	0.29%	0.31%	0.31%	0.31%	0.32%	0.31%	0.31%	0.30%
	A - K=KSS, AGC=KSS	0.62%	0.69%	0.71%	0.70%	0.72%	0.71%	0.69%	0.69%
	B - K=KSS, AGC=KSS	0.63%	0.71%	0.73%	0.71%	0.74%	0.73%	0.70%	0.70%
BILES									
	A - K=K, AGC=K	0.10%	0.12%	0.13%	0.13%	0.14%	0.14%	0.12%	0.13%
	B - K=K, AGC=K	0.11%	0.13%	0.13%	0.14%	0.14%	0.14%	0.13%	0.13%
	A - K=K, AGC=KSS	0.11%	0.13%	0.13%	0.14%	0.14%	0.14%	0.13%	0.13%
	B - K=K, AGC=KSS	0.11%	0.13%	0.14%	0.14%	0.15%	0.15%	0.13%	0.13%
	A - K=KSS, AGC=KSS	0.29%	0.35%	0.36%	0.37%	0.38%	0.38%	0.34%	0.35%
	B - K=KSS, AGC=KSS	0.30%	0.35%	0.37%	0.38%	0.39%	0.39%	0.35%	0.36%
MINE7									
	A - K=K, AGC=K	0.17%	0.15%	0.14%	0.13%	0.13%	0.13%	0.15%	0.14%
	B - K=K, AGC=K	0.17%	0.15%	0.14%	0.14%	0.14%	0.13%	0.15%	0.14%
	A - K=K, AGC=KSS	0.17%	0.15%	0.14%	0.13%	0.13%	0.13%	0.14%	0.14%
	B - K=K, AGC=KSS	0.17%	0.15%	0.14%	0.13%	0.13%	0.13%	0.15%	0.14%
	A - K=KSS, AGC=KSS	0.24%	0.22%	0.21%	0.20%	0.20%	0.19%	0.21%	0.21%
	B - K=KSS, AGC=KSS	0.25%	0.22%	0.21%	0.20%	0.20%	0.19%	0.22%	0.22%
BUTLR									
	A - K=K, AGC=K	0.28%	0.27%	0.27%	0.24%	0.26%	0.24%	0.26%	0.26%
	B - K=K, AGC=K	0.29%	0.27%	0.26%	0.25%	0.27%	0.25%	0.27%	0.27%
	A - K=K, AGC=KSS	0.28%	0.26%	0.27%	0.24%	0.26%	0.24%	0.26%	0.26%
	B - K=K, AGC=KSS	0.28%	0.27%	0.27%	0.25%	0.27%	0.24%	0.26%	0.26%
	A - K=KSS, AGC=KSS	0.29%	0.28%	0.28%	0.25%	0.27%	0.25%	0.27%	0.27%
	B - K=KSS, AGC=KSS	0.30%	0.28%	0.28%	0.26%	0.28%	0.26%	0.28%	0.28%
JENSN									
	A - K=K, AGC=K	0.35%	0.32%	0.31%	0.30%	0.29%	0.31%	0.32%	0.32%
	B - K=K, AGC=K	0.36%	0.33%	0.31%	0.31%	0.30%	0.32%	0.33%	0.33%
	A - K=K, AGC=KSS	0.35%	0.32%	0.30%	0.30%	0.29%	0.31%	0.32%	0.32%
	B - K=K, AGC=KSS	0.35%	0.32%	0.31%	0.31%	0.29%	0.31%	0.32%	0.32%
	A - K=KSS, AGC=KSS	0.53%	0.48%	0.46%	0.45%	0.43%	0.46%	0.48%	0.47%
	B - K=KSS, AGC=KSS	0.54%	0.49%	0.46%	0.46%	0.44%	0.47%	0.49%	0.48%
WHTCRK									
	A - K=K, AGC=K	0.21%	0.22%	0.21%	0.20%	0.19%	0.19%	0.21%	0.21%
	B - K=K, AGC=K	0.21%	0.22%	0.21%	0.20%	0.20%	0.19%	0.21%	0.21%
	A - K=K, AGC=KSS	0.20%	0.20%	0.20%	0.19%	0.19%	0.17%	0.20%	0.19%
	B - K=K, AGC=KSS	0.20%	0.21%	0.20%	0.19%	0.19%	0.19%	0.20%	0.20%
	A - K=KSS, AGC=KSS	0.35%	0.36%	0.34%	0.33%	0.32%	0.30%	0.34%	0.34%
	B - K=KSS, AGC=KSS	0.35%	0.37%	0.35%	0.34%	0.33%	0.31%	0.35%	0.35%

NOTES:
(<>) YEARLY AVERAGE ASBESTOS EROSION/YEARLY AVERAGE PRE-MINING ASBESTOS EROSION =

SOURCE: LEVINE-FRICKE

Reproduced with permission of the copyright owner. Further reproduction prohibited without permission.

Table 6-6F

INDIVIDUAL MINE IMPACT ON ASBESTOS SOIL EROSION SUMMARY - ADJUSTED K
PERCENTAGE OF INDIVIDUAL MINE IMPACT ON POST-ASBESTOS SOIL EROSION SUMMARY - ADJUSTED K

	ADJUSTED K	2 YR Mine Impact (<>)	5 YR Mine Impact (<>)	10 YR Mine Impact (<>)	25 YR Mine Impact (<>)	50 YR Mine Impact (<>)	100 YR Mine Impact (<>)	AVERAGE YEAR (<>)	YEARLY AVERAGE ASB. EROSION(<>)
CLNOR									
	A - K=K, AGC=K	0.32%	0.30%	0.31%	0.28%	0.31%	0.28%	0.30%	0.30%
	B - K=K, AGC=K	0.33%	0.31%	0.32%	0.29%	0.31%	0.29%	0.31%	0.31%
	A - K=K, AGC=KSS	0.32%	0.30%	0.31%	0.28%	0.30%	0.28%	0.30%	0.30%
	B - K=K, AGC=KSS	0.32%	0.31%	0.31%	0.28%	0.31%	0.28%	0.30%	0.30%
	A - K=KSS, AGC=KSS	0.32%	0.29%	0.30%	0.27%	0.30%	0.28%	0.30%	0.30%
	B - K=KSS, AGC=KSS	0.32%	0.30%	0.31%	0.28%	0.30%	0.28%	0.30%	0.30%
ATLAS									
	A - K=K, AGC=K	0.78%	0.82%	0.86%	0.91%	0.87%	0.86%	0.82%	0.84%
	B - K=K, AGC=K	0.80%	0.83%	0.88%	0.93%	0.89%	0.87%	0.84%	0.86%
	A - K=K, AGC=KSS	0.65%	0.64%	0.67%	0.70%	0.66%	0.65%	0.65%	0.66%
	B - K=K, AGC=KSS	0.66%	0.66%	0.68%	0.71%	0.67%	0.65%	0.66%	0.66%
	A - K=KSS, AGC=KSS	1.61%	1.73%	1.96%	2.12%	2.07%	2.06%	1.88%	1.98%
	B - K=KSS, AGC=KSS	1.63%	1.82%	1.99%	2.16%	2.11%	2.10%	1.92%	1.98%
BASIC									
	A - K=K, AGC=K	0.12%	0.14%	0.15%	0.15%	0.16%	0.16%	0.14%	0.14%
	B - K=K, AGC=K	0.12%	0.15%	0.15%	0.16%	0.16%	0.16%	0.15%	0.15%
	A - K=K, AGC=KSS	0.10%	0.12%	0.12%	0.12%	0.13%	0.13%	0.12%	0.12%
	B - K=K, AGC=KSS	0.10%	0.12%	0.12%	0.13%	0.13%	0.13%	0.12%	0.12%
	A - K=KSS, AGC=KSS	0.39%	0.39%	0.41%	0.42%	0.44%	0.44%	0.40%	0.40%
	B - K=KSS, AGC=KSS	0.39%	0.40%	0.41%	0.42%	0.44%	0.44%	0.40%	0.40%
BORDGE									
	A - K=K, AGC=K	0.10%	0.12%	0.13%	0.13%	0.14%	0.13%	0.12%	0.12%
	B - K=K, AGC=K	0.10%	0.12%	0.13%	0.13%	0.14%	0.14%	0.12%	0.12%
	A - K=K, AGC=KSS	0.11%	0.13%	0.13%	0.14%	0.14%	0.14%	0.13%	0.13%
	B - K=K, AGC=KSS	0.11%	0.13%	0.13%	0.14%	0.14%	0.14%	0.13%	0.13%
	A - K=KSS, AGC=KSS	0.28%	0.33%	0.34%	0.36%	0.37%	0.36%	0.34%	0.34%
	B - K=KSS, AGC=KSS	0.29%	0.34%	0.35%	0.36%	0.37%	0.37%	0.34%	0.34%
TROMBY									
	A - K=K, AGC=K	0.27%	0.30%	0.30%	0.29%	0.30%	0.29%	0.29%	0.29%
	B - K=K, AGC=K	0.29%	0.30%	0.31%	0.30%	0.31%	0.30%	0.30%	0.30%
	A - K=K, AGC=KSS	0.27%	0.30%	0.30%	0.30%	0.30%	0.30%	0.30%	0.30%
	B - K=K, AGC=KSS	0.28%	0.30%	0.31%	0.30%	0.31%	0.30%	0.30%	0.30%
	A - K=KSS, AGC=KSS	0.59%	0.66%	0.68%	0.67%	0.69%	0.68%	0.65%	0.66%
	B - K=KSS, AGC=KSS	0.61%	0.67%	0.69%	0.68%	0.70%	0.69%	0.67%	0.67%
BILES									
	A - K=K, AGC=K	0.10%	0.12%	0.13%	0.13%	0.14%	0.13%	0.12%	0.12%
	B - K=K, AGC=K	0.10%	0.12%	0.13%	0.13%	0.14%	0.14%	0.12%	0.12%
	A - K=K, AGC=KSS	0.11%	0.13%	0.13%	0.14%	0.14%	0.14%	0.13%	0.13%
	B - K=K, AGC=KSS	0.11%	0.13%	0.13%	0.14%	0.14%	0.14%	0.13%	0.13%
	A - K=KSS, AGC=KSS	0.29%	0.33%	0.34%	0.36%	0.37%	0.36%	0.34%	0.34%
	B - K=KSS, AGC=KSS	0.29%	0.34%	0.35%	0.36%	0.37%	0.37%	0.34%	0.34%
MINE7									
	A - K=K, AGC=K	0.16%	0.14%	0.14%	0.13%	0.13%	0.13%	0.14%	0.14%
	B - K=K, AGC=K	0.17%	0.15%	0.14%	0.13%	0.13%	0.13%	0.15%	0.14%
	A - K=K, AGC=KSS	0.16%	0.14%	0.14%	0.13%	0.13%	0.13%	0.14%	0.14%
	B - K=K, AGC=KSS	0.17%	0.15%	0.14%	0.13%	0.13%	0.13%	0.14%	0.14%
	A - K=KSS, AGC=KSS	0.23%	0.21%	0.20%	0.19%	0.19%	0.19%	0.20%	0.20%
	B - K=KSS, AGC=KSS	0.24%	0.21%	0.20%	0.19%	0.19%	0.19%	0.21%	0.21%
BUTLR									
	A - K=K, AGC=K	0.27%	0.26%	0.27%	0.24%	0.26%	0.24%	0.26%	0.26%
	B - K=K, AGC=K	0.28%	0.26%	0.27%	0.24%	0.26%	0.24%	0.26%	0.26%
	A - K=K, AGC=KSS	0.27%	0.26%	0.26%	0.23%	0.25%	0.23%	0.25%	0.25%
	B - K=K, AGC=KSS	0.28%	0.26%	0.27%	0.24%	0.26%	0.24%	0.26%	0.26%
	A - K=KSS, AGC=KSS	0.29%	0.27%	0.27%	0.24%	0.26%	0.24%	0.26%	0.26%
	B - K=KSS, AGC=KSS	0.29%	0.27%	0.28%	0.25%	0.27%	0.24%	0.27%	0.27%
JENSN									
	A - K=K, AGC=K	0.34%	0.32%	0.30%	0.30%	0.29%	0.30%	0.32%	0.31%
	B - K=K, AGC=K	0.35%	0.32%	0.30%	0.30%	0.29%	0.31%	0.32%	0.32%
	A - K=K, AGC=KSS	0.34%	0.31%	0.29%	0.29%	0.28%	0.30%	0.31%	0.30%
	B - K=K, AGC=KSS	0.35%	0.32%	0.30%	0.30%	0.29%	0.31%	0.32%	0.31%
	A - K=KSS, AGC=KSS	0.50%	0.46%	0.43%	0.43%	0.41%	0.44%	0.46%	0.45%
	B - K=KSS, AGC=KSS	0.51%	0.47%	0.44%	0.44%	0.42%	0.45%	0.47%	0.46%
WHTCRK									
	A - K=K, AGC=K	0.20%	0.21%	0.20%	0.20%	0.19%	0.19%	0.20%	0.20%
	B - K=K, AGC=K	0.21%	0.22%	0.21%	0.20%	0.19%	0.19%	0.21%	0.20%
	A - K=K, AGC=KSS	0.19%	0.20%	0.19%	0.19%	0.18%	0.17%	0.19%	0.19%
	B - K=K, AGC=KSS	0.20%	0.20%	0.20%	0.19%	0.18%	0.17%	0.20%	0.19%
	A - K=KSS, AGC=KSS	0.33%	0.34%	0.33%	0.32%	0.31%	0.29%	0.33%	0.32%
	B - K=KSS, AGC=KSS	0.34%	0.35%	0.33%	0.32%	0.31%	0.29%	0.34%	0.33%

NOTES: <> YEARLY AVERAGE ASBESTOS EROSION/YEARLY AVERAGE POST-MINING ASBESTOS EROSION * 100

SOURCE: LEVINE-FRICKE

Reproduced with permission of the copyright owner. Further reproduction prohibited without permission.

Table 6-7A
USLE INDIVIDUAL MINE IMPACT ON ASBESTOS SOIL EROSION SUMMARY - ADJUSTED K
YEARLY AVERAGE ASBESTOS EROSION

	ADJUSTED K	TYPE I STORM Pre-Mining (cu yd)	TYPE II STORM Pre-Mining (cu yd)	TYPE I STORM Post-Mining (cu yd)	TYPE II STORM Post-Mining (cu yd)	TYPE I STORM Mine Impact (cu yd)	TYPE II STORM Mine Impact (cu yd)	TYPE I STORM Mine Impact (%)	TYPE II STORM Mine Impact (%)	(MINE IMPACT)/POST. TYPE I STORM	(MINE IMPACT)/POST. TYPE II STORM
CLNOA											
	A - K=K, AOC=K	260.93	425.64	305.82	498.87	44.89	73.23	0.24%	0.24%	0.24%	0.24%
	B - K=K, AOC=K	260.93	425.64	305.82	498.87	44.89	73.23	0.25%	0.25%	0.24%	0.24%
	A - K=K, AOC=KSS	260.93	425.64	305.82	498.87	44.89	73.23	0.24%	0.24%	0.25%	0.25%
	B - K=K, AOC=KSS	260.93	425.64	305.82	498.87	44.89	73.23	0.24%	0.24%	0.24%	0.24%
	A - K=KSS, AOC=KSS	260.93	425.64	306.48	499.94	45.55	74.30	0.24%	0.24%	0.23%	0.23%
	B - K=KSS, AOC=KSS	260.93	425.64	306.48	499.94	45.55	74.30	0.25%	0.25%	0.23%	0.23%
ATLAS											
	A - K=K, AOC=K	6094.48	9941.55	6231.67	10246.90	137.19	305.35	1.01%	1.01%	0.99%	0.99%
	B - K=K, AOC=K	6062.79	9889.86	6249.59	10194.57	186.80	304.71	1.03%	1.03%	1.01%	1.01%
	A - K=K, AOC=KSS	6303.09	10281.62	6442.93	10509.95	133.84	218.33	0.71%	0.71%	0.69%	0.69%
	B - K=K, AOC=KSS	6275.89	10237.47	6409.31	10455.92	133.32	218.45	0.72%	0.72%	0.71%	0.71%
	A - K=KSS, AOC=KSS	6303.09	10281.62	6792.17	11089.42	489.08	797.80	2.59%	2.59%	2.46%	2.46%
	B - K=KSS, AOC=KSS	6275.89	10237.47	6763.62	11033.07	487.73	795.60	2.64%	2.64%	2.50%	2.50%
BASIC											
	A - K=K, AOC=K	6250.47	10196.06	6238.13	10257.51	37.66	61.45	0.20%	0.20%	0.20%	0.20%
	B - K=K, AOC=K	6218.78	10144.37	6256.45	10205.82	37.67	61.45	0.21%	0.21%	0.20%	0.20%
	A - K=K, AOC=KSS	6445.22	10513.75	6475.76	10563.59	30.54	49.85	0.16%	0.16%	0.16%	0.16%
	B - K=K, AOC=KSS	6412.02	10459.59	6442.71	10509.66	30.69	50.07	0.17%	0.17%	0.16%	0.16%
	A - K=KSS, AOC=KSS	6445.22	10513.75	6552.72	10689.12	107.50	175.37	0.57%	0.57%	0.54%	0.54%
	B - K=KSS, AOC=KSS	6412.02	10459.59	6519.45	10634.85	107.43	175.26	0.58%	0.58%	0.55%	0.55%
BORDOE											
	A - K=K, AOC=K	3083.73	5030.38	3116.39	5083.67	32.66	53.29	0.18%	0.18%	0.17%	0.17%
	B - K=K, AOC=K	3083.73	5030.38	3116.39	5083.67	32.66	53.29	0.18%	0.18%	0.18%	0.18%
	A - K=K, AOC=KSS	3153.81	5144.71	3188.53	5201.35	34.72	56.64	0.18%	0.18%	0.18%	0.18%
	B - K=K, AOC=KSS	3153.81	5144.71	3188.53	5201.35	34.72	56.64	0.19%	0.19%	0.18%	0.18%
	A - K=KSS, AOC=KSS	3153.81	5144.71	3246.24	5295.49	92.43	150.78	0.49%	0.49%	0.46%	0.46%
	B - K=KSS, AOC=KSS	3153.81	5144.71	3246.24	5295.49	92.43	150.78	0.50%	0.50%	0.47%	0.47%
TROMBY											
	A - K=K, AOC=K	4595.07	7495.75	4654.33	7592.52	59.32	96.77	0.32%	0.32%	0.31%	0.31%
	B - K=K, AOC=K	4595.07	7495.75	4654.33	7592.52	59.32	96.77	0.33%	0.33%	0.32%	0.32%
	A - K=K, AOC=KSS	4636.15	7560.65	4757.40	7760.57	61.25	99.92	0.32%	0.32%	0.32%	0.32%
	B - K=K, AOC=KSS	4636.15	7560.65	4757.40	7760.57	61.25	99.92	0.33%	0.33%	0.32%	0.32%
	A - K=KSS, AOC=KSS	4636.15	7560.65	4949.15	7308.59	152.00	247.94	0.81%	0.81%	0.76%	0.76%
	B - K=KSS, AOC=KSS	4636.15	7560.65	4849.15	7308.59	152.00	247.94	0.82%	0.82%	0.78%	0.78%
BILES											
	A - K=K, AOC=K	3083.73	5030.38	3116.39	5083.67	32.66	53.29	0.18%	0.18%	0.17%	0.17%
	B - K=K, AOC=K	3083.73	5030.38	3116.39	5083.67	32.66	53.29	0.18%	0.18%	0.18%	0.18%
	A - K=K, AOC=KSS	3153.81	5144.71	3188.53	5201.35	34.72	56.64	0.19%	0.19%	0.18%	0.18%
	B - K=K, AOC=KSS	3153.81	5144.71	3188.53	5201.35	34.72	56.64	0.19%	0.19%	0.18%	0.18%
	A - K=KSS, AOC=KSS	3153.81	5144.71	3246.24	5295.49	92.43	150.78	0.49%	0.49%	0.46%	0.46%
	B - K=KSS, AOC=KSS	3153.81	5144.71	3246.24	5295.49	92.43	150.78	0.50%	0.50%	0.47%	0.47%
MINE7											
	A - K=K, AOC=K	2142.44	3494.82	2161.17	3525.36	18.73	30.54	0.10%	0.10%	0.10%	0.10%
	B - K=K, AOC=K	2142.44	3494.82	2161.17	3525.36	18.73	30.54	0.10%	0.10%	0.10%	0.10%
	A - K=K, AOC=KSS	2155.66	3516.37	2174.51	3547.12	18.85	30.75	0.10%	0.10%	0.10%	0.10%
	B - K=K, AOC=KSS	2155.66	3516.37	2174.51	3547.12	18.85	30.75	0.10%	0.10%	0.10%	0.10%
	A - K=KSS, AOC=KSS	2155.66	3516.37	2183.76	3562.21	28.10	45.84	0.15%	0.15%	0.14%	0.14%
	B - K=KSS, AOC=KSS	2155.66	3516.37	2183.76	3562.21	28.10	45.84	0.15%	0.15%	0.14%	0.14%
BUTLR											
	A - K=K, AOC=K	359.44	586.33	395.09	644.48	35.65	58.15	0.19%	0.19%	0.19%	0.19%
	B - K=K, AOC=K	359.44	586.33	395.09	644.48	35.65	58.15	0.20%	0.20%	0.19%	0.19%
	A - K=K, AOC=KSS	359.44	586.33	395.09	644.48	35.65	58.15	0.19%	0.19%	0.19%	0.19%
	B - K=K, AOC=KSS	359.44	586.33	395.09	644.48	35.65	58.15	0.19%	0.19%	0.19%	0.19%
	A - K=KSS, AOC=KSS	359.44	586.33	397.53	648.46	38.09	62.13	0.20%	0.20%	0.19%	0.19%
	B - K=KSS, AOC=KSS	359.44	586.33	397.53	648.46	38.09	62.13	0.21%	0.21%	0.20%	0.20%
JENSN											
	A - K=K, AOC=K	1647.09	2686.78	1691.14	2758.64	44.05	71.86	0.24%	0.24%	0.23%	0.23%
	B - K=K, AOC=K	1647.09	2686.78	1691.14	2758.64	44.05	71.86	0.24%	0.24%	0.24%	0.24%
	A - K=K, AOC=KSS	1647.09	2686.78	1691.14	2758.64	44.05	71.86	0.23%	0.23%	0.23%	0.23%
	B - K=K, AOC=KSS	1647.09	2686.78	1691.14	2758.64	44.05	71.86	0.24%	0.24%	0.23%	0.23%
	A - K=KSS, AOC=KSS	1647.09	2686.78	1713.91	2795.78	66.82	109.00	0.35%	0.35%	0.34%	0.34%
	B - K=KSS, AOC=KSS	1647.09	2686.78	1713.91	2795.78	66.82	109.00	0.36%	0.36%	0.34%	0.34%
WHTCRK											
	A - K=K, AOC=K	307.68	1480.64	326.62	1527.84	28.94	47.20	0.16%	0.16%	0.15%	0.15%
	B - K=K, AOC=K	307.68	1480.64	336.62	1527.84	28.94	47.20	0.16%	0.16%	0.16%	0.16%
	A - K=K, AOC=KSS	319.30	1499.59	347.10	1544.94	27.80	45.35	0.15%	0.15%	0.14%	0.14%
	B - K=K, AOC=KSS	319.30	1499.59	347.10	1544.94	27.80	45.35	0.15%	0.15%	0.15%	0.15%
	A - K=KSS, AOC=KSS	319.30	1499.59	368.07	1579.15	48.77	79.56	0.26%	0.26%	0.25%	0.25%
	B - K=KSS, AOC=KSS	319.30	1499.59	368.07	1579.15	48.77	79.56	0.26%	0.26%	0.25%	0.25%
TOTAL MINES											
	A - K=K, AOC=K	18469.62	30129.42	18919.98	30863.07	450.36	734.65	2.44%	2.44%	2.38%	2.38%
	B - K=K, AOC=K	18105.12	29535.84	18554.20	30266.39	449.08	732.55	2.48%	2.48%	2.42%	2.42%
	A - K=K, AOC=KSS	18974.03	30788.11	19367.65	31430.21	393.62	642.10	2.09%	2.09%	2.04%	2.04%
	B - K=K, AOC=KSS	18503.52	30183.72	18896.45	30824.69	392.93	640.97	2.12%	2.12%	2.08%	2.08%
	A - K=KSS, AOC=KSS	18974.03	30788.11	19378.94	32427.37	1004.91	1638.26	5.30%	5.32%	5.06%	5.06%
	B - K=KSS, AOC=KSS	18503.52	30183.72	19505.73	31918.58	1002.21	1634.86	5.42%	5.42%	5.14%	5.14%
ROADS/PITS											
	A - K=K, AOC=K	18471.06	30130.79	18874.39	30788.63	403.33	657.31	2.18%	2.18%	2.14%	2.14%
	B - K=K, AOC=K	18106.48	29536.08	18499.37	30175.33	391.89	639.27	2.16%	2.16%	2.12%	2.12%
	A - K=K, AOC=KSS	18975.49	30790.48	19383.78	31456.46	408.27	665.98	2.15%	2.16%	2.12%	2.12%
	B - K=K, AOC=KSS	18504.88	30185.35	18901.56	30833.02	396.68	647.67	2.14%	2.14%	2.10%	2.10%

Reproduced with permission of the copyright owner. Further reproduction prohibited without permission.

Reproduced with permission of the copyright owner. Further reproduction prohibited without permission.

Table 6-7B

USLE INDIVIDUAL MINE IMPACT ON ASBESTOS SOIL EROSION SUMMARY - UNADJUSTED K

YEARLY AVERAGE ASBESTOS EROSION

UNADJUSTED K	TYPE I STORM Pre-Mining (cu yd)	TYPE II STORM Pre-Mining (cu yd)	TYPE I STORM Post-Mining (cu yd)	TYPE II STORM Post-Mining (cu yd)	TYPE I STORM Mine Impact (cu yd)	TYPE II STORM Mine Impact (cu yd)	TYPE I STORM Mine Impact (%)	TYPE II STORM Mine Impact (%)	(MINE IMPACT)/POST TYPE I STORM	(MINE IMPACT)/POST TYPE II STORM
CLNOA										
A - K=K, AOC=K	271.48	442.85	322.90	526.73	51.42	83.88	0.20%	0.20%	0.20%	0.20%
B - K=K, AOC=K	271.48	442.85	322.90	526.73	51.42	83.88	0.21%	0.21%	0.20%	0.20%
A - K=K, AOC=KSS	271.48	442.85	322.90	526.73	51.42	83.88	0.20%	0.20%	0.19%	0.19%
B - K=K, AOC=KSS	271.48	442.85	322.90	526.73	51.42	83.88	0.20%	0.20%	0.20%	0.20%
A - K=KSS, AOC=KSS	271.48	442.85	337.69	550.85	66.21	108.00	0.25%	0.25%	0.24%	0.24%
B - K=KSS, AOC=KSS	271.48	442.85	337.69	550.85	66.21	108.00	0.26%	0.26%	0.24%	0.24%
ATLAS										
A - K=K, AOC=K	9717.62	14220.50	9031.97	14733.29	314.35	512.79	1.24%	1.24%	1.21%	1.21%
B - K=K, AOC=K	9673.03	14147.77	8986.92	14659.00	313.89	512.03	1.25%	1.25%	1.22%	1.22%
A - K=K, AOC=KSS	9033.53	14745.62	9273.86	15127.97	234.33	382.25	0.90%	0.90%	0.88%	0.88%
B - K=K, AOC=KSS	8992.68	14669.19	9227.24	15051.82	234.56	382.63	0.92%	0.92%	0.90%	0.90%
A - K=KSS, AOC=KSS	9039.53	14745.62	9806.71	15997.07	767.18	1251.45	2.95%	2.95%	2.73%	2.73%
B - K=KSS, AOC=KSS	8992.68	14669.19	9757.96	15917.55	765.28	1240.36	2.99%	2.99%	2.82%	2.82%
BASIC										
A - K=K, AOC=K	8344.03	14539.34	8394.40	14672.10	50.37	82.16	0.20%	0.20%	0.19%	0.19%
B - K=K, AOC=K	8899.44	14517.20	8949.82	14599.39	50.38	82.19	0.20%	0.20%	0.20%	0.20%
A - K=K, AOC=KSS	9236.15	15066.46	9275.84	15131.20	39.69	64.74	0.15%	0.15%	0.15%	0.15%
B - K=K, AOC=KSS	9189.30	14990.03	9229.21	15055.14	39.91	65.11	0.16%	0.16%	0.15%	0.15%
A - K=KSS, AOC=KSS	9236.15	15066.46	9391.28	15319.52	155.13	253.06	0.60%	0.60%	0.56%	0.56%
B - K=KSS, AOC=KSS	9189.30	14990.03	9344.33	15242.92	155.03	252.89	0.61%	0.61%	0.57%	0.57%
BORDOE										
A - K=K, AOC=K	4450.38	7259.76	4494.24	7331.32	43.86	71.56	0.17%	0.17%	0.17%	0.17%
B - K=K, AOC=K	4450.38	7259.76	4494.24	7331.32	43.86	71.56	0.18%	0.18%	0.17%	0.17%
A - K=K, AOC=KSS	4555.50	7431.25	4602.45	7507.83	46.95	76.53	0.18%	0.18%	0.18%	0.18%
B - K=K, AOC=KSS	4555.50	7431.25	4602.45	7507.83	46.95	76.53	0.18%	0.18%	0.18%	0.18%
A - K=KSS, AOC=KSS	4555.50	7431.25	4689.02	7649.05	133.52	217.80	0.51%	0.51%	0.49%	0.49%
B - K=KSS, AOC=KSS	4555.50	7431.25	4689.02	7649.05	133.52	217.80	0.52%	0.52%	0.49%	0.49%
TROMBY										
A - K=K, AOC=K	6511.86	10622.54	6589.51	10749.21	77.65	126.67	0.31%	0.31%	0.30%	0.30%
B - K=K, AOC=K	6511.86	10622.54	6589.51	10749.21	77.65	126.67	0.34%	0.34%	0.30%	0.30%
A - K=K, AOC=KSS	6663.48	10869.88	6744.03	11001.28	80.55	131.40	0.31%	0.31%	0.30%	0.30%
B - K=K, AOC=KSS	6663.48	10869.88	6744.03	11001.28	80.55	131.40	0.31%	0.31%	0.31%	0.31%
A - K=KSS, AOC=KSS	6663.48	10869.88	6880.14	11223.31	216.66	353.43	0.85%	0.85%	0.79%	0.79%
B - K=KSS, AOC=KSS	6663.48	10869.88	6880.14	11223.31	216.66	353.43	0.86%	0.86%	0.80%	0.80%
BILES										
A - K=K, AOC=K	4450.38	7259.76	4494.24	7331.32	43.86	71.56	0.17%	0.17%	0.17%	0.17%
B - K=K, AOC=K	4450.38	7259.76	4494.24	7331.32	43.86	71.56	0.18%	0.18%	0.17%	0.17%
A - K=K, AOC=KSS	4555.50	7431.25	4602.45	7507.83	46.95	76.53	0.18%	0.18%	0.18%	0.18%
B - K=K, AOC=KSS	4555.50	7431.25	4602.45	7507.83	46.95	76.53	0.18%	0.18%	0.18%	0.18%
A - K=KSS, AOC=KSS	4555.50	7431.25	4689.02	7649.05	133.52	217.80	0.51%	0.51%	0.49%	0.49%
B - K=KSS, AOC=KSS	4555.50	7431.25	4689.02	7649.05	133.52	217.80	0.52%	0.52%	0.49%	0.49%
MINEF										
A - K=K, AOC=K	3016.30	4921.26	3042.63	4963.22	25.73	41.96	0.10%	0.10%	0.10%	0.10%
B - K=K, AOC=K	3016.30	4921.26	3042.63	4963.22	25.73	41.96	0.10%	0.10%	0.10%	0.10%
A - K=K, AOC=KSS	3036.72	4953.58	3062.64	4995.87	25.92	42.29	0.10%	0.10%	0.10%	0.10%
B - K=K, AOC=KSS	3036.72	4953.58	3062.64	4995.87	25.92	42.29	0.10%	0.10%	0.10%	0.10%
A - K=KSS, AOC=KSS	3036.72	4953.58	3076.51	5018.50	39.79	64.92	0.15%	0.15%	0.14%	0.14%
B - K=KSS, AOC=KSS	3036.72	4953.58	3076.51	5018.50	39.79	64.92	0.16%	0.16%	0.15%	0.15%
OUTLR										
A - K=K, AOC=K	372.12	607.01	408.07	665.65	35.95	58.64	0.14%	0.14%	0.14%	0.14%
B - K=K, AOC=K	372.12	607.01	408.07	665.65	35.95	58.64	0.14%	0.14%	0.14%	0.14%
A - K=K, AOC=KSS	372.12	607.01	408.07	665.65	35.95	58.64	0.14%	0.14%	0.14%	0.14%
B - K=K, AOC=KSS	372.12	607.01	408.07	665.65	35.95	58.64	0.14%	0.14%	0.14%	0.14%
A - K=KSS, AOC=KSS	372.12	607.01	411.73	671.62	39.61	64.61	0.15%	0.15%	0.14%	0.14%
B - K=KSS, AOC=KSS	372.12	607.01	411.73	671.62	39.61	64.61	0.15%	0.15%	0.15%	0.15%
JENSN										
A - K=K, AOC=K	1982.59	3234.05	2028.97	3309.54	46.29	75.49	0.18%	0.18%	0.18%	0.18%
B - K=K, AOC=K	1982.59	3234.05	2028.97	3309.54	46.29	75.49	0.19%	0.19%	0.18%	0.18%
A - K=K, AOC=KSS	1982.59	3234.05	2028.97	3309.54	46.29	75.49	0.18%	0.18%	0.17%	0.17%
B - K=K, AOC=KSS	1982.59	3234.05	2028.97	3309.54	46.29	75.49	0.18%	0.18%	0.18%	0.18%
A - K=KSS, AOC=KSS	1982.59	3234.05	2063.02	3365.25	80.44	131.20	0.31%	0.31%	0.29%	0.29%
B - K=KSS, AOC=KSS	1982.59	3234.05	2063.02	3365.25	80.44	131.20	0.31%	0.31%	0.30%	0.30%
WHTCRK										
A - K=K, AOC=K	1190.61	1942.16	1224.94	1998.16	34.33	56.00	0.14%	0.14%	0.13%	0.13%
B - K=K, AOC=K	1190.61	1942.16	1224.94	1998.16	34.33	56.00	0.14%	0.14%	0.13%	0.13%
A - K=K, AOC=KSS	1208.03	1970.58	1240.67	2023.82	32.64	53.24	0.13%	0.13%	0.12%	0.12%
B - K=K, AOC=KSS	1208.03	1970.58	1240.67	2023.82	32.64	53.24	0.13%	0.13%	0.12%	0.12%
A - K=KSS, AOC=KSS	1208.03	1970.58	1272.12	2075.13	64.09	104.55	0.25%	0.25%	0.23%	0.23%
B - K=KSS, AOC=KSS	1208.03	1970.58	1272.12	2075.13	64.09	104.55	0.25%	0.25%	0.24%	0.24%
TOTAL MINES										
A - K=K, AOC=K	25422.52	41470.30	26060.23	42510.56	637.71	1040.26	2.51%	2.51%	2.45%	2.45%
B - K=K, AOC=K	25012.60	40801.62	25648.31	41839.61	636.31	1037.99	2.54%	2.54%	2.48%	2.48%
A - K=K, AOC=KSS	26029.15	42459.95	26581.74	43361.27	552.61	901.44	2.12%	2.12%	2.08%	2.08%
B - K=K, AOC=KSS	25610.19	41776.44	26162.29	42677.05	552.10	900.61	2.16%	2.16%	2.11%	2.11%
A - K=KSS, AOC=KSS	26029.15	42459.95	27512.65	44879.92	1483.52	2419.99	5.70%	5.70%	5.39%	5.39%
B - K=KSS, AOC=KSS	25610.19	41776.44	27090.20	44190.70	1480.01	2414.26	5.78%	5.78%	5.46%	5.46%
ROADS/PITS										
A - K=K, AOC=K	25423.33	41472.69	25955.11	42339.09	531.13	866.40	2.09%	2.09%	2.05%	2.05%
B - K=K, AOC=K	25013.97	40803.96	25552.40	41648.55	538.43	845.63	2.07%	2.07%	2.03%	2.03%
A - K=K, AOC=KSS	26030.61	42462.24	26569.15	43340.73	538.54	878.49	2.07%	2.07%	2.03%	2.03%
B - K=K, AOC=KSS	25611.53	41779.70	26137.10	42636.03	525.60	857.39	2.05%	2.05%	2.01%	2.01%

Reproduced with permission of the copyright owner. Further reproduction prohibited without permission.

Table 6-8A

MUSLE TOTAL PRE-MINING ASBESTOS SEDIMENT YIELD CALCULATED BY THE MUSLE ADJUSTED AND UNADJUSTED K

PRE-MINING ADJUSTED K	2 YR (cu yd) (0.4)	5 YR (cu yd) (0.2)	10 YR (cu yd) (0.08)	25 YR (cu yd) (0.04)	50 YR (cu yd) (0.015)	100 YR (cu yd) (0.015)	AVERAGE YEAR (cu yd)	YEARLY AVERAGE (cu yd) (*)
MINES A K=K, AGC=K	2358.71	7398.85	12311.17	20027.73	26021.62	33031.75	4748.25	5095.06
MINES B K=K, AGC=K	2314.20	7257.07	12074.35	19628.07	25525.46	32383.80	4657.46	4996.80
MINES A K=K, AGC=KSS	2390.40	7514.31	12514.95	20373.13	26481.37	33624.96	4822.90	5176.74
MINES B K=K, AGC=KSS	2345.34	7370.68	12275.03	19968.25	25978.23	32967.92	4730.95	5077.20
MINES A K=KSS, AGC=KSS	2390.40	7514.31	12514.95	20373.13	26481.37	33624.96	4822.90	5176.74
MINES B K=KSS, AGC=KSS	2345.34	7370.68	12275.03	19968.25	25978.23	32967.92	4730.95	5077.20
ROADS/PITS A - K=K, AGC=K	2358.79	7399.17	11635.86	20028.74	26023.04	33033.60	4748.46	5041.22
ROADS/PITS B - K=K, AGC=K	2314.28	7257.37	11409.13	19629.04	25526.80	32385.54	4657.66	4943.76
ROADS/PITS A - K=K, AGC=KSS	2390.48	7514.62	11807.46	20374.16	26482.79	33626.83	4823.11	5120.32
ROADS/PITS B - K=K, AGC=KSS	2345.42	7370.98	11578.11	19969.23	25979.57	32969.87	4731.15	5021.62

PRE-MINING UNADJUSTED K	2 YR (cu yd)	5 YR (cu yd)	10 YR (cu yd)	25 YR (cu yd)	50 YR (cu yd)	100 YR (cu yd)	AVERAGE YEAR	YEARLY AVERAGE (cu yd)
MINES A K=K, AGC=K	3227.18	10133.93	16877.71	27456.44	35696.94	45275.27	6503.94	6980.72
MINES B K=K, AGC=K	3178.08	9977.00	16615.77	27015.12	35144.87	44554.87	6403.46	6871.98
MINES A K=K, AGC=KSS	3274.72	10307.12	17183.38	27974.55	36386.57	46165.08	6615.92	7103.24
MINES B K=K, AGC=KSS	3224.79	10147.42	16916.78	27525.40	35824.02	45431.05	6513.66	6992.58
MINES A K=KSS, AGC=KSS	3274.72	10307.12	17183.38	27974.55	36386.57	46165.08	6615.92	7103.24
MINES B K=KSS, AGC=KSS	3224.79	10147.42	16916.78	27525.40	35842.02	45431.05	6513.66	6992.85
ROADS/PITS A - K=K, AGC=K	3227.27	10134.25	15927.32	27457.47	35698.37	45277.15	6504.15	6904.68
ROADS/PITS B - K=K, AGC=K	3178.16	9977.30	15679.58	27016.09	35146.22	44556.65	6403.66	6797.28
ROADS/PITS A - K=K, AGC=KSS	3274.80	10307.44	16184.72	27975.59	36388.01	46166.99	6616.13	7023.53
ROADS/PITS B - K=K, AGC=KSS	3224.87	10147.73	15933.04	27526.38	35825.38	45432.83	6515.86	6914.07

NOTES:
(*) Equation for average yield: Yave = 0.015 x Y100 + 0.015 x Y50 + 0.04 x Y25 + 0.08 x Y10 + 0.2 x Y5 + 0.4 x Y2

SOURCE: LEVINE-FRICKE

Reproduced with permission of the copyright owner. Further reproduction prohibited without permission.

Table 6-8B

MUSLE TOTAL POST-MINING ASBESTOS SEDIMENT YIELD CALCULATED BY THE MUSLE ADJUSTED AND UNADJUSTED K

POST-MINING ADJUSTED K	2 YR (cu yd) (0.4)	5 YR (cu yd) (0.2)	10 YR (cu yd) (0.08)	25 YR (cu yd) (0.04)	50 YR (cu yd) (0.015)	100 YR (cu yd) (0.015)	AVERAGE YEAR (cu yd)	YEARLY AVERAGE (cu yd) (A)
MINES A								
K=K, AGC=K	2413.59	7574.12	12607.67	20511.32	26647.12	33815.81	4860.81	5216.27
B								
K=K, AGC=K	2368.90	7431.36	12370.18	20110.51	26149.43	33165.81	4769.79	5117.75
A								
K=K, AGC=KSS	2441.95	7676.37	12786.58	20812.77	27049.16	34330.57	4926.66	5288.17
B								
K=K, AGC=KSS	2396.83	7532.52	12546.27	20407.24	26544.15	33672.38	4834.56	5188.48
A								
K=KSS, AGC=KSS	2492.92	7858.48	13110.79	21371.04	27776.57	35257.00	5045.90	5418.07
B								
K=KSS, AGC=KSS	2447.65	7714.06	12863.46	20963.76	27270.24	34595.69	4953.51	5317.97
ROADS/PITS								
A - K=K, AGC=K	2424.74	7593.57	11941.66	20529.04	26669.14	33860.21	4872.88	5173.04
B - K=K, AGC=K	2378.80	7447.24	11707.53	20116.77	26157.09	33191.55	4779.20	5072.47
A - K=K, AGC=KSS	2456.92	7710.66	12115.67	20879.13	27135.09	34461.35	4948.59	5253.27
B - K=K, AGC=KSS	2410.41	7562.43	11878.83	20461.48	26615.86	33783.34	4853.69	5151.40

POST-MINING UNADJUSTED K	2 YR (cu yd)	5 YR (cu yd)	10 YR (cu yd)	25 YR (cu yd)	50 YR (cu yd)	100 YR (cu yd)	AVERAGE YEAR	YEARLY AVERAGE (cu yd)
MINES A								
K=K, AGC=K	3301.22	10372.40	17284.10	28124.50	36558.17	46353.68	6657.39	7146.35
B								
K=K, AGC=K	3252.00	10215.07	17021.44	27681.96	36004.47	45631.03	6556.64	7037.34
A								
K=K, AGC=KSS	3343.76	10525.77	17552.45	28576.68	37159.73	47125.82	6756.16	7254.20
B								
K=K, AGC=KSS	3293.79	10365.91	17285.57	28127.05	36596.55	46390.95	6653.79	7143.44
K=KSS, AGC=KSS	3422.85	10806.78	18052.10	29433.36	38279.63	48547.10	6940.13	7454.40
B								
K=KSS, AGC=KSS	3372.65	10646.08	17783.69	28901.12	37712.97	47807.54	6837.19	7343.02
ROADS/PITS								
A - K=K, AGC=K	3227.27	10134.25	16329.50	28116.14	36549.22	46364.08	6668.11	6992.46
B - K=K, AGC=K	3178.16	9977.30	16073.64	27660.95	35979.57	45620.78	6564.41	6883.06
A - K=K, AGC=KSS	3274.80	10307.44	16590.52	28641.27	37248.14	47265.79	6781.67	7112.01
B - K=K, AGC=KSS	3224.87	10147.73	16330.60	28178.03	36667.71	46508.47	6676.14	7000.71

SOURCE: LEVINE-FRICKE

Reproduced with permission of the copyright owner. Further reproduction prohibited without permission.

Table 6-8C

MUSLE TOTAL MINE AND ROADS/PITS IMPACT ON ASBESTOS SOIL EROSION - SUMMARY ADJUSTED AND UNADJUSTED K

ADJUSTED	2 YR <cu yd> <0.4>	5 YR <cu yd> <0.2>	10 YR <cu yd> <0.08>	25 YR <cu yd> <0.04>	50 YR <cu yd> <0.015>	100 YR <cu yd> <0.015>	AVERAGE YEAR <cu yd>	YEARLY AVERAGE <cu yd> <M>
MINES								
A K=K, AGC=K	54.88	175.27	296.51	483.59	825.50	784.06	112.58	121.21
B K=K, AGC=K	54.78	174.89	295.83	482.44	823.36	782.01	112.31	120.94
A K=K, AGC=KSS	51.56	162.06	271.63	439.63	566.79	705.61	103.76	111.44
B K=K, AGC=KSS	51.49	161.83	271.24	438.99	565.92	704.46	103.61	111.28
A K=KSS, AGC=KSS	102.52	344.17	595.84	997.90	1295.20	1632.04	223.08	241.35
B K=KSS, AGC=KSS	102.30	343.38	594.44	995.51	1292.01	1627.76	222.55	240.77
ROADS/PITS								
A - K=K, AGC=K	65.35	194.40	305.80	500.30	646.11	826.61	124.42	131.83
B - K=K, AGC=K	64.52	189.87	298.40	487.74	630.23	806.00	121.52	128.71
A - K=K, AGC=KSS	66.44	196.04	308.21	504.38	652.29	834.52	125.48	132.94
B - K=K, AGC=KSS	64.99	191.45	300.73	492.27	636.29	813.66	122.54	129.78

UNADJUSTED	2 YR	5 YR	10 YR	25 YR	50 YR	100 YR	AVERAGE YEAR	YEARLY AVERAGE
MINES								
A K=K, AGC=K	74.04	238.47	406.39	668.06	861.23	1078.41	153.45	165.64
B K=K, AGC=K	73.93	238.07	405.67	666.84	859.60	1076.22	153.18	165.35
A K=K, AGC=KSS	69.05	218.65	369.07	602.13	773.16	960.74	140.24	150.97
B K=K, AGC=KSS	69.00	218.49	368.79	601.65	772.53	959.90	140.13	150.85
A K=KSS, AGC=KSS	148.13	499.66	868.72	1458.81	1893.06	2382.01	324.20	351.16
B K=KSS, AGC=KSS	147.85	498.65	866.91	1455.72	1888.94	2376.49	323.53	350.43
ROADS/PITS								
A - K=K, AGC=K	87.08	256.27	402.18	658.67	850.84	1086.93	163.96	173.67
B - K=K, AGC=K	85.49	251.26	394.06	644.86	833.54	1064.15	160.75	170.23
A - K=K, AGC=KSS	87.80	258.72	405.80	665.68	860.13	1098.80	165.54	175.34
B - K=K, AGC=KSS	86.19	253.63	397.56	651.65	842.33	1075.64	162.28	171.84

NOTES:
<M> Equation for average yield: Yave = 0.015 H Y100 + 0.015 H Y50 + 0.04 H Y25 + 0.08 H Y10 + 0.2 H Y5 + 0.4 H Y2
(Yave = average yield, Y# = yield of that year)

SOURCE: LEVINE-FRICKE

Reproduced with permission of the copyright owner. Further reproduction prohibited without permission.

Table 6-8D

MUSLE TOTAL PRE-MINING AND POST-MINING ASBESTOS SEDIMENT YIELD CALCULATED BY THE MUSLE ADJUSTED AND UNADJUSTED K PORTION OF CURRENTLY ERODED ASBESTOS INCREASE TO NATURAL ASBESTOS EROSION

EFFECT ON NATURAL ASBESTOS EROSION

	(POST-PRE)/PRE (MINE IMPACT/PRE-MINING)							
ADJUSTED K	2 YR	5 YR	10 YR	25 YR	50 YR	100YR	AVERAGE YEAR	YEARLY AVERAGE
MINES A K=K, AGC=K	2.33%	2.37%	2.41%	2.41%	2.40%	2.37%	2.37%	2.38%
MINES B K=K, AGC=K	2.37%	2.41%	2.45%	2.46%	2.44%	2.41%	2.41%	2.42%
MINES A K=K, AGC=KSS	2.16%	2.16%	2.17%	2.16%	2.14%	2.10%	2.15%	2.15%
MINES B K=K, AGC=KSS	2.20%	2.20%	2.21%	2.20%	2.18%	2.14%	2.19%	2.19%
MINES A K=KSS, AGC=KSS	4.29%	4.58%	4.76%	4.90%	4.89%	4.85%	4.63%	4.66%
MINES B K=KSS, AGC=KSS	4.36%	4.66%	4.84%	4.99%	4.97%	4.94%	4.70%	4.74%
ROADS/PITS A - K=K, AGC=K	2.80%	2.63%	2.63%	2.50%	2.48%	2.50%	2.62%	2.61%
ROADS/PITS B - K=K, AGC=K	2.79%	2.62%	2.62%	2.48%	2.47%	2.49%	2.61%	2.60%
ROADS/PITS A - K=K, AGC=KSS	2.78%	2.61%	2.61%	2.48%	2.46%	2.48%	2.60%	2.60%
ROADS/PITS B - K=K, AGC=KSS	2.77%	2.60%	2.60%	2.47%	2.45%	2.47%	2.59%	2.58%

	(POST-PRE)/PRE							
UNADJUSTED K	2 YR	5 YR	10 YR	25 YR	50 YR	100 YR	AVERAGE YEAR	YEARLY AVERAGE
MINES A K=K, AGC=K	2.29%	2.35%	2.41%	2.43%	2.41%	2.38%	2.36%	2.37%
MINES B K=K, AGC=K	2.33%	2.39%	2.44%	2.47%	2.45%	2.42%	2.39%	2.41%
MINES A K=K, AGC=KSS	2.11%	2.12%	2.15%	2.15%	2.12%	2.08%	2.12%	2.13%
MINES B K=K, AGC=KSS	2.14%	2.15%	2.18%	2.19%	2.16%	2.11%	2.15%	2.16%
MINES A K=KSS, AGC=KSS	4.52%	4.85%	5.06%	5.21%	5.20%	5.16%	4.90%	4.94%
MINES B K=KSS, AGC=KSS	4.59%	4.91%	5.12%	5.29%	5.22%	5.23%	4.97%	5.01%
ROADS/PITS A - K=K, AGC=K	0.00%	0.00%	2.53%	2.40%	2.38%	2.40%	2.52%	1.27%
ROADS/PITS B - K=K, AGC=K	0.00%	0.00%	2.51%	2.39%	2.37%	2.39%	2.51%	1.26%
ROADS/PITS A - K=K, AGC=KSS	0.00%	0.00%	2.51%	2.38%	2.36%	2.38%	2.50%	1.26%
ROADS/PITS B - K=K, AGC=KSS	0.00%	0.00%	2.50%	2.37%	2.35%	2.37%	2.49%	1.25%

SOURCE: LEVINE-FRICKE

Reproduced with permission of the copyright owner. Further reproduction prohibited without permission.

Table 6-8E

MUSLE TOTAL PRE-MINING AND POST-MINING ASBESTOS SEDIMENT YIELD CALCULATED BY THE MUSLE ADJUSTED AND UNADJUSTED K PORTION OF CURRENTLY ERODED ASBESTOS

	(POST-PRE)/POST (MINE IMPACT/POST MINING)							
ADJUSTED K	2 YR	5 YR	10 YR	25 YR	50 YR	100YR	AVERAGE YEAR	YEARLY AVERAGE
MINES								
A K=K, AGC=K	2.27%	2.31%	2.35%	2.36%	2.35%	2.32%	2.32%	2.32%
B K=K, AGC=K	2.31%	2.35%	2.39%	2.40%	2.39%	2.36%	2.35%	2.36%
A K=K, AGC=KSS	2.11%	2.11%	2.12%	2.11%	2.10%	2.06%	2.11%	2.11%
B K=K, AGC=KSS	2.15%	2.15%	2.16%	2.15%	2.13%	2.09%	2.14%	2.14%
A K=KSS, AGC=KSS	4.11%	4.38%	4.54%	4.67%	4.66%	4.63%	4.42%	4.45%
B K=KSS, AGC=KSS	4.18%	4.45%	4.62%	4.75%	4.74%	4.71%	4.49%	4.53%
ROADS/PITS								
A - K=K, AGC=K	2.72%	2.56%	2.56%	2.44%	2.42%	2.44%	2.55%	2.55%
B - K=K, AGC=K	2.71%	2.55%	2.55%	2.42%	2.41%	2.43%	2.54%	2.54%
A - K=K, AGC=KSS	2.70%	2.54%	2.54%	2.42%	2.40%	2.42%	2.54%	2.53%
B - K=K, AGC=KSS	2.70%	2.53%	2.53%	2.41%	2.39%	2.41%	2.52%	2.52%

	(POST-PRE)/POST							
UNADJUSTED K	2 YR	5 YR	10 YR	25 YR	50 YR	100 YR	AVERAGE YEAR	YEARLY AVERAGE
MINES								
A K=K, AGC=K	2.24%	2.30%	2.35%	2.38%	2.36%	2.33%	2.30%	2.32%
B K=K, AGC=K	2.27%	2.33%	2.38%	2.41%	2.39%	2.36%	2.34%	2.35%
A K=K, AGC=KSS	2.06%	2.08%	2.10%	2.11%	2.09%	2.04%	2.08%	2.08%
B K=K, AGC=KSS	2.09%	2.11%	2.13%	2.14%	2.11%	2.07%	2.11%	2.11%
A K=KSS, AGC=KSS	4.33%	4.62%	4.81%	4.96%	4.95%	4.91%	4.67%	4.71%
B K=KSS, AGC=KSS	4.38%	4.68%	4.87%	5.02%	4.96%	4.97%	4.73%	4.77%
ROADS/PITS								
A - K=K, AGC=K	0.00%	0.00%	2.46%	2.34%	2.33%	2.34%	2.46%	1.25%
B - K=K, AGC=K	0.00%	0.00%	2.45%	2.33%	2.32%	2.33%	2.45%	1.25%
A - K=K, AGC=KSS	0.00%	0.00%	2.45%	2.32%	2.31%	2.32%	2.44%	1.24%
B - K=K, AGC=KSS	0.00%	0.00%	2.43%	2.31%	2.30%	2.31%	2.43%	1.24%

SOURCE: LEVINE-FRICKE

Reproduced with permission of the copyright owner. Further reproduction prohibited without permission.

Table 6-9

MINES IN THE LOS GATOS CREEK DRAINAGE BASIN

Mine and/or Mill	Location Sec. Twp. Rge/County	Commodity	Estimated Amount of Production/Date	Types of Working Tailings/Buildings	Estimated Surface Area	Comments Regarding SPLC MUSLE/USLE Modelling
Coalinga Asbestos Mill	1-19S-13E Fresno Co.	Asbestos	Asbestos mill operated by Coalinga Asbestos Co. 1964-74. Chromite mill operated by Harmac Resources from 1975-77. Amount of production unavailable.	Mill facilities and tailings site: In Sec 1-T 19S, R13E leased from Southern Pacific Co.	Mill/Tailings: 500' x 1200'	Includes ore and tailings from former milling operations.
Railroad Mine	NW 1/4 1-19S-13E Fresno Co.	Chromium	60 tons shipped, 1955-56	Two open cuts: 105' x 50' and 120' x 70'	----	----
Jensen Mine	34-18S-13E Fresno Co.	Asbestos	Production 1964-74, Amount of production unavailable.	Open Pit in SE 1/2 Sec 34.	Jensen Pit: 1000' x 1000'	----
Atlas Asbestos Co.	32, 31, 30-18S,13E 25-18S, 12E Fresno Co.	Asbestos	Production 1963-80 Amount of production unavailable.	Open Pits: Two Pits: Rover pit in NE 1/4 Sec 31, and Santa Cruz pit in NE 1/4 Sec 31 and 1/4 NW Sec 32 Tailings and Mill: located east, south, and northwest of Santa Cruz pit. Mill in Sec 32. Processed asbestos trucked to warehouse in Coalinga or beyond.	Tailings: 1500' x 4300' Rover pit; 800' x 1000'; Santa Cruz pit: 1000' x 1600'. Separate tailings area in Sec 30, T18S-13S and Sec 25, T18S-12E.	----
Basic Resources Corp.	S 1/2 30-18S-13E Fresno Co.	Asbestos	Pilot mining operation in 1959.	Surface ripping (bull-dozer); processing (screening) of ore at mining site; truck to pilot millsite in Coalinga	----	----

SOURCE: LEVINE-FRICKE

Reproduced with permission of the copyright owner. Further reproduction prohibited without permission.

MINES IN THE LOS GATOS CREEK DRAINAGE BASIN

Mine and/or Mill	Location Sec. Twp. Rge/County	Commodity	Estimated Amount of Production/Date	Types of Working Tailings/Buildings	Estimated Surface Area	Comments Regarding SPLC MUSLE/USLE Modelling
"Section 28 Mine"	S 1/2 28-18S-13E Fresno Co.	Asbestos	Operations probably by Union Carbide (as major claim holder in area).	----	----	Designated as Mine? by SPLC.
Big Ridge (Jeanne/ Condon Peak)	N 1/2 36-18S-12E Fresno Co.	Chromium	90 tons in 1917, 1268 tons in 1956-57.	Line of pits along crest of a ridge	----	----
Tromby No. 1 and 2	C36-18S-12E Fresno Co.	Chromium	----	----	----	Tromby No. 1 and 2 combined for modelling purposes.
Butler Estate (Histake; Koski; James/Thickston)	SW 1/4 34-18S-13E Fresno Co.	Chromium	Active ca 1900 to 1958. 202 carloads ore ($350,000) shipped Sept 1956-May 1958. Largest producer of chromite in Fresno Co. 1953-58 production 23,000 long tons. Still active in 1976	Deep open pit. Three mills that processed ore are on White Creek (Holman and Chambers/ Russell) and San Benito River (James). After 1952, all ore was trucked to Coalinga. In 1976, a mill for concentrating chromite was being built inside former asbestos mill (Coalinga Asbestos Co.) in Sec 1-19S-13E	850' x 550', 250' deep	----
White Creek Magnesite Mine	E 1/2 5-19S-13E Fresno Co.	Magnesium	----	----	----	----
Archer	NE 1/4 3-19S-13E Fresno Co.	Mercury	Discovered in 1904; worked until 1942, again in 1940's	Several open cuts, two adits, several drifts	----	Combined with James Corbett Byles Mine for modelling purposes.

Reproduced with permission of the copyright owner. Further reproduction prohibited without permission.

MINES IN THE LOS GATOS CREEK DRAINAGE BASIN

Mine and/or Hill	Location Sec. Twp. Rge/County	Commodity	Estimated Amount of Production/Date	Types of Working Tailings/Buildings	Estimated Surface Area	Comments Regarding SPLC MUSLE/USLE Modelling
James-Corbett (James-Corbett-Byles; Corbett-Byles)	NE 1/4 3-19S, 13E Fresno Co.	Chromium iron	Discovered in 1910. In 1945-55, shipped 11 tons lump ore, and 530 tons concentrates	Large benched cut 75 m long, 25 m deep - probable ore body is 10 m x 10 m x 5 m	----	Combined with Archer Mine for modelling purposes.

Source: Modified from "Inventory of Potential Asbestos Sources in the New Indria-Coalinga Study Region for the Atlas and Coalinga Sites Fresno County, California," (U.S. Environmental Protection Agency, September 15, 1987).

SOURCE: LEVINE-FRICKE

Reproduced with permission of the copyright owner. Further reproduction prohibited without permission.

Table 6-10
ESTIMATION OF CHROMITE MILLING SERPENTENITE SOIL MATRIX DISCHARGE

Chromite Mine	long tons shipped	long tons mined	calculated tons soil discharged	Estimated cu yd discharged	Estimated asbestos dis. cu yd
Butler Estate Chromite Mine	23000 B	63000 B	44000 C	32593 C	19556 C
Tromby No. 1 and 2	Records of quantities not available at this time - D				
James-Corbett/Byles Mine	530 A	1452 C	1014 C	751 C	601 C
Railroad Mine	60 A	164 C	115 C	85 C	68 C
Big Ridge	1358 A	3720 C	2598 C	1924 C	1540 C
			Totals 47727 tonsC	35353 cu yd C	21764 cu yd C

Calculation of discharge is based on the following relationships

1. (total chromite ore mined) = (total milled chromite ore) + (total asbestos soil matrix discharged)

Butler Estate Chromite material quantities were listed in Matthews R. A., 1961

Other mines assumed to have similar ratio of milled material to discharged tailings and mined materials as the Butler Estate Chromite Mine

2. 1cu ft soil = 100 lb

3. asbestos soil = 80% asbestos for all mines except Butler Estate which assumed 60% asbestos content

4. References and explanation of value origin

A-U.S. EPA, 1987, Inventory of Potential Asbestos Sourses in the New Idrea- Coalinga Study Region
B-Matthews, 1961, Geology of the Butler Estate Chromite Mine
C-Calculated
D-No reference available

SOURCE: LEVINE-FRICKE

Reproduced with permission of the copyright owner. Further reproduction prohibited without permission.

TABLE 6-11

MUSLE & USLE - CONSOLIDATION SUMMARY OF TOTAL MINE IMPACT, ROADS AND INDIVIDUAL MINE IMPACT ON SOIL EROSION IN PERCENTAGES

ANTHROPIC IMPACT	BEST ESTIMATE EVALUATED	WORST CASE K & ASBESTOS CONTENT ESTIMATE EVALUATED
Atlas Mine & Mill	1.63	2.99
Coalinga Mine & Mill (with Railroad Mine)	0.31	0.32
Basic Resources Mine	0.14	0.59
Bid Ridge Mine	0.13	0.52
Tromby Mines	0.30	0.85
James Corbett-Biles/Archer Mines	0.13	0.52
Mine?	0.14	0.26
Butler Estate Mine	0.26	0.28
Jensen Mine	0.31	0.54
White Creek Mine	0.20	0.37
All Mines & Mills	3.55	7.24
Roads & Pits	2.75	2.75
Total Anthropic Erosion Increases	6.30	9.99

SOURCE: LEVINE-FRICKE

Reproduced with permission of the copyright owner. Further reproduction prohibited without permission.

Table 6-12

ESTIMATED ASBESTOS CONCENTRATION INCREASE TO NATURAL ASBESTOS CONCENTRATIONS IN WATER DEPENDENT TRANSPORT PATHWAYS FROM ANTHROPIC ASBESTOS EROSION

ANTHROPIC IMPACT	WATER PATHWAY ASSUMING 50% ASBESTOS CA AQUEDUCT CONTRIBUTION				SEDIMENT DEPOSITION AREA	
	BEST ESTIMATE		WORST CASE ESTIMATE			
	37% EST.	62% EST.	37% EST.	62% EST.	15 SQ. MI.	8 SQ. MI.
Atlas Mine & Mill	0.513	0.310	0.942	0.568		X
Coalinga Mine & Mill (with Railroad Mine)	0.098	0.059	0.101	0.061		X
Basic Resources Mine	0.044	0.027	0.186	0.112	X	
Big Ridge Mine	0.041	0.025	0.164	0.099	X	
Tromby Mines	0.095	0.057	0.268	0.162	X	
James Corbett-Biles/Archer Mines	0.041	0.025	0.164	0.099	X	
Mine?	0.044	0.027	0.082	0.049		X
Butler Estate Mine	0.002	0.049	0.088	0.053	X	
Jensen Mine	0.098	0.059	0.170	0.103		X
White Creek Mine	0.063	0.038	0.117	0.070	X	
All Mines & Mills	1.118	0.675	2.281	1.376		
Roads & Pits	0.866	0.523	0.866	0.523	X	
Total Anthropic Erosion Increases	1.985	1.197	3.147	1.898		

SOURCE: LEVINE-FRICKE

Reproduced with permission of the copyright owner. Further reproduction prohibited without permission.

Table 6-13

INLETS AT FOOTHILL DRAINAGE AREAS WHERE RUNOFF ENTERS THE CALIFORNIA AQUEDUCT

FOOTHILL DRAINAGE AREAS					
LEGUNA SECA HILLS (23)	PANOCHE HILLS (2)	CIERVO HILLS (0)	BIG BLUE HILLS (2)	ARROYO PASAJERO (4) (SETTLING BASIN INLETS)	KETTLEMAN HILLS (14)
80.50 Mi.	102.24 Mi.	No Inlets	133.67 Mi. Cantua Creek	158.36 Mi.	165.38 Mi.
80.65 Mi.	102.63 Mi.		136.00 Mi. Salt Creek	158.37 Mi.	166.04 Mi.
81.00 Mi.				158.38 Mi.	166.90 Mi.
81.37 Mi.				158.39 Mi.	166.04 Mi.
81.70 Mi.					166.04 Mi.
82.12 Mi.					166.27 Mi.
82.67 Mi.					167.78 Mi.
83.24 Mi.					168.62 Mi.
83.25 Mi.					169.37 Mi.
83.87 Mi.					169.72 Mi.
84.60 Mi.					170.25 Mi.
85.05 Mi.					170.83 Mi.
86.97 Mi.					171.48 Mi.
87.30 Mi.					171.85 Mi.
87.45 Mi.					
87.98 Mi.					
88.38 Mi.					
89.27 Mi.					
90.47 Mi.					
92.58 Mi.					
93.41 Mi.					
94.88 Mi.					
96.57 Mi.					

NOTES:

Drainage inlets are indicated by Mile Post Number (designated Mi.).
Location of drainage inlets from California Department of Water Resources - See Chapter 4, Figure 4.
Number of inlet structures per foothill drainage area indicated in parentheses.

Leguna Seca Hills contain an estimated 15 square miles of Miocene and younger asbestos-containing sedimentary deposits.
Panoche Hills contain an estimated 68 square miles of Miocene and younger asbestos-containing sedimentary deposits.
Ciervo Hills contain an estimated 118 square miles of Miocene and younger asbestos-containing sedimentary deposits.
Big Blue Hills contain an estimated 85 square miles of Miocene and younger asbestos-containing sedimentary deposits.
Arroyo Pasajero contains an estimated 384 squrae miles of Miocene and younger asbestos-containing sedimentary deposits.
Kettleman Hills contain an estimated 30 square miles of Miocene and younger asbestos-containing sedimentary deposits.

Estimated square miles of miocene and younger sedimentary deposits based on geologic mapping by Jennings, 1971, and review of aerial photographs.
Area estimates include only those areas updip from the California Aqueduct to an elevation of approximately 1,000 feet.
Where applicable, area estimates include quaternary alluvial fan deposits updip of the Aqueduct.
Estimates do not include alluvial fan deposits down-dip from the California Aqueduct.
Estimates do not include ultramafic serpentinite deposits.

SOURCE: LEVINE-FRICKE

Reproduced with permission of the copyright owner. Further reproduction prohibited without permission.

Table 6-14

WATER QUALITY SAMPLING DATA

DATE	Asbestos Concentrations at Indicated Sampling Sites, MFL									CANAL FLOW AT MP 164 CU M/SEC	MP 164 FIBERS/FLOW
	MP 0	MP 3	MP 71	MP 143	MP 151	MP 162	MP 164	MP 171	MP 238		
Oct 81	110	190	190		740		1000		680	107	9
Nov 81		71	47	106			4700		1300	135	35
Dec 81	500	260	44		46		2400		1400	203	12
Jan 82		400	1200	2500			3100		810	137	23
Feb 82	830	340	1400		1200		6000		1800	142	42
Mar 82			510	870			1000		1100	108	9
Apr 82	310	650	820		940		1800		340	43	42
May 82		1300	140	550			1700		870	104	16
Jun 82	790	750	140		220		1700		1600	181	9
Jul 82		800	53	230			5300		3600	232	23
Aug 82	580	920	300		710		5700		2500	191	30
Aug 82					380	1345	2050	2300		137	15
Aug 82					240	1075	3200	4000		129	25
Aug 82					500	3200	3600	4300		123	29
Aug 82					215	1800	2500	3550		120	21
Sep 82			2900	880			2900		760	95	31
Sep 82					350	720	885	756		80	11
Oct 82	180	590	360		530		860		1200	88	10
Oct 82					145	690	330			69	5
Nov 82		470	450	320			710		520	57	12
Dec 82	250	180	340		420		340	520		141	2
Jan 83	240	110	37				370		420	25	15
Feb 83	96	150	210		610		840		740	11	76
Aug 83		850	386	1075			1450		3100	72	20
Aug 83					1967		4583	4867		63	73
Sep 83		450	405	1135			4050		955	15	270
Oct 83		1300	850	6150			18000		680	11	1636
Nov 83		825	515	5400			15000		1750	17	882
Dec 83		1160	600	3050			8100		6250	18	450
Jan 84		1210	910	1900			2850		1650	16	178
Feb 84		530	550	3250			9550		6200	73	131
Mar 84		495	485	1750			4250		4150	59	72
Apr 84		1900	1200	25500			18500		7450	107	173
May 84		950	115	3350			2900		3200	93	31
Jun 84		1120	720	6000			12500		8900	157	80
Jul 84		940	485	3950			3900		7050	157	25
Aug 84			1155		4700	5925	6200	5650	8900	142	44
Aug 84		500	164	2850			4800		3750	128	38
Aug 84			543		2950	2275	2725	2275		150	18
Sep 84		250	185	570			190		1000	58	3
Oct 84		300	250	885			780		1125	19	41

Source: Jones and McGuire, 1987.

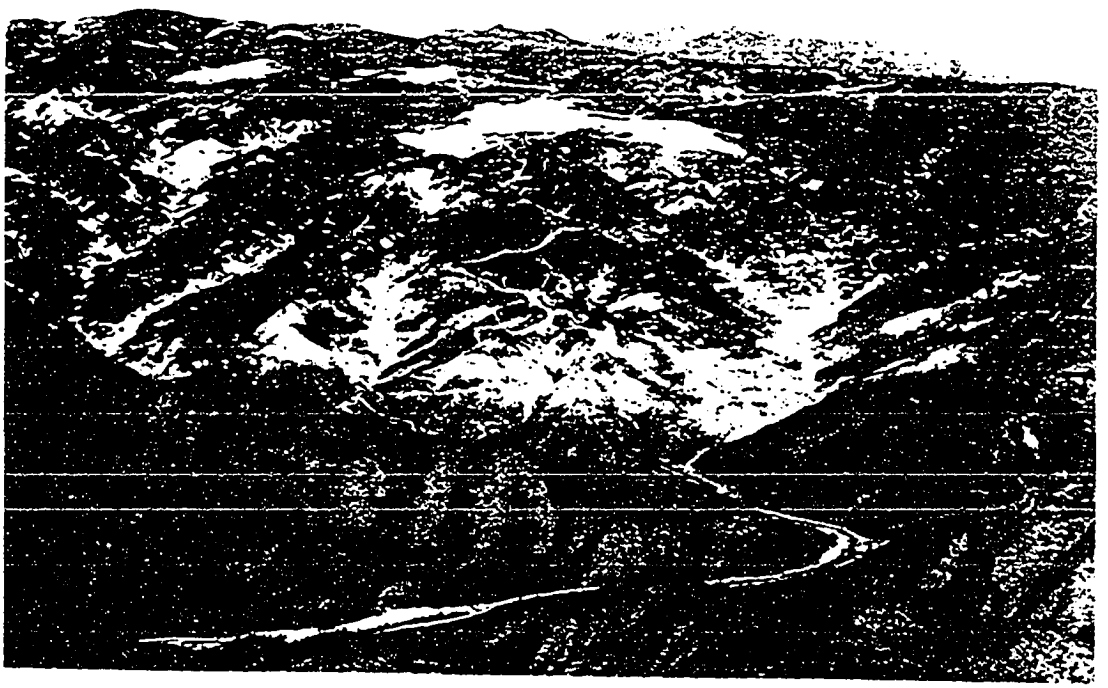
APPENDIX A

FIELD PHOTOGRAPHS

SOURCE: LEVINE-FRICKE

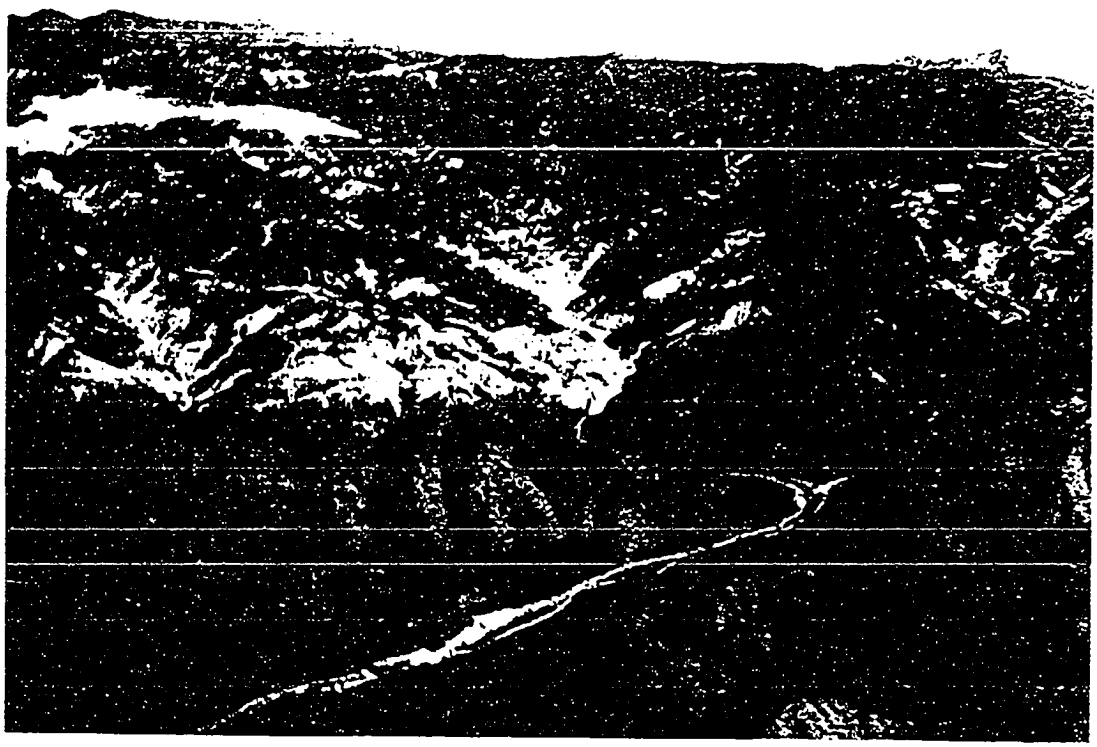
Reproduced with permission of the copyright owner. Further reproduction prohibited without permission.

Photo 1. Reconnaissance aerial photograph of serpentinite outcrop area in the White Creek drainage basin. This photo features the Atlas Site (top center), an extensive drainage network of barren erosional gullies (center), and the intermittent White Creek drainage channel which flows toward the reader. As illustrated, the serpentinite outcrop of the White Creek drainage has an extensive network of drainage gullies which have probably formed over long periods of geologic time (i.e., hundreds and/or thousands of years) in response to the headward erosion of the intermittent stream channels that drain the steeply sloped serpentinite outcrop surfaces of the New Idria Formation. Three of the gullies extend upslope from the White Creek channel (at the base of the serpentinite landslide and debris flow deposits) to the Atlas Site. This is a distance of more than 1.8 miles. Some of the sloping surfaces are inclined as much as 65 degrees. The location of an abandoned chromite mill site (as reported by Matthews, 1961) is evident in the White Creek streambed near the bottom center margin of the photo.



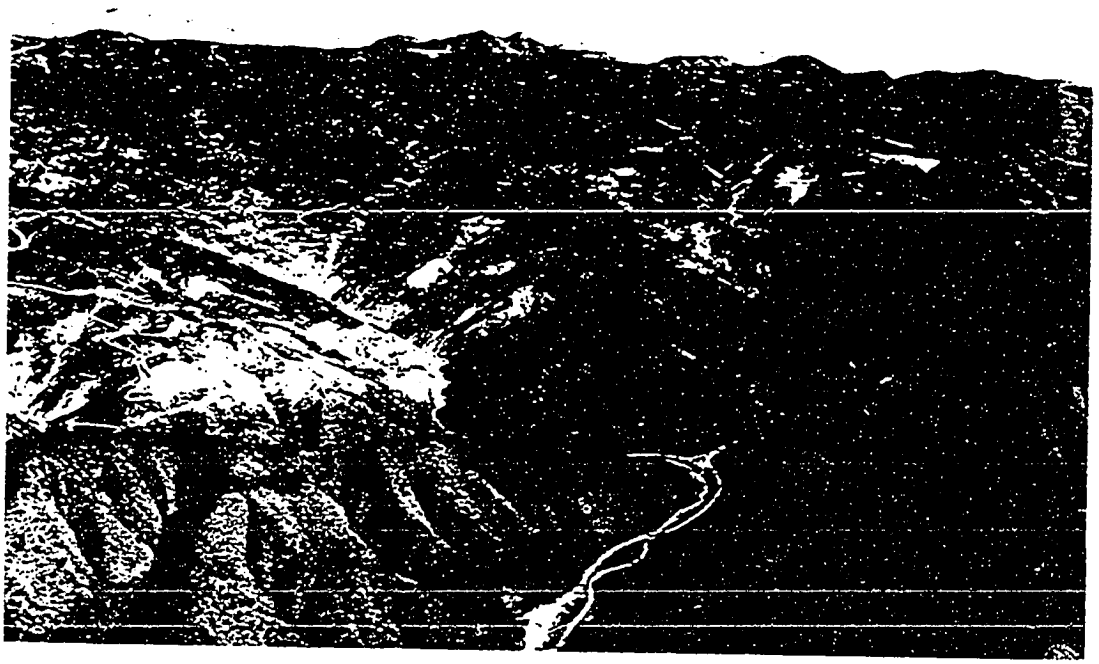
Reproduced with permission of the copyright owner. Further reproduction prohibited without permission.

Photo 2. Reconnaissance aerial photograph of serpentinite outcrop area in the White Creek drainage basin. This photo is similar to Photo 1 but includes more of the eastern portion of the White Creek drainage of the serpentinite outcrop area of Joaquin Ridge. This photo features the Atlas Site (top left), an extensive drainage network of barren erosional gullies (left center), and the intermittent White Creek drainage channel which flows toward the reader. As illustrated, the serpentinite outcrop of the White Creek drainage has an extensive network of drainage gullies which have probably formed over long periods of geologic time (i.e., hundreds and/or thousands of years) in response to the headward erosion of the intermittent stream channels that drain the steeply sloped serpentinite outcrop surfaces of the New Idria Formation. Some of the sloping surfaces are inclined as much as 65 degrees. The location of an abandoned chromite mill site (as reported by Matthews, 1961) is evident in the White Creek streambed near the bottom center margin of the photo.



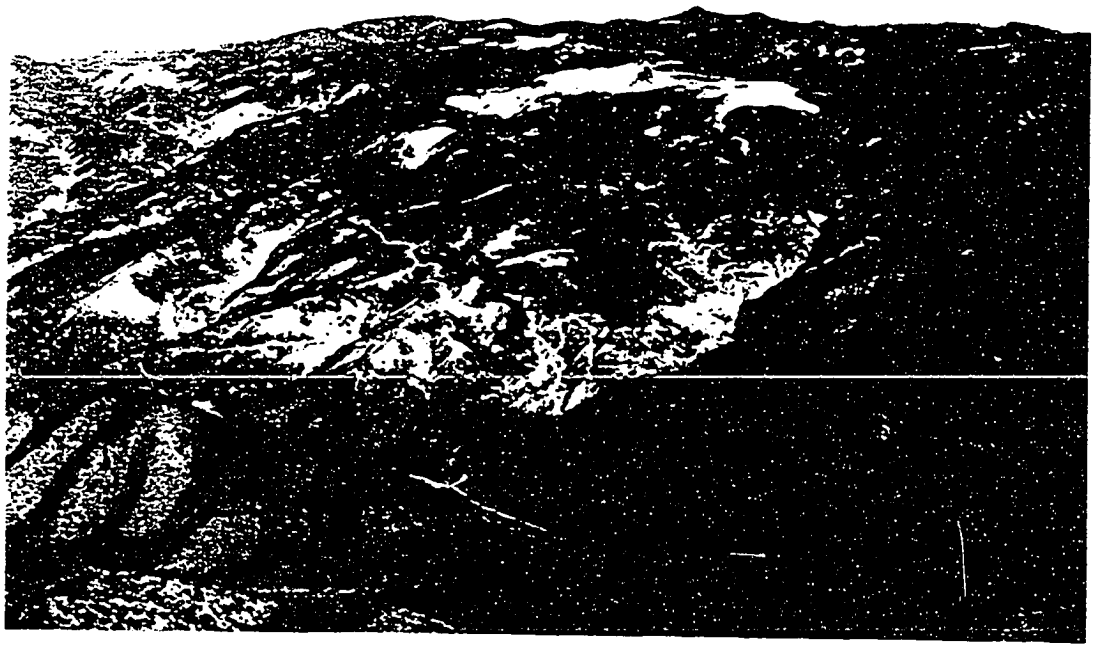
Reproduced with permission of the copyright owner. Further reproduction prohibited without permission.

Photo 3. Reconnaissance aerial photograph of eastern half of serpentinite outcrop area in the White Creek drainage basin. This photo is similar to Photos 1 and 2 but includes the far eastern margin of the serpentinite outcrop area which includes the James Corbett Byles Mine, the Butler Estate Chromite Mine, and the Jensen Mine. These mines are located in the upper right quarter of the photo. The James Corbett Byles Mine is located in the White Creek drainage. The Butler Mine is located on the drainage divide between the White Creek and Pine Canyon subbasins and the Jensen Mine is located in the Pine Canyon drainage. A barren erosional area in the White Creek drainage is featured in the left half of the picture.



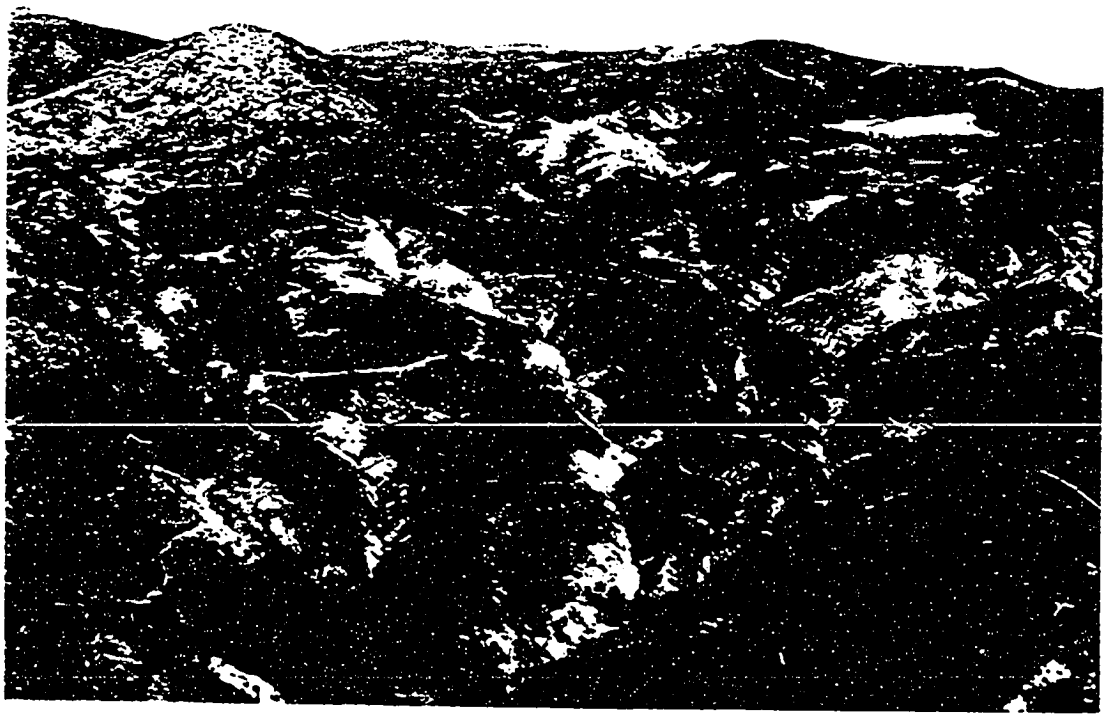
Reproduced with permission of the copyright owner. Further reproduction prohibited without permission.

Photo 4. Reconnaissance aerial photograph of White Creek drainage of serpentinite outcrop areas as described in Photos 1 and 2. This photo features the extent of some of the areas affected by gully erosion. The Atlas Site is at the upper center of the photo.



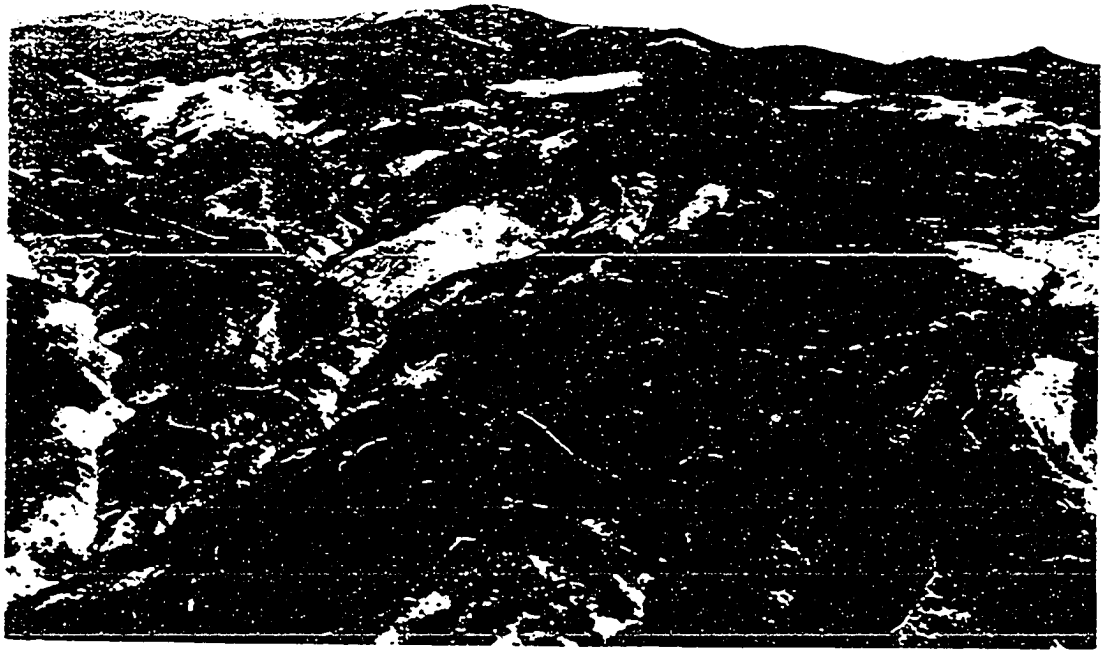
Reproduced with permission of the copyright owner. Further reproduction prohibited without permission.

Photo 5. Reconnaissance aerial photograph of the western half of the serpentinite outcrop in the White Creek drainage area. Condon Peak is in the upper left corner. This photo features some of the barren areas affected by gully erosion and several mines including the Big Ridge Mine (top center) Tromby Mine (upper right quadrant), and the Union Carbide Mine (top right quadrant near horizon).



Reproduced with permission of the copyright owner. Further reproduction prohibited without permission.

Photo 6. Reconnaissance aerial photograph of the western half of the serpentinite outcrop in the White Creek drainage area. This photo overlaps Photo 5 and includes part of the Atlas Mine (right center margin) and the Basic Resources Mine (upper right corner). Santa Rita Peak is in the upper right corner. This photo features some of the barren areas affected by gully erosion and several mines including the Big Ridge Mine (top left center), Tromby Mine (upper left quadrant below Big Ridge Mine), and the Union Carbide Mine (top center near horizon).



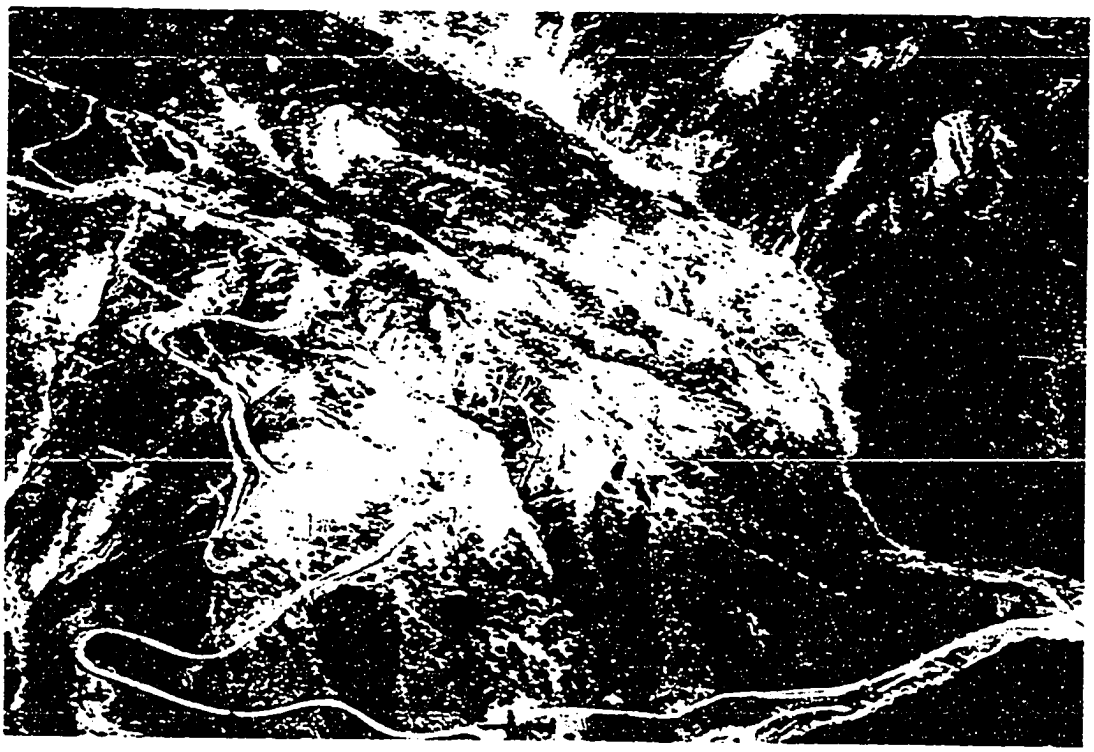
Reproduced with permission of the copyright owner. Further reproduction prohibited without permission.

Photo 7. Reconnaissance aerial photo of the Pine Canyon drainage area (upper right center) showing the Butler Mine (top center), Jensen Mine (top right), and the Coalinga Asbestos Mill area including the Railroad Mine (center). The White Creek outcrop area (and the Atlas Mine and Mill) is visible near the upper left margin of the photo.



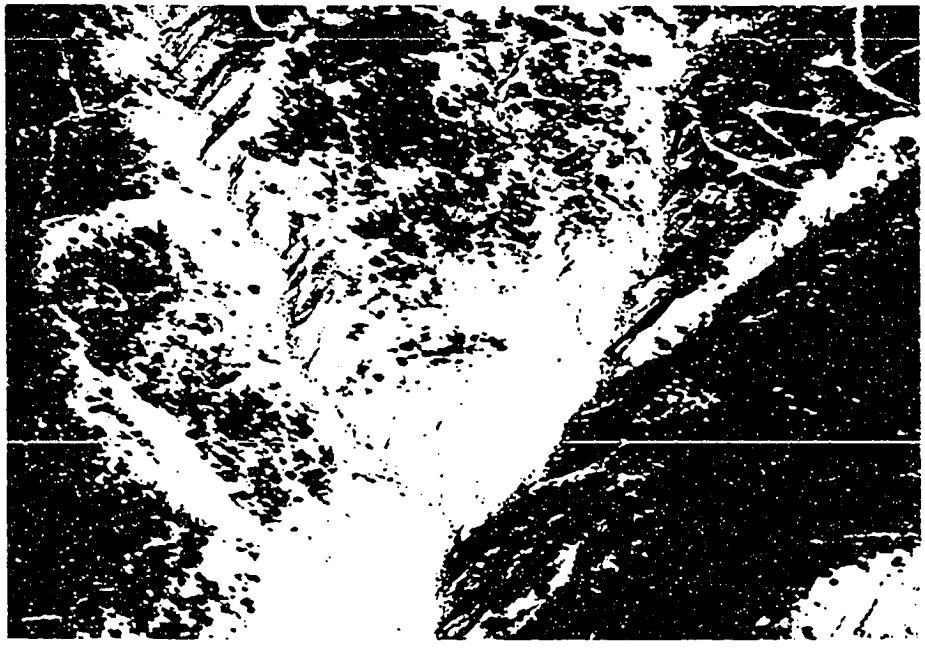
Reproduced with permission of the copyright owner. Further reproduction prohibited without permission.

Photo 8. Reconnaissance aerial photograph showing steep side slopes of serpentinite gullies in the White Creek watershed. Side slopes of gullies show evidence of scarring from slumping and mass wasting associated with undercutting of the serpentinite streambanks. Fresh serpentinite surfaces are white to yellowish gray and weathered surfaces are yellowish reddish brown.



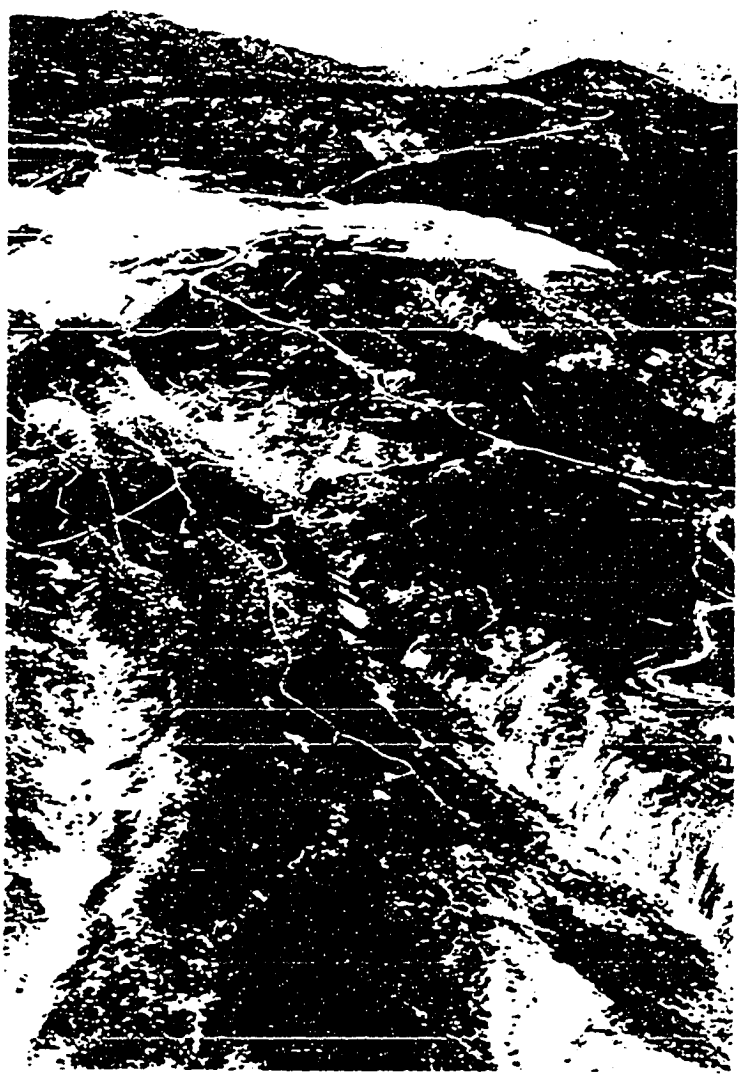
Reproduced with permission of the copyright owner. Further reproduction prohibited without permission.

Photo 9. Reconnaissance aerial photograph showing gullies that head into the Atlas Site in the White Creek watershed. This photo features barren gullies with steep sidewalls that are eroding as a result of slumping and mass wasting. Vegetation in some areas is very sparse.



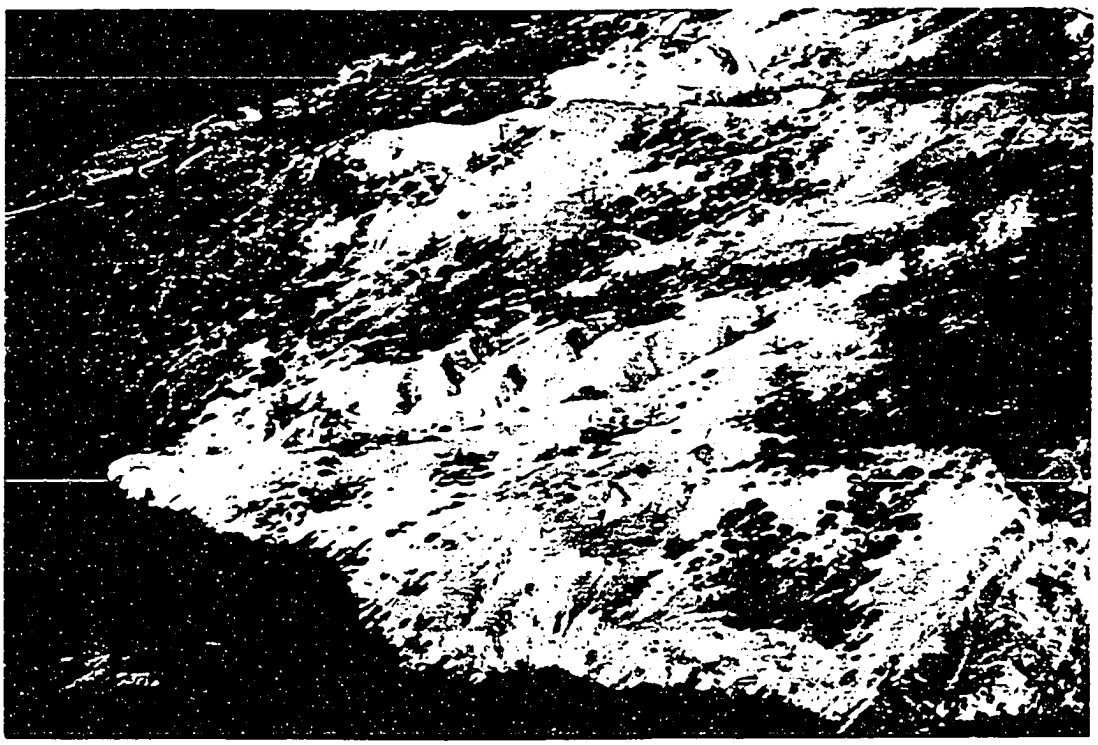
Reproduced with permission of the copyright owner. Further reproduction prohibited without permission.

Photo 10. Reconnaissance aerial photograph showing gullies that head into the Atlas Site in the White Creek watershed. This photo also features some of the unimproved exploration access roads that crisscross the serpentinite outcrop area. The Atlas Site and the crest of Joaquin Ridge are near the top of the photo. Asbestos-containing sedimentary formations are shown in the background at the top of the photo. These formations outcrop along the western margin of the central San Joaquin Valley. The sedimentary outcrops visible in this picture are about six miles distance from the crest of Joaquin ridge.



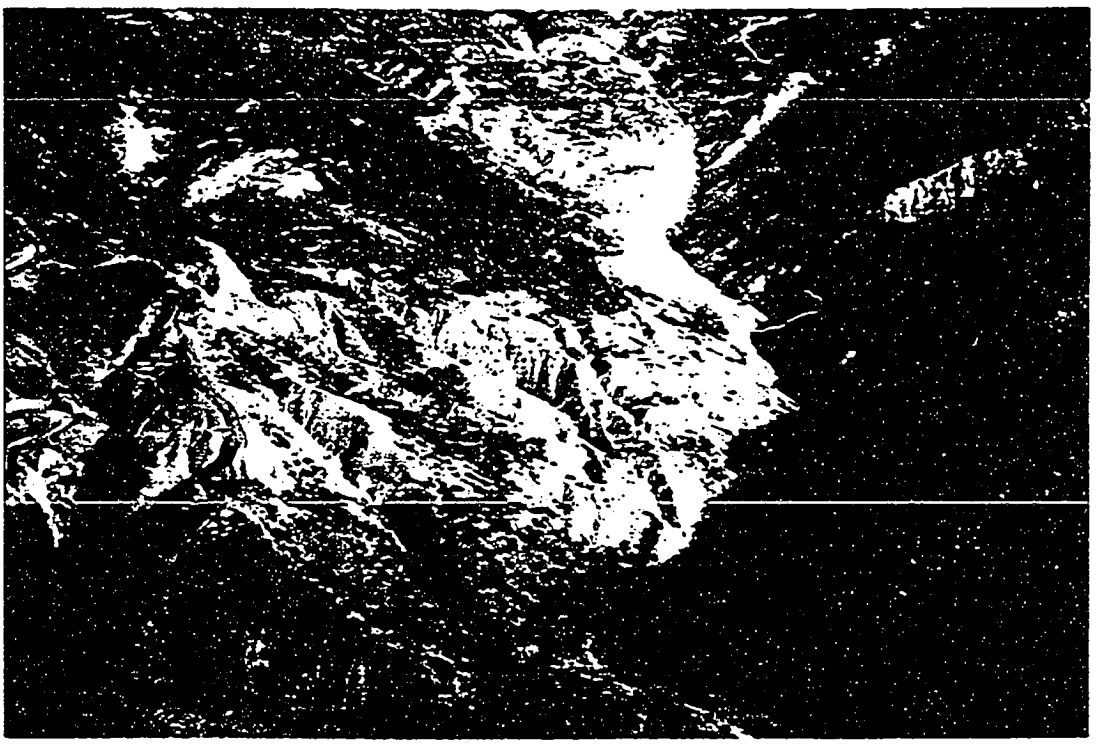
Reproduced with permission of the copyright owner. Further reproduction prohibited without permission.

Photo 11. Erosional serpentinite outcrop area in the White Creek drainage. This photo features slumping and mass wasting thhat has resulted from the headward erosion of gullies. Erosional areas are relatively barren of vegetation.



Reproduced with permission of the copyright owner. Further reproduction prohibited without permission.

Photo 12. Erosional serpentinite outcrop area in the White Creek drainage as described in Photo 11. Erosional areas like this have been mapped by SPLC as AGC - Atravesada Gully Complex.



Reproduced with permission of the copyright owner. Further reproduction prohibited without permission.

Photo 13. Close up of areas affected by gully erosion in the White Creek drainage.



Reproduced with permission of the copyright owner. Further reproduction prohibited without permission.

Photo 14. Close up of areas affected by gully erosion in the White Creek drainage. Some of the gully sidewalls are inclined as much as 65 degrees. These steeply inclined gully sidewalls are highly susceptible to slumping and mass wasting a result of the weak and fractured structure of the asbestos-containing serpentinite bedrock.



Reproduced with permission of the copyright owner. Further reproduction prohibited without permission.

Photo 15. Close up of one of the serpentinite outcrop areas affected by gully erosion in the White Creek drainage. This photo features the steep gully sidewalls which are highly susceptible to slumping and mass wasting.



Reproduced with permission of the copyright owner. Further reproduction prohibited without permission.

Photo 16. Close up of one of the serpentinite outcrop areas affected by gully erosion in the White Creek drainage. This photo features the steep gully sidewalls which are highly susceptible to slumping and mass wasting.



Reproduced with permission of the copyright owner. Further reproduction prohibited without permission.

Photo 17. This photo features an erosional serpentinite outcrop area associated with gullies and roads in the White Creek drainage. Some remnants of roads are visible in the barren area in the top half of the photo.



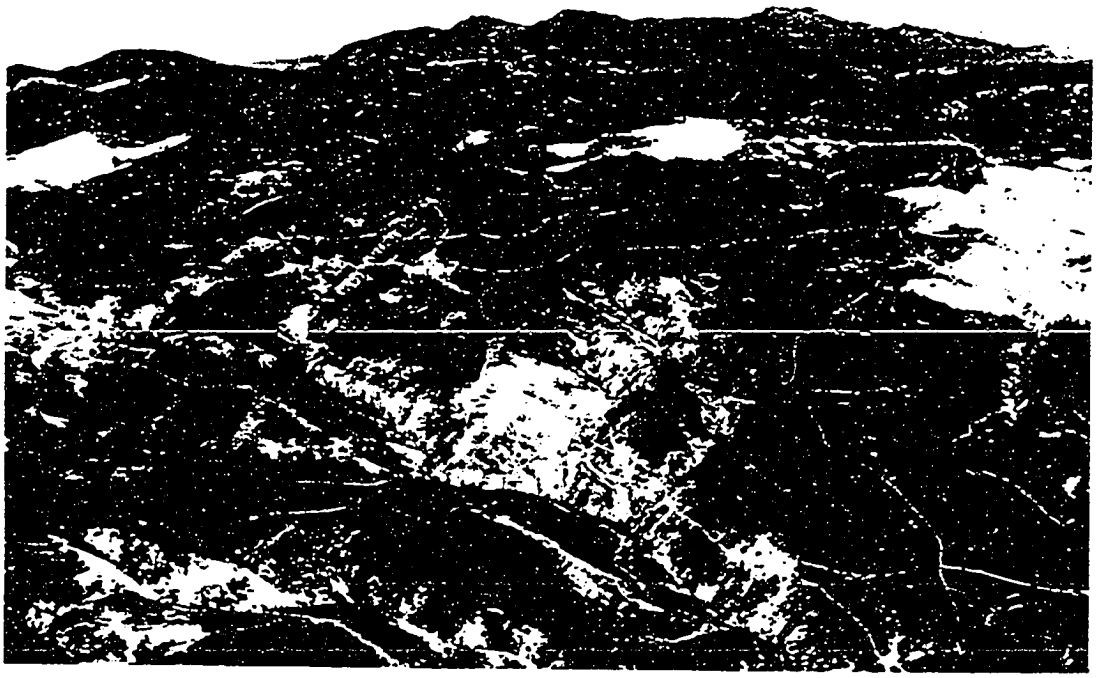
Reproduced with permission of the copyright owner. Further reproduction prohibited without permission.

Photo 18. This photo features an erosional serpentinite outcrop area in the White Creek drainage. The eroded areas are affected by slumping and mass wasting and are generally barren of vegetation. Some remnants of roads are visible in this picture.



Reproduced with permission of the copyright owner. Further reproduction prohibited without permission.

Photo 19. Erosional serpentinite outcrop areas associated with gullies and roads in the White Creek drainage. The Union Carbide Mine is visible in the upper left corner, the Basic Resources Mine is near the upper center, and the Atlas Mine is at the right margin of the photo. The asbestos-containing Big Blue Member of the Temblor and other asbestos-containing sedimentary formations are visible near the horizon at the top of the photo.



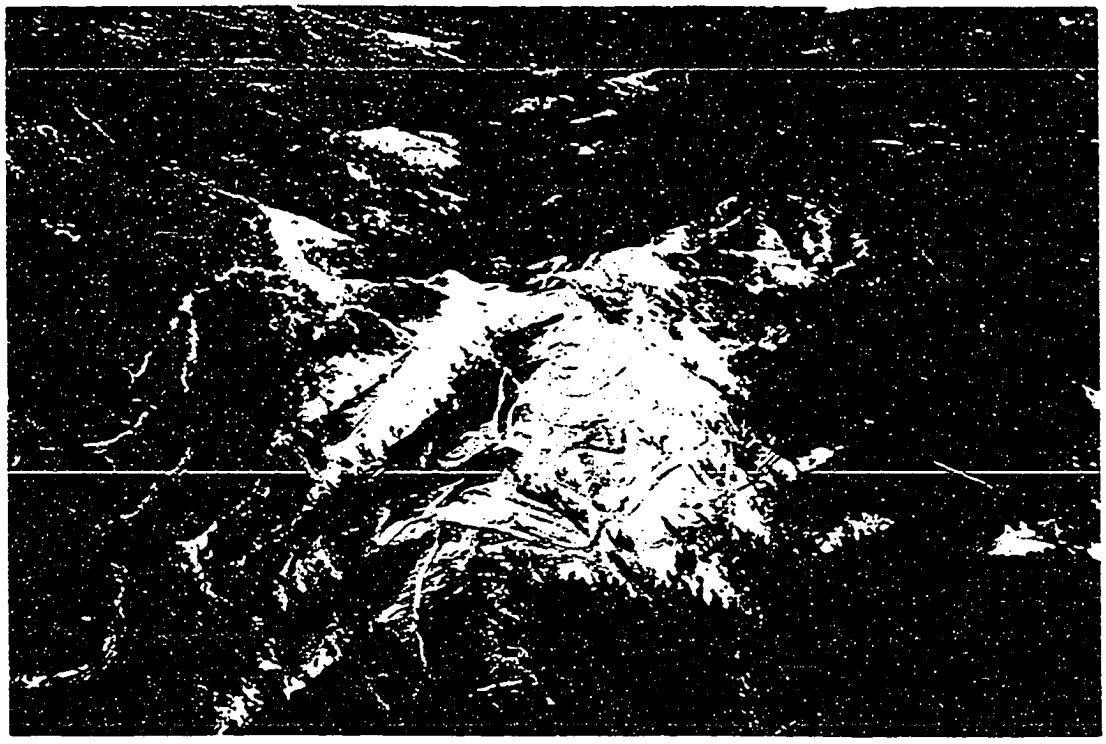
Reproduced with permission of the copyright owner. Further reproduction prohibited without permission.

Photo 20. Erosional serpentinite outcrop area affected by gullying, slumping, and mass wasting in the White Creek drainage. The barren area appears to have some terracing that may have been the result of surface mining activity.



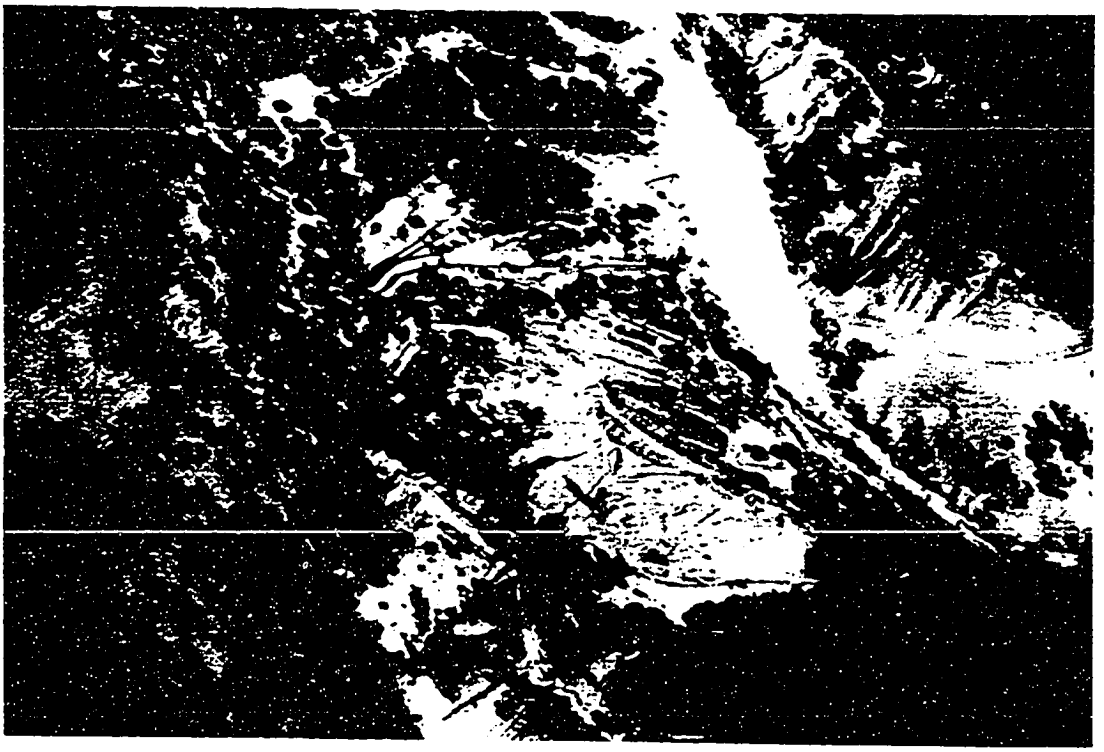
Reproduced with permission of the copyright owner. Further reproduction prohibited without permission.

Photo 21. Big Ridge Mine located on the northeastern flank of Condon Peak in the White Creek drainage area. This area was mined for disseminated chromite which can be found in economic quantities in some of the serpentinite deposits.



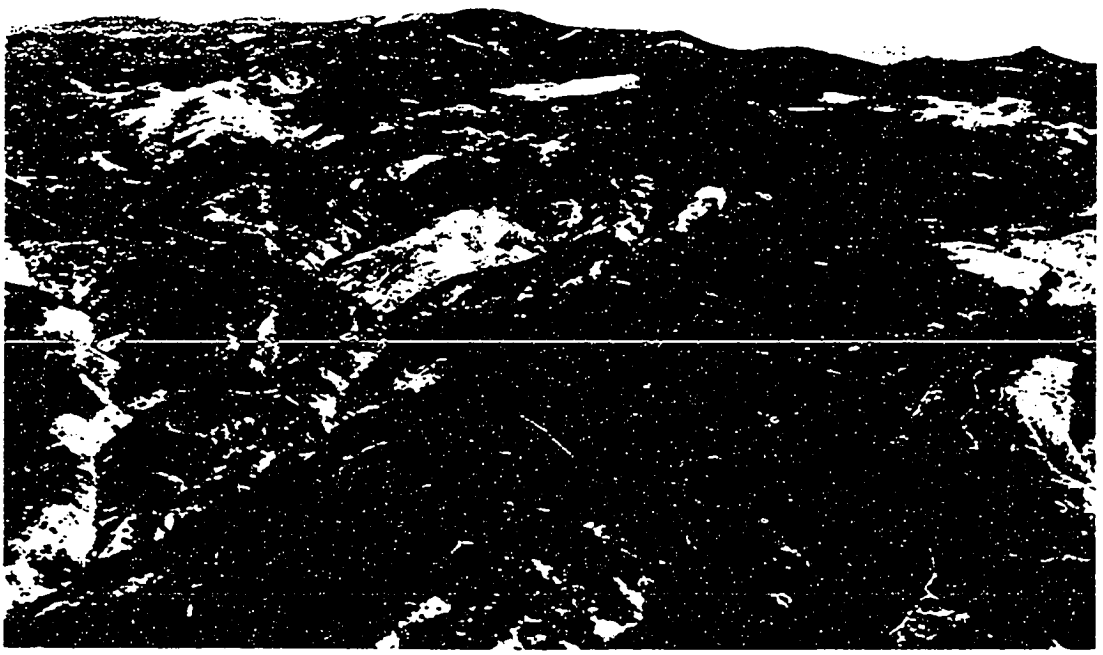
Reproduced with permission of the copyright owner. Further reproduction prohibited without permission.

Photo 22. This may be the location of the White Creek Magnesite Mine in the White Creek drainage area.



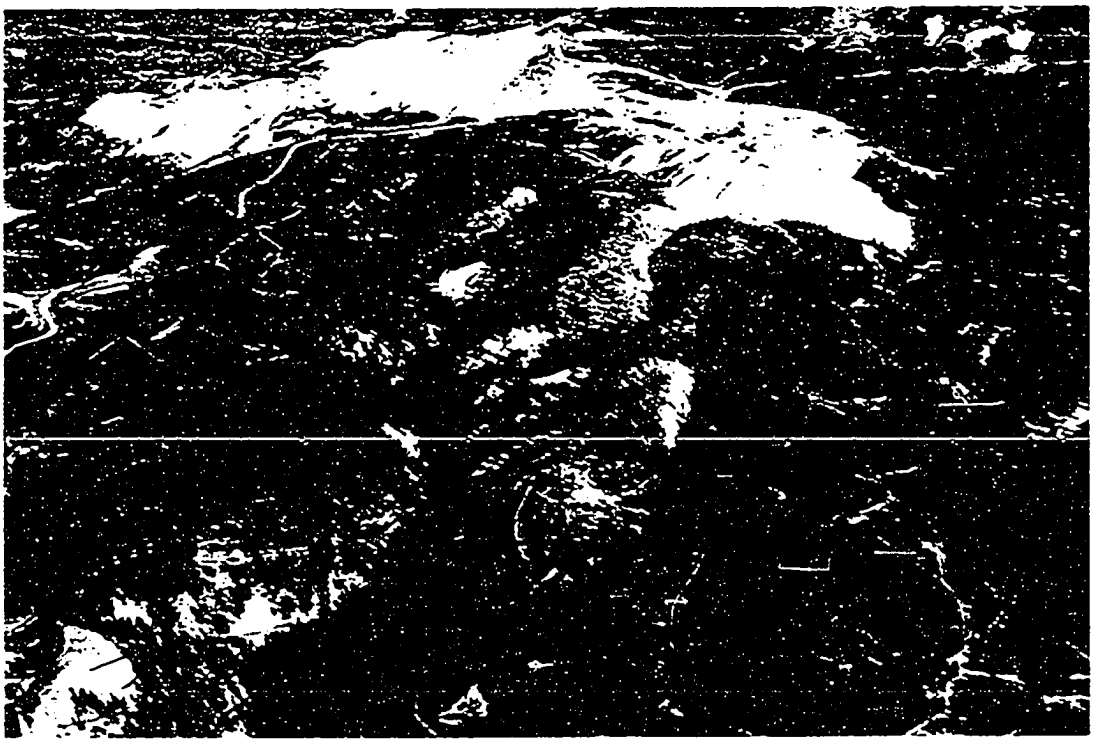
Reproduced with permission of the copyright owner. Further reproduction prohibited without permission.

Photo 23. The barren area in the left center of this photo is probably one of the Tromby Mines of the White Creek drainage. This photo also shows the Big Ridge Mine (upper left), the Union Carbide Mine (top center), the Basic Resources Mine (upper right corner), and part of the Atlas Site (right edge of photo).



Reproduced with permission of the copyright owner. Further reproduction prohibited without permission.

Photo 24A. This photo features the Atlas Site and several gullies that are encroaching on the tailings pile (upper right corner) and the mine areas (upper left). The front of the tailings pile has several gullies that are in the early formation stage. The far right side of the tailings pile appears to be a debris flow deposit that originated from an unstable pile.



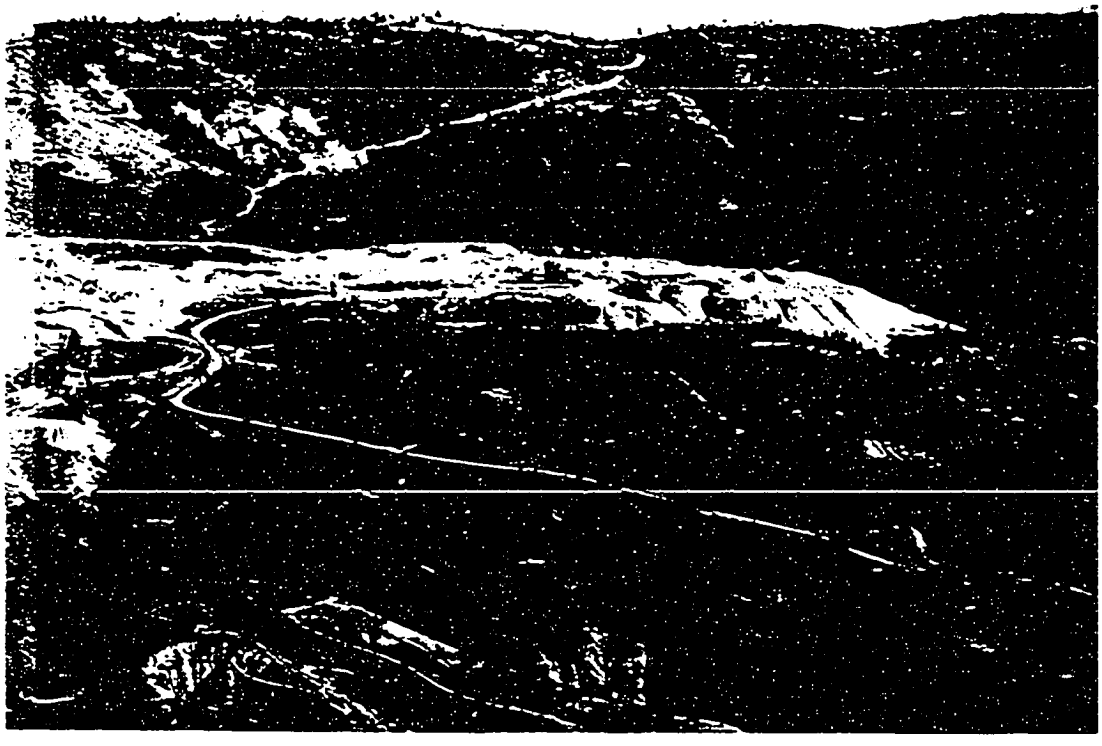
Reproduced with permission of the copyright owner. Further reproduction prohibited without permission.

Photo 24B. This photo features a side view of a gully that has formed near the front of the Atlas Mine. The side walls of the gully are subject to slumping and mass wasting.



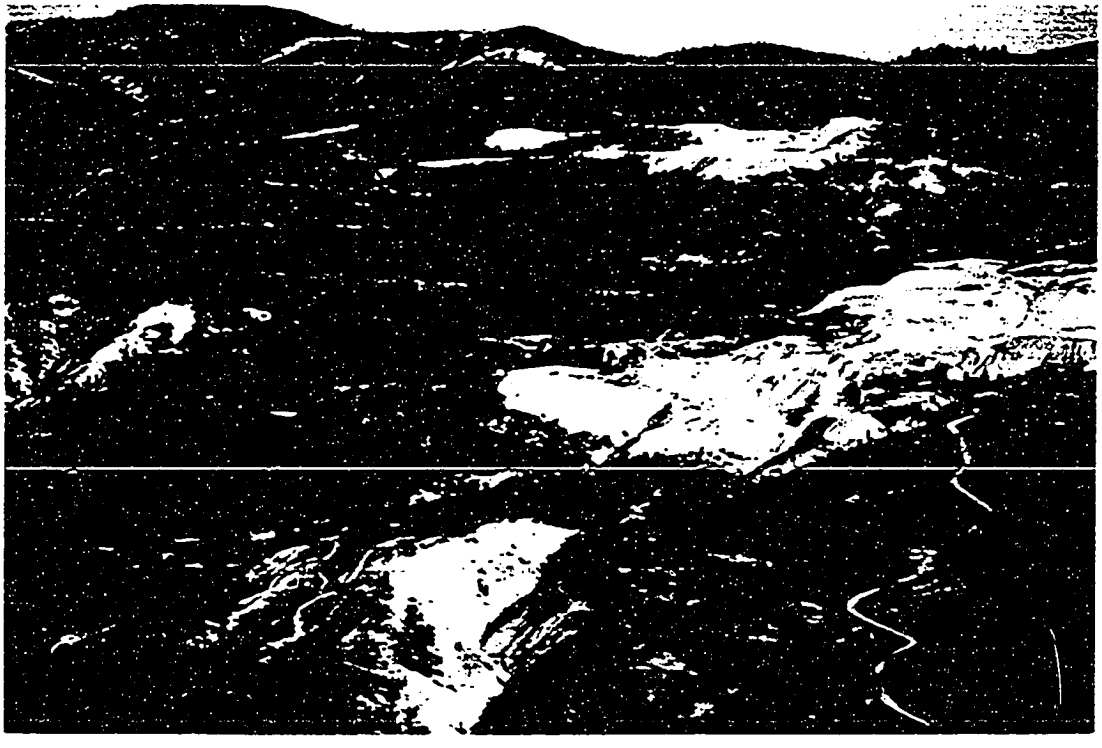
Reproduced with permission of the copyright owner. Further reproduction prohibited without permission.

Photo 25. This photo features the Atlas Mine and Mill including the tailings pile complex. The crest of Joaquin Ridge is visible at the upper margin of the photo.



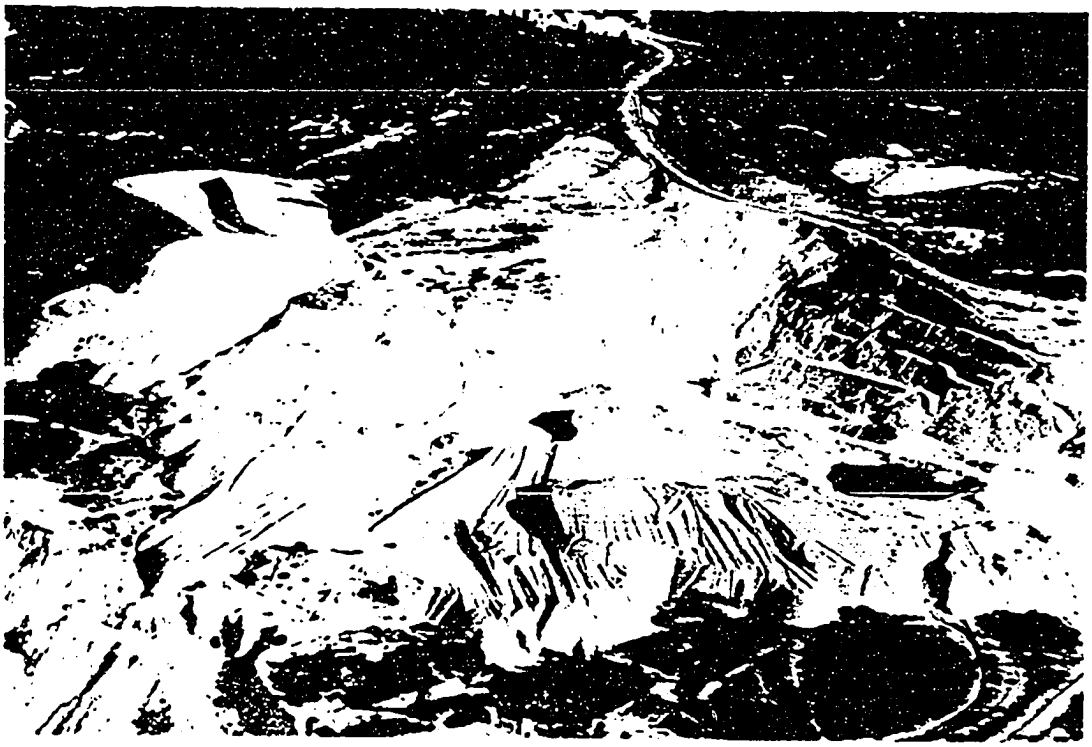
Reproduced with permission of the copyright owner. Further reproduction prohibited without permission.

Photo 26. This photo features an erosional gully that is encroaching on the Atlas Mine in the center right half of the photo. The Basic Resources Mine is in the upper right corner.



Reproduced with permission of the copyright owner. Further reproduction prohibited without permission.

Photo 27. Close up photo of the Atlas mining operation in the White Creek drainage. The mined areas are susceptible to erosion from slumping, mass wasting, and gully processes.



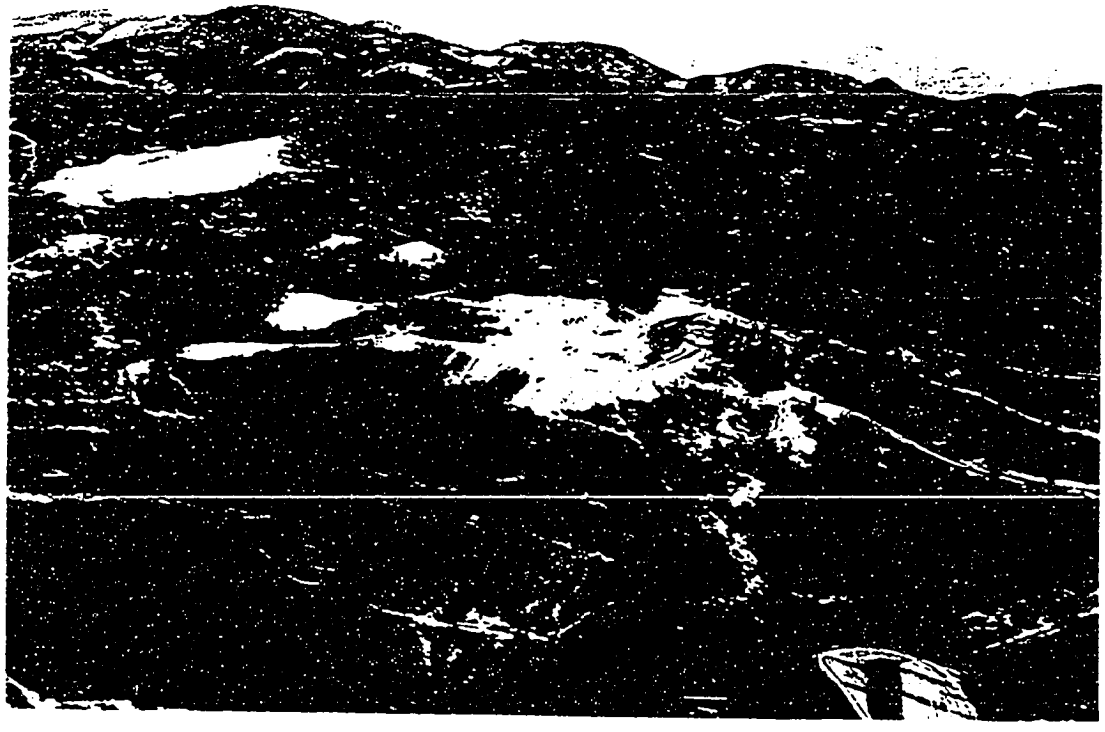
Reproduced with permission of the copyright owner. Further reproduction prohibited without permission.

Photo 28. Close up photo of the Atlas mining operation in the White Creek drainage. As illustrated in Photo 27, the mined areas are susceptible to erosion from slumping, mass wasting, and gully processes.



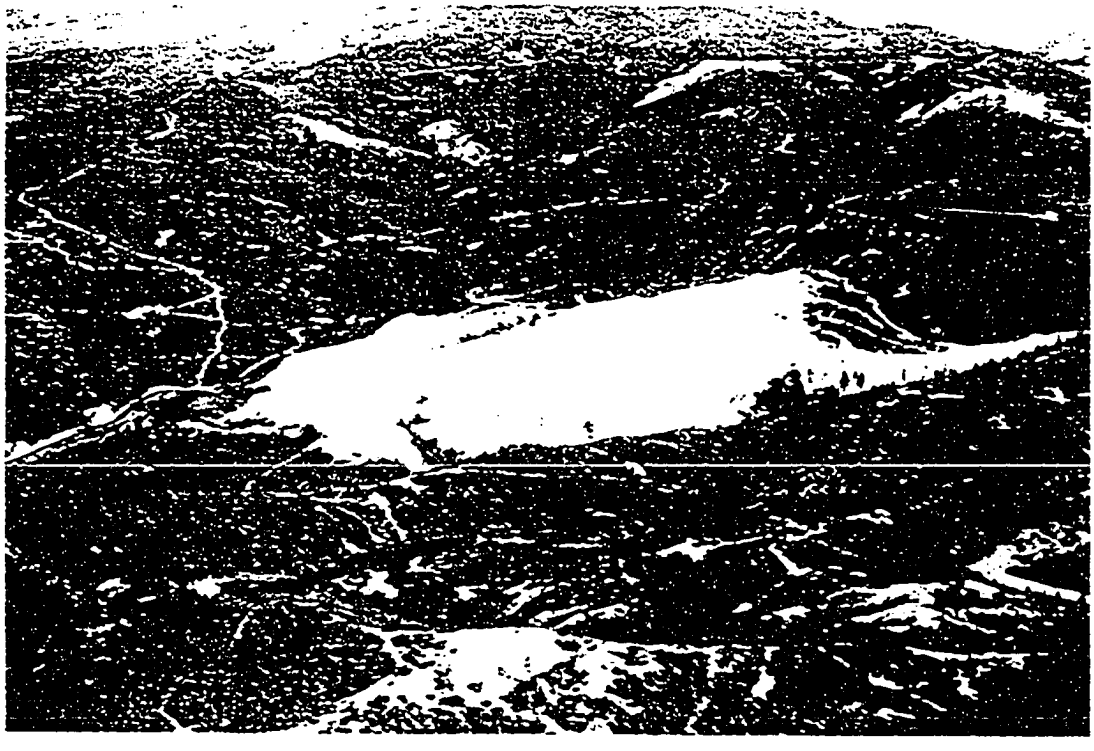
Reproduced with permission of the copyright owner. Further reproduction prohibited without permission.

Photo 29. This photo features the Basic Resources Mine (center of photo). The Union Carbide Mine appears in the upper left corner.



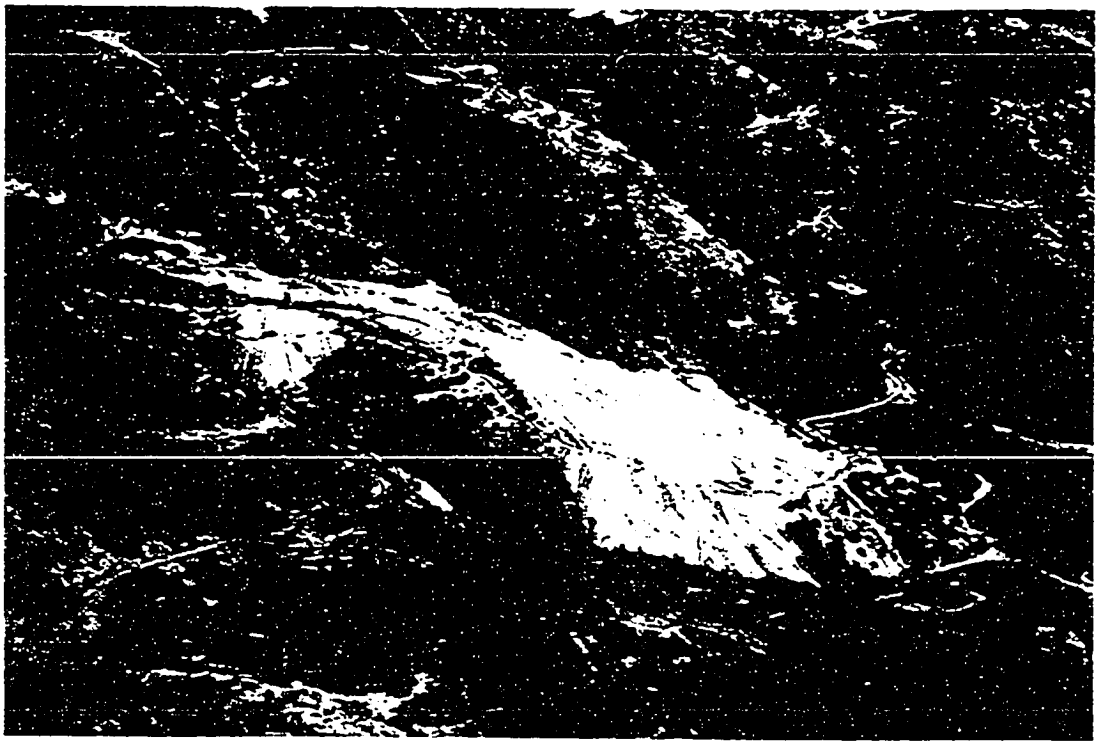
Reproduced with permission of the copyright owner. Further reproduction prohibited without permission.

Photo 30. Close up of the Union Carbide Mine. This asbestos mine is located in the San Benito River watershed which drains to the west to the Salinas Valley and Monterey Bay.



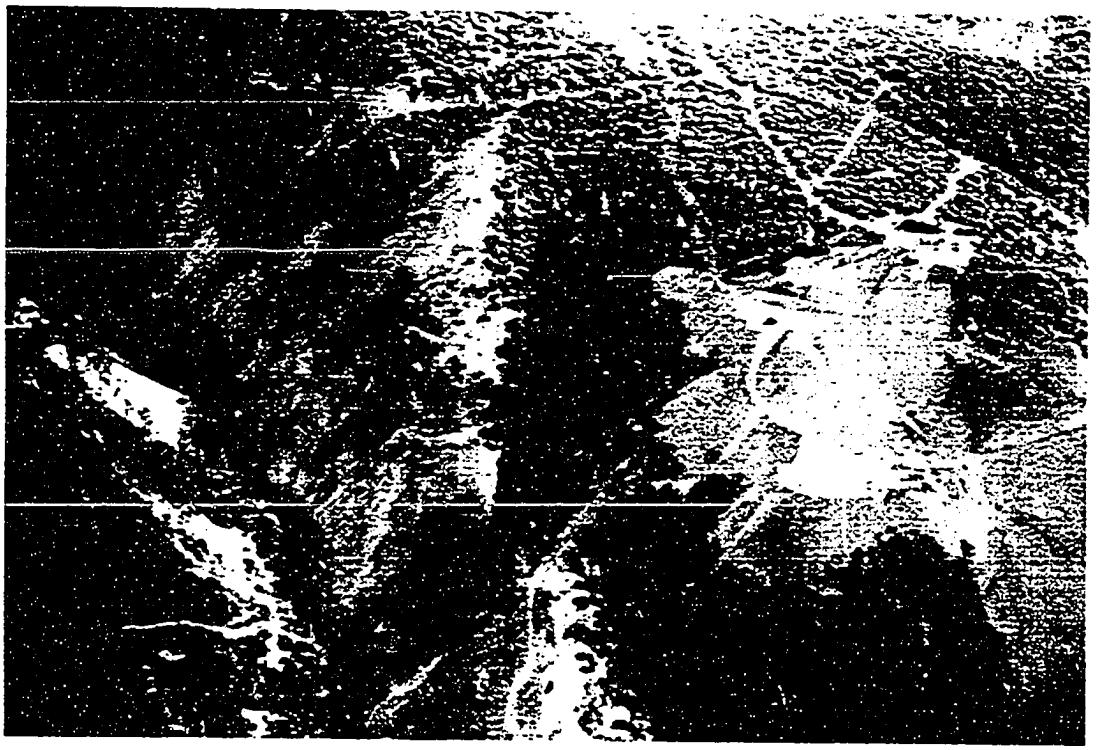
Reproduced with permission of the copyright owner. Further reproduction prohibited without permission.

Photo 31. An unmapped mine located to the east of the Atlas Site near the general vicinity of the James Corbett Byles Mine in the White Creek drainage area. This photo indicates the occurrence of a rich serpentinite deposit in a steeply sloping area which was easily mined with a bulldozer.



Reproduced with permission of the copyright owner. Further reproduction prohibited without permission.

Photo 32. This photo features the James Corbett Byles Mine in the eastern half of the White Creek serpentinite outcrop area. The mined area is located on the side of a steep slope that is adjacent to an erosional gully complex.



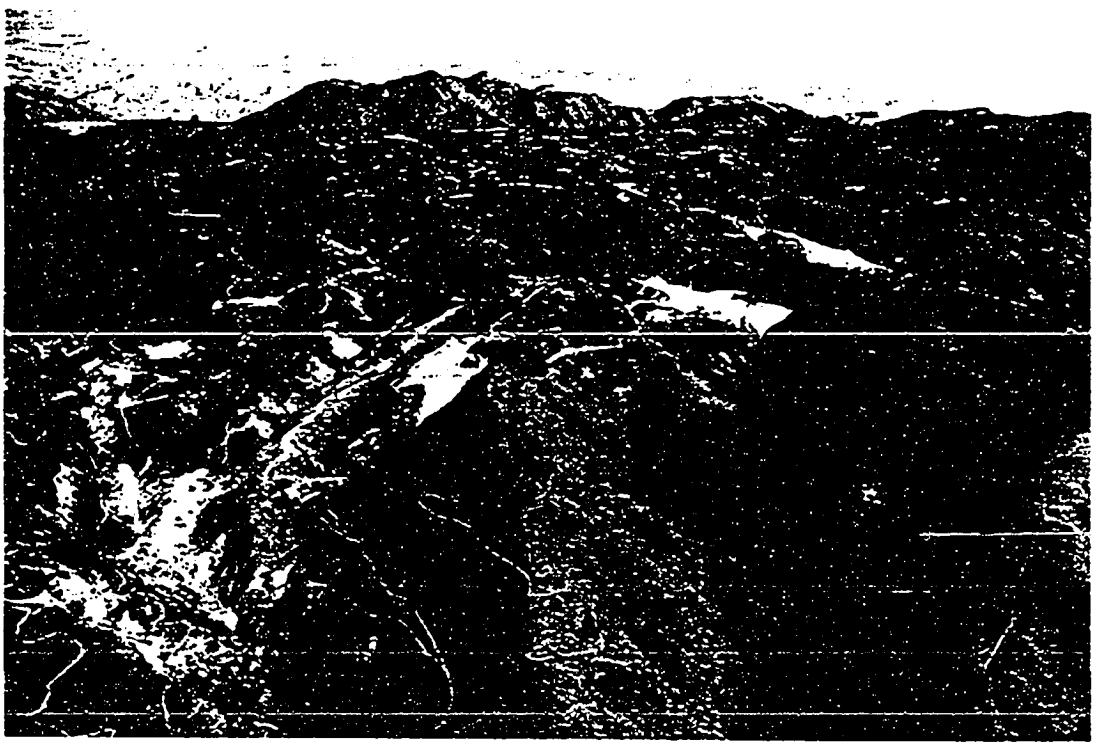
Reproduced with permission of the copyright owner. Further reproduction prohibited without permission.

Photo 33. This photo features the Christy Mine which is located on the northeast flank of Joaquin Ridge in the Cantua Creek drainage area.



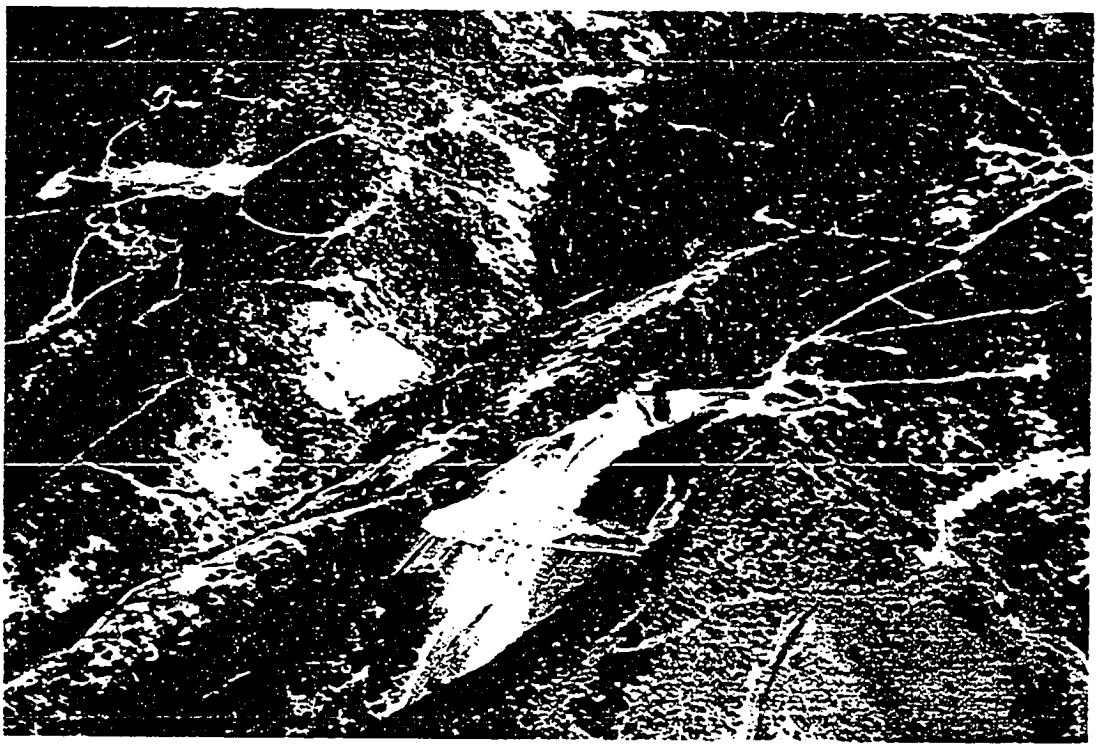
Reproduced with permission of the copyright owner. Further reproduction prohibited without permission.

Photo 34. Reconnaissance aerial photograph showing overburden that has been pushed downslope from the James Corbett Byles Mine (left center of photo) and the Butler Estate Chromite Mine (right center of photo). The Butler Mine is located on the drainage divide between the White Creek and Pine Canyon drainage areas. Most of the Butler mined area is in the Pine Canyon drainage area and some of the mine dumps material is located in the White Creek drainage area. The Jensen Mine (located in the Pine Canyon watershed) is shown in the distance (far center of picture).



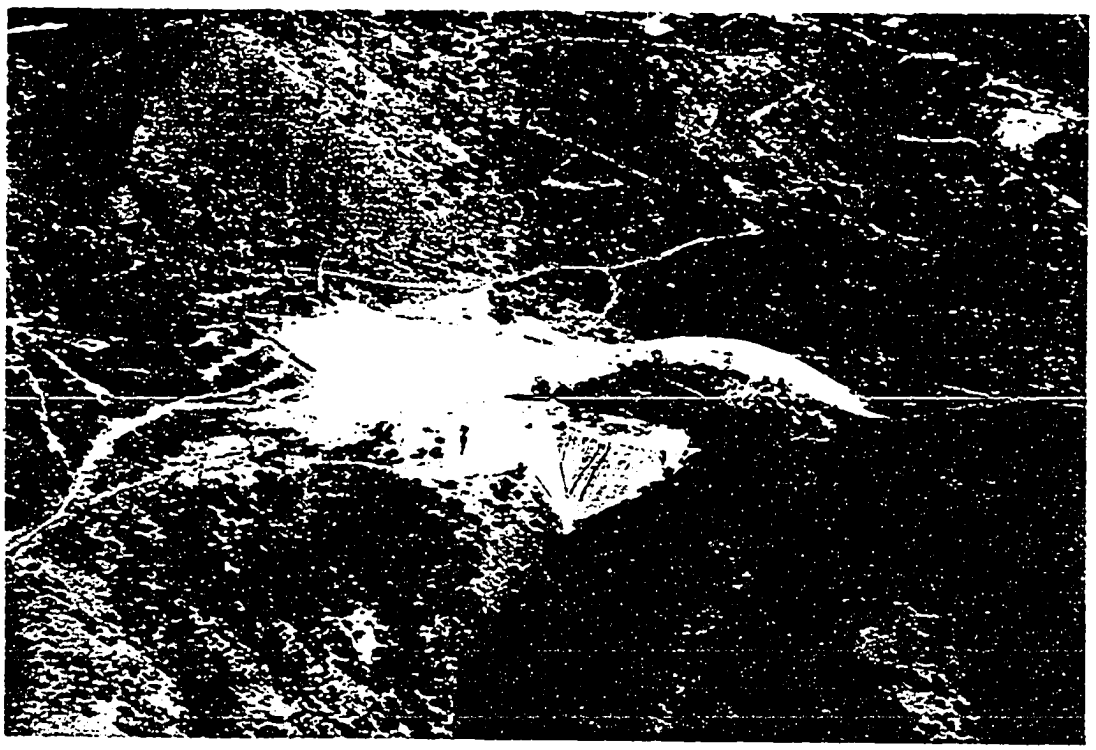
Reproduced with permission of the copyright owner. Further reproduction prohibited without permission.

Photo 35. Reconnaissance aerial photograph showing abandoned dumps and mined surfaces of the James Corbett Byles Mine in the White Creek drainage area. This mine is located in a steeply sloped area that is adjacent to a naturally occurring serpentinite gully.



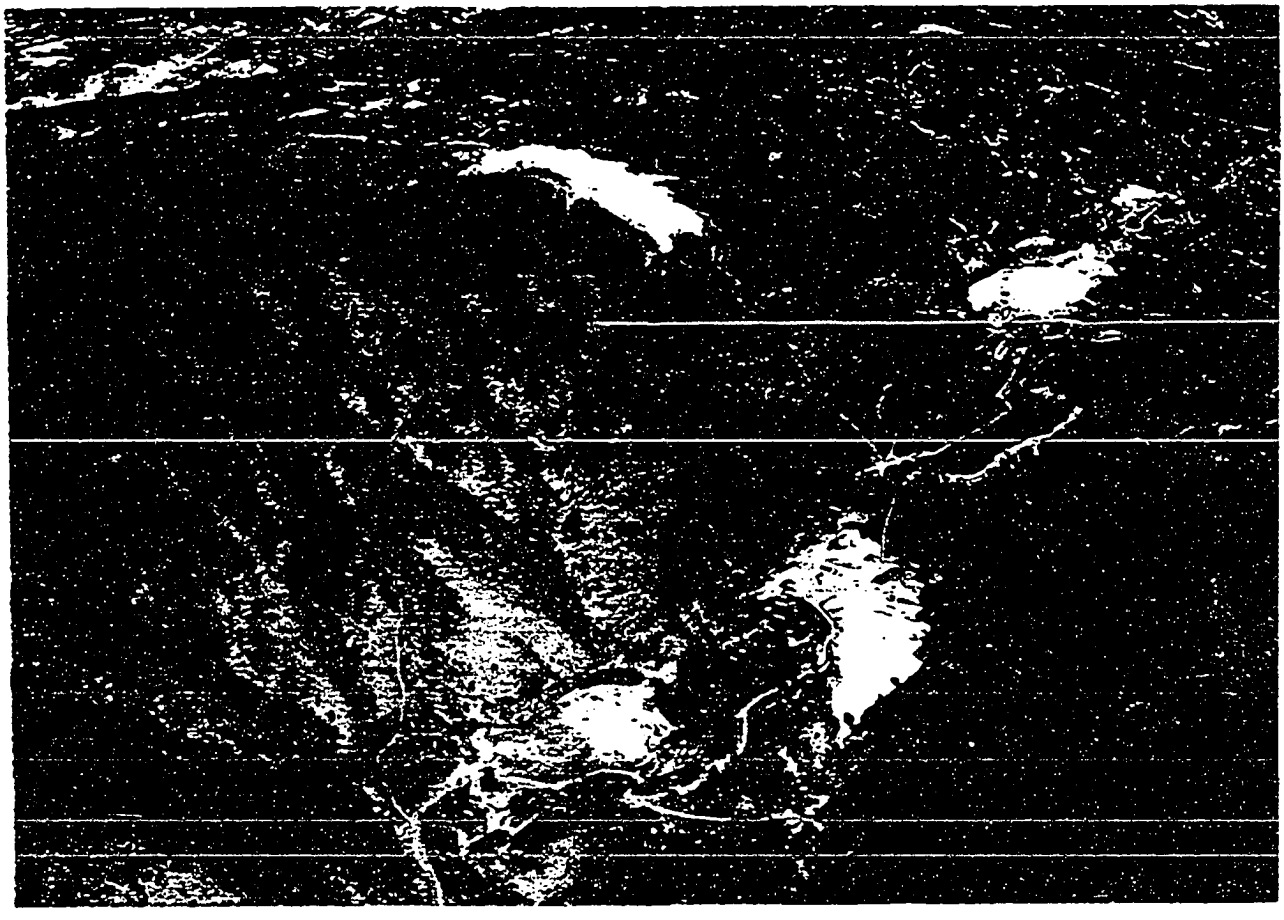
Reproduced with permission of the copyright owner. Further reproduction prohibited without permission.

Photo 36. Reconnaissance aerial photograph showing abandoned dumps, pits, and tailings associated with the Butler Estate Chromite Mine. The Butler Mine is located on the drainage divide between the White Creek and Pine Canyon watersheds. The White Creek drainage is towards the reader and the Pine Canyon drainage is towards the upper right of the photo (away from the reader).



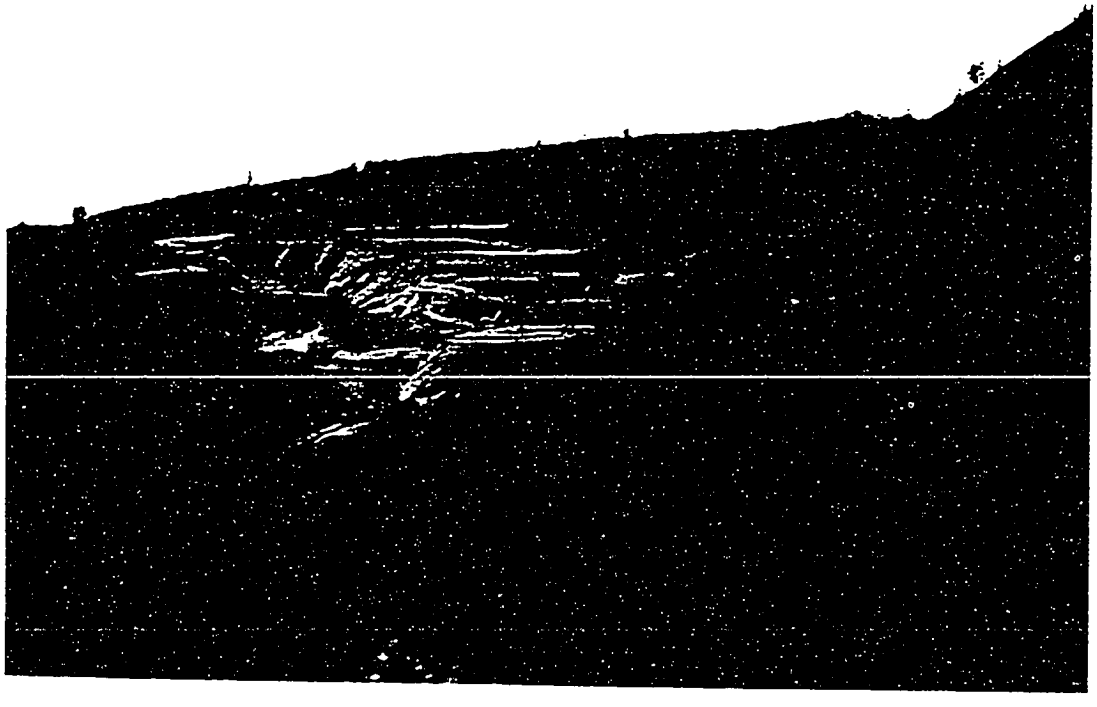
Reproduced with permission of the copyright owner. Further reproduction prohibited without permission.

Photo 37. Reconnaissance aerial photograph of Upper Pine Canyon showing some of the landslide and serpentinite debris flow deposits in relationship to some of the mining and milling operations including the Butler Estate Chromite Mine (upper left), the Jensen Mine (upper right), and the Coalinga Asbestos Mill Site (lower left).



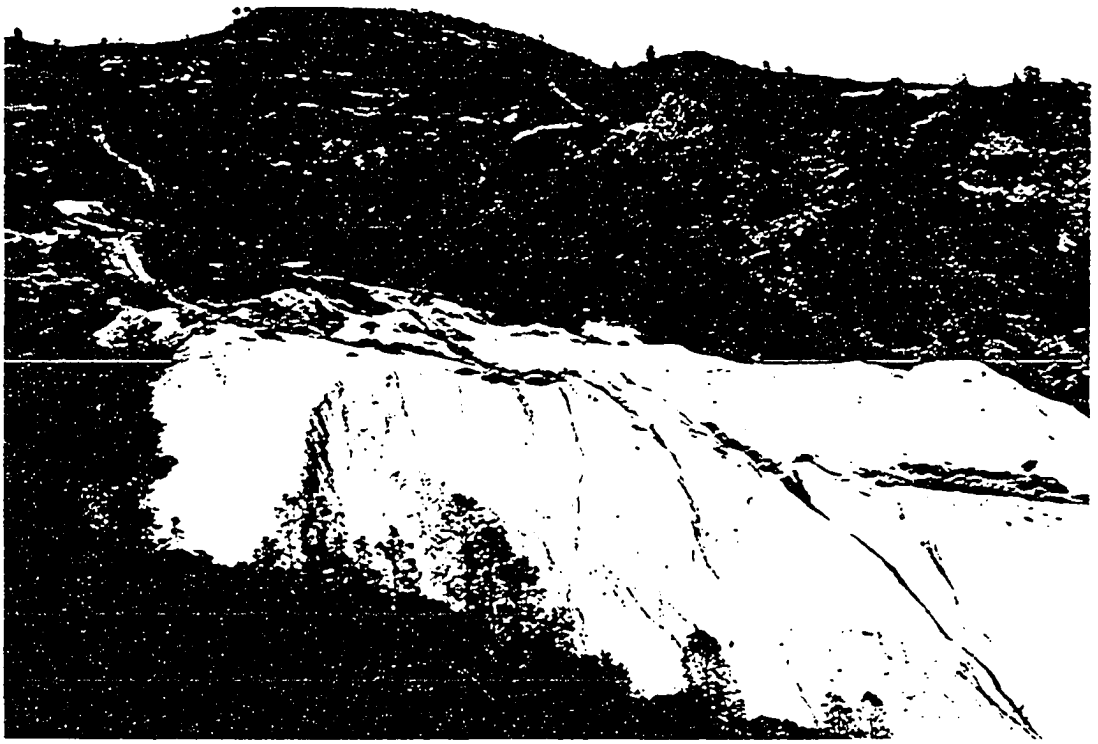
Reproduced with permission of the copyright owner. Further reproduction prohibited without permission.

Photo 38. Reconnaissance photo of Butler Estate Chromite Mine as viewed from ridge on eastern side of Pine Canyon (a distance of approximately 0.8 miles). Note the mass wasting and gully erosion that is occurring on the front of the Butler pile. This material is being washed into the western fork of the Upper Pine Canyon streambed.



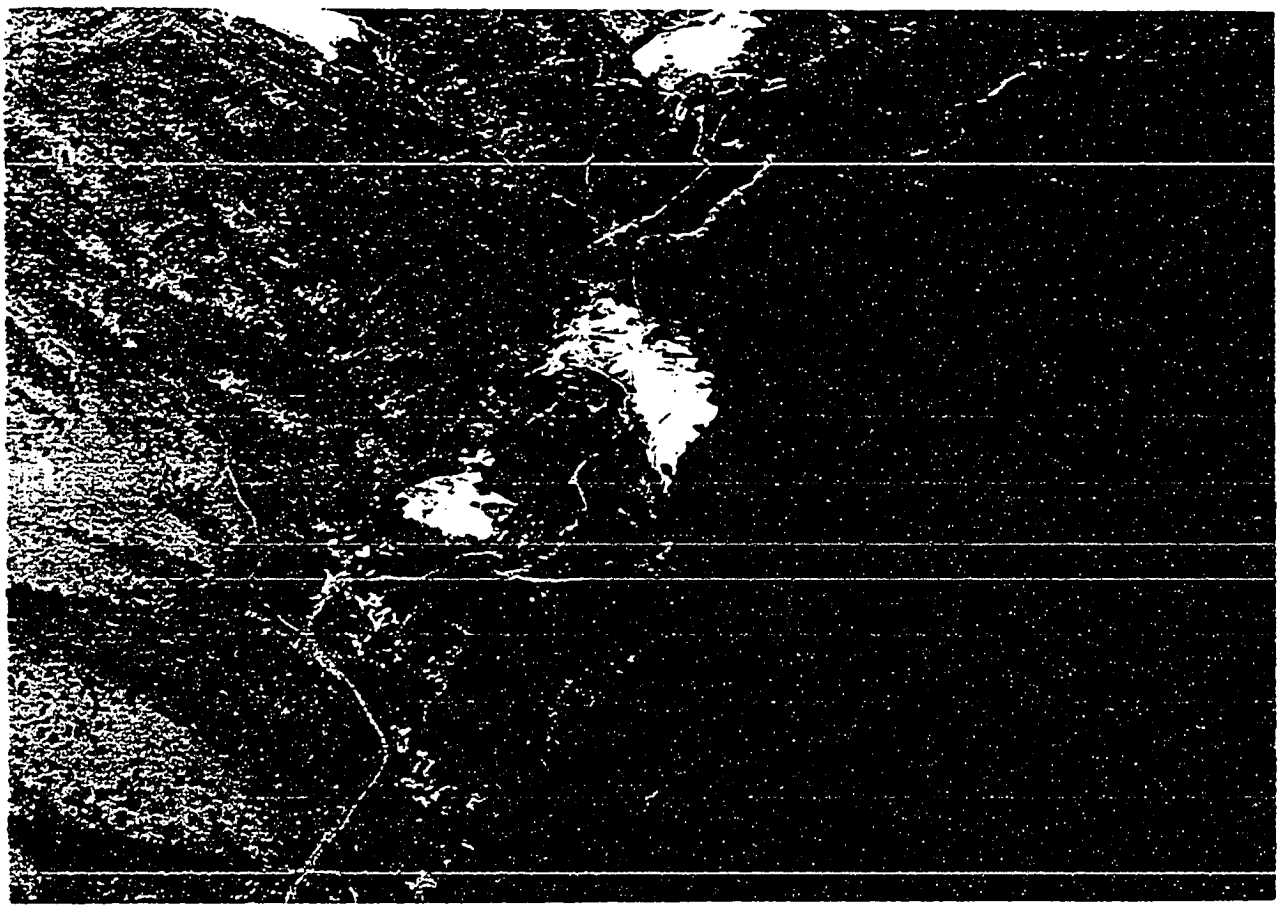
Reproduced with permission of the copyright owner. Further reproduction prohibited without permission.

Photo 39. Serpentinite debris and mine dump material pushed downslope from the Jensen Mine which is located approximately 0.6 miles upstream from the Coalinga Asbestos Mill Site in Upper Pine Canyon. A tributary to the western fork of the Upper Pine Canyon drainage network runs along the base of this pile. As illustrated, the front of this pile is subject to erosion and mass wasting from slumping. Serpentinite debris eroded from this mine dump is transported downslope into Upper Pine Canyon.



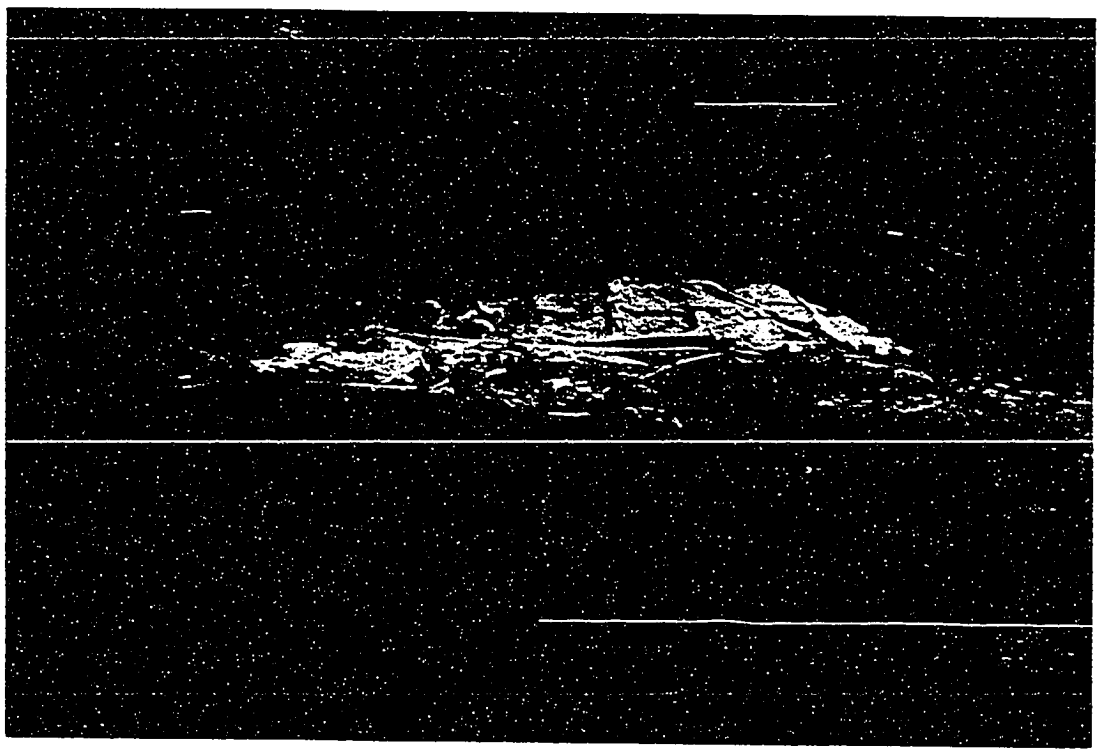
Reproduced with permission of the copyright owner. Further reproduction prohibited without permission.

Photo 40. Reconnaissance aerial photograph of Upper Pine Canyon showing part of the Butler Estate Chromite Mine (upper left), the Jensen Mine (upper center), the Coalinga Asbestos Mill tailings pile (center), and the Railroad Mine (left center). The photo also shows the extent of some of the landslide and serpentinite debris flow deposits that occur throughout the Upper Pine Canyon area, some of the deep gullies of the western fork, and part of the sediment retaining dam at the base of the tailings pile. Note the dense grassy covering that has developed on top of the undisturbed landslide surfaces in the vicinity of the Coalinga Mill. Before construction of the diversion from the east fork to the west fork (see center of photo), the east fork ran along the eastern margin of the serpentinite debris flow deposit that provided ore for the Jensen Mine. Erosion of the margin of this serpentinite deposit is the primary source of asbestos sediment in the east fork of Upper Pine Canyon upstream from the Coalinga Asbestos Mill tailings pile.



Reproduced with permission of the copyright owner. Further reproduction prohibited without permission.

Photo 41. Reconnaissance aerial photo of the Coalinga Site including the mill facility and the tailings pile and ore. The tailings pile has two bermed areas which were constructed by Marmac Resources Company/Mareco to capture runoff from the eastern fork of Pine Canyon for use in its chromite milling operations at the Coalinga Site.



Reproduced with permission of the copyright owner. Further reproduction prohibited without permission.

Photos 42. Close up photo of one of the two bermed ponding areas constructed by Marmac near the upstream end of the Coalinga tailings pile in the Eastern Fork of Pine Canyon Creek.



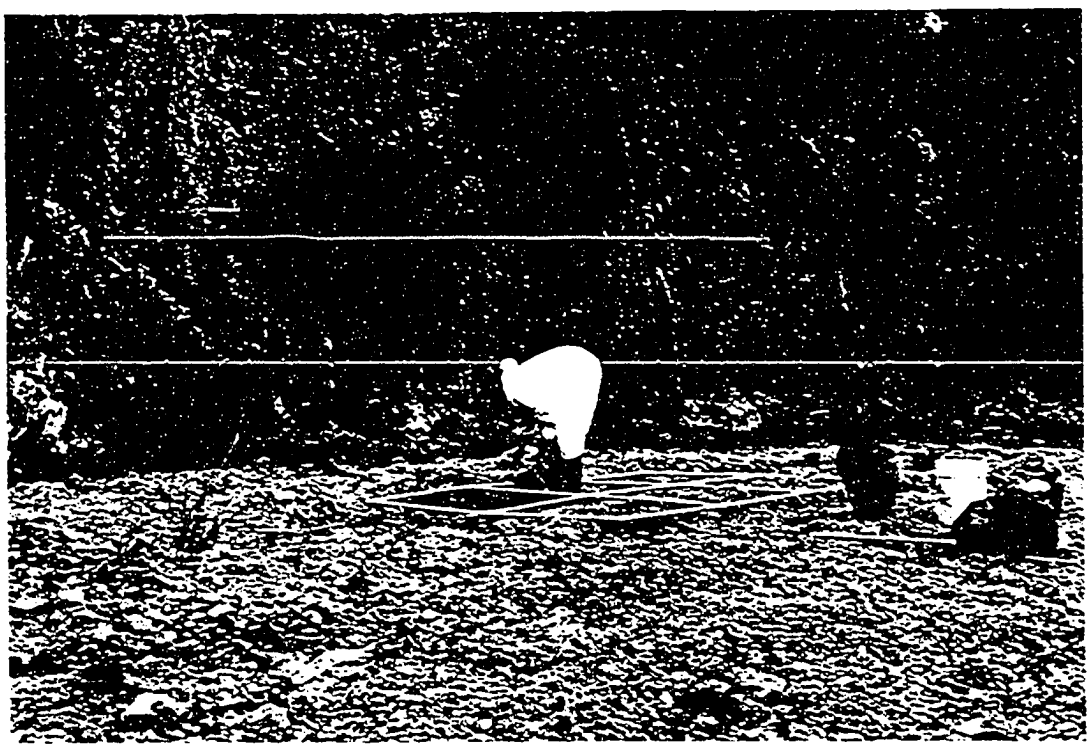
Reproduced with permission of the copyright owner. Further reproduction prohibited without permission.

Photo 43. Erosional gully that has formed on the lower sloping face of the Coalinga tailings pile in the eastern fork of Pine Canyon Creek. These tailing materials have a fine granular texture with a thin crust on the surface of undisturbed areas. The crustal material is generally one to two inches thick.



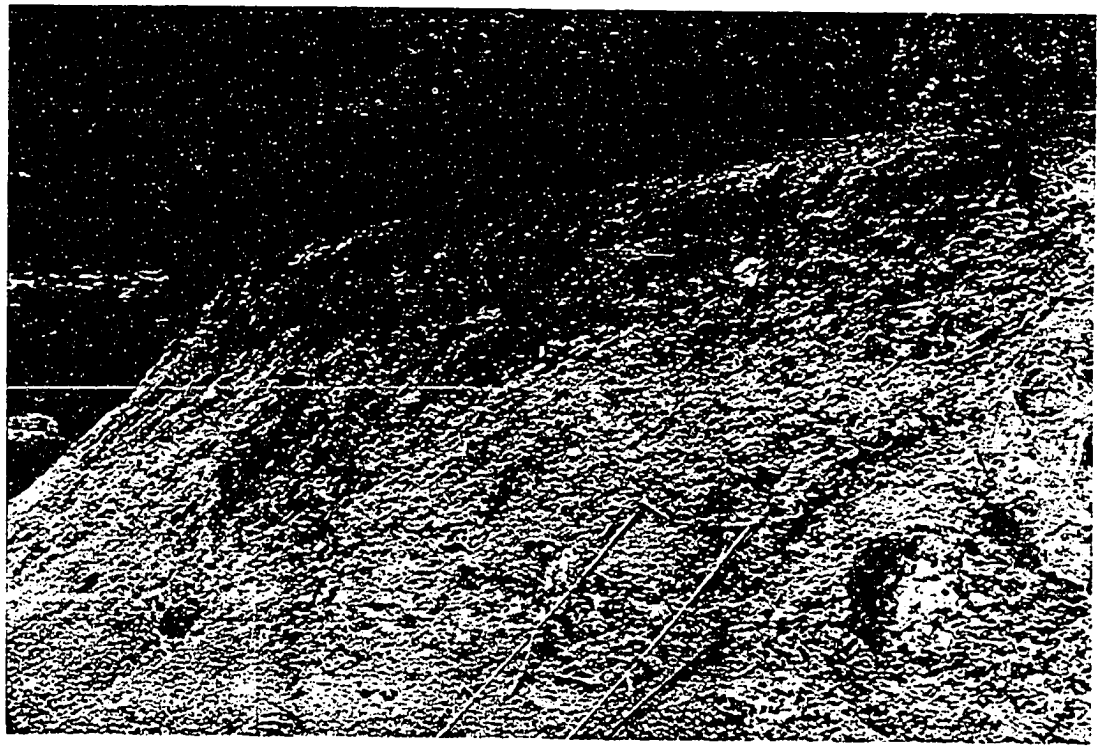
Reproduced with permission of the copyright owner. Further reproduction prohibited without permission.

Photo 44. Eroded serpentinite debris that has been deposited in the sediment retention basin constructed at the base of the Coalinga tailings pile in the Eastern Fork of Pine Canyon Creek. This serpentinite debris is trapped in a small arroyo. The sediment retaining dam is located approximately 100 yards downstream from this area. The sedimentary bedding planes of the exposed bedrock in the sidewalls of the arroyo are nearly vertical as a result of compressional tectonics.



Reproduced with permission of the copyright owner. Further reproduction prohibited without permission.

Photo 45. Exposed margins of asbestos-containing serpentinite debris flow deposit located approximately 80 yards upstream of the Coalinga Site. Serpentinite debris eroded from this deposit is transported into the eastern fork of Pine Canyon at the Coalinga Site. Note sparse manzanita vegetation without any grassy covering that has grown on top of the deposit. This type of restricted vegetation is characteristic of asbestos-containing serpentinite soils.



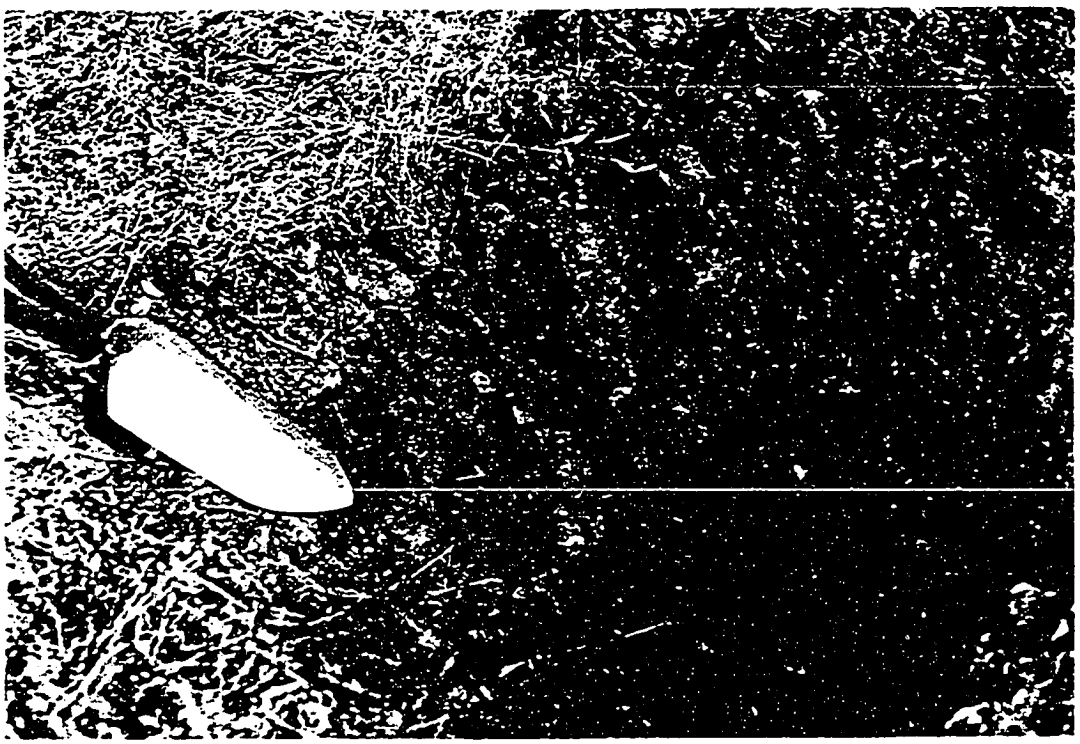
Reproduced with permission of the copyright owner. Further reproduction prohibited without permission.

Photo 46. This photo features the dark, clay rich soils that have developed on the surface of the landslide deposits in the vicinity of the Coalinga Site. The soil featured in this picture was excavated by a backhoe to a depth of approximately ten feet. These soils have been mapped by SPLC as LSS - Landslide Surface Soils. These soils support a thick covering of grass with rootlets that extend approximately three inches below the surface. There is little visible evidence of asbestos in these soils. This contrasts with the asbestos-containing soils associated with the serpentinite debris flow deposits illustrated in Photo 45.



Reproduced with permission of the copyright owner. Further reproduction prohibited without permission.

Photo 47. Close up photo of the dark, clay rich soil of the Coalinga Site. There is no visible evidence of asbestos in the soil of this shallow excavation pit which is approximately four inches deep.



Reproduced with permission of the copyright owner. Further reproduction prohibited without permission.

Photo 48. Sparsely vegetated serpentinite soil with some manzanita bushes and isolated Digger pine trees in the serpentinite outcrop area in the White Creek watershed. This is a natural area that has not been disturbed by anthropic activities and is typical of the sparsely vegetated natural slopes of the New Idria Formation in the Joaquin Ridge area. Note lack of any grassy ground covering.



Reproduced with permission of the copyright owner. Further reproduction prohibited without permission.

Photo 49. Sparsely vegetated serpentinite soil with isolated Digger pine trees. This picture was taken near the crest of Joaquin Ridge approximately 0.5 miles northeast of the Atlas Site in the White Creek drainage. This photo also features the blocky structure and the characteristic reddish-brown color of undisturbed serpentinite soils. Note lack of any grassy ground covering and gully-like drainage channel.



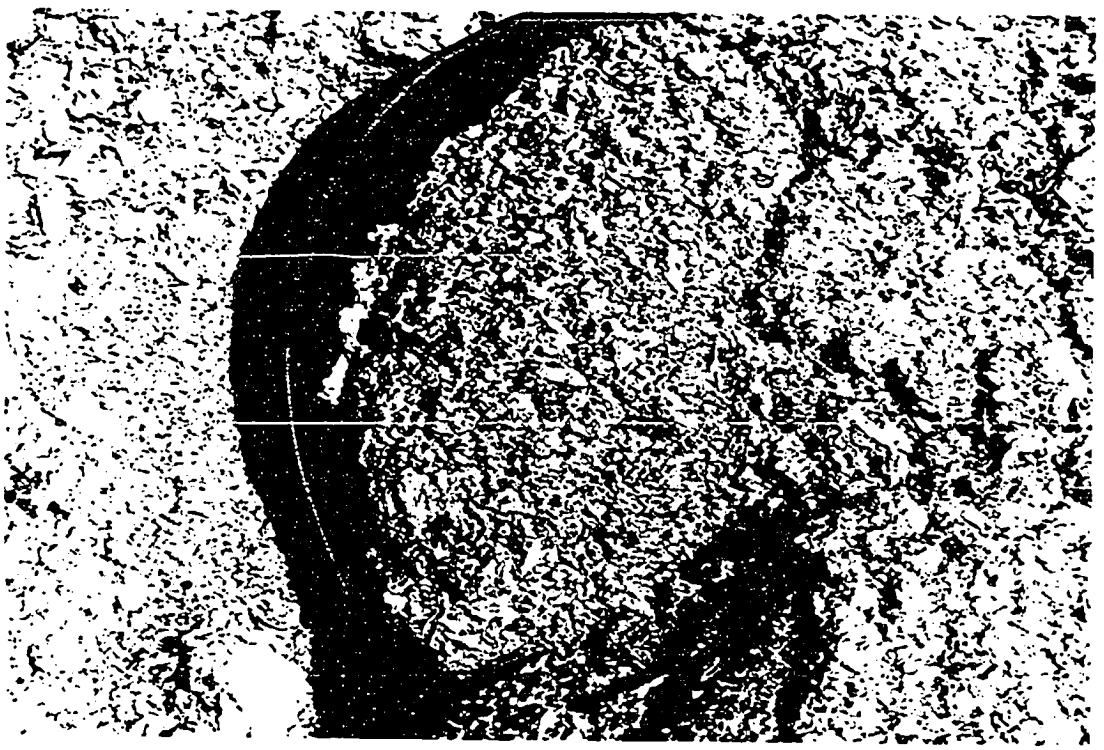
Reproduced with permission of the copyright owner. Further reproduction prohibited without permission.

Photo 50. Soil sampling station (OC-18) located approximately 0.8 miles west of Atlas Mine and Mill Site in the White Creek watershed. Note sparsely vegetated serpentinite soils with blocky soil structure evident in freshly sampled area at left of field geologist. Geologist is collecting soil samples using a one by two meter grid and a random sampling method as described in the SPLC QAPP (1987). This is a natural area that has not been disturbed by anthropic activities. Vegetation is naturally sparse in most of the serpentinite outcrop area.



Reproduced with permission of the copyright owner. Further reproduction prohibited without permission.

Photo 51. Coarse, sandy texture of platey serpentinite soils as exposed on the open-pit mine surfaces in the White Creek watershed. This photo was taken at one of the Atlas mines and is typical of the serpentinite materials that were mined throughout the Joaquin Ridge areas including the White Creek and Pine Canyon drainages.



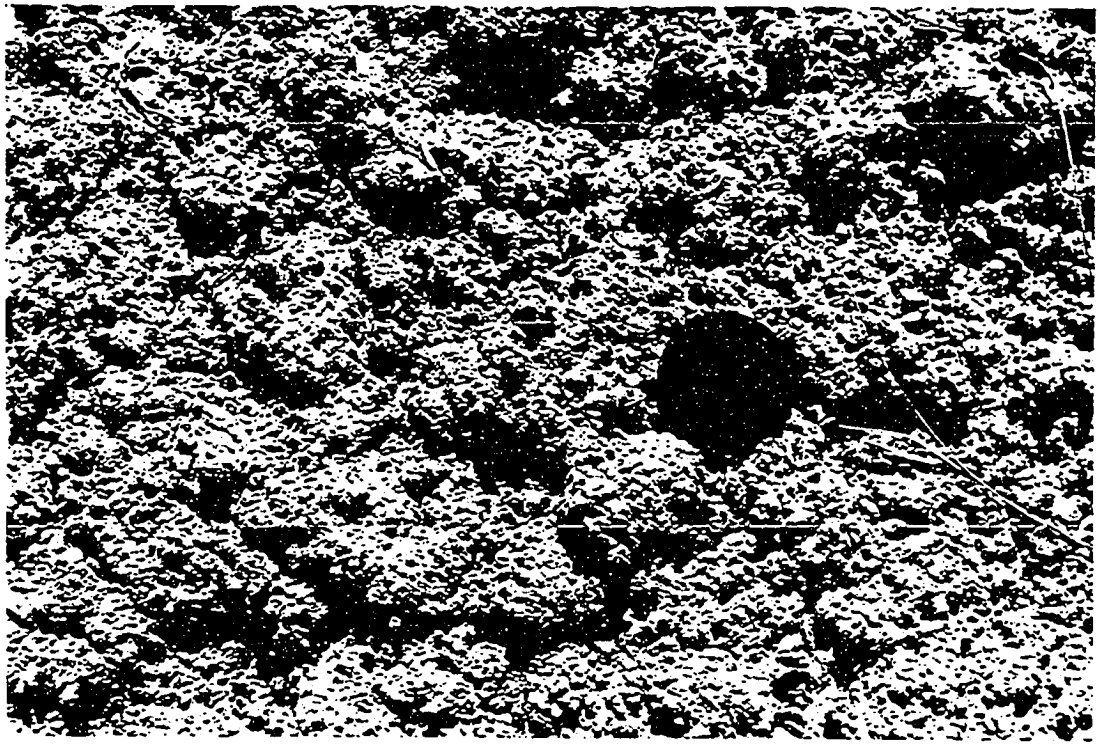
Reproduced with permission of the copyright owner. Further reproduction prohibited without permission.

Photo 52. Close up picture of the weakly-cemented crust that is commonly observed on anthropically disturbed surfaces of the New Idria Formation. This crust was generally not observed on the undisturbed serpentinite soils in the region. This type of crust was observed on open-pit mine surfaces and tailings piles in both the White Creek and Pine Canyon watersheds. This picture was taken at the Atlas Site in the White Creek drainage.



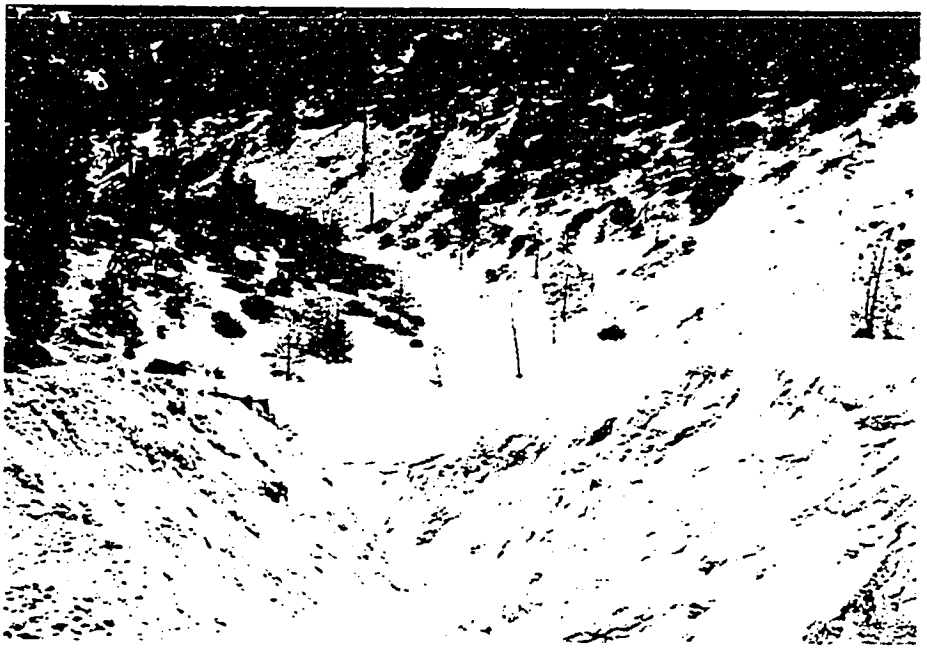
Reproduced with permission of the copyright owner. Further reproduction prohibited without permission.

Photo 53. Close up of serpentinite crust featured in Photo 52. Lens cap is useful for observing the scale of the nodular crust.



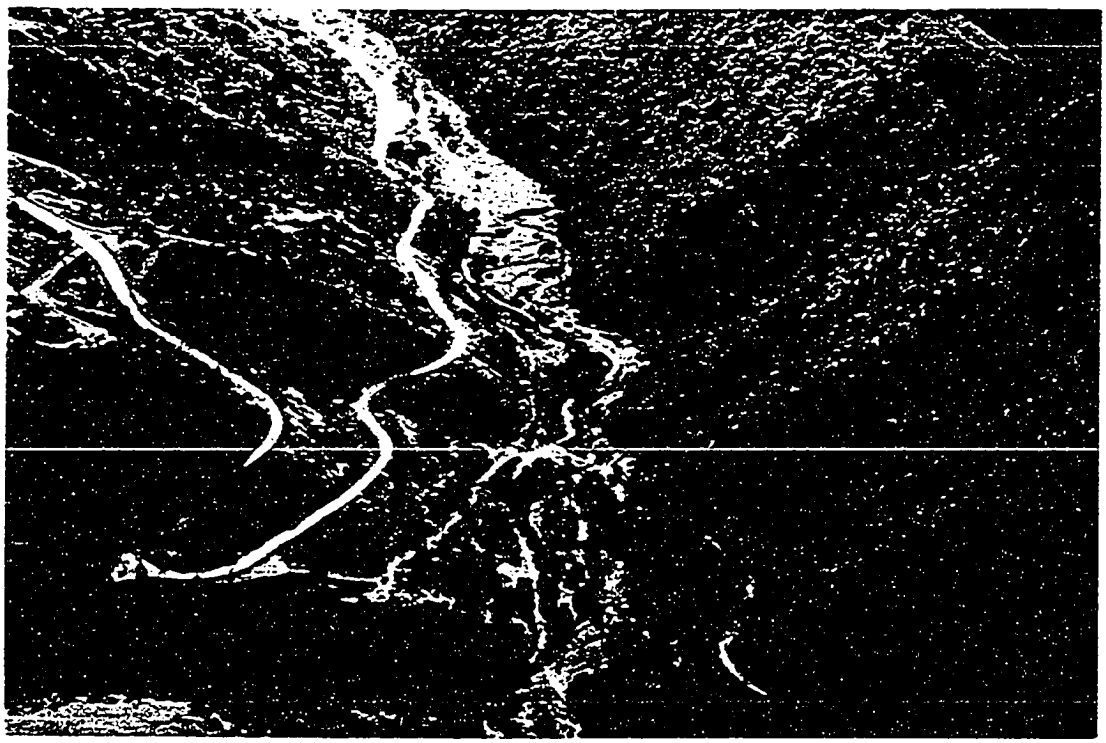
Reproduced with permission of the copyright owner. Further reproduction prohibited without permission.

Photo 54. Close up of gully that is forming on the southern margin of Atlas Site tailings pile. Because of fluvial and wind erosion and mass wasting, the uncontained Atlas pile is merging in dune-like fashion with the naturally occurring serpentinite soils of the New Idria Formation. This process has had a negative effect on near-by vegetation as illustrated in the center of the photo.



Reproduced with permission of the copyright owner. Further reproduction prohibited without permission.

Photo 55. This photo shows the location of an abandoned chromite mill site that was located along the upper reach of White Creek at the base of the serpentinite outcrop area. The mill site is located in White Creek (see top center). Intermittent flow in White Creek is towards the top of the photo.



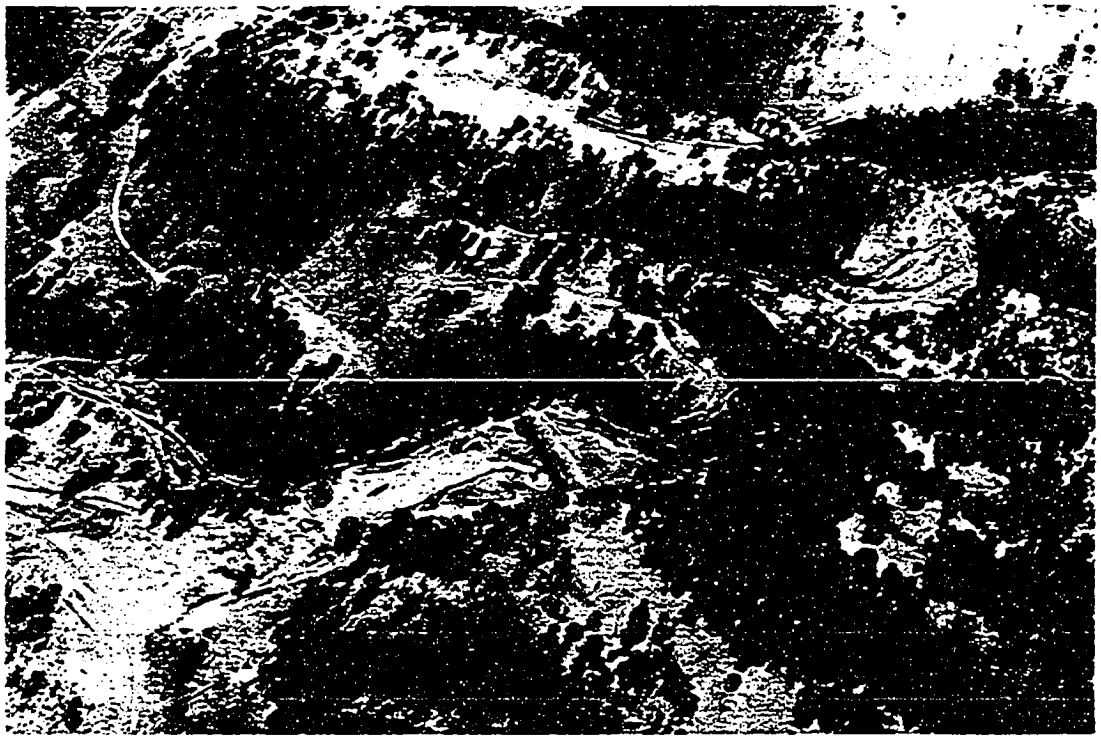
Reproduced with permission of the copyright owner. Further reproduction prohibited without permission.

Photo 56. This photo features the location of two abandoned chromite mill sites - one of which is featured in Photo 55. The chromite mill site of Photo 55 is visible in right center portion of this photo at the base of the serpentinite outcrop. The second abandoned chromite mill site appears as an abrupt widening of the White Creek streambed approximately one quarter mile downstream from the serpentinite outcrop area (see upper left center of photo in area covered by hillside shadow).



Reproduced with permission of the copyright owner. Further reproduction prohibited without permission.

Photo 57. This photo features an abandoned chromite mill site that is located in the intermittent drainage pathway of White Creek approximately two miles downstream from the serpentinite outcrop area. This photo shows an ore storage area (lower left), an earthen wier structure that was constructed across White Creek for the purposes of damming water for use in a water-based gravity settling milling process, and an abundance of grayish white serpentinite debris that has been deposited in the intermittent streambed.



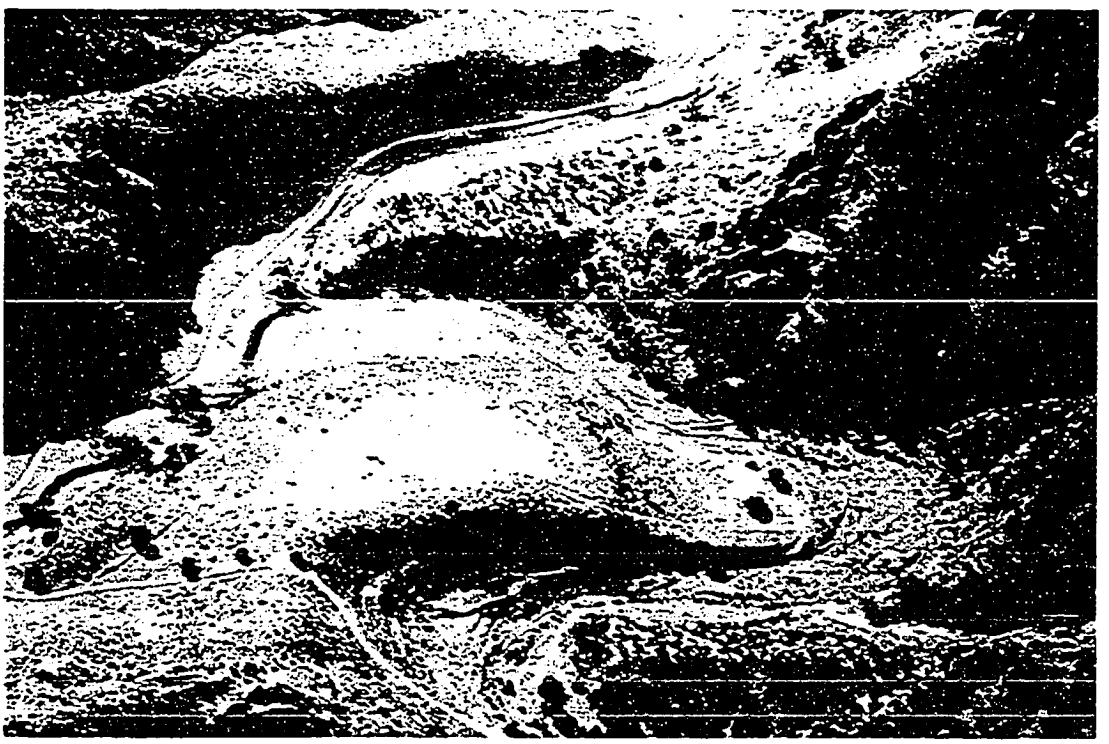
Reproduced with permission of the copyright owner. Further reproduction prohibited without permission.

Photo 58. This photo features an abandoned chromite mill site that is located in the intermittent drainage pathway of White Creek approximately three miles downstream from the serpentinite outcrop area - and approximately one mile downstream from the abandoned chromite mill site featured in Photo 57. Note the abundance of serpentinite debris that has been deposited in the intermittent streambed near the abandoned chromite milling sites.



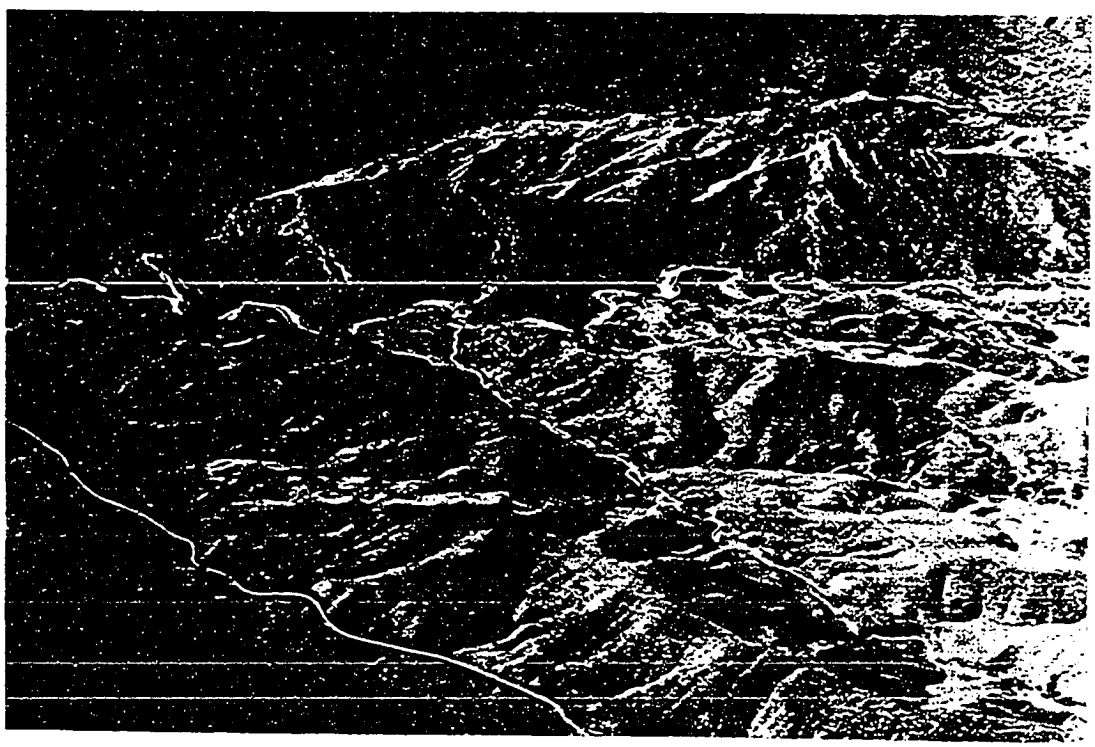
Reproduced with permission of the copyright owner. Further reproduction prohibited without permission.

Photo 59. This photo features the juncture of White Creek (flowing from the right and towards the top of the photo) with Pine Canyon Creek (flowing from the left and towards the top of the photo). Pine Canyon Creek is a minor tributary to White Creek as indicated by the comparative size of the intermittent drainage channels. An abandoned chromite mill site is located on the bank of White Creek at the bottom center. This abandoned mill site is approximately 300 yards upstream from the White Creek juncture with Pine Canyon Creek. In comparison with White Creek, there little visible evidence of asbestos in the Pine Canyon drainage pathway.



Reproduced with permission of the copyright owner. Further reproduction prohibited without permission.

Photo 60. This photo features the juncture of White Creek and Pine Canyon Creek as illustrated in Photo 59. In this photo, White Creek is flowing from right to left in a meandering channel that appears to have an abundance of grayish white sediment. Pine Canyon Creek is barely visible as a minor tributary to White Creek. Pine Canyon Creek flows from the lower right corner in a diagonal direction towards the upper left corner. The juncture is in the upper left quadrant. A dirt road runs adjacent to the Pine Canyon Creek in this area. As viewed from a distance, this road exaggerates the width of Pine Canyon Creek. The Diaz Canyon access road to the Upper Pine Canyon area is visible in the lower left quadrant of the photo.



Reproduced with permission of the copyright owner. Further reproduction prohibited without permission.

Photo 61. Close up of the Pine Canyon intermittent streambed at the point of its juncture with White Creek. Note the relative lack of sediment in the intermittent streambed. The channel at this point is approximately 15 feet wide. Stream gauge pipe in center of picture is approximately three feet high and is useful for scale.



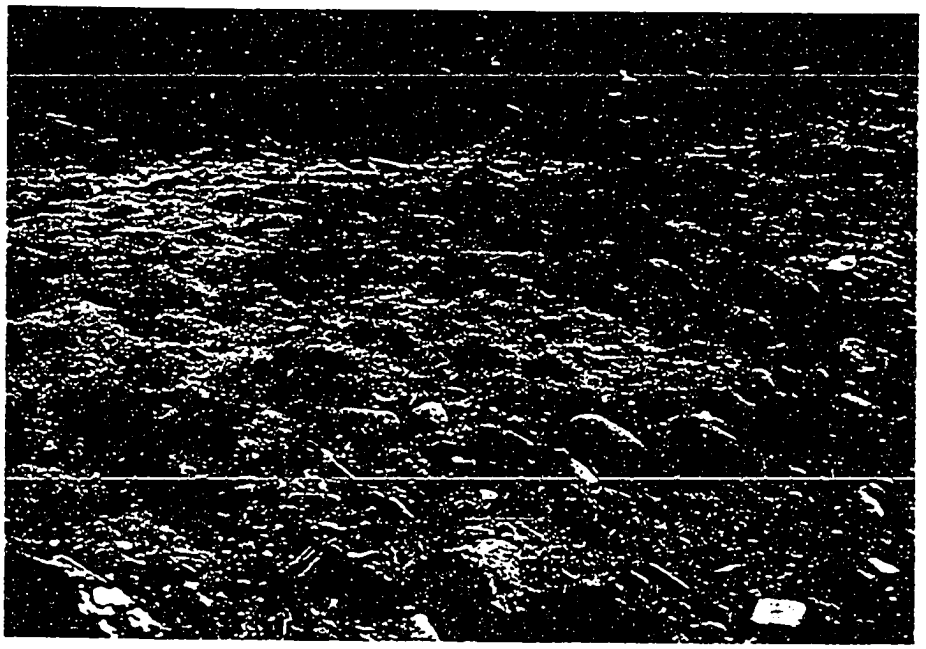
Reproduced with permission of the copyright owner. Further reproduction prohibited without permission.

Photo 62. Close up of juncture of White Creek and Pine Canyon Creek. White Creek is flowing from the left side of the photo and the Pine Canyon tributary is visible on the right side of the photo. The White Creek channel (including the first terrace which is covered by water during high run off events) is approximately 40 feet wide at this juncture.



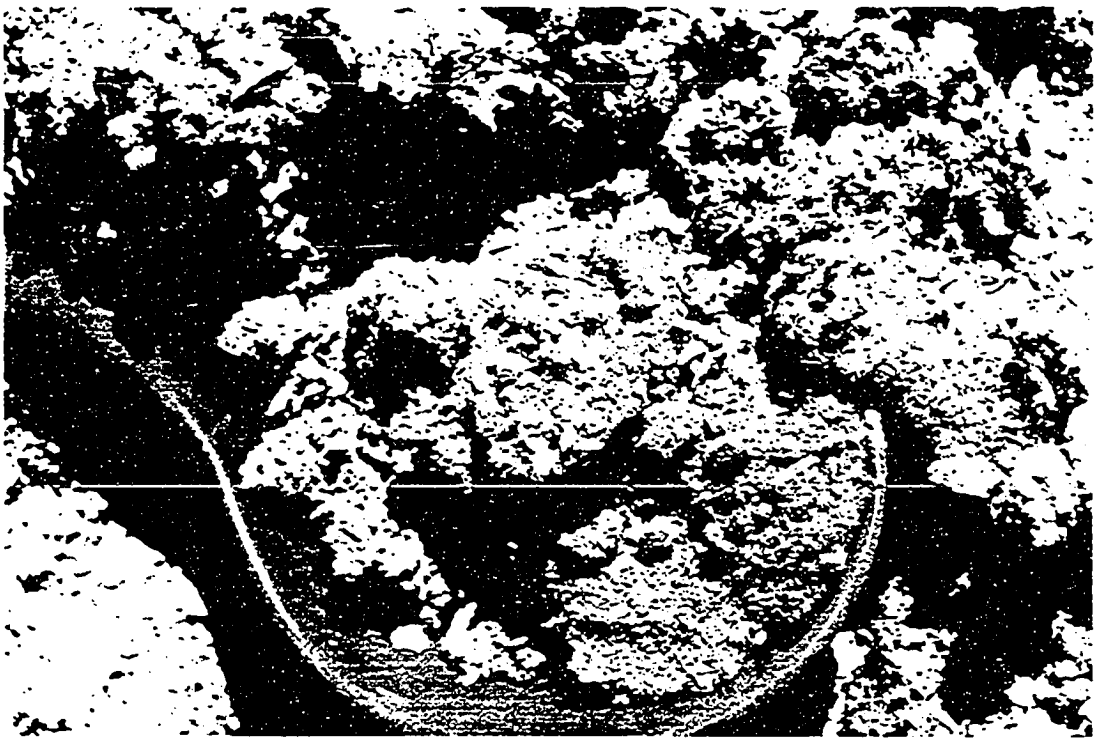
Reproduced with permission of the copyright owner. Further reproduction prohibited without permission.

Photo 63. Close up of grayish-white serpentinite debris that was deposited as a channel sand deposit on the margin of the White Creek streambed approximately 100 feet upstream from the juncture with Pine Canyon Creek.



Reproduced with permission of the copyright owner. Further reproduction prohibited without permission.

Photo 64. Coarse serpentinite debris collected from the western fork of Upper Pine Canyon upstream from the Coalinga Asbestos Mill Site. When wet, this material has a "mushy, fibrous" texture.



Reproduced with permission of the copyright owner. Further reproduction prohibited without permission.

Photo 65. Intermittent streambed channel of the eastern fork of Upper Pine Canyon approximately 0.3 miles downstream from the sediment retention dam at the base of the Coalinga Asbestos Mill Site tailings pile. Channel is about ten feet wide and is lined with a thick blanket of grass. There is little evidence of asbestos in the dark brown streambed sediment. Grassy areas are not normally associated with soils containing significant concentrations of asbestos. Photo is slightly over-exposed and this causes the soil at the right side of the picture to appear as white. The normal color of this is light tan when dry.



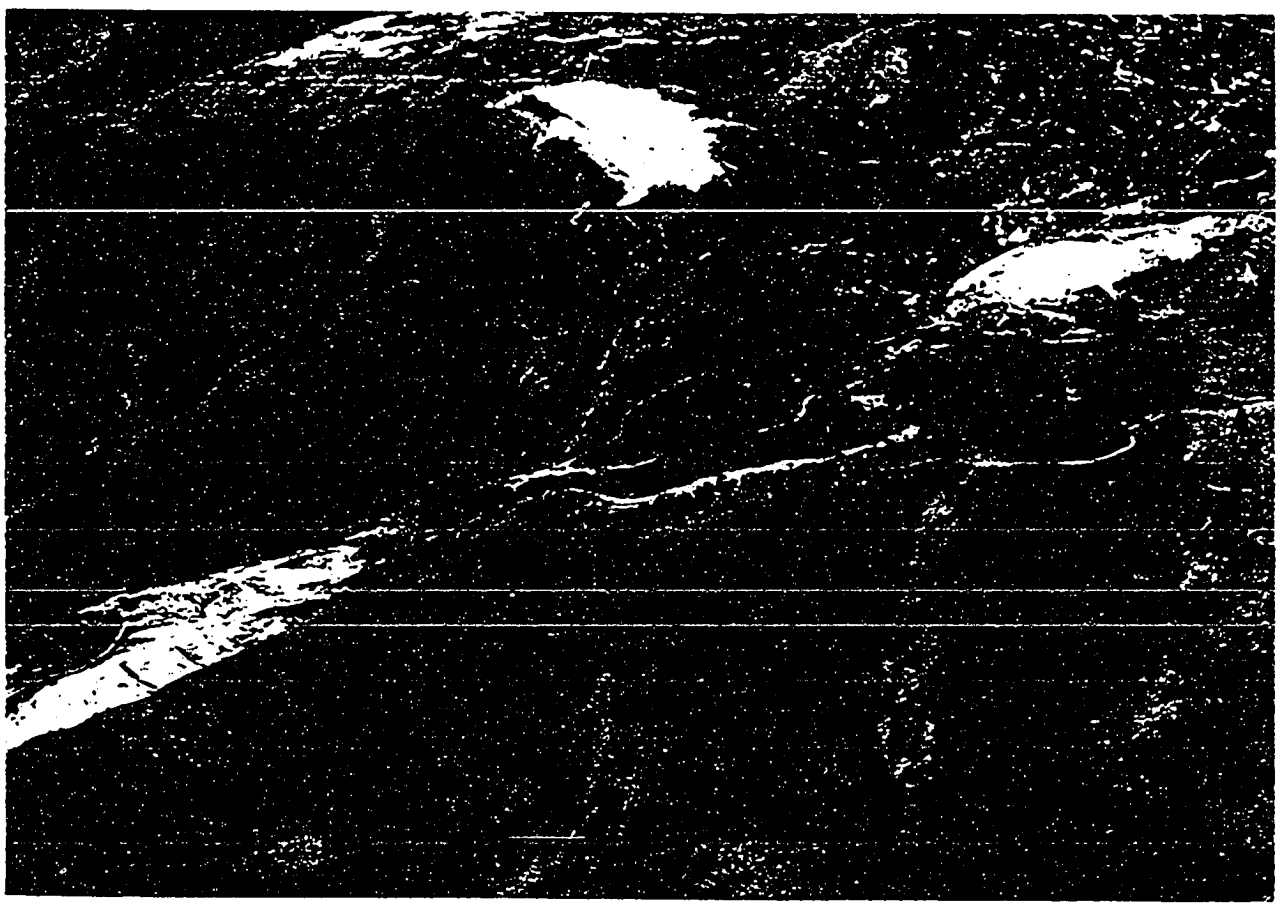
Reproduced with permission of the copyright owner. Further reproduction prohibited without permission.

Photo 66. Reconnaissance aerial photograph of Coalinga Asbestos Mill Site in Upper Pine Canyon showing the tailings pile in the eastern fork of Pine Canyon Creek (upper left corner); the Railroad Mine adjacent to the western fork (left center); and the deep gullies that have formed in the western fork on the margin of the landslide and/or serpentinite debris flow deposit that underlies most of the Coalinga Asbestos Mill area in Upper Pine Canyon. Some of the gullies are shown at the bottom of the picture.



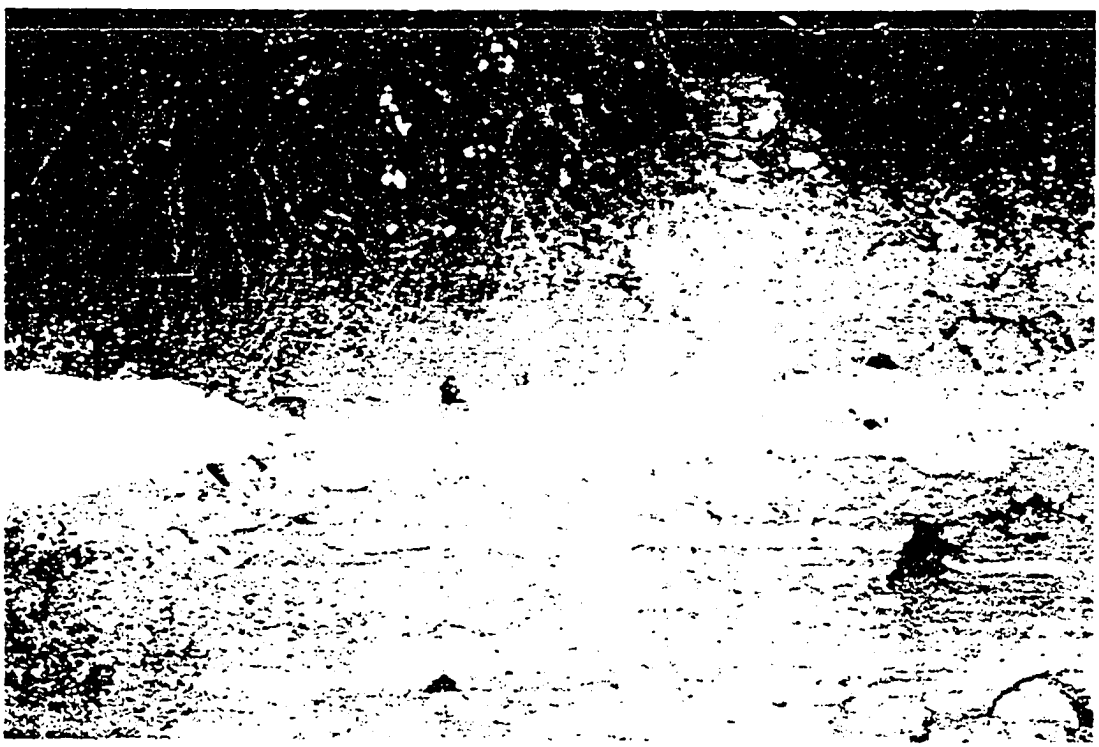
Reproduced with permission of the copyright owner. Further reproduction prohibited without permission.

Photo 67. Oblique aerial photograph of Upper Pine Canyon showing Butler Estate Chromite Mine (upper left center), the Jensen Mine (upper right), and the Coalinga Asbestos Mill tailings pile and ore (lower left). Note the dense grassy covering that has developed on top of the undisturbed landslide surfaces in the vicinity of the Coalinga Asbestos Mill area. These landslide soils have low concentrations of asbestos (generally less than 1%) and have been mapped by SPLC as LSS - Landslide Surface Soils. Before construction of the diversion from the east fork to the west fork (see center of photo to the right of the mill site), the east fork ran along the eastern margin of the serpentinite debris flow deposit that was the source of ore for the Jensen Mine. Erosion of the margin of this serpentinite deposit is the primary source of asbestos sediment in the east fork of Upper Pine Canyon upstream from the Coalinga Site tailings pile.



Reproduced with permission of the copyright owner. Further reproduction prohibited without permission.

Photo 68. Well laminated fluvial deposits of fine and coarse grained serpentinite debris that forms some of the streambank of the western fork of Upper Pine Canyon upstream from the Coalinga Site. Based on stratigraphic interpretation and what is known about the geology of the area, these laminated deposits may be thousands of years old.



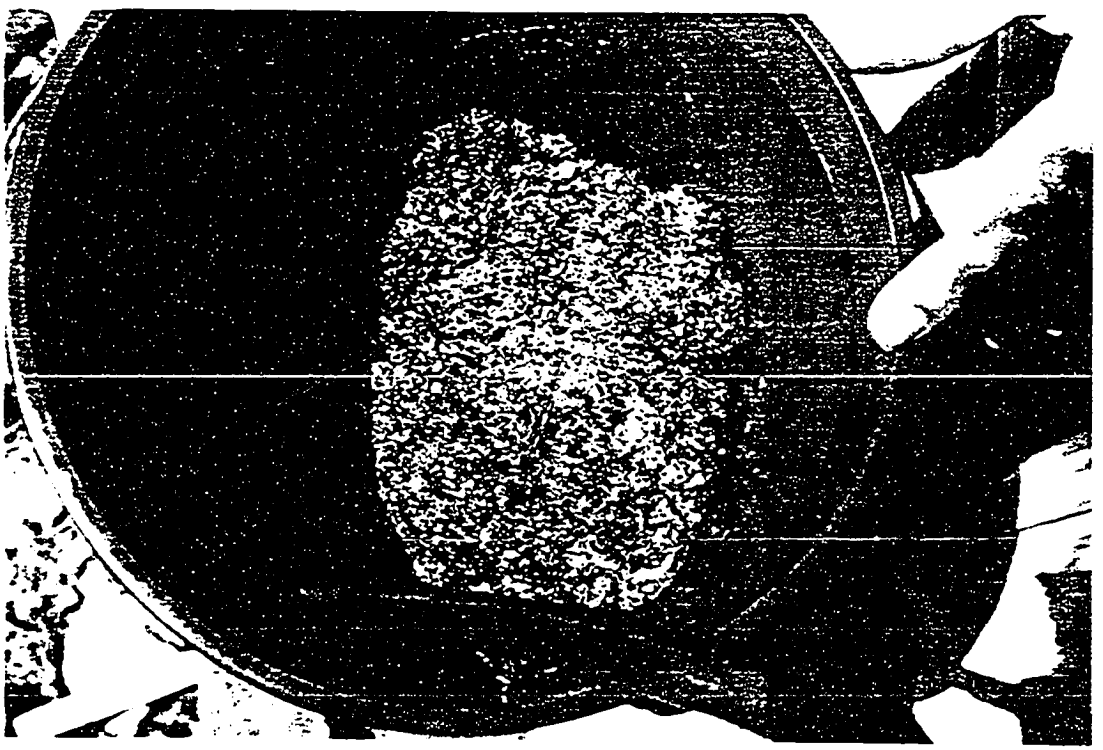
Reproduced with permission of the copyright owner. Further reproduction prohibited without permission.

Photo 69. Asbestos-containing streambed sediment sampled from Upper Pine Canyon approximately 0.3 miles downstream from the Jensen Mine and 0.3 miles upstream from the Coalinga Site. Asbestos concentration is estimated to be approximately 80% as indicated by the PLM results from streambed sediment sample PC41B.



Reproduced with permission of the copyright owner. Further reproduction prohibited without permission.

Photo 70. Asbestos-containing streambed sediment sampled from Upper Pine Canyon approximately 0.3 miles downstream from the Butler Mine and 0.2 miles upstream from the Coalinga Site. Coarse texture of grayish-white sediment resembles texture of serpentinite debris observed in tailings and dumps associated with the Butler pile. Asbestos concentration is estimated to be approximately 50% as indicated by the PLM results from streambed sediment sample PC2B.



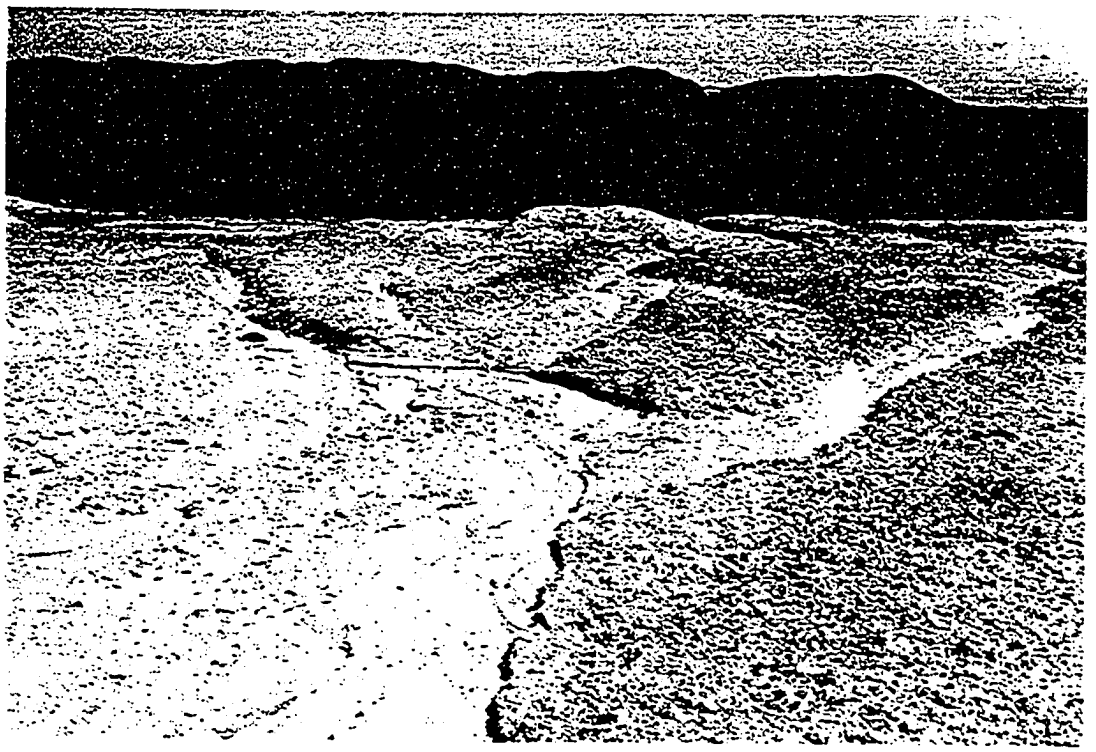
Reproduced with permission of the copyright owner. Further reproduction prohibited without permission.

Photo 71. Excavated pit of the Butler Mine which is approximately 200 to 300 feet deep. A small pond has formed at the bottom of the open-pit mine (lower right of picture). A mechanical shovel, barely visible in the background (left center of picture), is useful for scale.



Reproduced with permission of the copyright owner. Further reproduction prohibited without permission.

Photo 72. Coarse, friable, and crumbly serpentinite material exposed on the surface of the Jensen Mine. The exposed serpentinite minerals are coarse sand and gravel sized and have a pronounced blocky soil structure. These physical characteristics are common to other mines in the Joaquin Ridge area. This photo features one of the erosional drainage channels that has formed on the surface of the Jensen Mine. Intermittent flow is towards the top of the photograph (i.e., away from the reader).



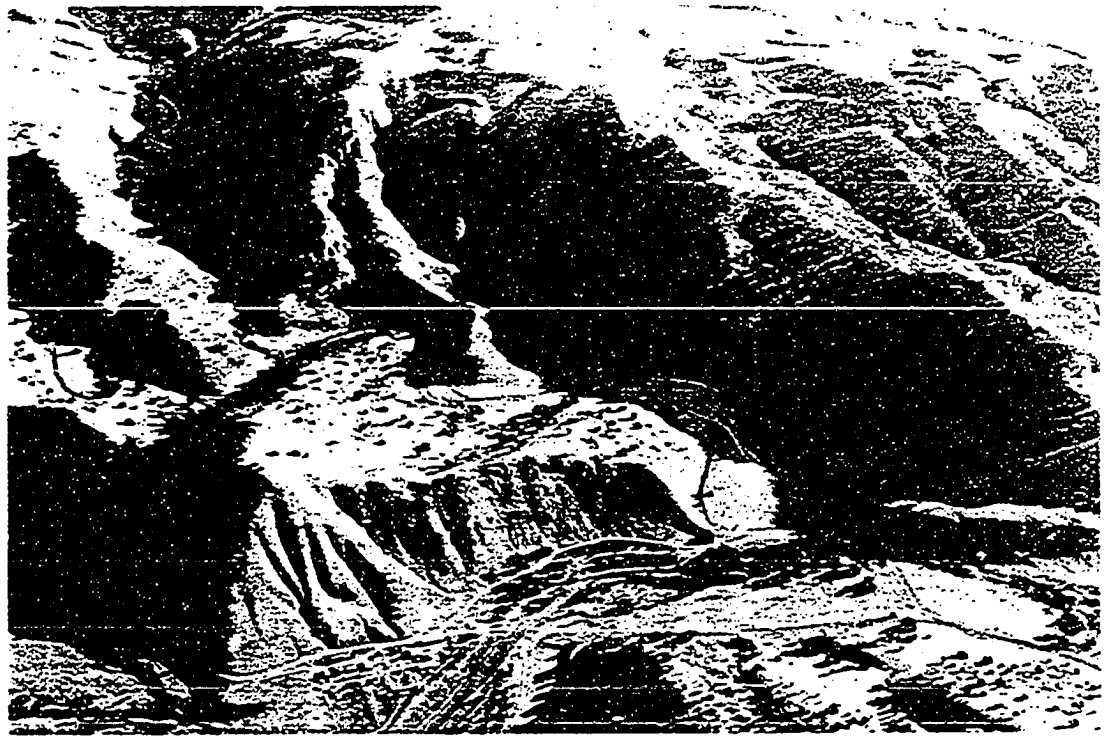
Reproduced with permission of the copyright owner. Further reproduction prohibited without permission.

Photo 73. Geologist compositing serpentinite sample collected from the surface of the Jensen Mine. Asbestos plates and bundles from fresh serpentinite surfaces are mostly sand and gravel sized.



Reproduced with permission of the copyright owner. Further reproduction prohibited without permission.

Photo 74. This photo features the juncture of White Creek with Los Gatos Creek. White Creek is in the center of the picture and flows from left to right. Los Gatos Creek is at the bottom of the photo and flows from left to right. The Birdwell Ranch houses are in the floodplain of Los Gatos Creek approximately a half mile upstream from the juncture of White Creek. White Creek has a diversion for direct drainage to Los Gatos Creek. This diversion protects the Pine Canyon access road from the effects of flooding during periods of high runoff. The diversion appears as a linear channel near the margin of the shadow in the lower right corner of the photo.



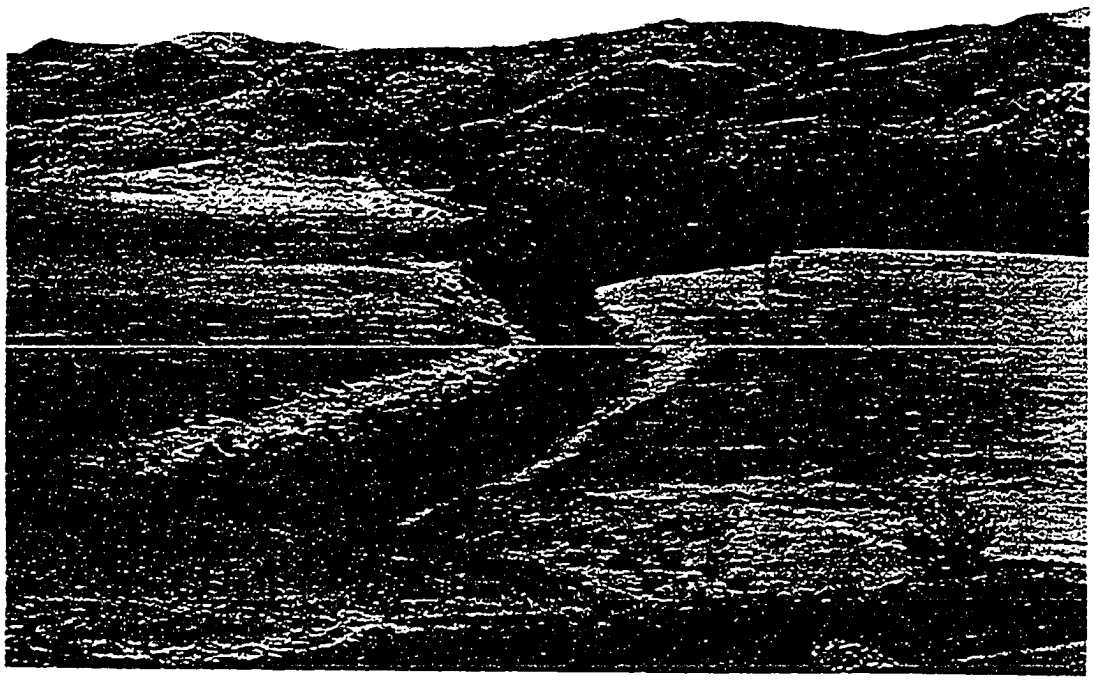
Reproduced with permission of the copyright owner. Further reproduction prohibited without permission.

Photo 75. This photo features Los Gatos Creek approximately two miles downstream from the juncture with White Creek. The Los Gatos Creek streambed ranges up to several hundred feet wide in some areas. The streambed interval shown in the lower left corner has been bulldozed probably for the purposes of protecting the streambank from erosion. The streambed sediment in this interval of Los Gatos Creek is mostly sandy gravel with an estimated asbestos concentration of approximately 5% to 20% as indicated by the PLM results of streambed sediment samples SS18 and SS19.



Reproduced with permission of the copyright owner. Further reproduction prohibited without permission.

Photo 76. Los Gatos Creek approximately four miles downstream from the juncture with White Creek. Flow in this picture is towards the reader. The streambed sediment is mostly sandy gravel with an estimated asbestos concentration of approximately 5% to 20% as indicated by the PLM results of streambed sediment samples SS18 and SS19.



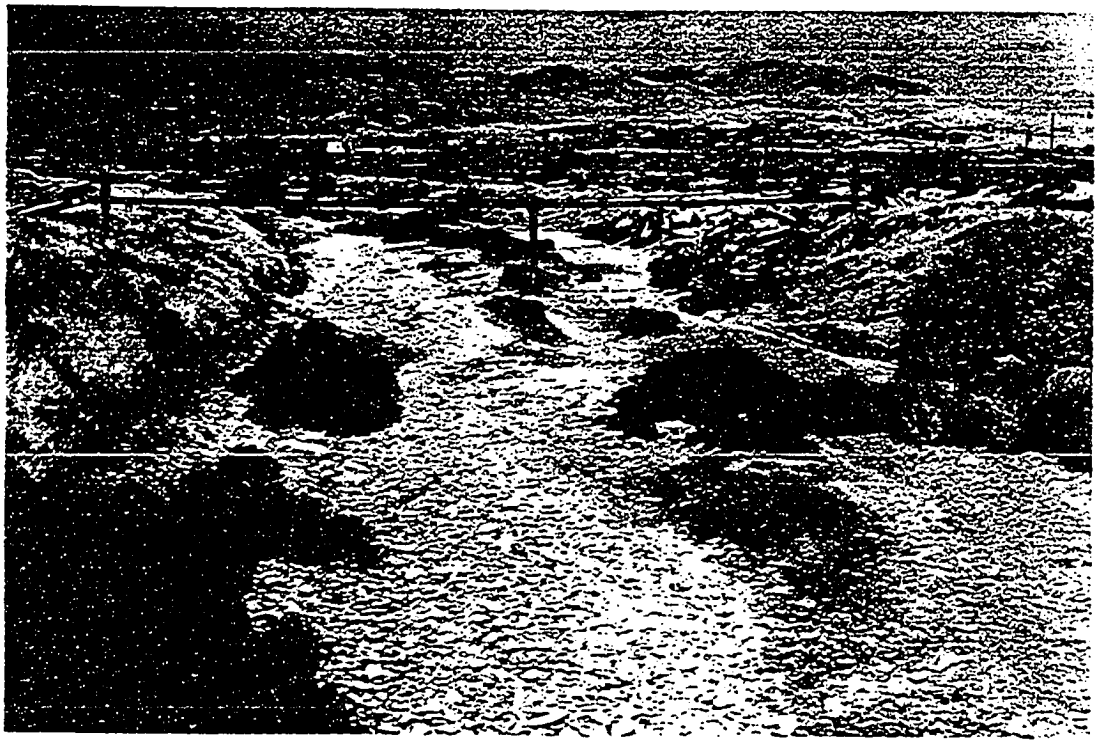
Reproduced with permission of the copyright owner. Further reproduction prohibited without permission.

Photo 77. This photo features Los Gatos Creek on the north side of the town of Coalinga in the vicinity of a quarry and the Coalinga general aviation airport. The intermittent streambed flows from the top of the picture towards the reader. The streambed sediment in this interval of Los Gatos Creek is mostly sandy gravel and gravelly sand with an estimated asbestos concentration of approximately 15% as indicated by the results of streambed sediment sample SS15.



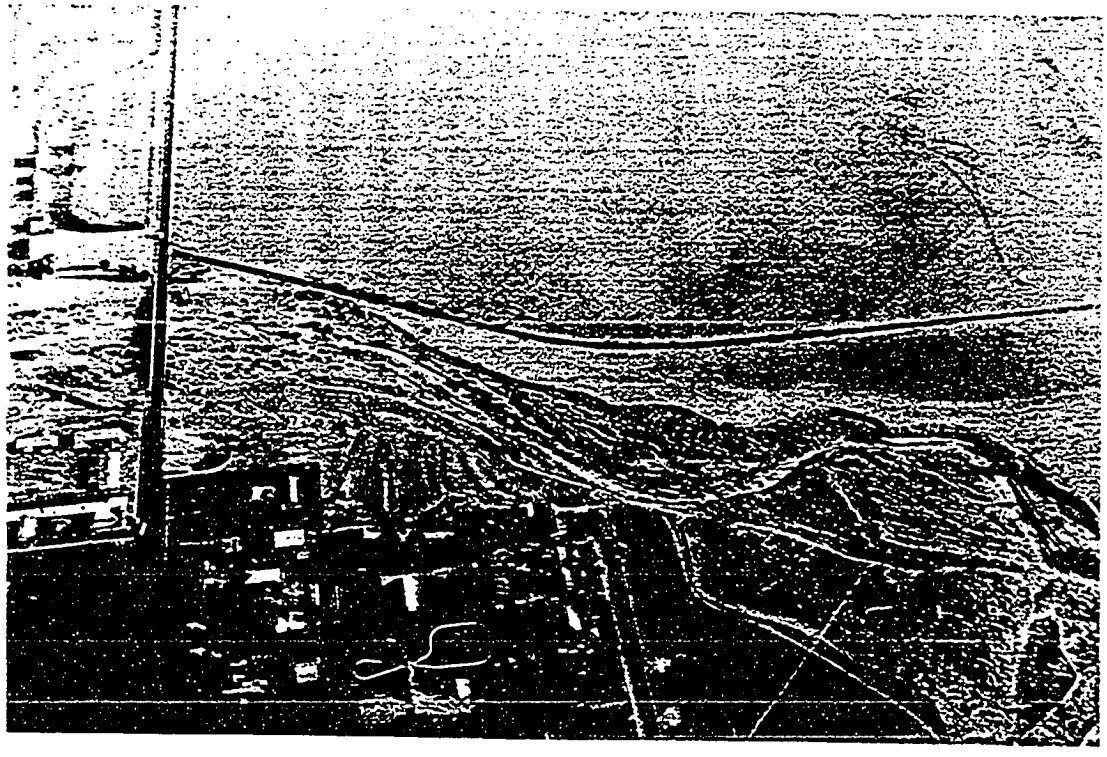
Reproduced with permission of the copyright owner. Further reproduction prohibited without permission.

Photo 78. Los Gatos Creek on the north side of the town of Coalinga. Flow in this picture is towards the reader. The streambed sediment is mostly sandy gravel with some channel sand deposits and the estimated asbestos concentration is approximately 15% as indicated by the results of streambed sediment sample SS15.



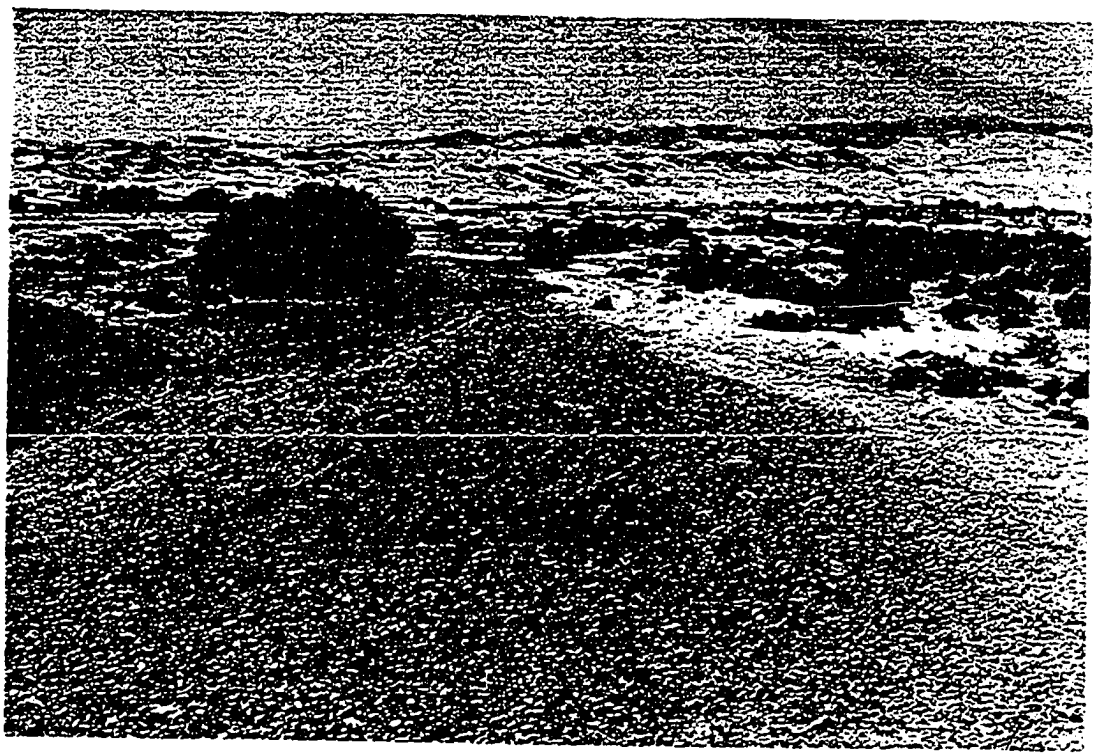
Reproduced with permission of the copyright owner. Further reproduction prohibited without permission.

Photo 79. Los Gatos Creek on the northeast side of the town of Coalinga. This photo shows the streambed interval on the east side of Highway 198/33. This is the area where Los Gatos Creek begins to head east towards Anticline Ridge by meandering in an easterly direction across the Pleasant Valley floodplain. The entrance to the Coalinga general aviation airport is shown in the upper left corner. The streambed sediment in this interval is mostly gravelly sand with an estimated asbestos concentration of approximately 1% to 10% as indicated by the PLM results of streambed sediment samples SS11 and SS12.



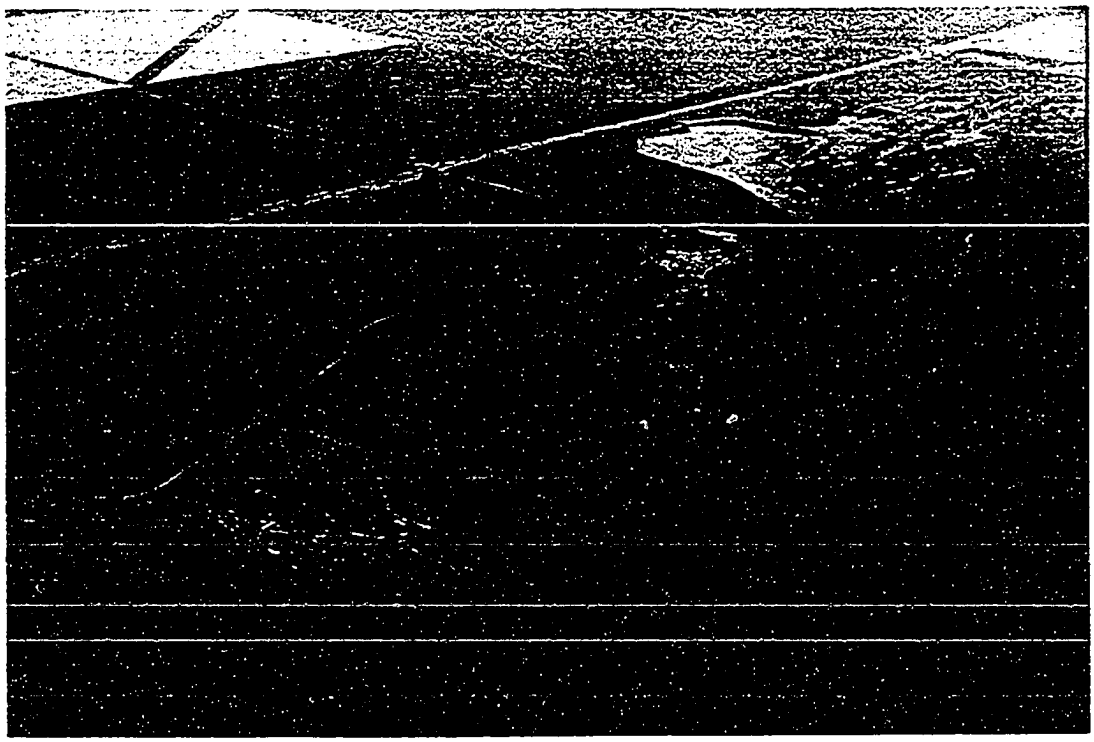
Reproduced with permission of the copyright owner. Further reproduction prohibited without permission.

Photo 80. Los Gatos Creek on the northeast side of the town of Coalinga near the Highway 198/33 bridge near the airport. The streambed sediment is mostly sandy gravel with an estimated asbestos concentration of approximately 1% to 10% as indicated by the PLM results of streambed sediment samples SS11 and SS12.



Reproduced with permission of the copyright owner. Further reproduction prohibited without permission.

Photo 81. Los Gatos Creek approximately three to four miles east of the town of Coalinga. In this interval, Los Gatos Creek is flowing in an easterly direction (towards the reader) towards the uplifted structural axis of the Coalinga Anticline. The streambed channel occurs in an entrenched, meandering floodplain that has several inset terraces. In this interval, the streambed is entrenched approximately 30 to 40 feet and the channel varies in width from approximately 500 to 1,200 feet. This interval is several miles downstream from the Los Gatos Creek juncture with Warthan Creek. Sediment from Warthan Creek contributes to dilution of the asbestos concentration of the streambed sediment in this interval. The streambed sediment in this reach is mostly sand and silt with an estimated asbestos concentration of less than 1% as indicated by the PLM results of streambed sediment samples SS8 and SS11.



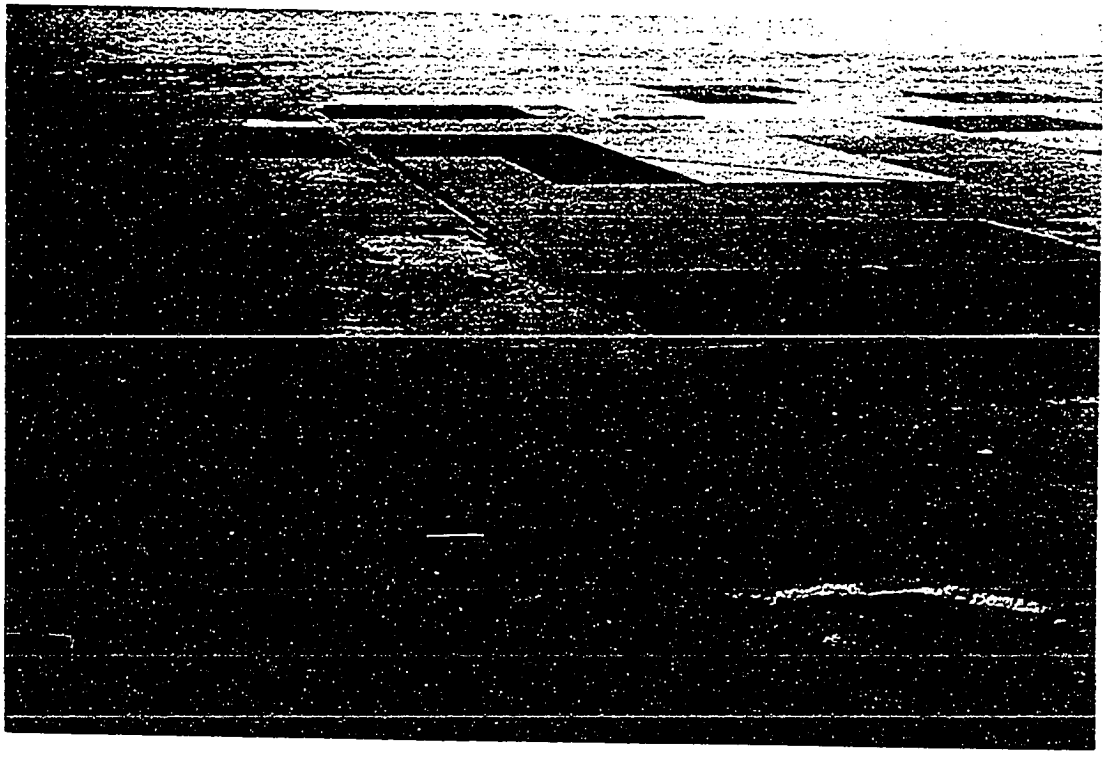
Reproduced with permission of the copyright owner. Further reproduction prohibited without permission.

Photo 82. Los Gatos Creek approximately three miles east of the town of Coalinga. This is the area where Los Gatos Creek is heading in an easterly direction across the Pleasant Valley alluvial plain and towards the Coalinga Anticline. The streambed sediment is mostly sand with about five to ten percent fine gravel. The asbestos concentration is estimated to be less than 1% as indicated by the PLM results of streambed sediment samples SS8 and SS11.



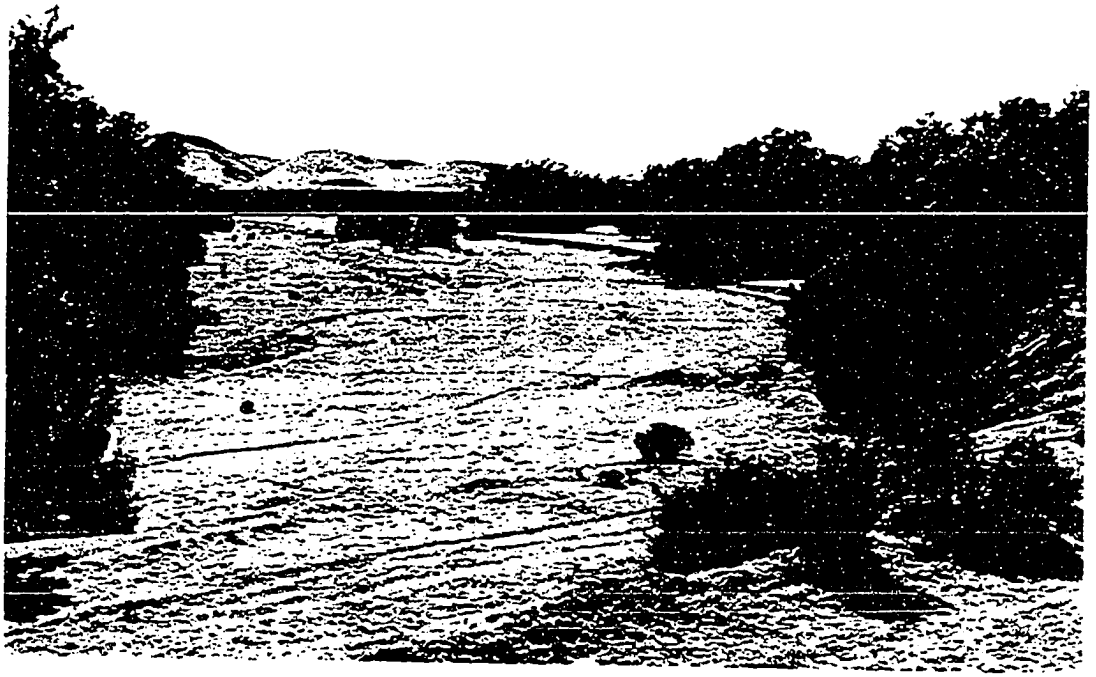
Reproduced with permission of the copyright owner. Further reproduction prohibited without permission.

Photo 83. This photo features Los Gatos Creek as it crosses the Pleasant Valley alluvial plain and the structural axis of the uplifted Coalinga Anticline. This is the area of maximum entrenchment. The town of Coalinga is in the upper left corner. The juncture of Jacalitos Creek with Los Gatos Creek is shown at the lower middle left of the picture and the highway is Interstate Five. The streambed sediment in this interval of Los Gatos Creek is mostly fine sand and silt with an estimated asbestos concentration of less than 1% as indicated by the PLM results of streambed sediment sample SS8.



Reproduced with permission of the copyright owner. Further reproduction prohibited without permission.

Photo 84. Los Gatos Creek in the area where the intermittent stream crosses the structural axis of the Coalinga Anticline. In this area, the intermittent stream occurs in an entrenched meander floodplain that has several inset terraces. This streambed interval is located approximately five miles east of the town of Coalinga. The streambed is entrenched approximately 30 to 40 feet (see nearly vertical cliff/streambank in far background). Two minor terraces are visible at the right margin of the streambed. The streambed sediment is mostly sand and silt with an estimated asbestos concentration of less than 1% as indicated by the PLM results of streambed sediment sample SS8.



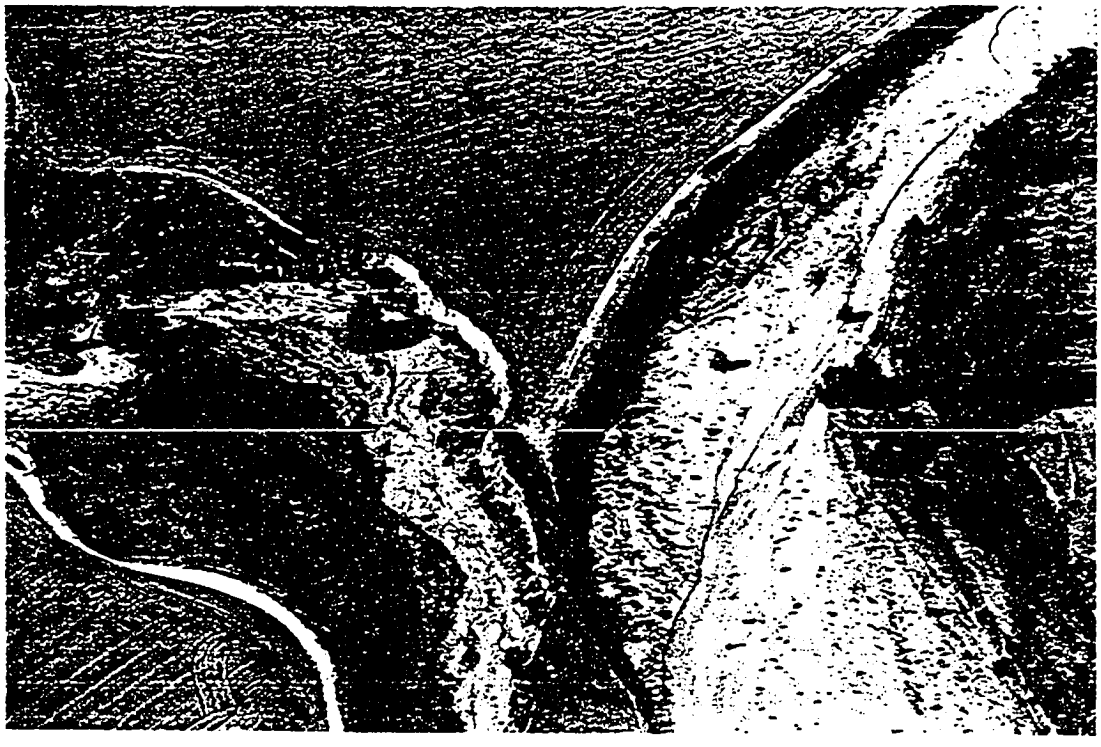
Reproduced with permission of the copyright owner. Further reproduction prohibited without permission.

Photo 85. Reconnaissance aerial photograph of Los Gatos Creek at the juncture with Zapato-Chino Creek which is located on the eastern flank of Anticline Ridge and the Guijarral Hills area. The broad, braided channels are subject to scouring and cut and fill depositional processes and are entrenched approximately twenty to thirty feet. Scouring from intermittent flow contributes to winnowing (and downstream transport) of the very fine silt and clay fractions. The highway is Interstate Five. The canal in the background is the Coalinga Canal which is connected to the California Aqueduct. The Coalinga Canal is the source of much of the water used for irrigation of the upper alluvial fan areas. Streambed sediment in this interval of Los Gatos Creek has an asbestos concentration of approximately less than 1% as indicated by the PLM results of streambed sediment samples SS3 and SS4.



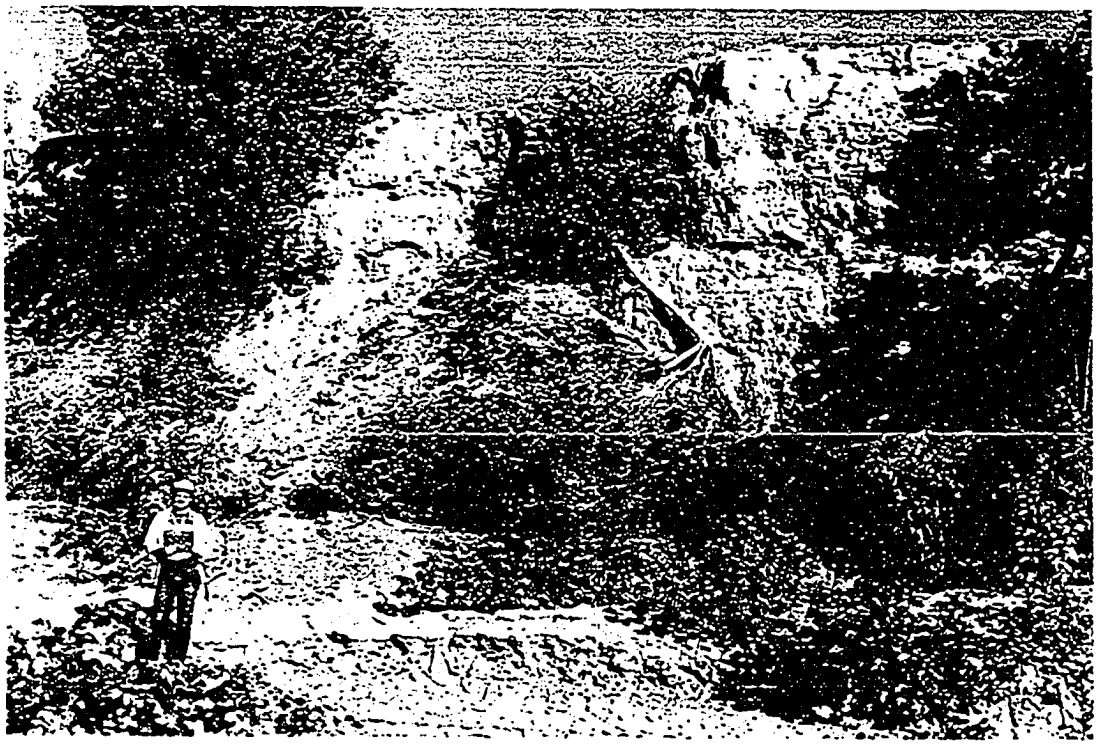
Reproduced with permission of the copyright owner. Further reproduction prohibited without permission.

Photo 86. Close up aerial photo of the juncture of Los Gatos and Zapato-Chino Creeks. This photo shows the braided streambed deposits of both channels which are subject to scouring and cut and fill depositional processes. The scouring and cut and fill processes tend to winnow the fine silt and clay sized sediments. The fine silt and clay sediments are then transported downstream.



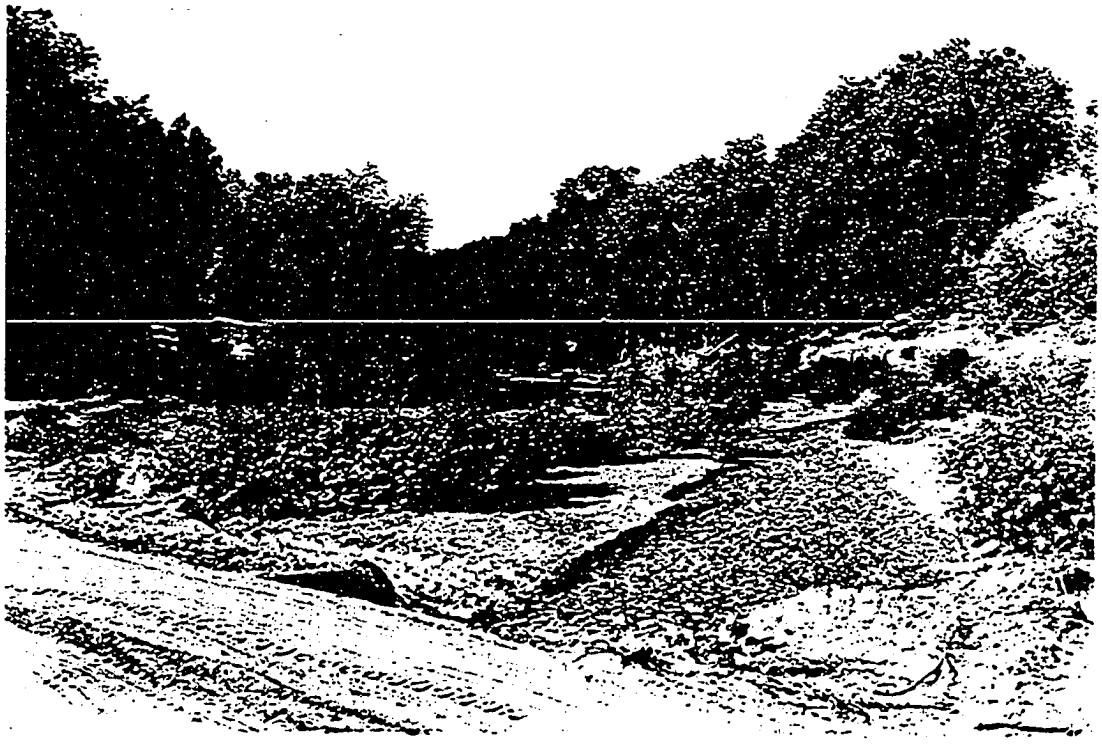
Reproduced with permission of the copyright owner. Further reproduction prohibited without permission.

Photo 87. Arroyo Pasajero channel near Butte Avenue approximately three miles east of Interstate Five. In this upper alluvial fan area, the Arroyo Pasajero is entrenched approximately twenty five to thirty five feet. The intermittent channel may be downcutting through the fine grained silt and sand sized sediment of the Tulare Formation (Pliocene-Pliestocene).



Reproduced with permission of the copyright owner. Further reproduction prohibited without permission.

Photo 88. Arroyo Pasajero channel near Butte Avenue approximately three miles east of Interstate Highway 5. Note yellowish-brownish color of fine grained streambed sediments with no visible evidence of the grayish-white asbestos sediment observed in the White Creek watershed (which is located approximately 40 miles upstream from the intersection of Butte Avenue and the Arroyo Pasajero channel). At this location, the concentration of the asbestos in the streambed sediment has been greatly diluted by sediment eroded from other areas of the Arroyo Pasajero watershed.



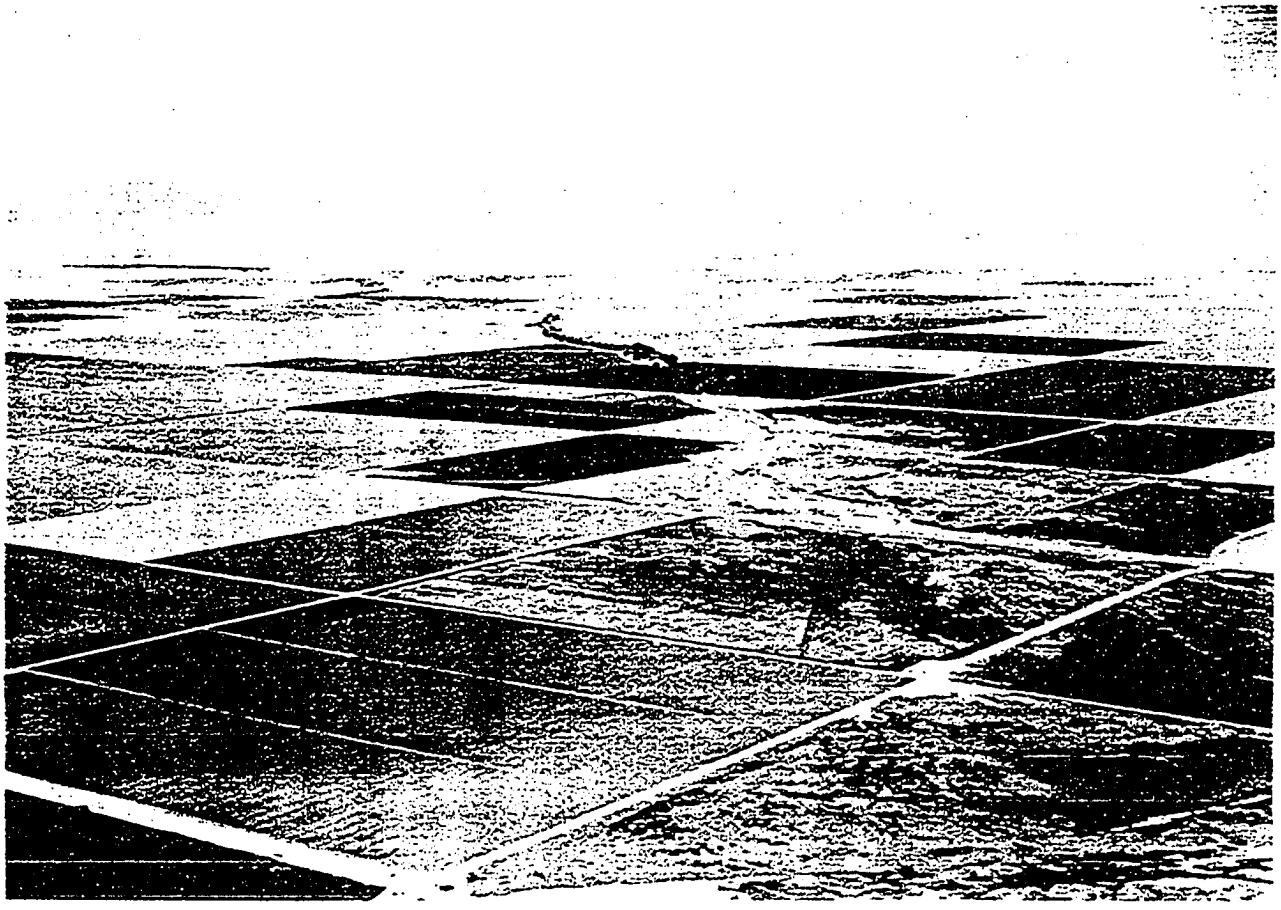
Reproduced with permission of the copyright owner. Further reproduction prohibited without permission.

Photo 89. Reconnaissance aerial photograph showing entrenched channel of the Arroyo Pasajero on the upper alluvial fan located approximately three to four miles downstream from the juncture of Los Gatos Creek with Zapato-Chino Creek. Apparent channel in the middle of the picture is probably an abandoned irrigation channel.



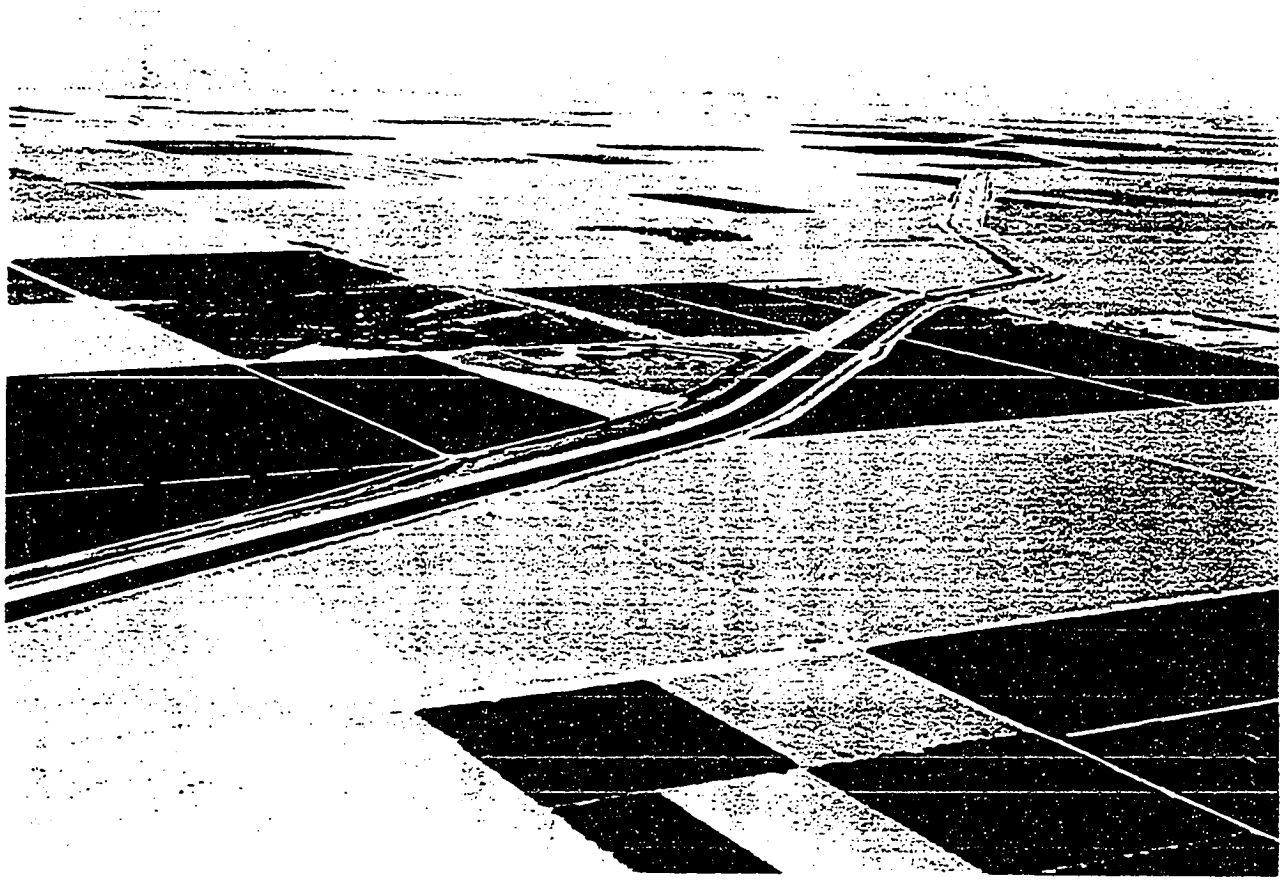
Reproduced with permission of the copyright owner. Further reproduction prohibited without permission.

Photo 90. Reconnaissance aerial photograph showing braided channel terminus of the Arroyo Pasajero channel on the northwest side of Huron. At this medial to upper alluvial fan location, fine grained alluvial fan sediments are deposited by sheet and flood flow processes.



Reproduced with permission of the copyright owner. Further reproduction prohibited without permission.

Photo 91. Reconnaissance aerial photograph showing flood waters in settling basin constructed adjacent to and upslope from the California Aqueduct. Earthen weir structure that restricts the northeastward flow of the Arroyo Pasajero floodwaters is barely visible in the center of the picture. This weir structure has been partly constructed from sediment removed from the settling basin. The Big Blue Hills are barely visible in the hazy background. Flow in the Aqueduct is towards the left.



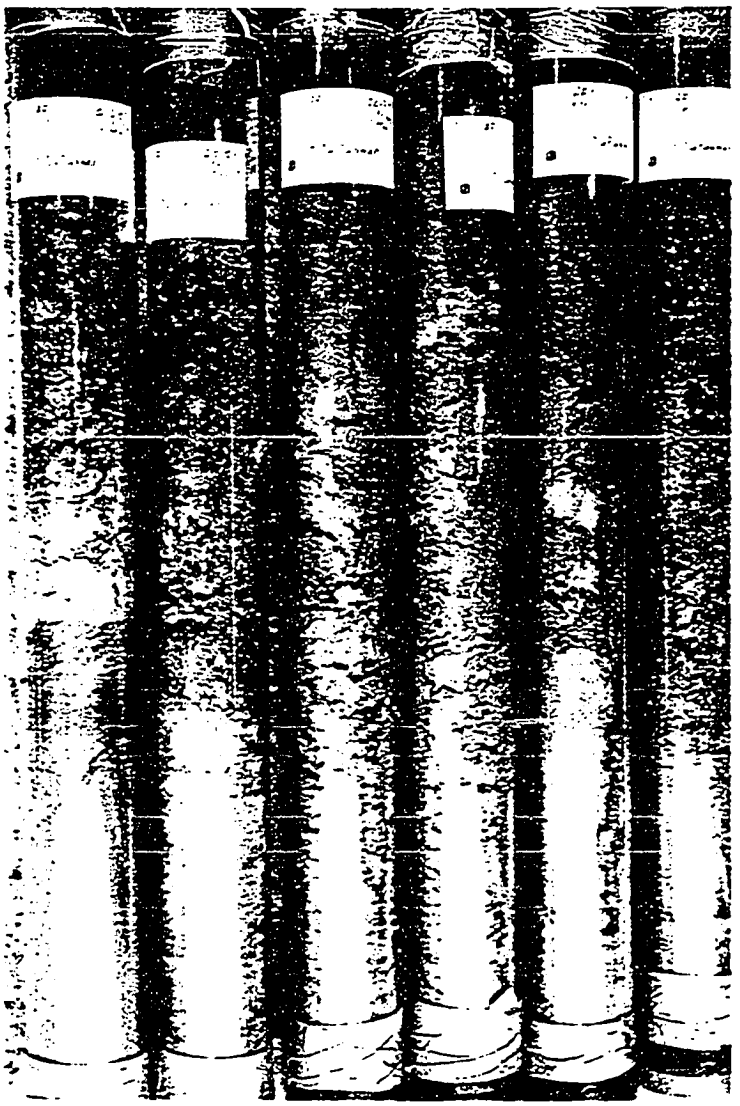
Reproduced with permission of the copyright owner. Further reproduction prohibited without permission.

Photo 92. Close up photo of fine grained silty clay material deposited in a medial to distal alluvial fan environment on the east side of the California Aqueduct. The high clay content of the soil is indicated by the deep mud cracks. There is no visible evidence of asbestos in this alluvial fan deposit.



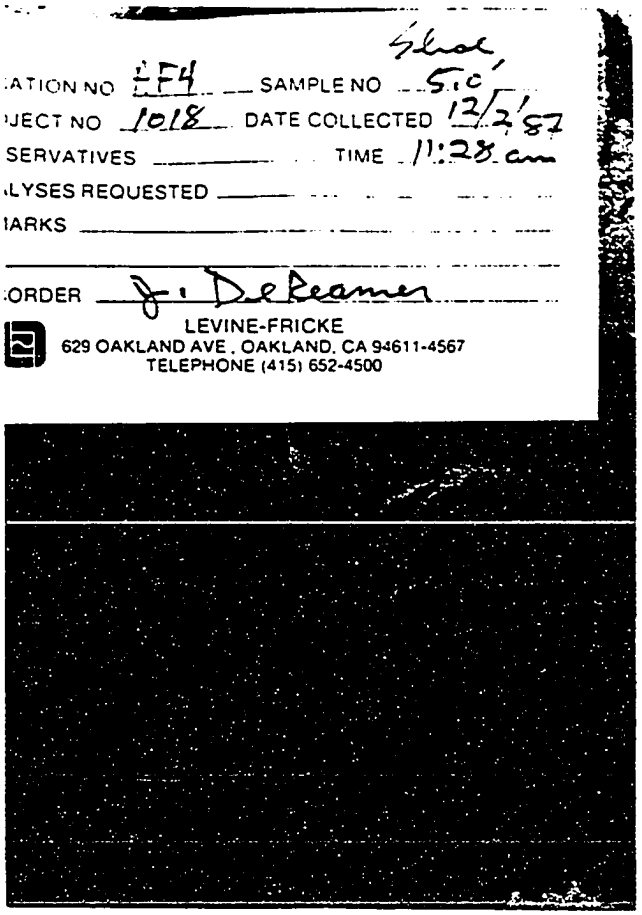
Reproduced with permission of the copyright owner. Further reproduction prohibited without permission.

Photo 93. Continuously cored soil boring from alluvial fan boring station AF-1 located on the east side of the California Aqueduct. Encountered sediments are mostly fine grained silts and clays with little or no visible evidence of stratified layering. See lithologic log for boring AF-1 in Appendix C.



Reproduced with permission of the copyright owner. Further reproduction prohibited without permission.

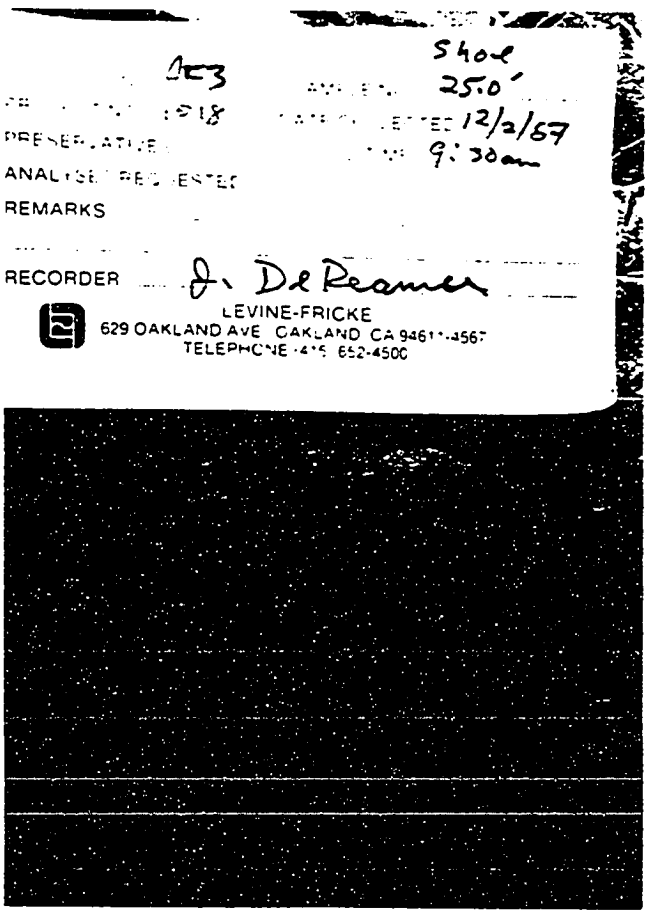
Photo 94 and 95. Close up photos of silty clay material sampled from alluvial fan boring AF-4 at a depth of five feet. There is no visible evidence of asbestos in this sample.

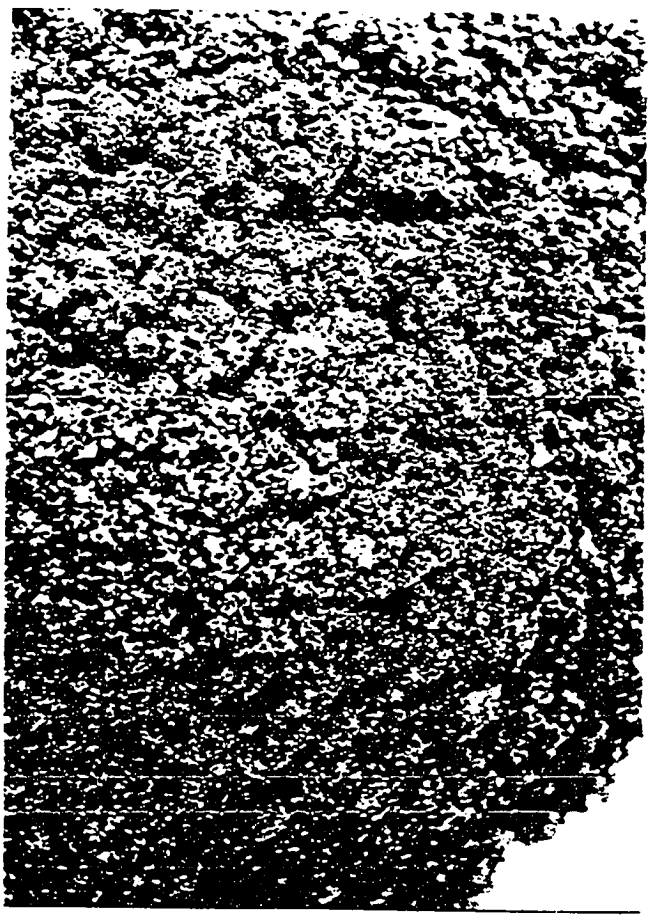




Reproduced with permission of the copyright owner. Further reproduction prohibited without permission.

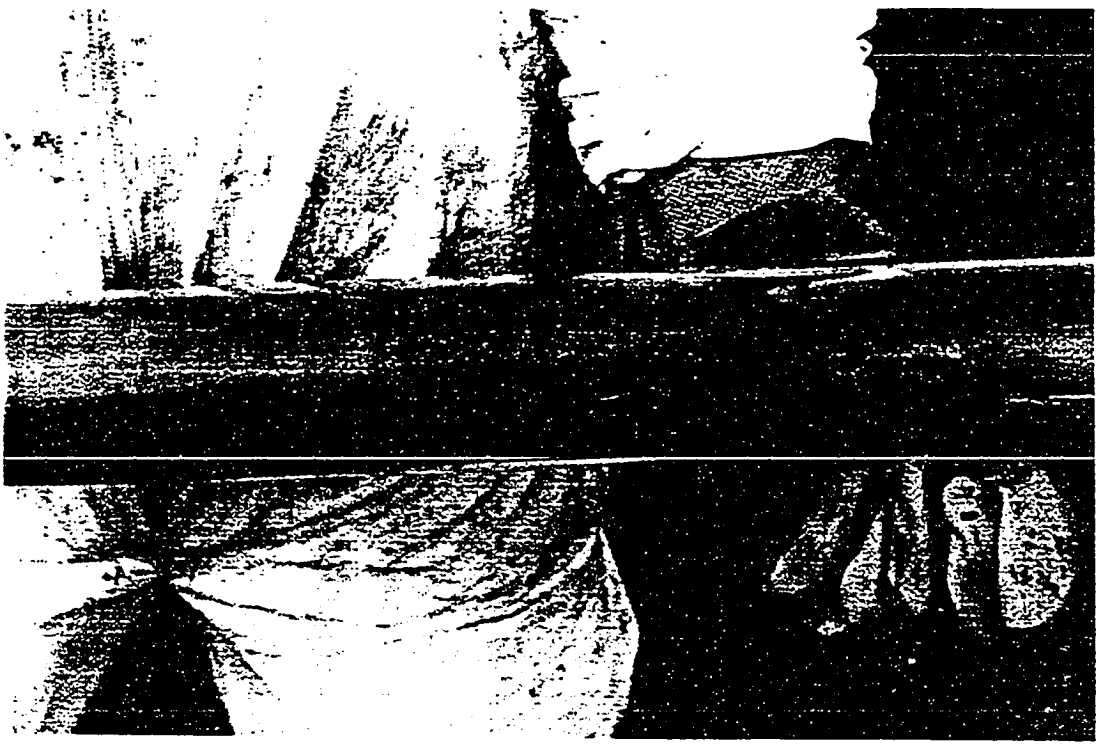
Photos 96 and 97. Close up photos of sandy interval from alluvial fan boring station AF-3 sampled from a depth of 25.0 feet. Sampled interval includes approximately two to three percent serpentine pebbles and a trace of lathe-shaped grains that are pale white to pale green in color. Serpentine pebbles range from 1/8 to 3/8 inch diameter. The coarse grain size indicates that these sediments were probably deposited by an old stream channel.





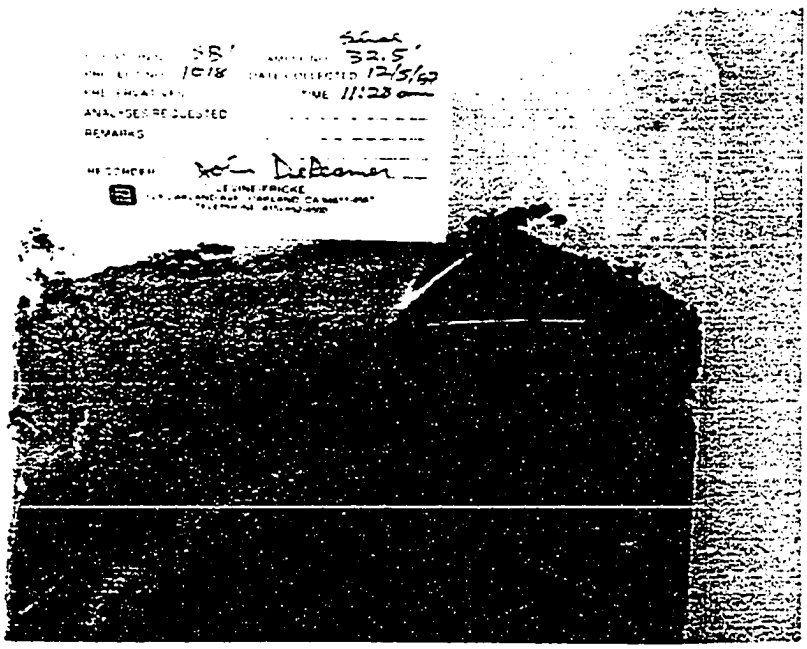
Reproduced with permission of the copyright owner. Further reproduction prohibited without permission.

Photo 98. Alluvial fan boring AF-5 showing "fluffy" sandy interval at a depth of approximately 13 feet. Other than a "fluffy" texture, there was no visible evidence of asbestos in the encountered sediments.



Reproduced with permission of the copyright owner. Further reproduction prohibited without permission.

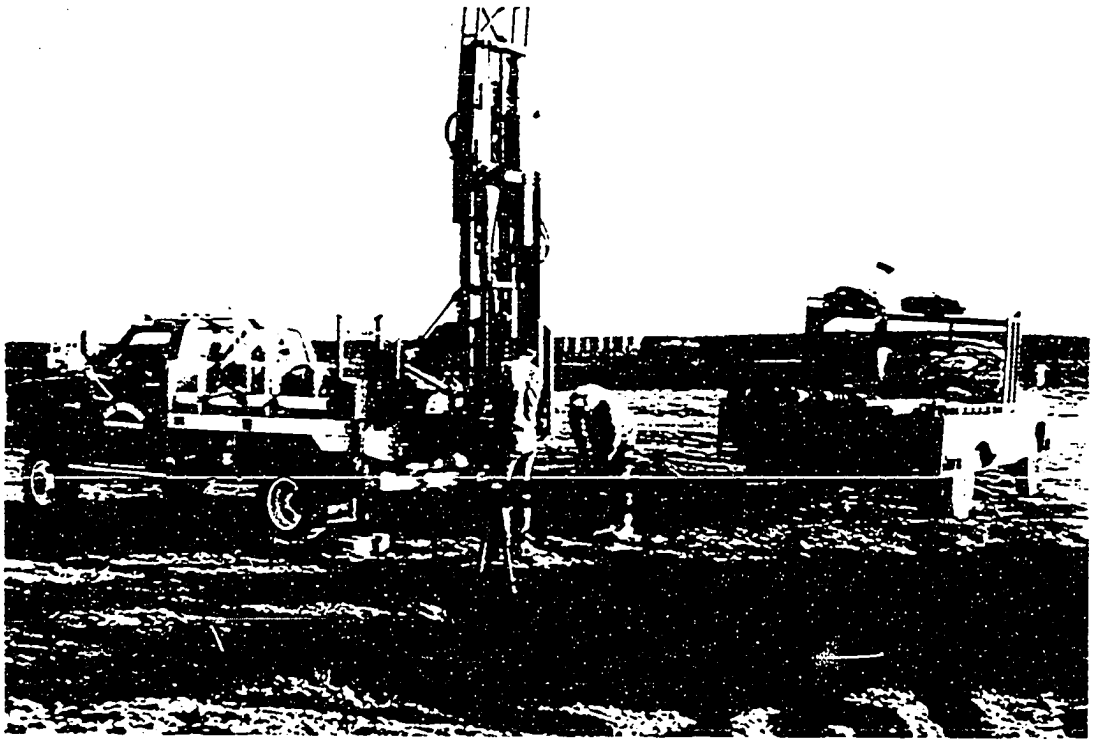
Photos 99 and 100. Silty sand sampled from settling basin boring SB-1 at a depth of 32.5 feet. There is no visible evidence of asbestos sediment in this sample.





Reproduced with permission of the copyright owner. Further reproduction prohibited without permission.

Photo 101. Settling basin boring station SB-2 with drill rig setting up in close proximity to the levy of the California Aqueduct which is visible in the background of photo.



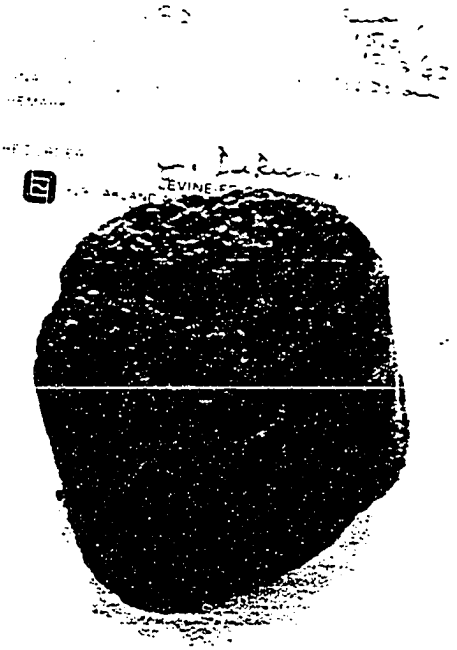
Reproduced with permission of the copyright owner. Further reproduction prohibited without permission.

Photo 102. Distilled water rinsing of core barrel "shoe" after scrubbing with an Alconox solution. This was standard procedure for alluvial fan subsurface soil sampling.



Reproduced with permission of the copyright owner. Further reproduction prohibited without permission.

Photo 103. Sample of stiff silty clay material encountered at a depth of 15 feet in settling basin boring SB-2. There is no visible evidence of asbestos sediment in this sample.



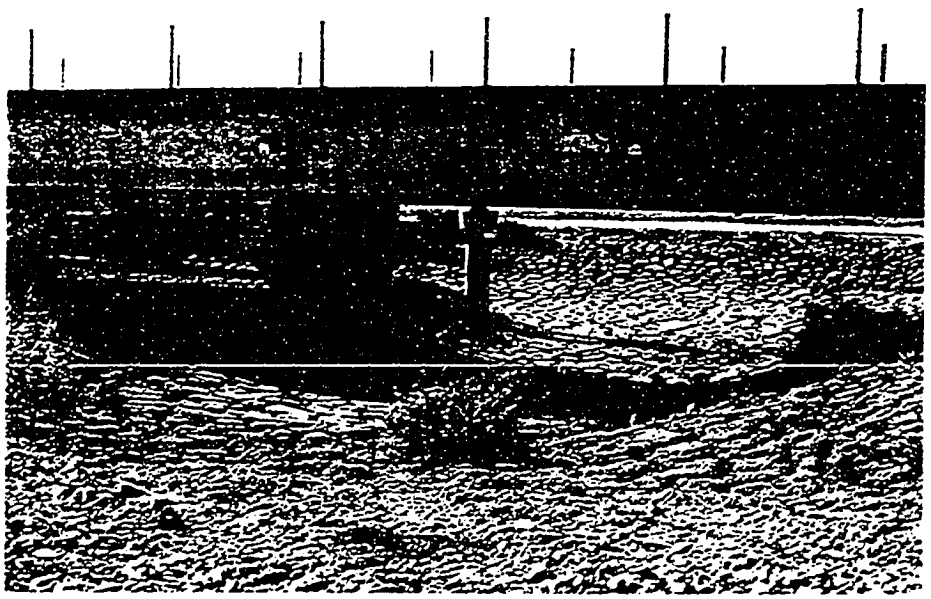
Reproduced with permission of the copyright owner. Further reproduction prohibited without permission.

Photo 104. This photo features the sediment that has been deposited in the settling basin area adjacent to and upslope from the California Aqueduct on the east side of Huron. The area appears to have recently been tilled and/or disked as indicated by the broken up soil. The sediment is generally yellowish brown with a high clay content and no visible evidence of asbestos. This is similar to the material that has been excavated from the settling basin in previous years. This photo (and Photos 105 and 106) was taken in August of 1987.



Reproduced with permission of the copyright owner. Further reproduction prohibited without permission.

Photo 105. This photo features the occurrence of deep mud cracks (more than 3 feet deep) that have formed in the sediment deposited near the Southern Pacific Railroad crossing over the Aqueduct. The deep mud cracks have formed from dewatering of the silty clay to clay sized sediments that have been deposited in the settling basin.



Reproduced with permission of the copyright owner. Further reproduction prohibited without permission.

Photo 106. This photo features a close up of the sediment that has been deposited in the settling basin near the Southern Pacific Railroad tracks and the Aqueduct. The sediment is mostly clay with no visible evidence of asbestos. The high clay content is indicated by the occurrence of the exceptionally large mud cracks which are three to four feet deep and several inches wide. Mud cracks of this size generally do not occur in silt and sand deposits.



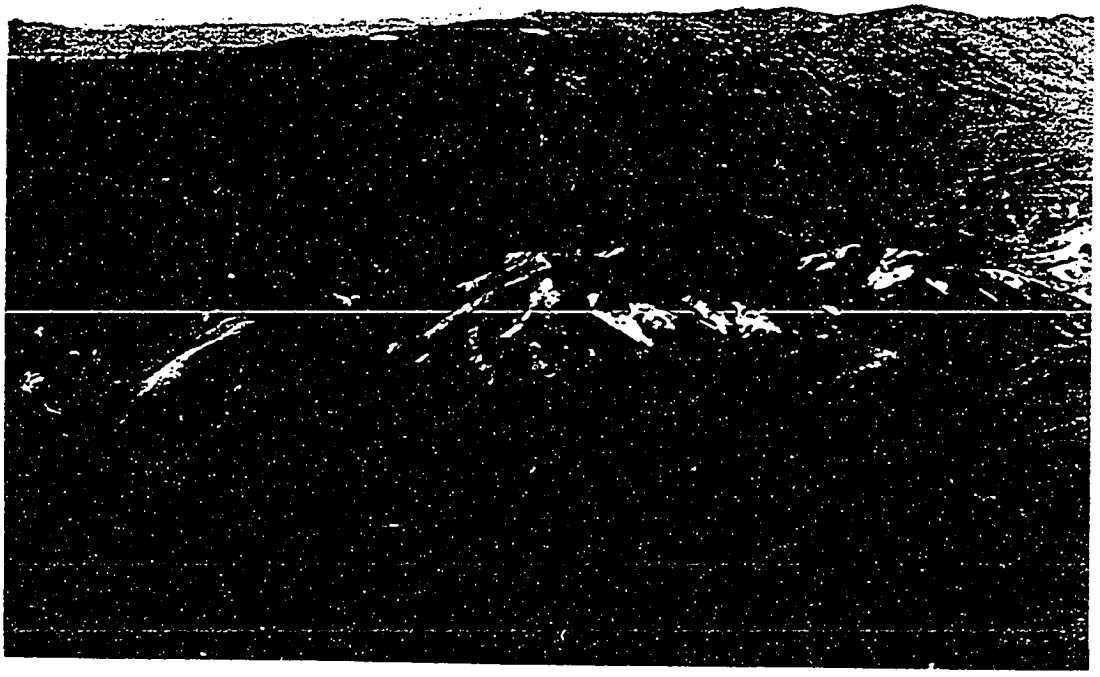
Reproduced with permission of the copyright owner. Further reproduction prohibited without permission.

Photo 107. Steeply sloping outcrop of the asbestos-containing Big Blue Member of the Temblor Formation as exposed in the Big Blue Hills on the north side of Coalinga. This asbestos-rich sedimentary formation is informally referred to as the "Big Blue". As illustrated in this picture, this soft, weakly consolidated formation mostly consists of detrital serpentinite debris that is susceptible to gully erosion and hillside slumping and mass wasting.



Reproduced with permission of the copyright owner. Further reproduction prohibited without permission.

Photo 108. Outcropping of the poorly vegetated Big Blue Member on the north side of Coalinga on the western margin of the San Joaquin Valley. Two asbestos mines located in the New Idria Formation on Joaquin Ridge are visible as white patches near the center horizon of the picture. The Joaquin Ridge area is located approximately eight miles west of the "Big Blue" outcrop.



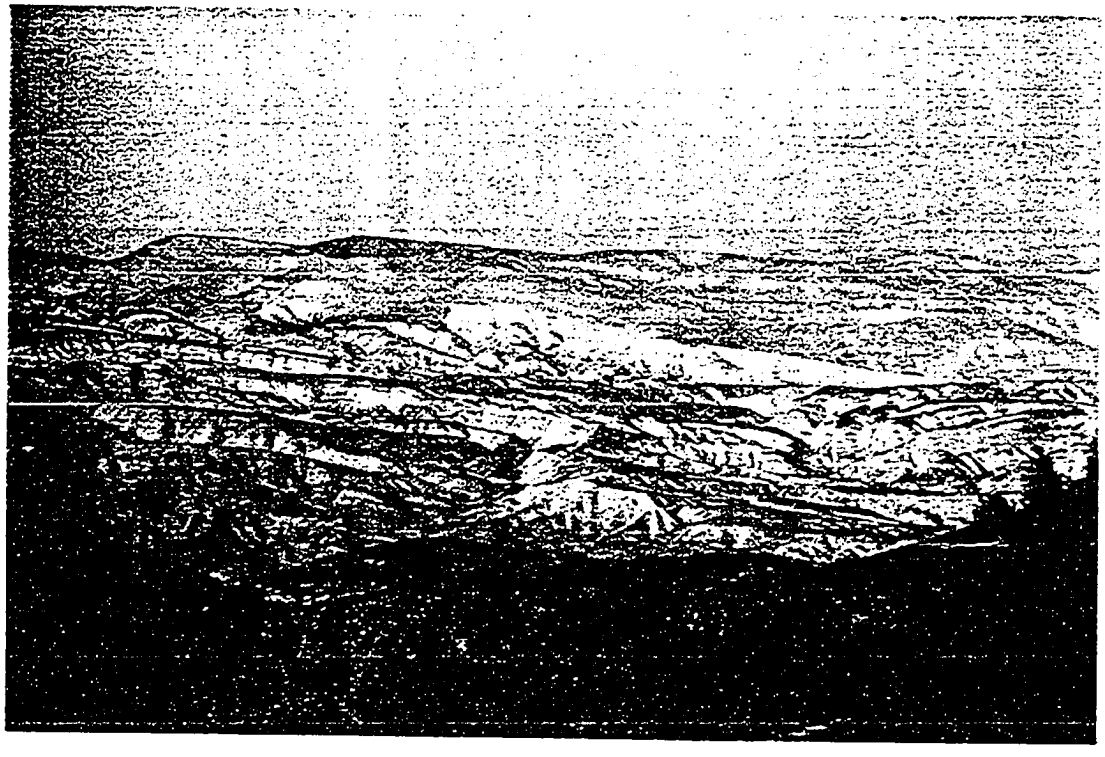
Reproduced with permission of the copyright owner. Further reproduction prohibited without permission.

Photo 109. In the Coalinga area, outcrops of the Big Blue Member are drained by the Martinez, Salt, and Cantua Creek intermittent stream systems. Some of these streams, such as Salt Creek illustrated in this picture, have cut deep gorges through this sedimentary serpentinite formation. Asbestos-containing sediment eroded from the Big Blue Member is be transported a short distance to the Cantua Creek and Salt Creek alluvial fans.



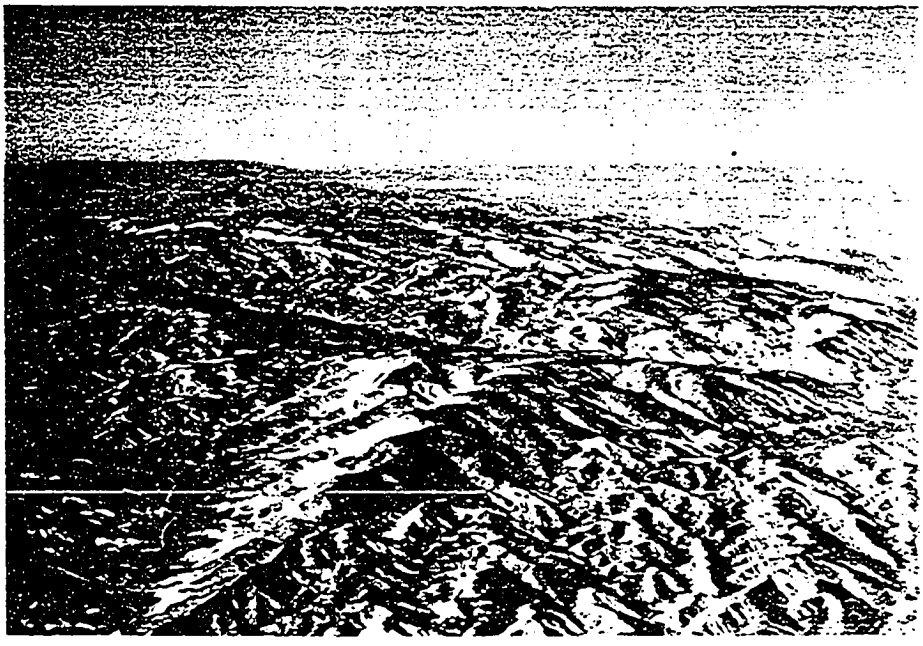
Reproduced with permission of the copyright owner. Further reproduction prohibited without permission.

Photo 110. Steeply sloping outcrops of the Big Blue Member and other undifferentiated sedimentary formations on the northeast side of the Joaquin Ridge Anticline. As illustrated, these generally unconsolidated, asbestos-containing formations are poorly vegetated and are highly susceptible to erosion and mass wasting. Much of this area is best characterized as "badlands".



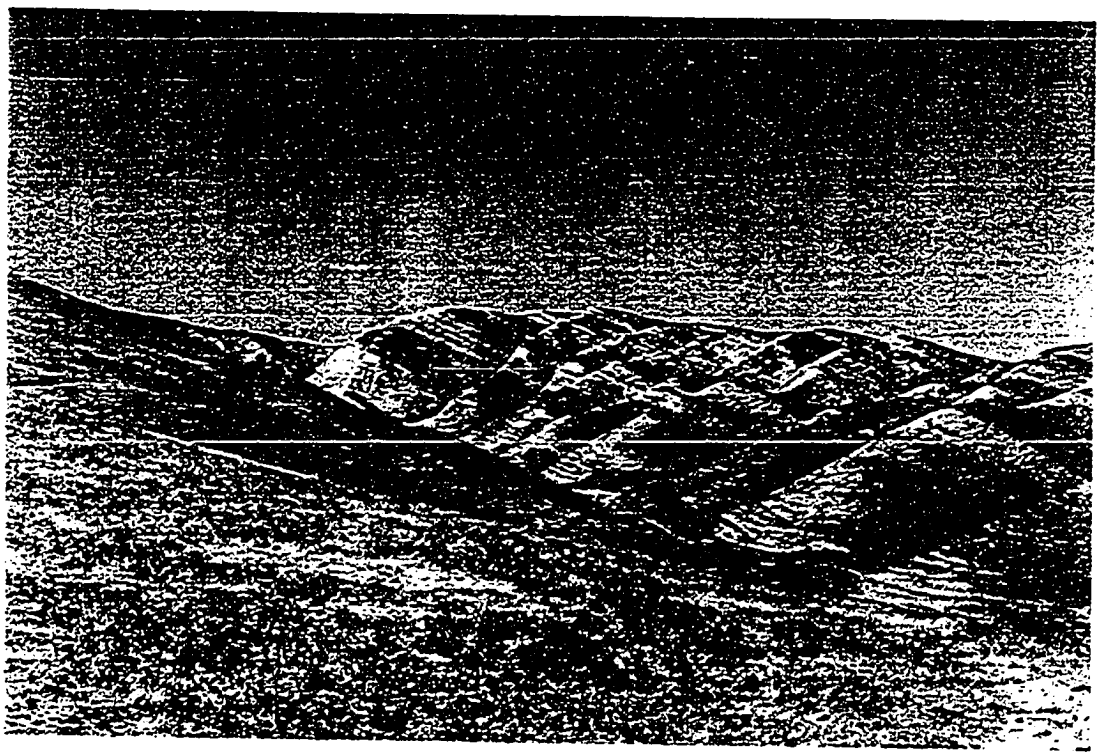
Reproduced with permission of the copyright owner. Further reproduction prohibited without permission.

Photo 111. "Badlands" complex formed by the Big Blue Member and other undifferentiated asbestos-containing sedimentary formations in the Cantua Creek and Arroyo Hondo watersheds. Cantua Creek is located in the lower left quadrant of this picture.



Reproduced with permission of the copyright owner. Further reproduction prohibited without permission.

Photo 112. Steeply dipping strata of the monoclinal structure that forms the western margin of the San Joaquin Valley on the north side of Coalinga. Strata are dipping to the east approximately 20 to 30 degrees. Because of this structure, the poorly consolidated sedimentary formations - including the Big Blue Member - are highly susceptible to erosion and mass wasting.



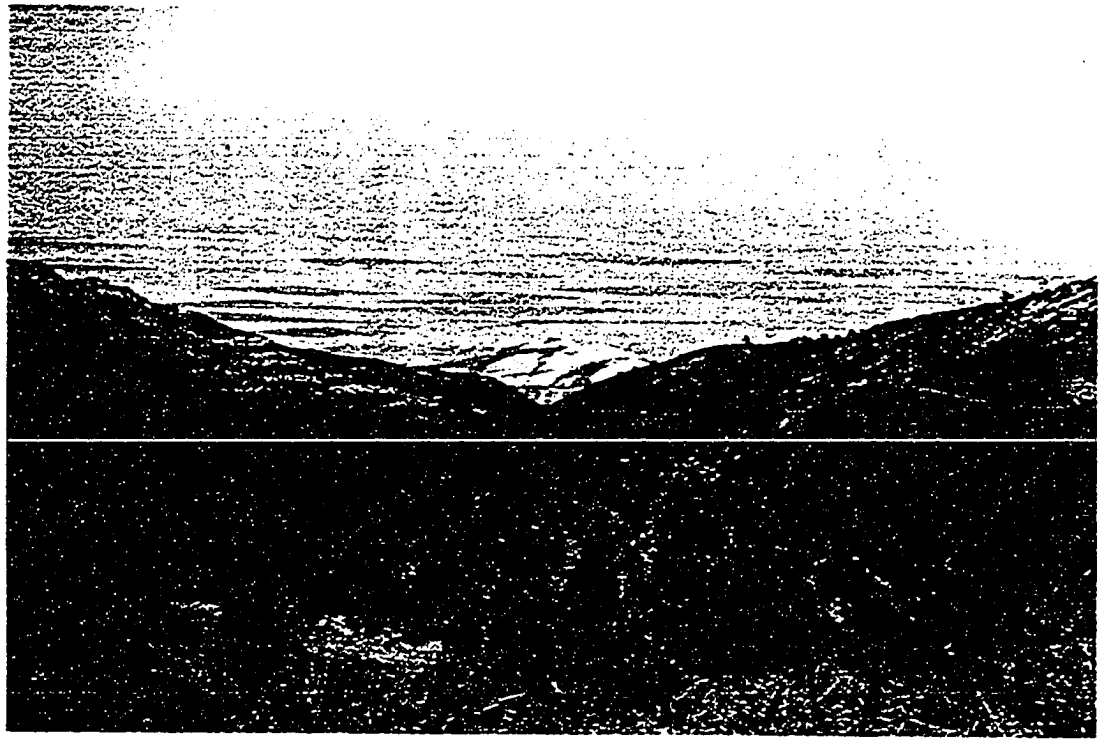
Reproduced with permission of the copyright owner. Further reproduction prohibited without permission.

Photo 113. This photo features a regional perspective of the Big Blue Hills and their relationship to the agricultural fields on the western margin of the central San Joaquin Valley. This picture was taken from Wright Mountain located on Joaquin Ridge. The Big Blue Hills featured in the distance near the center of the picture are approximately 8 miles away. Cantua Creek is barely visible as a meandering channel in the upper right quadrant.



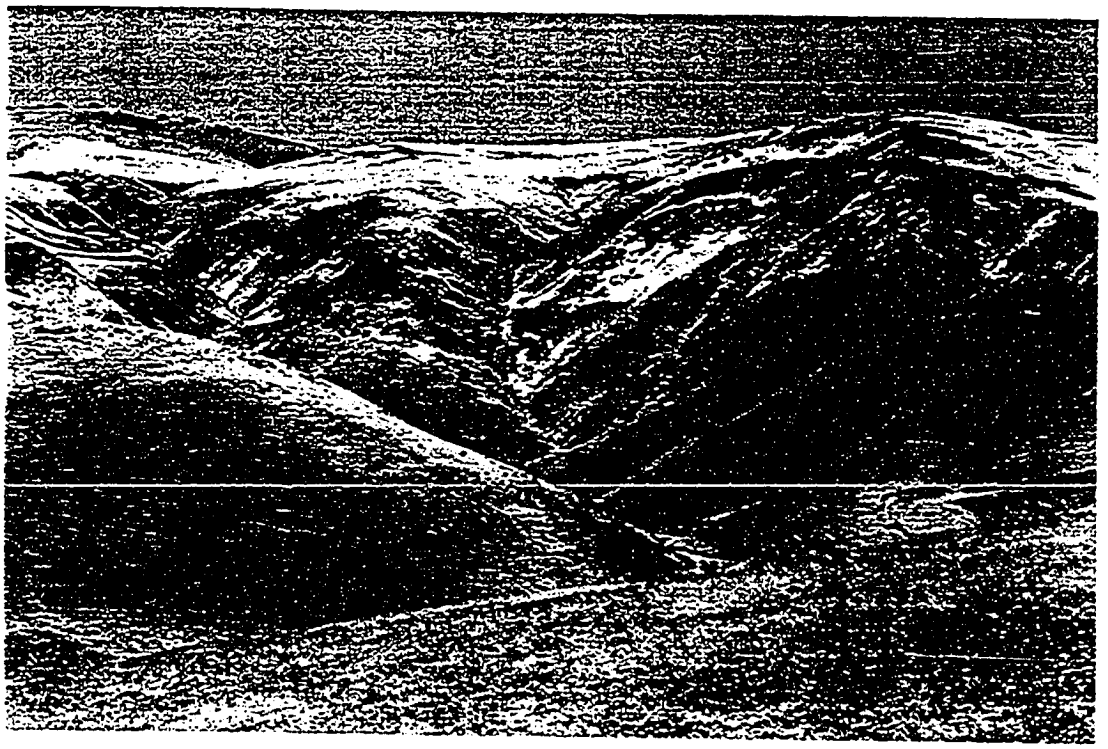
Reproduced with permission of the copyright owner. Further reproduction prohibited without permission.

Photo 114. This photo features an outcropping of the Big Blue Member as exposed on the western flank of the Big Blue Hills. This photo was taken from Wright Mountain near the crest of Joaquin Ridge. The Big Blue Hills are located approximately 8 miles to the east of Wright Mountain. The cultivated fields of the Cantua Creek alluvial fan are visible in far background.



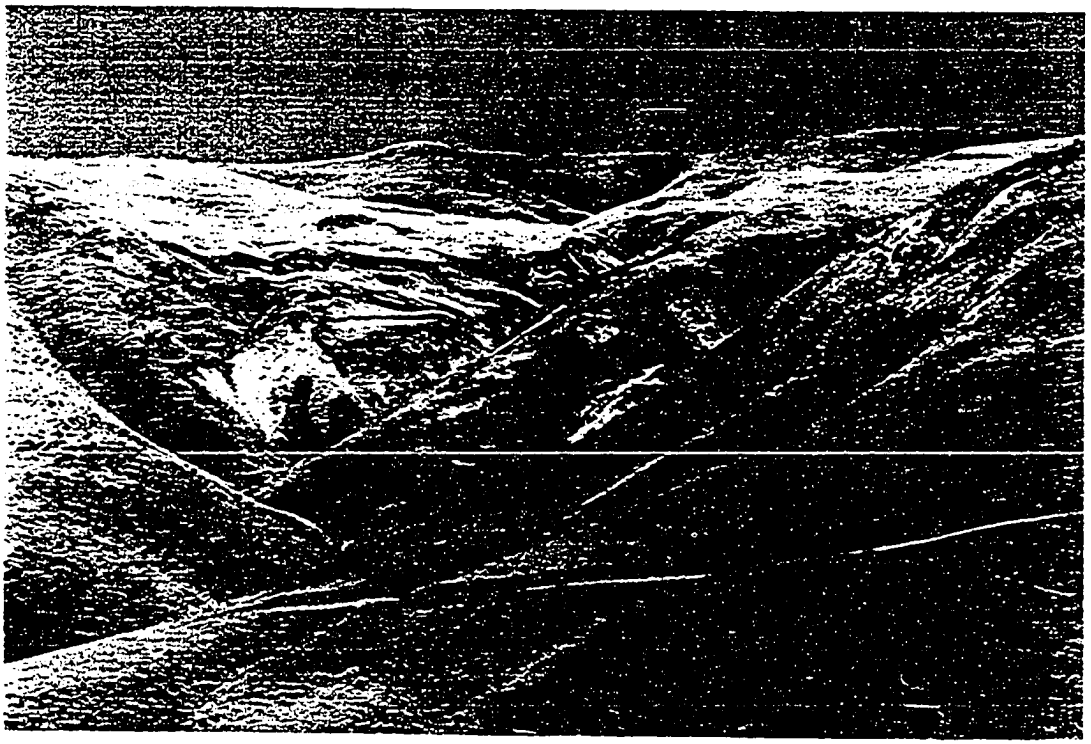
Reproduced with permission of the copyright owner. Further reproduction prohibited without permission.

Photo 115. Slumping hillside exposure of the asbestos-containing Big Blue Member in the Martinez Creek watershed area. In some areas, these hillside exposures are susceptible to severe gullying.



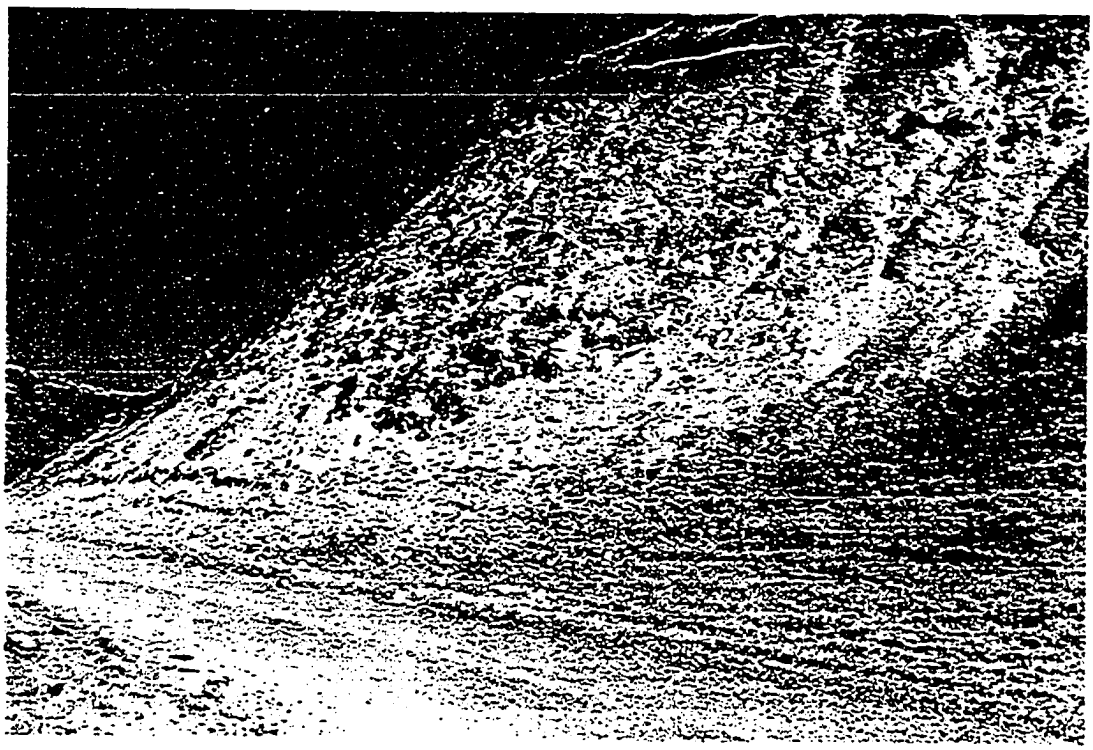
Reproduced with permission of the copyright owner. Further reproduction prohibited without permission.

Photo 116. Slumping hillside exposure of the Big Blue Member as exposed on the eastern flanks of the Big Blue Hills. Overgrazing in this area has contributed to increased erosion and slumping of the asbestos-containing sedimentary formations.



Reproduced with permission of the copyright owner. Further reproduction prohibited without permission.

Photo 117. Erosional outcrop of the Big Blue Member in the Cantua Creek watershed. The intermittent streambed of Cantua Creek is shown at the base of this outcrop in the lower left of Photo 118.



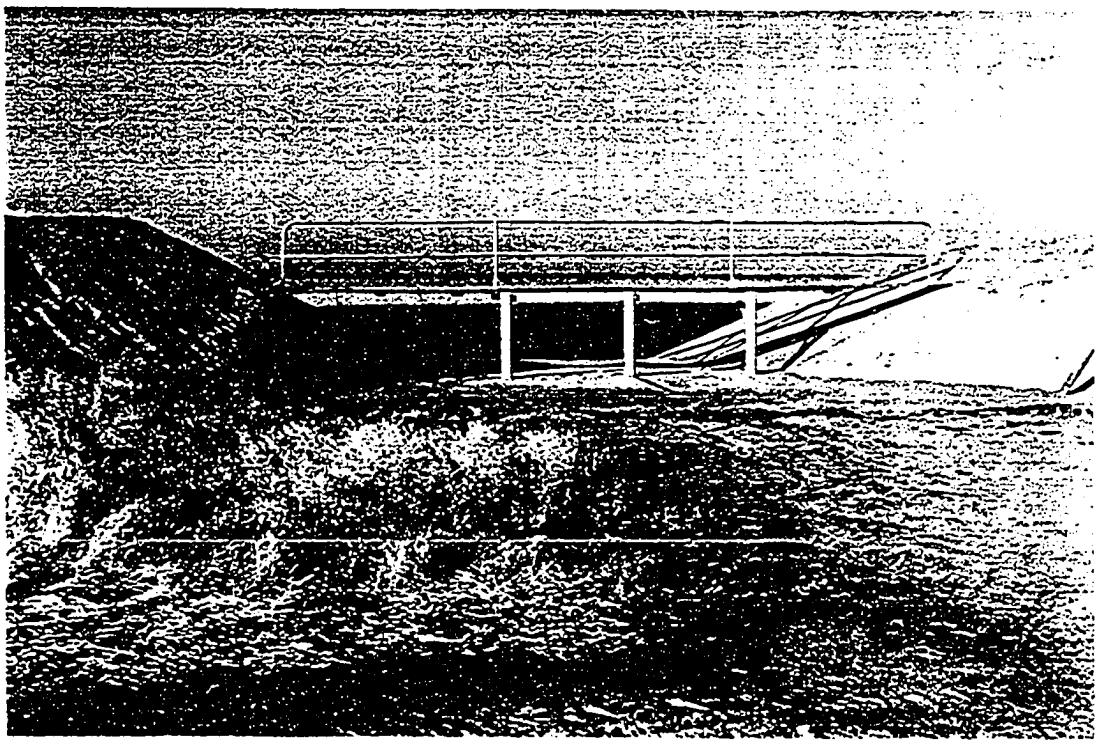
Reproduced with permission of the copyright owner. Further reproduction prohibited without permission.

Photo 118. Erosional outcrop of the Big Blue Member in the Cantua Creek watershed. This outcrop forms the streambank of Cantua Creek which flows at the base of this deposit.



Reproduced with permission of the copyright owner. Further reproduction prohibited without permission.

Photo 119. Ungated inlet structure to the California Aqueduct which is designed to capture runoff from the intermittent Cantua Creek.

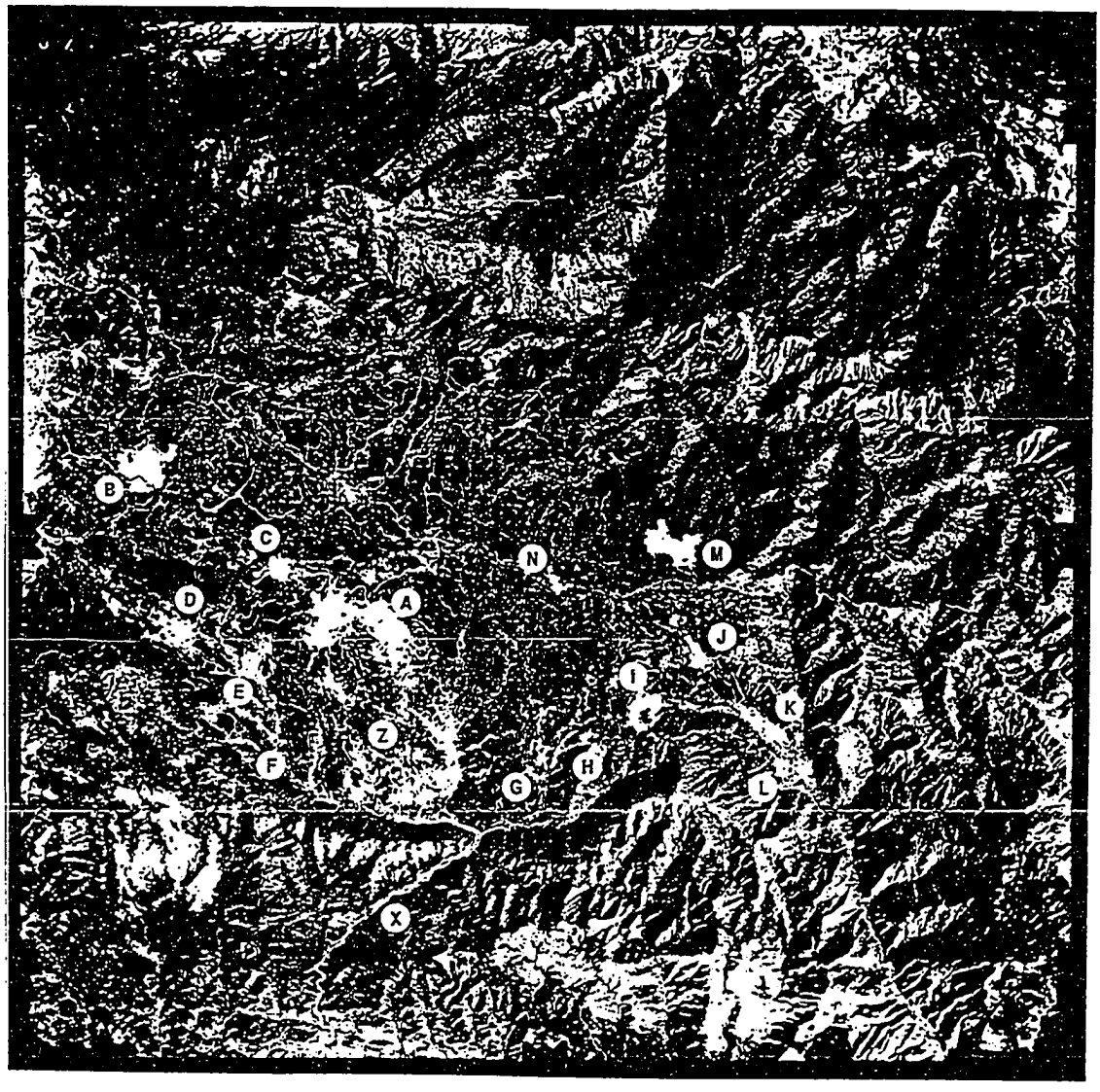


Reproduced with permission of the copyright owner. Further reproduction prohibited without permission.

APPENDIX B

AERIAL PHOTOGRAPHY AND INTERPRETATIONS

Reproduced with permission of the copyright owner. Further reproduction prohibited without permission.



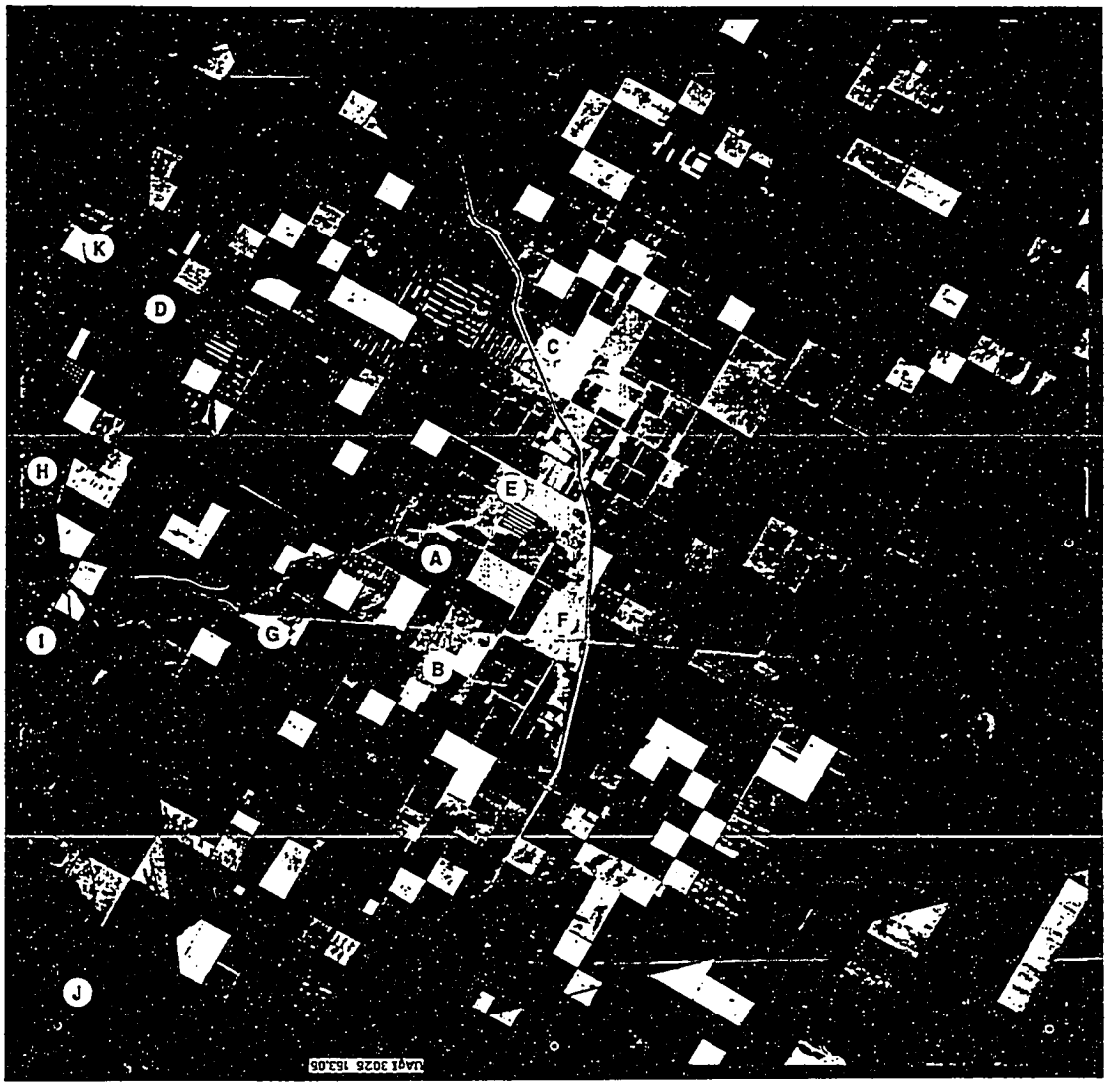
NHAP, August 1, 1981, Flight 81-455, Frame 079, Scale = 1:58,000

Color Infrared Image of Joaquin Ridge

This high altitude, color infrared image features the New Idria Formation serpentinite outcrop areas of the White Creek, Pine Canyon, and Cantua Creek drainages of Joaquin Ridge in western Fresno County. The New Idria Formation outcrops over an elliptically-shaped area (approximately 48 square miles) that forms the crest of Joaquin Ridge (see upper left quadrant of photo). Barren areas affected by mining or naturally occurring erosion appear as yellowish-white in this photo. Mines and other areas of interest are indicated by letters. Serpentinite gullies appear as a network of dendritic drainage channels. Roads appear as thin white lines. Vegetation in the serpentinite outcrop area appears as red and bluish-green. A high resolution enlargement of this image was used for numerical modelling of erosion in the White Creek and Pine Canyon drainages.

Explanation: A - Atlas Mine and Mill; B - Union Carbide Mine; C - Basic Resources Mine; D - Big Ridge Mine; E - Tromby Mines; F - White Creek Magnesite Mine; G - Archer Mine; H - James, Corbett, Byles Mine; I - Butler Estate Chromite Mine; J - Jensen Mine; K - Coalinga Asbestos Mill; L - Railroad Mine; M - Christie Mine; N - Unknown Mine. White Creek is indicated by X and some of the serpentinite gullies are near Z. Pine Canyon Creek is not visible without magnification. The thin white line leading from Upper Pine Canyon is a road and not a streambed.

Reproduced with permission of the copyright owner. Further reproduction prohibited without permission.



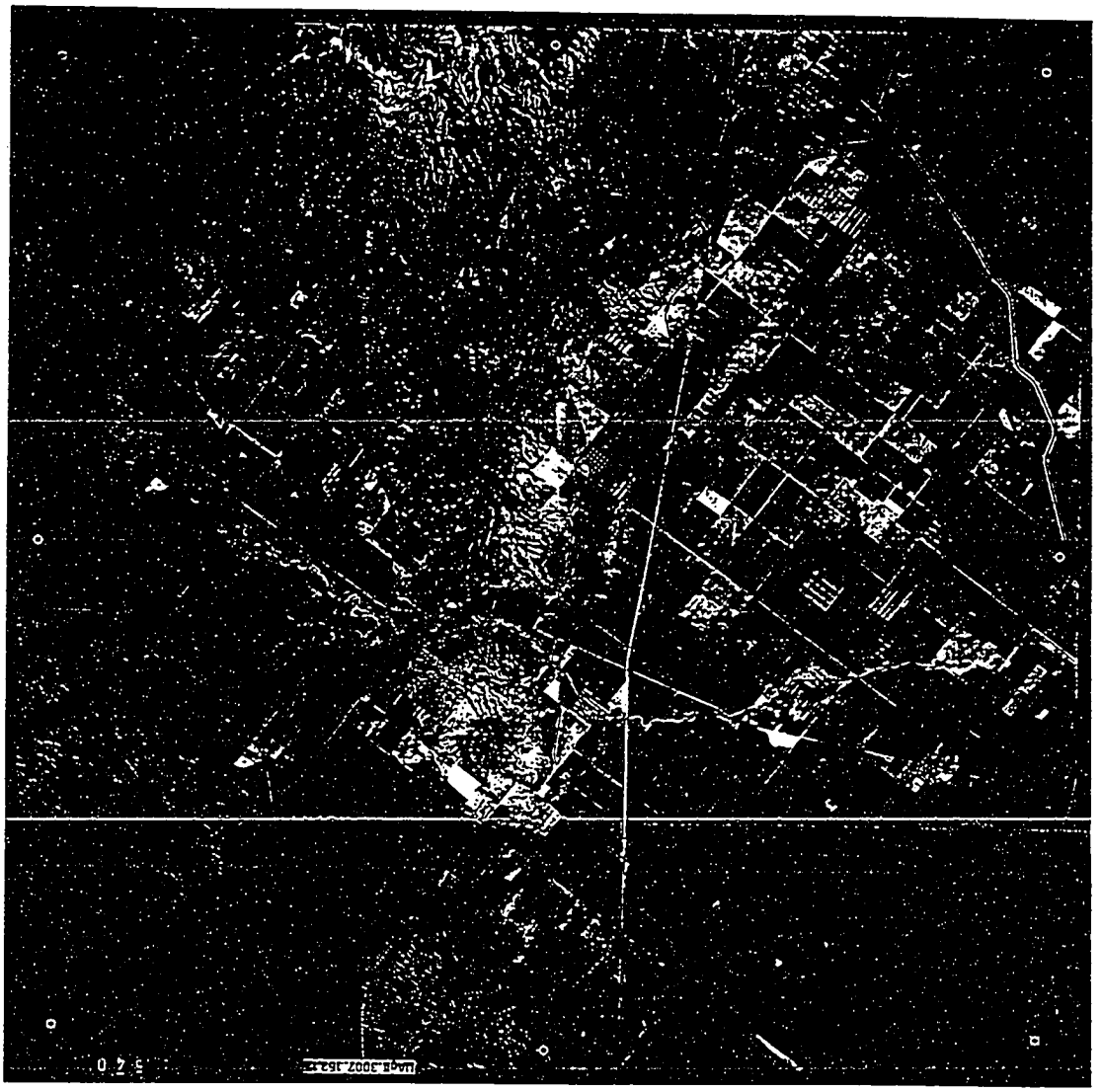
NASA, June 14, 1979, Flight 79-076, Frame 6584, Scale = 1:65,000

Color Infrared Image of Arroyo Pasajero Alluvial Fan

This photo features most of the Arroyo Pasajero alluvial fan including: A - the terminus of the Arroyo Pasajero channel; B - the town of Huron; C - California Aqueduct; D - Interstate Five; E - training dike; F - settling basin; G - railroad tracks (thin line line running east-west); H - Anticline Ridge; I - Guijarral Hills; J - Kettleman Hills; K - Coalinga Canal.

The entrenched channel of the Arroyo Pasajero is visible in the left center of the photo (near the letter G). Areas affected by sedimentation are to the northeast and east of Huron. Most of the upper alluvial fan surface has been cultivated as indicated by the patch-work of irrigated fields. Healthy vegetation appears as red. The Coalinga Canal (thin canal to the west of Interstate Five) provides water for irrigation of the upper and medial alluvial fan farming operations. Le Moore Naval Air Station is partially visible at the right center margin.

Reproduced with permission of the copyright owner. Further reproduction prohibited without permission.

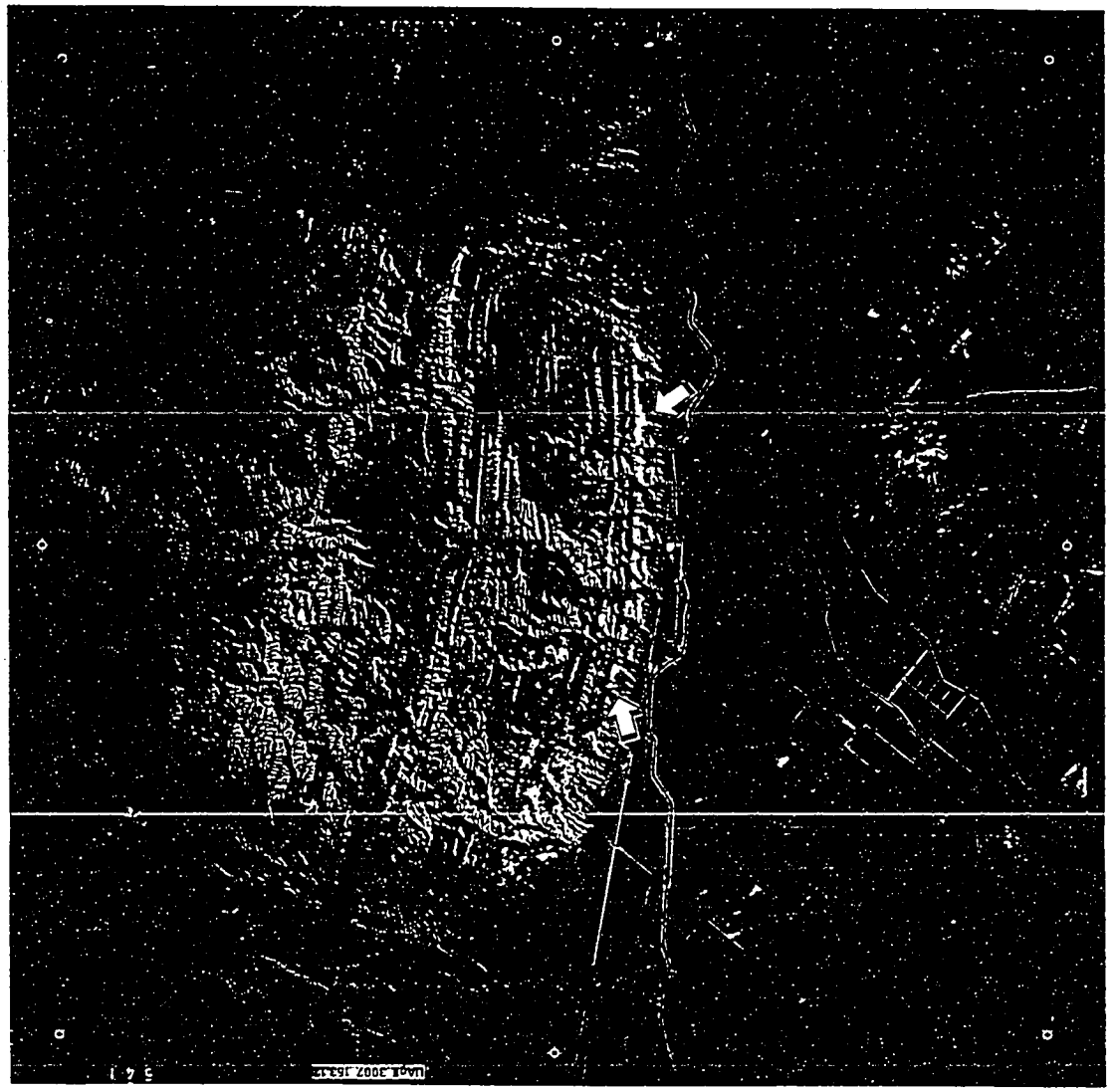


NASA, November 27, 1973, Flight 73-194, Frame 6406, Scale = 1:65,000

Color Infrared Image of Pleasant Valley, Anticline Ridge, and Arroyo Pasajero Alluvial Fan

This photo features the Los Gatos Creek and Arroyo Pasajero intermittent alluvial drainage channel as it flows through Pleasant Valley (left half of photo), across the structural axis of the Coalinga Anticline which is identified by the north-south trend of Anticline Ridge, Guijarral Hills, and Kettleman Hills; and the Arroyo Pasajero alluvial fan and the California Aqueduct (right half of photo). The town of Coalinga is visible at the western margin of Pleasant Valley and the town of Huron is visible in the lower right quadrant of the photo. Interstate 5 highway is on the eastern margin of Anticline Ridge.

Reproduced with permission of the copyright owner. Further reproduction prohibited without permission.



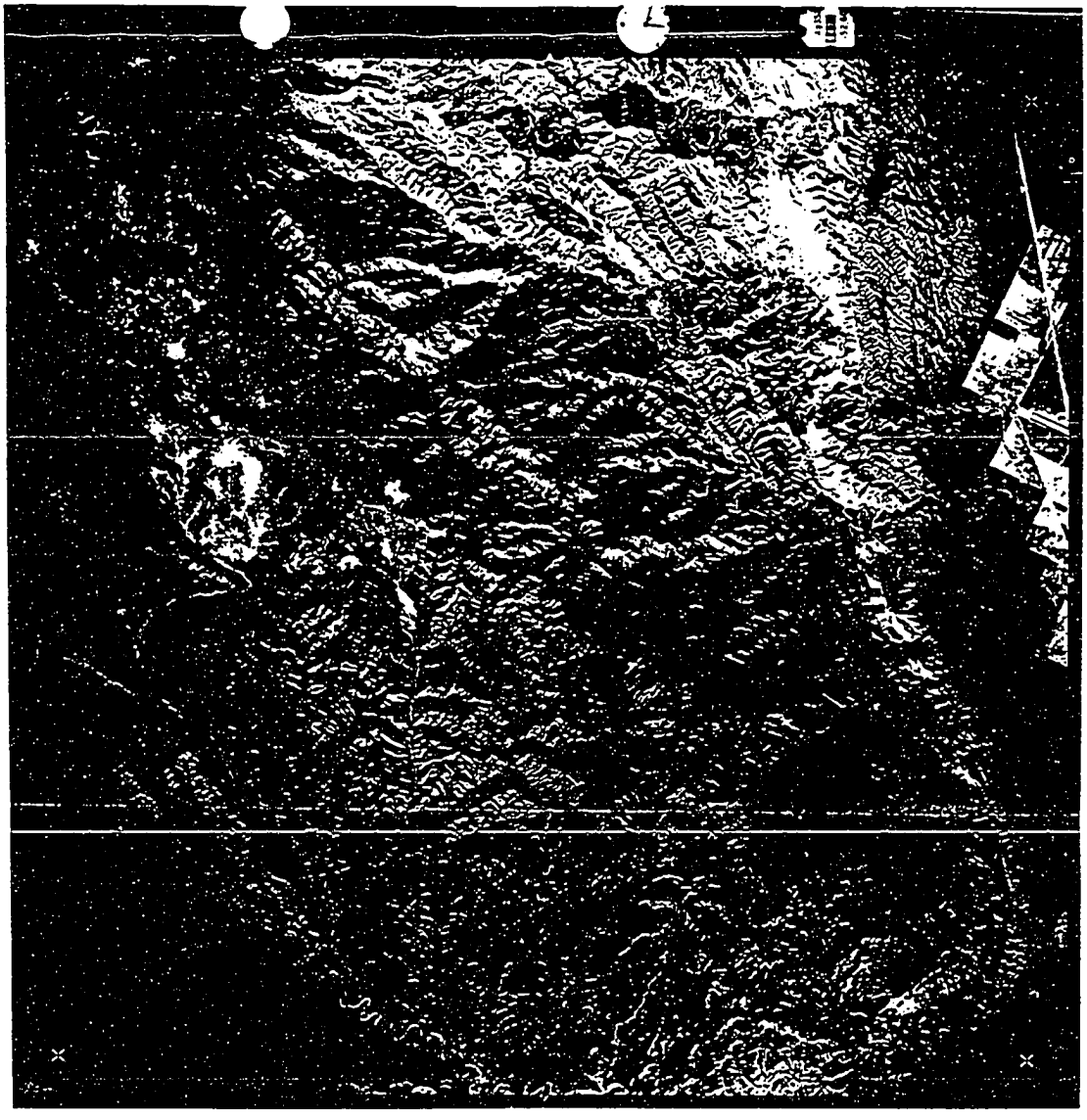
NASA, November 27, 1973, Flight 73-194, Frame 6414, Scale = 1:65,000

Color Infrared Image of Leguna Seca Hills and California Aqueduct

This photo features the California Aqueduct and the uplifted sedimentary formations that form the Leguna Seca Hills just south of the O'Neill Forebay (top center of photo). The uplifted formations adjacent to the Aqueduct (right center of photo) have near-infrared reflectance characteristics that are similar to that of the Big Blue Member of the Temblor Formation as exposed in the Big Blue Hills. The Leguna Seca Hills area is approximately 60 miles north of the Big Blue Hills. Interstate 5 highway is visible as a thin line (running north-south) between the Aqueduct and the foothills.

The geologic units indicated by the arrows probably contain asbestos based on reflectance characterisitics, stratigraphic position, and geologic mapping (Jenkins, 1971) and what is known about the geologic history of the central San Joaquin Valley.

Reproduced with permission of the copyright owner. Further reproduction prohibited without permission.



NASA, April 1, 1971, Flight MSC-164, Frame 3477, Scale = 1:60,000

Color Infrared Image of Joaquin Ridge and Big Blue Hills

Notable features in this picture include part of the New Idria Formation outcrop on the crest of Joaquin Ridge (upper left quadrant), the White Creek, Pine Canyon Creek, Los Gatos Creek drainage pathway leading downstream towards the Arroyo Pasajero (i.e., towards the lower right quadrant), outcrops of the asbestos-bearing Big Blue Member of the Temblor Formation (upper right quadrant), and the apex of the Salt Creek/Cantua Creek alluvial fan on the western margin of the cultivated fields of the San Joaquin Valley (center of right margin). This picture shows the close geographic relationship of the outcrops of the intrusive/extrusive New Idria Formation and the sedimentary Big Blue Member of the Temblor Formation. The distance between the outcrops of the New Idria Formation and the Big Blue Member is approximately eight miles.

In this photo, The New Idria Formation and the Big Blue Member both have a bright bluish white reflectance. The highly reflective serpentinite matrix of disturbed surfaces of the New Idria Formation facilitates identification of mines, tailings, and barren surfaces affected by geologic occurrences of gully erosion. Also visible are hundreds of exploration pits and many miles of exploration access roads. The restricted vegetation that grows on the magnesium-rich serpentinite soils appears as a dark bluish-green that is readily differentiated from the vegetation of non-serpentinite soils.

Note the ribbon of light bluish-gray sediment associated with the White Creek and Los Gatos Creek streambeds. This sediment has the same reflectance characteristics as the serpentinite outcrop of the New Idria Formation and the Big Blue Member. Particularly notable is the absence of similar light bluish-gray reflectance characteristics marking the pathway of Pine Canyon Creek. The visible pathway leading from Upper Pine Canyon is a dirt road and not a streambed. The tailings pile of the Coalinga Asbestos Mill in the east fork of Pine Canyon Creek can be seen as a small sliver of white material that is located approximately one half mile downslope from the lower right (southeastern) margin of the New Idria Formation outcrop. Close examination of the White Creek drainage pathway shows five areas where the streambed appears to widen. These are areas affected by chromite milling operations that were conducted along the banks of White Creek in the 1940's and 1950's.

Reproduced with permission of the copyright owner. Further reproduction prohibited without permission.

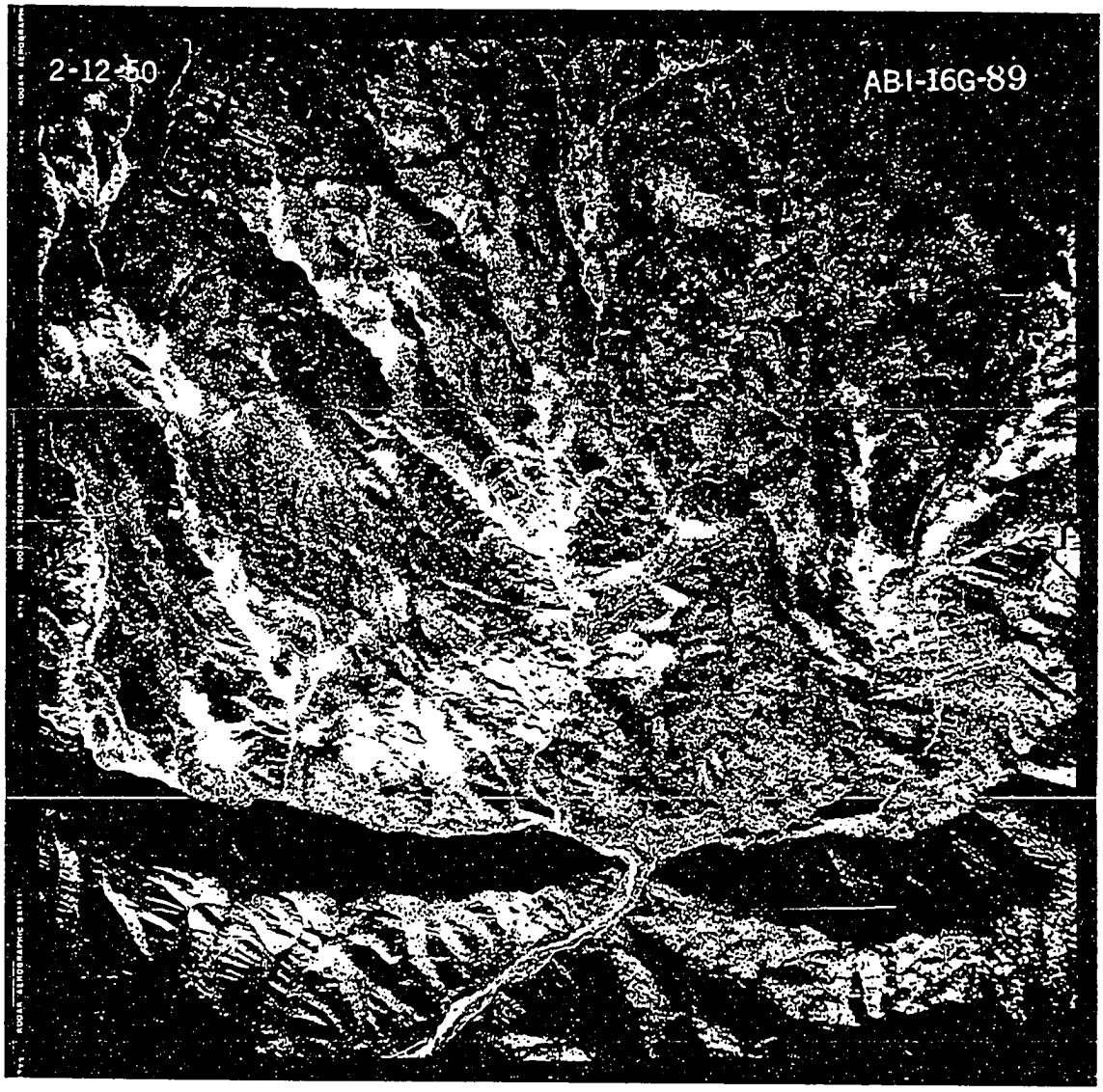


USDA/ABI, February 12, 1950, Flight 1242-50, Frame ABI-13G-57, Scale = 1:20,000

Black and White Image of White Creek Watershed of Joaquin Ridge

This photo features the occurrence of barren areas affected by gully erosion in the western portion of the White Creek drainage of the serpentinite outcrop of the New Idria Formation on Joaquin Ridge. Some of the barren areas may have been affected by mining that occurred prior to the date of this photo. These gullies and barren areas predate the occurrence of asbestos mining operations which began in the early 1960's. The gullies cover approximately 15% to 20% of the serpentinite outcrop area shown in the photo. For reference purposes, the Atlas Mine and Mill was constructed near the area shown in the far upper right corner of the photo. Drainage is downslope towards the bottom of the photo.

Reproduced with permission of the copyright owner. Further reproduction prohibited without permission.

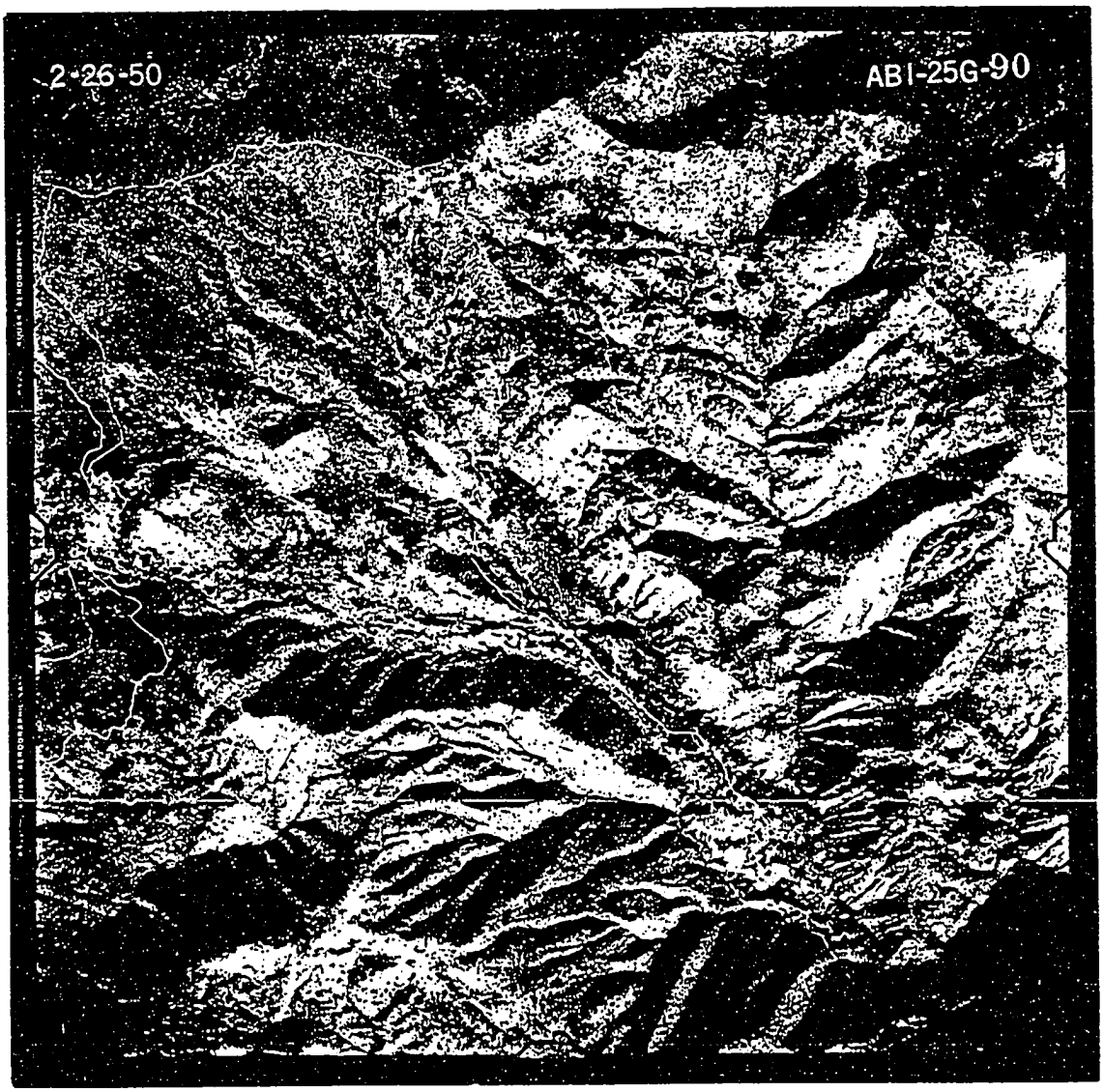


USDA/ABI, February 12, 1950, Flight 1242-50, Frame ABI-16G-89, Scale = 1:20,000

Black and White Image of White Creek Watershed of Joaquin Ridge

This photo features the occurrence of barren areas affected by gully erosion in the central portion of the White Creek drainage of the serpentinite outcrop of the New Idria Formation on Joaquin Ridge. This photo partially overlaps Frame ABI-13G-57. The gullies and barren areas featured in this photo predate the occurrence of asbestos mining operations which began in the early 1960's. The gullies and barren areas cover approximately 10% to 15% of the serpentinite outcrop area shown in the photo. This photo predates development of the Atlas Mine and Mill which was was constructed in the early 1960's near the area shown in the far upper left corner of the photo. Drainage is downslope towards the bottom of the photo.

Reproduced with permission of the copyright owner. Further reproduction prohibited without permission.



USDA/ABI, February 12, 1950, Flight 1242-50, Frame ABI-25G-90, Scale = 1:20,000

Black and White Image of Pine Canyon Watershed of Joaquin Ridge

This photo features the landslide and/or serpentinite debris flow deposits of the Upper Pine Canyon drainage area of the serpentinite outcrop area of Joaquin Ridge. Most of the landslide and/or serpentinite debris flow deposits originated from the serpentinite outcrop area shown in the upper left quadrant of the photo. The toe of the deposit has a snakehead-like diamond shape (lower right quadrant of photo). This photo predates development of the Butler Estate Chromite Mine, the Jensen Mine, the Railroad Mine, and the Coalinga Asbestos Mill. The present location of the Butler Estate Chromite Mine is near the left center margin of the photo; the Jensen Mine is located in the serpentinite debris flow deposit near the upper center of the photo; the Railroad Mine was is located near the toe of the deposit (light colored area in lower right quadrant); the Coalinga Asbestos Mill is located near the lower right center of the photo. Erosional gullies have formed at the margins of the landslide and/or debris flow deposits. A stereo pair of this photo was used as a basis for the field mapping of the landslide and/or debris flow deposits as illustrated in Figure 15 of Chapter 1.

Reproduced with permission of the copyright owner. Further reproduction prohibited without permission.

APPENDIX C

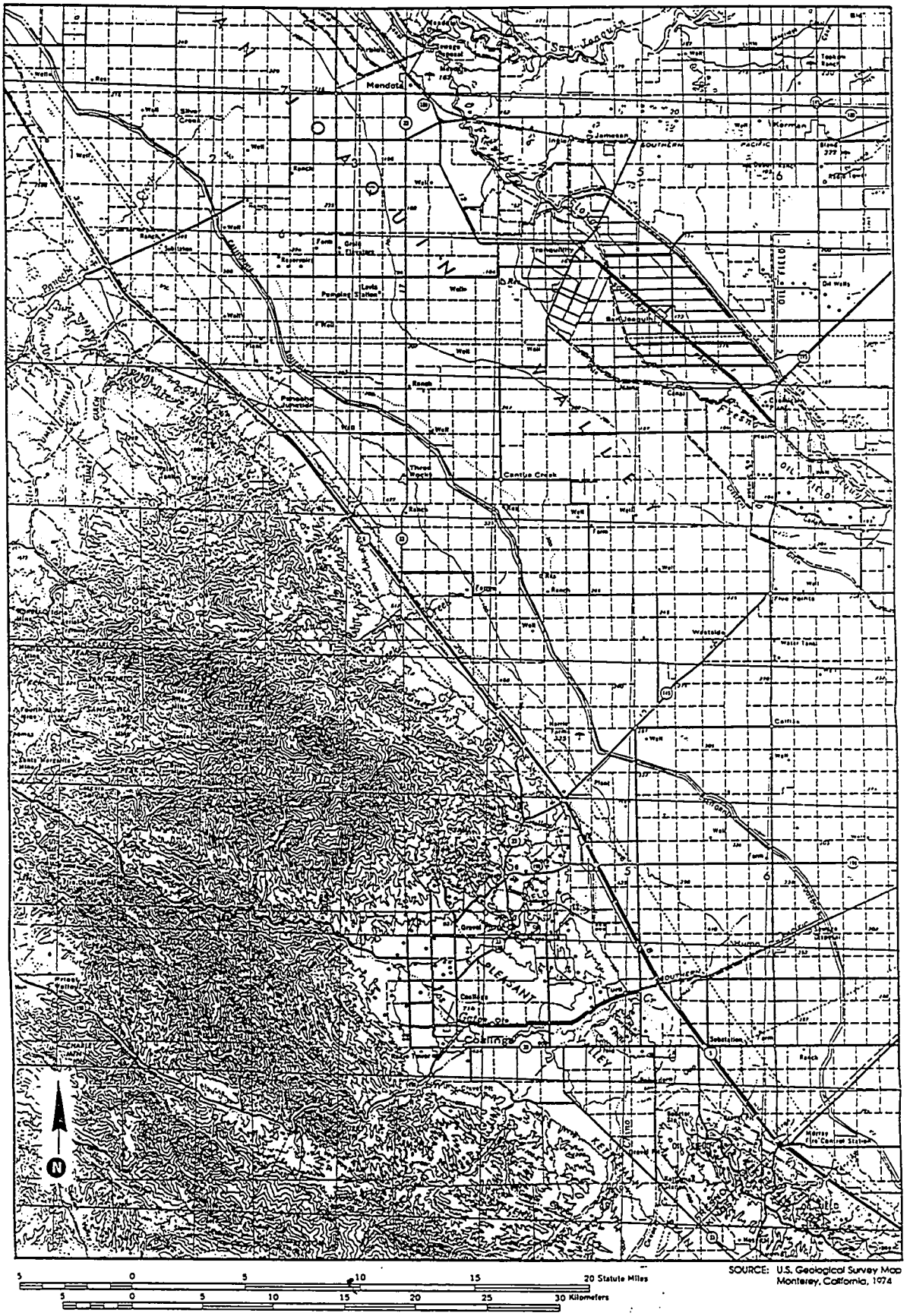
INVENTORY OF REVIEWED

AERIAL PHOTOGRAPHY

Reproduced with permission of the copyright owner. Further reproduction prohibited without permission.

REGIONAL LOCATION MAP

Reproduced with permission of the copyright owner. Further reproduction prohibited without permission.


Mendota
Coalinga
Oil City
Cantua Creek
Five Points
Huron
Guernsey
Kettleman City
Avenal
Lemoore
Hanford
Corcoran
Tulare
Visalia
Kingsburg
Selma
Fresno
Clovis
Madera
Chowchilla
Los Banos
Dos Palos
Gustine
Newman
Patterson
Crows Landing
Modesto
Turlock
Ripon
Manteca
Tracy
Livermore
Pleasanton
Dublin
San Leandro
Hayward
Oakland
Berkeley
Richmond
San Pablo
Martinez
Pittsburg
Antioch
Brentwood
Byron
Tracy
Stockton
Lodi
Galt
Elk Grove
Sacramento
Davis
Woodland
Winters
Vacaville
Fairfield
Suisun City
Benicia
Vallejo
Napa
Petaluma
Santa Rosa
Sebastopol
Healdsburg
Cloverdale
Ukiah
Willits
Fort Bragg
Point Arena
Gualala
Bodega Bay
Bodega Head
Point Reyes
Point Reyes Station
Inverness
Olema
Bolinas
Stinson Beach
Sausalito
Tiburon
Belvedere
Mill Valley
San Rafael
Novato
Petaluma
Sonoma
Glen Ellen
Kenwood
Santa Rosa
Windsor
Healdsburg
Geyserville
Cloverdale
Hopland
Ukiah
Willits
Laytonville
Leggett
Garberville
Redway
Miranda
Scotia
Rio Dell
Fortuna
Eureka
Arcata
Blue Lake
McKinleyville
Trinidad
Orick
Crescent City
Smith River
Gasquet
Hoopa
Willow Creek
Weitchpec
Orleans
Somes Bar
Happy Camp
Yreka
Montague
Tulelake
Alturas
Cedarville
Susanville
Westwood
Chester
Lassen Peak
Mineral
Red Bluff
Corning
Orland
Willows
Maxwell
Colusa
Williams
Arbuckle
Woodland
Dunnigan
Knights Landing
Marysville
Yuba City
Oroville
Chico
Paradise
Magalia
Butte Meadows
Forest Ranch
Cohasset
Stirling City
Paradise
Oroville
Gridley
Biggs
Chico
Durham
Dayton
Oroville
Marysville
Yuba City
Live Oak

SUMMARY AND DETAILED INDEXES

OF REVIEWED AERIAL PHOTOGRAPHS

Reproduced with permission of the copyright owner. Further reproduction prohibited without permission.

SUMMARY INDEX OF AERIAL PHOTOGRAPHS AND REMOTE SENSING DATA REVIEWED IN ARCHIVAL COLLECTIONS

Date	Agency and Flight Identification	Area Covered	
1928	Fairchild Collection, Flight C-353	AF	JR
1928	Fairchild Collection, Flight C-364	AF	
1937	Fairchild Collection, Flight C-4650	AF	
1942	USDA, ABI 2609-41	AF	
1950	USDA, ABI 1242-50	AF	JR
1951	Fairchild Collection, Flight C-17,000	AF	
1955	Division of Highways, ASC-97	AF	
1957	USDA, ABI CSS-3-57 DC	AF	JR
1960	Fairchild Collection, Flight C-23,763		JR
1961	USDA, Flight ABI	AF	
1969	DWR, WR-ABS (Flooded Area, w/Sed. Fan)	AF	
1971	NASA, MSC 164	AF	JR
1973	USGS, Flight GS-VDDI	AF	
1973	NASA, Flight 73-069	AF	JR
1973	NASA, Flight 73-094	AF	JR
1973	NASA, Flight 73-194	AF	
1974	NASA, Flight 74-139	AF	JR
1976	NASA, Flight 76-005	AF	
1976	NASA, Flight 76-060	AF	
1976	NASA, Flight 76-087	AF	
1977	NASA, Flight 77-112	AF	
1978	USGS, Flight GS-VEPW (Partial Coverage)	AF	JR
1979	NASA, Flight 79-076		JR
1981	NHAP, Flight 81-473	AF	JR
1982	NASA, Flight 82-149A	AF	
1983	DWR, WR-AOF (Wier Structure w/Flooding)	AF	
1983	NASA, Flight 83-149	AF	
1984	USGS, Radar Mosaic	AF	
1985	DWR, WR-APF-2 (Area Adjacent to Aqueduct)	AF	
1985	DWR, WR-APF-3 (Arroyo Pasajero Channel)	AF	
1987	DWR, WR-APF-4 (Training Dike)	AF	

Note: AF = Alluvial Fan
JR = Joaquin Ridge

Sources include the U.S. Geological Survey; Whittier College, Whittier, California; University of California at Santa Barbara, and the California Department of Water Resources, Sacramento, California

Reproduced with permission of the copyright owner. Further reproduction prohibited without permission.

Additional Coverage Available From National Archives, USDA ABI Series

1973 National Archives, USDA ABI Series
1939 National Archives, USDA ABI Series
1940 National Archives, USDA ABI Series

Additional Coverage Identified from Review of Cal Trans Index of Aerial Photography:

1964 Cal Index No. 192, San Luis Canal Service Area
1965 Cal Index No. 112, Alluvial Fan and Joaquin Ridge Areas
1967 Cal Index No. 247, Alluvial Fan Area
1973 Cal Index No. 189, Alluvial Fan Area
1976 Cal Index No. 73 (BLM CA 04-76), Joaquin Ridge Area
1977 Cal Index No. 108, Strip Coverage of Aqueduct
1978 Cal Index No. 18-06, Covers Rte. 198 and 269
1979 Cal Index No. 3-06-8, Strip Coverage of I-5
1980 Cal Index No. 60 (USDI BR-APA-1), Arroyo Pasajero Flooded Area

Reproduced with permission of the copyright owner. Further reproduction prohibited without permission.

DETAILED INDEX OF AERIAL PHOTOGRAPHS AND REMOTE SENSING DATA REVIEWED IN ARCHIVAL COLLECTIONS

Date:	1928
Agency:	Whittier College
Flight No.:	C-353
Frame Nos.:	Joaquin Ridge Area: 447 to 556; 472 to 483; 502 to 515; 536 to 547; 572 to 579; 604 to 608. Los Gatos Creek Area: 34, 35, 36, 55, 56, 57, 82, 83, 84, 85, 225, 226, 227, 271, 272, 273, 313, 314, 315, 353, 354, 355, 386, 387, 388, 423, 424, 452, 453, 479, 480, 481, 508, 509, 510, 511, 540, 541, 542, 572, 573, 574, 575, 604, 605.
Format:	Low Altitude, Black and White
Scale:	1" = 2,000'
Photo Index:	Yes
Area Covered:	Arroyo Pasajero Alluvial Fan and Joaquin Ridge
Comments:	Good coverage of entire study area including Los Gatos Creek from Pine Canyon and White Creek, downstream to the alluvial fan. Coverage is incomplete in the White Creek area and the Pine Canyon Creek area. The Coalinga Asbestos Mill Site landslide seems to appear in frame #75. Eastern margin of the flight line stops at Guijarral Hills. Coverage appears sharp with minimal cloud coverage.

Date:	1928
Agency:	Whittier College
Flight No.:	C-364
Frame Nos.:	457, 458, 459, 489, 490, 491, 492, 496, 497, 498, 520, 521, 522, 523, 524, 562, 563, 564, 565.
Format:	Low Altitude, Black and White
Scale:	1" = 2,000'
Photo Index:	Yes
Area Covered:	Alluvial Fan Area
Comments:	Good coverage of Los Gatos Creek below Coalinga down to about one mile east of Guijarral Hills. The index sheet shows other minor stream systems to the north debouching to the alluvial plain and contributing to a system of coalescing alluvial fans.

Reproduced with permission of the copyright owner. Further reproduction prohibited without permission.

Date:	1937
Agency:	Whittier College/USDA Agricultural Adjustment Administration
Flight No.:	C-4650/ABI AIS-15171
Frame No.:	
Format:	Low Altitude, Black and White
Scale:	
Photo Index:	Yes
Area Covered:	Coalinga and Los Gatos Creek
Comments:	Actual photos were not available. Index sheet 21 of 23 shows good coverage of Coalinga and Los Gatos Creek. Some abandoned meander channels are visible east of Coalinga. Index sheet 22 of 23 shows area east of Coalinga and Kettleman Hills and also shows Los Gatos Creek debouching to the alluvial fan. Whittier does not have many of the photos or negatives for flight C-4650, Fresno, CA. However, the photos of the Coalinga/Los Gatos Creek area are very good and may be useful for locating alluvial fan sampling stations that predate mining activities (these photos were taken in 1939). Index pages 18, 21, and 22 show Los Gatos Creek as it meanders and then splays into the outer alluvial fan. No good coverage of Pine Canyon (i.e.: no identifiable features). Index sheet 18 of 23 shows a weak pattern of outer fan deposition, but is largely obscured by farming.

Date:	June 6, 1942
Agency:	USDA Agricultural Adjustment Administration
Flight No.:	ABI USDA 2609-41
Frame Nos.:	5B-45 to 50; 5B-78 to 82; 12B-67 to 69;
Format:	Low Altitude, Black and White
Scale:	1 : 20,000
Photo Index:	Yes, Sheet 10
Area Covered:	Coverage includes the Guijarral Hills, Los Gatos Creek, and the Arroyo Pasajero Alluvial Fan

Date:	1947
Agency:	Whittier College
Flight No.:	C-11800
Frame No.	
Format:	Low Altitude, Black and White
Scale:	1" = 1,000'
Photo Index:	Yes
Area Covered:	White Creek
Comments:	Sheet 3 of 3. Good coverage of White Creek mining area but does not include Pine Canyon. Good index sheet showing San Benito/Fresno County borders north of the White Creek mining area.

Reproduced with permission of the copyright owner. Further reproduction prohibited without permission.

Date:	1950
Agency:	USDA Production and Marketing Administration
Flight No.:	ABI USDA 1242-50
Frame No.	ABI-28G-16,17, 40, 41, 42
Format:	Low Altitude, Black and White
Scale:	1 : 20,000
Photo Index:	Yes, Sheet No. 16
Area Covered:	Alluvial Fan
Comments:	Coverage of Coalinga, Los Gatos Creek, Guijarral Hills and the terminus of the Arroyo Pasajero Channel.

Date:	1950
Agency:	USDA Production and Marketing Administration
Flight No.:	ABI USDA 1242-50
Frame No.	13G-58 to 61; 15G-58 to 61; 16G-89 to 94; 25G-91 to 97; 29G-20 to 24; 29G-113 to 106
Format:	Low Altitude, Black and White
Scale:	1 : 20,000
Photo Index:	Yes, Sheet No. 15
Area Covered:	White Creek and Pine Canyon Area
Comments:	Coverage is limited to the White Creek and Pine Canyon Creek Area. Also includes coverage of the Coalinga Asbestos Mill Site. Index sheet 14 covers the area directly north of the White Creek Mining area. Index sheet 17 covers area east of sheet 16; it includes the outer alluvial fan.

Date:	1951
Agency:	Whittier College
Flight No.:	C-17000
Frame No.:	
Format:	Low Altitude, Black and White
Scale:	1" = 833'
Photo Index:	No
Area Covered:	Alluvial Fan and Pleasant Valley
Comments:	Good detailed coverage of Lower Los Gatos Creek showing juncture with Jacalitos Creek and entrenched meander plain north of Guijarral Hills.

Reproduced with permission of the copyright owner. Further reproduction prohibited without permission.

Date:	1954
Agency:	DWR
Flight No.:	ASC-55
Frame No.:	FRE-17- 207 to 211; FRE-18- 6 to 8; FRE-19- 106 to 112; FRE-25 -20 and 21.
Format:	Low Altitude, Black and White
Scale:	1" = 1,320'
Photo Index:	Yes, Sheet No. 30 of 53
Area Covered:	Guijarral Hills to Huron
Comments:	From the San Joaquin Valley Division of Highways Regional Subsidence Exploration. Good coverage of migrating channel in Los Gatos Creek flood plain. At Guijarral Hills, the channel seems to bifurcate to northeast and northwest.

Date:	1957
Agency:	USDA Commodity Stabilization Program
Flight No.:	ABI USDA CSS-3-57DC
Frame No.	26T - 47, 48, 49, 50 and 75, 76, 77, 78, 79
Format:	Low Altitude, Black and White
Scale:	1 : 20,000
Photo Index:	Yes, Sheet No. 13
Area Covered:	Coalinga and Alluvial Fan
Comments:	Coverage of Coalinga, Los Gatos Creek, Guijarral Hills, Huron, and areas east. Includes the terminus of the Arroyo Pasajero Channel

Date:	1957
Agency:	USDA Commodity Stabilization Program
Flight No.:	ABI USDA CSS-3-57DC
Frame No.	30T - 94 to 97; 32T - 7 to 11 and 50 to 54
Format:	Low Altitude, Black and White
Scale:	1 : 20,000
Photo Index:	Yes, Sheet No. 17
Area Covered:	Joaquin Ridge including White Creek and Pine Canyon
Comments:	Coverage includes the White Creek and Pine Canyon Mining area. Frames 30T - 95 and 96 show the Coalinga Asbestos Mill Site area with no evidence of milling. The Railroad Mine shows 3 excavation areas. There is no evidence of and tailings and no visible evidence of asbestos sediment in Pine Canyon Creek. Summary Note: The photos from this flight mission cover the Joaquin Ridge and Coalinga region. Index sheet #14 includes the canal in northeast quadrant and farmland (areas north of sheet #15). Index sheet #15 shows lower reaches of Los Gatos Creek debouching into the Arroyo Pasajero alluvial plain which includes Huron. Sheet #19 includes good coverage of White Creek and Pine Canyon Areas. Sheet #20 shows Los Gatos Creek to Coalinga.

Reproduced with permission of the copyright owner. Further reproduction prohibited without permission.

Date:	1960
Agency:	Whittier College
Flight No.:	C-23763
Frame No.	
Format:	Low Altitude, Black and White
Scale:	1" = 10,000'
Photo Index:	No
Area Covered:	Vicinity of Coalinga
Comments:	Coverage of most of the northern half of Santa Rita Peak and the mining areas just northwest of the Coalinga Asbestos Mill Site. Specific areas include: T18S, R12E, Secs. 15, 22-26, and 36, and T18S, R13E, Secs. 27-33. The client was Union Carbide Nuclear Corp., Grand Junction, Colorado. The photographs are somewhat overexposed and of poor quality.

Date:	1961
Agency:	UCSB/USDA Commodity Stabilization Service
Flight No.:	ABI No. CSS-7-61DC
Frame No.	IBB-4 to 17, 35 to 44, 58 to 64, and 2BB-13 to 9
Format:	Low Altitude, Color
Scale:	1 : 20,000
Photo Index:	Yes
Area Covered:	Fresno County
Comments:	Flight flown by Aeroflex Corp., Robinson Aerial Surveys Division, Newton, N.J. Coverage includes Coalinga to Guijarral Hills to the terminus of Los Gatos Creek. Coverage also includes Huron and LeMoore Naval Air Station.

Date:	1964
Agency:	DWR
Flight No.:	752838-11
Frame No.	
Format:	Low Altitude, Color
Scale:	
Photo Index:	No
Area Covered:	San Joaquin Valley Canal Routes
Comments:	Can No. 202, 203. Photos include strip coverage without any identifiable features.

Reproduced with permission of the copyright owner. Further reproduction prohibited without permission.

Date: 1964
Agency: DWR/Cal Index of Aerial Photography
Flight No.:
Frame No.
Format: Low Altitude, Color/Infrared
Scale: 1" = 1,667'
Photo Index: Yes #192
Area Covered: San Luis Canal Service Area
Comments: District #6, Fresno County.

Date: 1965
Agency: DWR/Cal Index of Aerial Photography
Flight No.:
Frame No.
Format:
Scale: 1" = 1,667'
Photo Index: Yes #112
Area Covered: Joaquin Ridge and Alluvial Fan
Comments: District #6, Fresno County. ASC #745.

Date: 1967
Agency: DWR/Cal Index of Aerial Photography
Flight No.:
Frame No.
Format:
Scale: 1" = 1,667'
Photo Index: Yes #247
Area Covered: Alluvial Fan
Comments: District #6, Fresno County.

Date: 1967
Agency: DWR
Flight No.: WR-AAQ 755092
Frame No.:
Format: Low Altitude, Color
Scale: 1" = 500'
Photo Index: Yes #1 and #2
Area Covered: Salt Creek
Comments: Can 282. Detailed coverage of Salt Creek drainage basin from the source area to the California Aqueduct, which is under construction. Index #1 shows the Source Area and Index #2 shows the Alluvial Plain and the California Aqueduct.

Reproduced with permission of the copyright owner. Further reproduction prohibited without permission.

Date: 1967
Agency: DWR/Cal Index of Aerial Photography
Flight No.:
Frame No.
Format:
Scale: 1" = 1,667'
Photo Index: Yes #247
Area Covered: Alluvial Fan Area
Comments: District #6, Fresno County.

Date: 1969
Agency: DWR
Flight No.: WR-ABS 757357
Frame No.
Format: Low Altitude, Color/Infrared
Scale:
Photo Index: No
Area Covered: Fresno County: vicinity of Huron
Comments: Can 378 - 379. Excellent coverage of Huron area after a flood event. Shows sediment fan and flooding of settling basin and area northeast of Huron and California Aqueduct. Source area to the California Aqueduct, which is under construction. Index #1 shows the Source Area and Index #2 shows the Alluvial Plain and the California Aqueduct.

Date: 1969
Agency: DWR
Flight No.: WR-ABN 757357
Frame No.
Format: Low Altitude, Color/Infrared
Scale:
Photo Index: Yes #5 of 9 and #3 of 3
Area Covered: San Luis Forebay to Kettleman City and California Aqueduct
Comments: Can 375. Detailed coverage of flooded area directly adjacent to the west side of the aqueduct. Streets and bridges are identified.

Date: 1969
Agency: DWR
Flight No.: WR-ABS 757357
Frame No.
Format: Low Altitude, Color/Infrared
Scale:
Photo Index: No
Area Covered: Huron: Fresno County
Comments: Can 379. Detailed coverage of flooded area directly adjacent to the west side of the aqueduct.

Reproduced with permission of the copyright owner. Further reproduction prohibited without permission.

Date: 1971
Agency: UCSB/NASA/MSC 164
Flight No.: #5, Roll 29
Frame No. 3450 to 3455
Format: High Altitude, Color/Infrared
Scale: 1 : 120,000
Photo Index: No
Area Covered: Coast Ranges of Site 254 and Site 260
Comments: Excellent coverage of mining area showing hundreds of prospecting pits.

Date: 1971
Agency: UCSB/NASA/MSC 164
Flight No.: #5, Roll 29
Frame No. 3289 to 3291
Format: High Altitude, Color/Infrared
Scale: 1 : 120,000
Photo Index: No
Area Covered: Coast Ranges of Site 254 and Site 260
Comments: Coverage includes medial fan, including Huron.

Date: 1971
Agency: UCSB/NASA/MSC 164
Flight No.: #5, Roll 29
Frame No. 3267 to 3270
Format: High Altitude, Color/Infrared
Scale: 1 : 120,000
Photo Index: No
Area Covered: Coast Ranges of Site 254 and Site 260
Comments: Coverage includes alluvial fan and outer fan.

Date: 1971
Agency: UCSB/NASA/MSC 164
Flight No.: #5, Roll 29
Frame No. 3479
Format: High Altitude, Color/Infrared
Scale: 1 : 120,000
Photo Index: No
Area Covered: Coast Ranges of Site 254 and Site 260
Comments: Coverage includes Los Gatos Creek and Coalinga.

Reproduced with permission of the copyright owner. Further reproduction prohibited without permission.

Date: 1971
Agency: UCSB/NASA/MSC 164
Flight No.: #5, Roll 29
Frame No. 3478
Format: CIR
Scale: 1 : 120,000
Photo Index: No
Area Covered: Coast Ranges of Site 254 and Site 260
Comments: Partial coverage of Joaquin Ridge, White Creek, Pine Canyon Creek Area including Big Blue to the northeast and Los Gatos Creek and Coalinga to the southeast.

Date: 1971
Agency: UCSB/NASA/MSC 164
Flight No.: #5, Roll 29
Frame No. 3477
Format: CIR
Scale: 1 : 120,000
Photo Index: No
Area Covered: Coast Ranges of Site 254 and Site 260
Comments: Coverage includes Joaquin Ridge, Pine Canyon, White Creek area, and Big Blue outcrop to the northeast.

Date: 1971
Agency: UCSB/NASA/MSC 164
Flight No.: #5, Roll 29
Frame No. 3476
Format: CIR
Scale: 1 : 120,000
Photo Index: No
Area Covered: Coast Ranges of Site 254 and Site 260
Comments: Coverage includes Joaquin Ridge, Pine Canyon, White Creek area, and a large portion of the Big Blue outcrop to the northeast.

Date: 1971
Agency: UCSB/NASA/MSC 164
Flight No.: #5, Roll 29
Frame No. 3474 and 3475
Format: CIR
Scale: 1 : 120,000
Photo Index: No
Area Covered: Coast Ranges of Site 254 and Site 260
Comments: Coverage includes Cantua Creek drainage area on the northeast side of the New Idria Formation.

Reproduced with permission of the copyright owner. Further reproduction prohibited without permission.

Date: 1971
Agency: UCSB/NASA/MSC 164
Flight No.: #4, Roll 21
Frame No. 3705
Format: CIR with red filter #24 (blue enhanced)
Scale: 1 : 120,000
Photo Index: No
Area Covered: Coast Ranges of Site 254 and Site 260
Comments: Coverage includes San Luis Reservoir.

Date: 1971
Agency: UCSB/NASA/MSC 164
Flight No.: #4, Roll 21
Frame No. 3704
Format: CIR with red filter #24 (blue enhanced)
Scale: 1 : 120,000
Photo Index: No
Area Covered: Coast Ranges of Site 254 and Site 260
Comments: Coverage includes San Luis Reservoir.

Date: 1971
Agency: UCSB/NASA/MSC 164
Flight No.: #4, Roll 21
Frame No. 3703
Format: CIR with red filter #24 (blue enhanced)
Scale: 1 : 120,000
Photo Index: No
Area Covered: Coast Ranges of Site 254 and Site 260
Comments: Coverage includes Interstate 5, California Aqueduct, and the Big Blue Formation.

Date: 1971
Agency: UCSB/NASA/MSC 164
Flight No.: #4, Roll 21
Frame No. 3702
Format: CIR with red filter #24 (blue enhanced)
Scale: 1 : 120,000
Photo Index: No
Area Covered: Coast Ranges of Site 254 and Site 260

Reproduced with permission of the copyright owner. Further reproduction prohibited without permission.

Comments: Coverage includes Interstate 5, California Aqueduct, and the Big Blue Formation.

Date: 1971
Agency: UCSB/NASA/MSC 164
Flight No.: #4, Roll 21
Frame No. 3699 - 3701
Format: CIR with red filter #24 (blue enhanced)
Scale: 1 : 120,000
Photo Index: No
Area Covered: Coast Ranges of Site 254 and Site 260
Comments: Coverage possibly includes the Panoche Fan.

Date: 1971
Agency: UCSB/NASA/MSC 164
Flight No.: #4, Roll 21
Frame No. 3698
Format: CIR with red filter #24 (blue enhanced)
Scale: 1 : 120,000
Photo Index: No
Area Covered: Coast Ranges of Site 254 and Site 260
Comments: Coverage includes the Cantua Creek Watershed with the New Idria Formation in part of the photo.

Date: 1971
Agency: UCSB/NASA/MSC 164
Flight No.: #4, Roll 21
Frame No. 3694 - 3696
Format: CIR with red filter #24 (blue enhanced)
Scale: 1 : 120,000
Photo Index: No
Area Covered: Coast Ranges of Site 254 and Site 260
Comments: Coverage includes the White Creek and Pine Canyon Drainage Area.

Date: 1971
Agency: UCSB/NASA/MSC 164
Flight No.: #4, Roll 22
Frame No. 071 & 072
Format: CIR with deep yellow filter #15
Scale: 1 : 120,000
Photo Index: No
Area Covered: Coast Ranges of Site 254 and Site 260
Comments: Coverage includes the Cantua Creek terminus at the California Aqueduct.

Reproduced with permission of the copyright owner. Further reproduction prohibited without permission.

Date: 1971
Agency: UCSB/NASA/MSC 164
Flight No.: #4, Roll 22
Frame No. 073 & 080
Format: CIR with deep yellow filter #15
Scale: 1 : 120,000
Photo Index: No
Area Covered: Coast Ranges of Site 254 and Site 260
Comments: Coverage includes the Arroyo Pasajero Alluvial Fan and the California Aqueduct.

Date: 1971
Agency: UCSB/NASA/MSC 164
Flight No.: #4, Roll 22
Frame No. 388 & 391
Format: CIR with deep yellow filter #15
Scale: 1 : 120,000
Photo Index: No
Area Covered: Coast Ranges of Site 254 and Site 260
Comments: Coverage includes the Table Mountain Serpentinite Outcrop.

Date: 1971
Agency: UCSB/NASA/MSC 164
Flight No.: #4, Roll 22
Frame No. 392 & 397
Format: CIR with deep yellow filter #15
Scale: 1 : 120,000
Photo Index: No
Area Covered: Coast Ranges of Site 254 and Site 260
Comments: Coverage includes Coalinga to the confluence of White Creek and Los Gatos Creek.

Date: 1971
Agency: UCSB/NASA/MSC 164
Flight No.: #4, Roll 22
Frame No. 398 & 403
Format: CIR with deep yellow filter #15
Scale: 1 : 120,000
Photo Index: No
Area Covered: Coast Ranges of Site 254 and Site 260
Comments: Coverage includes the Joaquin Ridge Area including Pine Canyon, part of White Creek (including the Atlas Site), and the northeast side of the ridge.

Reproduced with permission of the copyright owner. Further reproduction prohibited without permission.

Date: 1971
Agency: UCSB/NASA/MSC 164
Flight No.: #4, Roll 21
Frame No. 3510 to 3512
Format: Pink & Grey
Scale: 1 : 120,000
Photo Index: No
Area Covered: Coast Ranges of Site 254 and Site 260
Comments: Coverage of alluvial fan and outer areas.

Date: 1971
Agency: UCSB/NASA/MSC 164
Flight No.: #4, Roll 21
Frame No. 3531 to 3533
Format: Pink & Grey
Scale: 1 : 120,000
Photo Index: No
Area Covered: Coast Ranges of Site 254 and Site 260
Comments: Coverage of medial fan including Huron.

Date: 1971
Agency: UCSB/NASA/MSC 164
Flight No.: #4, Roll 21
Frame No. 3692 to 3696
Format: Pink & Grey
Scale: 1 : 120,000
Photo Index: No
Area Covered: Coast Ranges of Site 254 and Site 260
Comments: Excellent coverage of the mining area showing hundreds of prospecting pits.

Date: 1971
Agency: UCSB/NASA/MSC 164
Flight No.: #4, Roll 22
Frame No. 076 to 080
Format: Pink & Grey
Scale: 1 : 120,000
Photo Index: No
Area Covered: Coast Ranges of Site 254 and Site 260
Comments: Coverage of medial alluvial fan with the sediment backup at Interstate 5.

Reproduced with permission of the copyright owner. Further reproduction prohibited without permission.

Date: 1971
Agency: UCSB/NASA/MSC 164
Flight No.: #4, Roll 22
Frame No. 394 to 397
Format: Pink & Grey
Scale: 1 : 120,000
Photo Index: No
Area Covered: Coast Ranges of Site 254 and Site 260
Comments: Coverage of Coalinga to White Creek.

Date: 1971
Agency: UCSB/NASA/MSC 164
Flight No.: #4, Roll 22
Frame No. 398 to 400
Format: Pink & Grey
Scale: 1 : 120,000
Photo Index: No
Area Covered: Coast Ranges of Site 254 and Site 260
Comments: Excellent coverage of mining area showing hundreds of prospecting pits.

Date: 1973
Agency: DWR/Cal Index of Aerial Photography
Flight No.:
Frame No.
Format:
Scale: 1" = 3,333'
Photo Index: Yes #189
Area Covered: Fresno County
Comments: District #6, Fresno County. From the Agricultural Stabilization Commodity Service.

Date: 1973
Agency: UCSB/NASA
Flight No.: 73-094
Frame No. 2527 to 2529
Format:
Scale:
Photo Index: No
Area Covered: Coalinga Mill Site
Comments: Excellent detailed coverage of Coalinga to Mill Site including White Creek mining area and Pine Canyon.

Reproduced with permission of the copyright owner. Further reproduction prohibited without permission.

Date: 1973
Agency: UCSB/NASA
Flight No.: 73-094
Frame No. 2602 to 2605
Format:
Scale:
Photo Index: No
Area Covered: Coalinga
Comments: Coverage of medial fan including Guijarral Hills, Huron, the terminus of Los Gatos Creek, California Aqueduct, and the outer fan.

Date: 1973
Agency: UCSB/NASA
Flight No.: 73-069 flight line A - B
Frame No. 0634 to 0635
Format:
Scale:
Photo Index: No
Area Covered: Coalinga
Comments: Coverage of White Creek/Pine Canyon mining area and areas downstream including Los Gatos Creek and Coalinga.

Date: 1973
Agency: UCSB/NASA
Flight No.: 73-069 flight line A - B
Frame No. 0693 to 0695
Format:
Scale:
Photo Index: No
Area Covered: Coalinga
Comments:
Coverage of medial and outer fan including Huron, California Aqueduct, and LeMoore Naval Air Station.

Date: 1973
Agency: UCSB/NASA
Flight No.: 73-194
Frame No. 6369 to 6371
Format:
Scale:
Photo Index: No
Area Covered: Coast Ranges including site 254 and 260
Comments: Coverage of medial and outer fan areas including Huron and LeMoore Naval Air Station.

Reproduced with permission of the copyright owner. Further reproduction prohibited without permission.

Date: 1973
Agency: UCSB/NASA
Flight No.: 73-194 (ACC #01541)
Frame No. 6425, 6426, and 6427
Format: CIR
Scale:
Photo Index: No
Area Covered: Coast Ranges including site 254 and 260
Comments: Excellent coverage of the entire New Idria plug and regional structures.

Date: 1973
Agency: UCSB/NASA
Flight No.: 73-194 (ACC #01541)
Frame No. 6428, 6429, and 6430
Format: CIR
Scale:
Photo Index: No
Area Covered: Coast Ranges including site 254 and 260
Comments: Coverage of Table Mountain Serpentinite.

Date: 1973
Agency: UCSB/NASA
Flight No.: 73-194 (ACC #01541)
Frame No. 6405 and 6406
Format: CIR
Scale:
Photo Index: No
Area Covered: Coast Ranges including site 254 and 260
Comments: Coverage of Kettleman Hills and Polvadero Gap.

Date: 1973
Agency: UCSB/NASA
Flight No.: 73-194 (ACC #01541)
Frame No. 6407, 6408, and 6409
Format: CIR
Scale:
Photo Index: No
Area Covered: Coast Ranges including site 254 and 260
Comments: Coverage of Cantua Fan with the Big Blue Formation.

Reproduced with permission of the copyright owner. Further reproduction prohibited without permission.

Date: 1973
Agency: UCSB/NASA
Flight No.: 73-194 (ACC #01541)
Frame No. 6410 to 6414
Format: CIR
Scale:
Photo Index: No
Area Covered: Coast Ranges including site 254 and 260
Comments: Coverage of Panoche Fan with the Big Blue outcropping near the California Aqueduct.

Date: 1973
Agency: UCSB/NASA
Flight No.: 73-194 (ACC #01541)
Frame No. 6415 to 6417
Format: CIR
Scale:
Photo Index: No
Area Covered: Coast Ranges including site 254 and 260
Comments: Coverage of the San Luis Reservoir.

Date: 1973
Agency: UCSB/USDA
Flight No.: GS - VDDI
Frame No. 2-128
Format: B & W
Scale:
Photo Index: No
Area Covered: Coalinga
Comments: Coverage of Coalinga and lower Los Gatos Creek. Photo is of medium quality but is good for evaluating alluvial plain channel migration.

Date: 1974
Agency: UCSB/NASA
Flight No.: 74-139 (ACC #01894)
Frame No. 1150 & 1151
Format: CIR
Scale:
Photo Index: No
Area Covered: Coast Ranges including site 254 and 260
Comments: Coverage of Cantua Fan with the Big Blue Formation and the California Aqueduct.

Reproduced with permission of the copyright owner. Further reproduction prohibited without permission.

Date: 1974
Agency: UCSB/NASA
Flight No.: 74-139 (ACC #01894)
Frame No. 1147 to 1149
Format: CIR
Scale:
Photo Index: No
Area Covered: Coast Ranges including site 254 and 260
Comments: Coverage of Arroyo Pasajero Fan and the California Aqueduct.

Date: 1974
Agency: UCSB/NASA
Flight No.: 74-139 flight line A - B
Frame No. 1115 to 1119
Format: CIR
Scale:
Photo Index: No
Area Covered: Coalinga
Comments: Excellent coverage of White Creek and Pine Canyon mining area to Coalinga including Los Gatos Creek.

Date: 1974
Agency: UCSB/NASA
Flight No.: 74-139 flight line C - D
Frame No. 1147 to 1149
Format: CIR
Scale:
Photo Index: No
Area Covered: Coalinga
Comments: Good coverage of medial and outer fan areas including Coalinga, Huron, and east of the aqueduct.

Date: 1974
Agency: UCSB/NASA
Flight No.: 74-139 flight line E - F
Frame No. 1172 to 1174
Format: CIR
Scale:
Photo Index: No
Area Covered: Coalinga
Comments: Coverage of outer fan including LeMoore Naval Air Station and some of the aqueduct.

Reproduced with permission of the copyright owner. Further reproduction prohibited without permission.

Date:	1976
Agency:	DWR/Cal Index of Aerial Photography
Flight No.:	BLM CA 04-76
Frame No.	
Format:	
Scale:	1" = 1667'
Photo Index:	Yes #73
Area Covered:	White Creek/Pine Canyon
Comments:	Broad coverage of White Creek, Pine Canyon Creek, and the Clear Creek area.

Date:	1976
Agency:	DWR/Cal Index of Aerial Photography
Flight No.:	BLM CA 04-76
Frame No.	
Format:	
Scale:	1" = 1667'
Photo Index:	Yes #73
Area Covered:	Clear Creek
Comments:	District #6, Fresno County. Coverage includes the Clear Creek area. Flight flown by I. K. Curtis Services, Inc., for USDI. Adjacent to west side of aqueduct. Flight flown by Western Aerial Photos.

Date:	1976
Agency:	UCSB/NASA
Flight No.:	79-005 (ACC #02290)
Frame No.	7665 & 7664
Format:	CIR
Scale:	
Photo Index:	No
Area Covered:	Coast Ranges including site 254 and 260
Comments:	Coverage of Arroyo Pasajero and California Aqueduct with the LeMoore Naval Airbase.

Date:	1976
Agency:	UCSB/NASA
Flight No.:	79-005 (ACC #02290)
Frame No.	7656 to 7661
Format:	CIR
Scale:	
Photo Index:	No
Area Covered:	Coast Ranges including site 254 and 260
Comments:	Coverage of California Aqueduct on the western margin of the San Joaquin Valley.

Reproduced with permission of the copyright owner. Further reproduction prohibited without permission.

Date: 1976
Agency: UCSB/NHAP
Flight No.: 76-087 flight line E
Frame No.: 5300 to 5305
Format: CIR transparency
Scale:
Photo Index: No
Area Covered: Northern outer fan with the California Aqueduct
Comments:

Date: 1976
Agency: UCSB/NHAP
Flight No.: 76-087 flight line E
Frame No.: 5305 to 5308
Format: CIR transparency
Scale:
Photo Index: No
Area Covered: Northern outer fan with the California Aqueduct
Comments: Excellent coverage of outer fan with Huron, Aqueduct, and the terminus of Los Gatos Creek prior to the settling basins.

Date: 1976
Agency: UCSB/NHAP
Flight No.: 76-087 flight line E
Frame No.: 5308 to 5311
Format: CIR transparency
Scale:
Photo Index: No
Area Covered: Southern outer fan with the California Aqueduct
Comments:

Date: 1976
Agency: UCSB/NHAP
Flight No.: 76-087 flight line G
Frame No.: 5349 to 5351
Format: CIR transparency
Scale:
Photo Index: No
Area Covered: Los Gatos Creek, Coalinga, and Guijarral Hills
Comments:

Reproduced with permission of the copyright owner. Further reproduction prohibited without permission.

Date: 1976
Agency: UCSB/NHAP
Flight No.: 76-060 flight line A - B
Frame No.: 4786 to 4789
Format: CIR transparency
Scale:
Photo Index: No
Area Covered: Coalinga
Comments: Coverage of medial fan including Huron, the aqueduct, and LeMoore Naval Air Station.

Date: 1976
Agency: UCSB/NHAP
Flight No.: 76-060 flight line E - F
Frame No.: 4837 to 4838
Format: CIR transparency
Scale:
Photo Index: No
Area Covered: Huron
Comments: Coverage of Los Gatos Creek downstream of Huron.

Date: 1976
Agency: UCSB/NHAP
Flight No.: 76-005 flight line E - F
Frame No.: 7663 to 7666
Format: CIR transparency
Scale:
Photo Index: No
Area Covered: Huron
Comments: Coverage of medial and outer fan including Los Gatos Creek, Huron, the aqueduct, and LeMoore Naval Air Station.

Date: 1976
Agency: UCSB/NHAP
Flight No.: 76-005 flight line G - H
Frame No.: 7701 to 7703
Format: CIR transparency
Scale:
Photo Index: No
Area Covered: Coalinga
Comments: Coverage of Los Gatos Creek in the vicinity of Coalinga.

Reproduced with permission of the copyright owner. Further reproduction prohibited without permission.

Date: 1976
Agency: UCSB/NHAP
Flight No.: 79-076 flight line G - H
Frame No.: 1162 to 1164
Format: B & W
Scale:
Photo Index: No
Area Covered: Huron
Comments: Somewhat overexposed coverage of medial and outer fan areas including Los Gatos Creek, Huron, the aqueduct, and a small portion of LeMoore Naval Air Station.

Date: 1976
Agency: UCSB/NHAP
Flight No.: 79-076 flight line G - H
Frame No.: 6583 to 6585
Format: CIR
Scale:
Photo Index: No
Area Covered: Huron
Comments: Coverage of medial and outer fan areas including terminus of Los Gatos Creek, Huron, the aqueduct, and a small portion of LeMoore Naval Air Station.

Date: 1976
Agency: UCSB/NHAP
Flight No.: 79-076 flight line K - L
Frame No.: 1242 to 1246
Format: B & W
Scale:
Photo Index: No
Area Covered: Huron
Comments: Coverage of White Creek and Pine Canyon Area plus Los Gatos Creek to Coalinga.

Date: 1976
Agency: UCSB/NHAP
Flight No.: 79-076 flight line K - L
Frame No.: 6665 to 6667
Format: CIR
Scale:
Photo Index: No
Area Covered: Huron
Comments: Coverage of White Creek and Pine Canyon Area plus Los Gatos Creek to Coalinga.

Reproduced with permission of the copyright owner. Further reproduction prohibited without permission.

Date: 1977
Agency: UCSB/NHAP
Flight No.: 77-112 flight line I - J
Frame No.: 2065 to 2067
Format: CIR transparency
Scale:
Photo Index: No
Area Covered: Coalinga
Comments: Coverage includes the medial fan which includes Los Gatos Creek, Huron, and the California Aqueduct prior to the settling basins.

Date: 1977
Agency: UCSB/NHAP
Flight No.: 77-112 flight line G - H
Frame No.: 1968 to 1970
Format: CIR transparency
Scale:
Photo Index: No
Area Covered: Coalinga
Comments: Coverage includes the outer fan which includes LeMoore Naval Air Station, the California Aqueduct, Huron, and the terminus of Los Gatos Creek before the settling basins.

Date: 1977
Agency: UCSB/NHAP
Flight No.: 77-112 flight line K - L
Frame No.: 2096 to 2097
Format: CIR transparency
Scale:
Photo Index: No
Area Covered: Coalinga
Comments: Coverage of Coalinga to the mill site (on the far edge of photo) including Los Gatos Creek, White Creek, and Pine Canyon. Resolution of mill site is not very good. Other mining operations are not shown.

Reproduced with permission of the copyright owner. Further reproduction prohibited without permission.

Date: 1977
Agency: DWR/Cal Index of Aerial Photography
Flight No.: WR-AGM
Frame No.
Format:
Scale: 1" = 2,000'
Photo Index: Yes #108
Area Covered: Huron
Comments: Strip coverage of the California Aqueduct in the vicinity of Huron including the northern and southern sections plus the O'Neil Forebay to Kettleman City.

Date: 1977
Agency: DWR/Cal Index of Aerial Photography
Flight No.: WR-AGM
Frame No.
Format:
Scale: 1" = 2,000'
Photo Index: Yes #108 Sheet #1
Area Covered: California Aqueduct from O'Neil Forebay to Kettleman City
Comments: District #6, Fresno County. Detailed strip coverage of area adjacent to west side of aqueduct. Flight flown by Western Aerial Photos.

Date: 1977
Agency: UCSB/NASA
Flight No.: 77-112
Frame No. 2065-2067
Format:
Scale:
Photo Index: No
Area Covered: Coast Ranges of Site 254 and Site 260
Comments: Coverage includes the California Aqueduct and the Arroyo Pasajero Fan.

Date: 1977
Agency: UCSB/NASA
Flight No.: 77-112
Frame No. 2064
Format:
Scale:
Photo Index: No
Area Covered: Coast Ranges of Site 254 and Site 260
Comments: Coverage includes the California Aqueduct, Cantua Fan, and the Big Blue Formation.

Reproduced with permission of the copyright owner. Further reproduction prohibited without permission.

Date: 1977
Agency: UCSB/NASA
Flight No.: 77-112
Frame No. 2060 - 2063
Format:
Scale:
Photo Index: No
Area Covered: Coast Ranges of Site 254 and Site 260
Comments: Coverage includes the California Aqueduct, and the trend of the Big Blue Formation.

Date: 1977
Agency: UCSB/NASA
Flight No.: 77-112
Frame No. 2059 - 2056
Format:
Scale:
Photo Index: No
Area Covered: Coast Ranges of Site 254 and Site 260
Comments: Coverage includes the San Luis Reservoir.

Date: 1978
Agency: DWR/Cal Index of Aerial Photography
Flight No.:
Frame No.
Format:
Scale: 1" = 6,666'
Photo Index: Yes #18 and #23
Area Covered: Huron
Comments: Strip coverage of Route 269 and Route 198 in the vicinity of Huron. Tranquility USGS - VEPW 7/78 includes broad coverage of the Coalinga area with partial coverage of the site and the alluvial fan.

Date: 1978
Agency: DWR/Cal Index of Aerial Photography
Flight No.: ASC 13-7905-23
Frame No.
Format:
Scale: 1" = 200'
Photo Index: Yes #18-06
Area Covered: Fresno County
Comments: District 6, Fresno County. Coverage includes Route 198 and Route 269.

Reproduced with permission of the copyright owner. Further reproduction prohibited without permission.

Date: 1979
Agency: DWR
Flight No.: WR-AIS B-53002
Frame No.
Format:
Scale:
Photo Index: No
Area Covered: Salt Creek
Comments: Can 688. Strip coverage of the California Aqueduct and the Salt Creek drainage pathway.

Date: 1979
Agency: DWR
Flight No.: WR-AIS-2 B-53374
Frame No.
Format:
Scale:
Photo Index: No
Area Covered: Salt Creek
Comments: Can 734. Coverage includes only a small area of the Pastoria Siphon.

Date: 1979
Agency: DWR/Cal Index of Aerial Photography
Flight No.:
Frame No.
Format:
Scale: 1" = 200'
Photo Index: Yes #3-06-8
Area Covered: Fresno County
Comments: District #6, Fresno County. Coverage includes Interstate 5, between Route 198 and Kern County Line.

Date: 1979
Agency: DWR/Cal Index of Aerial Photography
Flight No.:
Frame No.
Format:
Scale: 1" = 200'
Photo Index: Yes #3-06-9
Area Covered: Fresno County
Comments: District #6, Fresno County. Coverage includes Interstate 5, between Route 3 and Route 5.

Reproduced with permission of the copyright owner. Further reproduction prohibited without permission.

Date: 1979
Agency: UCSB/NASA
Flight No.: 79-076 (ACC #02771)
Frame No. 1245 & 1246
Format: B&W Pan X
Scale:
Photo Index: No
Area Covered: Coast Ranges including site 254 and 260
Comments: Coverage of Joaquin Ridge, Pine Canyon, and White Creek Area.

Date: 1979
Agency: UCSB/NASA
Flight No.: 79-076 (ACC #02770)
Frame No. 6664 & 6665
Format: CIR
Scale:
Photo Index: No
Area Covered: Coast Ranges including site 254 and 260
Comments: Coverage of Coalinga including Los Gatos Creek with the abandoned channel of AF6.

Date: 1979
Agency: UCSB/NASA
Flight No.: 79-076 (ACC #02770)
Frame No. 6666 & 6667
Format: CIR
Scale:
Photo Index: No
Area Covered: Coast Ranges including site 254 and 260
Comments: Coverage of Los Gatos Creek, White Creek, and mining area (note burned area).

Date: 1979
Agency: UCSB/NASA
Flight No.: 79-076 (ACC #02770)
Frame No. 6668 & 6669
Format: CIR
Scale:
Photo Index: No
Area Covered: Coast Ranges including site 254 and 260
Comments: Coverage of Cantua Creek area.

Reproduced with permission of the copyright owner. Further reproduction prohibited without permission.

Date: 1979
Agency: UCSB/NASA
Flight No.: 79-076 (ACC #02770)
Frame No. 6670 to 6673
Format: CIR
Scale:
Photo Index: No
Area Covered: Coast Ranges including site 254 and 260
Comments: Coverage of Interstate 5, the Big Blue outcrop, and the San Luis Reservoir.

Date: 1979
Agency: UCSB/NASA
Flight No.: 79-076 (ACC #02770)
Frame No. 6582, 6588, 6589, and 6590
Format: CIR
Scale:
Photo Index: No
Area Covered: Coast Ranges including site 254 and 260
Comments: Coverage of the San Joaquin Valley with the Panoche Fan draining to the Fresno Slough.

Date: 1979
Agency: UCSB/NASA
Flight No.: 79-076 (ACC #02770)
Frame No. 6586
Format: CIR
Scale:
Photo Index: No
Area Covered: Coast Ranges including site 254 and 260
Comments: Coverage of the Cantua Fan, California Aqueduct, and the San Joaquin Valley.

Date: 1979
Agency: UCSB/NASA
Flight No.: 79-076 (ACC #02770)
Frame No. 6583 to 6585
Format: CIR
Scale:
Photo Index: No
Area Covered: Coast Ranges including site 254 and 260
Comments: Coverage of the Arroyo Pasajero Fan and the California Aqueduct.

Reproduced with permission of the copyright owner. Further reproduction prohibited without permission.

Date: 1980
Agency: DWR/Cal Index of Aerial Photography
Flight No.: BR-APA-1
Frame No.
Format:
Scale: 1" = 1,000'
Photo Index: Yes #60
Area Covered: Arroyo Pasajero Flood Area
Comments: District #6, Fresno County. Performed by Air Flight Service for the USDI.

Date: 1980
Agency: DWR/Cal Index of Aerial Photography
Flight No.:
Frame No.
Format:
Scale: 1" = 200'
Photo Index: Yes #3 and #6-80
Area Covered: Huron
Comments: Coverage of Interstate 5 in the vicinity of Huron.

Date: 1980
Agency: DWR/Cal Index of Aerial Photography
Flight No.:
Frame No.
Format:
Scale: 1" = 200'
Photo Index: Yes #3 and #6-80
Area Covered: Huron
Comments: Coverage of Interstate 5 in the vicinity of Huron.

Date: 1980
Agency: DWR/Cal Index of Aerial Photography
Flight No.: BR-APA-1
Frame No.
Format:
Scale:
Photo Index: Yes #60
Area Covered: Flood Area
Comments: From the USDI. Broad area coverage of Coalinga to Huron and east of the California Aqueduct flood area.

Reproduced with permission of the copyright owner. Further reproduction prohibited without permission.

Date: 1981
Agency: DWR/Cal Index of Aerial Photography
Flight No.: BR-APA-2
Frame No.
Format:
Scale:
Photo Index: No
Area Covered: Arroyo Pasajero
Comments: From the USBR.

Date: 1981
Agency: UCSB/NHAP
Flight No.: NHAP-81
Frame No.: 473-34, -35, -36
Format: Color
Scale:
Photo Index: No
Area Covered: Pine Canyon and White Creek
Comments: Excellent coverage of White Creek and Pine Canyon mining area. Greater detail may be found in transparency 445-74 to 77.

Date: 1981
Agency: UCSB/NHAP
Flight No.: NHAP-81
Frame No.: 445-36 & 38
Format:
Scale:
Photo Index: No
Area Covered: Los Gatos Creek and Nunez Canyon
Comments: Greater detail may be found in transparency 445-35 to 37.

Date: 1981
Agency: UCSB/NHAP
Flight No.: NHAP-81
Frame No.: 473-50, 51
Format:
Scale:
Photo Index: No
Area Covered: Coalinga and lower Los Gatos Creek
Comments: Greater detail may be found in transparency 465-53 to 52.

Reproduced with permission of the copyright owner. Further reproduction prohibited without permission.

Date: 1981
Agency: UCSB/NHAP
Flight No.: NHAP-81
Frame No.: 443-94 to 101
Format:
Scale:
Photo Index: No
Area Covered: Los Gatos Creek and Guijarral Hills and north to the Canal.
Comments:

Date: 1981
Agency: UCSB/NHAP
Flight No.: NHAP-81
Frame No.: 463-18 to 22
Format:
Scale:
Photo Index: No
Area Covered: Outer fan with the California Aqueduct.
Comments:

Date: 1981
Agency: UCSB/NHAP
Flight No.: NHAP-81
Frame No.: 473-34 to 35
Format: CIR
Scale:
Photo Index: No
Area Covered: White Creek and Pine Canyon sub-basin
Comments:

Date: 1981
Agency: UCSB/NHAP
Flight No.: NHAP-81
Frame No.: 473-36 to 38
Format:
Scale:
Photo Index: No
Area Covered: Lower White Creek and Los Gatos Creek
Comments:

Reproduced with permission of the copyright owner. Further reproduction prohibited without permission.

Date: 1981
Agency: UCSB/NHAP
Flight No.: NHAP-81
Frame No.: 473-42 to 45
Format:
Scale:
Photo Index: No
Area Covered: Medial and outer alluvial fan with the California Aqueduct
Comments:

Date: 1981
Agency: UCSB/NHAP
Flight No.: NHAP-81
Frame No.: 473-49 to 51
Format:
Scale:
Photo Index: No
Area Covered: Coalinga and lower Los Gatos Creek
Comments:

Date: 1981
Agency: UCSB/NHAP
Flight No.: NHAP-81
Frame No.: 473-94 to 99
Format:
Scale:
Photo Index: No
Area Covered: Guijarral Hills and Los Gatos Creek to northern outer fan areas
Comments:

Date: 1981
Agency: UCSB/NHAP
Flight No.: NHAP-81
Frame No.: 445-75 & 77
Format: CIR
Scale:
Photo Index: No
Area Covered: White Creek, Pine Canyon Creek, Los Gatos Creek
Comments: Coverage includes White Creek mining area.

Reproduced with permission of the copyright owner. Further reproduction prohibited without permission.

Date: 1981
Agency: UCSB/NHAP
Flight No.: NHAP-81
Frame No.: 440-29
Format: B & W
Scale:
Photo Index: No
Area Covered: Los Gatos Creek, Guijarral Hills and Arroyo Pasajero
Comments:

Date: 1981
Agency: UCSB/NHAP
Flight No.: NHAP-81
Frame No.: 438-29
Format: B & W
Scale:
Photo Index: No
Area Covered: Areas south of Huron
Comments:

Date: 1981
Agency: UCSB/NHAP
Flight No.: NHAP-81
Frame No.: 440-30
Format:
Scale:
Photo Index: No
Area Covered: Los Gatos Creek, Guijarral Hills, Huron, and Arroyo Pasajero
Comments:

Date: 1981
Agency: UCSB/NHAP
Flight No.: NHAP-81
Frame No.: 440-31
Format:
Scale:
Photo Index: No
Area Covered: Huron and northeast to LeMoore
Comments:

Reproduced with permission of the copyright owner. Further reproduction prohibited without permission.

Date: 1981
Agency: UCSB/NHAP
Flight No.: NHAP-81
Frame No.: 440-33
Format:
Scale:
Photo Index: No
Area Covered: North of Huron and east to LeMoore
Comments:

Date: 1981
Agency: UCSB/NHAP
Flight No.: NHAP-81
Frame No.: 440-57 and 58
Format:
Scale:
Photo Index: No
Area Covered: Not in area
Comments:

Date: 1981
Agency: UCSB/NHAP
Flight No.: NHAP-81
Frame No.: 440-92
Format:
Scale:
Photo Index: No
Area Covered: Coalinga to Guijarral Hills
Comments:

Date: 1981
Agency: UCSB/NHAP
Flight No.: NHAP-81
Frame No.: 440-94
Format:
Scale:
Photo Index: No
Area Covered: North of Coalinga
Comments:

Reproduced with permission of the copyright owner. Further reproduction prohibited without permission.

Date: 1981
Agency: UCSB/NHAP
Flight No.: NHAP-81
Frame No.: 440-96
Format:
Scale:
Photo Index: No
Area Covered: Salt Creek
Comments:

Date: 1981
Agency: UCSB/NHAP
Flight No.: NHAP-81
Frame No.: 440-130
Format:
Scale:
Photo Index: No
Area Covered: Coalinga and areas northeast
Comments:

Date: 1981
Agency: UCSB/NHAP
Flight No.: NHAP-81
Frame No.: 440-132
Format:
Scale:
Photo Index: No
Area Covered: Coalinga and northeast to Los Gatos Creek
Comments:

Date: 1981
Agency: UCSB/NHAP
Flight No.: NHAP-81
Frame No.: 440-134
Format:
Scale:
Photo Index: No
Area Covered: Panoche Creek
Comments:

Reproduced with permission of the copyright owner. Further reproduction prohibited without permission.

Date: 1981
Agency: UCSB/NHAP
Flight No.: NHAP-81
Frame No.: 440-156
Format:
Scale:
Photo Index: No
Area Covered: White Creek mining area
Comments:

Date: 1981
Agency: UCSB/NHAP
Flight No.: NHAP-81
Frame No.: 440-158
Format:
Scale:
Photo Index: No
Area Covered: White Creek/Pine Canyon
Comments:

Date: 1981
Agency: UCSB/NHAP
Flight No.: NHAP-81
Frame No.: 440-160
Format:
Scale:
Photo Index: No
Area Covered: Areas south of White Creek/Pine Canyon
Comments:

Date: 1981
Agency: UCSB/NHAP
Flight No.: NHAP-81
Frame No.: 445-73 to 76
Format:
Scale:
Photo Index: No
Area Covered:
Comments:

Reproduced with permission of the copyright owner. Further reproduction prohibited without permission.

on

Date: 1982
Agency: UCSB/NHAP
Flight No.: 82-149A flight line G - H
Frame No.: 1369 to 1371
Format:
Scale:
Photo Index: No
Area Covered: Outer fan areas from the California Aqueduct to LeMoore
Comments:

Date: 1982
Agency: UCSB/NHAP
Flight No.: 82-149A flight line I - J
Frame No.: 1377 to 1379
Format:
Scale:
Photo Index: No
Area Covered: Medial fan from Coalinga to the aqueduct
Comments:

Date: 1983
Agency: UCSB/NHAP
Flight No.: 83-149A flight line I - J
Frame No.: 5662 to 5664
Format:
Scale:
Photo Index: No
Area Covered: Coalinga
Comments:

Date: 1983
Agency: DWR
Flight No.: WR-AOF B-54250
Frame No.
Format:
Scale:
Photo Index: Yes #1 of 1 and #1 and 2 of 2
Area Covered: Arroyo Pasajero
Comments: Can No. 925. Detailed coverage of flooded area adjacent to wier structure and aqueduct. Photos show before and after floods.

Reproduced with permission of the copyright owner. Further reproduction prohibited without permission.

Date: 1984
Agency: DWR
Flight No.: WR-AOP-OB B-54556
Frame No.
Format:
Scale:
Photo Index: No
Area Covered: Salt Creek
Comments: Can 940. Coverage of Salt Creek in the vicinity of the off-stream storage site. Oblique coverage only.

Date: 1984/1985
Agency: DWR/Cal Trans
Flight No.: WR-APF-4
Frame No.
Format:
Scale:
Photo Index: Yes #36
Area Covered: Arroyo Pasajero: Training Dike
Comments: District #6.

Date: 1984/1985
Agency: DWR/Cal Index of Aerial Photography
Flight No.: WR-APE
Frame No.
Format:
Scale:
Photo Index: Yes #41
Area Covered: Coalinga
Comments: District #6. Small area northwest of Coalinga including Los Gatos Creek.

Date: 1984/1985
Agency: DWR/Cal Index of Aerial Photography
Flight No.:
Frame No.
Format:
Scale:
Photo Index: Yes #1
Area Covered: Coalinga
Comments: District #6. Coverage of State Road 198 northeast of Huron.

Reproduced with permission of the copyright owner. Further reproduction prohibited without permission.

Date: 1985
Agency: DWR
Flight No.: WR-APF and WR-APF-2 B-54926
Frame No.
Format:
Scale:
Photo Index: Yes #1 and #2 of both flights
Area Covered: Arroyo Pasajero Basin
Comments: Can 962. Excellent detailed coverage of medial and outer fan areas adjacent to the aqueduct. Detail is good enough to make out Jayne Ave. and Tractor Ave.

Date: 1985
Agency: DWR
Flight No.: WR-APF-3 B-54926
Frame No.
Format:
Scale:
Photo Index: No
Area Covered: Arroyo Pasajero Channel
Comments: Can 963. Detailed coverage of the Arroyo Pasajero Channel from Interstate 5 to a point near Huron.

Date: 1985
Agency: DWR
Flight No.: WR-APE B-54926
Frame No.
Format:
Scale:
Photo Index: Yes #1 of 1
Area Covered: Arroyo Pasajero: Los Gatos Dam Site
Comments: Can 958. Coverage includes Los Gatos Creek.

Date: 1985
Agency: DWR
Flight No.: WR-APE-2 B-54926
Frame No.
Format:
Scale:
Photo Index: Yes #1 of 1
Area Covered: Arroyo Pasajero: Los Gatos Reservoir Site
Comments: Can 958. Coverage includes Los Gatos Creek.

Reproduced with permission of the copyright owner. Further reproduction prohibited without permission.

Date: 1985
Agency: DWR
Flight No.: WR-APD-2 B-54926
Frame No.
Format:
Scale:
Photo Index: No
Area Covered: Arroyo Pasajero: Warthan Creek Dam Site
Comments: Can 958. Coverage includes Warthan Creek.

Date: 1985
Agency: DWR
Flight No.: WR-APD-2 B-54926
Frame No.
Format:
Scale:
Photo Index: No
Area Covered: Arroyo Pasajero: Warthan Creek Reservoir Site
Comments: Can 958. Coverage includes Warthan Creek.

Date: 1987
Agency: DWR
Flight No.: WR-APF-4 B-55883
Frame No.
Format:
Scale: 1" = 1,000'
Photo Index: No
Area Covered: Arroyo Pasajero: Training Dike
Comments: Can 963. Detailed coverage of a small area.

Reproduced with permission of the copyright owner. Further reproduction prohibited without permission.

DETAILED INTERPRETATIONS

OF REVIEWED AERIAL PHOTOGRAPHY

Reproduced with permission of the copyright owner. Further reproduction prohibited without permission.

INDEX OF LOW AND HIGH ALTITUDE AERIAL PHOTOGRAPHS DESCRIBED

Date	Agency and Flight Identification	Area Covered	
1986	Aerial Photometrics, Flight 8654 Series 1 of this report		JR
1981	NHAP, Flight 81-455 Series 2 of this report	AF	JR
1979	NASA, Flights 79-076, 77-112, 76-005 Series 3A, 3B, and 3C of this report	AF	JR
1973	NASA, Flight 73-194 Series 4 of this report	AF	JR
1971	NASA, MSC 164 Series 5A, 5B, and 5C of this report	AF	JR
1957	USDA, ABI CSS-3-57 Series 6 of this report	AF	JR
1950	USDA, ABI 1242-50 Series 7 of this report		JR

Note: AF = Alluvial Fan and/or Western Margin of Central San Joaquin Valley
JR = Joaquin Ridge and/or Upper Pine Canyon

Note: Appendix contains detailed descriptions for individual frames of the above photo series. Eight selected photos from the above series are included for general distribution with all copies of the SPLC Regional Report. These selected photos are identified on the following page and are included in Appendix The imagery of Appendix O is intended to provide a regional perspective of the Coalinga region including Joaquin Ridge, Pleasant Valley, and the Arroyo Pasajero alluvial fan. The photos also show the California Aqueduct and the Diablo Range foothills and alluvial fans of the western margin of the central San Joaquin Valley. One complete set of the aerial photographs described in Appendix G (Series 1 through 7) has been submitted to the EPA as supplemental information. Most of these photos are high resolution images with stereo pairs. Positive transparencies are available for analysis with magnification equipment.

Reproduced with permission of the copyright owner. Further reproduction prohibited without permission.

LIST OF SELECTED AERIAL PHOTOGRAPHS THAT ARE DESCRIBED

1. Color Infrared Image of Joaquin Ridge
   - NHAP, 1981, Flight 81-455, Frame No. 078
     See Descriptions of Series 2 Photos

2. Arroyo Pasajero Alluvial Fan and the California Aqueduct
   - NASA, 1979, Flight 79-076, Frame No. 6584
     See Descriptions of Series 3A Photos

3. Pleasant Valley, Anticline Ridge, and Arroyo Pasajero Alluvial Fan
   - NASA, 1973, Flight 73-194, Frame No. 6406
     See Descriptions of Series 4 Photos

4. Potential Sedimentary Serpentinite Deposits of Leguna Seca Hills Exposed in Outcrops Adjacent to California Aqueduct Near Fresno-Merced County Line and Los Banos Reservoir
   - NASA, 1973, Flight 73-194, Frame No. 6414
     See Descriptions of Series 4 Photos

5. Serpentinite Outcrops of the New Idria Formation and the Big Blue Member of the Temblor Formation
   - NASA, 1971, Flight MSC-164, Frame No. 6476
     See Descriptions of Series 5C Photos

6. Serpentinite Gullies in White Creek Drainage
   - USDA, 1950, Flight ABI 1242-50, Frame No. 13G-57
     See Descriptions of Series 7 Photos

7. Serpentinite Gullies in White Creek Drainage
   - USDA, 1950, Flight ABI 1242-50, Frame No. 13G-57
     See Descriptions of Series 7 Photos

8. Serpentinite Debris Flow Deposits in Pine Canyon
   - USDA, 1950, Flight ABI 1242-50, Frame No. 13G-57
     See Descriptions of Series 7 Photos

Reproduced with permission of the copyright owner. Further reproduction prohibited without permission.

DETAILED DESCRIPTIONS OF LOW AND HIGH ALTITUDE AERIAL PHOTOGRAPHS

SERIES 1

Date:	April 11, 1986
Agency:	Aerial Photometrics, Fresno, California
Flight No.:	8654
Scale:	1" = 600'
Format:	Low Altitude, Black and White
Photo Index:	No
Area Covered:	Upper Pine Canyon Including Coalinga Asbestos Mill Site, Butler Estate Chromite Mine, and Jensen Mine.

Comments: These photos show the relationship of the Coalinga Asbestos Mill Site with the asbestos and chromite mining operations located in the New Idria Formation outcrop area of Upper Pine Canyon.

Frame Descriptions:

Frame Nos. 8654-1 and 8654-2 feature the Coalinga Asbestos Mill Site in Upper Pine Canyon. Notable features in these pictures include the asbestos tailings in the east fork of Upper Pine Canyon Creek at the Coalinga Site and the sediment retaining dam constructed at the base of the tailings in the east fork. These photos also feature the Railroad Mine, milling structures, and ore storage areas.

Frame No. 8654-4 and 8654-5 illustrate the relationship of the Coalinga Asbestos Mill Site (lower center) with the Butler Estate Chromite Mine (left center) and the Jensen Mine (center), both of which are located in the New Idria Formation outcrop area approximately 0.6 miles upslope from the Coalinga Site. Other notable features include the Christie Mine (top right center), a network of exploration pits and access roads, and the landslide and serpentinite debris flow deposits that occupy the Coalinga Site and Upper Pine Canyon area.

Reproduced with permission of the copyright owner. Further reproduction prohibited without permission.

SERIES 2

Date: August 1, 1981
Agency: USGS-NHAP
Flight No.: 81-455
Scale: 1 : 58,000
Format: CIR
Photo Index: No
Area Covered: Arroyo Pasajero Alluvial Fan, Pleasant Valley Floodplain, and Joaquin Ridge including the New Idria Formation. Note: some of these photos are slightly over-exposed.

Frame Descriptions:

Frame Nos. 455-22 through 455-25 feature the cultivated fields of the Arroyo Pasajero alluvial fan including the braided channel terminus of the Arroyo Pasajero streambed, the earthen wier structure that diverts the northeasterly flow from the channel into a settling basin area adjacent to the California Aqueduct, and the town of Huron. (Note: the earthen wier structure is barely visible and almost appears as a dirt road). These pictures also illustrate the radial pathway of the California Aqueduct as it traverses the medial portion of the alluvial fan. The location of the Aqueduct correlates with an elevation contour of approximately 320 feet above sea level and consequently correlates with the radial profile of the alluvial fan surface.

Frame Nos. 443-94 through 443-98 feature the juncture of Los Gatos Creek and Zapato-Chino Creeks on the east side of Guijarral Hills. In this area, the streams have cut gaps through the hills formed by the trend of three anticlinal structures including Anticline Ridge, Guijarral Hills, and Kettleman Hills. Zapato-Chino Creek flows through the southerly (lower) gap which is known as Polvadero Gap. Los Gatos Creek flows through the northerly (upper) gap which is known as the Turk Narrows. On the east side of Guijarral Hills, the Los Gatos Creek - Arroyo Pasajero drainage pathway is entrenched approximately 30 to 40 feet as a result of uplift of the anticlinal strucutres.

Frame Nos. 443-185 through 443-187 feature the Pleasant Valley floodplain including the town of Coalinga and the meandering streambed of Los Gatos Creek on the east side of the town of Coalinga. On the southeast side of the town of Coalinga, Los Gatos Creek is joined by Warthan Creek. Los Gatos Creek is also joined by Jacalitos Creek on the west side of the gap that has been cut through the Guijarral Hills area.

Frame Nos. 445-35 through 445-37 feature the northwest quadrant of the Pleasant Valley floodplain including Los Gatos Creek as it flows through the Coalinga Oil Field.

Reproduced with permission of the copyright owner. Further reproduction prohibited without permission.

Frame Nos. 445-77 and 445-76 feature White Creek and the juncture of White Creek and Pine Canyon Creek, and the juncture of White Creek and Los Gatos Creek. At least 3 locations affected by chromite milling operations located along the banks and in the streambed of White Creek can be identified in Frame No. 445-76. These locations appear as a sudden noticeable widening of the White Creek streambed.

Frame Nos. 445-75 and 445-74 feature the New Idria Formation and the distribution and extent of barren areas affected by gully erosion and by mining activities including mines, exploration pits, exploration access roads, and asbestos mill sites. These anthropically affected areas can be visually differentiated from elongate shaped barren areas affected by naturally occurring gully erosion in the lower outcrop areas.

See Appendix For Flight Line Map.

Reproduced with permission of the copyright owner. Further reproduction prohibited without permission.

SERIES 3A

Date: June 14, 1979
Agency: NASA
Flight No.: 79-076
Format: CIR
Scale: 1 : 65,000
Photo Index: No
Area Covered: Pleasant Valley, Joaquin Ridge, Big Blue Hills, and Western Margin of San Joaquin Valley

Frame Descriptions:

Frame No. 6665 - Notable features in this photo include the Pleasant Valley floodplain flanked by the Coalinga Anticline (lower right quadrant), the Alcalde Hills (lower left quadrant), and the southeastern margin of the Joaquin Ridge Anticline. The Los Gatos Creek drainage pathway, including White Creek and Pine Canyon Creek, is visible in the upper left quadrant. The Coalinga Asbestos Mill Site is barely visible at the upper center margin of the picture. Outcrops of the Big Blue Member of the Temblor Formation are readily discernable in the upper right quadrant of the picture.

Frame No. 6666 - Same as above with 60% overlap to the north. Notable features in this picture include the White Creek and Pine Canyon drainage areas of the New Idria Formation outcrop at the crest of Joaquin Ridge (upper left quadrant). White Creek appears as a light bluish gray ribbon that has the same reflectance characteristics as the barren serpentinite surfaces of the New Idria Formation. Elongate barren areas are areas affected by naturally occurring gully erosion in steeply sloped drainage pathways in the New Idria Formation. Irregularly shaped ovoid barren areas are areas affected by mining operations and asbestos mill sites. Notable mines include the Atlas Mine and Mill Site, the Union Carbide Mine, the Gem Mine, the Big Ridge Mine, the Tromby Mines, the White Creek Magnesite Mine, the Archer Mine, the James-Corbett-Byles Mine, the Butler Estate Chromite Mine, the Jensen Mine, the Christie Mine, the Railroad Mine, and other un-named mines. Areas that appear as white dots are areas affected by exploration pits. Notable mill sites include the Atlas Mine and Mill Site in the White Creek drainage area and the Coalinga Asbestos Mill Site in the Pine Canyon drainage area. Four to five abandoned chromite milling operations can be identified in the streambed of White Creek. These locations can be identified by what appears as a sudden broadening of the White Creek streambed. This apparent widening is a result of asbestos debris deposited in ponding areas that were constructed in the streambeds. These ponding areas were constructed from earthen dams that were designed to retain water for the gravity settling chromite milling operations. The far right margin of this picture features the outcrop belt of the Big Blue Member of the Temblor Formation. The dark area in the upper right quadrant is an area affected by fire.

Reproduced with permission of the copyright owner. Further reproduction prohibited without permission.

Frame No. 6667 - Same as above with 60% overlap to the north.

Frame No. 6668 - Same as above with 60% overlap to the north.

Frame No. 6669 - This photograph features the northern end of Monocline Ridge (lower right quadrant with burned area), the Panoche Creek drainage basin (left center), and the southern half of the Panoche Hills area (top center). The mountainous area featured in the upper left quadrant of the picture is known as Gluacophane Ridge and may contain serpentine rocks. The Tumey Gulch area (which is known to drain outcrops of the Big Blue Member) is located just above the burned area in the lower right quadrant.

Frame No. 6670 - This picture features the Panoche Hills area including the Panoche Creek (lower right quadrant) and Little Panoche Creek (upper right quadrant) drainage basins.

Frame Nos. 6671 through 6673 feature the Little Panoche Creek, Laguna Seca, Ortigalita and Salt Creek drainage basins. (See USGS, Monterey, California 1:250,000 Scale Topographic Map - 1974 for geographic reference). As indicated in Frame No. 6672, these creeks drain an Upper Miocene formation that outcrops in a narrow strip that parallels the pathway of the California Aqueduct (see far right margin). The age, stratigraphic position, and reflectance characteristics of these units indicate that they may contain asbestos-bearing detrital serpentinite debris similar to the Big Blue Member near Coalinga.

Frame Nos. 6583, 6384, 6385. These photos feature most of the Arroyo Pasajero alluvial fan including the terminus of the Arroyo Pasajero channel, the town of Huron, and the California Aqueduct. Anticline Ridge and Interstate Five are visible at the far left margin. Most of the alluvial fan has been cultivated for agricultural purposes. This widespread cultivation has been made possible by the availability of irrigation water from the California Aqueduct via the Coalinga Canal.

Frame Nos. 6586, 6587, 6588. These photos feature the Salt and Cantua Creek alluvial fan areas and the California Aqueduct. This area is located immeadiately north of the Arroyo Pasajero in a drainage area that is known to contain asbestos-containing sedimentary serpentinite deposits (i.e., the Big Blue Member and other post-Miocene formations). Photos 6586 and 6587 show the terminus of the Cantua Creek alluvial channel and a sediment affected area adjacent to the Aqueduct. See upper left quadrant of Photo 6586.

Frame Nos. 6589 and 6590. These photos feature the California Aqueduct as it traverses the Panoche Creek alluvial fan. Drainage from the Panoche Creek alluvial channel is allowed to pass over the Aqueduct. The Fresno Slough is featured in the far right margins of the photos.

See Appendix for Flight Line Information and Data Sheets.

Reproduced with permission of the copyright owner. Further reproduction prohibited without permission.

SERIES 3B

Date: July 27, 1977
Agency: NASA
Flight No.: 77-112
Scale: 1 : 65,000
Format: CIR
Photo Index: No
Area Covered: Western Margin of the San Joaquin Valley and the California Aqueduct from the O'Neill Forebay south to the Arroyo Pasajero Alluvial Fan

Frame Descriptions:

Frame No. 2056, 2057, and 2058. These photos feature the California Aqueduct and the Diablo Range foothills of the western margin of the San Joaquin Valley. Notable features include the O'Neill Forebay and Los Banos Reservoir illustrated in Photo 2056 and some potential asbestos containing sedimentary formations as identified in Photos 2057 and 2058. These potential asbestos formations appear as bright white linear outcrops that parallel the California Aqueduct in the area between Ortigalita Creek to the north and the Little Panoche Creek to the south. This foothill area is known as the Leguna Seca Hills. Some intervals of the Aqueduct have a bright, bluish white reflectance characteristic that may be related to sediment deposition (?) in the Aqueduct.

Frame Nos. 2059, 2060, and 2061. These photos feature the California Aqueduct as it traverses the Panoche Creek alluvial fan and what appears to be some asbestos containing sedimentary formations in the Diablo Range foothills that form the western margin of the central San Joaquin Valley. The potential asbestos containing formations have a bright white reflectance characteristic that is similar to that of the New Idria Formation and the Big Blue Member of the Temblor Formation. These potential asbestos containing sedimentary formations are probably Miocene and/or younger in age and can be approximately correlated with the stratigraphic position of the Big Blue Member as exposed in the Big Blue Hills on the north side of Coalinga. The Panoche Creek alluvial channel is shown to extend towards the center of the Valley. The Arroyo Pasajero channel had similar drainage characteristics prior to construction of the California Aqueduct.

Reproduced with permission of the copyright owner. Further reproduction prohibited without permission.

Frame Nos. 2062, 2063, and 2064. These photos feature the California Aqueduct and some asbestos containing sedimentary formations in the Diablo Range foothills. See linear outcrops that have a very bright reflectance. Most of these outcrops are the Big Blue Member of the Temblor Formation as exposed in the Ciervo Hills and the Big Blue Hills. These hills are drained by several alluvial fan systems including Cantua Creek, Arroyo Hondo, and Tumey Gulch. Cantua Creek and the Big Blue Member are featured in Photo 2064. The outcrop of the Big Blue Member is observed to "wrap around" the structural axis of the Joaquin Anticline as illustrated in Photo 2064.

Frame Nos. 2065, 2066, and 2067. These photos feature the Arroyo Pasajero alluvial fan and the California Aqueduct as described in the above photo series.

See Appendix for Flight Line Map and Data Information Sheet.

Reproduced with permission of the copyright owner. Further reproduction prohibited without permission.

SERIES 3C

Date:	January 15, 1976
Agency:	NASA
Flight No.:	76-005
Scale:	1 : 65,000
Format:	CIR
Photo Index:	No
Area Covered:	Western Margin of the San Joaquin Valley and the California Aqueduct from the O'Neill Forebay south to the Arroyo Pasajero Alluvial Fan

Frame Descriptions:

Frame Nos. 7656 through 7665. These photos feature the California Aqueduct and the Diablo Range foothills of the western margin of the San Joaquin Valley as described in series 3A and 3B. The fotthills include (from north to south) Leguna Seca Hills, Panoche Hills, Ciervo Hills, Monocline Ridge, Big Blue Hills, Anticline Ridge, Guijarral Hills, and Kettleman Hills, Notable features in close proximity to the California Aqueduct include the the O'Neill Forebay and Los Banos Reservoir to the north and the Arroyo Pasajero alluvial fan to the south and the Diablo Range foothills that parallel the Aqueduct. Some potential asbestos containing sedimentary formations which appear as bright white linear outcrops that parallel the California Aqueduct, and a few intervals of the Aqueduct which have a bright, bluish white reflectance characteristic that may be related to sediment deposition (?) in the Aqueduct.

See Appendix for Flight Line Map and Data Information Sheet.

Reproduced with permission of the copyright owner. Further reproduction prohibited without permission.

SERIES 4

Date: November 27, 1973
Agency: NASA
Flight No.: 73-194
Scale: 1 : 65,000
Format: CIR
Photo Index: No
Area Covered: Western Margin of the San Joaquin Valley and the California Aqueduct from the O'Neill Forebay to the Arroyo Pasajero Alluvial Fan; and the Diablo Range Mountains including Joaquin Ridge and areas south to the San Andreas Fault Zone.

Frame Descriptions:

Frame No. 6405 - Kettleman Hills (lower center) and the southern portions of the Arroyo Pasajero alluvial fan and the Pleasant Valley region including the town of Coalinga.

Frame No. 6406 - Excellent coverage of the Arroyo Pasajero alluvial fan (right half of picture) and the Pleasant Valley region (left half of picture) including the braided terminus of the Arroyo Pasajero intermittent stream channel (far right center), the trend of the Coalinga Anticline (center) including Anticline Ridge, Turk Narrows, Guijarral Hills, Polvadero Gap, and Kettleman Hills. These photos also feature Pleasant Valley and the Los Gatos Creek stream group centered around the town of Coalinga. This picture illustrates the meandering pathway of Los Gatos Creek between Coalinga (far left center) and Turk Narrows - the gap between Guijarral Hills and Anticline Ridge.

Frame No. 6407 - Same as above with 60% overlap to the north. Image shows the intersection of the Coalinga Anticline (lower center) and the trend of the Joaquin Ridge Anticline (upper left quadrant). Outcrops of the Big Blue Member of the Temblor Formation are visible in the upper center.

Frame No. 6408 - Notable features in this image include the California Aqueduct and the terminus of Cantua Creek (left center), the Big Blue Hills and the north-south trending outcrops of the Big Blue Member of the Temblor Formation (center), and the uplifted sedimentary formations that flank the northwesterly trend of the Joaquin Anticline (geologic structure featured in left half of photo).

Frame Nos. 6409 through 6417 - These pictures feature the California Aqueduct and its relationship with the uplifted sedimentary formations that form the western margin of the San Joaquin Valley from the Cantua Creek region north to the O'Neill Forebay region in Merced County. Some of the formations featured in Frame No. 6414 have similar reflectance characteristics as the Big Blue Member and are in a similar stratigraphic position. These formations may include detrital serpentinite debris.

Reproduced with permission of the copyright owner. Further reproduction prohibited without permission.

Frame Nos. 6425 through 6430 - These pictures feature the Diablo Range Mountains in the vicinity of Coalinga including the New Idria Formation outcrop of Joaquin Ridge and areas south to the Table Mountain serpentinite deposits. Frame No. 6426 is a good image of the White Creek and Pine Canyon areas including the Atlas Mine and Mill Site, the Coalinga Asbestos Mill Site, and numerous mines and exploration pits. This image also illustrates the extent of the elongate barren areas affected by naturally-occuring (geologic) gully erosion.

See Appendix for Flight Line Information and Data Sheets.

Reproduced with permission of the copyright owner. Further reproduction prohibited without permission.

SERIES 5A

Date: April 1, 1971
Agency: NASA/MSC 164
Flight No.: No. 4, Roll 21
Scale: 1 : 60,000
Format: Red Filter, Blues Enhanced
Photo Index: No
Area Covered: Western Margin of San Joaquin Valley and California Aqueduct

Frame Descriptions:

Frame No. 3705 - San Luis Reservoir, O'Neill Forebay and California Aqueduct located on the western margin of the San Joaquin Valley in Merced County approximately 80 miles upstream from the Arroyo Pasajero alluvial fan and the Coalinga - Pleasant Valley region.

Frame No. 3704 - Same as above with 60% overlap to the south. Photo features San Luis Reservoir, O'Neill Forebay, and California Aqueduct located on the western margin of the San Joaquin Valley in Merced County approximately 80 miles upstream from the Arroyo Pasajero alluvial fan and the Coalinga - Pleasant Valley region.

Frame No. 3703 - Same as above with 60% overlap to the south. Notable features in this picture include the linear outcrops of the sedimentary formations that form the western margin of the central San Joaquin Valley and their close proximity to the California Aqueduct (right margin of picture). White reflectance characteristics of some of the formations can be correlated with outcrops of the asbestos-bearing Big Blue Member of the Temblor Formation (Miocene) as seen in Frame 3697 of this series. This suggests that some of these sedimentary units may contain asbestos-bearing detrital serpentinite debris. Some of the streams that drain this area are Ortigalita Creek, Laguna Seca Creek, and Little Panoche Creek. Some of these creeks drain directly into the California Aqueduct.

Frame No. 3702 - Same as above with 60% overlap to the south.

Frame No. 3701 - Same as above with 60% overlap to the south. A notable feature of this picture includes the radial pathway of the Aqueduct as it traverses the medial portion of the Panoche Alluvial Fan in Fresno County.

Frame No. 3700 - Same as above with 60% overlap to the south. A notable feature of this picture includes Little Panoche Creek (top right quadrant), Panoche Hills (center), and Panoche Valley and part of the Panoche Creek drainage system (lower left quadrant). The Panoche Hills area is being dissected by a radial dendritic drainage system. It is not known what the white reflectance area is in the center of the Panoche Hills area.

Reproduced with permission of the copyright owner. Further reproduction prohibited without permission.

Frame No. 3699 - Same as above with 60% overlap to the south. Notable features include the Panoche Hills (top right center), Panoche Creek and the Panoche Creek alluvial fan (lower center), the Ciervo Hills area (bottom right center), and Tumey Gulch which is draining an area that is known to contain exposed detrital serpentinite debris deposits of the Big Blue Member (see whitish area near bottom right hand margin of picture).

Frame No. 3698 - Same as above with 60% overlap to the south. This picture includes parts of the Cantua Creek drainage basin and part of the New Idria Formation which is visible in the lower left corner.

Frame No. 3697 - Same as above with 60% overlap to the south. Notable features include the badlands of the Arroyo Hondo and Cantua Creek drainage basins of the Monocline Ridge area (upper right center), parts of the Big Blue Hills (lower right quadrant), and the northeastern flank of the New Idria Formation near the mining town of Idria. Note the occurrence of elongate whitish areas which have resulted from gully erosion of the soft, serpentinite matrix of the New Idria Formation. The Atlas and Coalinga Asbestos Sites are not visible in this picture.

Frame No. 3696 - Same as above with 60% overlap to the south. Notable features include linear outcrops of the Big Blue Member (far right margin) the Cantua Creek and Arroyo Hondo drainage basins (upper right quadrant), and nearly the full extent of the New Idria Formation outcrop of Joaquin Ridge (left half of picture). The White Creek and Pine Canyon drainage areas are located in the lower left quadrant of the picture. The Atlas Mine and Mill Site is located near the center of the White Creek drainage area that is marked by the "C" shaped pathway of the intermittent White Creek streambed. The Coalinga Asbestos Mill Site (and the Jensen Mine and the Butler Estate Chromite Mine) is located near the far right margin of the New Idria Formation in the lower part of the lower left quadrant.

Frame No. 3695 - Same as above with 60% overlap to the south. Notable features of this picture include the New Idria Formation, the White Creek drainage area (left center) and the whitish streambed of White Creek and Los Gatos Creek (lower left quadrant). This photo also features outcrops of the Big Blue Member of the Temblor Formation as exposed around the margin of the structural axis of the Joaquin Ridge Anticline which is featured in the center of the photo. This area is located at the northern end of the Pleasant Valley floodplain which includes the town of Coalinga. Areas where White Creek is observed to widen and become more white are areas associated with chromite milling operations that existed in the 1940's and 1950's.

Reproduced with permission of the copyright owner. Further reproduction prohibited without permission.

Frame No. 3694 - Same as above with 60% overlap to the south. Notable features include the White Creek and Pine Canyon areas of the New Idria Formation (upper left center), the White Creek drainage pathway (left center), the Pleasant Valley floodplain (lower right quadrant), and outcrops of the Big Blue Member (upper right margin).

See Appendix for Flight Line and Data Information Sheets.

Reproduced with permission of the copyright owner. Further reproduction prohibited without permission.

SERIES 5B

Date: April 1, 1971
Agency: NASA/MSC 164
Flight No.: No. 4, Roll 22
Scale: 1 : 60,000
Format: CIR, Deep Yellow Filter (#15)
Photo Index: No
Area Covered: Pleasant Valley, Joaquin Ridge, and Badlands North of Cantua Creek

Frame Descriptions:

Frame No. 396 - This picture features the meandering pathway of Los Gatos Creek and the confluence of Los Gatos Creek and White Creek (upper left quadrant). Close inspection of this stream juncture shows a short (approximately 600 feet) diversion of White Creek to Los Gatos Creek. The drainage area in the lower right quadrant of the picture (i.e., part of the Pleasant Valley floodplain) has been uplifted in conjunction with the Joaquin Ridge and Coalinga Anticlines.

Frame No. 397 - Same as above with 60% overlap to the north.

Frame No. 398 - Same as above with 60% overlap to the north. The New Idria Formation is visible in the upper left quadrant of the picture. The Pine Canyon area including the Railroad Mine, the Coalinga Asbestos Mill Site, the Jensen Mine and the Butler Estate Chromite Mine are visible in the upper left center.

Frame No. 399 - Notable features of this picture include the southeastern outcrop of the New Idria Formation and disturbed areas associated with naturally occuring geologic erosion and mining operations. Areas associated with naturally occuring geologic erosion are elongated barren areas associated with gully erosional processes (see upper left quadrant of the outcrop area that is marginal to the White Creek streambed). Other disturbed areas include the Atlas Mine and Mill Site (top center of outcrop area), the Christie Mine (far upper right of outcrop area), and the mining operations of Pine Canyon as described in Frame No. 398.

Frame No. 400 - Same as above with 60% overlap to the north.

Frame No. 401 - The notable features of this picture include the New Idria Formation (upper left quadrant) and the unconsolidated, geologically undifferentiated sedimentary formations that form the "badlands" on the northeast flank of Joaquin Ridge near the monoclinal margin of the San Joaquin Valley. Most of this area is included in the Cantua Creek watershed.

Frame No. 402 - Same as above with 60% overlap to the north. Note areal extent of "badlands" described above. This area has very little vegetation and is

Reproduced with permission of the copyright owner. Further reproduction prohibited without permission.

highly susceptible to fluvial and wind erosion. Because of their stratigraphic position (i.e., post Miocene) and close proximity to the New Idria Formation and the "Big Blue", these unconsolidated sedimentary formations are expected to contain from trace to locally high concentrations of asbestos-bearing detrital serpentinite debris.

Frame No. 403 - Same as above with 60% overlap to the north.

See Appendix for Flight Line and Data Information Sheets.

Reproduced with permission of the copyright owner. Further reproduction prohibited without permission.

SERIES 5C

Date: April 1, 1971
Agency: NASA/MSC 164
Flight No.: No. 5, Roll 29
Scale: 1 : 60,000
Format: CIR
Photo Index: No
Area Covered: Pleasant Valley, Joaquin Ridge, and Badlands North of Cantua Creek.

Frame Descriptions:

Frame No. 3479 - Notable features in this picture include the town of Coalinga (center), the cultivated fields of the Pleasant Valley floodplain surrounded by the linearly folded foothills of the Diablo Range (left half of picture), the trend of the Coalinga Anticline (right half of picture), and the intermittent streambeds of the Arroyo Pasajero drainage system including Los Gatos Creek (upper left quadrant), Warthan Creek (left center of picture at town of Coalinga), and Jacalitos Creek (lower left center). These creeks join in the Pleasant Valley floodplain and flow through a gap between Anticline Ridge and Guijarral Hills. This gap is locally known as the Turk Narrows.

Frame No. 3478 - Notable Features in this picture include the New Idria Formation outcrop on the crest of Joaquin Ridge (upper left quadrant), the White Creek, Pine Canyon Creek, Los Gatos Creek drainage pathway leading to the town of Coalinga (botom center), outcrops of the asbestos-bearing Big Blue Member of the Temblor Formation (upper right quadrant), and the apex of the Salt Creek/Cantua Creek alluvial fan on the western margin of the cultivated fields of the San Joaquin Valley (far upper right corner). This picture shows the close geographic relationship of the New Idria Formation, the "Big Blue", and the town of Coalinga which is contained in the enclosed basin formed by the Pleasant Valley floodplain as described above. Note the ribbon of light bluish-gray sediment associated with the White Creek and Los Gatos Creek streambeds. This sediment has the same reflectance characteristics as the serpentinite outcrop of the New Idria Formation and the "Big Blue". Close examination of the White Creek drainage pathway shows five areas where the streambed appears to widen. These are likely areas associated with chromite milling operations that were conducted along the banks of White Creek in the 1940's and 1950's. The tailings pile of the Coalinga Asbestos Mill Site in Pine Canyon can be seen as a small sliver of white material that is located on the lower right margin of the New Idria Formation outcrop. Particularly notable is the absence of any light bluish-gray sediment marking the pathway of the Pine Canyon Creek. The visible pathway leading from the Coalinga Asbestos Mill Site is a dirt road and not a streambed.

Frame 3477 - Excellent detailed coverage of Joaquin Ridge including the New Idria Formation (left center of picture) and the sedimentary serpentinite

Reproduced with permission of the copyright owner. Further reproduction prohibited without permission.

deposits of the "Big Blue" (upper right quadrant of picture). The highly reflective serpentinite matrix of disturbed surfaces of the New Idria Formation facilitates identification of mines, tailings piles, and barren surfaces associated with geologic occurrences of gully erosion. Also visible are hundreds of exploration pits and many miles of exploration access roads. The restricted vegetation associated with the magnesium rich serpentinite soils appears as a dark bluish-green surface that is readily differentiated from the vegetation associated with non-serpentine soils. The Coalinga Asbestos Mill Site is located on the lower far right margin of the serpentinite outcrop and the Atlas Mine and Mill Site is located near the center of the serpentinite outcrop area that is drained by White Creek.

Frame No. 3476 - Same as the above picture with more of the "Big Blue" and the western margin of the San Joaquin Valley.

Frame No. 3475 - Notable features in this picture include the New Idria Formation (lower left corner), the Cantua Creek drainage network (center), the dendritic drainage network that is dissecting the uplifted sedimentary formations (including the "Big Blue") that form the monoclinal margin of the San Joaquin Valley on the north side of Coalinga, and the cultivated fields that are located near the apex of the coalescing alluvial fans formed by the Cantua Creek and Salt Creek intermittent stream systems (far right side of picture).

Frame No. 3474 - Same as above with more of the undifferentiated "badland" areas (top center of picture) that are located north of Cantua Creek. The geologic formations in this area are undifferentiated because the area is a massive complex of badlands associated with severe fluvial and wind erosion and mass wasting.

See Appendix for Flight Line Information and Data Sheets.

Reproduced with permission of the copyright owner. Further reproduction prohibited without permission.

SERIES 6

Date: October 24, 1957
Agency: USDA/ABI
Flight No.: CSS - 3 - 57 DC
Scale: 1 : 20,000
Format: Black and White
Photo Index: Yes - Sheet 19 of 25
Area Covered: Western Fresno County including Joaquin Ridge and the New Idria Formation

Frame Descriptions:

Frame Nos. 32T-7 through 32T-10 and 32T-49 through 32T-54 cover the White Creek and Pine Canyon outcrop areas of the New Idria Formation. These pictures are useful for illustrating the extent and distribution of barren areas associated with the naturally occuring geologic phenomenon of gully erosion of the soft serpentinite matrix of the New Idria Formation in areas associated with slopes of 30 degrees or more. These pictures are also useful for documenting the extent of chromite and other mining operations that preceded asbestos mining operations that were initiated in the early 1960's.

Frame Nos. 32T-53 and 32T-52 - These pictures feature the White Creek drainage area of the New Idria Formation including the area now occupied by the Atlas Mine and Mill Site. Notable features include barren areas associated with gully erosional processes and chromite mining operations and other mining operations.

Frame Nos. 32T-49 through 32T-53 and 32T-13 are useful for documenting the location of chromite milling operations on the banks and streambed of White Creek. A close analysis of these pictures, integrated with field observations and a review of the literature (i.e., Matthews, 1961), indicates that as many as five chromite mills operated on White Creek. Evidence of these mill sites can be seen in Frames 32T-52 (lower right center in streambed), 32T-31 (upper right quadrant in streambed), 32T-50 (center in streambed), 32T-49 (upper right quadrant in streambed), and 32T-13 (lower right quadrant in streambed).

Frame Nos. 32T-8 and 32T-9 show the location and extent of the Butler Estate Chromite Mine (center of photos) and the James-Corbett-Byles Mine and Archer Mine (both located to the left of the Butler Mine).

Frame No. 32T-95 features the Upper Pine Canyon area including the Railroad Mine and an undisturbed area now occupied by the Coalinga Asbestos Mill Site. Other than the Railroad Mine and the Butler Mine, no other mining operations are evident in Pine Canyon.

Photo Index Sheet Is Attached.

Reproduced with permission of the copyright owner. Further reproduction prohibited without permission.

SERIES 7

Date: 1950
Agency: USDA/ABI
Flight No.: 1242-50
Format: Black and White
Scale: 1 : 20,000
Photo Index: No
Area Covered: Joaquin Ridge Including White Creek and Pine Canyon

Comments: These photos are useful for documenting surface conditions, specifically the occurrence of erosional gullies in the serpentinite outcrop areas in White Creek and Pine Canyon drainage areas of the New Idria Formation prior to the initiation of asbestos mining activities in the late 1950's and early 1960's. Some of these photos were used as a basis for the mapping of landslide and serpentinite debris flow deposits of Upper Pine Canyon. These photos predate the occurrence of anthropic activities associated with the Railroad Mine and the Coalinga Asbestos Mill Site in the Pine Canyon drainage area and the Atlas Mine and Mill Site in the White Creek drainage area.

Frame Nos. 13G-58, -57, -56. These photos feature barren erosional areas associated with serpentinite gullies in the western portions of the New Idria Formation outcrop in the White Creek drainage basin. These gullies predate the occurrence of asbestos mining operations which began in the early 1960's. These photos are dated February 12, 1950. The gullies cover approximately 15% to 20% of the serpentinite outcrop areas shown in the photos. Drainage in the intermittent White Creek channel shown in Photo 13G-58 is towards the bottom of the image.

Frame Nos. 16G-87, -88, -89, -90. These photos feature the central portion of the serpentinite outcrop area in the White Creek drainage basin. Photos 16G-87 and 16G-88 feature the crest of Joaquin Ridge near Spanish Lake. The general area that became the Atlas Site in the early 1960's is approximately one mile southwest of Spanish Lake. As illustrated in this picture, at least three gullies are encroaching on this area. Photo 16G-89 features most of the central serpentinite outcrop area and a dendritic network of the erosional gullies. Intermittent flow in these gullies occurs as a response to runoff during storm events. Flow is towards White Creek towards the bottom of the image. The general area of the James Corbett Byles Mine is shown in the upper right quadrant of Photo 16G-90. The Butler Estate Chromite Mine, which is presently located less than one half mile northwest of the Byles Mine, was not yet in existence.

Frame Nos. 16G-90, -91, -92. These photos feature the intermittent drainage channel of White Creek at the base of the serpentinite outcrop area. These photos also feature the location of what appear to be four chromite milling operations that were set up in the intermittent streambed of White Creek. These chromite mill sites appear as sediment laden intervals associated with

Reproduced with permission of the copyright owner. Further reproduction prohibited without permission.

a noticeable broadening of the streambed. This was probably from ponding operations conducted in the streambed.

Frame Nos. 25G-95 and -94. These photos feature the middle reach of White Creek including the juncture of Pine Canyon Creek with White Creek (see lower right quadrant of 25G-95. The intermittent Pine Creek channel is barely visible. See USGS Santa Rita Peak 1:24,000 Scale Topographic Map for geographic reference.

Frame Nos. 25G-91, -90, -89. These photos feature the landslide and serpentinite debris flow deposits of the Upper Pine Canyon drainage area and were used as a basis for the geomorphic mapping of the this area prior to the initiation and affects of large-scale mining activities. Photo 25G-90 is the best reference photo for the analysis of the landslide and serpentinite debris complex. As illustrated in Photo 25G-90, there is little visible evidence of mining in the Upper Pine Canyon area at this time. However, the photos do show the occurrence of erosional areas associated with serpentinite gullies. These barren, erosional areas are not as extensive as in the White Creek drainage area.

Reproduced with permission of the copyright owner. Further reproduction prohibited without permission.

FLIGHT LINE DATA SHEETS

Reproduced with permission of the copyright owner. Further reproduction prohibited without permission.

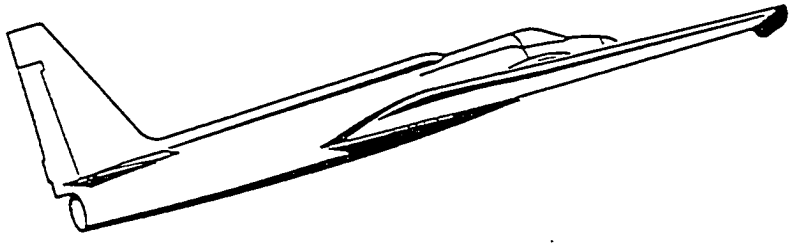
Airborne Instrumentation Research Project

Flight Summary Report

Flight No. 79-076

Date 14 June 1979

FSR- 1282



LIBRARY
UNIVERSITY OF CALIFORNIA
SANTA BARBARA
SEP 7 1979
MAP ROOM

NASA
National Aeronautics and
Space Administration

Ames Research Center
Moffett Field, California 94035

Airborne Missions and Applications Division

Reproduced with permission of the copyright owner. Further reproduction prohibited without permission.

FLIGHT SUMMARY REPORT

Flight No: 79-076

Date: 14 June 1979

FSR No: 1282

Julian Date: 165

Sensor Package: Dual RC-10
Aerosol Particulate Sampler (APS)

Aircraft No: 4

Purpose of Flight: #0666R Support
Requestor: Lumb/Bauer
#0047 Support
Requestor: Ferry

Area(s) Covered: Central California

SENSOR DATA

Accession No:	02770	02771	---
Sensor ID No:	031	033	024
Sensor Type:	RC-10	RC-10	APS
Focal Length:	6" 153.05mm	6" 153.17mm	---
Film Type:	High Definition Aerochrome Infrared, SO-127	Panatomic-X, 3400	---
Filtration:	CC .10B + 2.2AV	Wratten 12 + 2.2AV	---
Spectral Band:	510-900nm	510-700nm	---
f Stop:	4.0	5.6	---
Shutter Speed:	1/175	1/225	---
No. of Frames:	210	210	---
% Overlap:	60	60	---
Quality:	Excellent	Excellent	---
Remarks:	---	---	Non-imaging sensor

Reproduced with permission of the copyright owner. Further reproduction prohibited without permission.

FLIGHT SUMMARY

79-076

This flight was flown in support of Flight Requests #0666R (Lumb/Bauer, NASA/ARC) and #0047 (Ferry, NASA/ARC) under the FY 1979 Airborne Instrumentation Research Program (AIRP) plan. Photography was acquired over agricultural regions of central California (see Track Map). Aerosol Particulate Sampler (APS) data was collected throughout the flight but is not indicated on the track map.

The weather was clear over the entire area. However, some minor smoke was encountered along the first three data lines from agricultural burns and grass fires. The photography is of excellent quality with no camera or processing malfunctions noted.

The APS has been developed and is operated by Dr. Guy Ferry of the NASA-Ames Research Center Atmospheric Experiments Branch. The sampler is a non-imaging sensor designed to gather high altitude dust particles for laboratory research.

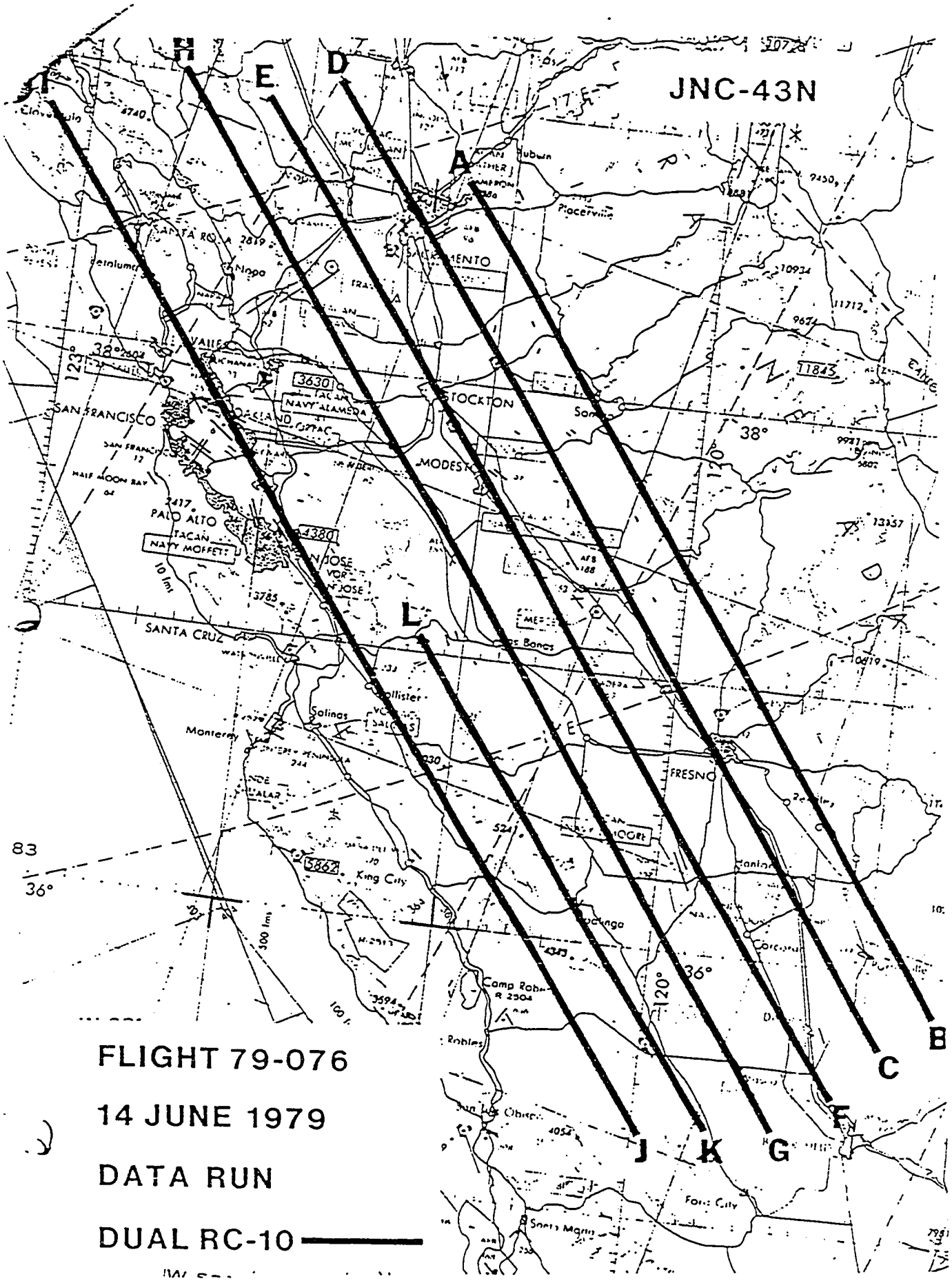
Reproduced with permission of the copyright owner. Further reproduction prohibited without permission.

Reproduced with permission of the copyright owner. Further reproduction prohibited without permission.

FLIGHT LINE DATA

FLIGHT NO. 79-076

	Check Points	Frame Numbers	Time (GMT – hr, min, sec) START	Time (GMT – hr, min, sec) END	Altitude, MSL feet/meters	Cloud Cover/Remarks
RC-10 #031	A-B	6465-6497	17:49:46	18:19:57	65,000/19800	Smoke, frs. 6479-6485
	C-D	6498-6534	18:23:38	18:57:36	"	Smoke, frs. 6532-6534
	E-F	6535-6574	19:01:08	19:38:02	"	Smoke, frs. 6537-6540
	G-H	6575-6615	19:41:05	20:18:58	"	Clear
	I-J	6616-6656	20:25:42	21:04:07	"	"
	K-L	6657-6674	21:07:32	21:23:10	"	"
RC-10 #033	A-B	1044-1076	17:49:15	18:19:31	65,000/19800	Smoke, frs. 1058-1064
	C-D	1077-1113	18:23:12	18:57:12	"	Smoke, frs. 1111-1113
	E-F	1114-1153	19:00:44	19:37:39	"	Smoke, frs. 1116-1119
	G-H	1154-1194	19:40:42	20:18:36	"	Clear
	I-J	1195-1235	20:25:20	21:03:45	"	"
	K-L	1236-1253	21:07:11	21:22:49	"	"
APS	---	---------	17:48:00	21:18:00	65,000/19800	APS #1 exposed near checkpoint "A" and sealed near checkpoint "L"



Reproduced with permission of the copyright owner. Further reproduction prohibited without permission.

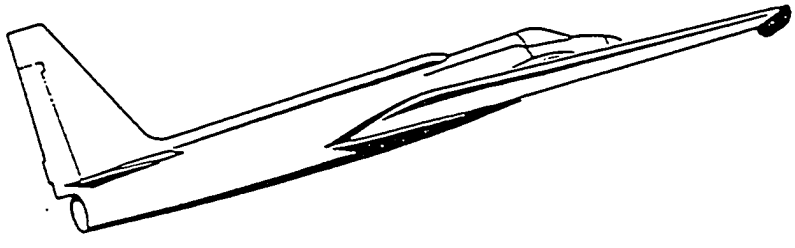
Airborne Instrumentation Research Project

Flight Summary Report

Flight No. 77-112

Date 27 July 1977

FSR- 1028



NASA
National Aeronautics and
Space Administration

Ames Research Center
Moffett Field, California 94035

Airborne Missions and Applications Division

Reproduced with permission of the copyright owner. Further reproduction prohibited without permission.

FLIGHT SUMMARY REPORT

Flight No: 77-112

Date: 27 July 1977

FSR No: 1028

Julian Date: 208

Sensor Package: RC-10 / Aerosol Particulate Sampler (APS)

Aircraft No: 5

Purpose of Flight: #0488 Support
Requestor: Robie
#0047 Support
Requestor: Ferry

Area(s) Covered: Sacramento and San Joaquin Valleys

SENSOR DATA

Accession No:	02520	---
Sensor ID No:	031	024
Sensor Type:	RC-10	APS
Focal Length:	6" 153.05mm	---
Film Type:	High Definition Aerochrome Infrared, SO-127	---
Filtration:	2.2 AV + CC .30M	---
Spectral Band:	510-900nm	---
f Stop:	5.6	---
Shutter Speed:	1/125	---
No. of Frames:	265	---
% Overlap:	60	---
Quality:	Excellent	---
Remarks:	---	Non-imaging sensor

Reproduced with permission of the copyright owner. Further reproduction prohibited without permission.

FLIGHT SUMMARY

77-112

This flight was flown in support of Flight Requests #0488 (Robie, California Department of Water Resources) and #0047 (Ferry, NASA/ARC) under the FY 1978 Airborne Instrumentation Research Program (AIRP) plan. Photographic coverage and Aerosol Particulate Sampler (APS) data were obtained over the Sacramento and San Joaquin Valleys in California (see Track Map). Because of the extensive flight track, the APS data track is not shown except at times the camera was operating.

The entire flight was cloud-free. The imagery is of excellent quality with no camera or processing malfunctions noted.

The APS has been developed and is operated by Dr. Guy Ferry of the NASA-Ames Research Center Atmospheric Experiments Branch. The sampler is a non-imaging sensor designed to gather high altitude dust particles for laboratory research.

Reproduced with permission of the copyright owner. Further reproduction prohibited without permission.

Reproduced with permission of the copyright owner. Further reproduction prohibited without permission.

FLIGHT LINE DATA

FLIGHT NO. 77-112

	Check Points	Frame Numbers	Time (GMT–hr, min, sec)		Altitude, MSL feet/meters	Cloud Cover/Remarks
			START	END		
RC-10	A-B	1833-1854	17:27:10	17:47:08	65,000/19800	Clear
	C-D	1855-1902	17:50:29	18:34:09	"	Clear
	E-F	1903-1954	18:37:19	19:24:03	"	Clear
	G-H	1955-2016	19:27:14	20:23:27	"	Clear
	I-J	2017-2080	20:26:27	21:24:00	"	10% smoke, frs. 2076-2077
	K-L	2081-2097	21:27:19	21:40:45	"	Clear
APS	---	---	17:16:00	21:36:00	"	APS #1 and #2 opened and closed

National Aeronautics and Space Administration

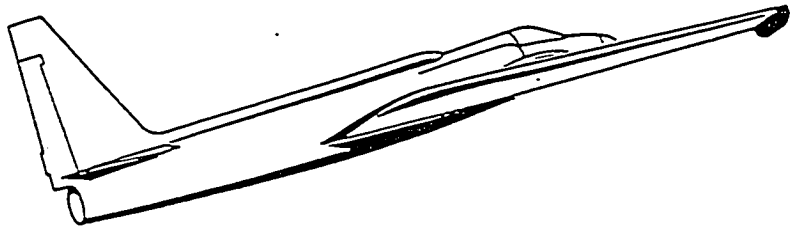
Earth Resources Aircraft Project

Flight Summary Report

Flight No. 76-005

Date 15 January 1976

FSR- 782



Airborne Science Office

Ames Research Center, Moffett Field, California

Reproduced with permission of the copyright owner. Further reproduction prohibited without permission.

FLIGHT SUMMARY REPORT

Flight No: 76-005 Date: 15 January 1976

FSR No: 782 Julian Date: 015

Sensor Package: RC-10 / Aerosol Particulate Sampler (APS) Aircraft No: 4

Purpose of Flight: #0303 Support
Requestor: Estes
#0047 Support
Requestor: Ferry

Area(s) Covered: Central California

SENSOR DATA

Accession No:	02290	---
Sensor ID No:	023	024
Sensor Type:	RC-10	APS
Focal Length:	6" 153.21mm	---
Film Type:	Aerochrome Infrared, 2443	---
Filtration:	WRATTEN 12 + CC .50M + 2.2 AV	---
Spectral Band:	510-900nm	---
f Stop:	5.6	---
Shutter Speed:	1/200	---
No. of Frames:	194	---
% Overlap:	60	---
Quality:	Good	---
Remarks:	---	Non-imaging sensor

Reproduced with permission of the copyright owner. Further reproduction prohibited without permission.

FLIGHT SUMMARY

76-005

This flight was flown in support of Flight Requests #0303 (Estes, University of California, Santa Barbara) and #0047 (Ferry, NASA/ARC) under the FY 1976 Airborne Instrumentation Research Program (AIRP) plan. Photographic and Aerosol Particulate Sampler (APS) data was collected over central California (see Track Map).

The weather over the entire area was clear except for some minor cirrus and haze in the San Joaquin Valley. The flight number displayed in the data annotation block on the imagery erroneously reads 76-015. The imagery obtained is good quality with no camera or processing malfunctions noted.

The Aerosol Particulate Sampler has been developed and is operated by Dr. Guy Ferry of the NASA-Ames Research Center Planetary Science and Applications Branch. The sampler is a non-imaging sensor designed to gather high altitude dust particles for laboratory research. The Track Map and Flight Line Data indicate those segments of the flight during which the sampler was activated.

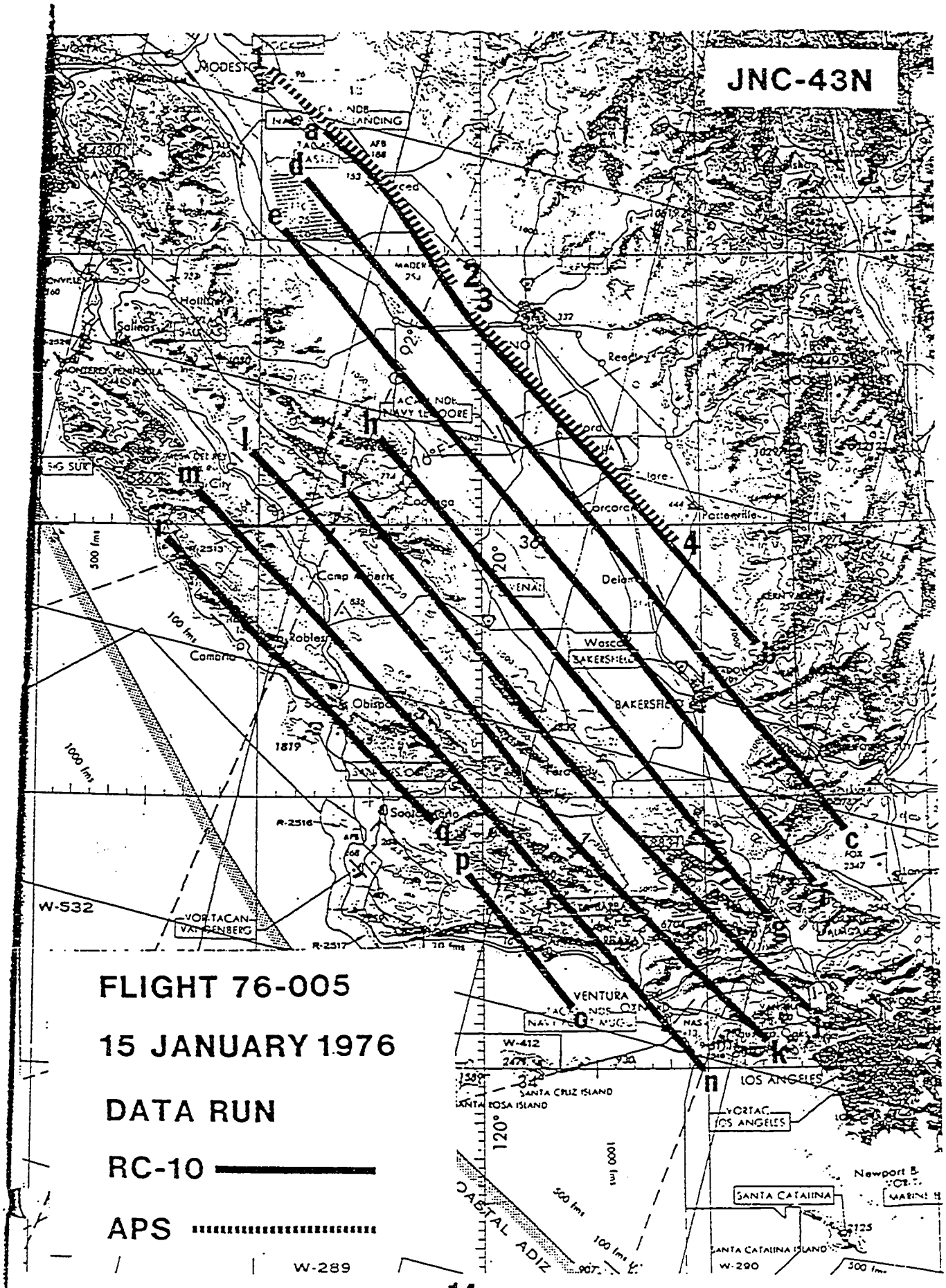
Reproduced with permission of the copyright owner. Further reproduction prohibited without permission.

Reproduced with permission of the copyright owner. Further reproduction prohibited without permission.

FLIGHT LINE DATA

FLIGHT NO. 76-005

	Check Points	Frame Numbers	Time (GMT – hr, min, sec) START	Time (GMT – hr, min, sec) END	Altitude, MSL feet/meters	Cloud Cover/Remarks
RC-10	a-b	7603-7625	19:00:26	19:19:56	65,000/19800	Light cirrus, frs. 7603-7608
	c-d	7626-7655	19:31:12	19:58:59	"	Light cirrus, frs. 7652-7655
	e-f	7656-7682	20:02:57	20:28:19	"	Clear
	g-h	7683-7703	20:31:22	20:50:36	"	Clear
	i-j	7704-7725	20:54:05	21:14:16	"	Clear
	k-l	7726-7752	21:18:09	21:42:59	"	Clear
	m-n	7753-7777	21:46:06	22:08:32	"	Clear
	o-p	7778-7782	22:15:55	22:19:48	"	Clear
	q-r	7783-7796	22:23:54	22:35:58	"	Clear
APS	1-2	---	18:56:--	19:06:--	"	APS #3 opened and closed
	3-4	---	19:07:--	19:17:--	"	APS #2 opened and closed
	3-r	---	19:07:--	22:35:--	"	APS #1 opened full time from start of photo data run and closed at the beginning of descent - not shown on Track Map



Reproduced with permission of the copyright owner. Further reproduction prohibited without permission.

UCSB MAP ROOM

National Aeronautics and Space Administration

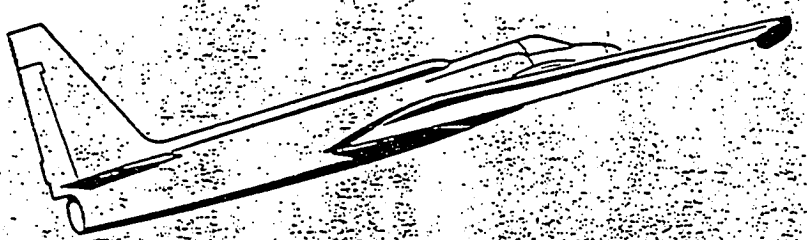
Earth Resources Aircraft Project

Flight Summary Report

Flight No. 73-194

Date 27 November 1973

FSR- 382



LIBRARY
UNIVERSITY OF CALIFORNIA
SANTA BARBARA
NOV 12 1974
MAP ROOM

Airborne Science Office

Ames Research Center, Moffett Field, California

Reproduced with permission of the copyright owner. Further reproduction prohibited without permission.

NASA/ARC Earth Resources Aircraft Project

FLIGHT SUMMARY REPORT

Flight No: 73-194

Date: 27 November 1973

Aircraft No: 5

Julian Date: 331

Sensor Package: Vinten System A/RC-10

Purpose of Flight: 74-SR-0102 Support
Requestor: Dr. Jack Estes
University of California, Santa Barbara

Area(s) Covered: San Joaquin Valley and South Coast Range, California

SENSOR DATA

Accession No:	01537	01538	01539	01540	01541
Sensor ID No:	001	002	003	004	017
Sensor Type:	Vinten	Vinten	Vinten	Vinten	RC-10
Lens Focal Length:	1-3/4"	1-3/4"	1-3/4"	1-3/4"	6"
Film Type:	Aerial Color, SO-242	Plus-X, 2402	Infrared, Aerographic, 2424	Aerochrome Infrared, 2443	Aerochrome Infrared, 2443
Spectral Band:	400-700nm	580-680nm	690-760nm	510-900nm	510-900nm
f Stop:	3.5	13.5	9.5	9.5	8
Shutter Speed:	1/250	1/250	1/250	1/250	1/225
No. of Frames:	278	278	278	278	242
% Overlap	60	60	60	60	60
Quality	Excellent	Excellent	Excellent	Excellent	Excellent
Remarks					

Reproduced with permission of the copyright owner. Further reproduction prohibited without permission.

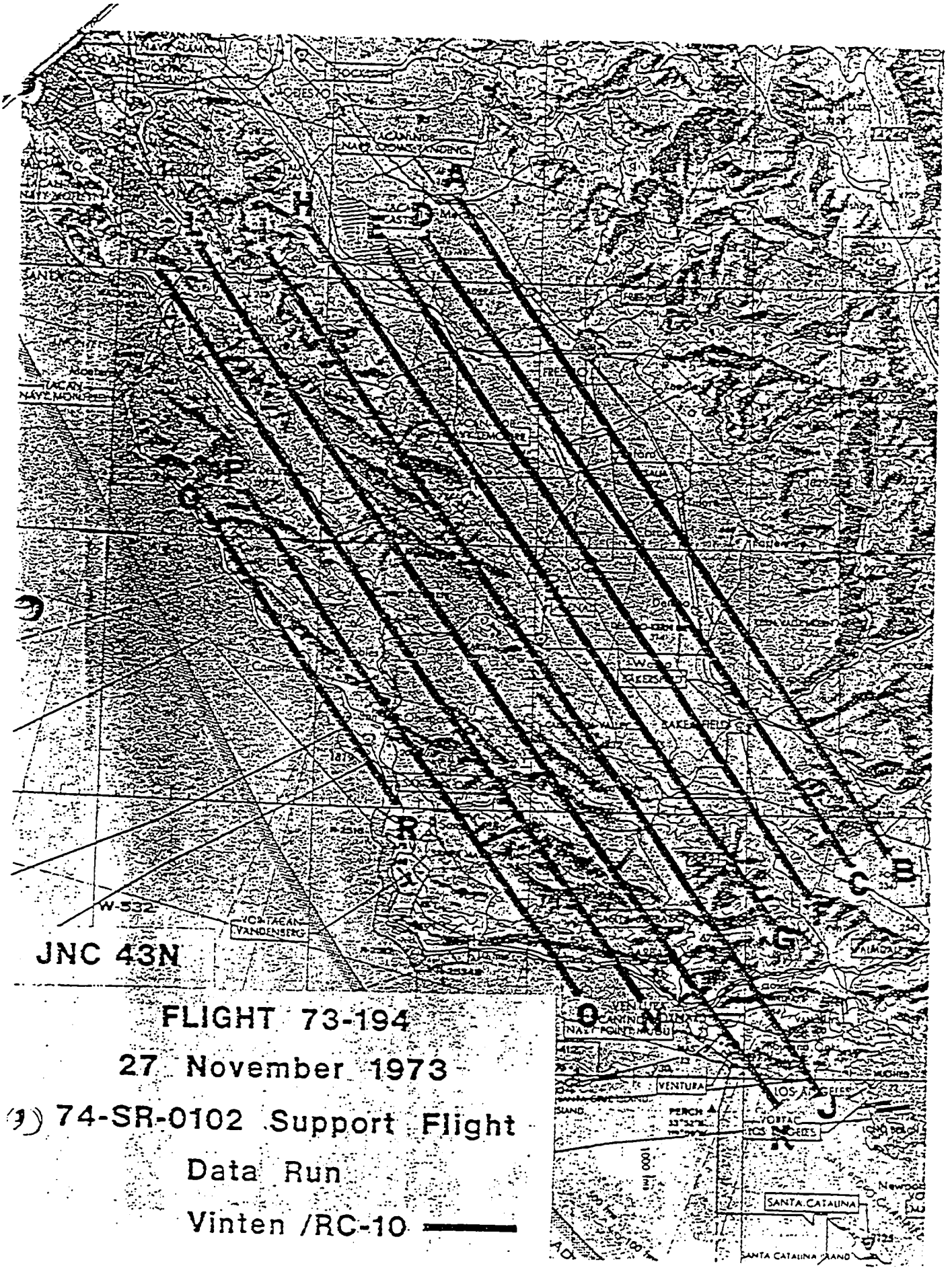
FLIGHT SUMMARY

73-194

This flight is in support of Flight Request 74-SR-0102 (Estes) under the calendar year 1974 Earth Observations Aircraft Program (EOAP) plan. The flight covers the San Joaquin Valley and south coast range areas of California (see Track Map).

All imagery is cloud-free and of excellent quality with no malfunctions noted. Due to a setting error of the Time Code Generator (TCG) the Vinten clock times show GMT minus one hour.

Reproduced with permission of the copyright owner. Further reproduction prohibited without permission.



Reproduced with permission of the copyright owner. Further reproduction prohibited without permission.

Reproduced with permission of the copyright owner. Further reproduction prohibited without permission.

FLIGHT LINE DATA

FLIGHT NO. 73-194

VINTENS

Check Points	Frame Numbers	* Time (GMT - hr, min, sec)		Altitude, MSL (feet)	Cloud Cover/Remarks
		START	END		
A-B	0001-0032	17:23:36	17:48:37	65,000	Clear
C-D	0033-0063	17:51:29	18:16:24	"	"
E-F	0064-0093	18:19:19	18:43:30	"	"
G-H	0094-0128	18:46:54	19:14:26	"	"
I-J	0129-0169	19:17:31	19:50:07	"	"
K-L	0170-0212	19:53:50	20:28:44	"	"
M-N	0213-0247	20:31:47	20:59:43	"	"
O-P	0248-0265	21:03:46	21:23:55	"	"
Q-R	0266-0270	21:27:11	21:37:02	"	"
		*Times listed are actual clock times (GMT minus 1 hour) To obtain correct GMT, add 1 hour to times listed			

FLIGHT LINE DATA

FLIGHT NO. 73-194

RC-10

Check Points	Frame Numbers	Time (GMT – hr, min, sec)		Altitude, MSL (feet)	Cloud Cover/Remarks
		START	END		
A-B	6308-6334	18:22:47	18:47:40	65,000	Clear
C-D	6335-6361	18:50:32	19:15:25	"	"
E-F	6362-6387	19:18:19	19:42:36	"	"
G-H	6388-6417	19:45:54	20:13:24	"	"
I-J	6418-6452	20:16:31	20:49:07	"	"
K-L	6453-6490	20:52:50	21:28:51	"	"
M-N	6491-6520	21:30:48	21:58:45	"	"
O-P	6521-6536	22:02:56	22:22:57	"	"
Q-R	6537-6549	22:26:13	22:36:10	"	"

Reproduced with permission of the copyright owner. Further reproduction prohibited without permission.

MSC-04883

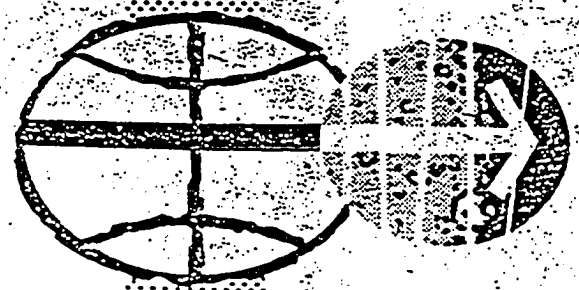
NATIONAL AERONAUTICS AND SPACE ADMINISTRATION

EARTH OBSERVATIONS AIRCRAFT PROGRAM

CATALOGING AND INDEXING REPORT

MISSION 164

TEST SITES 211, 254, AND 260



MANNED SPACECRAFT CENTER

HOUSTON, TEXAS

December 1971

Reproduced with permission of the copyright owner. Further reproduction prohibited without permission.

MISSION 164/TEST SITES 254 AND 260

Reproduced with permission of the copyright owner. Further reproduction prohibited without permission.

IMAGERY RECORD

AREA California -- Regions DATE FLOWN April 1, 1971

SCALE AT LINE OF FLIGHT 1: 120,000 (a) 1: _____ (b) 1: _____ (c)

FLIGHT I.D. NASA/MSC 164, Sites 254 & 260, Flight 4a, Roll 21

FILED BY same IN CATALOGUE FILED BY same IN COLLECTION

INDEX: MOSAIC _____ FLIGHT LINE X SPOT INDEX _____ OTHER _____

INDEX SCALE 1: CA. 1,000,000 SPECIAL LOCATION: IMAGERY INDEX ROLL FILM COLLECTION

IMAGERY

SIZE 9"x9" ENLARGEMENT _____ REDUCTION _____

VERTICAL X OBLIQUE: HIGH _____ LOW _____ RECTIFIED _____

OVERLAP 60% % SIDELAP _____ %

FILM TYPE SO-397 UV _____ B/W _____ B/W IR _____ COLOR X COLOR IR _____

SPECTRAL RANGE (S) 400-650nm _____

PRINT _____ POSITIVE X NEGATIVE _____

RESOLVING POWER & CONTRAST RATIO: 1.6:1 40 1000:1 80 LINE PAIRS PER MM _____

THERMAL IR _____ SPECTRAL RANGE (S) _____

MICROWAVE (TYPE & SPECTRAL RANGE) _____ POLARIZATION _____

FILTER (S) I.D. TYPE (S) 24 _____

GENERATION HELD BY LIBRARY 3rd LEVELING SCALE PRESENT _____

COMPUTER COMPATIBLE TAPES: ANALOG _____ DIGITAL _____

NUMBER OF TRACKS _____ BITS PER IN _____ TAPE WIDTH _____

TYPE OF TAPE: MAGNETIC _____ DISK _____ OTHER _____

SENSOR: CAMERA (TYPE & I.D.) RC-8, 4R LENS FOCAL LENGTH 6"

SCANNER (TYPE & I.D.) _____ DETECTOR SPECTRAL RANGES _____

RESEAU MARKS _____

EXPOSURE REMARKS: DENSITY _____ HUE _____ BRIGHTNESS _____

COLOR SATURATION _____ NOISE _____

GRAY SCALE WEDGE AVAILABLE _____ DENSITY STEP WEDGE AVAILABLE _____

FLIGHT CLOCK SET FOR G.M.T. _____ P.S.T. _____ OTHER _____

GENERAL SUBJECTIVE QUALITY _____

PLATFORM I.D. _____ DIRECTIONAL OREINTATION OF PLATFORM _____

SUN ANGLE TO PLATFORM _____ DEGREES AZIMUTH _____ DEGREES ELEVATION

ALTITUDE (S) (a) 60,000' (b) _____ (c) _____

FRAME NO.(S) (a) 3493-3706 (b) _____ (c) _____

CONTRACTOR OR REQUESTOR: Earth Observations Aircraft Program

FLOWN BY: NASA/MSC

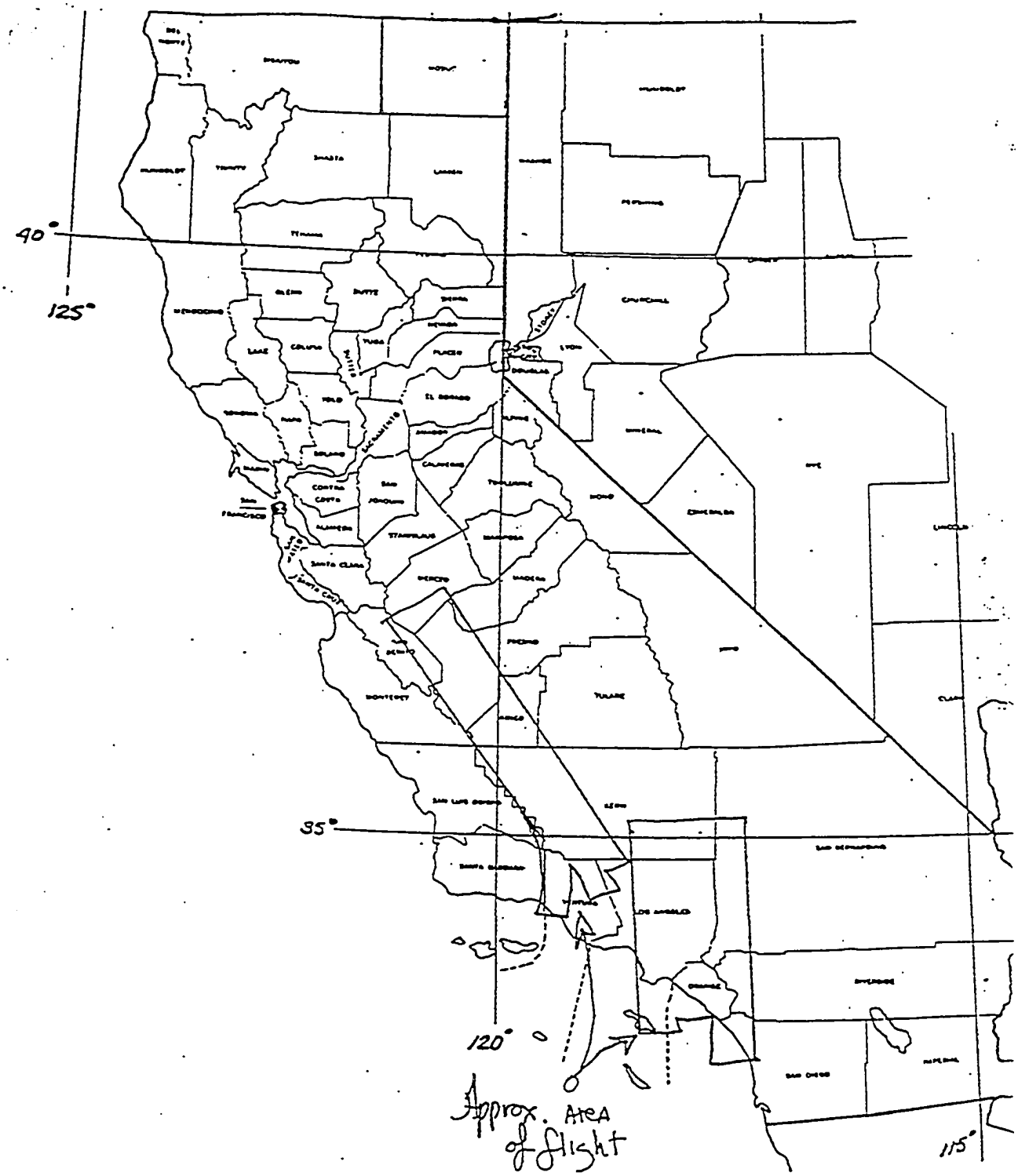
ACQUIRED FROM: UCSB/GRSU RECEIVED: 4/8

SUPPLEMENTAL INFORMATION: _____

CALIF. POL. SUB.

ORDER NUMBER (Lib-452

Reproduced with permission of the copyright owner. Further reproduction prohibited without permission.



Reproduced with permission of the copyright owner. Further reproduction prohibited without permission.

Reproduced with permission of the copyright owner. Further reproduction prohibited without permission.

PHOTOGRAPHIC COVERAGE PLOT LOG, FLIGHT 5

MISSION 164/254 (California Coastal Area)			DATE April 2, 1971									HOTES
SENSOR			RC-8/4L	RC-8/4R	Zeiss	Hasselblad 1	Hasselblad 2	Hasselblad 3	Hasselblad 4	Hasselblad 5	Hasselblad 6	Sites 254 and 260 overlap and flight lines coincide.
FOCAL LENGTH			6 in.	6 in.	12 in.	40 mm	40 mm	40 mm	40 mm	40 mm	40 mm	Film/filter configurations are identical.
FILM			2443	SO-397	2443	2402	2402	2424	SO-356	SO-356	2443	ASN-41 computer did not function.
FILTER			15	2A	15	25	58	89B	2E	W3	80B + 15	For RS-7 coverage, see Roll 40.
ROLL NO.			29	31	32	33	34	35	36	37	38	
LINE	RUN	Alt, ft	FRAMES	FRAMES	FRAMES	FRAMES	FRAMES	FRAMES	FRAMES	FRAMES	FRAMES	REMARKS
14	1	60 000	3469 3502	3711 3744	000 067	001 016	001 016	001 016	001 016	001 016	001 016	San Luis Flat southeast to Note Reservoir on San Luis Creek. (Not shown on map.) Rerun of Flight 4 Line 14
8b	1	60 000	3503 3515	3745 3757	068 093	017 022	017 022	017 022	017 022	017 022	017 022	Ford Point northwest to Purisima Pointe
9	1	60 000	3516 3553	3758 3795	094 168	023 041	023 041	023 041	023 041	023 041	023 041	Santa Cruz Channel northwest to 14 mi. northwest of Cypress Point (Monterey Bay)
8a	1	60 000	3554 3558	3796 3800	169 177	042 043	042 043	042 043	042 043	042 043	042 043	California Sea Otter Game Refuge. Vicinity of Point Sur
10	1	60 000	3559 3594	3801 3836	178 249	044 061	044 061	044 061	044 061	044 061	044 061	Monterey Bay southeast to Santa Cruz Island
11	1	60 000	3595 3634	3837 3876	250 329	062 081	062 081	062 081	062 081	062 081	062 081	Anacapa Passage northwest to Capitola. Frame 3595, oblique
12	1	60 000	3635 3671	3877 3913	330 403	082 086	082 086	082 086	082 086	082 086	082 006	Gilroy southeast to Anacap Island. Hasselblad film expended
13	1	60 000	3672 3694	3914 3936	404 439	087	087	087	087	087	087	Point Mugu northwest to Cholame Valley. Line incomplete. Film expended on completion of southern half. (See Flight 6)

Reproduced with permission of the copyright owner. Further reproduction prohibited without permission.

PHOTOGRAPHIC COVERAGE PLOT LOG, FLIGHT 4

MISSION 164/254 (California Coastal Area) 260 (California - Feather River Project) DATE April 1, 1971

SENSOR			RC-8/4L	RC-8/4R	Zeiss	Nase 1	Nase 2	Nase 3	Nase 4	Nase 5	Nase 6
FOCAL LENGTH			6 in.	6 in.	12 in.	40 mm	40 mm	40 mm	40 mm	40 mm	40 mm
FILM			2443	80-397	2443	2402	2402	2424	80-356	80-356	2443
FILTER			15	24	15	25	58	89B	2E	W3	80B + 15
ROLL NO.			19	21	22	23	24	25	26	27	28
LINE	RUN	Alt, ft	FRAMES	FRAMES	FRAMES	FRAMES	FRAMES	FRAMES	FRAMES	FRAMES	FRAMES
16	1	60 000	3251 3279	3493 3521	001 056	001 014	001 014	001 014	001 014	001 014	001 014
15	1	60 000	3280 3311	3522 3553	057 121	015 030	015 030	015 030	015 030	015 030	015 030
28	1	60 000	3312 3331	3554 3573	122 161	031 040	031 040	031 040	031 040	031 040	031 040
27	1	60 000	3332 3351	3574 3593	162 200	041 049	041 049	041 049	041 049	041 049	041 049
26	1	60 000	3352 3368	3594 3610	201 232	050 057	050 057	050 057	050 057	050 057	050 057
			3369 3372	3611 3614	233 239						
25	1	60 00	3373 3388	3615 3630	240 270	058 065	058 065	058 065	058 065	058 065	058 065
24	1	60 000	3389 3408	3631 3650	271 308	066 074	066 074	066 074	066 074	066 074	066 074
23	1	60 000	3409 3427	3651 3669	309 346	075 083	075 083	075 083	075 083	075 083	075 083
14	1	60 000	3428 3464	3670 3706	347 419	084 092	084 092	084 092	084 092	084 092	084 092

NOTES

Sites 254 and 260 overlap and flight lines coincide. Film/filter configurations are identical.

Line 14 was not flown within the sun angle constraints of Line 15 and was reflown on Flight 5.

The ASN-41 computer was not functioning. Cloud cover over Gulf of Santa Catalina. For RS-7 coverage, see Roll 30.

REMARKS
Grapevine Peak northwest to Santa Rita Park
Los Banos southeast to Whiteacre Peak
Four Corners south to Encinitas. Clouds along coast in the vicinity of Carlsbad
San Mateo Point north to Saddleback Mt. Clouds off shore in the vicinity of San Clemente
Peerless Valley south to Laguna Beach. Clouds off shore in the vicinity of Dana Point
Aborted. Oblique views of Long Beach and Los Angeles. Not plotted
Huntington Beach north to Mojave
Tehachapi south to Santa Catalina Island
Santa Catalina Island north to Tehachapi
Ventura north to San Luis Creek (reservoir). Off course 5 n. mi. west (reflown on Flight 5)

See also Line 14 Flight 5

AREA California -- Regions DATE FLOWN April 1, 1971

SCALE AT LINE OF FLIGHT 1: 60,000 (a) 1: (b) 1: (c)

FLIGHT I.D. NASA/MSC 164, Sites 254 & 260, Flight A, Roll 22

FILED BY same IN CATALOGUE FILED BY same IN COLLECTION

INDEX: MOSAIC FLIGHT LINE X SPOT INDEX OTHER

INDEX SCALE 1: CA. 1,000,000 SPECIAL LOCATION: IMAGERY INDEX ROLL FILM COLLECTION

IMAGERY

SIZE 9"x9" ENLARGEMENT REDUCTION

VERTICAL X OBLIQUE HIGH LOW RECTIFIED

OVERLAP 60% SIDELAP

FILM TYPE 2443 UV B/W B/W IR COLOR COLOR IR X

SPECTRAL RANGE(S) 510-900nm

PRINT POS. TRANS. X NEGATIVE

RESOLVING POWER & CONTRAST FACTOR: L & I 32 1000:1 63 LINE PAIRS PER MM

THERMAL IR SPECTRAL RANGE (S)

MICROWAVE (TYPE & SPECTRAL RANGE) POLARIZATION

FILTER(S) I.D. TYPE(S) 15

GENERATION HELD BY LIBRARY 3rd LEVELING SCALE PRESENT

COMPUTER COMPATIBLE TAPES: ANALOG DIGITAL

NUMBER OF TRACKS BITS PER IN TAPE WIDTH

TYPE OF TAPE: MAGNETIC DISK OTHER

SENSOR: CAMERA (TYPE & I.D.) Zeiss LENS FOCAL LENGTH 12"

SCANNER (TYPE & I.D.) DETECTOR SPECTRAL RANGES

RESEAU MARKS

EXPOSURE FORMULA: DENSITY HUE BRIGHTNESS

COLOR SATURATION NOISE

GRAY SCALE WEDGE AVAILABLE DENSITY STEP WEDGE AVAILABLE

FLIGHT CLOCK SET FOR: G.M.T. P.S.T. OTHER

GENERAL SUBJECTIVE QUALITY

PLATFORM I.D. DIRECTIONAL OREINTATION OF PLATFORM

SUN ANGLE TO PLATFORM DEGREES AZIMUTH DEGREES ELEVATION

ALTITUDE (S) (a) 60,000' (b) (c)

FRAME NO.(S) (a) 001-419 (b) (c)

CONTRACTOR OR REQUESTOR: Earth Observations Aircraft Program

FLOWN BY: NASA/MSC

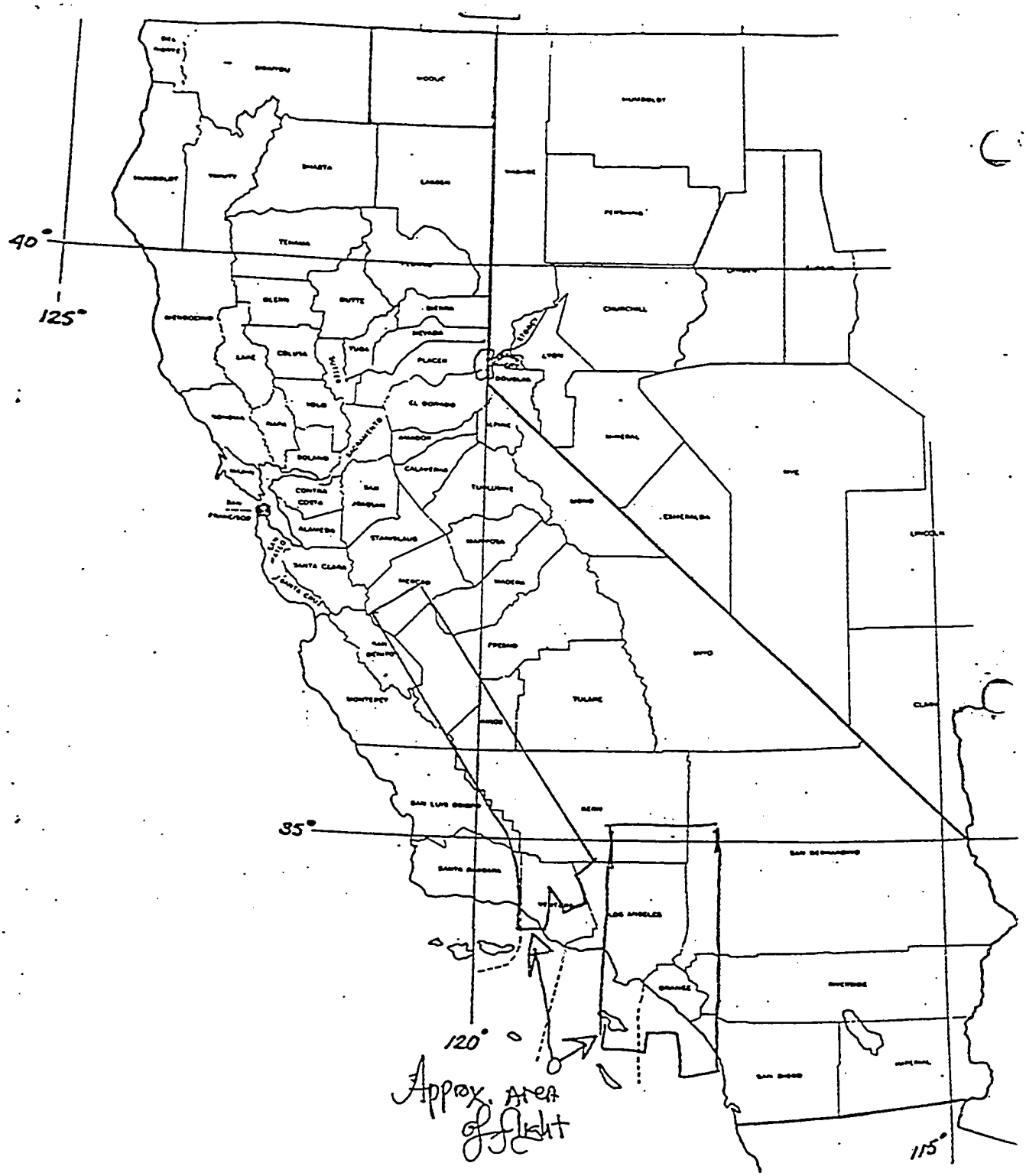
ACQUIRED FROM: UCSB/GRSU RECEIVED: 4/81

SUPPLEMENTAL INFORMATION:

CALIF. POL. SUB-

ORDER NUMBER (Lib-4

Reproduced with permission of the copyright owner. Further reproduction prohibited without permission.



Reproduced with permission of the copyright owner. Further reproduction prohibited without permission.

APPENDIX D

ANALYTICAL LABORATORY REPORTS OF RECONNAISSANCE PETROGRAPHIC, PLM, AND TEM ANALYSES

Reproduced with permission of the copyright owner. Further reproduction prohibited without permission.

mccrone environmental services, inc.
1412 OAKBROOK DRIVE • SUITE 100
NORCROSS, GA 30093 • 404-368-9600

September 24, 1987

Levine - Fricke
629 Oakland Avenue
Oakland, California 94611-4567

Attention: Mr. John DeReamer

Re: McCrone Project No. ME-4260; Levine-Fricke Job No. 1018

Dear Mr. DeReamer:

McCrone Environmental Services, Inc. has completed the analysis of five (5) samples of soil collected from the Coalinga site for total asbestos content utilizing polarized light microscopy/dispersion staining (PLM/DS). The samples were labeled P-SS-26-15, P-SS-26-35, P-SS-26-55, P-SS-26-75, and P-SS-26-95.

Each sample was separated into gravel (>2mm), sand (50um-2mm), silt (2um-50um) and clay (<2um) size functions by sieve and gravity settling techniques. Percent by weight of each size fraction was then determined for each sample (Table 1). Volume percentages of asbestos were estimated for each size fraction using stereo microscopic examination and PLM/DS (Table 2). Total asbestos was calculated by correcting percentages estimated in the various fractions for the respective weight ratios (Table 2).

Chrysotile asbestos was detected in the gravel, sand and silt fractions of all five samples. The asbestos percentages given in Table 2 include chrysotile and fibrous particles which displayed dispersion staining colors indicative of picrolite (fibrous antigorite, a polymorph of chrysotile). Macroscopically, chrysotile and apparent antigorite occur as white matted plates and white or green elongated chips which split readily into numerous fibrils upon crushing. No asbestos was positively identified by PLM/DS in the clay fractions.

Thank you for consulting McCrone Environmental Services. We hope that you have found this report helpful and informative. Photodocumentation of the analyses will be forwarded as soon as completed. If you have any questions, please contact our office.

Sincerely,

W. Randy Boltin

W. Randy Boltin
Manager, Optical Microscopy Lab

WRB/afw

1

a member of the mccrone group
850 PASQUINELLI DRIVE • WESTMONT, ILLINOIS 60559 • 312-887-7100

Reproduced with permission of the copyright owner. Further reproduction prohibited without permission.

mccrone environmental services, inc.
1412 OAKBROOK DRIVE • SUITE 100
NORCROSS, GA 30093 • 404-368-9600

08 October 1987

Levine-Fricke
629 Oakland Avenue
Oakland, California 94611-4567

Attention: Mr. John DeReamer

Re: McCrone Project No. ME-4260; Levine-Fricke
Job No. 1018

Dear Mr. DeReamer:

Attached is photodocumentation pertaining to the analysis of five (5) soil samples, the results of which are tabulated in our report dated September 24, 1987.

Figure 1 is a photograph which displays the abundance of gravel-and sand-sized fragments which typifies all five samples. The morphological character of the particles ranges from acicular fibers to rounded somewhat, flattened fragments. Many of the latter are easily crushed serpentine fragments that become quite fibrous upon doing so. Figure 2 is a stereophotograph of one of these serpentine fragments. The fibrous tendency is indicated by the horizontal lineation obvious on the surface. Fibrous mats of chrysotile are also common in the gravel and sand fractions of these samples (figure 3).

Various forms of fibrous serpentine detected in the sand fraction of these samples are displayed in figure 4. These included white fibrous mats of chrysotile and prismatic green or white bundles, some of which display central stop dispersion staining colors in 1.550 that are more consistent with fibrous antigorite serpentine (picrolite) (figure 5a,b; figure 6) than chrysotile. Figure 7 is a photomicrograph of a sand-sized blocky fragment of chrysotile which is easily fibrillated upon slight crushing.

Asbestos fibers are also apparent in the silt fraction of all five samples (figure 8) but are not positively identified in the clay fraction (figure 9) using PLM.

a member of the mccrone group
850 PASQUINELLI DRIVE • WESTMONT, ILLINOIS 60559 • 312-887-7100

Reproduced with permission of the copyright owner. Further reproduction prohibited without permission.

Thank you for consulting McCrone Environmental Services. I hope that this additional information will be helpful in your project. Please contact me if we can be of further service.

Sincerely,

W. Randy Boltin

W. Randy Boltin
Manager, Optical Microscopy Lab

WRB/afw

cc: 1) Levine-Fricke
Oakland CA
1) Mr. John DeReamer

Reproduced with permission of the copyright owner. Further reproduction prohibited without permission.



Figure 3. White fibrous mats of chrysotile from the gravel fraction of sample P-55-26-35. 7x.



Figure 4. Forms of fibrous serpentine from the sand fraction of sample P-55-26-35. 7x. c=chrysotile, p=possible fibrous antigorite (picrolite).

Reproduced with permission of the copyright owner. Further reproduction prohibited without permission.



Figure 5a. Fibrous bundle from sample P-55-26-95 displaying golden yellow colors corresponding to the index of refraction parallel to fiber length in mounting medium of index 1.550. Central stop dispersion staining. 100x.



Figure 5b. Same bundle as figure 5a but rotated 90° so that blue-magenta colors corresponding to the index of fraction perpendicular to fiber length in 1.550 are observed. The colors observed in figures 5a and 5b are consistent with those expected for fibrous antigorite (picrolite). Central stop dispersion staining. 100x.

Reproduced with permission of the copyright owner. Further reproduction prohibited without permission.

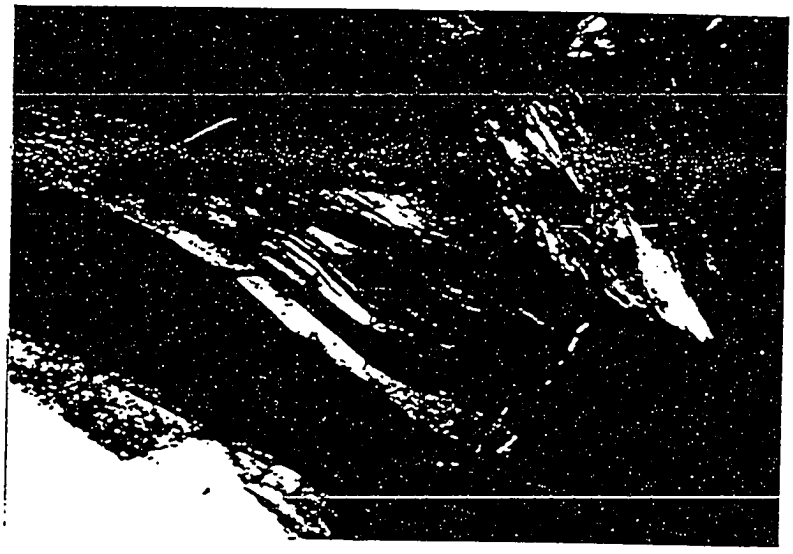


Figure 6. Photomicrograph of the same fiber bundle observed in figure 5 a,b. This crossed polars view details surface morphology of the fibers. 100x.

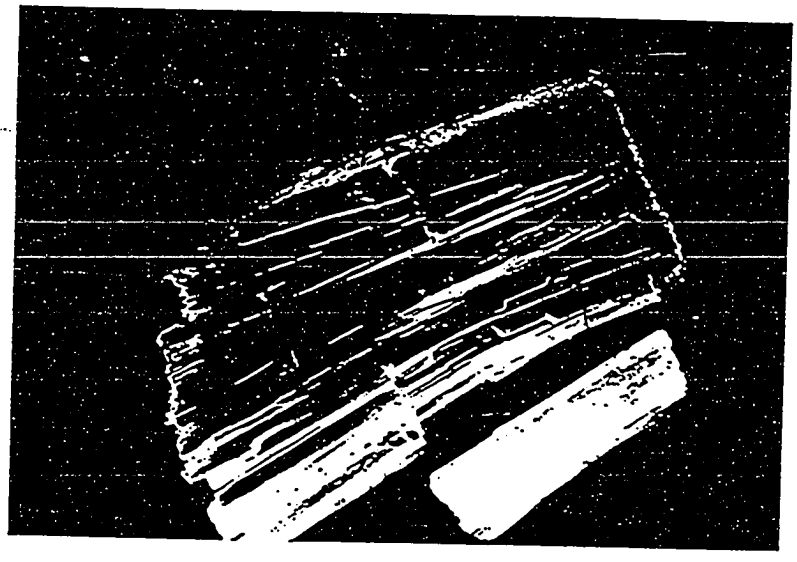


Figure 7. Blocky fragment of chrysotile in the sand fraction of sample P-55-26-55. Note the fibrils extending from the side of the fragment at the top of the photo. Crossed polars. 100x.

Reproduced with permission of the copyright owner. Further reproduction prohibited without permission.

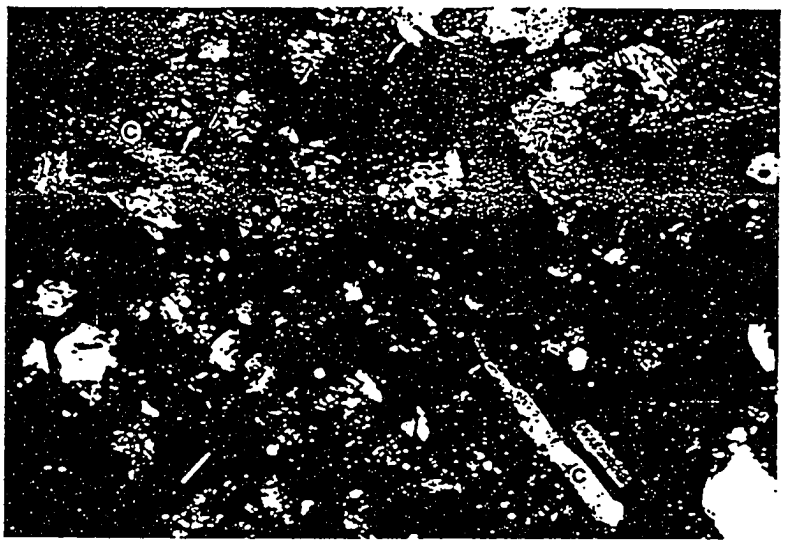


Figure 8. Chrysotile fibers (c) in the silt fraction of sample P-55-26-35. Slightly uncrossed polars. 200x.

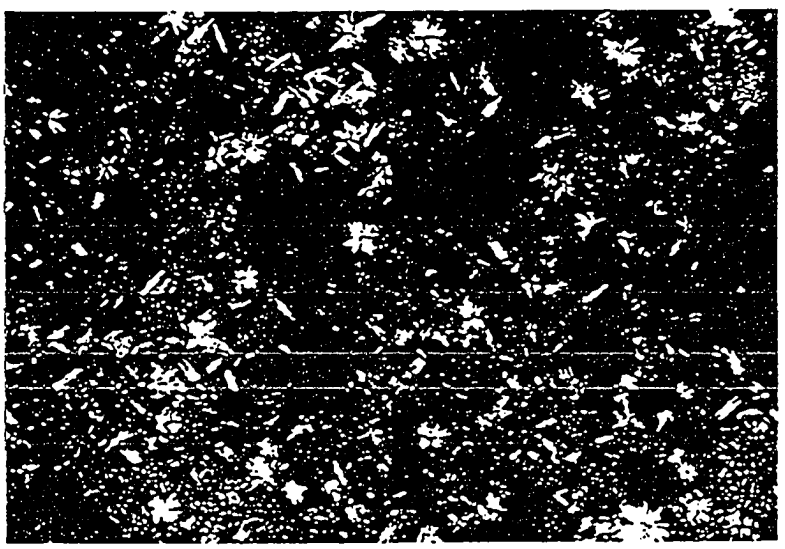


Figure 9. Clay fraction particles from sample P-55-26-35. Slightly uncrossed polars. 400x.

Reproduced with permission of the copyright owner. Further reproduction prohibited without permission.

TABLE 1

Breakdown By Weight % of Various Size Fractions in Coalinga Samples

	P-55-26-15	P-55-26-35	P-55-26-55	P-55-26-75	P-55-26-95
Gravel	31.5	48.1	43.7	36.3	35.9
Sand	64.6	49.4	53.5	60.5	60.9
Silt	3.4	2.5	2.8	3.2	3.2
Clay	<1.0	<1.0	<1.0	<1.0	<1.0

Reproduced with permission of the copyright owner. Further reproduction prohibited without permission.

TABLE 2

Volume % Estimates of Chrysotile (plus Fibrous antigorite?) Present in Various Size Fractions of Coalinga Samples

	P-55-26-15	P-55-26-35	P-55-26-55	P-55-26-75	P-55-26-95
Gravel	3-5	5-10	5-10	10-15	10-15
Sand	10-20	15-20	20-30	25-35	40-50
Silt	1-5	30-35	35-40	30-40	20-30
Total*	5-15	10-15	15-20	20-30	30-35

*Estimated Total Percent Asbestos in Samples (Corrected for weight percent of various size fractions)

Reproduced with permission of the copyright owner. Further reproduction prohibited without permission.

mccrone environmental services, inc.
1412 OAKBROOK DRIVE • SUITE 100
NORCROSS, GA 30093 • 404-368-9600

04 May 1988

Levine-Fricke
629 Oakland Avenue
Oakland, California 94611-4567

Attention: Mr. John DeReamer

Subject: Analysis of Seventy (70) Samples By Light Microscopy For Asbestos

Re: McCrone Project No. ME-4595

Dear Mr. DeReamer:

McCrone Environmental Services, Inc. has completed the analysis of seventy (70) samples of soil, mine tailings and stream sediment from the Coalinga area for total asbestos content as authorized by Levine-Fricke Purchase Order No. 1801-1223-JDR. In accordance with the Quality Assurance Project Plan 10% of the samples were divided into two aliquots; each was analyzed independently by separate analysts. All samples were analyzed by stereo microscopy and polarized light microscopy/dispersion staining. Methodology and analytical results are provided in the attached report.

Thank you for consulting McCrone Environmental Services, Inc. I hope that you will find the attached information beneficial. If you have any questions regarding the contents of the report or if we may be of further service please contact me at (404) 368-9600.

Sincerely,

Randy Boltin

Randy Boltin
Manager, Optical Microscopy Group

RB/mlj
Attachments

Reproduced with permission of the copyright owner. Further reproduction prohibited without permission.

ANALYTICAL REPORT

ANALYSIS OF SOIL, MINE TAILINGS AND

STEAM SEDIMENT FOR ASBESTOS

FROM

COALINGA ASBESTOS MILL SITE
COALINGA, CALIFORNIA

MCCRONE PROJECT NO. ME-4595

04 MAY 1988

MCCRONE ENVIRONMENTAL SERVICES, INC.
NORCROSS, GEORGIA

A SUBSIDIARY OF
THE MCCRONE GROUP
WESTMONT, ILLINOIS

Reproduced with permission of the copyright owner. Further reproduction prohibited without permission.

ANALYTICAL REPORT

Coalinga Asbestos Mill Site
Coalinga, California

McCrone Project No. ME-4595

Writer/Representative: Randy Boltin
Manager, Optical Microscopy Group

METHODOLOGY

Sample Preparation. An aliquot for each sample was obtained using a Humboldt Model H-3980 sample splitter. Two aliquots were prepared for 10% of the samples for Quality Control (QC) analysis. Forty-one (41) samples (including three QC aliquots) selected by Levine-Fricke were sieved to obtain gravel (>2mm), sand (50um-2m) and silt + clay (<50um) fractions. Percent by weight of each size fraction was determined for each of the sieved samples (Table 1).

Analytical Methods. All aliquots were examined by stereo microscopy and polarized light microscopy/dispersion staining (PLM/DS) to identify and estimate approximate percent by volume asbestos present in each. Gravel, sand and combined silt + clay fractions were analyzed separately for each of the sieved samples. A total asbestos percentage was estimated for these samples by multiplying the estimated range asbestos for each fraction by the respective weight % determined for each fraction. The resultant products were summed to give the estimated total % asbestos (Table 2).

Thirteen (13) of the sieved samples were specified by Levine-Fricke for more complete characterization according to morphology of asbestos and overall composition in an attempt to identify parameters which might be used to distinguish asbestos from various source areas (ie.. asbestos from tailings vs. asbestos from ancient serpentine landslide material)(Table 3.)

The remaining thirty-six (36) samples (including four QC aliquots) were analyzed as bulk material (Table 4). With the exception of one outcrop area sample, all of these specimens were mill site samples.

ANALYTICAL RESULTS

Serpentine asbestos was detected in various concentrations in all seventy (70) samples of soil, mine tailings and stream sediment from the Coalinga mill site. The asbestos occurs primarily as plates of matted fibers (Figure 1 a,b) which display more pronounced fibrosity upon crushing (Figure 2). Occurring in

Reproduced with permission of the copyright owner. Further reproduction prohibited without permission.

less abundance are somewhat harder green, elongated chips which become fibrous when crushed (Figure 3 a,b). Asbestiform serpentine was detected in gravel (Figure 4 a,b), sand (Figure 5 a,b) and silt + clay fractions of all samples except SS-2 (Table 2). The optical properties associated with Coalinga asbestos are not entirely consistent with those of more typical chrysotile (serpentine asbestos). Indices of refraction are generally higher for Coalinga asbestos than for most chrysotile asbestos; central stop dispersion staining colors observed for most specimens are more typically associated with antigorite, a normally non-fibrous form of serpentine.

Sieved Samples. Percent by weight size fractionation data for the 41 sieved samples is presented in table 1. Photodocumentation of these samples (total sample) is presented in figures 6-43. In general, Los Gatos Creek and Core Composite samples from unspecified source represented some of the lower asbestos percentages observed. Unprocessed asbestos ore (sample PG 4) and processed ore from the tailings pile (PG 5) contained the highest percentage asbestos of any samples of specified location from this group. Mill site samples displayed a wide range of estimated asbestos values though most contained a significant proportion. Results are summarized in table 2.

Sieved Samples For Characterization. Table 3 summarizes the morphological characteristics of serpentine asbestos and the associated mineralogy of the thirteen samples in this group. Plates of matted serpentine represent the predominant morphology of asbestos in all samples. Major associated minerals include massive serpentine (usually as subangular to rounded, massive, green grains), opaques (primarily magnetite) and carbonate (Figure 4 a,b). Yellow-brown to red-brown aggregates of sub-microscopic particles are also common. These aggregates may be clumps of clay or possibly one of the locally prevalent alteration products of the Coalinga District (1). Individual sub-microscopic particles (colorless, yellow, pale green in polarized light) are observed but have not been identified by PLM/DS. Quartz is observed in stream sediment samples. Brassy yellow and brown mica is observed in mill-site, off-site and stream sediment samples. Chlorite and actinolite are observed but not in sufficient quantity to be an indicator of source. Red-brown and dark brown microscopic dendritic crystals are also common and do not appear to be restricted to sample type or location.

Reproduced with permission of the copyright owner. Further reproduction prohibited without permission.

Neither asbestos morphology nor associated mineralogy appear to be effective parameters in determining the source(s) of asbestos in any particular sample based on light microscopic characterization of the 13 designated samples. One observation that is of potential use in the evaluation of source is the statistical decrease in grain size of precessed asbestos (sample PG 5) relative to unprocessed ore (sample PG 4) (compare figures 13 and 14). This observation may not be valid in the case of stream sediments samples due to the tendency towards mechanical grain size reduction during water-borne transport.

Mill Site Samples. Table 4 summarizes the results of analysis of bulk (non-sieved) mill site samples. Volume % estimates range from <2 to >85% asbestos. Sample OC 18 B is an outcrop area sample and contain >80% asbestos. Representative photodocumentation of this group is in figures 44-48.

Summary. Plates of matted serpentine asbestos were found to varying degrees in all 70 samples. Green elongated chips containing serpentine asbestos are subordinate. Within the limitations of this study. morphological and mineralogical characteristics observed on selected samples by PLM/DS are not sufficient for differentiation of source material for asbestos in any given sample.

References

(1) Mumpton, F.A. and Thompson, C.S., 1975. Mineralogy and origin of the Coalinga asbestos deposit. Clays and Clay Minerals, v. 23, pp. 131-143.

Reproduced with permission of the copyright owner. Further reproduction prohibited without permission.

TABLE 1
Breakdown By Weight % of Various Size
Fractions in Coalinga Samples

Sample ID	Gravel	Sand	Silt + Clay
SS-2	1.4	98.1	0.5
SS-12	22.2	76.1	1.7
SS-34	36.7	59.1	4.1
OC-17	23.7	73.3	3.0
OC-17 (QC)	20.3	77.4	2.3
OC-24	51.3	48.4	0.3
OC-28	46.4	52.9	0.7
XP1/2-3	17.5	78.8	3.7
XP1/4-5	23.7	72.6	3.7
XP1/5.5-6.5	32.5	65.2	2.2
XP3/2-3	77.5	19.9	2.6
XP3/4-5	80.5	18.0	1.5
XP3/6-7	73.8	24.4	1.8
XP5/1-2	87.8	11.2	1.0
XP5/4-5	65.3	32.7	2.0
XP6/4-5	74.9	23.9	1.2
PG 1	31.7	66.2	2.1
PG 2	31.8	63.2	5.0
PG 3A	57.0	42.2	0.8
PG 3A (QC)	50.2	48.5	1.3
PG 3B	19.1	76.9	4.0
PG 4	40.4	58.3	1.3
PG 5	4.1	90.3	5.6
PG 7	23.3	70.2	6.5
PG 8A[1]	29.4	70.0	0.6
PG 8A[2]	18.4	76.8	4.8
PG 8B	1.4	95.7	2.9
PC 1B	13.7	82.6	3.7
PC 2A	62.3	35.0	2.7
PC 2B	24.8	71.4	3.8
PC 2B (QC)	27.8	69.7	2.5
PC 2C	48.6	47.7	3.7
PC 2AX	50.3	45.3	4.4
PC 20A	29.4	68.2	2.4
PC 20B	46.4	51.4	2.2
PC 20C	53.7	44.0	2.3
AF1-14.5	0.4	93.5	6.1
SB3-7.0	37.0	58.5	4.5
SB3-15.0	1.8	96.3	1.9
SB3-27.5-27.8	3.1	96.3	0.6
SS-28	7.1	90.5	2.4

NOTE - [1]MES Lab ID: 880323001-17 [2]MES Lab ID: 880323001-18

Reproduced with permission of the copyright owner. Further reproduction prohibited without permission.

TABLE 2
Volume % Estimates of Serpentine Asbestos Present in Various Size Fractions of Selected Coalinga Samples

Sample ID	Location	Gravel	Sand	Silt + Clay	Total*
SS-2	Los Gatos Creek	Not Detected	≤ 1	≤1	≤ 1
SS-12	Los Gatos Creek	5-7	10-20	1-3	10-15
SS-34	Pine Creek	10-15	40-60	1-3	25-40
OC-17	Off-Site	40-60	>80	60-80	70-90
OC-17 (QC)		30-40	70-80	75-85	60-70
OC-24	Unspecified	50-70	60-80	60-80	55-75
OC-28	Off-Site	40-60	≥80	60-80	60-80
XP1/2-3	Unspecified	40-60	40-60	10-30	40-60
XP1/4-5	Unspecified	40-60	40-60	20-30	40-60
XP1/5.5-6.5	Unspecified	25-35	45-55	30-40	40-50
XP3/2-3	Unspecified	≤ 1	≤ 2	≤ 2	≤ 1
XP3/4-5	Unspecified	5-10	3-7	3-7	5-10
XP3/6-7	Unspecified	< 1	<1	<1	< 1
XP5/1-2	Unspecified	≤ 2	≤2	≤1	≤ 2
XP5/4-5	Unspecified	≤ 1	≤1	≤1	≤ 1
XP6/4-5	Unspecified	80-90	80-90	85-95	≥80
PG 1	Rail Road Mine -Central Deposit	70-80	>80	40-60	75-90
PG 2	Eastern Pine Canyon Above Tailings Pile	40-60	60-70	40-60	50-65
PG 3A	W. Fork of Pine Canyon Above Diversion	20-40	50-70	40-60	35-55
PG 3A (QC)	Same	25-35	70-80	25-35	45-55
PG 3B	Mill Site-W. Fork of Pine Canyon Draining Butler Pit	60-75	50-70	10-30	50-70

NOTE - [1]MES ID: 880323001-17 [2]MES ID: 880323001-18
*Estimated Total Percent Asbestos in Samples (Corrected for weight percent of various size fractions from Table 1).

Reproduced with permission of the copyright owner. Further reproduction prohibited without permission.

TABLE 2 (Cont'd)
Volume % Estimates of Serpentine Asbestos Present in
Various Size Fractions of Selected Coalinga Samples

Sample ID	Location	Gravel	Sand	Silt + Clay	Total*
PG 4	Unprocessed Asbestos Ore	≥80	≥80	60-80	≥80
PG 5	Tailings Pile -Processed Ore	≥80	≥80	60-65	≥80
PG 7	Lower Pine Canyon-Channel Sand Deposit	1-4	5-15	≤1	5-10
PG 8A[1]	White Creek-Channel Gravel Deposit	5-10	25-35	25-35	20-30
PG 8A[2]	White Creek-Channel Gravel Deposit	5-10	30-40	20-30	25-35
PG-8B	White Creek-Channel Sand Deposit	10-15	40-60	40-60	40-60
PC 1B	Mill Site	85-90	70-80	25-35	70-80
PC 2A	Mill Site	3-10	8-15	10-20	5-10
PC 2B	Mill Site	20-25	65-75	25-35	50-60
PC 2B (QC)	Same	25-35	60-80	30-50	50-65
PC 2C	Mill Site	1-3	5-10	10-15	3-7
PC 2AX	Mill Site	10-15	20-30	10-15	7-10
PC 20A	Mill Site	5-10	40-60	15-25	30-45
PC 20B	Mill Site	20-35	35-55	35-45	30-45
PC 20C	Mill Site	15-35	25-45	15-35	20-40
AF1-14.5	Unspecified	1-2	15-25	15-20	15-25
SB3-7.0	Unspecified Core Composite	1-3	1-2	1	1-2
SB3-15.0	Unspecified Core Composite	1-3	2-5	3-6	2-5
SB3-27.5 -27.8	Unspecified Core Composite	1	1-3	1-5	1-3
SS-28	White Creek	60-75	70-85	75-85	70-85

NOTE - [1]MES ID: 880323001-17 [2]MES ID: 880323001-18
*Estimated Total Percent Asbestos in Samples (Corrected for weight percent of various size fractions from Table).

Reproduced with permission of the copyright owner. Further reproduction prohibited without permission.

TABLE 3
Characterization Of Asbestos Morphology And Associated Mineralogy Of Selected Coalinga Samples

Sample ID	Location	Asbestos Morphology	Associated Minerals
OC-17	Off-Site	White-Pale Green Plates of Matted Fibers	1.2.4.5.7
OC-24	Unspecified	Same as OC-17	1.2.3.4.5.10
OC-28	Off-Site	Same as OC-17	1.2.3.4.5.7.8.10
PG 1	Rail Road Mine-Central Deposit	Same as OC-17	1.2.3.4.5.8.10
PG 2	Eastern Pine Canyon Above Tailings Pile	Tan Rounded Clumps + Tan-White Platy Clumps	1.2.3.4.5.9
PG 3A	W. Fork of Pine Canyon Above Diversion	White-Pale Green Plates of Matted Fibers	1.2.4.5.10
PG 3B	Mill Site - W. Fork of Pine Canyon Draining Butler Pit	Tan-White Plates of Matted Fibers	1.2.3.4.5.6.7

ASSOCIATED MINERALS CODES:

1 - Massive Serpentine
2 - Opaques
3 - Carbonate
4 - Yellow-brown to red-brown aggregates of sub-microscopic grains
5 - Equigranular individual grains, macroscopic to sub-microscopic
6 - Quartz ± Feldspar
7 - Mica
8 - Chlorite
9 - Actinolite
10 - Red-brown and dark brown microscopic dendritic particles

Reproduced with permission of the copyright owner. Further reproduction prohibited without permission.

TABLE 3 (Cont'd)
Characterization Of Asbestos Morphology And Associated Mineralogy Of Selected Coalinga Samples

Sample ID	Location	Asbestos Morphology	Associated Minerals
PG 4	Unprocessed Asbestos Ore	White Fibrous Plates and Clumps of Matted Fibers	1.2.3
PG 5	Tailings Pile - Processed Ore	White Plates of Matted Fibers	1.2.3
PG 7	Lower Pine Canyon Channel Sand Deposit	Tan-White Plates of Matted Fibers + Green Elongated Chips (Fibrous When Crushed)	1.2.3.4.5.6.7
PG 8A[1]	White Creek - Channel Gravel Deposit	Same as PG 7	1.2.4.5.6.8
PG 8A[2]	Same	Same as PG 7	1.2.3.4.5.6.7
PG 8B	White Creek - Channel Sand Deposit	Same as PG 7	1.2.4.5.6.7

ASSOCIATED MINERALS CODES:

1 - Massive Serpentine
2 - Opaques
3 - Carbonate
4 - Yellow-brown to red-brown aggregates of sub-microscopic grains
5 - Equigranular individual grains, macroscopic to sub-microscopic
6 - Quartz ± Feldspar
7 - Mica
8 - Chlorite
9 - Actinolite
10 - Red-brown and dark brown microscopic dendritic particles

NOTE - [1]MES ID: 880323001-17 [2]MES ID: 880323001-18

Reproduced with permission of the copyright owner. Further reproduction prohibited without permission.

TABLE 4
Volume % Estimates of Serpentine Asbestos Present in
Various Mill Site Samples

Sample ID	Asbestos %	Sample ID	Asbestos %
BP6/1.0	5-15	AL 17 B	>80
BP5/8-10	25-35	AL 18 A	40-50
BP14/11-12	15-30	AL 18 B	>80
BP14/13.3	≤2	AL 22 A	20-35
BP15/3-4	8-20	AL 22 B	45-60
BP15/10-11	3-8	AL 24 A	15-30
BS-9MC	5-15	AL 24 B	65-80
BP5/1.5	10-30	AL 31 A	1-3
AL 52	≥85	AL 31 B	≥80
AL 4 B	≥85	BS-29	20-40
AL 11 A	1-3	PC 41 A	70-80
AL 35 B	3-7	PC 41 B	55-70
AL 35 B (QC)[1]	3-5	PC 41 B (QC)	45-65
	1-3		
AL 17 A	45-65	PC 14 A	5-10
PC 11 A	10-20	PC 14 B	60-75
PC 11 A (QC)	5-15	PC 14 C	3-7
PC 11 B	70-85	OC 18 B[1]	≥85
PC 11 C	10-20	OC 18 B[1] (QC)	≥80

NOTE: [1]Sample AL 35B (QC) was analyzed by two analysts
[1] The location designated for sample OC 18B is `Outcrop Area', not `Mill Site'

Reproduced with permission of the copyright owner. Further reproduction prohibited without permission.



Figure 1a. Photomicrograph showing plate-like morphology of matted asbestos fibers from Sample PG8B. Crossed polars. 100X.



Figure 1b. Matted asbestos from OC 17. Crossed polars. 100X.

Reproduced with permission of the copyright owner. Further reproduction prohibited without permission.

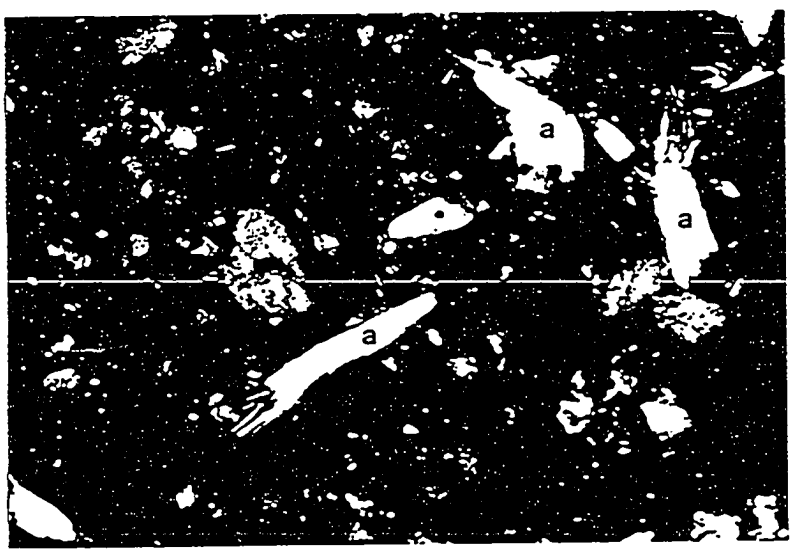


Figure 2. Bundles of serpentine asbestos (a) liberated from a mat of fibers by crushing. Sample PG88. Crossed polars. 40X.

Reproduced with permission of the copyright owner. Further reproduction prohibited without permission.

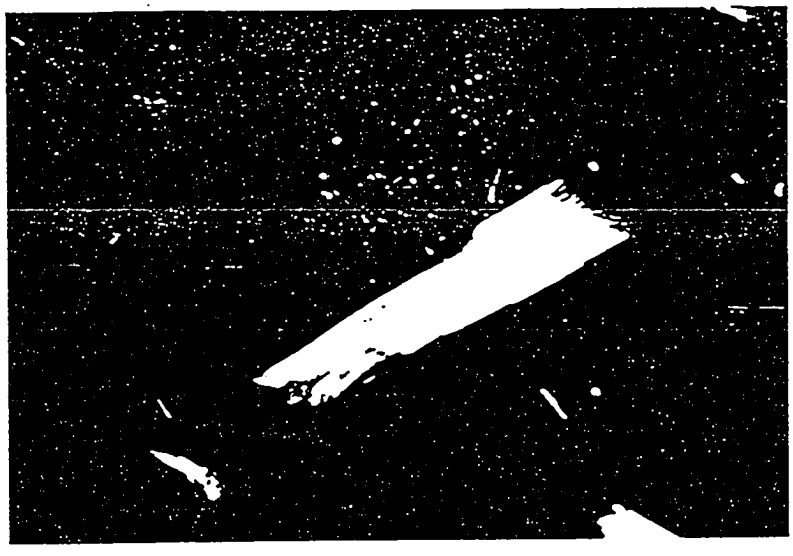


Figure 3a. Partially crushed green, elongated chip of serpentine asbestos from PG8B. Crossed polars. 40X.

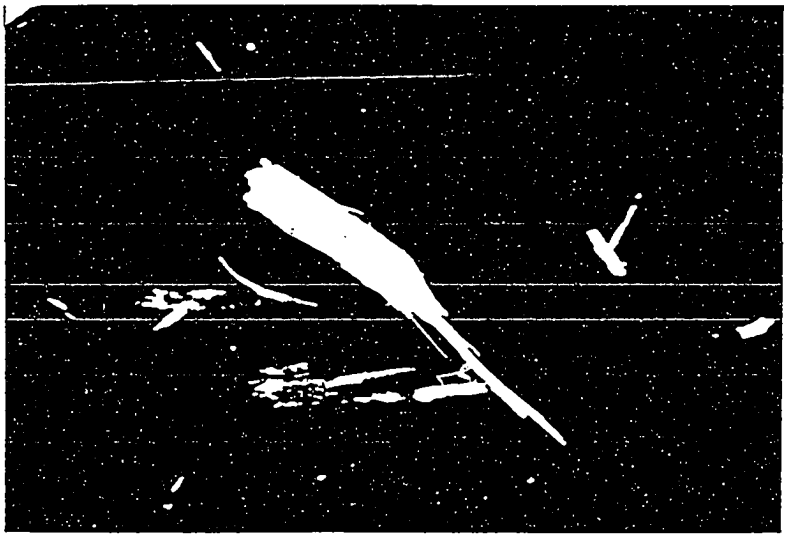


Figure 3b. Fibrous bundles liberated by crushing from a green, elongated chip of serpentine in PG8B. Crossed polars. 40X.

Reproduced with permission of the copyright owner. Further reproduction prohibited without permission.



Figure 4a. Photomicrograph of portion of gravel fraction from Sample PG4 (Unprocessed asbestos ore). Note the fibrous mats of serpentine (gray and white) and the presence of opaques (o) and carbonate grains (c). Crossed polars. 40X.

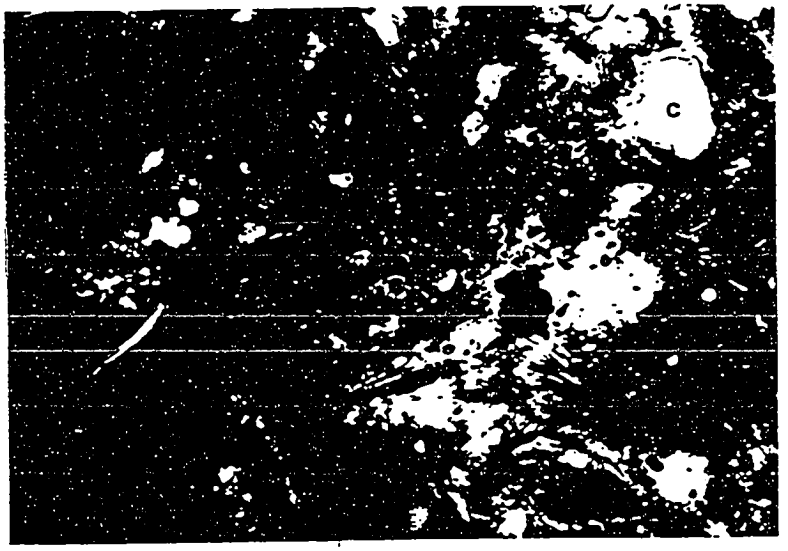


Figure 4b. Portion of gravel fraction from Sample PG5 (Processed ore from tailings pile). Note fibrous mats of serpentine (gray and white). abundance of opaques (black) and presence of carbonate (c). Crossed polars. 200X.

Reproduced with permission of the copyright owner. Further reproduction prohibited without permission.



Figure 5a. Photomicrograph showing serpentine asbestos (a) in sand fraction of Sample PG7. Crossed polars. 40X.

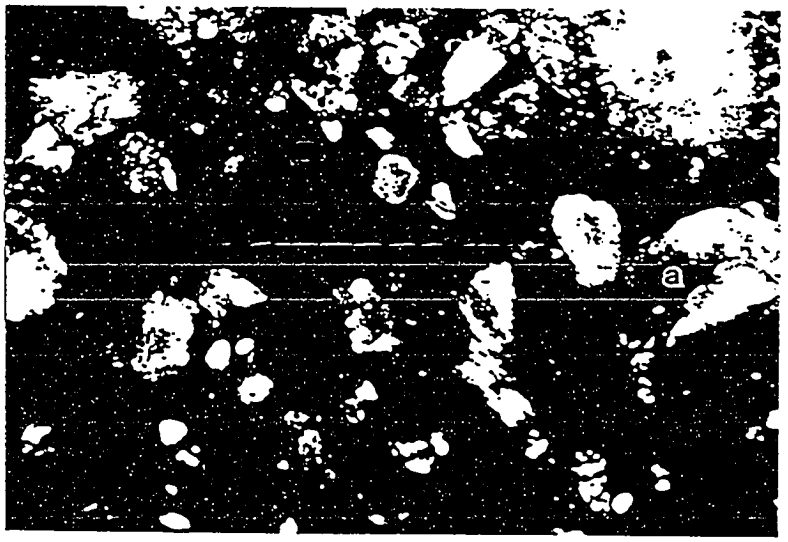


Figure 5b. Serpentine asbestos (a) in sand fraction of Sample PG3B. Crossed polars. 40X.

Reproduced with permission of the copyright owner. Further reproduction prohibited without permission.

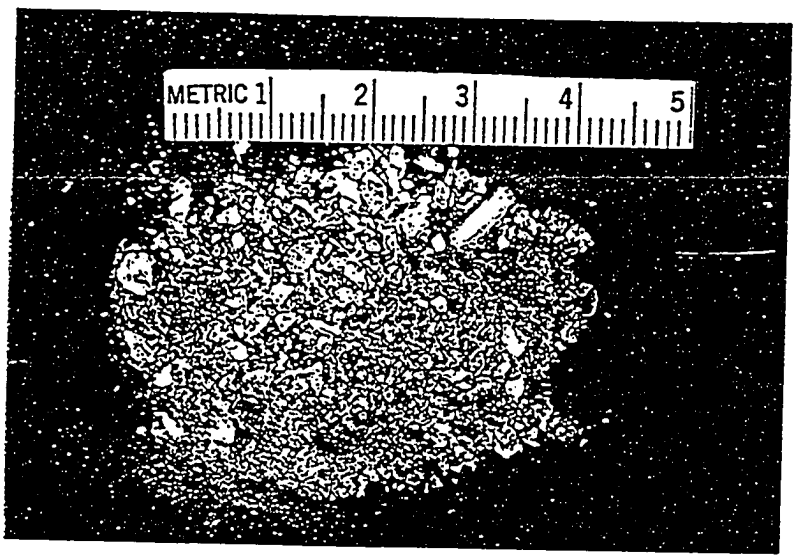


Figure 6. Sample OC 17.

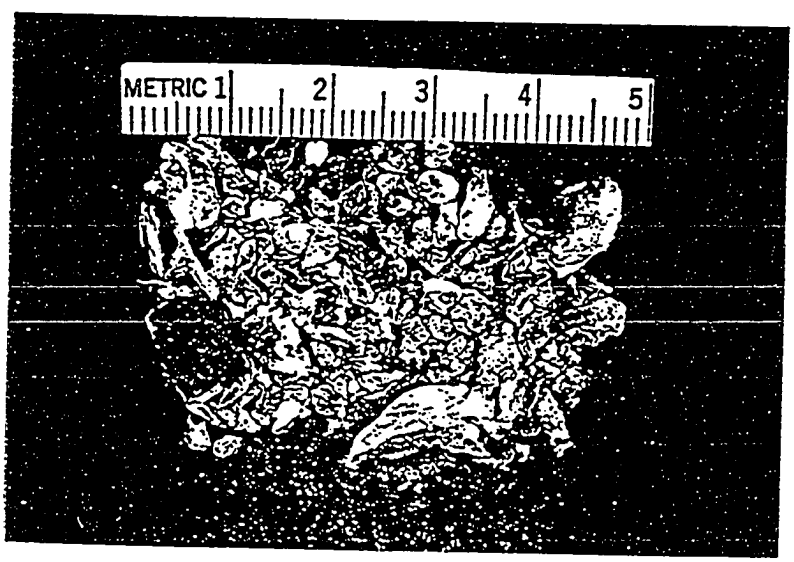


Figure 7. Sample OC 24.

Reproduced with permission of the copyright owner. Further reproduction prohibited without permission.

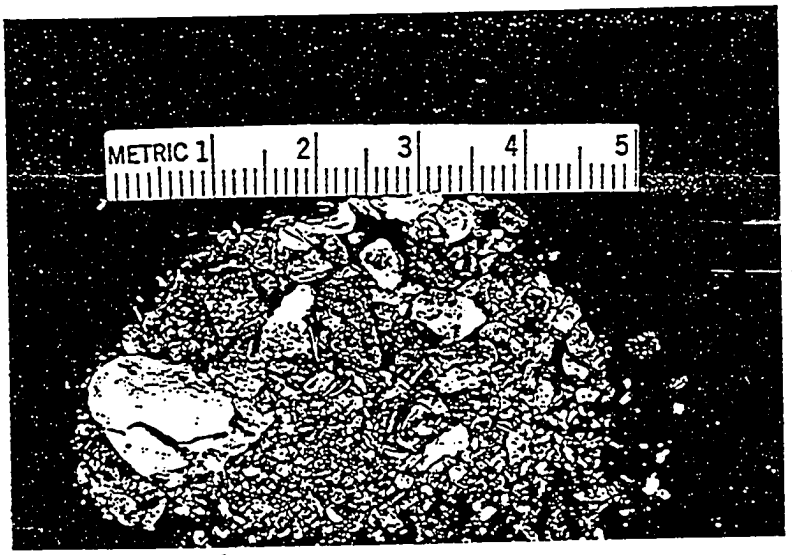


Figure 8. Sample OC 28.

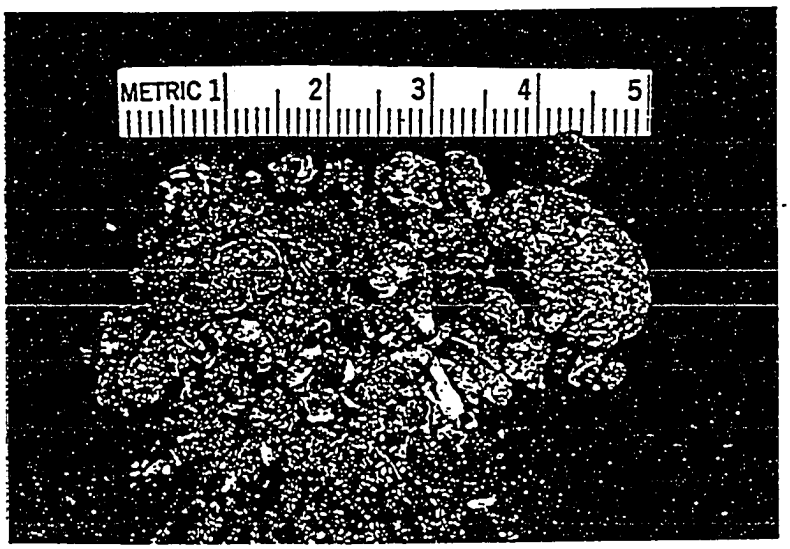


Figure 9. Sample PG 1.

Reproduced with permission of the copyright owner. Further reproduction prohibited without permission.

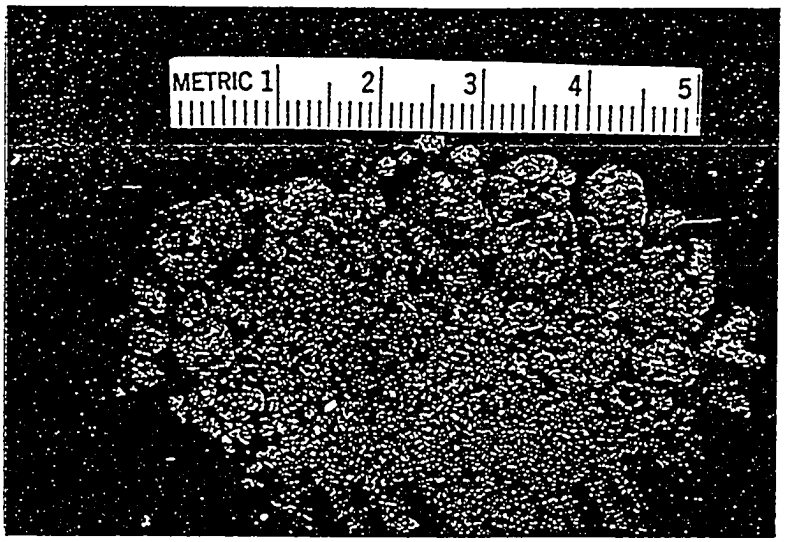


Figure 10. Sample PG 2.

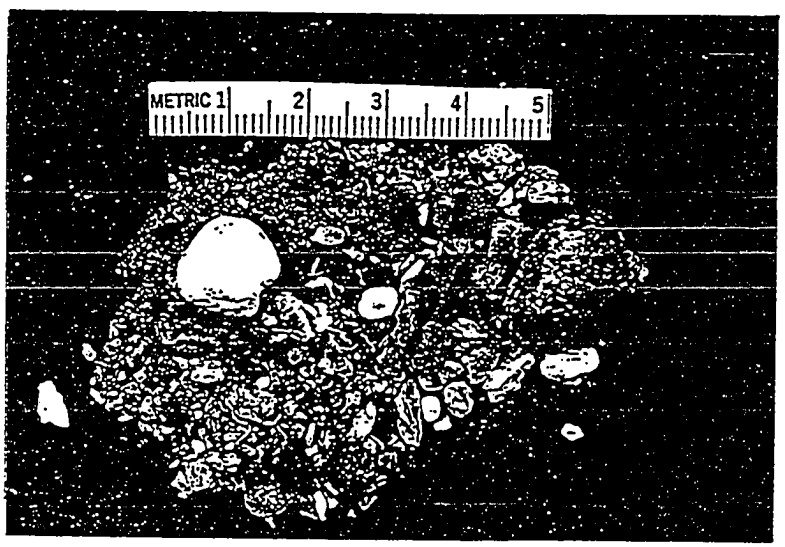


Figure 11. Sample PG 3A.

Reproduced with permission of the copyright owner. Further reproduction prohibited without permission.

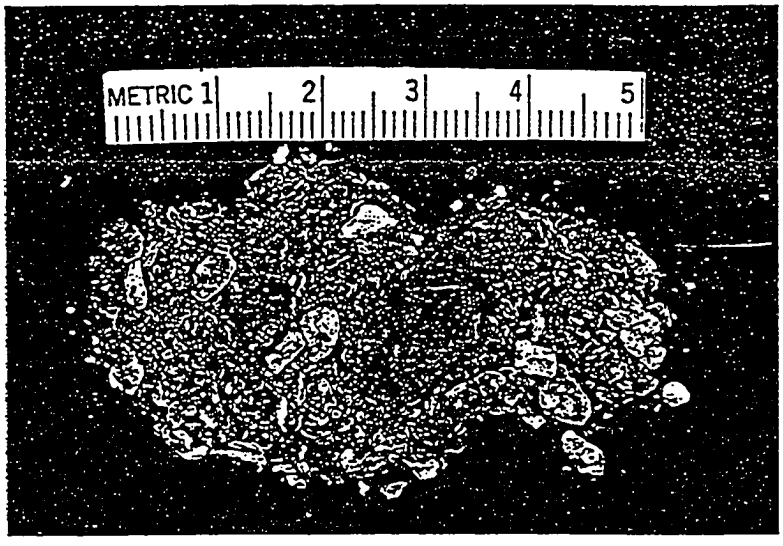


Figure 12. Sample PG 3B.

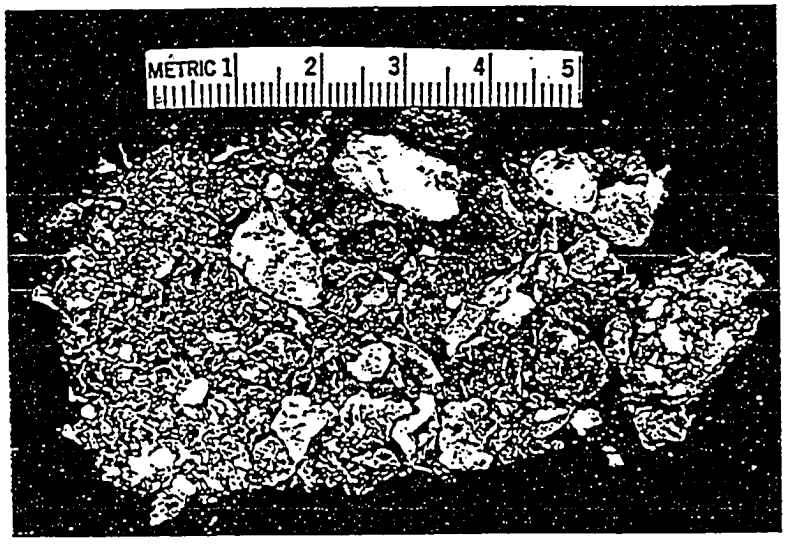


Figure 13. Sample PG 4.

Reproduced with permission of the copyright owner. Further reproduction prohibited without permission.

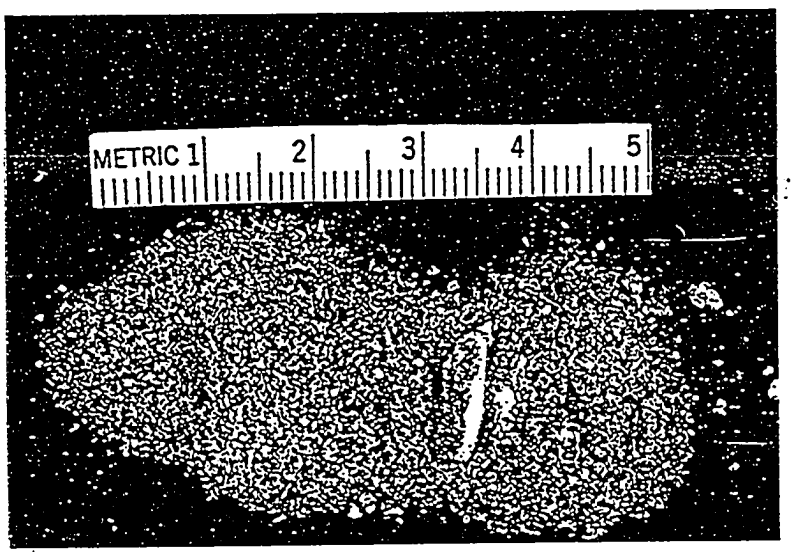


Figure 14. Sample PG 5.

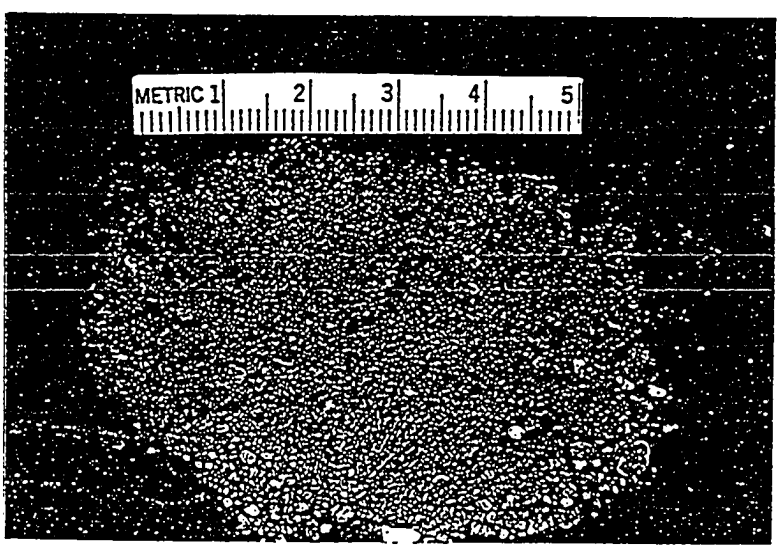


Figure 15. Sample PG 7.

Reproduced with permission of the copyright owner. Further reproduction prohibited without permission.

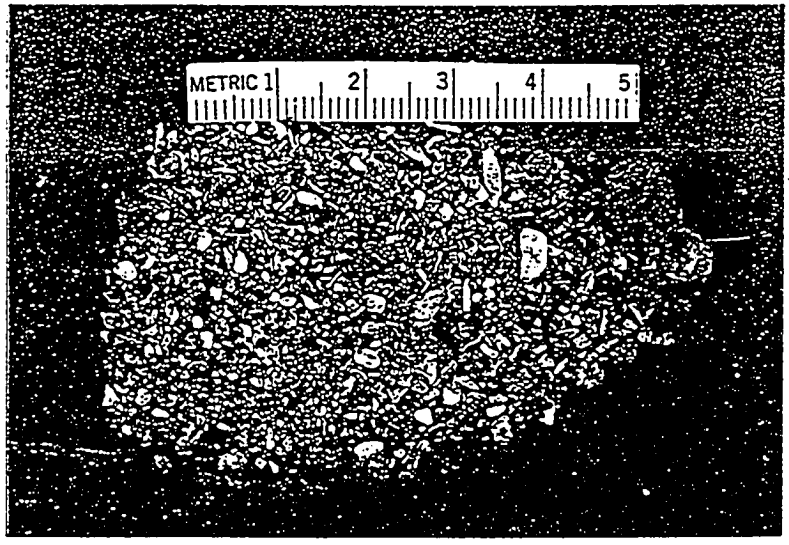


Figure 16. Sample 8A.
MES Sample No. 880323001-17.

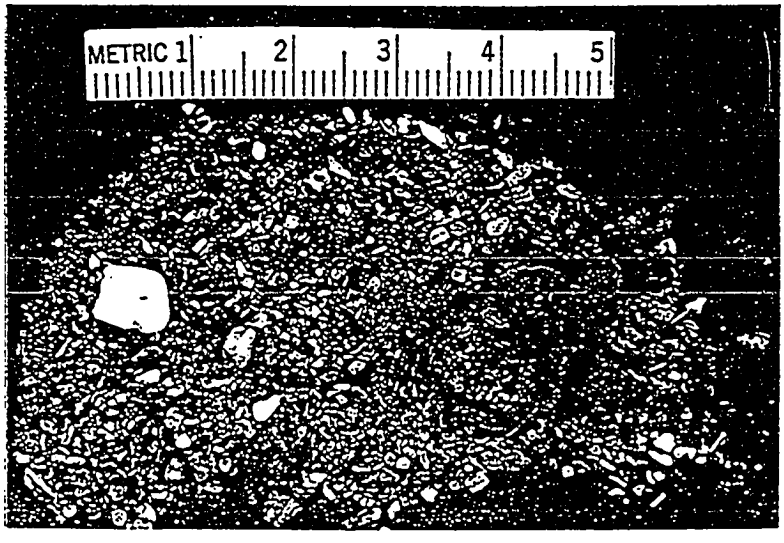


Figure 17. Sample 8A.
MES Sample No. 880323001-18.

Reproduced with permission of the copyright owner. Further reproduction prohibited without permission.

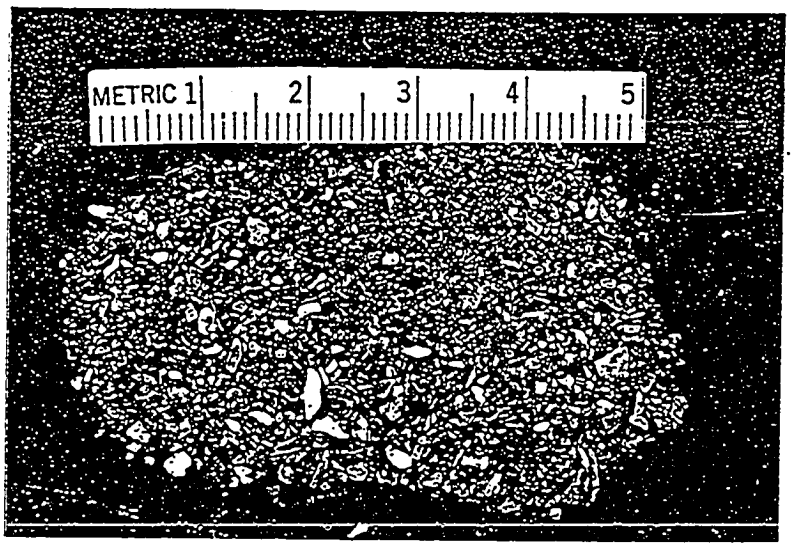


Figure 18. Sample PG 8B.

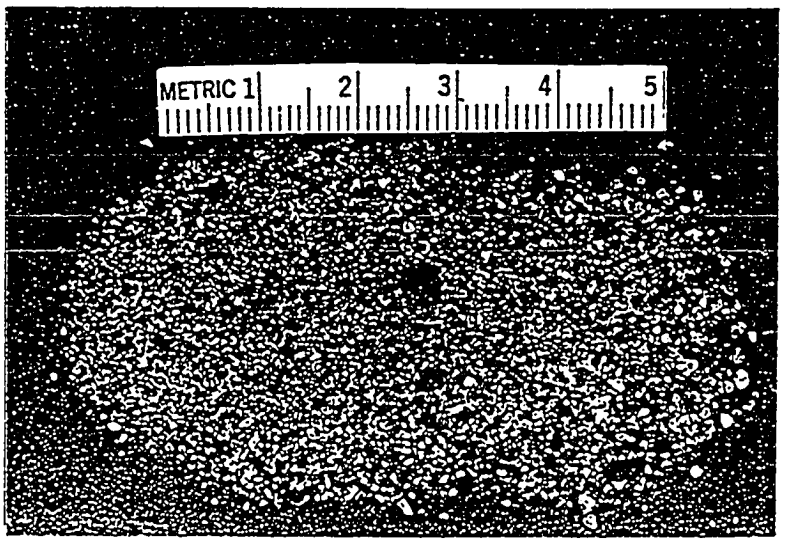


Figure 19. Sample SS 2.

Reproduced with permission of the copyright owner. Further reproduction prohibited without permission.

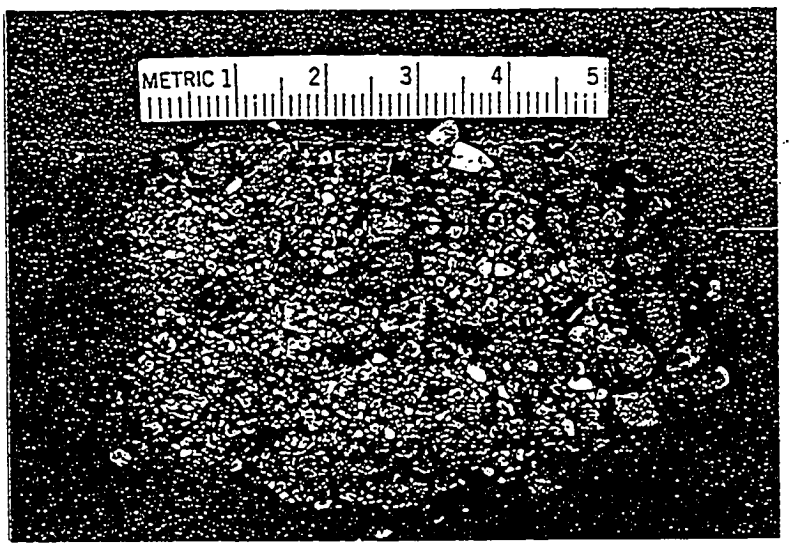


Figure 20. Sample SS 12.

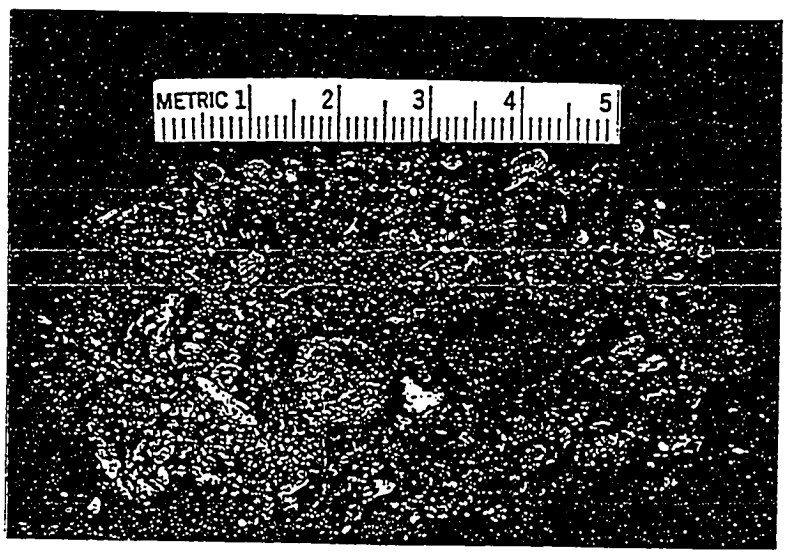


Figure 21. Sample SS 34.

Reproduced with permission of the copyright owner. Further reproduction prohibited without permission.

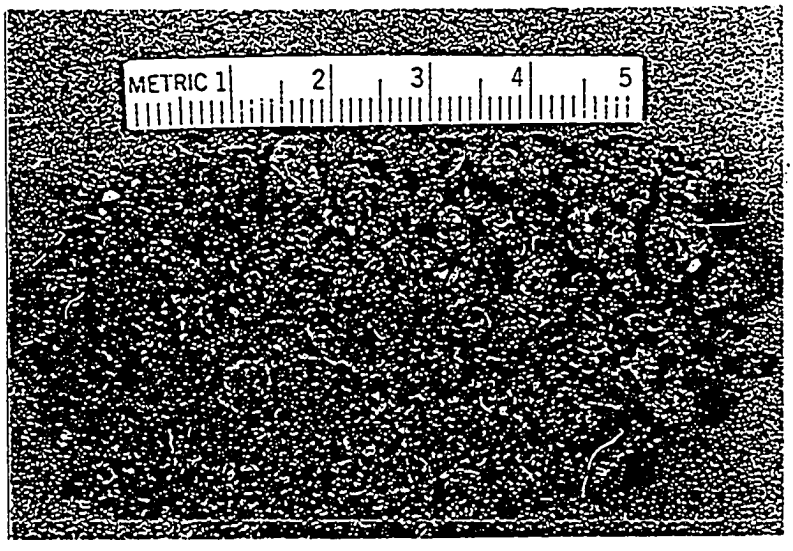


Figure 22. Sample XP1/2-3.

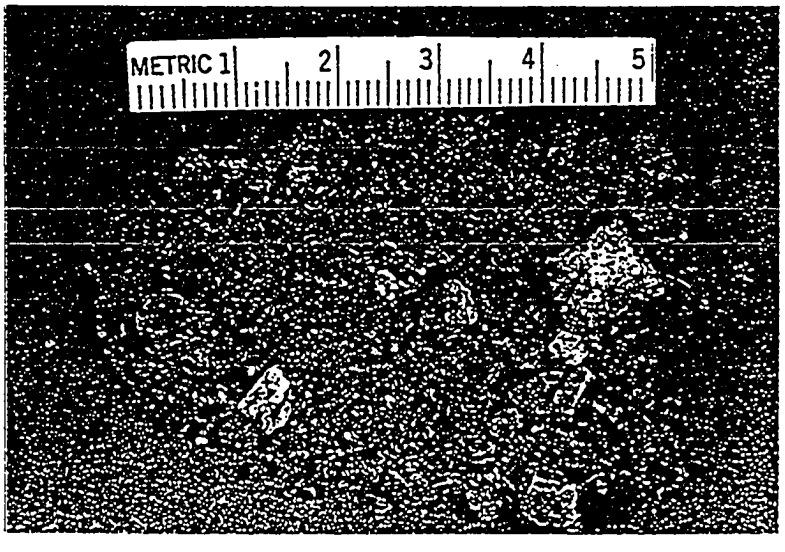


Figure 23. Sample XP1/4-5.

Reproduced with permission of the copyright owner. Further reproduction prohibited without permission.

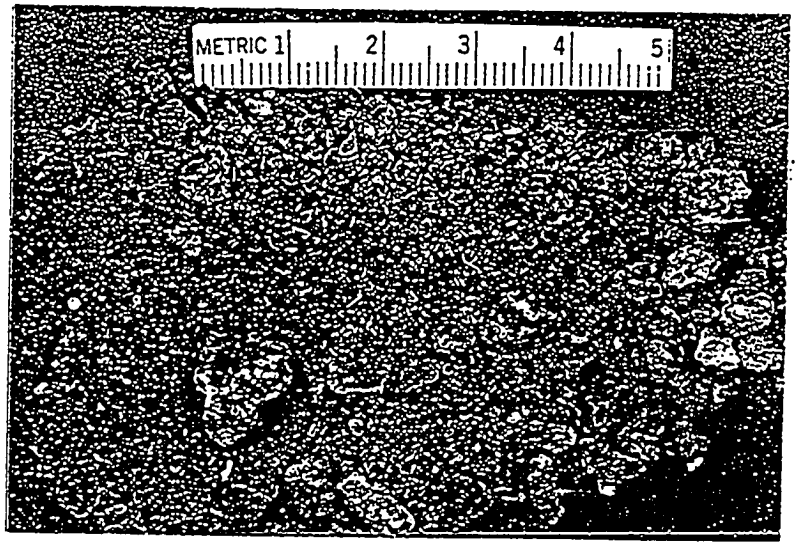


Figure 24. Sample XP1/5.5-6.5

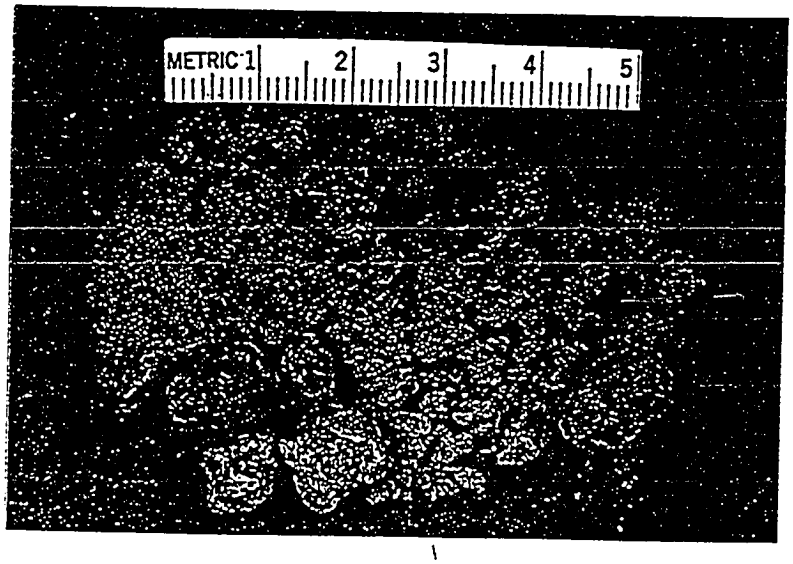


Figure 25. Sample XP3/2-3.

Reproduced with permission of the copyright owner. Further reproduction prohibited without permission.

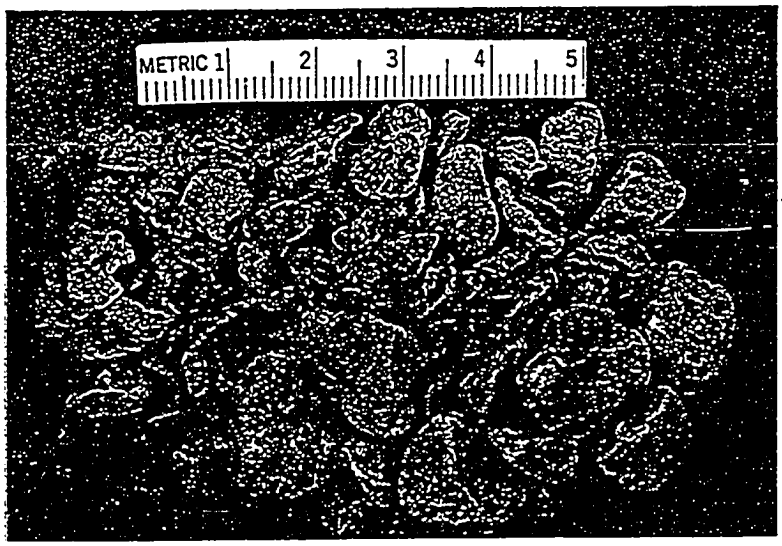


Figure 26. Sample XP3/4-5.

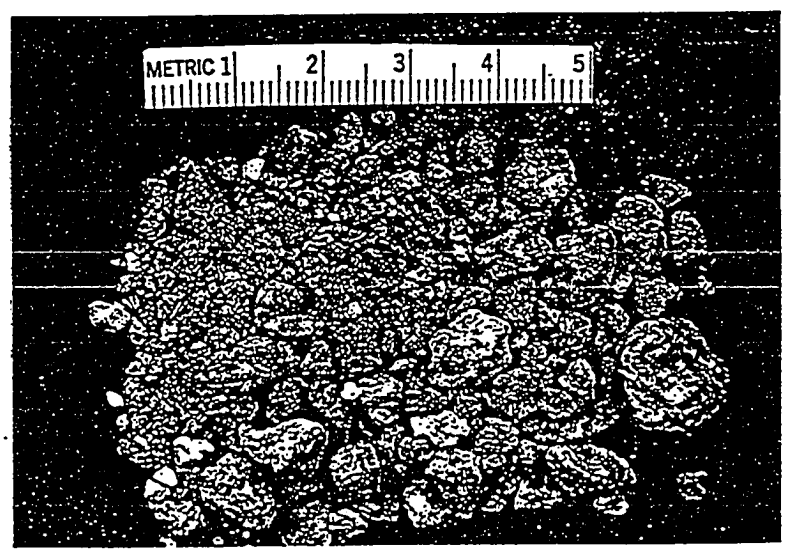


Figure 27. Sample XP3/6-7.

Reproduced with permission of the copyright owner. Further reproduction prohibited without permission.

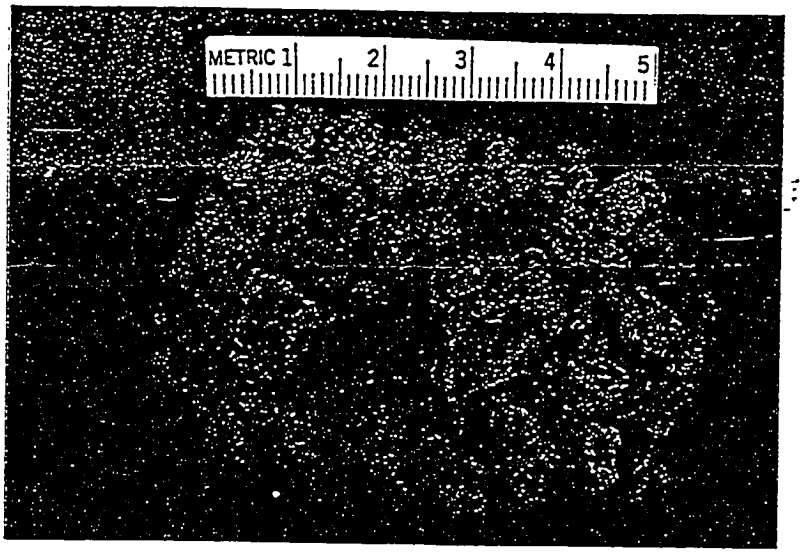


Figure 28. Sample XP5/1-2.

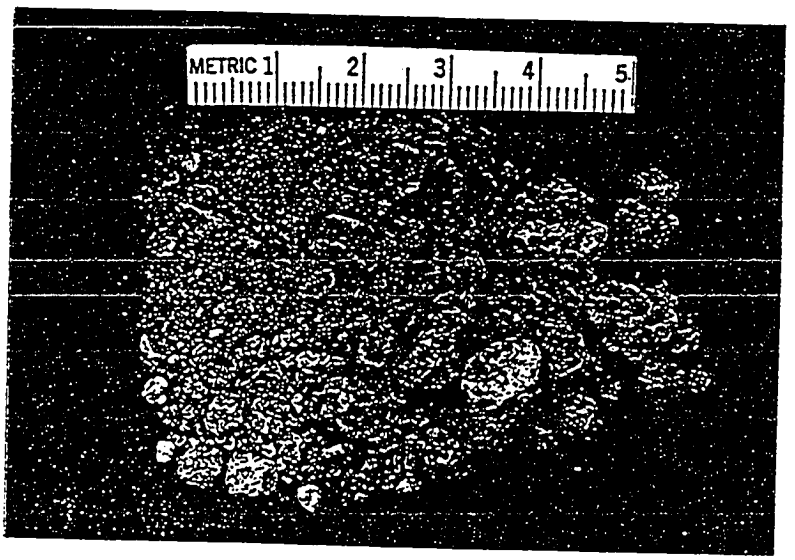


Figure 29. Sample XP5/4-5.

Reproduced with permission of the copyright owner. Further reproduction prohibited without permission.

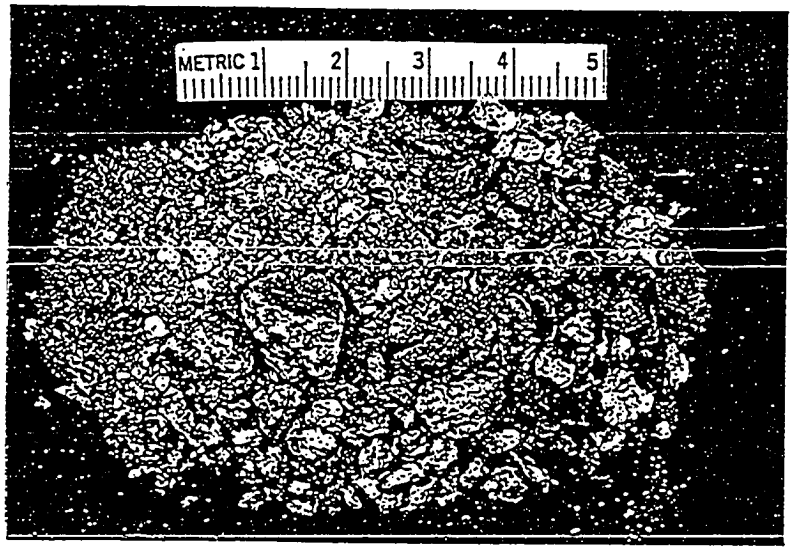


Figure 30. Sample XP6/4-5.

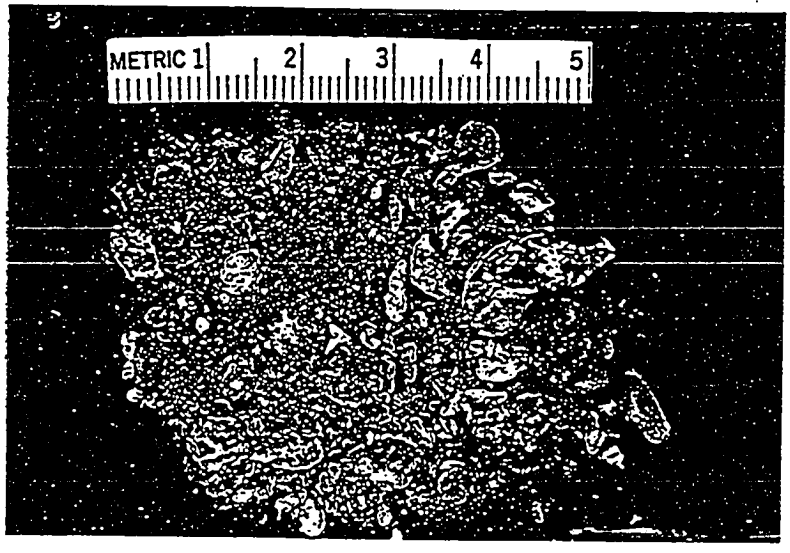


Figure 31. Sample PC 1B.

Reproduced with permission of the copyright owner. Further reproduction prohibited without permission.

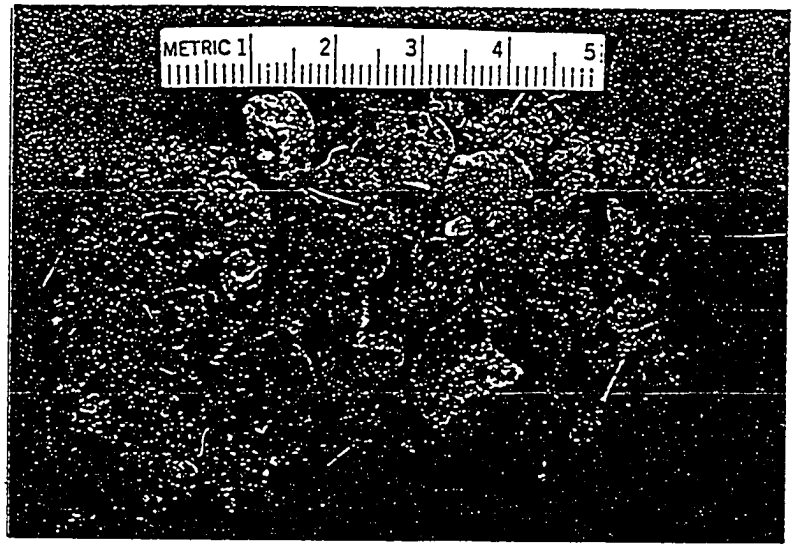


Figure 32. Sample PC 2A.

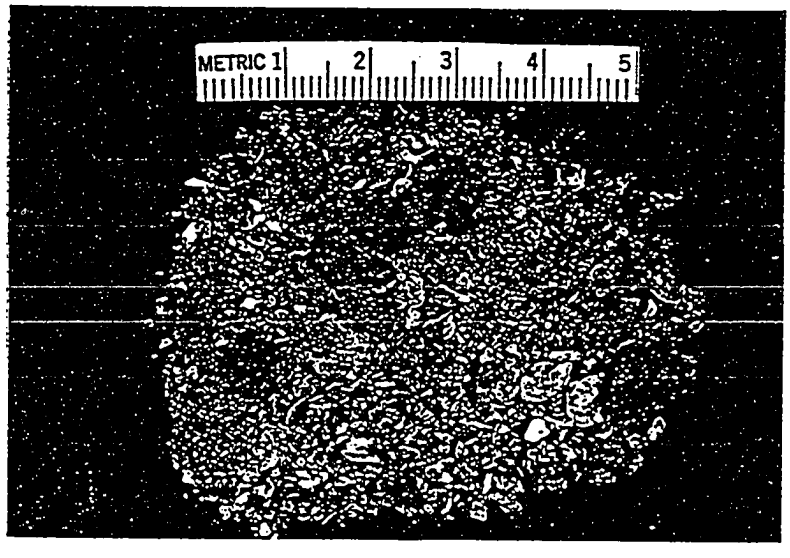


Figure 33. Sample PC 2B.

Reproduced with permission of the copyright owner. Further reproduction prohibited without permission.

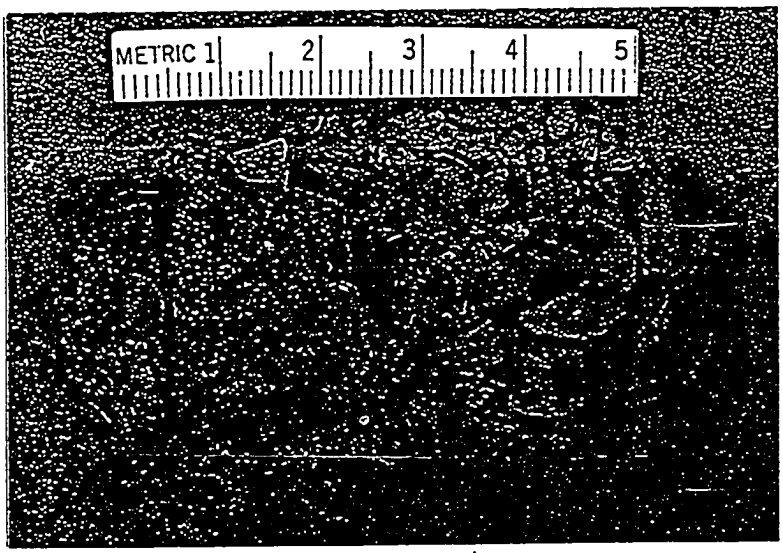


Figure 34. Sample PC 2C.

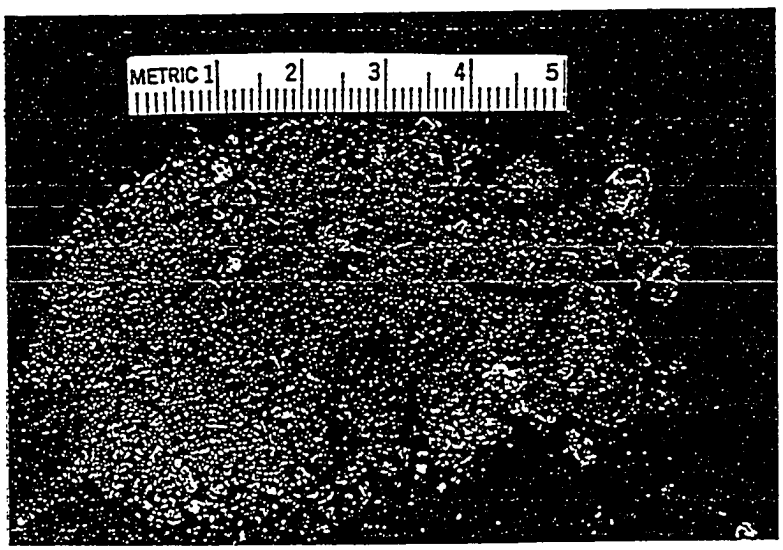


Figure 35. Sample PC 2AX.

Reproduced with permission of the copyright owner. Further reproduction prohibited without permission.

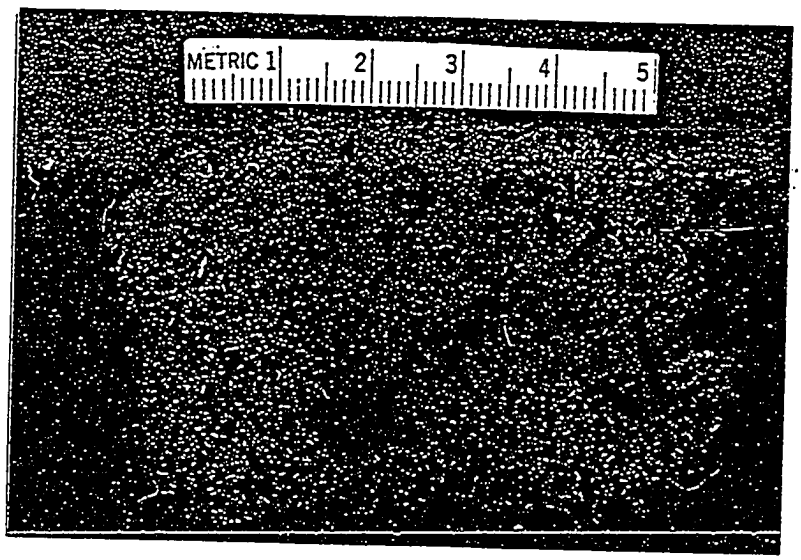


Figure 36. Sample PC 20A.

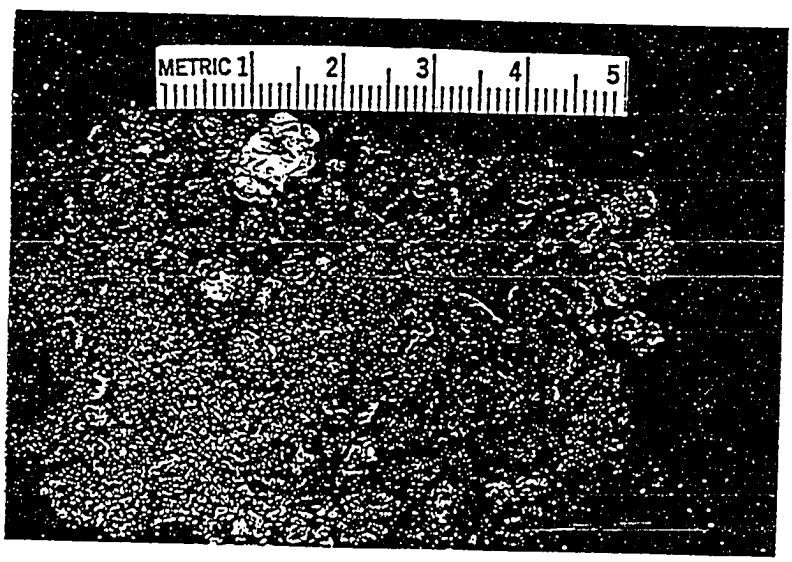


Figure 37. Sample PC 20B.

Reproduced with permission of the copyright owner. Further reproduction prohibited without permission.

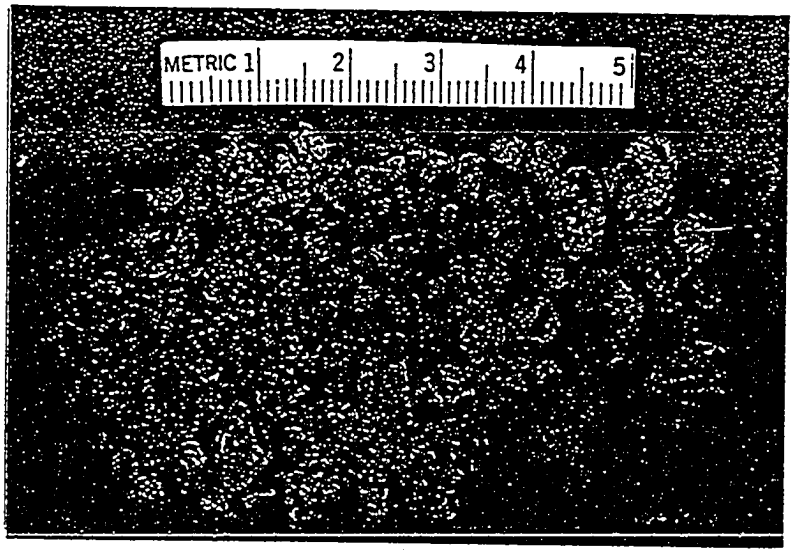


Figure 38. Sample PC 20C.

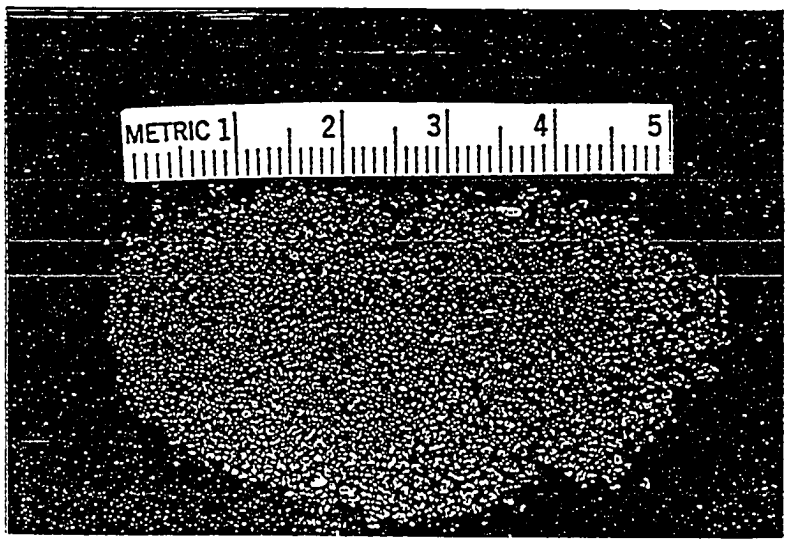


Figure 39. Sample AF1-14.5.

Reproduced with permission of the copyright owner. Further reproduction prohibited without permission.

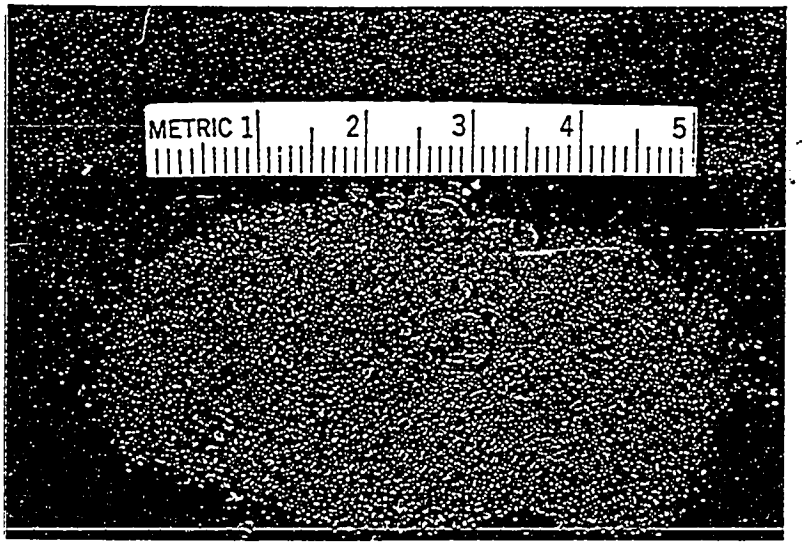


Figure 40. Sample SB3-7.0.

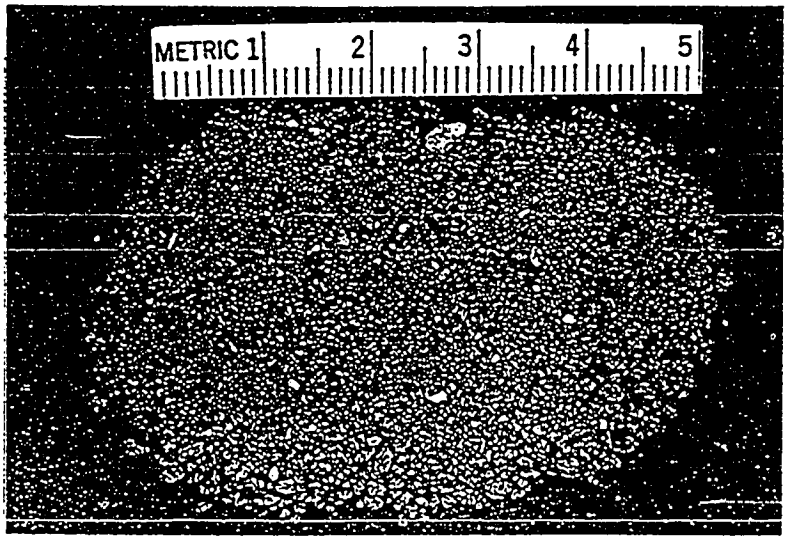


Figure 41. Sample SB3-15.0.

Reproduced with permission of the copyright owner. Further reproduction prohibited without permission.

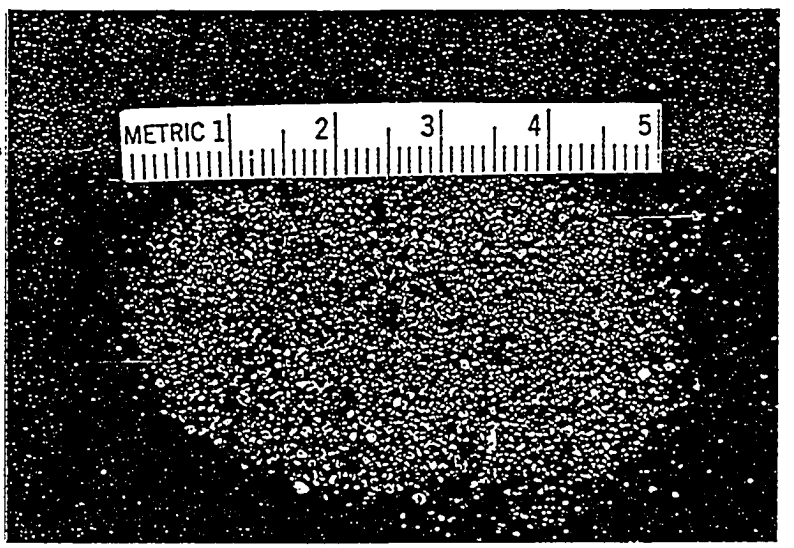


Figure 42. Sample SB3-27.5 - 27.8.

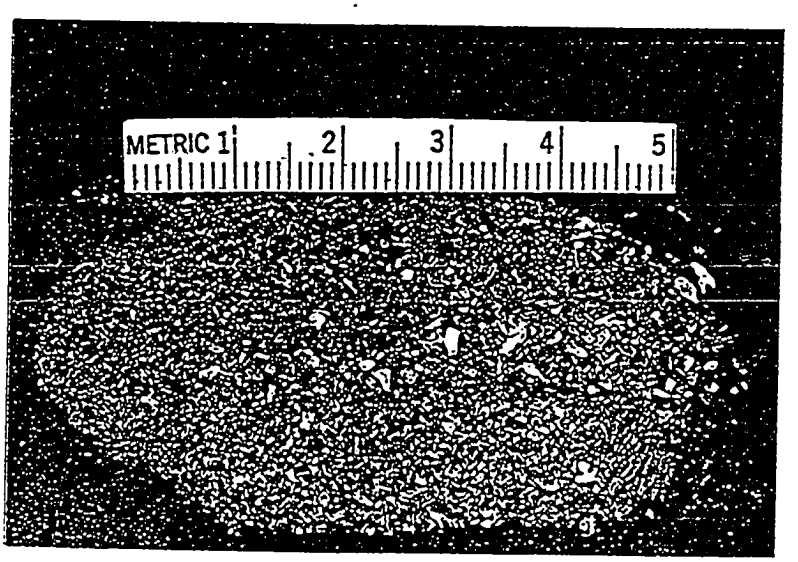


Figure 43. Sample SS 28.

Reproduced with permission of the copyright owner. Further reproduction prohibited without permission.

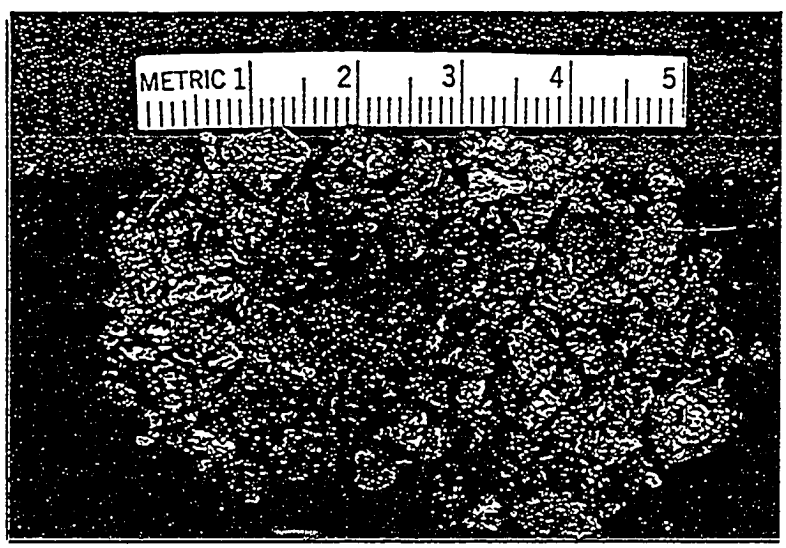


Figure 44. Sample BP6/1.0.

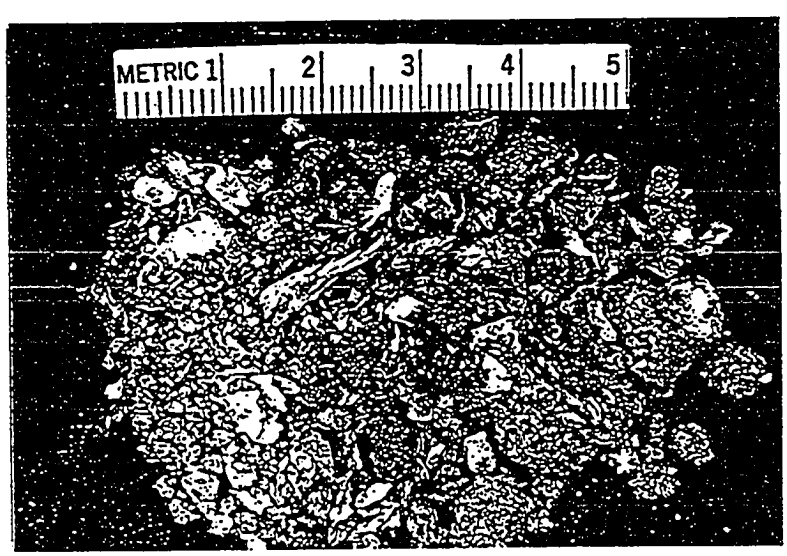


Figure 45. Sample AL 52.

Reproduced with permission of the copyright owner. Further reproduction prohibited without permission.

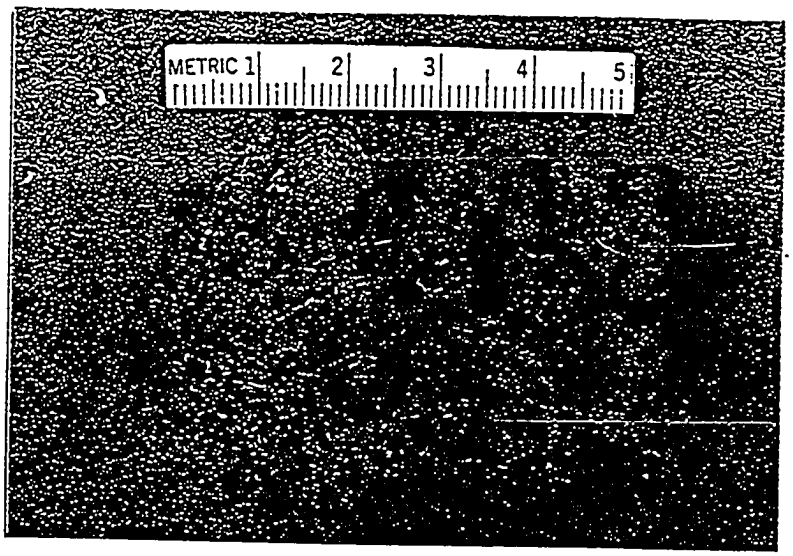


Figure 46. Sample BS 29.

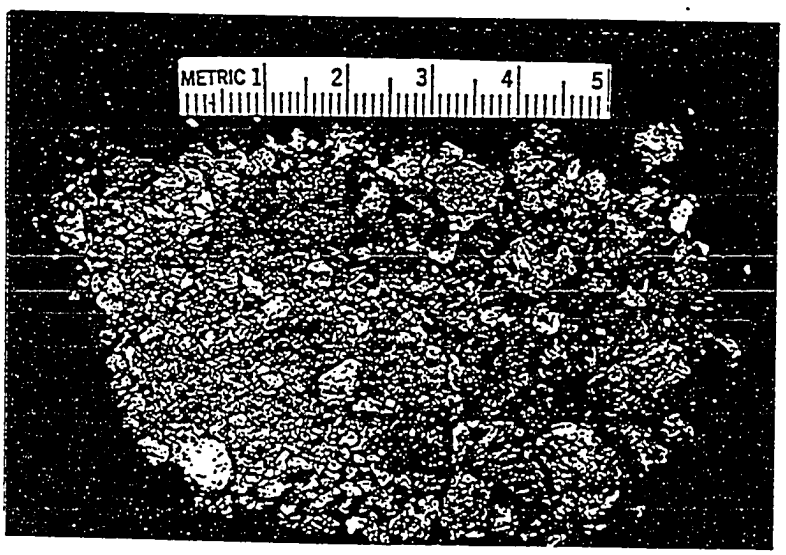


Figure 47. Sample PC 41A.

Reproduced with permission of the copyright owner. Further reproduction prohibited without permission.

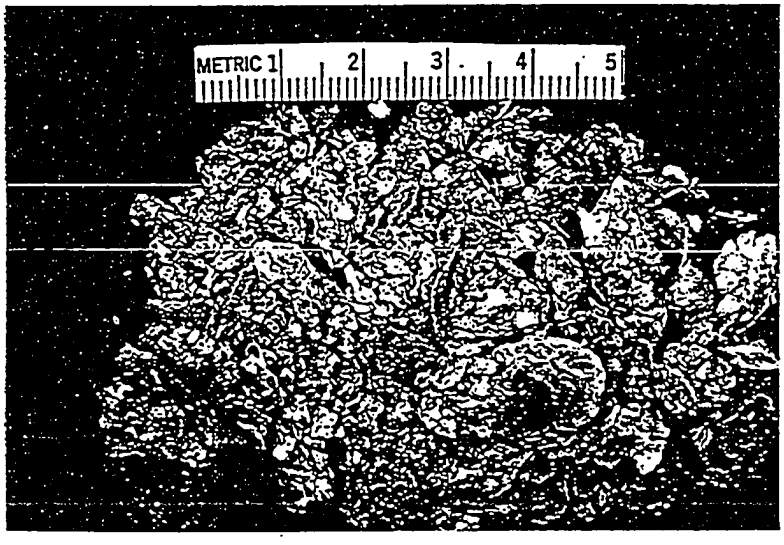


Figure 48. Sample OC 18B.

Reproduced with permission of the copyright owner. Further reproduction prohibited without permission.

1861 File

mccrone environmental services, inc.
1412 OAKBROOK DRIVE • SUITE 100
NORCROSS, GA 30093 • 404-368-9600

17 May 1988

Levine-Fricke
629 Oakland Avenue
Oakland, California 94611-4567

Attention: Mr. Glenn Leong

Subject: Estimate of Weight % Asbestos in Coalinga Samples

Re: McCrone Project No. ME-4595

Dear Mr. Leong:

Per our telephone conversation yesterday afternoon, I have reviewed the results of our analyses of seventy (70) soil, mine tailings and stream sediment samples (reference our report dated 04 May 1988). Regarding your request for further delineation of % asbestos present in these samples according to weight, this is a problem that the industry has faced since its inception. Even though EPA has defined asbestos-containing materials according to percent by weight asbestos present, they point out in their 1982 "Interim Method" that the point counting technique advocated by the method "provides a determination of the area percent asbestos". They also acknowledge that "reliable conversion of area percent to percent of dry weight is not currently feasible unless the specific gravities and relative volumes of the materials are known".

The analytical technique used by McCrone Environmental Services, Inc. (MES) establishes an approximate percentage or range of asbestos present based on a by volume estimate. As no attempt was made to quantify individual species of non-asbestos minerals in these samples it is not feasible to attempt a conversion to weight percent. It seems, however, that if the primary laboratory in this study utilized the point-count method or a PLM field of view estimating technique that their results may actually be area percent values. If this is the case, then the question becomes one of an approximation based on two-dimensional observation versus one based on three-dimensional observation. Correlation of results based on these two types of analysis, while not strictly valid, should yield results at least as compatible as trying to compare either an area % or volume % value to a true weight percent.

a member of the mccrone group
850 PASQUINELLI DRIVE • WESTMONT, ILLINOIS 60559 • 312-887-7100

Reproduced with permission of the copyright owner. Further reproduction prohibited without permission.

An examination of the approximate specific gravities of other mineral constituents detected in the thirteen (13) samples selected by Levine-Fricke for characterization according to composition and asbestos morphology reveals that none of the other identified constituents should have a lower specific gravity than serpentine.

Constituent	Specific Gravity
Serpentine	2.5-2.6
Chlorite	2.6-3.3
Mica	2.7-3.3
Actinolite	3.0-3.4
Feldspar	2.5-2.8
Quartz	2.65
Carbonate	2.7-3.5
Magnetite	5.2
Chromite	5.09

On the basis of this observation it is logical to assume that, if conversions to weight percent could be made, the volume percentages reported for asbestos by MES should be greater than or equal to the actual weight percent.

I hope that you have found this additional information useful. If you have further questions about these analyses please contact me at (404) 368-9600.

Sincerely,

Randy Boltin

Randy Boltin
Manager, Optical Microscopy Group

RB/mlj

Reproduced with permission of the copyright owner. Further reproduction prohibited without permission.

101 8

MED-TOX ASSOCIATES, INC.

MEMORANDUM

TO: Alan Leavitt, Levine Fricke

FROM: Tom Dagenhart, Med-Tox Associates, Inc.

DATE: June 3, 1988

RE: Points of Clarification on PLM and TEM Asbestos Analyses of Soils

1. TEM analyses of soil samples yield quite imprecise data when using a derivative of the Yamate EPA method or any other method that relies on calculated masses. This imprecision is indicated in our method description where the coefficient of variance is estimated as 1.0. Although imprecision limits the usefulness of TEM data, greater certainty in fiber identification and capability to resolve fibers too thin for PLM detection remain as two distinct advantages of TEM versus PLM. Imprecision results for two major reasons:

a. Mass calculation for counted fibers is an inexact process. The mass is derived from calculated volume and assumed density. Volume is calculated by assuming all fibrils and bundles are cylinders with diameter and length measurements as perceived on screen. Diameter measurements are crude at 20,000 X because perceived diameters range from a few tenths of a millimeter to a few millimeters on screen and because carbon deposited on asbestos structures during sample preparation significantly enhances the apparent diameter of thin fibers. The diameter measurement must be squared in calculating the volume of cylindrical fibers. Complex structures such as clusters and matrices add more uncertainty to mass calculations since the entire length of some fibers cannot be observed and the total number of fibers in some structures is not discernible. In summary mass calculations are imprecise due to unavoidable assumptions about particle density and shape and due to squaring of the least-well-known measurement, the diameter.

b. Counting statistics inject a certain level ofimprecision when selecting a small sample of fibers from a thinly dispersed fiber population. However sample size must remain small or else analytical costs become prohibitive.

2. Asbestos concentrations greater than 100% are obviously a physical impossibility. However, samples with true concentrations near 100% may yield analytical results greater than 100% due to method imprecision. Two samples in this study did yield results etween 200 and 300%. For a population of possible results with a log normal distribution, a coefficient of variance of 1.0, and a

Reproduced with permission of the copyright owner. Further reproduction prohibited without permission.

mean near 100%; these 200 to 300% results are well within the 95% confidence intervals.

3. Our PLM reports include the classifications "elongate serpentine" and "chrysotile" to deal with ambiguities arising during PLM asbestos analysis of soils in this study. Soils from the study area contain chrysotiles with a greater range of optical properties than is usually encountered during routine analysis. This increased range overlaps the range of optical properties characteristic of other serpentines. In addition these soils contain large percentages of these other serpentine minerals which are not present in routine insulation samples because milling normally removes most non-asbestiform serpentine (antigorite and lizardite) from the asbestiform serpentine (chrysotile) used commercially.

Many serpentine fragments exhibited morphologies clearly of a non-asbestiform nature; but because the fragments had aspect ratios of at least 3:1, the standard EPA method requires classification as fibers. To avoid conveying unjustifiably high values on asbestos content while adhering somewhat to the EPA fiber definition, the category "elongate serpentine" was created. Elongate serpentine includes all PLM-visible chrysotile asbestos and all other serpentine fragments which may be classified as asbestos fibers due to limitations of the standard EPA method. Elongate serpentine represents the upper limit on PLM-detectable asbestos in these soils (within the precision and accurracy limitations of the method).

Normal chrysotile was frequently encountered in these samples and these fibers were recorded in the "chrysotile" category which is a subset of the elongate serpentine category. Therefore chrysotile concentrations indicate the lower limit of possible asbestos concentrations (within the precision and accurracy limitations of the method). The true PLM-asbestos concentration in each sample obviously lies somewhere between the reported chrysotile and elongate serpentine levels.

4. Several factors must be considered in comparing TEM and PLM analyses of the same sample:

The majority of fibers detected by TEM were verified as chrysotile .
Most TEM analyses yielded higher asbestos concentrations than PLM analyses of the same samples.
Soil was ground more finely during TEM sample preparation than for PLM sample preparation
The PLM results generated by an independent QC laboratory correlated well with our PLM results but were somewhat higher (probably because elongate serpentine was lumped together with obvious chrysotile).

Reproduced with permission of the copyright owner. Further reproduction prohibited without permission.

MED-TOX ASSOCIATES, INC.

The observed results suggest two models to explain the relationship between TEM and PLM results:

a. Most elongate serpentine particles consist primarily of chrysotile. These fibers were released during TEM sample preparation and detected during TEM analysis. However the fibers were too thin or too tightly bound to be perceived as asbestos by PLM.

b. Most elongate serpentine particles consist of non-asbestos serpentine minerals, i.e. antigorite and lizardite and were reduced to non-fibrous powder during sample preparation. The excess chrysotile detected by TEM is present as naturally-occurring finely-divided chrysotile which escapes PLM detection due to resolution limitations. This model will alarm people because it requires the presence of asbestos in easily respirable small particles.

Both models probably contribute to the observed results. However neither model can be conclusively accepted or rejected based upon our limited data set. Both models can be evaluated with carefully designed analytical efforts somewhat different than standard procedures.

5. All QC data which you have requested has been forwarded under separate cover by Don Lyons.

cc: Don Lyons

Reproduced with permission of the copyright owner. Further reproduction prohibited without permission.

APPENDIX E

EXAMPLES OF TYPICAL LABORATORY DATA REPORTS

Reproduced with permission of the copyright owner. Further reproduction prohibited without permission.

Typical Asbestos PLM Reports

Reproduced with permission of the copyright owner. Further reproduction prohibited without permission.

LABORATORY REPORT

MED-TOX ASSOCIATES, INC.

LEVINE & FRICKE
7900 POWELL ST., 12TH FLOOR
EMERYVILLE, CA 94608
ATTN: JOHN DEREAMER

REPORT DATE: 4/22/88
SAMPLES RECEIVED: 4/12/88
MED-TOX JOB NO: 7L-8401-8/WP27
PURCHASE ORDER NO:

ANALYSIS: ASBESTOS IN BULK SAMPLES

METHOD: PLM (POLARIZED LIGHT MICROSCOPY/DISPERSION STAINING)
EPA 600/M4-82-020

Sample Identification Client	Lab No.	Brief Physical Description	Elongate* Serpentine Percent	Chrysotile* Asbestos Percent	Amphibole* Asbestos Percent
OC-30	73307	Greenish-gray soil	80	40	ND(1)
OC-32	73308	Tan soil	60	30	ND(1)
OC-81	73309	Greenish-gray soil	75	40	ND(1)
OC-82	73310	Gray soil	70	30	ND(1)
OC-83	73311	Greenish-gray soil	85	40	ND(1)
SS-30	73312	Gray soil	50	25	ND(1)
SS-15	73313	Tan soil	15	10	ND(1)
SS-17	73314	Brown soil	Trace	Trace	ND(1)
SS-16	73315	Brown soil	5	2	ND(1)
SS-18	73316	Tan soil	5	2	ND(1)
SS-19	73317	Dark gray soil	20	10	ND(1)
SS-20	73318	Dark brown soil	30	15	ND(1)
SS-21	73319	Tan soil with pebbles	Trace	Trace	ND(1)
SS-22	73320	Grayish-tan, sandy soil	Trace	ND(1)	ND(1)

David Reusswig/Julianne Rhodes
Laboratory Analyst

4/22/88
Date

Don Lyons
Laboratory Manager

"ND(1)" means no asbestos detected; method detection limit is 1%.
"Trace" means asbestos identified in sample; concentration less than method detection of 1%.
Other asbestos minerals sought but not detected include crocidolite, anthophyllite, tremolite, and actinolite.
* These samples contain serpentine minerals (antigorite and lizardite) which have optical properties similar to chrysotile. Chrysotile in these samples has optical properties more like fibrous antigorite than normal chrysotile. Given the limitations of the EPA PLM method, results are reported as both elongate serpentine and chrysotile. Elongate serpentine includes all serpentine fragments that have at least a 3:1 aspect ratio. Therefore elongate serpentine includes fibers of chrysotile, antigorite and lizardite and is the upper limit for PLM-detectable chrysotile. The chrysotile asbestos category only includes fibers with classical chrysotile properties and is our best professional judgement on PLM-detectable chrysotile.

1229 Morena Boulevard, San Diego, CA 92110 (619) 276-8843

received
MAY 2 1988

Reproduced with permission of the copyright owner. Further reproduction prohibited without permission.

LABORATORY REPORT

MED-TOX ASSOCIATES INC

LEVINE & FRICKE
1900 POWELL ST., 12TH FLOOR
EMERYVILLE, CA 94608
: JOHN DEREAMER

REPORT DATE: 4/22/88
SAMPLES RECEIVED: 4/12/88
MED-TOX JOB NO: 7L-6401-8/WP27
PURCHASE ORDER NO:

ANALYSIS: ASBESTOS IN BULK SAMPLES

METHOD: PLM (POLARIZED LIGHT MICROSCOPY/DISPERSION STAINING)
EPA 600/M4-82-020

Sample Identification Client	Lab No.	Brief Physical Description	Elongate* Serpentine Percent	Chrysotile* Asbestos Percent	Amphibole* Asbestos Percent
SS-23	73321	Tan soil, trace non-asbestiform actinolite	ND(1)	ND(1)	ND(1)
SS-20I	73322	Grayish-tan soil	75	30	ND(1)
SS-24	73323	Grayish-tan soil	65	30	ND(1)
SS-25	73324	Tan, pebbly soil	5	Trace	ND(1)
SS-26	73325	Gray, sandy soil	60	30	ND(1)
SS-33	73326	Tan soil, trace non-asbestiform actinolite	Trace	Trace	ND(1)
SS-36	73327	Tan soil	15	5	ND(1)
SS-34	73328	Tan soil	15	5	ND(1)
SS-1	73329	Tan soil	Trace	Trace	ND(1)
SS-2	73330	Tan soil	1	Trace	ND(1)
SS-81	73331	Tan soil	Trace	Trace	ND(1)
SS-3	73332	Tan soil	Trace	Trace	ND(1)
[illegible]	73333	Tan soil	Trace	Trace	ND(1)
[illegible]	73334	Tan soil	Trace	Trace	ND(1)
SS-6	73335	Tan soil, trace non-asbestiform actinolite	ND(1)	ND(1)	ND(1)
SS-7	73336	Tan soil, trace non-asbestiform actinolite	Trace	Trace	ND(1)

David Reussvig/Julianne Rhodes
Laboratory Analyst

4/22/88
Date

Don Lyons
Laboratory Manager

"ND(1)" means no asbestos detected; method detection limit is 1%.
"Trace" means asbestos identified in sample; concentration less than method detection of 1%.
Other asbestos minerals sought but not detected include crocidolite, anthophyllite, tremolite, and actinolite.
* These samples contain serpentine minerals (antigorite and lizardite) which have optical properties similar to chrysotile. Chrysotile in these samples has optical properties more like fibrous antigorite than normal chrysotile. Given the limitations of the EPA PLM method, results are reported as both elongate serpentine and chrysotile. Elongate serpentine includes all serpentine fragments that have at least a 3:1 aspect ratio. Therefore elongate serpentine includes fibers of chrysotile, antigorite and lizardite and is the upper limit for PLM-detectable chrysotile. The chrysotile asbestos category only includes fibers with classical chrysotile properties and is our best professional judgement on PLM-detectable chrysotile.

1229 Morena Boulevard, San Diego, CA 92110 (619) 276-8843

Reproduced with permission of the copyright owner. Further reproduction prohibited without permission.

LABORATORY REPORT

MED-TOX ASSOCIATES INC

LEVINE & FRICKE
1900 POWELL ST., 12TH FLOOR
[illegible]YVILLE, CA 94608
A..N: JOHN DEREAMER

REPORT DATE: 4/22/88
SAMPLES RECEIVED: 4/12/88
MED-TOX JOB NO:7L-6401-8/WP27
PURCHASE ORDER NO:

ANALYSIS: ASBESTOS IN BULK SAMPLES

METHOD: PLM (POLARIZED LIGHT MICROSCOPY/DISPERSION STAINING)
EPA 600/M4-82-020

Sample Identification Client	Lab No.	Brief Physical Description	Elongate* Serpentine Percent	Chrysotile* Asbestos Percent	Amphibole* Asbestos Percent
OC-9	73354	Greenish-gray soil	60	30	ND(1)
OC-10	73355	Greenish-gray soil	85	40	ND(1)
OC-10x	73356	Greenish-gray soil	65	45	ND(1)
OC-11	73357	Brown soil	ND(1)	ND(1)	ND(1)
OC-14	73358	Dark gray soil	90	50	ND(1)
OC-15	73359	Gray soil	80	50	ND(1)
OC-17	73360	Gray soil	80	50	ND(1)
OC-19	73361	Brown soil	60	20	ND(1)
OC-21	73362	Gray soil	60	30	ND(1)
OC-22	73363	Brown soil	ND(1)	ND(1)	ND(1)
OC-24	73364	Gray soil	85	50	ND(1)
OC-28	73365	Gray soil	80	45	ND(1)
OC-29	73366	Gray soil	90	50	ND(1)

David L. Reusswig
Laboratory Analyst

4/22/88
Date

Don Lyons
Laboratory Manager

"ND(1)" means no asbestos detected; method detection limit is 1%.
"Trace" means asbestos identified in sample; concentration less than method detection of 1%.
Other asbestos minerals sought but not detected include crocidolite, anthophyllite, tremolite, and actinolite.
* These samples contain serpentine minerals (antigorite and lizardite) which have optical properties similar to chrysotile. Chrysotile in these samples has optical properties more like fibrous antigorite than normal chrysotile. Given the limitations of the EPA PLM method, results are reported as both elongate serpentine and chrysotile. Elongate serpentine includes all serpentine fragments that have at least a 3:1 aspect ratio. Therefore elongate serpentine includes fibers of chrysotile, antigorite and lizardite and is the upper limit for PLM-detectable chrysotile. The chrysotile asbestos category only includes fibers with classical chrysotile properties and is our best professional judgement on PLM-detectable chrysotile.

1229 Morena Boulevard, San Diego, CA 92110 (619) 276-8843

Reproduced with permission of the copyright owner. Further reproduction prohibited without permission.

LABORATORY REPORT

MED-TOX ASSOCIATES, INC.

LEVINE & FRICKE
1900 POWELL ST., 12TH FLOOR
EMERYVILLE, CA 94608
ATTN: JOHN DEREAMER

REPORT DATE: 4/22/88
SAMPLES RECEIVED: 4/12/88
MED-TOX JOB NO:7L-8401-9/WP27
PURCHASE ORDER NO:

ANALYSIS: ASBESTOS IN BULK SAMPLES

METHOD: PLM (POLARIZED LIGHT MICROSCOPY/DISPERSION STAINING)
EPA 600/M4-82-020

Sample Identification Client	Lab No.	Brief Physical Description	Elongate* Serpentine Percent	Chrysotile* Asbestos Percent	Amphibole* Asbestos Percent
OC-2	73593	Gray, coarse-grained soil	70	35	ND(1)
OC-4	73594	Gray, coarse-grained soil	70	35	ND(1)
OC-6	73595	Gray, coarse-grained soil	85	45	ND(1)
OC-12	73596	Gray, coarse-grained soil	25	10	ND(1)
OC-13	73597	Gray, coarse-grained soil	25	10	ND(1)
OC-16	73598	Gray soil	25	5	ND(1)
OC-18	73599	Gray soil	90	65	ND(1)
OC-18B	73600	Gray soil	90	45	ND(1)
OC-26	73601	Brown soil	ND(1)	ND(1)	ND(1)
OC-27	73602	Tannish-gray, pebbly soil	85	45	ND(1)
OC-31	73603	Tannish-gray, pebbly soil	75	40	ND(1)
OC-25	73604	Gray soil	95	50	ND(1)
OC-25B	73605	Gray soil	95	50	ND(1)
OC-85	73606	Gray soil	95	50	ND(1)
SS-28	73607	Dark-gray soil	75	30	ND(1)
SS-29	73608	Gray soil	85	45	ND(1)
SS-30	73609	Gray soil	75	35	ND(1)
SS-31	73610	Brown soil	65	30	ND(1)
SS-32	73611	Brown soil	ND(1)	ND(1)	ND(1)
SS-27	73612	Brown soil	80	40	ND(1)
SS-83	73613	Dark-gray soil	ND(1)	ND(1)	ND(1)

Julianne Rhodes
Laboratory Analyst

5-25-88
Date

Don Lyons
Laboratory Manager

"ND(1)" means no asbestos detected; method detection limit is 1%.
"Trace" means asbestos identified in sample; concentration less than method detection of 1%.
Other asbestos minerals sought but not detected include crocidolite, anthophyllite, tremolite, and actinolite.

* These samples contain serpentine minerals (antigorite and lizardite) which have optical properties similar to chrysotile. Chrysotile in these samples has optical properties more like fibrous antigorite than normal chrysotile. Given the limitations of the EPA PLM method, results are reported as both elongate serpentine and chrysotile. Elongate serpentine includes all serpentine fragments that have at least a 3:1 aspect ratio. Therefore elongate serpentine includes fibers of chrysotile, antigorite and lizardite and is the upper limit for PLM-detectable chrysotile. The chrysotile asbestos category only includes fibers with classical chrysotile properties and is our best professional judgement on PLM-detectable chrysotile.

1229 Morena Boulevard, San Diego, CA 92110 (619) 276-8843

Reproduced with permission of the copyright owner. Further reproduction prohibited without permission.

LABORATORY REPORT

MED-TOX ASSOCIATES INC.

LEVINE & FRICKE
1900 POWELL ST., 12TH FLOOR
EMERYVILLE, CA 94608
ATTN: JOHN DEREAMER

REPORT DATE: 4/22/88
SAMPLES RECEIVED: 4/12/88
MED-TOX JOB NO:7L-6401-8/WP27
PURCHASE ORDER NO:

ANALYSIS: ASBESTOS IN BULK SAMPLES

METHOD: PLM (POLARIZED LIGHT MICROSCOPY/DISPERSION STAINING)
EPA 600/M4-82-020

Sample Identification Client	Lab No.	Brief Physical Description	Elongate* Serpentine Asbestos Percent	Chrysotile* Asbestos Percent	Amphibole* Asbestos Percent
SS-8	73337	Grayish-brown, sandy soil	Trace	ND(1)	ND(1)
SS-9	73338	Gray, sandy soil	ND(1)	ND(1)	ND(1)
SS-13	73339	Tan, pebbly soil	ND(1)	ND(1)	ND(1)
SS-12	73340	Tan, pebbly soil	10	5	ND(1)
SS-82	73341	Tan, pebbly soil	5	3	ND(1)
SS-11	73342	Gray, sandy soil	Trace	Trace	ND(1)
SS-10	73343	Gray, sandy soil	Trace	Trace	ND(1)
SS-14	73344	Brown, pebbly soil, trace non-asbestiform actinolite	ND(1)	ND(1)	ND(1)
SS-84	73345	Tan soil	15	5	ND(1)
SS-35	73346	Tan soil	ND(1)	ND(1)	ND(1)
SS-37	73347	Tan soil	10	5	ND(1)
SS-38	73348	Tan soil	20	5	ND(1)
SS-39	73349	Tan soil	25	10	ND(1)
SS-40	73350	Tan soil	25	15	ND(1)
OC-1	73351	Dark gray soil	85	50	ND(1)
OC-3	73352	Dark gray soil	60	30	ND(1)
OC-5	73353	Dark gray soil	65	25	ND(1)

David L. Reussvig
Laboratory Analyst

4/22/88
Date

Don Lyons
Laboratory Manager

"ND(1)" means no asbestos detected; method detection limit is 1%.
"Trace" means asbestos identified in sample; concentration less than method detection of 1%.
Other asbestos minerals sought but not detected include crocidolite, anthophyllite, tremolite, and actinolite.

* These samples contain serpentine minerals (antigorite and lizardite) which have optical properties similar to chrysotile. Chrysotile in these samples has optical properties more like fibrous antigorite than normal chrysotile. Given the limitations of the EPA PLM method, results are reported as both elongate serpentine and chrysotile. Elongate serpentine includes all serpentine fragments that have at least a 3:1 aspect ratio. Therefore elongate serpentine includes fibers of chrysotile, antigorite and lizardite and is the upper limit for PLM-detectable chrysotile. The chrysotile asbestos category only includes fibers with classical chrysotile properties and is our best professional judgement on PLM-detectable chrysotile.

1229 Morena Boulevard, San Diego, CA 92110 (619) 276-8843

Reproduced with permission of the copyright owner. Further reproduction prohibited without permission.

Typical Asbestos TEM Reports

Reproduced with permission of the copyright owner. Further reproduction prohibited without permission.

MED-TOX ASSOCIATES, INC.

ENVIRONMENTAL & OCCUPATIONAL HEALTH SERVICES

10366 BATTLEVIEW PARKWAY • MANASSAS, VA 22110 • (703) 368-7880

SOIL ASBESTOS ANALYSIS BY TRANSMISSION ELECTRON MICROSCOPY: AN EXPLANATION OF ANALYTICAL REPORTS

Definitions of Structures

Asbestos occurs not only as single fibers but also as complicated structures composed of many individual fibers in various states of aggregation. To assist in communicating information about asbestos and computing structural masses, asbestos structures are grouped into four structural classes illustrated in the attached figure.

Fibers or ultimate fibrils are the smallest units into which asbestos can subdivide. Fibers are typically 0.01 to 0.1 micrometers in diameter and 0.25 to 100 micrometers long. Bundles are structures composed of attached multiple fibers in parallel to sub-parallel orientation. Virtually all "fibers" seen by optical microscopists are actually bundles. Clumps (or clusters) of asbestos are structures composed of attached multiple fibers in non-parallel orientations. Matrix structures consist of any of the other types of structures attached to a matrix of cement or some other non-asbestos material.

Distinctions between the structural classes are not always simple, e.g. a large bundle with a tiny amount of attached cement, might be classified as a bundle by some analysts but as a matrix structure by others. Multiple fiber structures range in size from several centimeters down to the size range of fibers.

Definitions of Terms Used in Reports

Terms described by the following discussion are highlighted within a summary box on page one of the soil asbestos TEM reports. A brief explanation of each term is provided here to enhance understanding and to encourage proper use of the data. The title of each following section is an actual term used in the reports.

Total Asbestos Structure Concentration for All Structures

This figure indicates the number of asbestos structures found per gram of soil. All asbestos structures detected are included in the calculation regardless of size or structural

Reproduced with permission of the copyright owner. Further reproduction prohibited without permission.

classification. The results are reported in units of billions of structures per dry gram of soil.

Sample processing may change the particle size distribution of soil asbestos. Consequently, the measured structure concentration may not correlate directly with in situ structure concentrations. Soils containing high concentrations of asbestos or coarse particles require extensive grinding during sample preparation. These ground samples will definitely contain more structures per gram than the original sample as an unavoidable consequence of sample preparation.

The detection limit for structure concentrations is calculated based on four fibers observed per ten grid square openings. If less than four fibers are observed, a less than symbol followed by the calculated four fiber limit appears.

Total Asbestos Structure Concentration for Greater-than-Five-Micrometer Structures

This figure indicates the number of asbestos structures containing fibers longer than five micrometers found per gram of soil. These greater-than-five-micrometer structures are reported separately because the OSHA worker protection rules focus on fibers of this size. The results are reported in billions of structures per dry gram of soil.

As mentioned above, sample preparation may have greatly altered particle size distributions, especially in coarse-grained or asbestos rich samples. On any particular sample it is not feasible to predict whether the greater-than-five-micrometer fraction will increase or decrease due to sample treatment. When long fibers and bundles break across their length, the structures obviously become shorter and the concentration of short fibers increases while the concentration of long fibers decreases. When long bundles break parallel to their length, the length remains unchanged and only diameter decreases. Therefore, bundle separation along the length increases the number of long fibers and leaves the number of short fibers unchanged.

Observation of individual structures during sample preparation is not possible, and therefore, estimation of the frequency of breaking across bundles and along bundles is not feasible except by imprecise empirical methods. As a result, reported concentrations of both structures greater than five micrometers and total structures are only an approximation of in situ structure concentrations and cannot be back-calculated to original concentrations.

Total Asbestos Mass Concentration for All Structures

This soil TEM method is designed to maximize the accuracy of this particular result. The fine grinding which limits the

Reproduced with permission of the copyright owner. Further reproduction prohibited without permission.

accuracy of the structure concentrations enhances the accuracy of mass concentrations by producing a uniform material for TEM analysis.

TEM analysis determines mass indirectly by using a volume computed from structural dimensions and a density characteristic of the particular mineral. Errors in determining structure diameters propagate rapidly because diameters are squared when computing mass.

The mass concentrations are reported as micrograms of asbestos per dry gram of soil. This can also be read as parts per million or milligrams per kilogram if desired. Dividing the mass concentrations by 10,000 yields the percent asbestos.

Detection limits are not calculated for mass concentrations because the calculation would require specious assumptions about the size of the fibers that were not detected. Instead, if less than four fibers are detected, ND is printed in the column.

Total Asbestos Mass Concentrations for Greater-than-Five-Micrometer Structures

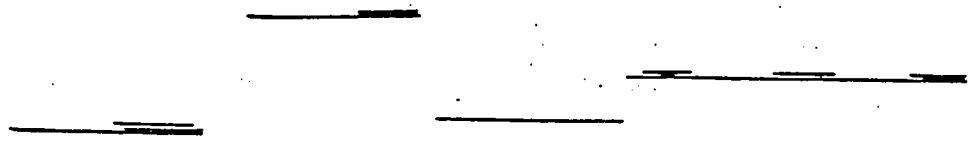
The mass concentration for greater-than-five-micrometer asbestos structures is computed from the calculated mass of all asbestos structures that contain fibers greater than five micrometers in the prepared sample. The same definitions, limitations, and detection limit considerations that apply to mass concentrations of all asbestos structures also apply to the mass concentration of these greater-than-five-micrometer structures. In addition, this data is further limited in accuracy by the considerations that apply to greater-than-five-micrometer asbestos structure concentrations.

To summarize, because the particle size distribution in the prepared sample is not identical to the distribution in the raw sample, the mass concentration of a certain particle size fraction in the prepared sample is only an approximation of the mass concentration of that particle size fraction in the raw sample.

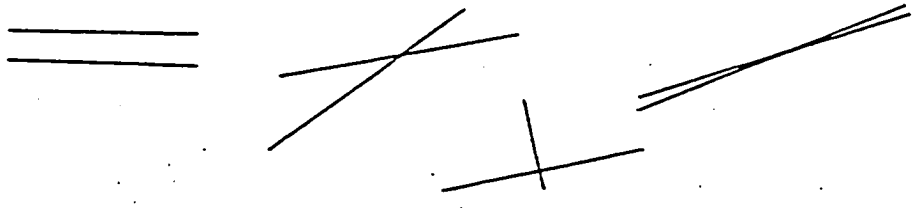
Reproduced with permission of the copyright owner. Further reproduction prohibited without permission.

FIGURE 5--COUNTING GUIDELINES USED IN DETERMINING ASBESTOS STRUCTURES

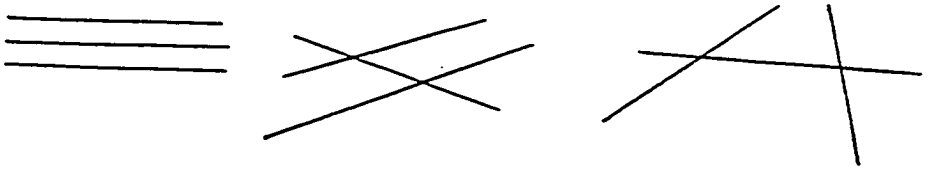
Count as 1 fiber; 1 Structure; no intersections.



Count as 2 fibers if space between fibers is greater than width of 1 fiber diameter or number of intersections is equal to or less than 1.



Count as 3 structures if space between fibers is greater than width of 1 fiber diameter or if the number of intersections is equal to or less than 2.

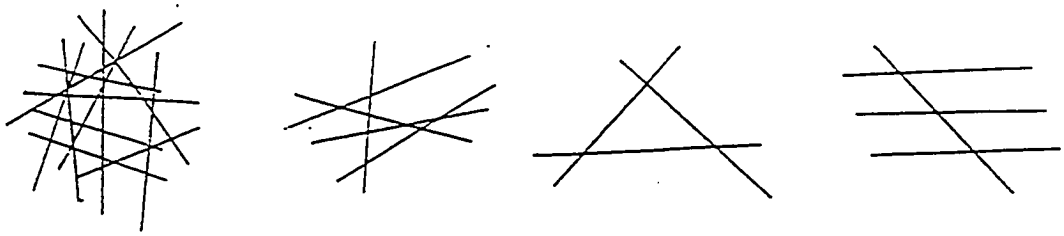


Count bundles as 1 structure; 3 or more parallel fibrils less than 1 fiber diameter separation.

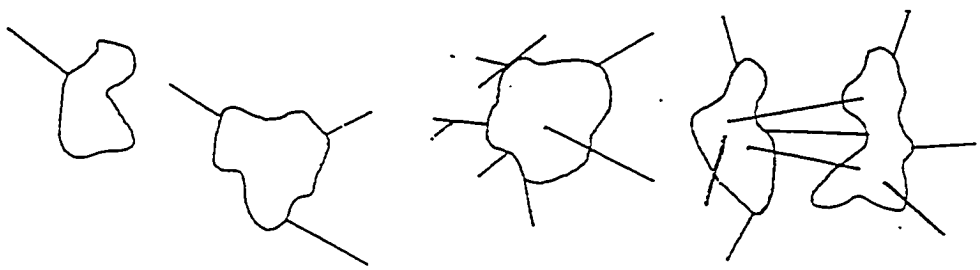


Reproduced with permission of the copyright owner. Further reproduction prohibited without permission.

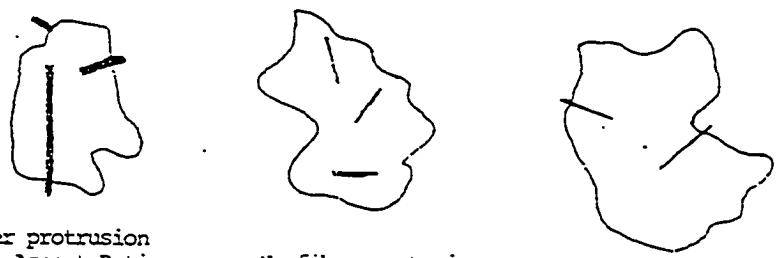
Count clusters as 1 structure; fibers having greater than or equal to 3 intersections.



Count matrix as 1 structure.



DO NOT COUNT AS STRUCTURES:



Fiber protrusion <5:1 Aspect Ratio

No fiber protusion

Fiber protrusion <0.5 micrometer

—— <0.5 micrometer in length
— <5:1 Aspect Ratio

BILLING CODE 6560-50-C

Reproduced with permission of the copyright owner. Further reproduction prohibited without permission.

SOIL ASBESTOS ANALYSIS BY TRANSMISSION ELECTRON MICROSCOPY (TEM)
EPA Level I Method (Yamate et al.; 1984)

MED-TOX ASSOCIATES INC.

EVIRE-FRICKE
629 OAKLAND AVE.
OAKLAND, CA 94511-4567
415-652-4500

Job Number : 6266-1
Client Number : AF1-10.0
Med-Tox Number: 67259
Receipt Date : DECEMBER 15, 1987
Report Date : JANUARY 25, 1988
Description :

FIELD OF VIEW METHOD

Analytical Sensitivity : 63.525 (bill.structures/g)
Total Area Scanned : 112 sq um
Magnification : 19400 x
Area of Original Filter : 2.01 sq cm
Dilution Factor : 0.0012
Area Ashed : <not ashed>
Area of Membrane : <not ashed>
Mass of Soil : 0.0227 g
Total number of structs : 31
Filter type : 0.1 um, polycarbonate

ASBESTOS SUMMARY

	All Structures	All > 5 um Structures
Total Asbestos Structure Concentration	1969.3 (bill.structures/g)	< 254.1 (bill.structures/g)
Total Asbestos Mass Concentration	26073.9 (ug/g)	ND (ug/g)

Additional Information by Structure Type

	Fiber	Bundle	Clump	Matrix	TOTAL
Structure Conc. (bill.structures/g)					
Chrysotile	1778.707	127.050	---	63.525	1969.283
Amphibole	---	---	---	---	---
Indeterminant	---	---	---	---	---
Mass Concentration (ug/g)					
Chrysotile	21403.9	2075.5	---	2594.4	26073.9
Amphibole	---	---	---	---	---
Indeterminant	---	---	---	---	---

- The structure concentration detection limit is 4 times the analytical sensitivity. Analytical sensitivity is defined by the EPA as the asbestos concentration represented by each fiber counter under the electron microscope.
- ND indicates insufficient structures detected to calculate mass concentration.
- TEM data is accurate to no more than one significant figure.
- bill.structures/g = billion structures per gram; ug/g = micrograms per gram or parts per million.
- Amphibole asbestos includes amosite (i.e. grunerite - cummingtonite), crocidolite (i.e. riebeckite - magnesioriebeckite), anthophyllite, tremolite and actinolite.

Analyst _____ Date 8/1/87

Lab Manager _____ Date 8/1/87

Reproduced with permission of the copyright owner. Further reproduction prohibited without permission.

SOIL ASBESTOS ANALYSIS BY TRANSMISSION ELECTRON MICROSCOPY (TEM) - DIMENSIONAL DATA
EPA Level I Method (Yamate et al.; 1984)

MED-TOX ASSOCIATES INC

LEVINE-FRICKE
629 OAKLAND AVE.
OAKLAND, CA 94511-4567
415-652-4500

Job Number : 6266-1
Client Number : AF1-10.0
Med-Tox Number: 67259

		Chrysotile	Amphibole	Indeterminant	Nonasbestos
Detailed Data For Structures Classified as FIBERS:					
Total Number of Structures Counted		28	0	0	0
Length	geometric mean	0.8008	0.0000	0.0000	0.0000
	standard deviation	1.2109	0.0000	0.0000	0.0000
Diameter	geometric mean	0.0595	0.0000	0.0000	0.0000
	standard deviation	0.0223	0.0000	0.0000	0.0000
Detailed Data For Structures Classified as BUNDLES:					
Total Number of Structures Counted		2	0	0	0
Length	geometric mean	1.0583	0.0000	0.0000	0.0000
	standard deviation	0.4283	0.0000	0.0000	0.0000
Diameter	geometric mean	0.0707	0.0000	0.0000	0.0000
	standard deviation	0.0359	0.0000	0.0000	0.0000
Detailed Data For Structures Classified as CLUMPS:					
No Structures Detected in This Category.					
Detailed Data For Structures Classified as MATRICES:					
Total Number of Structures Counted		1	0	0	0
Length	geometric mean	1.0000	0.0000	0.0000	0.0000
	standard deviation	0.0000	0.0000	0.0000	0.0000
Diameter	geometric mean	0.1000	0.0000	0.0000	0.0000
	standard deviation	0.0000	0.0000	0.0000	0.0000
DETAILED DATA FOR ALL STRUCTURES:					
Total Number of Structures Counted		31	0	0	0
Length	geometric mean	0.8212	0.0000	0.0000	0.0000
	standard deviation	1.1508	0.0000	0.0000	0.0000
Diameter	geometric mean	0.0611	0.0000	0.0000	0.0000
	standard deviation	0.0222	0.0000	0.0000	0.0000

Med-Tox Associates, Inc. 1229 Morena Blvd San Diego, CA 92110 619-276-8843

Reproduced with permission of the copyright owner. Further reproduction prohibited without permission.

SOIL ASBESTOS ANALYSIS BY TRANSMISSION ELECTRON MICROSCOPY (TEM) - DATA LISTING
EPA Level I Method (Yamate et al.; 1984)

MED-TOX ASSOCIATES INC.

EVINE-FRICKE
629 OAKLAND AVE.
OAKLAND, CA 94511-4567
415-652-4500

Job Number : 6266-1
Client Number : AF1-10.0
Med-Tox Number: 67259

Field No.	Structure No. per Field	Structure Type	Diameter (microns)	Length (microns)	Mass per Structure (pg)	Fibers per Structure	Structure Identification
1	1	fiber	0.05	0.80	0.004	1	chrysotile
2	1	fiber	0.10	1.00	0.020	1	chrysotile
3	1	fiber	0.05	0.60	0.003	1	chrysotile
3	2	fiber	0.05	0.60	0.003	1	chrysotile
4	1	fiber	0.05	0.60	0.003	1	chrysotile
4	2	fiber	0.05	0.80	0.004	1	chrysotile
5	1	fiber	0.05	0.60	0.003	1	chrysotile
5	2	fiber	0.05	0.60	0.003	1	chrysotile
5	3	matrix	0.10	1.00	0.041	2	chrysotile
6	1	fiber	0.10	0.80	0.016	1	chrysotile
7	1	fiber	0.05	1.00	0.005	1	chrysotile
7	2	fiber	0.05	1.20	0.006	1	chrysotile
8	1	fiber	0.05	0.60	0.003	1	chrysotile
8	2	fiber	0.05	0.80	0.004	1	chrysotile
9	1	bundle	0.10	1.40	0.029	15	chrysotile
11	1	fiber	0.05	0.60	0.003	1	chrysotile
11	2	fiber	0.05	0.60	0.003	1	chrysotile
12	1	fiber	0.05	0.80	0.004	1	chrysotile
12	2	fiber	0.05	0.60	0.003	1	chrysotile
13	1	bundle	0.05	0.80	0.004	5	chrysotile
14	1	fiber	0.10	1.20	0.025	1	chrysotile
15	1	fiber	0.10	0.60	0.012	1	chrysotile
16	1	fiber	0.10	7.00	0.143	1	chrysotile
16	2	fiber	0.05	0.60	0.003	1	chrysotile
17	1	fiber	0.05	0.60	0.003	1	chrysotile
17	2	fiber	0.05	0.80	0.004	1	chrysotile
18	1	fiber	0.05	0.60	0.003	1	chrysotile
20	1	fiber	0.10	1.00	0.020	1	chrysotile
20	2	fiber	0.10	1.20	0.025	1	chrysotile
21	1	fiber	0.05	0.60	0.003	1	chrysotile
21	2	fiber	0.05	0.80	0.004	1	chrysotile

- um = micron, a micron is one millionth of a meter.
- ug = microgram, a microgram is one millionth of a gram.
- pg = picogram, a picogram is one millionth of a microgram.
- Masses of indeterminate and non-asbestos fibers are estimated by assuming a density of 2.6 grams per cubic centimeter.

Med-Tox Associates, Inc. 1229 Morena Blvd San Diego, CA 92110 619-276-8843

Reproduced with permission of the copyright owner. Further reproduction prohibited without permission.

SOIL ASBESTOS ANALYSIS BY TRANSMISSION ELECTRON MICROSCOPY (TEM)
EPA Level I Method (Yamate et al.; 1984)

MED-TOX ASSOCIATES INC.

LEVINE-FRICKE
1900 POWELL ST., 12TH FLOOR
EMERYVILLE, CA 94608
JOHN DEREAMER 415-652-4500

Job Number : 7L-6401-9
Client Number : OC-25
Med-Tox Number: 73604
Receipt Date : APRIL 12, 1988
Report Date : APRIL 28, 1988
Description :

FIELD OF VIEW METHOD

Analytical Sensitivity : 131.792 (bill.structures/g)
Total Area Scanned : 62 sq um
Magnification : 20000 x
Area of Original Filter : 2.01 sq cm
Dilution Factor : 0.0012
Area Ashed : <not ashed>
Area of Membrane : <not ashed>
Mass of Soil : 0.0196 g
Total number of structs : 29
Filter type : 0.1 um, polycarbonate

ASBESTOS SUMMARY

	All Structures	All > 5 um Structures
Total Asbestos Structure Concentration	3822.0 (bill.structures/g)	< 527.2 (bill.structures/g)
Total Asbestos Mass Concentration	1640181.6 (ug/g)	ND (ug/g)

Additional Information by Structure Type

	Fiber	Bundle	Clump	Matrix	TOTAL
Structure Conc. (bill.structures/g)					
Chrysotile	131.792	3690.189	---	---	3821.982
Amphibole	---	---	---	---	---
Indeterminant	---	---	---	---	---
Mass Concentration (ug/g)					
Chrysotile	6189.9	1633991.7	---	---	1640181.6
Amphibole	---	---	---	---	---
Indeterminant	---	---	---	---	---

- The structure concentration detection limit is 4 times the analytical sensitivity. Analytical sensitivity is defined by the EPA as the asbestos concentration represented by each fiber counter under the electron microscope. ND indicates insufficient structures detected to calculate mass concentration.
- TEM data is accurate to no more than one significant figure.
- bill.structures/g = billion structures per gram; ug/g = micrograms per gram or parts per million.
- Amphibole asbestos includes amosite (i.e. grunerite - cummingtonite), crocidolite (i.e. riebeckite - magnesioriebeckite), anthophyllite, tremolite and actinolite.

Analyst _____ Date 5/1/88

Lab Manager _____ Date 5/1/88

AUG 16

Med-Tox Associates, Inc. 1229 Morena Blvd San Diego, CA 92110 619-276-8843

Reproduced with permission of the copyright owner. Further reproduction prohibited without permission.

SOIL ASBESTOS ANALYSIS BY TRANSMISSION ELECTRON MICROSCOPY (TEM) - DIMENSIONAL DATA
EPA Level I Method (Yamate et al.; 1984)

MED-TOX ASSOCIATES INC.

LEVINE-FRICKE
1900 POWELL ST., 12TH FLOOR
EMERYVILLE, CA 94608
JOHN DEREAMER 415-652-4500

Job Number : 7L-6401-9
Client Number : OC-25
Med-Tox Number: 73604

		Chrysotile	Amphibole	Indeterminant	Nonasbestos
Detailed Data For Structures Classified as FIBERS:					
Total Number of Structures Counted		1	0	0	0
Length	geometric mean	2.3000	0.0000	0.0000	0.0000
	standard deviation	0.0000	0.0000	0.0000	0.0000
Diameter	geometric mean	0.1000	0.0000	0.0000	0.0000
	standard deviation	0.0000	0.0000	0.0000	0.0000
Detailed Data For Structures Classified as BUNDLES:					
Total Number of Structures Counted		28	0	0	0
Length	geometric mean	1.5397	0.0000	0.0000	0.0000
	standard deviation	0.4940	0.0000	0.0000	0.0000
Diameter	geometric mean	0.2651	0.0000	0.0000	0.0000
	standard deviation	0.1716	0.0000	0.0000	0.0000

Detailed Data For Structures Classified as CLUMPS:

No Structures Detected in This Category.

Detailed Data For Structures Classified as MATRICES:

No Structures Detected in This Category.

DETAILED DATA FOR ALL STRUCTURES:

Total Number of Structures Counted		29	0	0	0
Length	geometric mean	1.5612	0.0000	0.0000	0.0000
	standard deviation	0.4823	0.0000	0.0000	0.0000
Diameter	geometric mean	0.2563	0.0000	0.0000	0.0000
	standard deviation	0.1706	0.0000	0.0000	0.0000

Med-Tox Associates, Inc. 1229 Morena Blvd San Diego, CA 92110 619-276-8843

Reproduced with permission of the copyright owner. Further reproduction prohibited without permission.

SOIL ASBESTOS ANALYSIS BY TRANSMISSION ELECTRON MICROSCOPY (TEM) - DATA LISTING
EPA Level I Method (Yamate et al.; 1984)

MED-TOX ASSOCIATES, INC.

LEVINE-FRICKE
1900 POWELL ST., 12TH FLOOR
EMERYVILLE, CA 94608
JOHN DEREAMER 415-652-4500

Job Number : 7L-6401-9
Client Number : OC-25
Med-Tox Number: 73604

Field No.	Structure No. per Field	Structure Type	Diameter (microns)	Length (microns)	Mass per Structure (pg)	Fibers per Structure	Structure Identification
1	1	bundle	0.20	2.30	0.188	3	chrysotile
2	1	bundle	0.15	1.00	0.046	3	chrysotile
3	1	bundle	0.40	1.40	0.457	15	chrysotile
3	2	bundle	0.15	1.60	0.074	3	chrysotile
3	3	bundle	0.60	2.30	1.691	15	chrysotile
3	4	bundle	0.20	1.00	0.082	10	chrysotile
4	1	bundle	0.80	2.30	3.006	15	chrysotile
6	1	bundle	0.20	2.00	0.163	5	chrysotile
6	2	bundle	0.40	1.00	0.327	15	chrysotile
6	3	bundle	0.30	1.20	0.221	6	chrysotile
7	1	bundle	0.50	2.20	1.123	15	chrysotile
9	1	bundle	0.40	2.30	0.751	5	chrysotile
9	2	bundle	0.20	2.00	0.163	10	chrysotile
10	1	bundle	0.15	1.20	0.055	5	chrysotile
11	1	bundle	0.20	2.00	0.163	5	chrysotile
12	1	bundle	0.20	1.00	0.082	5	chrysotile
12	2	bundle	0.20	1.60	0.131	5	chrysotile
12	3	bundle	0.50	1.00	0.511	10	chrysotile
13	1	bundle	0.50	1.80	0.919	10	chrysotile
13	2	bundle	0.10	2.00	0.041	3	chrysotile
13	3	bundle	0.20	1.20	0.098	5	chrysotile
14	1	bundle	0.30	2.00	0.368	10	chrysotile
14	2	bundle	0.20	1.40	0.114	5	chrysotile
14	3	bundle	0.30	1.60	0.294	5	chrysotile
14	4	bundle	0.20	1.00	0.082	5	chrysotile
14	5	bundle	0.20	1.00	0.082	5	chrysotile
15	1	bundle	0.50	2.00	1.021	15	chrysotile
15	2	fiber	0.10	2.30	0.047	1	chrysotile
15	3	bundle	0.20	1.80	0.147	3	chrysotile

- um = micron, a micron is one millionth of a meter.
- ug = microgram, a microgram is one millionth of a gram.
- pg = picogram, a picogram is one millionth of a microgram.
- Masses of indeterminate and non-asbestos fibers are estimated by assuming a density of 2.6 grams per cubic centimeter.

Med-Tox Associates, Inc. 1229 Morena Blvd San Diego, CA 92110 619-276-8843

Reproduced with permission of the copyright owner. Further reproduction prohibited without permission.

SOIL ASBESTOS ANALYSIS BY TRANSMISSION ELECTRON MICROSCOPY (TEM)
EPA Level I Method (Yamate et al.; 1984)

MED-TOX ASSOCIATES INC

LEVINE-FRICKE
1900 POWELL ST., 12TH FLOOR
EMERYVILLE, CA 94608
JOHN DEREAMER 415-652-4500

Job Number : 7L-6401-9
Client Number : OC-27
Med-Tox Number: 73602
Receipt Date : APRIL 12, 1988
Report Date : APRIL 28, 1988
Description :

FIELD OF VIEW METHOD

Analytical Sensitivity : 120.707 (bill.structures/g)
Total Area Scanned : 62 sq um
Magnification : 20000 x
Area of Original Filter : 2.01 sq cm
Dilution Factor : 0.0012
Area Ashed : <not ashed>
Area of Membrane : <not ashed>
Mass of Soil : 0.0214 g
Total number of structs : 31
Filter type : 0.1 um, polycarbonate

ASBESTOS SUMMARY

	All Structures	All > 5 um Structures
Total Asbestos Structure Concentration	3741.9 (bill.structures/g)	< 482.8 (bill.structures/g)
Total Asbestos Mass Concentration	1653196.3 (ug/g)	ND (ug/g)

Additional Information by Structure Type

	Fiber	Bundle	Clump	Matrix	TOTAL
Structure Conc. (bill.structures/g)					
Chrysotile	603.536	3138.385	---	---	3741.921
Amphibole	---	---	---	---	---
Indeterminant	---	---	---	---	---
Mass Concentration (ug/g)					
Chrysotile	27113.7	1626082.6	---	---	1653196.3
Amphibole	---	---	---	---	---
Indeterminant	---	---	---	---	---

- The structure concentration detection limit is 4 times the analytical sensitivity. Analytical sensitivity is defined by the EPA as the asbestos concentration represented by each fiber counter under the electron microscope.
  ND indicates insufficient structures detected to calculate mass concentration.
- TEM data is accurate to no more than one significant figure.
- bill.structures/g = billion structures per gram; ug/g = micrograms per gram or parts per million.
- Amphibole asbestos includes amosite (i.e. grunerite - cummingtonite), crocidolite (i.e. riebeckite - magnesioriebeckite), anthophyllite, tremolite and actinolite.

Analyst _____ Date 4/21/88

Lab Manager _____ Date 4/21/88

RECEIVED
APR 15

Med-Tox Associates, Inc. 1229 Morena Blvd San Diego, CA 92110 619-276-8843

Reproduced with permission of the copyright owner. Further reproduction prohibited without permission.

SOIL ASBESTOS ANALYSIS BY TRANSMISSION ELECTRON MICROSCOPY (TEM) - DIMENSIONAL DATA
EPA Level I Method (Yamate et al.; 1984)

MED-TOX ASSOCIATES INC

LEVINE-FRICKE
1900 POWELL ST., 12TH FLOOR
EMERYVILLE, CA 94608
JOHN DEREAMER 415-652-4500

Job Number : 7L-6401-9
Client Number : OC-27
Med-Tox Number: 73602

		Chrysotile	Amphibole	Indeterminant	Nonasbestos
Detailed Data For Structures Classified as FIBERS:					
Total Number of Structures Counted		5	0	0	0
Length	geometric mean	1.4333	0.0000	0.0000	0.0000
	standard deviation	0.4180	0.0000	0.0000	0.0000
Diameter	geometric mean	0.1149	0.0000	0.0000	0.0000
	standard deviation	0.0451	0.0000	0.0000	0.0000
Detailed Data For Structures Classified as BUNDLES:					
Total Number of Structures Counted		26	0	0	0
Length	geometric mean	1.4483	0.0000	0.0000	0.0000
	standard deviation	0.4521	0.0000	0.0000	0.0000
Diameter	geometric mean	0.3599	0.0000	0.0000	0.0000
	standard deviation	0.1402	0.0000	0.0000	0.0000

Detailed Data For Structures Classified as CLUMPS:

No Structures Detected in This Category.

Detailed Data For Structures Classified as MATRICES:

No Structures Detected in This Category.

DETAILED DATA FOR ALL STRUCTURES:					
Total Number of Structures Counted		31	0	0	0
Length	geometric mean	1.4459	0.0000	0.0000	0.0000
	standard deviation	0.4401	0.0000	0.0000	0.0000
Diameter	geometric mean	0.2994	0.0000	0.0000	0.0000
	standard deviation	0.1655	0.0000	0.0000	0.0000

Med-Tox Associates, Inc. 1229 Morena Blvd San Diego, CA 92110 619-276-8843

Reproduced with permission of the copyright owner. Further reproduction prohibited without permission.

SOIL ASBESTOS ANALYSIS BY TRANSMISSION ELECTRON MICROSCOPY (TEM) - DATA LISTING
EPA Level I Method (Yamate et al.; 1984)

MED-TOX ASSOCIATES INC.

LEVINE-FRICKE
1900 POWELL ST., 12TH FLOOR
EMERYVILLE, CA 94608
JOHN DEREAMER 415-652-4500

Job Number : 7L-6401-9
Client Number : OC-27
Med-Tox Number: 73602

Field No.	Structure No. per Field	Structure Type	Diameter (microns)	Length (microns)	Mass per Structure (pg)	Fibers per Structure	Structure Identification
1	1	bundle	0.30	2.30	0.423	10	chrysotile
2	1	bundle	0.20	1.40	0.114	5	chrysotile
2	2	fiber	0.10	1.00	0.020	1	chrysotile
3	1	fiber	0.10	1.40	0.029	1	chrysotile
3	2	bundle	0.20	2.00	0.163	5	chrysotile
5	1	bundle	0.70	2.30	2.301	25	chrysotile
5	2	bundle	0.50	1.20	0.613	10	chrysotile
5	3	fiber	0.20	1.20	0.098	1	chrysotile
5	4	bundle	0.50	1.40	0.715	10	chrysotile
6	1	bundle	0.30	1.20	0.221	5	chrysotile
7	1	bundle	0.40	2.30	0.751	10	chrysotile
7	2	bundle	0.30	1.00	0.184	5	chrysotile
7	3	bundle	0.40	1.00	0.327	10	chrysotile
9	1	bundle	0.30	1.80	0.331	10	chrysotile
9	2	bundle	0.40	1.00	0.327	10	chrysotile
9	3	bundle	0.40	1.40	0.457	5	chrysotile
10	1	bundle	0.50	2.30	1.174	15	chrysotile
11	1	bundle	0.40	1.40	0.457	5	chrysotile
11	2	bundle	0.30	1.60	0.294	10	chrysotile
12	1	bundle	0.20	1.40	0.114	15	chrysotile
12	2	bundle	0.30	1.40	0.257	5	chrysotile
12	3	bundle	0.30	1.00	0.184	10	chrysotile
12	4	fiber	0.10	1.80	0.037	1	chrysotile
14	1	bundle	0.40	2.00	0.653	5	chrysotile
14	2	bundle	0.30	1.20	0.221	10	chrysotile
14	3	bundle	0.30	1.00	0.184	10	chrysotile
14	4	bundle	0.40	1.80	0.588	5	chrysotile
14	5	bundle	0.80	1.20	1.568	15	chrysotile
15	1	bundle	0.40	1.40	0.457	5	chrysotile
15	2	bundle	0.40	1.20	0.392	10	chrysotile
15	3	fiber	0.10	2.00	0.041	1	chrysotile

- um = micron, a micron is one millionth of a meter.
- ug = microgram, a microgram is one millionth of a gram.
- pg = picogram, a picogram is one millionth of a microgram.
- Masses of indeterminate and non-asbestos fibers are estimated by assuming a density of 2.6 grams per cubic centimeter.

Med-Tox Associates, Inc. 1229 Morena Blvd San Diego, CA 92110 619-276-8843

Reproduced with permission of the copyright owner. Further reproduction prohibited without permission.

SOIL ASBESTOS ANALYSIS BY TRANSMISSION ELECTRON MICROSCOPY (TEM)
EPA Level I Method (Yamate et al; 1984)

MED-TOX ASSOCIATES, INC

LEVINE-FRICKE
1900 POWELL ST., 12TH FLOOR
EMERYVILLE, CA 94608
JOHN DEREAMER 415-652-4500

Job Number : 7L-6401-8
Client Number : OC-28
Med-Tox Number: 73365
Receipt Date : APRIL 7, 1988
Report Date : MAY 3, 1988
Description :

FIELD OF VIEW METHOD

Analytical Sensitivity : 14.023 (bill.structures/g)
Total Area Scanned : 597 sq um
Magnification : 20000 x
Area of Original Filter : 2.01 sq cm
Dilution Factor : 0.0012
Area Ashed : <not ashed>
Area of Membrane : <not ashed>
Mass of Soil : 0.0192 g
Total number of structs : 30
Filter type : 0.1 um, polcarbonate

ASBESTOS SUMMARY

	All Structures	All > 5 um Structures
Total Asbestos Structure Concentration	420.7 (bill.structures/g)	< 56.1 (bill.structures/g)
Total Asbestos Mass Concentration	157607.8 (ug/g)	ND (ug/g)

Additional Information by Structure Type

Structure Conc. (bill.structures/g)	Fiber	Bundle	Clump	Matrix	TOTAL
Chrysotile	84.137	308.502	28.046	---	420.685
Amphibole	---	---	---	---	---
Indeterminant	---	---	---	---	---
Mass Concentration (ug/g)					
Chrysotile	4123.5	145967.6	7516.7	---	157607.8
Amphibole	---	---	---	---	---
Indeterminant	---	---	---	---	---

- The structure concentration detection limit is 4 times the analytical sensitivity. Analytical sensitivity is defined by the EPA as the asbestos concentration represented by each fiber counter under the electron microscope. ND indicates insufficient structures detected to calculate mass concentration.
- TEM data is accurate to no more than one significant figure.
- bill.structures/g = billion structures per gram; ug/g = micrograms per gram or parts per million.
- Amphibole asbestos includes amosite (i.e. grunerite - cummingtonite), crocidolite (i.e. riebeckite - magnesioriebeckite), anthophyllite, tremolite and actinolite.

Analyst _____ Date 8/1/88

Lab Manager _____ Date 8/1/88

Received AUG 16

Reproduced with permission of the copyright owner. Further reproduction prohibited without permission.

SOIL ASBESTOS ANALYSIS BY TRANSMISSION ELECTRON MICROSCOPY (TEM) - DIMENSIONAL DATA
EPA Level I Method (Yamate et al; 1984)

MED-TOX ASSOCIATES INC

LEVINE-FRICKE
1900 POWELL ST., 12TH FLOOR
EMERYVILLE, CA 94608
JOHN DEREAMER 415-652-4500

Job Number : 7L-6401-8
Client Number : OC-28
Med-Tox Number: 73365

		Chrysotile	Amphibole	Indeterminant	Nonasbestos
Detailed Data For Structures Classified as FIBERS:					
Total Number of Structures Counted		6	0	0	0
Length	geometric mean	2.2372	0.0000	0.0000	0.0000
	standard deviation	0.9032	0.0000	0.0000	0.0000
Diameter	geometric mean	0.1000	0.0000	0.0000	0.0000
	standard deviation	0.0000	0.0000	0.0000	0.0000
Detailed Data For Structures Classified as BUNDLES:					
Total Number of Structures Counted		22	0	0	0
Length	geometric mean	2.7237	0.0000	0.0000	0.0000
	standard deviation	1.3739	0.0000	0.0000	0.0000
Diameter	geometric mean	0.2582	0.0000	0.0000	0.0000
	standard deviation	0.0648	0.0000	0.0000	0.0000
Detailed Data For Structures Classified as CLUMPS:					
Total Number of Structures Counted		2	0	0	0
Length	geometric mean	1.5811	0.0000	0.0000	0.0000
	standard deviation	1.0872	0.0000	0.0000	0.0000
Diameter	geometric mean	0.0707	0.0000	0.0000	0.0000
	standard deviation	0.0359	0.0000	0.0000	0.0000

Detailed Data For Structures Classified as MATRICES:

No Structures Detected in This Category.

DETAILED DATA FOR ALL STRUCTURES:					
Total Number of Structures Counted		30	0	0	0
Length	geometric mean	2.5254	0.0000	0.0000	0.0000
	standard deviation	1.3075	0.0000	0.0000	0.0000
Diameter	geometric mean	0.1959	0.0000	0.0000	0.0000
	standard deviation	0.0983	0.0000	0.0000	0.0000

Reproduced with permission of the copyright owner. Further reproduction prohibited without permission.

SOIL ASBESTOS ANALYSIS BY TRANSMISSION ELECTRON MICROSCOPY (TEM) - DATA LISTING
EPA Level I Method (Yamate et al; 1984)

MED-TOX ASSOCIATES, INC.

LEVINE-FRICKE
1900 POWELL ST., 12TH FLOOR
EMERYVILLE, CA 94608
JOHN DEREAMER 415-652-4500

Job Number : 7L-6401-8
Client Number : OC-28
Med-Tox Number: 73365

Field No.	Structure No. per Field	Structure Type	Diameter (microns)	Length (microns)	Mass per Structure (pg)	Fibers per Structure	Structure Identification
1	1	bundle	0.30	5.40	0.992	15	chrysotile
3	1	fiber	0.10	1.20	0.025	1	chrysotile
4	1	bundle	0.20	5.20	0.425	10	chrysotile
4	2	clump	0.05	1.00	0.026	5	chrysotile
5	1	bundle	0.25	3.80	0.485	5	chrysotile
6	1	fiber	0.10	1.40	0.029	1	chrysotile
6	2	bundle	0.30	1.20	0.221	10	chrysotile
7	1	bundle	0.15	4.00	0.184	5	chrysotile
7	2	bundle	0.15	2.20	0.101	5	chrysotile
8	1	bundle	0.20	1.00	0.082	5	chrysotile
8	2	bundle	0.25	4.00	0.511	10	chrysotile
9	1	bundle	0.25	3.20	0.408	10	chrysotile
9	2	bundle	0.30	1.40	0.257	15	chrysotile
9	3	bundle	0.30	1.40	0.257	15	chrysotile
9	4	fiber	0.10	2.80	0.057	1	chrysotile
10	1	bundle	0.30	4.00	0.735	15	chrysotile
11	1	bundle	0.40	4.80	1.568	10	chrysotile
11	2	bundle	0.30	2.20	0.404	5	chrysotile
12	1	fiber	0.10	2.80	0.057	1	chrysotile
12	2	fiber	0.10	3.40	0.069	1	chrysotile
13	1	bundle	0.25	4.40	0.562	3	chrysotile
13	2	fiber	0.10	2.80	0.057	1	chrysotile
14	1	bundle	0.20	2.00	0.163	5	chrysotile
14	2	bundle	0.30	1.80	0.331	10	chrysotile
14	3	bundle	0.25	3.40	0.434	10	chrysotile
15	1	clump	0.10	2.50	0.511	10	chrysotile
17	1	bundle	0.25	3.40	0.434	5	chrysotile
17	2	bundle	0.25	1.80	0.230	5	chrysotile
18	1	bundle	0.40	3.40	1.111	15	chrysotile
18	2	bundle	0.30	2.80	0.515	10	chrysotile

- um = micron, a micron is one millionth of a meter.
- ug = microgram, a microgram is one millionth of a gram.
  pg = picogram, a picogram is one millionth of a microgram.
- Masses of indeterminate and non-asbestos fibers are estimated by assuming a density of 2.6 grams per cubic centimeter.

Med-Tox Associates, Inc. 1229 Morena Blvd San Diego, CA 92110 619-276-8843

Reproduced with permission of the copyright owner. Further reproduction prohibited without permission.

Typical Particle Size Distribution Analysis Reports

Reproduced with permission of the copyright owner. Further reproduction prohibited without permission.

DELLAVALLE Laboratory, Inc.

Chemists and Consultants

1 W [illegible]ley, Suite 110 • Fresno, CA 93728 • (209) 233-6129

15 [illegible] Tulare Ave. • Tulare, CA 93274 • (209) 688-0608

File

REPORT OF ANALYSIS

Levine-Fricke #2932
1900 Powell Street, 12th Floor
Emeryville, CA 94608

Lab No. 68224
Sampled
Submitted 04/07/88
Submitted By
Reported 04/27/88
Office Fresno

Identification Soil

Ranch Coalinga Asbestos

Description	Sieve Size #	Sieve mm Opening	Hydrometer Reading Time	% Passing
OC - 10	4	4.75		66.9
Int. Wt. 245	8	2.36		60.9
	16	1.18		51.8
	30	0.60		40.3
	50	0.30		23.4
	100	0.150		9.8
	200	0.075		3.6
	pan	---		---
			1 min	3.5
			4 min	1.4
			19 min	1.1
			1 hr	0.9
			7 hr 15 min	0.5
			25 hr 45 min	0.2
OC - 10x	4	4.75		96
Int. Wt. 202.0	8	2.36		82.5
	16	1.18		50.7
	30	0.60		30.2
	50	0.30		14.6
	100	0.150		4.6
	200	0.075		1.6
	pan	---		---
			1 min	1.2
			4 min	0.6
			19 min	0.4
			1 hr	0.3
			7 hr 15 min	0.3
			25 hr 45 min	0.1

received
MAY 23 1988

Reproduced with permission of the copyright owner. Further reproduction prohibited without permission.

DELLAVALLE
Laboratory, Inc.
Chemists and Consultants
10 1 [illegible]ley, Suite 110 • Fresno, CA 93728 • (209) 233-6129
1. [illegible] Tulare Ave. • Tulare, CA 93274 • (209) 688-0608

REPORT OF ANALYSIS

Levine-Fricke #2932
1900 Powell Street, 12th Floor
Emeryville, CA 94608

Lab No. 68224
Sampled
Submitted 04/07/88
Submitted By
Reported 04/27/88
Office Fresno

Identification Soil

Ranch Coalinga Asbestos

Description	Sieve Size #	Sieve mm Opening	Hydrometer Reading Time	% Passing
OC - 11	4	4.75		65.2
Int. Wt. 352.8	8	2.36		52.6
	16	1.18		35.4
	30	0.60		20.2
	50	0.30		8.7
	100	0.150		3.7
	200	0.075		1.6
	pan	---		---
			1 min	1.5
			4 min	1.4
			19 min	1.2
			1 hr	0.9
			7 hr 15 min	0.9
			25 hr 45 min	0.4
OC - 14	4	4.75		100
Int. Wt. 183.7	8	2.36		99.3
	16	1.18		97.9
	30	0.60		95.1
	50	0.30		85.9
	100	0.150		55.3
	200	0.075		18.1
	pan	---		---
			1 min	12.9
			4 min	1.7
			19 min	1.3
			1 hr	0.8
			7 hr 15 min	0.7
			25 hr 45 min	0.8

Reproduced with permission of the copyright owner. Further reproduction prohibited without permission.

DELLAVALLE Laboratory, Inc.
Chemists and Consultants
1910 W. McKinley, Suite 110 • Fresno, CA 93728 • (209) 233-6129
1965 E. Tulare Ave • Tulare, CA 93274 • (209) 688-0608

REPORT OF ANALYSIS

Levine-Fricke #2932
1900 Powell Street, 12th Floor
Emeryville, CA 94608

Lab No. 68224
Sampled
Submitted 04/07/88
Submitted By
Reported 04/27/88
Office Fresno

Identification Soil

Ranch Coalinga Asbestos

No.	Description	Sieve Size #	Sieve mm Opening	Hydrometer Reading Time	% Passing
5.	OC - 15	4	4.75		74.4
	Int. Wt. 415	8	2.36		68.6
		16	1.18		59.6
		30	0.60		47.4
		50	0.30		31.4
		100	0.150		13
		200	0.075		4.4
		pan	---		---
				1 min	2.4
				4 min	0.6
				19 min	0.6
				1 hr	0.4
				7 hr 15 min	0.2
				25 hr 45 min	0.2
6.	OC - 17	4	4.75		80.1
	Int. Wt. 318.0	8	2.36		71.1
		16	1.18		53.5
		30	0.60		36.6
		50	0.30		19.9
		100	0.150		9.0
		200	0.075		3.2
		pan	---		---
				1 min	1.2
				4 min	0.8
				19 min	0.3
				1 hr	0.4
				7 hr 15 min	0.3
				25 hr 45 min	0.1

Reproduced with permission of the copyright owner. Further reproduction prohibited without permission.

DELLAVALLE
Laboratory, Inc.
Chemists and Consultants
10 Kinsley, Suite 110 • Fresno, CA 93728 • (209) 233-6129
Tulare Ave. • Tulare, CA 93274 • (209) 688-0608

REPORT OF ANALYSIS

Levine-Fricke #2932
1900 Powell Street, 12th Floor
Emeryville, CA 94608

Lab No. 68224
Sampled
Submitted 04/07/88
Submitted By
Reported 04/27/88
Office Fresno

Identification Soil

Ranch Coalinga Asbestos

Description	Sieve Size #	Sieve mm Opening	Hydrometer Reading Time	% Passing
OC - 22	4	4.75		62.0
Int. Wt. 429.3	8	2.36		47.6
	16	1.18		30.2
	30	0.60		18.3
	50	0.30		9.3
	100	0.150		4.8
	200	0.075		2.4
	pan	---		---
			1 min	2.1
			4 min	2.2
			19 min	1.2
			1 hr	1.3
			7 hr 15 min	1.0
			25 hr 45 min	0.6
OC - 24	4	4.75		79.8
Int. Wt. 192.8	8	2.36		60.8
	16	1.18		29.7
	30	0.60		14.6
	50	0.30		7.1
	100	0.150		3.6
	200	0.075		1.7
	pan	---		---
			1 min	1.1
			4 min	0.8
			19 min	0.5
			1 hr	0.2
			7 hr 15 min	0.0
			25 hr 45 min	0.2

Reproduced with permission of the copyright owner. Further reproduction prohibited without permission.

DELLAVALLE Laboratory, Inc.
Chemists and Consultants
1910 W. McKinley, Suite 110 • Fresno, CA 93728 • (209) 233-6129
1965 E. Tulare Ave. • Tulare, CA 93274 • (209) 688-0608

REPORT OF ANALYSIS

Levine-Fricke #2932
1900 Powell Street, 12th Floor
Emeryville, CA 94608

Lab No. 68224
Sampled
Submitted 04/07/88
Submitted By
Reported 04/27/88
Office Fresno

Identification Soil

Ranch Coalinga Asbestos

No.	Description	Sieve Size #	Sieve mm Opening	Hydrometer Reading Time	% Passing
9.	OC - 28	4	4.75		74.5
	Int. Wt. 199.8	8	2.36		66.5
		16	1.18		50.1
		30	0.60		31.9
		50	0.30		14.7
		100	0.150		5.8
		200	0.075		2.4
		pan	---		---
				1 min	2.0
				4 min	1.0
				19 min	0.0
				1 hr	0.3
				7 hr 15 min	0.0
				25 hr 45 min	0.3
10.	OC - 30	4	4.75		88.5
	Int. Wt. 238.0	8	2.36		81.7
		16	1.18		64.3
		30	0.60		42
		50	0.30		19.2
		100	0.150		7.7
		200	0.075		3.2
		pan	---		---
				1 min	3.2
				4 min	1.5
				19 min	0.6
				1 hr	0.9
				7 hr 15 min	0.0
				25 hr 45 min	0.3

Reproduced with permission of the copyright owner. Further reproduction prohibited without permission.

DELLAVALLE
Laboratory, Inc.
Chemists and Consultants
1011 Kinley, Suite 110 • Fresno, CA 93728 • (209) 233-6129
15... Tulare Ave. • Tulare, CA 93274 • (209) 688-0608

REPORT OF ANALYSIS

Levine-Fricke #2932
1900 Powell Street, 12th Floor
Emeryville, CA 94608

Lab No. 68224
Sampled
Submitted 04/07/88
Submitted By
Reported 04/27/88
Office Fresno

Identification Soil

Ranch Coalinga Asbestos

Description	Sieve Size #	Sieve mm Opening	Hydrometer Reading Time	% Passing
OC - 32	4	4.75		85.8
Int. Wt. 321.4	8	2.36		71.2
	16	1.18		51.6
	30	0.60		34.9
	50	0.30		18.9
	100	0.150		8.5
	200	0.075		3.3
	pan	---		---
			1 min	3.2
			4 min	1.9
			19 min	0.8
			1 hr	0.5
			7 hr 15 min	0.4
			25 hr 45 min	0.4
SS - 30	4	4.75		98.1
Int. Wt. 279.3	8	2.36		96.7
	16	1.18		95.6
	30	0.60		81.8
	50	0.30		44.1
	100	0.150		17.7
	200	0.075		5.6
	pan	---		---
			1 min	4.7
			4 min	1.7
			19 min	0.6
			1 hr	0.8
			7 hr 15 min	0.5
			25 hr 45 min	0.3

Sincerely,

Kathryn M. Graham
Systems & Methods Chemist

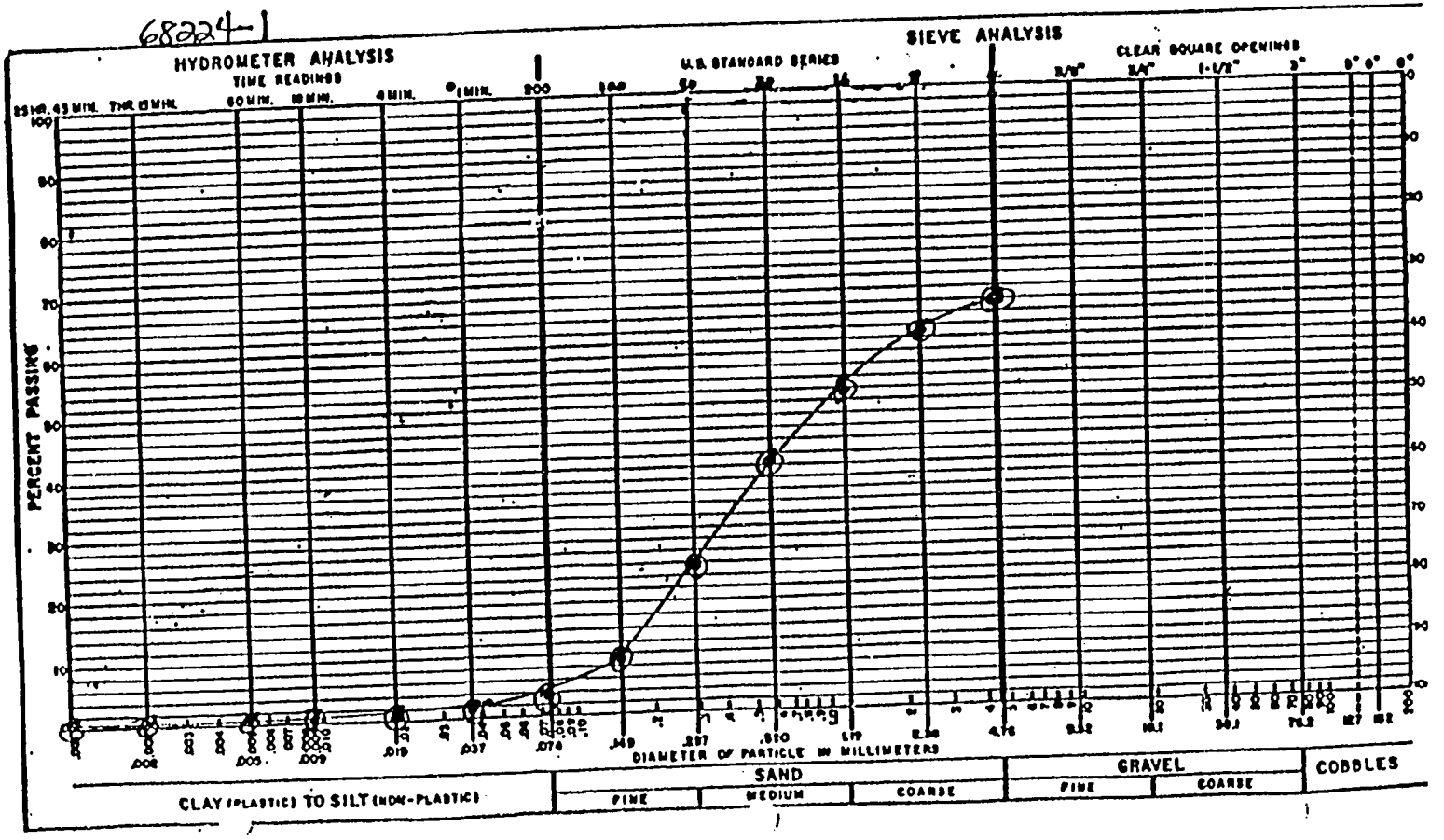
KMG:ae

Enclosures

Reproduced with permission of the copyright owner. Further reproduction prohibited without permission.

Reproduced with permission of the copyright owner. Further reproduction prohibited without permission.

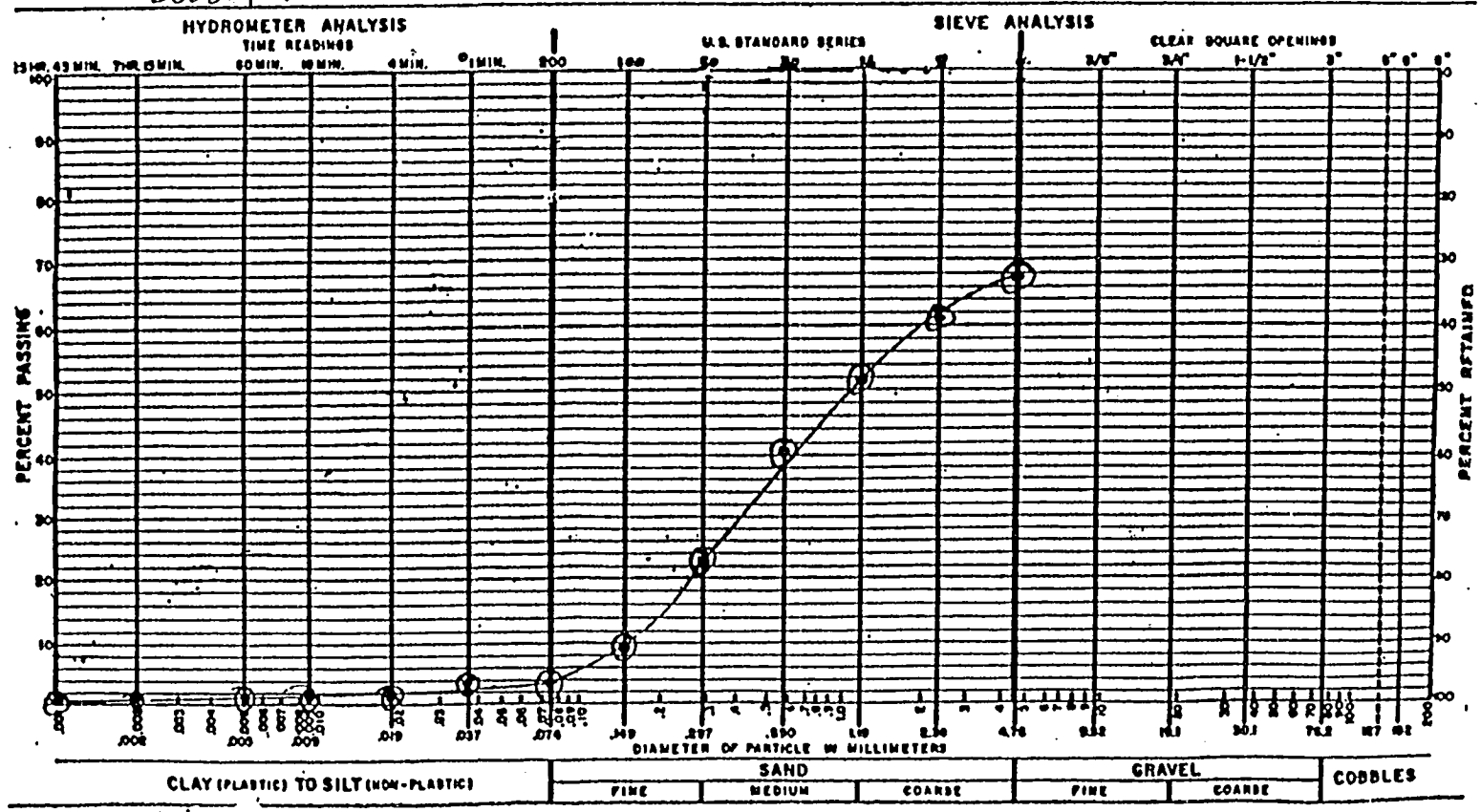
68224-1



OC-10

Reproduced with permission of the copyright owner. Further reproduction prohibited without permission.

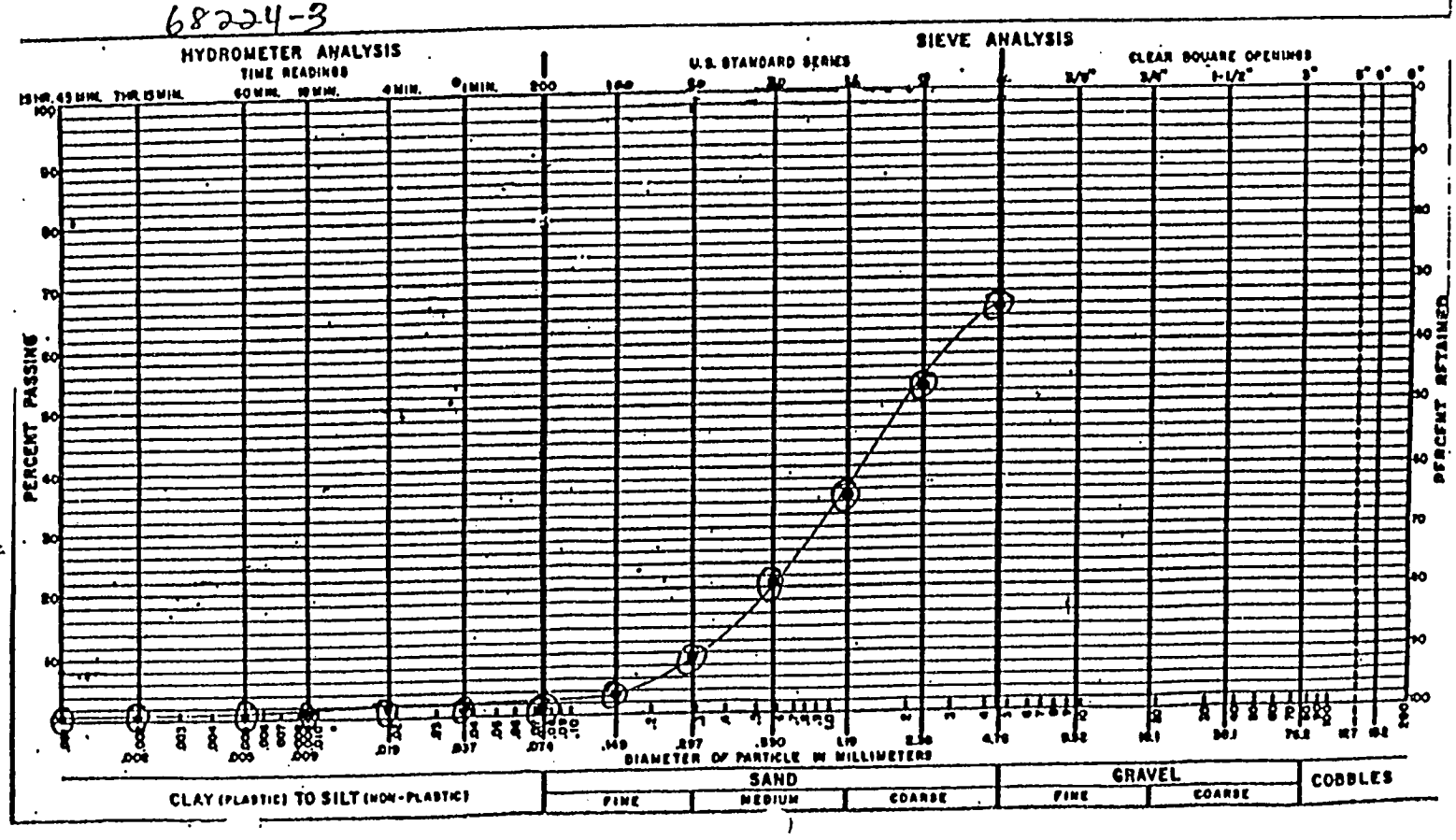
68224-2



OC-10X

Reproduced with permission of the copyright owner. Further reproduction prohibited without permission.

68224-3

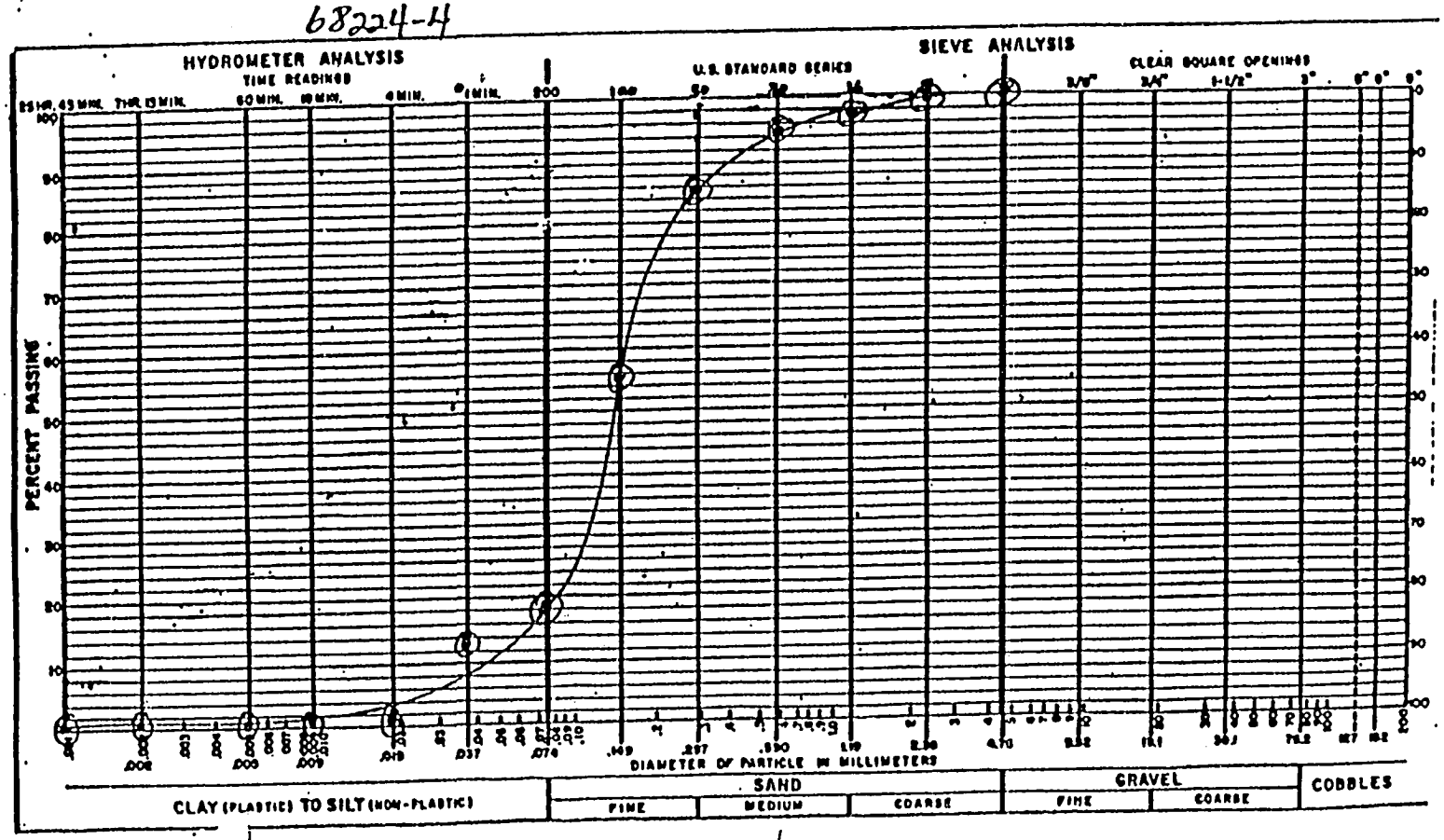


OC-11

6

Reproduced with permission of the copyright owner. Further reproduction prohibited without permission.

68224-4

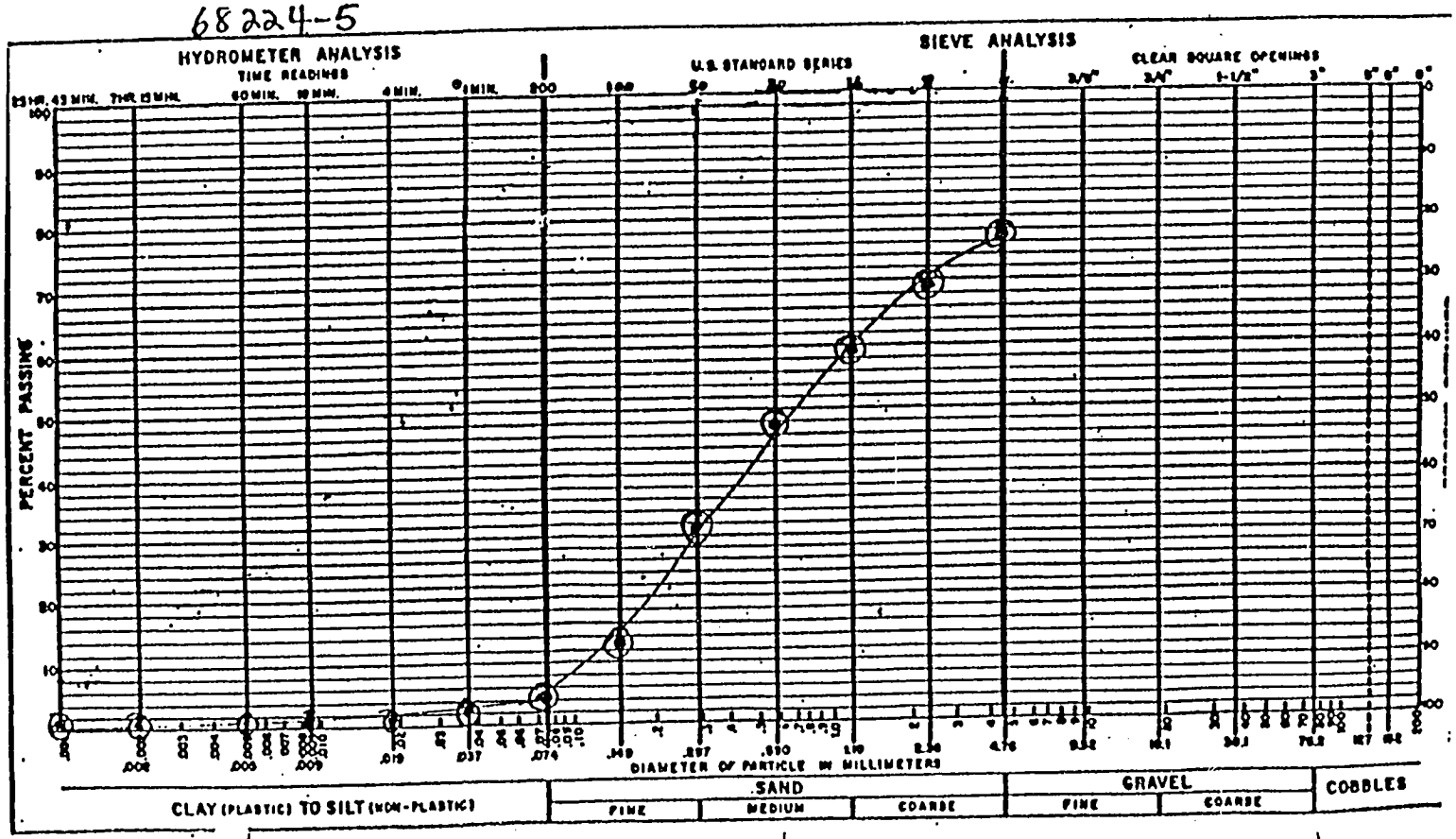


10

OC-14

Reproduced with permission of the copyright owner. Further reproduction prohibited without permission.

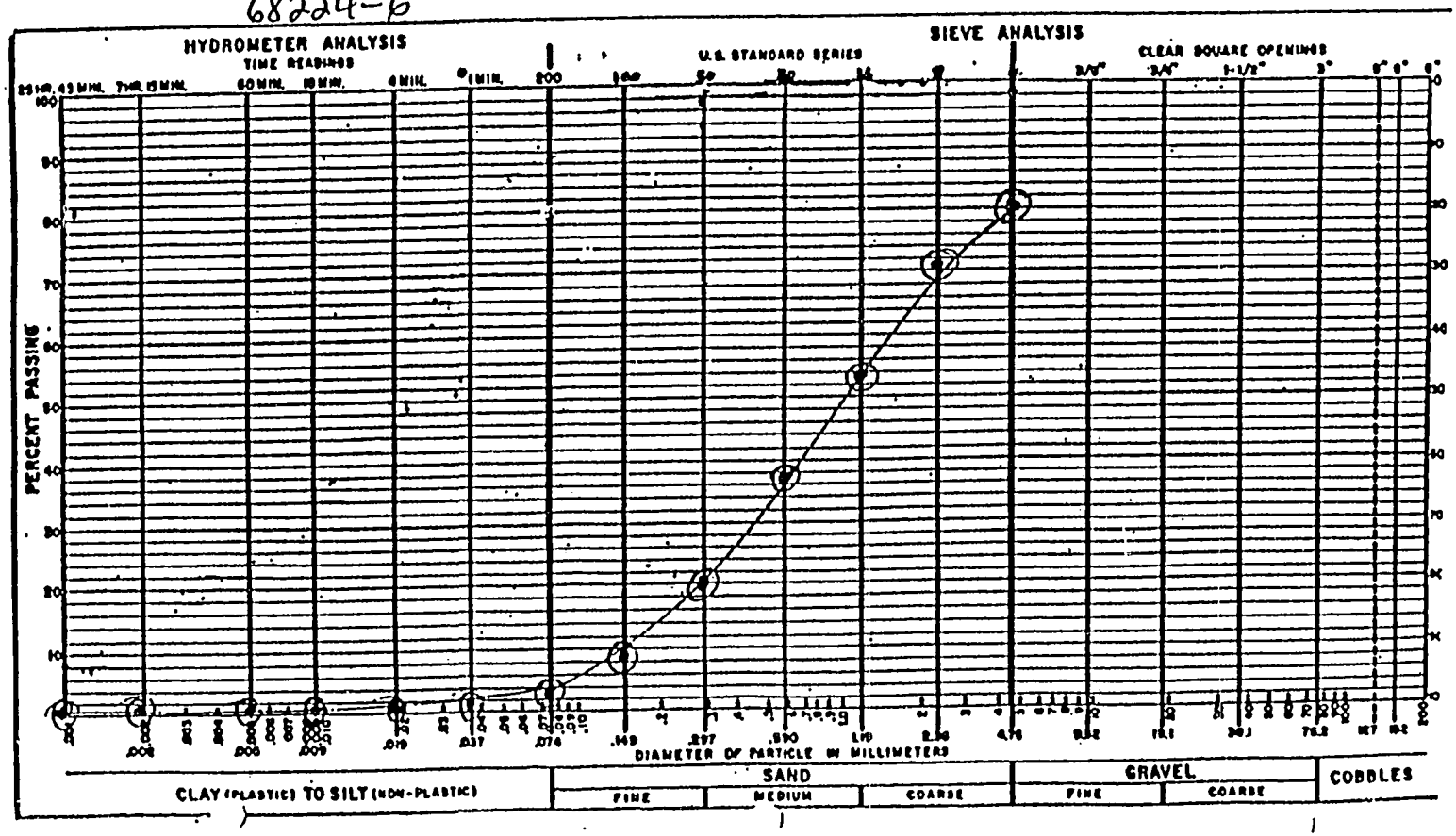
68224-5



OC-15

Reproduced with permission of the copyright owner. Further reproduction prohibited without permission.

68224-6

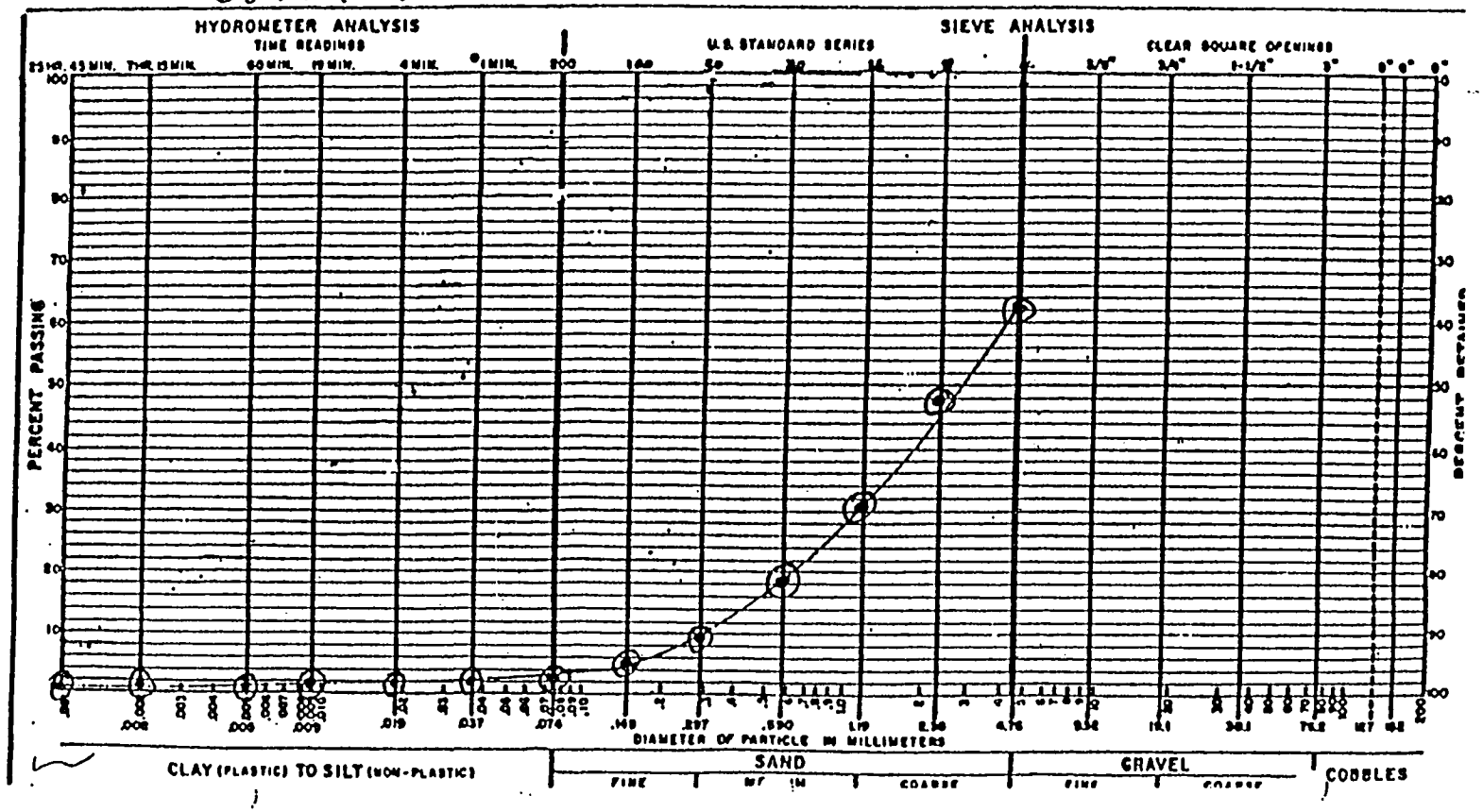


12

OC-17

Reproduced with permission of the copyright owner. Further reproduction prohibited without permission.

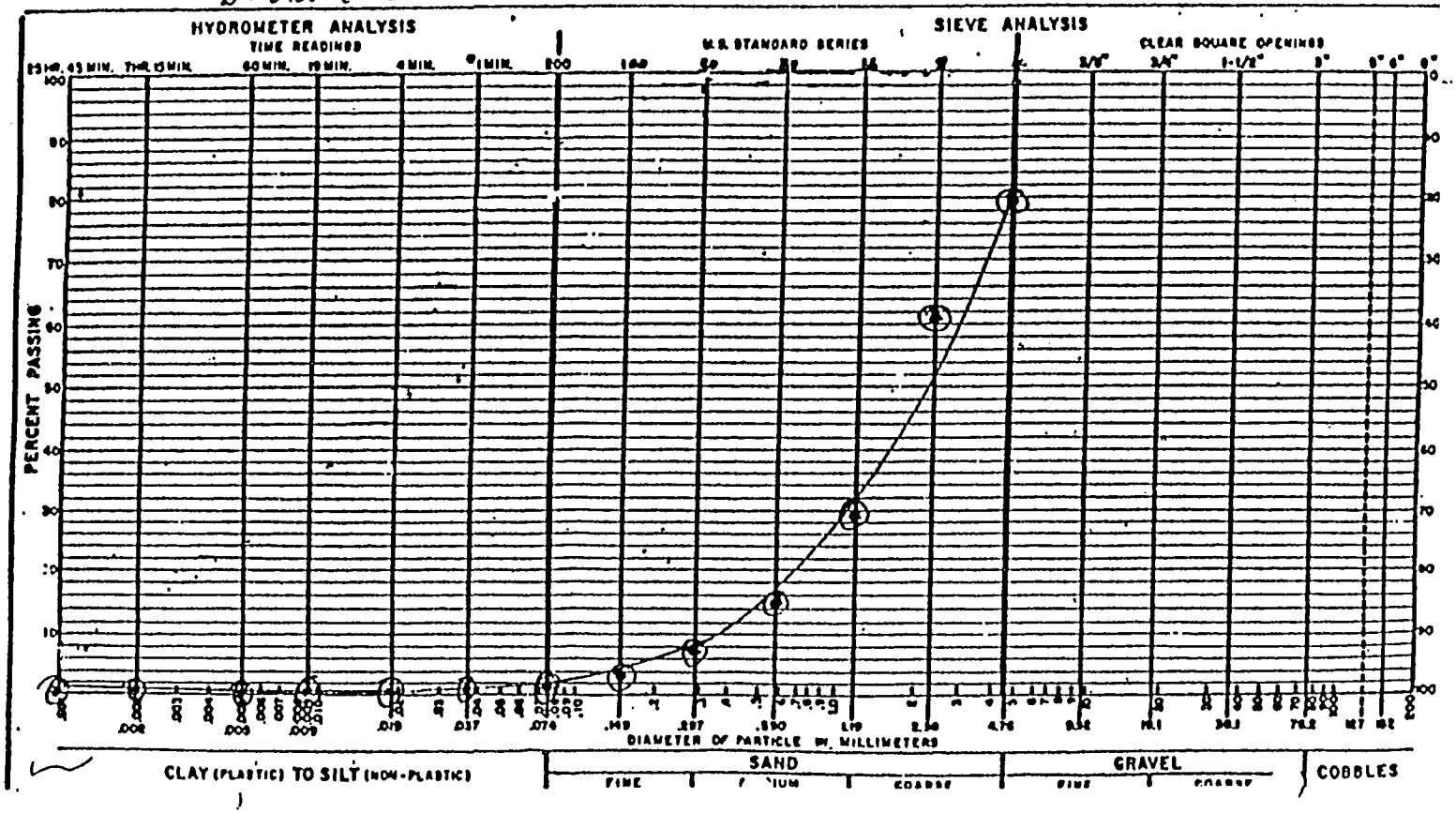
68224-7



OC-22

Reproduced with permission of the copyright owner. Further reproduction prohibited without permission.

68224-8

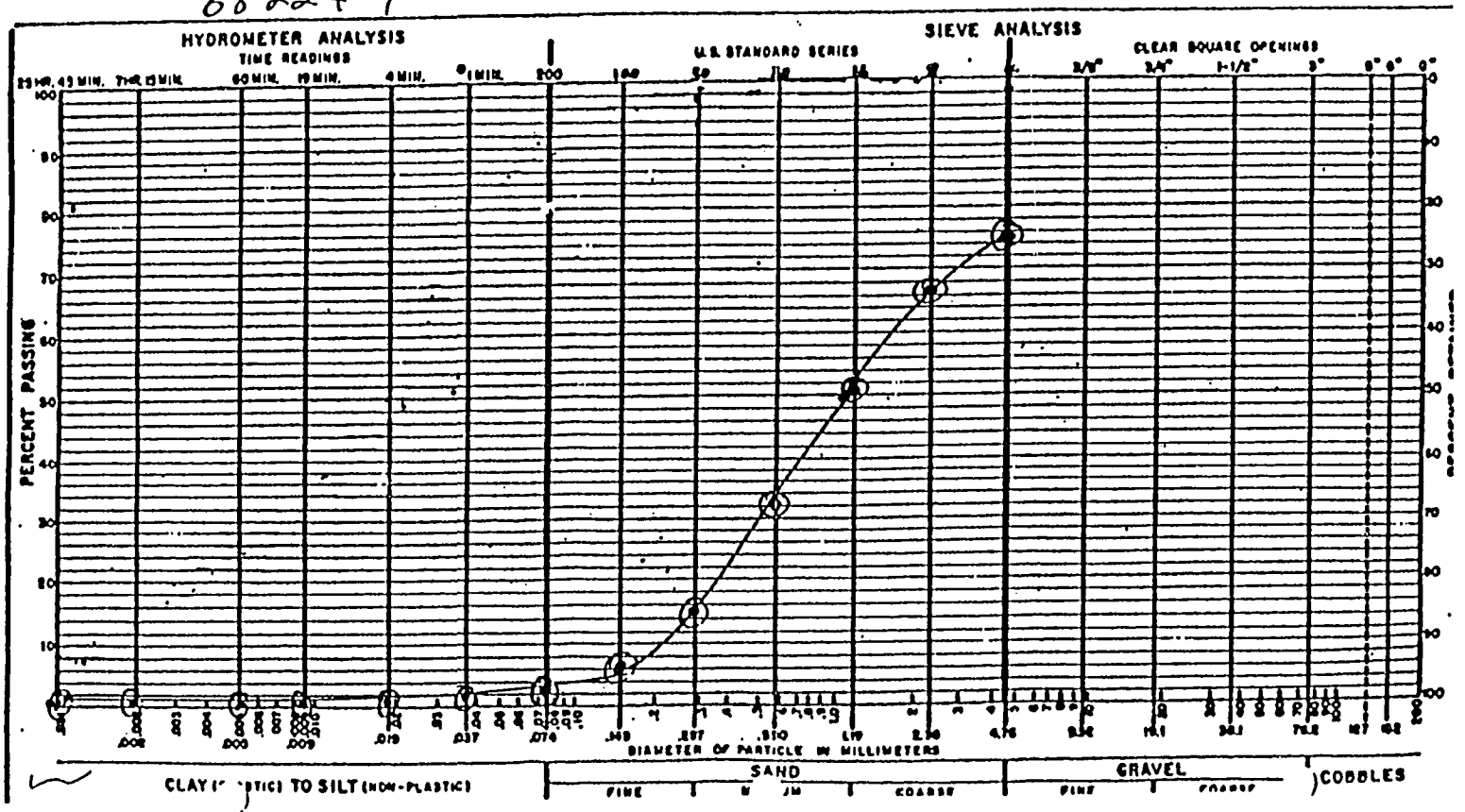


14

OC-24

Reproduced with permission of the copyright owner. Further reproduction prohibited without permission.

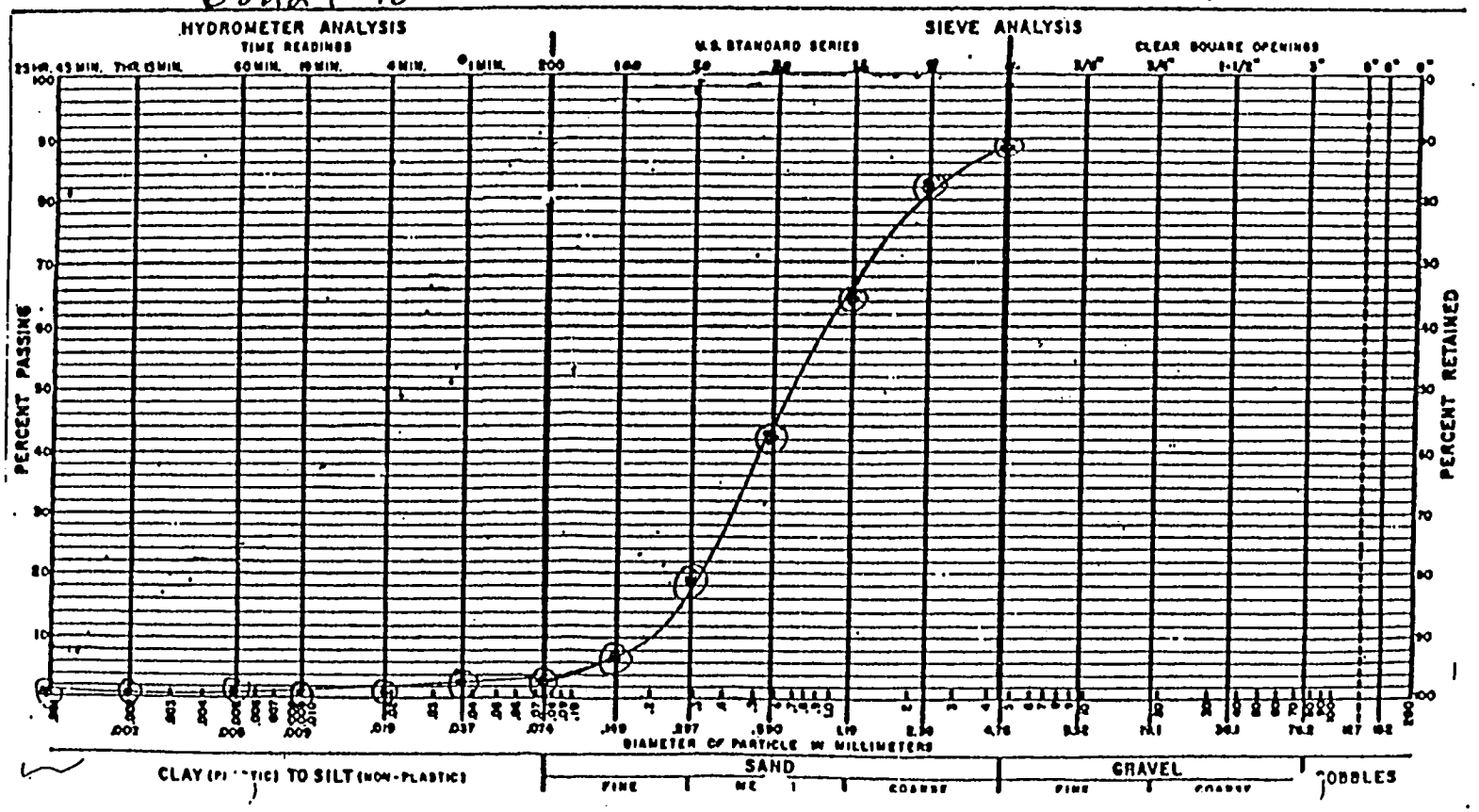
68224-9



OC-28

Reproduced with permission of the copyright owner. Further reproduction prohibited without permission.

68224-10

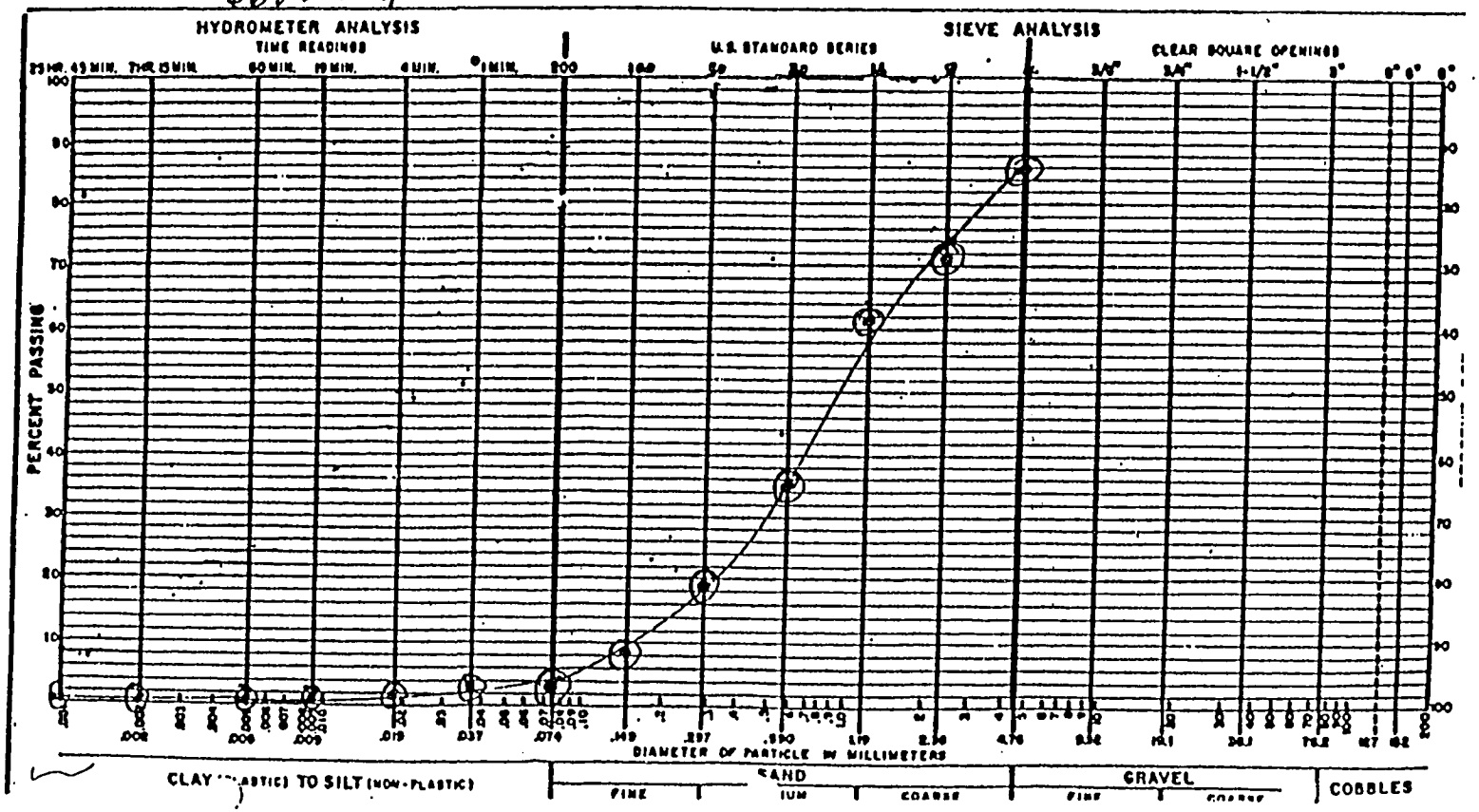


16

OC-30

Reproduced with permission of the copyright owner. Further reproduction prohibited without permission.

66224-11

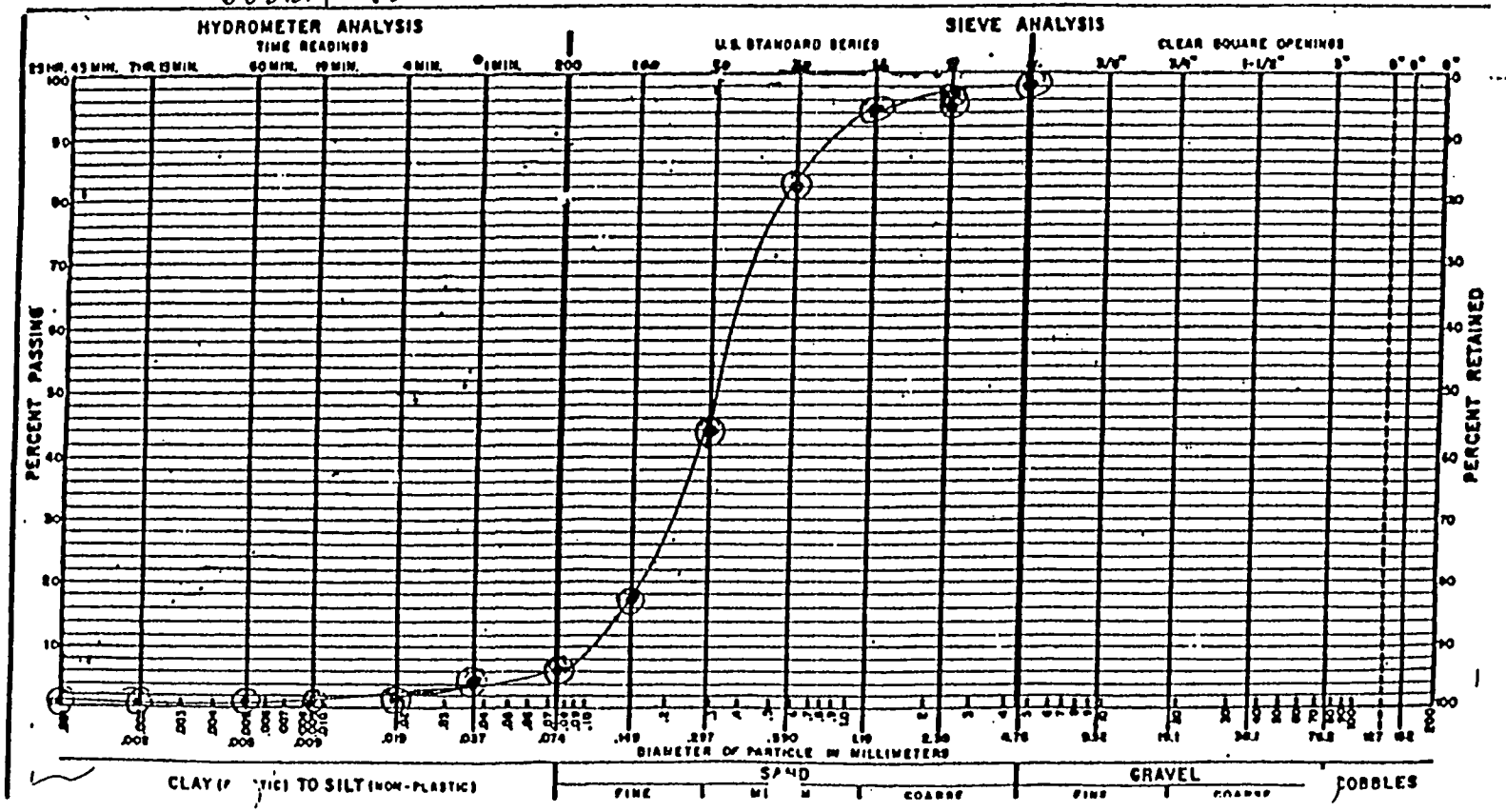


17

OC-32

Reproduced with permission of the copyright owner. Further reproduction prohibited without permission.

68224-12



18

SS-30

APPENDIX F

ALLUVIAL FAN SOIL BORING LOCATION MAP

AND SOIL BORING LITHOLOGIC LOGS

Reproduced with permission of the copyright owner. Further reproduction prohibited without permission.

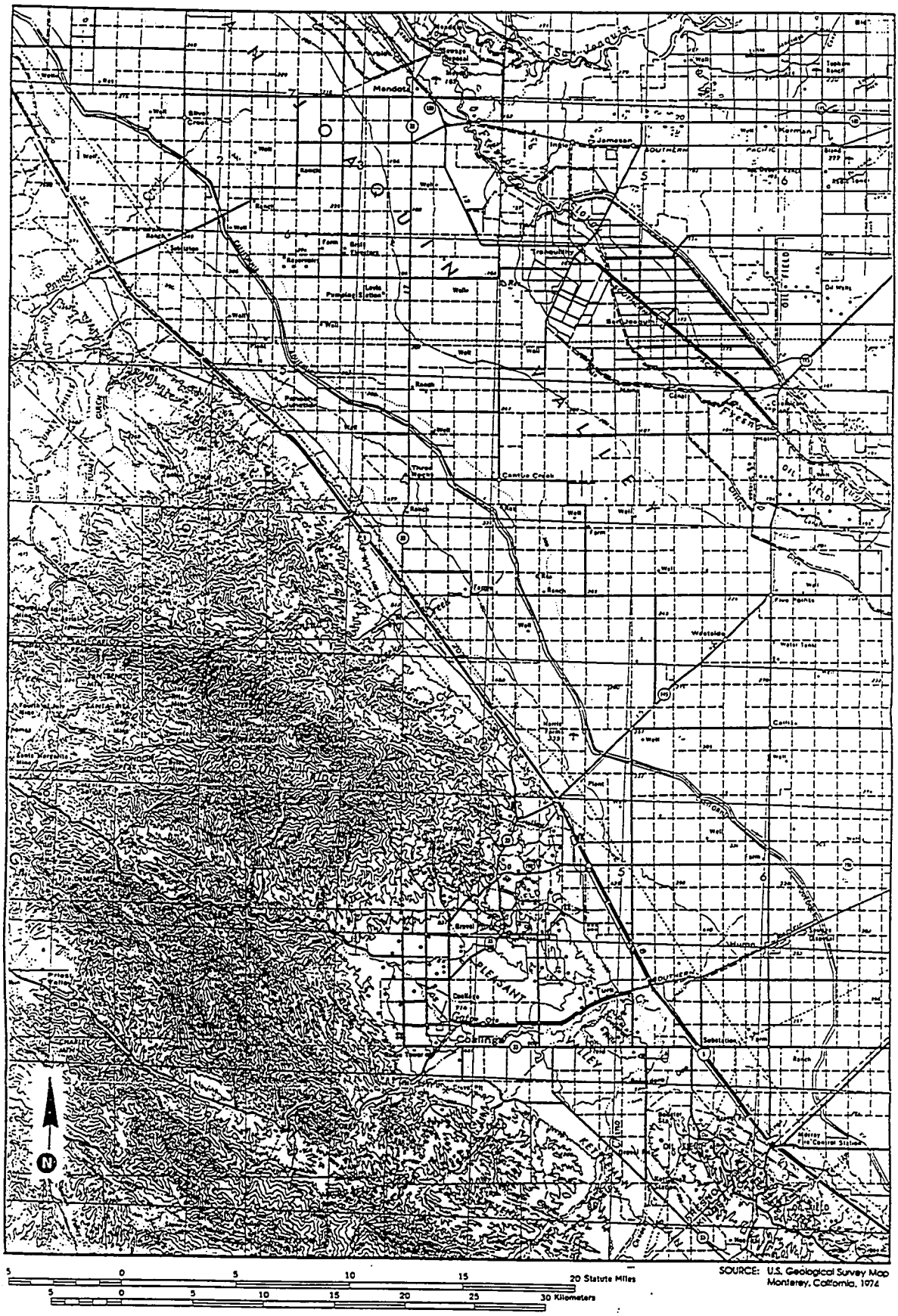


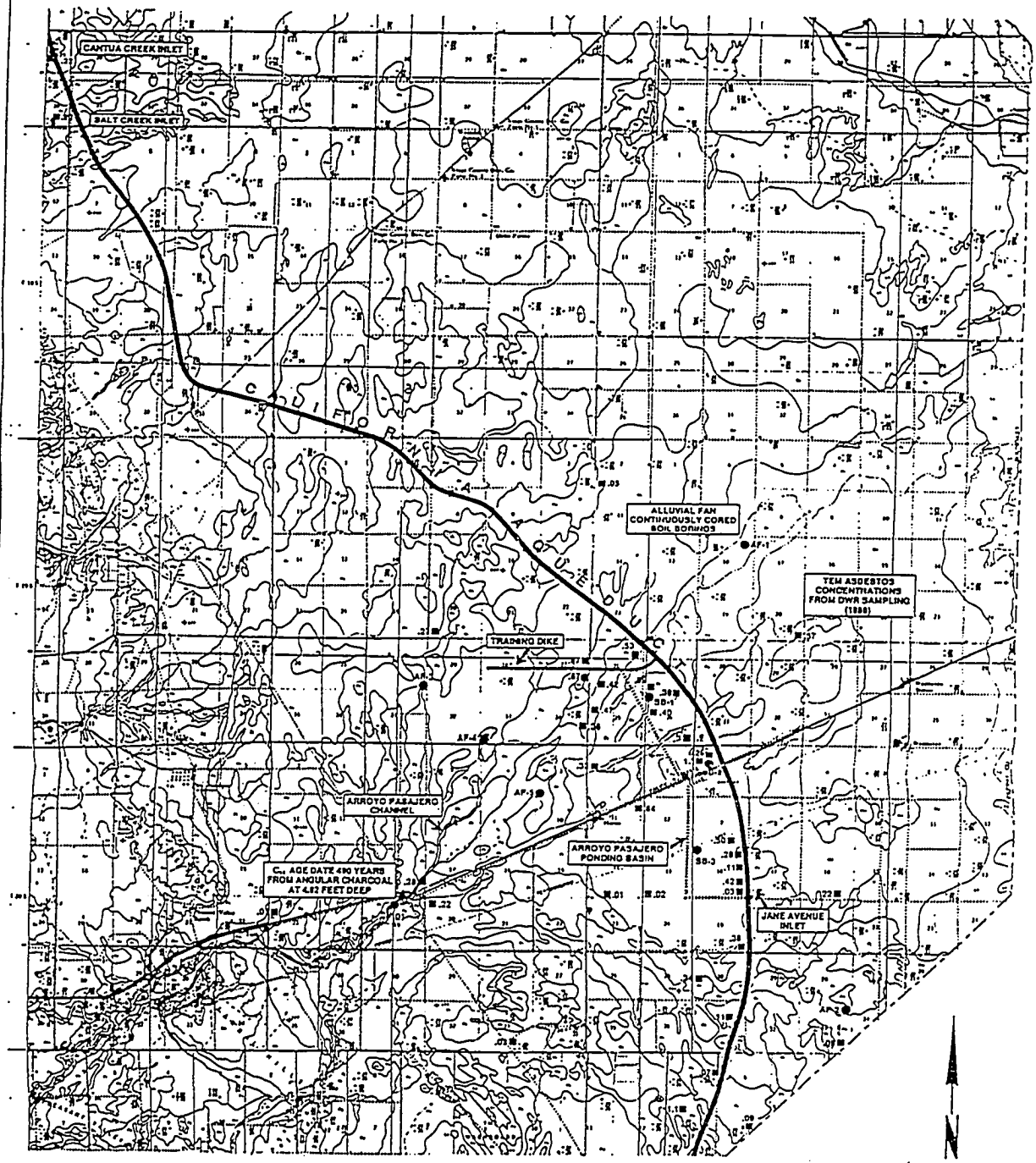
Figure F-1 : REGIONAL MAP OF COALINGA AREA INCLUDING JOAQUIN RIDGE AND WESTERN MARGIN OF SAN JOAQUIN VALLEY

Project No. 1802

LEVINE•FRICKE
CONSULTING ENGINEERS AND HYDROGEOLOGISTS

JDR11AUG88em

Reproduced with permission of the copyright owner. Further reproduction prohibited without permission.



EXPLANATION OF ADDED SYMBOLS

ALLUVIAL FAN BORINGS (Continuous Cores Drilled December, 1987)

- AF-1 ● Located in Medium Textured Alluvium (Pr) Deposited by Drainage Channel Floodwaters.
- AF-2 ● Located in Fine Textured Alluvium (Po) Deposited Near the Crest of a Very Low Ridge that Marks the General Vicinity of an Old Drainage Channel.
- AF-3 ● Located in Fine Textured Alluvium (Pk) Deposited by Floodwaters in Areas Near Stream Channels.
- AF-4 ● Located in Medium to Coarse Textured Alluvium (Pu) Deposited in Areas Adjacent to Stream Channels.
- AF-5 ● Located in Fine Textured Alluvium (Pr) Deposited by Drainage Channel Floodwaters.

SETTLING BASIN BORINGS (Continuous Cores Drilled December, 1987)

- SB-1 ●
- SB-2 ●
- SB-3 ● Located in Fine Textured Alluvium Deposited by Settling Basin Floodwaters.

ADDITIONAL DATA

- TEM ■ TEM Asbestos Concentrations by Percent Weight from Alluvial Fan Surface Samples Collected by the California Department of Water Resources (DWR) in 1986.
- C_{14} ▲ Age Date of 490 Years Before Present (60 Years) from Angular Charcoal Found at 4.92 Feet. This Indicates an Upper Alluvial Fan Depositional Rate of Approximately 0.01 Foot Per Year (Atwater et al, 1986).

1 0 1 2 3 MILES

APPROXIMATE SCALE

MAP SOURCE : Modified from USDA, Soil Survey, 1952.

FIGURE F-2

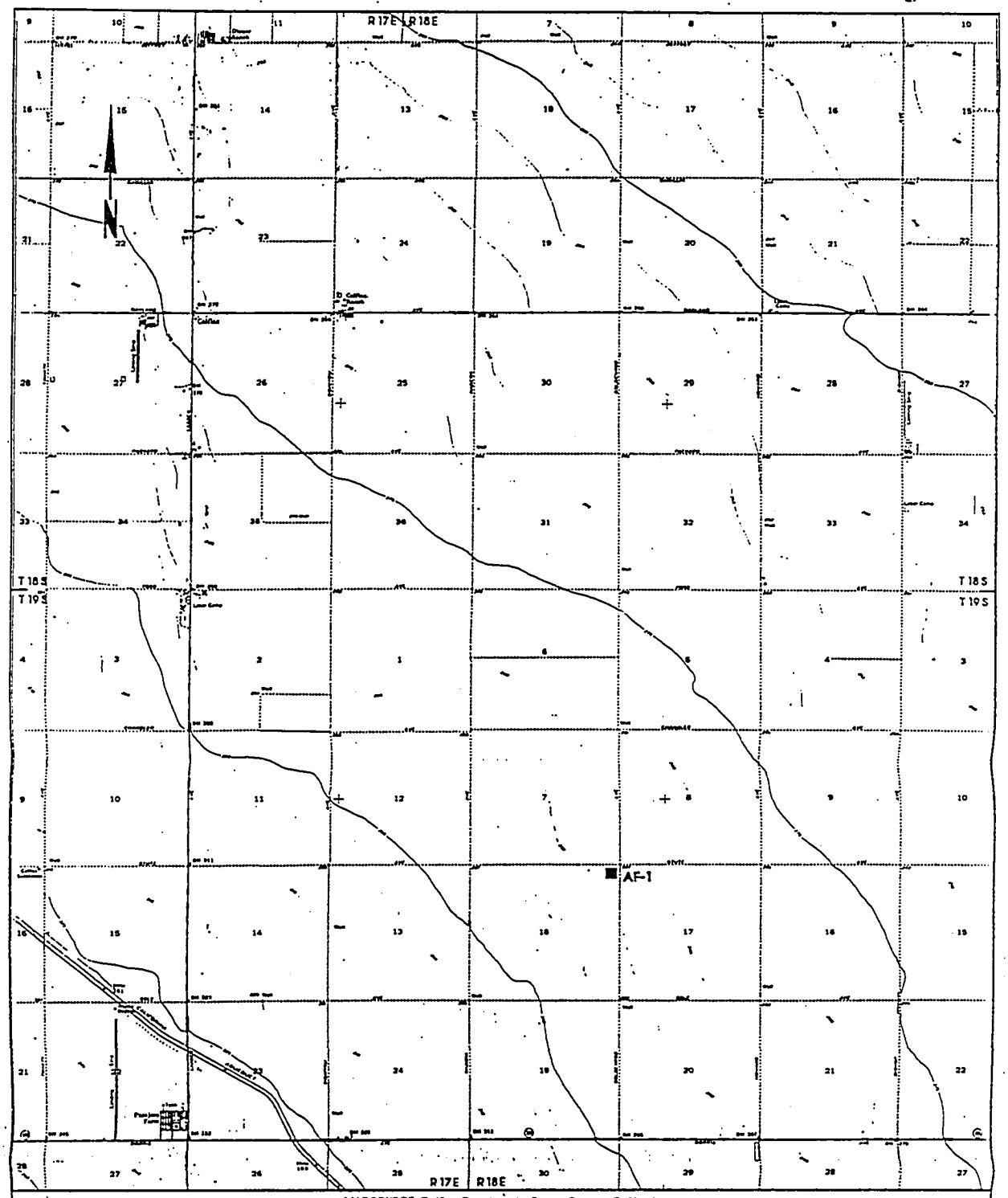
ARROYO PASAJERO
ALLUVIAL FAN SOIL MAP
WITH SAMPLING STATION DATA

Project No. 1802

LEVINE•FRICKE
CONSULTING ENGINEERS AND HYDROGEOLOGISTS

DE1585JHDR,MMK/mmk,tc

Reproduced with permission of the copyright owner. Further reproduction prohibited without permission.



MAP SOURCE: Caltax Quadrangle, Fresno County, California, 7.5 Minute Series (Topographic), U.S.G.S., Photorevised 1971

EXPLANATION

■ Alluvial Fan Boring Station

SCALE

0 1 2 MILES

CONTOUR INTERVAL = 25 FEET

SAMPLING STATION LOCATION

MAP "A"

Project No. 1802

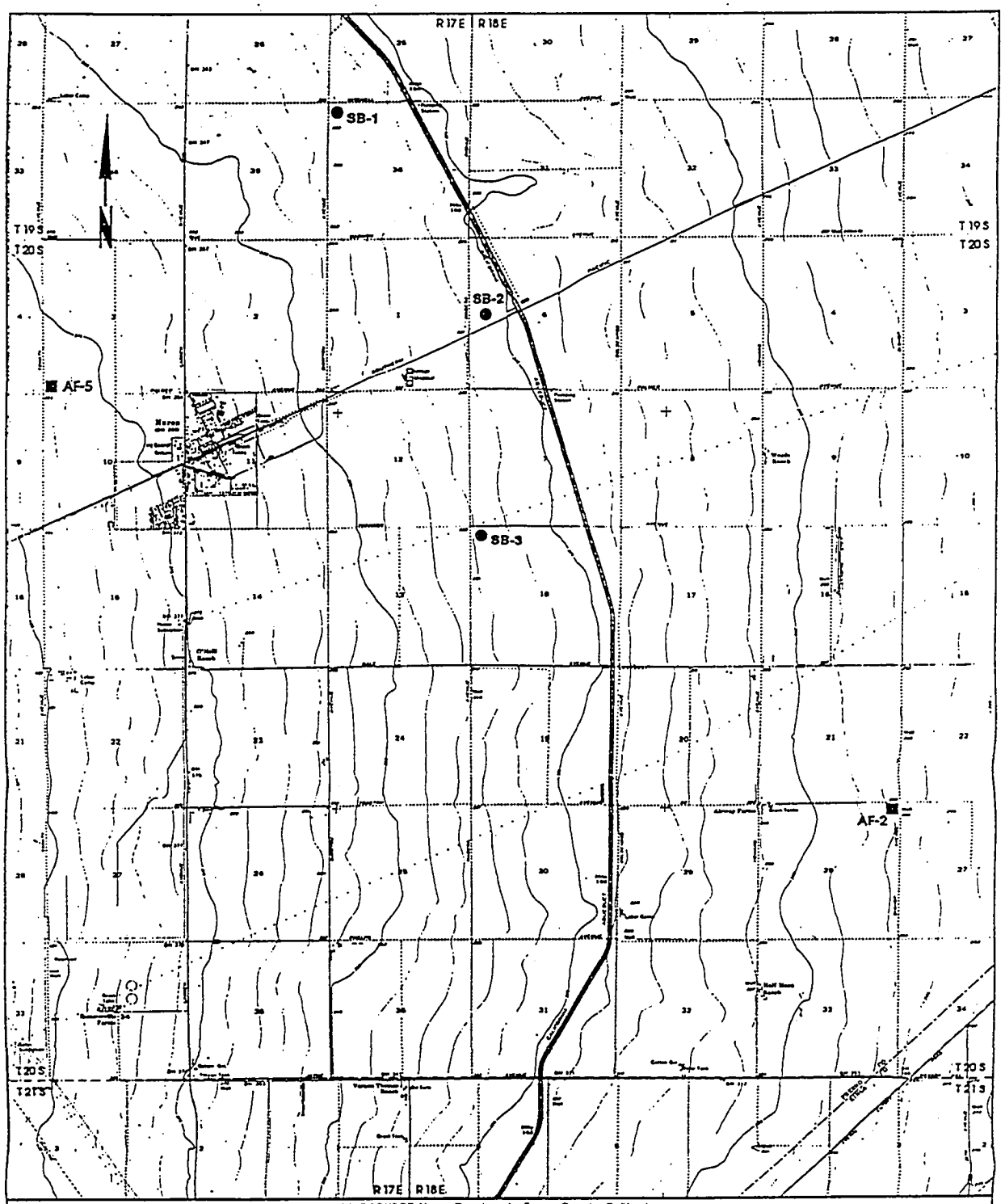
LEVINE•FRICKE

CONSULTING ENGINEERS AND HYDROGEOLOGISTS

083088JHDR/mmk,emt,scj

1802-01

Reproduced with permission of the copyright owner. Further reproduction prohibited without permission.



MAP SOURCE: Huron Quadrangle, Fresno County, California, 7.5 Minute Series (Topographic), U.S.G.S., Photorevised 1971.

EXPLANATION

- Alluvial Fan Boring Station
- Settling Basin Boring Station

SCALE

0 1 2 MILES

CONTOUR INTERVAL = 25 FEET

SAMPLING STATION LOCATION

MAP " B "

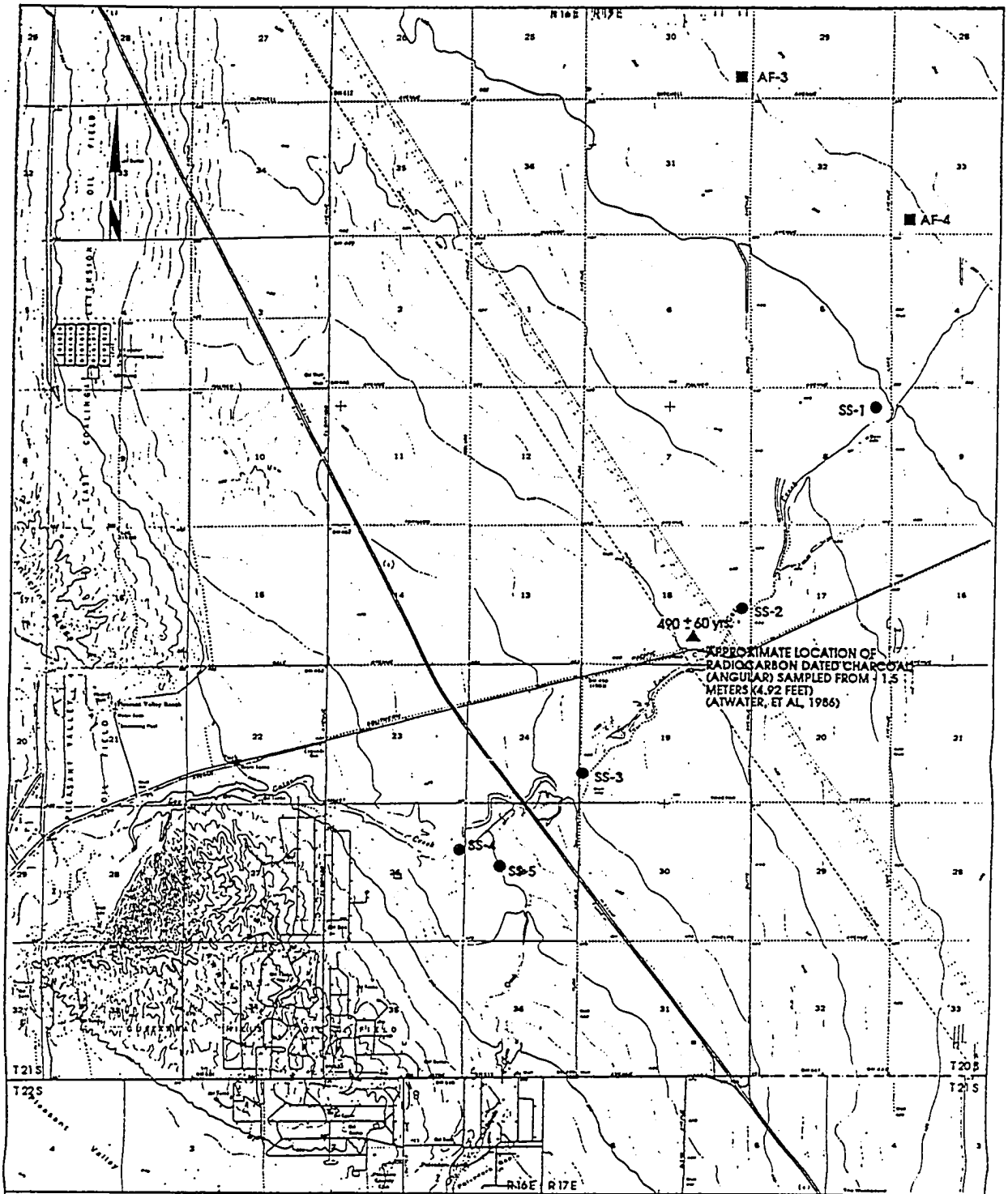
Project No. 1802

LEVINE•FRICKE

CONSULTING ENGINEERS AND HYDROGEOLOGISTS

1802-02

Reproduced with permission of the copyright owner. Further reproduction prohibited without permission.



MAP SOURCE: Guijarral Hills Quadrangle, Fresno County, California, 7.5 Minute Series (Topographic), U.S.G.S., Photorevised 1971.

EXPLANATION

- Alluvial Fan Boring Station
- Streambed Sampling Station
- Radiocarbon Dated Sample Location (Atwater, et al, 1986)

SCALE

0 1 2 MILES

CONTOUR INTERVAL = 20 FEET

SAMPLING STATION LOCATION

MAP "C"

Project No. 1802

LEVINE•FRICKE

CONSULTING ENGINEERS AND HYDROGEOLOGISTS

083088JHDR/mmk.eml.sc

1802-03

Reproduced with permission of the copyright owner. Further reproduction prohibited without permission.

COALINGA ASBESTOS - ALLUVIAL FAN BORING PROGRAM - SB1

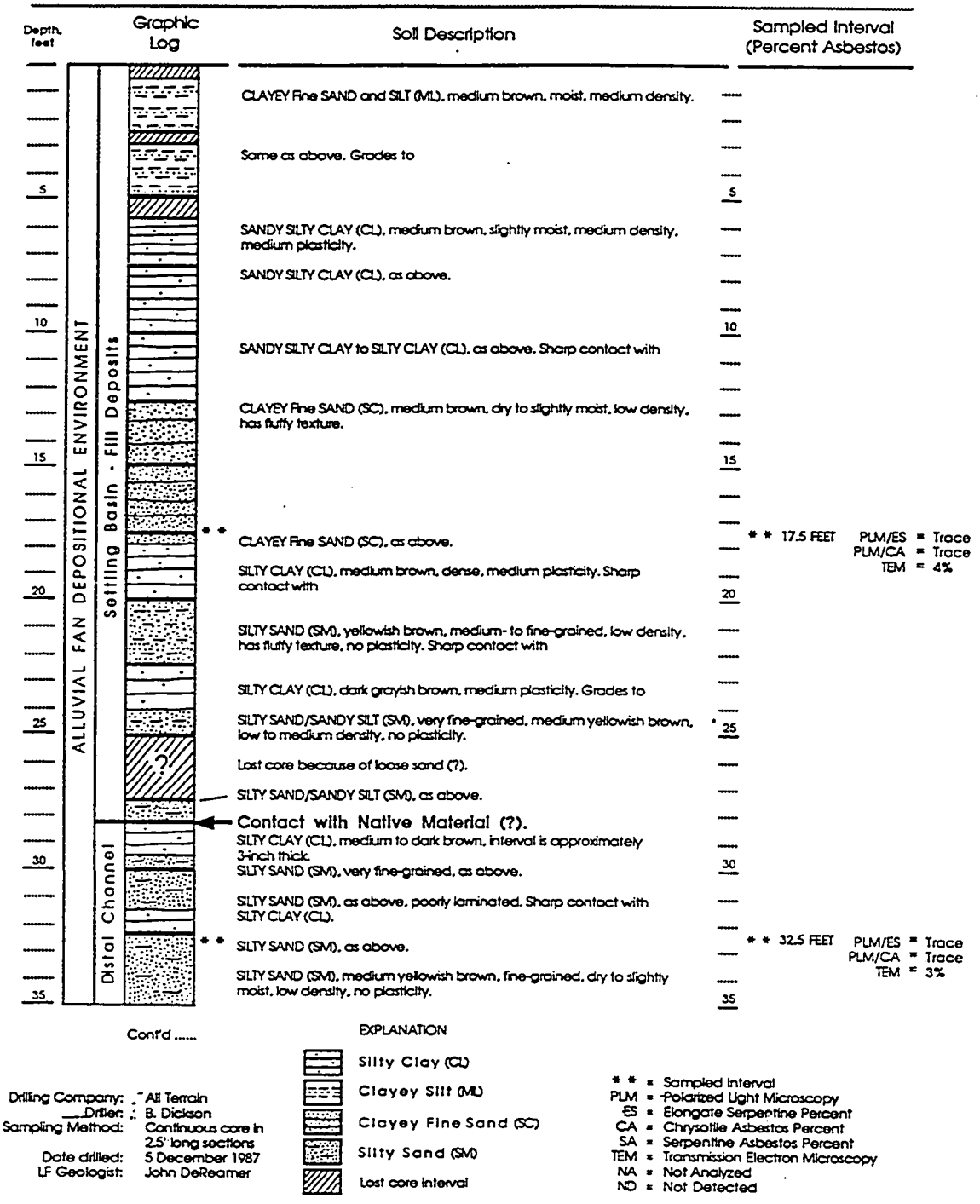


Figure A : LOG OF CONTINUOUSLY-CORED SOIL BORING SB1

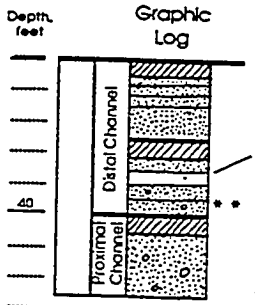
Project No. 1802 Settling Basin Boring Program

LEVINE•FRICKE
CONSULTING ENGINEERS AND HYDROGEOLOGISTS

1802JDR18OCT88em

Reproduced with permission of the copyright owner. Further reproduction prohibited without permission.

COALINGA ASBESTOS - ALLUVIAL FAN BORING PROGRAM - SB1



Soil Description	Sampled Interval (Percent Asbestos)
CLAYEY Fine SAND (SC), medium brown. Sharp contact with SAND (SP), yellowish grayish brown, medium- to coarse-grained, contains some light green, lath-shaped grains (approximately 1%). Sharp contact with SILTY CLAY (CL), medium brown, poorly laminated, approximately 2-inch thick. Sharp contact with	
* * SAND (SP), yellowish grayish brown, fine- to medium-grained.	40 * * 39.9 FEET PLM/ES = Trace PLM/CA = ND TEM = 1%
SAND (SP), yellowish grayish brown, medium- to coarse-grained with <3% fine gravel (up to 1/16-inch diameter). SAND (SP), yellowish grayish brown, medium- to coarse-grained with <3% coarse gravel (up to 1 1/2-inch diameter), loose, slightly moist, medium density.	
BOTTOM OF BORING AT 42.5 FEET.	45
Hole backfilled with native material with 1 foot of bentonite powder every 5 feet and at bottom of hole.	

Drilling Company: All Terrain
Driller: B. Dickson
Sampling Method: Continuous core in 2.5' long sections
Date drilled: 5 December 1987
LF Geologist: John DeReamer

EXPLANATION

- Silty Clay (CL)
- Clayey Fine Sand (SC)
- Sand (SP)
- Lost core interval

* * = Sampled Interval
PLM = Polarized Light Microscopy
ES = Elongate Serpentine Percent
CA = Chrysotile Asbestos Percent
SA = Serpentine Asbestos Percent
TEM = Transmission Electron Microscopy
NA = Not Analyzed
ND = Not Detected

Figure A : LOG OF CONTINUOUSLY-CORED SOIL BORING SB1 (CONT'D)

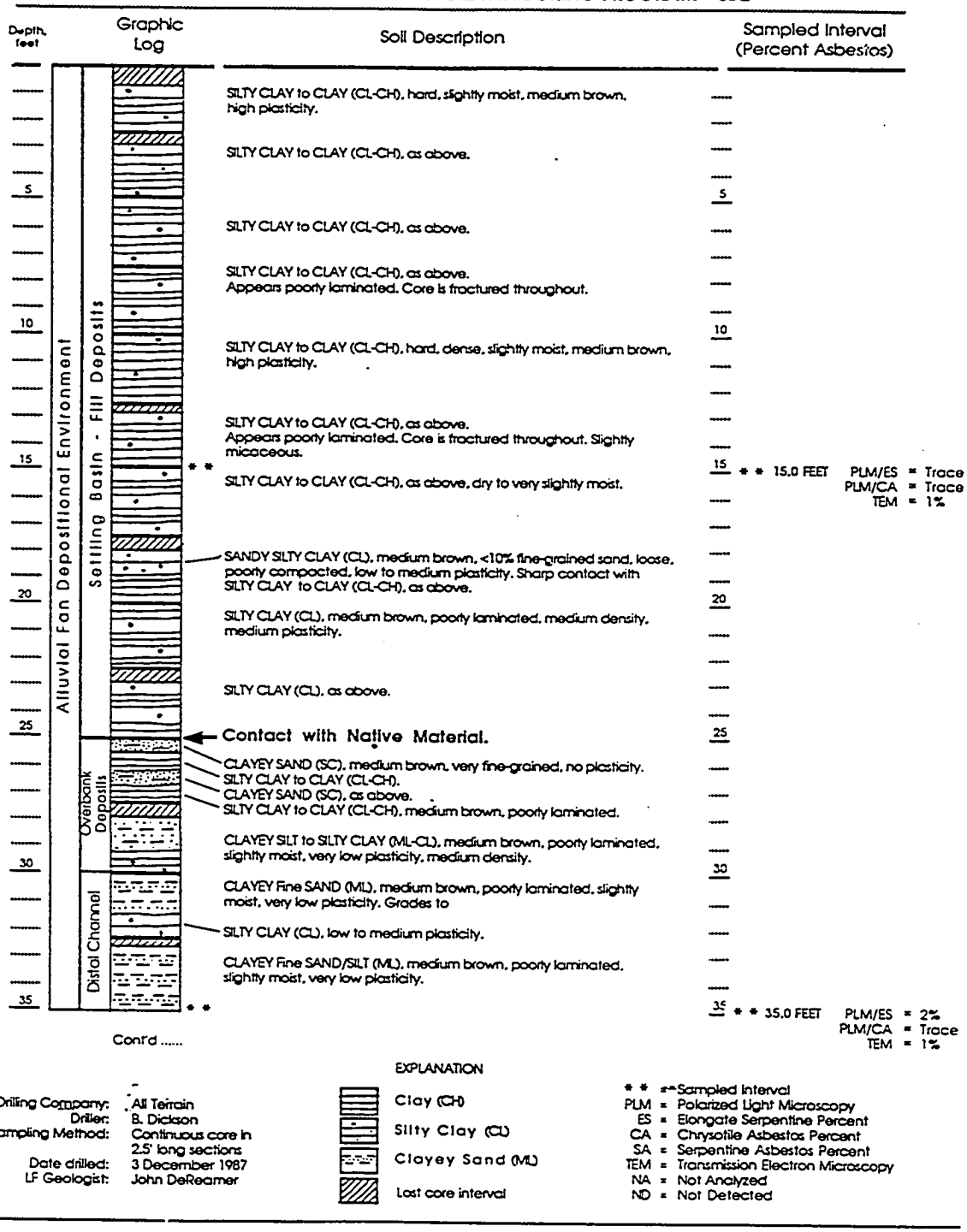
Project No. 1802 Settling Basin Boring Program

1802JDR18OC188em

LEVINE•FRICKE
CONSULTING ENGINEERS AND HYDROGEOLOGISTS

Reproduced with permission of the copyright owner. Further reproduction prohibited without permission.

COALINGA ASBESTOS - ALLUVIAL FAN BORING PROGRAM - SB2

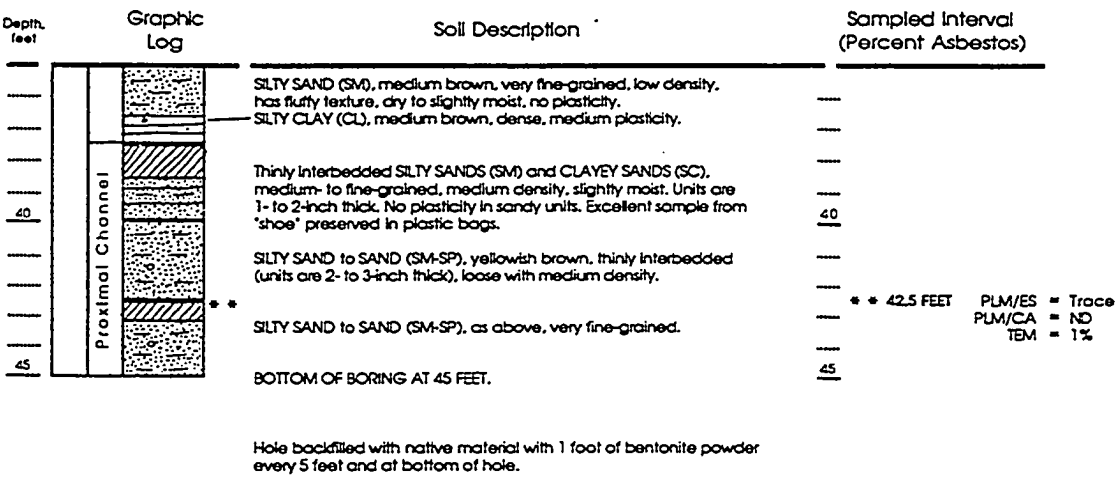


Drilling Company: All Terrain
Driller: B. Dickson
Sampling Method: Continuous core in 2.5' long sections
Date drilled: 3 December 1987
LF Geologist: John DeReamer

Figure B : LOG OF CONTINUOUSLY-CORED SOIL BORING SB2

Reproduced with permission of the copyright owner. Further reproduction prohibited without permission.

COALINGA ASBESTOS - ALLUVIAL FAN BORING PROGRAM - SB2



Drilling Company: All Terrain
Driller: B. Dickson
Sampling Method: Continuous core in 2.5' long sections
Date drilled: 3 December 1987
LF Geologist: John DeReamer

EXPLANATION

- Silty Clay (CL)
- Clayey Sand (SC)
- Silty Sand (SM)
- Sand (SP)
- Lost core interval

* * = Sampled Interval
PLM = Polarized Light Microscopy
ES = Elongate Serpentine Percent
CA = Chrysotile Asbestos Percent
SA = Serpentine Asbestos Percent
TEM = Transmission Electron Microscopy
NA = Not Analyzed
ND = Not Detected

Figure B : LOG OF CONTINUOUSLY-CORED SOIL BORING SB2 (CONT'D)

Project No. 1802 Settling Basin Boring Program

LEVINE-FRICKE
CONSULTING ENGINEERS AND HYDROGEOLOGISTS

1802JDR18OCT88em

Reproduced with permission of the copyright owner. Further reproduction prohibited without permission.

COALINGA ASBESTOS - ALLUVIAL FAN BORING PROGRAM - SB3

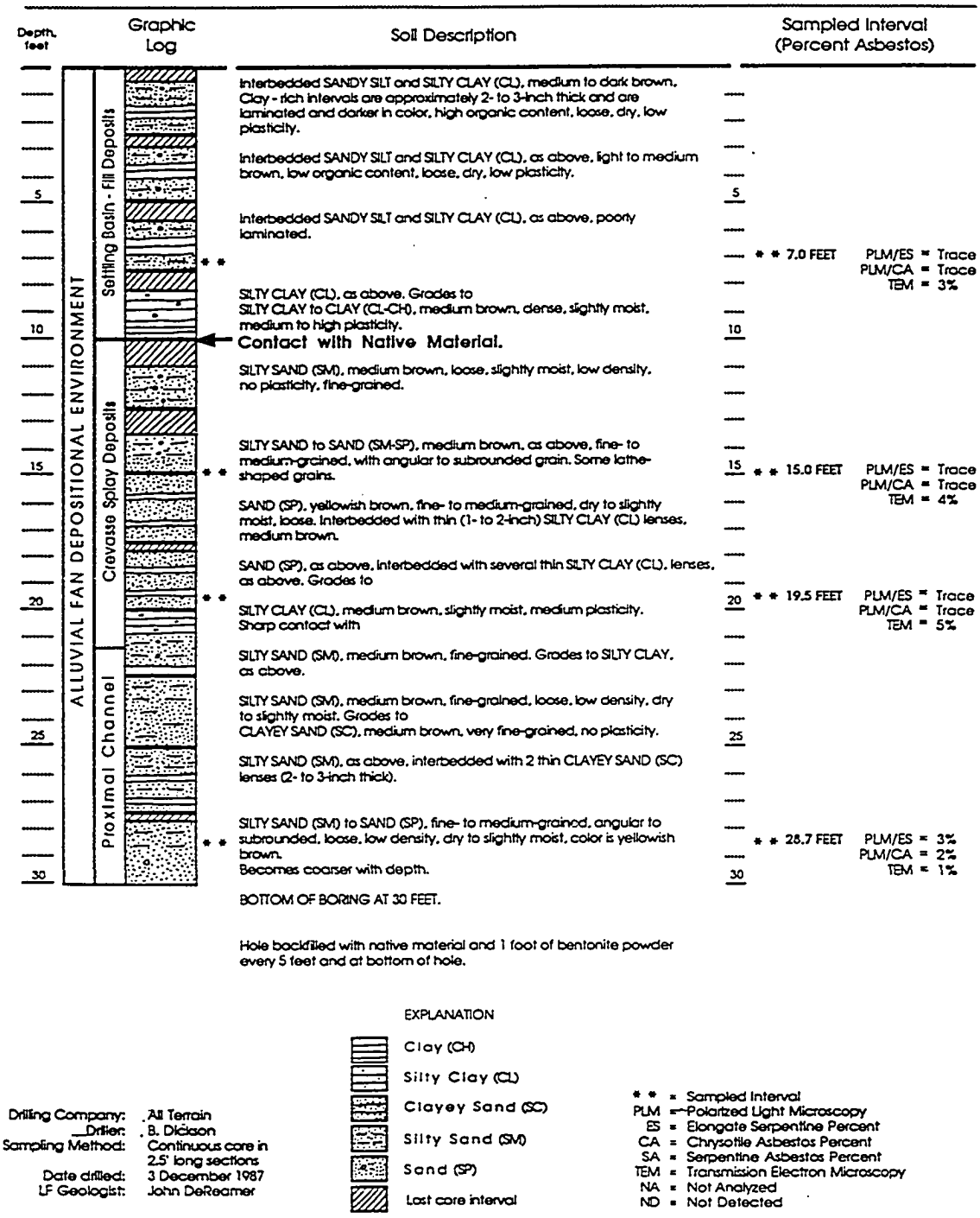


Figure C : LOG OF CONTINUOUSLY-CORED SOIL BORING SB3

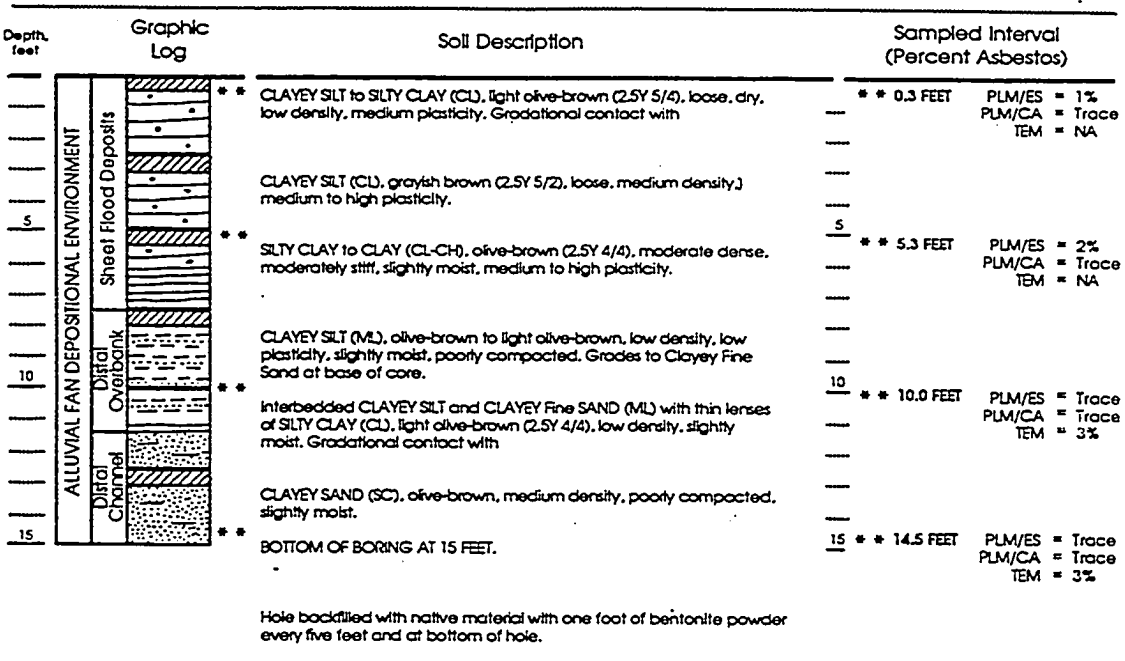
Project No. 1802 Settling Basin Boring Program

LEVINE•FRICKE
CONSULTING ENGINEERS AND HYDROGEOLOGISTS

1802JDR18OCT88em

Reproduced with permission of the copyright owner. Further reproduction prohibited without permission.

COALINGA ASBESTOS - ALLUVIAL FAN BORING PROGRAM - AF1



Drilling Company: All Terrain
Driller: B. Dickson
Sampling Method: Continuous core in 2.5' long sections
Date drilled: 1 December 1987
LF Geologist: John DeReamer

EXPLANATION

- Clay (CH)
- Silty Clay (CL)
- Clayey Silt (ML)
- Clayey Sand (SC)
- Lost core interval

* * = Sampled Interval
PLM = Polarized Light Microscopy
ES = Elongate Serpentine Percent
CA = Chrysotile Asbestos Percent
SA = Serpentine Asbestos Percent
TEM = Transmission Electron Microscopy
NA = Not Analyzed
ND = Not Detected

Figure D : LOG OF CONTINUOUSLY-CORED SOIL BORING AF1

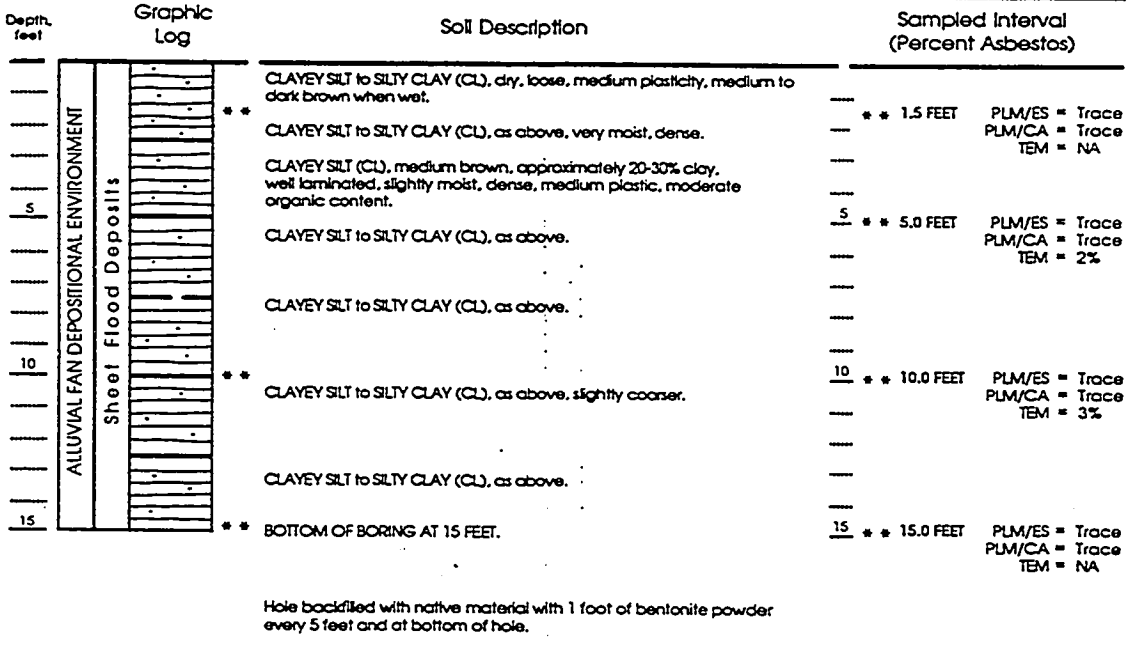
Project No. 1802 Settling Basin Boring Program

LEVINE•FRICKE
CONSULTING ENGINEERS AND HYDROGEOLOGISTS

1802JDR18OCT88em

Reproduced with permission of the copyright owner. Further reproduction prohibited without permission.

COALINGA ASBESTOS - ALLUVIAL FAN BORING PROGRAM - AF2



Hole backfilled with native material with 1 foot of bentonite powder every 5 feet and at bottom of hole.

Drilling Company: All Terrain
Driller: B. Dickson
Sampling Method: Continuous core in 2.5' long sections
Date drilled: 1 December 1987
LF Geologist: John DeReamer

EXPLANATION

Silty Clay (CL)

Lost core interval

** = Sampled Interval
PLM = Polarized Light Microscopy
ES = Elongate Serpentine Percent
CA = Chrysotile Asbestos Percent
SA = Serpentine Asbestos Percent
TEM = Transmission Electron Microscopy
NA = Not Analyzed
ND = Not Detected

Figure E : LOG OF CONTINUOUSLY-CORED SOIL BORING AF2

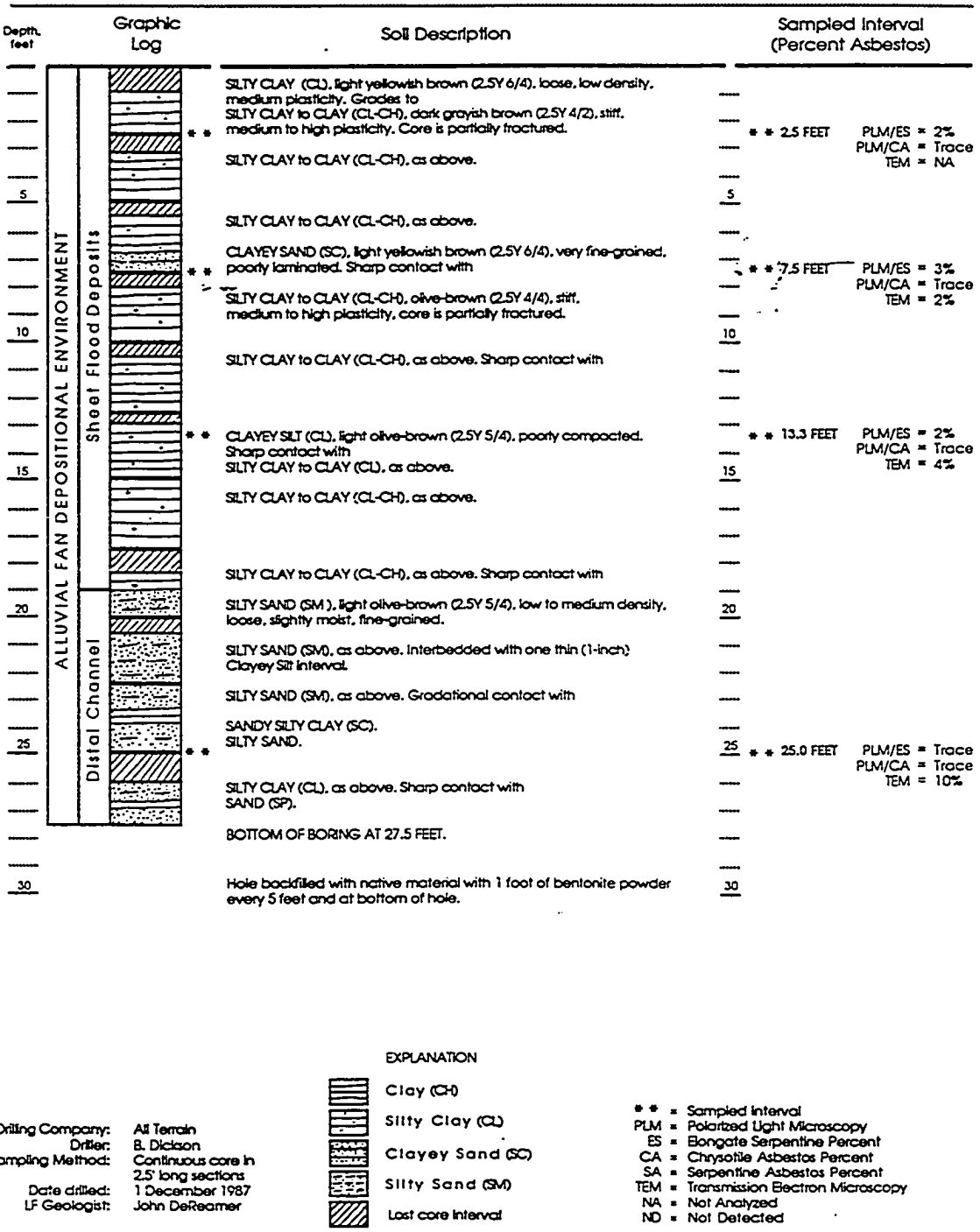
Project No. 1802 Settling Basin Boring Program

LEVINE•FRICKE
CONSULTING ENGINEERS AND HYDROGEOLOGISTS

1802JDR18OCT88em

Reproduced with permission of the copyright owner. Further reproduction prohibited without permission.

COALINGA ASBESTOS - ALLUVIAL FAN BORING PROGRAM - AF3



Drilling Company: All Terrain
Driller: B. Dickson
Sampling Method: Continuous core in 2.5' long sections
Date drilled: 1 December 1987
LF Geologist: John DeRoemer

EXPLANATION

- Clay (CH)
- Silty Clay (CL)
- Clayey Sand (SC)
- Silty Sand (SM)
- Lost core interval

* * = Sampled interval
PLM = Polarized Light Microscopy
ES = Elongate Serpentine Percent
CA = Chrysotile Asbestos Percent
SA = Serpentine Asbestos Percent
TEM = Transmission Electron Microscopy
NA = Not Analyzed
ND = Not Detected

Figure F : LOG OF CONTINUOUSLY-CORED SOIL BORING AF3

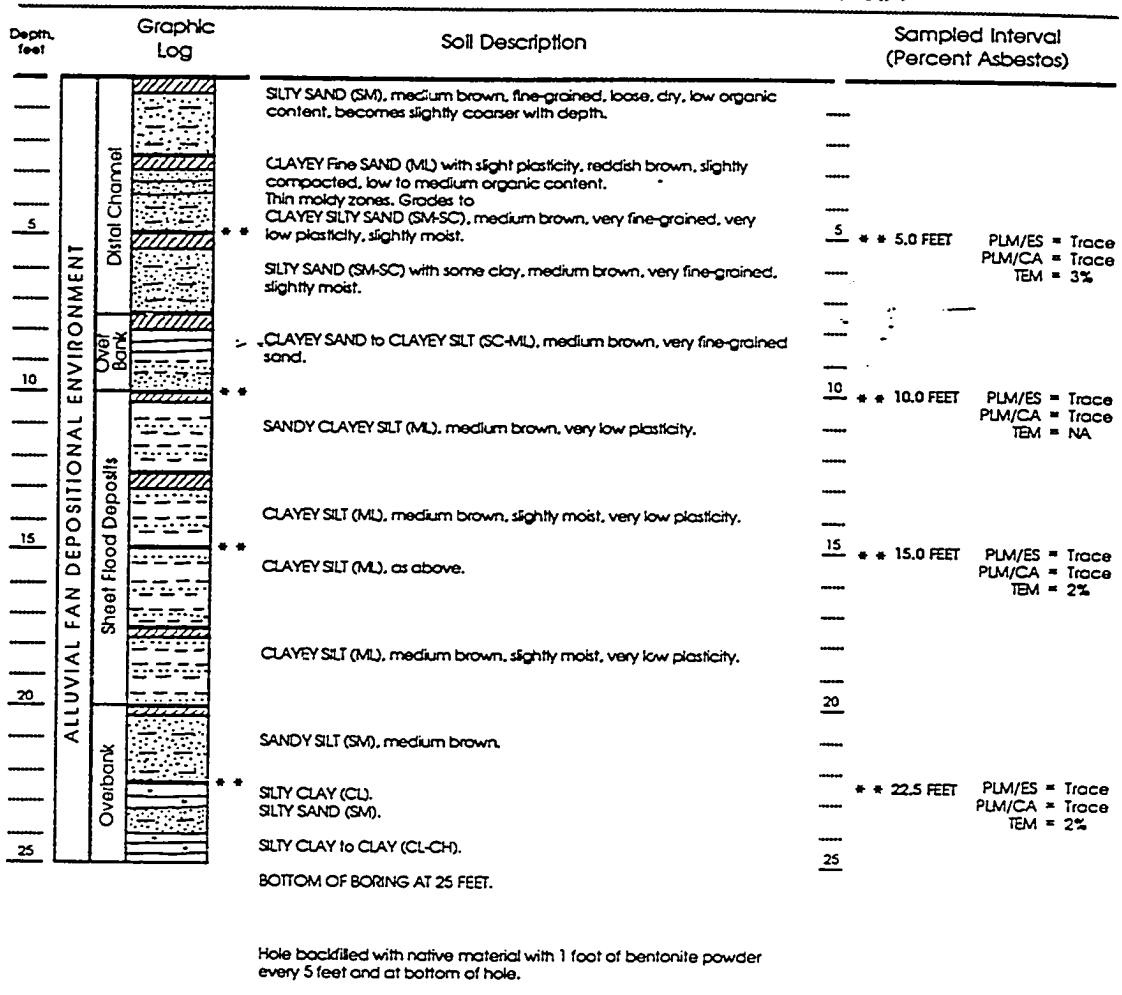
Project No. 1802 Settling Basin Boring Program

LEVINE•FRICKE
CONSULTING ENGINEERS AND HYDROGEOLOGISTS

1802JDR18OCT88em

Reproduced with permission of the copyright owner. Further reproduction prohibited without permission.

COALINGA ASBESTOS - ALLUVIAL FAN BORING PROGRAM - AF4



Hole backfilled with native material with 1 foot of bentonite powder every 5 feet and at bottom of hole.

EXPLANATION

- Clay (CH)
- Silty Clay (CL)
- Clayey Silt (ML)
- Clayey Sand (SC)
- Silty Sand (SM)
- Lost core interval

Drilling Company: All Terrain
Driller: B. Dickson
Sampling Method: Continuous core in 2.5' long sections
Date drilled:
LF Geologist: John DeReamer

* * = Sampled Interval
PLM = Polarized Light Microscopy
ES = Elongate Serpentine Percent
CA = Chrysotile Asbestos Percent
SA = Serpentine Asbestos Percent
TEM = Transmission Electron Microscopy
NA = Not Analyzed
ND = Not Detected

Figure G : LOG OF CONTINUOUSLY-CORED SOIL BORING AF4

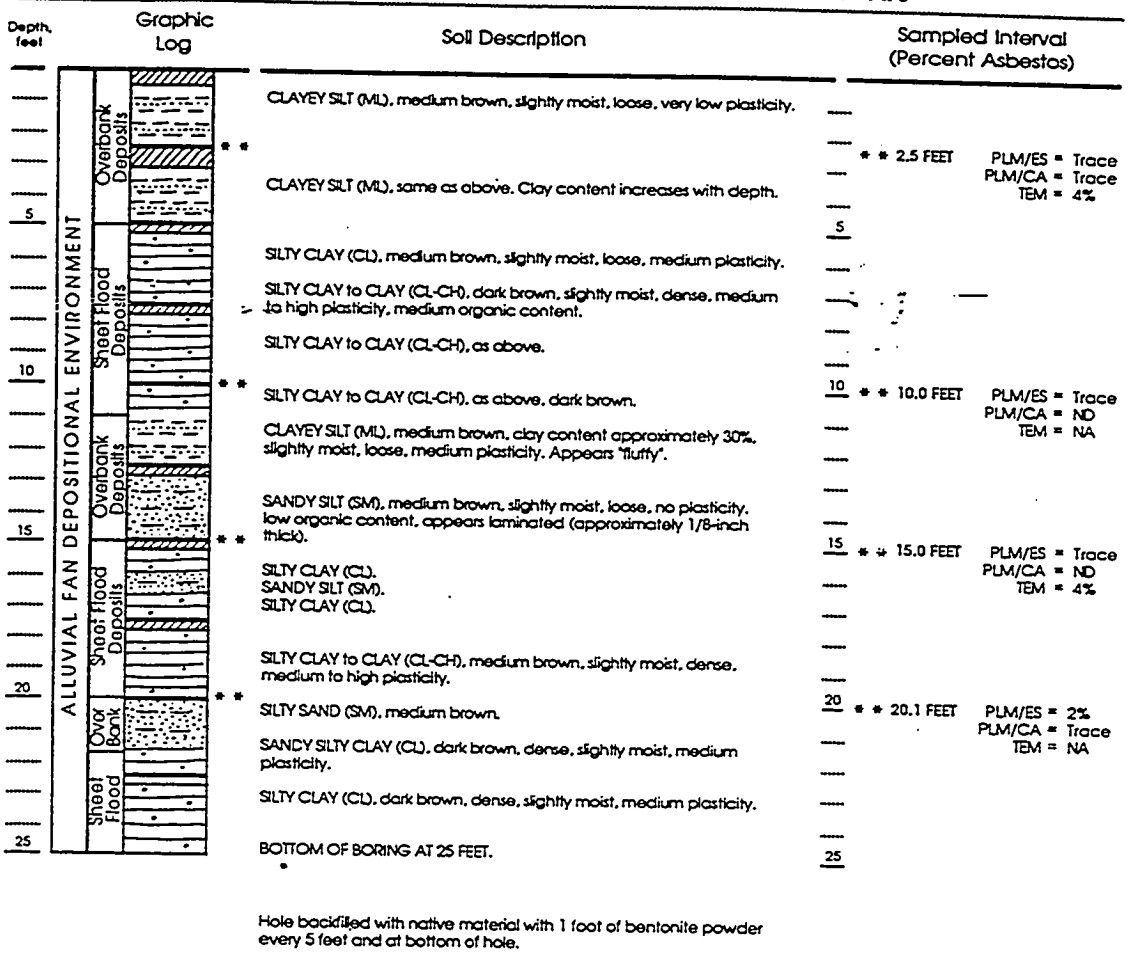
Project No. 1802 Settling Basin Boring Program

LEVINE•FRICKE
CONSULTING ENGINEERS AND HYDROGEOLOGISTS

1802JDR18OCT88em

Reproduced with permission of the copyright owner. Further reproduction prohibited without permission.

COALINGA ASBESTOS - ALLUVIAL FAN BORING PROGRAM - AF5



Hole backfilled with native material with 1 foot of bentonite powder every 5 feet and at bottom of hole.

Drilling Company: All Terrain
Driller: B. Dickson
Sampling Method: Continuous core in 2.5' long sections
Date drilled: 2 December 1987
LF Geologist: John DeReamer

EXPLANATION

- Clay (CH)
- Silty Clay (CL)
- Clayey Silt (ML)
- Sandy Silt (SM)
- Lost core interval

* * = Sampled Interval
PLM = Polarized Light Microscopy
ES = Elongate Serpentine Percent
CA = Chrysotile Asbestos Percent
SA = Serpentine Asbestos Percent
TEM = Transmission Electron Microscopy
NA = Not Analyzed
ND = Not Detected

Figure H : LOG OF CONTINUOUSLY-CORED SOIL BORING AF5

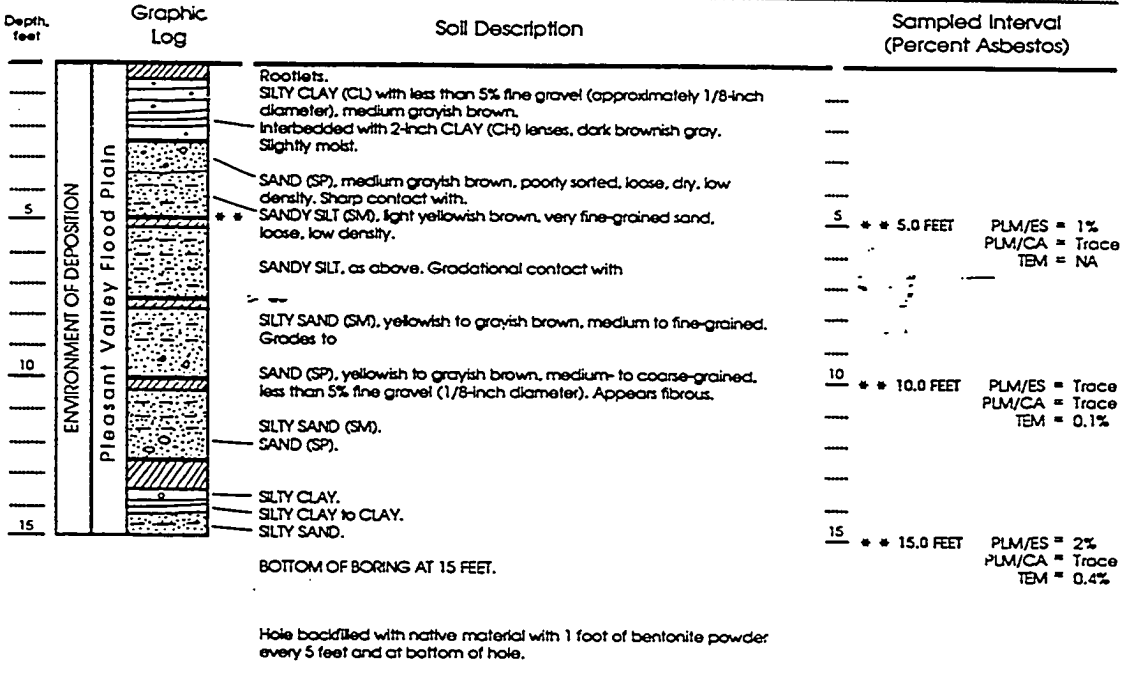
Project No. 1802 Settling Basin Boring Program

LEVINE•FRICKE
CONSULTING ENGINEERS AND HYDROGEOLOGISTS

1802JDR18OCT88em

Reproduced with permission of the copyright owner. Further reproduction prohibited without permission.

COALINGA ASBESTOS - ALLUVIAL FAN BORING PROGRAM - AF6



Hole backfilled with native material with 1 foot of bentonite powder every 5 feet and at bottom of hole.

Drilling Company: All Terrain
Driller: B. Dickson
Sampling Method: Continuous core in 2.5' long sections
Date drilled: 4 December 1987
LF Geologist: John DeReamer

EXPLANATION

- Clay (CH)
- Silty Clay (CL)
- Silty Sand (SM)
- Sand (SP)
- Lost core interval

* * = Sampled Interval
PLM = Polarized Light Microscopy
ES = Elongate Serpentine Percent
CA = Chrysotile Asbestos Percent
SA = Serpentine Asbestos Percent
TEM = Transmission Electron Microscopy
NA = Not Analyzed
ND = Not Detected

Figure 1 : LOG OF CONTINUOUSLY-CORED SOIL BORING AF6

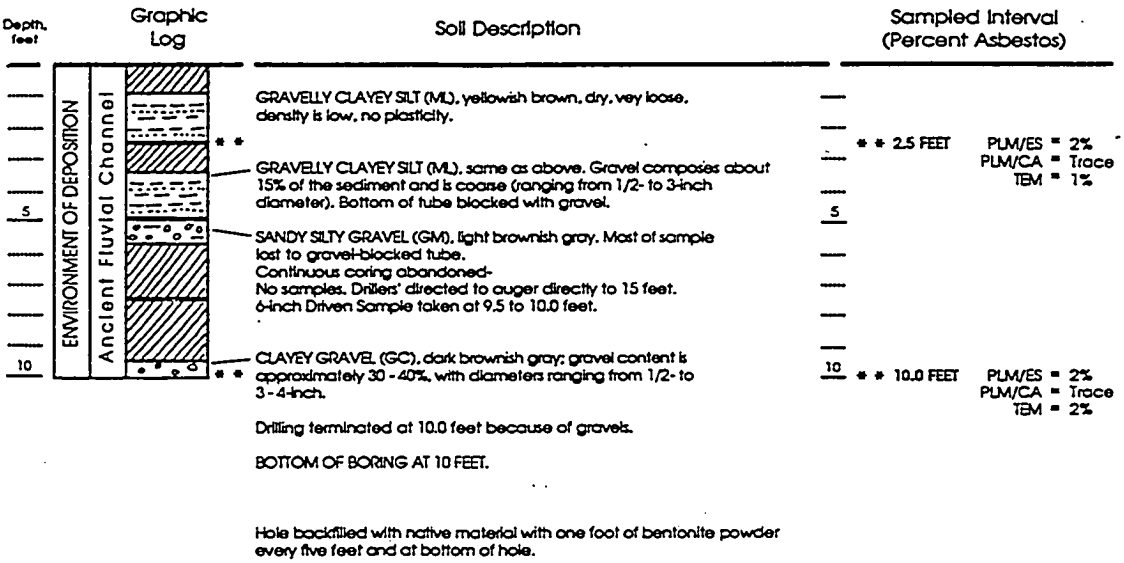
Project No. 1802 Settling Basin Boring Program

LEVINE•FRICKE
CONSULTING ENGINEERS AND HYDROGEOLOGISTS

1802JDR18OCT88em

Reproduced with permission of the copyright owner. Further reproduction prohibited without permission.

COALINGA ASBESTOS - ALLUVIAL FAN BORING PROGRAM - AF7



Drilling Company: All Terrain
Driller: B. Dickson
Sampling Method: Continuous core in 2.5' long sections
Date drilled: 4 December 1987
LF Geologist: John DeRearmer

EXPLANATION

- Gravelly Clayey Silt (ML)
- Sandy Silty Gravel (GM)
- Clayey Gravel (GC)
- Lost core interval

* * = Sampled Interval
PLM = Polarized Light Microscopy
ES = Elongate Serpentine Percent
CA = Chrysotile Asbestos Percent
SA = Serpentine Asbestos Percent
TEM = Transmission Electron Microscopy
NA = Not Analyzed
ND = Not Detected

Figure J : LOG OF CONTINUOUSLY-CORED SOIL BORING AF7

Project No. 1802 Settling Basin Boring Program

LEVINE•FRICKE
CONSULTING ENGINEERS AND HYDROGEOLOGISTS

1802JDR18OCT88em

Reproduced with permission of the copyright owner. Further reproduction prohibited without permission.

Reproduced with permission of the copyright owner. Further reproduction prohibited without permission.

Table F - 1

TEXTURAL CHARACTERISTICS, DEPOSITIONAL ENVIRONMENTS, AND ASBESTOS RESULTS FROM ALLUVIAL FAN AND SETTLING BASIN SUBSURFACE BORING PROGRAM

Number of Samples	General Textural Characteristics	Alluvial Fan Depositional Environments	Sampled Core Interval		******** Asbestos Results ******** PLM/ES	PLH/CA	TEM
11	Silty Clay to Clay Silty Clay	Sheet Flood Deposits	AF1-0.3		1 %	TR	NA
			AF1-5.3		2 %	TR	NA
			AF2-1.5		TR	TR	NA
			AF2-5.0		TR	TR	2 %
			AF2-10.0		TR.	TR	3 %
			AF2-15.0		TR	TR	NA
			AF3-2.5		2 %	TR	NA
			AF3-7.5		3 %	TR	2 %
			AF3-13.3		2 %	TR	4 %
			AF4-15.0		TR	TR	2 %
			AF5-10.0		TR	ND	NA
				Average	1.2 %	TR	2.6 %
19	Clayey Silt Clayey Fine Sand Silty Sand	Distal Overbank, Distal Alluvial Channel, and Crevasse Splay Deposits	SB1-32.5		TR	TR	3 %
			SB1-39.9	(Duplicate)	TR	ND	1 %
			SB1-40.0	(Duplicate)	TR	ND	0.5 %
			SB2-35.0		2 %	TR	1 %
			SB3-15.0	(Quadruplicate)	TR	TR	4 %
			SB3-15.1	(Quadruplicate)	TR	TR	1 %
			SB3-15.2	(Quadruplicate)	TR	TR	6 %
			SB3-15.3	(Quadruplicate)	TR	TR	1 %
			SB3-19.7		TR	TR	5 %
			SB3-28.7		3 %	2 %	1 %
			AF1-14.5		TR	TR	3 %
			AF3-7.5		3 %	TR	2 %
			AF3-25.0		TR	TR	10 %

Reproduced with permission of the copyright owner. Further reproduction prohibited without permission.

TEXTURAL CHARACTERISTICS, DEPOSITIONAL ENVIRONMENTS, AND ASBESTOS RESULTS FROM ALLUVIAL FAN AND SETTLING BASIN SUBSURFACE BORING PROGRAM

Number of Samples	General Textural Characteristics	Alluvial Fan Depositional Environments	Sampled Core Interval		******** Asbestos Results ******** PLM/ES	PLM/CA	TEM
(continued)	Clayey Silt Clayey Fine Sand Silty Sand	Distal Overbank, Distal Alluvial Channel, and Crevasse Splay Deposits	AF4-5.0		TR	TR	3 %
			AF4-10.0		TR	TR	NA
			AF4-15.0		TR	TR	2 %
			AF4-22.5		TR	TR	2 %
			AF5-2.4	(Duplicate)	TR	ND	3 %
			AF5-2.5	(Duplicate)	TR	TR	4 %
				Average	TR	TR	2.9 %
7	Medium Sand	Proximal Alluvial Channel and Overbank Deposits	SB2-42.5		TR	ND	1.%
			SB3-19.7		TR	TR	5 %
			SB3-27.8		3 %	2 %	1 %
			AF4-22.5		TR	TR	2 %
			AF5-15.0		TR	ND	4 %
			AF5-20.1		2 %	TR	NA
			AF5-20.2		TR	TR	1 %
				Average	1.1 %	TR	2.3 %
2	Clay, Silt, and Sand with Gravel	Fluvial Channel Deposits	AF7-2.5		2 %	TR	1 %
			AF7-10.0		2 %	TR	2 %
				Average	2 %	TR	1.5 %
3	Clay, Silt, and Fine Sand	Abandoned Channel and Floodplain Deposits	AF6-5.0		1 %	TR	NA
			AF6-10		TR	TR	0.1 %
			AF6-15.0		2 %	TR	0.4 %
				Average	1.2 %	TR	TR
7	Clay, Silt, and Fine Sand	Settling Basin Fill · Flood Water Deposits	SB1-17.5		TR	TR	3 %

Reproduced with permission of the copyright owner. Further reproduction prohibited without permission.

TEXTURAL CHARACTERISTICS, DEPOSITIONAL ENVIRONMENTS, AND ASBESTOS RESULTS FROM ALLUVIAL FAN AND SETTLING BASIN SUBSURFACE BORING PROGRAM

Number of Samples	General Textural Characteristics	Alluvial Fan Depositional Environments	Sampled Core Interval		******** Asbestos Results ******** PLM/ES	PLM/CA	TEM
(continued)	Clay, Silt, and Fine Sand	Settling Basin Fill - Flood Water Deposits	SB2-15.0		TR	TR	1 %
			SB2-15.0		TR	TR	4 %
			SB3-6.7	(Quadruplicate)	TR	TR	2 %
			SB3-6.8	(Quadruplicate)	TR	TR	4 %
			SB3-6.9	(Quadruplicate)	2 %	1 %	2 %
			SB3-7.0	(Quadruplicate)	TR	TR	3 %
				Average	0.7 %	TR	2.7 %

Notes:
ES = Elongate Sepentine Asbestos
CA = Chrysotile Asbestos

ND = Not detected
TR = Trace, less than 1%
NA = Not Analyzed

SBX-XX = Settling Basin Core Number and Depth of Sampled Interval
AFX-XX = Alluvial Fan Core Number and Depth of Sampled Interval

PLM = Polarized Light Microscopy Analytical Method
TEM = Transmission Electron Microscopy Analytical Method

Textural characteristics are based on field classification of hand samples.

Depositional environments based on interpretation of textural characteristics, bedding characteristics, vertical sequences, and the geometry of alluvial fan deposits. See Boring Logs of Appendix C-3.

Averages were calculated by using a value of 0.5% for trace concentrations (TR), and 0.0% for not detected (ND).

Averages less than 1% were reported as TR.

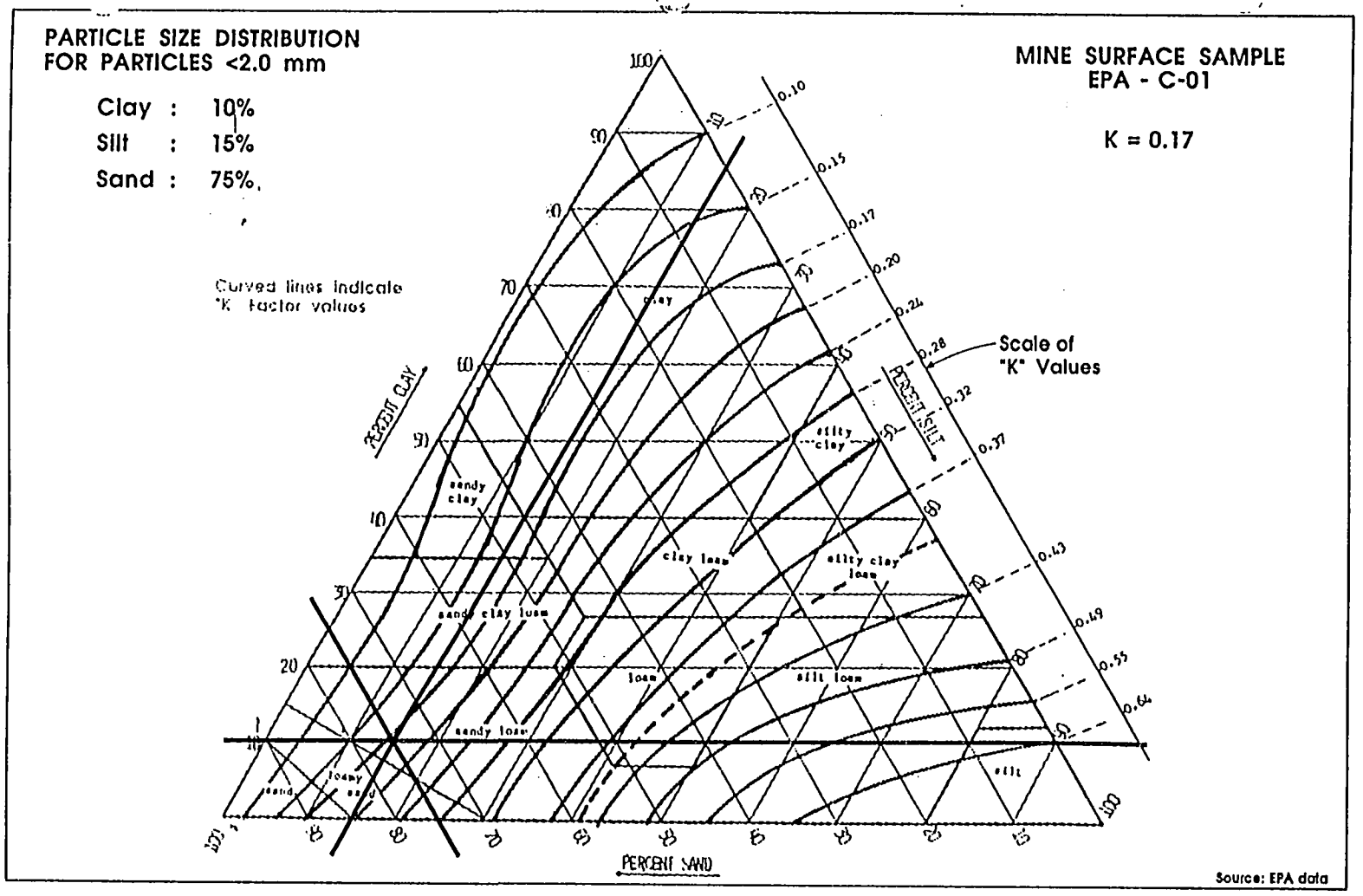
SOURCE: LEVINE-FRICKE

APPENDIX G

K - FACTOR NOMOGRAPHS

Reproduced with permission of the copyright owner. Further reproduction prohibited without permission.

Reproduced with permission of the copyright owner. Further reproduction prohibited without permission.



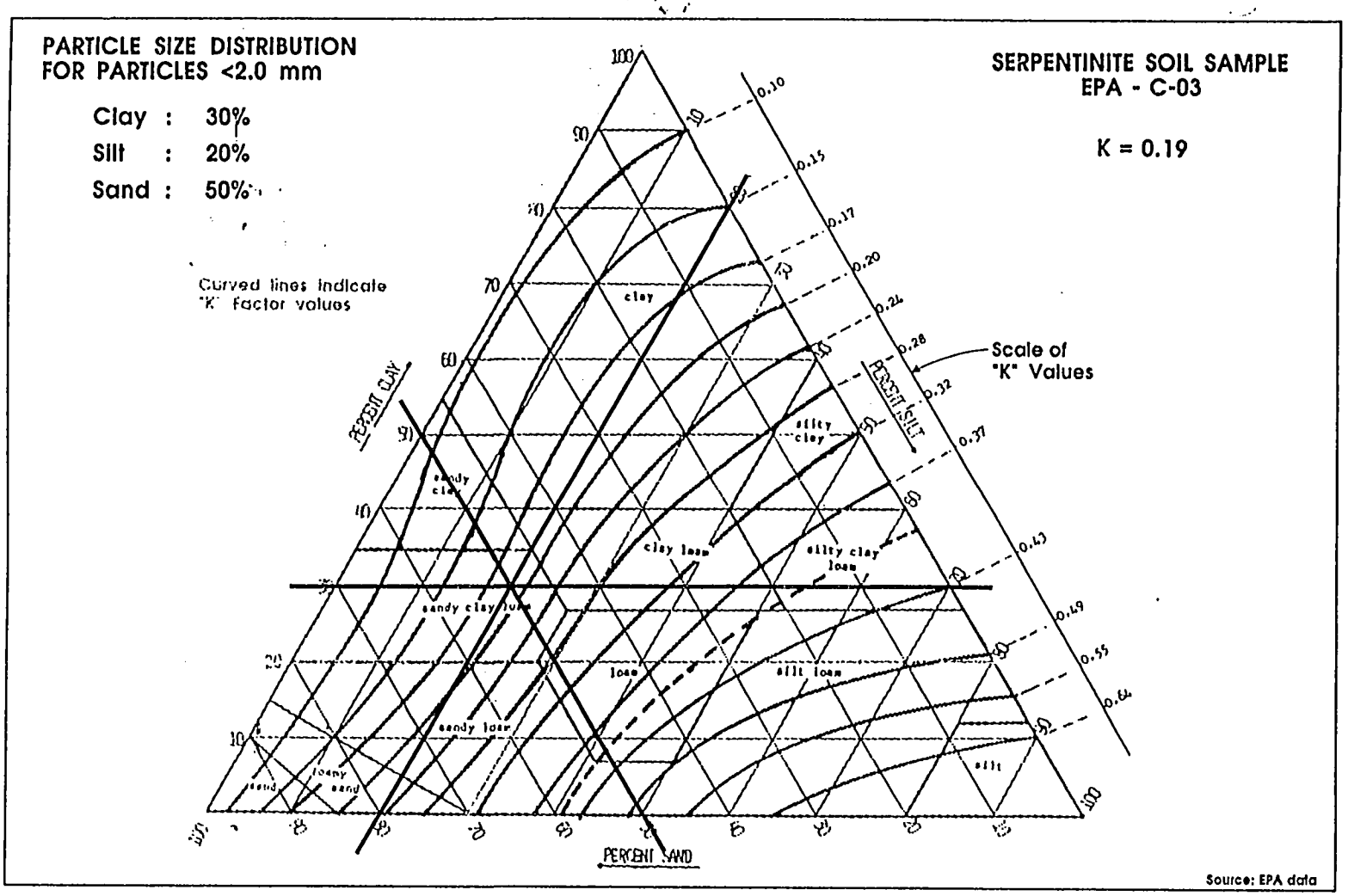
TRIANGULAR NOMOGRAPH METHOD FOR DETERMINING K FACTOR VALUES - SAMPLE EPA - C-01

Project No. 1802

LEVINE • FRICKE
CONSULTING ENGINEERS AND HYDROGEOLOGISTS

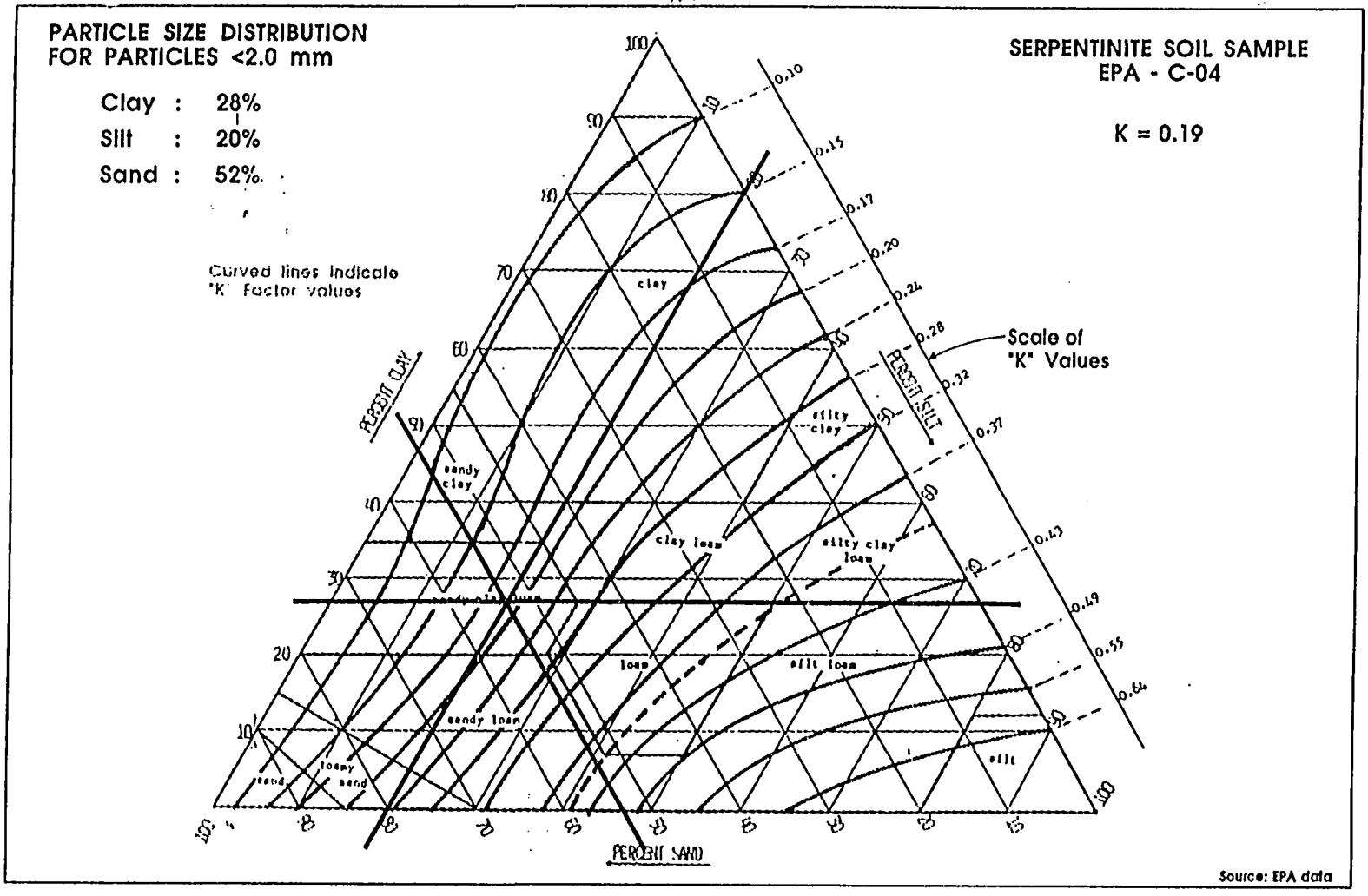
1802JDR24OCT88DT•MSS-EPA

Reproduced with permission of the copyright owner. Further reproduction prohibited without permission.



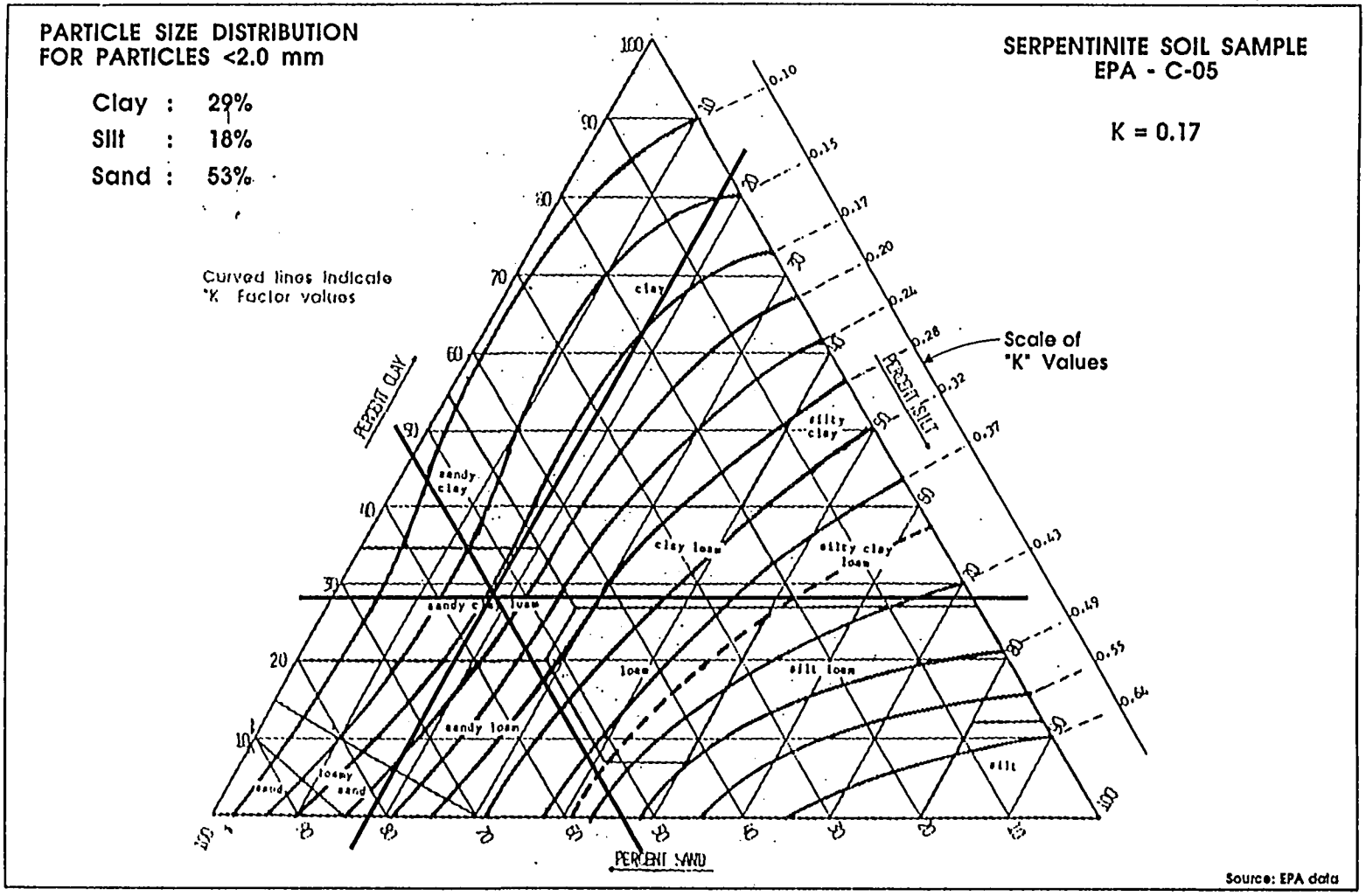
TRIANGULAR NOMOGRAPH METHOD FOR DETERMINING K FACTOR VALUES - SAMPLE EPA - C-03

Reproduced with permission of the copyright owner. Further reproduction prohibited without permission.



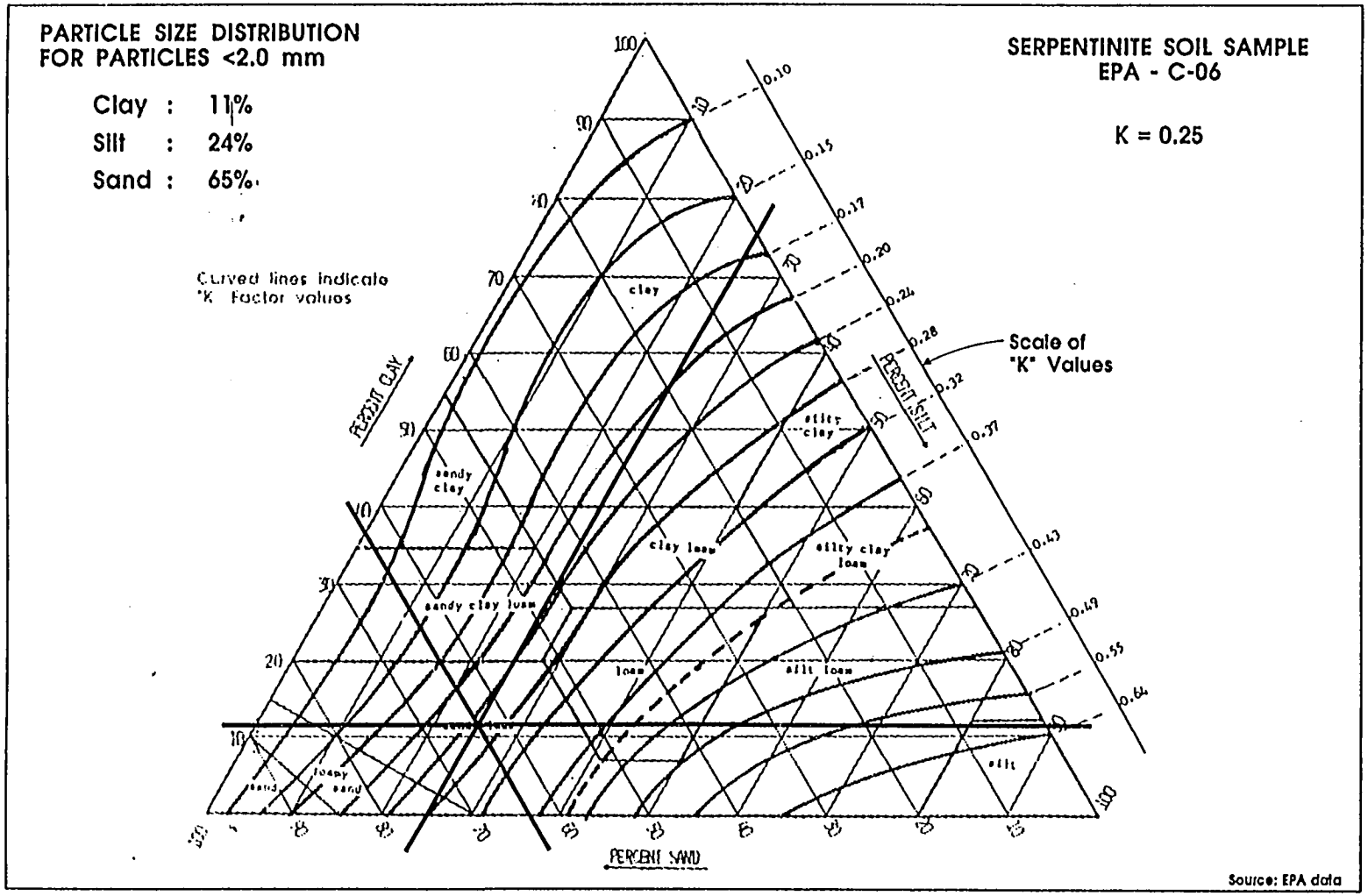
TRIANGULAR NOMOGRAPH METHOD FOR DETERMINING K FACTOR VALUES - SAMPLE EPA - C-04

Reproduced with permission of the copyright owner. Further reproduction prohibited without permission.



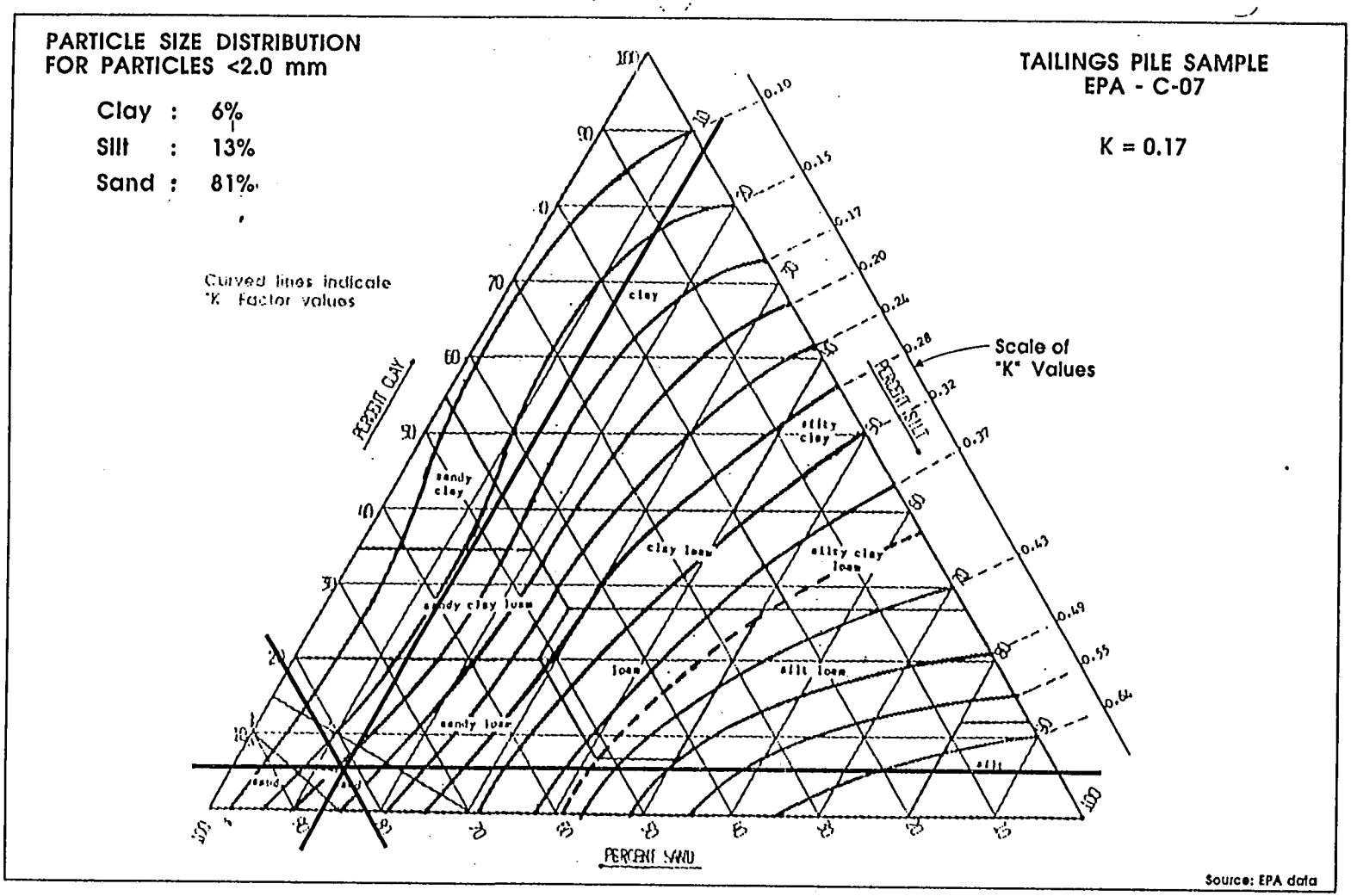
TRIANGULAR NOMOGRAPH METHOD FOR DETERMINING K FACTOR VALUES - SAMPLE EPA - C-05

Reproduced with permission of the copyright owner. Further reproduction prohibited without permission.



TRIANGULAR NOMOGRAPH METHOD FOR DETERMINING K FACTOR VALUES - SAMPLE EPA - C-06

Reproduced with permission of the copyright owner. Further reproduction prohibited without permission.



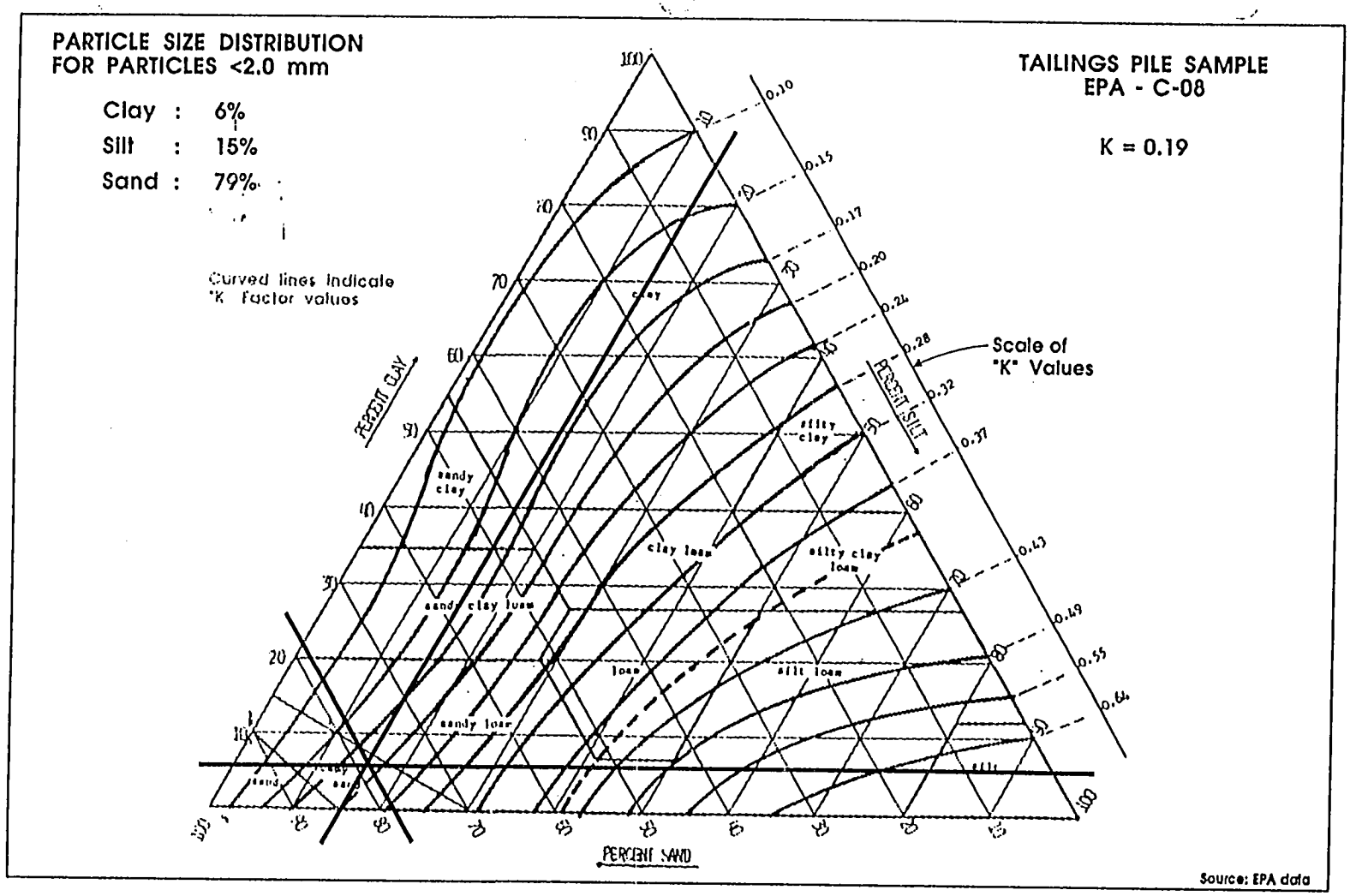
TRIANGULAR NOMOGRAPH METHOD FOR DETERMINING K FACTOR VALUES - SAMPLE EPA - C-07

Project No. 1802

LEVINE • FRICKE
CONSULTING ENGINEERS AND HYDROGEOLOGISTS

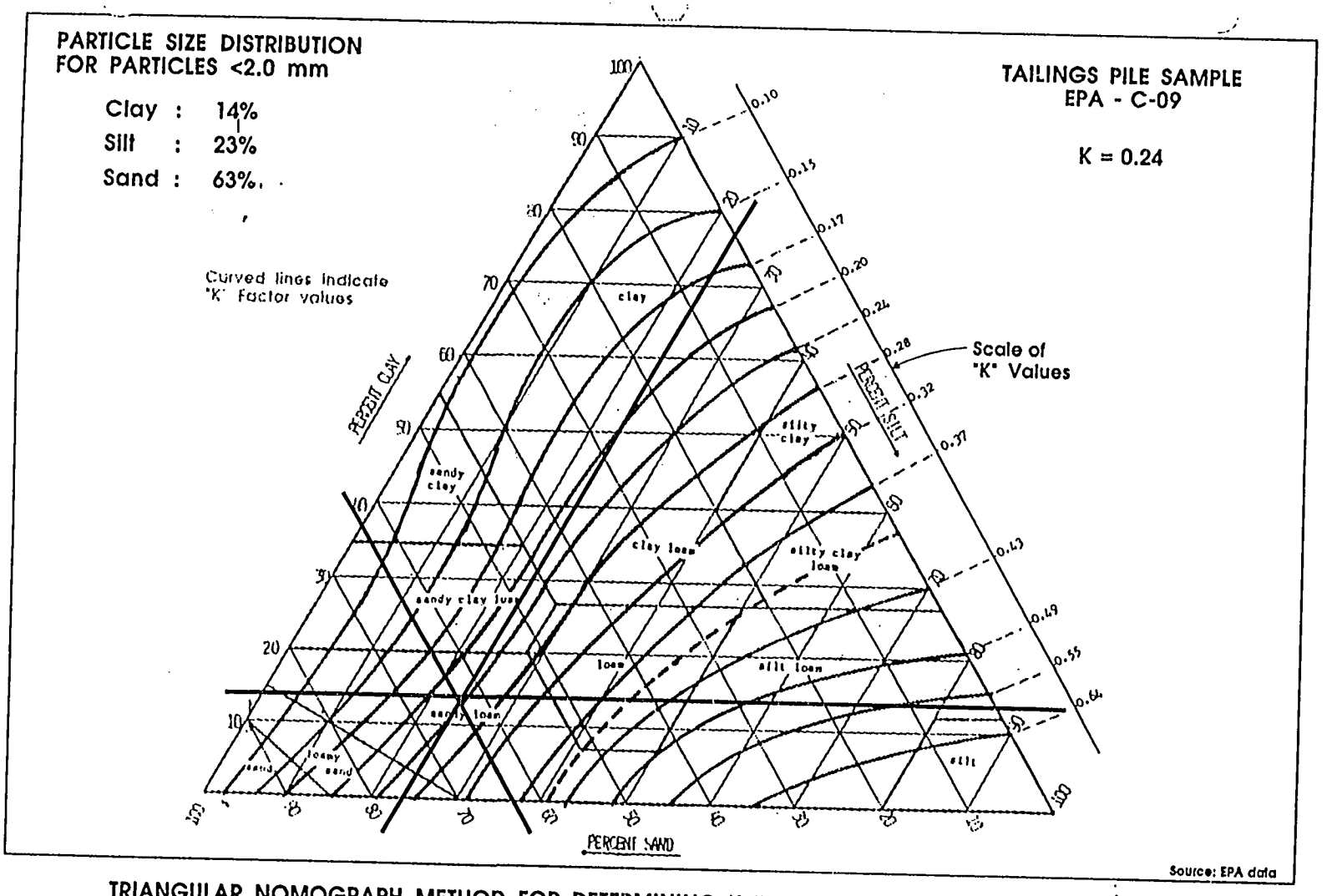
1802JDR24OCT88DT•TPS-EPA

Reproduced with permission of the copyright owner. Further reproduction prohibited without permission.



TRIANGULAR NOMOGRAPH METHOD FOR DETERMINING K FACTOR VALUES - SAMPLE EPA - C-08

Reproduced with permission of the copyright owner. Further reproduction prohibited without permission.



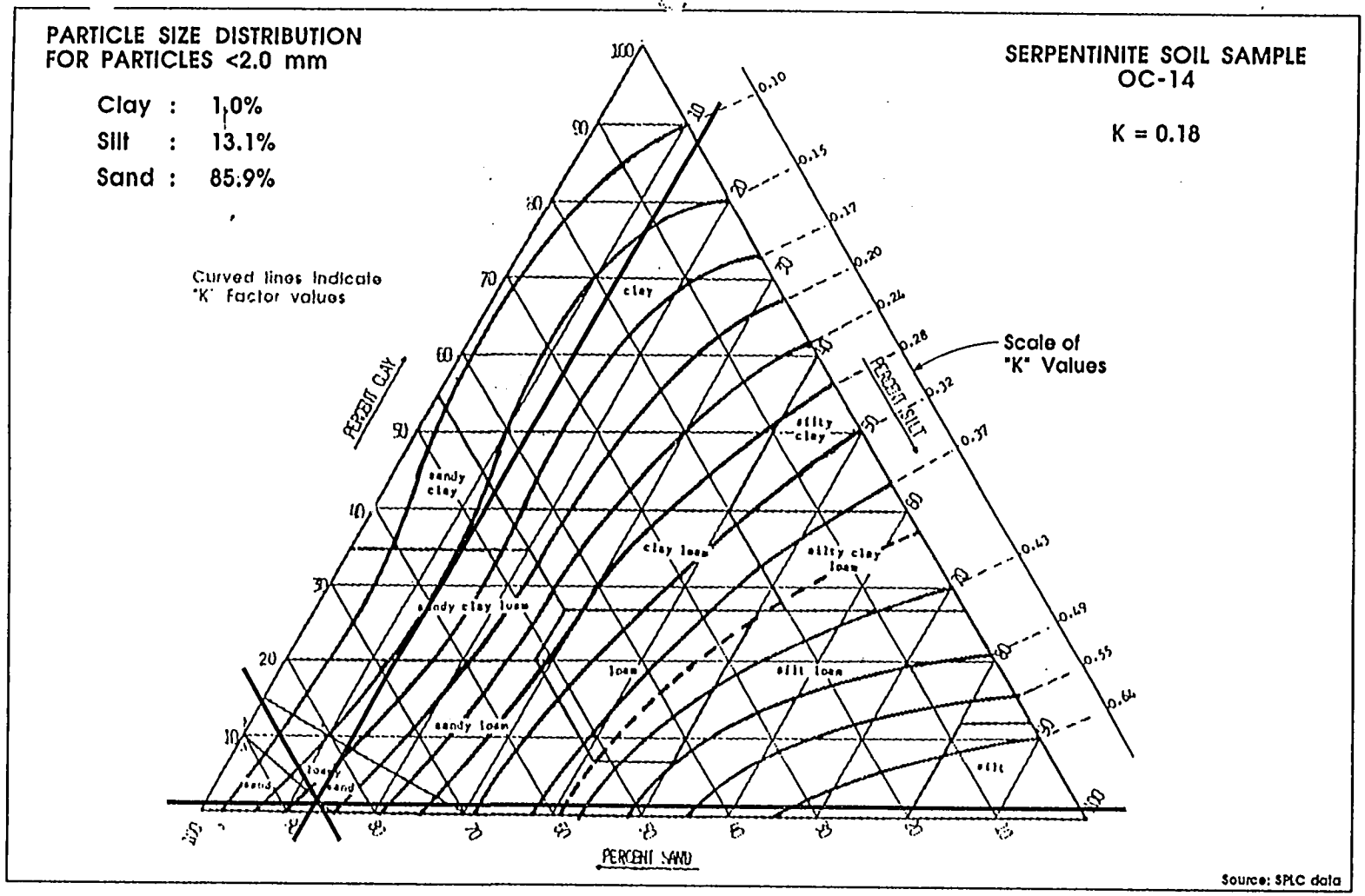
TRIANGULAR NOMOGRAPH METHOD FOR DETERMINING K FACTOR VALUES - SAMPLE EPA - C-09

Project No. 1802

1802JDR24OCT88DT•TPS-EPA

LEVINE • FRICKE
CONSULTING ENGINEERS AND HYDROGEOLOGISTS

Reproduced with permission of the copyright owner. Further reproduction prohibited without permission.



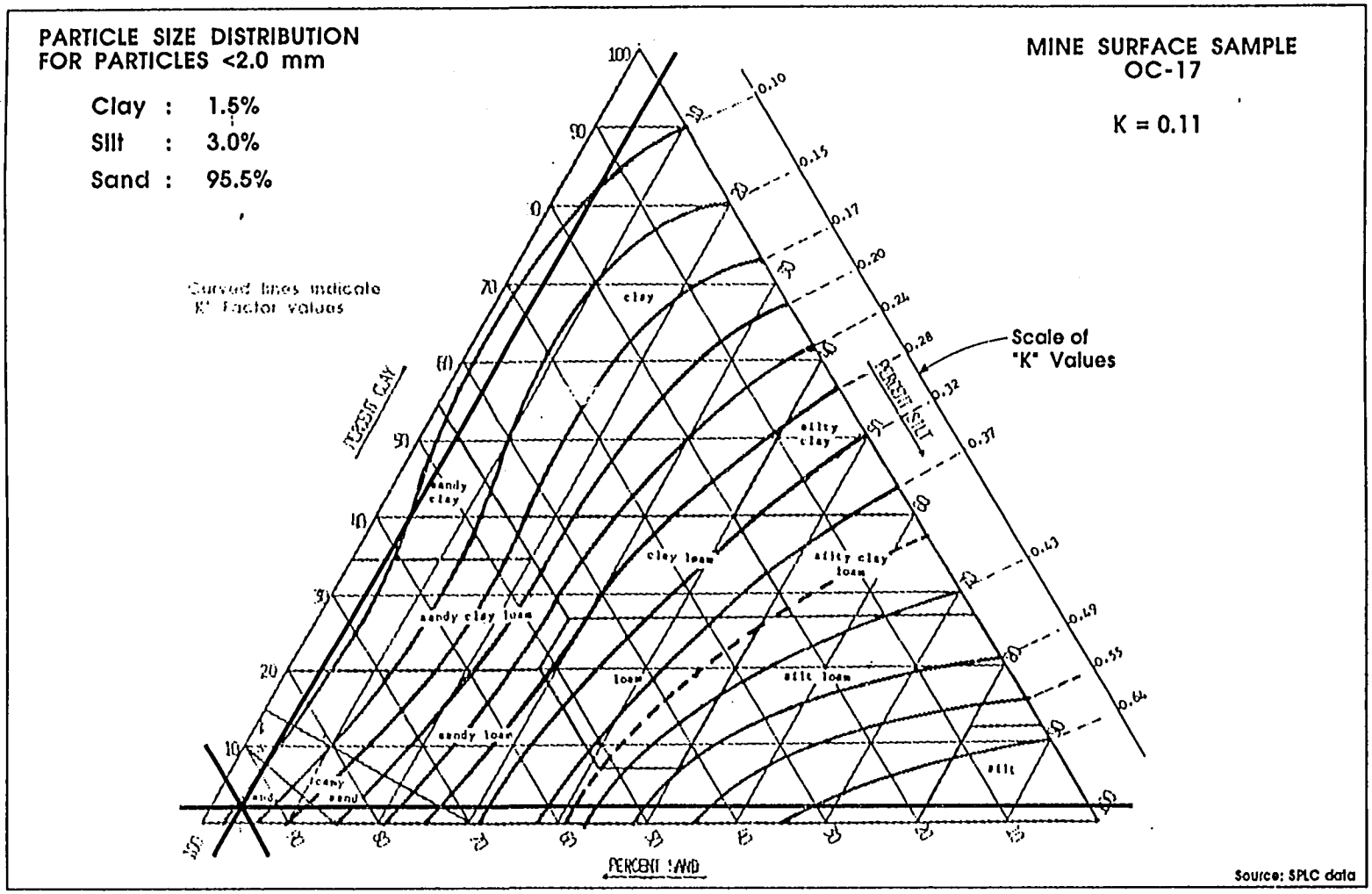
TRIANGULAR NOMOGRAPH METHOD FOR DETERMINING K FACTOR VALUES - SAMPLE OC-14

Project No. 1802

LEVINE • FRICKE
CONSULTING ENGINEERS AND HYDROGEOLOGISTS

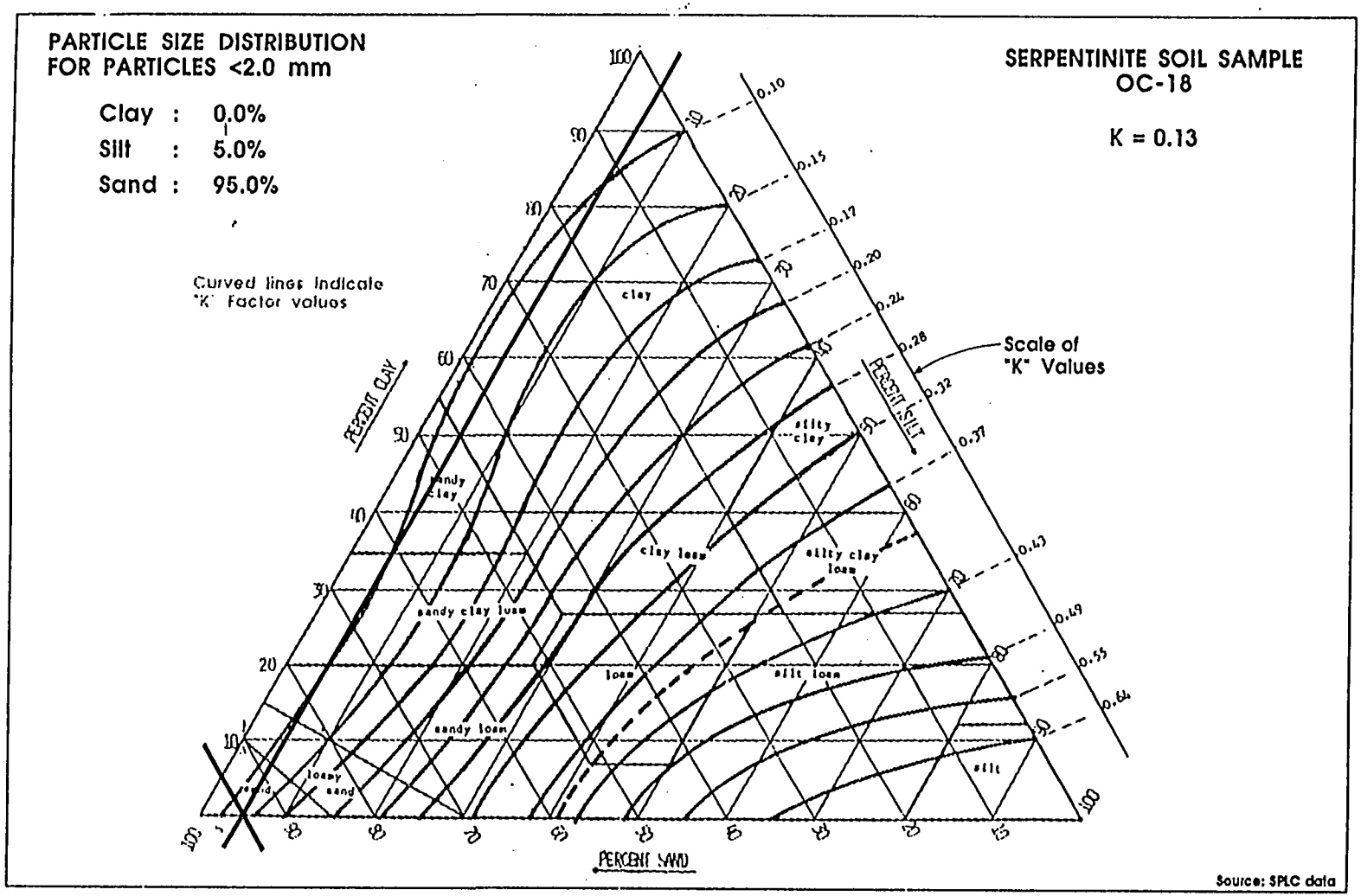
1802JDR24OCT88DT•SSS-OC-SPLC

Reproduced with permission of the copyright owner. Further reproduction prohibited without permission.



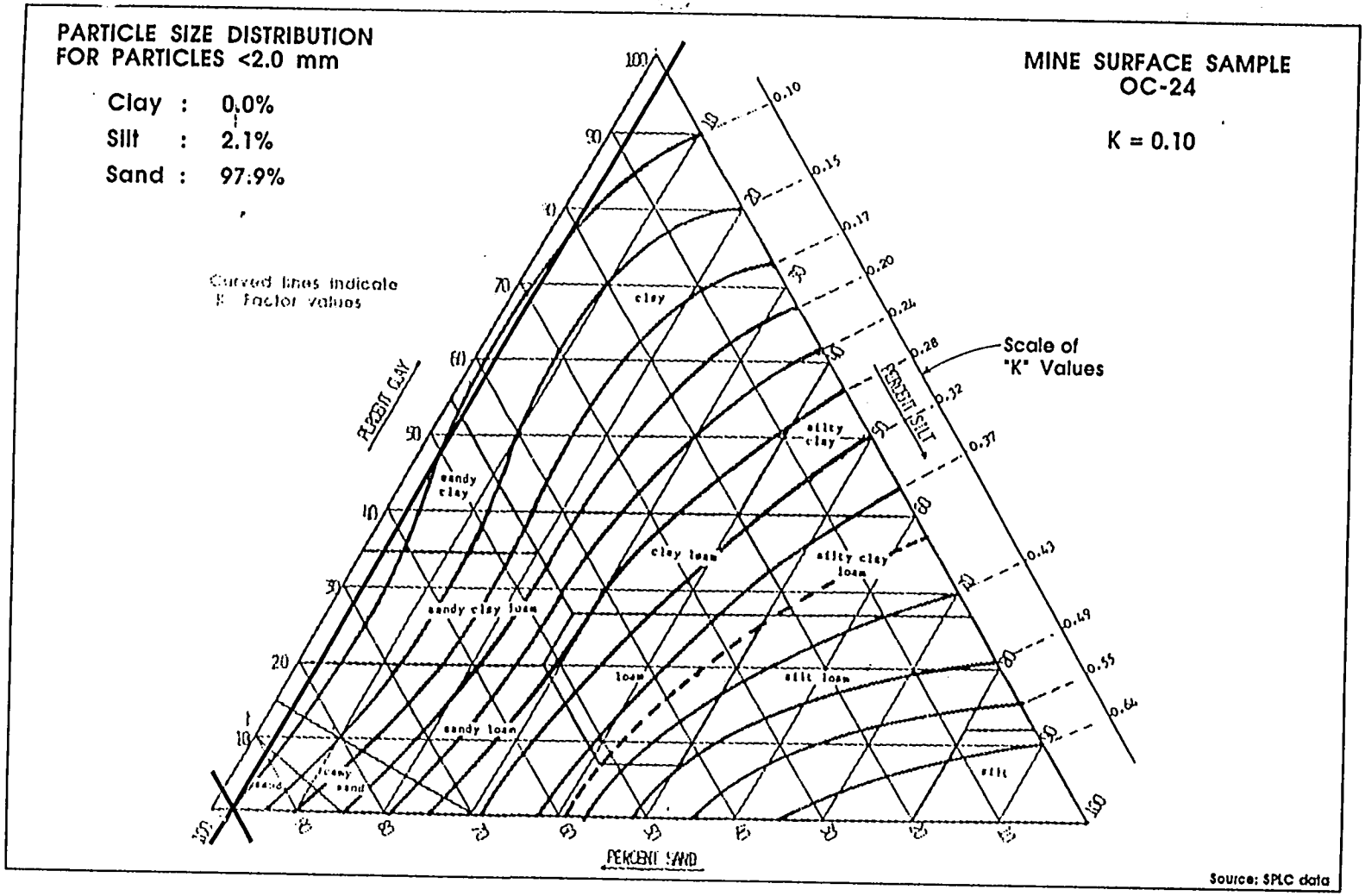
TRIANGULAR NOMOGRAPH METHOD FOR DETERMINING K FACTOR VALUES - SAMPLE OC-17

Reproduced with permission of the copyright owner. Further reproduction prohibited without permission.



TRIANGULAR NOMOGRAPH METHOD FOR DETERMINING K FACTOR VALUES - SAMPLE OC-18

Reproduced with permission of the copyright owner. Further reproduction prohibited without permission.



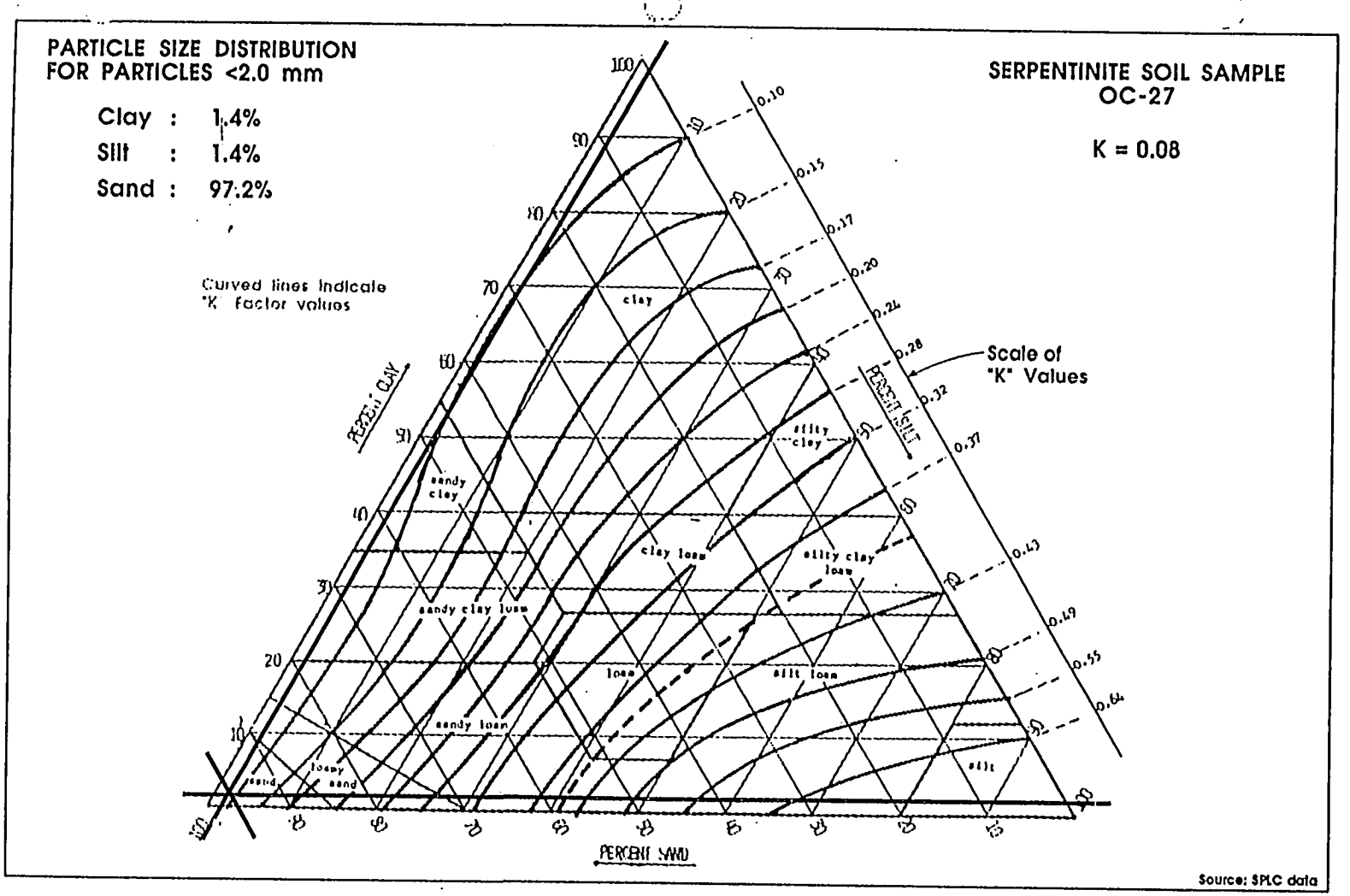
TRIANGULAR NOMOGRAPH METHOD FOR DETERMINING K FACTOR VALUES - SAMPLE OC-24

Project No. 1802

1802JDR24OCT88D1•MSS-OC-SPLC

LEVINE•FRICKE
CONSULTING ENGINEERS AND HYDROGEOLOGISTS

Reproduced with permission of the copyright owner. Further reproduction prohibited without permission.



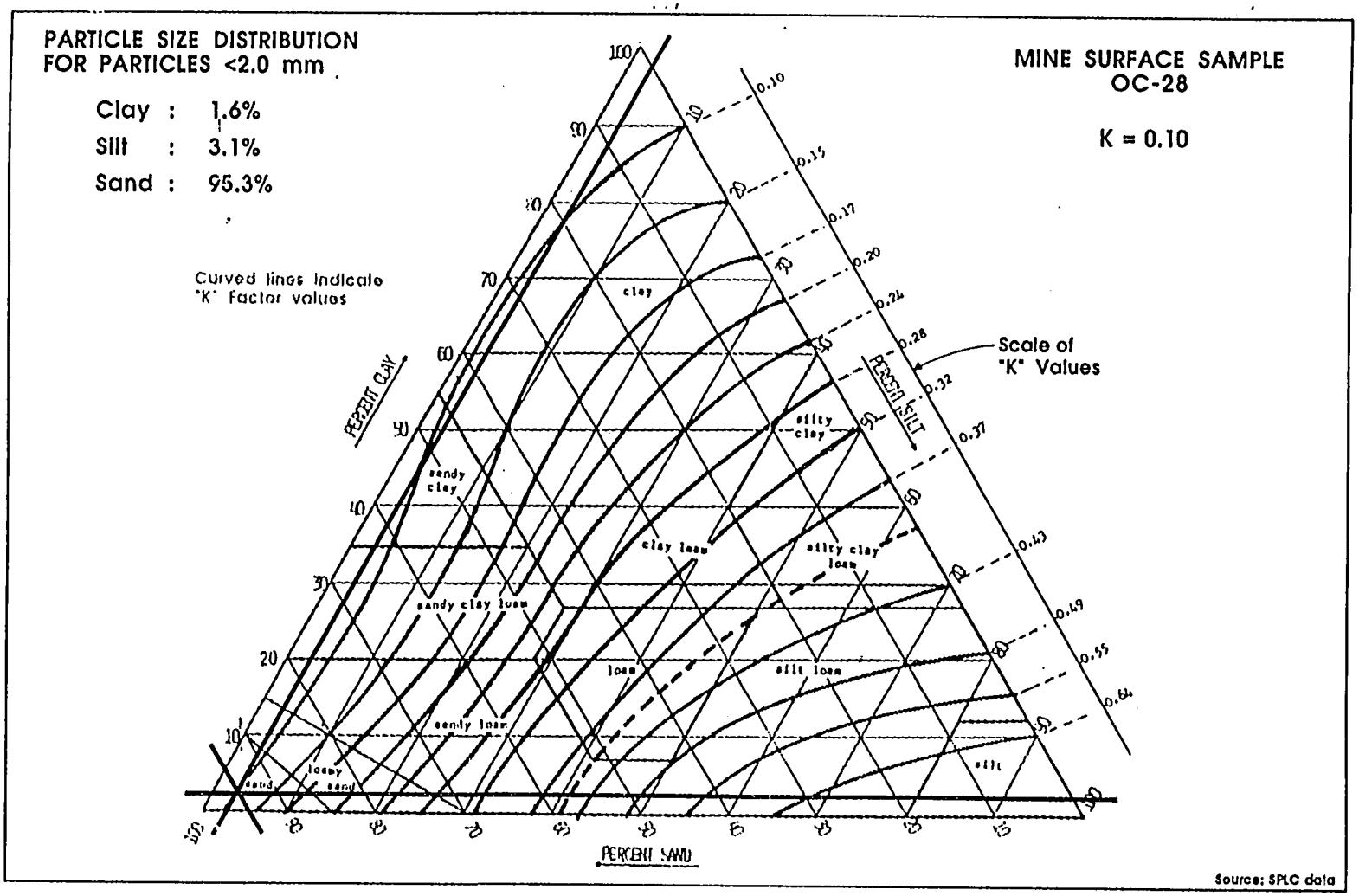
TRIANGULAR NOMOGRAPH METHOD FOR DETERMINING K FACTOR VALUES - SAMPLE OC-27

Project No. 1802

LEVINE • FRICKE
CONSULTING ENGINEERS AND HYDROGEOLOGISTS

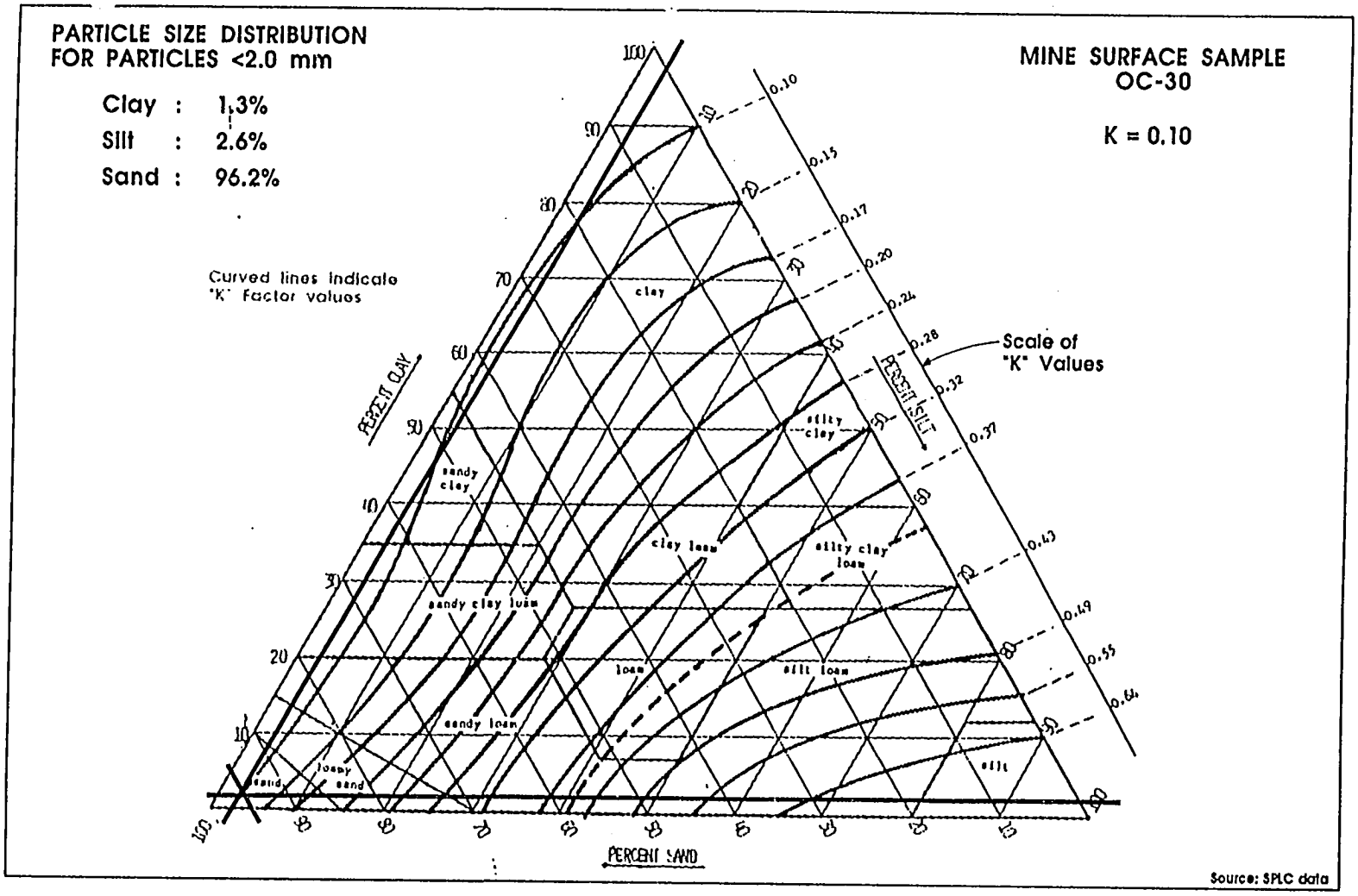
1802JDR24OCT88DT+SSS-OC-SPLC

Reproduced with permission of the copyright owner. Further reproduction prohibited without permission.



TRIANGULAR NOMOGRAPH METHOD FOR DETERMINING K FACTOR VALUES - SAMPLE OC-28

Reproduced with permission of the copyright owner. Further reproduction prohibited without permission.



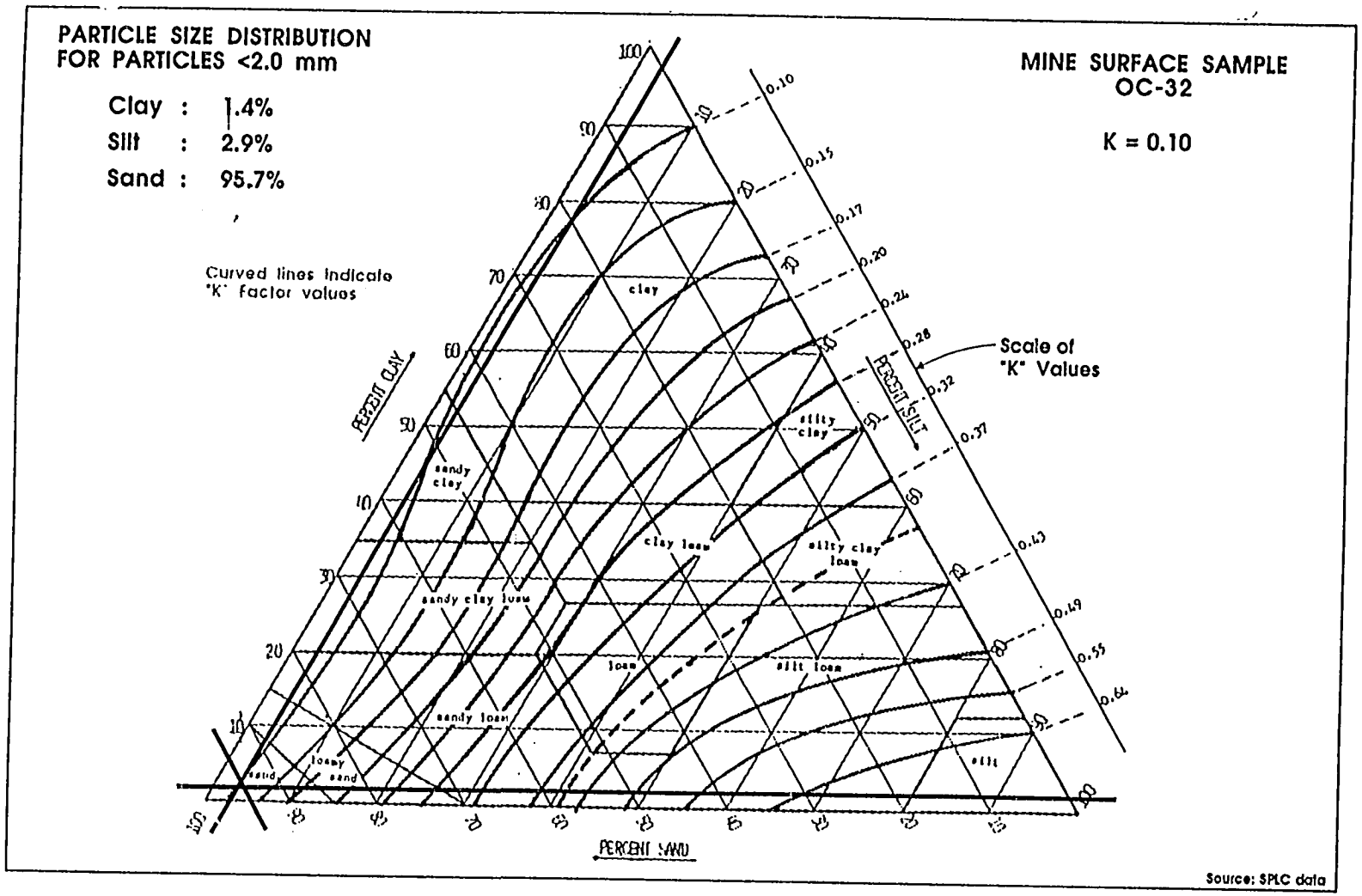
TRIANGULAR NOMOGRAPH METHOD FOR DETERMINING K FACTOR VALUES - SAMPLE OC-30

Project No. 1802

LEVINE•FRICKE
CONSULTING ENGINEERS AND HYDROGEOLOGISTS

1802JDR24OCT88DT•MSS-OC-SPLC

Reproduced with permission of the copyright owner. Further reproduction prohibited without permission.



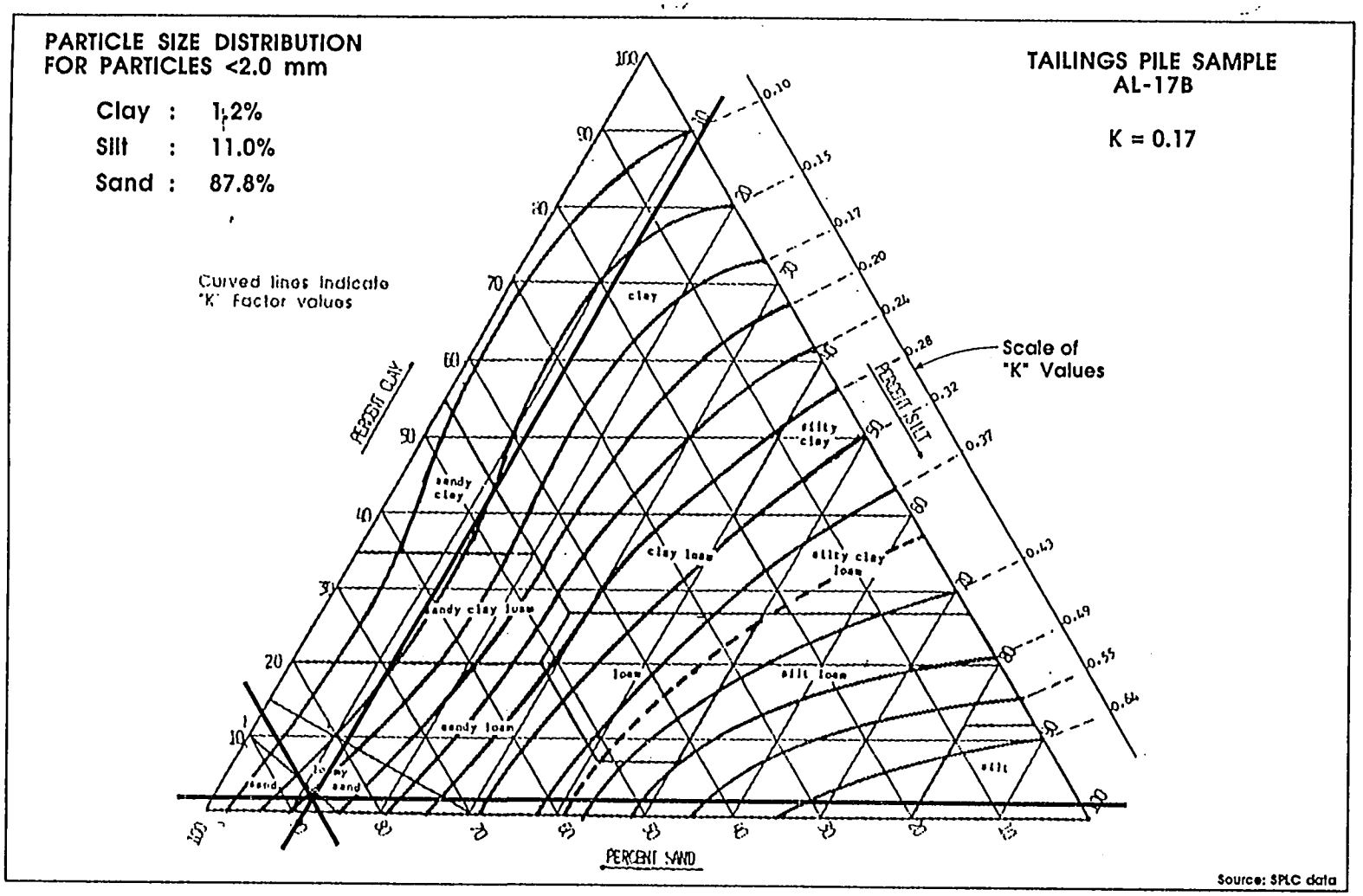
TRIANGULAR NOMOGRAPH METHOD FOR DETERMINING K FACTOR VALUES - SAMPLE OC-32

Project No. 1802

1802JDR24OCT88DT•MSS-OC-SPLC

LEVINE•FRICKE
CONSULTING ENGINEERS AND HYDROGEOLOGISTS

Reproduced with permission of the copyright owner. Further reproduction prohibited without permission.



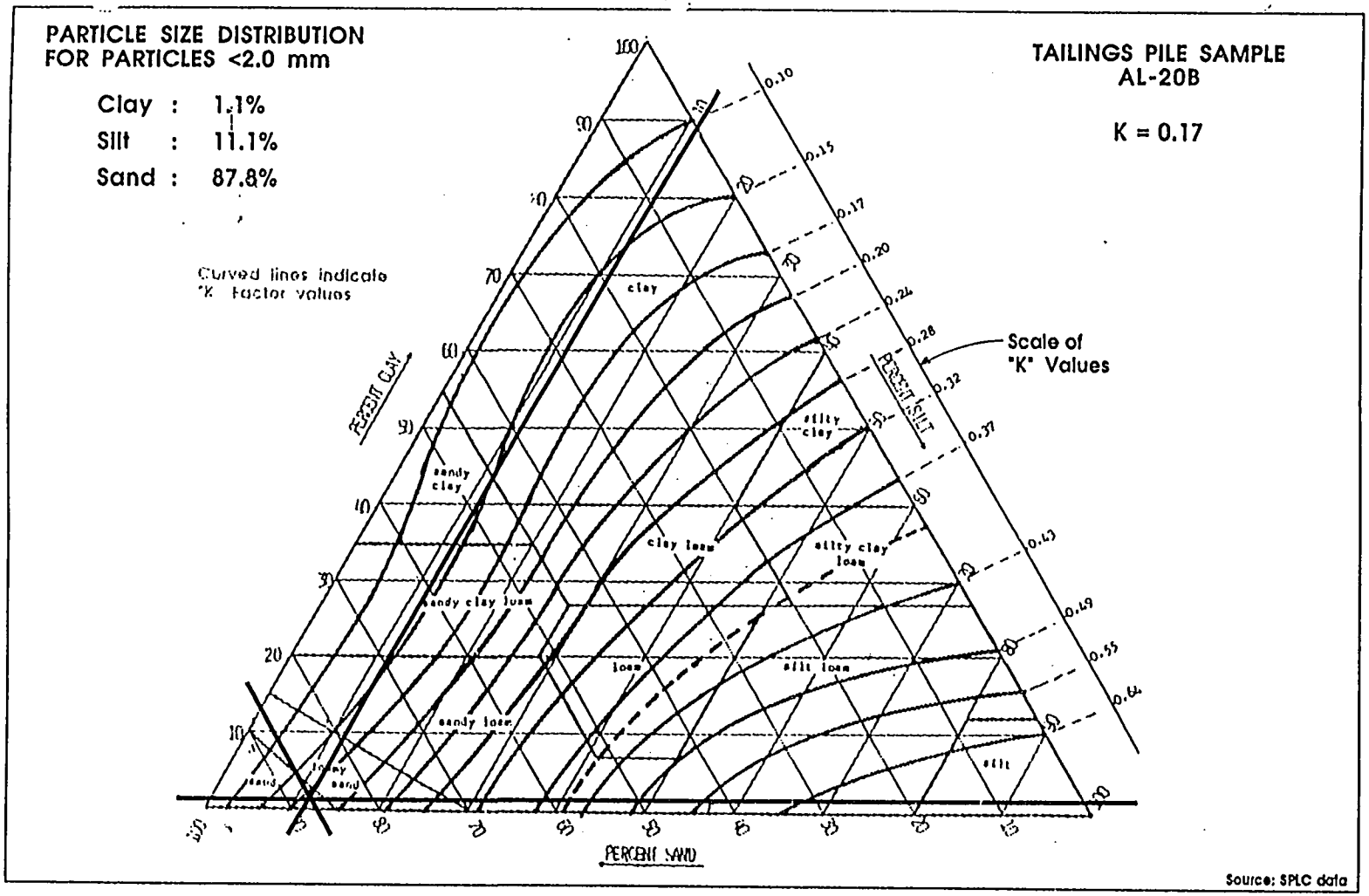
TRIANGULAR NOMOGRAPH METHOD FOR DETERMINING K FACTOR VALUES - SAMPLE AL-17B

Project No. 1802

LEVINE • FRICKE
CONSULTING ENGINEERS AND HYDROGEOLOGISTS

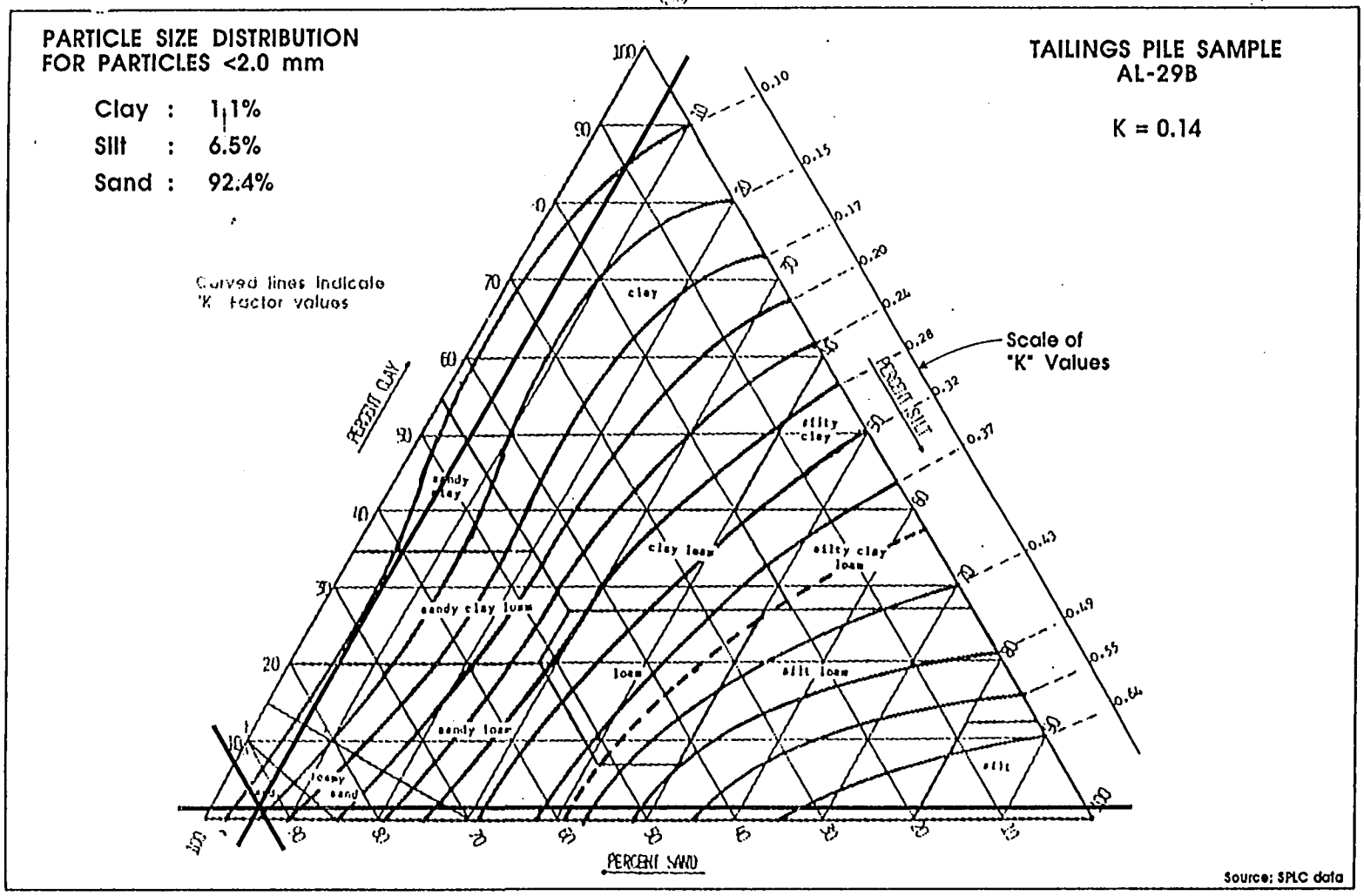
1802JDR24OCT88D1•TP3-AL-SPLC

Reproduced with permission of the copyright owner. Further reproduction prohibited without permission.



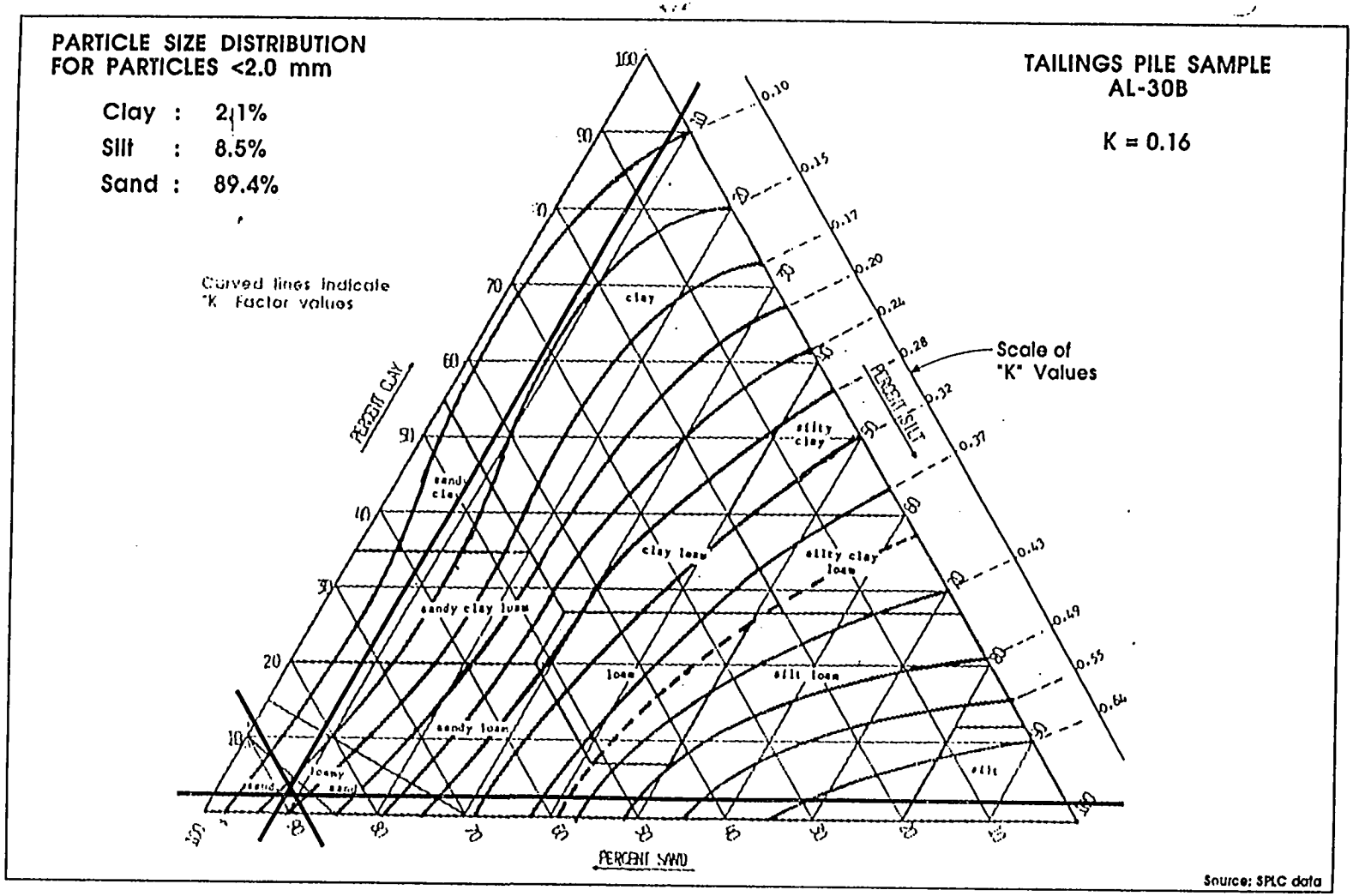
TRIANGULAR NOMOGRAPH METHOD FOR DETERMINING K FACTOR VALUES - SAMPLE AL-20B

Reproduced with permission of the copyright owner. Further reproduction prohibited without permission.



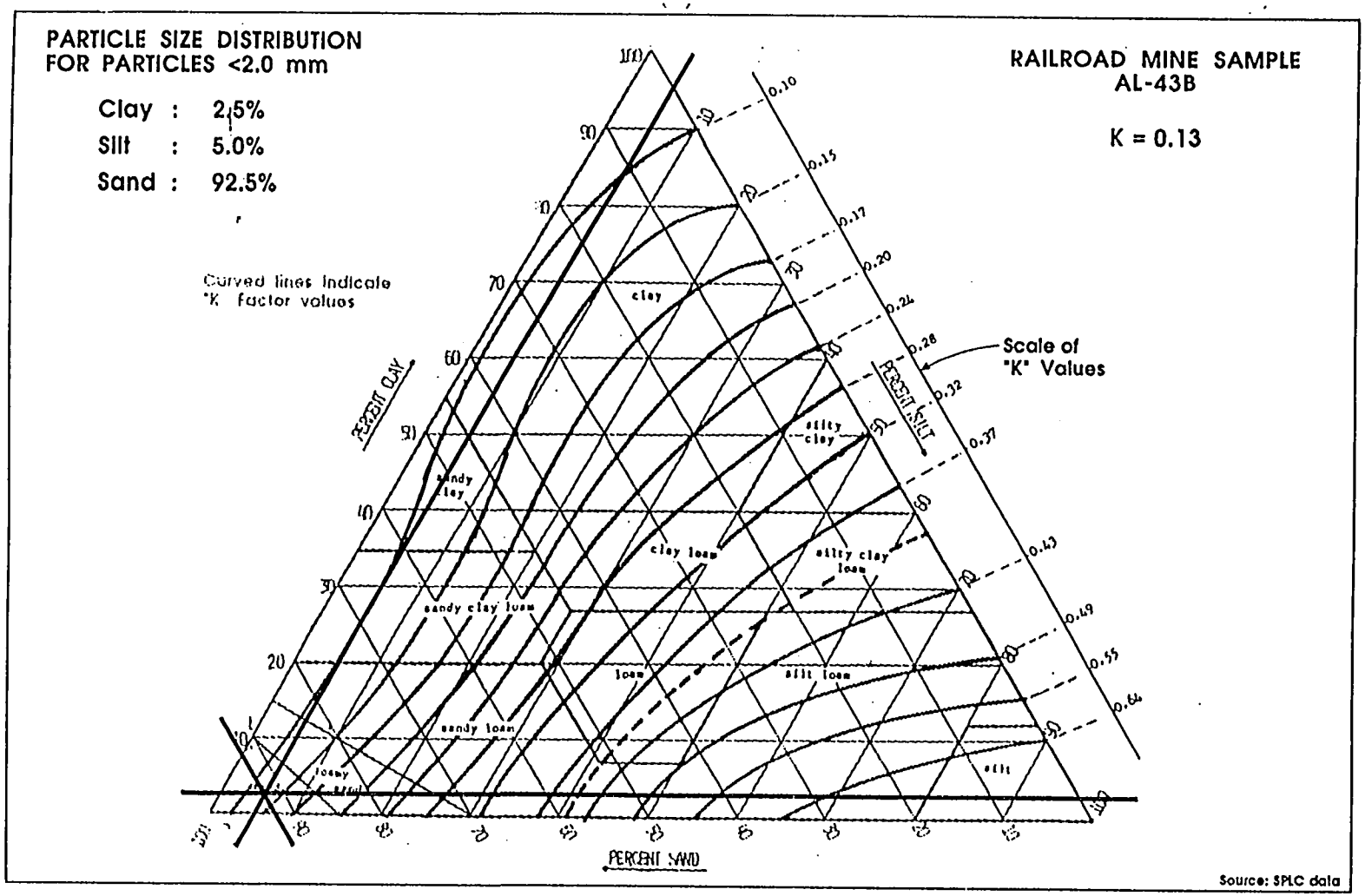
TRIANGULAR NOMOGRAPH METHOD FOR DETERMINING K FACTOR VALUES - SAMPLE AL-29B

Reproduced with permission of the copyright owner. Further reproduction prohibited without permission.



TRIANGULAR NOMOGRAPH METHOD FOR DETERMINING K FACTOR VALUES - SAMPLE AL-30B

Reproduced with permission of the copyright owner. Further reproduction prohibited without permission.



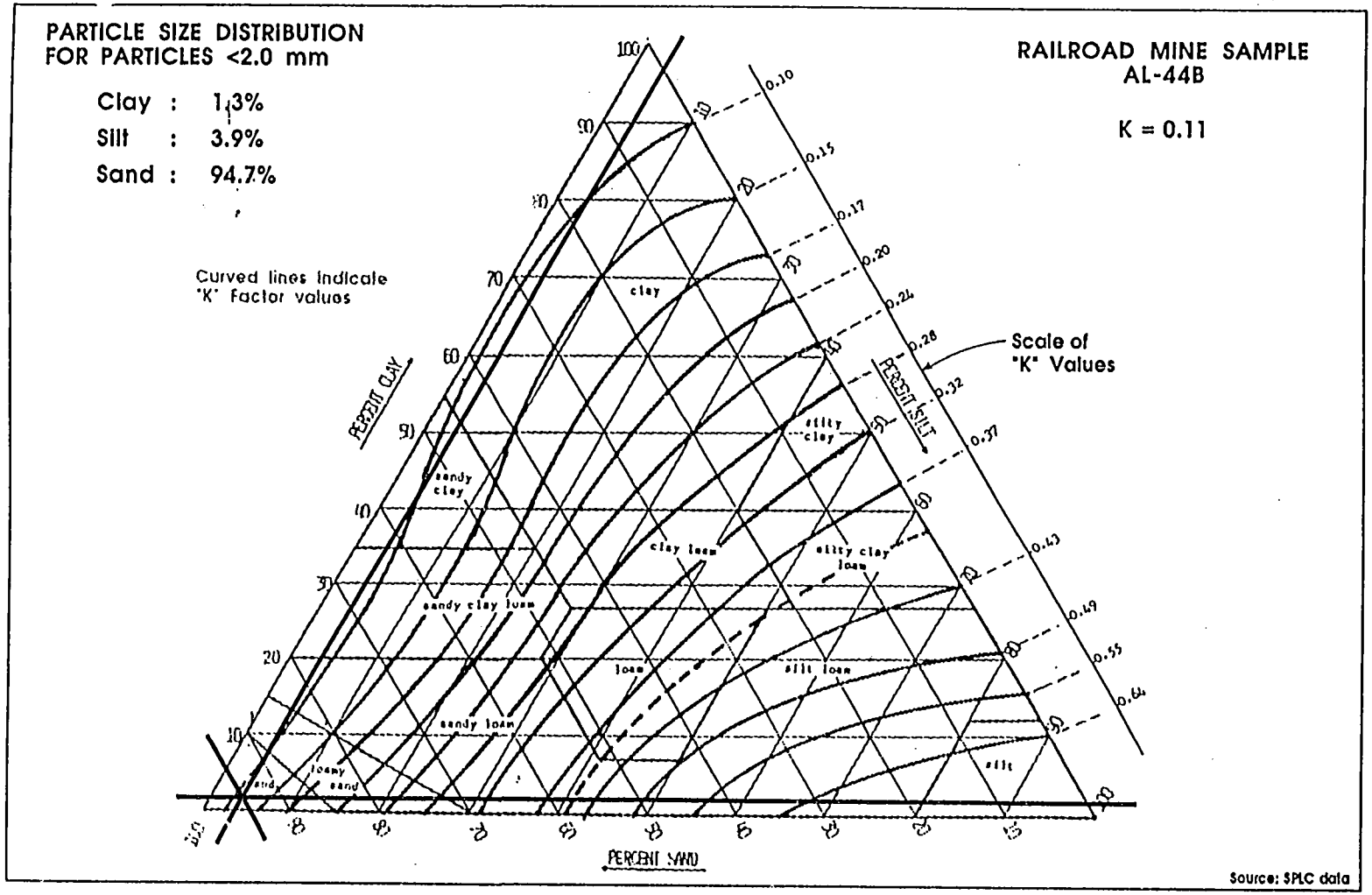
TRIANGULAR NOMOGRAPH METHOD FOR DETERMINING K FACTOR VALUES - SAMPLE AL-43B

Project No. 1802

LEVINE • FRICKE
CONSULTING ENGINEERS AND HYDROGEOLOGISTS

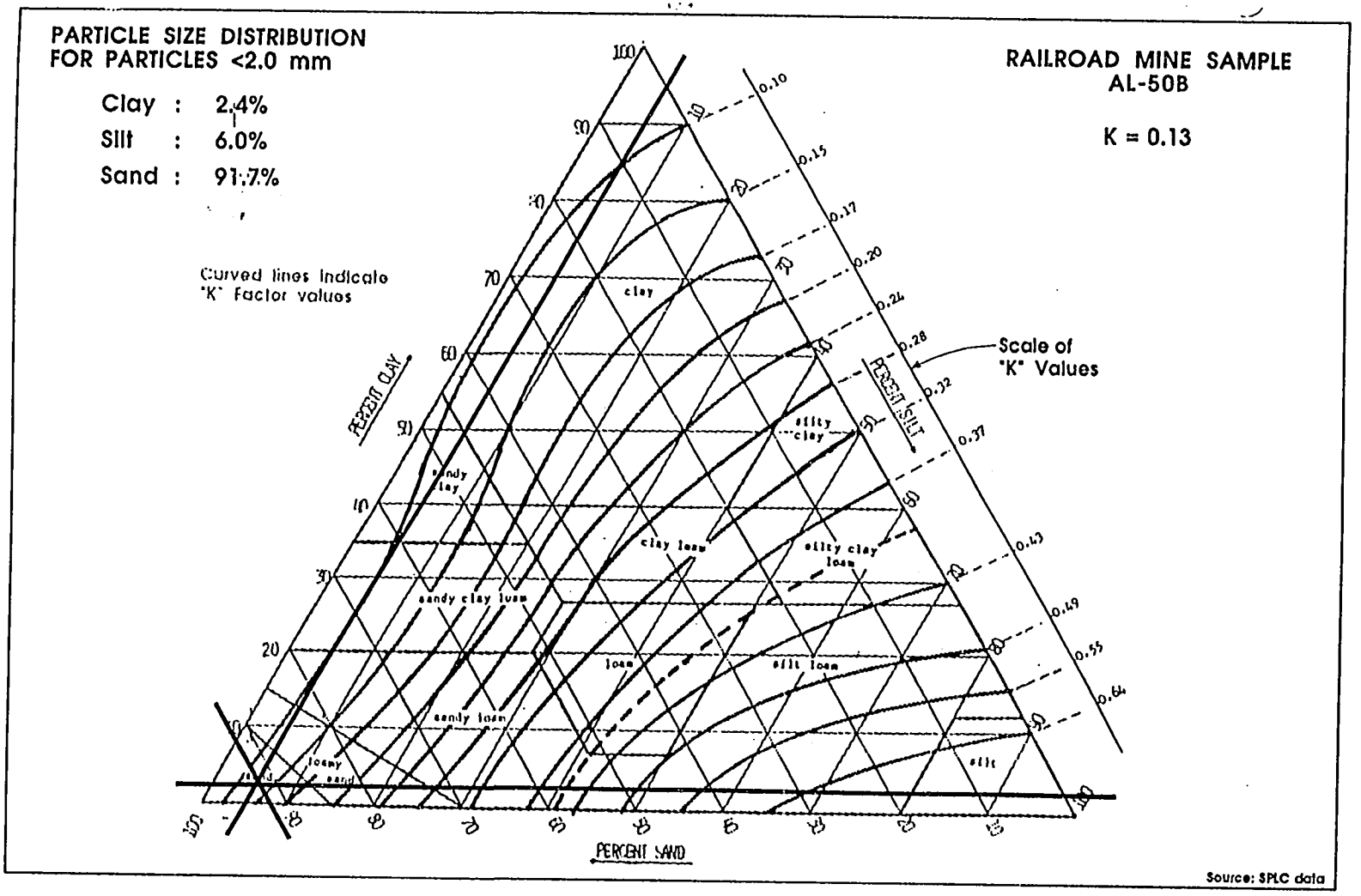
1802JDR24OCT88DT•RM3-AL-SPLC

Reproduced with permission of the copyright owner. Further reproduction prohibited without permission.



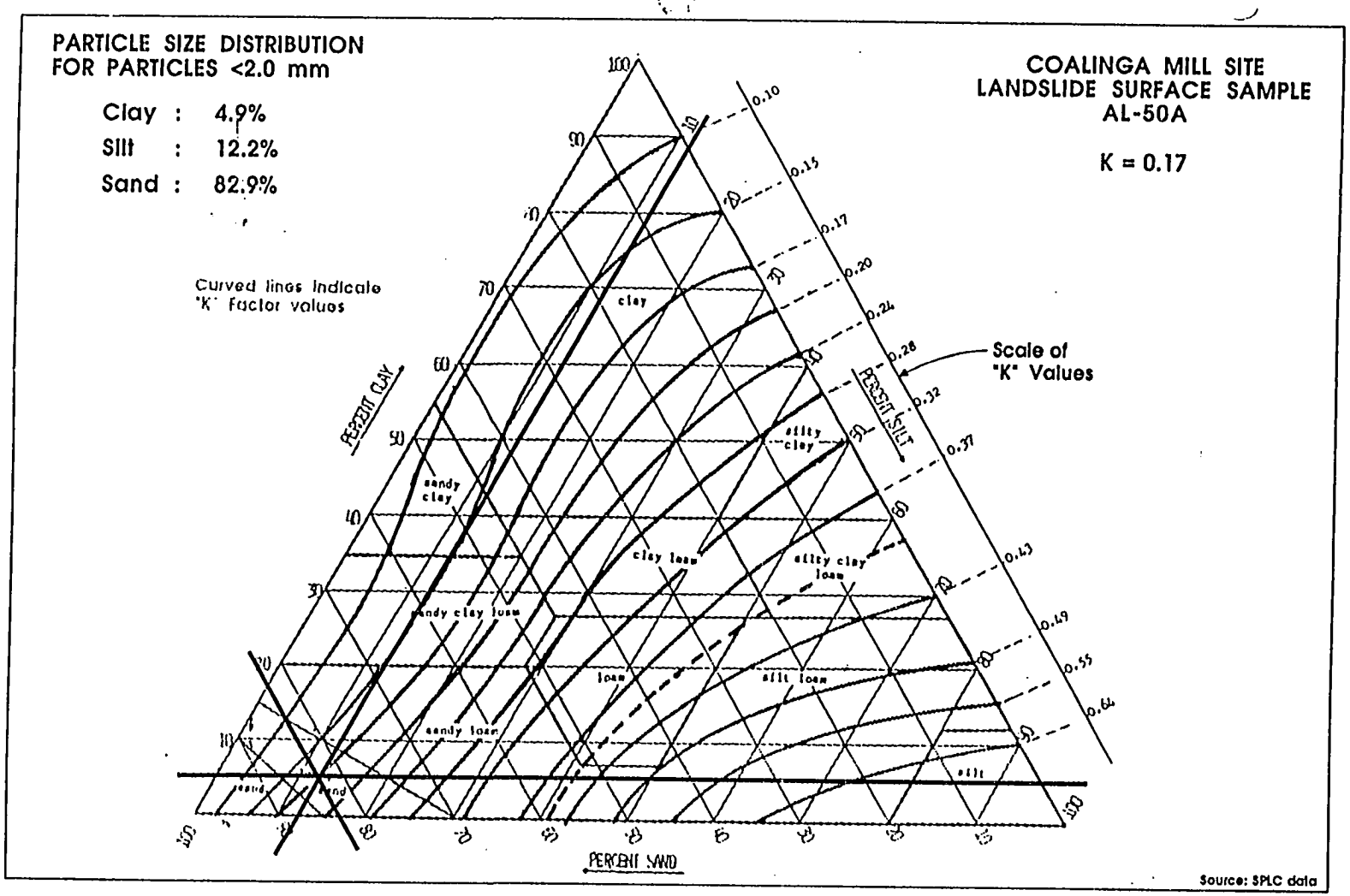
TRIANGULAR NOMOGRAPH METHOD FOR DETERMINING K FACTOR VALUES - SAMPLE AL-44B

Reproduced with permission of the copyright owner. Further reproduction prohibited without permission.



TRIANGULAR NOMOGRAPH METHOD FOR DETERMINING K FACTOR VALUES - SAMPLE AL-50B

Reproduced with permission of the copyright owner. Further reproduction prohibited without permission.



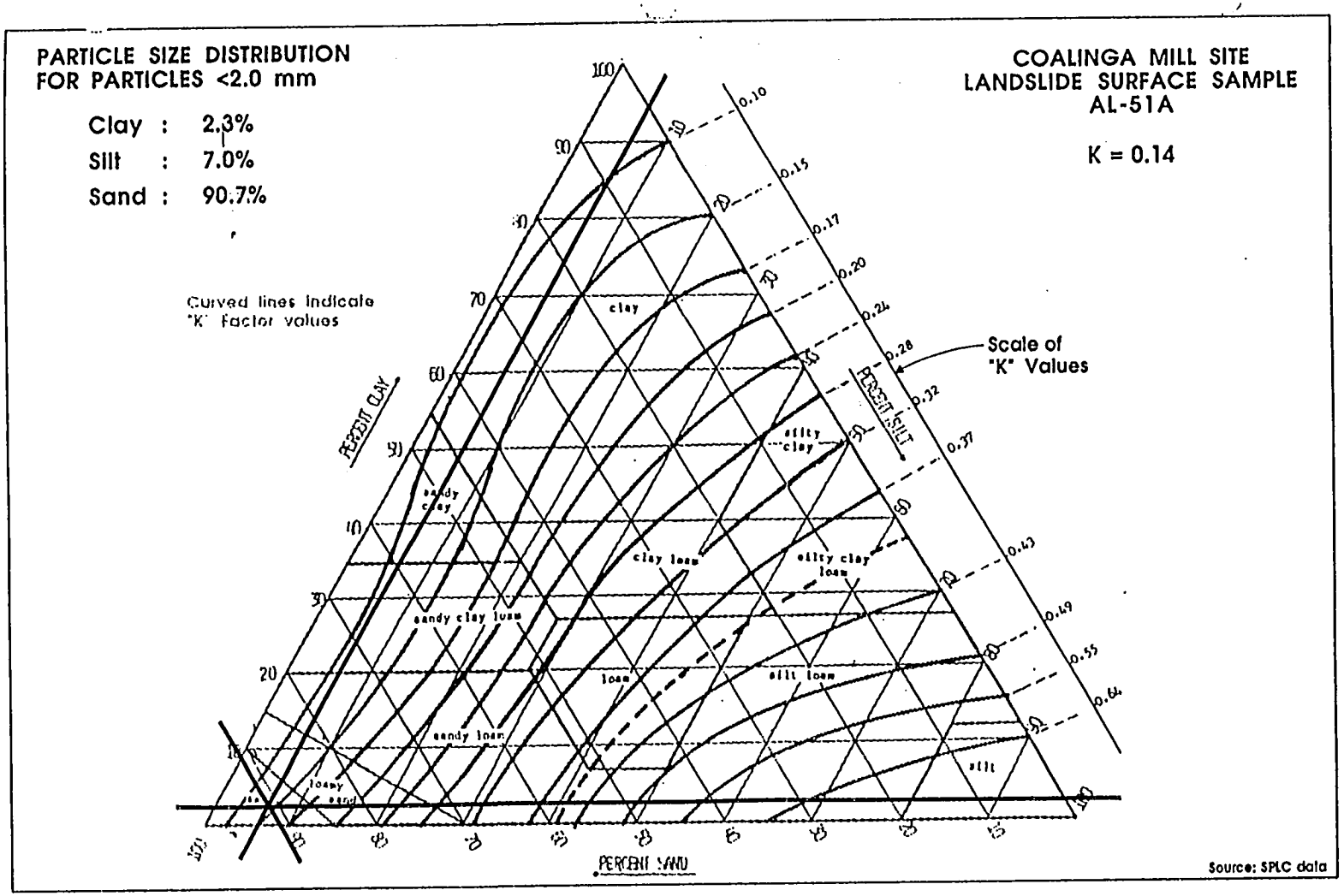
TRIANGULAR NOMOGRAPH METHOD FOR DETERMINING K FACTOR VALUES - SAMPLE AL-50A

Project No. 1802

LEVINE • FRICKE
CONSULTING ENGINEERS AND HYDROGEOLOGISTS

1802JDR24OCT88DT-LSS-SS-SPLC

Reproduced with permission of the copyright owner. Further reproduction prohibited without permission.



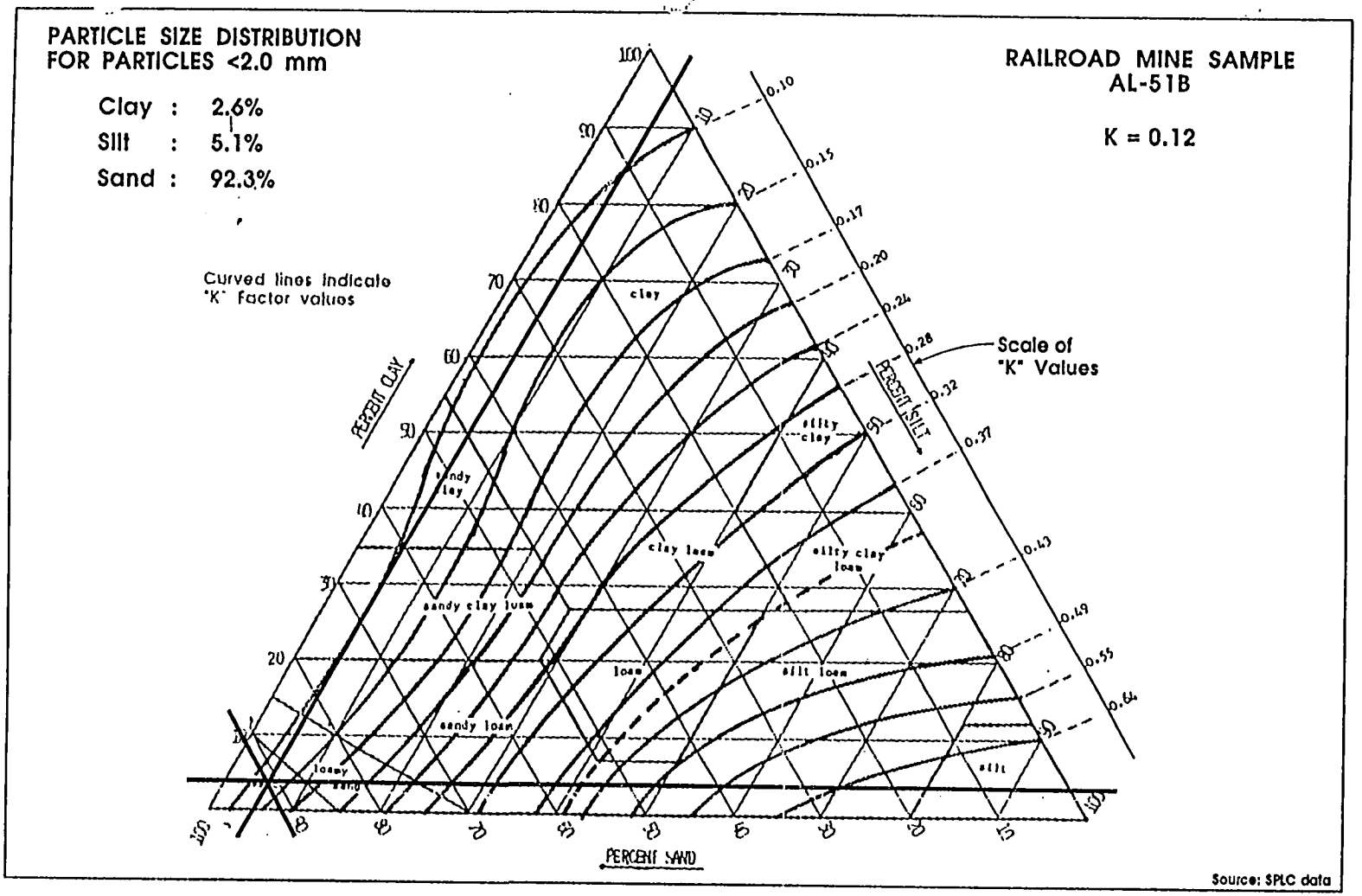
TRIANGULAR NOMOGRAPH METHOD FOR DETERMINING K FACTOR VALUES - SAMPLE AL-51A

Project No. 1802

LEVINE • FRICKE
CONSULTING ENGINEERS AND HYDROGEOLOGISTS

1802JDR24OCT88DT+LSS-BS-SPLC

Reproduced with permission of the copyright owner. Further reproduction prohibited without permission.



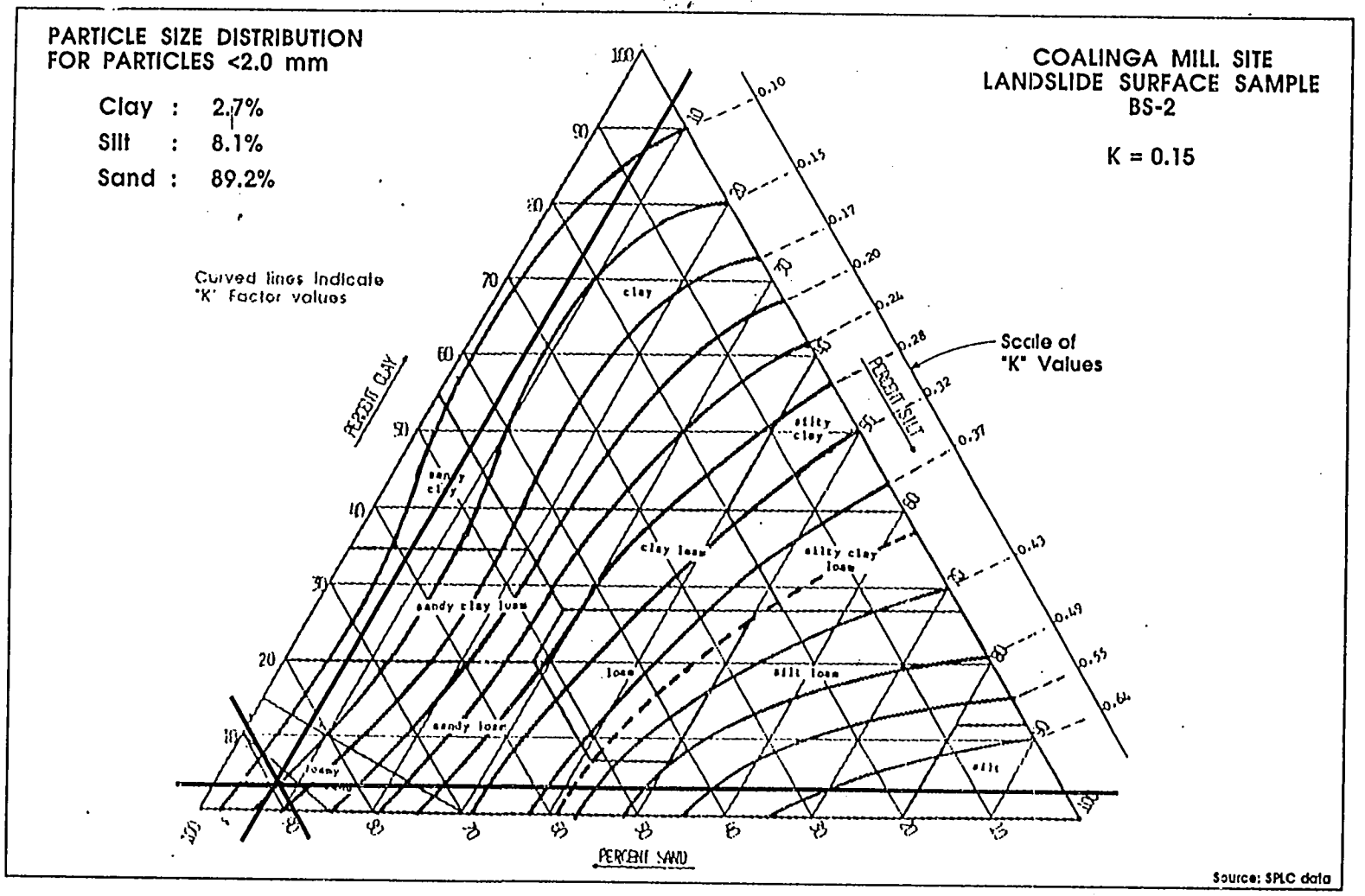
TRIANGULAR NOMOGRAPH METHOD FOR DETERMINING K FACTOR VALUES - SAMPLE AL-51B

Project No. 1802

LEVINE • FRICKE
CONSULTING ENGINEERS AND HYDROGEOLOGISTS

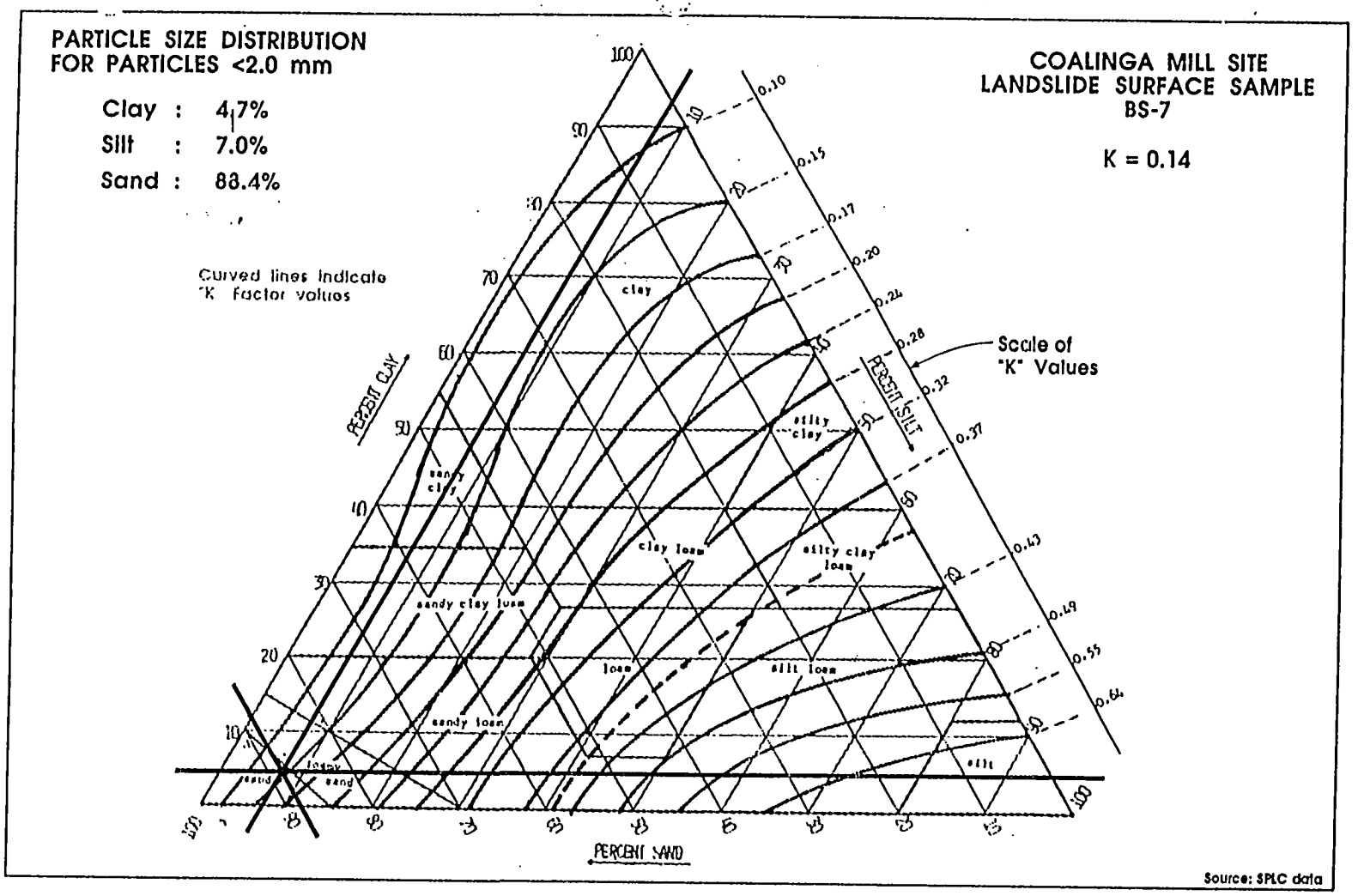
1802JD824OCT88DT•RMS-AL-SPLC

Reproduced with permission of the copyright owner. Further reproduction prohibited without permission.



TRIANGULAR NOMOGRAPH METHOD FOR DETERMINING K FACTOR VALUES - SAMPLE BS-2

Reproduced with permission of the copyright owner. Further reproduction prohibited without permission.



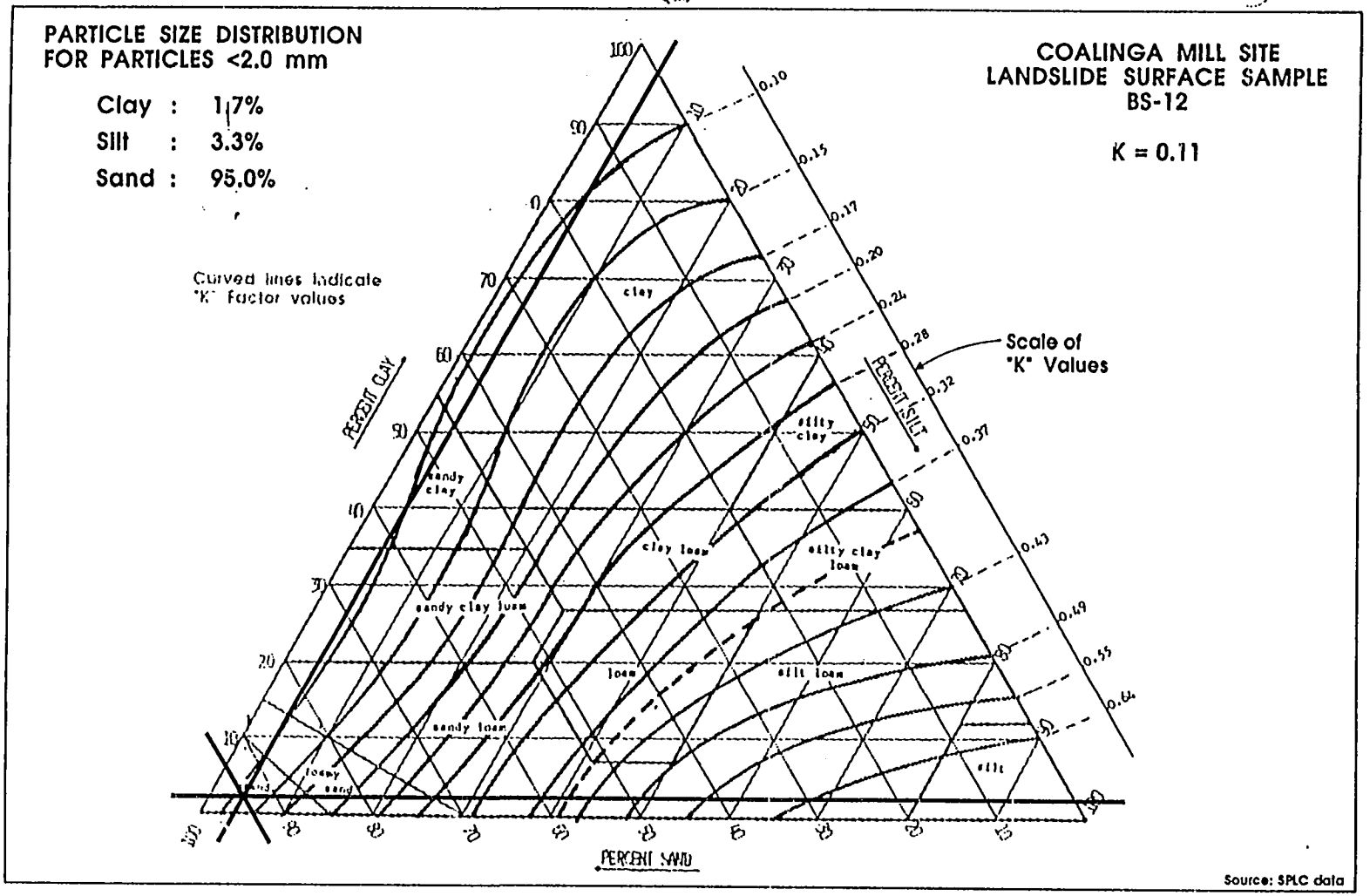
TRIANGULAR NOMOGRAPH METHOD FOR DETERMINING K FACTOR VALUES - SAMPLE BS-7

Project No. 1802

LEVINE • FRICKE
CONSULTING ENGINEERS AND HYDROGEOLOGISTS

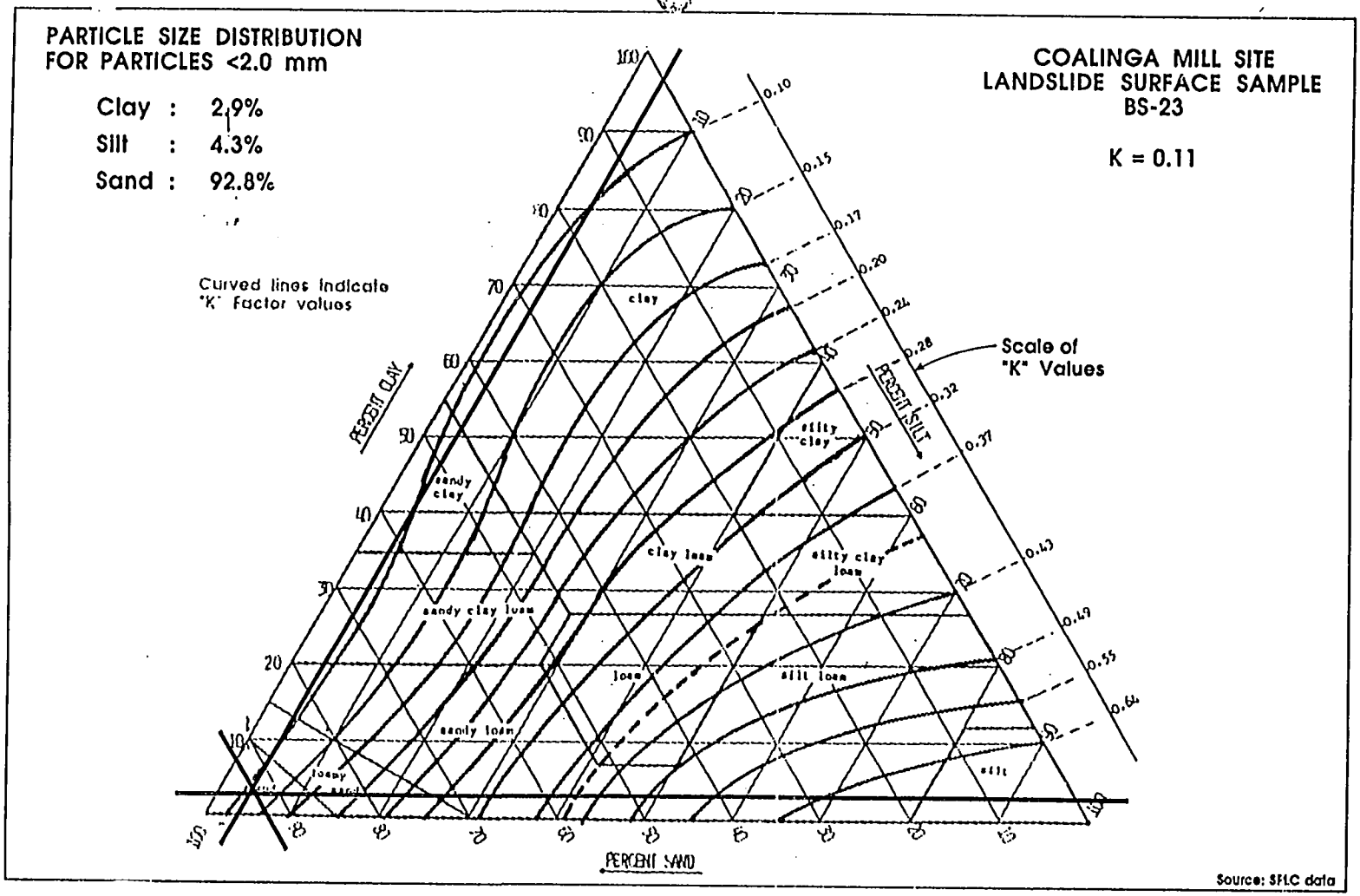
1802JDR24OCT88DI•LSS-BS-SPLC

Reproduced with permission of the copyright owner. Further reproduction prohibited without permission.



TRIANGULAR NOMOGRAPH METHOD FOR DETERMINING K FACTOR VALUES - SAMPLE BS-12

Reproduced with permission of the copyright owner. Further reproduction prohibited without permission.



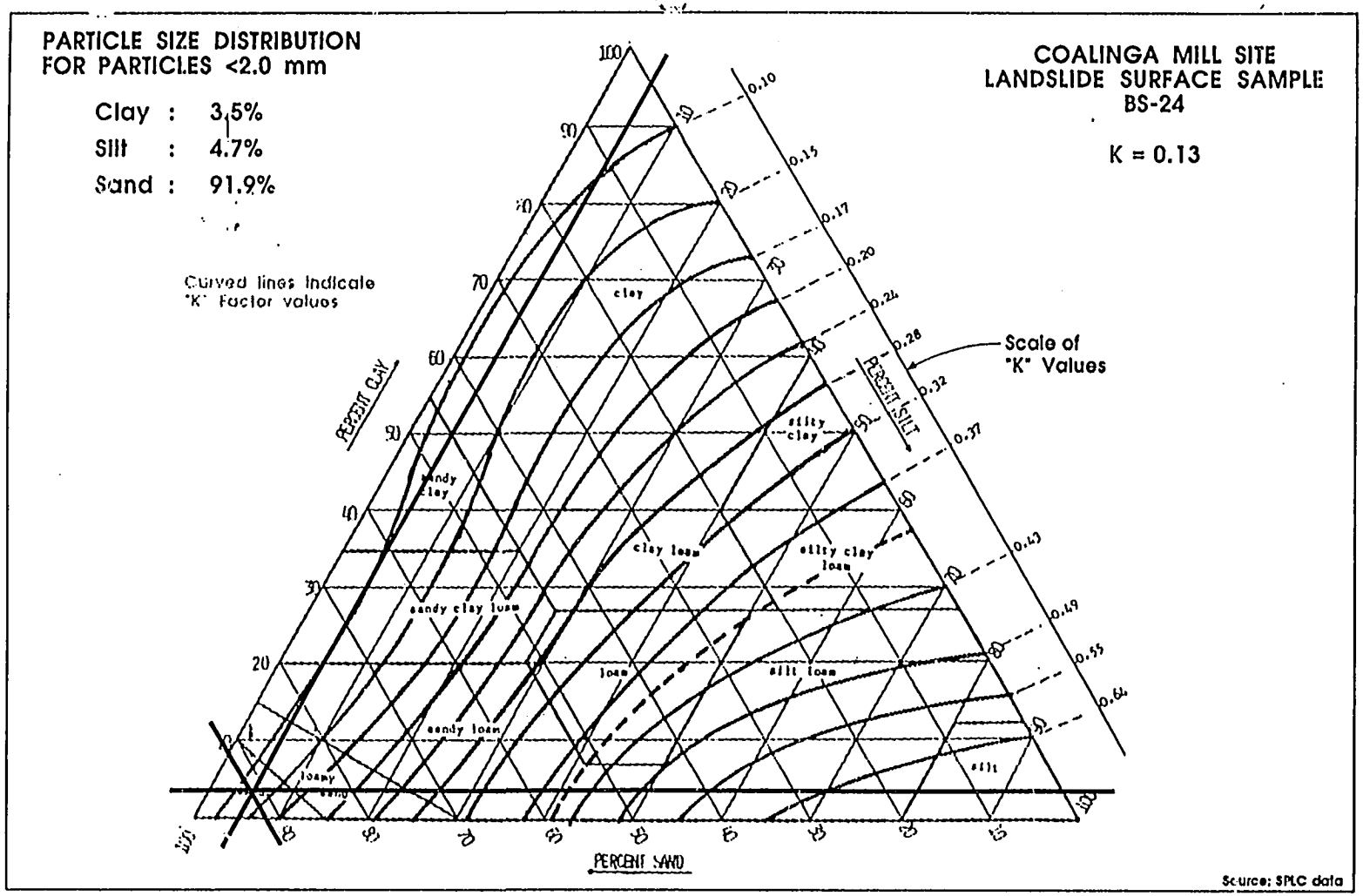
TRIANGULAR NOMOGRAPH METHOD FOR DETERMINING K FACTOR VALUES - SAMPLE BS-23

Project No. 1802

LEVINE • FRICKE
CONSULTING ENGINEERS AND HYDROGEOLOGISTS

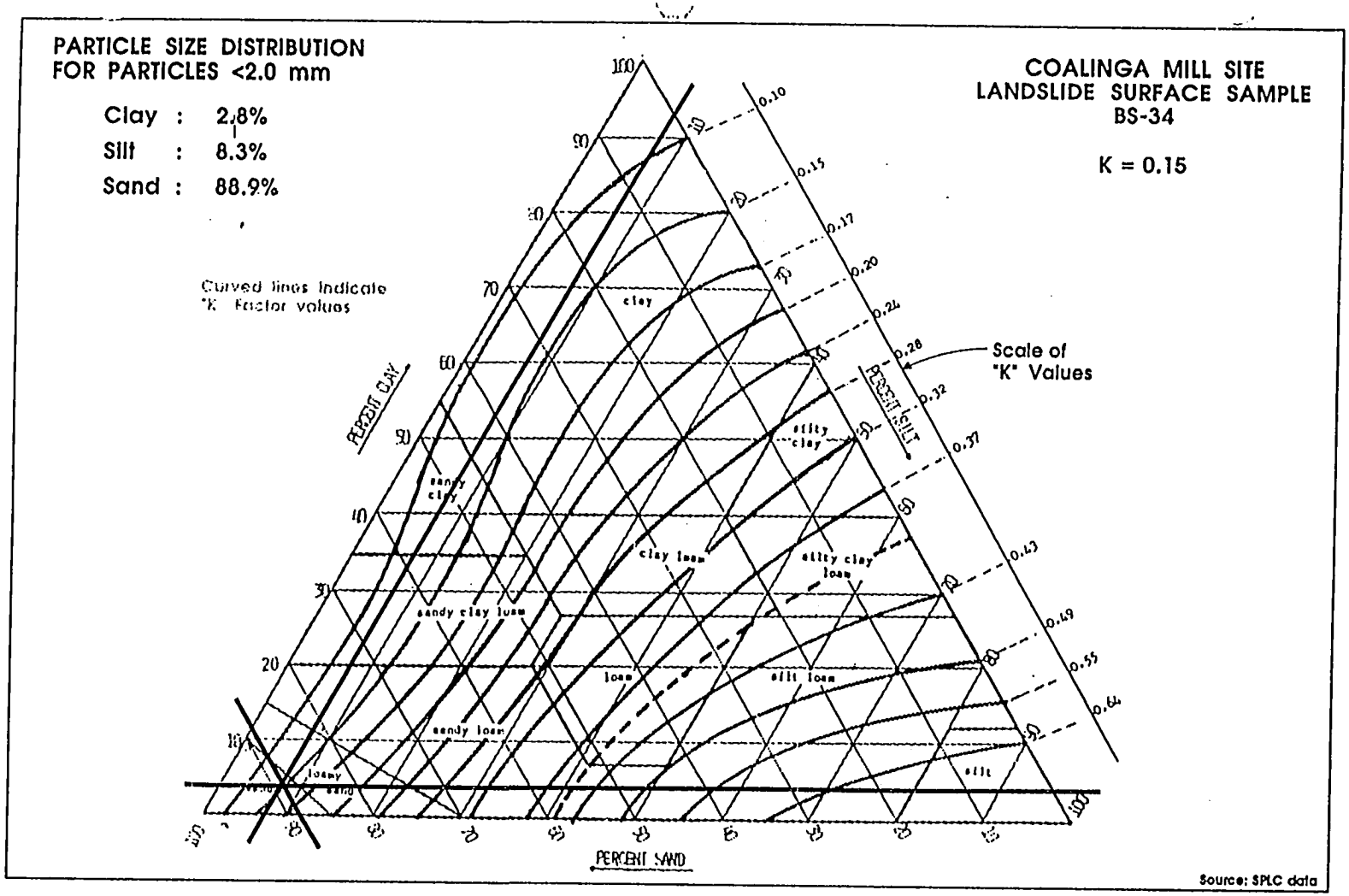
1802JDR24OCT88DF•LSS-BS-SFLC

Reproduced with permission of the copyright owner. Further reproduction prohibited without permission.



TRIANGULAR NOMOGRAPH METHOD FOR DETERMINING K FACTOR VALUES - SAMPLE BS-24

Reproduced with permission of the copyright owner. Further reproduction prohibited without permission.



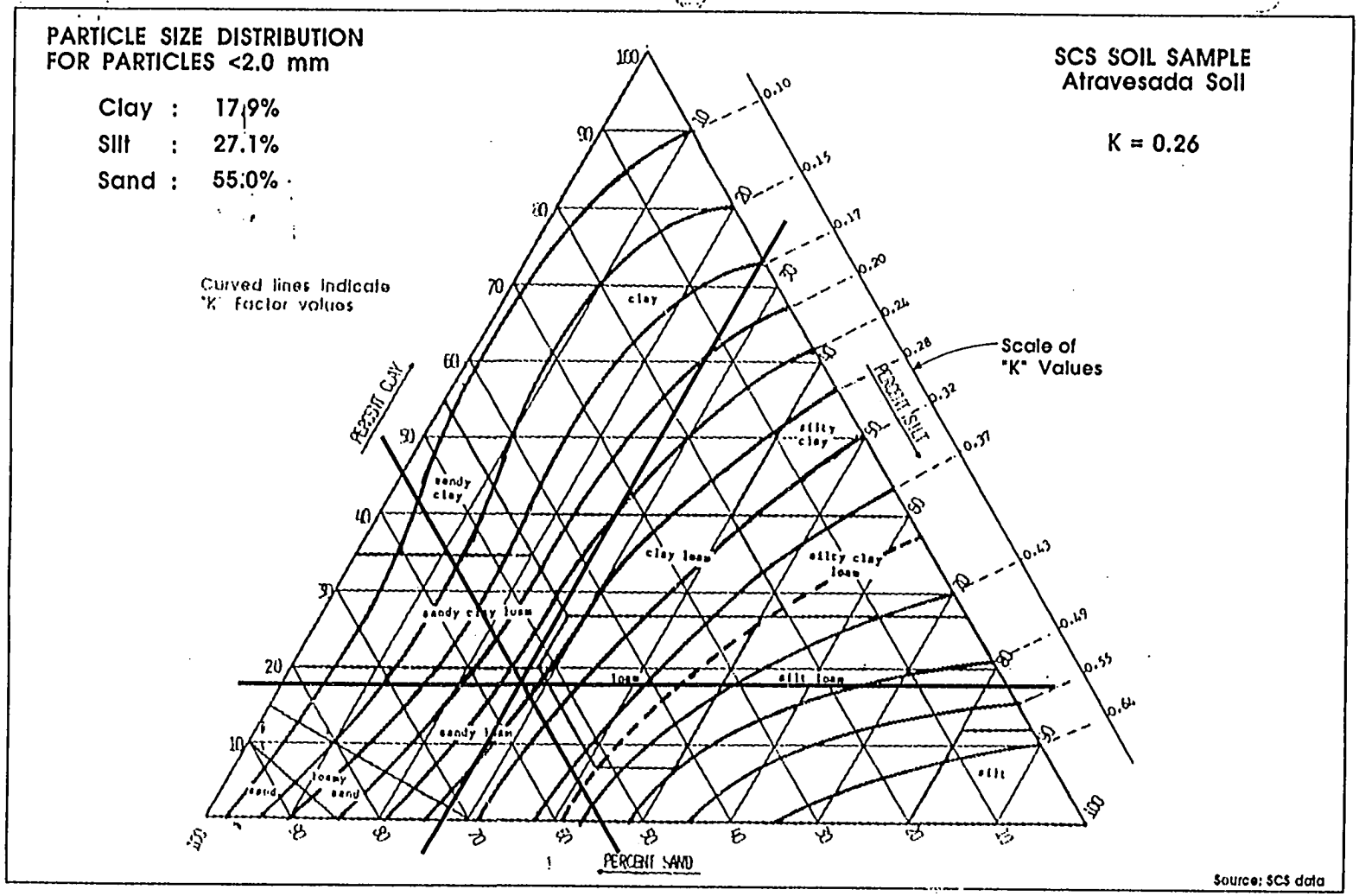
TRIANGULAR NOMOGRAPH METHOD FOR DETERMINING K FACTOR VALUES - SAMPLE BS-34

Project No. 1802

LEVINE • FRICKE
CONSULTING ENGINEERS AND HYDROGEOLOGISTS

1802JDR24OCT88DT•LSS-BS-SPLC

Reproduced with permission of the copyright owner. Further reproduction prohibited without permission.



TRIANGULAR NOMOGRAPH METHOD FOR DETERMINING K FACTOR VALUES - SAMPLE SCS - Atravesada